SHOUT
SHARE
IT

MBL

Volume 203
Number 1

# THE
# BIOLOGICAL
# BULLETIN

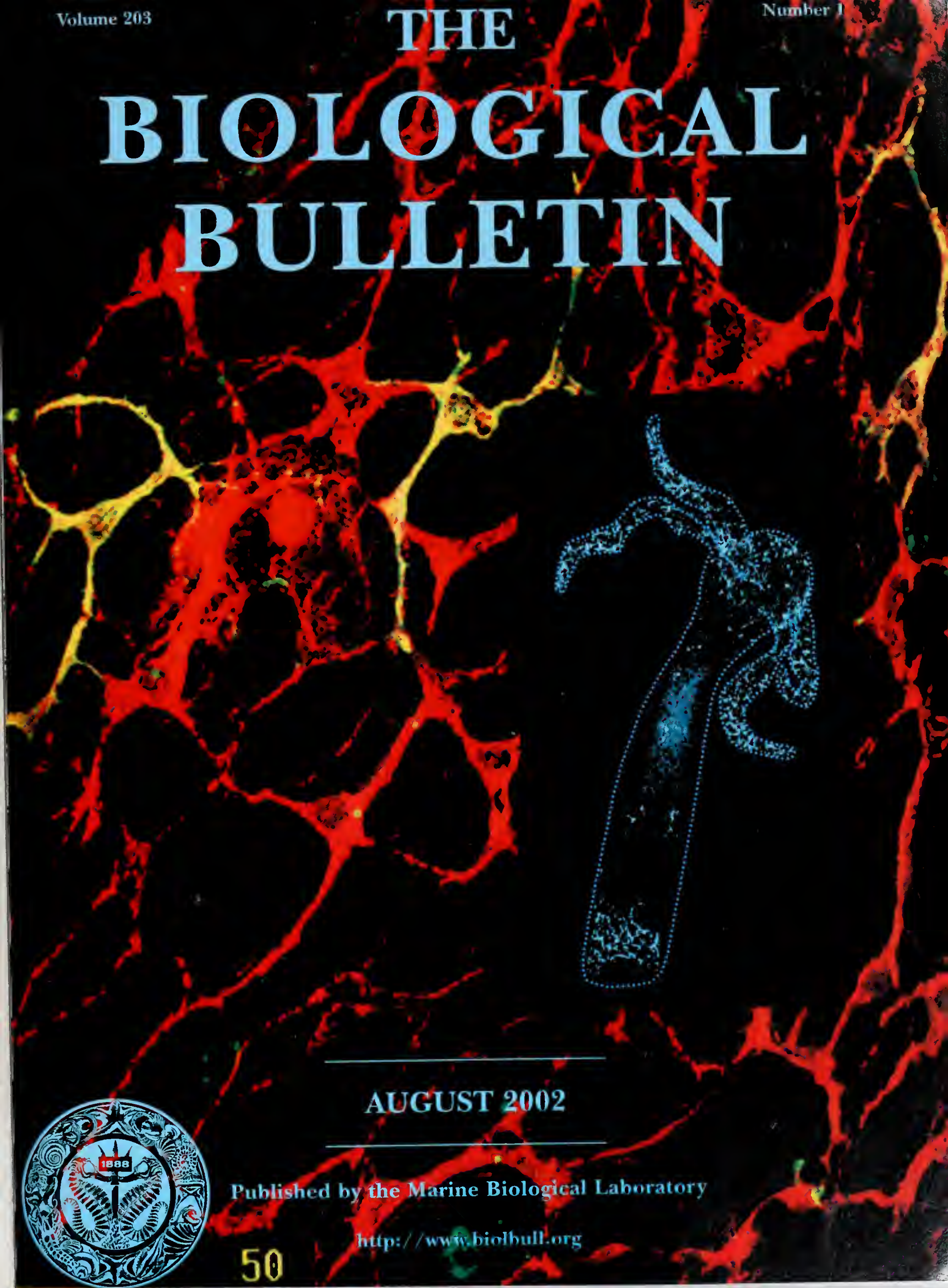

AUGUST 2002

Published by the Marine Biological Laboratory

http://www.biolbull.org

50

INVERTED MICROSCOPES

ERGONOMIC 25° EYEPIECE TUBE
ERGONOMIC TILTING TUBE
EXTENDIBLE INFINITY DESIGN PERMITTING ADDITION OF ILLUMINATION SOURCES/ATTACHMENTS
Nikon

# DRAWN FROM EXPERIENCE

## ONLY NIKON COULD REINVENT INVERTED MICROSCOPY WITH THE NEW ECLIPSE TE2000 SERIES.

When they were launched, Nikon's Eclipse TE microscopes set new standards in optical performance, continuing a tradition of over twenty years of excellence in inverted microscopy.

Now, Nikon proudly introduces the next generation of Eclipse research inverted microscopes. The Eclipse TE2000 series incorporates past successes into a new design with innovations that are exactly what today's varied research techniques require.

Here are just some of the special features built into this extraordinary microscope:

- Multi-part design permitting addition of optional illumination sources and other attachments without modifying the microscope.
- Unique "Noise Terminator" thoroughly eliminates stray light for greater S/N ratio in fluorescence imaging.
- Super-nanoprecision Z-access control and increased stability for superior 3D imaging.
- Modular motorized components for automated control.
- Exclusive CFI60™ infinity optical system for excellent resolution with high numerical apertures and longer working distances.

The Eclipse TE2000 is available in three models, each configured to meet your research needs. Draw on Nikon's experience.
For more information, call 1-800-52-NIKON, ext. 392
or visit www.nikonusa.com
In Canada, call 1-866-99-NIKON.

Visit MicroscopyU at
www.nikonusa.com to learn more
about inverted microscopy.

CFI60
ECLIPSE

Nikon

©2002 Nikon Instruments Inc.

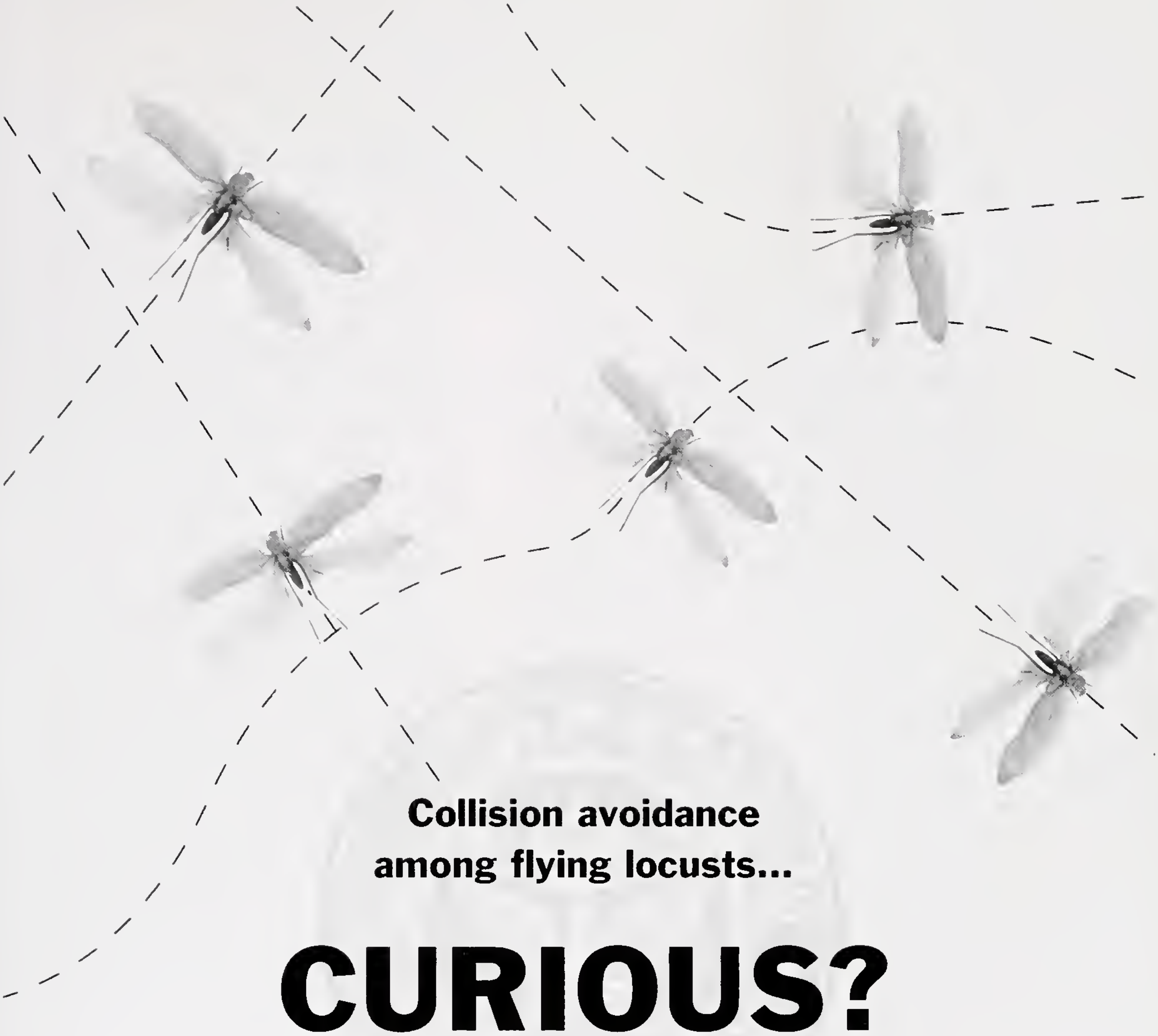

**Collision avoidance among flying locusts...**

**CURIOUS?**

- More than 12 million searchable journal articles
- World's largest collection of free full-text articles
- 4 different search tools to locate what you need
- Online archives of *The Biological Bulletin* plus more than 330 other journals covering the sciences and medicine

Find what you need at Stanford University's
www.highwire.org

HighWire LIBRARY OF THE SCIENCES AND MEDICINE

SEP 0 6 2002

# THE BIOLOGICAL BULLETIN
# ONLINE

The Marine Biological Laboratory is pleased to announce that the full text of *The Biological Bulletin* is available online at

http://www.biolbull.org

*The Biological Bulletin* publishes outstanding experimental research on the full range of biological topics and organisms, from the fields of Neurobiology, Behavior, Physiology, Ecology, Evolution, Development and Reproduction, Cell Biology, Biomechanics, Symbiosis, and Systematics.

Published since 1897 by the Marine Biological Laboratory (MBL) in Woods Hole, Massachusetts, *The Biological Bulletin* is one of America's oldest peer-reviewed scientific journals.

The journal is aimed at a general readership, and especially invites articles about those novel phenomena and contexts characteristic of intersecting fields.

*The Biological Bulletin Online* contains the full content of each issue of the journal, including all figures and tables, beginning with the February 2001 issue (Volume 200, Number 1). The full text is searchable by keyword, and the cited references include hyperlinks to Medline. PDF files are available beginning in February 1990 (Volume 178, Number 1), some abstracts are available beginning with the October 1976 issue (Volume 151, Number 2), and some Tables of Contents are online beginning with the October 1965 issue (Volume 129, Number 2).

Each issue will be placed online approximately on the date it is mailed to subscribers; therefore the online site will be available prior to receipt of your paper copy. Online readers may want to sign up for the eTOC (electronic Table of Contents) service, which will deliver each new issue's table of contents *via* e-mail. The web site also provides access to information about the journal (such as Instructions to Authors, the Editorial Board, and subscription information), as well as access to the Marine Biological Laboratory's web site and other *Biological Bulletin* electronic publications.

The free trial period for access to *The Biological Bulletin* online has ended. Individuals and institutions who are subscribers to the journal in print or are members of the Marine Biological Laboratory Corporation may now activate their online subscriptions. All other access (*e.g.*, to Abstracts, eTOCs, searching, Instructions to Authors) remains freely available. Online access is included in the print subscription price.

For more information about subscribing or activating your online subscription, visit <www.biolbull.org/subscriptions>.

---

http://www.biolbull.org

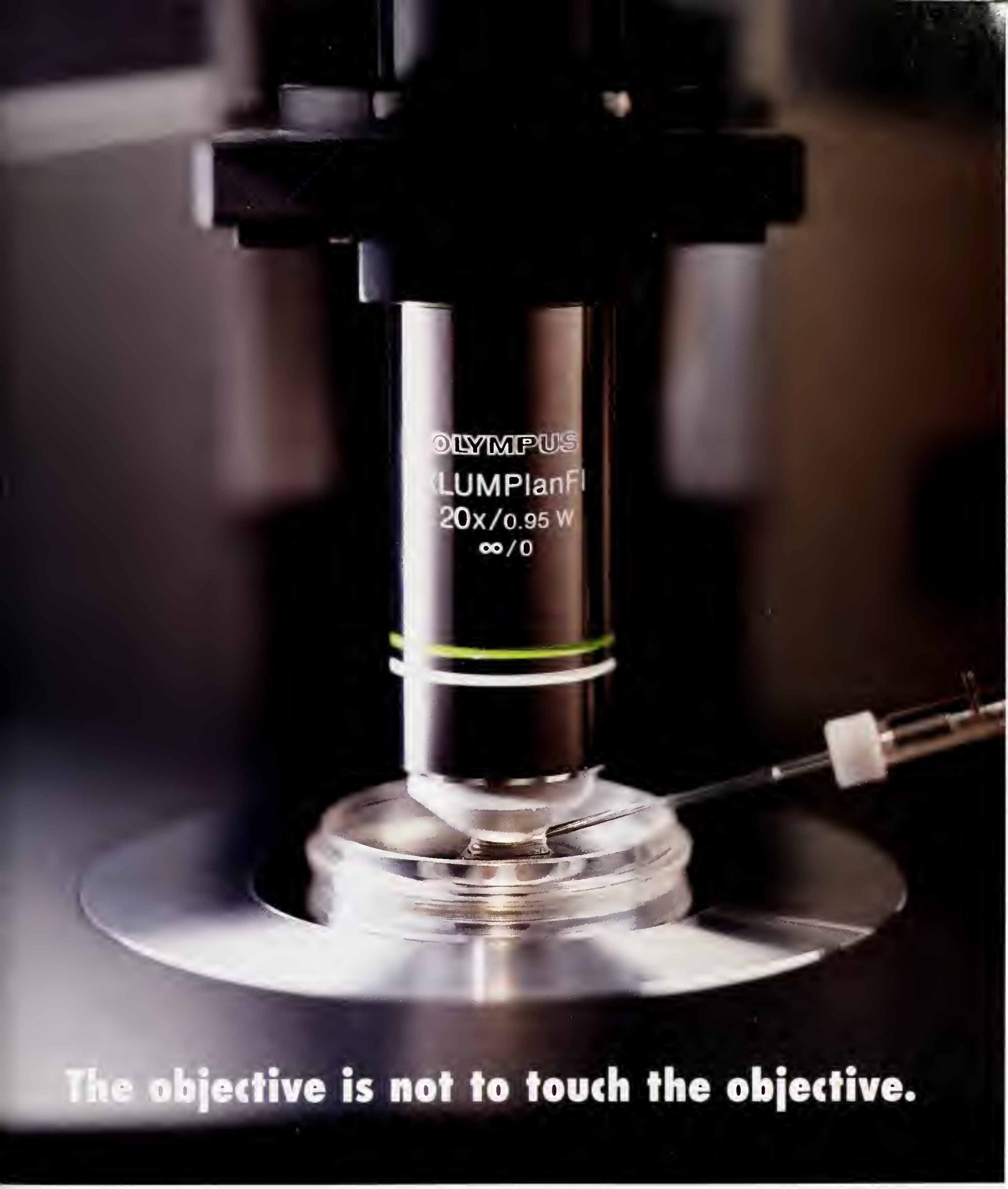
OLYMPUS
LUMPlanFl
20x/0.95 W
∞/0
The objective is not to touch the objective.

**The BX51WI.** A single 20x water immersion objective. A high N.A. of 0.95. A W.D. of 2.0mm. An intermediate magnification changer. Switch between low and high magnifications. Objective is untouched. Vibrations eliminated. Electrodes unmoved. It's a new movement in microscopy. **How Original. How Olympus.** Visit us at olympusamerica.com or call 1-800-446-5967.

OLYMPUS®
FOCUS ON LIFE

## *Cover*

The size of neuronal populations in developing metazoan nervous systems is thought to be influenced by two processes: overproduction of nerve cells, which ensures that all necessary and appropriate connections are made; and programmed cell death, which culls the excess neurons that have not found a target. Programmed cell death during neural development has been described in many metazoans—both vertebrates and invertebrates. The Cnidaria are among the most primitive metazoans with a nervous system; and, indeed, the molecular mechanism for apoptosis, a type of programmed cell death, is uniformly expressed among the cells of *Hydra vulgaris*[1].

Gordon B. Brumwell and Vicki J. Martin have raised embryos of *Hydra vulgaris* from fertilized eggs and have counted defined neuronal populations throughout development. They report in this issue of *The Biological Bulletin* (p. 70) that from the time that neurons of a particular type appear in the embryo, until development is complete, the population of these cells increases. From embryo to adult, no losses in any of the neuronal populations were detected. These data open the possibility, therefore, that no large-scale programmed cell death occurs in hydra during the development of the nervous system. Moreover, this study also suggests that culling of excess neurons—as a critical process in nervous system development—may have arisen in evolution after the appearance of the Cnidaria.

The neuronal populations described by Brumwell and Martin were first identified on the basis of their immunoreactivity to two antibodies, and then divided into subpopulations on morphological criteria. One of the immunoreactivities—to an antiserum raised to RFamide (Arg-Phe-$NH_2$)—occurs early in development; and, in an embryo 5 days after hatching, defines a pair of well-developed networks in the base and oral region. Such a 5-day embryo (about 0.9 mm from base to mouth) is shown on the cover, in the inset (blue). The larger image on the cover shows a nerve net in the base of an adult stained with both antibodies (the scale, in micrometers, is about 10 times that of the inset). Immunoreactivity to anti-RFamide (red) dominates the net, but a few neurons (yellow) are also reactive to the second antibody—a monoclonal to JD1, an uncharacterized antigen (green).

The cover images were provided by Gordon Brumwell and Vicki Martin. The inset image, from Fig. 2b, p. 74, was modified with Adobe PhotoShop by Beth Liles, MBL, who designed the cover.

---

[1] **Cikala, M., B. Wilm, E. Hobmeyer, A. Bottger, and C. N. David. 1999.** Identification of caspases and apoptosis in the simple metazoan Hydra. *Curr. Biol.* **9:** 959–962.

# THE
# BIOLOGICAL BULLETIN
## AUGUST 2002

| | | |
|---|---|---|
| **Editor** | Michael J. Greenberg | The Whitney Laboratory, University of Florida |
| **Associate Editors** | Louis E. Burnett | Grice Marine Laboratory, College of Charleston |
| | R. Andrew Cameron | California Institute of Technology |
| | Charles D. Derby | Georgia State University |
| | Michael LaBarbera | University of Chicago |
| **Section Editor** | Shinya Inoué, *Imaging and Microscopy* | Marine Biological Laboratory |
| **Online Editors** | James A. Blake, *Keys to Marine Invertebrates of the Woods Hole Region* | ENSR Marine & Coastal Center, Woods Hole |
| | William D. Cohen, *Marine Models Electronic Record and Compendia* | Hunter College, City University of New York |
| **Editorial Board** | Peter B. Armstrong | University of California, Davis |
| | Ernest S. Chang | Bodega Marine Lab., University of California, Davis |
| | Thomas H. Dietz | Louisiana State University |
| | Richard B. Emlet | Oregon Institute of Marine Biology, Univ. of Oregon |
| | David Epel | Hopkins Marine Station, Stanford University |
| | Kenneth M. Halanych | Woods Hole Oceanographic Institution |
| | Gregory Hinkle | Cereon Genomics, Cambridge, Massachusetts |
| | Nancy Knowlton | Scripps Inst. Oceanography & Smithsonian Tropical Res. Inst. |
| | Makoto Kobayashi | Hiroshima University of Economics, Japan |
| | Esther M. Leise | University of North Carolina Greensboro |
| | Donal T. Manahan | University of Southern California |
| | Margaret McFall-Ngai | Kewalo Marine Laboratory, University of Hawaii |
| | Mark W. Miller | Institute of Neurobiology, University of Puerto Rico |
| | Tatsuo Motokawa | Tokyo Institute of Technology, Japan |
| | Yoshitaka Nagahama | National Institute for Basic Biology, Japan |
| | Sherry D. Painter | Marine Biomed. Inst., Univ. of Texas Medical Branch |
| | J. Herbert Waite | University of California, Santa Barbara |
| | Richard K. Zimmer | University of California, Los Angeles |
| **Editorial Office** | Pamela Clapp Hinkle | Managing Editor |
| | Victoria R. Gibson | Staff Editor |
| | Carol Schachinger | Editorial Associate |
| | Wendy Child | Subscription & Advertising Administrator |

Published by
Marine Biological Laboratory
Woods Hole, Massachusetts

http://www.biolbull.org

chnology you can count o

# Exceptional Clusters, Superior Tech Support

## Microway's Reputation is Your Guarantee!

Harness Dual Athlon Power with a Microway® Scalable 25 Node 50 Processor Cluster Using Dual Athlon MP 2100+ and Myrinet Interconnect, Yielding Peak Throughput of 170 Gigaflops.

Microway® 1U Dual Athlon MP 2100+ RuggedRack™ Chassis Featuring Proprietary Across the Board™ Cooling plus 3 PCI Slots

## Athlon, Xeon, and Alpha Clusters for Life Sciences

Microway is the market leader in clusters for science. We offer innovative, competitively priced solutions, incorporating state of the art processors, and high speed interconnects. We provide customized solutions for both fine and coarse grain parallel applications, plus MCMS — Microway's monitoring and control package — which allows the system administrator to monitor the cluster via a web-based GUI. Since 1982, Microway has been the vendor of choice for scientists at universities, research labs, Fortune 500 and financial institutions worldwide. We understand that on-time delivery, out-of-the-box reliability and excellent ongoing technical support are critical to our users. Call us first for quotations and benchmarking capabilities. Find information, testimonials, and solutions at www.microway.com.

## *Over 17,000 Satisfied Customers Since 1982 Include:*

**CORPORATIONS**
AT&T
Carnegie Institute of Washington
Cray Research
EOS Biotechnology
Exxon
Federal Aviation Administration
General Electric
General Motors
Grumman Aerospace
Hughes Aircraft
Johnson & Johnson
Lion Bioscience
Lockheed Martin
Millennium Pharmaceuticals
Morgan Stanley
Myricom
Raytheon Missile Systems
RIB-X Pharmaceuticals

**LABORATORIES**
Ames
Argonne National Laboratory
Jet Propulsion Lab
Lawrence Livermore
Los Alamos National Laboratory
MBL - Woods Hole
NASA
NIH
NIST
NOAA
NSF
Naval Research Lab
Oak Ridge National Laboratory
Sandia National Laboratory
US Air Force, Army, Navy
US Department of Defense
US Geological Survey

**UNIVERSITIES**
California (Berkeley, UCLA, UCSD, UCSF)
Carnegie Mellon
Chicago
Colorado
Colorado State
Columbia
Connecticut
Cornell
Dartmouth
Duke
Florida
Georgia Tech
Harvard
Illinois
Maine
Maryland
Massachusetts
McGill
MIT
Northwestern
Pennsylvania
Pittsburgh
Princeton
Purdue
Rockefeller
Rutgers
South Carolina
Stanford
Texas
Tufts
Utah
Virginia
Vermont
Washington
Wisconsin
Yale

## *Expert Integration ~ Cost Effective Solutions*

"Our committee chose Microway over other vendors because of their reputation in the HPC community for delivering high quality, fully integrated clusters. Our decision was based also on their extensive technical expertise with Myrinet, demonstrated financial stability and ability to quickly deliver the 208 node cluster we required."

*— Jake Ward, Director, Department of Industrial Cooperation, University of Maine at Orono*

**SEE THE FUTURE...**

**Microway Symposium:**

**NEW DIRECTIONS IN CLUSTER TECHNOLOGIES**

**September 18-19
Plymouth,
Massachusetts, USA**

***Visit us at ISMB,***
**Edmonton,
August 3-7
Booth 18**

**Call us: 508-746-7341**
*For a technical salesperson who speaks your language*
**Visit us: www.microway.com**

Microway®
*Technology you can count on*℠

# CONTENTS

Volume 203, No. 1: August 2002

## PHYSIOLOGY AND BIOMECHANICS

**Denny, Mark, and Loretta Roberson**
Blade motion and nutrient flux to the kelp, *Eisenia arborea* . . . . 1

**Thompson, Joseph T., and William M. Kier**
Ontogeny of squid mantle function: changes in the mechanics of escape-jet locomotion in the oval squid, *Sepioteuthis lessoniana* Lesson, 1830 . . . . 14

**Marshall, Jennifer, Wayne P. Kelley, Stanislav S. Rubakhin, Jon-Paul Bingham, Jonathan V. Sweedler, and William F. Gilly**
Anatomical correlates of venom production in *Conus californicus* . . . . 27

**Burnett, Louis, Nora Terwilliger, Amy Carroll, Darwin Jorgensen, and David Scholnick**
Respiratory and acid-base physiology of the purple sea urchin, *Strongylocentrotus purpuratus,* during air exposure: presence and function of a facultative lung . . . . 42

## DEVELOPMENT AND REPRODUCTION

**Farley, Gregory S.**
Helical nature of sperm swimming affects the fit of fertilization-kinetics models to empirical data. . . . . 51

**Staver, Jennifer M., and Richard R. Strathmann**
Evolution of fast development of planktonic embryos to early swimming . . . . 58

**Brumwell, Gordon B., and Vicki J. Martin**
Immunocytochemically defined populations of neurons progressively increase in size through embryogenesis of *Hydra vulgaris* . . . . 70

**Chaparro, O. R., J. L. Charpentier, and R. Collin**
Embryonic velar structure and function of two sibling species of *Crepidula* with different modes of development . . . . 80

**Okusu, Akiko**
Embryogenesis and development of *Epimenia babai* (Mollusca Neomeniomorpha) . . . . 87

**Martynova, Marina G., and Olga A. Bystrova**
Undifferentiated cells in the snail myocardium are capable of DNA synthesis and myodifferentiation. . . . . 104

## NEUROBIOLOGY AND BEHAVIOR

**Delgado, Gabriel A., Robert A. Glazer, and Nicola J. Stewart**
Predator-induced behavioral and morphological plasticity in the tropical marine gastropod *Strombus gigas* . . . . 112

* * *

**Annual Report of the Marine Biological Laboratory** . . . . R1

THE BIOLOGICAL BULLETIN

THE BIOLOGICAL BULLETIN is published six times a year by the Marine Biological Laboratory, 7 MBL Street, Woods Hole, Massachusetts 02543.

Subscriptions and similar matter should be addressed to Subscription Administrator, THE BIOLOGICAL BULLETIN, Marine Biological Laboratory, 7 MBL Street, Woods Hole, Massachusetts 02543. Subscription includes both print and online journals. Subscription per year (six issues, two volumes): $260 for libraries; $105 for individuals. Subscription per volume (three issues): $130 for libraries; $52.50 for individuals. Back and single issues (subject to availability): $45 for libraries; $20 for individuals.

Communications relative to manuscripts should be sent to Michael J. Greenberg, Editor-in-Chief, or Pamela Clapp Hinkle, Managing Editor, at the Marine Biological Laboratory, 7 MBL Street, Woods Hole, Massachusetts 02543. Telephone: (508) 289-7428. FAX: 508-289-7922. E-mail: pclapp@mbl.edu.

http://www.biolbull.org

THE BIOLOGICAL BULLETIN is indexed in bibliographic services including *Index Medicus* and MEDLINE, *Chemical Abstracts, Current Contents, Elsevier BIOBASE/Current Awareness in Biological Sciences*, and *Geo Abstracts*.

Printed on acid free paper,
effective with Volume 180, Issue 1, 1991.

POSTMASTER: Send address changes to THE BIOLOGICAL BULLETIN, Marine Biological Laboratory,
7 MBL Street, Woods Hole, MA 02543.

Copyright © 2002, by the Marine Biological Laboratory

Periodicals postage paid at Woods Hole, MA, and additional mailing offices.
ISSN 0006-3185

# INSTRUCTIONS TO AUTHORS

*The Biological Bulletin* accepts outstanding original research reports of general interest to biologists throughout the world. Papers are usually of intermediate length (10–40 manuscript pages). A limited number of solicited review papers may be accepted after formal review. A paper will usually appear within four months after its acceptance.

Very short, especially topical papers (less than 9 manuscript pages including tables, figures, and bibliography) will be published in a separate section entitled "Research Notes." A Research Note in *The Biological Bulletin* follows the format of similar notes in *Nature*. It should open with a summary paragraph of 150 to 200 words comprising the introduction and the conclusions. The rest of the text should continue on without subheadings, and there should be no more than 30 references. References should be referred to in the text by number, and listed in the Literature Cited section in the order that they appear in the text. Unlike references in *Nature*, references in the Research Notes section should conform in punctuation and arrangement to the style of recent issues of *The Biological Bulletin*. Materials and Methods should be incorporated into appropriate figure legends. See the article by Lohmann *et al.* (October 1990, Vol. **179:** 214–218) for sample style. A Research Note will usually appear within two months after its acceptance.

The Editorial Board requests that regular manuscripts conform to the requirements set below; those manuscripts that do not conform will be returned to authors for correction before review.

1. ***Manuscripts.*** Manuscripts, including figures, should be submitted in quadruplicate, with the originals clearly marked. (Xerox copies of photographs are not acceptable for review purposes.) If possible, please include an electronic copy of the text of the manuscript. Label the disk with the name of the first author and the name and version of the wordprocessing software used to create the file. If the file was not created in some version of Microsoft Word, save the text in rich text format (rtf). The submission letter accompanying the manuscript should include a telephone number, a FAX number, and (if possible) an E-mail address for the corresponding author. The original manuscript must be typed in no smaller than 12 pitch or 10 point, using double spacing (*including* figure legends, footnotes, bibliography, etc.) on one side of 16- or 20-lb. bond paper, 8 by 11 inches. Please, no right justification. Manuscripts should be proofread carefully and errors corrected legibly in black ink. Pages should be numbered consecutively. Margins on all sides should be at least 1 inch (2.5 cm). Manuscripts should conform to the *Council of Biology Editors Style Manual*, 5th Edition (Council of Biology Editors, 1983) and to American spelling. Unusual abbreviations should be kept to a minimum and should be spelled out on first reference as well as defined in a footnote on the title page. Manuscripts should be divided into the following components: Title page, Abstract (of no more than 200 words), Introduction, Materials and Methods, Results, Discussion, Acknowledgments, Literature Cited, Tables, and Figure Legends. In addition, authors should supply a list of words and phrases under which the article should be indexed.

2. ***Title page.*** The title page consists of a condensed title or running head of no more than 35 letters and spaces, the manuscript title, authors' names and appropriate addresses, and footnotes listing present addresses, acknowledgments or contribution numbers, and explanation of unusual abbreviations.

3. ***Figures.*** The dimensions of the printed page, 7 by 9 inches, should be kept in mind in preparing figures for publication. We recommend that figures be about 1 times the linear dimensions of the final printing desired, and that the ratio of the largest to the smallest letter or number and of the thickest to the thinnest line not exceed 1:1.5. Explanatory matter generally should be included in legends, although axes should always be identified on the illustration itself. Figures should be prepared for reproduction as either line cuts or halftones. Figures to be reproduced as line cuts should be unmounted glossy photographic reproductions or drawn in black ink on white paper, good-quality tracing cloth or plastic, or blue-lined coordinate paper. Those to be reproduced as halftones should be mounted on board, with both designating numbers or letters and scale bars affixed directly to the figures. All figures should be numbered in consecutive order, with no distinction between text and plate figures and cited, in order, in the text. The author's name and an arrow indicating orientation should appear on the reverse side of all figures.

*Digital art: The Biological Bulletin* will accept figures submitted in electronic form; however, digital art must conform to the following guidelines. Authors who create digital images are wholly responsible for the quality of their material, including color and halftone accuracy.

*Format.* Acceptable graphic formats are TIFF and EPS. Color submissions must be in EPS format, saved in CMKY mode.

*Software.* Preferred software is Adobe Illustrator or Adobe Photoshop for the Mac and Adobe Photoshop for Windows. Specific instructions for artwork created with various software programs are available on the Web at the Digital Art Information Site maintained by Cadmus Professional Communications at http://cpc.cadmus.com/dal/

*Resolution.* The minimum requirements for resolution are 1200 DPI for line art and 300 for halftones.

*Size.* All digital artwork must be submitted at its actual printed size so that no scaling is necessary.

*Multipanel figures.* Figures consisting of individual parts (*e.g.*, panels A, B, C) must be assembled into final format and submitted as one file.

*Hard copy.* Files must be accompanied by hard copy for use in case the electronic version is unusable.

*Disk identification.* Disks must be clearly labeled with the following information: author name and manuscript number; format (PC or Macintosh); name and version of software used.

*Color: The Biological Bulletin* will publish color figures and plates, but must bill authors for the actual additional cost of printing in color. The process is expensive, so authors with more than one color image should—consistent with editorial concerns, especially citation of figures in order—combine them into a single plate to reduce the expense. On request, when supplied with a copy of a color illustration, the editorial staff will provide a pre-publication estimate of the printing cost.

4. ***Tables, footnotes, figure legends, etc.*** Authors should follow the style in a recent issue of *The Biological Bulletin* in preparing table headings, figure legends, and the like. Because of the high cost of setting tabular material in type, authors are asked to limit such material as much as possible. Tables, with their headings and footnotes, should be typed on separate sheets, numbered with consecutive Roman numerals, and placed after the Literature Cited. Figure legends should contain enough information to make the figure intelligible separate from the text. Legends should be typed double spaced, with consecutive Arabic numbers, on a separate sheet at the end of the paper. Footnotes should be limited to authors' current addresses, acknowledgments or contribution numbers, and explanation of unusual abbreviations. All such footnotes should appear on the title page. Footnotes are not normally permitted in the body of the text.

5. ***Literature cited.*** In the text, literature should be cited by the Harvard system, with papers by more than two authors cited as Jones *et al.*, 1980. Personal communications and material in preparation or in press should be cited in the text only, with author's initials and institutions, unless the material has been formally accepted and a volume number can be supplied. The list of references following the text should be headed Literature Cited, and must be typed double spaced on separate pages, conforming in punctuation and arrangement to the style of recent issues of *The Biological Bulletin*. Citations should include complete titles and inclusive pagination. Journal abbreviations should normally follow those of the U. S. A. Standards Institute (USASI), as adopted by Biological Abstracts and Chemical Abstracts, with the minor differences set out below. The most generally useful list of biological journal titles is that published each year by Biological Abstracts (biosis List of Serials; the most recent issue). Foreign authors, and others who are accustomed to using The World List of Scientific Periodicals, may find a booklet published by the Biological Council of the U.K. (obtainable from the Institute of Biology, 41 Queen's Gate, London, S.W.7, England, U.K.) useful, since it sets out the World List abbreviations for most biological journals with notes of the USASI abbreviations where these differ. Chemical Abstracts publishes quarterly supplements of additional abbreviations. The following points of reference style for The Biological Bulletin differ from USASI (or modified World List) usage:

A. Journal abbreviations, and book titles, all underlined (for *italics*)

B. All components of abbreviations with initial capitals (not as European usage in World List *e.g., J. Cell. Comp. Physiol.* NOT *J. cell. comp. Physiol.*)

C. *All* abbreviated components must be followed by a period, whole word components *must not* (*i.e., J. Cancer Res.*)

D. Space between all components (*e.g., J. Cell. Comp. Physiol.*, not *J.Cell.Comp.Physiol.*)

E. Unusual words in journal titles should be spelled out in full, rather than employing new abbreviations invented by the author. For example, use *Rit Vísindafjélags Islendinga* without abbreviation.

F. All single word journal titles in full (*e.g., Veliger, Ecology, Brain*).

G. The order of abbreviated components should be the same as the word order of the complete title (*i.e., Proc.* and *Trans.* placed where they appear, not transposed as in some BIOLOGICAL ABSTRACTS listings).

H. A few well-known international journals in their preferred forms rather than WORLD LIST or USASI usage (*e.g., Nature, Science, Evolution* NOT *Nature, Lond., Science, N.Y.; Evolution, Lancaster, Pa.*)

6. ***Reprints, page proofs, and charges.*** Authors may purchase reprints in lots of 100. Forms for placing reprint orders are sent with page proofs. Reprints normally will be delivered about 2 to 3 months after the issue date. Authors (or delegates for foreign authors) will receive page proofs of articles shortly before publication. They will be charged the current cost of printers' time for corrections to these (other than corrections of printers' or editors' errors). Other than these charges for authors' alterations, *The Biological Bulletin* does not have page charges.

Reference: *Biol. Bull.* **203:** 1–13. (August 2002)

# Blade Motion and Nutrient Flux to the Kelp, *Eisenia arborea*

MARK DENNY* AND LORETTA ROBERSON

*Hopkins Marine Station, Stanford University, Pacific Grove, California 93950*

**Abstract.** Marine algae rely on currents and waves to replenish the nutrients required for photosynthesis. The interaction of algal blades with flow often involves dynamic reorientations of the blade surface (pitching and flapping) that may in turn affect nutrient flux. As a first step toward understanding the consequences of blade motion, we explore the effect of oscillatory pitching on the flux to a flat plate and to two morphologies of the kelp *Eisenia arborea*. In slow flow (equivalent to a water velocity of 2.7 cm $s^{-1}$), pitching increases the time-averaged flux to both kelp morphologies, but not to the plate. In fast flow (equivalent to 20 cm $s^{-1}$ in water), pitching has negligible effect on flux regardless of shape. For many aspects of flux, the flat plate is a reliable model for the flow-protected algal blade, but predictions made from the plate would substantially underestimate the flux to the flow-exposed blade. These measurements highlight the complexities of flow-related nutrient transport and the need to understand better the dynamic interactions among nutrient flux, blade motion, blade morphology, and water flow.

## Introduction

Lacking the means to transport water actively, marine algae rely on currents and waves to move water over their surfaces, thereby replenishing the supply of nutrients required for photosynthesis. In areas of slow flow, the flux of nutrients to the algal blade can be a limiting factor in primary production (*e.g.*, Gerard and Mann, 1979; Wheeler, 1980; Gerard, 1982; Koehl and Alberte, 1988; Koch, 1993; Gonen *et al.*, 1995), and it has been hypothesized that in some species (*e.g.*, *Macrocystis pyrifera*, *Macrocystis integrifolia*, *Eisenia arborea*) the morphology of the blade has adapted to increase mixing (and consequently, flux) at low water velocities (Wheeler, 1980; Hurd *et al.*, 1996; Roberson, 2001). The efficacy of these morphological adaptations has been debated (for reviews, see Hurd, 2000; Roberson, 2001), and their effect in nature remains an open question.

The exploration of nutrient flux to marine algae has often involved a comparison of the mixing over algal blades to the mixing over a flat, rigid plate (Wheeler, 1980; Hurd and Stevens, 1997). Flow over a smooth flat plate has been studied extensively by fluid dynamicists (through both theory and empirical measurements), and it indeed provides a handy model for the flow over an algal blade. It has been taken as evidence of adaptation if the flux to an alga is greater than that predicted for a flat plate of comparable size (*e.g.*, Wheeler, 1980). This comparison may not always be appropriate, however. The theory of flow relative to a smooth, flat plate (Schlichting, 1979) assumes that the plate is precisely planar, has a distinct leading edge, and has a width (perpendicular to flow) much greater than its length (parallel to flow)—criteria met by few algal blades. It is not surprising, then, that the flow over even smooth algal blades deviates substantially from the predictions of flat-plate theory (Koehl and Alberte, 1988; Hurd and Stevens, 1997).

Simple boundary-layer theory also assumes that the plate is rigid and parallel to flow (Schlichting, 1979), again criteria that few algal blades fulfill. Algal blades and stipes are flexible, and their interaction with flow often causes waves of deformation to pass through the stipe and blade. When the wavelength of this deformation is large compared to the length of the blade, the blade appears to pitch up and down (Gerard, 1982). When the wavelength of deformation is equal to or less than the length of the blade, the blade "flutters" or "flaps" in a manner similar to a wind-blown flag (Koehl and Alberte, 1988; Hurd and Stevens, 1997). These hydroelastic motions have long been thought to affect mixing over algal blades, and Koehl and Alberte (1988)

---

Received 21 December 2001; accepted 29 April 2002.

* To whom correspondence should be addressed. E-mail: mwdenny@leland.stanford.edu

have shown that flux to a *Nereocystis* blade increased when they forcibly flapped the blade. However, the hydrodynamic basis of a flap-induced increase in flux and its generality among algae have not been studied.

The dynamic reorientation of algal blades in flow, and the consequent effects on nutrient flux, pose exceedingly complex questions in fluid dynamics and structural mechanics. It is often advantageous in this type of situation to perform a series of preliminary laboratory experiments on simple models. These experiments may not be able to precisely duplicate the complexities of the natural world, but this disadvantage is offset by the ability to control and quantify the various parameters that might contribute to the phenomenon. Here we report on such laboratory experiments that explore the effects of dynamic blade reorientation on the flow-mediated flux to algal blades. Our intent is to draw attention to the potential importance of these effects, to introduce a method by which the effects can be quantified, and thereby to set the stage for future research in which the actual rates of nutrient flux can be measured under the natural conditions found in the wave-swept environment.

We compare the dynamic flux to models of two flow-related morphologies of the kelp *Eisenia arborea*, and find that cyclic pitching indeed increases the flux to these blades. The effect is more substantial at low water velocities than at high water velocities. In addition to the measurements made on model kelp blades, a comparison is made between the flow around kelps and that around a flat, smooth, rigid plate. Flux to the flow-protected morphology of *Eisenia* (which is thought to be adapted to increase overall flux at low flow; Roberson, 2001) more closely resembles the flux to a flat plate than does the flux to the flow-exposed morphology. These measurements highlight the complexities of flow-related nutrient transport and the need for further research if we are to understand the dynamic interaction among nutrient flux, blade motion, blade morphology, and water flow.

## Materials and Methods

*Eisenia arborea* (Ruprecht) was collected near the Wrigley Institute of Environmental Science on Catalina Island, California. At this site, the kelp occurs in two distinct morphologies that are correlated with the maximal flow to which the alga is exposed (Roberson, 2001). In relatively high-flow environments (mean velocity $> 0.1$ m s$^{-1}$) *E. arborea* produces long, narrow, straplike blades that are characterized by rows of relatively low ridges and valleys oriented more or less parallel to flow (Roberson, 2001). The valley-to-ridge height of these blades is about 1 mm, and the distance between ridges is about 5 mm. In contrast, in areas of low water velocity (mean flow $< 0.03$ m s$^{-1}$), blades are short, wide, and triangular, and are characterized by relatively large-amplitude bullations ("bumps"; Roberson, 2001). In this case, the valley-to-ridge height is about 2.4 mm and the ridge-to-ridge distance is 10–20 mm. A representative blade of the flow-exposed morphology was obtained at a depth of 5 m and the flow-protected morphology at a depth of 20 m. Both blades were returned to the laboratory, blotted dry, sprayed with cooking oil, and cast in plaster. A sheet of copper foil (0.5 mm thick) was then pressed into the casts to form a rigid, thermally conductive model of each algal blade (Fig. 1).

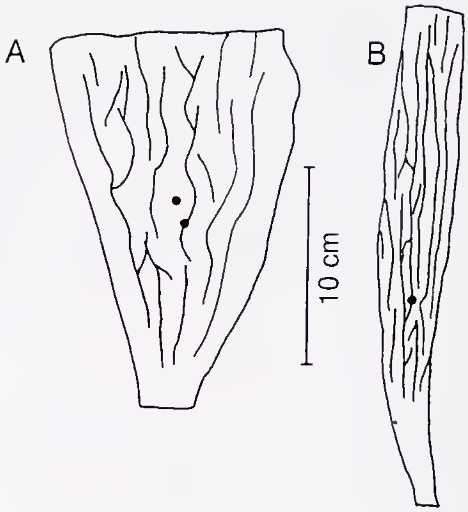

**Figure 1.** Tracings of the two *Eisenia arborea* blades used in this study. (A) the flow-protected morphology; (B) the flow-exposed morphology. The lines show the location of the midline of crests, and the dots show where heat flux was measured. In both blades, the proximal end of the blade is toward the bottom of the page, and flow is toward the top of the page.

Each copper model was sealed to a watertight jacket milled from a block of PVC (Fig. 2A). To minimize the effect of the jacket on the flow past the model, the upstream end of the jacket was recessed about 2 cm from the upstream end of the model and was beveled to make the jacket more streamlined. Water from a constant-temperature bath (Neslab Endocal model RTE 220) was rapidly circulated through this jacket to maintain the surface of the model at a constant temperature. Given this arrangement, the flux of heat to or from the model's surface is analogous to the flux of nutrients to or from the blade of an actual alga, and depends on the characteristics of the boundary-layer flow (Bird *et al.*, 1960; Denny, 1993; Vogel, 1994). These models thus provide a means for a quantitative exploration of the interaction between fluid flow and nutrient flux.

For convenience, experiments were conducted in air rather than in water. The shift from one medium to another is a common tool in fluid mechanics, and relies on the fact that the pattern of flow relative to an object remains constant across media if the Reynolds number, $Re_x$, is held constant (Denny, 1993; Vogel, 1994). Reynolds number (the ratio of inertial to viscous forces in flow) is

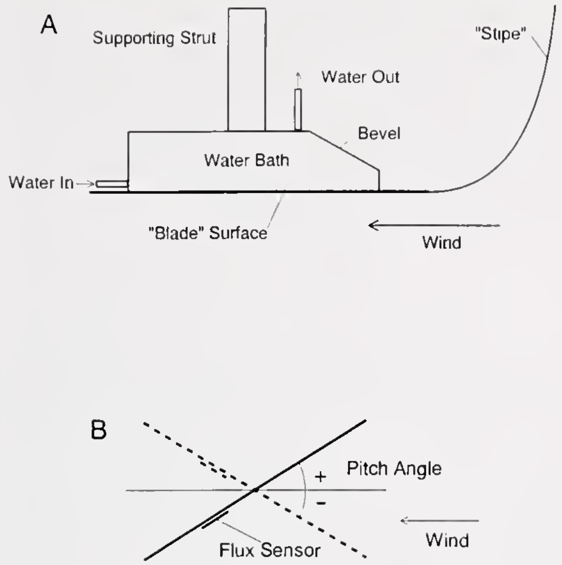

**Figure 2.** (A) Schematic drawing of a model used to measure heat flux (not drawn to scale). The water bath kept the blade surface at a constant temperature. (B) Definition of the pitch angle (= angle of incidence). When the pitch angle is positive, the heat flux sensor is on the windward face of the model.

$$\mathrm{Re}_x = \frac{ux}{\nu}, \qquad \text{(Eq. 1)}$$

where $u$ is the velocity of the fluid relative to the object, $x$ is a characteristic length (here taken to be the distance from the upstream end of the blade to the point at which flux is measured), and $\nu$ is the kinematic viscosity of the fluid. In the terms of Denny (1993) and Vogel (1994), this is a "local" Reynolds number. The kinematic viscosity of seawater at 20 °C (a typical temperature for *E. arborea* at Catalina) is $1.06 \times 10^{-6}$ $\mathrm{m^2\ s^{-1}}$, whereas the kinematic viscosity of air at 20 °C (the temperature of the laboratory) is $15.1 \times 10^{-6}$ $\mathrm{m^2\ s^{-1}}$ (Denny, 1993). Thus for a given $x$, the Reynolds number (and therefore the pattern of flow) is the same if $u$ in air is 14.2 times that in water.

Experiments were conducted in a low-speed wind tunnel (Bell, 1993, 1995) with a working cross-section 60 cm square. Each model kelp was mounted in the center of the cross-section with its exposed surface down (to ensure that within the water jacket no bubbles were in contact with the copper foil) and its proximal end upstream (Fig. 2A). The pitch angle of the blade (its angle of incidence to the oncoming flow) was measured as shown in Figure 2B.

To mimic the presence of the narrow proximal end of the blade and the stipe, one end of a flexible strip of plastic was attached to the proximal end of the model blade. The other end of the plastic strip was attached to the ceiling of the wind tunnel. The width of the plastic strip was constant along its length and equal to the width of the model blade at its proximal end.

Each model was held in place by an aluminum frame that could be rotated about a horizontal axis perpendicular to flow (Fig. 3). The pitch of models relative to flow could thus be varied as the frame rotated. In turn, the rotation of the frame was controlled by a linkage attached to a motor-driven eccentric arm. The length of the eccentric arm was such that the pitch of the frame varied by about ±20° as the motor turned. Through this arrangement, we caused the model to pitch up and down in flow in a pattern of motion roughly analogous to the dynamic reorientation of blades in nature. By varying the speed of the motor, we could vary the frequency of oscillation. In the absence of accurate measurements of pitching frequency in nature, an arbitrary range of frequencies (0.13, 0.20, 0.39, and 0.59 Hz) was used. The instantaneous angle of the frame was measured using a linearly variable differential transformer (LVDT, Schaevitz model 500HR) connected by a string to a capstan as shown in Figure 3A. The voltage output from the LVDT was recorded on one channel of a Kipp and Zonen BD112 potentiometric chart recorder.

For comparison, a rigid, smooth, flat brass plate (15.2 cm wide by 23.0 cm long by 0.05 cm thick) was fitted with a water jacket and mounted in the wind tunnel as for the blade

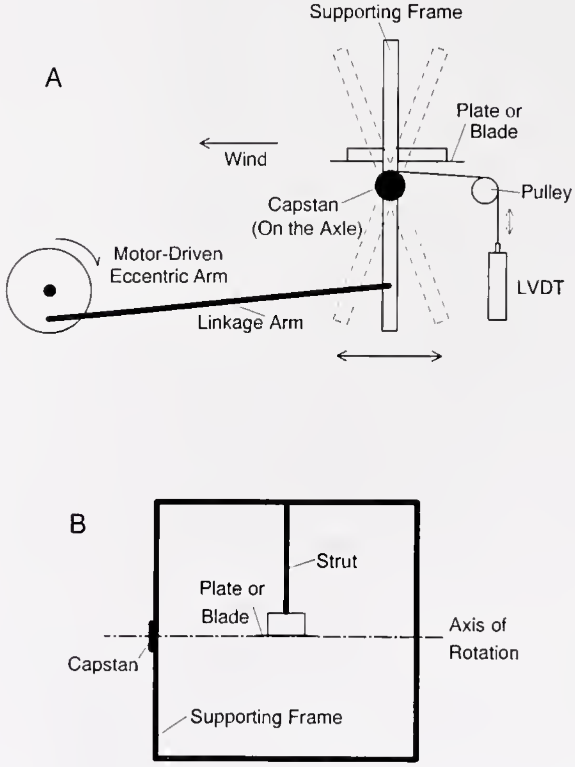

**Figure 3.** A schematic diagram of the apparatus used to vary the pitch angle. (A) Side view. Rotation of the motor-driven eccentric arm causes the supporting frame to oscillate through an angle of ±20°. The extent of rotation is measured with the linearly variable differential transformer (LVDT), whose core is raised and lowered by a string attached to the capstan. (B) View of the apparatus looking downwind.

models. No plastic strip was attached to the plate, thereby retaining its distinct, sharp leading edge.

Water at a constant high temperature was circulated through the water bath of each experimental model, and the flux of heat from the model was measured using a Micro Foil heat flux sensor (part number 20450-1, RdF Inc., Hudson, NH). This device is a small thermopile (about 1 mm square) mounted in a 12-mm long by 7.5-mm wide piece of thin insulating foil. The thermopile produces a voltage linearly proportional to the temperature difference between the faces of the foil, and thereby (through the thermal equivalent of Ohm's law) a voltage proportional to heat flux. Voltage was amplified and recorded on the second channel of the chart recorder. The heat flux sensor was held in good thermal contact with the blade by double-sided adhesive tape. According to the manufacturer, the time response of the sensor is about 0.01 s.

The temperature at the model's surface was measured with a 40-gauge thermocouple taped to the surface downstream of the heat flux sensor. Surface temperature was constant (within 0.5 °C) through a series of measurements on a given model (that is, across pitching frequencies and between wind velocities), but among series (both within and among models) the temperature ranged from 45° to 50 °C. Given the ambient air temperature of 20 °C, the temperature differential between the models and the ambient air thus varied by as much as 20%. All other factors being equal, this variability in temperature differential could lead to variation in heat flux among the models of as much as 20%, and this potential variation is taken into account in comparisons among models as described in the Results. Repeated trials on the flat plate at the beginning and end of experimentation ensured that there had been no long-term drift in the meter's output.

We have not attempted to use the voltage records from the heat flux sensor to calculate the actual heat flux. If it were practical to measure absolute heat flux simultaneously with the temperature gradient adjacent to our models, we could (*via* Fick's 1st law of diffusion) calculate the turbulent thermal diffusivity (Denny, 1993), and from the diffusivity we could estimate the rate of nutrient transport to kelp blades. Unfortunately, accurate dynamic measurements of the temperature gradient were not feasible, and in the absence of these measurements there is little advantage to calculating absolute heat flux. Instead, we report flux in arbitrary units (the amplified voltage output from the heat sensor) and confine our interpretation of the data to relative measurements: flux in one blade morphology relative to that in the other morphology, flux in kelp blades relative to that in a flat plate, and flux while pitching relative to flux while stationary.

For each object, the heat flux sensor was placed about 10 cm downstream of the "leading edge" (see the dots in Fig. 1). For the kelp models, distance was measured from the point of attachment of the flexible faux stipe. The flow-protected morphology of *E. arborea* is deeply bullate, and measurements were conducted both on the crest of a typical bullation and in an adjacent trough downstream. The crest was 10.5 cm from the leading edge, and the trough was 12 cm from the leading edge. The flow-exposed blade was also bullate, but the bullations were too narrow to allow reliable attachment of the heat flux sensor in a trough. As a result, measurements were conducted only on a crest 11 cm behind the leading edge. On the flat plate, the meter was installed 10 cm behind the leading edge.

**Table 1**

*Radii at the heat flux sensor*

| Model | Location | Radius (cm) |
|---|---|---|
| Flat plate | | 6.23 |
| Flow-protected blade | crest | 6.62 |
| | trough | 5.96 |
| Flow-exposed blade | crest | 5.43 |

Two wind velocities were used: 0.38 m $s^{-1}$ (corresponding to a velocity of 2.7 cm $s^{-1}$ in water and a local Reynolds number of about 2700) and 2.82 m $s^{-1}$ (corresponding to a water velocity of 20 cm $s^{-1}$ and $Re_x$ of 20,000). The lower velocity is in the $Re_x$ range at which photosynthesis in kelps may be limited by nutrient flux (Wheeler, 1980; Gerard, 1982; Hurd, 2000). The higher wind velocity corresponds to a water velocity well above that at which nutrient flux is thought to saturate (about 6–10 cm $s^{-1}$; Hurd, 2000), but is a velocity found commonly in the more flow-exposed sites inhabited by *E. arborea*. Wind velocity was measured upstream of the model, using a Kurz model 441S heated-probe anemometer. The turbulence intensity in the free-stream flow of the tunnel is low. The standard deviation of velocity is 0.7% of the mean at 0.38 m $s^{-1}$ and 1.4% of the mean at 2.8 m $s^{-1}$. Turbulence intensity has not been measured in actual beds of *Eisenia*, so it is not known how the turbulence intensity in these tests compares to that in the field.

The axis about which each model pitched was not coincident with the heat flux sensor. As a result, the pitching motion of the model was associated with a tangential velocity that alternately added to and subtracted from the mainstream velocity (a situation that may also pertain to blades as they pitch in the field on the end of a flexible stipe). In each case, the maximum tangential velocity is

$$u_t = 2\alpha\pi fR \qquad \text{(Eq. 2)}$$

where $\alpha$ is the amplitude of the pitching oscillation (0.362 radians), $f$ is the frequency of the oscillation (in cycles per second) and $R$ is the radial distance from the center of the axle to the sensor (see Table 1). At the maximum pitching frequency used in our experiments (0.59 Hz), tangential velocity is about 0.08 m $s^{-1}$, roughly 20% of the slow mainstream velocity (0.38 m $s^{-1}$) and 3% of the fast mainstream velocity (2.82 m $s^{-1}$).

Experiments were conducted as follows. The heat flux was measured in nominally still air with the surface of the model horizontal. This flux value was subtracted from all subsequent values. In other words, the fluxes reported here are an estimate of the increase in flux associated with mainstream flow. (Even at zero mainstream velocity, some flow is induced by the buoyancy of air in contact with the heated model, and the associated flux would not be present in actual kelp blades.) The wind velocity was then brought to the appropriate value, and the pitch motor was turned on. The variation in heat flux was recorded for 25 cycles at one rate of pitch oscillation. The rate of oscillation was then changed, and flux was recorded for another 25 cycles. After the full range of oscillation frequencies had been used, flux was then measured at a series of 13–15 static angles spanning the full range of pitch. For each angle, the model was held stationary for about 30 s, and this measurement of static heat flux was recorded. At the end of this series of measurements, the heat flux in still air was again recorded to ensure that the output of the meter had not drifted.

Recordings were analyzed in two fashions. The average heat flux across several cycles of pitch was calculated for each model and wind velocity as a function of the rate of pitching. Averages were calculated from measurements ($n \approx 50$) of the instantaneous flux taken every 0.2 s. The corresponding average for an object with an infinite period of oscillation was calculated from the measurements of static flux by weighting each value at a given pitch angle (an average of 40–65 measurements) by the relative time that the object would spend at that angle were the plate to pitch up and down sinusoidally. For example, when the pitch of a model is near its extreme, the rate of change of pitch is relatively slow, and the flux corresponding to these angles is maintained for a relatively long time. Consequently, these values are weighted heavily. In contrast, when the model is nearly horizontal, the rate of change of pitch is relatively large, and the flux corresponding to these angles is maintained for only a short time. These values are weighted lightly. The details of the calculation are given in the Appendix. The arrangement of the linkage and eccentric shown in Figure 3A is such that the pitch of the models is not exactly sinusoidal (to be precisely sinusoidal, the linkage would have to be infinitely long), but the deviation from sinusoidal fluctuation is negligible and has been ignored in these calculations.

To examine the instantaneous change in heat flux through the course of an individual pitch oscillation, a pitching frequency of 0.20 Hz was used and seven cycles were chosen from the middle of the record. In each of these seven cycles, the instantaneous heat flux was measured at times corresponding to a set of 13–14 angles spanning the full range of pitch angle. The average and standard deviation of the seven measurements at each angle provided an index of instantaneous flux ("dynamic" flux) and the variability in flux (an index of turbulence) at that angle. These measurements of instantaneous flux during oscillation could then be compared to static measurements in which the model was held fixed at a set of angles spanning the same range.

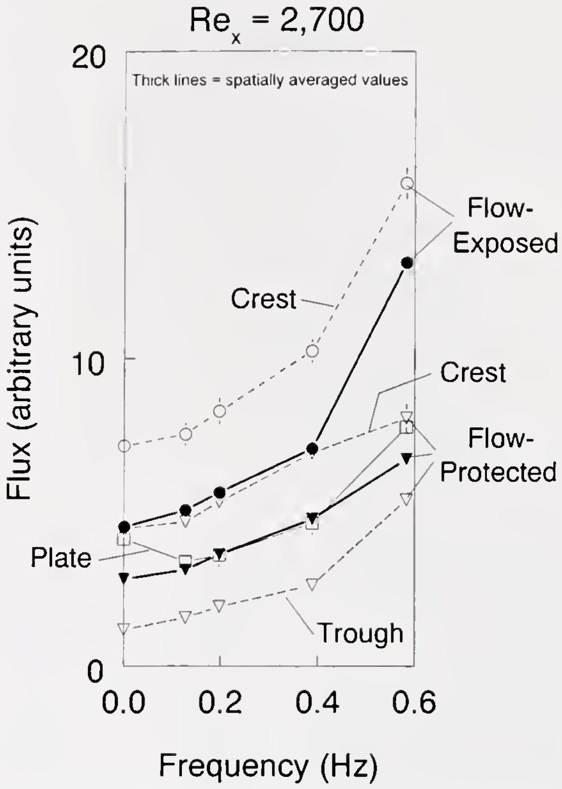

**Figure 4.** In slow flow, flux from the models varies with frequency of pitch oscillation. Data shown are for $Re_x = 2700$. The vertical bars (which in many cases do not protrude beyond the symbols) are standard errors.

The statistical significance of differences between means of measurements (flux on a crest *versus* flux in a trough, flux to a plate *versus* flux to a blade, etc.) was determined using the Wilcoxon paired-sample signed-rank test, incorporating a Bonferroni correction in the case of multiple comparisons.

## Results

### *Flux versus frequency: slow flow*

Average flux at slow flow is shown as a function of pitch frequency in Figure 4. All fluxes increased significantly with increasing pitching frequency (Table 2), at least in part due to the tangential velocity of the model. Flux is on average higher on the crests of the flow-protected blade than in the troughs ($P < 0.001$); the ratio of the two fluxes is 2.7. If we assume that flux varies linearly between crest and trough, we can average these two values to estimate the

**Table 2**

*The correlation between heat flux and pitch frequency*

| Reynolds number | Model | Correlation coefficient | Probability |
|---|---|---|---|
| 2700 | Flat plate | 0.842 | <0.05 |
| | Flow-protected crest | 0.986 | <0.001 |
| | Flow-protected trough | 0.943 | <0.005 |
| | Flow-protected average | 0.980 | <0.001 |
| | Flow-exposed crest | 0.945 | <0.005 |
| | Flow-exposed average | 0.925 | <0.01 |
| 20,000 | Flat plate | 0.888 | <0.02 |
| | Flow-protected crest | 0.524 | >0.05 |
| | Flow-protected trough | 0.579 | >0.05 |
| | Flow-protected average | −0.823 | <0.05 |
| | Flow-exposed crest | 0.150 | >0.05 |
| | Flow-exposed average | 0.226 | >0.05 |

overall flux across blade topography, and this value closely approximates the value for a flat plate.

Flux to the crest of the flow-exposed blade is higher than that to the crest of the flow-protected blade ($P < 0.001$); the ratio of fluxes is 1.6. These two sets of measurements were made with the models at the same surface temperature, so that none of this difference in flux can be accounted for by a difference in temperature differential between the models' surface and the ambient air. If we assume that the flux to the troughs of the flow-exposed blade shows the same ratio to the flux at the crest as that observed in the flow-protected blade, we can estimate an overall flux to the flow-exposed blade. This estimated average flux is higher than that to either the flat plate or the flow-protected blade ($P < 0.001$).

### *Flux versus frequency: fast flow*

Flux in fast flow is shown as a function of pitch frequency in Figure 5. At this high flow speed, fluxes do not change substantially with increasing pitching frequency, perhaps because the tangential velocity of the pitching model is such a small fraction of the mainstream velocity. Flux to the flat plate shows a statistically significant positive trend with increasing pitch frequency, while the average flux to the flow-exposed blade shows a statistically significant negative trend (Table 2), but in neither case does the trend have a major effect on the overall flux.

Flux is again substantially higher on the crest of the flow-protected blade than in the troughs ($P < 0.001$); the ratio of fluxes is 2.4. If we again assume that flux varies linearly between crest and trough, we can average these two values to estimate the overall flux across blade topography. In this case, the time-averaged flux to the flow-protected blade is slightly less than that for a flat plate ($P < 0.001$).

Flux to the crest of the flow-exposed blade is again substantially higher than that to the crest of the flow-protected blade ($P < 0.001$); the ratio of fluxes is 2.5. If we assume that the flux to the troughs of the flow-exposed blade shows the same ratio to the flux at the crest as that observed in the flow-protected blade, we can again estimate an overall flux to the flow-exposed blade. This estimated average flux is substantially higher than that to either the flat plate or the flow-protected blade ($P < 0.001$).

In summary, flux increases substantially with increasing frequency of pitching at $Re_x = 2700$ but not at $Re_x = 20{,}000$. The flux to the flow-exposed blade is higher than would be predicted from a pitching flat plate, whereas the flux to the flow-protected blade could be predicted with reasonable accuracy from measurements on a flat plate.

### *Angle-specific flux: slow flow*

Angle-specific flux to a flat plate in slow flow is shown in Figure 6. The open circles refer to static measurements, and the vertical bars show the standard deviation of fluxes measured among cycles. Static flux is low and relatively constant for positive angles of pitch (that is, when the flux sensor is on the windward face of the plate, Fig. 2B). The small standard deviations indicate that flow in the boundary

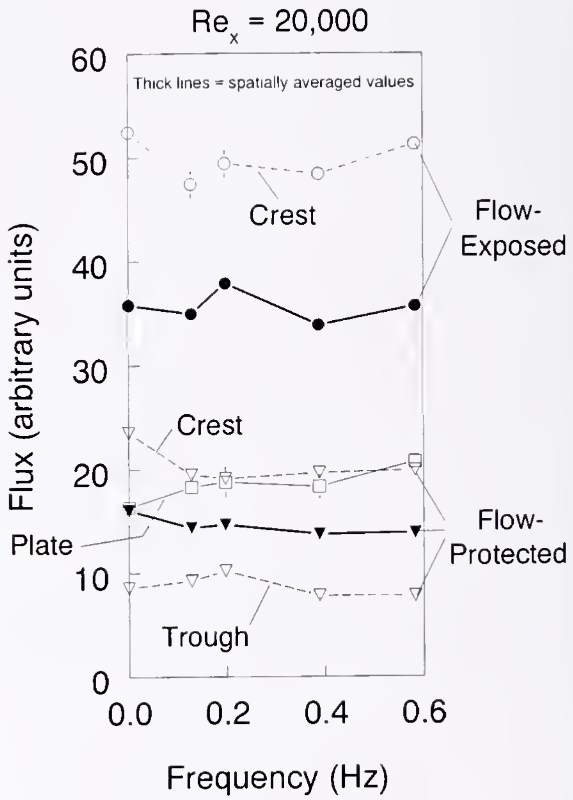

**Figure 5.** In rapid flow, flux from the models does not vary substantially with frequency of pitch oscillation. Data shown are for $Re_x = 20{,}000$. The vertical bars (which in many cases do not protrude beyond the symbols) are standard errors.

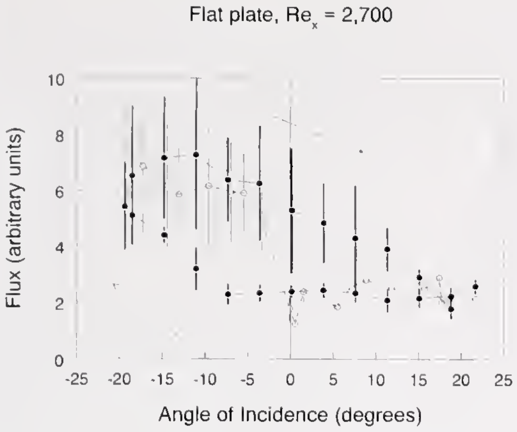

**Figure 6.** Angle-specific flux from a smooth flat plate at $Re_x = 2700$. Open circles show the static response of the model; filled circles, the dynamic response. The vertical bars are the standard deviation of measurements among seven cycles, an index of the intensity of turbulent mixing over the model. The arrows indicate the order in which angles were achieved during a cycle of pitching.

layer adjacent to the flux sensor has a relatively low turbulence intensity at these angles of incidence. In contrast, fluxes at negative angles of incidence (with the sensor on the leeward face of the plate) are high and associated with relatively high turbulence intensities (evidenced by the large standard deviation among cycles). This turbulence (and the associated high flux) is probably due to the shedding of vortices from the leading edge.

Measurements of instantaneous flux to the flat plate during pitching (filled circles, Fig. 6) show a different pattern. As pitch angle decreases from its maximum, the dynamic flux remains close to the static flux until the plate is parallel to flow (pitch angle = 0). Whereas the static flux shifts to higher values at negative angles of incidence, the dynamic flux remains low through a considerable angle. The standard deviations associated with these low fluxes are small, indicating the lack of substantial turbulence. Only at the extreme negative angles used here (about −20°) does the dynamic flux increase to approximate that of the static flux. An increase in standard deviation (evidence of an increase in turbulence) is associated with the increase in flux at large negative angles. This pattern of flux at negative, decreasing pitch angles is probably due to the time required for turbulence to be established in the lee of the leading edge. As initially bound vortices begin to break down and are shed from the plate (in effect, as the plate "stalls"), the mixing in the vicinity of the flux sensor (and hence the flux itself) increases. A similar pattern of "delayed stall" has been observed in flapping insect wings at Reynolds numbers in the range of about 1000 to 7000, similar to the Reynolds number in this experiment ($Re_x = 2700$; for a review, see Ellington, 1984a, b).

As the pitch angle reaches its negative extreme and begins to become more positive, the dynamic flux initially closely approximates the static flux: the flux is high in association with a large standard deviation. In contrast to the static flux, however, the dynamic flux during a positive rate of pitching remains high even at positive angles. As the angle continues to increase, the flux gradually subsides to match that of the static plate.

The net result is that the flux during active pitching is sometimes lower and sometimes higher than that of a static plate, and the overall cyclic average is virtually identical between the static and dynamic cases: the ratio of dynamic flux to static flux for the plate is 0.98 (Table 3).

At slow flow, the pattern of static flux to the crest of the flow-protected blade (Fig. 7A) is substantially different from that to a flat plate. Static flux generally increases with pitch angle (either positive or negative), and the standard deviation of fluxes among cycles at negative angle of incidence is much smaller than that seen for the plate. It seems likely that in the absence of a well-defined leading edge (due both to the presence of the "stipe" and the triangular shape of the blade), the shedding of vortices on the leeward face of the kelp blade is different from that on a flat plate.

In contrast to the static measurements, the pattern of dynamic fluxes measured on the flow-protected blade show a pattern that is in general terms similar to that of a flat plate (filled circles, Fig. 7A). Flux is substantially below the maximum and relatively constant as pitch angle decreases, and flux is initially low even at negative angles of incidence. Flux and standard deviation of flux both increase at extreme negative angles as the angle decreases, and remain high as the blade begins to pitch back up. High fluxes are maintained during positive rates of pitching (even at positive angles up to 5°), decreasing thereafter to values near the static level.

The pattern of flux to the trough of the flow-protected blade is shown in Figure 7B, and is very similar to that of the crest, albeit at a substantially lower absolute value of flux.

The ratios of dynamic to static flux for the flow-protected blade are high—1.33 and 1.44 for the crest and trough, respectively—due in large part to the low flux values measured for the static blade. In summary, when the flow is slow, the flow-protected blade appears to receive a substantial increase in average flux if its pitch angle oscillates.

**Table 3**

*The ratio of dynamic flux to static flux at a pitching frequency of 0.2 Hz*

| Model | Location | Re = 2700 | Re = 20,000 |
|---|---|---|---|
| Plate | | 0.976 | 1.145 |
| Flow-protected blade | Crest | 1.333 | 1.083 |
| | Trough | 1.437 | 1.187 |
| Flow-exposed blade | Crest | 1.177 | 1.022 |

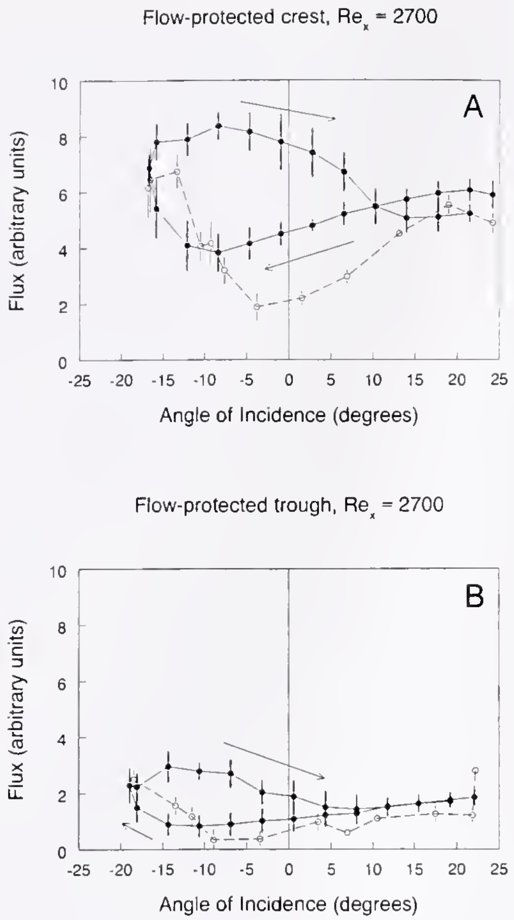

**Figure 7.** Angle-specific flux from a flow-protected blade at $Re_x$ = 2700. Open circles show the static response of the model; filled circles, the dynamic response. The vertical bars are the standard deviation of measurements among seven cycles, an index of the intensity of turbulent mixing over the model. (A) Crest. (B) Trough. The arrows indicate the order in which angles were achieved during a cycle of pitching.

The pattern of flux at $Re_x$ = 2700 for the flow-exposed blade is more complex than that of the other models (Fig. 8). Static flux (open circles) is very low when the blade is parallel to flow (lower than the small-angle values for either the plate or the flow-protected blade), but increases with increasingly positive angle of pitch to values higher than those for the other models. (The surface temperature during this series of measurements was 8% higher than the comparable measurements for the flow-protected blade, but this difference in temperature differential between surface and ambient temperature is not sufficient to account for the difference in flux between models.) The standard deviation of flux to the flow-exposed model is relatively small at positive angles, indicative of suppressed turbulence. Static flux initially increases steeply with increasingly negative pitch angle (again to values high relative to the other models), but reaches a peak at about −15°, decreasing sharply thereafter. This decrease in flux at extreme negative angles is associated with an increase in standard deviation. An explanation for this anomalous negative correlation between flux and turbulence at high negative angles is not readily apparent. It should be kept in mind, however, that the width of this blade is small relative to its length, and as a consequence there is substantial potential for three-dimensional flow in the vicinity of the heat-flux sensor. At large angles of incidence, eddies may curl around the sides of the blade with unpredictable effects.

The pattern of dynamic flux to the flow-exposed blade is for the most part similar to that discussed above for other models. As the blade pitches down from its positive extreme, the flux gradually decreases and remains low until extreme negative angles of incidence. The flux then remains high as the blade pitches back up. In this case, however, the flux associated with a positive rate of pitching is relatively low at positive angles of pitch. Again, low flux values are often associated with high standard deviations of flux among cycles.

At this slow flow, the crest of the flow-exposed blade receives a relatively minor benefit from flapping. The ratio of dynamic to static flux is 1.18, apparently less than that for the crest of the flow-protected blade (1.33, Table 3), although we have not attempted to attach a level of statistical confidence to the difference of these ratios.

### *Angle-specific flux: fast flow*

Flux to our models at a local Reynolds number of about 20,000 is much higher than at $Re_x$ = 2700 and shows a simpler pattern of variation across angles. For example, the static flux to a smooth, flat plate (open circles, Fig. 9) is lowest at the maximum positive angle of incidence and

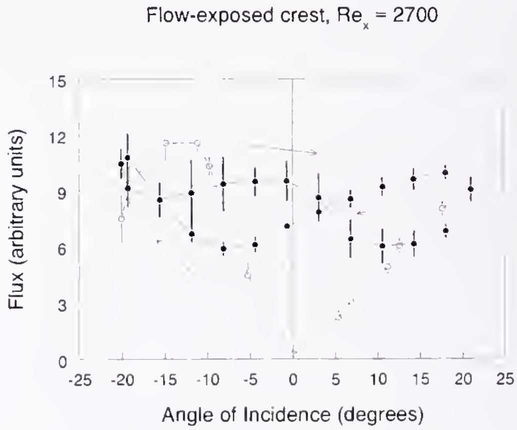

**Figure 8.** Angle-specific flux from the crest of a flow-exposed blade at $Re_x$ = 2700. Open circles show the static response of the model; filled circles, the dynamic response. The vertical bars are the standard deviation of measurements among seven cycles, an index of the intensity of turbulent mixing over the model. The arrows indicate the order in which angles were achieved during a cycle of pitching.

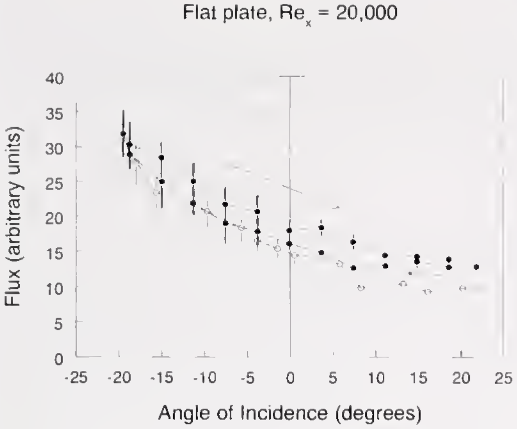

**Figure 9.** Angle-specific flux from a smooth flat plate at $Re_x$ = 20,000. Open circles show the static response of the model; filled circles, the dynamic response. The vertical bars are the standard deviation of measurements among seven cycles, an index of the intensity of turbulent mixing over the model. The arrows indicate the order in which angles were achieved during a cycle of pitching.

increases monotonically with decreasing pitch angle. The abrupt increase in both flux and standard deviation of flux seen near 0° in slow flow (Fig. 6) is absent in this case—turbulent mixing gradually increases as pitch angle decreases. The cyclically averaged static flux at $Re_x$ = 20,000 (16.95) is about 4.5 times that at $Re_x$ = 2700 (3.74).

Dynamic flux to the flat plate during decreasing pitch angle is virtually identical to the static flux (filled circles, Fig. 9). When pitch angle is increasing, dynamic flux is slightly higher than static flux, although the difference between the two is never large. The average dynamic flux at high flow (19.40) is about 5.3 times that at low flow (3.65). The ratio of dynamic to static flux for the flat plate at high $Re_x$ is 1.15, compared to 0.98 for the same plate at lower $Re_x$ (Table 3).

In summary, at a Reynolds number of 20,000, where boundary-layer turbulence intensity is expected to be relatively large, flux to a flat plate is relatively high. The higher the angle of incidence, the lower the flux.

Flux to a crest of the flow-protected blade is shown in Figure 10A. Static flux varies little with angle of incidence, showing slightly elevated values at the pitch extremes and for a small range of angles near 0°. The cyclic average static flux at $Re_x$ = 20,000 (23.52) is about 2.7 times that at $Re_x$ = 2700 (8.59). Dynamic flux to the crest (filled circles, Fig. 10) varies little with pitch angle. The dynamic flux at high local Reynolds number (25.47) is about 2.5 times that at lower $Re_x$ (10.2). The ratio of dynamic to static flux at high $Re_x$ is 1.08, apparently less than that at lower $Re_x$ (1.33), although we have again not attempted to attach a level of statistical confidence to the difference of these ratios.

Both static and dynamic flux to a trough of the flow-protected blade (Fig. 10B) vary little with pitch angle. Dynamic flux (filled circles) is slightly higher than static flux (open circles) at negative angles of incidence, but the difference is small. Flux to the trough at $Re_x$ = 20,000 is higher than that at $Re_x$ = 2700: 8.59 compared to 1.19 (a ratio of 7.2) for cyclic average static flux, 10.20 compared to 1.71 (a ratio of 6.0) for dynamic flux. The ratio of dynamic to static flux for the trough at high $Re_x$ is 1.19, apparently less than the comparable ratio at lower $Re_x$ (1.44).

The angle-specific pattern of flux to the flow-exposed blade at $Re_x$ = 20,000 is similar to that of a flat plate at lower Reynolds number (Fig. 11). Static flux (open circles) is low for large, positive angles of incidence (>+5°), and there is a jump to higher fluxes at negative angles of incidence. Dynamic flux shows the same sort of "hysteresis" seen in the flat plate at $Re_x$ = 2700. When the angle of incidence is decreasing, dynamic flux at positive pitch angles is similar to static flux, but is lower than static flux for

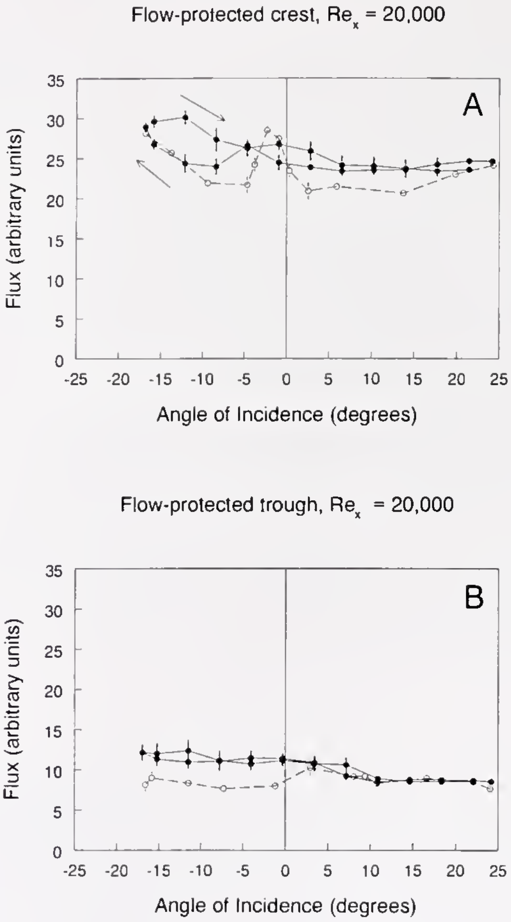

**Figure 10.** Angle-specific flux from a flow-protected blade at $Re_x$ = 20,000. (A) Crest. (B) Trough. Open circles show the static response of the model; filled circles, the dynamic response. The vertical bars are the standard deviation of measurements among seven cycles, an index of the intensity of turbulent mixing over the model. The arrows indicate the order in which angles were achieved during a cycle of pitching.

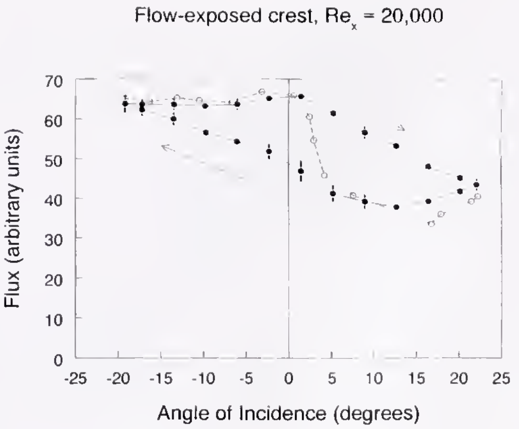

**Figure 11.** Angle-specific flux from the crest of a flow-exposed blade at $Re_x$ = 20,000. Open circles show the static response of the model; filled circles, the dynamic response. The vertical bars are the standard deviation of measurements among seven cycles, an index of the intensity of turbulent mixing over the model. The arrows indicate the order in which angles were achieved during a cycle of pitching.

negative angles of incidence. When the angle of incidence is increasing, dynamic flux at negative pitch is similar to static flux, but is greater than static flux for positive angles of incidence. The reason for the similarity of the flux pattern between the flow-exposed blade at high $Re_x$ and the flat plate at low $Re_x$ is not readily apparent. High flux values for the blade are not associated with high standard deviations of flux. Thus, the explanation invoked for the flat plate at low $Re_x$ (temporal hysteresis in the creation and subsequent dissipation of turbulence in the plate's wake) is unlikely to apply to the flow-exposed blade.

Cyclic average static flux to the flow-exposed blade at $Re_x$ = 20,000 (52.45) is about 7.3 times that at $Re_x$ = 2700 (7.16). Dynamic flux at high $Re_x$ (53.60) is 6.4 times that at lower $Re_x$ (8.43). The ratio of dynamic to static flux at high $Re_x$ is 1.02 for the flow-exposed blade, apparently slightly lower than that at $Re_x$ = 2700 (1.18), although we have again not attempted to attach a level of statistical confidence to the difference of these ratios.

### *Overall flux versus static angle*

In steady, unidirectional flow, a kelp blade may be oriented at a fixed pitch angle. In this case, the overall flux to the blade can be estimated from our measurements as the sum of the static flux to the blade's upstream and downstream faces at that angle relative to flow. That is, for a fixed pitch angle of 5°, we sum our measured static fluxes for +5° (representing the upstream face of the blade) and −5° (representing the lee side of the blade). Values for overall static flux to a blade are shown in Figure 12 for the range of angles used in our experiments. In some cases, we have interpolated between measured values to estimate the flux at the specified angles. At $Re_x$ = 2700 (Fig. 12A), overall flux to a flat plate is low at zero angle of incidence but constant at a somewhat higher value for angles between 5° and 20°. Overall flux to the flow-protected blade (a linear average of crest and trough) increases with increasing angle, but is always less than or equal to that to a flat plate. Thus, at fixed angles of incidence, the morphology of the flow-protected blade does not appear to provide any advantage over that of a smooth, flat plate. The estimated overall flux to the flow-exposed blade (calculated using the same crest/trough ratio as for the flow-protected blade and a linear average of crest and trough values) increases with increasing angle of incidence; it is lower than that for a flat plate at low angles, higher at high angles.

At a local Reynolds number of 20,000, the overall fluxes to the flat plate and the flow-protected blade vary little with the angle of incidence, and the two fluxes are virtually identical (Fig. 12B). Again, the morphology of the flow-protected blade does not appear to provide any advantage relative to a flat plate. At high $Re_x$, the estimated overall flux to the flow-exposed blade (calculated used the crest/trough ratios for the flow-protected blade and a linear average) is about twice that of either the flow-protected blade or the flat plate, and it decreases slightly with increasing angle of incidence.

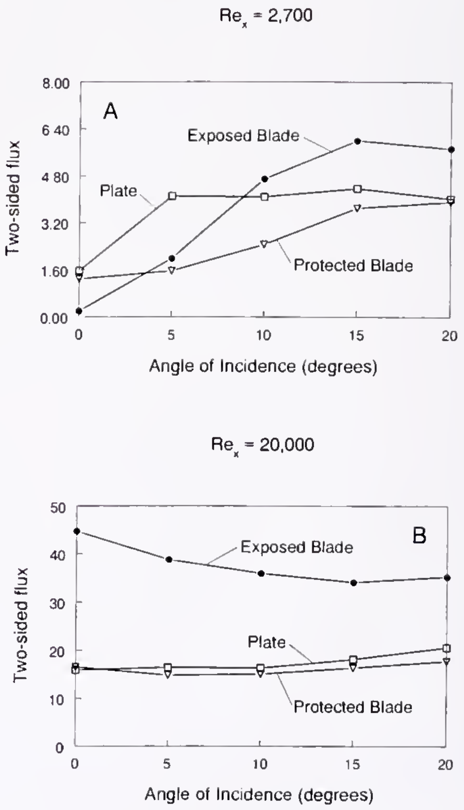

**Figure 12.** Overall flux to blades held at a fixed angle of incidence. (A) $Re_x$ = 2700. (B) $Re_x$ = 20,00.

In summary, at $Re_x = 2700$, it appears to be advantageous for any of our models to have a nonzero static pitch angle. At least up to a pitch of 20°, the higher the static angle of a kelp blade, the greater the estimated overall flux. At $Re_x = 20{,}000$, the static angle of incidence has little effect on overall flux.

## Discussion

Four conclusions can be drawn from these results:

1. *At a relatively low local Reynolds number (2700), dynamic pitching can indeed increase the flux to algal blades.* Thus, in the slow flows where nutrient flux can potentially limit blade growth, dynamic pitching may be advantageous. It is important to note, however, that the experiments conducted here on rigid models are at best a rough approximation of the dynamic pitching that flexible blades undergo in nature and an even rougher approximation of the flapping and flutter that can occur within a blade. In actual blades in the field, orientation responds to the flow itself, and the flow simultaneously responds to the blade. In our experiments, this interaction is one-way—pitch is imposed and the flow is forced to respond. As a result, extrapolations from the measurements made here should be made with caution. Furthermore, it is an open question as to how widespread flapping and flutter are in algal blades. In their laboratory study of 10 species of kelps, Hurd and Stevens (1997) reported flow-induced motions of blades in velocities as low as 0.5–1.5 cm/s, but they also noted that flapping was more common at velocities greater than 5 cm/s. Accurate measurement of the frequency and angle of blade pitching in the field has not been attempted for any kelp.
2. *At a relatively high local Reynolds number (20,000), dynamic pitching has very little effect on flux.* Similar results have been obtained for the leaves of terrestrial plants flapping in wind (Parlange *et al.*, 1971). However, it seems unlikely that this lack of flapping-induced enhancement of flux at high Reynolds numbers will have substantial biological consequences. Even in low-nutrient water, kelps are able to extract sufficient nutrients when flow is greater than 5–10 cm $s^{-1}$ (equivalent to a local Reynolds number of 5000–10,000 in the experiments conducted here; Wheeler, 1980; Gerard, 1982; Hurd, 2000). As a result, nutrient limitation may not be a factor for Reynolds numbers at which flapping does not affect flux.
3. *At low local Reynolds numbers, the angle of attack can have a large effect on flux to algal blades.* This effect was seen in all three models here (Fig. 12A), although it is most evident in the flow-exposed morphology (Fig. 8). This effect can color the conclusions drawn regarding blade morphology. For example, near zero pitch angle, the flow-exposed morphology has a lower flux than the wave-protected morphology, and one might conclude that the deep bullations of the flow-protected blade have afforded a selective advantage. This conclusion is in accord with experiments carried out in the field (Roberson, 2001): in areas where the nutrient content of the water is low, flow-exposed plants transplanted to flow-protected sites wither and die while adjacent flow-protected plants thrive. Roberson (2001) suggests that this effect is due to differential flux of nutrients to the two morphologies. However, our measurements in slow flow suggest that for an angle of incidence as little as ±5°, the flow-exposed morphology has a flux equal to or higher than that of the flow-protected blade. Thus, unless blades in slow flow are oriented precisely parallel to flow, the measurements made here are at odds with the inferred nutrient uptake. As noted above, the angle of incidence of blades in the field has not yet been accurately measured (for this or any other species), and the experiments reported here suggest that these measurements should be an important consideration in future studies.
4. *A flat plate is often not an appropriate analogue to an algal blade.* For example, at a $Re_x$ of 2700, the dynamic flux to a pitching flat plate is roughly the same as the cyclic-average static flux (Table 2); based on this evidence, one might predict that dynamic pitching of algal blades has little if any effect on nutrient transport in slow flow. In fact, direct measurements on model blades show that in slow flow the dynamic flux is substantially larger than the cyclic average static flux. In another example (Fig. 12B), in fast flow the static flux to a flat plate is very similar to the static flux to the flow-protected blade, whereas the flux to a flat plate is substantially less than that to the flow-exposed blade. It appears that only after direct measurements have been made on both a blade and a plate can we know whether the plate is an appropriate model. If this is true, the utility of the flat plate as an experimental proxy is severely limited.

## Caveats

These conclusions should be viewed with caution for several reasons.

1. We have measured heat flux at only one small range of distances from the upstream edge of the blade, only near the blade's center line, and on only one representative blade of each morphology. Thus, it would be rash to extrapolate from our results to more general conclusions. Much work remains before the precise overall pattern of flux to even these particular models will be known (especially, its three-dimensional na-

ture), and more work still before we can accurately generalize our findings to different morphological groups within the species. Only when these more robust findings are in hand will we be able to compare the selective pressures that accompany morphological effects on nutrient flux in *Eisenia*.

2. The flux values reported here have been measured relative to the flux at zero mainstream flow. However, as noted, this zero-flow flux includes the free-convective flux due to the buoyancy of air induced by the heated model. In making our calculations, we have implicitly assumed that the free-convective flux remains constant when a mainstream flow is applied. In fact, forced convection may interfere with the free convection, and in that case the values recorded here may underestimate the actual flux to our models. In essence, forced convective interference might result in a downward shift in the abscissa of Figures 4–12. However, such a shift (if necessary) would have minimal impact on the conclusions drawn here. The ratios we cite between flapping and stationary blades would be closer to 1 than we have calculated, but all other comparisons would be unaffected. Accurate measurement of the effect of forced convection on the flux due to free-convection will be tricky, and we have not attempted it here.
3. Our measurements were conducted at a low level of ambient turbulence. It is not known how this level compares to that in the field, and we have made no attempt to explore how variation in turbulence could affect the dynamics of flux. It seems likely that such an exploration will be a productive, although complex, area for future research. Turbulence in a bed of *Eisenia* may vary drastically from one location to another (at least in part due to the turbulence caused by vortex shedding in the wakes of upstream kelps) and from one time to another as waves pass overhead. Considerable work will be necessary to determine how this temporal and spatial variation is coupled to the dynamics of blade reorientation and nutrient flux.

Although the measurements we report here are only a step toward understanding the complex interaction of algal blades with flow, they highlight the necessity for more thorough experimentation. In particular, simultaneous measurements of flow-induced blade motions and instantaneous flux (perhaps using the field-deployable shear-stress transducers of Gust, 1988) will be invaluable in the interpretation of flow-related blade morphology.

## Acknowledgments

We thank Jeff Koseff for bringing our attention to heat flux sensors, and John Lee for assistance with the electronics. This work was funded in part by NSF grants OCE-9633070 and OCE-9985946 to MD. This is contribution 82 of PISCO (Partnership for the Interdisciplinary Study of Coastal Oceans).

## Literature Cited

**Bell, E. C. 1993.** Photosynthetic response to temperature and desiccation of the intertidal macroalga, *Mastocarpus papillatus*. *Mar. Biol.* **117:** 337–346.

**Bell, E. C. 1995.** Environmental and morphological influences on thallus temperature and desiccation of the intertidal alga *Mastocarpus papillatus* Kützing. *J. Exp. Mar. Biol. Ecol.* **191:** 29–55.

**Bird, R. B., W. E. Stewart, and E. N. Lightfoot. 1960.** *Transport Phenomena.* Wiley, New York.

**Denny, M. W. 1993.** *Air and Water.* Princeton University Press, Princeton, NJ.

**Ellington, C. P. 1984a.** The aerodynamics of hovering flight. IV. Aerodynamic mechanisms. *Philos. Trans. R. Soc. Lond.* **B 305:** 79–113.

**Ellington, C. P. 1984b.** The aerodynamics of flapping animal flight. *Am. Zool.* **24:** 95–105.

**Gerard, V. A. 1982.** *In situ* water motion and nutrient uptake by the giant kelp *Macrocystic pyrifera*. *Mar. Biol.* **69:** 51–54.

**Gerard, V. A., and K. H. Mann. 1979.** Growth and production of *Laminaria longicruris* (Phaeophyta) populations exposed to different intensities of water movement. *J. Phycol.* **15:** 33–41.

**Gonen, Y., E. Kimmel, and M. Friedlander. 1995.** Diffusion boundary layer transport in *Gracilaria conferta* (Rhodophyta). *J. Phycol.* **31:** 768–773.

**Gust, G. 1988.** Skin friction probes for field applications. *J. Geophys. Res.* **93:** 14121–14132.

**Hurd, C. L. 2000.** Water motion and marine macroalgal physiology and production. *J. Phycol.* **36:** 453–472.

**Hurd, C. L., and C. L. Stevens. 1997.** Flow visualization around single- and multiple-bladed seaweeds with various morphologies. *J. Phycol.* **33:** 360–367.

**Hurd, C. L., P. J. Harrison, and L. Druehl. 1996.** Effect of seawater velocity on inorganic nitrogen uptake by morphologically distinct forms of *Macrocystis integrifolia* from wave-sheltered and exposed sites. *Mar. Biol.* **126:** 205–214.

**Koch, E. W. 1993.** The effect of water flow on photosynthetic processes of the alga *Ulva lactuca L. Hydrobiologia* **260/261:** 457–462.

**Koehl, M. A. R., and R. S. Alberte. 1988.** Flow, flapping, and photosynthesis of *Nereocystis luetkeana*: a functional comparison of undulate and flat blade morphologies. *Mar. Biol.* **99:** 435–444.

**Parlange, J.-Y., P. E. Waggoner, and G. H. Heichel. 1971.** Boundary layer resistance and temperature distribution on still and flapping leaves. *Plant Physiol.* **48:** 437–442.

**Roberson, L. M. 2001.** Evolution of kelp morphology in response to local physical factors: the effect of small-scale water flow on nutrient uptake, growth, and speciation in the southern sea palm, *Eisenia arborea*. Ph.D. Dissertation, Stanford University.

**Schlichting, H. 1979.** *Boundary-Layer Theory.* McGraw-Hill, New York.

**Vogel, S. 1994.** *Life in Moving Fluids.* Princeton University Press, Princeton, NJ.

**Wheeler, W. N. 1980.** Effect of boundary layer transport on the fixation of carbon by the giant kelp *Macrocystis pyrifera*. *Mar. Biol.* **56:** 103–110.

## Appendix

Measurements of flux at a series of static angles are converted to the corresponding flux during one cycle of oscillation through the following calculations.

At any time $t$, the instantaneous angle of the model $\phi$ is

$$\phi = \alpha \cos(\omega t) + \beta\,, \qquad \text{(Eq. 3)}$$

where $\alpha$ is the amplitude of pitch oscillation,

$$\alpha = \frac{\phi_{\max} - \phi_{\min}}{2}\,, \qquad \text{(Eq. 4)}$$

and $\beta$ is the average pitch around which the model oscillates (nominally 0, but, in our experiments, a few degrees).

$$\beta = \frac{\phi_{\max} + \phi_{\min}}{2}\,. \qquad \text{(Eq. 5)}$$

The radian frequency $\omega$ is,

$$\omega = \frac{2\pi}{T} \qquad \text{(Eq. 6)}$$

where $T$ is the period of the oscillation (in seconds).

Solving eq. 3 for $t$, we find that the time corresponding to a given angle is

$$t = \frac{1}{\omega}\cos^{-1}\left(\frac{2\phi - \phi_{\max} - \phi_{\min}}{\phi_{\max} - \phi_{\min}}\right). \qquad \text{(Eq. 7)}$$

The calculation of the cyclic flux begins with $F(\phi_1)$, the static flux measured at the positive extreme of pitch ($\phi_1$) and $F(\phi_2)$, the static flux measured at the next most positive angle ($\phi_2$). $F(\phi_1)$ occurs at time $t(\phi_1)$ and $F(\phi_2)$ at $t(\phi_2)$, both times calculated using eq. 7. Our estimate of the heat transferred as the model pitches from $\phi_1$ to $\phi_2$ is the product of the average flux and the period between $t(\phi_1)$ and $t(\phi_2)$:

$$\text{heat transfer} = \left(\frac{F(\phi_1) + F(\phi_2)}{2}\right) \times (t(\phi_1) - t(\phi_2))\,. \qquad \text{(Eq. 8)}$$

The flux $F(\phi_3)$ is then calculated for the next most positive angle, and the calculation of eq. 8 is repeated using $\phi_2$ and $\phi_3$. This process is repeated for all adjacent pairs of angles until the negative extreme angle is reached. Summing the heat transferred in each of these periods provides the total heat transferred, and dividing by the period of the half cycle (the time to go from one extreme of pitch to the other) provides the average cyclic flux.

Reference: *Biol. Bull.* **203:** 14–26. (August 2002)

# Ontogeny of Squid Mantle Function: Changes in the Mechanics of Escape-Jet Locomotion in the Oval Squid, *Sepioteuthis lessoniana* Lesson, 1830

JOSEPH T. THOMPSON* AND WILLIAM M. KIER

*Department of Biology, CB#3280 Coker Hall, University of North Carolina,*
*Chapel Hill, North Carolina 27599-3280*

**Abstract.** In *Sepioteuthis lessoniana,* the oval squid, ontogenetic changes in the kinematics of the mantle during escape-jet locomotion imply a decline in the relative mass flux of the escape jet and may affect the peak weight-specific thrust of the escape jet. To examine the relationship between ontogenetic changes in the kinematics of the mantle and the thrust generated during the escape jet, we simultaneously measured the peak thrust and the kinematics of the mantle of squid tethered to a force transducer. We tested an ontogenetic series of *S. lessoniana* that ranged in size from 5 to 40 mm dorsal mantle length (DML). In newly hatched squids, thrust peaked 40 ms after the start of the escape jet and reached a maximum of between 0.10 mN and 0.80 mN. In the largest animals, thrust peaked 70 ms after the start of the escape jet and reached a maximum of between 18 mN and 110 mN. Peak thrust was normalized by the wet weight of the squid and also by the cross-sectional area of the circumferential muscle that provides power for the escape jet. The weight-specific peak thrust of the escape jet averaged 0.36 in newly hatched squid and increased significantly to an average of 1.5 in the largest squids measured ($P < 0.01$). The thrust per unit area of circumferential muscle averaged 0.25 mN/mm$^2$ in hatchlings and increased significantly to an average of 1.4 mN/mm$^2$ in the largest animals tested ($P < 0.01$). The impulse of the escape jet was also lowest in newly hatched individuals (1.3 mN · s) and increased significantly to 1000 mN · s in the largest squids measured ($P < 0.01$). These ontogenetic changes in the mechanics of the escape jet suggest (1) that propulsion efficiency of the exhalant phase of the jet is highest in hatchlings, and (2) that the mechanics of the circumferential muscles of the mantle change during growth.

## Introduction

The kinematics and mechanics of locomotion change significantly during the growth of many aquatic animals, especially in those that are small at hatching and grow to large body size. The ontogeny of the kinematics and mechanics of locomotion may reflect a change in the hydrodynamic environment of the animal as it grows (Weihs, 1974; Batty, 1984; Webb and Weihs, 1986; Osse, 1990; Williams, 1994; Müller and Videler, 1996). The size of the animal or its propulsor, the speed of the animal or its propulsor, and the kinematic viscosity of water all affect the forces experienced by an aquatic animal (*e.g.*, Lighthill, 1975). The Reynolds number (Re) describes the relationship among these three factors,

$$\mathrm{Re} = lU/\nu \qquad \text{(Lighthill, 1975)} \qquad \text{(Eq. 1)}$$

where $l$ is a characteristic length of the organism (*e.g.*, body or propulsor length), $U$ is the velocity of the organism (or a portion of the organism) relative to the surrounding water, and $\nu$ is the kinematic viscosity of the fluid (*i.e.*, the ratio of water viscosity to water density). The Reynolds number characterizes the relative importance of inertial forces and viscous forces on the swimming animal (Vogel, 1994). Thus, when the Reynolds number is high ($>10^3$), inertial forces dominate locomotion; when the Reynolds number is low ($<1$), viscosity dominates. In an intermediate Reynolds number fluid regime ($1 < \mathrm{Re} < 10^3$), inertial forces dom-

---

Received 25 July 2001; accepted 30 May 2002.

* To whom correspondence should be addressed. E-mail: joethomp@email.unc.edu

*Abbreviation:* DML, dorsal mantle length.

inate, but the effects of viscosity are considerable (Daniel *et al.*, 1992).

The hydrodynamic environment influences the mechanics of locomotion during ontogeny. For example, newly hatched larval brine shrimp and fish swim in a fluid regime between Re = 1 and Re = 20 (Batty, 1984; Williams, 1994; Müller *et al.*, 2000), where inertial and viscous forces are nearly equal. In such a hydrodynamic environment, inertial modes of locomotion, such as burst-and-coast swimming, are hypothesized to be energetically costly compared with drag-based modes of locomotion, such as steady anguilliform swimming (Weihs, 1974; Müller *et al.*, 2000). Thus, hydrodynamic considerations may explain the observed change from drag-based to inertial locomotion during the growth of larval brine shrimp and fish (Batty, 1984; Williams, 1994; Müller *et al.*, 2000).

Locomotion in some animals may be fixed, despite shifts in their hydrodynamic regime during growth. For example, the jet propulsion used by squids is analogous to the inertia-dependent burst-and-coast swimming employed by some fish. A squid produces a burst of thrust as the mantle contracts and expels water from the mantle cavity, followed by a coasting phase as the mantle expands and the mantle cavity refills. Because squids are limited to inertia-dependent jet propulsion for rapid swimming, the mechanics and energetics of locomotion for small hatchling squids may be compromised given the near parity of inertia and viscosity of their intermediate Re fluid environment ($1 < \text{Re} < 100$, unpub. obs. of *Sepioteuthis lessoniana* during fast and slow jetting). For instance, unlike adults, newly hatched individuals of *S. lessoniana* (unpub. obs.) and *Loligo vulgaris* (Packard, 1969) coast only a short distance after a burst of thrust. Because inertia-based modes of locomotion are unfavorable in the hydrodynamic environment of the hatchlings (Müller *et al.*, 2000), we might expect compensatory changes in the kinematics of the mantle and the mechanics of jet locomotion as squid grow.

Indeed, the amplitude of mantle movement during jet locomotion changes as a squid grows. In *Loligo vulgaris* (Packard, 1969), *L. opalescens* (Gilly *et al.*, 1991; Preuss *et al.*, 1997), and *S. lessoniana* (Thompson and Kier, 2001a), the maximum amplitude of mantle movement during the escape jet decreases dramatically during ontogeny. In *S. lessoniana*, the maximum contraction and hyperinflation of the mantle (both measured as the percent change from the resting mantle diameter) are significantly greater during an escape jet in small hatchlings than in the larger animals (Thompson and Kier, 2001a). The maximum contraction and hyperinflation of the mantle decrease exponentially until the squid reach a dorsal mantle length (DML) of about 15 mm. In squids larger than 15 mm DML, the maximum contraction and hyperinflation of the mantle during the escape jet remain unchanged (Thompson and Kier, 2001a). In addition, the maximum rate of contraction of the mantle during the escape jet is highest in hatchling squids and decreases exponentially until the animals reach 15 mm DML. In *S. lessoniana* specimens larger than 15 mm DML, the maximum rate of contraction of the mantle does not change significantly (Thompson and Kier, 2001a).

*Specific problem.* The ontogenetic changes in the kinematics of the mantle in *S. lessoniana* may affect the performance and the mechanical efficiency of escape-jet locomotion. Specifically, changes in the kinematics of the mantle result in higher relative mass flux (= mass of water exiting the mantle cavity per unit time, relative to body mass) in newly hatched squids than in larger animals (Thompson and Kier, 2001a). Because the thrust produced during the escape jet is proportional to the product of mass flux and the velocity of water exiting the funnel aperture (averaged over the funnel aperture; Vogel, 1994), a change in the relative mass flux may affect the thrust generated during the escape jet.

To explore how changes in the kinematics of the mantle impact escape-jet locomotion, we measured the peak thrust generated during the escape jet in an ontogenetic series of *S. lessoniana*. We examined the implications of an ontogenetic change in jet thrust on the propulsion efficiency of escape-jet locomotion, and on the mechanics of the circumferential muscles that power the jet. We also discuss the possibility that the evolution of ontogenetic changes in the morphology and kinematics of the mantle and funnel might reflect the scale effects of jet locomotion.

## Materials and Methods

### *Animals*

We obtained an ontogenetic series of *Sepioteuthis lessoniana* Lesson, 1830, the oval squid. Wild embryos collected from Izo, Japan, in September 1999 and August 2000 were raised by the National Resource Center for Cephalopods (NRCC) at the University of Texas Medical Branch, Galveston, Texas. The cohort consisted of thousands of embryos from six to eight different egg mops. Thus, it is likely that the sample populations were not the offspring of a few closely related individuals, but were representative of the natural population at the collection site.

The embryos were transported from the field to the NRCC and reared (Lee *et al.*, 1994). Commencing at hatching and at regular intervals thereafter, live squid were sent *via* overnight express shipping from the NRCC to the University of North Carolina. The squids ranged in size from 5 to 40 mm dorsal mantle length (DML) and in age from newly hatched to 6 weeks after hatching.

Prior to the start of the experiments, the animals were allowed at least 30 min to equilibrate in an 80-l circular holding tank. The temperature (23 °C) and salinity (35 ppt) of the water matched the temperature and salinity of the water in which the squid were raised. Circular water flow in the tank helped keep the squid swimming parallel to the sides of the tank to prevent injury. No animal remained in the holding tank for longer than 2 h.

Every animal used for the experiments was in excellent condition. The coloration and activity of the squids were qualitatively similar to those of animals in the large culture tanks at the NRCC (pers. obs.). Many of the animals in this study captured and consumed prey (feeder guppies or mysid shrimp) while in the holding tank. None of the squids inked during shipping or during the anesthesia prior to the experiments.

### *The tether*

We measured the thrust produced during escape-jet locomotion in squid tethered to a force transducer. Squid were tethered (see Thompson and Kier, 2001a) as follows. Individual squid were removed from the holding tank and anesthetized lightly in a 1:1 solution of 7.5% $MgCl_2$ : artificial seawater (Messenger *et al.*, 1985). A needle (0.3-mm-diameter insect pin for small animals or 0.7-mm-diameter hypodermic needle for large animals) was inserted through the brachial web of the squid, anterior to the brain cartilage and posterior to the buccal mass. The needle was positioned between these two rigid structures to prevent it from tearing the soft tissue of the squid. The needle was inserted into a hollow stainless steel post (hypodermic tubing) attached to a force transducer. Flat, polyethylene washers on the post and needle were positioned above and below the head to prevent vertical movement.

Insertion of the needle through the anesthetized squid was rapid and required minimal handling of the animal. Individuals of *S. lessoniana* become nearly transparent under anesthesia, making the buccal mass and the brain cartilage readily visible. Needle placement was verified after the experiment by examination of the location of the needle entrance and exit wounds.

The tethered squid and force transducer were transferred to an aquarium (0.4 m by 0.2 m by 0.2 m) filled with 20° to 23 °C artificial seawater and were allowed to recover. Recovery, which was judged by the return of normal chromatophore patterning and fin activity, normally occurred within 10 min. Tethered squid remained alive and in apparent good health for up to several hours, though most squid were tethered for fewer than 20 min.

Although tethering is an invasive technique, it did not appear to be unduly traumatic to the squid. First, tethered squid behaved similarly to the animals in the holding tank. Both the tethered and free-swimming squid spent most of the time hovering, using the fins and low-amplitude jets. Second, unlike squid that are in distress or startled, more than 90% of the tethered squid did not eject ink. Third, the chromatophore patterns of tethered squid did not differ qualitatively from the patterns exhibited by freely swimming squid in the holding tank. Finally, when removed from the tether and returned to the holding tank, squid swam normally, and their survival was similar to that of undisturbed specimens. All experiments met the animal care guidelines of the University of North Carolina at Chapel Hill.

### *Critique of the method*

Previously published methods of estimating the thrust produced by jetting squids require measuring the funnel aperture during jet locomotion (see Johnson *et al.*, 1972; O'Dor, 1988a; Anderson and DeMont, 2000). Because a squid can adjust both the orientation of the funnel and the size and shape of the funnel aperture during the jet (Zuev, 1966; O'Dor, 1988a), accurate measurement of funnel diameter is difficult. These problems are exacerbated in newly hatched squid by their inability to maintain position in a flow tank, by their small size, and by the small funnel aperture. In addition, the method employed by Johnson *et al.* (1972) and O'Dor (1988a) is not applicable to hatchling squid because it is not currently possible to monitor mantle cavity pressure in these small animals without substantially altering normal mantle kinematics.

The tethering approach adopted here was chosen to bypass these difficulties. Tethering to a force transducer is particularly effective for small animals (see Svetlichnyy and Svetlichnyy, 1986; Lenz and Hartline, 1999), and the method has the considerable advantage of not requiring the small and dynamic funnel aperture of hatchling and juvenile squids to be measured to calculate thrust. Nevertheless, a potential disadvantage of this approach is its interference with the movement of the mantle during the escape jet. Because the tether did not touch the mantle and the kinematics of the mantle of tethered squids were qualitatively similar to those of untethered squids swimming in the holding tank (see Thompson and Kier, 2001a), it is unlikely that this was a source of significant error. Another possible disadvantage is that the flow field around a tethered squid is stationary. During an escape jet, an untethered squid has a velocity relative to the water, and this velocity affects the magnitude of the thrust required to keep a squid jetting at a given velocity (Vogel, 1994). Because we were investigating the maximum thrust that a squid can generate and not the variations in thrust produced during jetting, the stationary flow field is not an issue. The final potential disadvantage is that the post of the tether, which was located downstream of the funnel aperture (Fig. 1A), could alter thrust by interfering with the fluid exiting the funnel aperture. Significant alterations in thrust caused by the post are considered unlikely because of its small size relative to the funnel aperture and the distance of the post from the funnel aperture. Additionally, there were no significant differences between the thrust measured using either of our force trans-

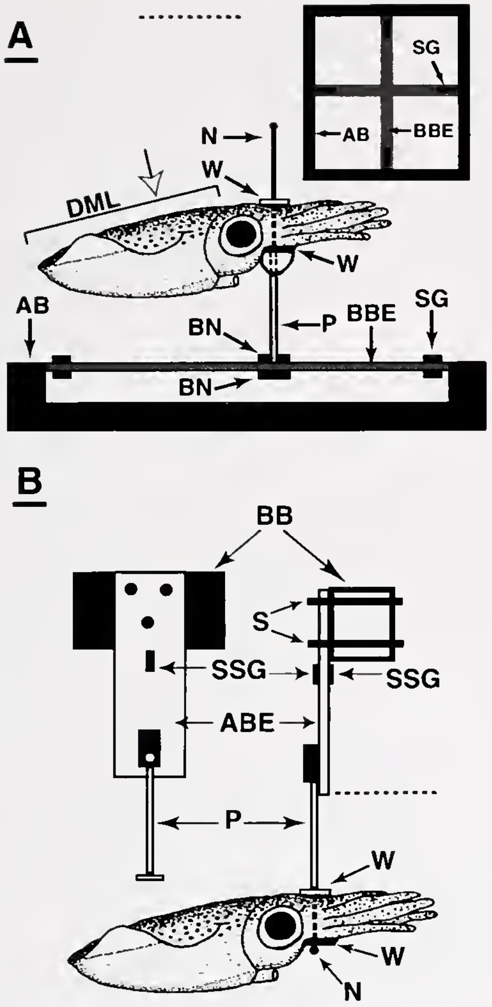

**Figure 1.** The tethering apparatus and the force transducers. The dashed lines indicate the water level during the experiments. (A) Transducer 1. The inset at top right is a plan view of the schematic with the squid and tether apparatus removed. The bracket above the squid indicates the dorsal mantle length (DML), and the white arrow points to 1/3 DML. AB, aluminum base; BBE, brass blade element; BN, brass nut; N, needle; P, stainless steel post; SG, thin foil strain gauge; W, plastic washer. (B) Transducer 2. The inset at left is a front view of the transducer with the squid removed. Abbreviations same as in A except as follows: ABE, aluminum blade element; BB, box beam; S, screws; SSG, semiconductor strain gauge.

ducers: one which had the post located downstream of the funnel and one which did not (see Fig. 1).

### *The force transducers*

We built two force transducers to measure the thrust produced by the squid. The first force transducer (transducer 1) consisted of thin foil strain gauges, wired as a full bridge (see Biewener and Full, 1992), and glued to two brass blade elements (Fig. 1A; see Appendix for details). We used long, thin blade elements to obtain the sensitivity necessary to measure the small thrust forces of the hatchlings. Thus, the resonant frequency of the force transducer was fairly low (about 55 Hz when unloaded in air).

We also built a second force transducer (transducer 2) with a higher resonant frequency (about 110 Hz when unloaded in air). It consisted of a single aluminum blade element with semiconductor strain gauges wired as a half bridge (Fig. 1B, see Appendix). The higher gauge factor of the semiconductor strain gauges allowed the stiffness of the blade element to be increased without sacrificing sensitivity.

Using analysis of covariance (Glantz and Slinker, 2001), we compared the data from the two force transducers. The adjusted slopes and means of the two data sets did not differ significantly (ANCOVA, $P = 0.82$). Therefore, we pooled the data from both transducers.

Each force transducer was calibrated in air after completion of the day's experiments.

### *Thrust measurement and mantle kinematics*

Escape-jet behavior of squids tethered to the force transducers was videotaped using an S-VHS video camera (Panasonic AG-450 Professional). A light-emitting diode (LED) flashing at 15 Hz was placed in the field of view of the camera to aid in aligning the video fields with the transducer output. The video output, the pre-amplified output voltage from the force transducer, and the 15-Hz signal from the function generator connected to the LED were collected simultaneously on a magnetic tape data recorder (A. R. Vetter Co., Rebersburg, PA).

Escape-jet data were digitized from the magnetic tape at 500 Hz using MacScope MAC-600 (Thornton Associates, Waltham, MA) and DATAQ DI-700 (DATAQ Instruments Inc, Akron, OH) analog-to-digital converters, and analyzed using MacScope and WinDAQ waveform analysis software.

Prior to digitization, the raw thrust-time data from transducer 1 were filtered with a 45-Hz low-pass filter (4 pole Butterworth; Ithaco, Inc., Ithaca, NY). Because (1) the fundamental frequency of the escape jets varied from 5 to 10 Hz, and (2) the contribution to the raw thrust-time data by harmonics above the 4th order was negligible for all the escape jets measured (indeed, the raw thrust-time data of most escape jets were composed of the fundamental and only the first two harmonics), the filtering did not affect the peak forces recorded. The raw data from transducer 2 were not filtered because the signal-to-noise ratio was very high.

Video sequences of escape-jet behavior were viewed using a Panasonic AG-1980P professional S-VHS videocassette recorder. Individual video fields were digitized with a frame grabber card (Imagenation, Beaverton, OR) and changes in mantle diameter measured using morphometrics software (SPSS Science, Chicago, IL). During an escape jet, the outer diameter of the mantle at 1/3 DML (from the anterior margin of the mantle; see Fig. 1A) was measured in each video field from the S-VHS videotapes and plotted against time. The diameter at 1/3 DML was selected because this location experiences the largest amplitude change during the escape jet (Thompson and Kier, 2001a). Time was estimated from the video camera capture rate of 60 fields per second.

The LED and its voltage spike were used to align the mantle kinematics and thrust data. The plot of thrust *versus* time (*i.e.*, the calibrated output of the force transducer) for the same escape jet was compared with the mantle kinematics.

### *Data analysis*

The peak thrust produced during an escape jet was measured as the difference between the baseline and the highest thrust achieved during the escape jet. The average of the 25 digitized data points (50 ms) immediately preceding the start of the escape jet was used as the baseline. The average of five digitized data points (10 ms) at the highest thrust produced was considered the peak thrust. The peak thrust was measured in a minimum of eight escape jets for each squid and only the largest thrust reported.

We also determined the average rate of thrust increase during each escape jet. This rate was calculated as the average slope of the thrust-time trace over the interval from the start of the jet to the peak thrust. Only the highest average rate for each squid was reported. In most instances, the escape jet that yielded the highest peak thrust also had the highest average slope.

We calculated impulse over the interval from the start of the escape jet to the point at which the thrust-time trace returned to the baseline (see arrows in Fig. 2B). Impulse is the integral of the product of force and time, and is a measure of the change in momentum of a squid during an escape jet. The impulse was calculated for a minimum of eight escape jets for each squid, and only the largest impulse was reported.

### *Morphometrics of mantle and funnel*

We normalized the thrust data for each squid in two ways. First, we divided the peak thrust of the escape jet by the wet weight of the squid to yield the weight-specific thrust. To determine weight, squids were anesthetized, lifted from the anesthetic by the posterior tip of the mantle (to permit water to drain from the mantle cavity), blotted dry, and weighed to the nearest 5 mg on an electronic balance.

Second, we divided the peak thrust by the cross-sectional area of the mitochondria-poor circumferential muscles of the mantle. These muscles, analogous to the white muscle fibers of mammals (Bone *et al.*, 1981; Mommsen *et al.*, 1981), are a relevant measure because it is likely that they provide the power for escape-jet locomotion (Gosline *et al.*, 1983; Bartol, 2001). Cross-sectional area of the "white" circumferential muscles was estimated as follows. The thickness of the ventral midline of the mantle at 1/2 DML was measured in unfixed squids. The squids were anesthetized in 7.5% $MgCl_2$ and killed by decapitation. Blocks of tissue from the midline of the ventral mantle were then fixed and embedded in paraffin. Sections parallel to the sagittal plane (*i.e.*, transverse to the long axes of the circumferential muscle fibers) were cut at 5 $\mu$m and stained. The ratio of the thickness of the band of white circumferential muscle fibers to the thickness of the entire mantle wall was measured from stained sections. Using the initial measurement of mantle thickness in unfixed animals, the width of the white circumferential muscle band could then be determined. The cross-sectional area of the muscles was estimated by multiplying the DML by the width of the white muscle band.

We also measured the maximum funnel aperture in a subset of the sample population. The diameter was measured with an ocular micrometer in squids that had been anesthetized following tethering.

### *Statistics*

The sample population used in this study was subdivided into the life-history stages described by Segawa (1987). The life-history stages were selected as an independent organization scheme upon which to base many of the statistical analyses. Segawa (1987) studied the life cycle of *S. lessoniana* from embryo to adult and divided the life cycle into seven stages based on morphological and ecological characters. These stages include hatchling (up to 10 mm DML), juvenile 1 (11–25 mm DML), juvenile 2 (26–40 mm DML), young 1 (41–60 mm DML), young 2 (61–100 mm DML), subadult (100–150 mm DML), and adult (>150 mm DML). In this classification, external adult morphology is achieved around 40 mm DML (the end of the juvenile 2 stage), and onset of sexual maturity occurs at 150 mm DML. The sample population of *S. lessoniana* used in the current investigation included the hatchling, juvenile 1, and juvenile 2 stages.

Nonparametric statistics were used for most of the analyses. For comparisons among the life-history stages, Kruskal-Wallis one-way analysis of variance on ranks was used with Dunn's method of pairwise multiple comparisons (Zar, 1996). Comparisons among all squid in the ontogenetic series were made using the Spearman rank order correlation (Zar, 1996).

All log-transformed (base 10) data passed normality and homoscedasticity tests. Regression lines were fitted to the data using an ordinary least squares approximation. All statistical analyses were completed using SigmaStat 1.01 (SPSS Science, Chicago, IL) and JMP (SAS, Cary, NC).

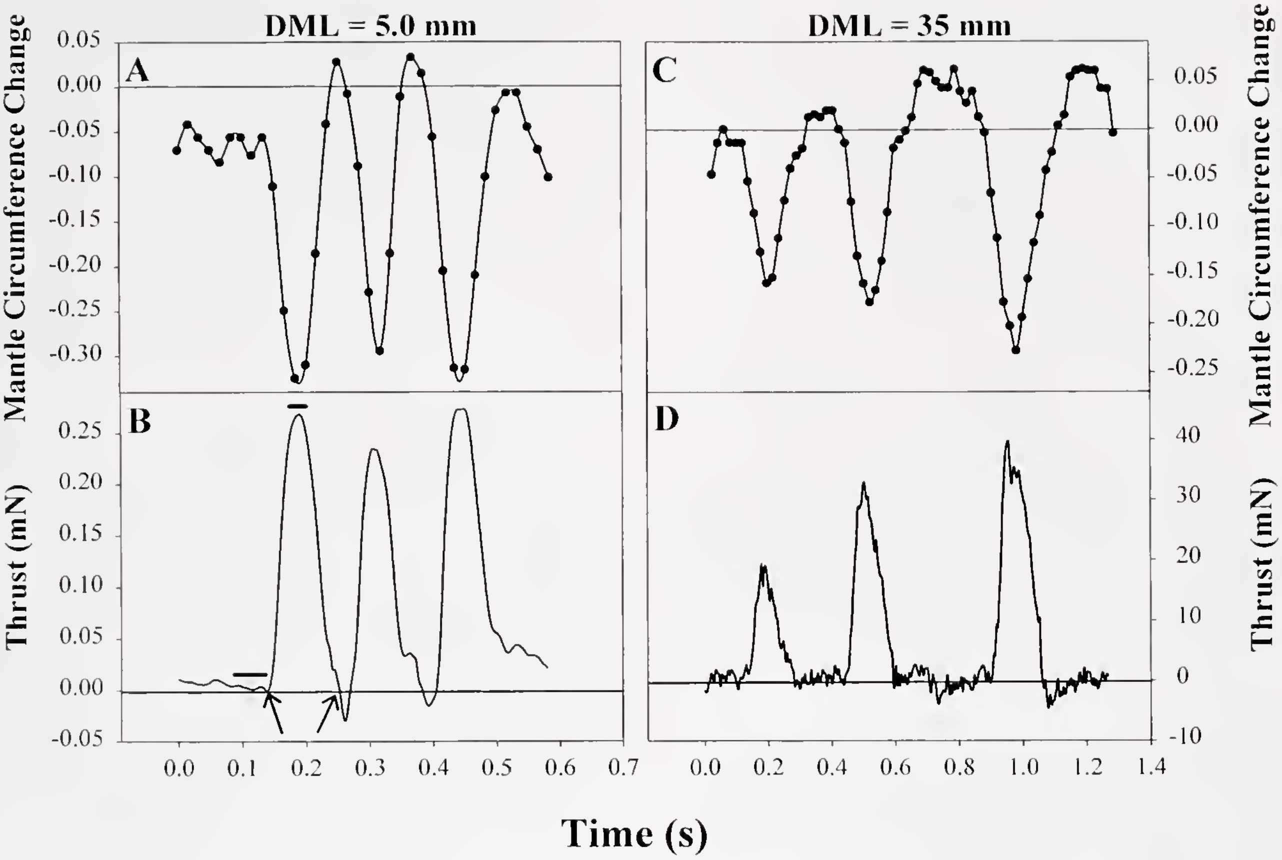

**Figure 2.** Plot of mantle circumference change and thrust *versus* time during three escape jets in a hatchling (DML, 5 mm) and a juvenile 2 (DML, 35 mm) stage of the squid *Sepioteuthis lessoniana*. (A and C) Mantle circumference change was normalized by the resting mantle diameter at 1/3 DML (represented by the horizontal lines) in the anesthetized squid. Negative values indicate contraction of the mantle; positive values indicate hyperinflation. Each data point represents the mantle circumference measurement from a single video field. (B and D) Plots of thrust *versus* time for the same sequences of escape-jetting in panels A and C, respectively. The trace in panel B was from transducer 1. The raw data were filtered at 45 Hz (low pass). The arrows on the plot indicate the interval over which the impulse was calculated. The black bar to the left of the first escape jet indicates the 50-ms interval used to calculate the average baseline thrust. The small bar at the top of the first escape jet indicates the 10-ms interval used to calculate the peak thrust. The trace in panel D is from transducer 2. The raw data are presented.

## Results

### *Thrust-time traces*

There were no major qualitative differences in the shape of the thrust-time traces during ontogeny. At the start of an escape jet the mantle usually expands beyond its resting diameter. During this "hyperinflation," water fills the mantle cavity through large openings along the left and right anterior edges of the mantle. The plots of thrust *versus* time often showed negative thrust that was correlated with hyperinflation of the mantle as observed in the video records (Fig. 2).

Next in the escape-jet sequence, the mantle contracts rapidly and ejects water from the mantle cavity through the funnel aperture. Concurrent with contraction of the mantle, thrust increased rapidly (Figs. 2B, D). In hatchling stage squid, the thrust peaked within 40 ms ± 7.4 ms (mean ± standard deviation) of the start of the escape-jet, whereas in juvenile 2 stage squid thrust peaked within 71 ms ± 14 ms.

In the final event of the escape-jet sequence, the mantle re-expands to its original shape and the mantle cavity is refilled. At the end of the mantle contraction and during mantle refilling, the thrust decreased rapidly, though at a lower rate than the force increase during the early phase of mantle contraction (Fig. 2B, D). In many of the thrust-time traces, though most noticeably in the juvenile 1 and juvenile 2 stage animals, the thrust decreased below the baseline during refilling of the mantle cavity, implying reverse thrust (the end of jet 1 in Fig. 2B; at the end of jet 3 in Fig. 2D).

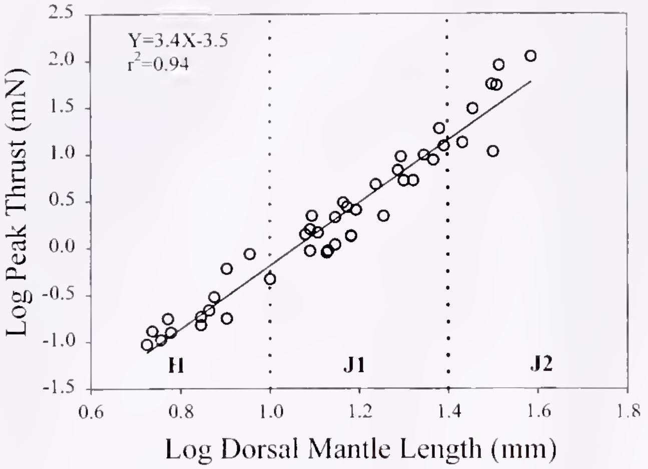

**Figure 3.** The log of the peak thrust generated during the escape jet *versus* the log of dorsal mantle length. Each data point represents the highest peak thrust produced by one squid, and thus there are no error bars. Log peak thrust was regressed against the log of the DML, using an ordinary least-squares method. The equation is indicated in the upper left corner of the plot. H, Hatchling stage squids; J1, Juvenile 1 stage; J2, Juvenile 2 stage.

### *Peak thrust*

As expected, the peak thrust produced during the escape jet increased with dorsal mantle length (Spearman rank order correlation, $r = 0.97$, $P < 0.001$, $n = 54$). Newly hatched *S. lessoniana* produced between 0.10 mN and 0.80 mN of thrust during the escape jet, whereas the largest squids studied generated between 18 mN and 110 mN of thrust (Fig. 3; see Table 1 for descriptive statistics based on life-history stage). Sorting the data by the life-history stages of Segawa (1987) indicated that hatchling stage squid generated lower peak thrust than either the juvenile 1 or juvenile 2 stage squid ($P < 0.01$; Table 1). Juvenile 1 stage squid produced lower peak thrust than juvenile 2 stage animals during the escape jet ($P < 0.01$; Table 1).

The peak thrust data were normalized by the wet weight of each squid. The weight-specific peak thrust of the escape jet increased significantly with DML (Spearman rank order correlation, $r = 0.68$, $P < 0.001$, $n = 54$), from 0.20 to 0.40 in hatchlings to between 1.0 and 2.5 in the largest squids tested (Fig. 4A). Sorting the data by the life-history stages of Segawa (1987) indicated that the mean of 0.36 in the hatchling stage squid was significantly lower than the averages of 0.55 and 1.5 in the juvenile 1 and juvenile 2 stage squids, respectively ($P < 0.01$; Table 1). In addition, the juvenile 1 stage animals produced lower weight-specific thrust during the escape-jet than did the juvenile 2 stage squids ($P < 0.01$; Table 1).

The peak thrust data were also normalized by the cross-sectional area of the "white" circumferential muscle fibers (*i.e.*, the muscles that probably provide the power for escape-jet thrust; see Gosline *et al.*, 1983, and Bartol, 2001). Newly hatched squids generated much lower thrust per unit area of white circumferential muscle than did older, larger animals (Fig. 4B). Sorting the normalized thrust data by the life-history stages of Segawa (1987) indicated that hatchling stage squids produced significantly lower thrust per unit area of white circumferential muscle (0.25 $mN/mm^2$) than either the juvenile 1 (0.47 $mN/mm^2$) or juvenile 2 (1.4 $mN/mm^2$) stage squids ($P < 0.01$; Table 1). In addition, the juvenile 1 stage squids produced lower normalized thrust than juvenile 2 stage animals ($P < 0.01$; Table 1).

### *Rate of thrust increase*

The average rate of thrust increase of the escape jet increased significantly with dorsal mantle length (Spearman rank order correlation, $r = 0.92$, $P < 0.001$, $n = 54$). The mean rate of thrust increase varied from 3 to 18 mN/s in hatchlings and increased rapidly to between 300 and 1800 mN/s in the largest squids studied (Fig. 5). Sorting the data by the life-history stages of Segawa (1987) indicated that the average rate of thrust increase in hatchling stage animals (13 mN/s) was significantly lower than in either the juvenile

**Table 1**

*A comparison of the mechanics of the escape jet among squid divided into the life-history stages of Segawa (1987)*

| Stage | *n* | Peak thrust (mN) | Weight-specific peak thrust | Thrust/unit area muscle ($mN/mm^2$) | Mean rate thrust increase (mN/s) | Mean impulse (mN · s) |
|---|---|---|---|---|---|---|
| Hatchling | 17 | 0.28 ± 0.24 | 0.36 ± 0.15 | 0.25 ± 0.10 | 13 ± 13 | 1.3 ± 1.2 |
| Juvenile 1 | 27 | 4.0 ± 3.2 | 0.55 ± 0.24 | 0.47 ± 0.18 | 170 ± 240 | 30 ± 32 |
| Juvenile 2 | 10 | 45 ± 32 | 1.5 ± 0.78 | 1.4 ± 0.72 | 960 ± 190 | 600 ± 370 |

The means of the peak thrust, the weight-specific peak thrust, the thrust per unit area of "white" circumferential muscle, the rate of thrust increase, and impulse during the escape jet are listed in each column ± the standard deviation of the mean. The highest thrust, weight-specific thrust, thrust/unit area muscle, rate of thrust increase, and impulse for each squid in a life-history stage were pooled to calculate the mean and the standard deviation. In each column, the mean value for the hatchling stage squids was significantly less than the mean for the juvenile 1 and juvenile 2 life-history stages (one-way ANOVA on ranks, $P < 0.01$). In each column, the mean value for the juvenile 1 stage squids was significantly less than the mean for the juvenile 2 stage animals (one-way ANOVA on ranks, $P < 0.01$).

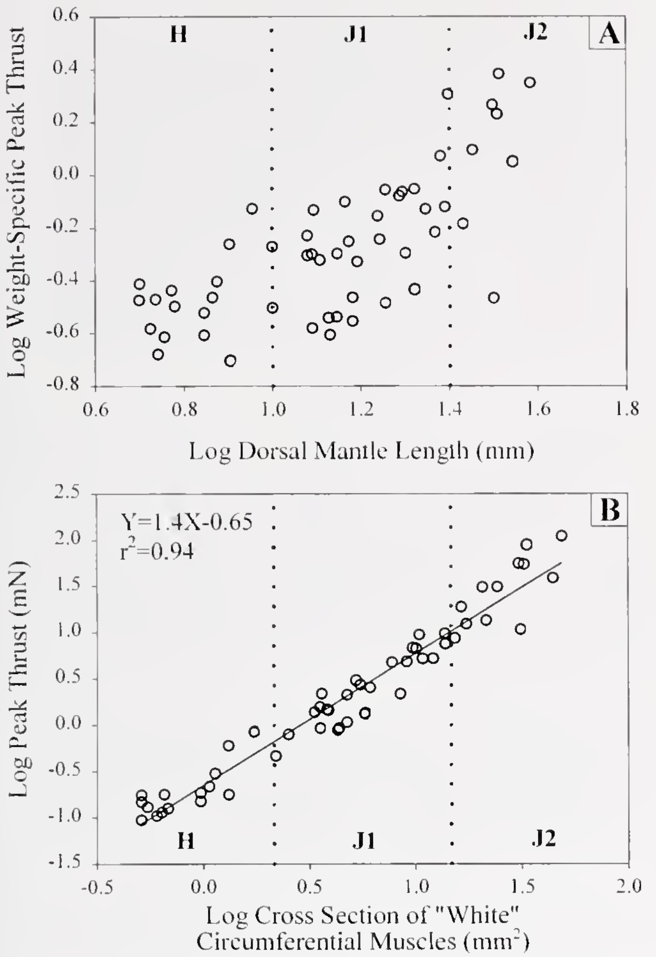

**Figure 4.** The peak thrust of the escape jet normalized by different measures of squid size. H, Hatchling stage squids; J1, Juvenile 1 stage; J2, Juvenile 2 stage. (A) The log of weight-specific peak thrust produced during the escape jet *versus* the log of dorsal mantle length. Weight-specific peak thrust was calculated by dividing the peak thrust generated by an individual squid (data in Fig. 3) by the wet weight (in mN) of the squid. Weight-specific peak thrust was positively correlated with DML (Spearman rank order correlation, $r = 0.68$, $P < 0.001$, $n = 54$). (B) The log of the peak thrust of the escape jet *versus* the log of the cross-sectional area of the "white" circumferential muscles. Log peak thrust was regressed against the log of the cross-sectional area of the white circumferential muscles, using an ordinary least-squares method. The equation is indicated in the upper left corner of the plot.

1 (170 mN/s) or juvenile 2 (960 mN/s) stages ($P < 0.01$; Table 1). The rate of thrust increase was also lower in juvenile 1 stage animals than in juvenile 2 stage squids ($P < 0.01$; Table 1).

### *Impulse*

The impulse produced during the escape jet increased rapidly with DML (Spearman rank order correlation, $r = 0.88$, $P < 0.001$, $n = 54$). Impulse ranged from 0.25 to 5.0 mN · s in newly hatched animals and increased exponentially during ontogeny to between 100 and 1000 mN · s in the largest squids studied (Fig. 6). Sorting the data into the life-history stages of Segawa (1987) indicated that the mean impulse of 1.3 mN · s in the hatchling stage squid was significantly less than the impulses of 30 mN · s and 600 mN · s in the juvenile 1 and 2 stage animals, respectively ($P < 0.01$; Table 1). In addition, the juvenile 1 stage squid

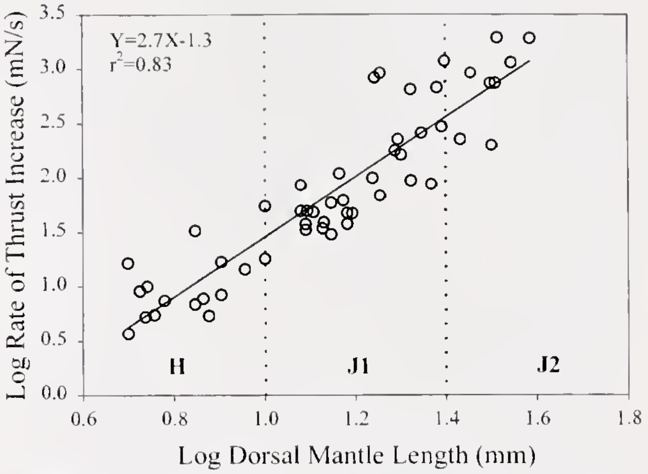

**Figure 5.** Plot of the log rate of thrust increase *versus* the log of dorsal mantle length. Each point represents the highest rate of thrust increase for one squid. Log rate of thrust increase was regressed against the log of DML, using an ordinary least-squares method. The regression equation is located in the upper left corner of the plot. H, Hatchling stage squids; J1, Juvenile 1 stage; J2, Juvenile 2 stage.

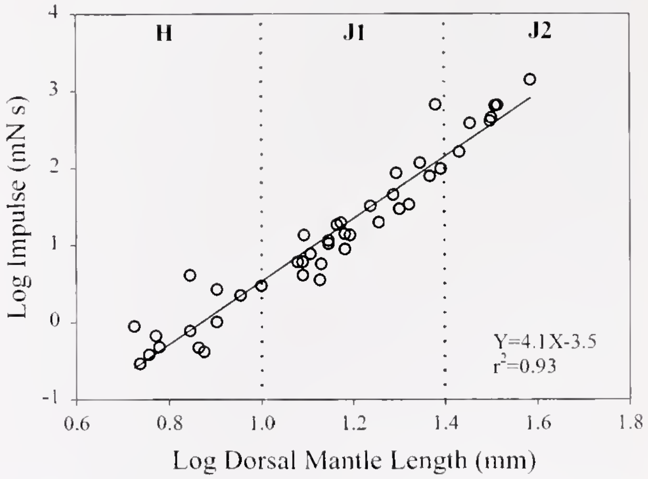

**Figure 6.** Plot of log impulse *versus* log dorsal mantle length. Each point represents the highest impulse produced during an escape jet by one squid. The impulse (the integral of force · time) was calculated from the force and time data for each escape jet. In most cases, the highest impulse was produced during the same escape jet that yielded the peak thrust. Log impulse was regressed against the log of DML, using an ordinary least-squares method. The regression equation is located in the lower right corner of the plot. H, Hatchling stage squids; J1, Juvenile 1 stage; J2, Juvenile 2 stage.

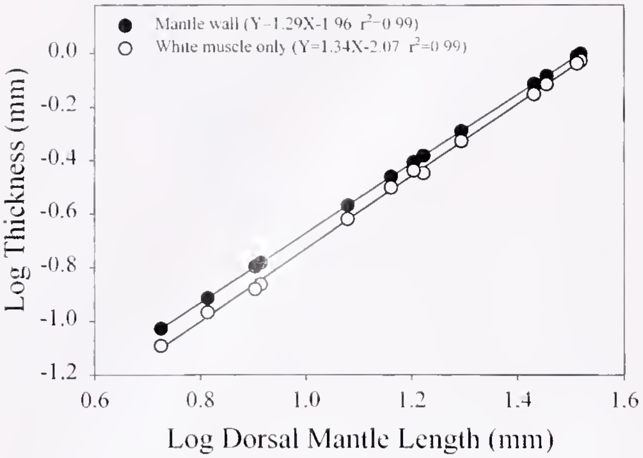

**Figure 7.** Mantle morphometric data. Log thickness of the mantle wall (filled symbols) and log thickness of the layer of "white" circumferential mantle muscles (open symbols) *versus* log dorsal mantle length. The thickness of both the entire mantle wall and the layer of white circumferential muscles was measured at ½ dorsal mantle length along the ventral midline. See the materials and methods section for details. Log mantle thickness and log thickness of the white muscles were regressed against the log DML, using an ordinary least-squares method. The regression equations are located in the upper left corner of the plot. Note the positive allometry: relative to mantle length, both the thickness of the mantle wall and the layer of white muscles are highest in the oldest, largest animals studied.

produced less impulse during the escape jet than the juvenile 2 stage animals ($P < 0.01$; Table 1).

### *Morphometrics of mantle and funnel*

The thickness of the mantle wall increased from between 0.070 mm and 0.13 mm in hatchlings, up to 2.5 mm in the largest animals studied (Fig. 7). The slope (1.29) of the regression of the thickness of the mantle wall against DML and the slope (1.34) of the regression of the thickness of the white circumferential muscle layer against DML were significantly greater than 1.0 ($P < 0.01$). This indicates positive allometry of mantle thickness, relative to DML, during growth (Fig. 7). In addition, the slopes of the two regressions were not significantly different ($P > 0.05$), suggesting that the positive allometric increase in mantle wall thickness (relative to DML) was due, in large part, to the ontogenetic allometric increase in the width of the white circumferential muscle layer (Fig. 7).

The diameter of the funnel aperture in anesthetized squids increased during growth. The slope (0.65) of the regression of funnel aperture against DML was, however, less than unity, indicating that the aperture of the funnel relative to body length decreased with growth (Fig. 8). Indeed, the average funnel aperture in anesthetized newly hatched squids is about 1.8 times larger (relative to mantle length) than the average aperture in anesthetized juvenile 2 stage squids.

## Discussion

The peak thrust, weight-specific peak thrust, rate of thrust increase, and impulse of the escape jet all increase significantly during the growth of *S. lessoniana*. These changes in the mechanics of the escape jet correlate strongly with striking ontogenetic changes in (1) the morphology of the mantle (Thompson and Kier, 2001b) and funnel, and (2) the maximum amplitude and rate of mantle movement during the jet (Thompson and Kier, 2001a). Furthermore, the changes in the mechanics of the escape jet have implications for circumferential muscle mechanics and the propulsion efficiency of the jet.

### *Ontogeny of muscle mechanics*

The large increase in the relative thickness of the musculature of the mantle wall (Fig. 7) may help explain the ontogenetic increase in the weight-specific thrust of the escape jet (Fig. 4A). For a pressurized cylinder such as the mantle, the relationship between the stress in the wall, the pressure, and the radius is given by the following equation (after Fung, 1994):

$$\sigma = r_i\, p/t \qquad \text{(Eq. 2)}$$

where $\sigma$ is the average circumferential stress in the wall, $p$ is the internal pressure, $r_i$ is the radius of the inner edge of the mantle wall, and $t$ is the thickness of the mantle wall. Solving equation (2) for pressure ($p$),

$$p = \sigma t/r_i \qquad \text{(Eq. 3)}$$

and substituting measured values of mantle radius (Thompson

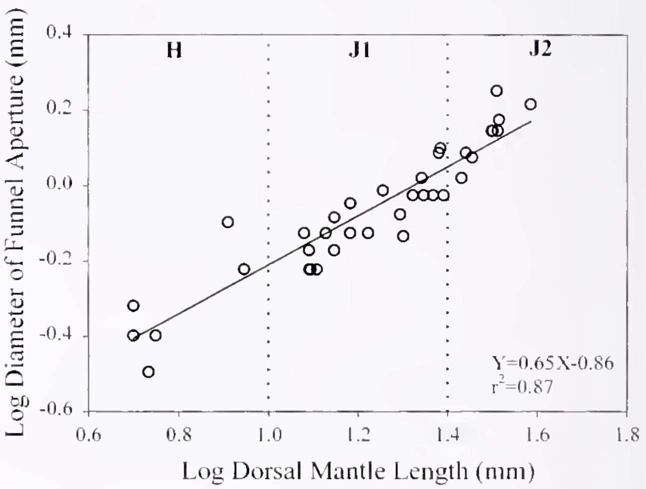

**Figure 8.** Log diameter of the funnel aperture *versus* log dorsal mantle length. Maximum funnel aperture was measured in anesthetized squids. The regression was done using an ordinary least squares method, and the equation is listed in the lower right corner of the plot. Note the negative allometry of the relationship: the funnel aperture is largest (relative to mantle length) in the smallest squids. H, Hatchling stage squids; J1, Juvenile 1 stage; J2, Juvenile 2 stage.

and Kier, 2001a), of mantle wall thickness (Fig. 7A), and of the peak isometric stress generated by the circumferential mantle muscles of squids (Milligan *et al.*, 1997), the maximum mantle cavity pressure that can be generated during the escape jet can be calculated. The peak isometric stress produced by the "white" circumferential mantle muscles of adult *Loligo vulgaris* was measured to be 262 mN/mm$^2$, but it may range as high as 400 mN/mm$^2$ (Milligan *et al.*, 1997). Using those values and assuming that the peak isometric stress of the circumferential muscles does not change during ontogeny, we calculate that a newly hatched squid (DML = 5 mm) should generate mantle cavity pressures between 2 and 3 kPa during the escape jet, whereas a juvenile squid (DML = 40 mm) should produce pressures between 6 and 9 kPa. This threefold difference in the maximum mantle cavity pressure during the escape jet results from a substantial ontogenetic increase in the relative thickness of the mantle wall musculature and may explain part of the ontogenetic increase in the weight-specific peak thrust of the escape jet that we observed.

The ontogenetic difference in the relative thickness of the mantle wall alone is insufficient to explain the growth-related changes in the mechanics of the escape jet. Our data also suggest that the contractile properties of the circumferential mantle muscles of *S. lessoniana* change during growth. Newly hatched squid generated 0.25 mN thrust per square millimeter of circumferential muscle during the escape jet, whereas the largest squids studied were able to produce nearly 6 times as much thrust per unit area of muscle (Fig. 4B; Table 1). Although the mantles of hatchlings contain a slightly lower proportion of the white circumferential muscle fibers that provide the power for the escape jet than the mantles of adults (Thompson and Kier, 2001b), ontogenetic differences in the proportions of "red" and "white" circumferential muscle fibers are insufficient to explain the sixfold difference in thrust per unit area that we observed. Indeed, normalizing the peak thrust data by the entire thickness of the mantle wall (*i.e.*, both the red and white circumferential muscles) does not change the result.

The thrust produced per unit area of circumferential muscle depends not only on the contractile properties of the circumferential muscles (*e.g.*, thick myofilament length), but also on the funnel aperture. Control of the funnel aperture affects the peak thrust of the escape jet and, therefore, the measurement of the "unit thrust output" of the circumferential musculature. Thus, the ontogenetic differences in the magnitude of thrust per unit area of the circumferential muscles may depend on several variables.

An additional observation, however, supports the proposal that the contractile properties of the mantle muscle change with growth. Thompson and Kier (2001a) reported that the shortening velocity of the circumferential muscles (measured indirectly from the contraction velocity of the entire mantle during an escape jet) ranged from a high of 13 lengths per second (L/s) in hatchling *S. lessoniana* to a low of 4 L/s in mature squids. The shortening velocity of muscle varies inversely with the load on the muscle and the lengths of the thick filaments and sarcomeres, and in direct proportion to the rate of cross-bridge cycling (Schmidt-Nielsen, 1997). The force generated by a muscle varies in proportion with its cross-sectional area and the length of its thick filaments (Schmidt-Nielsen, 1997). Thus, shorter thick filaments in hatchling *S. lessoniana* than in older, larger squids would be consistent with the observations that (1) the shortening velocity of the circumferential muscles is highest in hatchlings, and (2) the peak thrust generated per unit area circumferential muscle is lowest in hatchlings. We plan to measure the contractile properties and myofilament dimensions of the circumferential muscles from an ontogenetic series of *S. lessoniana* to examine the possibility of a change in performance of the muscle during ontogeny.

### *Propulsion efficiency*

The propulsion efficiency of jet locomotion may be higher in newly hatched individuals of *S. lessoniana* than in older, larger animals. Propulsion efficiency is the ratio of the power output by the animal (the product of thrust and the velocity of the animal) to the power input by the animal (the kinetic energy input per unit time). The hydrodynamic propulsion efficiency ($\eta$) of the exhalant phase of the jet stroke can be calculated using the following equation of rocket-motor propulsion efficiency:

$$\eta = (2VV_j)/(V^2 + V_j^2), \text{ (Anderson and DeMont, 2000)} \qquad \text{(Eq.4)}$$

where $V$ is the velocity of flow past the squid and $V_j$ is the velocity of the jet relative to the squid. According to equation (4), the highest propulsion efficiency is achieved when $V_j$ approximates $V$. Because $V_j$ must be greater than $V$ for a squid to accelerate, a relatively lower jet velocity increases propulsion efficiency.

Our results support the hypothesis that $V_j$ is relatively lower in hatchling than in larger *S. lessoniana* individuals. First, the funnel is proportionately larger (about 1.8 times, relative to body size) in anesthetized newly hatched squids than in older, larger squids (Fig. 8; also see Clarke, 1966; Packard, 1969; Boletzky, 1974). By the principle of continuity, for a given volume of water exiting the mantle cavity per unit time, a larger funnel aperture will decrease the average water velocity, while a narrow nozzle will increase the average water velocity.

Second, steady-state jet thrust is proportional to the product of mass flux (= mass of water per unit time that exits the mantle cavity) and the difference between the velocity of water exiting the funnel aperture and the velocity of the animal (Vogel, 1994). In previous work on *S. lessoniana* (Thompson and Kier, 2001a), we showed that significant differences in the relative volume of water in the mantle cavity and both the amplitude and the rate of mantle contraction during escape-jet locomotion result in much greater relative mass flux in hatchlings than in larger squid. Because the peak weight-specific thrust produced during the escape jet is lowest in newly hatched squid (Fig. 4A, Table 1) but relative mass flux is highest (Thompson and Kier, 2001a), the velocity of water exiting the funnel aperture ($V_j$) must be relatively slower in the hatchlings than in the adults. This observation supports the assumption that the funnel apertures of hatchling squids are relatively larger than the apertures of mature squids, not only in anesthetized animals but also during escape-jet locomotion (see also O'Dor and Hoar, 2000).

Is the propulsion efficiency of the escape jet higher in newly hatched squid than in larger animals? Anderson and DeMont (2000) emphasize that the overall propulsion efficiency of the jet includes both the efficiency of the jet stroke and the efficiency of refilling the mantle cavity. The thrust-time traces for the escape jets of many squid showed that a substantial thrust, opposite in direction to the escape-jet thrust, occurs during the refilling of the mantle cavity. We suspect that these forces are associated with refilling following the escape jet. However, further work with higher time resolution video data is required to begin to measure the efficiency of refilling.

If the propulsion efficiency of the exhalant phase of the escape jet is higher in newly hatched squid than in larger animals, is the cost of transport during escape-jet locomotion lower in hatchlings? Most likely, it is not. Mass-specific metabolic rate is higher in hatchling ommastrephid and loliginid squids than in the adults (O'Dor and Webber, 1986; O'Dor, 1988b). In addition, hydromechanical costs other than propulsion efficiency, such as drag and the acceleration reaction, may be relatively higher in the intermediate Reynolds number (Re) fluid regime of the hatchling squid. For example, Müller *et al.* (2000) hypothesized that burst-and-coast swimming was much less efficient hydrodynamically in larval zebra danios (*Brachydanio rerio*) than in the adult fish. Because the larval fish swim in an intermediate Re fluid regime, Müller *et al.* (2000) suggested that the high relative viscous drag on the larvae during the coasting phase contributed to the reduction in hydrodynamic efficiency relative to the adult. Indeed, *B. rerio* larvae coast for less than half a body length, but adult fish coast for several body lengths following a burst (Müller *et al.*, 2000).

Escape-jet locomotion is analogous to burst-and-coast swimming. In escape-jet locomotion, there is a brief period of thrust generation (*i.e.*, rapid contraction of the mantle) followed by mantle cavity refilling and coasting. Given their small size and low absolute swimming speeds, newly hatched squids swim in an intermediate Re fluid regime (unpub. obs. of *S. lessoniana*; Hoar *et al.*, 1994; Preuss *et al.*, 1997). Because viscous drag is relatively high at intermediate Re, newly hatched individuals of *S. lessoniana* may experience lower hydrodynamic efficiency relative to the adult during escape-jet locomotion. Unfortunately, it is not possible to analyze this issue further because, to our knowledge, there are no data on the hydrodynamics of escape-jet locomotion in hatchling squid. Nevertheless, higher propulsion efficiency for hatchlings of *S. lessoniana* will reduce the cost of transport, compared to a hypothetical case in which the kinematics and mechanics of the escape jet in hatchlings are identical to those of the adults.

Finally, the relatively large funnel apertures of hatchlings of *S. lessoniana* will result in lower velocities of water exiting the funnel ($V_j$) at all jetting speeds, not only in escape-jet locomotion. Indeed, it is likely that natural selection for high propulsion efficiency during the escape jet is not strong in hatchlings (*i.e.*, the cost of being eaten is zero fitness). Thus, the relatively large funnel apertures in hatchlings may represent selection for high propulsion efficiency at low-speed jetting, with the associated trade-off of low weight-specific thrust of the escape jet. An alternative hypothesis is that size-related differences in the physics of locomotion may constrain funnel aperture in the tiny hatchlings.

### *An effect of scale on jet locomotion?*

In *S. lessoniana*, ontogenetic changes in the mantle kinematics of the escape jet occur concomitantly with a reorganization of the intramuscular (IM) collagen fibers that store elastic energy and help limit the deformation of the mantle during jet locomotion (Thompson and Kier, 2001b). One consequence of these changes in mantle morphology and function is that the average mass flux of the escape jet, relative to body mass, is highest in hatchling squids and declines significantly during growth (Thompson and Kier, 2001a). As mentioned previously, jet thrust is proportional to the product of mass flux and the velocity of water exiting the funnel aperture (Vogel, 1994). Because the weight-specific peak thrust of the escape jet is lowest in hatchlings, the velocity of water exiting the funnel must be disproportionately low in newly hatched animals. Thus, tiny squid must keep the funnel aperture relatively large during the escape jet.

If mass flux remains unchanged, hatchlings could increase the weight-specific peak thrust generated during the escape jet by narrowing the funnel aperture. Given the potential benefits of increasing the weight-specific thrust, why don't hatchlings narrow the funnel aperture during the escape jet? One possibility is that newly hatched squid are unable to modulate the aperture of the funnel, perhaps due to mechanical or neuromuscular limitations of the funnel musculature. However, because the pressure required to pump water through a pipe (*e.g.*, a funnel) at a given rate of flow varies inversely with the 4th power of the radius of the pipe (Vogel, 1994), two alternative hypotheses are also possible. First, the circumferential muscles (that create the pressure that forces water through the funnel) of hatchlings might not produce sufficient force to maintain relatively high mass flux through a smaller funnel aperture. Second, the circumferential muscles of hatchlings might be able to generate sufficient force, but the energetic costs of forcing water through a relatively smaller funnel may be higher. Thus, an effect of scale may have constrained the evolution of funnel aperture in *S. lessoniana*. We are attempting to address this issue by measuring the mechanics of the circumferential muscles in an ontogenetic series of *S. lessoniana* and by using a comparative approach to study the prevalence of ontogenetic changes in the organization of IM collagen fibers in the mantles of a variety of cephalopods.

### *Summary and future directions*

In conclusion, we observed significant ontogenetic changes in the mechanics of the escape jet in squid tethered to a force transducer. These growth-related alterations in the mechanics of the escape-jet may be correlated with changes in the mechanics of the circumferential muscles of the mantle. The changes reveal an apparent trade-off in jet locomotion during growth—hatchling squids achieve high propulsion efficiency, but at the expense of the thrust. This apparent trade-off may be indicative of an effect of scale on jet locomotion.

As the next step, we intend to measure the ontogeny of locomotor performance (peak escape velocity, acceleration, *etc.*) in untethered specimens of *S. lessoniana*. We also plan to measure the contractile properties and myofilament dimensions of the circumferential muscles from an ontogenetic series of *S. lessoniana* in order to examine the possibility of a change in performance of the muscle during ontogeny. In addition, because the elastic energy stored during mantle hyperinflation may be returned to augment the thrust produced during the escape jet, future studies should examine the ontogeny of radial muscle contraction in hyperinflation. These experiments will help us achieve our ultimate goal of understanding the fitness consequences of ontogenetic variation in morphology, physiology, and locomotion in soft-bodied invertebrates.

## Acknowledgments

This research was supported by NSF grants to W.M.K. (IBN-9728707 and IBN-9219495). Grants and fellowships to J.T.T. from the Wilson Fund, the American Malacological Society, and Sigma Xi helped defray research expenses. The research was also supported by a Seeding Postdoctoral Innovators in Research and Education (SPIRE) fellowship to J.T.T. from the Minority Opportunities in Research Division of the National Institute of General Medical Sciences (Grant No. GM000678). H. Hsiao, R. Goldberg, and S. Vogel provided ideas for the force transducers, and J. Goldman supplied the circuit diagram for the instrumentation amplifier that we built to amplify the thrust-time signals. We thank L. Walsh at the NRCC for her expertise in shipping squid cross-country. We thank J. Taylor, T. Uyeno, J. Voight, and two anonymous reviewers for excellent comments and suggestions.

## Literature Cited

**Anderson, E. J., and M. E. DeMont. 2000.** The mechanics of locomotion in the squid *Loligo pealei*: locomotory function and unsteady hydrodynamics of the jet and intramantle pressure. *J. Exp. Biol.* **203:** 2851–2863.

**Bartol, I. K. 2001.** Role of aerobic and anaerobic circular mantle muscle fibers in swimming squid: electromyography. *Biol. Bull.* **200:** 59–66.

**Batty, R. S. 1984.** Development of swimming movements and musculature of larval herring (*Clupea harengus*). *J. Exp. Biol.* **110:** 217–229.

**Biewener, A. A., and R. J. Full. 1992.** Force platform and kinematic analysis. Pp. 45–73 in *Biomechanics: Structures and Systems. A Practical Approach*. A. A. Biewener, ed. IRL Press at Oxford University Press, New York.

**Boletzky, S. V. 1974.** The "larvae" of Cephalopoda: a review. *Thalassia Jugosl.* **10:** 45–76.

**Bone, Q., A. Pulsford, and A. D. Chubb. 1981.** Squid mantle muscle. *J. Mar. Biol. Assoc. UK* **61:** 327–342.

**Clarke, M. R. 1966.** A review of the systematics and ecology of oceanic squids. *Adv. Mar. Biol.* **4:** 91–300.

**Daniel, T., C. Jordan, and D. Grunbaum. 1992.** Hydromechanics of swimming. Pp. 17–49 in *Advances in Comparative and Environmental Physiology. Vol. II. Mechanics of Animal Locomotion*, R. M. Alexander, ed. Springer-Verlag, New York.

**Fung, Y. C. 1994.** *A First Course in Continuum Mechanics: For Physical and Biological Scientists and Engineers*. 3rd ed. Prentice Hall, Englewood Cliffs, NJ.

**Gilly, W. F., B. Hopkins, and G. O. Mackie. 1991.** Development of giant motor axons and neural control of escape responses in squid embryos and hatchlings. *Biol. Bull.* **180:** 209–220.

**Glantz, S. A., and B. K. Slinker. 2001.** *Primer of Applied Regression and Analysis of Variance*. 2nd ed. McGraw-Hill, New York.

**Gosline, J. M., J. D. Steeves, A. D. Harman, and M. E. DeMont. 1983.** Patterns of circular and radial mantle muscle activity in respiration and jetting of the squid *Loligo opalescens*. *J. Exp. Biol.* **104:** 97–109.

**Hoar, J. A., E. Sim, D. M. Webber, and R. K. O'Dor. 1994.** The role of fins in the competition between squid and fish. Pp. 27–43 in *Mechanics and Physiology of Animal Swimming*, L. Maddock, Q. Bone, and J. M. V. Rayner, eds. Cambridge University Press, Cambridge.

**Johnson, W., P. D. Soden, and E. R. Trueman. 1972.** A study in jet propulsion: an analysis of the motion of the squid, *Loligo vulgaris*. *J. Exp. Biol.* **56:** 155–165.

**Lee, P. G., P. E. Turk, W. T. Yang, and R. T. Hanlon. 1994.** Biological characteristics and biomedical applications of the squid *Sepioteuthis lessoniana* cultured through multiple generations. *Biol. Bull.* **186:** 328–341.

**Lenz, P. H., and D. K. Hartline. 1999.** Reaction times and force production during escape behavior of a calanoid copepod. *Undinula vulgaris*. *Mar. Biol.* **133:** 249–258.

**Lighthill, J. 1975.** *Mathematical Biofluiddynamics*. Society for Industrial and Applied Mathematics, Philadelphia.

**Messenger, J. B., M. Nixon, and K. P. Ryan. 1985.** Magnesium chloride as an anaesthetic for cephalopods. *Comp. Biochem. Physiol.* **82C:** 203–205.

**Milligan, B. J., N. A. Curtin, and Q. Bone. 1997.** Contractile properties of obliquely striated muscle from the mantle of squid (*Alloteuthis subulata*) and cuttlefish (*Sepia officinalis*). *J. Exp. Biol.* **200:** 2425–2436.

**Mommsen, T. P., J. Ballantyne, D. MacDonald, J. Gosline, and P. W. Hochachka. 1981.** Analogues of red and white muscle in squid mantle. *Proc. Natl. Acad. Sci. USA* **78:** 3274–3278.

**Müller, U. K., and J. J. Videler. 1996.** Inertia as a 'safe harbour': Do fish larvae increase length growth to escape viscous drag? *Rev. Fish Biol. Fish.* **6:** 353–360.

**Müller, U. K., E. J. Stamhuis, and J. J. Videler. 2000.** Hydrodynamics of unsteady fish swimming and the effects of body size: comparing the flow fields of fish larvae and adults. *J. Exp. Biol.* **203:** 193–206.

**O'Dor, R. K. 1988a.** The forces acting on swimming squid. *J. Exp. Biol.* **137:** 421–442.

**O'Dor, R. K. 1988b.** The energetic limits on squid distributions. *Malacologia* **29:** 113–119.

**O'Dor, R. K., and J. A. Hoar. 2000.** Does geometry limit squid growth? *ICES J. Mar. Sci.* **57:** 8–14.

**O'Dor, R. K., and D. M. Webber. 1986.** The constraints on cephalopods: why squid aren't fish. *Can. J. Zool.* **64:** 1591–1605.

**Osse, J. W. M. 1990.** Form changes in fish larvae in relation to changing demands of function. *Neth. J. Zool.* **40:** 362–385.

**Packard, A. 1969.** Jet propulsion and the giant fibre response of *Loligo*. *Nature* **221:** 875–877.

**Preuss, T., Z. N. Lebaric, and W. F. Gilly. 1997.** Post-hatching development of circular mantle muscles in the squid *Loligo opalescens*. *Biol. Bull.* **192:** 375–387.

**Schmidt-Nielsen, K. 1997.** *Animal Physiology. Adaptation and Environment.* 5th ed. Cambridge University Press, Cambridge.

**Segawa, S. 1987.** Life history of the oval squid, *Sepioteuthis lessoniana* in Kominato and adjacent waters central Honshu, Japan. *J. Tokyo Univ. Fish.* **74:** 67–105.

**Svetlichnyy, L. S., and A. S. Svetlichnyy. 1986.** Measurement of the locomotion characteristics of copepods attached to a dynamometer sensor. *Oceanology* **26:** 646–647.

**Thompson, J. T., and W. M. Kier. 2001a.** Ontogenetic changes in mantle kinematics during escape-jet locomotion in the oval squid, *Sepioteuthis lessoniana* Lesson, 1830. *Biol. Bull.* **201:** 154–166.

**Thompson, J. T., and W. M. Kier. 2001b.** Ontogenetic changes in fibrous connective tissue organization in the oval squid, *Sepioteuthis lessoniana* Lesson, 1830. *Biol. Bull.* **201:** 136–153.

**Vogel, S. 1994.** *Life in Moving Fluids.* 2nd ed. Princeton University Press, Princeton.

**Webb, P. W., and D. Weihs. 1986.** Functional locomotor morphology of early life history stages of fishes. *Trans. Am. Fish. Soc.* **115:** 115–127.

**Weihs, D. 1974.** Energetic advantages of burst swimming of fish. *J. Theor. Biol.* **48:** 215–229.

**Williams, T. A. 1994.** A model of rowing propulsion and the ontogeny of locomotion in *Artemia* larvae. *Biol. Bull.* **187:** 164–173.

**Zar, J. H. 1996.** *Biostatistical Analysis.* Prentice Hall, Upper Saddle River, NJ.

**Zuev, G. V. 1966.** Characteristic features of the structure of cephalopod molluscs associated with controlled movements. Ekologo-Morfologicheskie Issledovaniya Nektonnykh Zhivotnykh. Kiev, Special Publication. (Canadian Fisheries and Marine Services Translation series 1011, 1968).

---

## Appendix

Description of the two force transducers used to measure the thrust produced by tethered squid.

### *Transducer 1*

Force transducer 1 consisted of two brass blade elements (152 mm long, 6.4 mm wide, 0.25 mm thick) arranged at a right angle (*i.e.*, a cross) and attached to a 150-mm by 150-mm by 25-mm aluminum base (Fig. 1A). A hole drilled in the center of each blade element permitted insertion of a 10-mm length of 3.4-mm diameter threaded brass rod. The center of the threaded rod was drilled to accept the stainless steel post of the tether, which was glued in place using waterproof contact cement. The threaded rod was inserted through each blade element and held firmly by a brass nut on either side of the blade elements (Fig. 1A). The nuts also held the blade elements together tightly.

The tip of each blade element was clamped to the aluminum base. Slots were milled in the base to prevent the blade elements from contacting the base when deformed.

Four thin foil strain gauges (model CEA-13-250UW-350, The Measurement Group, Wendell, NC) were attached near the end of each blade element (*i.e.*, where the blade element was clamped to the aluminum base) and wired as a full Wheatstone bridge (see Biewener and Full, 1992). The strain gauges were waterproofed with several coats of silicone aquarium sealant.

The perpendicular arrangement of the blade elements permitted the magnitude of the thrust vector to be calculated using the Pythagorean theorem

$$F_T = \sqrt{(B_1{}^2 + B_2{}^2)}\,, \qquad \text{(Eq. 5)}$$

where $F_T$ is the magnitude of the thrust vector, $B_1$ is the output of bridge 1, and $B_2$ is the output of bridge 2.

### *Transducer 2*

Force transducer 2 consisted of a single aluminum blade element (57 mm long by 18 mm wide by 1.6 mm thick) screwed securely to a length of 26-mm by 26-mm steel box beam (Fig. 1B). The box beam was bolted to a steel frame positioned over the experimental arena.

A small aluminum block, which had been drilled to accept the stainless steel post of the tether, was screwed to the distal end of the blade element (Fig. 1B). A setscrew in the block held the post in place. The post extended 40 mm beyond the end of the blade element.

Two semiconductor strain gauges (model ESU-025-1000, Entran Sensors, Fairfield, NJ) were attached near the base of the blade element (Fig. 1B) and wired as a half Wheatstone bridge.

Reference: *Biol. Bull.* **203:** 27–41. (August 2002)

# Anatomical Correlates of Venom Production in *Conus californicus*

JENNIFER MARSHALL[1], WAYNE P. KELLEY[2], STANISLAV S. RUBAKHIN[2], JON-PAUL BINGHAM[3], JONATHAN V. SWEEDLER[2], AND WILLIAM F. GILLY[1,*]

[1]*Hopkins Marine Station and Department of Biological Sciences of Stanford University, Pacific Grove, California 93950;* [2]*Department of Chemistry and the Beckman Institute, University of Illinois, Urbana, Illinois 61801; and* [3]*Department of Pharmacology, Yale University School of Medicine, New Haven, Connecticut 06520*

**Abstract.** Like all members of the genus, *Conus californicus* has a specialized venom apparatus, including a modified radular tooth, with which it injects paralyzing venom into its prey. In this paper the venom duct and its connection to the pharynx, along with the radular sac and teeth, were examined using light and transmission electron microscopy. The general anatomy of the venom apparatus resembles that in other members of the genus, but several features are described that have not been previously reported for other species. The proximal (posterior) quarter of the venom duct is composed of a complex epithelium that may be specialized for active transport rather than secretion. The distal portion of the duct is composed of a different type of epithelium, suggestive of holocrine secretion, and the cells display prominent intracellular granules of at least two types. Similar granules fill the lumen of the duct. The passageway between the lumen of the venom duct and pharynx is a flattened branching channel that narrows to a width of 10 $\mu$m and is lined by a unique cell type of unknown function. Granular material similar to that in the venom duct was also found in the lumen of individual teeth within the radular sac. Mass spectrometry (MALDI-TOF) demonstrated the presence of putative peptides in material derived from the tooth lumen, and all of the more prominent species were also evident in the anterior venom duct. Radular teeth thus appear to be loaded with peptide toxins while they are still in the radular sac.

## Introduction

Predatory marine snails of the genus *Conus* have long been of interest because their highly evolved hunting strategies employ peptide toxins that paralyze prey (Bergh, 1895; Shaw, 1914; Kohn, 1956; reviewed by Halstead, 1988). The gastropod radula is typically equipped with rows of chitinous teeth that scrape or bite during feeding. In cone snails, however, the radular teeth are unattached and resemble barbed hypodermic needles that are used to inject venom into the prey. When resting, the snail holds its proboscis retracted inside the rostrum. When prey is sensed by waterborne chemical signals (Spengler and Kohn, 1995), searching behavior commences with the proboscis extended and a tooth held near the tip by a sphincter (Kohn, 1956; Greene and Kohn, 1989). When prey is contacted, the tooth is forcibly inserted into the victim, and venom is injected.

Each of the more than 500 *Conus* species (Röckel *et al.*, 1995; Kohn, 1998) is thought to contain a large number of distinct peptide toxins in the venom duct (Olivera, 1997; McIntosh *et al.*, 1999), and contemporary *Conus* research has primarily focused on purifying and characterizing these toxins. *Conus* toxins are typically 10–30 amino acids in length and belong to one of several families defined by highly conserved cysteine frameworks and internal disulfide linkages (Olivera *et al.*, 1995; McIntosh *et al.*, 1999; Duda and Palumbi, 1999; Conticello *et al.*, 2001). Most of these peptides target voltage- and ligand-gated ion channels.

Production and delivery of *Conus* venom involves three general steps: (1) synthesis, processing, and packaging of peptide toxins; (2) generation and storage of radular teeth and transfer of a tooth to the tip of the proboscis; and (3) the final insertion of the tooth and ejection of venom. These

Received 26 October 2001; accepted 25 June 2002.

[*] To whom correspondence should be addressed. E-mail: lignje@stanford.edu

*Abbreviations:* MALDI-TOF, matrix-assisted laser desorption-ionization time of flight mass spectrometry; *m/z*, mass-to-charge ratio.

processes are carried out within an anatomically complex venom apparatus in conjunction with the anterior regions of the digestive tract. These features are relatively invariable between *Conus* species (see Halstead, 1988), and a schematic venom apparatus is illustrated in Figure 1.

Some events listed above can be assigned to specific anatomical components:

1. Production of venom takes place in a long, convoluted venom duct. The proximal end of the duct is equipped with a muscular bulb. Distally the duct enters the pharynx just anterior to its border with the esophagus. Proximal and distal portions of the duct differ in gross structure and venom content (Endean and Duchemin, 1967; Bingham *et al.*, 1996), but the sites of synthesis, post-translational modification, and presumed packaging of peptides into large "venom granules" (Maguire and Kwan, 1992) remain unclear. Although these granules are undoubtedly associated with toxin production, there is no compelling evidence that they contain active peptides.
2. Teeth are generated in the long arm of the radular sac, and mature teeth are stored in the short arm, the lumen of which enters the pharynx slightly anterior to the venom duct opening (Marsh, 1977). In preparation for use, an individual tooth is transported into the pharynx by an unknown mechanism, where it is probably surrounded by the retracted proboscis and then grasped around the basal spur by a subterminal sphincter (Hermitte, 1946; Greene and Kohn, 1989). At this point, the lumen of the tooth is thought to be empty (Marsh, 1977) and ready to be filled with venom that has moved into the pharynx directly from the venom duct (Kohn *et al.*, 1960). Finally, the proboscis extends with the venom-loaded tooth held at the tip.
3. The muscular bulb is generally thought to take little or no part in the secretion of venom (see Halstead, 1988). Although the bulb has often been hypothesized to provide the force for final venom ejection out of the tooth (see Halstead, 1988; Endean and Duchemin, 1967; Freeman *et al.*, 1974; Olivera, 1997), there is no direct evidence for this idea. It is more likely that the muscular proboscis provides the necessary positive pressure to mediate venom ejection (Songdahl, 1973; Greene and Kohn, 1989; Kohn and Hunter, 2001). The mechanics of this action are unclear, and the function of the muscular bulb remains enigmatic.

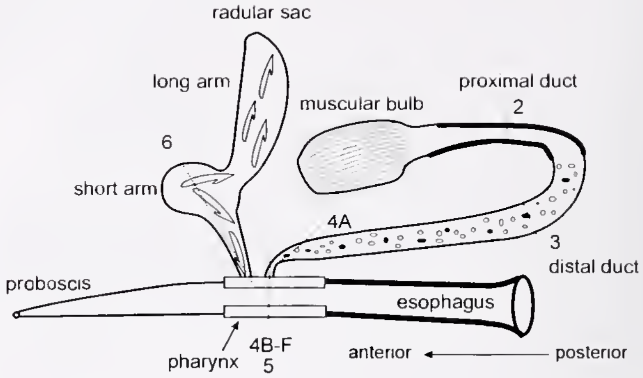

**Figure 1.** Schematic representation of the main parts of a generic *Conus* venom apparatus and the anterior digestive tract. The figure is not to scale. Only a few of the many teeth are indicated in the short and long arms of the radular sac. Numbered dotted lines indicate the approximate position and orientation of the sections described in Figures 2–6.

We have been studying the biology of venom production in *Conus californicus*, a local species. Toxic components exist in the venom, but they have not been studied in detail (Whysner and Saunders, 1963, 1966; Cottrell and Twarog, 1972; Elliot and Kehoe, 1978; Elliot and Raftery, 1979; Bingham *et al.*, 2000). Anatomical studies are also limited (Hinegardner, 1958; Halstead, 1988), and cellular details that might be correlated with biochemical data are lacking.

This report describes some new features of the venom apparatus in *C. californicus* as revealed by conventional light and transmission electron microscopy. First, we have found that the proximal portion of the venom duct has a unique structure and may be specialized for active transport rather than secretion. Second, we have discovered a novel and unusually narrow passageway between the venom duct and the pharynx through which venom must pass prior to ejection. Third, complex, granular material resembling that in the lumen of the venom duct is found packaged inside the lumen of individual teeth while they are still in the radular sac. Furthermore, mass spectrometry demonstrates that presumptive peptides can be identified in material isolated from the venom duct and from the lumen of single radular teeth. Although the sequences of these peptides are unknown, equivalence in their apparent molecular weights suggests that some of the same peptides are present in both locations.

## Materials and Methods

Specimens of *Conus californicus* were obtained from Monterey Bay, California (Sea Life Supply, Sand City, CA), and maintained in the laboratory for as long as several weeks in a flow-through seawater system (13–15°C) or in an aerated, closed system at room temperature (22–24°C). Results obtained from the two sets of animals were equivalent.

### *Light and electron microscopy*

In preparation for light microscopy, two animals were relaxed in seawater containing 2% $MgCl_2$, and the shells were cracked with vise-grips and removed. The complete venom apparatus and anterior digestive tract as depicted in Figure 1 were dissected under seawater. Tissue samples were fixed overnight at 4°C in 2% glutaraldehyde made up in 80% filtered seawater containing 100 m*M* HEPES (pH 7.3) and then dehydrated in a graded ethanol series. Tissues were then cut into smaller pieces (several cubic millimeters) and embedded in Spurs resin. Sections (0.5–2 μm) were cut with an ultramicrotome equipped with a glass knife, stained with 1% methylene blue dissolved in 0.1 N NaOH, and examined with an Olympus BH-2 microscope. The venom duct was examined at several places along its length, and anatomical locations and orientations of all sections figured in this paper are indicated in Figure 1.

For transmission electron microscopy (TEM), tissue was fixed and embedded as described above, except a post-fixation step of 1% $OsO_4$ in seawater for 1 h was added. Sections were cut with a diamond knife, stained with saturated uranyl acetate and lead citrate in 0.1 N NaOH, and viewed on a Phillips CM12 microscope at Stanford University School of Medicine.

Living animals were also relaxed and dissected as described above to reveal the junction between the short arm of the radular sac and the pharynx. An incision was made at the junction and several teeth were carefully removed with a fine forceps. The teeth were rinsed well in seawater and examined using water immersion optics.

### *Matrix-assisted laser desorption-ionization time of flight mass spectrometry (MALDI-TOF)*

A complete venom apparatus was removed as described above, and the distalmost thin segment of venom duct (area 4 in Fig. 1) was ligated with fine surgical silk close to where it enters the pharyngeal wall; this ligation prevents any leakage of venom into the proboscis and potentially into the radular sac. Most of the proboscis and esophagus were removed, and the pharynx was then slit longitudinally and the lumen was washed with seawater. This semi-intact venom duct (with bulb) and radular sac preparation was then shipped in iced seawater to the University of Illinois by overnight carrier.

Individual teeth from the short arm of the radular sac were dissected upon arrival in Illinois and washed well in isotonic NaCl. Single teeth were broken open with forceps and mashed onto a MALDI target into 0.5 μl of matrix solution (10 mg $ml^{-1}$ 2,5-dihydroxybenzoic acid (ICN Pharmaceuticals, Costa Mesa, CA)) in deionized water. Short (~1 mm) segments of the venom duct were also cut from locations corresponding to areas 2, 3, and 4 in Figure 1. Some of the luminal contents of these sections was squeezed into the same volume of matrix solution on additional target spots.

MALDI-TOF MS analysis was carried out as previously described (Sweedler *et al.*, 2000; Li *et al.*, 2000) using a Voyager DE STR (PE Biosystems, Framingham, MA). A pulsed, nitrogen laser (337 nm) served as the desorption/ionization source, and positive-ion mass spectra were obtained with both linear and reflection modes of operation. The former mode has greater sensitivity, whereas the latter is more accurate in establishing mass. Mass-to-charge ratio (*m/z*) calibrations were performed externally with a standard calibration mixture including angiotensin and bovine insulin (Sequazyme, PE Biosystems, Framingham, MA). For data presented in this paper, the *m/z* parameter is equivalent to molecular weight (Bingham *et al.*, 1996). The spectra shown are representative examples from several hundred spectra acquired from several snails.

## Results

### *The proximal venom duct*

Near its junction with the muscular bulb, the proximal (*i.e.*, posterior) venom duct, in an animal of 30–35 mm shell-length, is orange-pink and about 250 μm in diameter. Light microscopy reveals three distinct zones in this region (Fig. 2A): an outermost layer of connective tissue (c), a cellular, epithelial layer (ep), and an inner lumen (l).

Electron microscopy (Fig. 2B) shows that the outer layer is composed mostly of collagen-like fibrils (c), which are themselves layered according to their direction of orientation. Scattered profiles of presumptive muscle cells (m) are embedded in the collagen layer and appear to be associated with certain sublayers. This collagen-rich layer is not covered by a distinct outer cellular layer, although cells that are probably fibroblasts can be found on the outer surface.

The inner surface of this collagenous layer is an amorphous basal lamina (see also Fig. 3B) that covers the cellular layer (ep). Cells in this epithelium contain numerous mitochondria (mt, white pointers) that are concentrated on the basal surface facing the collagen layer. Nuclei also tend to be located here (n in Fig. 2A). The apical surface of the epithelial cells is densely covered with microvilli that protrude into the lumen (mv in Fig. 2B). Boundaries between these interdigitating cells are highly complex in this region, and tight junctions are also present along the apical surface (black arrow).

Much cellular debris (cd) and many mitochondrial fragments (mt) are found in the lumen of the duct (Fig. 2C), and this material probably derives from more distal regions of the duct as described below. Profiles of cilia in small clusters are fairly common (arrow), but it is unclear whether they are part of the debris or whether they emerge from cells in the epithelial layer. A few venom granules (g) are found in the lumen, but they are relatively uncommon in this region of the duct.

### *The distal venom duct*

About one-quarter of the distance to the pharynx, the venom duct enlarges to a diameter of about 375 μm and

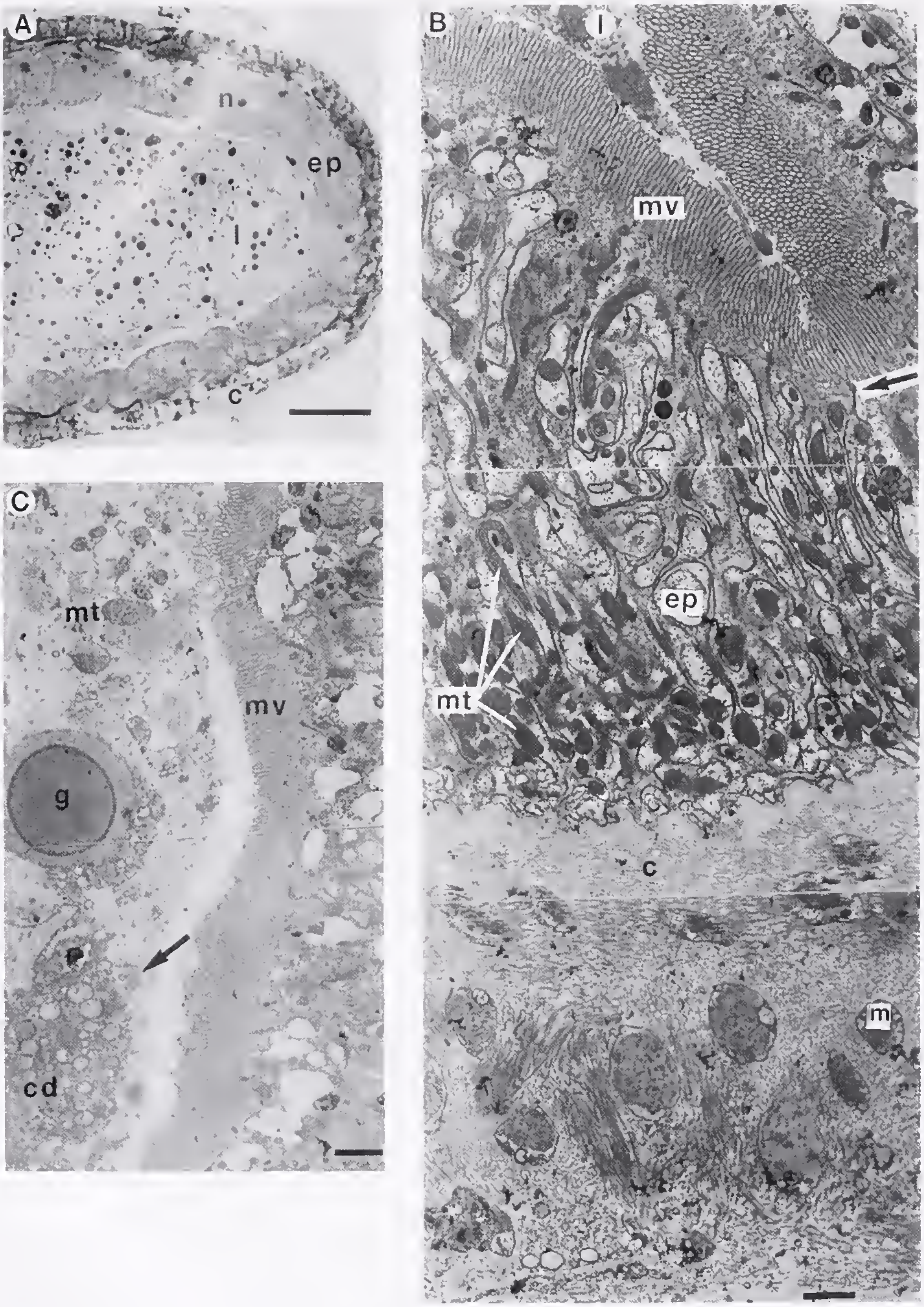

**Figure 2.** Proximal portion of the venom duct. (A) Low-power light micrograph showing overall view of the duct in this region. A collagenous layer (c) covers an epithelium (ep) composed of large cells with prominent nuclei (n). The lumen (l) contains noncellular material. Scale bar is 50 $\mu$m. (B) TEM image of the complete collagenous and epithelial layers. Muscle-cell (m) profiles occur in the collagenous layer; mitochondria (mt) densely pack the basal end of the epithelial cells (ep); and microvilli (mv) cover the apical surfaces. Tight junctions (arrow) exist along this surface. Scale bar is 1 $\mu$m. (C) TEM image of apical edge of the epithelial cells and the lumen. There are large amounts of cellular debris (cd) in the lumen and mitochondrial fragments (mt) as well as cross sections of ordinary "9+2" cilia (5 indicated by arrow) and sparse venom granules (g). Scale bar is 1 $\mu$m.

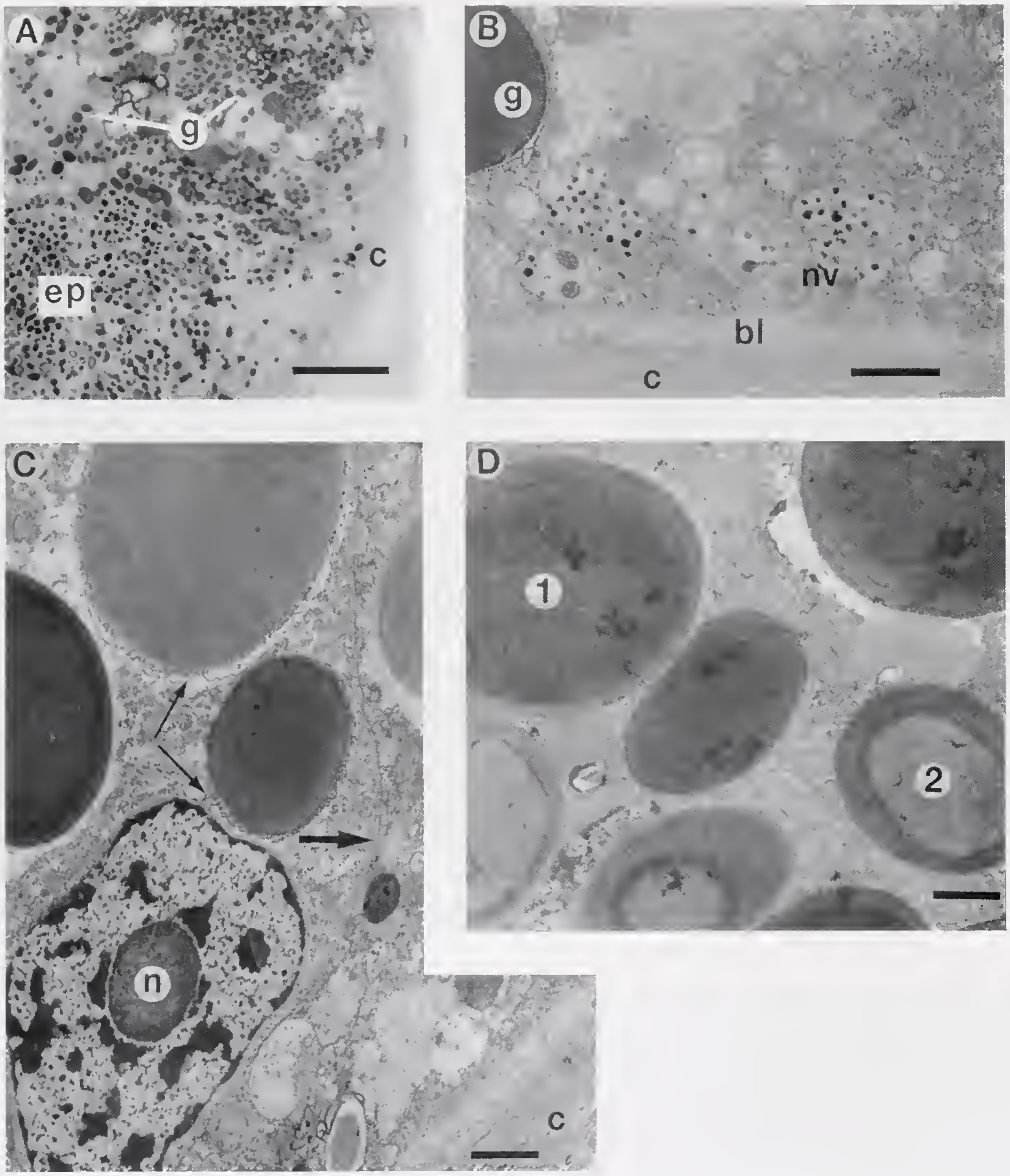

**Figure 3.** Middle region of the distal venom duct. (A) Light micrograph of the collagenous layer (c) and epithelial cells (ep). Venom granules (g) are prominent. Scale bar is 50 μm. (B) TEM image of the basal surface of epithelial cells, basal lamina (bl), and collagen fibrils (c). Profiles of neural processes (nv) containing dense vesicles are apparent. A portion of a venom granule is visible (g). Scale bar is 1 μm. (C) TEM image of a nucleus (n) and intracellular venom granules. Large arrow points to the cell membrane. Thinner arrows point to the membranous coating of venom granules. Scale bar is 1 μm. (D) TEM image of venom granules of two different types (1 and 2). The area of this section is in the central region of the duct near the lumen, where unambiguous distinction between extracellular and intracellular regions is difficult due to the breakdown of cell membranes associated with secretion. Scale bar is 1 μm.

becomes creamy white. Duct morphology also dramatically changes, as evidenced by the light micrograph in Figure 3A. The outer layer is still collagenous (c), but the nature of the epithelium is quite different. Large, vaguely columnar epithelial cells with poorly demarcated luminal and lateral boundaries (ep in Fig. 3A) are present, and these cells are filled with deeply stained (blue) venom granules (g) as large as 5 μm or more in diameter.

Electron microscopy confirms that the mitochondrion-rich cells with apical microvilli as described above are

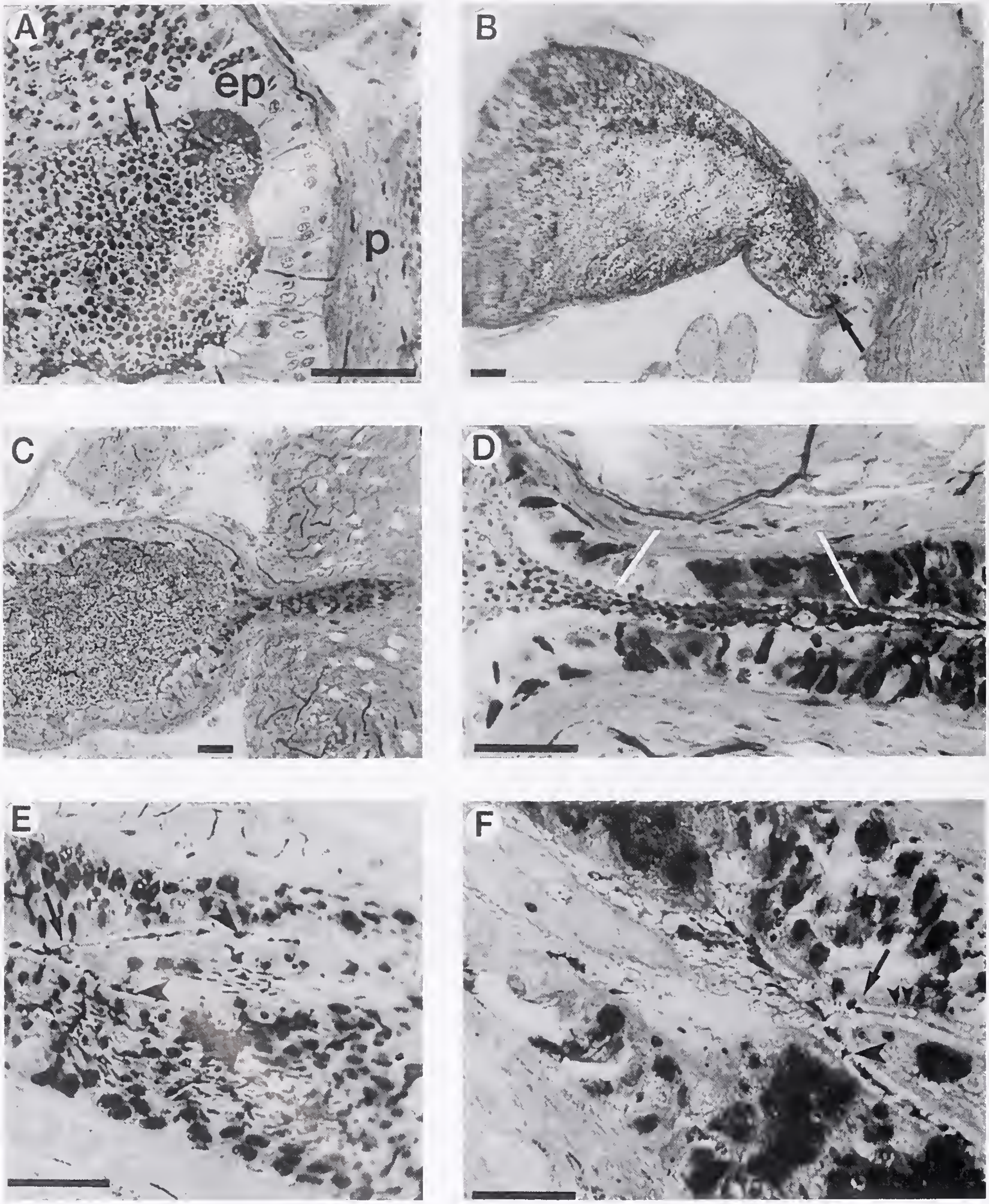

absent from this more distal region. Figure 3B shows the external border of the duct where the basal lamina (bl) separates the cellular and collagenous (c) layers that again run in at least two directions. Immediately beneath the basal lamina (bl, Fig. 3B), cross-sections of presumptive neuronal processes (nv) are sometimes found. Many of these processes are filled with electron-dense vesicles, which are much smaller than the venom granules (g) and are not resolvable by light microscopy.

Epithelial cells just inside the external surface of the duct in this region contain numerous intracellular venom granules. A nucleus (n) and several granules can be seen within the same membrane-limited cellular unit in Figure 3C. Granules in these more peripheral epithelial cells tend to be covered with a membranous coating (small arrows). Closer to the lumen of the duct, cellular boundaries become difficult to define, even by TEM, probably because the cells are breaking down in a holocrine-type secretory process (see Halstead, 1988).

Extracellular granules well within the central duct lumen in this region are substantially more abundant than in the proximal region described above. Analysis of 50 × 50 $\mu m^2$ areas in light micrographs at the magnification of Figure 3A yielded granule counts of 58.3 ± 48.3 (distal) *versus* 13 ± 4 (proximal; mean ± SD, $n = 3$ in both cases). Density in the distal lumen was quite variable, and the area in the upper left of Figure 3A, which was included in the analysis, is at the low end of the range (25–84).

Within this deeper region of the distal venom duct, individual venom granules display distinct ultrastructure and can be separated into at least two classes (Fig. 3D). The first (1 in Fig. 3D) has an electron-dense core surrounded by a more intensely stained ring, which in turn is covered by a diffuse coating of lightly stained material. There is no sign of the membranous coating. The second class (2) has a core that stains much more lightly, but displays a similar coating of the ring and external diffuse layer. The relationship of the two granule classes to each other or to venom production in general is not obvious from the anatomy, but presumably granules without a membranous coat derive from the clearly intracellular granules described above.

Profiles of cilia are also occasionally found in the distal lumen. In living material examined with water-immersion optics, clumps of motile cilia can be seen to create microscopic vortices but not directional fluid flow. Neither the origin nor functional significance of these processes is known.

### *The anteriormost venom duct and the connection to the pharynx*

In general, the above description of the distal duct region applies up to its anterior end, just before it joins the pharynx, where the duct diameter is about 475 $\mu m$. Figure 4A shows an oblique, but generally longitudinal, section through this region. Some of the columnar-type epithelial cells contain intracellular granules similar to those found in the lumen of the duct (arrows), but the relative cellular *versus* luminal distribution of granules is opposite to that in Figure 3A. Here the lumen of the duct is densely packed with granules (84.7 ± 2.1 per 2500 $\mu m^{-2}$; mean ± SD, $n = 3$), and intracellular granules are sparse. Epithelial cells adjacent to the pharynx (p) appear to contain no granules at all.

As the venom duct approaches the pharynx, it narrows rapidly to a diameter of about 125 $\mu m$ (Fig. 4B). At the point where the duct begins to penetrate the pharyngeal musculature, most epithelial cells resemble those cells lacking granules as described in conjunction with Figure 4A. In addition, a distinct type of smaller epithelial cell is interspersed in this region. These cells are filled with extremely small particles that are intensely stained purple by methylene blue (Fig. 4B, arrow). They are very evident in Figure 4C–F. These metachromatic "purple cells" become more numerous as the duct proceeds across the pharyngeal wall and narrows to a luminal width of about 20 $\mu m$ (Fig. 4D). Venom granules in the lumen here (between white pointers in Fig. 4D) resemble those in the distal venom duct. Light- and dark-blue granules are evident in light microscopy, and they presumably correspond to the two ultrastructural classes described above.

At a distance of about 250 $\mu m$ into the pharyngeal wall, the narrow venom duct passageway branches into two smaller channels, each about 10 $\mu m$ wide (arrows in Fig. 4E, F). Just before the branch point, blue-stained granules are largely replaced by smaller, clear granules that continue into the finer channels. These clear granules appear to line the channel, with a few larger, stained profiles persisting in the core (single arrowheads in Fig. 4E, F). The latter objects lack the smooth profiles of venom granules, and they are

**Figure 4.** Anteriormost zone of distal venom duct, and the penetration of the duct into the pharyngeal wall (light micrographs). (A) Oblique section through the duct in the region of the pharynx. Epithelial cells (ep) of the duct display intracellular venom granules (upward arrow), and similar granules (downward arrow) fill the lumen as well. Epithelial cells facing the pharynx (p) do not contain granules, and prominent nuclei are evident. Scale bar is 50 $\mu m$. (B–F) Successive longitudinal sections through the venom duct as it crosses the pharyngeal wall. Scale bars are 50 $\mu m$ throughout. (B) The duct as it barely penetrates the proboscis wall. At this site small epithelial cells that intensely stain purple first appear (arrow). (C) The section grazes through the metachromatic purple cells lining the venom duct as it penetrates more deeply into the pharynx. (D) Magnified view of the duct entering the pharyngeal muscle with the lumen narrowing down. Purple cells line both sides of the duct in this region. The duct becomes densely packed with blue-staining venom granules as it narrows (between white pointers). (E, F) Two views of the venom duct branching into two finer tracts inside the pharyngeal wall (arrows). Smooth, blue-staining granules (large arrowheads) become sparse after the branching point, and small, clear vesicles (small arrowheads) become more prominent and appear to line the fine channels. See text for additional details.

stained more intensely purple like the metachromatic cells. These features suggest that the stained granular material in the core of these fine channels is distinct from either of the two types of venom granules described above, but any relationship to the metachromatic cells is uncertain. In some cases, only clear granules are evident, although some amorphous material, which appears to be matted cilia, persists in the channel core (double arrowhead in Fig. 4F).

After the duct's bifurcation, each of the branches continues for about another 500 $\mu$m before opening into the lumen of the pharynx. Two such channels are visible in Figure 5A. The proximal ends are marked by ovals (the branch point is not visible in Fig. 5A), and the distal ends (stars) open into a common space connected to the pharyngeal lumen (l). Purple cells continue to line the channel epithelium to a point about halfway from the bifurcation to the distal opening. Beyond this point (bold arrows), the clear granules in the lumen of the channels become infrequent, and the passageways, which here are ciliated, grow a bit in width. The cuboidal epithelium forming the channels in this region is contiguous with the highly folded, ciliated epithelium of the pharynx. Thus, two pharyngeal folds extend particularly deeply and merge with the fine venom duct channels. It is at this junction that the novel purple cells lining the final venom duct passageway give way to the pharyngeal epithelium. A schematic summary of the nature of the venom duct as it crosses the pharyngeal wall is given in Figure 5B.

### *The radular sac*

Teeth are manufactured in the long arm of the radular sac, but this complex region was not studied in the present work. The short arm of the radula sac is thought to contain only mature teeth that are ready for use (Marsh, 1977) and is bounded by an outer epithelial layer about 7.5 $\mu$m thick (oe in Fig. 6A), a narrow layer of connective tissue, and an inner epithelial (ie) layer composed of cells about 25 $\mu$m long. The inner epithelium is complex, highly folded, and thick (up to 125 $\mu$m in Fig. 6A).

Many radular teeth in the short arm are in close contact with this inner cellular layer. Basal spurs are easily recognized (*), and a majority of the teeth are oriented with their points towards the pharynx (Fig. 6E), but other orientations can be found (Fig. 6A,C). The space around the teeth contains a mixture of granular, cellular, and unidentifiable material, and similar materials are evident in the lumen of individual teeth (Fig. 6B). In some cases, clusters of darkly stained granules are present within the inner epithelium, and similar granules can be found inside teeth (Fig. 6D, arrows).

At the site where the teeth enter the channel passing into the pharynx, they all point anteriorly (Fig. 6E) and are enveloped by muscle of the pharyngeal wall (m). At the connection between the radular sac and the pharynx, the two structures are in intimate contact, and folds of the pharyngeal epithelium wrap around the sac (p in Fig. 6E; arrow in Fig. 6F). The packing of the basal spurs evident in Fig. 6E suggests that the teeth enter this connecting channel in a tight queue. The lumen of every tooth in this region is densely packed with a rich mixture of granules and other noncellular material (Fig. 6F).

Teeth taken from this final portion of unfixed radular sacs were also studied. Examination of such teeth under water-immersion optics confirms the presence of a large amount of granular material in the lumen (Fig. 7). This granular content does not leak out to any visually noticeable extent during several hours of observation, although FITC-dextran (fluorescein isothiocyanate-dextran, 19,000 mw) can enter the lumen and after an exchange of bathing solution can be visualized by fluorescence microscopy.

### *MALDI-TOF analysis of individual teeth and venom duct sections*

Individual radular teeth taken from within the short arm of the radular sac, and samples of the venom duct from regions corresponding to anatomical sections 2–4 (Fig. 1), were also analyzed by mass spectrometry. Mass spectra obtained with the linear mode (positive polarity) of MALDI-TOF are illustrated in Figure 8. Reflectron-mode results were comparable (not illustrated). Although major peaks in these spectra undoubtedly represent peptide toxins, neither the amino acid composition nor the toxicity of any of these species is known. However, several general trends are evident in the distribution of peaks of specific molecular weights in different samples:

1. The most prominent peaks are not the same peptide species in different regions of the venom duct (Fig. 8A–C). The 3218 *m/z* peak is really the only one that constitutes a major presence in all three duct samples, although peaks at 2996 and 4043 *m/z* are also detectable in all samples. Most of the prominent species in the proximal duct (2275, 3370, 3460, 5088, 5285 *m/z*) are essentially absent in the distal duct samples. Methods employed in this study yield a mass accuracy for direct biological samples of typically 0.05%, and the several dalton differences between some of the peaks for the different samples shown in Figure 8 are thus insignificant.
2. The mid-distal (Fig. 8B) and anteriormost (Fig. 8C) duct samples are quite similar to one another. However, relative to the 3218 *m/z* peak, the anteriormost material appears to contain much less of the 2352 and 2525 *m/z* species and considerably more of the 4781 *m/z* peak. Many previously identified *Conus* peptides fall into this *m/z* range (Bingham *et al.*, 1996). However, due to the different composition of these sam-

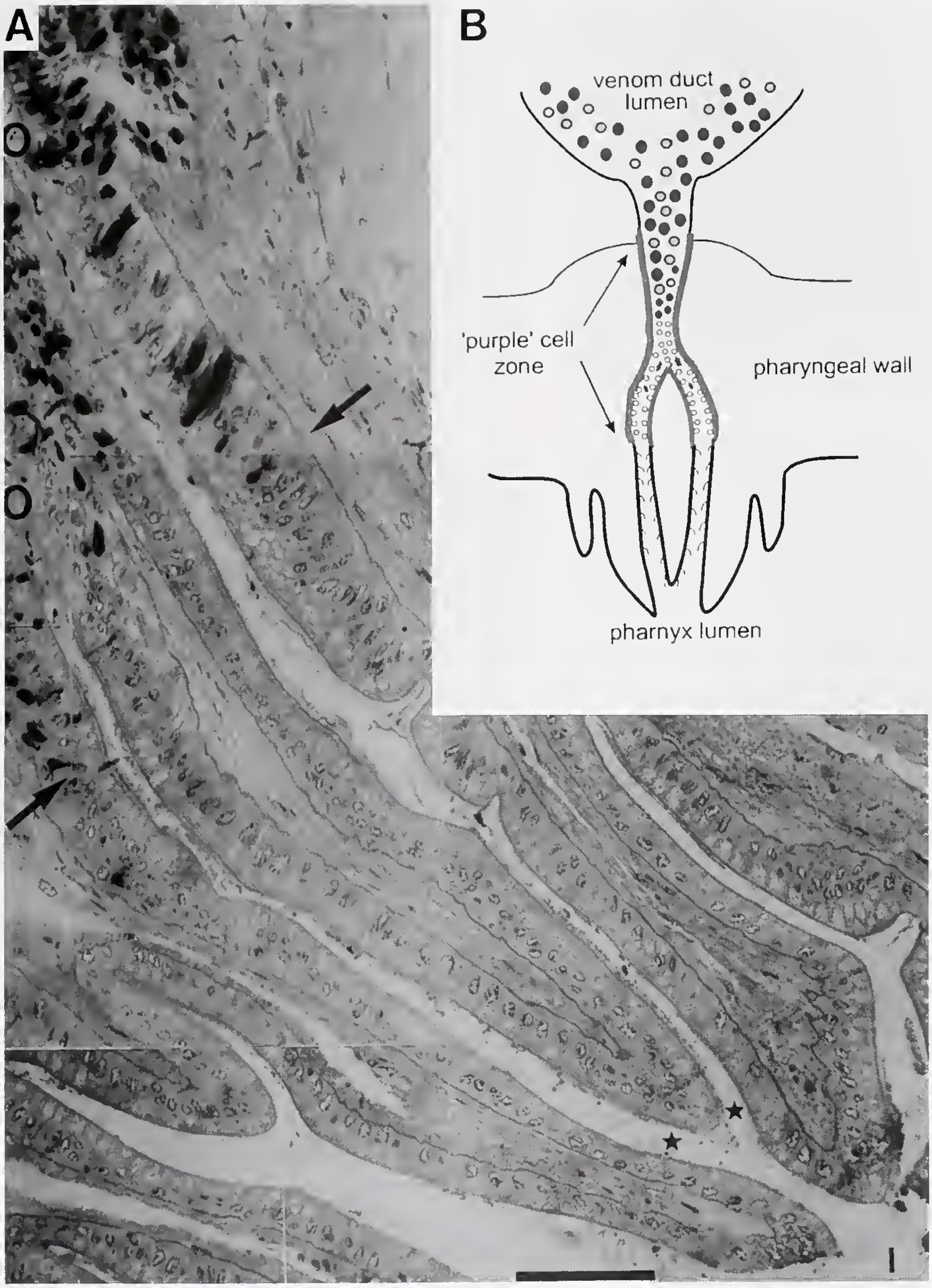

**Figure 5.** Longitudinal section through the fine venom duct channels as they cross the medial half of the pharyngeal wall and enter the lumen of the pharynx. (A) Ovals at the left edge of the image indicate the proximal ends of the two fine channels discussed in the text; the more proximal bifurcation where the channels are formed is not visible in this section. The two channels merge distally (*) to form a common passage that opens into the lumen of the pharynx (l). The deeply infolded pharyngeal epithelium merges proximately with the venom duct epithelium, which contains purple cells (bold arrows). Scale bar is 50 $\mu$m. (B) Schematic interpretation of the micrographs in Figures 4 and 5. See text for details. Diagram is not to scale.

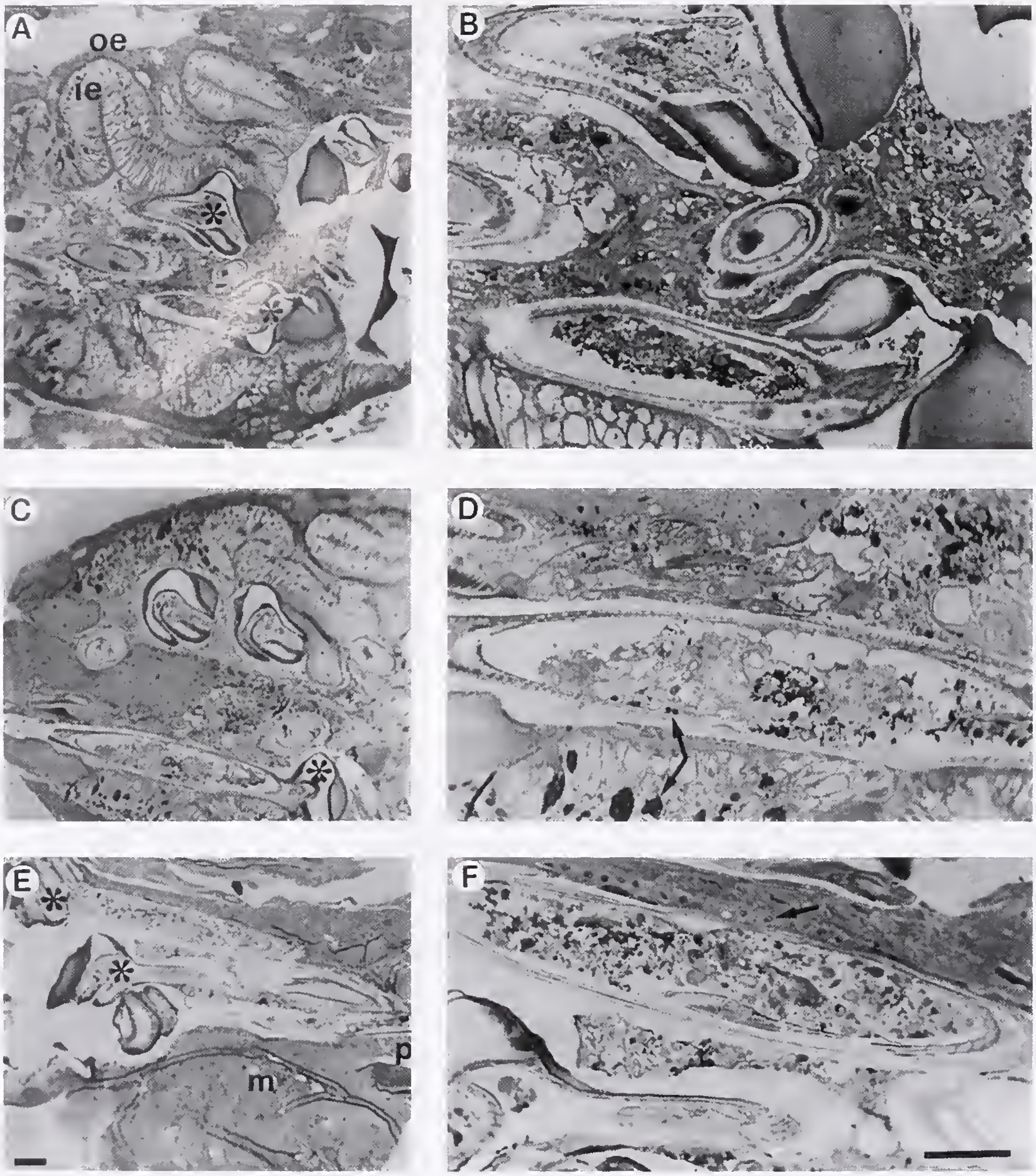

**Figure 6.** Short arm of the radular sac and teeth within it. Three views of teeth are shown. Each panel on the right is a magnified image of that on the left. The pharynx would be on the right side of all panels. Scale bars in E and F are 50 $\mu$m and also apply to A, C and B, D, respectively. (A, B) Comparison of radular sac content with tooth content. The basal ends (*) of two teeth are visible. Granular materials inside and outside the teeth are similar in appearance. (C, D) Dense granules (stained blue) occur in clusters within the inner epithelium of the radular sac, and similar granules are evident in the lumen of a tooth (arrows). (E, F) Three teeth in the passage through the muscle (m) of the pharyngeal wall. Pharyngeal epithelium (p [in E] and arrow [in F]) appears to line this passageway. The teeth point towards the pharynx and are all filled with granular material.

ples, the extraction and ionization efficiencies may not be identical, and this makes more quantitative comparisons of even the same peptide peak between sample types difficult.

3. The tooth sample (Fig. 8D) reveals a spectrum similar to that of the distal venom duct samples. Thus, the three most prominent peaks (2996, 3218, and 4046 *m/z*) are also present in both duct samples. However, the 4781 *m/z* peak is greatly diminished in the tooth, although it may be obscured by sodium adducts of these compounds. Although procedural differences complicate quantitative comparison of intensities between tooth and duct samples, the *m/z* values are directly comparable. Thus, these data strongly suggest that the tooth lumen contains some, but perhaps not all, of the peptides found in the venom duct.

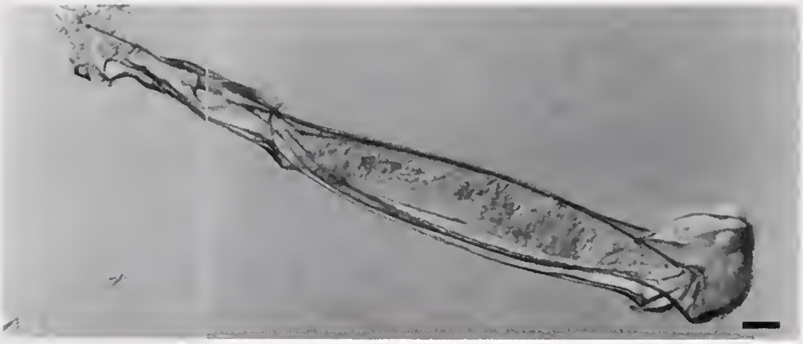

**Figure 7.** Non-fixed tooth dissected from the short arm of the radular sac at the site closest to the pharynx (*i.e.*, as in Fig. 6E, F) and examined with water-immersion optics. Granular material in the lumen is clearly visible. Connective tissue at the tip of the tooth was not always present. Scale bar is 50 $\mu$m.

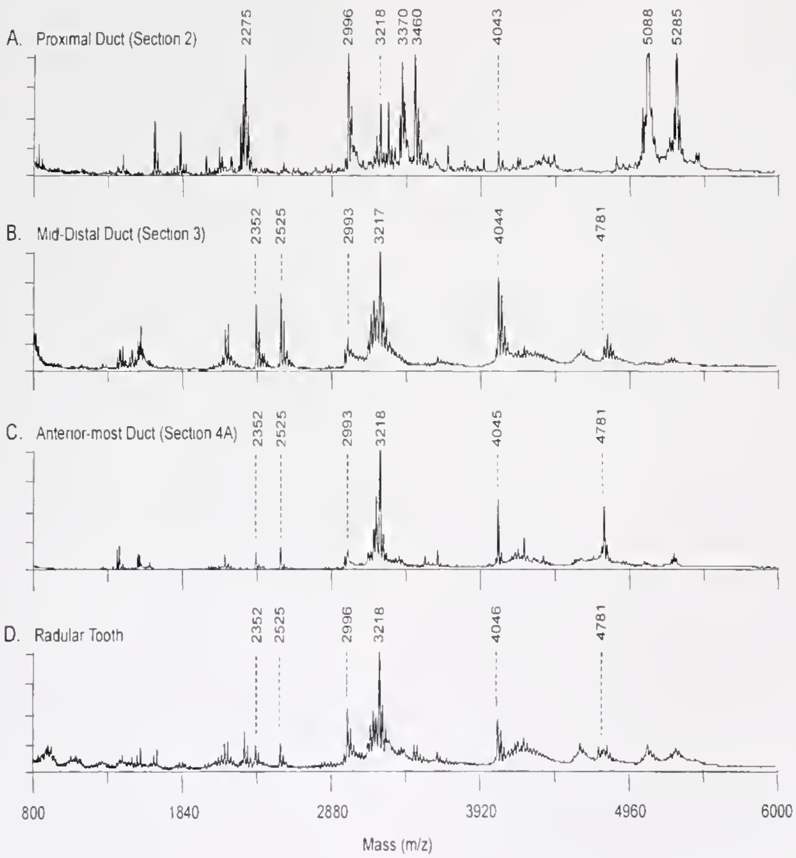

**Figure 8.** Representative mass spectra (MALDI-TOF) for selected regions of the venom duct and for a single tooth from the short arm of the radular sac. (A) Proximal venom duct (corresponding to section 2 in Fig. 1). (B) Mid-distal venom duct (section 3 in Fig. 1). (C) Anteriormost venom duct (section 4A in Fig. 1). (D) Luminal contents of tooth. Presumptive peptide peaks from the tooth are a subset of those contained in venom duct. See text for additional details. Comparable spectra were obtained from other radular teeth from the same snail (not illustrated).

## Discussion

As described in this paper, the general anatomy of the venom apparatus of *Conus californicus* is similar to that in other *Conus* species. This is noteworthy, because *C. californicus* is an atypical member of the genus. The vast majority of tropical species, including all of those previously studied anatomically, are highly specific for certain prey types (Kohn, 1956, 1966; Nybakken, 1970, 1990). However, *C. californicus*, a temperate species, is a generalized feeder (Kohn, 1966) with unusual radular teeth (Kohn *et al.*, 1999) and a variety of feeding strategies (Saunders and Wolfson, 1961).

Along with the general anatomical similarities, we have identified several features in *C. californicus* that have not been described in other species. Whether these features are characteristic of other *Conus* species remains to be established:

1. The proximal venom duct is composed of a well-organized epithelium that is highly specialized, and the lumen contains a great deal of cellular debris and few venom granules.
2. The distal venom duct is composed of a poorly organized epithelium. The lumen contains both cellular debris and many venom granules.
3. The connection between the venom duct and the pharynx is a complex, branching channel that is extremely narrow for most of the distance across the pharyngeal wall. A unique type of epithelial cell is found only in this region.
4. Teeth within the radular sac contain luminal granular material, and mass spectrometry reveals putative peptides in the tooth lumen that are also found in the venom duct.

### *The proximal venom duct*

Previous studies have indicated that material extracted from the proximal portion of the *Conus* venom duct has different peptides (Bingham *et al.*, 1996), venom granules, and pharmacological properties (Endean and Duchemin, 1967) than that extracted from the distal duct. However, the role of this region in venom production remains vague, and no anatomical specialization suggestive of a secretory function has been reported.

TEM images described in this paper reveal that the proximal duct is structurally unique. The high concentration of mitochondria found in the basal region of the epithelial cells must be associated with a high level of energy production, and microvilli greatly increase the apical surface area. Although both features might be associated with secretion, there are no other structural aspects of these cells that support this idea.

In contrast, the above structural features suggest that this tissue mediates active transport. In particular, the epithelium of the proximal venom duct is strikingly similar to the proximal tubule of the mammalian kidney. The latter epithelium absorbs glucose and amino acids along with sodium through apical microvilli and actively transports sodium into the bloodstream across the basal surface with energy provided by numerous mitochondria. Although the nature of the postulated transport process in the proximal venom duct is unknown, it is possible that this epithelium functions in a similar manner to take up ions and small organic molecules (*e.g.*, amino acids, fatty acids) from the duct lumen as part of a recycling mechanism. An attractive source for these molecular substrates is the prominent cellular debris in the lumen.

### *The distal venom duct*

Few venom granules or obvious precursor materials exist in the lumen of the proximal duct, and this suggests that venom granules are manufactured elsewhere, presumably in more anterior duct regions. Numerous venom granules characterize the entire distal venom duct, and they are found both within epithelial cells and in the lumen. Over the length of the distal duct, the relative abundance of granules changes from primarily intracellular proximally to extracellular distally. Cellular debris is also abundant in the lumen of the initial segment of the distal duct (*i.e.*, the more posterior region).

These features strongly suggest that venom granules originate in the distal venom duct. The epithelial cells of this region probably express the genes encoding specific peptides, and granules appear to be assembled in the same cells. The disorganized nature of this epithelium, the poorly defined cell membranes, and the cellular debris in the lumen are all consistent with holocrine secretion, as suggested by previous authors (Halstead, 1988; see also dos Santos *et al.*, 2000). Thus, the abundant cellular debris in the lumen of the proximal duct probably derives from this distal secretory region.

Our analysis of *C. californicus* contrasts somewhat with work on *C. magus* by Endean and Duchemin (1967) in which "immature" venom granules were identified within the distal duct and extremely large "mature" granules (up to 20 $\mu$m long and 5 $\mu$m wide) were found in the proximal duct. On the basis of the presumed developmental progression, those authors suggested that granules did not originate in the posterior duct. Although we agree with that conclusion, we find few granules of any sort in the proximal duct and no extremely large granules anywhere in *C. californicus*. Reasons for these differences are not clear, and subcellular anatomical studies on other species are inadequate to permit a meaningful comparative analysis.

### *The connection between the venom duct and proboscis*

An important contribution of this paper is the description of the passageway taken by the venom duct into the pharynx (see Fig. 5C). Two features of this region are likely to be important to the manufacture and delivery of venom.

First, the venom duct narrows to channels only 10 $\mu$m or less in width as they cross the pharyngeal wall. This appearance can last through 100 $\mu$m of serial sections cut parallel to the long axis of the passage. This suggests that the passage is not a cylindrical duct, but rather a flat channel that is much larger in one dimension than the other. The course of these channels becomes somewhat convoluted after the bifurcation, making it impossible to capture the entire length across the pharynx in a single section. Thus, the number of such channels is uncertain, but there are at least two. These channels merge once again upon reaching the lumen of the pharynx, and presumably this is where venom enters the pharynx *in vivo* (* in Fig. 5A).

The small diameter and considerable length of the fine connecting channels suggest that venom ejection is not likely to involve high flow rates or large volumes. Possibly the cilia lining the distal portions of the fine channels are involved in transport of venom into the pharynx (see also below). A very narrow opening into the pharynx and an associated ciliated tuft were also described in *C. magus* (Endean and Duchemin, 1967), but the passage within the pharyngeal wall was not elaborated upon.

The second important feature is the unique type of epithelial cell that surrounds the fine duct channels over their course through the pharyngeal wall. These metachromatic cells, which we call purple cells, appear in the wall of the duct just before it enters the pharynx, and they line the passageway to the point at which this epithelium meets the infolded pharyngeal epithelium (see Fig. 5B). The specialized nature and localization of the purple cells suggest that they play a critical role in the production or delivery of venom. It is possible that these cells are secretory and contribute a specific component to the final venom for ejection. Such components could be peptides not found elsewhere in the venom duct (Bingham *et al.*, 1996), enzymes such as phospholipases (McIntosh *et al.*, 1995), or simply mucus.

Alternatively, the purple cells could play an active role in "simplifying" venom from the duct in preparation of the final material to be injected into a victim. Venom "milked" from living *Conus* of several species contains a much simpler complement of peptidic toxins than that found in crude venom isolated from the duct (Hopkins *et al.*, 1995; Bingham *et al.*, 1996). Our anatomical data suggest that some kind of granule breakdown or sorting process may occur in the fine channels of the venom duct, because at the final branching point, large blue granules are replaced by smaller, clear ones (Fig. 4D–F). Purple cells might selectively take up materials or release specific products that act to break down or modify the granules. In turn, this action could lead to simplification of the peptide complement of the final venom. The purple-cell zone may well represent the site of this process, but the underlying biochemical mechanisms remain to be elucidated.

### *The radular sac and teeth*

As demonstrated in this paper, radular teeth of *C. californicus* are filled with a rich assortment of granules and other material. This is true for teeth well within the short arm of the radular sac as well as those that are ready to be passed to the proboscis. Examination of non-fixed teeth confirms the presence of granular material. Morphological similarities with material in the lumen of the venom duct make it plausible that peptide toxins exist in both places. This idea is directly supported by mass spectrometry analysis. Thus, *C. californicus* teeth in the radular sac appear to be "pre-loaded" with peptidic components of venom before being passed to the proboscis for use in hunting. This hypothesis obviously contrasts with the ideas discussed in the Introduction.

### *A summary model for venom manufacture and delivery in* Conus californicus

Profound ultrastructural differences between the proximal and distal portions of the venom duct suggest major functional differences for these regions. We propose that peptide toxins are synthesized and assembled into venom granules within the epithelial cells of the distal venom duct, and that the contents of these cells are discharged into the lumen of the duct, probably by holocrine secretion. Cellular debris resulting from this process would be recycled through an uptake pathway in the proximal venom duct. If so, the muscular bulb may play some role in the reuptake process.

Venom granules are extremely abundant in the lumen of the anteriormost region of the distal venom duct. However, they are prevented from free passage into the pharynx by the network of specialized narrow channels that connects the duct and the pharynx. Slow and limited transport of venom probably occurs across these channels, and some material may be directed into the radular sac, where teeth can be loaded with at least some venom components. This postulated transport need not involve a complex mechanism, and a specialized ciliary tract in a typhlosole-like structure could easily move the requisite material along the highly folded pharyngeal epithelium and into the radular sac.

During the slow passage of venom through the fine duct channels in the purple-cell zone, the granule content and peptide complement of the crude venom could be simplified as hypothesized above. This simplification would appear to be a requirement for *in vivo* preparation of the final venom for injection. This important feature is difficult to explain if large volumes of material from the anterior venom duct are quickly passed into the pharynx.

Finally, our model is compatible with the possibility that venom injection involves more material than could be contained in the lumen of a single tooth. We are unaware of quantitative data demanding this capability for any *Conus* species, but it seems likely to be true. Neuronal control over the richly innervated pharyngeal musculature might permit sufficient dilation of the fine duct channels to move a bit of extra venom into the pharynx once the pre-loaded tooth was passed from the radular sac. This bolus of venom could be carried along at the base of the tooth to the tip of the proboscis for final ejection. In this case, if the extra venom were limited to the material of unique granular content contained in the narrow channels, it could still retain a simplified peptide composition.

## Acknowledgments

We are grateful to Chris Patton of Hopkins Marine Station for assistance with TEM sectioning, other microscopic techniques, and photographic work. We thank Dr. Joseph Schulz for critically evaluating the manuscript, and Drs. Barbara Block, Simon Hathaway, and William C. Pitts for helpful suggestions. This work was partially supported by a Stanford University Undergraduate Research Opportunity award sponsored by the Howard Hughes Medical Institute to J.M., by NIH grants NS-17510 (W.F.G.) and NS-31609 (J.V.S.), and by NSF grant IBN-0131788 (W.F.G.).

## Literature Cited

**Bergh, R. 1895.** Beiträge zur Kenntniss der Coniden. *Nova Acta Leopold.* **65**(2): 69–214.

**Bingham, J.-P., A. Jones, R. J. Lewis, P. R. Andrew, and P. F. Alewood. 1996.** *Conus* venom peptides (conopeptides): inter-species, intra-species and within individual variation revealed by ionspray mass spectrometry. Pp. 13–27 in *Biomedical Aspects of Marine Pharmacology*, E. Lazarovici, M.E. Spira, and E. Zlotkin, eds. Alaken, Fort Collins, CO.

**Bingham, J.-P., A. Burlingame, E. Moczydlowski, and W. F. Gilly. 2000.** A new highly selective conotoxin from *Conus californicus* that targets voltage-gated neuronal Na$^+$ channels of squid. *J. Gen. Physiol.* **116:** 12A.

**Conticello, S. G., Y. Gilad, N. Avidan, E. Ben-Asher, Z. Levy, and M. Fainzilber. 2001.** Mechanisms for evolving hypervariability: the case of conopeptides. *Mol. Biol. Evol.* **18:** 120–131.

**Cottrell, G. A., and B. M. Twarog. 1972.** Active factors in the venom duct of *Conus californicus*. *Br. J. Pharmacol.* **44:** 365P–366P.

**dos Santos, V. L. P., C. R. V. Franco, R. L. L. Viggiano, R. B. da Silveira, M. P. Cantao, O. C. Mangili, S. S. Veiga, and W. Gremski. 2000.** Structural and ultrastructural description of the venom gland of *Loxosceles intermedia* (brown spider). *Toxicon* **38:** 265–285.

**Duda, T. F., and S. R. Palumbi. 1999.** Molecular genetics of ecological diversification: duplication and rapid evolution of toxin genes of the venomous gastropod *Conus*. *Proc. Natl. Acad. Sci. USA* **96:** 6820–6823.

**Elliot, E. J., and J. Kehoe. 1978.** Cholinergic receptors in *Aplysia* neurons: activation by a venom component from the marine snail *Conus californicus*. *Brain Res.* **156:** 387–390.

**Elliot, E. J., and M. A. Raftery. 1979.** Venom of marine snail *Conus californicus*: biochemical studies of a cholinomimetic component. *Toxicon* **17:** 259–268.

**Endean, R., and C. Duchemin. 1967.** The venom apparatus of *Conus magus*. *Toxicon* **4:** 275–284.

**Freeman, S. E., R. J. Turner, and S. R. Silva. 1974.** The venom and venom apparatus of the marine gastropod *Conus striatus* Linne. *Toxicon* **12:** 587–592.

**Greene, J. L., and A. J. Kohn. 1989.** Functional morphology of the *Conus* proboscis (Mollusca: Gastropoda). *J. Zool. Lond.* **219:** 487–493.

**Halstead, B. W. 1988.** *Poisonous and Venomous Marine Animals of the World.* Darwin Press, Princeton, NJ. Pp. 243–263.

**Hermitte, L. C. D. 1946.** Venomous marine molluscs of the genus *Conus*. *Trans. R. Soc. Trop. Med. Hyg.* **39:** 485–512.

**Hinegardner, R. T. 1958.** The venom apparatus of the cone shell. *Hawaii Med. J.* **17:** 533–536.

**Hopkins, C., M. Grilley, C. Miller, K. Shon, L. J. Cruz, W. R. Gray, J. Dykert, J. Rivier, D. Yoshikami, and B. M. Olivera. 1995.** A new family of *Conus* peptides targeted to the nicotinic acetylcholine receptor. *J. Biol. Chem.* **270:** 22361–22367.

**Kohn, A. J. 1956.** Piscivorous gastropods of the genus *Conus*. *Proc. Natl. Acad. Sci.* **42:** 168–172.

**Kohn, A. J. 1966.** Food specialization in *Conus* in Hawaii and California. *Ecology* **47:** 1041–1043.

**Kohn, A. J. 1998.** Superfamily Conoidae. Pp. 846–854 in *Mollusca: The Southern Synthesis. Part B. Fauna of Australia*, Vol. 5. P. L. Beesley, G. J. B. Ross, and A. Wells, eds. CSIRO Publishing, Melbourne.

**Kohn, A. J., and C. Hunter. 2001.** The feeding process in *Conus imperialis*. *Veliger* **44:** 232–234.

**Kohn, A. J., M. Nishi, and B. Pernet. 1999.** Snail spears and scimitars: a character analysis of *Conus* radular teeth. *J. Molluscan Stud.* **65:** 461–481.

**Kohn, A. J., P. R. Saunders, and S. Weiner. 1960.** Preliminary studies on the venom of the marine snail, *Conus*. *Ann. NY Acad. Sci.* **90:** 706–725.

**Li, L., R. W. Garden, and J. V. Sweedler. 2000.** Single-cell MALDI: a new tool for direct peptide profiling. *Trends Biotechnol.* **18:** 151–160.

**Maguire, D., and J. Kwan. 1992.** Cone shell venoms—synthesis and packaging. Pp. 11–18 in *Toxins and Targets: Effects of Natural and Synthetic Poisons on Living Cells and Fragile Ecosystems*, D. Watters, M. Lavin, D. Maguire, and J. Pearn, eds. Harwood Academic Publishers, Philadelphia.

**Marsh, H. 1977.** The radular apparatus of *Conus*. *J. Molluscan Stud.* **43:** 1–11.

**McIntosh, J. M., F. Ghomashchi, M. H. Gelb, D. J. Dooley, S. J. Stoehr, A. B. Giordani, S. R. Naisbitt, and B. M. Olivera. 1995.** Conodipine-M, a novel phospholipase A$_2$ isolated from the venom of the marine snail *Conus magus*. *J. Biol. Chem.* **270:** 3518–3526.

**McIntosh, J. M., A. D. Santos, and B. M. Olivera. 1999.** *Conus* peptides targeted to specific nicotinic acetylcholine receptors subtypes. *Annu. Rev. Biochem.* **68:** 59–88.

**Nybakken, J. 1970.** Correlation of radula tooth structure and food habits of three vermivorous species of *Conus*. *Veliger* **12:** 316–318.

**Nybakken, J. 1990.** Ontogenetic change in the *Conus* radula, its form, distribution among the radula types, and significance in systematics and ecology. *Malacologia* **32:** 35–54.

**Olivera, B. M. 1997.** *Conus* venom peptides, receptor and ion channel targets, and drug design: 50 million years of neuropharmacology. *Mol. Biol. Cell* **8:** 2101–2109.

**Olivera, B. M., D. R. Hillyard, M. Marsh, and D. Yoshikami. 1995.**

Combinatorial peptide libraries in drug design: lesson from venomous cone snails. *Trends Biotechnol.* **13:** 422–426.

**Röckel, D., W. Korn, and A. J. Kohn. 1995.** *Manual of the Living Conidae. Vol. 1. Indo-Pacific Region.* Verlag Christa Hemmen, Wiesbaden, Germany. 517 pp.

**Saunders, P. R., and F. Wolfson. 1961.** Food and feeding behavior in *Conus californicus* Hinds, 1844. *Veliger* **3:** 73–76.

**Shaw, H. Q. 1914.** On the anatomy of *Conus tulipa* Linn., and *Conus textile* Linn. *Q. J. Microsc. Sci.* **60:** 1–60.

**Songdahl, J. H. 1973.** The venom and venom apparatus of the Atlantic cone, *Conus spurius atlanticus* (Clench). *Bull. Mar. Sci.* **23:** 600–612.

**Spengler, H. A., and A. J. Kohn. 1995.** Comparative external morphology of the *Conus* osphradium. *J. Zool. (Lond.)* **235:** 439–453.

**Sweedler, J. V., L. Li, P. Floyd, and W. Gilly. 2000.** Mass-spectrometric survey of peptides in cephalopods with an emphasis on the FMRFamide-related peptides. *J. Exp. Biol.* **203:** 3565–3573.

**Whysner, J. A., and P. R. Saunders. 1963.** Studies of the venom of the marine snail *Conus californicus. Toxicon* **1:** 113–122.

**Whysner, J. A., and P. R. Saunders. 1966.** Purification of the lethal fraction of the venom of the marine snail *Conus californicus. Toxicon* **4:** 177–181.

Reference: *Biol. Bull.* **203:** 42–50. (August 2002)

# Respiratory and Acid-Base Physiology of the Purple Sea Urchin, *Strongylocentrotus purpuratus*, During Air Exposure: Presence and Function of a Facultative Lung

LOUIS BURNETT[1,2,*], NORA TERWILLIGER[3], AMY CARROLL[1], DARWIN JORGENSEN†, AND DAVID SCHOLNICK[1]

[1]*Department of Biology, University of San Diego, Alcala Park, San Diego, California 92110;* [2]*Grice Marine Laboratory, College of Charleston, 205 Fort Johnson, Charleston, South Carolina 29412; and* [3]*Oregon Institute of Marine Biology, University of Oregon, Charleston, Oregon 97420*

**Abstract.** Upon exposure to air (emersion), the purple sea urchin *Strongylocentrotus purpuratus* releases an "emersion fluid" from its esophagus. Release of this fluid causes air to appear within the test (or calcareous theca), most likely inside the intestine. The air space is large, occupying 33.5% of the volume of the intrathecal space. The intestine containing air forms a facultative lung and contributes to the oxygenation of the perivisceral coelomic fluid (PCF) during emersion. During emersion, the mean partial pressure of oxygen ($Po_2$) of the PCF declined from 56 to 24 torr (1 torr = 0.1333 kPa) after 2 h, remained relatively unchanged after 4 h, and rose to 39 torr after 8 h. The partial pressure of carbon dioxide ($Pco_2$) rose from 2.6 to 3.8 torr after 2 h, remained unchanged after 4 h, and declined to 2.7 after 8 h. Due to the elevation of $Pco_2$ PCF pH declined from 7.41 to 7.17. PCF osmotic concentration, calcium ion concentration, chloride ion concentration, ammonium ion concentration, and protein concentration were unchanged by air exposure. Lactate levels in the PCF were undetectable. *S. purpuratus* was an osmoconformer and a chloride ion conformer at salinities down to 20.9 ppt. Below this salinity, the sea urchins died. The respiratory acidosis resulting from air exposure was uncompensated, supporting the hypothesis that compensation for a respiratory acidosis induced by air exposure does not occur in organisms that are unable to regulate ions in a dilute environment. We suggest that the facultative lung ensures a minimal $Po_2$ in the PCF, which may be especially important when the intrathecal space is full of ripe gonads, allowing the gonads to be more reliant on aerobic metabolism.

## Introduction

Intertidal organisms experience bouts of exposure to air, or emersion; these bouts vary in duration with the motility of the organism and the magnitude of the tide. Many intertidal organisms take up oxygen from the air during air exposure and thus sustain aerobic metabolism (deFur, 1988). Other organisms, poorly adapted for exchanging gases in an aerial medium, revert either wholly or in part to anaerobic metabolism (*e.g.*, deFur and McMahon, 1984; Spicer *et al.*, 1988) or reduce their metabolism (Burnett and McMahon, 1987).

The responses of intertidal invertebrates to periodic emersion have been well-studied in decapod crustaceans (see Burnett, 1988 for review) and bivalve molluscs (Widdows *et al.*, 1979; Booth *et al.*, 1984; Walsh *et al.*, 1984; Widdows and Shick, 1985; Shick *et al.*, 1986; Dwyer and Burnett, 1996). In every crustacean and mollusc studied, the hemolymph $Po_2$ increased substantially, generating a so-called respiratory acidosis. The molluscs partially compensated for this acidosis (Booth *et al.*, 1984; Dwyer and Burnett, 1996), and all but one of the crustaceans studied compensated nearly completely. The exceptional crustacean was the mud crab *Eurytium albidigitum*, which is also an osmoconformer (Burnett and McMahon, 1987). We hypothesize that the acid-base compensation observed in the crustaceans and the relatively weak compensation observed in

Received 18 January 2000; accepted 10 April 2002.

* To whom correspondence should be addressed. E-mail: burnettl@cofc.edu

† Current address: Department of Biology, Roanoke College, Salem, VA 24153.

the molluscs is correlated with the strong regulation of hemolymph ionic concentration by the crustaceans and the weak regulation by the molluscs.

Burnett and McMahon (1987) speculated that the uncompensated acidosis in the crab *E. albidigitum* is responsible for the decline in oxygen uptake that occurs in this animal during air exposure. The mechanisms of compensation for acid-base disturbances are thought to involve the transport of ions such as sodium, chloride, and bicarbonate between the organism and its environment or between fluid compartments within the organism (Burnett and McMahon, 1987; Burnett, 1988). Since osmoregulation in crustaceans occurs primarily through the transport of sodium and chloride ions, it is suggested that osmoregulators (or more properly ion regulators) also possess the capacity to compensate for acid-base disturbances. An acidosis during air exposure that is left uncompensated could depress metabolism and decrease overall activity (Burnett and McMahon, 1987). These ideas suggest that good ion regulators have the best chance of compensating for an emersion-induced acidosis, and could thereby maintain aerobic metabolism and activity during emersion. Therefore, we hypothesize that osmoregulation is correlated in various intertidal animals with the capacity to compensate for a respiratory acidosis during emersion.

The purple sea urchin *Strongylocentrotus purpuratus* (Stimpson) inhabits the intertidal zone along the west coast of North America, where it may occur in great numbers. The water vascular system of echinoids constitutes their primary means for external gas exchange (Farmanfarmaian, 1966). The system terminates externally in tube feet, which make up the major surface for gas exchange with the ambient medium. When they are immersed in water, echinoids appear to be well adapted for exchanging oxygen and carbon dioxide through their tube feet (Fenner, 1973). The tube feet are waved in the water between the spines of the urchin; oxygen is taken up, and $CO_2$ is released from fluid that is circulated in the tube feet. This fluid then circulates to the ampullae (Fenner, 1973; Smith, 1978), where gases are exchanged with the perivisceral coelomic fluid. When the urchin is exposed to air, however, the tube feet withdraw almost completely and collapse; and the exchange of gases is greatly inhibited (Fenner, 1973).

A few studies have been done on sea urchins that were air exposed. The research of Webster and Giese (1975) and Johansen and Vadas (1967) touched briefly on the oxygen uptake and the $Po_2$ in the coelomic fluid in three species of *Strongylocentrotus*. Johansen and Vadas (1967) measured a coelomic fluid $Po_2$ substantially higher than that measured by Webster and Giese (1975), who showed that coelomic fluid $Po_2$ dropped rapidly and approached zero during emersion. More recently, Spicer *et al.* (1988) investigated acid-base status as a function of air exposure in two species of sea urchins. Their study revealed a mild respiratory acidosis that was completely compensated in both species. These studies plus the interesting findings of Bookbinder and Shick (1986), who demonstrated that the gonads of sea urchins are heavily dependent on anaerobic metabolism, led us to investigate the internal environment of the sea urchin during emersion. We aimed to determine whether a respiratory acidosis would occur, whether it would be compensated for, and whether these responses would be related to the ability of the sea urchin to osmoregulate.

We were especially intrigued by the large amount of fluid that sea urchins lose when they are air exposed. Since the tests of sea urchins are rigid, we reasoned that the fluid lost from within the test must be replaced by air. We thought that the air space appearing during emersion might be important to the urchin during a period of air exposure, serving essentially as a "facultative lung." Thus, we identified the source of the fluid lost during emersion, documented in detail the presence of an air space within the sea urchin, and gathered physiological data that would suggest a functional role for this facultative lung.

## Materials and Methods

### *Collection*

Purple sea urchins *Strongylocentrotus purpuratus* were collected by hand from tide pools along the southwestern coast of Charleston, Oregon, during the last two weeks of May 1990. The sea urchins were transported to the Oregon Institute of Marine Biology where they were kept on sea tables in flowing seawater (12°C and 32 ppt salinity). All animals were used within 3 weeks of collection.

Animals used to determine the source of emersion fluid were collected by hand in and around exposed rock jetties at South Mission Beach, San Diego, California, in June 1991. The animals were taken to the University of San Diego and held in recirculating seawater at 15°C, 34 ppt salinity (Instant Ocean salts).

### *Determination of the volume of fluid lost during emersion*

For purposes of clarity and consistency, we use the term intrathecal space to designate the whole space contained within the calcareous theca or test (Hyman, 1955) of an urchin. This space encloses numerous compartments, including the perivisceral coelomic space and the gut. We noticed that, shortly after emersion, all urchins lost a relatively large amount of fluid from the intrathecal space; we call this emersion fluid (EF). Because the test is rigid, we surmised that the loss of this much fluid volume would create an air space somewhere within the theca. We used several different approaches to measure the volume of the EF and the resulting air space in the same urchins. First, the volume of fluid lost from each urchin during 8 h of air exposure was measured directly by placing the urchin over a funnel, collecting the fluid released, and then measuring its volume (Row B in Table 1; fluid volume is milliliters per gram of sea urchin fresh weight, Row A). Second, individuals were weighed immediately upon air exposure (Row A in Table 1) and then emersed for 8 h. After this period of air exposure, the animals were again weighed, and the difference between the pre-emersion and post-emersion weights was taken as a measure of the EF lost during air exposure (using the density of water = 1 g $ml^{-1}$; Row C in Table 1). Third, several holes were drilled into the aboral surface to drain fluid from the intrathecal space of the emersed urchins. The holes were about 2 cm in diameter and located roughly 2–5 cm from the anal opening (depending on the diameter of the individual). The sea urchins were then inverted, the EF was drained, and its volume was measured in a graduated cylinder (Row E in Table 1). Once thoroughly drained, the urchins were submerged in seawater and allowed to fill completely. The seawater in the intrathecal space was subsequently drained and its volume measured (Row D in Table 1). The difference in the volume of seawater filling the intrathecal space and the volume of fluid remaining in the intrathecal space after emersion (Row D − Row E) is another measure of the air space (or fluid lost) during air exposure (Row F in Table 1).

### *Source of the emersion fluid (EF)*

In separate experiments, we injected blue dextran (M.W. = 2,000,000) dissolved in seawater into each of two body compartments: the espohagus and the perivisceral coelomic cavity. We suspected these compartments of being the origin of the emersion fluid. We chose blue dextran because its color is easy to see in solution, and its large molecular weight makes it unlikely to be metabolized during the short duration (minutes) of these experiments, or to cross membranes between fluid compartments. In one experiment, we injected the blue dextran solution into the perivisceral coelomic cavity, air exposed the sea urchin, and collected the EF and examined it for the presence of blue dextran. In a second experiment, we injected the esophagus with the blue dextran solution, air exposed the animals, and collected the emersion fluid and examined it for the presence of blue dextran.

The concentration of blue dextran was 25 mg $ml^{-1}$ in seawater (pH = 7.9), and 0.5 ml of this solution was injected into both compartments while the animal was submerged. The perivisceral coelomic cavity was injected through the aboral surface with a 1-ml syringe and 26-gauge needle. The sea urchin was placed in a holding tank, which contained seawater of 34 ppt salinity at 15°C. After being allowed to move about freely for 30 min, the animal was air exposed for up to 15 min at 15°C and the EF was collected. After air exposure, a 1-ml sample of perivisceral coelomic fluid was also drawn (as described below). The presence of blue dextran was confirmed by measuring the absorbance of the perivisceral coelomic fluid samples at 618 nm, the absorption maximum of blue dextran in seawater.

In the second set of experiments, individuals were injected with blue dextran into the esophagus with a 1-ml glass syringe connected to a short length of PE-50 tubing. While submerged, the animal was inverted and gently touched around the mouth, which induced the jaws to open. The thin tubing was then inserted about 1 cm into the esophagus, the dye slowly injected, and the tubing immediately withdrawn. After injection, there was no obvious leakage of fluid from the mouth, and the animals were either immediately air exposed (oral side down), or allowed to remain submerged for intervals between 1 and 10 min before being exposed to air. After air exposure, EF was collected at intervals for up to 10 min and evaluated for the presence of blue dextran, as described above.

### *Coelomic cavity pressure*

Hydrostatic pressure within the intrathecal space was measured while the animals were submerged and, subsequently, during air exposure. For each trial, an individual was placed in well-aerated seawater (Instant Ocean salts) thermostatically set to 12°C. A hypodermic needle was inserted through the aboral surface extending into the main coelomic cavity of a submerged animal. The needle was connected *via* polyethylene tubing (PE 100) to a pressure transducer (Statham p23dB) coupled to a four-channel recorder (Beckman RA511). The pressure-measuring unit was calibrated statically. The animal was then emersed by draining water from the holding tank. The hydrostatic pressure in the perivisceral coelomic fluid was monitored continuously during the emersion period. All readings were in torr (1 torr = 0.1333 kPa).

Simultaneously the volume of EF lost by the sea urchin during emersion was measured. Fluid lost from the urchin after emersion was collected in a glass buret, open at the top and closed on the bottom with a three-way stopcock, that was connected *via* tubing to a second pressure transducer (Statham P23dB) with output to the recorder. The pressure of water in the buret increased with the volume and was calibrated prior to the experiment; thus we could simultaneously measure the volume of fluid released and the pressure in the perivisceral coelomic fluid.

### *Osmotic and ionic regulation at low salinities*

We exposed *S. purpuratus* to salinities ranging from 17 to 32.5 ppt for 2 d; salinities were produced by diluting seawater with deionized water. Samples of perivisceral coelomic fluid (PCF) from individual urchins were withdrawn anaerobically with a 1-ml glass syringe equipped with a 22-gauge needle, which was inserted into the main coelomic cavity through the membrane surrounding the anus. These samples of coelomic fluid, as well as samples of ambient water, were assayed as follows: osmotic concentration was measured with a vapor pressure osmometer (Wescor Model 5100C); chloride ion concentration was measured with a chloride titrator (Radiometer CMT10); and calcium ion concentration was measured with a calcium ion selective electrode (Radiometer ISE25Ca).

### *Measurement of respiratory variables during emersion*

We exposed sea urchins to air by draining the sea tables of seawater. Plastic bags filled with ice were placed in the vicinity of the air-exposed animals to maintain them at a constant 12 ± 1°C ambient temperature. Care was taken to ensure adequate air spaces around the sea urchins.

Perivisceral coelomic fluid samples were drawn from animals after 0, 2, 4, and 8 h of air exposure. The samples were extracted as described above. Volumes ranging from 0.5–1 ml were typically drawn from each individual at each exposure period.

The pH of the coelomic fluid was measured with a microcapillary pH electrode (Radiometer BMS2). The total $CO_2$ content in the coelomic fluid ($Cco_2$) was determined by the method of Cameron (1971). The partial pressure of carbon dioxide ($Pco_2$) was determined with a $Pco_2$ electrode (Radiometer, Copenhagen) (deFur and McMahon, 1984), and that of oxygen was measured with an $O_2$ electrode (Radiometer, E5046). All electrodes (pH, $Pco_2$, $Po_2$) were maintained at 12 ± 0.1°C.

### *Measurements of chloride, calcium, ammonia, lactate, osmotic, and protein concentration during emersion*

The coelomic fluid remaining after the respiratory variables had been sampled was assayed as follows: chloride and calcium ion concentrations were measured as described above; the ammonia content of each sample was assayed spectrophotometrically by the method of Solorzano (1969); lactic acid was converted to pyruvate with lactate dehydrogenase, and reduced NAD was measured spectrophotometrically (Sigma Technical Bulletin No. 826-UV); the remaining fluid was frozen and assayed later for protein concentration (a colorimetric assay; Sigma Technical Bulletin 541–2).

### *Determination of gonadal index*

In May, 13 individual sea urchins from Oregon were removed from the water, blotted, and weighed immediately. After weighing, the sea urchins were carefully dissected; the gonads were removed, rinsed with cold seawater, blotted dry, and weighed. The gonadal index (percent wet weight of gonads per wet body weight) was then calculated. Animals used in all experiments were collected in late May or June. For comparison, we measured the gonadal index of sea urchins collected in Oregon in February 1997, a time when the gonads are larger and when *S. purpuratus* spawns along the Oregon coast (Gonor, 1973).

### *Statistical analysis*

Many variables were analyzed for changes as a function of emersion time. Data were analyzed for normality and equal variance with SigmaStat 2.0 statistical software. Where data were normally distributed, and where variances were equal, a one-way analysis of variance was used to assess differences as a function of emersion time. Where significant differences were found, variables at different times of emersion were compared with the pre-emersion value, using Dunnett's method. When the data were not normally distributed, they were analyzed using a Kruskal-Wallis one-way analysis of variance on ranks. In this case, when differences were detected, pre-emersion values and values at an emersion time were compared by Dunn's method.

## Results

### *Fluid lost during emersion*

Since the test of the sea urchin is rigid, we surmised that the fluid lost during emersion must have been displaced by air. We measured the volume of this air (= fluid lost) in several independent ways. Direct measurement of the volume of fluid released (emersion fluid) when the urchin was air exposed resulted in an averaged weight-specific volume of 0.078 ml $g^{-1}$ wet weight of urchin (Table 1, Row B). This was slightly, although not significantly (Wilcoxon signed rank test, $P = 0.064$), lower than the volume of 0.101 ml $g^{-1}$ calculated from the weight difference between sea urchins weighed immediately after emersion and the same animals weighed after 8 h of air exposure (Table 1, Row C). We also independently measured the volume of the fluid in the intrathecal space (Table 1, Row D), as well as the volume of fluid contained within the intrathecal space after air exposure (Table 1, Row E). The difference between these two volumes approximates the intrathecal volume occupied by air (Table 1, Row F). This volume of air was 0.102 ml $g^{-1}$ wet weight of urchin and takes up 33.5% of the intrathecal fluid volume. There is excellent agreement in the measurements of emersion fluid lost using the three techniques.

Our experiments with blue dextran revealed that the esophagus was the source of the EF. Blue dextran injected into the perivisceral coelom was not detected in the EF at any time. Blue dextran injected into the esophagus appeared in the EF within minutes of air exposure (Fig. 1). However, if the urchin was kept submerged after the injection, the longer it remained submerged prior to air exposure, the more dilute the blue dextran was in the EF that was finally released upon emersion (Fig. 1). Therefore, the dye in the esophagus is either rapidly absorbed by the walls of the esophagus, passed through the esophagus to the stomach, or diluted with ambient seawater.

Pressure in the perivisceral coelom of three different sea

**Table 1**

*Volume of fluid released upon emersion and the size or volume of various parts or compartments of the sea urchin*

| Row | Part or component | Size or volume | | | |
|---|---|---|---|---|---|
| | | Mean | Min | Max | SEM |
| A | Weight of sea urchin immediately upon emersion (g) | 147.1 | 95.6 | 235.5 | 11.2 |
| B | Emersion fluid (ml $g^{-1}$) (from volume of fluid collected) | 0.078 | 0.054 | 0.107 | 0.004 |
| C | Emersion fluid (ml $g^{-1}$) (from pre-emersion − post-emersion weight difference) | 0.101 | 0.065 | 0.258 | 0.016 |
| D | Intrathecal space fluid volume (ml $g^{-1}$) | 0.304 | 0.255 | 0.423 | 0.015 |
| E | Post-emersion intrathecal space Fluid Volume (ml $g^{-1}$) | 0.202 | 0.136 | 0.314 | 0.015 |
| F (D − E) | Air space or emersion fluid volume (ml $g^{-1}$) | 0.102 | 0.080 | 0.144 | 0.005 |
| G | Gonad weight (g) | 4.44 | 2.55 | 5.57 | 0.34 |
| H (G/A – 100) | % Gonads | 3.1 | 2.1 | 4.3 | 0.2 |

Volume is expressed per unit of pre-emersion urchin weight (Row A). Gonad weight and gonadal index are also given. All measurements were made on each of 10 animals.

urchins was slightly positive throughout submersion (pressure traces of one urchin are shown in Fig. 2) and showed some variation with the movement of the urchin. During emersion, the pressure within the perivisceral coelom fell to ambient and remained there throughout the exposure period (Fig. 2).

### *Osmotic and ionic regulation*

Sea urchins did not survive 17 ppt salinity, the lowest level tested. At salinities of 20.9 ppt (568 mOsm $kg^{-1}$; 311 mmol $Cl^{-}$ $l^{-1}$) and above, however, they were strict conformers with respect to osmotic, chloride, and calcium ion concentrations (Table 2).

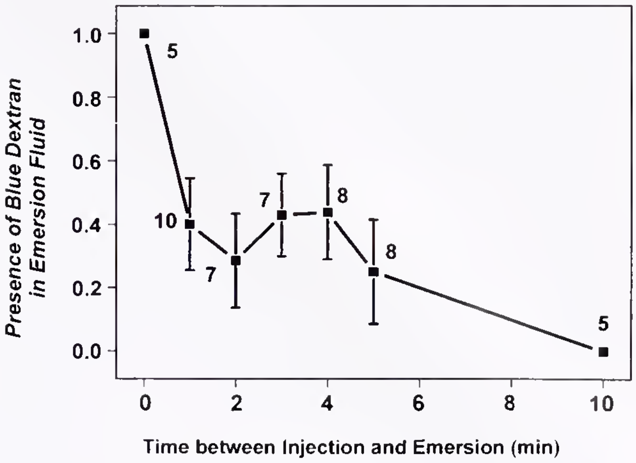

**Figure 1.** A solution of blue dextran injected into the esophagus of *Strongylocentrotus purpuratus* appears in the emersion fluid, but only if the time interval between injection and emersion is short. Blue dextran in the emersion fluid was scored as 0 (absent), 0.5 (present, but dilute), or 1 (present). Values are mean ± SEM. The number of observations is given next to each data point.

### *Respiratory and chemical variables*

Monitoring of respiratory and chemical variables in the PCF during emersion revealed changes in some, but not all variables. During the first 2 h of air exposure, the $Po_2$ in the PCF fell significantly from 56 to 24 torr (Fig. 3); then from the 2nd to the 4th h, the $Po_2$ remained relatively unchanged, but still different from pre-emersion values. Finally, after 8 h, the $Po_2$ rose to 39 torr, still significantly different from pre-emersion values.

$Pco_2$ rose significantly within the first 2 h of air exposure from 2.6 to 3.8 torr (Fig. 3); it then remained significantly elevated after 4 h, and finally declined to 2.7 torr after 8 h, a value not significantly different from pre-emersion conditions. Coelomic fluid pH fell significantly during the 2nd and 4th h of emersion, but was no different from pre-emersion values after 8 h. Total carbon dioxide did not change significantly at any time as a result of air exposure.

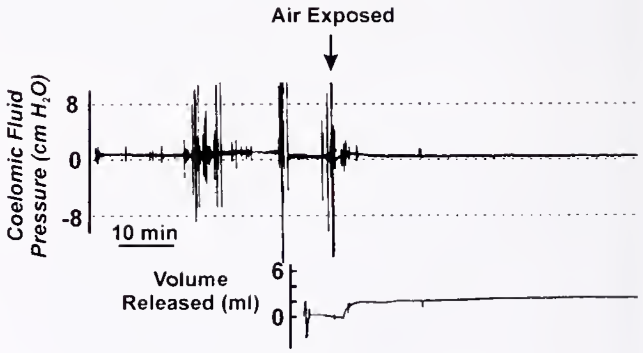

**Figure 2.** Perivisceral coelomic fluid pressure in *Strongylocentrotus purpuratus* before and during air exposure. The time of emersion is indicated by the arrow. The volume of emersion fluid released is measured simultaneously; note that the fluid is released within minutes of emersion. Oscillations in the pressure trace prior to air exposure are caused by the movement of the sea urchin.

Table 2

*Osmotic, calcium ion, and chloride ion concentrations of the perivisceral coelomic fluid (PCF) in* Strongylocentrotus purpuratus *as a function of ambient salinity values are mean ± standard error of the mean (SEM)*

| Variable | Ambient salinity (ppt) | | |
|---|---|---|---|
| | 19.9 | 25.0 | 32.0 |
| Osmolality (mOsm $kg^{-1}$) | | | |
| medium (seawater) | 594 | 839 | 921 |
| PCF | 568 ± 3.62 | 746 ± 1.44 | 943 ± 4.41 |
| *n* | 10 | 10 | 10 |
| Calcium (mmol $l^{-1}$) | | | |
| medium (seawater) | 5.9 | 8.6 | 10.3 |
| PCF | 5.6 ± 0.08 | 7.9 ± 0.08 | 9.3 ± 0.15 |
| *n* | 9 | 10 | 9 |
| Chloride (mmol $l^{-1}$) | | | |
| medium (seawater) | 326 | 448 | 506 |
| PCF | 311 ± 2.14 | 390 ± 0.94 | 499 ± 1.44 |
| *n* | 10 | 10 | 10 |

We were able to obtain gas samples from within the intestine of two urchins exposed to air for 9 h. The $Po_2$ values for the two samples were 122 and 125 torr, respectively.

The osmotic concentration in the coelomic fluid did not change during air exposure, nor did protein, $Cl^-$, $Ca^{++}$, or ammonia concentration (Table 3). There was never detectable lactate in the coelomic fluid.

### *Gonadal index*

The gonads were small and occupied little of the intrathecal space. They constituted 3.11% of the wet body weight in animals collected in early June 1990 from the low intertidal of the Oregon coast (Table 1). This is much lower than the 8.04 gonadal index (SEM = 0.58; $n = 6$) that we measured on urchins collected from the same area in February 1997. These data are consistent with those of Gonor (1973), who reported gonadal indices of 8.4 in early March and 4.2 in June.

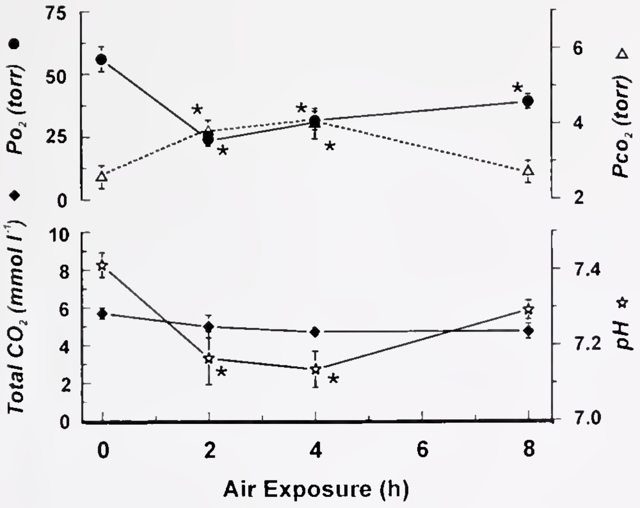

**Figure 3.** Respiratory and acid-base variables in the perivisceral coelomic fluid of *Strongylocentrotus purpuratus* as a function of the duration of air exposure. Values are mean ± SEM, $n = 10$. Significant differences ($P < 0.05$) from 0 h air exposure are indicated by *.

## Discussion

The most striking finding of this study is that, when the sea urchin is emersed, air enters its gut, displacing 33.5% of the volume of the intrathecal space. We suggest that the intestine, containing air with a high oxygen capacitance, constitutes a facultative lung within the intrathecal space and oxygenates the perivisceral coelomic fluid.

Upon emersion, urchins rapidly release a large amount of emersion fluid (EF). This EF originates in the esophagus and perhaps a part of the stomach proximal to the esophagus, a conclusion we base on the appearance, once the urchin is emersed, of dextran blue previously injected into the esophagus (Fig. 1). We suggest that the muscles of the esophagus are not strong enough to hold its contained fluid when the urchin is emersed.

The long stomach and intestinal regions of the gut of regular echinoids are thin, delicate, and lightly muscled, and filled with a relatively constant volume of gut fluid and food (Buchanan, 1969). The fluid volume of the gut has been estimated to be between 6% and 14% of the total volume of the perivisceral coelomic cavity, depending on whether the animals were fed or starved (Buchanan, 1969). Buchanan's (1969) estimates are low because the fluid volume of the gut was measured after the urchin was dissected and the PCF had drained from around the gut; these conditions would have caused some EF to leak out of the gut from each end. The important point is that the gut contains a large amount

**Table 3**

*Perivisceral coelomic fluid variables in* Strongylocentrotus purpuratus *as a function of the duration of air exposure; no significant differences were found*

| | Duration of emersion (h) | | | |
|---|---|---|---|---|
| Variable | 0 | 2 | 4 | 8 |
| Osmolality (mOsm $kg^{-1}$) | | | | |
| Mean | 943.1 | 942.9 | 944.9 | 944.1 |
| SEM | 4.41 | 3.49 | 1.44 | 6.11 |
| Calcium (mmol $l^{-1}$) | | | | |
| Mean | 9.31 | 9.03 | 8.83 | 8.74 |
| SEM | 0.15 | 0.23 | 0.25 | 0.12 |
| Chloride (mmol $l^{-1}$) | | | | |
| Mean | 499.2 | 492.4 | 490.5 | 494.4 |
| SEM | 2.18 | 1.38 | 2.35 | 2.78 |
| Ammonium (mmol $l^{-1}$) | | | | |
| Mean | 0.038 | 0.046 | 0.041 | 0.056 |
| SEM | 0.02 | 0.03 | 0.03 | 0.03 |
| Protein (mg $ml^{-1}$) | | | | |
| Mean | 0.448 | 0.319 | 0.242 | 0.488 |
| SEM | 0.05 | 0.07 | 0.05 | 0.06 |

Number of observations (*n*) is 10 in all cases.

of EF that, when released upon emersion, is replaced by air. The fact that no negative hydrostatic pressures occur within the coelomic cavity when sea urchins lose this fluid (Fig. 2) suggests that air displaces the lost fluid easily. We submit that the air enters the anal opening and resides in the intestine with a volume occupying 33.5% of the volume of the perivisceral coelomic cavity (Table 1).

In echinoids the digestive tract is long and coiled and is the most likely place for this relatively large volume of air to reside. The stomach is the longest part of the digestive tract (Anderson, 1966), and makes almost a complete circuit of the body, hanging in five "bag-like festoons" from its attachments to the body wall. The intestine is next, turning and making a reverse circuit alongside the stomach before joining the rectum. A hemal system associated with the gut is particularly well developed in echinoids (Anderson, 1966) and would facilitate the diffusion of oxygen from the lumen of the gut into the PCF. One of us (A. Carroll) has observed that the posterior intestine of many specimens of emersed *Strongylocentrotus droebachiensis* is distended with air upon dissection, supporting our hypothesis that air enters the gut through the anus.

The function of this facultative lung is clearly respiratory. Gas sampled from the intestine of two sea urchins 9 h after emersion has a $Po_2$ of 122 and 125 torr, about 30 torr below the partial pressure of ambient air (155 torr). These results indicate that the oxygen taken into the sea urchin is being consumed by the animal. Oxygenated PCF may be especially important to *S. purpuratus* when the gonads occupy a significant mass within the urchin, and it may be adaptive in minimizing the dependence of the gonads on anaerobic metabolism. We return to this point below.

The $Po_2$ of the PCF of immersed *S. purpuratus* is similar to previous measurements in this species (Johansen and Vadas, 1967; Webster, 1975; Webster and Giese, 1975). Although Bookbinder and Shick (1986) measured a slightly higher gonadal index (about 4%) in *S. droebachiensis,* the PCF $Po_2$ and pH were nearly identical to those measured in the present study. The PCF pH of *S. purpuratus* was somewhat higher than values reported by Spicer *et al.* (1988) for two other species of sea urchins, *Psammechinus miliaris* and *Echinus esculentus* (pH 7.05 to 7.17). Spicer *et al.* (1988) also reported values of total $CO_2$ in the PCF that are lower than those reported here; but their values for $Pco_2$ are very similar to ours. The reasons for these differences are unclear. Temperature is probably not a factor, since Spicer *et al.* (1988) conducted their experiments at 10°C, close to the 12°C used in the present study. Although they make no mention of the presence of gonads, their animals may have had a different gonadal index. Bookbinder and Shick (1986) have shown that $Po_2$ and pH can vary with gonadal index, and this variation may explain some of the differences between the results of Spicer *et al.* (1988) and the present study.

Components of the PCF changed when urchins were emersed, and these changes were consistent with a reduction of gas exchange. PCF $Po_2$ declined while $Pco_2$ increased, and the rise in $Pco_2$ was accompanied by a decrease in pH. A similar decline in PCF $Po_2$ was measured by Johansen and Vadas (1967), with values of about 20 torr after 5 h of air exposure. A decline of PCF $Po_2$ was also measured by Webster and Giese (1975), but their values declined to about zero after 3 h. These low values might well be attributed to the needle oxygen electrode used in these experiments. The electrode was inserted into the coelomic cavity but may have penetrated a gonad or some other tissue, producing a low reading. In fact, Bookbinder and Shick (1986) measured 0 torr of oxygen in the center of the ovary using an oxygen microelectrode.

Spicer *et al.* (1988) measured an increase in PCF $Pco_2$ during air exposure in the two species used in their study, and these pressure changes were not accompanied by a decrease in pH. This is in contrast to the results obtained in the present study, where PCF $Pco_2$ increased significantly and pH declined. The results of Spicer *et al.* (1988) indicate a rapid pH compensation for the $Pco_2$ increase in their urchins. They measured small but significant increases in PCF calcium and magnesium ion concentrations in both species, which may account for a part of this compensation. In *S. purpuratus,* we detected no significant changes in any of the ionic concentrations during emersion (Table 3), nor did we observe compensation to the respiratory acidosis. An interesting trend in the respiratory variables suggested that the urchins were exchanging gases more efficiently after 4 h than in the initial stages of emersion (Fig. 3). For example, PCF $Po_2$ after 8 h was elevated above the levels at 2 h, and $Po_2$ had returned to pre-emersion levels; and pH also showed a moderate increase. Another possible explanation for these changes is a reduction in oxygen demand. This hypothesis remains to be tested, but *S. purpuratus* is rarely exposed to air much longer than 4 h (N. B. Terwilliger, pers. obs.).

Bookbinder and Shick (1986) concluded that 76% to 92% of the overall metabolism of the ovaries is anaerobic at the physiological partial pressures of oxygen within the PCF. They reasoned that oxygen is consumed primarily in the superficial tissues and not deep in the ovary (Bookbinder and Shick, 1986). Gut tissues also metabolize anaerobically, but not to the extent of the ovaries. Interestingly, Bookbinder and Shick (1986) detected only very small amounts of lactate within the PCF, a result similar to our own; but when they incubated gonads under anoxic conditions, lactate production rose dramatically. On the basis of their measurements of gonad heat dissipation in a calorimeter, they concluded that the metabolism had a large anaerobic component (Bookbinder and Shick, 1986). However, this conclusion is called into question by the lack of lactate production at physiological $Po_2$. The production of anaerobic endproducts other than lactate (Ellington and Lawrence, 1973; Bookbinder and Shick, 1986) could explain the lack of lactate accumulation at physiological $Po_2$, but additional studies are needed to confirm this. However, the energy demands of the unfertilized egg in *S. purpuratus* are extremely small (Leong and Manahan, 1997); a low oxygen demand means that only the eggs deep within the gonad experience a very low concentration of oxygen. In any event, the diffusion of oxygen from the surface of the gonads to the deep tissues must be limited by the $Po_2$ in the PCF. Therefore, the higher the $Po_2$ in the PCF, the greater the amount of gonad that could remain aerobic. During emersion, a facultative lung full of air would serve to maintain aerobic metabolism, at least on the surface of the gonads.

Other tissues bathed by the PCF would also benefit from a well oxygenated medium. The gut of *S. droebachiensis* is less dependent on anaerobic metabolism than the ovaries (Bookbinder and Shick, 1986) and may benefit from direct contact with the air filling the gut. Webster and Giese (1975) reported that the isolated body wall of *S. purpuratus* has a high rate of oxygen uptake, suggesting that it consumes oxygen when oxygen is readily available.

The presence of air somewhere within the urchin explains why Webster and Giese (1975) were able to account for only 10% of the oxygen taken up by the internal tissues during air exposure. Their measurement of the rate of the depletion of oxygen in the PDF showed a rate slower than that expected if the intrathecal space were completely sealed from a supply of oxygen—the basis of their calculation. Thus, oxygen-rich air residing in the intestine—located within the intrathecal space—would prevent a rapid decline in oxygen in the PCF.

These results suggest that, in the sea urchin, the intestine participates in respiration. Others have also suggested that the digestive tract could serve as a respiratory surface in echinoids (Perrier, 1875; Cuénot, 1948, as cited by Farmanfarmaian, 1966). But Farmanfarmaian (1966) dismissed this possibility for a number of reasons that may still apply, provided sea urchins are immersed in seawater. Stott (1955) demonstrated clearly that water circulates through the mouth, esophagus, siphon, and intestine during periods when the animal is not feeding, and he suggested that this circulating water serves a respiratory function. In a similar manner, the air within the gut can play an important role in keeping the PCF oxygenated during emersion.

Finally, we return to one of the ideas that drove this study in the first place, that is, the proposed relationship between osmotic and ionic regulation, compensation for respiratory acidosis, and activity during emersion. Sea urchins are thought to be stenohaline (Binyon, 1966), and it is not surprising that in this study they did not tolerate salinities below 50% seawater. Our results (Table 2) are similar to those obtained by Giese and Farmanfarmaian (1963), who showed that *S. purpuratus* did not survive low salinity. Like the mud crab *Eurytium albidigitum* (Burnett and McMahon, 1987), which is also an osmoconformer, *S. purpuratus* undergoes a respiratory acidosis during emersion, and this acidosis, as in *E. albidigitum,* remains uncompensated after 8 h (Fig. 3).

Acid-base compensation occurred in the urchins studied by Spicer *et al.,* (1988); pH was maintained as $Pco_2$ rose.

The mechanism for this compensation was probably related to the small increase in calcium and magnesium in the PCF. However, this increase may be more related to a passive response of the calcified sea urchin test to the respiratory (*i.e.*, $CO_2$-induced) acidosis. Such responses have been documented in bivalves (Booth *et al.*, 1984; Dwyer and Burnett, 1996) and at least one crustacean (deFur and McMahon, 1984) in response to a respiratory acidosis induced by emersion, and they are thought to be passive (Booth and Mangum, 1978). The lack of any significant changes in the PCF variables during emersion in *S. purpuratus* (Table 3) suggests that no mechanisms, active or passive, are used to compensate for the acidosis.

These findings support our general hypothesis that intertidal organisms that remain active during emersion compensate for the respiratory acidosis induced by air exposure, and this compensation occurs only if the organism is also a good osmotic and ionic regulator. *S. purpuratus* is indeed not active during air exposure, and thus the hypothesis is supported. On the other hand, lack of activity during emersion of this species of sea urchin may reflect poor anatomical design for movement and respiration in air, rather than an inability to compensate for an emersion-related acidosis.

### Acknowledgments

Contribution No. 196 of the Grice Marine Laboratory.

### Literature Cited

**Anderson, J. M. 1966.** Aspects of nutritional physiology. Pp. 329–357 in *Physiology of Echinodermata.* R. A. Boolootian, ed., John Wiley, New York.

**Binyon, J. 1966.** Salinity tolerance and ionic regulation. Pp. 359–377 in *Physiology of Echinodermata.* R. A. Boolootian, ed., John Wiley, New York.

**Bookhinder, L. H., and J. M. Shick. 1986.** Anaerobic and aerobic energy metabolism in ovaries of the sea urchin *Strongylocentrotus droebachiensis. Mar. Biol.* **93:** 103–110.

**Booth, C. E., and C. P. Mangum. 1978.** Oxygen uptake and transport in the lamellibranch mollusc *Modiolus demissus. Physiol. Zool.* **51:** 17–32.

**Booth, C. E., D. G. McDonald, and P. J. Walsh. 1984.** Acid-base balance in the sea mussel, *Mytilus edulis.* I. Effects of hypoxia and air-exposure on hemolymph acid-base status. *Mar. Biol. Lett.* **5:** 347–358.

**Buchanan, J. B. 1969.** Feeding and the control of volume within the tests of regular sea urchins. *J. Zool. Lond.* **159:** 51–64.

**Burnett, L. E. 1988.** Physiological response to air exposure: Acid-base balance and the role of branchial water stores. *Am. Zool.* **28:** 125–135.

**Burnett, L. E., and B. R. McMahon. 1987.** $O_2$ uptake, acid-base balance and branchial water $CO_2$ content during air exposure in intertidal crabs. *Physiol. Zool.* **60:** 27–36.

**Cameron, J. N. 1971.** Rapid method for determination of total carbon dioxide in small blood samples. *J. Appl. Physiol.* **31:** 632–634.

**Cuénot, L. 1948.** Anatomie, éthologie et systématique des échinodermes. Pp. 3–372, Vol. 11 in *Traité de Zoologie,* P. Grassé, ed., Paris, Masson. (Cited in Farmanfarmaian, 1966.)

**deFur, P. L. 1988.** Systemic respiratory adaptations to air exposure in intertidal decapod crustaceans. *Am. Zool.* **28:** 115–124.

**deFur, P. L., and B. R. McMahon. 1984.** Physiological compensation to short-term air exposure in red rock crabs *Cancer productus* Randall, from littoral and sublittoral habitats. II. Acid-base balance. *Physiol. Zool.* **57:** 151–160.

**Dwyer, J. J., and L. E. Burnett. 1996.** Acid-base status of the oyster, *Crassostrea virginica,* in response to air exposure and to infections by *Perkinsus marinus. Biol. Bull.* **190:** 139–147.

**Ellington, W. R., and J. M. Lawrence. 1973.** Malic and lactic dehydrogenase activities and ratios in regular and irregular echinoids. *Comp. Biochem. Physiol.* **45B:** 727–730.

**Farmanfarmaian, A. 1966.** The respiratory physiology of echinoderms. Pp. 245–265 in *Physiology of Echinodermata.* R. A. Boolootian, ed., John Wiley, New York.

**Fenner, D. H. 1973.** The respiratory adaptations of the podia and ampullae of echinoids (Echinodermata). *Biol. Bull.* **145:** 323–339.

**Giese, A. C., and A. Farmanfarmaian. 1963.** Resistance of the purple sea urchin to osmotic stress. *Biol. Bull.* **124:** 182–192.

**Gonor, J. J. 1973.** Reproductive cycles in Oregon populations of the echinoid, *Strongylocentrotus purpuratus* (Stimpson). II. Seasonal changes in oocyte growth and in abundance of gametogenic stages in the ovary. *J. Exp. Mar. Biol. Ecol.* **12:** 65–78.

**Hyman, L. H. 1955.** *The Invertebrates: Echinodermata.* McGraw-Hill, New York. 763 pp.

**Johansen, K., and R. L. Vadas. 1967.** Oxygen uptake and responses to respiratory stress in sea urchins. *Biol. Bull.* **132:** 16–22.

**Leong, P. K. K., and D. T. Manahan. 1997.** Metabolic importance of $Na^+/K^+$-ATPase activity during sea urchin development. *J. Exp. Biol.* **200:** 2881–2892.

**Perrier, E. 1875.** L'appareil circulatoire des oursins. *Arch. Zool. Exp. Gén.* **4:** 605–643.

**Shick, J. M., E. Gnaiger, J. Widdows, B. L. Bayne, and A. de Zwaan. 1986.** Activity and metabolism in the mussel *Mytilus edulis* L. during intertidal hypoxia and aerobic recovery. *Physiol. Zool.* **59:** 627–642.

**Smith, A. B. 1978.** A functional classification of the coronal pores of regular echinoids. *Palaeontology* **21:** 759–789.

**Solorzano, L. 1969.** Determination of ammonia in natural waters by the phenolhypochlorite method. *Limnol. Oceanogr.* **14:** 799–801.

**Spicer, J. I., A. C. Taylor, and A. D. Hill. 1988.** Acid-base status in the sea urchins *Psammechinus miliaris* and *Echinus esculentus* (Echinodermata: Echinoidea) during emersion. *Mar. Biol.* **99:** 527–534.

**Stott, F. C. 1955.** The food canal of the sea-urchin *Echinus esculentus* L. and its functions. *Proc. Zool. Soc. Lond.* **125:** 63–85.

**Walsh, P. J., D. G. McDonald, and C. E. Booth. 1984.** Acid-base balance in the sea mussel, *Mytilus edulis.* II. Effects of hypoxia and air-exposure on intracellular acid-base status. *Mar. Biol. Lett.* **5:** 359–369.

**Webster, S. K. 1975.** Oxygen consumption in echinoderms from several geographical locations, with particular reference to the Echinoidea. *Biol. Bull.* **148:** 57–164.

**Webster, S. K., and A. C. Giese. 1975.** Oxygen consumption of the purple sea urchin with special reference to the reproductive cycle. *Biol. Bull.* **148:** 165–180.

**Widdows, J., and J. M. Shick. 1985.** Physiological responses of *Mytilus edulis* and *Cardium edule* to aerial exposure. *Mar. Biol.* **85:** 217–232.

**Widdows, J., B. L. Bayne, D. R. Livingstone, R. I. E. Newell, and P. Donkin. 1979.** Physiological and biochemical responses of bivalve molluscs to exposure to air. *Comp. Biochem. Physiol.* **62A:** 301–308.

Reference: *Biol. Bull.* **203:** 51–57. (August 2002)

# Helical Nature of Sperm Swimming Affects the Fit of Fertilization-Kinetics Models to Empirical Data

GREGORY S. FARLEY

*Department of Biological Science, The Florida State University, Tallahassee, Florida 32306*

**Abstract** Models of fertilization kinetics rely upon estimates of the swimming velocity of sperm to predict collision rates between egg and sperm. Most investigators measure sperm swimming velocity without accounting for the helical motion of sperm, thereby obtaining an inflated estimate of the velocity with which sperm approach eggs. In turn, models of fertilization predict inflated rates of sperm/egg collision. I observed sea urchin sperm colliding with eggs, quantified the rate of sperm/egg collision, and measured sperm velocity as a component of the helix through which they swim. I also adjusted the "target size" of eggs to reflect the diameter of the helix. My estimate of sperm swimming velocity is an order of magnitude lower than other estimates for the same species. By using helical parameters in fertilization kinetics models and accounting for dead sperm in laboratory trials, I was able to accurately predict lower rates of sperm/egg collision. Moreover, making these adjustments in the model increased the estimated proportion of sperm that initiate fertilization by 6- to 7-fold, suggesting that a better understanding of sperm swimming might lead to a more complete understanding of fertilization biology and natural selection on gamete traits.

## Introduction

Broadcast-spawning marine invertebrates release both eggs and sperm into the water column, where fertilization and development consequently take place. Variation in the proportion of eggs fertilized in nature has long been postulated (Lillie, 1915; Mortensen, 1938; Thorson, 1950), and variability in fertilization success has been empirically quantified in the laboratory (Pennington, 1985; Havenhand, 1991; Levitan *et al.*, 1991; Oliver and Babcock, 1992; Levitan, 1993, 1996a, 2000; Benzie and Dixon, 1994), in field experiments (Pennington, 1985; Levitan *et al.*, 1992; Babcock *et al.*, 1992, 1994; Levitan and Young, 1995; Levitan, 1996a, 1998), and in *in situ* surveys of spawning events (Babcock and Mundy, 1992; Babcock *et al.*, 1992, 1994; Brazeau and Lasker, 1992; Oliver and Babcock, 1992; Sewell and Levitan, 1992; Lasker *et al.*, 1996; Coma and Lasker, 1997). Much of this empirical work has confirmed that fertilization success rarely approaches 100% in nature, where factors such as water-flow velocity (Pennington, 1985; Levitan *et al.*, 1992; Benzie *et al.*, 1994; Levitan, 1996a, 1998), turbulence (Benzie *et al.*, 1994), the distance among spawning animals (Pennington, 1985; Grosberg, 1987; Levitan, 1991, 1998; Yund, 1990; Babcock *et al.*, 1992, 1994; Benzie *et al.*, 1994), and synchrony of spawning (Oliver and Babcock, 1992; Babcock *et al.*, 1992, 1994) all affect the mixing of male and female gametes.

Variation in fertilization success can contribute to selection on gamete characteristics (Levitan, 1993, 1996b), and efforts to understand the evolution of gamete phenotype have relied in part upon models of fertilization kinetics. There have been three principal attempts to model the proportion of eggs fertilized in still water in the laboratory (Rothschild and Swann, 1951; Hultin, 1956; Vogel *et al.*, 1982). The Rothschild and Swann (1951) and Vogel *et al.* (1982) models are at least partially derived from models of molecular kinetics, which assume random motion of all particles involved and estimate reaction rates based upon the rates at which molecules collide. Hultin (1956) predicted laboratory fertilization based upon the proximity of sperm to virgin eggs, although he did not address the manner by which sperm approach eggs.

Of these three attempts to model fertilization, the model of Vogel *et al.* (1982) has received the most attention. Vogel and colleagues recognized three possible sperm-egg interactions: (1) permanent adhesion of a sperm to the first egg found ("Don Ottavio"); (2) adhesion to the first egg for a

Received 25 October 2001; accepted 21 May 2002.
E-mail: farley@bio.fsu.edu

negligible time, followed by resumed swimming ("Don Giovanni"); and (3) adhesion for some "longer-than-negligible" period, after which nonfertilizing sperm detach and resume searching ("Masetto"). They state that, during their observations, sperm behavior closely matched the first alternative (collision with, and permanent adhesion to, the first available egg), and subsequent authors have used their "Don Ottavio" model (hereafter VCCW) almost exclusively. The model has been modified by several authors (Denny, 1988; Denny and Shibata, 1989; Denny *et al.*, 1992; Babcock *et al.*, 1994; Benzie *et al.*, 1994; Levitan and Young, 1995) to predict fertilization success under turbulent flow conditions in nature. Styan (1998) also adapted the VCCW model to incorporate the negative effects of polyspermy on fertilization success at high sperm concentrations; however, his model uses the framework of the VCCW model to predict sperm-egg collision rates prior to fertilization.

The VCCW model predicts the proportion of eggs fertilized in a sample ($\Phi$) by first predicting the number of sperm colliding with a single egg:

$$\text{\# of sperm colliding} = S_0(1 - \exp(-\beta_0 E_0 \tau)) \qquad \text{(1, VCCW Eq. 10)}$$

where $S_0$ is the initial sperm concentration (sperm/$\mu$l), $E_0$ is the initial concentration of virgin eggs (eggs/$\mu$l), $\tau$ is sperm half-life (seconds), and $\beta_0$ is a rate constant for sperm-egg collisions (mm$^3$/s). $\beta_0$ is estimated by multiplying sperm swimming speed ($v$, mm/second) and the area of the egg cross-section ($\sigma$, mm$^2$):

$$\beta_0 = v\sigma \qquad \text{(2,VCCW Eq. 7)}$$

where $\sigma = \pi$ (egg radius)$^2$. The time of sperm-egg exposure, $t$, can be substituted for sperm half-life ($\tau$) when $t$ is less than $\tau$. This substitution probably reflects natural conditions, where sperm longevity may exceed contact time due to rapid dilution of gametes.

The proportion of eggs fertilized is then a function of the number of sperm-egg collisions and a rate constant describing fertilization ($\beta$, mm$^3$/s):

$$\phi = 1 - \exp[(-\beta S_0/\beta_0 E_0)(1 - \exp(-\beta_0 E_0 \tau))] \qquad \text{(3,VCCW Eq. 14)}$$

Again, $t$ can be substituted for $\tau$ when $t$ is less than $\tau$. The value of the fertilization rate constant ($\beta$) is estimated by iterating the model, using empirical estimates for the proportion of eggs fertilized in a sample ($\Phi$), the initial sperm concentration ($S_0$), the initial egg concentration ($E_0$), the time of sperm-egg exposure ($t$), and the rate constant describing collisions ($\beta_0$, mm$^3$/s).

Estimates of $\beta_0$ are likely to be inflated because the VCCW model, like the models of chemical reaction kinetics upon which it is based, assumes that the motion of eggs and sperm is Brownian—that is, completely random. However, sperm swimming is far from random; rather, sperm (and other microbiota) both translate and simultaneously rotate about their long axis, and so describe a helix as they swim (Jennings, 1901; Bullington, 1925; Gray, 1955; Gray and Hancock, 1955; Crenshaw, 1993a, b, 1996; Crenshaw and Edelstein-Keshet, 1993). The velocity of sperm swimming through helices can therefore be estimated in two ways. The absolute velocity of a swimming sperm describes the velocity with which a sperm passes through a helical trajectory. However, the velocity of a sperm relative to a target such as an egg is better estimated as the rate of advance of the helix (analogous to the "pitch" of a screw) through which the sperm swims. Investigators measuring sperm swimming velocity typically measure the former quantity, which may inflate estimates of the collision rate constant $\beta_0$.

In contrast to any inflation caused by considerations of sperm velocity, estimates of $\beta_0$ can also be deflated when the helical swimming of sperm is not considered. As sperm pass through a helix, they sweep out a cylindrical volume of water; the diameter of that cylinder is equal to the diameter of the helix through which they swim. If the diameter of the helix is less than or equal to the diameter of the egg, then the additional volume of water searched by sperm might increase the likelihood that sperm will collide with eggs. In the VCCW model, this quantity should be added to the area of the egg cross-section ($\sigma$), such that

$$\sigma = \pi(\text{egg radius}^2) + \pi(\text{helix radius}^2) \qquad (4)$$

This will increase the estimate of the collision rate constant $\beta_0$ relative to estimates that do not incorporate the helical nature of sperm swimming.

Changes to the estimated value of $\beta_0$ also affect estimates of the fertilization rate constant, $\beta$, in the VCCW model, as well as the value of the ratio between the two rate constants ($\beta/\beta_0$). This ratio is important, because investigators ascribe biological importance to $\beta/\beta_0$. The ratio $\beta/\beta_0$ describes the proportion of sperm that are capable of initiating fertilization, or the fraction of the egg surface area available for fertilization (Vogel *et al.*, 1982). Estimates of $\beta/\beta_0$ range from 0.01 (Vogel *et al.*, 1982) to 0.17 (Levitan, 1993), but these estimates are very sensitive to estimates of the collision rate constant $\beta_0$ (Vogel *et al.*, 1982; Styan and Butler, 2000).

Although the ability of the VCCW model to predict fertilization has been comprehensively tested in the laboratory by varying sperm age, sperm concentration, egg concentration, and sperm-egg contact time (Vogel *et al.*, 1982; Levitan *et al.*, 1991), the ability of the model to predict the quantity underlying fertilization—collisions between sperm and eggs—has never been tested. In this study, I measure the rate at which helically swimming sperm approach eggs, estimate sperm-egg collision rate by observing gametes of the sea urchin *Lytechinus variegatus*, and test the ability of the VCCW model to predict sperm-egg collision rates by comparing predictions with empirical estimates. I then re-estimate fertilization efficiency ($\beta/\beta_0$) to compensate for reducing sperm swimming velocity in the VCCW model.

## Methods and Materials

### *Gamete manipulation*

Using modified syringes, I injected 90 single *Lytechinus variegatus* eggs into 1-ml pools of sperm on the stage of a trinocular microscope (Farley and Levitan, 2001). The microscope was fitted with a low-light-level video camera, which was in turn connected to a video monitor and a videocassette recorder. I videotaped eggs until fertilization had occurred (marked by the complete expansion of the fertilization membrane); among eggs that were not fertilized, I terminated the videotape after 20 min. The ability of *L. variegatus* sperm to fertilize eggs declines after 20 min (Levitan, 2000); the same is true for many other species (Vogel *et al.*, 1982; Levitan *et al.*, 1991; Benzie and Dixon, 1994). Using a hemacytometer, I quantified the sperm concentration for each trial.

From a frame-by-frame analysis of the videotapes, I quantified the number of sperm colliding with each egg or egg jelly coat (Farley and Levitan, 2001) and estimated the radius and rate of forward advance of the helix through which *L. variegatus* sperm swim. Because I removed the jelly coats from one-half of the eggs tested, and because eggs that were not fertilized were exposed to sperm for longer than eggs that were fertilized, I compensated for variation in the sizes of egg targets and in the time of exposure to sperm: collisions were standardized by the time of sperm-egg exposure and by the area of egg cross-section, yielding a final unit of collisions/s/mm$^2$. Because the data showed a skewed distribution, I used a 4th-root transformation to de-emphasize non-normality (Downing, 1981), then regressed transformed standardized collisions on 4th-root transformed sperm concentration using a least-squares regression to ascertain relationships between the two variables. I performed two such regressions—first regressing standardized collisions on the sperm concentrations that I quantified, and then regressing standardized collisions on 60% of the quantified sperm concentration. The second method was based on the observation (Levitan, 2000) that about 40% of *L. variegatus* sperm are inactive on microscope slides in the laboratory.

### *Fertilization assays*

I assayed fertilization across a gradient of sperm concentration represented by seven serial dilutions (Farley and Levitan, 2001). I extracted eggs and sperm from dissected *L. variegatus* gonads, adjusted egg concentration to about 200 eggs/ml, and exposed eggs from each female to seven serial dilutions of sperm from a single male. Ten seconds after adding sperm to each vial, I added 5 ml of 0.55 *M* KCl and swirled vials to ensure thorough mixing. Potassium chloride immobilizes sperm without interrupting the development of fertilized eggs (Schuel, 1984), and it does not induce fertilization in unfertilized eggs.

After incubating the vials in running seawater in a wet table for 2 h following the introduction of KCl, I counted at least 200 eggs from each vial, scoring each egg as fertilized or unfertilized. The 2-h wait allowed embryos to develop to the two- or four-cell stage, making fertilized/developed eggs distinct from unfertilized eggs. I collected data from 17 male-female urchin pairs, using urchins whose gametes were not used in videotaped observations of sperm-egg interactions.

### *Predictions of sperm-egg collisions*

I predicted collisions of sperm to eggs using the portion of the VCCW model designed for this purpose (Eq. 1, above). I generated two sets of predictions. In the first set, the collision rate constant ($\beta_0$, estimated as $v\sigma$) was estimated using absolute sperm swimming speed ($v$ = 0.2 mm/s, Levitan, unpubl. data) and the diameter of eggs without jelly coats (0.0994 mm, Farley and Levitan, 2001). This yielded $\beta_0$ = 0.00155 mm$^3$/s. In the second set of predictions, the rate of forward advance of the helix ($v$ = 0.027 mm/s) was used in place of absolute sperm velocity, and the area of helical cross-section (0.00190 mm$^2$) was added to the egg target size (Eq. 4 above). This yielded $\beta_0$ = 0.000261. In both cases, $t$ was set equal to 10 s and $E_0$ to 0.001 eggs/$\mu$l. Predicted collisions were standardized by time of exposure and egg target size, and the predictions were 4th-root-transformed to make them comparable to the empirical data. I then plotted both predictions and empirical data as a function of sperm concentration and used analyses of covariance to search for congruence between the two.

### *Estimation of fertilization efficiency*

I fitted fertilization assay data to the Styan (1998) model using SAS (1996; proc nlin) to estimate the fertilization rate constant $\beta$ for *L. variegatus* eggs with intact jelly coats. Sperm velocity was set equal to the rate of forward helical advance ($v$ = 0.027 mm/s). To estimate $\sigma$, the diameter of eggs with intact jelly coats (193.6 $\mu$m; Farley and Levitan, 2001) was used and the area of helical cross-section (0.00190 mm$^2$) was added. This yielded $\sigma$ = 0.0313 and $\beta_0$ = 0.000846. Empirical estimates of $E_0$ were used (0.1–0.28 eggs/$\mu$l), and $t$ was set equal to 10 s to reflect laboratory conditions.

I also fitted fertilization assay data to the Styan (1998) model and estimated the fertilization rate constant $\beta$ for *L.*

*variegatus* eggs without jelly coats. Values for sperm velocity and $\sigma$ were as specified above except that the diameter of eggs without jelly coats (99.4 $\mu$m; Farley and Levitan, 2001) was substituted in estimating $\sigma$, which yielded $\sigma = 0.00966$ and $\beta_0 = 0.000261$. Again, empirical estimates of $E_0$ were used (0.1–0.272 eggs/$\mu$l), and $t$ was set equal to 10 s to reflect laboratory conditions.

Iterating the Styan (1998) model in SAS provided estimates of $\beta$ for eggs with and without jelly coats, and also generated 95% confidence intervals about mean assayed fertilization success for both egg types. I used the estimates of $\beta_0$ above and the iterated estimates of $\beta$ to generate predictions of fertilization success using the Styan (1998) model, and plotted predictions and 95% confidence intervals together to compare model predictions to the data.

## Results

### *Predictions of sperm-egg collision rates*

Sperm concentration was a good predictor of the number of collisions (standardized for time and size differences between targets) between sperm and eggs; increasing sperm concentration yielded increased sperm-egg collision rates in my trials. When standardized collision rates were plotted as a function of sperm concentration, variation in sperm concentration explained 27% of the variation in collision rates (Fig. 1A; $y = 0.279x + 0.127$; $r^2 = 0.270$; $P < 0.0001$). However, the empirical collision rate is significantly lower than that predicted by the VCCW model [ANCOVA; $r^2 = 0.859$; $P$(interaction term) $< 0.0001$].

Because I estimated sperm concentration by counting killed sperm on a hemacytometer, I may have overestimated the proportion of active spermatozoa in my samples. About 40% of *Lytechinus variegatus* sperm on microscope slides are inactive (Levitan, 2000). To determine whether variation in sperm concentration could be driving differences between empirical and predicted sperm-egg collision rates, I plotted the predicted and empirical numbers of collisions (adjusted by target size and area) as a function of 60% of the estimated sperm concentration (Fig. 1B). This also yielded a significant positive relationship ($y = 0.317x + 0.127$; $r^2 = 0.270$; $P < 0.0001$), which was greater in slope but similar in intercept than the relationship in Figure 1A. By accounting for dead sperm, I reduced the disparity between the slope predicted by the model and the slope of empirical data, but the empirically estimated collision rate was still significantly lower than the VCCW model predicted [ANCOVA; $r^2 = 0.859$; $P$(interaction term) $< 0.0001$].

The power of the VCCW model to predict sperm-egg collisions (Eq. (1) above) improved when I substituted the helical rate of advance for the absolute sperm swimming velocity and added the helical cross-section to the egg target size. I plotted standardized sperm-egg collision rate as a function of 60% sperm concentration (Fig. 2), and used the parameters of the helix to generate a predicted collision rate. Empirical collision rate was similar to model predictions [ANCOVA, $r^2 = 0.585$; $P$(sperm concentration) $< 0.0001$; $P$(data type: empirical or predicted) $= 0.692$; $P$(sperm concentration $\times$ data type) $= 0.261$], indicating that the VCCW model accurately predicted rates of encounter between sperm and eggs when helical sperm swimming was considered.

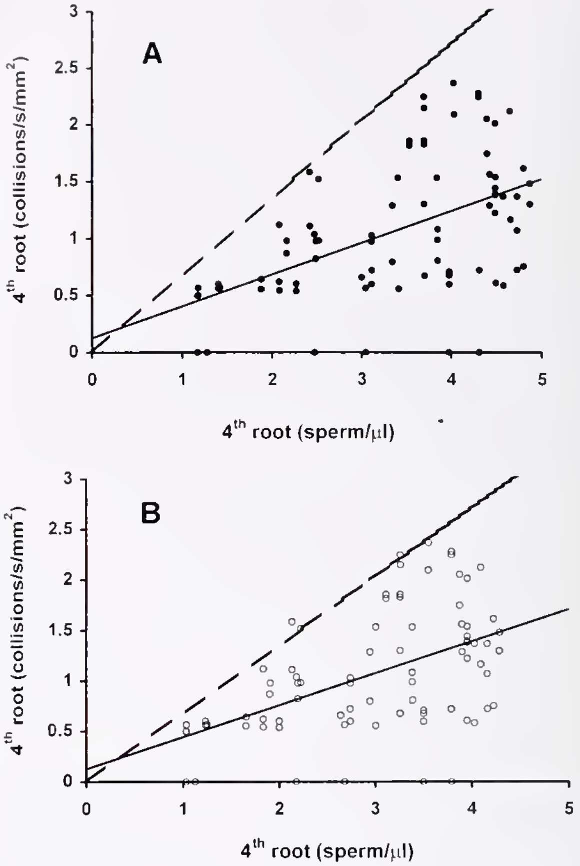

**Figure 1.** Sperm-egg collision rates as a function of sperm concentration. Predicted rates (dashed line) are compared to empirical data (solid line). The collision rates predicted by the VCCW model (Eq. 1 in text) using absolute sperm swimming velocity were significantly greater than the observed rates, whether the latter were based on counts of killed sperm on a hemacytometer (A: closed circles) or calculated by plotting the empirical data against 60% of the empirical sperm concentration to account for dead sperm in laboratory trials (B: open circles).

### *Estimation of fertilization efficiency*

I fitted empirical data to Styan's (1998) model to estimate fertilization efficiency in *L. variegatus* eggs with intact jelly coats. Using $\beta_0 = 0.000846$ to reflect helix parameters resulted in a value of 0.000070 for $\beta$, making $\beta/\beta_0 = 0.0827$. Predictions using $\beta/\beta_0 = 0.0827$ fell within the 95% confidence interval about empirical fertilization rates

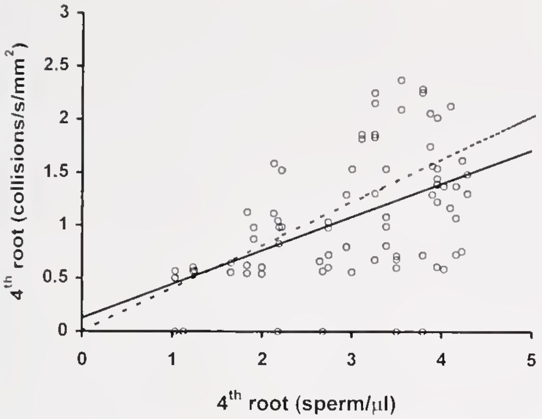

**Figure 2.** As in Figure 1, with empirical data (open circles, solid line) plotted against 60% of empirical sperm concentration. Dashed line: Collision rate predicted by the VCCW model (Eq. 1 in the text), using the rate of forward progression of sperm swimming through a helix. The model predictions are similar to the data.

for *L. variegatus* eggs with intact jelly coats in the laboratory (Fig. 3A).

To estimate $\beta$ for eggs without jelly coats, I fitted an estimate of $\beta_0 = 0.000261$ and empirical fertilization data to Styan's (1998) model. This yielded an estimate of $\beta = 0.000044$, and $\beta/\beta_0 = 0.169$. Again, predictions of fertilization success fell within the 95% confidence interval about empirical fertilization rates for *L. variegatus* eggs without jelly coats in the laboratory (Fig. 3B).

## Discussion

Consideration of the helical nature of sperm swimming significantly improves the ability of the VCCW model (and the Styan (1998) model, which is derived from the VCCW model) to predict sperm-egg collisions. Adjusting sperm velocity in fertilization-kinetics models to reflect the rate of helical advance, rather than the absolute speed of sperm in the water, adjusting egg "target size" ($\sigma$) to reflect the diameter of the helix, and adjusting sperm concentration to reflect dead sperm in laboratory conditions, all contribute to significant improvements in the accuracy with which sperm-egg collision rates are predicted.

An improved understanding of sperm swimming may affect our understanding of sperm viability. In fertilization kinetics models (Vogel *et al.*, 1982; Styan, 1998), the quantity $\beta/\beta_0$ is interpreted as the quantity of viable sperm, or as the proportion of colliding sperm that initiate fertilization ("fertilization efficiency"; Styan, 1998; Styan and Butler, 2000). Typical estimates of $\beta/\beta_0$ from laboratory data range from 0.01 to 0.1, indicating that 1%–10% of sperm are thought to be viable (see, *e.g.*, Vogel *et al.*, 1982; Levitan, 1993; Styan and Butler, 2000; Farley and Levitan, 2001). The highest recorded value of $\beta/\beta_0$ for eggs with intact jelly coats is 0.17 (the sea urchin *Strongylocentrotus droebachiensis*, Levitan, 1993).

In this study, incorporating helical swimming characteristics into estimates of sperm-egg collision rates increases $\beta/\beta_0$. For *Lytechinus variegatus* eggs with intact jelly coats, the previous estimate of $\beta/\beta_0$ was 0.0119 (Farley and Levitan, 2001). Incorporating helical parameters into the Styan (1998) fertilization-kinetics model increased $\beta/\beta_0$ to 0.0827, a 7-fold increase in the estimate of fertilization efficiency for this species. Among *L. variegatus* eggs without jelly coats, the increase is similar: $\beta/\beta_0$ is increased from 0.0284 (Farley and Levitan, 2001) to 0.169. This constitutes a 6-fold increase in fertilization efficiency.

When sperm swim through a helix, their rate of forward progress is much less than their absolute swimming speed: in *L. variegatus*, the rate of forward progress (0.027mm/s) is an order of magnitude less than the absolute swimming

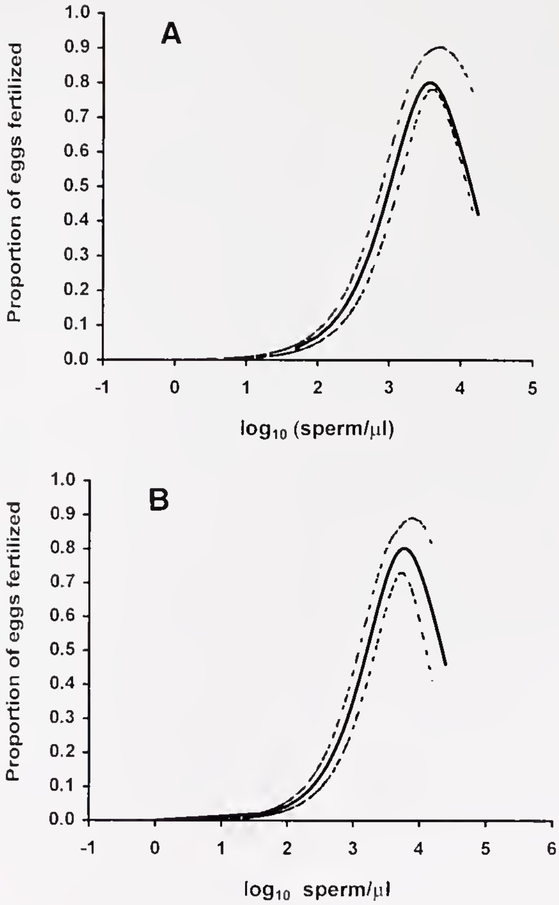

**Figure 3.** Fertilization success in *Lytechinus variegatus* eggs, plotted as a function of sperm concentration, for eggs with intact jelly coats (A), and for eggs without jelly coats (B). Dashed lines: upper and lower 95% confidence intervals about mean fertilization in laboratory assays. Heavy solid lines: predicted fertilization using helical sperm velocity and a newly fitted value for fertilization efficiency ($\beta/\beta_0 = 0.368$). Reducing sperm swimming velocity to reflect helical swimming prompts a reappraisal of fertilization efficiency in this species.

speed (0.2 mm/s). The fact that the lower, helical-advance velocity results in a higher fertilization efficiency may be a mathematical artifact of model fitting, or it may indicate that sperm swimming "architecture" is adaptive. In spatially explicit, three-dimensional computer simulations of helically swimming and randomly moving sperm (Farley, 1999), helically swimming sperm that collide with eggs take less time to "find" eggs than do randomly swimming sperm (although helical swimmers find eggs less frequently than do random swimmers when sperm are more than 100 $\mu$m from eggs). Because sperm expire quickly, particularly at low concentration (Levitan *et al.*, 1991), the time that sperm need to collide with an egg may be critical to fertilization.

The movement of sperm in nature is probably more strongly affected by turbulent mixing of the water column than by sperm swimming (Denny, 1988; Denny and Shibata, 1989). Here, I have measured the helical parameters of sperm swimming in still water, a condition that is probably rare in nature. This raises the possibility that helical swimming is a hydrodynamic constraint imposed on small swimming bodies. However, if turbulent motion were sufficient for fertilization, then we would expect little variation in the swimming characteristics of sperm. Inverse relationships between egg size and absolute sperm swimming speed in congeneric urchins (Levitan, 1993) suggest that sperm swimming is important, even if only at very small spatial scales, and that it might be shaped by natural selection.

If sperm swimming is adaptive (Levitan, 2000), selection may act on sperm swimming to maximize the probability of fertilization. Variation in flagellar motion can affect the characteristics of the helix through which sperm swim (Brokaw, 1962; Crenshaw, 1993a, b). Flagellar motion depends on the number and placement of proteins (dynein) on the microtubules that make up flagellae (Alberts *et al.*, 1989), so genetic mutation may affect helix characteristics, and such quantities as the rate of forward progress and the diameter of the helix may be subject to variation and selection. Moreover, unlike variation in egg size and number, there is no *a priori* reason to suspect trade-offs between helix characteristics and other characteristics of sperm, such as abundance or longevity. Investigators interested in selection on gamete traits should consider the helical nature of sperm swimming and variations in helix characteristics, as well as variation in egg size and number.

## Acknowledgments

I thank the two anonymous reviewers who thoughtfully critiqued the manuscript. This research was supported by an NSF grant to D.R. Levitan, who also provided the SAS model for estimating $\beta$. The FSU Marine Laboratory donated space and materials to the project.

## Literature Cited

**Alberts, B., D. Bray, J. Lewis, M. Raff, K. Roberts, and J. D. Watson. 1989.** *The Molecular Biology of the Cell*, 2nd ed. Garland Publishing, New York.

**Babcock, R. C., and C. N. Mundy. 1992.** Reproductive biology, spawning and field fertilization rates of *Acanthaster planci*. *Aust. J. Mar. Freshw. Res.* **43:** 525–534.

**Babcock, R., C. Mundy, J. Keesing, and J. Oliver. 1992.** Predictable and unpredictable spawning events: *in situ* behavioural data from free-spawning coral reef invertebrates. *Invertebr. Reprod. Dev.* **22:** 213–228.

**Babcock, R. C., C. N. Mundy, and D. Whitehead.** 1994. Sperm diffusion models and *in situ* confirmation of long-distance fertilization in the free-spawning asteroid *Acanthaster planci*. *Biol. Bull.* **186:** 17–28.

**Benzie, J. A. H., and P. Dixon. 1994.** The effects of sperm concentration, sperm: egg ratio, and gamete age on fertilization success in crown-of-thorns starfish (*Acanthaster planci*) in the laboratory. *Biol. Bull.* **186:** 139–152.

**Benzie, J. A. H., K. P. Black, P. J. Moran, and P. Dixon. 1994.** Small-scale dispersion of eggs and sperm of crown-of-thorns starfish (*Acanthaster planci*) in a shallow coral reef habitat. *Biol. Bull.* **186:** 153–167.

**Brazeau, D. A., and H. R. Lasker. 1992.** Reproductive success in a benthic marine invertebrate, the Caribbean octocoral *Briareum asbestinum*. *Mar. Biol.* **114:** 157–163.

**Brokaw, C. J. 1962.** Studies on isolated flagella. Pp. 269–283 in *Spermatozoan Motility*, D.W. Bishop, ed. American Association for the Advancement of Science, Washington, DC.

**Bullington, W. E. 1925.** A study of spiral movement in the ciliate infusoria. *Arch. Protistenkd.* **50:** 219–274.

**Coma, R., and H. R. Lasker. 1997.** Effects of spatial distribution and reproductive biology on *in situ* fertilization rates of a broadcast-spawning invertebrate. *Biol. Bull.* **193:** 20–29.

**Crenshaw, H. C. 1993a.** Orientation by helical motion. I. Kinematics of the helical motion of organisms with up to six degrees of freedom. *Bull. Math. Biol.* **55:** 197–212.

**Crenshaw, H. C. 1993b.** Orientation by helical motion. III. Microorganisms can orient to stimuli by changing the direction of their rotational velocity. *Bull. Math. Biol.* **55:** 231–255.

**Crenshaw, H. C. 1996.** A new look at locomotion in microorganisms: rotating and translating. *Am. Zool.* **36:** 608–618.

**Crenshaw, H. C., and L. Edelstein-Keshet. 1993.** Orientation by helical motion - II. Changing the direction of the axis of motion. *Bull. Math. Biol.* **55:** 213–230.

**Denny, M. W. 1988.** *Biology and Mechanics of the Wave-Swept Environment*. Princeton University Press, Princeton, NJ.

**Denny, M. W., and M. F. Shibata. 1989.** Consequences of surf-zone turbulence for settlement and external fertilization. *Am. Nat.* **134:** 859–889.

**Denny, M. W., J. Dairiki, and S. Destefano. 1992.** Biological consequences of topography on wave-swept rocky shores: I. Enhancement of external fertilization. *Biol. Bull.* **183:** 220–232.

**Downing, J. A. 1981.** How well does the fourth-root transformation work? *Can. J. Fish. Aquat. Sci.* **38:** 127–129.

**Farley, G. S. 1999.** *Sperm-egg collisions and fertilization in the sea urchin* Lytechinus variegatus. Master's thesis, The Florida State University. 142 pp.

**Farley, G. S., and D. R. Levitan. 2001.** The role of jelly coats in sperm-egg encounters, fertilization success, and selection on egg size in broadcast spawners. *Am. Nat.* **157:** 626–636.

**Gray, J. 1955.** The movement of sea-urchin spermatozoa. *J. Exp. Biol.* **32:** 775–801.

**Gray, J., and G. J. Hancock. 1955.** The propulsion of sea-urchin spermatozoa. *J. Exp. Biol.* **32:** 802–814.

**Grosberg, R. 1987.** Limited dispersal and proximity-dependent mating success in the colonial ascidiam *Botryllus schlosseri*. *Evolution* **45:** 130–142.

**Havenhand, J. N. 1991.** Fertilisation and the potential for the dispersal of gametes and larvae in the solitary ascidian *Ascidia mentula*. *Ophelia* **33:** 1–15.

**Hultin, E. 1956.** Mechanism of fertilization by rate determinations. *Exp. Cell Res.* **10:** 286–293.

**Jennings, H. S. 1901.** On the significance of the spiral swimming of organisms. *Am. Nat.* **35:** 369–378.

**Lasker, H. R., D. A. Brazeau, J. Calderon, M. A. Coffroth, R. Coma, and K. Kim. 1996.** *In situ* rates of fertilization among broadcast spawning gorgonian corals. *Biol. Bull.* **190:** 45–55.

**Levitan, D. R. 1991.** Influence of body size and population density on fertilization success and reproductive output in a free-spawning invertebrate. *Biol. Bull.* **181:** 261–268.

**Levitan, D. R. 1993.** The importance of sperm limitation to the evolution of egg size in marine invertebrates. *Am. Nat.* **141:** 517–536.

**Levitan, D. R. 1996a.** Effects of gamete traits on fertilization in the sea and the evolution of sexual dimorphism. *Nature* **382:** 153–155.

**Levitan, D. R. 1996b.** Predicting optimal and unique egg sizes in free-spawning marine invertebrates. *Am. Nat.* **148:** 174–188.

**Levitan, D. R. 1998.** Does Bateman's principle apply to broadcast-spawning organisms? Egg traits influence *in situ* fertilization rates among congeneric sea urchins. *Evolution* **52:** 1043–1056.

**Levitan, D. R. 2000.** Sperm velocity and longevity trade off each other and influence fertilization in the sea urchin *Lytechinus variegatus*. *Proc. R. Soc. Lond. B* **267:** 531–534.

**Levitan, D. R., and C. M. Young. 1995.** Reproductive success in large populations: empirical measures and theoretical predictions of fertilization in the sea biscuit *Clypeaster rosaceus*. *J. Exp. Mar. Biol. Ecol.* **190:** 221–241.

**Levitan, D. R., M. A. Sewell, and F.-S. Chia. 1991.** Kinetics of fertilization in the sea urchin *Strongylocentrotus franciscanus*: interaction of gamete dilution, age, and contact time. *Biol. Bull.* **181:** 371–378.

**Levitan, D. R., M. A. Sewell, and F. -S. Chia. 1992.** How distribution and abundance influence fertilization success in the sea urchin *Strongylocentrotus franciscanus*. *Ecology* **73:** 248–254.

**Lillie, F. R. 1915.** Studies of fertilization VII: analysis of variations in the fertilizing power of sperm suspensions of *Arbacia*. Biol. Bull. **28:** 229–251.

**Mortensen, T. 1938.** Contributions to the study of the development and larval form of echinoids. *K Dan. Vidensk. Selsk. Biol. Skr.* **7:** 1–59.

**Oliver, J., and R. Babcock. 1992.** Aspects of the fertilization ecology of broadcast spawning corals: sperm dilution effects and *in situ* measurements of fertilization. *Biol. Bull.* **183:** 409–417.

**Pennington, J. T. 1985.** The ecology of fertilization of echinoid eggs: the consequences of sperm dilution, adult aggregation, and synchronous spawning. *Biol. Bull.* **169:** 417–430.

**Rothschild, L., and M. M. Swann. 1951.** The fertilization reaction in the sea-urchin: the probability of a successful sperm-egg collision. *J. Exp. Biol.* **28:** 403–416.

**SAS Institute. 1996.** *SAS/Stat User's Guide*, release 6.03. SAS Institute, Cary, NC.

**Schuel, H. 1984.** The prevention of polyspermic fertilization in sea urchins. *Biol. Bull.* **167:** 271–309.

**Sewell, M. A., and D. R. Levitan. 1992.** Fertilization success in a natural spawning of the dendrochirote sea cucumber *Cucumaria miniata*. Bull. Mar. Sci. **51:** 161–166.

**Styan, C. A. 1998.** Polyspermy, egg size, and the fertilization kinetics of free-spawning marine invertebrates. *Am. Nat.* **152:** 290–297.

**Styan, C. A., and A. J. Butler. 2000.** Fitting fertilisation kinetics models for free-spawning marine invertebrates. *Mar. Biol.* **137:** 943–951.

**Thorson, G. 1950.** Reproduction and larval biology of marine bottom invertebrates. *Biol. Rev.* **25:** 1–45.

**Vogel, H., G. Czihak, P. Chang, and W. Wolf. 1982.** Fertilization kinetics of sea urchin eggs. *Math. Biosci.* **58:** 189–216.

**Yund, P. 1990.** An *in situ* measurement of sperm dispersal in a colonial marine hydroid. *J. Exp. Zool.* **253:** 102–106.

Reference: *Biol. Bull.* **203:** 58–69. (August 2002)

# Evolution of Fast Development of Planktonic Embryos to Early Swimming

JENNIFER M. STAVER AND RICHARD R. STRATHMANN*

*Friday Harbor Laboratories and Department of Zoology, University of Washington,*
*620 University Road, Friday Harbor, Washington 98250*

**Abstract.** Planktonic embryos of marine animals swim at an early stage and age. Although natural selection has apparently favored rapid development of structures for swimming, taxa have not converged on the same, minimal time from first cell division to first swimming. Comparisons of 34 species with planktonic embryos in 10 phyla revealed factors that account for variation in time to swimming. Time to first swimming correlated significantly with time from first to second cleavage (first cell cycle) in analyses of all embryos sampled and separately within the Spiralia and Echinodermata. Time to first swimming also correlated significantly with egg diameter in some clades, but not in all. Correlations between egg diameter and cell cycle duration were low except for the three species of Urochordata. Development to a feeding or nonfeeding larva did not affect time to first swimming beyond effects attributable to egg size. Time to first swimming did not correlate with type of locomotion developed (uniciliated cells, multiciliated cells, or muscle). Nonetheless, differences in locomotion are associated with changes in cell cycle durations prior to swimming. The ratios of time to first swimming and time for first cell cycle suggests that allocation of time to multiplication of cells *versus* differentiation of cells is resolved differently in species with different types of locomotion.

## Introduction

Many marine invertebrates release their eggs individually into the plankton, where each embryo develops with little protection. A common feature of such embryos is rapid development of locomotion. We expect that the factors influencing age and stage at first swimming have influenced the evolution of most animal embryos. Multicellular animals originated and diverged into most major existing clades in the sea, and development *via* small, solitary embryos is inferred to be an ancient and persisting mode of development. We also expect that planktonic development of more recent origin has converged to some extent on similar early swimming. Here we examine the degree of convergence and divergence in rates of development and time to first swimming by comparing diverse planktonic embryos.

Solitary embryos are at risk. Embryos contain rich nutrient stores for predators but are more limited than larvae in means of defense or flight. Although planktonic embryos have extra-embryonic envelopes or coats (Strathmann, 1987), some contain toxins (Lindquist, 1996; McClintock and Baker, 1997), and the plankton may be a safer environment than the bottom, planktonic embryos lack the parental care, protective gel, or tough envelope that shields most benthic embryos. Planktonic embryos are therefore among the least protected and most vulnerable embryos of marine animals.

Sources of mortality for planktonic embryos include predation (Pennington and Chia, 1984); ultraviolet radiation (Morgan and Christy, 1996; Epel *et al.*, 1999); advection from suitable adult habitat (Jackson and Strathmann, 1981); and deposition on the bottom, where risks may be even greater for single embryos. Although mortality rates for planktonic embryos have not been estimated, they are presumably at least as great as those of small larvae (Pennington *et al.*, 1986). Estimates of instantaneous mortality rates for small planktonic larvae are high, ranging from 0.04 to 1.0 per day (Strathmann, 1985; Rumrill, 1990).

There are no obvious benefits from prolonging planktonic embryonic development. Planktonic embryos have limited opportunities for growth or reproduction. Active transport

---

Received 3 December 2001; accepted 25 April 2002.

* To whom correspondence should be addressed. E-mail: rrstrath@u.washington.edu

of dissolved organic molecules from the environment is well documented in larvae (Manahan and Crisp, 1982; Jaeckle and Manahan, 1989; Manahan, 1990) and may be common in embryos (Chia, 1972; DeBurgh and Burke, 1983; Manahan, 1983; Shilling and Bosch, 1994). However, there is little growth before a functional gut develops and feeding begins (Strathmann, 1987; Fenaux *et al.*, 1994).

With no apparent benefit and substantial risk to prolonging planktonic embryonic development, natural selection should favor a reduction in the duration of this high-risk life-history stage (Shine, 1989). Comparisons of early embryonic cell cycle durations of planktonic and protected benthic embryos in several independent evolutionary divergences confirm that cell cycles are shorter in planktonic embryos and that the range of cell cycle durations is less for the planktonic than for the benthic protected embryos (Strathmann *et al.*, 2002). The vulnerability of planktonic embryos is indeed associated with rapid development.

Comparisons also indicate that selection has favored early swimming in development of planktonic embryos. Developmental times prior to first swimming in planktonic embryos are especially short. Planktonic embryos swim at earlier stages than more protected embryos, and the structures in the first locomotory stages are less developed in broadcasting species than in species that brood or deposit egg masses (Strathmann, 1987; Kiørboe and Sabatini, 1994; Satoh, 1994; Strathmann *et al.*, 2002). Development of locomotory cilia is one of the earliest morphogenetic activities of the zygotic genome in diverse planktonic embryos. In spiralian embryos, the trochoblasts are the first cells to differentiate during embryonic development (Kooij *et al.*, 1998). Ciliogenesis is the first zygotically programmed morphogenetic event in sea urchin embryos (Stephens, 1995). First swimming occurs at different stages of development in different planktonic embryos (Strathmann, 1987). Of ciliary swimmers, some asteroids first swim as blastulae, others as gastrulae; spiralians swim before or after gastrulation, or even as veliger larvae. Some must develop muscles, as in the tunicate tadpole. However, in all these groups, planktonic development of single embryos is associated with earlier development of locomotory structures relative to other structures.

Although comparative evidence for advantages to early swimming in planktonic development is strong, the costs and benefits of early swimming, as opposed to passively sinking or floating, are unclear. Swimming, if faster than sinking, could increase encounters with ambush predators (Gerritsen and Strickler, 1977; Gerritsen, 1980), but swimming may also confer some protection against capture by some pelagic predators (Pennington *et al.*, 1986). Moreover, models of vertical swimming by flagellates in a wind-mixed water column (Yamazaki and Kamykowski, 1991) indicate that even the slow upward swimming of sea urchin blastulae (Mogami *et al.*, 1988) should often reduce encounters with benthic predators, relative to the slow downward sinking prior to swimming. The quantitative effects of swimming depend on swimming speed, adjustments in orientation, and rates of turbulent mixing, but first swimming is nevertheless an important life-history event. Prior to swimming, these embryos drift passively. Most sink slowly in still water, while some larger embryos float upwards. When they begin to swim, they can adjust their position in the water column (Yamazaki and Kamykowski, 1991; Eckman *et al.*, 1994; Kelman and Emlet, 1999; Metaxas, 2001). First swimming marks a transition into a new set of capabilities and selective pressures.

To examine trade-offs and constraints that limit the evolution of rapid embryonic development, we examined time to swimming of disparate, distantly related planktonic embryos. We took similarity in time as a measure of convergence. We investigated egg size, cell cycle duration, type of locomotion, and larval nutrition as factors that could account for the variation. Correlations of these factors with time to first swimming then point to limits on convergence of distantly related embryos.

### *Egg size*

Some studies have reported longer times to swimming in species with larger eggs (*e.g.*, tunicates: Berrill, 1935; copepods: McLaren, 1966; fish: Duarte and Alcaraz, 1989; gastropods: Kohn and Perron, 1994). Others have found no relationship (echinoids: Dickie *et al.*, 1989; asteroids: Hoegh-Guldberg and Pearse, 1995; copepods: Kiørboe and Sabatini, 1995). Berrill (1935) and McLaren (1966) interpreted exceptions to the trend of longer times with larger eggs as the result of differences in "yolkiness," as indicated by optical density. Berrill (1935) also found a significant correlation between egg size and cell cycle duration in tunicates, which could partially explain the correlation he found between egg diameter and time to swimming. Among species that swim with cilia, time to first swimming might correlate with egg diameter if larger embryos need more cilia for propulsion (Emlet, 1994) and if there is a time constraint to building many cilia.

### *Cell cycle duration*

The duration of the first cell cycle (first to second cleavage) may correlate with time to first swimming if cell multiplication is a primary factor limiting rapid development to swimming. The first cell cycle is among the fastest in an animal's life history. The durations of other early cell cycles are nearly proportional to the durations of this first cell cycle; thus the first cell cycle is representative of others in early development, within a species at different temperatures (Dettlaff, 1964) or between closely related species (Schneider *et al.*, 1992). Although there is some early transcription of the zygotic genome in at least some planktonic embryos (Davidson, 1986), the earliest cell cycles of diverse rapidly developing embryos include synthesis of new DNA and mitosis without measurable gap phases (Murray and Hunt, 1993). Differences in early cell cycle duration may result from constraints or trade-offs at a molecular level (Strathmann *et al.*, 2002).

### *Type of locomotion*

Planktonic embryos swim in disparate ways, using very different structures (Chia *et al.*, 1984). The locomotory structures at first swimming can be very conservative traits, unchanged in many lineages since the divergence of phyla and classes. Echinoderms swim as uniformly ciliated blastulae or gastrulae with only one cilium on each cell. Most spiralians (annelids, molluscs, nemerteans, etc.) form specialized regions of cilia for propulsion, with many cilia on each cell. Other animals, such as tunicates and crustaceans, start to swim using muscle. The type of locomotory structure that an embryo differentiates might affect the time for development to a swimming stage. For example, embryos with many cilia per cell might be expected to swim with fewer cells and perhaps earlier than embryos that have only one cilium per cell. Conversely, embryos that incorporate multiciliated cells into specialized swimming structures (*e.g.*, ciliated bands or ctene rows) might be expected to take longer to construct their swimming apparatus than embryos that swim with simple, uniciliated cells. Animals that swim with muscles might be expected to swim later than those that use cilia, because they must develop more complex tissues.

### *Mode of larval nutrition*

Some embryos develop into larvae that swim and feed in the plankton. Others form nonfeeding larvae and rely primarily on nutrients stored in the egg for energy (Thorson, 1950). Embryos that develop into feeding larvae might be expected to take longer to develop to swimming if developing feeding structures were to compromise development of early locomotion. Conversely, the benefit of earlier feeding might outweigh other costs of rapid embryonic development and result in earlier swimming. Or there could be no effect of larval feeding because species with feeding larvae and planktonic development start to swim well before they start to feed (Strathmann, 1987).

## Materials and Methods

We investigated the embryonic development of 34 species in 10 phyla (Table 1). Species identification followed Kozloff (1987). Identification of *Henricia leviuscula* and *Henricia* (gray armpit) followed M. Strathmann (pers. comm., 1998). *Henricia* (gray armpit) is an undescribed species with a distinctive color pattern. All animals were collected in the San Juan Archipelago and nearby areas of Washington State and are native to the region. Methods for obtaining eggs and sperm and rearing embryos are described in Strathmann (1987), except that zygotes of *Membranipora membranacea* were obtained by dissection, as in the method for *Phoronis vancouverensis*, and spawning of the protobranch bivalve *Acila castrensis* followed Zardus and Morse (1998).

Inseminated eggs were distributed into ~80 ml of 0.45-$\mu$m filtered seawater. Developing embryos in beakers were incubated in water baths at 10, 14, and 18 °C (accurate to within ± 0.3 °C). Since many embryos did not develop to swimming at 18 °C, data only from 10 °C and 14 °C will be discussed here. Seasonal and geographic comparisons indicate that although temperature tolerances vary within species, there is little acclimation (Fujisawa, 1995; Nomaguchi *et al.*, 1997) or adaptation (Bosch *et al.*, 1987; Hoegh-Guldberg and Pearse, 1995) of development rates. Selection at two temperatures produced little change in duration of pupal stages of fruit flies (Partridge *et al.*, 1994). Nevertheless, temperature acclimations have been reported (copepods: Landry, 1975; Hart and McLaren, 1978; Tester, 1985; echinoids: Johnson *et al.*, 1990). We therefore compared rates for embryos from one region and at two temperatures to avoid unrecognized bias from acclimation or adaptation.

In most cases a sufficient number of embryos was obtained from a single pair of parents (or one self-fertile hermaphroditic parent) to divide between the two temperatures. We limited the number of embryos per beaker so that development rates would not be oxygen limited (Strathmann and Strathmann, 1995). Video cameras mounted on dissecting microscopes over the water baths and a time-lapse recorder recorded development of the embryos. Accuracy in time measurements was limited to 1.5 min.

For each group of embryos, we measured the diameter of about 10 eggs and recorded the mean. For some cases there was more than one spawn, and the spawn means were averaged as an estimate of egg size for the species. In some cases our reported mean egg diameter for a species differs slightly between temperatures because different groups of embryos were observed at each temperature.

Hatching and swimming do not coincide in all species. Polychaetes often incorporate the egg envelope into the larva and thus never truly hatch (Strathmann, 1987). The appendicularean tadpoles hatched and then twitched as long as 45 min before they swam. In all but one species (*Calliostoma ligatum*), we defined first swimming as the time when an embryo moved away from its position, though many rotated in place before swimming. We recorded the time to rotation instead of time to swimming for *C. ligatum*. Trochophores of the gastropod *C. ligatum* rotate in capsules several days at 12 °C before hatching as veligers (Strathmann, 1987). For each treatment of embryos, we recorded the time from first to second cleavage and the time from first

**Table 1**

*Age and stage at first swimming and other features of development for 34 species with planktonic embryos*

| PHYLUM<br>Class<br>*Species* | Mean egg diameter (μm) | | Time from 2-cell to 4-cell (h) | | Time to first swimming (h)[1] | | Type of locomotion[2] | Mode of larval nutrition[3] | Stage at first swimming[4] |
|---|---|---|---|---|---|---|---|---|---|
| | 10 °C | 14 °C | 10 °C (*n*) | 14 °C (*n*) | 10 °C (*n*) | 14 °C (*n*) | | | |
| CNIDARIA | | | | | | | | | |
| *Aglantha digitale* | 142.0 | 136.4 | 1.38 (18) | 0.97 (17) | 10.53 (19) | 7.72 (17) | UC | NF | planula |
| *Mitrocoma cellularia* | 153.1 | 153.1 | 1.28 (15) | 0.85 (15) | 16.73 (15) | 10.77 (15) | UC | NF | planula |
| CTENOPHORA | | | | | | | | | |
| *Pleurobrachia bachei* | 144.0 | | 0.95 (6) | | 28.47 (4) | | MC | F | cydippid |
| NEMERTEA | | | | | | | | | |
| *Micrura alaskensis* | 69.7 | 69.7 | 1.52 (18) | 0.92 (25) | 29.95 (16) | 16.43 (25) | MC | F | blastula* (a) |
| ANNELIDA | | | | | | | | | |
| Polychaeta | | | | | | | | | |
| *Owenia fusiformis* | 68.6 | 71.3 | 0.88 (8) | 0.63 (17) | 29.33 (11) | 18.23 (23) | UC | F | trochophore |
| *Serpula columbiana* | 68.0 | 67.9 | 1.20 (13) | 0.66 (14) | 12.90 (10) | 7.35 (19) | MC | F | trochophore |
| *Arctonoe fragilis* | 75.8 | 75.8 | 1.00 (13) | 0.65 (10) | 9.27 (13) | 6.42 (8) | MC | F | trochophore |
| *Sabellaria cementarium* | 77.5 | 77.5 | 1.58 (9) | 0.92 (5) | 17.28 (8) | 10.72 (5) | MC | F | gastrula* |
| MOLLUSCA | | | | | | | | | |
| Bivalvia | | | | | | | | | |
| *Mytilus trossulus* | 61.2 | 61.2 | 1.22 (13) | 0.75 (8) | 11.28 (13) | 7.02 (10) | MC | F | blastula* |
| *Chlamys hastata* | 68.1 | 67.7 | 1.71 (23) | 1.04 (23) | 27.96 (22) | 17.53 (23) | MC | F | gastrula* |
| *Acila castrensis* | 126.0 | 126.0 | 2.18 (5) | 1.47 (4) | 40.65 (5) | 25.2 (4) | MC | NF | blastula* (b) |
| Polyplacophora | | | | | | | | | |
| *Mopalia muscosa* | 204.7 | 206.0 | 1.37 (9) | 0.80 (7) | 36.30 (18) | 21.12 (8) | MC | NF | gastrula* |
| Gastropoda | | | | | | | | | |
| *Tectura scutum* | 138.2 | 138.2 | 0.87 (10) | 0.55 (9) | 19.77 (10) | 14.72 (10) | MC | NF | trochophore |
| *Calliostoma ligatum* | 233.1 | 233.1 | 1.57 (10) | 1.03 (6) | 41.32 (9)† | 26.13 (5)† | MC | NF | veliger |
| PHORONIDA | | | | | | | | | |
| *Phoronis pallida* | 62.6 | 62.6 | 1.25 (6) | 0.68 (7) | 11.03 (6) | 6.37 (7) | UC | F | blastula (c) |
| BRACHIOPODA | | | | | | | | | |
| *Terebrotalia transversa* | 160.2 | 160.2 | 1.03 (10) | 0.63 (14) | 14.25 (8) | 10.65 (13) | UC | NF | blastula |
| BRYOZOA | | | | | | | | | |
| *Membranipora membranacea* | 60.2 | 59.6 | 1.38 (16) | 0.87 (7) | 32.96 (14) | 18.43 (3) | MC | F | early larva (c) |
| ECHINODERMATA | | | | | | | | | |
| Echinoidea | | | | | | | | | |
| *Strongylocentrotus purpuratus* | 85.8 | 85.8 | 1.95 (8) | 1.40 (7) | 23.63 (11) | 17.12 (9) | UC | F | blastula |
| *Strongylocentrotus franciscanus* | 131.2 | 131.2 | 1.58 (12) | 1.05 (12) | 22.88 (14) | 14.97 (13) | UC | F | blastula |
| *Strongylocentrotus droebachiensis* | 163.4 | 163.4 | 1.48 (22) | 1.09 (12) | 22.25 (29) | 17.22 (13) | UC | F | blastula |
| *Dendraster excentricus* | 130.0 | 130.0 | 1.67 (15) | 0.97 (12) | 23.22 (15) | 13.63 (13) | UC | F | blastula |
| Holothuroidea | | | | | | | | | |
| *Parastichopus californicus* | 191.3 | 191.3 | 2.03 (12) | 1.27 (5) | 40.72 (12) | 25.52 (5) | UC | F | blastula |
| Asteroidea | | | | | | | | | |
| *Luidia foliolata* | 152.0 | 152.0 | 1.93 (7) | 1.13 (11) | 39.92 (10) | 25.63 (11) | UC | F | early gastrula (d) |
| *Orthasterias koehleri* | 148.2 | 148.2 | 2.00 (7) | 1.40 (8) | 39.73 (7) | 27.63 (10) | UC | F | blastula |
| *Evasterias troschelii* | 162.5 | 162.5 | 1.50 (3) | 1.18 (9) | 32.23 (5) | 21.95 (6) | UC | F | blastula |
| *Pisaster ochraceus* | 178.0 | 177.5 | 1.57 (8) | 1.13 (6) | 33.95 (8) | 22.43 (6) | UC | F | blastula |
| *Crossaster papposus* | 796.5 | | 2.03 (5) | | 57.12 (5) | | UC | NF | gastrula (d) |
| *Pteraster tesselatus* | 1175.0 | | 1.68 (6) | | 63.32 (3) | | UC | NF | gastrula (e) |
| *Henricia* (grey armpit) | 1087.0 | | 1.73 (6) | | 65.12 (6) | | UC | NF | gastrula (d) |
| *Henricia leviuscula* | 1342.0 | | 1.98 (8) | | 72.53 (8) | | UC | NF | gastrula (d) |
| Ophiuroidea | | | | | | | | | |
| *Ophiopholis aculeata* | 96.5 | 96.5 | 1.45 (7) | 1 20 (4) | 18.93 (7) | 14.22 (5) | UC | F | blastula |
| UROCHORDATA | | | | | | | | | |
| Appendicularia | | | | | | | | | |
| *Oikopleura dioica* | 76.0 | 76.0 | 0.33 (4) | 0.23 (9) | 8.87 (7) | 6.00 (4) | M | NF | tadpole |
| Ascidiacea | | | | | | | | | |
| *Boltenia villosa* | 155.7 | 156.9 | 0.92 (12) | 0.59 (10) | 30.62 (13) | 18.75 (16) | M | NF | tadpole |
| *Ascidia paratropa* | 169.3 | 167.9 | 1.08 (13) | 0.70 (12) | 45.80 (17) | 28.92 (10) | M | NF | tadpole |

[1] If more than one batch of eggs was observed per species, the mean of the median times to swimming is reported.

[2] UC = uniciliated cells; MC = multiciliated cells; M = muscle.

[3] NF = nonfeeding larvae; F = feeding larvae.

[4] Stages at swimming are from Strathmann (1987) except (a) S. Stricker (Univ. of Washington, pers. comm); (b) Zardus and Morse (1998); (c) R. Zimmer (Univ. of Southern California, pers. comm); (d) unpubl. obs.; (e) Kelman and Emlet (1999).

* Most of the spiralians began to swim as trochophores (with ciliated trochoblasts). Some sources indicate stage with regard to gastrulation.

† Times to rotation are reported for *Calliostoma ligatum*.

cleavage to first swimming for a minimum of 3 and a maximum of 15 embryos. Cleavage furrows were at similar stages for recorded times for first and second cleavage. We did not use time from spawning, fertilization, or egg activation, because the interval between these events and first cleavage includes different developmental events, such as meiotic divisions, in different species.

We used the median times from each treatment to limit the effects of unusually slow embryos. There was little variation among median times within a species at a given temperature. For many species, two or three spawns were recorded at each temperature. The median values for first cell cycle duration and time to first swimming from each treatment were averaged to yield one value per species per temperature for each variable.

For general patterns, we examined the relationship of each variable with time to first swimming in all sampled species with egg diameters less than 250 $\mu$m. To remove the potentially large effect of large eggs in one taxon, the four asteroids with very large eggs were included only in analyses of the Asteroidea. For *C. ligatum*, times to rotation are reported in Table 1 and included in Figures 2–3, but are not included in any of the statistical analyses of time to first swimming.

To discern whether any patterns observed were from a few among-clade differences and also to examine evolutionary patterns repeated among clades, we compared species within narrower clades for each continuous variable (egg diameter and cell cycle duration). These included the Spiralia, Echinodermata, Asteroidea, and Urochordata. For the discrete factors (type of locomotion and mode of larval nutrition), we identified several pairwise comparisons that represent independent evolutionary divergences.

Relationships among many phyla are still uncertain (Adoutte *et al.*, 2000). Ideally, one should compare sister taxa that differ in the trait of interest. Sampling metazoan phyla from one geographic region compared species adapted to a similar environment, but limited the number of species that could be sampled from most phyla. Nonetheless, phylogenetic hypotheses from morphological and molecular data (Halanych *et al.*, 1995; Stechmann and Schlegel, 1999; Adoutte *et al.*, 2000) and distributions of traits suggest that our comparisons represent independent evolutionary divergences (Fig. 1). Though recent evidence suggests the lophophorates are polyphyletic (Halanych *et al.*, 1995), the relationships within the group remain uncertain (Adoutte *et al.*, 2000). On the basis of morphology, however, brachiopods, phoronids, and bryozoans have been grouped together as the Lophophorata (Hyman, 1959). Thus, we included comparisons within the lophophorates.

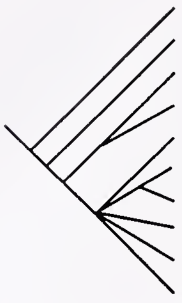

| | Locomotion | Nutrition |
|---|---|---|
| Cnidaria | UC | NF |
| Ctenophora | MC | F |
| Echinodermata | UC | F&NF |
| Urochordata | M | NF |
| Bryozoa | MC | F |
| Brachiopoda | UC | NF |
| Phoronida | UC | F |
| Nemertea | MC | F |
| Annelida | MC&UC | F |
| Mollusca | MC | F&NF |

**Figure 1.** A phylogeny of the phyla used in this study. Type of locomotion and mode of larval nutrition are indicated for species sampled. UC = uniciliated cells; MC = multiciliated cells; M = muscles. NF = nonfeeding larva; F = feeding larva. See text for details of independent evolutionary comparisons.

We examined the effect of type of locomotion on time to first swimming in four comparisons of animals with uniciliated or multiciliated cells: the cnidarians *versus* the ctenophore, other lophophorates *versus* the bryozoan, echinoderms *versus* the Lophotrochozoa with multiciliated cells (the bryozoan, nemertean, annelids, and molluscs), and the oweniid *versus* other polychaetes. Occurrence of uniciliated and multiciliated cells is reviewed by Gardiner (1978) and Nielsen (1995). Urochordates with muscular locomotion provide a fifth independent divergence in locomotory structure. For mode of larval nutrition, we compared species with feeding and nonfeeding larvae within the Mollusca, the Echinodermata, and the Lophophorata, and between the Cnidaria and Ctenophora.

## Results

Time to first swimming, egg diameter, and cell cycle duration are summarized in Table 1. The $Q_{10}$ values (a measure of the increase in rate for each 10 °C rise in temperature) for cell cycle duration and time to first swimming ranged from about 2 to 4. Although the effect of temperature varied greatly among species, general trends in the results were consistent at 10 °C and 14 °C. Moreover, there was little differential effect of temperature on different stages of development: the mean of [(time to swimming)/(time for first cell cycle) at 14 °C]/[(time to swimming)/(time for first cell cycle) at 10 °C] for 29 species was 0.999 ± 0.083 SD ($n$ = 29). This sample of species includes all those observed at both 10 °C and 14 °C. The figures depict data at 10 °C. Similar patterns were observed at 14 °C (Table 2).

Although planktonic embryos first swim at an early stage and young age, they have not converged on a similar minimum time to swimming. For the species with egg diameters less than 250 $\mu$m, the minimum and maximum times to first swimming were 10.5 and 45.8 h at 10 °C and 7.7 and 28.9 h at 14 °C. Two covariates account for about half of the variation in time to first swimming.

Time to first swimming was significantly correlated with both egg diameter and first cell cycle duration overall,

**Table 2**

*Pearson correlations for data shown in Figure 1*

| | 10 °C | | 14 °C | |
|---|---|---|---|---|
| | *r* | *P* | *r* | *P* |
| Time to swimming *vs.* Cell cycle duration | | | | |
| Overall | 0.500 (29) | **0.006** | 0.568 (28) | **0.002** |
| Spiralia | 0.572 (10) | **0.004** | 0.612 (10) | 0.060 |
| Echinodermata | 0.657 (10) | **0.039** | 0.496 (10) | 0.145 |
| Asteroidea | 0.990 (4) 0.381 (8) | **0.010** 0.352 | 0.715 (4) | 0.271 |
| Urochordata | 0.976 (3) | 0.138 | 0.972 (3) | 0.152 |
| Time to swimming *vs.* Egg diameter | | | | |
| Overall | 0.502 | **0.006** | 0.569 | **0.002** |
| Spiralia | 0.530 | 0.115 | 0.564 | 0.089 |
| Echinodermata | 0.675 | **0.032** | 0.632 | 0.050 |
| Asteroidea | −0.772 0.980 | 0.228 **<0.001** | −0.834 | 0.166 |
| Urochordata | 0.959 | 0.182 | 0.940 | 0.222 |
| Cell cycle duration *vs.* Egg diameter | | | | |
| Overall | 0.196 | 0.308 | 0.264 | 0.175 |
| Spiralia | 0.098 | 0.788 | 0.093 | 0.798 |
| Echinodermata | 0.081 | 0.825 | −0.180 | 0.619 |
| Asteroidea | −0.823 0.206 | 0.177 0.625 | −0.607 | 0.393 |
| Urochordata | 0.998 | **0.044** | 0.994 | 0.070 |

Underlined values include the four asteroid species with eggs greater than 250 $\mu$m. Sample sizes are indicated in parentheses for the first comparison and are the same in subsequent analyses. Bold type indicates statistical significance ($P < 0.05$).

though these two factors were not consistently correlated with each other (Fig. 2 and Table 2). In a multiple regression of time to first swimming on egg diameter and cell cycle duration, the combined effect of egg diameter and first cell cycle duration explained approximately half of the variation in time to first swimming (at 10 °C: $r^2 = 0.496$, $P < 0.001$, $n = 27$; at 14 °C: $r^2 = 0.598$, $P < 0.001$, $n = 26$). This regression included all species with eggs less than 250 $\mu$m except the urochordates. The urochordates were not included in this calculation because of their high correlation between egg diameter and cell cycle duration.

### *Cell cycle duration*

Time to first swimming was positively correlated with cell cycle duration (first to second cleavage) in almost all clades, phyla, and classes considered, but the correlation was not always significant (Table 2). The only exception to the trend was within the polychaetes, because *Owenia fusiformis* has an anomalously long time to first swimming. It may have initially benthic development of clustered eggs (unpubl. obs.).

### *Egg size*

Time to first swimming was positively correlated with egg diameter overall and for the Spiralia, Echinodermata, and Urochordata (Table 2). The positive correlation was not significant in the spiralians or urochordates, perhaps because of the small sample sizes. If the times to rotation for *Calliostoma ligatum* are included, the correlation in the spiralians is significant ($r = 0.659$, $P = 0.028$). Overall, time to first swimming was positively correlated with egg diameter when species with feeding and nonfeeding larvae were considered separately (Table 3). The correlation was negative for asteroids with feeding larvae but positive when species with nonfeeding larvae were included, which greatly increased range in egg sizes and times to swimming (Tables 2 and 3). Within the echinoids there was also a negative correlation for the four species with feeding larvae. Again, this may be due to small sample sizes and a narrow range of egg sizes within these groups.

Egg diameter and cell cycle duration were not correlated with each other overall or for the spiralians or echinoderms (Table 2). Within the urochordates, the correlation coefficient for egg diameter and cell cycle duration was high but not significant with the small sample of three species. For the four species of echinoids, the correlation was negative, but sample size and ranges were small.

### *Type of locomotion*

There was no significant difference in time to swimming among species that swim using uniciliated cells, multiciliated cells, or muscle at either temperature (Kruskal-Wallis test, 10 °C: $H = 0.771$, $P = 0.680$; 14 °C: $H = 0.300$, $P = 0.861$). Similarly, there was no consistent pattern

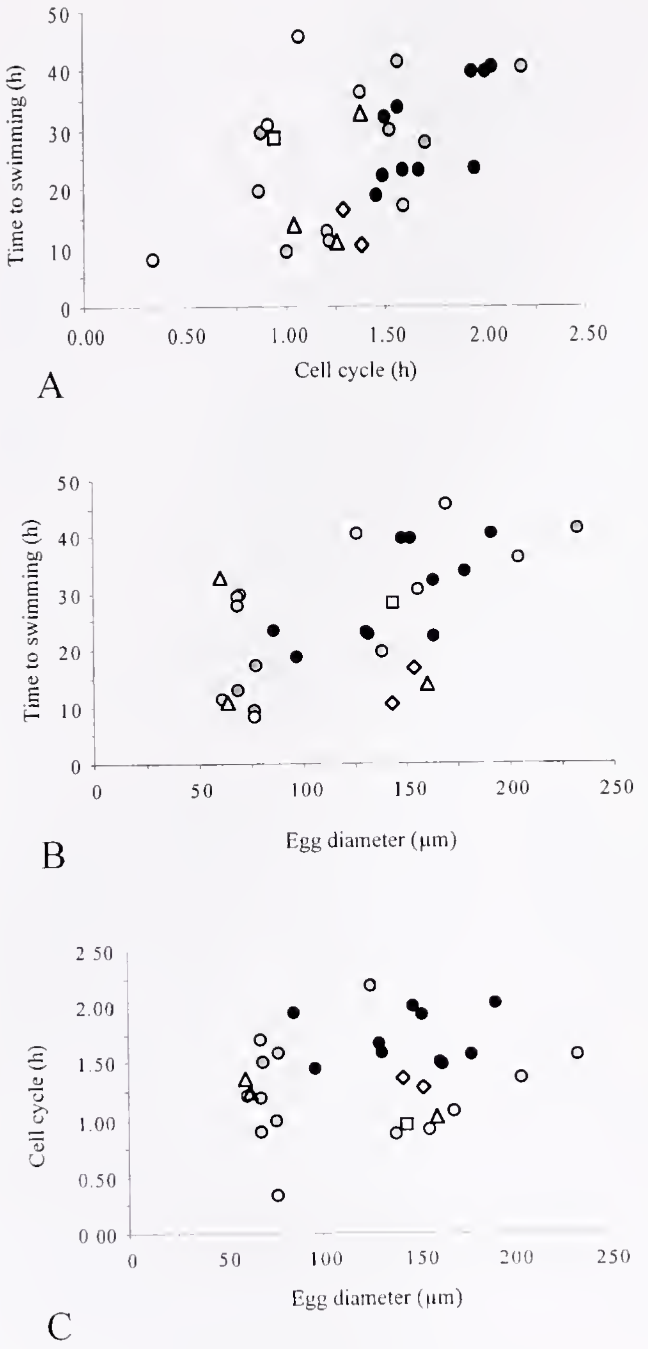

**Figure 2.** Relationships among time to swimming and two continuous variables at 10 °C. Four asteroid species with eggs greater than 250 $\mu$m are not shown. (A) Time to swimming is significantly correlated with cell cycle duration ($P = 0.006$). (B) Time to swimming is significantly correlated with egg diameter ($P = 0.006$). (C) Cell cycle duration is not significantly correlated with egg diameter ($P = 0.308$). Diamonds = Cnidaria; square = Ctenophora; gray circles = Spiralia; triangles = Lophophorata; black circles = Echinodermata; open circles = Urochordata. See Table 2 for statistical analyses.

relating time to first swimming to type of locomotion among pairwise comparisons. The ctenophore with multiciliated cells took 1.7 to 2.7 times longer to develop to swimming than the two cnidarians with uniciliated cells. Within the Lophophorata, the bryozoan with multiciliated cells took 1.7 to 3 times longer to develop to swimming than the phoronid and brachiopod with uniciliated cells. The times to first swimming for echinoderms with uniciliated cells overlapped broadly with those for the Lophotrochozoa with multiciliated cells (echinoderms 18.9 to 40.7 h, lophotrochozoans 9.3 to 40.6 h for 10 °C and eggs less than 250 $\mu$m). The three polychaetes with multiciliated cells developed to swimming 1.7 to 3.2 times faster than the polychaete with uniciliated cells. Two of the three urochordates, which swim with muscle, developed to swimming in the same time as species that first swim with cilia. The cell cycles and egg diameters of groups with muscle, multiciliated cells, and uniciliated cells overlapped broadly (Table 1) indicating that the effects of egg diameter and cell cycle were not obscuring a relation between type of locomotion and time to first swimming. Within the pairwise comparisons, the species with the longest time to swimming in each comparison often had an egg diameter and cell cycle duration toward the lower end of the range of species included in the comparison. (An exception occurred in the lophophorates, in which the bryozoan had the longest time to swimming as well as the longest cell cycle.)

### *Mode of larval nutrition*

Times to first swimming for species with feeding larvae and species with nonfeeding larvae were not significantly different at either temperature (Mann-Whitney test, 10 °C: $U = 95$, $P = 0.115$; 14 °C: $U = 89$, $P = 0.783$). For within-clade comparisons, there was no consistent pattern relating time to swimming to type of larval nutrition. The times to swimming for the two molluscs with feeding overlapped those for the three with nonfeeding larvae. The four echinoderms with nonfeeding larvae took longer to develop to swimming than did the nine with feeding larvae. Within the Lophophorata, the times to first swimming for the feed-

**Table 3**

*Pearson correlations for time to first swimming and egg diameter with feeding or nonfeeding larvae*

| | 10 °C | | 14 °C | |
|---|---|---|---|---|
| | $r$ | $P$ | $r$ | $P$ |
| NF overall | 0.497 (9) | 0.173 | 0.494 (9) | 0.176 |
| F overall | 0.614 (20) | **0.004** | 0.705 (19) | **0.001** |
| F Asteroidea | −0.772 (4) | 0.228 | −0.834 (4) | 0.166 |
| NF Asteroidea | 0.940 (4) | 0.060 | | |

Four asteroid species with eggs greater than 250 $\mu$m are not included except in nonfeeding asteroid analyses. Sample size is in parentheses. Bold type indicates statistical significance ($P < 0.05$). NF = nonfeeding larvae. F = feeding larvae.

ing phoronid and bryozoan bracketed that of the nonfeeding brachiopod. The feeding ctenophore took longer to develop to swimming than the two nonfeeding cnidarians.

The cell cycles of groups with feeding and nonfeeding larvae overlapped broadly, indicating that the effect of cell cycle duration was not obscuring a relation between mode of larval nutrition and time to first swimming. The ctenophore took longer to develop to swimming than the cnidarians but had a shorter cell cycle. The bryozoan took longer to swim than the other lophophorates and had a longer cell cycle. The cell cycles of the feeding and nonfeeding molluscs overlapped.

Apparent effects of larval nutrition, where they occur, may be attributable to effects of egg size. In general, egg diameters of species with feeding and nonfeeding larvae overlapped. Within the lophophorate and cnidarian/ctenophore comparisons, the species with the longest time to swimming had an egg diameter at the lower end of the range of egg diameters in the comparison. However, in comparisons of more closely related species, the nonfeeding bivalve and asteroids took longer to develop to swimming than their within-class relatives with feeding larvae, but they also had larger eggs. Overall, time to first swimming was positively correlated with egg diameter in species with feeding and nonfeeding larvae (Table 3). The trend holds in feeding echinoderms and nonfeeding urochordates (Table 2). (The trend was not significant in the urochordates, perhaps because of the small sample size.) However, in feeding echinoids and feeding asteroids, time to first swimming was not positively correlated with egg diameter. In nonfeeding asteroids, the positive correlation was not significant (Tables 2 and 3). This could be a result of the small sample sizes. In any case, it is difficult to separate any effect of mode of larval nutrition from that of egg diameter.

### *Asteroidea*

In analyses of asteroids with eggs less than 250 $\mu$m in diameter, time to first swimming was significantly correlated with cell cycle but not with egg diameter (Table 2). However, the range of egg diameters in the comparison (30 $\mu$m) may not be large enough to reveal an effect of egg size (Table 1). If the four species with eggs greater than 250 $\mu$m are considered as well, time to first swimming was significantly correlated with egg diameter, but not with cell cycle. In this broader comparison of asteroids, the ranges in egg diameters and time to swimming were much larger, but the range in cell cycle durations was not (Table 1). Cell cycle and egg diameter were not significantly correlated with each other in any of the asteroid comparisons. The asteroids with nonfeeding larvae take almost twice as long to develop to swimming as do the asteroids with feeding larvae, and they have much larger egg diameters.

## Discussion

Time to first swimming correlated with egg diameter overall and within most groups considered. Time to first swimming also correlated with cell cycle duration (first to second cleavage). Cell cycle duration and egg diameter did not correlate with each other in most of the groups we observed. Thus the hypothesis that egg diameter correlates with time to first swimming simply because larger eggs take longer to divide is rejected.

Species with nonfeeding larvae often have larger eggs than species with feeding larvae (Strathmann, 1987). Though egg size often correlated with time to first swimming in this data set, mode of larval nutrition did not correlate with time to first swimming overall or within most groups considered. Limited indications that species with nonfeeding larvae take longer to develop to swimming were confounded with egg size. The relationship between time to first swimming and mode of larval nutrition remains uncertain, and clarification requires additional independent comparisons of related species with feeding and nonfeeding larvae that overlap in egg size. However, the correlation between time to first swimming and egg diameter appears to be independent of the mode of larval nutrition.

Egg diameter correlates with time to first swimming in ciliated swimmers, presumably because there is a time constraint to making cilia and it takes more cilia to propel a larger object through the water (Emlet, 1994). The ciliated species that we observed are almost spherical when they first swim. The diameter of embryos at first swimming increases with egg diameter. At low Reynolds numbers, the drag on a moving sphere increases with the diameter of the sphere (Vogel, 1994). In a ciliated embryo, one might also expect the number of cilia necessary for swimming to increase as the diameter of the embryo increases (Emlet, 1994). In embryos with uniciliated cells, the number of cilia depends on the number of cells, and the limiting factor may be the construction of new cells. In embryos with multiciliated cells, production of cilia still requires time, even if fewer cell divisions are required. In each case, construction of cilia requires the expression of tubulin genes (Tansey and Ruderman, 1983; Gong and Brandhorst, 1988; Damen *et al.*, 1994). Production of more cilia by larger embryos may delay time to swimming, whether each of many cells makes one cilium or each of few cells makes many cilia.

For species that swim with cilia, large egg diameters may delay swimming while other development proceeds. The four asteroids with very large eggs start swimming nearly 20 h later than the slowest asteroid with eggs less than 250 $\mu$m in diameter, and they start to swim as gastrulae rather than as blastulae. Within the Spiralia, species with larger eggs also started swimming at later ages and stages (Table 1).

Cell cycle duration correlated with time to first swimming

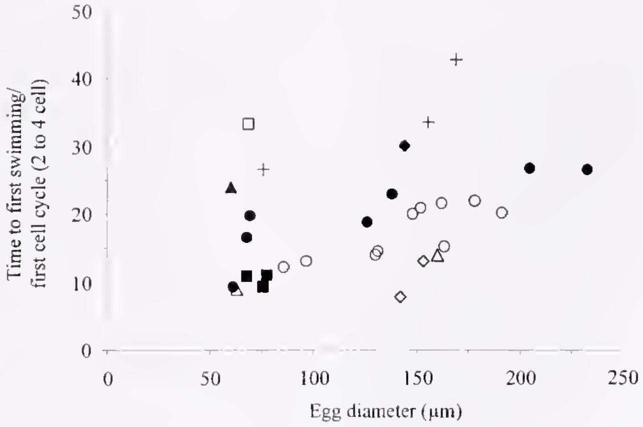

**Figure 3.** Relationship between the extrapolated maximum number of cell cycles prior to swimming (if all were as brief as the first cell cycle) and egg diameter. Data from 10 °C. Open symbols = uniciliated cells; filled symbols = multiciliated cells; + = muscle. Groups of taxa within these categories are indicated by diamonds = Cnidaria and Ctenophora; squares = Polychaeta; triangles = Lophophorata; + = Urochordata; circles = other species (open = Echinodermata; filled = Mollusca, Nemertea).

overall and within most groups considered. The simplest explanation for this pattern is that the number of cells embryos need to swim determines time to first swimming. The duration of the first cell cycle (first to second cleavage) gives an indication of the maximum speed at which a species' egg can be divided into cells. In general, cell cycles slow as development progresses and transcription increases. If, however, embryos continued to multiply cells at the same rate as in the first cell cycle in all cell lineages, the maximum number of cells at first swimming would be $2^n$, where $n$ is the extrapolated number of cell cycles (time to first swimming divided by first cell cycle duration).

These extrapolated maximum cell numbers at swimming range over 10 orders of magnitude in this sample of species. When these extrapolated cell numbers are plotted against egg diameter, the embryos cluster by type of locomotion (Fig. 3). If the cell cycles of *Ascidia paratropa*, an ascidian, continued from fertilization to swimming at the initial rate, the tadpole would have approximately one trillion cells (an average of ~41 cell divisions in a cell lineage) at swimming—an absurdly large number. *Aglantha digitale*, a cnidarian, would have only 200 cells (an average of ~8 divisions in a cell lineage)—a remarkably small number. In general, for a particular egg size, if species sustained their initial rates of cell division through development to swimming, species with uniciliated cells would have fewer cells than those with multiciliated cells, which would have fewer cells than the animals that swim with muscle (Fig. 3). Instead, cell cycles appear to lengthen differentially.

Estimates of cell number indicate that species that swim with different equipment lengthen their cell cycles differently prior to swimming. The number of cells in tadpole larvae of solitary ascidians is fairly constant among species (Yamada and Nishida, 1999). Thus, *Boltenia villosa* and *Ascidia paratropa* probably have approximately 2500–3000 cells at first swimming, implying that, on average, cell lineages undergo only 11 or 12 divisions instead of the projected maximum number of 32 and 42 respectively. Cell cycles lengthen to different extents in other species. Cell counts in two echinoids with uniciliated cells that start swimming as simple blastulae suggest relatively little lengthening of cell cycles. *Dendraster excentricus* has approximately 1200–1500 cells at swimming (K. Tanaka, pers. comm., Univ. of Washington, 2000). *Strongylocentrotus purpuratus* has approximately 350 cells at swimming (Hinegardner, 1967). In each echinoid, the embryos completed about 70% of the maximum number of cell cycles projected. Estimates of cell numbers at first swimming in species with multiciliated cells suggest that they may be intermediate to the echinoderms and urochordates in lengthening later cell cycles (E. Edsinger-Gonzales, pers. comm., Univ. of Utrecht, 2000; Morrill, 1982).

These results point to differences in allocation of time to multiplying compared with differentiating cells that are associated with different means of achieving early swimming. Preliminary comparisons of number of cells at first swimming suggest that animals that first swim as very simple embryos, such as echinoids and cnidarians, may spend a large fraction of their time simply dividing cells, because they have little need for cell differentiation. Species that swim with multiciliated cells often incorporate their cilia into specialized swimming structures. These animals may spend less time simply multiplying cells and more time differentiating them, than do species with uniciliated cells. Similarly, animals that start swimming using muscles (*e.g.*, tunicates, chaetognaths, crustaceans, and fish) may spend even more time differentiating cells relative to multiplying them. Urochordates appear to invest a large proportion of their development time prior to swimming in processes other than multiplying cells. Indeed, developmental studies suggest the neural tube is the only tissue with continuing cell division after gastrulation. Muscle and notochord lineages stop dividing after the 9th cell cycle and differentiate (Nishida, 1997). Cell counts for other animals at first swimming could test the hypothesis that mode of locomotion affects a trade-off between differentiation and multiplication of cells.

In our sample of animals with planktonic development, the urochordates had the shortest cell cycles at a given time to first swimming. The short cell cycles and other developmental devices permit swimming as a tadpole (with muscles, notochord, and nerves) as early as other animals swim as a hollow ball of ciliated cells. Selection for early swimming with muscles may have selected for especially short early cell cycles in the urochordates. Comparisons with other planktonic embryos that develop muscles for first swimming, as in copepods and chaetognaths, could test the hypothesis that short early cell cycles have generally evolved as part of rapid development to swimming with muscles.

The high correlation between egg diameter and cell cycle duration in the urochordates, though nonsignificant in this sample of three species, is consistent with past studies (Berrill, 1935). If egg size and cell cycle duration are correlated only for embryos with the shortest cell cycles, then possibly egg size does set the lowest limits on early cell cycle durations. The rate of these concentrated cell divisions may be limited by cellular factors related to egg size, for example, construction of the cytoskeleton; and evolution may have shortened the early cell cycles to a limit imposed by egg size. However, asteroids with eggs that are larger by a factor of 6 have cell cycles that are only twice as long as those of urochordates (Table 1).

The combined effect of egg diameter and early embryonic cell cycle explained nearly half of the variation in time to swimming in this diverse group of animal embryos. Many factors could account for the remaining variation. Differences in vulnerability among embryos may explain some of the variation. Protected embryos begin swimming at a later age and stage than their less protected relatives (Strathmann *et al.*, 2002). Though among the least protected of marine invertebrate embryos, planktonic embryos differ in buoyancy, extra-embryonic membranes, and chemical defenses (Szollosi, 1969; Lucas *et al.*, 1979; Strathmann, 1987; Young, 1995; Lindquist, 1996; McClintock and Baker, 1997).

Within several groups, related animals start to swim at very different ages and stages. In planktonically developing gastropods, for example, both *Tectura scutum* and *Calliostoma ligatum* have formed trochophores when their cilia start to beat. However, *T. scutum* swims as a trochophore nearly a day before *C. ligatum* starts to rotate in its capsule, and it rotates in its capsule for several days before hatching as a veliger. The planktonically developing abalones, such as *Haliotis kamtschatkana*, also hatch as trochophores (Strathmann, 1987). *Tegula funebralis* (like *C. ligatum* a trochoidean from the northeast Pacific) has a 1-h cell cycle from first to second cleavage at 13–15 °C (like *C. ligatum*) but hatches as a pretorsional veliger at 40 h, a much earlier stage and age than for *C. ligatum* (Moran, 1997). Perhaps the egg capsule of *C. ligatum* provides protection that relieves selection for early swimming. Rotation of *C. ligatum* in its capsule for several days before hatching suggests that early ciliary motion may have benefits other than swimming. Ancestral benthic development may account for the long time to first swimming for the free-spawning *C. ligatum*. Some species of trochoidean gastropods have benthic egg masses, and others have individual planktonic embryos (Hadfield and Strathmann, 1990). Evolutionary transitions between benthic egg masses and single planktonic embryos could have occurred many times in this group. More extensive comparisons could test the hypothesis that a late stage at hatching of a planktonic embryo is associated with a more protected development in the ancestry.

Times to first swimming for diverse embryos of distantly related species were remarkably similar. The comparisons presented here represent extremely ancient divergences among clades of animals. The structures formed for first swimming are highly disparate. Nonetheless, major structural and functional differences in embryos and larvae appear to have little influence on embryonic durations. Instead, egg size and cell cycle length appear to most reliably predict times to swimming for these animals. However, as discussed above, the trade-offs and devices that allowed such convergence in times to swimming have shaped the development and life histories of major groups of metazoans. The evolution of early swimming is associated with the evolution of cell cycle durations, timing of transcription and differentiation in cell lineages, parental investment in protection of offspring, developmental stage at first locomotion, and first locomotory capabilities.

## Acknowledgments

National Science Foundation grants OCE-9633193 and IBN-0113603 and the Friday Harbor Laboratories of the University of Washington supported this research. We are grateful to D. O. Duggins, E. Edsinger-Gonzales, G. Freeman, D. Grunbaum, S. Y. Henderson, M. B. Hille, J. R. Hoffman, P. Hohenlohe, E. V. Iyengar, M. D. Lamare, C. C. Lambert, G. Lambert, J. B. Marcus, C. E. Mills, G. M. Odell, D. K. Padilla, S. Santagata, J. L. Schwartz, C. Staude, M. F. Strathmann, S. A. Stricker, B. J. Swalla, K. Tanaka, and others at the Friday Harbor Laboratories for discussion of hypotheses or for expert advice and help with obtaining and rearing a wide variety of embryos.

## Literature Cited

**Adoutte, A., G. Balavoine, N. Lartillot, O. Lespinet, B. Prud'homme, and R. de Rosa. 2000.** The new animal phylogeny: reliability and implications. *Proc. Nat. Acad. Sci. USA* **97:** 4453–4456.

**Berrill, N. J. 1935.** Studies in tunicate development. Part iii. Differential retardation and acceleration. *Philos. Trans. R. Soc. Lond. B Biol. Sci.* **225:** 255–326.

**Bosch, I., K. A. Beauchamp, M. E. Steele, and J. S. Pearse. 1987.** Development, metamorphosis, and seasonal abundance of embryos and larvae of the Antarctic sea urchin *Sterechinus neumayeri. Biol. Bull.* **173:** 126–135.

**Chia, F.-S. 1972.** Note on the assimilation of glucose and glycine from seawater by the embryos of a sea anemone, *Actinia equina. Can. J. Zool.* **50:** 1333–1334.

**Chia, F. S., J. Buckland-Nicks, and C. M. Young. 1984.** Locomotion of marine invertebrate larvae: a review. *Can. J. Zool.* **62:** 1205–1222.

**Damen, W. G. M., L. A. van Grunsven, and A. E. van Loon. 1994.** Transcriptional regulation of tubulin gene expression in differentiating trochoblasts during early development of *Patella vulgata. Development* **120:** 2835–2845.

**Davidson, E. H. 1986.** *Gene Activity in Early Development*, 3rd ed. Academic Press, Orlando, FL. 670 pp.

**DeBurgh, M. E., and R. D. Burke. 1983.** Uptake of dissolved amino acids by embryos and larvae of *Dendraster excentricus* (Eschscholtz) (Echinodermata: Echinoidea). *Can. J. Zool.* **61:** 349–354.

**Dettlaff, T. A. 1964.** Cell divisions, duration of interkinetic states and differentiation in early stages of embryonic development. *Adv. Morphog.* **3:** 323–362.

**Dickie, L., M. Hart, and R. Helling. 1989.** Pre-feeding larval development time is not correlated with egg size in regular echinoids (*Strongylocentrotus* species). *Invertebr. Reprod. Dev.* **15:** 229–232.

**Duarte, C. M., and M. Alcaraz. 1989.** To produce many small or few large eggs: a size independent reproductive tactic of fish. *Oecologia* **80:** 401–404.

**Eckman, J. E., F. E. Werner, and T. F. Gross. 1994.** Modelling some effects of behavior on larval settlement in a turbulent boundary layer. *Deep-Sea Res. II.* **41:** 185–208.

**Emlet, R. B. 1994.** Body form and patterns of ciliation in nonfeeding larvae of echinoderms: functional solutions to swimming in the plankton? *Am. Zool.* **34:** 570–585.

**Epel, D., K. Hemela, M. Shick, and C. Patton. 1999.** Development in the floating world: defenses of eggs and embryos against damage from UV radiation. *Am. Zool.* **39:** 271–278.

**Fenaux, L., M. F. Strathmann, and R. R. Strathmann. 1994.** Five tests of food-limited growth of larvae in coastal waters by comparisons of rates of development and form of echinoplutei. *Limnol. Oceanogr.* **39:** 84–98.

**Fujisawa, H. 1995.** Variation in embryonic temperature sensitivity among groups of the sea urchin, *Hemicentrotus pulcherimmus*, which differ in their habitats. *Zool. Sci.* **12:** 583–589.

**Gardiner, S. L. 1978.** Fine structure of the ciliated epidermis on the tentacles of *Owenia fusiformis* (Polychaeta Oweniidae). *Zoomorphologie* **91:** 37–48.

**Gerritsen, J. 1980.** Adaptive responses to encounter problems. Pp. 52–62 in *Evolution and Ecology of Zooplankton Communities*, W. C. Kerfoot, ed. The University Press of New England, Hanover, NH.

**Gerritsen, J., and J. R. Strickler. 1977.** Encounter probability and community structure in zooplankton: a mathematical model. *J. Fish. Res. Board Can.* **34:** 73–82.

**Gong, Z., and B. P. Brandhorst. 1988.** Multiple levels of regulation of tubulin gene expression during sea urchin embryogenesis. *Dev. Biol.* **130:** 144–153.

**Hadfield, M. G., and M. F. Strathmann. 1990.** Heterostrophic shells and pelagic development in trochoideans: implications for classification, phylogeny, and paleoecolgy. *J. Molluscan Stud.* **56:** 239–256.

**Halanych, K. M., J. D. Bacheller, A. M. Aguinaldo, S. M. Liva, D. M. Hills, and J. A. Lake. 1995.** Evidence from 18S ribosomal DNA that the lophophorates are protostome animals. *Science* **267:** 1641–1643.

**Hart, R. C., and I. A. McLaren. 1978.** Temperature acclimation and other influences on embryonic duration in the copepod *Pseudocalanus* sp. *Mar. Biol.* **45:** 23–30.

**Hinegardner, R. T. 1967.** Echinoderms. P. 148 in *Methods in Developmental Biology*, F. J. Wilt and N. K. Wessels, eds. Crowell-Collier, New York.

**Hoegh-Guldberg, O., and J. S. Pearse. 1995.** Temperature, food availability, and the development of marine invertebrate larvae. *Am. Zool.* **35:** 415–425.

**Hyman, L. H. 1959.** *The Invertebrates*. Vol. 5. McGraw Hill, New York. 783 pp.

**Jackson, G. A., and R. R. Strathmann. 1981.** Larval mortality from offshore mixing as a link between precompetent and competent periods of development. *Am. Nat.* **118:** 16–26.

**Jaeckle, W. B., and D. T. Manahan. 1989.** Growth and energy imbalance during the development of a lecithotrophic molluscan larva (*Haliotis rufescens*). *Biol. Bull.* **177:** 237–246.

**Johnson, L. G., J. E. Chenoweth, and B. L. Bingham. 1990.** Population differences and thermal acclimation in temperature responses of developing sea urchin embryos. *Proc. S. D. Acad. Sci.* **69:** 99–108.

**Kelman, D., and R. B. Emlet. 1999.** Swimming and buoyancy in ontogenetic stages of the cushion star *Pteraster tesselatus* (Echinodermata: Asteroidea) and their implications for distribution and movement. *Biol. Bull.* **197:** 309–314.

**Kiørboe, T., and M. Sabatini. 1994.** Reproductive and life cycle strategies in egg-carrying cyclopoid and free-spawning calanoid copepods. *J. Plankton Res.* **16:** 1353–1366.

**Kiørboe, T., and M. Sabatini. 1995.** Scaling of fecundity, growth and development in marine planktonic copepods. *Mar. Ecol. Prog. Ser.* **120:** 285–298.

**Kohn, A. J., and F. E. Perron. 1994.** *Life History and Biogeography: Patterns in* Conus. Clarendon Press, Oxford. 106 pp.

**Kooij, A. van der, C. P. W. M. Veraart, and A. E. van Loon. 1998.** Cyclin A, cyclin B and stringlike are regulated separately in cell cycle arrested trochoblasts of *Patella vulgata* embryos. *Dev. Genes Evol.* **207:** 524–534.

**Kozloff, E. N. 1987.** *Marine Invertebrates of the Pacific Northwest*. University of Washington Press, Seattle. 511 pp.

**Landry, M. R. 1975.** Seasonal temperature effects and predicting development rates of marine copepod eggs. *Limnol. Oceanogr.* **20:** 434–440.

**Lindquist, N. 1996.** Palatability of invertebrate larvae to corals and sea anemones. *Mar. Biol.* **126:** 745–755.

**Lucas, J. S., R. J. Hart, M. E. Howden, and R. Salathe. 1979.** Saponins in eggs and larvae of *Acanthaster planci* (L.) (Asteroidea) as chemical defenses against planktivorous fish. *J. Exp. Mar. Biol. Ecol.* **40:** 155–165.

**Manahan, D. T. 1983.** The uptake of dissolved glycine following fertilization of oyster eggs (*Crassostrea gigas* Thunberg). *J. Exp. Mar. Biol. Ecol.* **68:** 53–58.

**Manahan, D. T. 1990.** Adaptations by invertebrate larvae for nutrient acquisition from seawater. *Am. Zool.* **30:** 147–160.

**Manahan, D. T., and D. J. Crisp. 1982.** The role of dissolved material in the nutrition of pelagic larvae: amino acid uptake by bivalve veligers. *Am. Zool.* **22:** 635–682.

**McClintock, J. B., and B. J. Baker. 1997.** Palatability and chemical defense of eggs, embryos, and larvae of shallow-water Antarctic marine invertebrates. *Mar. Ecol. Prog. Ser.* **154:** 121–131.

**McLaren, I. A. 1966.** Predicting development rate of copepod eggs. *Biol. Bull.* **131:** 457–469.

**Metaxas, A. 2001.** Behaviour in flow: perspectives on the distribution and dispersion of meroplanktonic larvae in the water column. *Can. J. Fish. Aquat. Sci.* **58:** 86–98.

**Mogami, Y., C. Oohayashi, T. Yamaguchi, Y. Osigo, and S. A. Baba. 1988.** Negative geotaxis in sea urchin larvae: a possible role of mechanoreception in the late stage of development. *J. Exp. Biol.* **137:** 141–156.

**Moran, A. L. 1997.** Spawning and larval development of the black turban snail *Tegula funebralis* (Prosobranchia: Trochidae). *Mar. Biol.* **128:** 107–114.

**Morgan, S. G., and J. H. Christy. 1996.** Survival of marine larvae under the countervailing selective pressures of photodamage and predation. *Limnol. Oceanogr.* **41:** 498–504.

**Morrill, J. B. 1982.** Development of the pulmonate gastropod, *Lymnaea*. Pp. 399–483 in *Developmental Biology of Freshwater Invertebrates*, F. W. Harrison and R. R. Cowden, eds. Alan R. Liss, New York.

**Murray, A. W., and T. Hunt. 1993.** *The Cell Cycle: an Introduction*. W. H. Freeman, New York. 251 pp.

**Nielsen, C. 1995.** *Animal Evolution.* Oxford University Press, Oxford. 467 pp.

**Nishida, H. 1997.** Cell lineage and timing of fate restriction, determination and gene expression in ascidian embryos. *Semin. Cell Dev. Biol.* **8:** 359–365.

**Nomaguchi, T. A., C. Nishijima, S. Minowa, M. Hashimoto, C. Haraguchi, S. Amemiya, and H. Fujisawa. 1997.** Embryonic thermosensitivity of the ascidian, *Ciona savignyi. Zool. Sci.* **14:** 511–515.

**Partridge, L., B. Barrie, K. Fowler, and V. French. 1994.** Thermal evolution of pre-adult life history traits in *Drosophila melanogaster. J. Evol. Biol.* **7:** 645–663.

**Pennington, J. T., and F. S. Chia. 1984.** Morphological and behavioral defenses of trochophore larvae of *Sabellaria cementarium* (Polychaeta) against four planktonic predators. *Biol. Bull.* **167:** 168–175.

**Pennington, J. T., S. S. Rumrill, and F. S. Chia. 1986.** Stage-specific predation upon embryos and larvae of the Pacific sand dollar, *Dendraster excentricus,* by 11 species of common zooplanktonic predators. *Bull. Mar. Sci.* **39:** 234–240.

**Rumrill, S. S. 1990.** Natural mortality of marine larvae. *Ophelia* **32:** 163–198.

**Satoh, N. 1994.** *Developmental Biology of Ascidians.* Cambridge University Press, Cambridge. 254 pp.

**Schneider, S., A. Fischer, and A. W. C. Dorresteijn. 1992.** A morphometric comparison of dissimilar early development in sibling species of *Platynereis* (Annelida, Polychaeta). *Roux's Arch. Dev. Biol.* **201:** 243–256.

**Shilling, F. M., and I. Bosch. 1994.** 'Pre-feeding' embryos of antarctic and temperate echinoderms use dissolved organic material for growth and metabolic needs. *Mar. Ecol. Prog. Ser.* **109:** 173–181.

**Shine, R. 1989.** Alternative models for the evolution of offspring size. *Am. Nat.* **134:** 311–317.

**Stechmann, A., and M. Schlegel. 1999.** Analysis of the complete mitochondrial DNA sequence of the brachiopod *Terebratulina retusa* places Brachiopoda within the protostomes. *Proc. R. Soc. Lond.* **266:** 2043–2052.

**Stephens, R. E. 1995.** Ciliogenesis in sea urchin embryos- a subroutine in the program of development. *BioEssays* **17:** 331–341.

**Strathmann, M. F., ed. 1987.** *Reproduction and Development of Marine Invertebrates of the Northern Pacific Coast.* University of Washington Press, Seattle. 670 pp.

**Strathmann, R. R. 1985.** Feeding and nonfeeding larval development and life history evolution in marine invertebrates. *Annu. Rev. Ecol. Syst.* **16:** 339–361.

**Strathmann, R. R., and M. F. Strathmann. 1995.** Oxygen supply and limits on aggregation of embryos. *J. Mar. Biol. Assoc. UK* **75:** 413–428.

**Strathmann, R. R., J. M. Staver, and J. R. Hoffman. 2002.** Risk and the evolution of cell cycle durations of embryos. *Evolution* **56:** 708–720.

**Szollosi, D. 1969.** Unique envelope of a jellyfish ovum: the armed egg. *Science* **163:** 586–587.

**Tansey, T. R., and J. V. Ruderman. 1983.** Differential mRNA accumulation and translation during *Spisula* development. *Dev. Biol.* **99:** 338–351.

**Tester, P. A. 1985.** Effects of parental acclimation temperature and egg-incubation temperature on egg-hatching time in *Acartia tonsa* (Copepoda: Calanoida). *Mar. Biol.* **89:** 45–53.

**Thorson, G. 1950.** Reproductive and larval ecology of marine bottom invertebrates. *Biol. Rev.* **25:** 1–45.

**Vogel, S. 1994.** *Life in Moving Fluids: the Physical Biology of Flow,* 2nd ed. Princeton University Press, Princeton. 352 pp.

**Yamada, A., and H. Nishida. 1999.** Distinct parameters are involved in controlling the number of rounds of cell division in each tissue during ascidian embryogenesis. *J. Exp. Zool.* **284:** 379–391.

**Yamazaki, H., and D. Kamykowski. 1991.** The vertical trajectories of motile phytoplankton in a wind-mixed water column. *Deep-Sea Res.* **38:** 219–241.

**Young, C. M. 1995.** Behavior and locomotion during the dispersal phase of larval life. Pp. 249–277 in *Ecology of Marine Invertebrate Larvae,* L. McEdward, ed. CRC Press, Boca Raton, FL.

**Zardus, J. D., and M. P. Morse. 1998.** Embryogenesis, morphology and ultrastructure of the pericalymma larva of *Acila castrensis* (Bivalvia: Protobranchia: Nuculoida). *Invertebr. Biol.* **117:** 221–244.

Reference: *Biol. Bull.* **203:** 70–79. (August 2002)

# Immunocytochemically Defined Populations of Neurons Progressively Increase in Size Through Embryogenesis of *Hydra vulgaris*

GORDON B. BRUMWELL[1] AND VICKI J. MARTIN[2]

*Department of Biological Sciences, University of Notre Dame, Notre Dame, Indiana 46556*

**Abstract.** The hydra nervous system shares many features with nervous systems of more complex organisms but serves as a unique model system due to its simplicity and constant regeneration. Development of neuron populations during and after hydra embryogenesis is not well understood. In this study, neurons were identified at prehatching and posthatching stages with RFamide or JD1 antisera. These populations were further subdivided into ganglion, sensory, or unclassifiable neurons, and all identified populations were statistically analyzed over developmental time. RFamide-positive neurons appeared 20 days after the cuticle formed around the embryo. The JD1-positive neuron population appeared just after hatching, but by adulthood it had surpassed the size of the RFamide-positive population. All neuron populations progressively increased through their adult levels. Density of most of the populations, however, did not. For instance, during the 5-fold increase in size that the hydra experienced between 5 days posthatching and adulthood, the number of RFamide-positive neurons rose approximately 2-fold and the number of JD1-positive neurons 4-fold. However, the density of neurons in each of these populations fell. These data do not support the hypothesis that large-scale culling of neurons during development, frequently found in other animals, occurs in hydra.

## Introduction

Cnidarian nervous systems are simple nervous systems with relatively few neurons and synapses (Grimmelikhuijzen *et al.*, 1988; Spencer, 1989, 1995). However, individual cnidarian neurons and synapses exhibit many characteristics of more advanced systems. These commonalities include multiple immunochemically defined neuronal subsets (including subsets reactive to RFamide antisera and to the monoclonal antibody (Ab) JD1) and the presence of chemical and electrical synapses, action potentials, temporal and spatial summation, and miniature end-plate potentials (Roberts and Mackie, 1980; Grimmelikhuijzen *et al.*, 1980, 1982; Dunne *et al.*, 1985; Grimmelikhuijzen, 1985; Kerfoot *et al.*, 1985; Yu *et al.*, 1986; Fraser *et al.*, 1987; Anderson and Spencer, 1989; Green, 1989; Spencer, 1989; Umbriaco *et al.*, 1990; Sakaguchi *et al.*, 1996; Westfall, 1996). Thus, cnidarians are useful for studying basic nervous system phenomena such as development and synaptic transmission in isolation from the added complexity of large numbers of neurons. Hydra are a particularly good model in which to study nervous system development because they have a few easily observed morphologically and immunochemically defined neuron types.

Adult hydra continually develop and integrate numerous subsets of neurons. This ongoing development occurs by continual translocation of the neurons along the body length axis, which in turn is due to the continual translocation of the tissues in which the neurons are embedded (Campbell, 1966, 1974; Bode *et al.*, 1988a). Some of the neuronal subsets have been defined by their immunoreactivities (Grimmelikhuijzen, 1983a, 1984; Koizumi *et al.*, 1992). For instance, immunoreactivity to the neuropeptide FMRFamide is broadly distributed in cnidarians and has been detected in the head (in both the hypostome and tentacles), base, and body column of hydra (Grimmelikhuijzen, 1983b; Grimmelikhuijzen *et al.*, 1989). Antisera to the RFamide carboxyterminus of FMRFamide (Grimmelikhuijzen and Graff, 1985) yield a similar staining pattern. However, FMRFamide is not the only neuropeptide ending in RF-

---

Received 2 August 2001; accepted 10 April 2002.

[1] To whom correspondence should be addressed. E-mail: gordon.b.brumwell.1@nd.edu

[2] Present address: Department of Biology, Appalachian State University, Boone, North Carolina 28608.

amide in hydra (Mitgutsch *et al.*, 1999). In adult *Hydra magnipapillata*, three separate genes code for four different carboxyterminus RFamides (Mitgutsch *et al.*, 1999). Although the RFamide genes are expressed in different subpopulations of neurons, RFamide immunoreactivity coincides with the total distribution of expression of the three genes (Grimmelikhuijzen and Graff, 1985; Mitgutsch *et al.*, 1999). Thus, RFamide Ab detects a family of RFamide-positive neurons.

Neurons identified by markers other than RFamide can show different staining and developmental patterns in adult hydra. The monoclonal Ab JD1 recognizes an uncharacterized antigen (Dunne *et al.*, 1985), and though the JD1 and RFamide Abs both recognize neurons, the distribution of their immunoreactivities is not identical. For instance, whereas RFamide antisera label neurons in the head, base, and body column in *Hydra vulgaris* (Grimmelikhijzen, 1983b, 1985), JD1 stains neurons only in the head and base of *Hydra oligactis* (Dunne *et al.*, 1985). This may simply be an interspecific difference, however. Also, the hypostomal nerve ring of *H. oligactis* contains neurons that are both RFamide-positive and JD1-positive, but although all JD1-positive neurons are RFamide-positive, the opposite is not true (Koizumi *et al.*, 1992).

Though hydra are generally known as animals that reproduce by budding, some also reproduce sexually. Sexual reproduction in hydra involves gametogenesis that results in external eggs, spermaries, or both, and is followed by external fertilization, development of a spherical embryo (initially attached to the mother), addition of a protective cuticle, and hatching (Martin, 1997; Martin *et al.*, 1997). Cuticle deposition is complete 48 h after fertilization; the cuticle stage lasts between 2 and 24 weeks (Martin *et al.*, 1997). Two days before hatching, two distinct layers of cells appear in the embryo (Martin *et al.*, 1997). This subphase of the cuticle stage is termed the minus-2-d stage. At hatching, the hydra, which has not yet formed tentacles, is roughly cigar-shaped and is described as being in the cigar stage. Complete embryonic development can take as little as about 3 weeks or as long as about 25 weeks. The tentacle bud stage begins when tentacle formation is apparent—as early as 15 min after hatching—and lasts until the animal is 1 day old.

The architecture and development of the nervous system and the distribution of neuronal subpopulations have been extensively studied in the adult hydra but not in the embryonic animal. It is known that neurons appear 2 d prior to hatching in maceration studies of sequentially aged hydra embryos (Martin *et al.*, 1997). At that stage, RFamide-positive neuron clusters are found at both the head and base ends (Martin, 1997). A better, and quantitative, understanding of when neuron subpopulations arise and how their pool sizes change during and after embryogenesis is important because it will help frame questions about relationships between neuronal subsets and about relationships between neuronal subsets and development itself.

The population dynamics of developing nervous systems throughout the animal kingdom display culling *via* programmed cell death (PCD) (Galliresta and Resta, 1992). Virtually all developing vertebrate nervous systems use this mechanism, which in many subpopulations is so prevalent that about half the neurons undergo PCD (Burek and Oppenheim, 1996; Sastry and Rao, 2000). PCD is also found in developing nervous systems of invertebrates. In the larval moth *Manduca sexta*, 10% to 70% of the neurons in the central nervous system (CNS) undergo PCD, and eclosion of the adult is followed by PCD of up to 50% of the CNS neurons (Booker *et al.*, 1996; Ewer *et al.*, 1998). Flies, nematodes, grasshoppers, and leeches also exhibit neuronal PCD (Stewart *et al.*, 1987; Shankland and Martindale, 1989; Robinow *et al.*, 1993; Sanders and Wride, 1995). Finally, PCD of peptidergic neurons has been observed in the fly and the moth (Ewer *et al.*, 1998; Draizen *et al.*, 1999). Apoptosis, a type of PCD, has recently been reported to result in the loss of the whole interstitial cell lineage in a hydra mutant (Cikala *et al.*, 1999). The same paper also identifies two enzymes belonging to the caspase 3 family of asparate-specific cysteinyl proteases, and holds that both are apparently expressed in all hydra cell types (Cikala *et al.*, 1999). Because caspase activity is associated with apoptosis in nematodes, flies, and mammals (Cikala *et al.*, 1999), the presence of caspases in all hydra cell types suggests all these cells, including neurons, have the capacity to undergo apoptosis. Given that culling of developing nervous systems is widespread in the animal kingdom and that all hydra cells are apparently capable of PCD, it is interesting that PCD (or culling as an indicator of PCD) has not been reported for the developing nervous system of any part of the hydra's life history. Perhaps large-scale PCD occurs in hydra neuroembryogenesis, as it does in many other embryonic systems. If so, an indicator that this is occurring would be a significant decrease in neuron numbers at some point in nervous system development. Therefore, we characterized the development of the RFamide-positive and JD1-positive neuron subpopulations of hydra embryos, posthatching hydra, and adults to understand their population dynamics. This is the first study in which subpopulations of neurons in sexually derived hydra have been studied over developmental time.

## Materials and Methods

Stock cultures of *Hydra vulgaris* were maintained in "hydra" water (1 m*M* $CaCl_2$, 1.5 m*M* $NaHCO_3$, 0.1 m*M* $MgCl_2$, 0.08 m*M* $MgSO_4$, and 0.03 m*M* $KNO_3$ in double-distilled water, pH 7.0) at 18°C on a cycle of 12 h of light and 12 h of dark. The female hydra strain, designated PA2, was isolated from a pond on the Haverford College campus near Philadelphia, Pennsylvania. The male strain, CA7, was collected from Boulder Creek, near Susanville, California. Embryos were obtained by placing spermary-carrying males with egg-carrying females. Embryos were cut from the mother with a surgical knife after the formation of the protective cuticle, placed in petri dishes of hydra water, and allowed to develop. Adult hydra were fed once a week with the brine shrimp *Artemia salina*, and the medium was changed twice a week. The following pre-adult stages were stained to characterize the temporal distribution of the JD1-positive and RFamide-positive neurons ($n = 5$ for single staining, $n = 1$ for double staining): embryos that had formed cuticles 10 d earlier (10-d cuticles), 20-d cuticles, minus-2-d cuticles, cigar stage, tentacle bud stage, and 5-d-old hatchlings. For the JD1 study, the adults stained were gameteless CA7 *H. vulgaris*. For the RFamide study, gameteless adult *H. vulgaris* from CA7/PA2 crosses were stained. This adult stock was created by allowing the hydra resulting from sexual crosses to bud, thus creating genetic clones of hatchlings. Adults were starved at least 48 h before fixing, and the younger animals were never fed.

Wholemounts of the aforementioned developmental stages were stained for RFamide, the JD1 antigen, or dual (RFamide and JD1) immunoreactivity. Staining with the anti-RFamide polyclonal Ab was based on the procedure of Bode *et al.* (1988b), and staining with the monoclonal Ab JD1 was based on the procedure of Dunne *et al.* (1985). Because the protocols are very similar, they are presented together, with any variations noted. All cuticled stages were fixed in Zamboni's fixative (2.0% paraformaldehyde and 0.2% picric acid in 0.1 *M* phosphate buffer, pH 7.0) for the RFamide procedure or in Lavdowsky's fixative (50 units ethanol:10 formalin:4 acetic acid:40 $ddH_2O$) for the JD1 procedure for 2–3 h, then placed in phosphate-buffered saline (PBS; 0.15 *M* NaCl, 0.008 *M* $Na_2HPO_4$, and 0.002 *M* $NaH_2PO_4 \cdot H_2O$, pH 7.0), where the cuticles were surgically removed from the embryos with a scalpel. All post-hatching hydra were relaxed for 1–2 min in 2% urethane in hydra water. De-cuticled embryos were then further fixed, and posthatching relaxed hydra were fixed for the first time (overnight, 7 °C). After fixation, all animals were treated sequentially as follows (room temperature (21 °C) at 80 rpm on an orbital shaker unless otherwise noted): PBS-Tween (0.05% Tween 80 in PBS; 3 × 20 min for RFamide procedure, 3 × 10 min for JD1 procedure); 0.4 *M* glycine, pH 7.0 (1 h, RFamide procedure only); PBS-Triton (0.25% Triton X-100 in PBS; 3 × 20 min for RFamide procedure, 3 × 10 min for JD1 procedure); 10% fetal bovine serum (FBS) (in 0.1% $NaN_3$ in PBS, pH 7.0; overnight, 7 °C); primary antiserum (overnight, 7 °C; RFamide antiserum 146 III (Grimmelikhuijzen, 1985) diluted 1:1000 in 0.1 *M* PBS, pH 7.2, containing 0.05% Tween 80 and 0.25% human serum albumin or JD1 monoclonal Ab (Dunne *et al.*, 1985)); PBS-Triton (3 × 20 min); secondary Ab (in total dark as were all subsequent incubations, 1 h, FITC conjugated goat anti-rabbit IgGs 1:60 in 10% FBS for RFamide procedure and FITC conjugated goat anti-mouse IgGs 1:50 in 10% FBS for JD1 procedure (Boehringer Mannheim)); PBS-Triton (3 × 20 min); and PBS (10 min). Wholemounts from cigar stage through adult were double-stained for RFamide and JD1 in a procedure similar to that of Koizumi *et al.* (1992). The first half of the procedure was the same as that for RFamide staining except that the primary Ab was JD1 and the secondary Ab was that used in the JD1 procedure. The second half of the double-staining procedure was the RFamide staining procedure (beginning with the incubation in RFamide antisera), except that the secondary Ab was rhodamine-conjugated goat anti-rabbit IgG and diluted 1:600. Controls for the single-staining procedures included omission of the primary Ab. Also, adult hydra were stained as controls with all younger stages in both the single- and double-staining procedures.

The positive-staining ganglion, sensory, and unclassifiable neurons were counted (JD1 also stained interstitial cells and nematoblasts, but only the neuron work is presented here). After staining, each hydra was placed in mounting medium (5% *n*-propyl gallate and 50% glycerin in PBS) and between two coverslips (the coverslip-hydra-coverslip sandwich was attached to the microscope slide by a drop of oil). Because each sandwich could be flipped over, both sides of a hydra were equally visible under the microscope, thus allowing the number of positive-staining neurons in each animal to be counted (Zeiss IV FL epi-fluorescence condenser, 450–490 nm and 546 nm filters). After the neurons in an animal were counted, the area of the body was measured with Universal Imaging's Image-1 software. Densities were then calculated for each neuron type at each stage. Sizes of each neuron population, densities of each population, and the sizes of the animal itself (in square millimeters) were compared among the developmental stages *via* one-way ANOVA and Tukey's honestly significant difference *post-hoc* test. Also, the total (ganglion cells + sensory cells + unclassifiable neurons) number of RFamide-positive neurons was compared to the total number of JD1-positive neurons, and the density of the total RFamide-positive population was compared to the density of the total JD1-positive population at each stage. These pairs of RFamide-positive and JD1-positive total neuron numbers or total neuron population densities within a stage were compared *via* *t* tests run as independent and not assuming equal variances. Differences were considered significant at $P \leq 0.05$.

## Results

The total number of RFamide-positive neurons and the total number of JD1-positive neurons increased throughout the hydras' development (Fig. 1a). In contrast, the total densities of each population increased, then decreased (Fig.

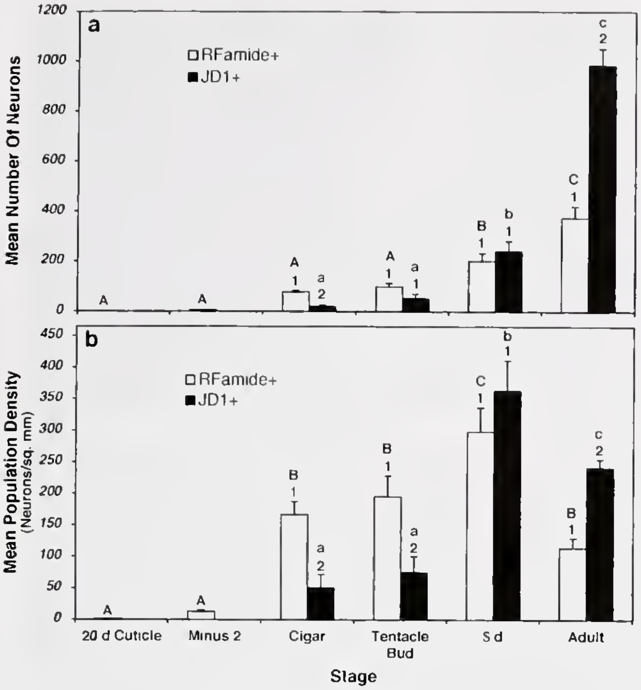

**Figure 1.** Mean (±standard error of the mean (SEM)) total numbers (a) and population densities (b) of RFamide-immunoreactive neurons and JD1-immunoreactive neurons in different developmental stages of *Hydra vulgaris* ($n = 5$). One-way ANOVA for RFamide-positive neurons across all stages and for JD1-positive neurons across the last four stages showed significant differences (for number of RFamide-positive neurons $F = 36.75$, df $= 5$, $P = 0.001$; for number of JD1-positive neurons $F = 129.39$, df $= 3$, $P = 0.001$; for density of RFamide-positive neuron population $F = 23.67$, df $= 5$, $P = 0.001$; for density of JD1-positive neuron population $F = 24.52$, df $= 3$, $P = 0.001$). Results of *post-hoc* Tukey's honestly significant difference tests are indicated with letters (uppercase for RFamide results and lower case for JD1 results). Within-stage differences between the RFamide-positive population and the JD1-positive population were compared for each of the last four stages *via t* tests. The cigar stage (separate variances $t = 8.79$, df $= 8$, and $P = 0.001$) and adult (separate variances $t = -7.61$, df $= 7$, $P = 0.001$) each showed a significant difference between the total RFamide-positive population and the total JD1-positive neuron population. The cigar stage (separate variances $t = 3$, df $= 8$, and $P = 0.001$), tentacle bud stage (separate variances $t = 2.88$, df $= 7$, and $P = 0.02$), and adult (separate variances $t = -6.27$, df $= 8$, and $P = 0.001$) also each showed a significant difference between the two neuron population densities. Results of the $t$ test are indicated by numbers. Bars that share a letter or number within the range of an ANOVA or $t$ test are not significantly different ($P > 0.05$).

1b). All significant changes in the number of RFamide-positive neurons and in the number of JD1-positive neurons were increases (Fig. 1a). The density of each population declined significantly after the 5-d stage (Fig. 1b). The RFamide-positive population was initially more numerous and dense than the JD1-positive population, but the ratios later reversed such that the JD1-positive population was more numerous and dense (Fig. 1). In the cigar stage, the numbers of RFamide-positive neurons exceeded those of JD1-positive neurons significantly, but the adult stage showed the opposite with JD1-positive neurons significantly more prevalent. Similarly, in the cigar stage the RFamide-positive population was significantly more dense than the JD1-positive neuron population but the adult showed the opposite result.

RFamide-positive neurons were not present in the 10-d cuticle stage but were in every stage examined thereafter. They were first seen in some of the 20-d cuticle stage hydra, and in later stages both the number of RFamide-positive neurons and the complexity of the RFamide-positive nerve net increased (Figs. 1, 2a–c). However, the size of the RFamide-stained hydra did not increase until after the 5-d stage. Areas of the pre-adult stages in which RFamide-positive neurons were found ranged from 0.3 $\text{mm}^2$ (+/− 0.03 $\text{mm}^2$ standard error of the mean (SEM)) for the 20-d cuticle to 0.7 $\text{mm}^2$ (+/− 0.1 $\text{mm}^2$ SEM) for the 5-d and did not differ significantly. The increase from 5 d to adult (3.5 $\text{mm}^2$ +/−0.6 $\text{mm}^2$ SEM) was significant ($P < 0.001$). In contrast to the RFamide-positive neurons, JD1-positive neurons first appeared in the cigar stage. However, like the RFamide-positive neuron population, once the JD1-positive population arose, both the number of JD1-positive neurons and the complexity of the JD1-positive nerve net increased (Figs. 1, 2d–f). Pre-adult hydra stained for JD1 did not differ in area, but the adults stained for JD1 were significantly larger than the 5-d stage ($P < 0.001$).

The population trends of RFamide-positive neuron subtypes reflected the trends of total RFamide-positive neuron numbers and densities (Fig. 3). Like the RFamide-positive neuron population as a whole, all significant changes in the RFamide-positive ganglion cell, RFamide-positive sensory cell, and RFamide-positive unclassifiable neuron numbers between stages were increases (Fig. 3a). Furthermore, the population density of the RFamide-positive ganglion cells declined significantly after the 5-d stage (Fig. 3b), as was seen in the density dynamics of the whole RFamide-positive neuron population. Finally, neither the mean population density of the RFamide-positive sensory cells nor that of the RFamide-positive unclassifiable neurons decreased significantly after the 5-d stage. However, the shape of the graphs of each of these populations over time is reminiscent of the density dynamics of the whole RFamide-positive neuron population (Figs. 1b, 3b).

The population trends of the JD1-positive neuron subtypes reflected the trends of total JD1-positive neuron numbers and densities (Fig. 4). All significant changes in JD1-positive ganglion cell, JD1-positive sensory cell, and JD1-positive unclassifiable neuron numbers between stages were increases (Fig. 4a), mirroring the population dynamics of the JD1-positive neuron population as a whole. Also, there were significant increases in the population densities of JD1-positive ganglion cells, JD1-positive sensory cells, and JD1-positive unclassifiable neurons by the 5-d stage (Fig. 4b). But the JD1-positive ganglion cell and JD1-positive

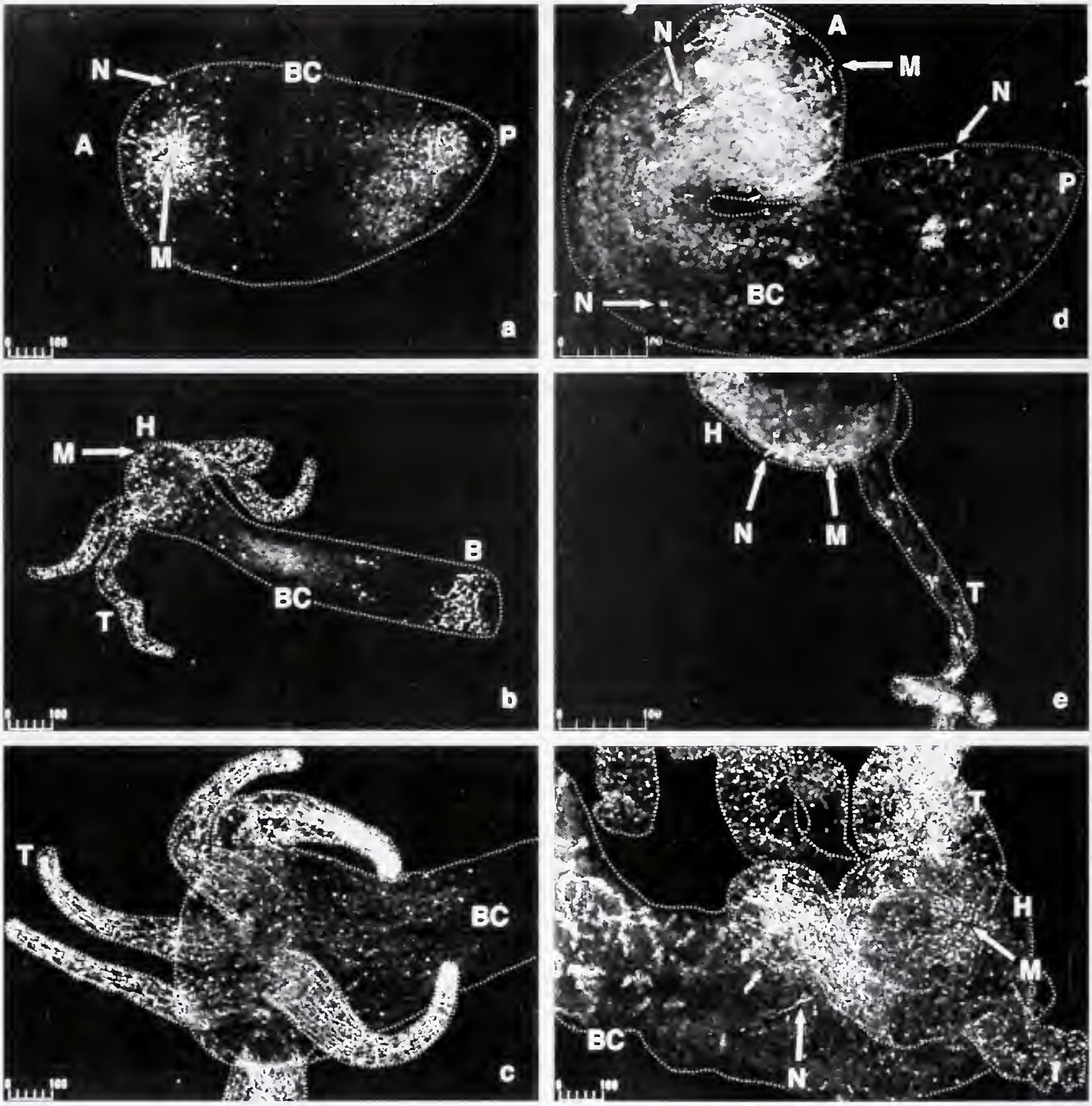

**Figure 2.** Single-plane confocal images of RFamide-positive and JD1-positive nerve net development. A, anterior; P, posterior; H, hypostome; M, mouth; T, tentacle; BC, body column; B, base; N, individual neuron. Scale bars are in $\mu$m. (a, b, c) The left column indicates the increasing numbers of neurons and complexity of the RFamide-positive nerve net as it progressed from the cigar stage (a) to the 5-d stage (b) to the adult (c, only shows upper body column and head). (d, e, f) The right column indicates the increasing numbers of neurons and complexity of the JD1-positive nerve net as it progressed from the cigar (d) to the 5-d stage (e, only shows head) to the adult (f, only shows upper body column and head).

unclassifiable neuron population densities both decreased significantly after the 5-d stage (Fig. 4b), reflecting the density dynamics of the total JD1-positive neuron population. Finally, the mean JD1-positive sensory cell population density did not decrease significantly after the 5-d stage, but the shape of the graph of this population over time is reminiscent of the density dynamics of the whole JD1-positive population (Figs. 1b, 4b).

The RFamide staining protocol labeled a population of neurons largely distinct from that labeled by the JD1 stain-

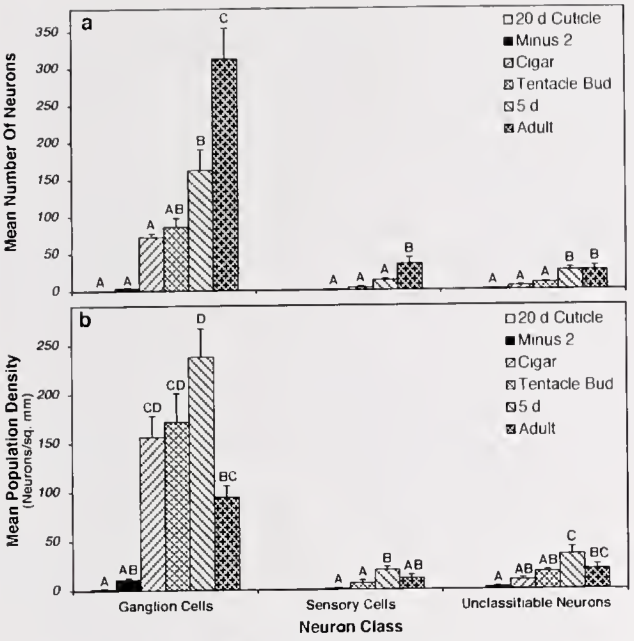

**Figure 3.** Mean (± SEM) numbers (a) and population densities (b) of RFamide-positive ganglion cells, sensory cells, and unclassifiable neurons in different developmental stages of *Hydra vulgaris* ($n = 5$). One-way ANOVA for numbers and population densities of ganglion cells across all six stages studied, sensory cells across the last four stages, and unclassifiable neurons across the last five stages showed significant differences (RFamide-positive ganglion cell number, $F = 31.73$, df = 5, $P = 0.001$; density of RFamide-positive ganglion cell population, $F = 23.02$, df = 5, $P = 0.0001$; RFamide-positive sensory cell number, $F = 13.02$, df = 3, $P = 0.001$; density of RFamide-positive sensory cell population, $F = 8.77$, df = 3, $P = 0.001$; RFamide-positive unclassifiable neuron number, $F = 15.94$, df = 4, $P = 0.001$; density of RFamide-positive unclassifiable neuron population, $F = 8.76$, df = 4, $P = 0.001$). Results of *post-hoc* Tukey's honestly significant differences test are indicated with letters—bars sharing a letter within an ANOVA series are not significantly different ($P > 0.05$).

ing protocol. Though some double labeling was observed in each of the posthatching stages ($n = 1$ for double staining), the numbers of double-labeled neurons were minimal compared to the average total RFamide-positive and JD1-positive neuron populations found in the single-stained samples ($n = 5$) of those stages. The percentage of double-labeled neurons ranged from a low of 1% of RFamide-positive neurons and 1% of JD1-positive neurons in the 5-d stage to a high of 5% of RFamide-positive neurons and 10% of JD1-positive neurons in the tentacle bud stage.

Adult hydra stained *via* the RFamide or JD1 procedures minus their respective primary Abs displayed no stained cells (Fig. 5). Also, positive-staining adults were present as controls in every assay that produced nonstaining embryos.

## Discussion

This study provides evidence based on neuron counts over developmental time that large-scale programmed cell death might not occur in the RFamide-positive or JD1-positive neuron populations of developing hydra. Similar evidence is provided that large-scale PCD might not occur during the development of the RFamide-positive or JD1-positive subpopulations (ganglion, sensory, or unclassifiable). If massive neuron culling were occurring in these populations, then their neuron counts would decrease (excepting the possibility that PCD and neurogenesis are concurrent but that neurogenesis outpaces PCD). The results showed that the neuron counts did not decrease during (or after) embryogenesis (Figs. 1, 3, 4). Therefore, culling *via* PCD might not occur on a large scale in these neuron populations during or after hydra embryogenesis.

This hypothesis is consistent with whole-neuron counts in two other modes of hydra development—budding and head regeneration. In five stages of bud development the total neuron number progresses as follows: 350, 500, 750, 1500,

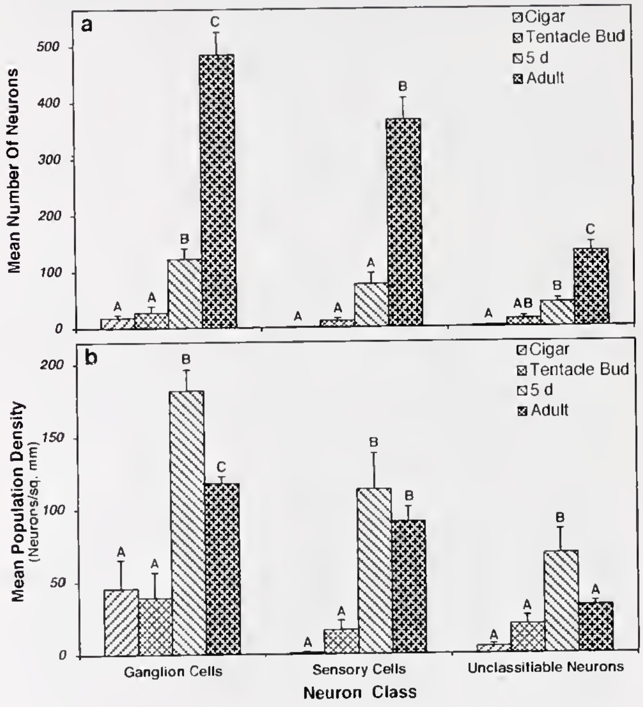

**Figure 4.** Mean (±SEM) numbers (a) and population densities (b) of JD1-positive ganglion cells, sensory cells, and unclassifiable neurons in different developmental stages of *Hydra vulgaris* ($n = 5$). One-way ANOVA for numbers and population densities of ganglion cells, sensory cells, and unclassifiable neurons across the JD1-positive stages showed significant differences (JD1-positive ganglion cell number, $F = 88.96$, df = 3, $P = 0.001$; density of JD1-positive ganglion cell population, $F = 19.45$, df = 3, $P = 0.001$; JD1-positive sensory cell number, $F = 61.08$, df = 3, $P = 0.001$; density of JD1-positive sensory cell population, $F = 15.87$, df = 3, $P = 0.001$; JD1-positive unclassifiable neuron number, $F = 46.52$, df = 3, $P = 0.001$; density of JD1-positive unclassifiable neuron population, $F = 9.39$, df = 3, $P = 0.001$). Results of *post-hoc* Tukey's honestly significant differences test are indicated with letters—bars sharing a letter within an ANOVA series are not significantly different ($P > 0.05$).

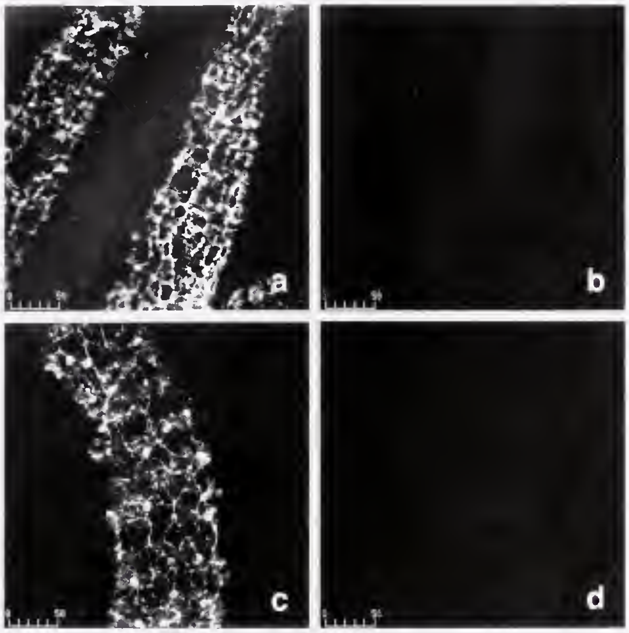

**Figure 5.** Single-plane confocal images of controls. Scale bars are in μm. (a, b) Tentacles processed with the RFamide antibody revealed a nerve net (a), whereas tentacles processed without the RFamide antibody did not (b). (c, d) Tentacles stained with the JD1 antibody revealed a nerve net (c), whereas tentacles processed using the same protocol minus the JD1 antibody did not (d).

2500 (Bode *et al.*, 1973). The authors report 5600 neurons in the adult. Similarly, regenerating heads show no decreases in neuron number. A decapitated hydra generates its new head from the tissue below the old head (Bode *et al.*, 1988a). Initially about 250 neurons populate the subhead region, and this number increases to 300, 500, and 700 as this tissue becomes head; the adult head contains about 800 neurons (Bode *et al.*, 1973). Thus, in embryological development, budding, and head regeneration, the hydra neuron populations studied show no culling. This indicates that continuous increase in neuron numbers through adult levels may be a common mechanism of neurodevelopment in hydra.

The hypothesis that large-scale neuronal PCD might not be part of adult hydra development is also supported by studies of tissue dynamics. First, loss of tissue to buds and to sloughing at the extremities balances the constant neuron production occurring in the adult hydra (David and Gierer, 1974; Bode *et al.*, 1988a; Sakaguchi *et al.*, 1996). If massive neuronal culling were occurring in the constantly developing adult, then neuron loss through budding and sloughing would not balance neuron production. However, calculations suggest that these two activities do balance neuron production (David and Gierer, 1974; Bode *et al.*, 1988a). This leaves little room for large-scale PCD of neurons between neurogenesis and sloughing. Second, if many neurons died between genesis and sloughing in adults, then neurons would be less long-lived than if they made the whole journey. However, quantitative studies of the whole neuron populations of the hypostome and the region of the body column apical to the budding zone (the gastric region) indicate that neurons in these regions live at least several times the mass-doubling period of an adult hydra's tissue and perhaps live indefinitely (David and Gierer, 1974). Thus, the lack of neuron population decrease in embryos, buds, and regenerating heads is consistent with the finding of David and Gierer (1974) that neurons of adult hydra are long-lived in the hypostome and gastric region. David and Gierer's results also suggest neurons live long enough to reach an extremity and be sloughed or to reach a bud. So, the normal tissue dynamics of the adult hydra leave very little room for large-scale PCD of neurons and are therefore consistent with the hypothesis that neuronal culling does not occur during embryogenesis.

The combination of neuron counts and studies of tissue dynamics outlined above indicates that massive neuron death might not occur during the development of the hydra nervous system, though it does in many more advanced nervous systems. Individual neurons and synapses of cnidarian nervous systems exhibit basic characteristics like those of more evolved systems (Roberts and Mackie, 1980; Kerfoot *et al.*, 1985; Fraser *et al.*, 1987; Anderson and Spencer, 1989; Grimmelikhuijzen and Westfall, 1995; Westfall, 1996). But greater numbers of neurons, more complex architectures, more specialized neurons, and a lesser emphasis on peptides appeared in nervous systems later in evolution (Grimmelikhuijzen and Westfall, 1995; Grimmelikhuijzen *et al.*, 1996). Large-scale culling of neurons during development may also have evolved later.

However, it appears hydra cells, including neurons, actually do come fully equipped with apoptotic machinery (Cikala *et al.*, 1999). This apoptotic machinery in hydra neurons may be used for any number of purposes other than culling neurons overproduced during development. PCD operates in contexts such as responding to DNA damage, defending against viruses and cancer, splitting of tissues in development, and shedding old tissue (Shikone *et al.*, 1997; Ahmad and Golic, 1999; Mire and Venable, 1999; Simon *et al.*, 1999; Gartner *et al.*, 2000; Ollmann *et al.*, 2000; Ramachandran *et al.*, 2000; Sastry and Rao, 2000). More specifically, PCD facilitates fission in sea anemones (Mire and Venable, 1999); perhaps it has a similar function during budding in hydra. Finally, PCD is important in the shedding of mammalian endometrial and intestinal epithelia (Shikone *et al.*, 1997; Simon *et al.*, 1999; Ramachandran *et al.*, 2000); perhaps it is similarly important in the continual sloughing of hydra cells (including neurons).

It may be possible to explain the apparent constant increase in hydra neuron numbers and also invoke massive culling of neuron populations that could not be detected by neuron counts. An organism as plastic as the hydra could be undergoing the massive neuroapoptosis associated with other model systems but still produce enough new neurons to mask culling. A study of cell-death markers during development of the hydra nervous system is required to examine this possibility.

Differentiation and maintenance of neuron populations in hydra does not keep pace with the animal's growth in size. If it did, neuron densities would remain constant throughout development. However, most of the neuron population densities studied in the sexually derived hydra decreased significantly (Figs. 1, 3, 4), failing to keep up with the 5-fold increase in size the present study has shown to occur after the 5-d stage. Similarly, in asexual reproduction, neurons compose 6.5% of the total cell number of a recently dropped *H. vulgaris* bud, but only 4.5% of an adult's total cell number (Bode *et al.*, 1973). As the bud adds mass after being dropped, this decrease in the percentage of neurons probably also represents a decrease in the density of neurons (measured as number per unit of tissue). So, RFamide-positive neurons and JD1-positive neurons of sexually derived hydra and, probably, the whole neuron population of buds differentiate less quickly relative to growth in size after the 5-d stage or bud dropping. This indicates that a mechanism common to both hydra embryogenesis and budding may be involved in regulating neuronal density.

Increased feeding of adult hydra moderately increases the proportion of epithelial cells to neurons (Bode *et al.*, 1973). The same may apply to buds and young sexually derived hydra and would explain why their neuron populations differentiate less quickly relative to growth in size after either the 5-d stage or bud dropping. In the present study, no developmental stages were fed. But, by the 2-d stage, hydra have both nematocytes mounted on tentacles and tentacles long enough to function in feeding (Martin *et al.*, 1997). Sexually derived hydra in the wild, or in the laboratory if allowed, increase their food intake after this stage. Likewise, buds may increase their food consumption as their cell-type distribution and morphology mature. As maturing buds and sexually derived hydra eat more, the proportion of epithelial cells to neurons will increase moderately, assuming that the cell-type proportions are regulated as in the adult. If neurons and epithelial cells were the same size, then this increase in the proportion of epithelial cells to neurons would moderately decrease neuron density measured as number of neurons per unit of tissue. However, because epithelial cells are much larger than neurons, a moderate increase in the number of epithelial cells to the number of neurons may be magnified into a significant decrease in the density of neurons per unit area (as seen in maturing sexually derived hydra). Perhaps neurite arborization is increased during this time of rapid growth and decreasing neuron density to maintain connectivity to the increasing bulk of tissue.

RFamide-positive neurons arose much earlier than JD1-positive neurons and, when the two types were present concurrently, were greater in number and density in early stages than JD1-positive neurons (Fig. 1). These proportions reversed in later stages. RFamide-positive neurons appear 1/2 d to 2 d prior to the first signs of head regeneration in adult *H. vulgaris* (Bode *et al.*, 1988b; Koizumi *et al.*, 1990), and the RFamide-positive neuron *network* already exists at the future head end of the minus-2 stage (Martin, 1997), 2 d before tentacles arise. Thus, RFamide-positive neurons appear before head formation in the regenerating adult and in the embryo. On the other hand, studies of *H. oligactis* indicate that JD1-positive neurons may appear concurrently with head structures in both budding hydra and hydra regenerating heads (Dunne *et al.*, 1985). In the embryo, JD1-positive neurons were first seen in the cigar stage. If, indeed, those neurons did appear at or near hatching, then neurogenesis of JD1-positive neurons correlates with the appearance of the embryo's head morphology, because tentacle buds form within a few minutes of hatching. Thus, the sequence of differentiation of RFamide-positive and JD1-positive neurons might occur with similar timing in embryos, buds, and regenerating heads.

In summary, the neuron subpopulations quantified in this study show no evidence of large-scale PCD during or after hydra embryogenesis; neither do neuron counts nor studies of tissue dynamics in budding, head regeneration, or the constantly developing adult hydra. Neuron population densities decrease after reaching a maximum in both embryonic and bud development, and the sequence of RFamide-positive and JD1-positive neurogenesis might be the same in embryos, buds, and regenerating heads. These commonalities indicate that neurodevelopment strategy may be highly conserved among the various modes of hydra development.

## Acknowledgments

The authors thank Bill Archer (University of Notre Dame) for technical assistance, Dr. Cornelis Grimmelikhuijzen (Department of Cell Biology, University of Copenhagen) for the RFamide antibody, Dr. Hans Bode (Developmental Biology Center, University of California, Irvine) for the JD1 Ab, and Dr. Scott Gilbert (Swarthmore College) for assistance in collecting hydra. This work was supported in part by a grant from Sigma Xi (GBB) and by NSF grants DCB-8702212 (VJM), DCB-8711245 (VJM), and DUE-9552116 (VJM).

## Literature Cited

**Ahmad, K., and K. G. Golic. 1999.** Telomere loss in somatic cells of *Drosophila* causes cell cycle arrest and apoptosis. *Genetics* **151:** 1041–1051.

**Anderson, P. A., and A. N. Spencer. 1989.** The importance of cnidarian synapses for neurobiology. *J. Neurobiol.* **20:** 435–457.

**Bode, H., S. Berking, C. N. David, A. Gierer, H. Schaller, and E. Trenkner. 1973.** Quantitative analysis of cell types during growth and morphogenesis in hydra. *Wilhelm Roux's Arch. Dev. Biol.* **171:** 269–285.

**Bode, H., S. Heimfeld, O. Koizumi, C. L. Littlefield, and M. S. Yaross. 1988a.** Maintenance and regeneration of the nerve net in hydra. *Am. Zool.* **28:** 1053–1063.

**Bode, P., T. A. Awad, O. Koizumi, Y. Nakashima, C. J. P. Grimmelikhuijzen, and H. R. Bode. 1988b.** Development of the two-part pattern during regeneration of the head in hydra. *Development* **102:** 223–235.

**Booker, R., J. Babashak, and J. B. Kim. 1996.** Postembryonic neurogenesis in the central nervous system of the tobacco hornworm, *Manduca sexta*. III. Spatial and temporal patterns of proliferation. *J. Neurobiol.* **29:** 233–248.

**Burek, M. J., and R. W. Oppenheim. 1996.** Programmed cell death in the developing nervous system. *Brain Pathol.* **6:** 427–446.

**Campbell, R. D. 1966.** Tissue dynamics of steady state growth in *Hydra littoralis*. III. Behavior of specific cell types during tissue movements. *J. Exp. Zool.* **164:** 379–392.

**Campbell, R. D. 1974.** Cell movements in Hydra. *Am. Zool.* **14:** 523–535.

**Cikala, M., B. Wilm, E. Hohmayer, A. Bottger, and C. N. David. 1999.** Identification of caspases and apoptosis in the simple metazoan Hydra. *Curr. Biol.* **9:** 959–962.

**David, C. N., and A. Gierer. 1974.** Cell cycle kinetics and development of *Hydra attenuatta*. III. Nerve and nematocyte differentiation. *J. Cell Sci.* **16:** 359–375.

**Draizen, T. A., J. Ewer, and S. Robinow. 1999.** Genetic and hormonal regulation of the death of peptidergic neurons in the *Drosophila* central nervous system. *J. Neurobiol.* **38:** 455–465.

**Dunne, J. F., L. C. Javois, L. W. Huang, and H. R. Bode. 1985.** A subset of cells in the nerve net of *Hydra oligactis* defined by a monoclonal antibody: its arrangement and development. *Dev. Biol.* **109:** 41–53.

**Ewer, J., C. M. Wang, K. A. Klukas, K. S. Mesce, J. W. Truman, and S. E. Fahrbach. 1998.** Programmed cell death of identified peptidergic neurons involved in ecdysis behavior in the moth, *Manduca sexta*. *J. Neurobiol.* **37:** 265–280.

**Fraser, S. E., C. R. Green, H. R. Bode, and N. B. Gilula. 1987.** Selective disruption of gap junctional communication interferes with a patterning process in hydra. *Science* **237:** 49–55.

**Galliresta, L., and G. Resta. 1992.** A quantitative model for the regulation of naturally-occurring cell-death in the developing vertebrate nervous system. *J. Neurosci.* **12:** 4586–4594.

**Gartner, A., S. Milstein, S. Ahmed, and J. Hodgkin. 2000.** A conserved checkpoint pathway mediates DNA damage-induced apoptosis and cell cycle arrest in *C. elegans*. *Mol. Cell* **5:** 435–443.

**Green, C. R. 1989.** Cnidarian gap junctions: structure, function and evolution. Pp. 3–20 in *Evolution of the First Nervous Systems*, P. A. V. Anderson, ed. Advanced Science Institute Series, Vol. 188. Plenum Press, New York.

**Grimmelikhuijzen, C. J. 1983a.** Coexistence of neuropeptides in hydra. *Neuroscience* **9:** 837–845.

**Grimmelikhuijzen, C. J. 1983b.** FMRFamide immunoreactivity is generally occurring in the nervous system of coelenterates. *Histochemistry* **78:** 361–381.

**Grimmelikhuijzen, C. J. 1984.** Peptides in the nervous systems of coelenterates. Pp. 39–58 in *Evolution and Tumor Pathology of the Neuroendocrine System*, S. Falkmer, R. Hakanson, and R. Sandler, eds. Elsevier, New York.

**Grimmelikhuijzen, C. J. P. 1985.** Antisera to the sequence Arg-Phe-amide visualize neuronal centralization in hydroid polyps. *Cell Tissue Res.* **241:** 171–182.

**Grimmelikhuijzen, C. J. P., and D. Graff. 1985.** Arg-Phe-amide-like peptides in the primitive nervous systems of coelenterates. *Peptides* **6:** 447–483.

**Grimmelikhuijzen, C. J., and J. A. Westfall. 1995.** The nervous systems of cnidarians. *Exper. Suppl. (Basel)* **72:** 7–24.

**Grimmelikhuijzen, C. J., F. Sundler, and J. F. Rehfeld. 1980.** Gastrin/CCK-like immunoreactivity in the nervous system of coelenterates. *Histochemistry* **69:** 61–68.

**Grimmelikhuijzen, C. J., K. Dierickx, and G. J. Boer. 1982.** Oxytocin/vasopressin-like immunoreactivity is present in the nervous system of hydra. *Neuroscience* **7:** 3191–3199.

**Grimmelikhuijzen, C. J., D. Graff, and A. N. Spencer. 1988.** Structure, location and possible actions of Arg-Phe-amide peptides in coelenterates. Pp. 199–217 in *Neurohormones in Invertebrates*, M. C. Thorndyke and G. J. Goldsworthy, eds. Society for Experimental Biology Seminar Series, Vol. 33. Cambridge University Press, Cambridge.

**Grimmelikhuijzen, C. J., D. Graff, O. Koizumi, J. A. Westfall, and I. D. McFarlane. 1989.** Neurons and their peptide transmitters in coelenterates. Pp. 95–109 in *Evolution of the First Nervous Systems*, P. A. V. Anderson, ed. Advanced Science Institute˚Series, Vol. 188. Plenum Press, New York.

**Grimmelikhuijzen, C. J., I. Leviev, and K. Carstensen. 1996.** Peptides in the nervous systems of cnidarians: structure, function, and biosynthesis. *Int. Rev. Cytol.* **167:** 37–89.

**Kerfoot, P. A., G. O. Mackle, R. W. Meech, A. Roberts, and C. L. Singla. 1985.** Neuromuscular transmission in the jellyfish *Aglantha digitale*. *J. Exp. Biol.* **116:** 1–25.

**Koizumi, O., H. Mizumoto, T. Sugiyama, and H. R. Bode. 1990.** Nerve net formation in the primitive nervous system of Hydra—an overview. *Neurosci. Res. Suppl.* **13:** S165–170.

**Koizumi, O., M. Itazawa, H. Mizumoto, S. Minobe, L. C. Javois, C. J. P. Grimmelikhuijzen, and H. R. Bode. 1992.** Nerve ring of the hypostome in Hydra. I. Its structure, development, and maintenance. *J. Comp. Neurol.* **326:** 7–21.

**Martin, V. J. 1997.** Cnidarians, the jellyfish and hydras. Pp. 57–86 in *Embryology: Constructing the Organism*, S. F. Gilbert and A. M. Raunio, eds. Sinauer Associates, Sunderland, MA.

**Martin, V. J., C. L. Littlefield, W. E. Archer, and H. R. Bode. 1997.** Embryogenesis in hydra. *Biol. Bull.* **192:** 345–363.

**Mire, P., and S. Venable. 1999.** Programmed cell death during longitudinal fission in a sea anemone. *Invertebr. Biol.* **118:** 319–331.

**Mitgutsch, C., F. Hauser, and C. J. P. Grimmelikhuijzen. 1999.** Expression and developmental regulation of the Hydra-RFamide and Hydra-LWamide preprohormone genes in hydra: evidence for transient phases of head formation. *Dev. Biol.* **207:** 189–203.

**Ollmann, M., L. M. Young, C. J. DiComo, F. Karim, M. Belvin, S. Robertson, K. Whittaker, M. Demsky, W. W. Fisher, A. Buchman, G. Duyk, L. Friedman, C. Prives, and C. Kopczynski. 2000.** Drosophila p53 is a structural and functional homolog of the tumor suppressor p53. *Cell* **101:** 91–101.

**Ramachandran, A., M. Madesh, and K. A. Balasubramanian. 2000.** Apoptosis in the intestinal epithelium: its relevance in normal and pathophysiological conditions. *J. Gastroenterol. Hepatol.* **15:** 109–120.

**Roberts, A., and G. O. Mackie. 1980.** The giant axon escape system of a hydrozoan medusa, *Aglanthe digitale*. *J. Exp. Biol.* **84:** 303–318.

**Robinow, S., W. S. Talbot, D. S. Hogness, and J. W. Truman. 1993.** Programmed cell death in the *Drosophila* CNS is ecdysone-regulated and coupled with a specific ecdysone receptor isoform. *Development* **119:** 1251–1259.

**Sakaguchi, M., A. Mizusina, and Y. Kobayakawa. 1996.** Structure, development, and maintenance of the nerve net of the body column in Hydra. *J. Comp. Neurol.* **373:** 41–54.

**Sanders, E. J., and M. A. Wride. 1995.** Programmed cell death in development. *Int. Rev. Cytol.* **163:** 105–173.

**Sastry, P. S., and K. S. Rao. 2000.** Apoptosis and the nervous system. *J. Neurochem.* **74:** 1–20.

**Shankland, M., and M. Q. Martindale. 1989.** Segmental specificity and lateral asymmetry in the differentiation of developmentally homologous neurons during leech embryogenesis. *Dev. Biol.* **135:** 431–448.

**Shikone, T., K. Kokawa, M. Yamoto, and R. Nakano. 1997.** Apoptosis of human ovary and uterine endometrium during the menstrual cycle. *Horm. Res.* **48:** 27–34.

**Simon, C., J. C. Martin, A. Galan, D. Valbuena, and A. Pellicer. 1999.** Embryonic regulation in implantation. *Semin. Reprod. Endocrinol.* **17:** 267–274.

**Spencer, A. N. 1989.** Chemical and electrical synaptic transmission in the Cnidaria. Pp. 33–53 in *Evolution of the First Nervous Systems*, P. A. V. Anderson, ed. Advanced Science Institutes Series, Vol. 188. Plenum Press, New York.

**Spencer, A. N. 1995.** Modulatory mechanisms at a primitive neuromuscular synapse: membrane currents, transmitter release and modulation by transmitters in a cnidarian motor neuron. *Am. Zool.* **35:** 520–528.

**Stewart, R. R., W. Q. Gao, A. Peinado, B. Zipser, and E. R. Macagno. 1987.** Cell death during gangliogenesis in the leech: bipolar cells appear and then degenerate in all ganglia. *J. Neurosci.* **7:** 1919–1927.

**Umbriaco, D., M. Anctil, and L. Descarries. 1990.** Serotonin-immunoreactive neurons in the cnidarian *Renilla koellikeri*. *J. Comp. Neurol.* **291:** 167–178.

**Westfall, J. A. 1996.** Ultrastructure of synapses in the first-evolved nervous systems. *J. Neurocytol.* **25:** 735–746.

**Yu, S. M., J. A. Westfall, and J. F. Dunne. 1986.** Use of a monoclonal antibody to classify neurons isolated from the head region of Hydra. *J. Morphol.* **188:** 79–90.

Reference: *Biol. Bull.* **203:** 80–86. (August 2002)

# Embryonic Velar Structure and Function of Two Sibling Species of *Crepidula* With Different Modes of Development

O. R. CHAPARRO[1,*], J. L. CHARPENTIER[1], AND R. COLLIN[2,†]

[1]*Instituto de Biología Marina Dr. J. Winter, Facultad de Ciencias, Universidad Austral de Chile, Valdivia, Chile; and* [2]*Committee on Evolutionary Biology, University of Chicago, 1025 E. 57th St., Chicago, Illinois 60637, and the Field Museum, 1400 S. Lake Shore Dr., Chicago, Illinois 60605*

**Abstract.** The structure and function of the embryonic velum of two closely related species of *Crepidula* with different modes of development are examined. The velum of *C. dilatata*, a direct developer whose embryos feed on nurse eggs, does not differ substantially from the velum of *C. fecunda*, a species with planktotrophic larvae. Although velar ciliation develops earlier in embryos of *C. dilatata*, embryos of both species were able to feed on small particles, using the opposed-band ciliary mechanism. However, the embryos of *C. dilatata* lose this ability as they grow. The embryos of *C. dilatata* were not able to swim, whereas those of *C. fecunda* swam consistently in vials of seawater. This difference in swimming ability is probably due to differences in velum-body size allometry between the two species.

## Introduction

In marine invertebrates, the evolution of direct development from the putative ancestral state of development with planktotrophic larvae is often accompanied by modifications of morphological structures associated with swimming and feeding (Strathmann, 1978; Hadfield and Iaea, 1989; Emlet, 1994; Byrne, 1995; Byrne and Cerra, 1996; Wray, 1996; Hadfield *et al.*, 1997). The functional modifications associated with the loss of feeding in pelagic echinoderm larvae are relatively well understood. For example, the ciliary bands that are arranged into complex loops along larval arms in feeding larvae are reorganized into transverse bands or fields of cilia around a cylindrical body in nonfeeding larvae (Emlet, 1994). Among echinoderm larvae, such modifications are believed to maximize feeding efficiency in planktotrophic larvae and maximize swimming efficiency in nonfeeding planktonic larvae (Emlet, 1994). Modifications or loss of larval feeding or swimming structures are often so extreme that re-evolution of such structures appears to be difficult. Loss of these complex structures is cited as evidence that feeding larvae, once lost, cannot be regained (Strathmann, 1978). The morphological modifications associated with the loss of feeding larvae in other groups of marine invertebrates are less well understood. In marine gastropods, for example, the evolution of nonfeeding or direct development is usually associated with encapsulated development. The functional requirements of development within a capsule may be very different from the requirements of free-living development. For example, the embryo may need structures to circulate intracapsular fluid (Strathmann and Chaffee, 1984), ingest intracapsular fluid (Fioroni, 1966; Morrill, 1982; Rivest, 1992; Moran, 1999), or ingest nurse eggs or siblings (Rivest, 1981).

The morphological structure associated with both feeding and swimming in gastropod larvae is the velum. In planktotrophic larvae, the velum is normally a pair of large flat lobes of tissue edged with two opposed bands of compound cilia, extending from behind the head. The anterior band of cilia, the preoral band, and the posterior, postoral band flank a "food groove" lined with shorter cilia (Werner, 1955; Strathmann and Leise, 1979). Gastropods with planktotrophic larvae, and especially those with long-lived planktotrophic larvae, often have large elaborate vela with as many as six or eight lobes (Fretter and Pilkington, 1970; DiSalvo,

---

Received 10 July 2001; accepted 23 May 2002.

* To whom correspondence should be addressed. E-mail: ochaparr@uach.cl

† Current address: Smithsonian Tropical Research Institute, P.O. Box 2072, Balboa, Ancon, Republic of Panama. E-mail: collinr@naos.si.edu

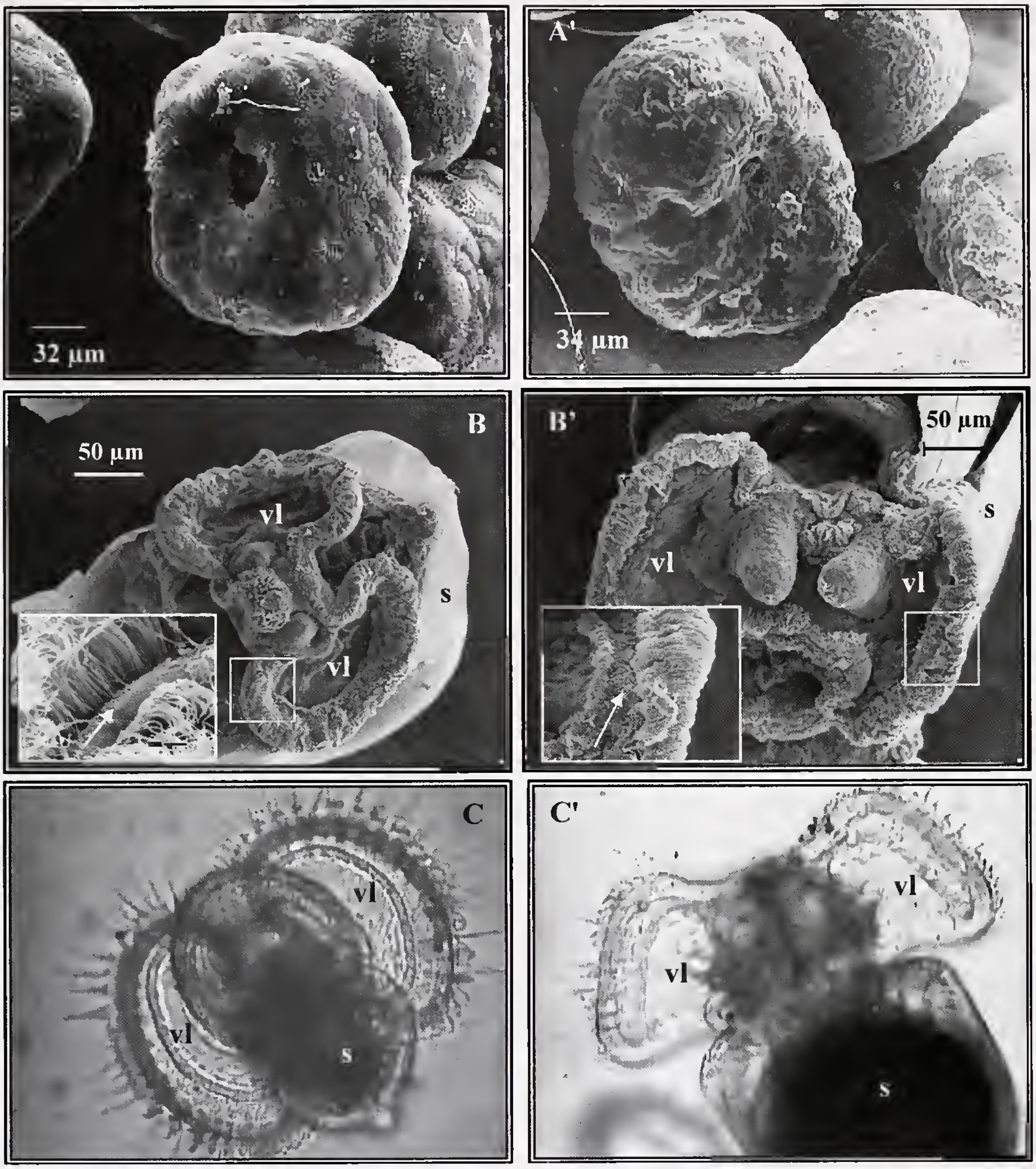

**Figure 1.** Scanning electron micrographs of different developmental stages of *Crepidula fecunda* (left side pictures: A–C) and *C. dilatata* (right side pictures: A′–C′). (A) Gastrula. (B) Intracapsular veliger; arrow in enlarged area indicates the food groove. (C) Light micrograph of the same stage as in B, showing the opposed-band ciliation and organized metachronal wave in both species.

1988). In larvae of *Crepidula fornicata*, the velar lobes grow significantly larger, in relation to shell size, when larvae are cultured with low concentrations of food rather than with high concentrations (Klinzing and Pechenik, 2000). In swimming larvae, the velum is lost at metamorphosis. Those species with abbreviated pelagic phases or complete intracapsular development often show a reduction in the size of the velum, loss of ciliary bands, and shortening of cilia (Fioroni, 1966). Hadfield *et al.* (1997) showed that "archaeogastropod" larvae, which are characterized by swimming, nonfeeding larvae, have well developed preoral cilia but lack the food groove. In embryos of *Crepidula adunca*, a species with direct development from large yolky eggs, the velum is reduced to a small ridge with cilia only slightly longer than those on the surrounding mouth, tentacles, and head vesicle (Collin, 2000).

The absence of a feeding, swimming larval stage is not always associated with the loss of function of the velum. In some species of *Littorina*, the embryonic velum is used to ingest albumin from the egg capsules (Moran, 1999). In these species the velum is as large, relative to embryonic body size, as the velum in species with planktotrophic larvae (Moran 1999), suggesting that this novel function is selecting against loss of structure and function of the velum. In embryos of *Petaloconchus montereyensis*, the velum is modified to ingest intracapsular yolk but has lost the preoral cilia. Other embryonic modifications associated with intracapsular development are reviewed in Fioroni (1966). In species with direct, nonswimming development, the velum is lost before hatching.

The present study was undertaken to examine structural and functional modifications of the embryonic velum associated with the evolution of nurse-egg feeding. We compare the embryonic development, especially the velar development, of two closely related species of gastropods with differing modes of development: *Crepidula fecunda* Gallardo 1979, a species with planktotrophic development, and *C. dilatata* Lamarck 1822, a species with direct development in which the embryos consume nurse eggs (Gallardo, 1976, 1977, 1979; Chaparro and Paschke, 1990). We measured the ability, relative to velar morphology, of the embryos to capture particles and to swim.

## Materials and Methods

Adult *Crepidula dilatata* were collected subtidally in the estuary of Rio Quempillen at the north end of Chiloé Island, Chile (41°52′S, 73°44′W), and *C. fecunda* were collected from the intertidal of Bahía de Yaldad in the south of Chiloé Island (43°08′S, 73°44′W).

Prior to examination by electron microscopy, broods were removed from the females, individually incubated for 5 min in 0.5% solution of chloral hydrate, fixed in a 3% solution of gluteralderhyde with cacodylate buffer (pH = 7.4), and maintained at 4 °C for 1 h. Embryos were subsequently excapsulated, rinsed for 10 min in phosphate buffer, dehydrated in a graded acetone series, and critical-point dried. They were attached to stubs with double-sided tape, gold-coated, and examined with a Bausch & Lomb Nanolab 2000 scanning electron microscope.

To test for the ability of the embryos to feed on small particles, the embryos were excapsulated and placed in seawater at ambient temperature. Nontoxic red beads 2–10 $\mu$m in diameter (Chaparro *et al.*, 1993) were added to the solution. After 2 h the embryos were removed from the solution and fixed in formalin until they were analyzed. The presence of red particles in the larval or embryonic stomach was determined after fixation. One hundred embryos at each stage of development were examined under a compound microscope, and the percentage of embryos that had ingested particles (as indicated by red particles in the gut) was recorded. The method of particle capture was observed and recorded using an inverted microscope connected to a Sony DXC-C1 video camera and a Sony PVM-1953MD monitor. Similarly, to test for swimming ability, embryos were excapsulated, and groups of 20 were placed in 20 ml of seawater. After 5 min, the number of embryos swimming above the bottom of the vial was recorded. The shell length and velar characteristics of embryos used in both experiments were measured, using Scion Image PC (Scion Corporation, Frederick, MD), from video images.

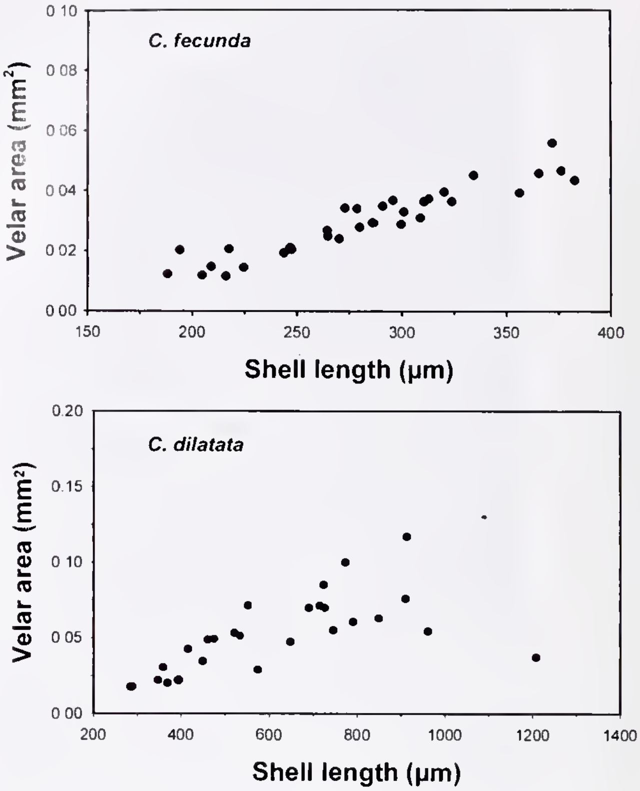

**Figure 2.** Scatter plot of velum area *versus* shell length for *Crepidula fecunda* and *C. dilatata*.

## Results

### *Embryonic morphology*

Embryos of both *Crepidula dilatata* and *C. fecunda* develop from eggs with average diameters of 250 and 212 $\mu$m respectively (Gallardo, 1977). However, the embryos of *C. dilatata* consume uncleaved nurse eggs (Gallardo, 1977) and hatch as crawling juveniles of about 1100–1200 $\mu$m shell length (Chaparro and Paschke, 1990), whereas those of *C. fecunda* do not consume nurse eggs, and they hatch as planktotrophic larvae at a size of 400–500 $\mu$m. Despite this difference in mode of development, the embryonic morphologies of both species are similar.

In both species, spiral cleavage and gastrulation by epiboly result in a very slightly flattened gastrula with a central

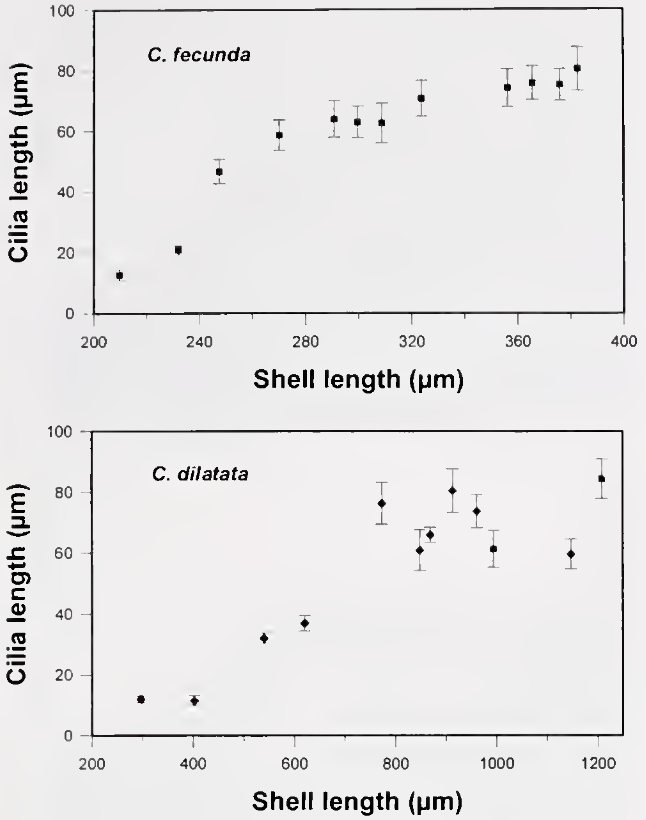

**Figure 3.** A comparison of cilia length *versus* shell length for *Crepidula fecunda* and *C. dilatata*. The vertical bars represent the standard deviation.

blastopore. In *C. dilatata* (Fig. 1A′), the gastrula is somewhat more elongate than the round gastrula of *C. fecunda* (Fig. 1A). The initial gastrula is not ciliated, but patches of cilia in the area of the presumptive velum and head vesicle can be seen in scanning electron micrographs of later gastrulas.

In both species, an intracapsular trochophore stage follows the gastrula. This stage is characterized by elongation of the embryo and flattening of the posterior dorsal area where the shell begins to form. In *C. dilatata*, clearly defined patches of cilia around the mouth, at the ventral anterior (presumptive head vesicle) and ventral posterior (telotroch) areas of the embryo, and lateral to the mouth (presumptive velum) begin to develop. In *C. fecunda*, these cilia are less obvious, and their elaboration occurs later, relative to other morphological events, than in the embryos of *C. dilatata*.

As the edge of the velum extends laterally from the body wall, the distinct bands of cilia can be observed along its edge in *C. dilatata*. It is at this stage that the preoral cilia first appear in *C. fecunda*; the postoral and oral cilia appear slightly later. At this stage, in both species, the embryonic kidney is clearly visible on each side of the embryo, the shell begins to grow around the posterior end of the embryo, and the foot begins to differentiate and becomes ciliated. In embryos of both species of 200–300 μm, the small head vesicle is distinct and covered with cilia, the velum clearly shows opposed band ciliation, and the foot has an operculum and a medial band of ventral cilia (Fig. 1B, B′, 1C, C′). Subsequent development reflects the growth and elaboration of these structures. The shell grows to contain the yolk and developing viscera. The lobes of the velum grow wider, and the preoral cilia grow to a length of 80 μm. Larvae of *C. fecunda* hatch at a shell length of 400–500 μm, after the reabsorption of the embryonic kidneys and the head vesicle.

In *C. dilatata*, further morphogenesis occurs in the capsule. The tentacles begin to form at a shell length of about 500 μm. Both tentacles are large and the apical ciliarly tufts are well developed, as is the foot, in embryos with a shell length of 700 μm. At this stage the velar cilia reach their maximal length of 80 μm. Embryos between 800 and 1100 μm in shell length undergo intracapsular metamorphosis. The pedal glands become visible, and the velum gradually shrinks. By the time the embryo is about 1000 μm in shell length, the velum and embryonic kidneys are no longer visible. This is also near the length at which the embryos usually exhaust the supply of nurse eggs (Chaparro and Paschke, 1990). Among advanced embryos, the shell length

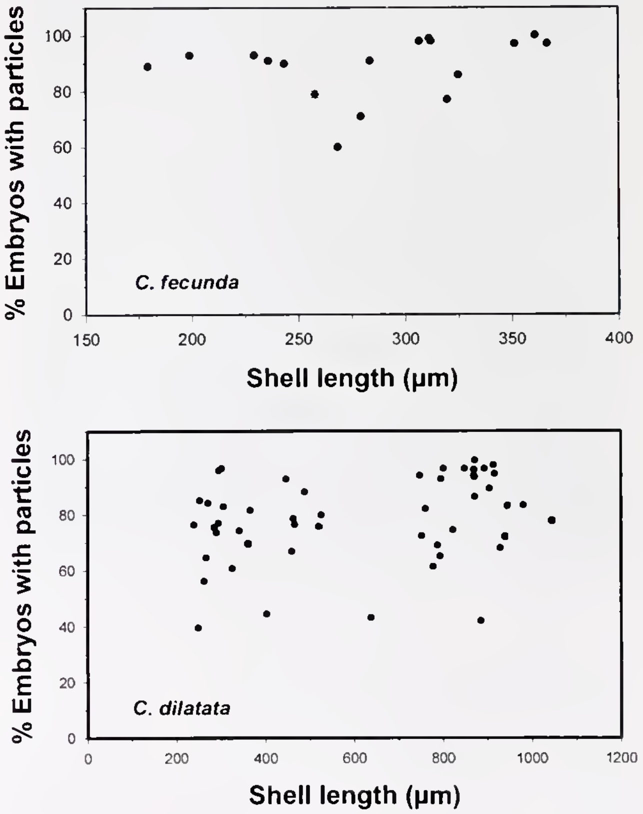

**Figure 4.** Scatter plot of the proportion of embryos that ingested particles *versus* shell length for *Crepidula fecunda* and *C. dilatata*. Each point represents a trial with 100 embryos.

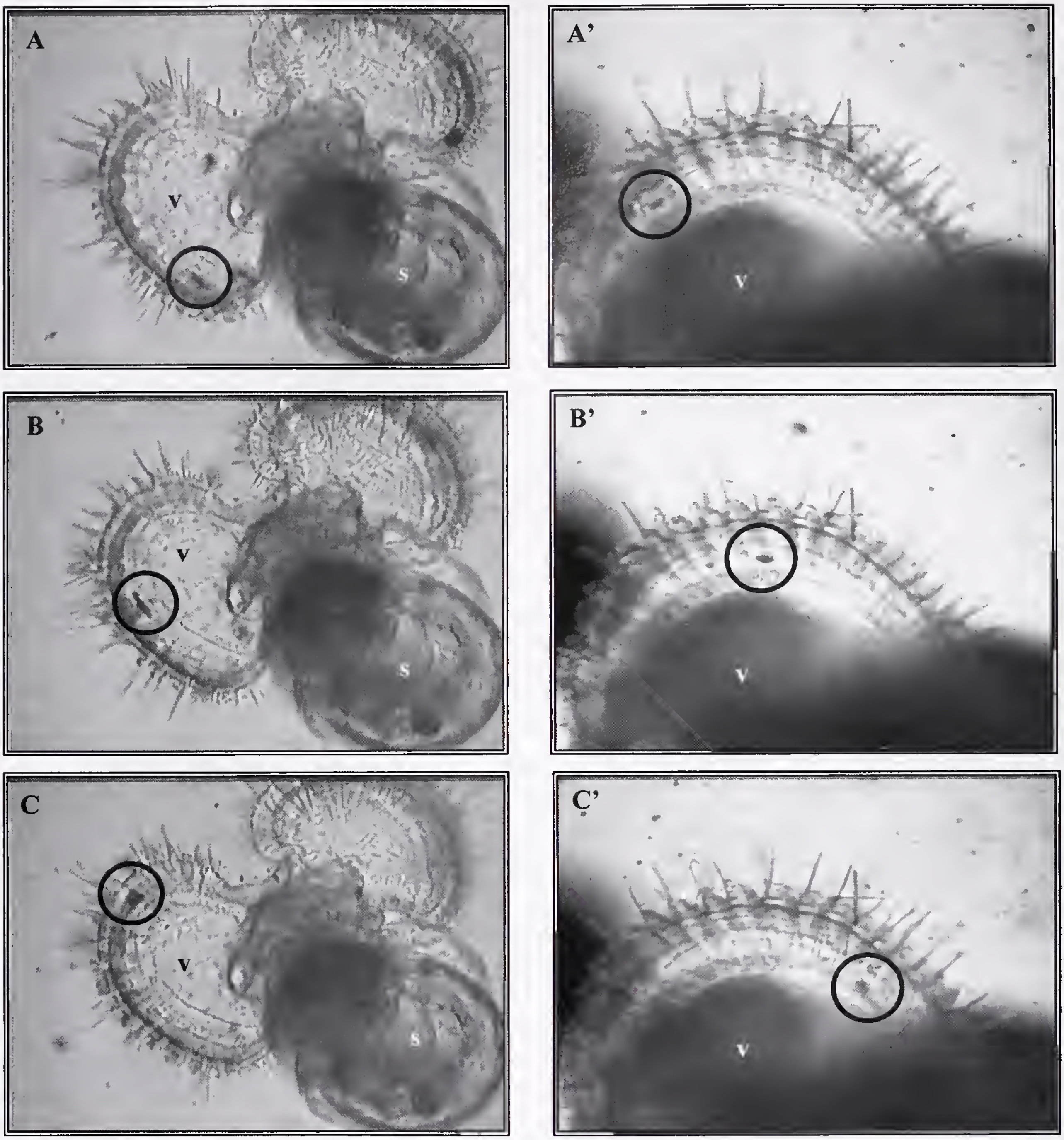

**Figure 5.** Video sequence of a captured particle (encircled) moving along the food groove towards the mouth. Left side (A–C): *Crepidula fecunda* embryo. Right side (A′–C′): *C. dilatata* embryo.

at any given developmental stage shows variation due to differences in the number of nurse eggs consumed by each embryo.

### *Allometry*

In *C. fecunda*, the velum grows throughout intracapsular development. The velar area increases linearly with respect to shell length (Fig. 2), and it reaches its maximal size, about 0.06 mm$^2$, near hatching. The size of the velum relative to shell length in *C. dilatata* is initially the same as in *C. fecunda*, but the velum grows more slowly relative to shell length. Comparisons of larvae at a comparable shell length ($<600$ $\mu$m) showed a significant difference in velum size relative to shell length (ANCOVA, $n = 374$; $f =$

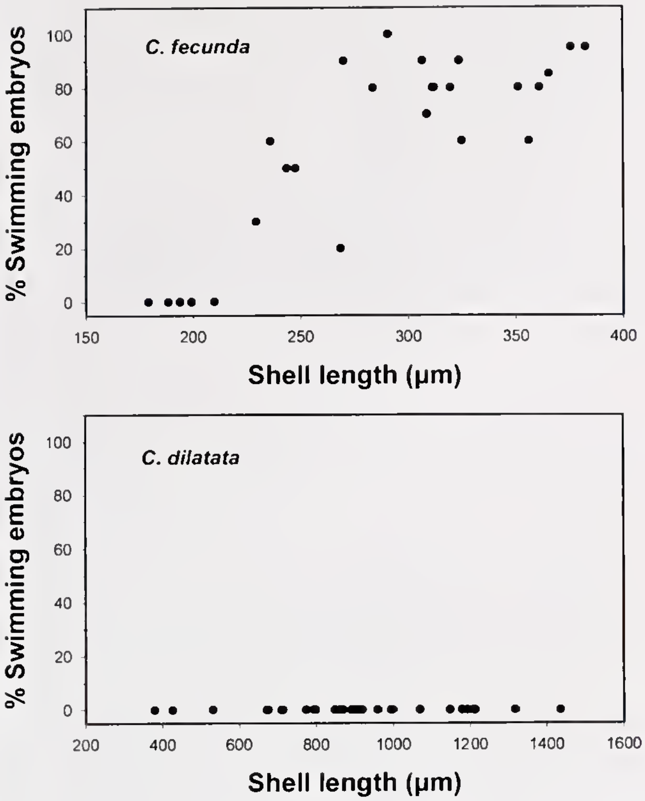

**Figure 6.** Scatter plot of the number of embryos that showed swimming ability *versus* shell length for *Crepidula fecunda* and *C. dilatata*.

227.987, $P < 0.001$). The velum in *C. dilatata* continues to grow until it reaches an area of about 0.12 mm$^2$. At large shell sizes the velar area decreases as the velum is absorbed prior to hatching.

The preoral cilia grow to a length of about 80–90 $\mu$m in embryos of both species (Fig. 3), but the relationship between the lengths of cilia and shell differs between the two species. In *C. dilatata,* the direct developer, the cilia reach their maximal length at a shell length of approximately 700 $\mu$m (near the size of maximal velar area); the same maximal length is attained in *C. fecunda* at a shell length of about 320 $\mu$m. The velar cilia of *C. fecunda* continue growing until hatching, as does the velum.

### *Feeding and swimming*

The embryos of both *C. dilatata* and *C. fecunda* were able to capture and ingest small particles from suspension in seawater (Fig. 4). A high percentage of *C. fecunda* embryos from a shell length of 175 $\mu$m to the hatching size of 350–450 $\mu$m showed the ability to capture and ingest beads. In *C. dilatata,* the small embryos (shell length less than 400 $\mu$m) ingested particles with high frequency. Observation of both species showed that the embryos use the opposed-band ciliary mechanism to capture particles and to move them along the food groove to the mouth (Fig. 5A, A′, 5B, B′, 5C, C′).

There was a striking difference between the species in swimming ability: embryos of *C. dilatata* never swam, whereas embryos of *C. fecunda* larger than 270 $\mu$m swam consistently in our experiment (Fig. 6).

## Discussion

Our observations of *Crepidula* embryos show that the embryonic morphology of the direct-developing *C. dilatata* is little modified from that of the planktotrophic *C. fecunda.* After consuming many nurse eggs, the embryos of *C. dilatata* are larger than those of *C. fecunda,* and the relative size of the velum is smaller; however, the operculum is not lost, and there is no elaboration of the embryonic kidneys or massive enlargement of the head vesicle as has been reported for embryos of another direct-developing *Crepidula* species (Moritz, 1939; Collin, 2000). The velum of *C. dilatata* is not lost or greatly reduced in absolute size as it is in many gastropods with direct development, and it appears to be structurally similar to the velum of the closely related planktotrophic *C. fecunda.* It retains the bands of both preoral and postoral cilia and has a ciliated food groove. In addition, *C. dilatata* retains the ability to use the opposed-band ciliation to capture and transport particles along the food groove.

The lack of change in the embryonic development in the direct-developing *C. dilatata* could be the result of several factors. It is possible that there are few overall modifications of development because direct development has evolved recently in this species. Gallardo (1979) suggested that *C. fecunda* and *C. dilatata* were recently diverged sibling species The retention of a well-developed velum with a functional opposed-band ciliary mechanism in direct developing species is unusual in North American *Crepidula* that do not consume nurse eggs (RC, pers. obs.) It is probable that the continued use of this structure to feed on material within the capsule has maintained the velum as a functional structure. Small particles of yolk from abnormal or damaged embryos pass along the velum of young embryos of *C. dilatata* in the same manner as the artificial particles described here. Nurse eggs are ingested in a different manner. In *C. dilatata,* the nurse eggs are generally consumed after the embryos have reached a shell length of 500 $\mu$m (Chaparro and Paschke, 1990) and have developed a large ciliated velum (see above). The embryo rotates the nurse egg on the velum. The egg deforms as the cilia of the buccal region slowly draw the egg into the esophagus (OC and RC, pers. obs.). The ability of *C. dilatata* embryos to capture small particles before the stage at which they actively feed on nurse eggs suggests that small particles from damaged embryos may be an important source of early nutrition in young embryos.

The energetic contributions of these different feeding mechanisms should be examined in greater detail.

A previous study that addressed the possibility of the re-evolution of feeding gastropod larvae concluded that *Petaloconchus montereyensis* has lost the velar structures necessary for swimming and feeding, making the re-evolution of feeding larvae that use the opposed-band ciliary mechanism on the velum unlikely (Hadfield and Iaea, 1989). Because, as demonstrated here, *C. dilatata* embryos retain the ability to capture particles by using the opposed-band mechanism, the re-evolution of feeding larvae from this species is not impossible. However, changes in the velum-body size allometry and hatching size would probably be necessary to produce a larva capable of swimming. Because the hatching size for *C. dilatata* is determined by the number of nurse eggs per embryo in each capsule, it is possible that velum-body size allometry is determined by the number of nurse eggs consumed. If this is the case, a drastic reduction in the number of nurse eggs per capsule could change this allometry enough to produce embryos capable of swimming.

## Acknowledgments

We thank the staff of the Quempillen field station for help with field work, and R. Silva for help with electron microscopy. O. Chaparro's research was funded by grants from Fondecyt—Chile1980984 and Dirección de Investigación—Universidad Austral de Chile. R. Collin's travel to Chile was supported by a grant from the National Geographic Society. B. Pernet made helpful comments on the manuscript.

## Literature cited

**Byrne, M. 1995.** Changes in larval morphology in the evolution of benthic development by *Patiriella exigua* (Asteroidea: Asterinidae), a comparison with the larvae of *Patiriella* species with planktonic development. *Biol. Bull.* **188:** 293–305.

**Byrne, M., and A. Cerra. 1996.** Evolution of intragonadal development in the diminutive asterinid sea stars *Patiriella vivipara* and *P. parvivipara* with an overview of development in the Asterinidae. *Biol. Bull.* **191:** 17–26.

**Chaparro, O. R., and K. A. Paschke. 1990.** Nurse egg feeding and energy balance in embryos of *Crepidula dilatata* Lamarck during intracapsular development. *Mar. Ecol. Prog. Ser.* **65:** 183–191.

**Chaparro, O. R., R. J. Thompson, and J. E. Ward. 1993.** *In vivo* observations of larval brooding in the Chilean oyster, *Ostrea chilensis* Philippi, 1845. *Biol. Bull.* **185:** 365–372.

**Collin, R. 2000.** Sex change, reproduction, and development of *C. adunca* and *C. lingulata*. *Veliger* **43:** 24–33.

**DiSalvo, L. H. 1988.** Observations on the larval and post-metamorphic life of *Concholepas concholepas* (Brugiere, 1789) in laboratory culture. *Veliger* **30:** 358–368.

**Emlet, R. B. 1994.** Body form and patterns of ciliation in non-feeding larvae of echinoderms—functional solutions to swimming in the plankton. *Am. Zool.* **34:** 570–585.

**Fioroni, P. 1966.** Zur Morphologie und Embryogeneses des Darmtraktes und der transitorischen Organe bei Prosobranchiern (Mollusca, Gastropoda). *Rev. Suisse Zool.* **73:** 621–876.

**Fretter, V., and M. C. Pilkington. 1970.** Prosobranchia: veliger larvae of the Taenioglossa and Stenoglossa. *Cons. Int. Explor. Mer. Zooplankton Sheets* 129–132.

**Gallardo, C. S. 1976.** Historia natural y reproducción de *Crepidula dilatata* Lamarck en una población de Bahía Mehuin (Prov. Valdivia, Chile). *Medio Ambiente* **2:** 44–50.

**Gallardo, C. S. 1977.** Two modes of development in the morphospecies *Crepidula dilatata* (Gastropoda: Calyptraeidae) from Southern Chile. *Mar. Biol.* **39:** 241–251.

**Gallardo, C. S. 1979.** Especies gemelas del genero *Crepidula* (Gastropoda, Calyptraeidae) en la costa de Chile: una redescripción de *C. dilatata* Lamarck y descripción de *C. fecunda* n. sp. *Stud. Neotrop. Fauna Environ.* **14:** 215–226.

**Hadfield, M. G., and D. K. Iaea. 1989.** Velum of encapsulated veligers of *Petaloconchus* (Gastropoda), and the problem of re-evolution of planktotrophic larvae. *Bull. Mar. Sci.* **45:** 377–386.

**Hadfield, M. G., M. F. Strathmann, and R. R. Strathmann. 1997.** Ciliary currents of non-feeding veligers in putative basal clades of gastropods. *Invertebr. Biol.* **116:** 313–321.

**Klinzing, M. S. E., and J. A. Pechenik. 2000.** Evaluating whether velar lobe size indicates food limitation among larvae of the marine gastropod *Crepidula fornicata*. *J. Exp. Mar. Biol. Ecol.* **252:** 255–279.

**Moran, A. 1999.** Intracapsular feeding by embryos of the gastropod genus *Littorina*. *Biol. Bull.* **196:** 229–244.

**Moritz, C. E. 1939.** Organogenesis in *Crepidula adunca* Sowerby. *Univ. Calif. Publ. Zool.* **43:** 217–248.

**Morrill, J. B. 1982.** Development of the pulmonate gastropod, *Lymnaea*. Pp. 399–483 in *Developmental Biology of Freshwater Invertebrates*, G. W. Harrison and R. W. Cowden, eds. Alan R. Liss, New York.

**Rivest, B. R. 1981.** Nurse egg consumption and the uptake of albumen in the embryonic nutrition of marine snails. Ph.D. dissertation. University of Washington, 185 pp.

**Rivest, B. R. 1992.** Studies on the structure and function of the larval kidney complex of prosobranch gastropods. *Biol. Bull.* **182:** 305–325.

**Strathmann, R. R. 1978.** The evolution and loss of feeding larval stages of marine invertebrates. *Evolution* **32:** 894–906.

**Strathmann, R. R., and C. Chaffee. 1984.** Constraints on egg masses. II. Effect of spacing, size, and number of eggs on ventilation of masses of embryos in jelly, adherent groups, or thin-walled capsules. *J. Exp. Mar. Biol. Ecol.* **84:** 85–93.

**Strathmann, R. R., and E. Leise. 1979.** On feeding mechanism and clearance rates of molluscan veligers. *Biol. Bull.* **157:** 524–535.

**Werner, B. 1955.** Über die anatomie, die Entwicklung und Biologie des Veligers und der Veliconcha von *Crepidula fornicata* L. (Gastropoda, Prosobranchia). *Helgol. Wiss. Meeresunters.* **5:** 169–217.

**Wray, G. 1996.** Parallel evolution of nonfeeding larvae in echinoids. *Syst. Biol.* **45:** 308–322.

Reference: *Biol. Bull.* **203:** 87–103. (August 2002)

# Embryogenesis and Development of *Epimenia babai* (Mollusca Neomeniomorpha)

AKIKO OKUSU

*Organismic and Evolutionary Biology, Harvard University, Cambridge, Massachusetts 02138*

**Abstract.** Neomenioid aplacophorans (= Solenogastres) constitute one of the main lineages of molluscs. Developmental data of early embryogenesis and larval development of neomenioids are available for some species based on histological sections. I used other techniques to study the development of *Epimenia babai* Salvini-Plawen, 1997, and here I report new data on neomenioid development. The embryos of *E. babai* are lecithotrophic and cleavage is spiral, unequal, and holoblastic. Two polar lobes are formed, one at the first cleavage stage and one at the second cleavage stage. No evidence of external metameric iteration is visible through scanning electron microscopy or histology at any stage. A ciliated foot, a pedal pit, and aragonitic spicules develop from the definitive ectoderm. A spicule begins as a solid tip, continues to an open-ended hollow spicule, and finally becomes a closed-ended hollow spicule.

The free-swimming trochophore larvae of *E. babai* have been considered unusual in lacking the characteristic neomenioid cellular test, an outer locomotory structure within which the entire definitive adult body develops. However, through the use of scanning electron and light microscopy, semithin sections, Hoechst nuclear staining, and programmed cell death staining to study the ontogeny and fate of the apical cells, I show that the entire pre-oral sphere (the apical cap) of the larvae is similar to the test of the other neomenioids. The results suggest that the test of the neomenioid larvae is an enlarged pre-oral sphere of a trochophore. The test morphologies of neomenioid larvae are compared to those of pericalymma larvae of protobranch bivalves, and the homology and evolution of molluscan larval tests is discussed.

Received 25 July 2001; accepted 30 May 2002.

Email: aokusu@oeb.harvard.edu

## Introduction

Neomenioid aplacophorans (= Solenogastres) are shell-less vermiform molluscs with a ciliated foot and an epidermal cuticle covered by many calcareous spicules. Given that aplacophorans are hypothesized to hold a basal position among molluscs (Götting, 1980; Salvini-Plawen, 1985; Salvini-Plawen and Steiner, 1996; Ivanov, 1996; Waller, 1998; Haszprunar, 2000), their development may provide the key to answering outstanding questions in the evolution of molluscan larvae. However, little is known about the developmental processes and features of neomenioid aplacophorans. Larval descriptions are based on five neomenioid aplacophoran species: *Epimenia babai* Salvini-Plawen, 1997 (as *E. verrucosa*); *Halomenia gravida* Heath, 1918; *Neomenia carinata* Tullberg, 1875; *Nematomenia* (= *Dondersia*) *banyulensis* Pruvot, 1890; and *Rhopalomenia* (= *Proneomenia*) *aglaopheniae* Kowalewsky and Marion, 1887 (Pruvot, 1890, 1892; Heath, 1918; Baba, 1938, 1940, 1951; Thompson, 1959, 1960). Early cleavage pattern is known only for *E. babai* (Baba, 1940, 1951; and herein). Nothing has been reported on the early embryology of chaetodermomorph aplacophorans (= Caudofoveata), and their larval descriptions are based on a drawing of *Scutopus robustus* (Salvini-Plawen, 1990), on drawings based on Gustafson's unpublished sketches (Nielsen, 2001), and on scanning electron micrographs of *Chaetoderma nitidulum* larva (Nielsen, presented at World Congress of Malacology 2002).

Neomenioid aplacophorans are hermaphroditic and either brood juveniles (Heath, 1918; Salvini-Plawen, 1978) or have free-swimming lecithotrophic larvae with an outer locomotory larval test, within which the definitive adult structures develop (Pruvot, 1890, 1892; Thompson, 1960). A similar enveloping test, or "pericalymma," has also been described for the larvae of protobranch bivalves (Drew, 1897, 1899a, b, 1901; Gustafson and Reid, 1986, 1988a, b; Gustafson, 1987; Gustafson and Lutz, 1992; Zardus and

Morse, 1998). The homology of larvae with tests among protobranch bivalves and neomenioid aplacophorans remains uncertain because the phylogenetic relationships of these groups are still debatable, the morphology of these larvae is quite diverse, and the morphology of the neomenioid test is poorly understood (Pruvot, 1890, 1892; Drew, 1899b; Gustafson and Reid, 1986; Thompson, 1959, 1960; Gustafson and Lutz, 1992; Zardus and Morse, 1998).

The neomenioid aplacophoran *Epimenia babai* from Japan is considered to have a unique larval form among neomenioid aplacophorans in that it lacks the true test structure characteristic of neomenioid pericalymma larvae (Baba, 1938, 1940, 1951, 1999; Thompson, 1960; Nielsen, 2001). Baba (1938, 1940, 1951) was the first to describe the larval development of *E. babai*, and he suggested that the morphology and fate of the apical cells of the species do not resemble the pericalymma test cells of other neomenioid aplacophorans. Because of its unique development, the larval form of *E. babai* has been suggested to be an intermediate form between pericalymma and trochophore larvae (Baba, 1938, 1940, 1951, 1999) called "stenocalymma" by Salvini-Plawen (1973, 1980). The descriptions by Baba were based primarily on histological sections, but details of morphology and cell fate during embryogenesis were not studied, and thus such differentiation is not certain.

Adult specimens of *E. babai* are easily collected and maintained in the laboratory. Whereas most aplacophorans are small (1–5 mm) and inhabit the deep sea where they are not easily obtainable for developmental studies, *E. babai* can reach 30 cm in length and lives in relatively shallow water from 20 to 70 m in depth (Salvini-Plawen, 1997). The embryos are relatively large (*ca.* 250 μm) and can be maintained at room temperature. Taking advantage of the accessibility of *E. babai*, this study reexamines the early and late development of the species to elucidate some of the unknown developmental features of a neomenioid aplacophoran, such as the morphology and fate of the pericalymma test.

## Materials and Methods

### *Animal collection and culture*

Adult specimens of *E. babai* were collected offshore near Amakusa Marine Biological Laboratory (Kumamoto, Japan) in 1999 and 2000 during the most active breeding period between June and September (Baba, 1938, 1940, 1951). These specimens were up to 20 cm in length and 1 cm in diameter. The exemplars were collected from synthetic gill nets (3 m width, 500 m length, 5 × 5 cm mesh size) that were set on a rocky bottom at a depth of 20 to 30 m among beds of the soft coral *Alcyonium gracillimum*.

The adults were maintained in an aquarium with running seawater at ambient temperature, about 26 °C, and were supplied with fresh *Alcyonium gracillimum* for food. The animals spawned spontaneously several hours after sunset or were induced to spawn by turning off the light after 12–14 h of constant light. Spawned egg sheets (see Fig. 1a) were transferred to culture jars containing filtered seawater (0.45-μm mesh) with streptomycin (50 mg/ml) and penicillin (35 mg/ml) to reduce bacterial growth (Strathmann, 1987). Cultures were kept at both ambient temperature and 16 °C, and their development was compared. Developmental descriptions are based on cultures maintained at 16 °C. More than 1000 embryos from three adults were analyzed.

### *Scanning electron microscopy*

Egg capsules were freed from a jelly mucous casing by gentle agitation, and the embryos were dissected out of their capsules with fine forceps. The embryos were fixed in 1% osmium tetroxide ($OsO_4$) in filtered seawater and washed twice in 0.2 *M* sodium cacodylate buffer solution (pH 7.4). They were then dehydrated through a series of ethanol washes (20%, 50%, 75%) and transported from Amakusa to Woods Hole, Massachusetts, where dehydration in ethanol (100%, 100%) was completed. The samples were critical-point-dried (SAMDRI-780), mounted on aluminum stubs with double-sided tape, coated with gold in a sputter-coater (SAMSPUTTER-2a), and imaged using a JEOL scanning electron microscope (JSM-840).

### *Semithin sections*

Dissected embryos were first fixed in a solution of 3% gluteraldehyde in 0.2 *M* sodium cacodylate buffer at pH 7.4, washed in 0.2 *M* sodium cacodylate buffer, postfixed in 1% osmium tetroxide ($OsO_4$), and washed in the buffer again. The embryos were then dehydrated, transported as above, embedded in Araldite/Epon (EMbed-812), and sectioned with glass knives into semithin sections (0.30–1.0 μm). The sections were mounted onto clean slides on a hot plate (60 °C), stained with a mixture of methylene blue and azure II (Richardson *et al.*, 1960), washed under tap water, and imaged on a Zeiss light microscope.

### *Hoechst nuclear staining*

Larvae were incubated overnight at 4 °C in Hoechst solution (1 μg/ml) in 4% formalin (in seawater). The larvae were then washed in 1× phosphate buffered saline (PBS), mounted on a glass slide, and examined with fluorescence under a microscope with a UV filter set.

### *Programmed cell death determination*

Cell viability and apoptosis in the larvae were detected *in vivo* using acridine orange/ethidium bromide staining according to the method described by Martin *et al.* (1996) with slight modifications. Programmed cell death (PCD) occurs frequently during animal development when larval tissues

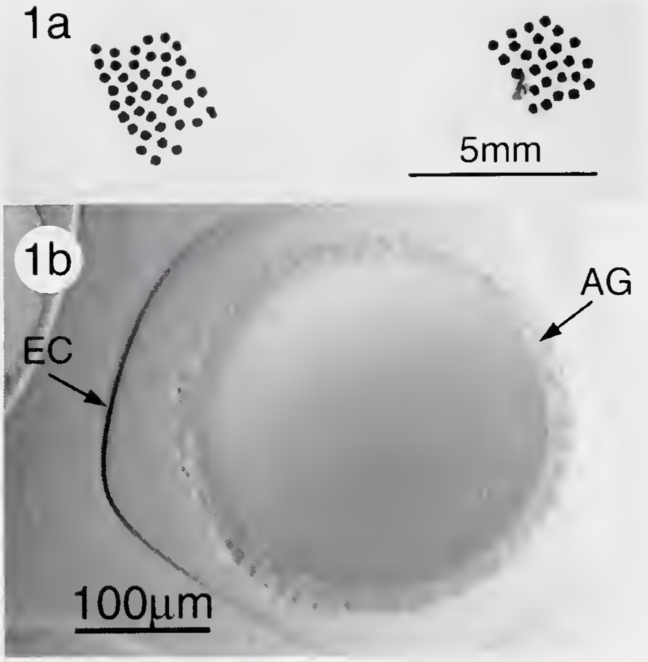

**Figure 1.** Eggs of *Epimenia babai*. (a) A pair of egg sheets (3 × 3 mm). Each sheet contained 20 to 50 fertilized eggs. (b) A fertilized egg (~250 μm in diameter) in a single egg capsule (EC) membrane. Numerous accessory granules (AG) were observed within the capsule.

are degenerated and lost during the transformation into the adult body form. Live larvae were incubated for 10 min in acridine orange (100 μg/ml) + ethidium bromide (100 μg/ml) in seawater. The larvae were washed in clean seawater for an hour and, while alive, were examined on a glass slide under a fluorescence microscope with a UV filter set.

The acridine orange intercalates into the DNA of live cells with intact membranes, and the cells fluoresce bright green. As apoptosis progresses, ethidium bromide enters the cells, and they fluoresce bright orange. Late apoptotic cells have a uniform bright orange color (Martin *et al.*, 1996).

## Results

### *Reproduction and spawning*

Three individuals of *Epimenia babai* laid approximately 20,000 eggs over 90 consecutive nights in the laboratory. One individual that was isolated for more than 90 days laid viable eggs. Sperm transfer was not observed.

Fertilized eggs were laid in pairs of square gelatinous sheets (3 × 3 mm) containing a single layer of 20–50 eggs (Fig. 1a). One individual laid one to four pairs of egg-sheets every night, one pair at a time, at intervals of about an hour. The egg sheets were always laid in pairs, presumably one from each of the paired gametoducts that open into the mantle cavity at the posterior end of the animal. At the time of deposition, the fertilized eggs were always at the single-cell stage. No brooding was observed.

### *Early development*

The early development of *E. babai* was followed using both scanning electron and light microscopy. Development was slower at 16 °C than at room temperature (26 °C) (Table 1). However, hatching time observed at 16 °C was the same as at 26 °C, with larvae reared at 16 °C hatching at a much earlier stage of development than those at 26 °C. The lower temperature did not cause any abnormalities in further development.

Observations of early embryogenesis are generally consistent with those of Baba (1940). The eggs are oval at first and become spherical within 30 min at a diameter of 250 μm. Each egg is enclosed in a tough transparent egg capsule 300–350 μm in diameter (Fig. 1b). The eggs are opaque yellow, presumably from high yolk content, and were surrounded by numerous accessory granules. Formation of two polar bodies, as reported by Baba (1938, 1940, 1951), was not observed.

Cleavage is spiral, unequal, and asynchronous (Figs. 2–9). First cleavage was meridional (= parallel to animal-vegetal axis) and unequal (Fig. 3). Just before the first cleavage was completed, the first polar lobe protruded from the vegetal side of the embryo (Fig. 3). The polar lobe appeared whiter and less yolky than the rest of the contents of the CD cell. The first polar lobe was soon absorbed by one of the two blastomeres, making this blastomere (CD) slightly larger than the other (AB).

Second cleavage was also meridional and unequal, forming blastomeres A–D. Cleavage was slightly asynchronous, with the larger blastomere (CD) dividing slightly later than the AB cell (Figs. 4, 5). The cross-furrow of the four blastomeres was visible but indistinct (Fig. 4). A second polar lobe protruded from the vegetal region during CD

**Table 1**

*Approximate timing of early development of* Epimenia babai *at 16–18 °C and ambient temperature (26 °C)*

| Developmental stage | 16–18 °C | 26 °C |
|---|---|---|
| Spawning | 0 h | 0 h |
| 2-cell | 2 h | 1 h |
| 4-cell | 4 h | 2.5 h |
| 8-cell | 6 h | 3.5 h |
| 16-cell | 8 h | 4.5 h |
| 32-cell | 10 h | 5.5–6 h |
| Blastula | 15 h | 7–9 h |
| Gastrula | 20–24 h | 10–13 h |
| Trochophore | 48 h | 24 h |
| Hatching | 3 d | 3 d |
| Metamorphosis | 11–13 d | 5–7 d |

2

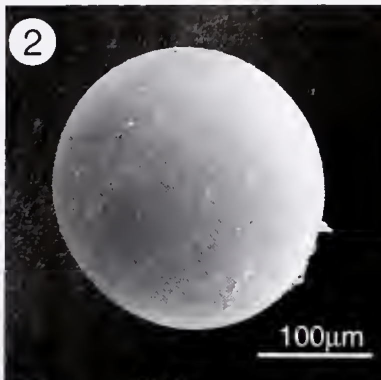

3

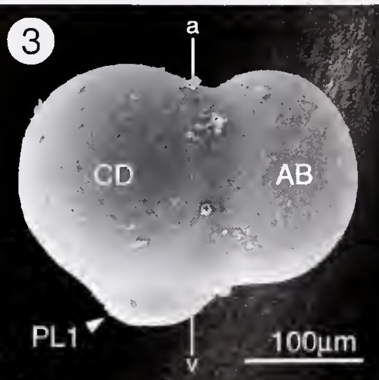
a
CD
AB
PL1
v
100µm

4

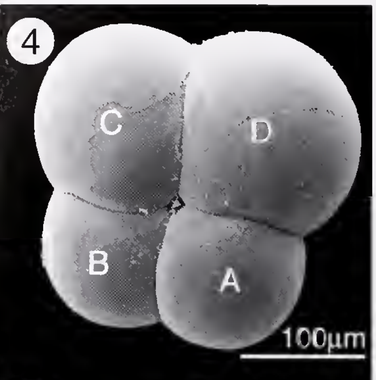

5

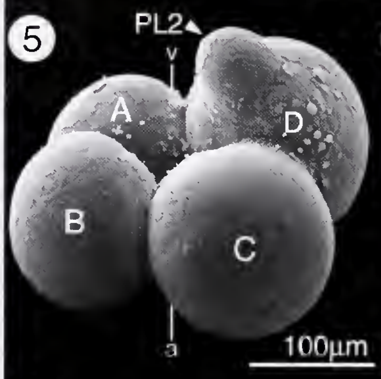
PL2
v
A
D
B
C
a
100µm

6

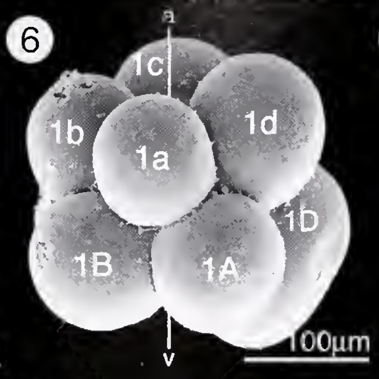
a
1c
1b
1a
1d
1D
1B
1A
v
100µm

7

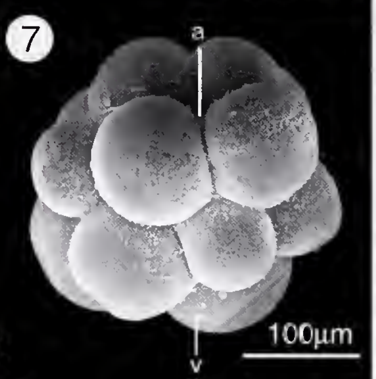

8

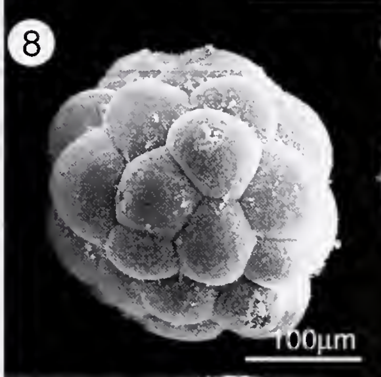

9

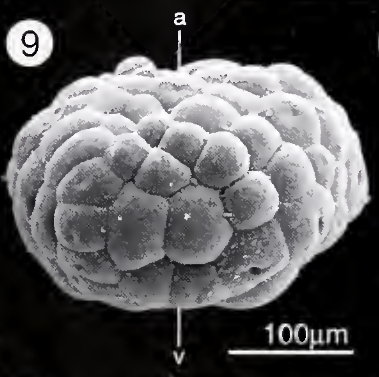

10

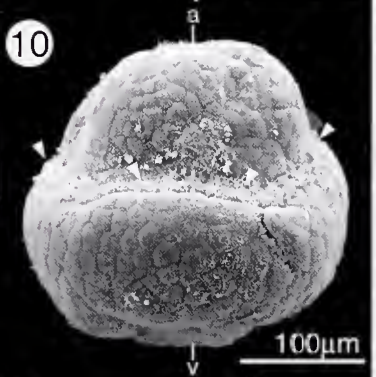

11

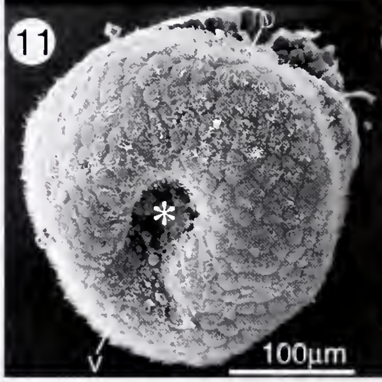

12

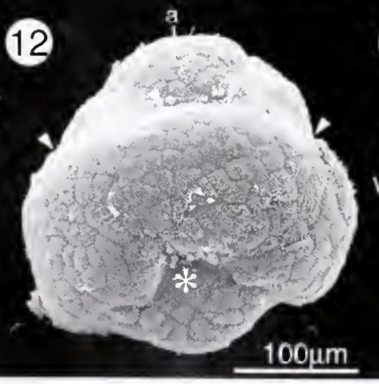

13

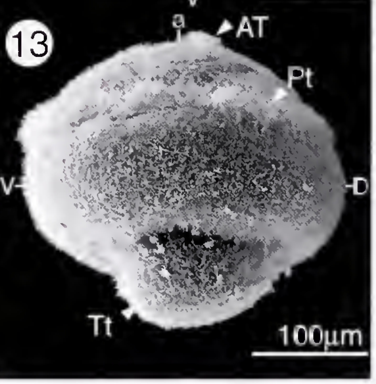
a
AT
Pt
V
D
Tt
100µm

division. Within 30 min, it was absorbed by the D blastomere (Fig. 5), making it the largest of the four.

Third cleavage was equatorial (= perpendicular to the animal-vegetal axis), resulting in four micromeres at the animal pole (1a–1d); the four macromeres remained at the vegetal pole (1A–1D) (Fig. 6). The chirality of spiral cleavage displaced the four micromeres dextrally (clockwise from the animal pole) relative to the four macromeres. Cell 1D seemed to be slightly larger than the rest of the macromeres, but the difference was not substantial. Cleavage continued to be slightly asynchronous by alternation of chirality: the fourth cleavage was sinistral (anti-clockwise from the animal pole), producing 16 cells (Fig. 7); and the fifth cleavage was dextral, producing 32 cells (Fig. 8).

The embryos reached 64 cells about 15 h after they were laid and became flattened animal-vegetally, forming a blastula (Fig. 9). Further cleavage stages until gastrulation were difficult to follow owing to the asynchronous nature of cleavage.

Within 24 h after oviposition, while the embryos were still within the capsule, gastrulation occurred at the vegetal pole by means of both epiboly and invagination (Figs. 10, 11). Cells between the blastopore and presumptive prototrochal cells thickened to form a broad lip around the vegetal side of the gastrula (Fig. 10). Patches of short cilia covered the surface of the gastrula. Cells within the blastopore proliferated to form an outgrowth of a definitive ectodermal bud beneath. From this elongation of ectoderm, the blastopore diminished and migrated toward the future ventral side of the larva (Fig. 12).

Two days after oviposition, the presumptive apical tuft and prototroch on the apical region, and the telotroch at the caudal end of the ectodermal trunk, became evident (Figs. 13, 27a). The unciliated ectodermal trunk bent slightly towards the ventral side.

### *Larval development*

Three days after oviposition, the larvae hatched and swam forward and spirally, using the prototroch, until they reached metamorphosis 9 to 13 days after oviposition (7- to 11-day-old larvae) (see below). It is not certain whether the telotroch was directly involved in swimming or not. The larvae did not seem to be phototactic.

*Larvae aged 1 to 3 days.* The free-swimming larvae had three distinct body regions: apical cap, trunk, and caudal region (Figs. 14a, 27b). The entire pre-oral sphere of the larvae, the apical cap, was completely ciliated and was divided into a pretrochal and a post-trochal region by a prominent row of compound prototroch cilia at its equator (Figs. 14a, b, 16, 17, 27b). The pretrochal hemisphere of the apical cap originated most larval structures, such as the apical tuft, also composed of compound cilia (Figs. 14a, 15), and secretory globules (Figs. 17, 21a, b; morphology discussed below in detail). Cerebral ganglial depressions formed on the pretrochal hemisphere of the apical cap, and they persisted through metamorphosis (Figs. 14a, 17, 19a, 22a, b, 23a, b, 24a, 27, 28; development discussed below in detail).

The trunk region of the larvae was unciliated. The trunk gave rise to definitive ectodermal structures, such as cuticle and epidermis. A ciliated stomodeum formed on the ventral side of the unciliated ectodermal trunk directly below the apical cap (Figs. 14b, 20a, b, 27b, 28a).

The caudal region was covered with short cilia. Globules, similar to those of the pretrochal hemisphere of the apical cap, were present (Figs. 14b, 18). The cilia at the periphery and the center of the caudal region were composed of compound cilia, and the cilia were longer (*ca.* 15 $\mu$m) than on the flat bottom surface (*ca.* 10 $\mu$m) (Figs. 14b, 18).

*Larvae aged 4 to 6 days.* The post-trochal region of the apical cap narrowed and the cerebral depressions became deeper as the trunk grew longer (Figs. 19, 27c). A wide midventral longitudinal band (15–20 $\mu$m across) of the trunk region of the larvae became ciliated, forming a foot (Figs. 19, 27b). At the animal end of the long foot, a pedal pit formed sharp-ended cilia, longer (3–4 $\mu$m) than the cilia on the foot, which had blunt ends (1–2 $\mu$m) (Fig. 19b). Epidermal papillae formed covering the entire trunk region (Fig. 19a, morphology discussed later in detail).

### *Larval morphology*

*Secretory organs.* The function of the globules that covered the pretrochal hemisphere of the apical cap and the entire surface of the caudal region (Figs. 14a, b, 17, 18)

**Figures 2–13.** Scanning electron micrographs (SEM) of the early embryological development of *Epimenia babai* before hatching. Animal vegetal axis (a–v) and dorsal ventral axis (D–V) are indicated. 2. A fertilized egg just after spawning; polar bodies not detected. 3. The beginning of first cleavage (lateral view). The first polar lobe (PL1) has protruded from the vegetal side as the two cells (AB/CD) divide meridionally. The polar lobe was then absorbed by the CD cell, making it larger than AB. 4. Animal view of the 4-cell embryo (A–D). 5. Vegetal view of the 4-cell (A–D) embryo. The second polar lobe (PL2) protruded from the vegetal side of the D cell, and was soon absorbed by the D cell. 6. Lateral view of the 8-cell stage (1a–1d, 1A, 1B, 1D). 7. Lateral view of 8- to 16-cell stage. 8. Animal view of 16- to 32-cell stage. 9. Lateral view of 64-cell to blastula stage. The embryo has flattened in animal-vegetal direction. 10. Lateral view of gastrula. The arrowheads indicate ciliated presumptive prototrochal cells. The entire embryo is covered with short microvilli. 11. Vegetal view of the gastrula showing the blastopore opening (*). 12. Lateroventral view of embryo showing proliferation of the unciliated ectodermal cells dorsal to the blastopore. This outgrowth of the cells has shifted the ventral opening of the blastopore (*) towards the ventral side of the larva. 13. Tip of the outgrowth has become ciliated and forms the presumptive telotroch. The presumptive apical tuft and prototroch are apparent on the apical cap. The trunk is bent slightly towards the ventral side. a, animal pole; AT, apical tuft; D, dorsal; Pt, prototroch; Tt, telotroch; v, vegetal pole; V, ventral.

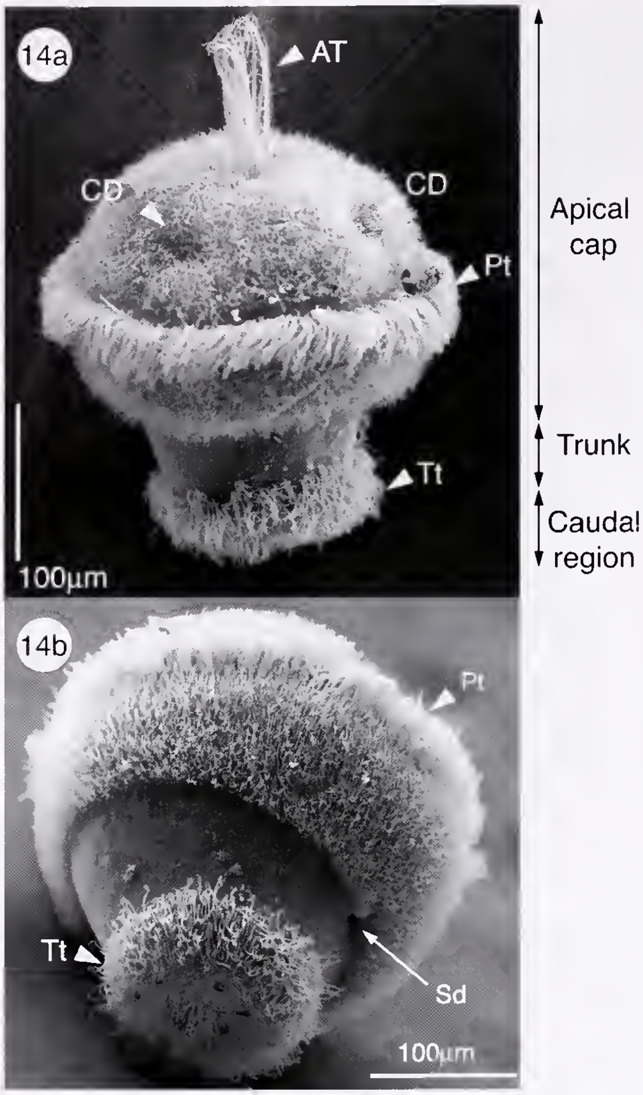

**Figure 14.** Larvae after hatching from the egg capsule (3 days after ovipositon, 1-day-old larvae). (a) Ventral view of the larva with three distinct body regions: ciliated pre-oral apical cap, unciliated trunk, and ciliated caudal region. (b) Vegetal (caudal) view of the trochophore larva showing the small invagination of the stomodeum on the ventral side of the trunk. AT, apical tuft; CD, cerebral depression; Pt, prototroch; Sd, stomodeum; Tt, telotroch.

appears to be secretory, because the cilia-free membranes covering the globules were often ruptured (Fig. 21a, b). The globules appeared iridescent under the light microscope. The globules disappeared at metamorphosis, as the apical cap and the caudal region were withdrawn into the trunk (Fig. 24b).

One to two hundred small epidermal papillae appeared on the trunk (Figs. 19a, 23a, 24b). Like the globules mentioned above, these papillae are suspected to be secretory in function. Unlike the globules, the papillae persisted after metamorphosis (Figs. 24b, 25a). Protonephridia were not observed in the light micrographs of semithin sections.

*Nervous system.* The cells underneath a pair of depressions on the pretrochal region of the apical cap on the future ventral side of the adult (Figs. 14a, 17, 19a, 22a, 23a, b, 24a, 27, 28) became internalized to differentiate into definitive cerebral ganglia (Fig. 22b). These depressions were free of white globules, but the surface ciliation was not different from that of the rest of the apical area (Figs. 17, 22a). Pedal ganglia arose (Fig. 22b); however, the process by which they were formed is uncertain. Development of terminal sense organs was not apparent, although may have been present.

### *Metamorphosis*

*Larvae aged 7 to 8 days: beginning of metamorphosis.* In spite of active ciliary movement of the prototroch and apical tuft, larvae at this point were no longer able to swim, and they sank to the bottom of the culture jars. The unciliated trunk grew longer, the epidermal papillae increased in number and size, and presumptive spicules formed (Fig. 23c, d). Spicules seemed still to be under the cuticle just along the foot groove and beneath the apical cap (Fig. 23). Although the post-trochal region of the test narrowed as the trunk grew, lengthening of the trunk appeared to be due to proliferation of definitive ectodermal trunk cells and not to any material supplied by the larval test (Figs. 23a, 27; later discussed in the programmed cell death determination of the test). Larval structures, such as the apical tuft and telotroch, were diminished. The apical cap and the prototroch occasionally became withdrawn into the trunk (Figs. 23b, 27d, e, 28b).

*Larvae aged 9 to 11 days: completion of metamorphosis.* The trunk was now completely covered with epidermal papillae and spicules that extended well beyond the cuticle (Fig. 24a). The whole caudal region and the cap became enclosed within the trunk and covered by the posterior and anterior extensions of definitive ectoderm (Fig. 24b).

The post-metamorphic juveniles crawled on the ciliated foot located in the midventral pedal groove. A rudiment of the adult anterior atrium developed as an invagination above the mouth. In adults, the invagination was often open, with the anterior end and half the length of the entire body raised above the substrum. The juveniles seemed to be sensitive to vibration, but not to light.

The juveniles grew more transparent as the original yolky yellow color became internally restricted. The animals lived for up to 1 month without any particulate food source, and the gut was not differentiated in histological sections during the period.

*Development of hollow spicules.* Juvenile spicules are different from adult spicules in shape and distribution. The spicules of adults are solid and bladelike along the foot

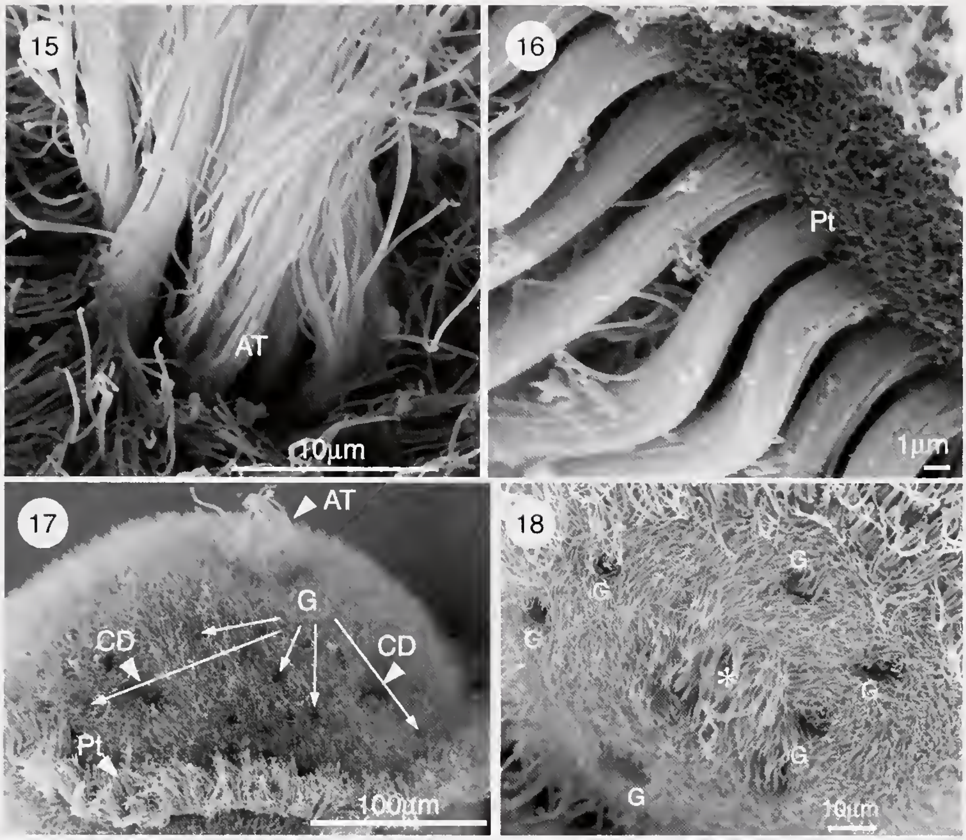

**Figures 15–18.** Larval structures of 1- to 3-day-old larvae. 15. Apical tuft composed of several bundles of compound cilia. 16. Compound cilia of prototroch. 17. Ventral view of the apical cap. The two lateral depressions (CD) mark where cells are proliferating internally to form the cerebral ganglia. Unciliated globules are scattered between and on both sides of the depressions. 18. Bottom surface of the caudal region. The entire surface is ciliated except for scattered unciliated globules. The cilia at the periphery and in the center of the caudal region (*) are longer than the rest of the cilia on the caudal surface. AT, apical tuft; CD, cerebral depression; G, globules; Pt, prototroch.

groove and near the mouth, but the rest of the body is covered by hollow, needlelike spicules forming a crisscrossed meshwork within the cuticle. In juveniles, however, flat bladelike spicules were distributed evenly over the entire body along with upright and needlelike spicules (Fig. 25a, c). The juvenile pedal spicules were flat and bladelike as in the adults (Fig. 25b, c), and the head region also was covered with flat, bladelike spicules (Fig. 25d).

The development of hollow spicules in early juveniles was observed for the first time in aplacophorans (Fig. 26) by observing within the cuticle of live larvae on a glass slide using polarized light microscopy. The first part of the spicules to be secreted was the solid distal tip (Fig. 26a). The spicules continued to grow at the proximal end, becoming hollow with an open end (Fig. 26b). The proximal end finally closed to form a closed-ended hollow spicule with solid base (Fig. 26c). This type of hollow spicule formation is known to continue throughout the growth of adult neomenioids (Hoffman, 1949).

### *Morphology and fate of apical cells*

*Hoechst nuclear staining.* Hoechst nuclear staining showed that cells of the apical cap were much larger than cells of the trunk region and stayed relatively constant in size (Fig. 27). It also showed that the number of the cells in the apical cap decreased as the apical cap degenerated, while the cells in the trunk region decreased in size and increased in number through proliferation (Fig. 27).

*Programmed cell death determination.* Cell viability and apoptotic index of apical cells were determined using programmed cell death (PCD) staining. At a stage as early as the first day of hatching, the entire pre-oral region of the embryos, including the prototrochal cells, stained orange (Fig. 28a), thus indicating PCD. The cerebral ganglial depressions, however, remained green and thus viable (Fig. 28a). The definitive ectodermal trunk also remained green and viable (Fig. 28a). The caudal region stained orange (Fig. 28a), indicating that the caudal cells also were degenerating.

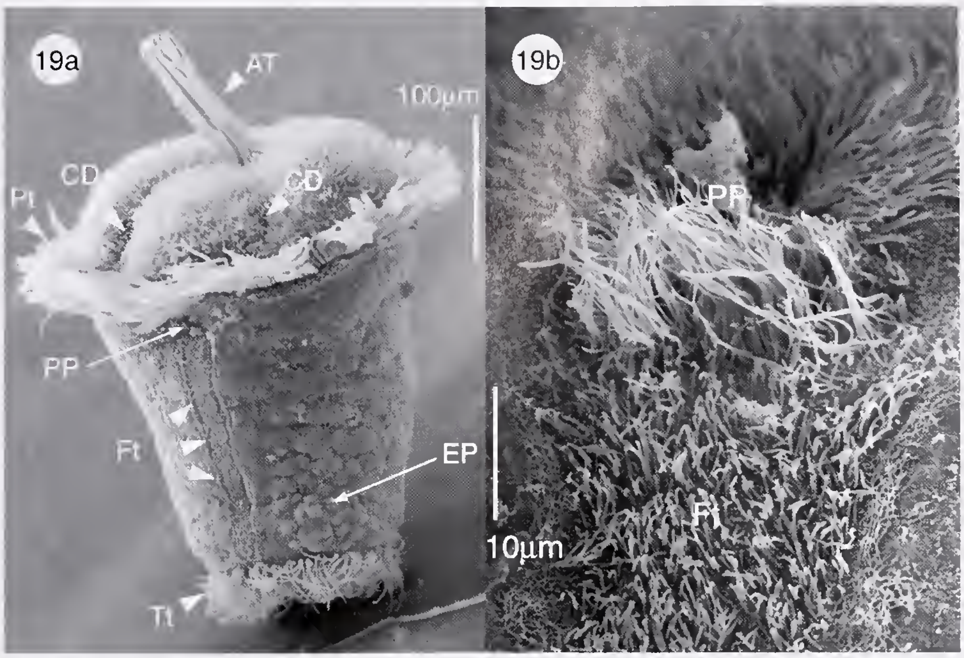

**Figure 19.** Larvae aged 4 to 6 days. (a) Ventral view. The ciliated foot has formed midventrally on the trunk, and the pedal pit has formed at its apical end. Epidermal papillae are beginning to form on the trunk. The post-trochal region of the apical cap is diminishing as the trunk region elongates. (b) Cilia in the pedal pit are longer (3–4 $\mu$m) and more slender than those on the foot (1–2 $\mu$m). AT, apical tuft; CD, cerebral depression; EP, epidermal papilla; Ft, foot; PP, pedal pit; Pt, prototroch; Tt, telotroch.

The pre-oral region of larvae at later stages, 5 to 7 days old, stained in brighter orange to red as it became withdrawn into the definitive ectoderm (Fig. 28b), indicating that these cells entered later stages of apoptosis. The caudal telotroch, partially withdrawn, also stained brighter orange. The elongated ectodermal trunk still remained green, indicating viable cells, but the epidermal papillae stained in orange to red, presumably because they are secretory and undergoing rapid turnover and cell death.

## Discussion

### *Observations and remarks on reproduction and development*

As observed in this study, reproduction and spawning in *Epimenia babai* were mostly consistent with Baba's descriptions (1938, 1940, 1951). *E. babai* is hermaphroditic, and although the time of sperm transfer is not known, fertilization is assumed to have occurred internally while the posterior ends of animals were entwined. This behavior has also been reported in *E. australis* (Scheltema and Jebb, 1994). However, an observation that one individual isolated for more than 90 days laid viable fertilized eggs suggests either that *E. babai* can self-fertilize, or that sperm were held for that period in the seminal receptacles.

Although brooding was not observed in *E. babai* during this study, the capacity to keep embryos within the posterior mantle cavity in fast water currents cannot be refuted. Brooding of larvae in the posterior mantle cavity was previously reported in *E. babai* (Baba, 1938, 1951), as well as in *E. australis* (Scheltema and Jebb, 1994), *Halomenia gravida* (Heath, 1918), and some perimeniid (= "pruvotinid") neomenioids (Thiele, 1913; Salvini-Plawen, 1978). During this study, *E. babai* individuals tightly curled their posterior part around the alcyonarian corals, thus pressing closed the mantle cavity opening and keeping their eggs within the mantle cavity. In their natural habitat, *E. babai* and other species of *Epimenia* live and feed on the alcyonarian corals that prefer strong swift water currents (Baba, 1938, 1940, 1951; Salvini-Plawen, 1972; Salvini-Plawen and Benayahu, 1991; Scheltema and Jebb, 1994). Therefore, brooding may take place in the natural habitat.

### *Homology of tests among neomenioid aplacophorans*

On the basis of similarity in cell type, ontogeny, ciliation pattern, and cell fate of the apical cap, the larva of *E. babai* is here proposed to have a test-like apical cap with cells similar to the test cells of larvae of other neomenioid aplacophorans: *Neomenia carinata, Nematomenia banyulensis,* and *Rhopalomenia aglaopheniae* (Pruvot, 1890, 1892; Thompson, 1960) (Fig. 29a). The apical cap of *E. babai* and the tests of the other neomenioids are composed of large yolky cells that are larval in fate and pre-oral in origin, are

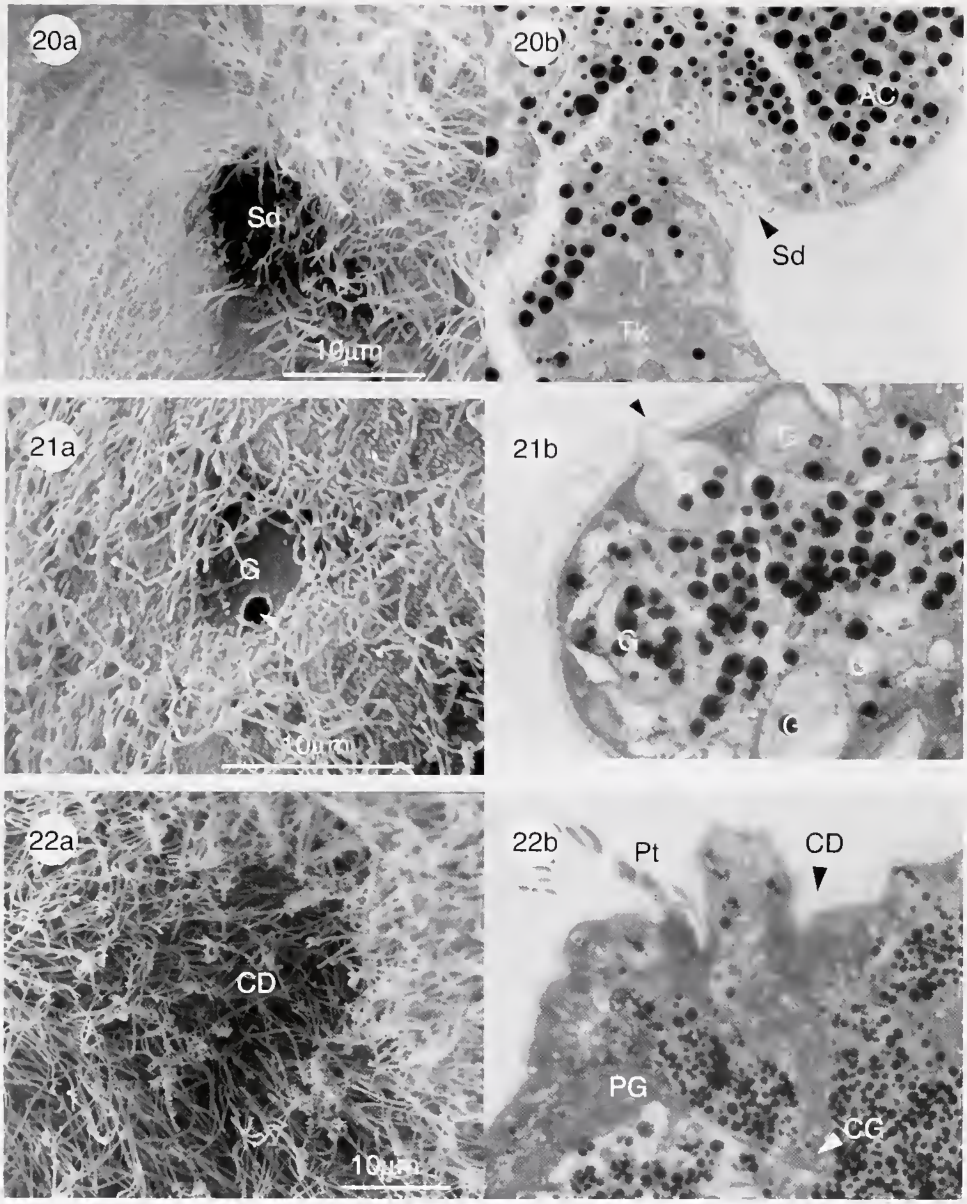

**Figures 20–22.** Development of stomodeum, globules, and cerebral depression of 1- to 3-day-old larvae. 20a. SEM image at the first sign of the stomodeal invagination on the trunk just beneath the apical cap. 20b. Light microscope image of a histological section through the ciliated stomodeum. 21a. SEM image of a globule (Figs. 17, 18) with an unciliated surface and a hole (arrowhead) that remained after the globule had ruptured. 21b. Light microscope image of a histological section of a globule as it ruptured (arrowhead). 22a. SEM image of the surface of one of the two cerebral depressions on the apical cap. The surface ciliation of the depression was not different from the surrounding area. 22b. Light microscope image of cells beneath the depression (arrowhead) that have proliferated into a cerebral ganglion, which connects to a pedal ganglion. AC, apical cap; CD, cerebral depression; CG, cerebral ganglion; G, globule; Sd, stomodeum; PG, pedal ganglion; Pt, prototroch; Tk, trunk.

covered with uniform short cilia, have a row of prototrochal cells and an apical tuft, and have cerebral ganglia depressions that persist through metamorphosis. The "test" of *E. babai* is less obvious because its cells are much smaller than those of other neomenioid tests, thus leaving the developing definitive ectodermal trunk underneath more exposed (Fig. 29).

The apical cap cells of the *E. babai* larvae are entirely apoptotic and, like the tests of other neomenioid aplacophorans, presumably do not contribute to development of any definitive adult structures except for the cerebral ganglia. The tests of *Nematomenia banyulensis* and *Rhopalomenia aglaopheniae* were said by Pruvot (1890, 1892) to be cast off and discarded at metamorphosis. The test cells of

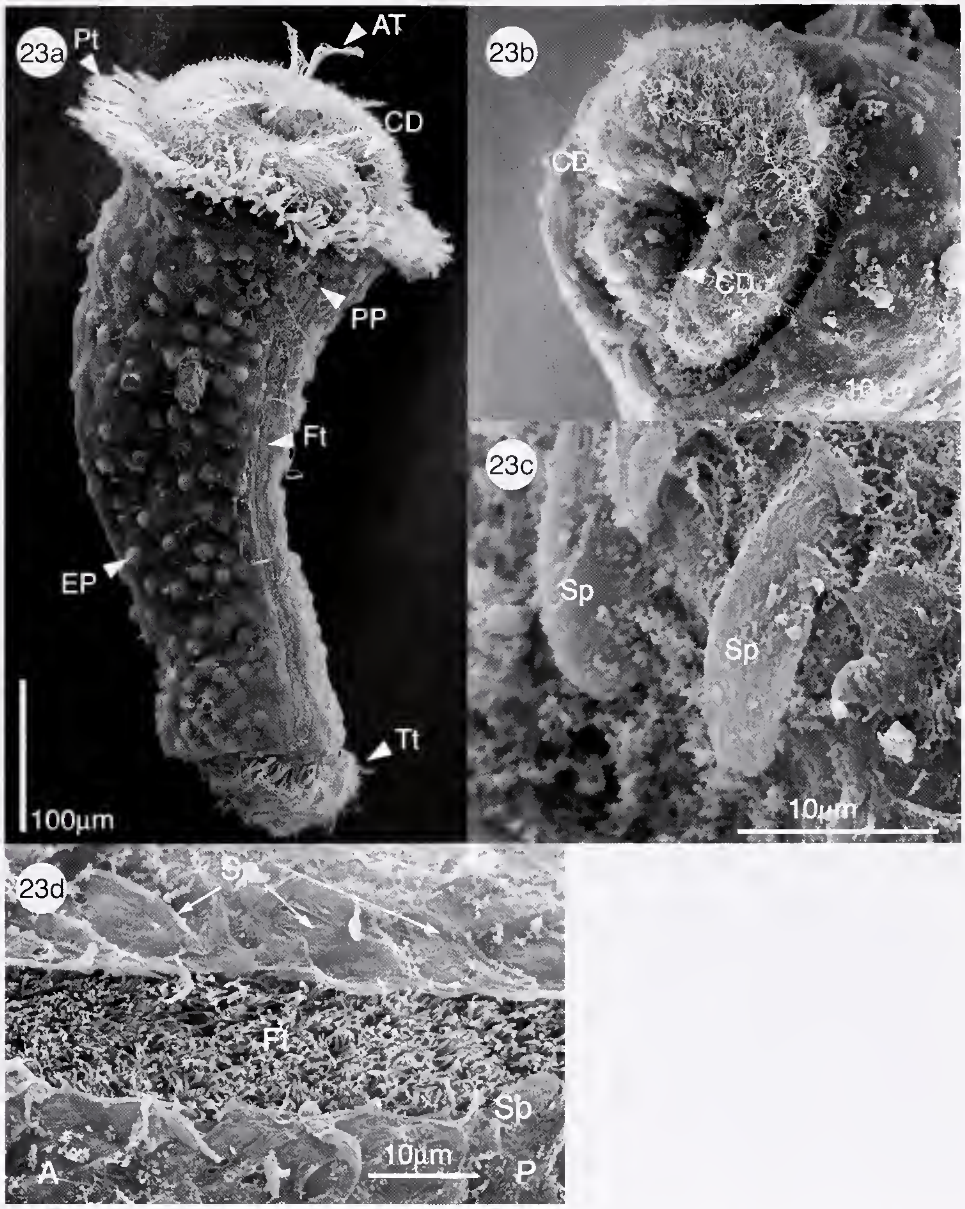

**Figure 23.** Beginning of the gradual process of metamorphosis (7- to 8-day-old larvae). (a) The post-trochal region of the apical cap has completely disappeared. The trunk has become covered with numerous large epidermal papillae. (b) A larva with its apical region withdrawn into the trunk. (c) Aragonitic larval spicules, restricted to the trunk region, have started to appear underneath the cuticle. (d) Regularly arranged spicules underneath the cuticle beside the foot. AT, apical tuft; CD, cerebral depression; EP, epidermal papilla; Ft, foot; Sp, spicule; PP, pedal pit; Pt, prototroch; Tt, telotroch.

*Neomenia carinata* are absorbed by the animal at metamorphosis, as are the apical cap cells of *E. babai*; they degenerate and in *N. carinata* are known to be the main food reserve of post-larvae (Thompson, 1960). The fate of the cells in the brooded larvae of *Halomenia gravida* is not clear, although Heath (1918) observed in histological sections that they become reduced in size at later stages, indicating resorption.

There are some differences among neomenioid aplacophoran species in the number of "test" cells and in number of pairs of cerebral ganglia that proliferate from the test (Table 2). Test cells are arranged in six regular tiers of cells in *Nematomenia banyulensis* and *Rhopalomenia aglaopheniae* (Pruvot, 1890, 1892) and in five regular tiers of cells in *Neomenia carinata* (Thompson, 1960), whereas the apical cap cells of *E. babai* are numerous and irregularly arranged. The number of cerebral ganglia invaginations also varies: there is one pair in *E. babai*, *Nematomenia banyulensis*

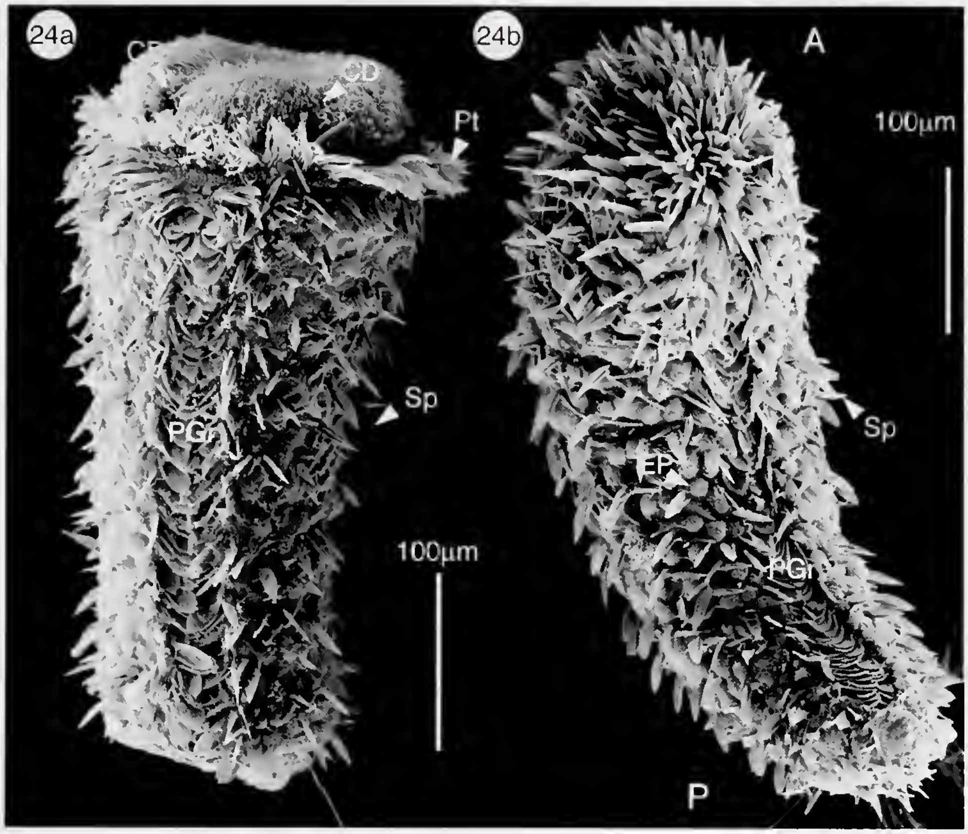

**Figure 24.** Larvae during the completion of metamorphosis (9- to 11-day-old larvae). (a) The larva covered by spicules on the trunk. The apical cap has diminished, and the apical tuft is being resorbed at the apical end. (b) Post-metamorphic juvenile. The apical cap and caudal regions have been completely engulfed by the trunk, leaving the trunk as the only definitive juvenile structure. A, anterior; CD, cerebral depression; EP; epidermal papilla; Sp, spicule; P, posterior; PGr, pedal groove; Pt, prototroch.

and *R. aglaopheniae* (Pruvot, 1890, 1892), whereas there are three pairs in *Neomenia carinata*, the third pair corresponding to the pedal ganglia (Thompson, 1960). In *Nematomenia banyulensis* and *R. aglaopheniae*, the pedal ganglia proliferate and split off from the cerebral ganglia internally (Pruvot, 1890, 1892). The process of pedal ganglia formation was not clear for *E. babai*.

*Phylogenetic affinities of pericalymma larvae*

Tests or test-like structures also occur in other molluscan taxa. Diverse forms of tests are described from six protobranch species: *Acila castrensis* (Zardus and Morse, 1998), *N. delphinodonta* (Drew, 1901), *Nucula proxima* (Drew, 1899a), *Solemya reidi* (Gustafson and Reid, 1986), *S. velum* (Gustafson and Lutz, 1992), and *Yoldia limatula* (Drew, 1899b). Protobranch bivalve tests are composed of large yolky cells, and the tests engulf the larvae entirely (*N. delphinodonta, S. reidi, S. velum*, and *Y. limatula*) or only partly (*A. castrensis* and *N. proxima*). The protobranch tests are larval and are cast off and ingested through the mouth at metamorphosis. The ciliation pattern of protobranch bivalve larvae is diverse: *A. castrensis, N. proxima*, and *Y. limatula* have an apical tuft and three rows of ciliary bands, whereas *N. delphinodonta, S. reidi*, and *S. velum* have no apical tuft and no ciliary bands. The tests of *A. castrensis, N. delphinodonta, N. proxima*, and *Y. limatula* are composed of five rows of cells, whereas the tests of *S. reidi* and *S. velum* are composed of nine. The caudal organ also seems to be diverse among protobranchs: *A. castrensis* and *S. reidi* have a ciliated caudal organ, *N. proxima* has an unciliated caudal organ, and *S. velum* and *Y. limatula* have no caudal organ.

Test-like structures are also found among trochophore larvae of scaphopods, described as having an apical tuft and three or six ciliary bands (Lacaze-Duthiers, 1856; Geilenkirchen *et al.*, 1970; Guerrier *et al.*, 1978; Wanninger and Haszprunar, 2001). No ciliated caudal structure has been reported. The test of scaphopods, in later developmental stages, becomes pushed anteriorly to form a velum (Lacaze-Duthiers, 1856). The scaphopod velum has been homologized with the lamellibranch bivalve velum. However, the scaphopod velum functions solely in locomotion, as in the

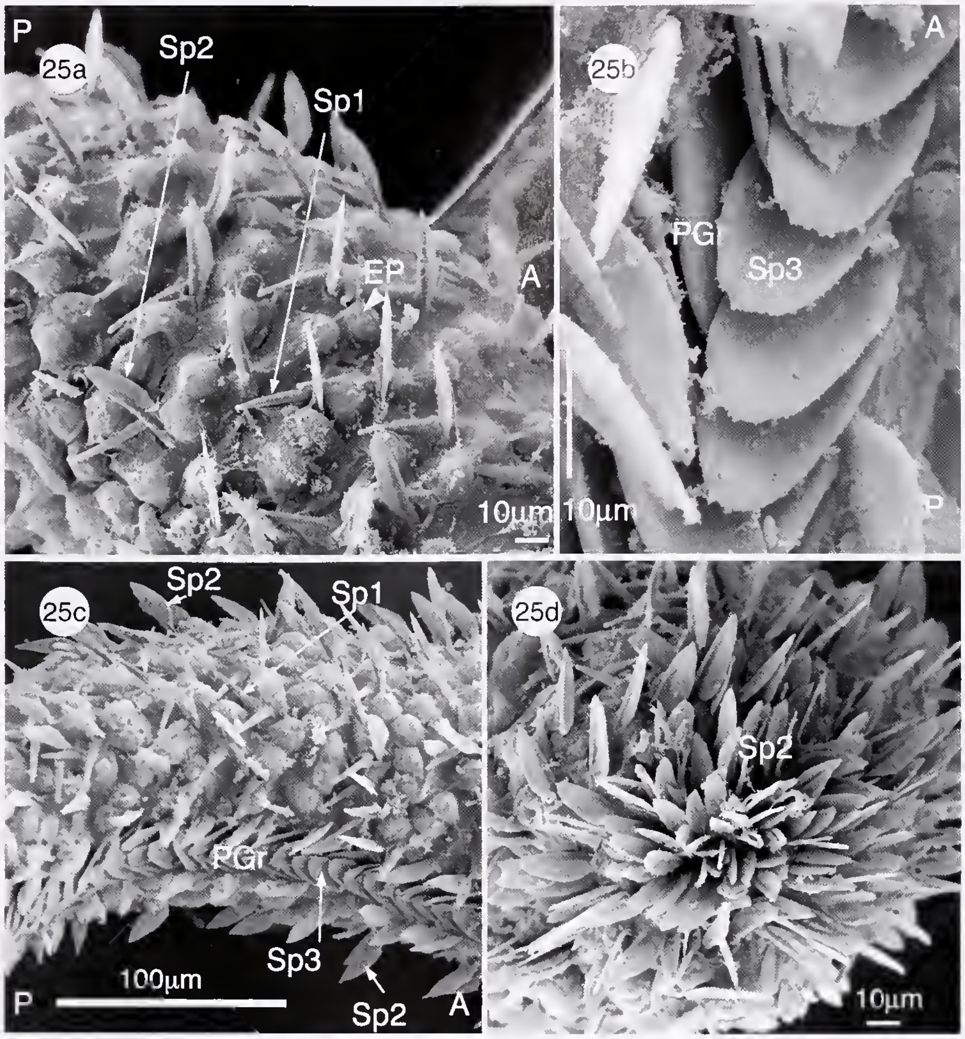

**Figure 25.** Three types of larval spicules right after metamorphosis. (a) Dorsal view. Two types of spicules are equally abundant over the entire body of the juvenile: hollow upright spicules (Sp1) lie against the body, while bladelike solid spicules (Sp2) project outwards from the body. (b) The third type of larval spicule (Sp3) is broad and solid, forming a single row on each side of the pedal groove. (c) Ventral view. (d) Anteriormost region covered with Sp2-type spicules. A, anterior; EP; epidermal papilla; P, posterior; PGr. pedal groove; Sp1, spicule type 1; Sp2, spicule type 2; Sp3, spicule type 3.

pericalymma tests, whereas the lamellibranch bivalve velum also functions in feeding, and the homology is not certain.

Polyplacophorans (Grave, 1932; Eernisse and Reynolds, 1994), archaegastropods (Patten, 1886; Kessel, 1964), and chaetoderm aplacophorans (Nielsen, 2001) have trochophore larvae with a ciliated circular velum. Polyplacophoran vela are composed of one to three rows of prototrochal bands (Grave, 1932; pers. obs.). The ventral side of the ciliated apical region of polyplacophorans becomes absorbed at metamorphosis, while the dorsal side of the apical region gives rise to adult features such as the anteriormost shell valve and spicules (Grave, 1932). The archaegastropod vela also have three rows of prototrochal bands, which function in both locomotion and feeding. There seem to be several rows of ciliary bands on the chaetoderm aplacophoran vela; however, lack of complete developmental descriptions of the group limits speculation.

The question of the ancestral larval type among molluscs has been important in many discussions of their origin and diversification. The pericalymma of neomenioid aplacophorans and protobranch bivalves has been regarded as plesiomorphic by some authors (*e.g.*, Drew, 1901; Thompson, 1960; Salvini-Plawen, 1972, 1973, 1980), although the trochophore has been generally considered plesiomorphic (Haszprunar *et al.*, 1995; Rouse, 1999) and the pericalymma as derived. It has also been suggested that the lamellibranch velum could have arisen from the coalescence of perica-

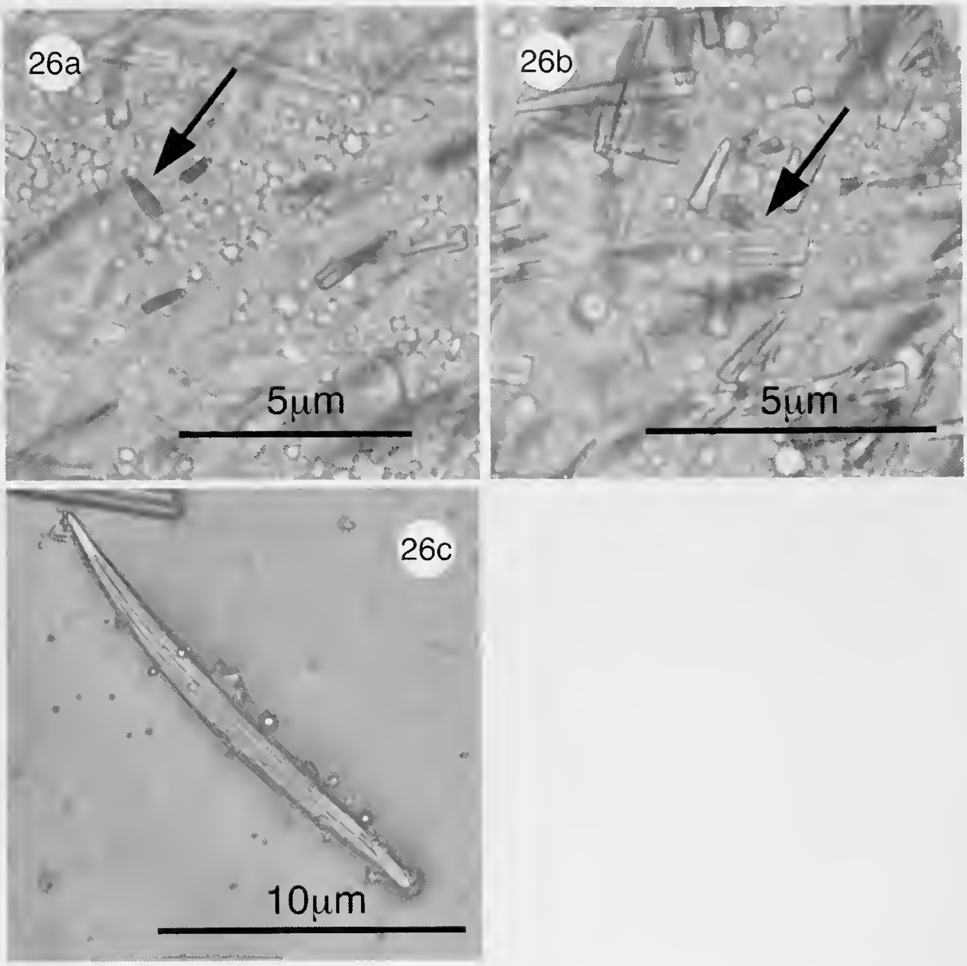

**Figure 26.** Developmental sequence of hollow spicules in *Epimenia babai* juveniles. Spicule begins as a solid tip (a), develops to a hollow, open spicule (b), and finally becomes a hollow, closed spicule (c).

lymma test (Drew, 1899b, 1901). However, there are as yet neither sufficient morphological data nor any cell lineage data to resolve the question of homology among the tests and homology of the tests to the velum.

Trochophore larvae seem to have gone through many modifications, not only within the clade Mollusca, but also in other spiralian taxa. Test-like structures are also found among lecithotrophic larvae of non-molluscan spiralians: the "serosa" of the sipunculid *Sipunculus nudus* (Rice, 1988); the "endolarva" of the polychaete *Phyllodoce mucosa* (Cazaux, 1970) and other Phyllodocidae spp. (Dawydoff, 1959); the "Iwata's larva" of a heteronemertean (Korschelt, 1936; Iwata, 1958; Jägersten, 1968); and the lecithotrophic nemertean larvae of *Emplectonema gracile* (Delsman, 1915), *Geonemertes australiensis* (Hickmann, 1963), and *Tetrastemma candidum* (Maslakova and Malakhov, 1999).

Given that test-like structures occur across various distant taxa within Spiralia that have lecithotrophic larvae, that their tests are composed of yolk cells, and that the tests are merely an enlarged pre-oral region of a trochophore larva, the tests could have arisen independently in each clade by adaptation to lecithotrophy. Homology among larval tests within molluscs and among spiralians and the pattern in which they evolved within the clade can probably be ascertained by more detailed developmental data analyzed within a well-corroborated phylogenetic framework. However, the phylogeny of Mollusca is controversial; cladistic analysis of a limited number of morphological characters (Salvini-Plawen and Steiner, 1996; Waller, 1998; Haszprunar, 2000) and available molecular sequence data on 18S rRNA (Winnepenninckx *et al.*, 1996) have not yet resolved the issue. Larval development of other neomenioids and the Chaetodermomorpha needs to be studied in order to understand the diversity of developmental processes among aplacophorans. In addition, cell lineage tracing would help to ascertain the exact ontogeny of the tests among molluscs and other spiralians. Furthermore, developmental descriptions of monoplacophoran larvae, which are entirely lacking, are desired.

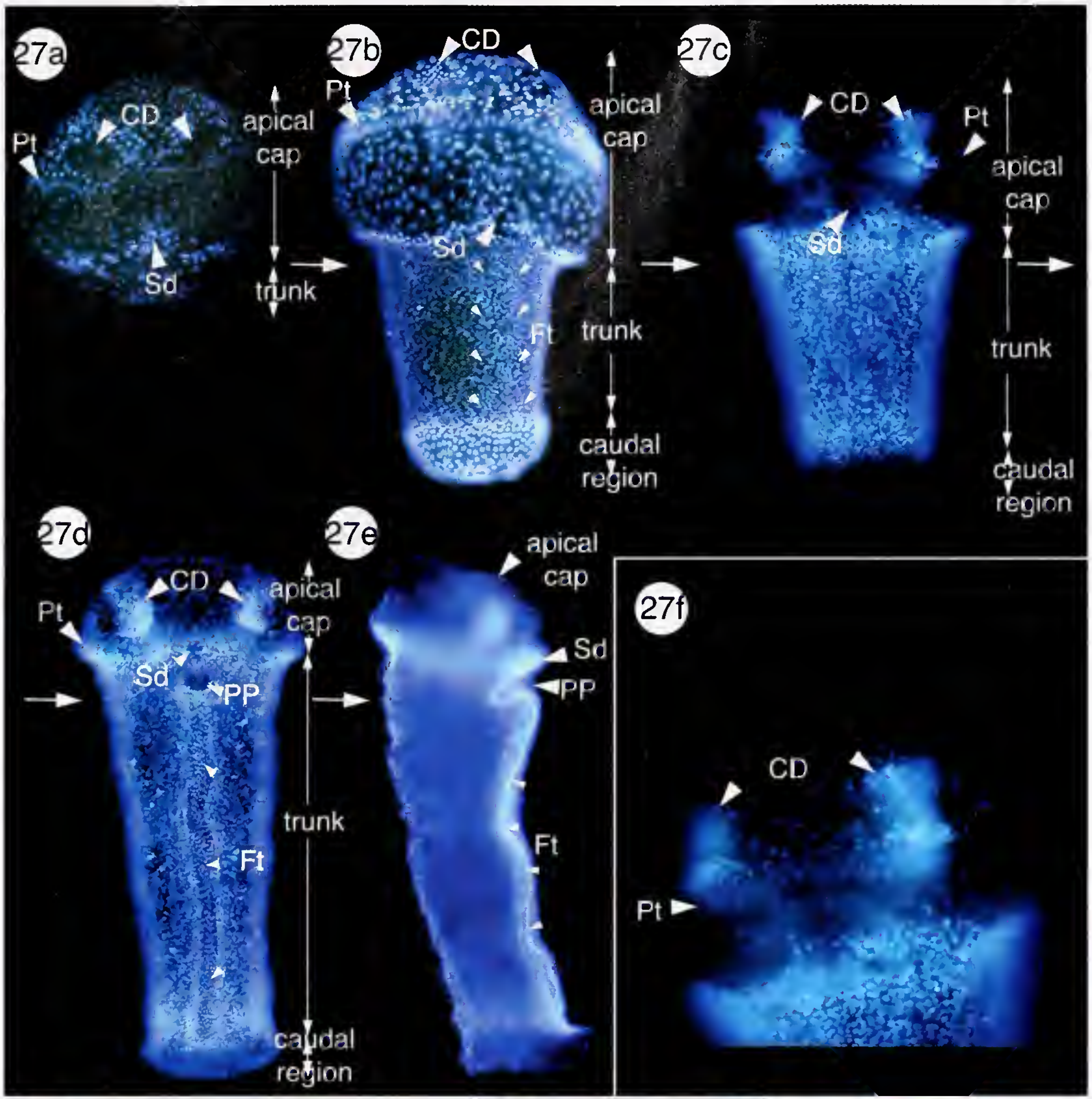
27a
CD
Pt
Sd
apical cap
trunk
27b
CD
Pt
Sd
Ft
apical cap
trunk
caudal region
27c
CD
Pt
Sd
apical cap
trunk
caudal region
27d
CD
Pt
Sd
PP
Ft
apical cap
trunk
caudal region
27e
apical cap
Sd
PP
Ft
27f
CD
Pt

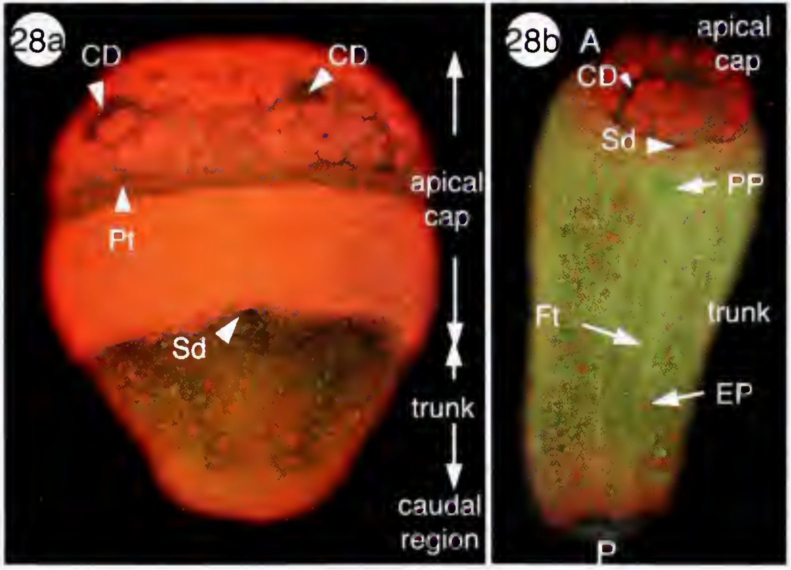
28a
CD
CD
Pt
Sd
apical cap
trunk
caudal region
28b
A
CD
Sd
PP
Ft
EP
P
apical cap
trunk

**29**

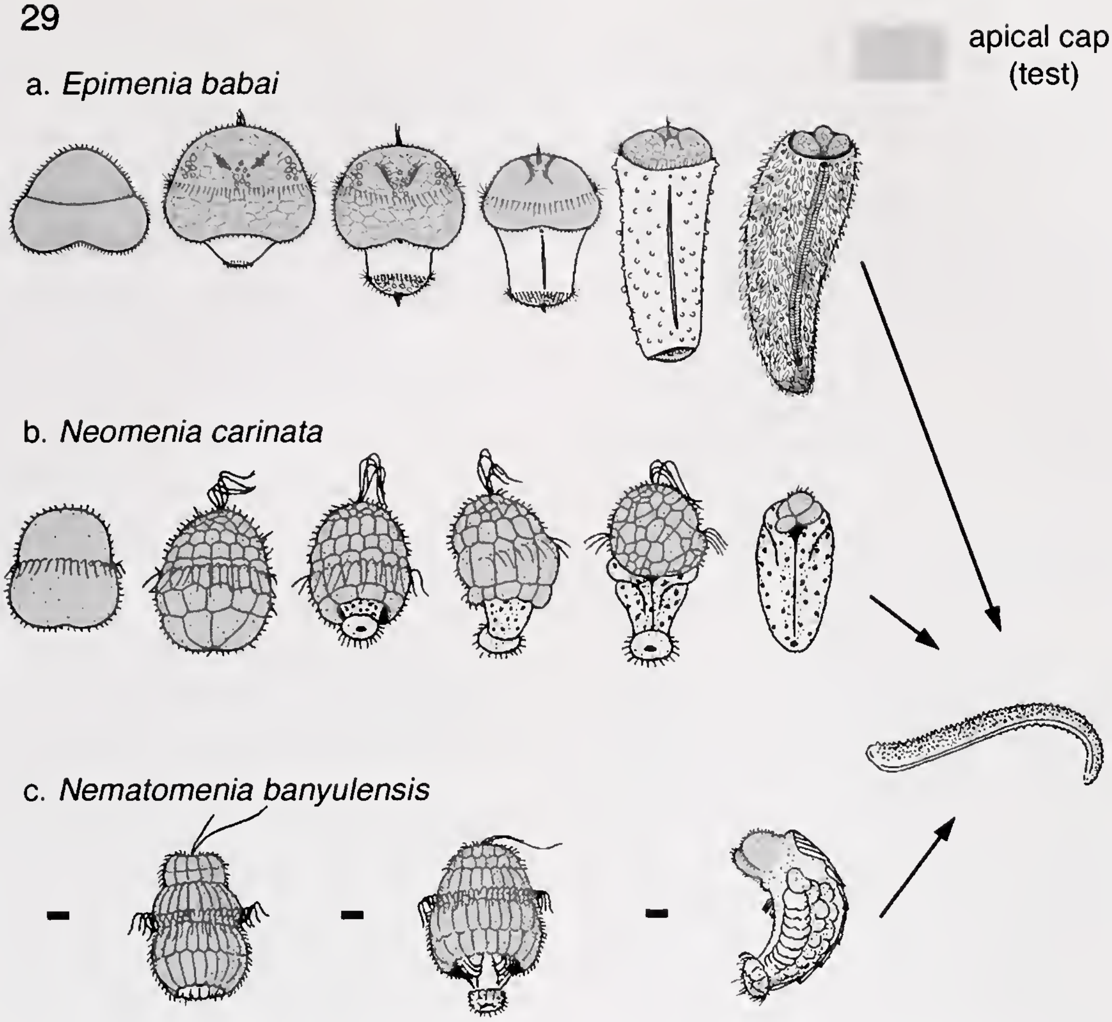

**Figure 29.** Developmental sequences of free-swimming larvae compared among the three neomenioid aplacophorans: (a) *Epimenia babai*. (b) *Neomenia carinata* (modified from Thompson, 1960). (c) *Nematomenia banyulensis* (modified from Pruvot, 1890). The gray shading indicates apical cap (test) structure.

---

**Figure 27.** Hoechst nuclear staining showing the development of larvae and the degeneration of large apical cap cells. (a) Ventral view of a larva right before hatching, showing apical cap and trunk (*cf.* Fig. 13). (b) Ventral view of a 3- to 4-day-old larva (*cf.* Figs. 14, 19). Cells of the apical cap are larger than cells on the trunk. Arrowheads indicate the broad ciliated foot starting to form. (c) Ventral view of a 5-day-old-larva (*cf.* Fig. 19). The size of the cells in the apical cap has not changed, whereas the cells in the trunk region have become smaller and fewer in number as they proliferated and differentiated. (d) Ventral view of a 7-day-old larva (*cf.* Fig. 23). The number of cells in the apical cap has decreased; post-trochal region of the apical cap has diminished. The cells in the apical cap still remain large. The foot narrows as the trunk elongates. (e) The lateral view of a 7-day-old larva. The apical cap is being withdrawn into the trunk. (f) Apical cap of a 5-day-old larva. The cells of the apical cap remain large, and they appear to be transparent and degenerating. CD, cerebral depression; Ft, foot; PP, pedal pit; Pt, prototroch; Sd, stomodeum.

**Figure 28.** Programmed cell death (PCD) of apical cap cells and caudal region of *Epimenia babai* larvae. (a) 2-day-old larva. The entire pre-oral apical cap is stained orange to red, indicating PCD, except for the cerebral depressions, which remained green, indicating viable cells. The definitive ectodermal trunk has remained green, also indicating viable cells. The caudal region also stained orange to red, indicating PCD. (b) 8-day-old larva. The apical cells indicating PCD are withdrawing into the definitive trunk. The trunk remains green and thus viable; however, the epidermal papillae are stained for PCD. A, anterior; CD, cerebral depression; EP, epidermal papillae; Ft, foot; P, posterior; PP, pedal pit, Pt, protroch; Sd, stomodeum.

Table 2

*Modes of development of neomenioid aplacophorans*

| | | | Test Morphology | | | | | | |
|---|---|---|---|---|---|---|---|---|---|
| | Egg diameter ($\mu$m) | Mode of larval nutrient | Apical tuft | No. cell rows in prototroch | No. pairs of ectodermal cerebral depressions | No. rows of test cells | No. cells in test | Test fate | Telotroch/ caudal organ |
| *Nematomenia banyulensis*[1] | 110–120 | lecithotrophic | + | 1 | ? | 6 | 56 | cast off? | ciliated telotroch |
| *Rhopalomenia aglaopheniae*[1] | 260 | lecithotrophic | + | 1 | ? | 6 | ? | cast off? | ciliated telotroch |
| *Halomenia gravida*[2] | 320 | lecithotrophic (brooded) | ? | ? | ? | ? | ? | ? | ciliated telotroch |
| *Neomenia carinata*[3] | ? | lecithotrophic | + | 1 | 3 | 5 | ~80 | resorbed | ciliated telotroch |
| *Epimenia babai*[4] | 250 | lecithotrophic (brooded?) | + | 1 | 1 | no regularity | >100 | resorbed | ciliated telotroch |

[1] Pruvot, 1890, 1892; [2] Heath, 1918; [3] Thompson, 1960; [4] Baba, 1938, 1940, 1951, present study.

## Acknowledgments

I thank Dr. Amélie Scheltema and Kikutarô Baba for guidance in working with aplacophorans. I also thank Dr. Mark Martindale for assistance and support in determining cell fate, and Dr. John Zardus for advice in SEM and sectioning techniques. I thank Dr. Satoshi Nojima and students at Amakusa Marine Biological Laboratories and the fishermen Mr. Kawamoto and Mr. and Mrs. Togawa for their cooperation while collecting in Japan. This work benefited from discussions and comments given by Drs. Amélie Scheltema, Gonzalo Giribet, Damhnait McHugh, Thomas Dahlgren, and Kenneth Halanych. Finally, I thank the reviewers for their helpful comments. The research was supported by a Putnam Grant in animal systematics from the Museum of Comparative Zoology, Harvard University, a National Science Foundation (NSF) Dissertation Improvement Grant in Systematic Biology (#0073312), and an NSF PEET grant (#9521930). This is contribution No. 10754 of the Woods Hole Oceanographic Institution.

## Literature Cited

**Baba, K. 1938.** The later development of a solenogastre, *Epimenia verrucosa*. *J. Dep. Agric.* **6:** 21–41.

**Baba, K. 1940.** The early development of a Solenogastre, *Epimenia verrucosa* (Nierstrasz). *Annot. Zool. Jpn.* **19:** 107–113.

**Baba, K. 1951.** General sketch of the development in a Solenogastre, *Epimenia verrucosa* (Nierstrasz). *Misc. Rep. Res. Inst. Nat. Resour.* (Tokyo) **19–21:** 38–46.

**Baba, K. 1999.** Solenogastres (= Neomeniina, Ventroplicida). Pp. 55–107 In *Mollusca I*. (Nakayama Shoten, Tokyo, Japan). [In Japanese.]

**Cazaux, C. 1970.** Recherches sur l'écologie et le développement larvaires des Polychètes de la région d' Arcachon, Vol. 295. Thèse Fac. Sci. Univ. Bordeaux, France.

**Dawydoff, C. 1959.** Ontogenèse des Annélides. Pp. 594–686 In *Traité de Zoologie*, P. Grassé, ed. Masson, Paris.

**Delsman, H. C. 1915.** Eifurchung and Gastrulation bei *Emplectonema gracile* Stimpson. *Tijdschr. Ned. Dierk. Ver.* **14:** 68–109.

**Drew, G. A. 1897.** Notes on the embryology, anatomy, and habits of *Yoldia limatula*, Say. *Johns Hopkins Univ. Circ.* **17:** 11–14.

**Drew, G. A. 1899a.** Some observations on the habits, anatomy and embryology of members of the Protobranchia. *Anat. Anz.* **15:** 493–519.

**Drew, G. A. 1899b.** The anatomy, habits, and embryology of *Yoldia limatula*, Say. *Mem. Biol. Lab. Johns Hopkins Univ.* **4:** 1–37.

**Drew, G. A. 1901.** The life-history of *Nucula delphinodonta* (Mighels). *Quart. J. Microsc. Sci.* **44:** 313–392.

**Eernisse, D. J., and P. D. Reynolds. 1994.** Polyplacophora. Pp. 55–110 in *Microscopic Anatomy of Invertebrates, Vol. 5: Mollusca I*, F. W. Harrison and A. J. Kohn, eds. Wiley-Liss, New York.

**Geilenkirchen, W. L. M., N. H. Verdonk, and L. P. M. Timmermans. 1970.** Experimental studies on morphogenetic factors localized in the first and the second polar lobe of *Dentalium* eggs. *J. Embryol. Exp. Morphol.* **23:** 237–243.

**Götting, K. J. 1980.** Origin and relationships of the Mollusca. *Z. Zool. Syst. Evoltionsforsch.* **18:** 24–27.

**Grave, B. H. 1932.** Embryology and life history of *Chaetopleura apiculata*. *J. Morphol.* **54:** 153–160.

**Guerrier, P., J. A. M. v. D. Biggelaar, C. A. M. v. Dongen, and N. H. Verdon. 1978.** Significance of the polar lobe for the determination of dorsoventral polarity in *Dentalium vulgare* (da Costa). *Dev. Biol.* **63:** 233–242.

**Gustafson, R. G. 1987.** Phylogenetic implications of the molluscan pericalymma larva. *Am. Zool.* **27:** 301A.

**Gustafson, R. G., and R. A. Lutz. 1992.** Larval and early post-larval development of the protobranch bivalve *Solemya velum* (Mollusca: Bivalvia). *J. Mar. Biol. Assoc.* UK **72:** 383–402.

**Gustafson, R. G., and R. G. B. Reid. 1986.** Development of the pericalymma larva of *Solemya reidi* (Bivalvia: Cryptodonta: Solemyidae) as revealed by light and electron microscopy. *Mar. Biol.* **93:** 411–427.

**Gustafson, R. G., and R. G. B. Reid. 1988a.** Association of bacteria with larvae of the gutless protobranch bivalve *Solemya reidi* (Cryptodonta: Solemyidae). *Mar. Biol.* **97:** 389–401.

**Gustafson, R. G., and R. G. B. Reid. 1988b.** Larval and post-larval morphogenesis in the gutless protobranch bivalve *Solemya reidi* (Cryptodonta: Solemyidae). *Mar. Biol.* **97:** 373–387.

**Haszprunar, G., L. v. Salvini-Plawen, and R. M. Rieger. 1995.** Larval planktotrophy—a primitive trait in the Bilateria? *Acta Zool.* **76:** 141–154.

**Haszprunar, G. 2000.** Is the Aplacophora monophyletic? A cladistic point of view. *Am. Malacol. Bull.* **15:** 115–130.

**Heath, H. 1918.** Solenogastres from the eastern coast of North America. *Mem. Mus. Comp. Zool. Harv.* **45:** 185–263.

**Hickman, V. V. 1963.** The occurrence in Tasmania of the land nemertine, *Geonemertes australiensis* Dendy, with some account of its distribution, habits, variations and development. *Pap. Proc. R. Soc. Tasmania* **97:** 63–75.

**Hoffman, S. 1949.** Studien über das Integument der Solenogastren, nebst Bemerkungen über die Verwandtschaft zwischen den Solenogastres und Placophoren. *Zool. Bidr. Uppsala* **27:** 293–427.

**Ivanov, D. L. 1996.** Origin of Aculifera and problems of monophyly of higher taxa in molluscs. Pp. 59–65 in *Origin and Evolutionary Radiation of the Mollusca,* J. Taylor, ed. Oxford University Press, Oxford.

**Iwata, F. 1958.** On the development of the nemertean *Micrura akkeshiensis. Embryologia* **4:** 103–131.

**Jägersten, G. 1968.** *Livcykelns Evolution hos Metazoa.* Scandinav. University Books, Lund, Sweden.

**Kessel, M. M. 1964.** Reproduction and larval development of *Acmea testudinalis* (Müller). *Biol. Bull.* **127:** 294–303.

**Korschelt, E. 1936.** *Vergleichende Entwicklungsgeschichte der Tiere.* G. Fischer, Jena.

**Lacaze-Duthiers, F. J. H. 1856.** Historie de l'organisation et du développement du Dentale. *Ann. Sci. Nat. Zool. Biol. Anim.* **4:** 171–255.

**Martin, S. J., C. P. M. Reutelingsperger, and D. R. Green. 1996.** A specific probe for apoptotic cells. Pp. 107–120 in *Techniques in Apoptosis: A User's Guide,* T. G. Cotter and S. J. Martin, eds. Portland Press, London.

**Maslakova, S. A., and V. V. Malakhov. 1999.** Hidden larva in the Hoplonemertini order of nemerteans. *Dokl. Akad. Nauk.* **366:** 849–852.

**Nielsen, C. 2001.** *Animal Evolution: Interrelationships of the Living Phyla.* Oxford University Press, Oxford.

**Patten, W. 1886.** The embryology of *Patella. Arb. Zool. Inst. Wien* **6:** 149–174.

**Pruvot, G. 1890.** Sur le développement d'un solénogastre. *C. R. Acad. Sci. Paris* **3:** 689–692.

**Pruvot, G. 1892.** Sur l'embryogénie d'une *Proneomenia. C. R. Acad. Sci. Paris* **114:** 1211–1214.

**Rice, M. E. 1988.** Observations on development and metamorphosis of *Siphonosoma cumanense* with comparative remarks on *Sipunculus nudus* (Sipuncula, Sipunculidae). *Bull. Mar. Sci.* **42:** 1–15.

**Richardson, K. C., L. Jarrett, and E. H. Finke. 1960.** Embedding in epoxy resins for ultrathin sectioning in electron microscopy. *Stain Technol.* **35:** 313–323.

**Rouse, G. W. 1999.** Trochophore concepts: ciliary bands and the evolution of larvae in spiralian Metazoa. *Biol. J. Linn. Soc.* **66:** 411–464.

**Salvini-Plawen, L. v. 1972.** Cnidaria as food-sources for marine invertebrates. *Cah. Biol. Mar.* **13:** 385–400.

**Salvini-Plawen, L. v. 1973.** Zur Klärung des "Trochophora"-Begriffes. *Experientia* **29:** 1434–1436.

**Salvini-Plawen, L. v. 1978.** Antarktische und subantarktische Solenogastres (Eine Monographie: 1898–1974). *Zoologica* **128:** 1–315.

**Salvini-Plawen, L. v. 1980.** Was ist eine Trochophora? Eine Analyse der Larventypen mariner Prostomier. *Zool. Jahrb. Abt. Anat. Ont. Tiere* **103:** 389–423.

**Salvini-Plawen, L. v. 1985.** Early evolution and the primitive groups. Pp. 59–150 in *The Mollusca: Evolution,* E. R. Trueman and M. R. Clarke, eds. Academic Press, Orlando, FL.

**Salvini-Plawen, L. v. 1990.** Origin, phylogeny and classification of the Phylum Mollusca. *Iberus* **9:** 1–33.

**Salvini-Plawen, L. v. 1997.** Systematic revision of the Epimeniidae (Mollusca: Solenogastres). *J. Molluscan Stud.* **63:** 131–155.

**Salvini-Plawen, L. v., and Y. Benayahu. 1991.** *Epimenia arabica* spec. nov. a Solenogaster (Mollusca) feeding on the Alcyonacean *Scleronephthya corymbosa* (Cnidaria) from shallow waters of the Red Sea. *Mar. Ecol.* **12:** 139–152.

**Salvini-Plawen, L. v., and G. Steiner. 1996.** Synapomorphies and plesiomorphies in higher classification of Mollusca. Pp. 29–51 in *Origin and Evolutionary Radiation of the Mollusca,* J. Taylor, ed. Oxford University Press, Oxford.

**Scheltema, A. H., and M. Jebb. 1994.** Natural history of a solenogaster mollusc from Papua New Guinea, *Epimenia australis* (Thiele) (Aplacophora: Neomeniomorpha). *J. Nat. Hist.* **28:** 1297–1318.

**Strathmann, M. F. 1987.** *Reproduction and Development of Marine Invertebrates of the Northern Pacific Coast.* Univ. Washington Press, Seattle.

**Thiele, J. 1913.** Antarktische Solenogastren. *Dtsch. Südpolar-Exp. 1901–1903* 14, *Zool., Heft* **1:** 35–65.

**Thompson, T. E. 1959.** Development of the aplacophorous mollusc *Neomenia carinata* Tullberg. *Nature* **184:** 122–123.

**Thompson, T. E. 1960.** The development of *Neomenia carinata* Tullberg. *Proc. R. Soc. B* **153:** 263–278.

**Waller, T. R. 1998.** Origin of the molluscan class Bivalvia and a phylogeny of major groups. Pp. 1–45 in *Bivalves: An Eon of Evolution—Palaeobiological Studies Honoring Norman D. Newell,* P. A. Johnston and J. W. Haggart, eds. University of Calgary Press, Calgary, Alberta.

**Wanninger, A., and G. Haszprunar. 2001.** The expression of an engrailed protein during embryonic shell formation of the tusk-shell, *Antalis entalis* (Mollusca, Scaphopoda). *Evol. Dev.* **3:** 312–321.

**Winnepenninckx, B., T. Backeljau, and R. D. Wachter. 1996.** Investigation of molluscan phylogeny on the basis of 18s rRNA sequences. *Mol. Biol. Evol.* **13:** 1306–1317.

**Zardus, J. D., and M. P. Morse. 1998.** Embryogenesis, morphology and ultrastructure of the pericalymma larva of *Acila castrensis* (Bivalvia: Protobranchia: Nuculoida). *Invertebr. Biol.* **117:** 221–244.

Reference: *Biol. Bull.* **203:** 104–111. (August 2002)

# Undifferentiated Cells in the Snail Myocardium Are Capable of DNA Synthesis and Myodifferentiation

MARINA G. MARTYNOVA* AND OLGA A. BYSTROVA

*Institute of Cytology of the Russian Academy of Sciences, 194064 St. Petersburg, Russia*

**Abstract.** Cellular mechanisms of heart-muscle growth in the snail *Achatina fulica* have been studied using cytophotometry and electron microscopic autoradiography. Cytophotometric DNA measurements showed that the snail cardiomyocytes are mononucleated cells with diploid nuclei. Ultrastructural analysis of the snail myocardium revealed that, in addition to mature myocytes, it contains small roundish undifferentiated cells (UCs) and poorly differentiated muscle cells. EM autoradiography detected silver grains over the nuclei of UCs 2 h after injection of tritiated thymidine ([$^3$H]Tdr), while the nuclei of both mature and poorly differentiated myocytes remained unlabeled. In EM autographs of the myocardial tissue fixed 14 days after [$^3$H]Tdr administration, labeled myonuclei were evident, which may suggest some myodifferentiation of prelabeled UCs. Many labeled UCs persist for 14 days after a single [$^3$H]Tdr injection, suggesting that not all UCs undergo myodifferentiation after passing through the cell cycle, and that those that do not can enter the next cycle. UCs in the snail myocardium presumably provide not only reserve but also stem cells for myocytes. Thus, the heart muscle of the adult snail consists of mononucleated diploid myocytes with blocked proliferative activity and a renewable population of precursor myogenic cells. The results obtained suggest that the growth of this muscle involves a myoblastic mechanism of myogenesis; this mechanism differs from that of vertebrate cardiac muscle growth, which is non-myoblastic—that is, based on proliferation or polyploidization of cardiomyocytes. Evolutionary aspects of cellular mechanisms of the heart-muscle growth are discussed.

## Introduction

In vertebrates, developing and mature cardiac muscles lack a pool of morphologically undifferentiated myoblasts. This is in contrast with skeletal muscle, which possesses an obvious pool of satellite cells. Differentiated cardiomyocytes of vertebrates retain their ability to synthesize DNA, and vertebrate heart muscle grows non-myoblastically, through hyperplasia or hypertrophy of myofibril-containing cells (reviewed by Rumyantsev, 1991).

In many respects the molluscan heart resembles that of vertebrates. This striking convergence involves myogenic automatism, high heart volume, beat frequency, and some other physiological features. In addition, such morphological peculiarities as the location of the heart in the pericardial cavity, a chambered heart construction, the availability of valves and trabeculae, and a rich supply of nerve endings are worth mentioning (Martin, 1980). Some cephalopods have a relatively closed circulatory system (Kling and Schipp, 1987; Schipp, 1987), as well as a pacemaker zone in the heart and coronary vasculature (Wells and Smith, 1987). As in the vertebrate myocardium, the cellular unit of molluscan heart muscle is a mononucleated muscle cell linked to its neighbors by intercalated discs (North, 1963; Watts *et al.*, 1981; Okland, 1982; Kling and Schipp, 1987). In other invertebrates, the heart muscle is formed either by multinucleated muscle fibers, as in arthropods (Nylund, 1981; Nylund *et al.*, 1986; Martynova *et al.*, 1986); or by myoepithelial cells, as in brachiopods (Martynova and Chaga, 1997), annelids (Hama, 1960; Jensen, 1974), pogonophorans (Jensen and Myklebust, 1975), hemichordates (Lester, 1982; Balser and Ruppert, 1990), and ascidians (Martynova and Nylund, 1996).

Although the molluscan heart muscle has been the subject of many ultrastructural and physiological studies, little is known so far about the cellular mechanisms that underlie its growth.

---

Received 27 June 2001; accepted 4 June 2002.

* To whom correspondence should be addressed. E-mail: heartdev@mail.cytspb.rssi.ru

In our previous ultrastructural study of molluscan heart muscle (Bystrova *et al.*, 1996), the presence of a population of undifferentiated cells (UCs) was revealed in the bivalve *Crenomytilus grayanus*, the gastropod *Helix aspersa*, and the cephalopod *Rossia macrosoma*. These cells were assumed to be myogenic stem cells involved in the growth of the molluscan heart muscle. The goal of the present work was to validate this assumption and attempt to understand the mode of heart-muscle growth in molluscs. For this purpose we examined the DNA-synthesizing capacity of UCs by means of electron microscope autoradiography with tritiated thymidine as a precursor and followed the fate of labeled UCs in tests with delayed fixation. We also studied the ploidy levels of cardiomyocytes in the snail heart.

## Materials and Methods

### *Experimental animals*

We used a gastropod mollusc, the land snail *Achatina fulica*, which we reared in the laboratory. The snails were kept at room temperature in large glass vessels and fed a vegetable diet.

### *Cytophotometry*

Tissue samples from the atria and ventricles of three mature snails (about 40 g body weight) were fixed in 10% formalin and then treated with 50% KOH. Smears of isolated cells were postfixed in Carnoy solution and stained by the Feulgen technique. DNA was measured using a Morphoquant scanning cytophotometer (Germany) at a wavelength of 550 nm on 200 muscle nuclei from each heart chamber. The quantity of DNA in the blood cell nuclei available in the same smears served as a standard of the diploid DNA value.

### *Scintillation counting*

A Beckman LS-8100 $\beta$-scintillation counter was used to determine the time of $[^3H]$Tdr (tritiated thymidine) circulation in the body fluid. After a single $[^3H]$Tdr injection at a dose of 10 $\mu$Ci/g live weight, 0.1 ml of hemolymph was taken at regular intervals (each time from a different animal), placed on a paper filter, and left to dry. The filters were then put into standard glass vials with the scintillation liquid, and the radioactivity was measured. The results were expressed as percent clearance of radioactivity as related to the first sample taken immediately after the isotope injection.

### *Autoradiography*

$[^3H]$Tdr (State Institute for Applied Chemistry, St. Petersburg, Russia) with a specific activity of 16 Ci/$\mu$mole was injected at a dose of 10 $\mu$Ci per gram of body weight into the pericardial cavity of small 2-week-old snails (about 0.2 g body weight) through a small hole drilled in the shell. In 2 h (test I) or 14 days (test II), the heart tissues were fixed in a cacodylate-buffered solution of 2.5% glutaraldehyde, pH 7.4, postfixed in 1% $OsO_4$, dehydrated in a series of ethanols, and embedded in a mixture of Epon and Araldite. Four animals were used in each test for EM autoradiography. EM autographs were prepared by the method of Larra and Droz (1970) with an exposure time of 60 days. Observations were made with a JEM 7A electron microscope.

For two animals in each test (four animals in all), the percentage of $[^3H]$Tdr-labeled nuclei from the total number of nuclei of undifferentiated cells (UCs) was calculated from EM autoradiographs. Over 100 UC nuclei from each animal were examined. From the same autoradiographs, the percentage of UC nuclei related to the total population of myocardial nuclei (namely, muscle nuclei plus those of UCs) was estimated. The average number of myocardial nuclei counted for each of four animals was 1000.

## Results

### *Ultrastructure of the snail heart*

The snail *Achatina fulica* has a two-chambered heart. The atrial and ventricular walls consist of an outer single-cell layer of coelomic epithelium (epicardium), a myocardium, and an inner discontinuous layer of endothelial cells (Fig. 1). The myocardium is intensely penetrated by nerve fibers (Fig. 2), which are particularly numerous in the atrium. The myocardium is formed of a compact part that underlies the epicardium and a spongy trabecular part that faces the lumen. In the atrium, the compact part is less expressed, and the trabeculae are thinner and more loosely arranged than in the ventricle. Mature cardiomyocytes (Fig. 2) are tightly packed with obliquely striated myofibers and contact each other by small desmosomes and intercalated discs (Fig. 3). Dense bodies and attachment plaques form Z-material. The nuclei are normally located in the lateral luminal protrusions of the sarcoplasm. The karyoplasm is filled with condensed chromatin blocks, located predominantly under the plasma membrane, and with finely dispersed chromatin. Sometimes a poorly developed Golgi complex and centrioles are seen near the nucleus.

Small oval cells devoid of myofilaments were observed in the myocardium beside the muscle cells and in close association with them (Fig. 4). These undifferentiated cells (UCs) were usually tightly adjacent to the luminal surface of the myocardial trabeculae. Sometimes spot desmosomes were between UCs and adjacent myocytes (Fig. 4, inset). These cells were quite common, and in the heart muscle of 4-week-old snails made up as much as about 10% of the total population of myocardial nuclei. Each UC consists of a single nucleus surrounded by scanty cytoplasm. A set of cytoplasmic organelles includes a few mitochondria, ribo-

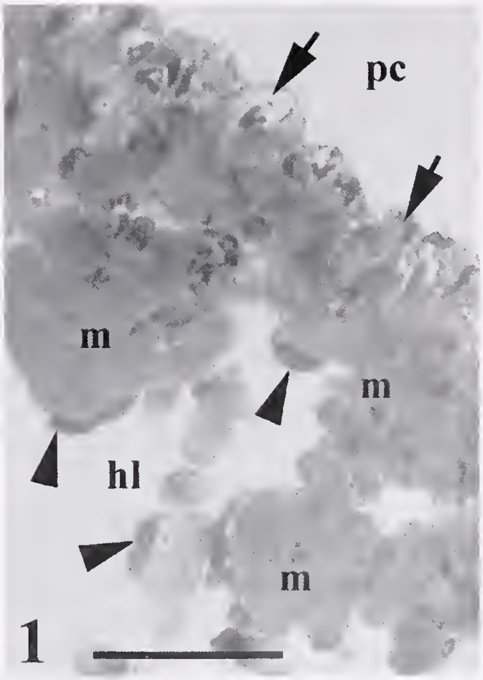

**Figure 1.** Light micrograph of semithin section through the atrium of the snail *Achatina fulica*. The heart wall consists of epicardium (arrows) facing the pericardial cavity (pc) and a myocardium (m). The endothelial cells (arrowheads) adjoin the luminal surface of the myocardial trabeculae. hl, heart lumen. Scale bar = 0.05 mm.

somes, and a number of small vesicles. UCs were easy to distinguish from other nonmuscle cells in the heart, such as endothelial cells, gliointerstitial cells accompanying nerve fibers, and blood cells, by this extreme paucity of cytoplasmic organelles and the presence of a spherical "empty" nucleus whose chromatin is not dispersed but clumped immediately beneath the nuclear envelope. These peculiar nuclei were commonly surrounded by fragments of evidently destroyed cytoplasm, which may presumably result from occasional damage of UCs during fixation. A high fragility of UCs probably accounts for the fact that these were missed in many earlier relevant publications on the ultrastructure of the molluscan heart.

Sometimes small muscle cells were seen containing only a few myofilaments randomly arranged and embedded into some amorphous material (Fig. 5). Moderately differentiated myocytes were also seen (Figs. 6, 7). Thus, all morphological intermediate stages may be observed in the molluscan heart—from small oval cells with no or only a few myofilaments to well-differentiated cardiomyocytes—and a series of cells representing the process of transformation of undifferentiated cell into mature muscle cell can be identified.

We failed to observe any mitotic figures in UCs or myocytes.

### *Ploidy analysis*

Cytophotometric measurements of DNA contents in KOH-dissociated, Feulgen-stained cells showed that both atrial and ventricular myocytes of the snail heart are exclusively mononucleated, with the nuclei being diploid.

### *Scintillation counting*

The data on [$^3$H]Tdr availability are presented in Figure 8. Of the amount of [$^3$H]Tdr injected at a dose of 10 $\mu$Ci/g into the body cavity of the snail, about half was consumed within the first 10 min, and by 2 h almost all of the isotope was used up. Then the curve reached a plateau, which may indicate the presence of some other labeled compounds into which [$^3$H]Tdr could be converted or of blood cells that also might incorporate thymidine. So, [$^3$H]Tdr is available for only about 2 h.

### *Electron microscope autoradiography*

*Test I.* The first series of experiments was aimed at examining the DNA-synthesizing capacity in UCs and myocytes of the *Achatina* heart. Electron microscope autographs of the heart tissue fixed 2 h after [$^3$H]Tdr injection showed labeling of some nuclei in UCs (Fig. 9). The labeled UC nuclei composed 4.2% and 4.3% (for each animal) of the total population of UC nuclei. No silver grains were detected over the nuclei of either poorly or well-differentiated muscle cells. In addition to the UCs, the nuclei of some epicardial, endothelial, and gliointerstitial cells in the heart tissue demonstrated [$^3$H]Tdr incorporation.

*Test II.* To follow the fate of [$^3$H]Tdr-labeled UCs, the heart tissue was examined 14 days after the isotope injection. Electron microscope autographs showed the appearance of labeled nuclei in both moderately differentiated (Fig. 10) and mature myocytes (Fig. 11). It is noteworthy that, along with labeled myocytes, labeled UCs were also observed. For one snail, the number of [$^3$H]Tdr-labeled nuclei composed 13.0% of the total UC population; labeled muscle and UC nuclei made up 9.5% and 3.5%, respectively. For another snail, the number of labeled nuclei amounted to 17.2% of the total UC population; labeled muscle and UC nuclei composed 8.5% and 9.7%, respectively. The nuclear labeling was also seen in some endothelial, epicardial, and gliointerstitial cells. Similar patterns of labeling were observed in both the atrium and ventricle.

## Discussion

The electron microscope study has shown that the snail myocardium contains a population of undifferentiated cells (UCs) and a number of poorly and moderately differentiated myocytes. All these myocardial cells can be arranged successively into a series of stages representing a process of myodifferentiation, which indicates that the UCs in the snail

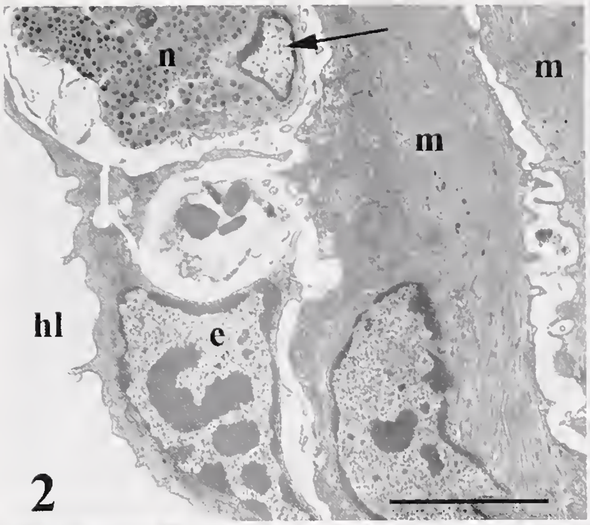

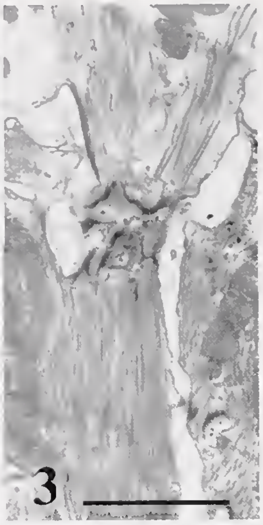

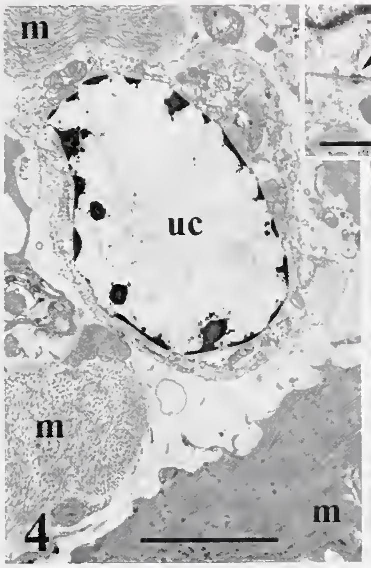

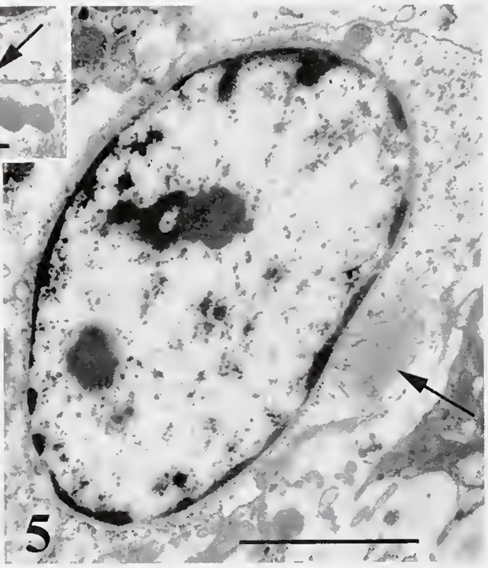

**Figure 2.** Electron micrograph of mature cardiomyocytes (m) of *Achatina*. Nerve ending (n) with glio-interstitial cell (arrow) and endothelial cell (e) adjoin the luminal surface of the cardiomyocyte. hl, heart lumen. Scale bar = 2 μm.

**Figure 3.** Electron micrograph showing a primitive intercalated disc between cardiomyocytes. Scale bar = 1 μm.

**Figure 4.** Electron micrograph of an undifferentiated cell (uc) adjoining cardiomyocytes (m) in the *Achatina* myocardium. Scale bar = 2 μm. Inset: a spot desmosome (arrow) between the undifferentiated cell (at the upper part of the figure) and a mature cardiomyocyte (at the lower part of the figure). Scale bar = 0.5 μm.

**Figure 5.** Electron micrograph of a cardiomyocyte at the early stage of myodifferentiation. A few myofilaments embedded in an amorphous material (arrow) can be seen. Scale bar = 2 μm.

heart are myogenic. The autoradiographic experiments supported this view. As evident from test I with a short [$^3$H]Tdr-pulse, UCs are capable of DNA synthesis, but muscle cells, including those at the earliest stages of myodifferentiation, are not. The appearance of labeled myonuclei in test II with a delayed fixation indicates that UCs underwent mitosis and myodifferentiation within the first several hours after [$^3$H]Tdr injection. Furthermore, the labeled UCs were also present in the heart tissue fixed 14 days after isotope injection. Since [$^3$H]Tdr was available in hemolymph for only 2 h, it may be that not all UCs differentiated into myocytes after DNA synthesis and mitosis: that some daughter UCs might remain undifferentiated and compose a defined population. Thus, in the snail heart, UCs could produce a renewable population and eventually function not only as a reserve but also as stem cells for the myocytes. The counts of labeled nuclei showed that their numbers increased by a factor of 4 over 2 weeks, suggesting that, for a given time, the prelabeled UCs could undergo about two cell cycles. Other nonmuscle cells of the snail

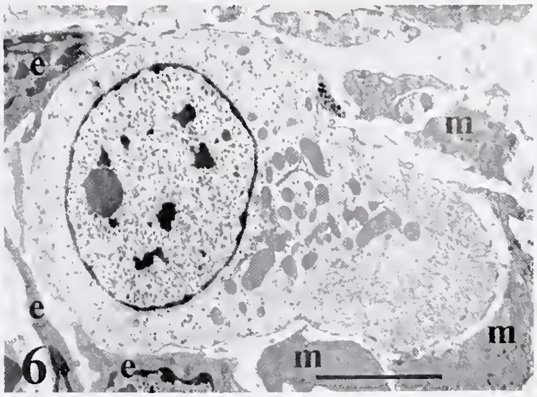

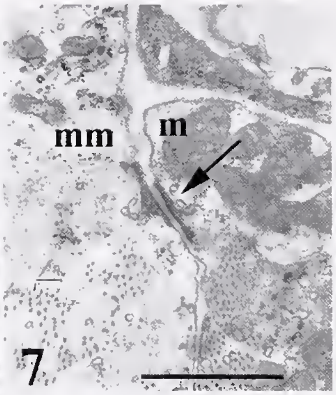

**Figure 6.** Electron micrograph of a moderately differentiated cardiomyocyte in the *Achatina* myocardium. m, mature cardiomyocytes, e, endothelial cells. Scale bar = 2 $\mu$m.

**Figure 7.** Electron micrograph showing a desmosome (arrow) between moderately differentiated (mm) and mature (m) cardiomyocytes. Scale bar = 1 $\mu$m.

heart do not demonstrate any morphological indications of transformation into myocytes, so they could not be serving as stem cells for muscle differentiation.

The present study of the *Achatina* heart muscle provided no evidence about whether the examined UCs are remnants of the original, embryonic myoblasts or represent new cells of another origin, which invaded the heart only later in its development. Recent data on the participation of bone-marrow-derived cells in cardiac muscle regeneration in Duchenne dystrophic mice demonstrate that adult vertebrate myocardium has a source of myogenic stem cells located outside the organ (Bittner *et al.*, 1999).

A population of undifferentiated cells was found also in the myocardia of bivalve and cephalopod molluscs (Bystrova *et al.*, 1996). It may be assumed that the mosaic distribution of myogenic cells is a characteristic feature of the molluscan myocardium shared by representatives of different classes. This shared feature enables us to classify the molluscan heart muscle as a special muscle type consisting of discrete mononucleated diploid myocytes and, at the same time, possessing myogenic UCs. Such a cellular organization makes it possible to differentiate the molluscan heart muscle from all other muscle types so far described in either vertebrates or invertebrates.

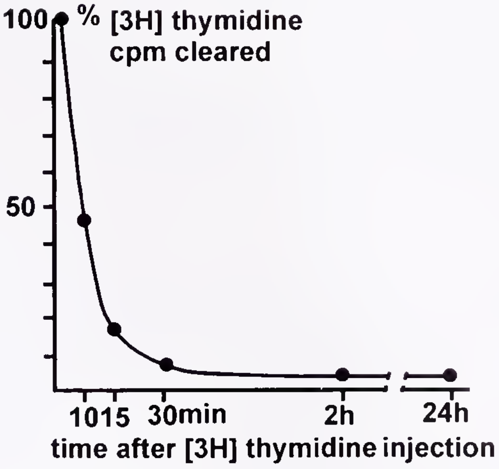

**Figure 8.** Percent radioactivity in the hemolymph of the snail plotted against time after tritiated thymidine injection. Results are expressed as percent clearance of the first sample radioactivity (immediately after isotope injection).

It is well known that in warm-blooded vertebrates—birds (Anatskaya *et al.*, 2001), mammals (Kudryavtsev *et al.*, 1997), and humans (Adler, 1991)—polyploidization of cardiomyocytes is an essential component of heart-muscle growth. The mere presence of undifferentiated myogenic elements in the snail myocardium does not preclude the possibility that polyploidy may occur in molluscan cardiomyocyte nuclei. In many adult tissues of gastropod molluscs, such as nervous tissue (Bulloch, 1985; Moffett, 1995), connective tissue, various gland and gonad tissues, gut and skin epithelia (Anisimov, 1999), the occurrence of undifferentiated stem cells is suprisingly accompanied by a high level of ploidy in their differentiated cells. Even though the cardiomyocytes of adult snails do not synthesize DNA, polyploidization might be able to occur at earlier stages of development. To check this possibility, we examined nuclear DNA content in snail cardiomyocytes and found that the snail myocardium was composed exclusively of mononucleated diploid myocytes. This is another proof for repression or irreversible loss of DNA-synthesizing capacity in the molluscan cardiomyocytes.

In vertebrate cardiomyocytes, syntheses of DNA and cell-specific proteins are not mutually exclusive. Myogenic stem cells are absent from the vertebrate myocardium (Rumyantsev, 1991). In contrast, all protostome invertebrates so far examined in this respect demonstrate the pres-

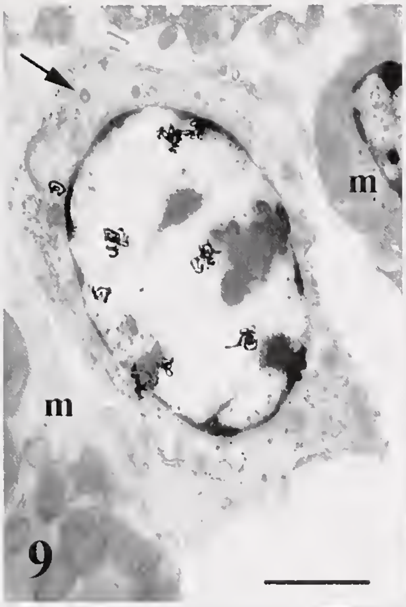

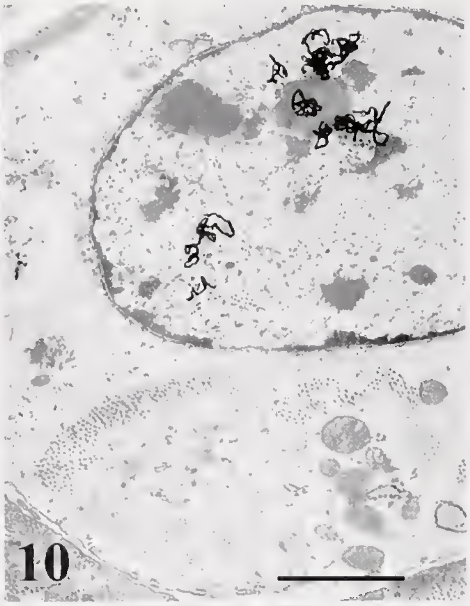

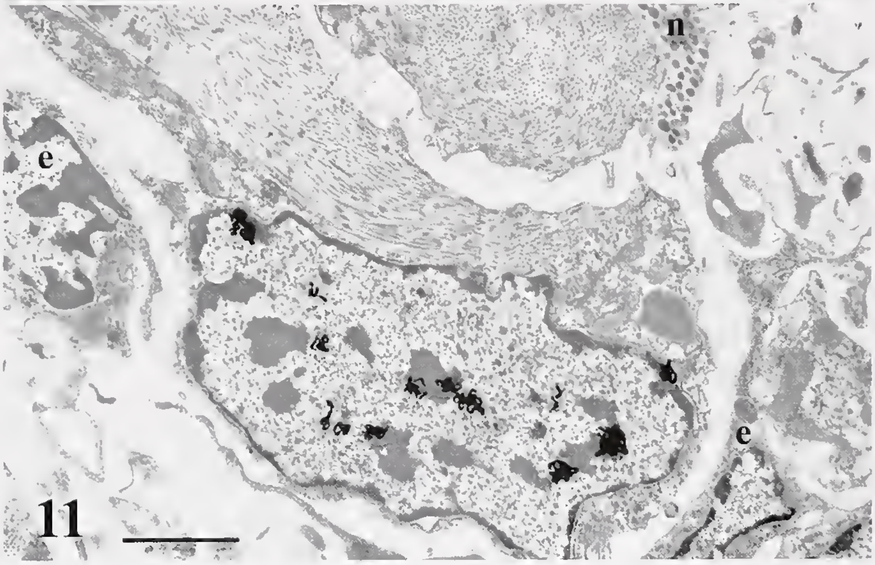

**Figure 9.** Electron-microscopic autoradiograph of a labeled undifferentiated cell from the *Achatina* heart fixed 2 h after injection of tritiated thymidine. m, mature cardiomyocytes. Arrow points to centriole. Scale bar = 1 $\mu$m.

**Figure 10.** Electron-microscopic autoradiograph of a labeled moderately differentiated cardiomyocyte from the *Achatina* heart fixed 14 days after injection of tritiated thymidine. Scale bar = 1 $\mu$m.

**Figure 11.** Electron-microscopic autoradiograph of a labeled mature cardiomocyte from the *Achatina* heart fixed 14 days after tritiated thymidine injection. n, nerve ending, e, endothelial cells. Scale bar = 1 $\mu$m.

ence of myogenic precursor cells in the heart muscle and the absence of DNA synthesis in myocytes, even though the cellular organization of heart muscles in different groups of invertebrates varies significantly. Thus, brachiopod myocardium consists of alternating myoepithelial and epithelial cells, the latter being myogenic (Martynova and Chaga, 1997). Crustacean heart muscle, like vertebrate skeletal muscle, is composed of multinucleated myofibers and mononucleated undifferentiated satellite cells, which function as myogenic stem cells (Martynova, 1993). Crustacean heart myonuclei have no DNA synthetic activity. In deuterostome invertebrates such as ascidians, the myocardium consists of a homogeneous population of myoepithelial cells and contains myogenic precursor cells localized in a region of transition from pericardium to myocardium. At the same time, myoepithelial cells of the ascidian myocardium are capable of DNA synthesis (Martynova and Nylund, 1996). Thus, it can be suggested that DNA blocking in muscle cells, combined with the occurrence of a pool of undifferentiated myogenic cells, is the common feature of the heart muscle in protostomes (the myoblastic mechanism of myogenesis), whereas the cardiomyocytes capable of DNA synthesis developed only in deuterostomians and as early as the emergence of ascidians. Further development of the cardiac muscle in deuterostomians was accompanied by an ultimate loss of undifferentiated myogenic elements in vertebrates (the non-myoblastic mechanism of myogenesis). The principal difference in cellular mechanisms of heart-muscle growth between Deuterostomia and Proterostomia may be accounted for by different origin and development of cardiogenic mesoderm in these two main phylogenic taxa.

To gain an insight into the behavior of myogenic stem cells, it is necessary to identify components involved in regulation of their activity. It has been well established that in vertebrate skeletal muscle myogenic stem cells (*i.e.*, satellite cells) participate not only in growth but also in regenerative processes. The injury of skeletal muscle fibers causes reactive proliferation of satellite cells (Grounds and McGeachie, 1989; Roberts *et al.*, 1989). Our attempts to activate DNA synthesis in molluscan UCs by mechanical injury of the heart were not successful. The only observed reaction was the filling of the wounded heart wall with a cluster of blood cells (unpubl. data). A similar reaction to mechanical injury was observed in the crayfish heart (Martynova and Khaitlina, 1991). Thus, the regenerative process in crustacean and molluscan heart muscles, unlike that in vertebrate skeletal muscle, does not trigger proliferation of precursor myogenic cells. DNA synthesis and myodifferentiation of satellite cells in the crayfish heart was initiated by ecdysterone, an arthropod molting hormone, both intrinsically and applied exogenously (Martynova, 1993, 1997). Furthermore, ecdysteroids have been detected in snails (Romer, 1979; Whitehead and Sellheyer, 1982; Nolte *et al.*, 1986), and the presence of ecdysteroid receptors was recently demonstrated in the heart of *Helix aspersa* (Bugaeva *et al.*, 1999). These data suggest that ecdysteroids are probably a trigger factor activating mitoses and myodifferentiation of myogenic stem cells in the molluscan myocardium. Experiments are in progress on the effect of ecdysterone on biosynthetic processes in cells of the snail heart.

## Literature Cited

**Adler, C. P. 1991.** Polyploidization and augmentation of heart muscle cells during normal cardiac growth and in cardiac hypertrophy. Pp. 227–252 in *The Development and Regenerative Potential of Cardiac Muscle*, J. O. Oberpriller, J. C. Oberpriller, and A. Mauro, eds. Harwood Academic, Chur, Switzerland.

**Anatskaya, O. V., A. E. Vinogradov, and B. N. Kudryavtsev. 2001.** Cardiomyocyte ploidy levels in birds with different growth rates. *J. Exp. Zool.* **289:** 48–58.

**Anisimov, A. P. 1999.** Cell proliferation and somatic polyploidy in tissues of the gastropod molluscs: a review. VI. General regularities of cell proliferation and endoreproduction. *Tsitologija* **41:** 23–31 (In Russian, English summary).

**Balser, E. J., and E. E. Ruppert. 1990.** Structure, ultrastructure, and function of the preoral heart-kidney in *Saccoglossum kowalevskii* (Hemichordata: Enteropneusta) including new data on the stomochord. *Acta Zool.* **71:** 235–249.

**Bittner, R. E., C. Schöfer, K. Weipoltshammer, S. Ivanova, B. Streubel, E. Hauser, M. Freilinger, H. Höger, A. Elbe-Bürger, and F. Wachtler. 1999.** Recruitment of bone-marrow-derived cells by skeletal and cardiac muscle in adult dystrophic *mdx* mice. *Anat. Embryol.* **199:** 391–396.

**Bugaeva, E. A., O. A. Bystrova, and M. G. Martynova. 1999.** Ecdysteroid receptors in the heart of *Helix aspersa* (Gastropoda). *Tsitologija* **41:** 132–134.

**Bulloch, A. G. M. 1985.** Development and plasticity of the molluscan nervous system. Pp. 335–410 in *The Mollusca*. Vol. 8. *Neurobiology and Behavior*. Pt. 1, K. M. Wilbur, ed. Academic Press, New York.

**Bystrova, O. A., M. G. Martynova, and A. Nylund. 1996.** Stem muscle cells in the molluscan heart muscle. *Tsitologija* **38:** 440–444 (In Russian, English summary).

**Grounds, M. D., and J. K. McGeachie. 1989.** Myogenic cells of regenerating adult chicken muscle can fuse into myotubes after a single cell division *in vivo*. *Exp. Cell Res.* **180:** 429–439.

**Hama, K. 1960.** The fine structure of some blood vessels of the earth worm *Eisenia foetida*. *J. Biophys. Biochem. Cytol.* **7:** 717–724.

**Jensen, H. 1974.** Ultrastructural studies on the heart in *Arenicola marina* L. (Annelida: Polychaeta). *Cell Tissue Res.* **150:** 355–369.

**Jensen, H., and R. Myklebust. 1975.** Ultrastructure of the muscle cells in *Siboglinum fiordicum* (Pogonophora). *Cell Tissue Res.* **163:** 185–197.

**Kling, G., and R. Schipp. 1987.** Comparative ultrastructural and cytochemical analysis of the cephalopod systemic heart and its innervation. *Experientia* **43:** 502–511.

**Kudryavtsev, B. N., O. V. Anatskaya, V. K. Nilova, and S. A. Komarov. 1997.** Interrelation between myofibrillar and mitochondrial apparatus and cardiomyocyte polyploidy and hypertrophy in mammals with different body weight. *Tsitologija* **39:** 946–964 (In Russian, English summary).

**Larra, F., and B. Droz. 1970.** Techniques radioautographiques et leur application a l'étude du renouvellement des constituants cellulaires. *J. Microsc.* **9:** 845–880.

**Lester, S. M. 1982.** Fine structure of the heart vesicle and pericardium in the pterobranch *Rhabdopleura* (Hemichordata). *Am. Zool.* **22:** 938.

**Martin, A. W. 1980.** Some invertebrate myogenic hearts: the hearts of worms and molluscs. Pp. 1–40 in *Heart and Heart-like Organs*. Vol. 1. *Comparative Anatomy and Development*, G. H. Borne, ed. Academic Press, New York.

**Martynova, M. G. 1993.** Satellite cells in the crayfish heart muscle function as stem cells and are characterized by molt-dependent behaviour. *Zool. Anz.* **230:** 181–190.

**Martynova, M. G. 1997.** The influence of ecdysterone on DNA synthesis in heart satellite cells of the *Astacus astacus*. *Tsitologija* **39:** 979–982 (In Russian, English summary).

**Martynova, M. G., and O. Y. Chaga. 1997.** Ultrastructural study of the heart and its relationship with the connective tissue sheath of the stomach in *Rhynchonella psittacea* (Tentaculata, Brachiopoda). *J. Morphol.* **234:** 69–77.

**Martynova, M. G., and S. Yu. Khaitlina. 1991.** Attempt to stimulate regenerative processes in the heart of the crayfish *Astacus astacus*: an autoradiographic and electrophoretic study. *Tsitologija* **33:** 23–28 (In Russian, English summary).

**Martynova, M. G., and A. Nylund. 1996.** DNA-synthesizing cells in the heart of *Ascidia obliqua* (Tunicata). *Biol. Bull.* **190:** 410–417.

**Martynova, M. G., S. Okland, P. P. Rumyantsev, and A. Tjonneland. 1986.** The ultrastructure of the myocardium and myocardial satellite cells in *Hyas areneus* L., *Carcinas maenas* L., and *Cancer pagurus* L. (Crustacea, Decapoda). *Zool. Anz.* **216 (5/6):** 357–366.

**Moffett, S. B. 1995.** Neural regeneration in gastropod molluscs. *Progr. Neurobiol.* **46:** 289–330.

**Nolte, A., J. Kollman, M. Dorlöchter, and H. Straub. 1986.** Ecdysteroids in the dorsal bodies of pulmonates (Gastropoda): synthesis and release of ecdysone. *Comp. Biochem. Physiol.* **84A:** 777–782.

**North, R. J. 1963.** The fine structure of the myofibers in the heart of the snail *Helix aspersa. J. Ultrastruct. Res.* **8:** 206–218.

**Nylund, A. 1981.** The heart ultrastructure of *Praunus flexuosus* (Müller) and *Mysis relicta* (Lovén) (Crustacea, Mysidacea). *J. Crustac. Biol.* **1:** 558–566.

**Nylund, A., N. I. Komarova, P. P. Rumyantsev, A. Tjonneland, and S. Okland. 1986.** Heart ultrastructure in *Petrobius brevistylis* (Archaeognatha: Microcoryphia). *Entomol. Gener.* **11 (3/4):** 263–272.

**Okland, S. 1982.** The ultrastructure of the heart complex in *Patella vulgata* L. (Archaeogastropoda, Prosobranchia). *J. Molluscan Stud.* **48:** 331–341.

**Roberts, P., J. K. McGeachie, M. D. Graunds, and E. R. Smith. 1989.** Initiation and duration of myogenic precursor cell replication in transplants of intact skeletal muscle: an autoradiographic study in mice. *Anat. Rec.* **224:** 1–6.

**Romer, F. 1979.** Ecdysteroids in snails. *Naturwissenschaften* **66:** 471–472.

**Rumyantsev, P. P. 1991.** *Growth and Hyperplasia of Cardiac Muscle Cells.* Harwood Academic, Chur, Switzerland, 376 pp.

**Schipp, R. 1987.** General morphological and functional characteristics of the cephalopod circulatory system. An introduction. *Experientia* **43:** 474–477.

**Watts, J. A., R. A. Koch, M. J. Greenberg, and S. K. Pierce. 1981.** Ultrastructure of the heart of the marine mussel, *Geukensia demissa. J. Morphol.* **170:** 301–319.

**Wells, M. J., and P. J. S. Smith. 1987.** The performance of the octopus circulatory system: a triumph of engineering over design. *Experientia* **43:** 487–499.

**Whitehead, D. L., and K. Sellheyer. 1982.** The identification of ecdysterone (20-hydroxyecdysone) in 3 species of molluscs (Gastropoda: Pulmonata). *Experientia* **38:** 1249–1251.

Reference: *Biol. Bull.* **203:** 112–120. (August 2002)

# Predator-Induced Behavioral and Morphological Plasticity in the Tropical Marine Gastropod *Strombus gigas*

GABRIEL A. DELGADO*, ROBERT A. GLAZER, AND NICOLA J. STEWART†

*Florida Fish and Wildlife Conservation Commission, Florida Marine Research Institute,*
*2796 Overseas Highway, Suite 119, Marathon, Florida 33050*

**Abstract.** Florida queen conch stocks once supported a significant fishery, but overfishing prompted the state of Florida to institute a harvest moratorium in 1985. Despite the closure of the fishery, the queen conch population has been slow to recover. One method used in the efforts to restore the Florida conch population has been to release hatchery-reared juvenile conch into the wild; however, suboptimal predator avoidance responses and lighter shell weights relative to their wild counterparts have been implicated in the high mortality rates of released hatchery juveniles. We conducted a series of experiments in which hatchery-reared juvenile conch were exposed to a predator, the spiny lobster (*Panulirus argus*), to determine whether they could develop behavioral and morphological characteristics that would improve survival. Experiments were conducted in tanks with a calcareous sand substrate to simulate a natural environment. Conditioned conch were exposed to caged lobsters while conch in the control tanks were exposed to empty cages. Conditioned conch moved significantly less and buried themselves more frequently than the naive control conch. Morphometric data indicated that the conditioned conch grew at a significantly slower rate than the naive conch, but the shell weights of the two groups were not significantly different. This implies that the conditioned conch had thicker or denser shells than the control group. As a result, the conditioned conch had significantly higher survival than naive conch in a subsequent predation experiment in which a lobster was allowed to roam free in each tank for 24 hours. In the future, the conditioning protocols documented in this study will be used to increase the survival of hatchery-reared conch in the wild.

## Introduction

A growing body of evidence suggests that predators elicit behavioral and morphological responses in their prey. Predators have been shown to influence burial depth, respiration rates, and filtration in clams (Doering, 1982a, b); feeding in copepods (Bollens and Stearns, 1992) and damselflies (Koperski, 1997); foraging behavior and growth rates in intertidal snails (Yamada *et al.*, 1998); behavior and growth rates in larval frogs (Relyea and Werner, 1999); and byssal attachment strength in blue mussels (Reimer and Tedengren, 1997). Additionally, morphological plasticity has been predator-induced in a wide variety of taxa from protozoans to crustaceans (Havel, 1987; Appleton and Palmer, 1988; Adler and Harvell, 1990; Spitze, 1992; Reimer and Tedengren, 1996; Arnqvist and Johansson, 1998; Yamada *et al.*, 1998). In many cases, these responses result in increased fitness or survival of the prey organism (Doering, 1982a; Adler and Harvell, 1990; Reimer and Tedengren, 1996; Yamada *et al.*, 1998).

The queen conch (*Strombus gigas*) is a tropical marine gastropod common to shallow-water seagrass habitats throughout the Caribbean bio-province. Queen conch populations have supported a substantial commercial fishery in the region; however, overfishing has depleted stocks to the point that the species has been included in the Convention on the International Trade in Threatened and Endangered Flora and Fauna (CITES) Appendix II (Bräutigam, 1992). In Florida, a moratorium on harvest was instituted in 1985,

---

Received 1 February 2002; accepted 30 April 2002.

* To whom correspondence should be addressed. E-mail: gabriel.delgado@fwc.state.fl.us

† Current address: University of California-Berkeley, Department of Health and Medical Sciences, 570 University Hall MC1190, Berkeley, California 94720.

but conch stocks have not recovered. This has caused many investigators to propose releasing hatchery-reared juvenile conch as a strategy to replenish impoverished stocks (see Stoner, 1997, and Stoner and Glazer, 1998, for reviews). The hatchery's role is to (1) establish or re-establish populations, and (2) supplement or enhance natural production through the release and survival of hatchery-reared juveniles. To accomplish these goals, a successful stock-enhancement program requires a hatchery than can produce not just large quantities of juveniles, but large quantities of high-quality juveniles. Furthermore, after release, these "outplants" must survive and grow to reproduce. Unfortunately, behavioral and morphological deficits have been associated with the husbandry process in queen conch (see Stoner, 1997, and Stoner and Glazer, 1998, for reviews). For example, conch have evolved predator avoidance strategies that include an infaunal early life-history stage (Iversen *et al.*, 1986); however, researchers have observed that released hatchery-reared juvenile conch have lower burial rates than their wild counterparts. Ultimately, this has resulted in higher mortalities in the hatchery cohort (Appeldoorn and Ballantine, 1983; Coulston *et al.*, 1989; Stoner and Davis, 1994). Additionally, the decreased shell weight and shorter apical spines of hatchery-reared *S. gigas* were implicated in their higher mortality relative to wild conch (Stoner and Davis, 1994). To overcome these disadvantages, optimal culture and release strategies are essential.

The extent to which the behavior and morphology of hatchery-reared queen conch can be manipulated before release to maximize survival after release is unknown. However, the survival benefits of exposing laboratory-reared animals to a predator prior to their release have been demonstrated in studies with salmon (Olla *et al.*, 1998) and flounder (Kellison *et al.*, 2000). The present study was initiated to investigate predator-mediated behavioral and morphological plasticity and to determine if any observed phenotypic variations will affect queen conch survival.

## Materials and Methods

We conducted two laboratory experiments to determine the behavioral and morphological effects on queen conch after exposure to one of their main predators, *Panulirus argus*, a species of spiny lobster. We used lobsters 60–80 mm in carapace length for the experiments. Each experiment consisted of two treatments: a conditioned group exposed to a lobster in a cage and a naive control group exposed to an empty cage. Each treatment consisted of three replicates (*i.e.*, tanks) of 20 conch each. Conch were randomly assigned to each tank, and tanks were randomly assigned to each treatment. The first experiment examined differences in burial rates, movement, and shell morphology between the treatments. The second experiment examined the differences in predator-avoidance and conch survival between the conditioned and naive treatments after a lobster had been allowed to roam free in the tank.

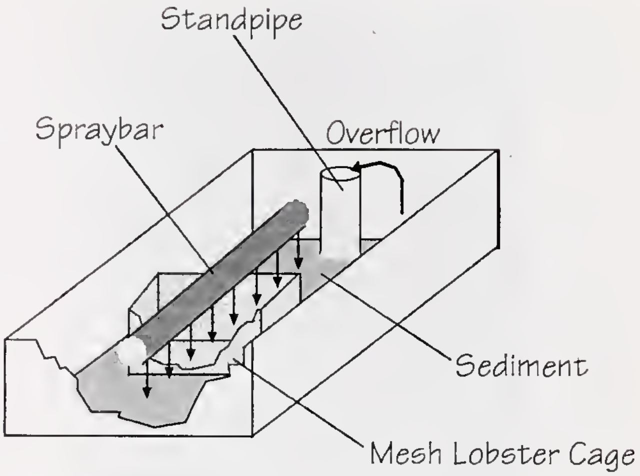

**Figure 1.** Cut-away view of one of the tanks used to condition queen conch. Tank dimensions were 182 cm long × 51 cm wide × 27 cm deep. The lobster was placed in the center of the tank in a mesh cage that allowed water to flow through it. Water entered the tank *via* the spraybar and exited through the standpipe. The sediment was supported off the bottom of the tank by a plastic grid and screen. Drawing not to scale.

We conducted all the experiments at the Florida Fish and Wildlife Conservation Commission's (FWC) queen conch hatchery at the Keys Marine Laboratory on Long Key in the Florida Keys. All conch used in the experiments were cultured from egg masses collected in the wild. We used well-described husbandry techniques (see Davis, 1994, for review). The experiments were conducted in six fiberglass tanks with a centralized, flow-through water system (Fig. 1). Each tank had substrate 4 cm to 5 cm deep, consisting of calcareous sand collected from locations that supported wild populations of conch. Before use, the sand was disinfected with dilute chlorine and rinsed with fresh water. The sand was then rinsed with salt water and placed on 1.8-mm mesh supported by a plastic grid about 2 cm off the bottom of the tank. The water circulation and plastic grid minimized the anoxic effects commonly associated with substrate placed directly on the tank bottom.

### *Experiment I: Conditioning*

From a pool of about 300 individuals, 120 conch ranging in size from 35 mm to 40 mm were randomly selected for inclusion in this study. Each day, we fed the conch a diet consisting of a commercially available koi feed (Mazuri Koi Platinum, Purina Feeds, St. Louis, MO), ground and supplemented with 15% oyster shell by dry weight. A uniquely numbered tag was secured to the spire of each conch with Monel wire (Fig. 2), which allowed us to track individuals throughout the duration of the experiments. We measured

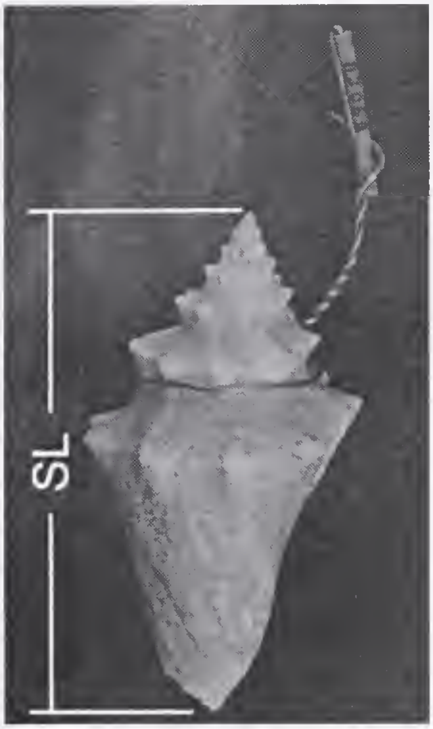

**Figure 2.** Juvenile queen conch showing the numbered tag used to distinguish individuals. The tag was attached to the spire of the conch by Monel stainless-steel wire. The shell length (SL) is defined as the linear distance between the tip of the spire and the end of the siphonal canal.

the shell length of each conch to 0.1 mm (Fig. 2) at the onset and completion of the experiments.

Conditioning was initiated by placing a spiny lobster confined within a plastic mesh cage into the tanks. The cage effectively isolated the lobster from the conch while permitting water exchange and visual contact between the two (Fig. 1). Additional juvenile conch similar in size to those in the tank were supplied as food to the predator, thus permitting any chemical alarm substance produced by the feed conch to contact the juveniles being conditioned. Depending on the treatment, juvenile conch were exposed to either a caged predator or an empty cage for 6 h each day (1100 to 1700 hours) for 2 weeks. At 1700, the caged lobsters and empty cages were removed from all tanks.

To facilitate the calculation of conch movements, a quadrat subdivided into 37 × 11 blocks (roughly 5 cm × 5 cm) was placed on top of each tank. At the initiation of the experiments, we distributed the conch in each tank uniformly, using this Cartesian coordinate grid system. Conch in all tanks were redistributed every morning after their positions were noted. This permitted daily movement information to be unbiased by the final location from the previous day.

We recorded the number of completely buried conch and the position of all individuals at 2-h intervals beginning at 0900 and ending at 1900 hours. These data were used to assess predator avoidance responses (*i.e.*, burial and mean daily movement) and optimal conditioning time as a function of temporal exposure (*i.e.*, days). A two-way repeated measures ANOVA was used to test for differences in the proportion of buried conch between the two treatments (independent factor) over the duration of the experiment (14 conditioning days = repeated factor). A two-way repeated measures ANOVA of the same design was used to examine the mean daily movement of the individual conch in the two treatments. Planned multiple-comparison *t* tests with a Bonferroni adjustment were used to compare burial and movement between the two treatments for each day.

At the end of 2 weeks, the shell length of each individual was recorded for growth calculation. In addition, 10 randomly selected juveniles from each tank were sacrificed. The foot and viscera were removed, and the shell was placed in a drying oven for 24 h at 70 °C; dry shell weight was then recorded. Morphological comparisons (initial shell length, growth, and shell dry weight) of the conch in the two treatments were made using a one-way nested ANOVA (the tanks or replicates were the nested factor).

The conditioning experiment was repeated to determine whether predator-induced morphological changes would arise in a one-week period; however, in this experiment, each treatment (conditioned and naive) contained only two replicates of 20 conch due to the limited inventory of 35-mm to 40-mm conch. No movement or burial data were recorded during this run, but as with the 2-week experiment, growth for all 20 conch and the shell dry weight of 10 randomly selected individuals from each tank were recorded and tested using a one-way nested ANOVA.

The conditioning experiment was repeated once again. This run was designed to test whether predator-induced morphological changes would arise in the presence of lobsters fed on non-molluscan prey (*i.e.*, frozen shrimp). Conditioning lasted 2 weeks. Due to the limited number of animals available, slightly smaller conch (approximately 30 mm) were used than in previous experimental runs, and each treatment (conditioned and naive) contained three replicates of eight conch. No movement or burial data were recorded during this run, but growth for all 24 conch was recorded and tested using a one-way nested ANOVA. We did not examine shell dry weight.

### *Experiment II: Predator-avoidance and conch survival*

The second experiment was conducted to determine whether any behavioral or morphological differences between the conditioned and naive conch would translate into differences in predation and mortality rates. We used the remaining conch from the one-week conditioning experiment. The conch were left in their respective tanks (two treatments with two replicates, each replicate containing 10

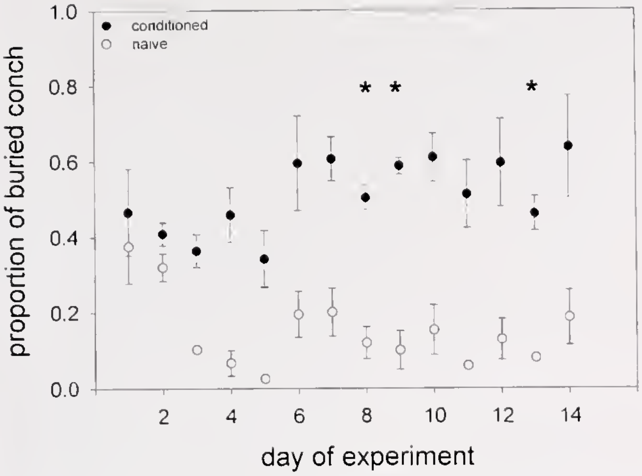

**Figure 3.** The proportion of buried conditioned and buried naive queen conch over the duration of the 2-week conditioning experiment. Error bars represent one standard error. A two-way repeated measures ANOVA showed that conditioned conch buried at significantly higher rate than naive conch ($P = 0.002$) and that there was a significant difference in burial among the days of the experiment ($P = 0.003$). An asterisk indicates that the Bonferroni adjusted planned comparison $t$ test between the two treatments was significant for that day.

conch), and one lobster was allowed to forage throughout each tank for 24 h.

At the end of the 24 h, the numbers of dead conch, live conch with damaged shells, and live conch with undamaged shells were counted. Those categories were used to assess survival and predator-avoidance as a function of conditioning. Fisher's exact test was used to examine the differences between the two treatments. We compared the number of dead conch to the number of live conch (damaged and undamaged combined) to examine differences in survival between treatments. The numbers of dead conch and live conch with damaged shells were compared against the number of live conch with undamaged shells to examine avoidance through burial. We assumed that conch with undamaged shells escaped detection by burying themselves, although it is possible that the lobsters detected and handled these conch, but did not damage them.

## Results

### *Conditioning: Burial and movement*

There was a significant difference in the proportion of buried conch between the two treatments and among the days of the 2-week conditioning experiment (repeated measures ANOVA: $F_{\text{btwn treatments } [1, 4]} = 55.1$, $P = 0.002$; $F_{\text{among days } [13, 52]} = 2.92$, $P = 0.003$). The proportion of buried conch in the conditioned treatment increased dramatically on day 6 of the experiment and remained relatively constant afterwards (Fig. 3). Meanwhile, the proportion of buried conch in the naive treatment was fairly steady throughout the conditioning experiment (Fig. 3). The Bonferroni adjusted multiple comparison $t$ tests showed that the proportion of buried conch in the conditioned treatment was significantly higher on days 8, 9, and 13 only, although burial diverged after day 3 (Fig. 3).

There was a significant difference in the mean movement of conch in the two treatments and among the days of the 2-week conditioning experiment (repeated measures ANOVA: $F_{\text{btwn treatments } [1, 4]} = 15.1$, $P = 0.018$; $F_{\text{among days } [13, 1598]} = 12.9$, $P < 0.001$). The mean movement of the conditioned conch diverged from the naive individuals on day 3 and continued to decrease throughout the rest of the experiment (Fig. 4). The Bonferroni adjusted multiple comparison $t$ tests showed that the conditioned conch moved significantly less than the naive conch on days 3 through 6 and days 8 through 14 (Fig. 4).

### *Conditioning: Morphology*

There was no significant difference in initial shell length among the conch chosen for the conditioning experiment (Nested ANOVA: $F_{\text{btwn treatments } [1, 4]} = 0.536$, $P = 0.505$) (Fig. 5a). At the end of 2 weeks, the conditioned conch had grown significantly less than the control group (Nested ANOVA: $F_{\text{btwn treatments } [1, 4]} = 295$, $P < 0.001$), but the shell weights of the two groups were not significantly different (Nested ANOVA: $F_{\text{btwn treatments } [1, 4]} = 0.128$, $P = 0.738$) (Fig. 5a). None of the nested factors (*i.e.*, the tanks) within these ANOVAs were significantly different (initial shell length: $F_{\text{among replicates } [4, 112]} = 1.11$, $P = 0.354$;

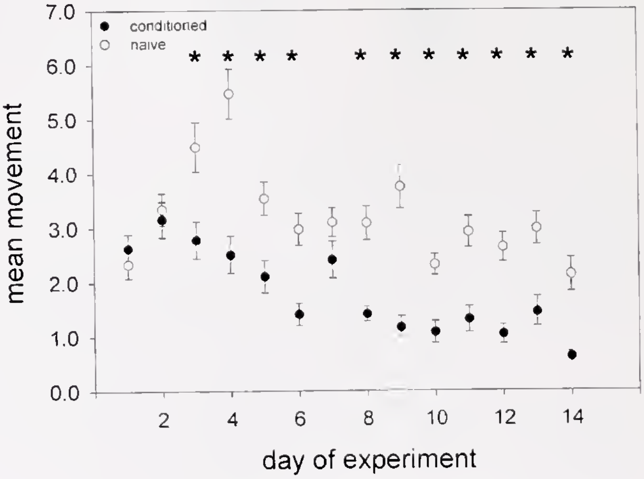

**Figure 4.** The mean movement of conditioned and naive queen conch over the duration of the 2-week conditioning experiment. Error bars represent one standard error. A two-way repeated measures ANOVA showed that conditioned conch moved significantly less than naive conch ($P = 0.018$) and that there was a significant difference in movement among the days of the experiment ($P < 0.001$). An asterisk indicates that the Bonferroni adjusted planned comparison $t$ test between the two treatments was significant for that day.

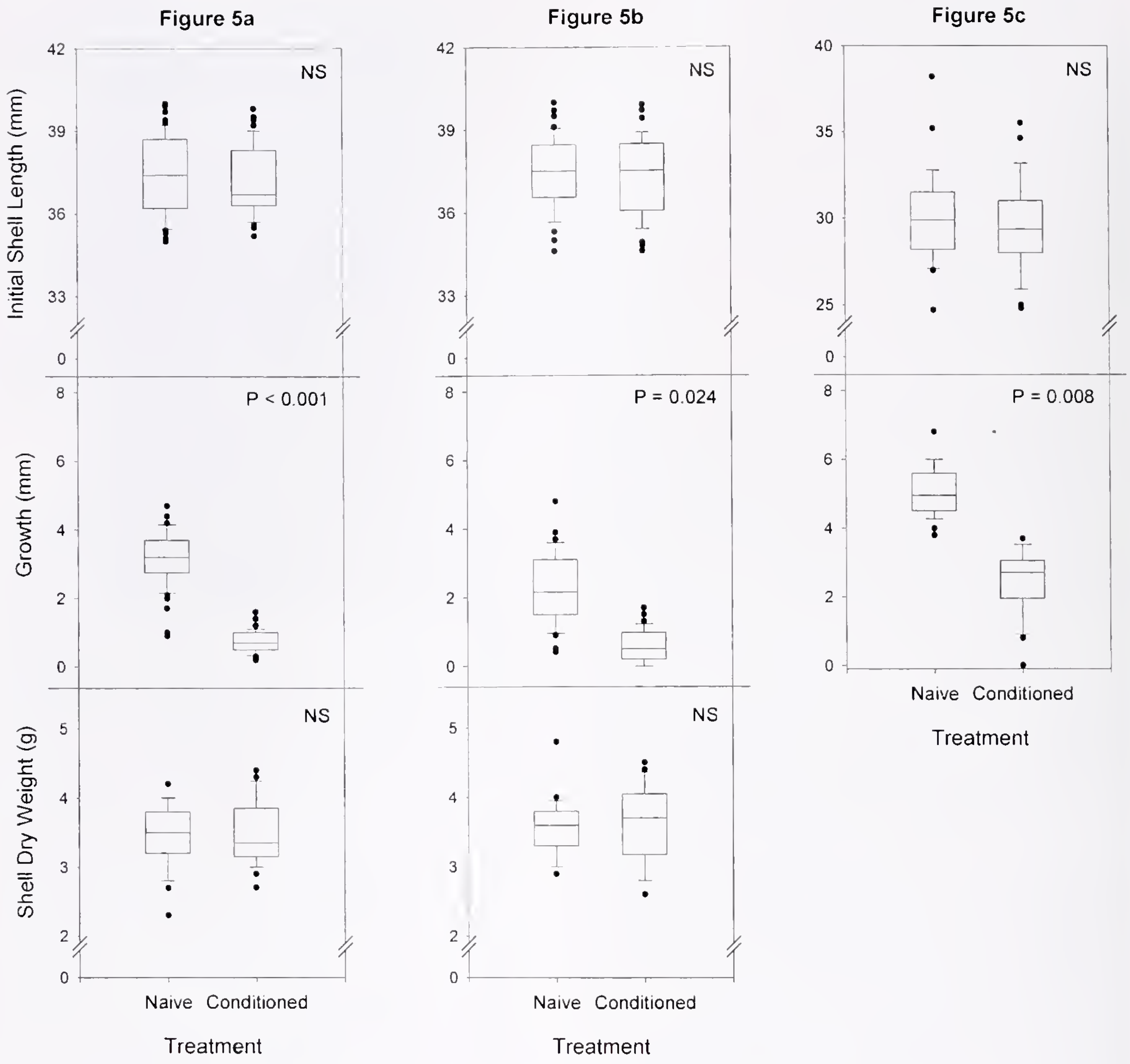

**Figure 5.** Initial shell length, growth, and shell dry weight of naive and conditioned queen conch in the 2-week conditioning experiment (5a), the 1-week conditioning experiment (5b), and the 2-week conditioning experiment in which the lobsters were fed non-molluscan prey (*i.e.*, frozen shrimp) (5c). Shell dry weight was not examined in the third experiment (5c). The boxes represent the interquartile ranges, which contain 50% of the values. The line bisecting the box represents the median. The whiskers extend to the 90th percentile. Dots represent outliers. When significant, *P* values from the nested ANOVAs are given in the upper right-hand corner of each graph; NS indicates that the test was not significant.

growth: $F_{\text{among replicates }[4,\,112]} = 1.56$, $P = 0.191$; shell weight: $F_{\text{among replicates }[4,\,52]} = 0.270$, $P = 0.896$). Two conch in the conditioned treatment were not included in these analyses because they buried themselves under the sand and the plastic grid, and were not found until the experiment was disassembled.

The conditioning experiment was repeated to determine whether these predator-induced morphological changes would arise in a one-week period. Again, there was no significant difference in initial shell length among the conch chosen for the two predator treatments (Nested ANOVA: $F_{\text{btwn treatments }[1,\,2]} = 0.360$, $P = 0.609$) (Fig. 5b). After one week, the conditioned conch had grown significantly less than the control group (Nested ANOVA: $F_{\text{btwn treatments [1, 2]}} = 40.7$, $P = 0.024$), and again, the shell weights of the two groups were not significantly different (Nested ANOVA: $F_{\text{btwn treatments [1, 2]}} = 0.013$, $P = 0.921$) (Fig. 5b). None of the nested factors within the ANOVAs were significantly different (initial shell length: $F_{\text{among replicates [2, 75]}} = 0.832$, $P = 0.439$; growth: $F_{\text{among replicates [2, 75]}} = 1.96$, $P = 0.149$; shell weight: $F_{\text{among replicates [2, 35]}} = 2.59$, $P = 0.090$). One juvenile in the conditioned treatment was not included in these analyses because it buried itself under the sand and the plastic grid, and was not found until the experiment was disassembled.

The next run was designed to determine whether predator-induced morphological changes would arise after 2 weeks of conditioning in the presence of lobsters fed on frozen shrimp. There was no significant difference in initial shell length among the conch chosen for the two predator treatments (Nested ANOVA: $F_{\text{btwn treatments [1, 4]}} = 0.295$, $P = 0.616$) (Fig. 5c). The nested factor (*i.e.*, the tanks) within this ANOVA was not significantly different ($F_{\text{among replicates [4, 42]}} = 0.910$, $P = 0.467$). After 2 weeks, the conditioned conch had grown significantly less than the control group (Nested ANOVA: $F_{\text{btwn treatments [1, 4]}} = 24.7$, $P = 0.008$) (Fig. 5c). However, the nested factor within this ANOVA was significantly different ($F_{\text{among replicates [4, 42]}} = 7.14$, $P < 0.001$). The conch in one of the tanks within the conditioning treatment had much less growth (1.35 ± 0.795 mm) than the other two conditioned tanks (3.00 ± 0.537 mm and 2.89 ± 0.464 mm). When this tank was removed from the analysis, the conditioned conch still had significantly slower growth.

### *Predator-avoidance and conch survival*

Predator-avoidance was independent of conditioning (Fisher's exact test: $P = 1.0$); only two individuals (one from each treatment: conditioned and naive) avoided detection through burial (Fig. 6a). However, survival was dependent on conditioning (Fisher's exact test: $P = 0.014$). Conditioned conch survived their encounter with the lobster 50% of the time, whereas only 10% of the naive conch survived (Fig. 6b).

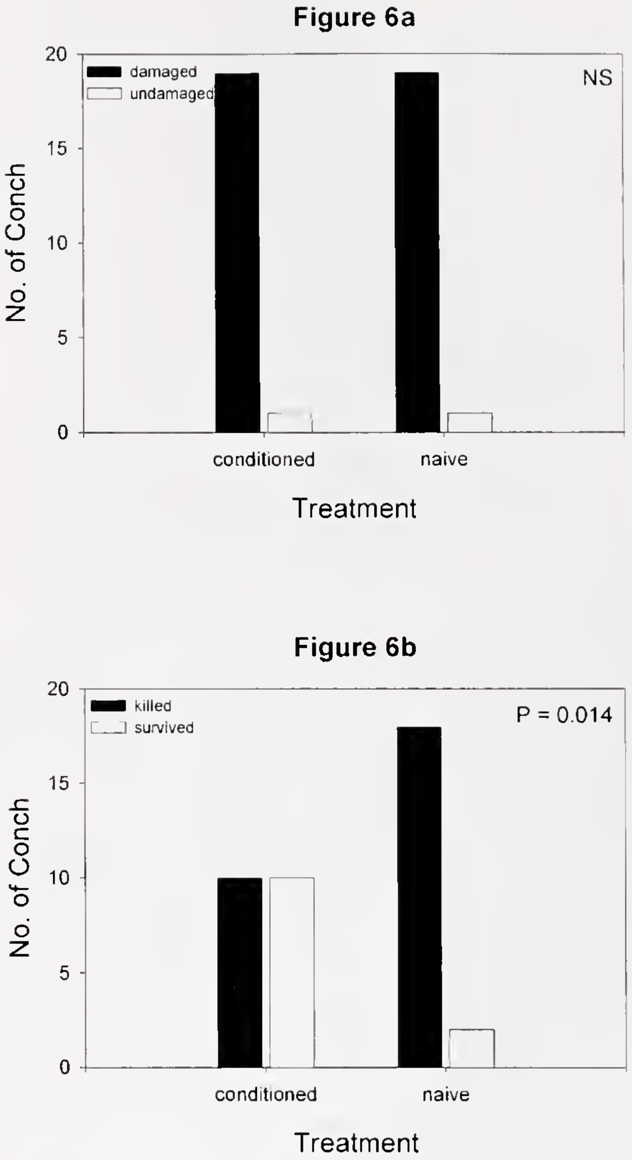

**Figure 6.** The number of conditioned and naive queen conch damaged (6a) and killed (6b) during the predator-avoidance and conch survival experiment. We assumed that conch with undamaged shells escaped detection *via* burial. Fisher's exact test showed that predator-avoidance was independent of conditioning (6a, $P = 1.0$); however, conditioned conch had significantly higher survival than their naive counterparts (6b, $P = 0.014$).

## Discussion

Many organisms have been shown to produce adaptive phenotypes in response to environmental changes or stimuli (see Havel, 1987, and Adler and Harvell, 1990, for reviews). In the queen conch, shell morphology is plastic depending on environmental conditions (environmental induction) (Alcolado, 1976; Stoner and Davis, 1994; Martin-Mora *et al.*, 1995). Therefore, by altering the culture environment in the hatchery, it may be possible to induce the expression of different phenotypes (phenotypic plasticity). Predator-mediated changes in behavior and morphology have been described for a variety of species, and the present experiments demonstrate that these alterations can be induced in hatchery-raised queen conch as well.

We have shown that conch exposed to a predator for 2 weeks grew significantly slower; but their shell weights were practically identical to naive conch, implying that conditioned animals had thicker or denser shells. These morphological changes in conditioned conch were also induced after exposure to the lobster for just one week. The aim of the study was not to determine the mechanism of the changes in behavior and morphology, but to determine whether the changes could be predator-induced in queen conch. Nevertheless, the mechanism for the morphological responses may have been visual or mechanical cues from the lobster, odor cues produced by the lobster, a chemical alarm substance excreted by the feed conch, or a combination of these. However, it is unlikely that a species-specific alarm substance was the sole cause of the morphological variability, because conditioned conch exposed to lobster fed on frozen shrimp also had slower growth rates than naive individuals. A study conducted on the intertidal gastropod *Thais lamellosa* produced similar results. *Thais* developed predator-resistant thicker shells when in the presence of crabs fed conspecific snails and in the presence of crabs fed frozen fish (Appleton and Palmer, 1988). Queen conch probably detect predators through their chemosensitive tentacles and use their keen eyesight to orient the escape response correctly, as reported with *Strombus maculatus* (Field, 1977).

The shell's primary function is protection; as a protective structure, the molluscan shell must be able to resist breakage. Spiny lobsters peel shells with their greatly enlarged mandibles by breaking off successive pieces of shell, beginning at the outer lip (Davis, 1992); small conch are especially prone to this type of breakage because of their thin shells. The conditioned conch grew at a slower rate than the control group, yet they had thicker or denser shells. Therefore, exposure to a predator before release will probably improve survival, because juvenile queen conch with thicker or denser shells would be better adapted to resist having their shells crushed or peeled. However, a thicker shell will not necessarily reduce all predation mortality; for example, it will not deter crustaceans and molluscs that attack through the aperture (Ray and Stoner, 1995). Therefore, a conch's ability to detect, recognize, and avoid predators (by burying themselves) is also important in reducing predation mortality.

Glazer and Jones (1997) reported that hatchery-reared juvenile conch incurred significantly higher mortalities during the first week after release. We were able to significantly alter the morphology and behavior of hatchery-raised conch in a week's time. It is apparent from the results of both studies that the first week after release is crucial. Evidently, it takes about one week for outplants to adjust to life in the wild; however, conditioning may be able to reduce this period of adjustment and decrease the level of mortality associated with the first week after release. This is especially likely considering that we have shown that both optimal burial and movement responses are induced after one week of exposure to the lobster (Figs. 3 and 4).

The predator-induced morphological and behavioral differences documented in this study are interrelated, as buried conch have a tendency to move less. It is no coincidence then that the conditioned conch also had slower growth and thicker or denser shells. In gastropods, shell material is deposited along the aperture in the spiral direction with the mantle lying at the growing edge (Vermeij, 1993). The inner layer of shell is added last, well back from the growing edge and is deposited by the mantle's surface, not the mantle's margin (Vermeij, 1993). When growth in the spiral direction is not occurring, the mantle margin withdraws from the edge, and new shell material is deposited only on the innermost layer (Vermeij, 1993). A conch that is sedentary and buried does not have its mantle at the growing edge but continues to deposit calcium carbonate on the inner layer of the shell, which explains the slower growth and coincidental thicker or denser shells of the conditioned conch. Therefore, by inducing changes in the conch's behavior, their morphology was changed as well.

Other studies have also shown that predator-induced changes in prey behavior affect prey activity and growth. Searching for food increases the risk of predation; therefore, many taxa reduce activity when in the presence of predators (Doering, 1982b; Lima and Dill, 1990; Bollens and Stearns, 1992; Koperski, 1997; Yamada *et al.*, 1998; Relyea and Werner, 1999). These changes in prey behavior are presumed to reduce (1) the rate of predator encounters, (2) the time spent vulnerable to attack, and (3) the probability of death in an encounter (Lima and Dill, 1990). We have demonstrated that by conditioning hatchery-raised conch to one of their principal predators, they can develop behavior and morphology that may accomplish all three survival strategies. Burial will decrease the rate of predator encounters by reducing exposure time, and thicker shells will reduce the probability of mortality if confronted by a shell-peeling or shell-crushing predator.

These predator-induced defense mechanisms were tested in our second experiment (predator-avoidance and conch survival). This experiment showed that the anti-predator morphological changes that took place in conditioned conch were enough to significantly increase their survival over their naive counterparts. A closer inspection of the data showed that most (83.3%) of the conch that survived had incurred some shell damage but escaped being eaten, presumably because their thicker or denser shells were able to resist the shell-peeling lobsters. Davis (1992) reported that hatchery-raised queen conch less than 40 mm in shell length were consumed by lobsters similar in size to those used in this study, whereas larger juvenile conch (>50 mm) suffered damage, but survived. Jory and Iversen (1988) reported that shell strength increased exponentially once conch reached 55 mm in shell length. Therefore, by conditioning juveniles and inducing adaptive morphologies by changing their behavior, the effective size or shell strength of hatchery-reared conch is increased, resulting in survival rates similar to those of larger conch.

The increased burial frequency of the conditioned conch proved to be ineffective in our predator-avoidance and conch survival experiment; only 16.7% of the conch that survived escaped detection through burial. This predator-avoidance behavior should have allowed more individuals to remain undiscovered. A similar study with the hard clam *Mercenaria mercenaria* showed that the clams burrowed deeper into the sediment when subjected to predacious sea stars, and that this behavior increased survival over individuals that were not allowed to burrow more deeply (Doering, 1982a). The sediment in our tanks may not have been deep enough for the buried conch to avoid detection or the conch density may have been artificially high, allowing the lobster to efficiently forage the entire tank. Deeper sediment or reduced conch densities might have yielded different results.

Stock enhancement through mariculture may be one of the only ways to restore queen conch populations in the Florida Keys. Because of high monetary costs, the usual objective of most conch hatchery operations is to produce the largest product in the quickest time possible. However, this strategy may not be effective in a restoration context. The results of our experiments have shown that the production of fast-growing individuals should not necessarily be the determining factor in the success of a stock-enhancement facility. Rather, it is crucial to release well-adapted individuals in the appropriate habitat to maximize survival. The conditioning protocols documented in this study will be integrated into future releases of hatchery-raised conch to increase outplant survival and increase the cost-effectiveness of our stock rehabilitation program for queen conch.

## Acknowledgments

This project was funded by the Florida Fish and Wildlife Conservation Commission and by the U.S. Fish and Wildlife Service's Partnerships for Wildlife grants program (federal grant #P-1; state grant #FO633). Bill Arnold, John Ransier, Greg Vermeer, and two anonymous reviewers made valuable suggestions that improved the manuscript. Lyn French, Judy Leiby, and Jim Quinn provided editorial comments. Jim Kidney and Kevin McCarthy assisted with the experiments. The authors would also like to thank all of The Nature Conservancy volunteers at the hatchery, especially Dr. David Hawtof and Elsie Weber.

## Literature Cited

**Adler, F. R., and C. D. Harvell. 1990.** Inducible defenses, phenotypic variability, and biotic environments. *Trends Ecol. Evol.* **5:** 407–410.

**Alcolado, P. M. 1976.** Crecimiento, variaciones morfologicas de la concha y algunas datos biologicos del cobo *Strombus gigas* L. (Mollusca, Mesogastropoda). *Acad. Cienc. Cuba, Ser. Oceanol.* **34:** 1–36.

**Appeldoorn, R. S., and D. L. Ballantine. 1983.** Field release of cultured queen conch in Puerto Rico: implications for stock restoration. *Proc. Gulf Caribb. Fish. Inst.* **35:** 89–98.

**Appleton, R. D., and A. R. Palmer. 1988.** Water-borne stimuli released by predatory crabs and damaged prey induce more predator-resistant shells in a marine gastropod. *Proc. Natl. Acad. Sci. USA* **85:** 4387–4391.

**Arnqvist, G., and F. Johansson. 1998.** Ontogenetic reaction norms of predator-induced defensive morphology in dragonfly larvae. *Ecology* **79:** 1847–1858.

**Bollens, S. M., and D. E. Stearns. 1992.** Predator-induced changes in the diel feeding cycle of a planktonic copepod. *J. Exp. Mar. Biol. Ecol.* **156:** 179–186.

**Bräutigam, A. 1992.** *CITES: A Conservation Tool.* 3rd ed. Center for Marine Conservation, Washington, DC.

**Coulston, M. L., R. W. Berey, A. C. Dempsey, and P. Odum. 1989.** Assessment of the queen conch (*Strombus gigas*) population and predation studies of hatchery reared juveniles in Salt River Canyon, St. Croix, USVI. *Proc. Gulf Caribb. Fish. Inst.* **38:** 294–305.

**Davis, M. 1992.** Predation of hatchery-reared juvenile queen conch, *Strombus gigas* (L.) by juvenile spiny lobsters, *Panulirus argus* (L.). Master's thesis. Florida Institute of Technology, Melbourne, FL.

**Davis, M. 1994.** Mariculture techniques for queen conch (*Strombus gigas* L.): egg mass to juvenile stage. Pp. 231–252 in Strombus gigas: *Queen Conch Biology, Fisheries, and Mariculture,* R. S. Appeldoorn and B. Rodriguez, eds. Fundacion Cientifica Los Roques, Caracas, Veneznela.

**Doering, P. H. 1982a.** Reduction of sea star predation by the burrowing response of the hard clam *Mercenaria mercenaria* (Mollusca: Bivalvia). *Estuaries* **5:** 310–315.

**Doering, P. H. 1982b.** Reduction of attractiveness to the sea star *Asterias forbesi* (Desor) by the clam *Mercenaria mercenaria* (Linnaeus). *J. Exp. Mar. Biol. Ecol.* **60:** 47–61.

**Field, L. H. 1977.** An experimental analysis of the escape response of the gastropod *Strombus maculatus. Pac. Sci.* **31:** 1–11.

**Glazer, R. A., and R. Jones. 1997.** Temporal factors influencing survival of hatchery-raised queen conch outplants. Final Report (FO 507-95-9X-F), Project P-1, U.S. Fish and Wildlife Service, Partnerships for Wildlife Grants Program. Florida Marine Research Institute, Marathon, FL.

**Havel, J. E. 1987.** Predator-induced defenses: a review. Pp. 263–278 in *Predation: Direct and Indirect Impacts on Aquatic Communities,* W. C. Kerfoot and A. Sih, eds. University Press of New England, Hanover, NH.

**Iversen, E. S., D. E. Jory, and S. P. Bannerot. 1986.** Predation on queen conch, *Strombus gigas,* in the Bahamas. *Bull. Mar. Sci.* **39:** 61–75.

**Jory, D. E., and E. S. Iversen. 1988.** Shell strength of queen conch, *Strombus gigas* L.: aquaculture implications. *Aquacult. Fish. Manage.* **19:** 45–51.

**Kellison, G. T., D. B. Eggleston, and J. S. Burke. 2000.** Comparative behaviour and survival of hatchery-reared versus wild summer flounder (*Paralichthys dentatus*). *Can. J. Fish. Aquat. Sci.* **57:** 1870–1877.

**Koperski, P. 1997.** Changes in feeding behavior of the larvae of the damselfly *Enallagma cyathigerum* in response to stimuli from predators. *Ecol. Entomol.* **22:** 167–175.

**Lima, S. L., and L. M. Dill. 1990.** Behavioural decisions made under the risk of predation: a review and prospectus. *Can. J. Zool.* **68:** 619–640.

**Martin-Mora, E., F. C. James, and A. W. Stoner. 1995.** Developmental plasticity in the shell of the queen conch *Strombus gigas. Ecology* **76:** 981–994.

**Olla, B. L., M. W. Davis, and C. H. Ryer. 1998.** Understanding how the hatchery environment represses or promotes the development of behavioral survival skills. *Bull. Mar. Sci.* **62:** 531–550.

**Ray, M., and A. W. Stoner. 1995.** Predation on a tropical spinose gastropod: the role of shell morphology. *J. Exp. Mar. Biol. Ecol.* **187:** 207–222.

**Reimer, O., and M. Tedengren. 1996.** Phenotypical improvement of morphological defences in the mussel *Mytilus edulis* induced by exposure to the predator *Asterias rubens. Oikos* **75:** 383–390.

**Reimer, O., and M. Tedengren. 1997.** Predator-induced changes in byssal attachment, aggregation and migration in the blue mussel, *Mytilus edulis. Mar. Freshw. Behav. Physiol.* **30:** 251–266.

**Relyea, R. A., and E. E. Werner. 1999.** Quantifying the relation between predator-induced behavior and growth performance in larval anurans. *Ecology* **80:** 2117–2124.

**Spitze, K. 1992.** Predator-mediated plasticity of prey life-history and morphology: *Chaoborus americanus* predation on *Daphnia pulex. Am. Nat.* **139:** 229–247.

**Stoner, A. W. 1997.** The status of queen conch, *Strombus gigas*, research in the Caribbean. *Mar. Fish. Rev.* **59:** 14–22.

**Stoner, A. W., and M. Davis. 1994.** Experimental outplanting of juvenile queen conch, *Strombus gigas*: comparison of wild and hatchery-reared stocks. *Fish. Bull.* **92:** 390–411.

**Stoner, A. W., and R. A. Glazer. 1998.** Variation in natural mortality: Implications for queen conch stock enhancement. *Bull. Mar. Sci.* **62:** 427–442.

**Vermeij, G. J. 1993.** *A Natural History of Shells.* Princeton University Press, Princeton, NJ.

**Yamada, S. B., S. A. Navarrete, and C. Needham. 1998.** Predation induced changes in behavior and growth rate in three populations of the intertidal snail, *Littorina sitkana* (Philippi). *J. Exp. Mar. Biol. Ecol.* **220:** 213–226.

# Marine Biological Laboratory Woods Hole Massachusetts

## One Hundred and Fourth Report for the Year 2001 One Hundred and Thirteenth Year

### Officers of the Corporation

Sheldon J. Segal, *Chairman of the Board of Trustees*
Alfred M. Zeien, *Vice Chair of the Board of Trustees*
John E. Dowling, *President of the Corporation*
William T. Speck, *Director and Chief Executive Officer*
Mary B. Conrad, *Treasurer of the Corporation*
Thomas S. Crane, *Clerk of the Corporation*

## Contents

Report of the Director and CEO . . . . . . . . . . . . . . . . R1
Research and Education Highlights . . . . . . . . . . . . . R4
Report of the Treasurer . . . . . . . . . . . . . . . . . . . . . . R7
Financial Statements . . . . . . . . . . . . . . . . . . . . . . . . . R8
Report of the Library Director . . . . . . . . . . . . . . . . R20
Educational Programs
  Summer Courses . . . . . . . . . . . . . . . . . . . . . . . . . R22
  Special Topics Courses . . . . . . . . . . . . . . . . . . . . R26
  Other Programs . . . . . . . . . . . . . . . . . . . . . . . . . . R33
Summer Research Programs
  Principal Investigators . . . . . . . . . . . . . . . . . . . . R36
  Other Research Personnel . . . . . . . . . . . . . . . . . R37
  Library Readers . . . . . . . . . . . . . . . . . . . . . . . . . R38
  Institutions Represented . . . . . . . . . . . . . . . . . . R40
Resident Research Programs . . . . . . . . . . . . . . . . . R44
Honors . . . . . . . . . . . . . . . . . . . . . . . . . . . . . . . . . . . R58
Board of Trustees and Committees . . . . . . . . . . . R66
Administrative Support Staff . . . . . . . . . . . . . . . . . R70
Members of the Corporation
  Life Members . . . . . . . . . . . . . . . . . . . . . . . . . . . R73
  Members . . . . . . . . . . . . . . . . . . . . . . . . . . . . . . . R74
  Associate Members . . . . . . . . . . . . . . . . . . . . . . . R84
Certificate of Organization . . . . . . . . . . . . . . . . . . R87
Articles of Amendment . . . . . . . . . . . . . . . . . . . . . . R87
Bylaws . . . . . . . . . . . . . . . . . . . . . . . . . . . . . . . . . . . R87
Publications . . . . . . . . . . . . . . . . . . . . . . . . . . . . . . R92

**Photo credits:**
E. Armstrong—R1, R4, R26, R31, R47, R57, R70, R73
R. Barlow—R39
M. Downs—R2
R. Hanlon—R23, R54
A. Hawkins—R7
R. Howard—R66
H. Luther—R22, R28, R49, R58
D. Patterson—R92
V. Steger–R53

# Report of the Director and Chief Executive Officer

The year 2001 was a year of momentum, self-study, and pride at the Marine Biological Laboratory. Our resident research program took a major step forward with the establishment of an exciting new program in global infectious diseases. We embarked on a strategic planning process and spent much of the fall reviewing current research and educational programs and thinking about how the MBL can best serve science and continue to have a disproportionate impact on the life sciences. And we celebrated when we learned that one of our own had won the 2001 Nobel Prize in Physiology or Medicine for a discovery made in one of the MBL's teaching laboratories.

### *Tim Hunt Wins Nobel Prize for Work Done in MBL Course*

On October 8, 2001, Tim Hunt of Cancer Research UK, Clare Hall Laboratories, was awarded the 2001 Nobel in Physiology or Medicine for a discovery that he made at the Marine Biological Laboratory while teaching in the Physiology course during the summer of 1982. Tim, a member of the MBL Corporation, was recognized for his discovery of cyclins, proteins that figure prominently in the cascade of events that regulate the cell cycle, the process by which cells, including the billions that make up the human body, grow and divide. Tim's exciting discovery at the MBL has helped lay the foundation for subsequent studies on the cell cycle and mitosis, important work that continues at the MBL today.

### *New Resident Research Program Established in Global Infectious Disease*

In 2001, the Marine Biological Laboratory received a grant of nearly $5 million from the Ellison Medical Foundation of Bethesda, Maryland, to establish a new interdisciplinary Program in Molecular Pathogenesis and Global Infectious Diseases. This new program will create a unique international center for research and training dedicated to studying organisms that cause tropical disease and the complex relationships these pathogens have with their hosts. The program will be in the Josephine Bay Paul Center for Comparative Molecular Biology and Evolution at the MBL, and will take advantage of the Center's existing strengths in molecular evolution and comparative genomics.

Stephen L. Hajduk, a leading parasitologist and molecular biologist, will direct the new program. Steve is currently a Professor in the Department of Biochemistry and Molecular Genetics and Senior Scientist in the AIDS Center and the Comprehensive Cancer Center at the University of Alabama at Birmingham. His research program in the molecular and biochemical basis of pathogenesis focuses on African trypanosomes, which cause human sleeping sickness, a fatal disease that has re-emerged as a major health problem in sub-Saharan Africa. Steve's appointment at the MBL will become effective in the summer of 2002, when members of his current laboratory staff will occupy the program's newly renovated space on the third floor of the MBL's Lillie building.

At the MBL, Steve and his colleagues will study the molecular basis of disease mechanisms, the evolution of virulence factors, pathogen diversity, and infectious disease dispersal in the environment. This will be a unique research environment that fosters interactions between scientists who study disease-causing organisms, and experts in molecular biology, phylogenetics, and environmental microbiology.

The MBL has a rich history in studying the basic science of parasitism and infectious disease. Twenty years ago, the laboratory launched the field of molecular parasitology with the establishment of its Biology of Parasitism course, which continuously reinvents itself as it trains new investigators in this ever-expanding field. In addition, tropical health and infectious disease specialists from around the world travel to the MBL annually to attend the Immunoparasitology Meeting and Molecular

Susan Rainey

Parasitology Meeting, held in the spring and fall, respectively.

In addition, the MBL's Josephine Bay Paul Center, directed by Mitchell Sogin, has an active research program with strong ties to infectious disease. Center scientists have contributed many important insights about the evolution of parasitic protists. Recently, they embarked upon the sequence analysis of the *Giardia* genome. *Giardia* is the principal cause of diarrheal disease in children and adults around the world. The availability of the *Giardia* genome will facilitate the development of new techniques for diagnosing and treating giardial infection.

## *Looking Ahead: Developing a Strategic Plan for the MBL*

The satisfactory completion of the Marine Biological Laboratory's Discovery Campaign and the recognition that the Laboratory was in a strong position financially, programmatically, and spiritually created a climate conducive to contemplation. As a result, the Board of Trustees decided in 2001 to begin a review process that would result in the creation of a strategic plan for the Laboratory.

The Board asked John Dowling and me to direct the planning process with the help of outside consultants. Following a competitive review process, a selection committee chose the international firm of McKinsey and Company to assist us. We were impressed with the McKinsey team, specifically their familiarity and commitment to the MBL, and their experience in facilitating strategic planning processes in the for-profit and not-for-profit sectors of the scientific community.

The Board has charged us with assessing both the reputation and the impact of the MBL within the broader scientific community. They asked us to develop a clear vision for how we will maintain and build on our research and educational strengths. This includes our aspirations for areas we will focus on, a description of how we will organize, and a plan to meet our financial requirements.

The broad participation of the MBL community is crucial to the success of this effort. During the first phase of the process, which began in the fall of 2001, we established a 19-person Steering Committee composed of MBL scientists and Trustees. The McKinsey group also interviewed individuals representing the MBL's various constituencies to gather background data on the laboratory and perspectives on MBL strategy today and in the future.

In early November of 2001, the Steering Committee met for the first time. We discussed the preliminary data gathered by the McKinsey team and developed a set of shared beliefs about the MBL's future:

- The MBL is a year-round institution
- The MBL should make a disproportionate contribution to the advancement of the biological sciences
- MBL leadership should actively enhance the collaborative strength of the institution
- External talent should be more proactively recruited
- The MBL should focus on building its external reputation
- The MBL should continue to build the effectiveness of its governing bodies

The Committee also wrote a first draft of an aspiration statement to help guide the laboratory going forward:

*Our aspiration is to be recognized for having a disproportionate impact on the advancement of biological sciences that improve the human condition. The MBL will achieve this impact along two interdependent dimensions:*

1. *Driving fundamental advances in biological sciences through both resident and visiting research. The MBL will target areas where it has (or can reasonably develop) a distinctive position that benefits from the collaborative and cross-disciplinary strengths of the MBL.*
2. *Catalyzing the scientific careers and contributions of the most promising and important scientists in biological sciences by providing a unique opportunity to interact with leading scientists and collaborate across disciplines. The MBL's educational programs, its research programs, and its scientific interactions are all expected to contribute to this mission.*

The Steering Committee then embarked on Phase II of the process, establishing three Task Forces charged with addressing a series of "researchable questions" that were framed during the interviews and the Steering Committee meeting. The first, chaired by John Dowling and George Logan, examined questions associated with "Ensuring distinctiveness and collaboration in resident (year-round) research." The second, chaired by Kerry Bloom and Howard Jacobson, explored "Ensuring excellence in education." And the third, chaired by Joan Ruderman and Vin Ryan, looked at "Attracting the next generation of visiting scientists" to the summer research program.

Since December of 2001, these Task Forces have been busy gathering data, conducting surveys, and meeting regularly to develop a fact base from which they generated a series of recommendations that were presented to, and endorsed by, the Steering Committee at a meeting on April 26, 2002. These recommendations were presented to the Board of Trustees in May. John Dowling and I will host regular meetings during the summer of 2002 in Woods Hole to answer questions and keep the community informed of our progress.

This is a momentous time for the Marine Biological Laboratory. As always, I value your comments as we all work towards preparing the Marine Biological Laboratory for an exciting and prosperous future.

—William T. Speck, M.D.

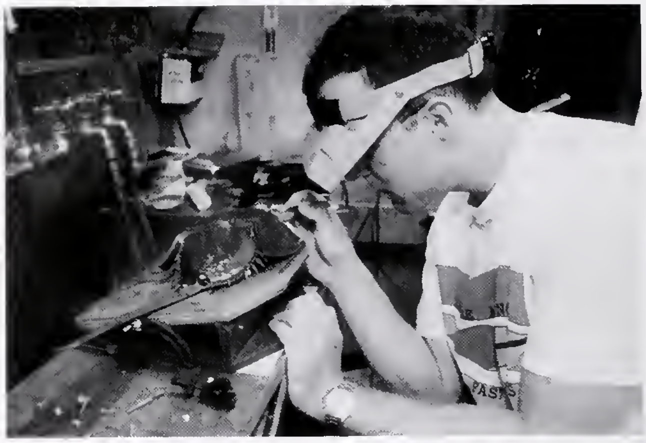

# Research and Education Highlights

## *The Ecosystems Center*

Scientists and staff of The Ecosystems Center, the MBL's largest resident research program, moved their offices and laboratories into the new C. V. Starr Environmental Sciences Building during the summer of 2001. The MBL dedicated the building on August 3, bringing to a close the final chapter of the MBL's very successful Discovery Campaign.

The work of the Center continues at field sites around the globe, including two Long Term Ecological Research sites located at Toolik Lake in Alaska and Plum Island Sound on the Northeast coast of Massachusetts. Research is also being conducted closer to home, on Martha's Vineyard, where Assistant Scientist Chris Neill and his colleagues are attempting to understand more about how development is affecting biological diversity and ecological functioning and what conservation efforts are needed to ensure the survival of remaining natural ecosystems.

## *Marine Resources Center*

Research in the Marine Resources Center over the past year focused on studies of cephalopod behavior and sensory biology, learning and memory in molluscs, understanding and developing treatments for diseases of aquatic animals, and developing tools to aid scientific and commercial aquaculture efforts. An international search also began in 2001 for a director and scientific staff of the Scientific Aquaculture Program.

MBL Veterinarian Roxanna Smolowitz continued her studies of Quahog Parasite Unknown, a devastating parasite that has infected quahogs throughout the Cape and southeastern Massachusetts. In addition to studying four diseases of the Eastern oyster, Smolowitz is also investigating the cause of epizootic shell disease in lobsters on the east coast of the U.S. using traditional histopathology, bacterial culture, and scanning electron microscopy.

Associate Scientist Alan Kuzirian is using DNA fingerprinting techniques to determine whether the genetic distinctiveness of bay scallop (*Argopecten irradians*) populations can be used to determine the effectiveness of seeding programs. He has found that this technology can be used to distinguish feral animals from hatchery stocks, allowing shellfish managers to assess the success and economic viability of their aquaculture efforts. Kuzirian is also studying learning and memory using the nudibranch mollusc, *Hermissenda crassicornis*, as a model. New results show that calexcitin, an important calcium regulator, increases with the acquisition of long-term memory but not with short-term memory. It was also negatively affected by lead, a heavy metal that causes learning deficits. These findings are important in understanding how memory is formed and also how and why it decays with age.

## *BioCurrents Research Center*

Research on calcium and other ion channels continues in the MBL's BioCurrents Research Center (BRC), directed by Peter Smith. One of the MBL's newest resident researchers, Assistant Scientist Stefan McDonough, is focusing his research on understanding the physiology and pharmacology of the voltage-gated calcium channels found in the heart and nervous system. These channels are targets for drugs that treat pain, hypertension, epilepsy, and brain damage after stroke. McDonough's colleague, Orian Shirihai, also an Assistant Scientist in the BRC, studies ion channels as well, particularly the role that potassium and calcium channels play in activating microglia and brain macrophages to release specific neurotoxic substances implicated in Alzheimer's disease.

*Architectural Dynamics in Living Cells Program*

Shinya Inoué continues to lead an exciting program in cell biology and architectural dynamics at the MBL. During the summer of 2001 he hosted the Cell Division Group led by Drs. Ted Salmon and Tim Mitchison. In collaboration with Drs. Makoto Goda and Phong Tran, he discovered the striking fluorescence anisotropy exhibited by crystals of native GFP (green fluorescent protein), provided by Dr. Osamu Shimomura. The group presented early reports of their findings at the Biophysical Society Meeting in Boston, the MBL's General Scientific Meeting, and the MBL Cell Group Seminar. A short report on the work was featured in the October 2001 issue of *The Biological Bulletin*, and a full paper appeared in the spring of 2002 in the *PNAS*.

### *Independent Research*

Resident researchers at the MBL are also addressing a variety of other scientific and medical questions. They are defining how environmental toxins and carcinogens target cells during development and how they alter normal cell function (Carol Reinisch); trying to understand the molecular basis of synaptic plasticity, which also has implications for learning and memory (Ayse Dosemici); studying the synthesis and function of a special amino acid found in blood clotting proteins (Bruce and Barbara Furie); investigating the mechanisms underlying female infertility (David Keefe); and exploring the molecular defense mechanisms exhibited by marine organisms in response to invading bacteria, viruses, and fungi (Norman Wainwright).

### *Osamu Shimomura Retires*

The MBL bid farewell to one of its long-time resident researchers in the fall of 2001. Senior Scientist Osamu Shimomura retired from the MBL after 19 years of conducting top-flight research. Dr. Shimomura's contributions to biology are legendary. He discovered green fluorescent protein and aequorin, biological markers that are now staples in the biologist's toolbox. Since his discovery of aequorin 40 years ago, Shimomura's life's work has been devoted to shedding light on luminescence—a complex chemical reaction within an organism's cells that results in the release of energy in the form of light instead of heat. Shimomura determined years ago that aequorin glows blue when tiny amounts of calcium bind to it.

This discovery led to the use of aequorin as an important biomedical tool for tracking the movement of calcium within cells. Calcium plays a crucial role in the regulation of a variety of biological processes including fertilization, muscle contraction, and the transmission of nerve impulses. Clinicians also recognize that calcium is significant in the pathology of a number of neurological diseases. A symposium celebrating Shimomura's outstanding contributions to science will be held at the MBL on July 27, 2002.

### *Summer/Visiting Research*

During the summer of 2001, we hosted a full complement of scientists from institutions around the world. Of the 112 Principal Investigators working at the MBL last summer, 74% were full professors, 16% were Associate Professors, 6% were Assistant Professors, and 4% were postdocs. These figures include investigators sponsored by the Grass and MBL Research Fellowship Programs.

Studies in the summer research program ranged from axonal transport in squid to cell division and mitosis in clams, from exploring the evolution of chordates to understanding muscle fiber design in the toadfish.

For example, Harvey Fishman, a biophysicist at the University of Texas Medical Branch, spent the summer of 2001 at the MBL studying how individual nerve cells heal naturally, using the squid giant axon as a model. Fishman's research begins to answer questions about why nerve repair is possible and how scientists may eventually augment the process. Fishman studies how to forecast nerve cell survival after a spinal cord injury. He is also expanding his research to look at axon injury, repair, and survival in the neurons of mammals. Understanding these cell membrane repair processes may help lead to therapeutics that will prevent nerve cell damage or death. This, along with an understanding of how vesicles form and aid in cell repair, may eventually help doctors treat spinal cord injuries and diseases that destroy the nervous system.

Larry Cohen of Yale University spent his summer examining how animals, including humans, recognize scents. Hundreds of scents—a freshly baked cookie or a rotten egg, for example—are immediately recognizable, but scientists have no clear idea of how we identify and remember these smells. Cohen studies the activity of the olfactory bulb, the first way station in the olfactory system that provides us with our sense of smell. An organism smells something when odor molecules attach to receptor proteins on the ends of neurons in the nose. The binding causes the neuron to send an impulse to the olfactory bulb. Cohen uses special dyes that change colors in response to nerve impulses and a fast camera to record an organism's reaction to different scents. The resulting pictures of the activity of the neurons in the olfactory lobe show that for every odor there is a particular pattern of receptor cells and neurons sending impulses to the olfactory bulb.

Diane Heck of Rutgers University spent her days in Woods Hole watching sea urchins develop from clear spherical eggs to adulthood. She studies how estrogens influence sea urchin development to determine whether these common environmental contaminates harm the urchins and, ultimately, humans. The development of the sea urchin is well known, so aberrations can be easily identified under the microscope. Heck exposes healthy sea urchin eggs to various estrogenic compounds at different developmental stages and then watches them grow. Because the estrogen effects are limited to early development, Heck hypothesizes that estrogen disrupts the function of a family of proteins that control these developmental stages: fibroblast growth factors. The next step in her research is to isolate which growth factors are altered by estrogen. Fibroblast growth factors control both early development and cell repair. Mistakes in the system cause not only developmental defects but also unregulated cellular repair, or cancer. Heck hopes that by pinpointing the pathways disrupted by estrogens during sea urchin development, she can begin to understand how these environmental pollutants cause cancer in humans.

### *Education*

The MBL's Education Program welcomed 435 students and 598 faculty to the MBL's 6 summer and 13 special topics courses in 2001. According to tradition, the leadership of all MBL courses must rotate every five years to ensure that the courses we teach are always fresh and up-to-date. The year 2001 was the final year of teaching for a number of course directors, including Ed Pearce of the Biology of Parasitism course; Marianne Bronner-Fraser and Scott Fraser of the Embryology course; John Dowling of the Neural Development and Genetics of Zebrafish course; and Jerry Schatten, Kelly Mayo, and Joan Hunt of the Frontiers in Reproduction course. They will be replaced in 2002 by Asgerally Fazleabas, Patricia Hunt, and Theresa Woodruff in Frontiers in Reproduction; Cecilia Moens in Neural Development and Genetics of Zebrafish; Richard Harland and Joel Rothman in Embryology; and Elisabetta Ullu in Biology of Parasitism. We thank all retiring course directors for their tireless efforts on behalf of the MBL and our students, and welcome our incoming course directors and wish them all the best.

The MBL's Semester in Environmental Science Program for undergraduates hosted its fourth class of students during the fall of 2001. Thirteen students from a variety of small colleges and universities participated in the program, which is taught by faculty from the MBL's Ecosystems Center.

# Report of the Treasurer

The financial results for the year 2001 were mixed. Operating results and investment portfolio results were disappointing. On the other hand, our diversified portfolio enabled us to perform better than the market. Also philanthropic support was strong last year, and we were able to make significant improvements to the Laboratory's physical plant, including the completion of the new C.V. Starr Environmental Sciences building.

The Unrestricted Operating results showed a 4.7% decline in revenues while expenses grew by 10.1%. As a consequence, the Laboratory reported a $3 million operating loss. All revenue categories showed a decline except for Unrestricted Contributions, which were up 3.6% and Government Grants, which grew a modest 4.3%, compared to double-digit growth in the previous three years. Net Assets Released from Restrictions had the greatest decline (35%), resulting in part from the correction of a premature release of restricted funds. Also Investment Income declined 11.7% and Rental Income declined 10.3% due to a reduction in the space used by the Boston University Marine Program. Another cause of the overall decline was due to September 11th when the Laboratory lost over $250 thousand in revenues as a result of cancelled fall Conferences.

On the expense side, increases in Equipment purchases (51%), Utilities (26%), Professional Services (22%), and Subcontracts (13%) were the major contributors to the growth. Salaries and Fringe Benefits grew a modest 4.3%, but even that was overstated due to an accounting adjustment to the Fringe that added $290 thousand in adjustments to 2001 results. Our accrual for Depreciation rose $250 thousand as a result of the plant improvements. We also funded less Depreciation from operations due to the slowing in indirect recoveries from research grants and because of a one-half percent reduction in the annual draw from our Long-Term Investments.

In our Non-Operating Activities, Contributions to Plant remained strong and when combined with the Bond proceeds enabled us to make over $10 million in building and equipment improvements to the Laboratory in 2001. On the other hand, MBL experienced $2.9 million, or 5.9%, in realized and unrealized investment losses as a result of the decline in the Equity Markets. Total Contributions, which exceeded $13.3 million for this year after the close of the Discovery Campaign, enabled the MBL to report the seventh year of a positive Change in Net Assets of $2.1 million.

MBL's Balance Sheet Assets continue to grow, rising $3 million in 2001. Improved cash management is demonstrated by the two-fold increase in Short-Term Investments and reduced Cash. The increase in Plant Assets, Net reflects over $15 million in improvements since the Bond offering in March 2000. The $3.6 million growth in Permanently Restricted Net Assets reflects our growing endowment.

Looking at some financial performance ratios, our Return on Average Net Assets was a fairly weak 2.8%. Our Leverage Ratio (Unrestricted & Temporarily Restricted Net Assets/Debt) remains sound at 5.12× at year-end 2001. Both our Debt Service Coverage (3.24×) for 2001 and our Cash & Investments of $23.1 million as of March 31, 2002 are well in excess of the financial covenants of the Letter of Credit supporting the Bond issue.

In summary, although disappointing, more than half of the operating loss reported in 2001 was due to exceptional, non-recurring items. On a positive note, we continued to receive strong support from the private sector and were able to put significant resources into improving our physical plant. Although it was a challenging year, the Marine Biological Laboratory remains financially sound.

—Mary B. Conrad

PRICEWATERHOUSECOOPERS

PricewaterhouseCoopers LLP
One International Place
Boston MA 02110
Telephone (617) 478 5000
Facsimile (617) 478 3900

## REPORT OF INDEPENDENT ACCOUNTANTS

To the Board of Trustees of
Marine Biological Laboratory:

In our opinion, the accompanying balance sheet of the Marine Biological Laboratory (the "Laboratory") at December 31, 2001 and the related statements of activities and of cash flows for the year then ended present fairly, in all material respects, the financial position of the Laboratory at December 31, 2001, and the changes in its net assets and its cash flows for the year then ended in conformity with accounting principles generally accepted in the United States of America. These financial statements are the responsibility of the Laboratory's management; our responsibility is to express an opinion on these financial statements based on our audit. The prior year summarized comparative information has been derived from the Laboratory's 2000 financial statements, and in our report dated April 6, 2001, we expressed an unqualified opinion on those financial statements. We conducted our audit of these statements in accordance with auditing standards generally accepted in the United States of America, which require that we plan and perform the audit to obtain reasonable assurance about whether the financial statements are free of material misstatement. An audit includes examining, on a test basis, evidence supporting the amounts and disclosures in the financial statements, assessing the accounting principles used and significant estimates made by management, and evaluating the overall financial statement presentation. We believe that our audit provides a reasonable basis for our opinion.

Our audit was conducted for the purpose of forming an opinion on the basic financial statements taken as a whole. The supplemental schedule of functional expenses as of December 31, 2001 is presented for the purpose of additional analysis and is not a required part of the basic financial statements. Such information has been subjected to the auditing procedures applied in the audit of the basic financial statements and, in our opinion, is fairly stated, in all material respects, in relation to the basic financial statements taken as a whole.

April 1, 2002

# MARINE BIOLOGICAL LABORATORY

## BALANCE SHEET

### As of December 31, 2001 and 2000

| **ASSETS** | **2001** | **2000** |
|---|---|---|
| Cash and cash equivalents | $ 315,132 | $ 3,583,033 |
| Short-term investments, at market | 8,677,416 | 3,599,833 |
| Accounts receivable, net of allowance for doubtful accounts of $47,541 in 2001 and $47,222 in 2000 | 817,749 | 1,109,706 |
| Current portion of pledges receivable | 3,249,823 | 5,026,750 |
| Receivables due for costs incurred on grants and contracts | 2,520,421 | 2,036,734 |
| Other current assets | 512,115 | 352,983 |
| Total current assets | 16,092,656 | 15,709,039 |
| Assets held by bond trustee | 268,743 | 5,423,615 |
| Long-term investments, at market | 42,180,828 | 44,494,649 |
| Pledges receivable, net of current portion | 3,956,301 | 2,230,344 |
| Charitable remainder trusts | 414,147 | 202,948 |
| Plant assets, net | 31,519,247 | 23,423,156 |
| Other assets | 199,287 | 206,280 |
| Total long-term assets | 78,538,553 | 75,980,992 |
| Total assets | $94,631,209 | $91,690,031 |
| **LIABILITIES AND NET ASSETS** | | |
| Accounts payable and accrued expenses | $ 2,825,799 | $ 2,073,375 |
| Deferred income | 1,044,500 | 1,016,060 |
| Total current liabilities | 3,870,299 | 3,089,435 |
| Annuities and unitrusts payable | 1,383,241 | 1,393,735 |
| Long-term debt | 10,200,000 | 10,200,000 |
| Advances on contracts | 1,273,095 | 1,230,743 |
| Total long-term liabilities | 12,856,336 | 12,824,478 |
| Total liabilities | 16,726,635 | 15,913,913 |
| Commitments and contingencies | | |
| Net assets: | | |
| Unrestricted | 22,261,451 | 22,903,287 |
| Temporarily restricted | 29,940,986 | 30,752,413 |
| Permanently restricted | 25,702,137 | 22,120,418 |
| Total net assets | 77,904,574 | 75,776,118 |
| Total liabilities and net assets | $94,631,209 | $91,690,031 |

*The accompanying notes are an integral part of the financial statements.*

# MARINE BIOLOGICAL LABORATORY

## STATEMENT OF ACTIVITIES

For the Year Ended December 31, 2001

(With Comparative Totals for the Year Ended December 31, 2000)

---

| | Unrestricted | Temporarily Restricted | Permanently Restricted | 2001 | 2000 |
|---|---|---|---|---|---|
| Operating support and revenues: | | | | | |
| Government grants | $14,648,426 | $ — | $ — | $14,648,426 | $14,048,464 |
| Private contracts | 1,675,293 | — | — | 1,675,293 | 1,697,062 |
| Laboratory rental income | 1,434,419 | — | — | 1,434,419 | 1,598,373 |
| Tuition, net | 519,135 | — | — | 519,135 | 543,305 |
| Fees for conferences and services | 4,382,525 | — | — | 4,382,525 | 4,407,311 |
| Contributions | 1,754,793 | 5,149,660 | 3,981,059 | 10,885,512 | 5,949,444 |
| Investment income | 1,533,757 | 788,095 | — | 2,321,852 | 2,330,716 |
| Miscellaneous revenue | 277,077 | — | — | 277,077 | 468,482 |
| Present value adjustment to annuities | — | (43,541) | — | (43,541) | 55,176 |
| Net assets released from restrictions | 2,678,816 | (2,719,162) | 40,346 | — | — |
| Total operating support and revenues | 28,904,241 | 3,175,052 | 4,021,405 | 36,100,698 | 31,098,333 |
| Expenses: | | | | | |
| Research | 20,465,308 | — | — | 20,465,308 | 17,799,627 |
| Instruction | 5,650,893 | — | — | 5,650,893 | 5,626,223 |
| Conferences and services | 1,133,390 | — | — | 1,133,390 | 1,307,458 |
| Other programs (Note 2) | 4,674,499 | — | — | 4,674,499 | 4,261,327 |
| Total expenses | 31,924,090 | — | — | 31,924,090 | 28,994,635 |
| Change in net assets before nonoperating activity | (3,019,849) | 3,175,052 | 4,021,405 | 4,176,608 | 2,103,698 |
| Nonoperating revenue (expense): | | | | | |
| Change in value of interest rate swap | (120,000) | — | — | (120,000) | — |
| Contributions to Plant: | | | | | |
| Private | 1,485,215 | 992,026 | — | 2,477,241 | 4,638,615 |
| Released from restrictions | 1,376,486 | (1,376,486) | — | — | — |
| Contributions invested in Plant | 2,861,701 | (384,460) | — | 2,477,241 | 4,638,615 |
| Investment Income and Gains/Losses: | | | | | |
| Total investment income and gains/losses | (296,451) | (2,194,013) | (439,686) | (2,930,150) | (2,139,838) |
| Less: investment earnings used for operations | (67,237) | (1,408,006) | — | (1,475,243) | (1,415,871) |
| Investment income and gains/losses | (363,688) | (3,602,019) | (439,686) | (4,405,393) | (3,555,709) |
| Total change in net assets | (641,836) | (811,427) | 3,581,719 | 2,128,456 | 3,186,604 |
| Net assets, beginning of year | 22,903,287 | 30,752,413 | 22,120,418 | 75,776,118 | 72,589,514 |
| Net assets, end of year | $22,261,451 | $29,940,986 | $25,702,137 | $77,904,574 | $75,776,118 |

*The accompanying notes are an integral part of the financial statements.*

# MARINE BIOLOGICAL LABORATORY

## STATEMENT OF CASH FLOWS

### For the Year Ended December 31, 2001

### (With Comparative Totals for the Year Ended December 31, 2000)

| | **2001** | **2000** |
|---|---|---|
| Cash flows from operating activities: | | |
| Change in net assets | $ 2,128,456 | $ 3,186,604 |
| Adjustments to reconcile change in net assets to net cash provided by (used in) operating activities: | | |
| Depreciation | 1,943,381 | 1,791,975 |
| Unrealized depreciation on investments | 1,961,505 | 6,700,396 |
| Realized (gain) loss on investments | 1,924,025 | (3,886,669) |
| Present value adjustment to annuities and unitrusts payable | 43,541 | (55,176) |
| Contributions restricted for long-term investment and annuities | (4,973,085) | (2,033,528) |
| Provision for bad debt | 319 | — |
| Provision for uncollectible pledges | (15,000) | 423,982 |
| Unrealized appreciation in charitable remainder trusts | (211,199) | |
| Change in certain balance sheet accounts: | | |
| Accounts receivable | 291,638 | 48,367 |
| Pledges receivable | 65,970 | (410,852) |
| Grants and contracts receivable | (483,687) | (655,968) |
| Other current assets and other assets | (152,139) | (252,745) |
| Accounts payable and accrued expenses | 752,424 | 115,867 |
| Deferred income | 28,440 | 359,315 |
| Annuities and unitrusts payable | (56,002) | (73,167) |
| Advances on contracts | 42,352 | (344,015) |
| Net cash provided by operating activities | 3,290,939 | 4,914,386 |
| Cash flows from investing activities: | | |
| Purchase of property and equipment | (10,039,472) | (5,096,406) |
| Proceeds from sale of investments | 39,553,943 | 68,837,634 |
| Purchase of investments | (41,048,363) | (76,930,252) |
| Net cash used in investing activities | (11,533,892) | (13,189,024) |
| Cash flows from financing activities: | | |
| Payments on annuities and unitrusts payable | (96,891) | (96,316) |
| Receipt of permanently restricted gifts | 4,973,085 | 2,033,528 |
| Annuity and unitrusts donations received | 98,858 | 102,270 |
| Proceeds from issuance of bonds | — | 10,200,000 |
| Payments on long-term debt | — | (2,324,096) |
| Net cash provided by financing activities | 4,975,052 | 9,915,386 |
| Net (decrease) increase in cash and cash equivalents | (3,267,901) | 1,640,748 |
| Cash and cash equivalents at beginning of year | 3,583,033 | 1,942,285 |
| Cash and cash equivalents at end of year | $ 315,132 | $ 3,583,033 |

*The accompanying notes are an integral part of the financial statements.*

# *Marine Biological Laboratory*

## *Notes to Financial Statements*

1. *Background*

The Marine Biological Laboratory (the "Laboratory") is a private, independent not-for-profit research and educational institution dedicated to establishing and maintaining a laboratory and station for scientific study and investigation, and a school for instruction in biology and natural history. The Laboratory was founded in 1888 and is located in Woods Hole, Massachusetts.

2. *Significant Accounting Policies*

*Basis of Presentation*

The accompanying financial statements have been prepared on the accrual basis of accounting and in accordance with the principles outlined in the American Institute of Certified Public Accountants' Audit Guide, "Not-For-Profit Organizations." The financial statements include certain prior-year summarized comparative information in total but not by net asset class. Such information does not include sufficient detail to constitute a presentation in conformity with generally accepted accounting principles. Accordingly, such information should be read in conjunction with the Laboratory's financial statements for the year ended December 31, 2000, from which the summarized information was derived.

The Laboratory classifies net assets, revenues, and realized and unrealized gains and losses based on the existence or absence of donor-imposed restrictions and legal restrictions imposed under Massachusetts State law. Accordingly, net assets and changes therein are classified as follows:

*Unrestricted*

Unrestricted net assets are not subject to donor-imposed restrictions of a more specific nature than the furtherance of the Laboratory's mission. Revenues from sources other than contributions are generally reported as increases in unrestricted net assets. Expenses are reported as decreases in unrestricted net assets. Gains and losses on investments and other assets or liabilities are reported as increases or decreases in unrestricted net assets unless their use is restricted by explicit donor stipulations or law. Expirations of temporary restrictions on net assets, that is, the donor-imposed stipulated purpose has been accomplished and/or the stipulated time period has elapsed, are reported as reclassifications between the applicable classes of net assets and titled "Net assets released from restrictions."

*Temporarily Restricted*

Temporarily restricted net assets are subject to legal or donor-imposed stipulations that will be satisfied either by the actions of the Laboratory, the passage of time, or both. These assets include contributions for which the specific, donor-imposed restrictions have not been met and pledges, annuities, and unitrusts for which the ultimate purpose of the proceeds is not permanently restricted. As the restrictions are met, the assets are released to unrestricted net assets. Also, realized/unrealized gains/losses associated with permanently restricted gifts which are not required to be added to principal by the donor are classified as temporarily restricted and maintain the donor requirements for expenditure.

*Permanently Restricted*

Permanently restricted net assets are subject to donor-imposed stipulations that they be invested to provide a permanent source of income to the Laboratory. These assets include contributions, pledges and trusts which require that the corpus be invested in perpetuity and only the income be made available for program operations in accordance with donor restrictions.

*Performance Indicator*

Nonoperating revenues include realized and unrealized gains on investments during the year as well as investment income on the master pooled investments and revenues that are specifically for the acquisition or construction of plant assets. Investment income from short-term investments and investments held in trust by others are included in operating support and revenues. To the extent that nonoperating investment income and gains are used for operations as determined by the Laboratory's total return utilization policy (see below), they are reclassified from nonoperating as "Investment earnings used for operations" to operating as "Investment income" on the statement of activities. All other activity is classified as operating revenue.

*Cash and Cash Equivalents*

Cash equivalents consist of resources invested in overnight repurchase agreements and other highly liquid investments with original maturities of three months or less.

Financial instruments which potentially subject the Laboratory to concentrations of risk consist primarily of cash and investments. The Laboratory maintains cash accounts with one banking institution.

*Investments*

Investments are carried at market value. The cost basis of donated investments is recorded as fair market value at the date of the gift. For closely held non-publicly traded investments, management determines the fair value based upon the most recent information available from the limited partnership. For determination of gain or loss upon disposal of investments, cost is determined based on the first-in, first-out method. Investments with an original maturity of three months to one year, or those that are available for operations within the next fiscal year, are classified as short-term. All other investments are considered long-term. Investments are maintained primarily with three institutions.

In 1924, the Laboratory became the beneficiary of certain investments, included in permanently restricted net assets, which are held in trust by others. The Laboratory has the continuing rights to the income produced by these funds in perpetuity, subject to the contractual restrictions on the use of such funds. Accordingly, the trust has established a process to conduct a review every ten years by an independent committee to ensure the Laboratory continues to perform valuable services in biological research in accordance with the restrictions placed on the funds by the agreement. The committee met in 1994 and determined that the Laboratory has continued to meet the contractual requirements. The market values of such investments are $7,458,425 and $7,904,545 at December 31, 2001 and 2000, respectively. The dividend and interest income on these investments, included in unrestricted support and revenues, totaled $293,494 and $201,407 in 2001 and 2000, respectively.

*Investment Income and Distribution*

For the master pooled investments, the Laboratory employs a total return utilization policy that establishes the amount of the investment return made available for spending each year. The Finance Committee of the Board of Trustees has approved a spending policy that the withdrawal will be based on a percentage of the 12 quarter average ending market values of the funds. The market value includes the principal plus reinvested income, realized and unrealized gains and losses. Spending rates in excess of 5%, but not exceeding 7%, can be utilized if approved in advance by the Finance Committee of the Board of Trustees. For fiscal 2001 and 2000, the Laboratory obtained approval to expend 5.5% and 6%, respectively, of the latest 12 quarter average ending market values of the long-term investments.

The net appreciation on permanently and temporarily restricted net assets is reported together with temporarily restricted net assets until such time as all or a portion of the appreciation is distributed for spending in accordance with the total return utilization policy and applicable state law.

Investment income on the pooled investment account is allocated to the participating funds using the market value unit method (Note 4).

*Assets Held by Bond Trustee*

Assets held by bond trustee relate to assets held by an outside trustee under the March 1, 2000 loan and trust agreement. Per the prospectus, these funds may be used solely for capital projects as determined by the Laboratory's Board of Directors. At December 31, 2001 and 2000, these assets were invested in a qualified GIC under a funding agreement with an insurance company.

*Plant Assets*

Buildings and equipment are recorded at cost. Donated facility assets are recorded at fair market value at the date of the gift. Depreciation is computed using the straight-line method over the asset's estimated useful life. Estimated useful lives are generally three to five years for equipment and 20 to 40 years for buildings and improvements. Depreciation is not recorded for those assets classified as construction-in-process as they have not yet been placed into service. Depreciation expense for the years ended December 31, 2001 and 2000 amounted to $1,943,381 and $1,791,975, respectively, and has been recorded in the statement of activities in the appropriate functionalized categories. When assets are sold or retired, the cost and accumulated depreciation are removed from the accounts and any resulting gain or loss is included in unrestricted income for the period.

*Annuities and Unitrusts Payable*

Amounts due to donors in connection with gift annuities and unitrusts are determined based on remainder value calculations, with varied assumptions of rates of return and payout terms.

*Deferred Income*

Deferred income includes prepayments received on Laboratory publications and funding received for grants and contracts before it is earned.

*Advances on Contracts*

Advances on contracts represents funds held by the Laboratory for the benefit of research projects conducted by certain scientists associated with the Laboratory. The funds are invested in the master pooled account until they are expended.

*Revenue Recognition*

Sources of revenue include grant payments from governmental agencies, contracts from private organizations, and income from the rental of laboratories and classrooms for research and educational programs. The Laboratory recognizes revenue associated with grants and contracts at the time the related direct costs are incurred or expended. Recovery of related indirect costs is recorded at predetermined fixed rates negotiated with the government. Revenue related to conferences and services is recognized at the time the service is provided, while tuition revenue is recognized as classes are offered. The tuition income is net of student financial aid of $507,263 and $579,790 in 2001 and 2000, respectively. Fees for conferences and other services include the following activities: housing, dining, library, scientific journals, aquatic resources and research services.

*Contributions*

Contribution revenue includes gifts and pledges. Gifts are recognized as revenue upon receipt. Pledges are recognized as temporarily or permanently restricted revenue in the year pledged and are recorded at the present value of expected future cash flows, net of allowance. Gifts and pledges, other than cash, are recorded at fair market value at the date of contribution.

*Expenses*

Expenses are recognized when incurred and charged to the functions to which they are directly related. Expenses that relate to more than one function are allocated among functions based upon either modified total direct cost or square footage allocations.

Other programs expense consists primarily of fundraising, year-round labs and library room rentals, costs associated with aquatic resource sales and scientific journals. Total fund-raising expense for 2001 and 2000 is $1,164,151 and $1,156,656, respectively.

*Use of Estimates*

The preparation of financial statements in conformity with generally accepted accounting principles requires management to make estimates and assumptions that affect the reported amounts of assets and liabilities and disclosure of contingent assets and liabilities at the date of financial statements and the reported amounts of revenues and expenses during the reporting period. Actual results could differ from those estimates.

*Tax-Exempt Status*

The Laboratory is exempt from federal income tax under Section 501(c)(3) of the Internal Revenue Code.

*Reclassification*

Certain prior year balances have been reclassified to conform with the current year presentation.

### 3. *Investments*

The following is a summary of the cost and market value of all investments at December 31, 2001 and 2000:

| | *Market* | | *Cost* | |
|---|---|---|---|---|
| | *2001* | *2000* | *2001* | *2000* |
| Certificates of deposit | $ 40,000 | $ 40,000 | $ 40,000 | $ 40,000 |
| Money market securities | 1,744,599 | 764,969 | 1,745,024 | 764,969 |
| U.S. Government securities | 3,907,574 | 2,300,738 | 3,815,421 | 2,165,197 |
| Corporate fixed income | 2,691,557 | 2,412,548 | 2,918,577 | 2,537,913 |
| Common stocks | 10,386,280 | 16,144,089 | 11,352,220 | 16,318,538 |
| Mutual funds | 23,707,865 | 19,909,549 | 24,204,730 | 19,306,250 |
| Limited partnerships | 8,380,369 | 6,522,589 | 7,248,480 | 5,324,442 |
| Total investments | $50,858,244 | $48,094,482 | $51,324,452 | $46,457,309 |

Investments portfolios for the years ended December 31, 2001 and 2000 are as follows:

| | *Market* | | *Cost* | |
|---|---|---|---|---|
| | *2001* | *2000* | *2001* | *2000* |
| *Short-Term Investments* | | | | |
| Certificates of deposit | $ 40,000 | $ 40,000 | $ 40,000 | $ 40,000 |
| Money market | 1,385,126 | 377,654 | 1,385,126 | 377,654 |
| Mutual funds | 7,247,744 | 3,102,515 | 7,255,408 | 3,085,445 |
| Common stocks in transit | 4,546 | 79,664 | 4,546 | 79,664 |
| Total short-term | 8,677,416 | 3,599,833 | 8,685,080 | 3,582,763 |
| *Long-Term Investments* | | | | |
| Pooled investments: | | | | |
| Master pooled investments | 32,348,774 | 34,116,704 | 32,874,382 | 33,153,390 |
| Separately invested: | | | | |
| General Friendship Trust | 5,851,051 | 6,204,107 | 5,607,858 | 5,654,623 |
| Library Friendship Trust | 1,607,374 | 1,700,438 | 1,534,760 | 1,543,691 |
| Annuity and unitrusts investments | 2,373,629 | 2,473,400 | 2,622,372 | 2,522,842 |
| Total long-term | 42,180,828 | 44,494,649 | 42,639,372 | 42,874,546 |
| Total investments | $50,858,244 | $48,094,482 | $51,324,452 | $46,457,309 |

For the years ended December 31, 2001 and 2000, the Laboratory recorded net realized (losses) gains of ($1,924,025) and $3,886,669 and net unrealized (losses) gains of ($1,961,505) and ($6,700,396), respectively. Dividend and interest income totaled $1,820,312 and $1,588,734, for the years ended December 31, 2001 and 2000, respectively.

## 4. *Accounting for Pooled Investments*

Certain net assets are pooled for investment purposes. Investment income from the pooled investment account is allocated on the market value unit basis, and each fund subscribes to or disposes of units on the basis of the market value per unit at the beginning of the calendar quarter within which the transaction takes place. The unit participation of the funds at December 31, 2001 and 2000 is as follows:

| | *2001* | *2000* |
|---|---|---|
| Unrestricted | 10,386 | 11,290 |
| Temporarily restricted | 37,936 | 40,042 |
| Permanently restricted | 79,716 | 73,724 |
| Advances on contracts | 5,214 | 5,396 |
| | 133,252 | 130,452 |

Pooled investment activity on a per-unit basis was as follows:

| | *2001* | *2000* |
|---|---|---|
| Unit value at beginning of year | $261.53 | $283.37 |
| Unit value at end of year | 242.76 | 261.53 |
| Total return on pooled investments | $ (18.77) | $ (21.84) |

## 5. *Long-Term Debt*

Long-term debt consisted of the following at December 31:

| | *2001* | *2000* |
|---|---|---|
| Variable rate (1.45% as of December 31, 2001) Massachusetts Development Finance Agency Bonds payable in annual installments from 2006 through 2030 | $10,200,000 | $10,200,000 |

The aggregate amount of principal due on long-term debt for each of the next five years ending December 31, and thereafter is as follows:

| | |
|---|---|
| 2002–2005 | $ — |
| 2006 | 215,000 |
| Thereafter | 9,985,000 |
| | $10,200,000 |

In March 2000, the Massachusetts Development Finance Agency issued on behalf of the Laboratory a series of Variable Rate Revenue Bonds (the "Bonds") in the amount of $10,200,000. The initial interest rate on the issue was 3.65% and is reset weekly. The bonds are scheduled to mature on February 1, 2030. The proceeds of these bonds were used to finance the capital improvements of the Laboratory's educational, research and administrative facilities, specifically the construction and equipping of the Environmental Sciences building. A portion of the proceeds were also used to extinguish all of the Laboratory's prior debt obligations.

During 2001, the Laboratory entered into an interest rate swap agreement with a commercial bank. Under the terms of this agreement, the Laboratory effectively changed its interest rate exposure on the nominal amount of $10,200,000 from a variable rate to a fixed rate of 3.9%. The agreement expires in 2006.

As collateral for the bonds, the Laboratory has entered into a Letter of Credit Reimbursement Agreement which is set to expire on March 15, 2007. The Letter of Credit is in an amount sufficient to pay the aggregate principal amount of the bonds and up to 46 days' interest.

The Laboratory is required to make interest payments only for the first five years. The first principal payment is due February 1, 2006 with incremental increases through maturity.

The agreements related to these bonds subject the Laboratory to certain covenants and restrictions. Under the most restrictive covenant of this debt, the Laboratory is required to maintain a minimum debt service coverage ratio of 1.20.

The Laboratory has an unsecured line of credit agreement with a commercial bank from which it may draw up to $1,000,000. The line of credit has an interest rate of prime plus ½ percent. The line expired February 15, 2002. No amounts were outstanding under this agreement at December 31, 2001 and 2000.

### 6. *Plant Assets*

Plant assets consist of the following at December 31:

| | *2001* | *2000* |
|---|---|---|
| Land | $ 753,708 | $ 702,908 |
| Buildings | 47,145,199 | 35,236,087 |
| Equipment | 5,463,003 | 5,059,022 |
| Construction in process | 2,357,208 | 4,681,629 |
| Total | 55,719,118 | 45,679,646 |
| Less: Accumulated depreciation | (24,199,871) | (22,256,490) |
| Plant assets, net | $31,519,247 | $23,423,156 |

### 7. *Retirement Plan*

The Laboratory participates in the defined contribution pension plan of TIAA-CREF (the "Plan"). The Plan is available to permanent employees who have completed two years of service. Under the Plan, the Laboratory contributes 10% of total compensation for each participant. Contributions amounted to $898,698 and $862,850 for the years ended December 31, 2001 and 2000, respectively.

### 8. *Pledges*

Unconditional promises to give are included in the financial statements as pledges receivable and the related revenue is recorded in the appropriate net asset category. Unconditional promises to give are expected to be realized in the following periods:

| | *2001* | *2000* |
|---|---|---|
| In one year or less | $3,249,823 | $5,026,750 |
| Between one year and five years | 4,644,381 | 2,818,804 |
| After five years | 80,000 | — |
| Total | 7,974,204 | 7,845,554 |
| Less: discount of $363,080 in 2001 and $168,460 in 2000 and allowance of $405,000 in 2001 and $420,000 in 2000 | (768,080) | (588,460) |
| | $7,206,124 | $7,257,094 |

### 9. *Postretirement Benefits*

The Laboratory accounts for its postretirement benefits under Statement No. 106, "Employers' Accounting for Postretirement Benefits Other than Pensions," which requires employers to accrue, during the years that the employee renders the necessary service, the expected cost of benefits to be provided during retirement. As permitted, the Laboratory has elected to amortize the transition obligation over 20 years commencing on January 1, 1994.

The Laboratory's policy is that all current retirees and certain eligible employees who retired prior to June 1, 1994 will continue to receive postretirement health benefits. The remaining current employees will receive benefits; however, those benefits will be limited as defined by the Plan.

Employees hired on or after January 1, 1995 will not be eligible to participate in the postretirement medical benefit plan.

| | 2001 | 2000 |
|---|---|---|
| Change in benefit obligation | | |
| Postretirement benefit obligation at beginning of year | $1,991,669 | $2,043,659 |
| Service cost | 22,594 | 23,020 |
| Interest cost | 150,209 | 149,574 |
| Actuarial loss (gain) | 83,114 | (87,740) |
| Benefits paid | (153,711) | (136,844) |
| Postretirement benefit obligation at end of year | 2,093,875 | 1,991,669 |
| Change in plan assets | | |
| Fair value of plan assets at beginning of year | 1,038,546 | 936,149 |
| Employer contribution | 175,237 | 182,776 |
| Actual return on plan assets | 41,589 | 56,465 |
| Benefits paid | (153,711) | (136,844) |
| Fair value of plan assets at end of year | 1,101,661 | 1,038,546 |
| Funded status | (992,214) | (953,123) |
| Unrecognized actuarial gain | (60,615) | (185,377) |
| Unrecognized net transition obligation | 1,041,869 | 1,128,691 |
| Accrued postretirement benefit cost | (10,960) | (9,809) |
| Less estimated amount payable within one year and classified as a current liability | — | — |
| Accrued postretirement benefit cost, net of current portion | $ (10,960) | $ (9,809) |
| Weighted-average assumptions as of December 31 | | |
| Discount rate | 7.50% | 7.50% |
| Expected long-term rate of return on plan assets | 7.25% | 7.25% |

For purposes of measuring the benefit obligation, a 7.5% annual rate of increase in the per capita cost of covered health benefits was assumed for 2001. The rate was assumed to decrease gradually to 5% in 2006 and remain at that level thereafter.

| | 2001 | 2000 |
|---|---|---|
| Components of net periodic benefit cost | | |
| Service cost | $ 22,594 | $ 23,020 |
| Interest cost | 150,209 | 149,574 |
| Expected return on assets | (76,469) | (69,524) |
| Amortization of net obligation at transition | 86,822 | 86,822 |
| Recognized net actuarial loss | (6,768) | (14,655) |
| Net periodic benefit cost | $176,388 | $ 175,237 |
| Impact of 1% increase in health care cost trend: | | |
| on interest cost plus service cost during past year | $ 12,913 | $ 14,271 |
| on accumulated postretirement benefit obligation | 163,035 | 41,263 |
| Impact of 1% decrease in health care cost trend: | | |
| on interest cost plus service cost during past year | (10,877) | (11,946) |
| on accumulated postretirement benefit obligation | (140,601) | (233,324) |

Pension plan assets consist of investments in a money market fund.

10. *Subsequent Events*

The Laboratory is the beneficiary of two trusts, the General Friendship Trust and the Library Friendship Trust, that were established to support the Laboratory's mission. The trusts name a bank as trustee and custodian. On December 17, 2001, at the request of the trusts' grantor, Friendship Trust, Inc. and the Laboratory, the Bank resigned as Trustee and custodian. The grantor assumed the role of Trustee as of that date and delegated its investment responsibilities to the Laboratory. As a result of the transfer of trusteeship, the Bank commenced transferring the trust funds to the Laboratory's investment custodian on January 3, 2002.

On February 15, 2002, the Laboratory established a $2.1 million committed line of credit with a bank. The line of credit matures one year from the date of issuance and has a borrowing rate equal to the lessor of 1) a variable rate of interest equal to the Prime Rate or 2) a rate equal to LIBOR plus 0.75% per annum fixed against the prevailing LIBOR rate for the interest period selected. The interest period may be a one-, two-, three- or six-month period at the discretion of the Laboratory. In addition, the agreement provides that the Laboratory is required to pay a service fee equal to ¼ % of the total letter of credit. As collateral for this credit facility, the Laboratory pledged $3 million in securities.

# MARINE BIOLOGICAL LABORATORY

## SUPPLEMENTAL SCHEDULE OF FUNCTIONAL EXPENSES

For the Year Ended December 31, 2001

(With comparative Totals for the Year Ended December 31, 2000)

| | *Research* | *Instruction* | *Conferences* | *Other* | *Facilities Maintenance* | *Administration* | *Library Services* | *Research Services* | *Aquatic Research Services* | *2001 Total* | *2000 Total* |
|---|---|---|---|---|---|---|---|---|---|---|---|
| Salaries | $ 4,452,544 | $ 425,122 | $ 542,470 | $ 503,548 | $1,479,073 | $2,067,297 | $424,709 | $419,040 | $277,290 | $10,591,093 | $10,258,516 |
| Fringe benefits | 1,326,902 | 127,111 | 162,199 | 157,153 | 442,243 | 811,602 | 126,988 | 125,293 | 82,910 | 3,362,401 | 3,125,722 |
| Professional services | 206,010 | 438,179 | 26,454 | 47,822 | 12,009 | 397,482 | 9,568 | 10,140 | — | 1,147,664 | 940,626 |
| Subcontracts | 2,212,974 | 52,820 | 1,811,770 | — | — | 144 | — | — | — | 4,077,708 | 3,604,836 |
| Equipment | 1,111,474 | 35,327 | 7,009 | — | 7,514 | 15,026 | 4,022 | 11,544 | — | 1,191,916 | 788,580 |
| Supplies | 1,105,742 | 498,412 | 107,213 | 154,332 | 310,058 | 155,058 | 22,660 | 408,391 | 48,099 | 2,809,965 | 2,767,852 |
| Travel | 461,562 | 351,682 | 3,958 | 60,692 | 3,195 | 77,663 | 10,203 | 5,181 | — | 974,136 | 1,021,661 |
| Serials | 3,805 | 15,636 | 273 | 5,798 | 2,240 | 1,547 | 729,221 | (25,200) | — | 733,320 | 659,692 |
| Utilities | 6,433 | 597 | 275,215 | 3,068 | 921,889 | 84,679 | — | 877 | 1,629 | 1,294,387 | 1,026,893 |
| Depreciation | — | — | — | — | 1,943,381 | — | — | — | — | 1,943,381 | 1,791,975 |
| Other | 582,643 | 415,357 | 266,943 | 334,299 | 1,071,265 | 639,704 | 139,740 | 226,486 | 121,682 | 3,798,119 | 3,008,282 |
| *Internal direct charges, net | 1,728,977 | 1,417,309 | (2,094,163) | 552,779 | (241,956) | (178,642) | (121,755) | (862,973) | (199,576) | — | — |
| Total | 13,199,066 | 3,777,552 | 1,109,341 | 1,819,491 | 5,950,911 | 4,071,560 | 1,345,356 | 318,779 | 332,034 | 31,924,090 | 28,994,635 |
| **Overhead expense allocations | 7,266,242 | 1,873,341 | 24,049 | 2,855,008 | (5,950,911) | (4,071,560) | (1,345,356) | (318,779) | (332,034) | — | — |
| Total expenses | $20,465,308 | $5,650,893 | $1,133,390 | $4,674,499 | $ — | $ — | $ — | $ — | $ — | $31,924,090 | $28,994,635 |

* Internal direct charges are net expenses from one functional area to another based upon the actual use of goods and services.

** Overhead expense allocations include the costs allocated from the Laboratory's functional areas to the final cost objectives.

*The accompanying notes are an integral part of the financial statements.*

# Report of the Library Director

The days of measuring a research library's success by the number of books or journals the library owns and circulates are gone. A major transition has taken place as libraries shift dollars toward "licensing access to" materials rather than "purchasing and owning" those materials. This shift to "access *versus* ownership" presents both changing economic models and significant legal challenges to libraries. While many costs have yet to be elucidated, perhaps of greatest concern to librarians and scientists are issues of how and where viable information archives will be maintained. We have joined other libraries in a discourse with publishers about this important topic. Also, increased automation and use of digital resources precipitate different space needs for libraries and patrons. So the balancing act continues as new technologies change the way libraries do business.

Technology gave us many opportunities to expand and broaden the Library's reach beyond our walls. We now deliver many services and resources directly to the desktops of scientists 24 hours a day, 7 days a week. In 2001 the Library launched several new services for the Woods Hole scientific community including remote access to electronic journals and databases, desktop delivery of electronic documents, and patron-initiated interlibrary loan requests. We also gave patrons the ability to borrow books directly from a variety of partner libraries, which are delivered to our patrons' Woods Hole offices.

We aggressively moved more Library content and supporting services to the web to make such direct delivery possible. We added important new resources such as *Current Contents, Current Protocols in Molecular Biology, Psychinfo, SciFinder Scholar* and *Zoological Record* to our web site. By the end of 2001 the MBL/WHOI Library was delivering approximately 52% of our serials and 100% of our databases in distributed electronic format. This extended the Library's reach and gave us significantly greater return on our investment for these resources.

Much emphasis was placed on revamping the Library's web site, as it is the gateway to our electronic products and services. The site was redesigned considerably and was brought into compliance with the Americans with Disabilities Act. We created many new interactive forms for services like interlibrary loan, created space and readership applications, and constructed internal intranets for working documents, computer inventories and staff development information.

Librarians saw these changes as another opportunity to demonstrate their instructional role within the institutions. They developed short training courses to familiarize and train scientists how to best utilize electronic resources, and they spread the word through departmental visits, laboratory meetings, and one-on-one training.

### *Collections and Space*

The book collection in the Lillie Building was shifted to provide additional space for the Special Collections. The WHOI Data Library and Archives completed an installation of compact shelving, which greatly enhanced our ability to curate important data collections. We continued to move serial titles to the Harvard Depository. (Materials for which we have electronic access were considered suitable candidates for offsite storage.) Staff devoted considerable effort to programming and database development as we cataloged our myriad electronic resources and provided access to them *via* logical links on the Library's web site. Searching in major databases like *PubMed* was enhanced by building links from citations to the full text of the article whenever the Library had licensed access to the journal title. In our continuing effort to dispel the myth that everything on the Internet is free, we "branded" electronic resources and database search results with the Library logo so patrons could readily see that these resources were paid for and licensed through the auspices of the Library. We continued to negotiate license agreements that guaranteed that the Woods Hole scientific community had access to our resources.

### *Rare Books and Special Collections*

The Library purchased a significant volume for the Rare Books Room: Comte Luigi Ferdinando Marsilli's

*Histoire Physique de la Mer* (c1725), which is recognized as the first oceanographic treatise. We also found a 1999 companion volume that provides a page-by-page English translation, thus allowing researchers to make better use of this historically important work.

The MBL/WHOI Library could not accomplish all we do without a cadre of willing and able volunteers. The Rare Books Room volunteers served as our goodwill ambassadors and spent the year identifying volumes that needed preservation and conservation. In July of 2001 the MBL Associates established a Restoration Program campaign and sponsored a special program to celebrate both the MBL Rare Books Room and to honor Millie Huettner and the memory of Robert Huettner for their volunteer efforts in this part of the Library. Jean Ashton, Director of Columbia University's Rare Book and Manuscript Library, gave a lecture at this event. In addition, Ann Weissmann curated a black and white photograph collection, from the archives, of turn-of-the-century scenes and scientists, which was exhibited in the MBL's Meigs Room in 2001.

On behalf of the MBL Archives, we accepted the papers of Viktor Hamburger, who taught in the Embryology course in the 1930s and is considered to be one of the leaders in the field. We also received and processed the papers of Ruth Sager and Sally Schrader—important female MBL scientists. The WHOI Data Library and Archives, under a grant from the American Institute of Physics, processed papers of seven WHOI scientists; and their dedicated and talented volunteers continued an Oral History Project that seeks to record the recollections and personal insights of WHOI scientists and staff.

### *Cooperating Libraries*

The Boston Library Consortium continues to serve the Woods Hole community well, and Williams College was welcomed as the newest member of the Consortium. With help from the Jewett Foundation, we established a virtual consortium of libraries with the American Museum of Natural History, Rockefeller University, Cold Spring Harbor, and the New York Botanical Gardens. These consortial memberships not only considerably expand the resources available to our scientific staff, but also allow us to share our unique and valuable resources with other scholars.

The library continues to support informatics for the National Library of Medicine and finished its tenth year with the establishment of a roving wireless classroom.

There is no doubt that 2002 will be an exciting year for the library with these new initiatives.

—Catherine Norton

# Educational Programs

## *Summer Courses*

### *Biology of Parasitism: Modern Approaches*

### *(June 7–August 4, 2001)*

*Directors*

Pearce, Edward, Cornell University
Tschudi, Christian, Yale University School of Medicine

*Faculty*

Bangs, Jay, University of Wisconsin, Madison
Fraunholz, Martin, University of Pennsylvania
Grencis, Richard, University of Manchester, United Kingdom
Guiliano, David, University of Edinburgh
Kissinger, Jessica, University of Pennsylvania
McFadden, Geoffrey Ian, University of Melbourne, Australia
Parsons, Marilyn, Seattle Biomedical Research Institute
Rathod, Pradip, Catholic University of America
Roos, David, University of Pennsylvania
Tarleton, Rick, University of Georgia
Ullu, Elisabetta, Yale University School of Medicine

*Lecturers*

Beverley, Stephen, Washington University School of Medicine
Burleigh, Barbara, Harvard School of Public Health
Deitsch, Kirk, Cornell Medical School
Dobbelaere, Dirk, University of Bern, Switzerland
Dunne, David, University of Cambridge, United Kingdom
Englund, Paul, John Hopkins Medical School
Goldberg, Daniel, Washington University School of Medicine
Hajduk, Stephen, University of Alabama, Birmingham
Harn, Don, Harvard University
Hoffman, Steve, Celera Genomics
Hunter, Chris, University of Pennsylvania
Johnson, Patricia, University of California, Los Angeles
Matthews, Keith, University of Manchester, United Kingdom
Nutman, Thomas, National Institutes of Health
Pearlman, Eric, Case Western Reserve University
Petri, William, University of Virginia Health System
Phillips, Margaret, UT Southwestern Medical Center
Reiner, Steve, University of Pennsylvania
Roditi, Isabel, University of Bern, Switzerland
Sacks, David, National Institutes of Health
Scherf, Artur, Institut Pasteur, France
Scott, Phillip, University of Pennsylvania
Seebeck, Thomas, University of Bern, Switzerland
Soldati, Dominique, University of Heidelberg, Germany
Striepen, Boris, University of Georgia
Ward, Gary, University of Vermont
Waters, Andrew, Leiden University, The Netherlands

*Teaching Assistants*

Alexander, David, University of Wisconsin, Madison
Artis, David, University of Pennsylvania
Djikeng, Appolinaire, Yale University
Ganesan, Karthikeyan, Catholic University of America
Helmby, Helena, University of Manchester, United Kingdom
Hubby, Bolyn, University of Georgia
Jensen, Bryan, Seattle Biomedical Research Institute
Keeling, Patrick, University of British Columbia, Canada
Mair, Gunnar, Queens University, United Kingdom
Martin, Diana, University of Georgia
Ralph, Stuart, University of Melbourne, Australia

*Course Assistant*

Chipperfield, Caitlin, Cornell University

*Students*

Adoro, Stanley, University of Ibadan
Arastu, Shirin, Oregon Health Sciences University
Barak, Efrat, Technion-Israel Institute of Technology
Blair, Peter, University of Notre Dame
Boscardin, Silvia, Universidade Federal de São Paulo
Brown, Mark, Brookhaven National Laboratory
Echeverria, Pablo, Inst. di Parasit. Fatale, Buenos Aires, Argentina
Foth, Bernardo, University of Melbourne
Frischknecht, Friedrich, Institut Pasteur
Kriek, Neline, University of Oxford
Motyka, Shawn, Johns Hopkins University School of Medicine
Rottenberg, Sven, Institute of Animal Pathology
Sherrer, Rita, University of Alabama, Birmingham
Silva, Neide, Universidade Federal de Minas Gerais
Uzureau, Pierrick, Institut Pasteur
Westwood, Nick, Harvard Medical School

### *Embryology: Concepts and Techniques in Modern Developmental Biology*

### *(June 17–July 29, 2001)*

*Directors*

Bronner-Fraser, Marianne, California Institute of Technology
Fraser, Scott, California Institute of Technology

*Faculty*

Adoutte, Andre, Centre Natl. de la Recherche Scientifique, France
Carroll, Sean, University of Wisconsin, Madison
Collazo, Andres, House Ear Institute
Ettensohn, Charles, Carnegie Mellon University
Halpern, Marnie, Carnegie Institution of Washington
Harland, Richard, University of California, Berkeley
Henry, Jonathan, University of Illinois, Urbana
Krumlauf, Robb, Stowers Institute for Medical Research
Levine, Michael, University of California, Berkeley
Niswander, Lee, Memorial Sloan-Kettering Cancer Center
Patel, Nipam, University of Chicago
Rothman, Joel, University of California, Santa Barbara
Sanes, Joshua, Washington University Medical School
Saunders, Jr., John, Marine Biological Laboratory
Shankland, Martin, University of Texas, Austin
Wieschaus, Eric, Princeton University
Wray, Gregory, Duke University
Zeller, Robert, San Diego State University

*Lecturers*

Davidson, Eric, California Institute of Technology
Holland, Linda, University of California, San Diego
Hopkins, Nancy, Massachusetts Institute of Technology
Joyner, Alexandra, New York University School of Medicine
Robertson, Elizabeth, Harvard University
Rosenthal, Nadia, Massachusetts General Hospital, East
Smith, William, University of California, Santa Barbara
Stern, Claudio, University College London
Turnbull, Dan, New York University School of Medicine

*Teaching Assistants*

Baker, Clare, California Institute of Technology
Bui, Yen Kim, California Institute of Technology
Casey, Elena, University of California, Berkeley
Cowden, John, University of California, Berkeley
Davis, Gregory, University of Chicago
De Rosa, Renaud, Centre National de la Recherche Scientifique, France
Gamse, Joshua, Carnegie Institution of Washington
Garcia-Castro, Martin, California Institute of Technology
Gendreau, Steve, Exelixis, Inc.
Gross, Jeffrey, Duke University
Khokha, Mustafa, University of California, Berkeley
Kuhlman, Julie, University of Oregon
Lane, Mary Ellen, Rice University
Lespinet, Olivier, National Institutes of Health
Liu, Karen, University of California, Berkeley
Mariani, Francesca, University of California, Berkeley
Nakatani, Yuki, University of California
Ober, Elke, University of California, San Francisco
Stathopoulos, Angela, University of California, Berkeley
Tabin, Clifford, Harvard Medical School
Tobey, Allison, Memorial Sloan-Kettering Cancer Center
Trainor, Paul, Medical Research Council, United Kingdom
Wallingford, John, University of California, Berkeley
Walsh, Emily, University of California, San Francisco
Walter, Brian, University of Illinois
Williams, Terri A., Yale University
Wilson, Valerie, University of Edinburgh, United Kingdom

*Course Assistants*

Hurwitz, Mark, Marine Biological Laboratory
Wylie, Michael, Marine Biological Laboratory
Wylie, Sara, Marine Biological Laboratory

*Students*

Alexander, Tara, University of Houston
Babbitt, Courtney, University of Chicago
Bachler, Monika, IMP
Chang, Chenbei, The Rockefeller University
Cooper, Kimberly, University of Washington
Kelly, Kristie, Cornell University Medical College
Liu, Feng, University of Southern California
Lu, Carole, California Institute of Technology
Luria, Victor, Columbia University
Lynch, Jeremy, New York University
Medina, Mónica, California Academy of Sciences
Neill, Anna, Scripps Institution of Oceanography
Nelson, Brenden, Montana State University
Osborne, Nicholas, University of California, San Francisco
Patten, Iain, University of Sheffield
Prince, Frédéric, University of Basel Biocenter
Ricci, Giulia, La Sapienza University of Rome
Sen, Anindya, Tata Institute of Fundamental Research
Sousa Nunes, Rita, National Institute for Medical Research
Van Raay, Terrence, University of Utah
Wandelt, Jessica, University of Arizona
Xanthos, Jennifer, University of Minnesota
Yan, Irene, The Rockefeller University
Yu, Jr-Kai, Scripps Institution of Oceanography

## *Microbial Diversity (June 10–July 27, 2001)*

*Directors*

Harwood, Caroline, University of Iowa
Spormann, Alfred, Stanford University

*Faculty*

Armitage, Judith, University of Oxford
Brahamsha, Bianca, University of California, San Diego
Buckley, Daniel, University of Connecticut
Ditty, Jayna, Texas A&M University
Gibson, Jane, Professor Emeritus
Golden, Susan, Texas A&M University
Golden, James W., Texas A&M University
Lory, Steve, Harvard Medical School
Palenik, Brian, University of California, San Diego

*Lecturers*

DeLong, Edward, Monterey Bay Aquarium Research Institute
Forney, Larry, University of Idaho
Gerlt, John A., University of Illinois
Greenberg, Everett, University of Iowa
Larimer, Frank W., Oak Ridge National Laboratory
LaRossa, Robert, E. I. Du Pont de Nemours and Company
Lovley, Derek, University of Massachusetts
Margulis, Lynn, University of Massachusetts
Schmidt, Thomas, Michigan State University
Weinstock, George, Baylor College of Medicine

*Teaching Assistants*

Mueller, Jochen, Stanford University
Pelletier, Dale, Stanford University
Schaefer, Amy, University of Iowa

*Course Coordinator*

Hawkins, Andrew, University of Iowa

*Lab Assistant*

Waterbury, Matt, Marine Biological Laboratory

*Students*

Baumgartner, Laura, University of Connecticut
Behrens, Sebastian, Max-Planck-Institute for Marine Microbiology
Coby, Aaron, Indiana University
Fleming, Erich, University of Oregon
Gerlach, Robin, Montana State University
Giegerich, Jennifer, Pennsylvania State University
Harris, Jonathan, University of Colorado, Boulder
Hughes, Jennifer, Brown University
Kellogg, Laurie, University of Notre Dame
Kelman, Dovi, Tel Aviv University
Lim, Grace, Scripps Institution of Oceanography
Lupp, Claudia, University of Hawaii
Martiny, Adam, Technical University of Denmark
Pilcher, Carl, NASA Headquarters
Rash, Brian, Louisiana State University
Reed, Andrew, Rutgers University
Riemann, Lasse, Scripps Institution of Oceanography
Robidart, Julie, Scripps Institution of Oceanography
Schuster, Martin, University of Iowa
Whitaker, Rachel, University of California, Berkeley

## *Neural Systems and Behavior*

### *(June 10–August 4, 2001)*

*Directors*

Carr, Catherine, University of Maryland
Levine, Richard, University of Arizona, Tucson

*Faculty*

Calabrese, Ronald L., Emory University
Chen, Shanping, House Ear Institute
Chitwood, Raymond, Baylor College of Medicine
Davis, Graeme, University of California, San Francisco
French, Kathleen, University of California, San Diego
Glanzman, David, University of California, Los Angeles
Golowasch, Jorge, Rutgers University
Kristan, William, University of California, San Diego
Mandelstam-Manor, Yair, Ben-Gurion University of the Negev
McAnelly, Lynne, University of Texas, Austin
Mooney, Richard, Duke University Medical Center
Nadim, Farzan, Rutgers University
Prusky, Glen, The University of Lethbridge, Canada
Reyes, Alexander, New York University
Roberts, William, University of Oregon
Szczupak, Lidia, Ciudad Universitaria
Weeks, Janis, University of Oregon
Wenning-Erxleben, Angela, Emory University
Wessel, Ralf, University of California, San Diego
Wood, Emma, University of Edinburgh, United Kingdom
Zakon, Harold, University of Texas, Austin
Zirpel, Lance, University of Utah School of Medicine

*Lecturers*

Augustine, George, Duke University
Barnes, Carol, University of Arizona
Nusbaum, Michael, University of Pennsylvania School of Medicine
O'Dowd, Diane, University of California, Irvine
Perkel, David, University of Washington
Simon, Jonathan, University of Maryland

*Teaching Assistants*

Beenhakker, Mark, University of Pennsylvania
Blitz, Dawn Marie, Harvard Medical School
Bradford, Yvonne, University of Oregon
Coleman, Melissa, St. Joseph's Hospital
Few, Preston, University of Texas
Goodman, Miriam, Columbia University
Kittelberger, Matthew, Duke University Medical Center
Lewis, John, University of Ottawa
Li, Quan, University of California, Los Angeles
MacLeod, Katrina, University of Maryland
Marek, Kurt, University of California, San Francisco
Melville, Johnathan, University of Oregon
Paradis, Suzanne, University of California, San Francisco
Philpot, Benjamin, Brown University
Rosen, Merri, Duke University Medical Center
Villareal, Greg, University of California, Los Angeles
Zee, M. Jade, University of Oregon

*Course Assistant*

Rodrigues, Elizabeth, University of Oregon

*Students*

Bee, Mark, University of Missouri
Bertetto, Lisa, Wesleyan University
Brome, Clint, University of California, San Francisco
de Hoz, Livia, University of Edinburgh
Elliott, Taffeta, Columbia University
Garcia de Polavieja, Gonzalo, University of Cambridge
Garza, Annette, University of Texas, San Antonio
Halabisky, Brian, Case Western Reserve University
Hertzberg, Shari, University of Pennsylvania School of Medicine
Karpova, Alla, Harvard Medical School
Ludwar, Bjoern, Universität zu Köln
Martinez-Conde, Susana, Harvard Medical School
Monroy, Jenna, Northern Arizona University
Moore, Timothy, Clark Atlanta University
Nader, Karim, New York University
Palmer, Stephanie, University of California, San Francisco
Siegel, Jennifer, Bowling Green State University

Sumbre, German, Hebrew University of Jerusalem
Woodward, Owen, University of Washington
Yu, Angela, University College London

## Neurobiology *(June 10–August 11, 2001)*

*Directors*
Faber, Donald, Albert Einstein College of Medicine
Lichtman, Jeff W., Washington University School of Medicine

*Faculty*
Conchello, Jose-Angel, Washington University
DeFranco, Donald, University of Pittsburgh School of Medicine
Denk, Winfried, Max-Planck-Institute for Medical Research, Germany
Engisch, Kathrin, Emory University School of Medicine
Gan, Wenbiao, New York University School of Medicine
Geschwind, Daniel, University of California, Los Angeles
Grabowski, Paula, University of Pittsburgh
Harris, Kristen, Boston University
Hart, Anne, Massachusetts General Hospital Cancer Center
Huguenard, John, Stanford University School of Medicine
Jacob, Michele, Tufts University
Johnston, Daniel, Baylor College of Medicine
Kaprielian, Zaven, Albert Einstein College of Medicine
Kauer, Julie, Brown University
Khodakhah, Kamran, University of Colorado School of Medicine
Lambert, Nevin, Medical College of Georgia
Lin, Jen-Wei, Boston University
Lipscombe, Diane, Brown University
Littleton, Troy, Massachusetts Institute of Technology
Lohmann, Christian, Washington University
Mellon, Pamela, University of California, San Diego
Nichols, A-Paula, University of Pittsburgh School of Medicine
Nicolelis, Miguel, Duke University Medical Center
Nowak, Linda, Cornell University
Preuss, Thomas, Albert Einstein College of Medicine
Price, Donald, Johns Hopkins University
Reese, Thomas, National Institutes of Health
Sanes, Joshua, Washington University Medical School
Schweizer, Felix, University of California, Los Angeles
Stanciu, Madalina, University of Pittsburgh School of Medicine
Terasaki, Mark, University of Connecticut Health Center
Thompson, Wesley J., University of Texas
Tully, Tim, Cold Spring Harbor Laboratory
Wong, Rachel, Washington University School of Medicine

*Lecturers*
Betz, Bill, University of Colorado School of Medicine
Harlow, Mark, Stanford University School of Medicine
Marshall, Robert, Stanford University Medical School
McMahan, Uel, Stanford University School of Medicine
Miller, Chris, Brandeis University
Posakony, James, University of California, San Diego
Ress, David, Stanford University
Sigworth, Fred, Yale University
Smith, Stephen, Stanford University School of Medicine
Tsien, Roger, University of California, San Diego

*Teaching Assistants*
Bishop, Derron, Washington University School of Medicine
Guan, Zhuo, Massachusetts Institute of Technology
Walsh, Mark, Washington University School of Medicine

*Course Assistants*
Satterlee, Danielle, Marine Biological Laboratory
Szabo, Theresa, Texas A&M University

*Students*
Adolfsen, William, Massachusetts Institute of Technology
Barreto, Ernest, George Mason University
Coyle, Joseph, McLean Hospital
Datta, Debkanya, National Centre for Biological Sciences
Emond, Michelle, Stanford University
Follett, Pamela, Children's Hospital, Boston
Haspel, Gal, Ben Gurion University
Kasthuri, Narayanan, Oxford University
Mahoney, Melissa, Cornell University
Rasse, Tobias, Max-Planck-Institut für Biophysikalische
Rinberg, Dima, Bell Laboratories, Lucent Technologies
Zuo, Yi, Northwestern University Medical School

## Physiology: The Biochemical and Molecular Basis of Cell Signaling *(June 10–July 21, 2001)*

*Directors*
Garbers, David, University of Texas Southwestern Medical Center
Reed, Randall, Johns Hopkins University School of Medicine

*Faculty*
Comerford, Sarah, University of Texas Southwestern Medical Center
Ehrlich, Barbara, Yale University
Furlow, John, University of California, Davis
Gardner, Kevin, University of Texas Southwestern Medical
Megraw, Timothy, Indiana University
Prasad, Brinda, New York University School of Medicine
Scholl, Jason, University of Texas Southwestern Medical Center
Schultz, Nikolaus, University of Texas Southwestern Medical Center
Zielinski, Raymond, University of Illinois, Urbana

*Isenberg Lecturer*
Lifson, Richard, Yale University School of Medicine

*A. K. Parpart Lecturer*
Michael Welsh, University of Iowa

*Lecturers*
Bennett, Anton, Yale University Medical Center
Berkowitz, Gerald, University of Connecticut
Buck, Linda, Harvard Medical School

Clapham, David, Harvard Medical School
Hammer, Robert, University of Texas Southwestern Medical Center
Hepler, Peter, University of Massachusetts
Hynes, Richard, Massachusetts Institute of Technology
Kaupp, U. B., Institut für Biologische Informationsverarbeitung
Mangelsdorf, David, University of Texas Southwestern Medical Center
Oprian, Daniel, Brandeis University
Sheen, Jen, Massachusetts General Hospital
Spiegelman, Bruce, Harvard Medical School
Stock, Ann, Center for Advanced Biotechnology and Medicine
Turek, Fred, Northwestern University
Welsh, Michael, University of Iowa College of Medicine
Wilkie, Thomas, University of Texas Southwestern Medical Center

*Teaching Assistants*

Buaboocha, Teerapong, University of Illinois at Urbana-Champaign
Croy, Jennifer, University of Texas Southwestern Medical Center
Janowitz, Tobias, Marine Biological Laboratory
Johenning, Friedrich, Yale University School of Medicine
Lim, Wayland, University of California, Davis

*Course Coordinator*

Rossi, Kristen, University of Texas Southwestern Medical Center

*Course Assistant*

Knutson, Casey, Marine Biological Laboratory

*Students*

Dhingra, Anuradha, University of Pennsylvania
Dowell, Joshua, Riley Hospital for Children, Indiana
Griffis, Eric, Emory University School of Medicine
Herve, Maxime, Institut Pasteur de Lille
Kalinowski, Rebecca, University of Connecticut Health Center
Karres, Janina, University of Massachusetts
Kulisz, Andre, Iowa State University
Labunskiy, Dmitriy, Institute of Neurology, Moscow
Lutton, Bram, Boston University
Maritz, Christine, University of Pretoria
Melnick, Richard, University of Vermont
Nakauchi, Sakura, Tokyo University Pharmacy and Life Science
Ramsey, David, University of Illinois at Chicago
Selak, Sanya, University of Calgary
Sell, Anne, Woods Hole Oceanographic Institution
Sigal, Irina, UMDNJ-New Jersey Medical School
Silverstein, Robert, University of Washington, Seattle
Vidaltamayo, Roman, National University of Mexico
Yanochko, Gina, University of Arizona

# Special Topics Courses

## Analytical and Quantitative Light Microscopy (May 10–18, 2001)

*Directors*

Sluder, Greenfield, University of Massachusetts Medical School
Wolf, David, Sensor Technologies

*Faculty*

Abramowitz, Mort, Olympus Corporation
Amos, William B., Medical Research Council, United Kingdom
Cardullo, Richard, University of California, Riverside
Gall, Joseph, Carnegie Institute of Washington
Gelles, Jeff, Brandeis University
Hinchcliffe, Edward, University of Massachusetts Medical School
Hinsch, Jan, Leica Microsystems Inc.
Inoué, Shinya, Marine Biological Laboratory
Keller, Ernst, Carl Zeiss, Inc.
Moomaw, Butch, Hamamatsu Photonic Systems
Nordberg, Joshua, University of Massachusetts Medical School
Oshiro, Masafumi, Hamamatsu Photonic Systems
Pollard, Angela, BioHybrid Technologies
Reichelt, Stefanie, Medical Research Council, United Kingdom
Rottenfusser, Rudi, Marine Biological Laboratory
Salmon, Edward, University of North Carolina, Chapel Hill
Sears, Kathryn, Sensor Technologies
Silver, Randi, Cornell University Medical College
Spring, Kenneth, National Institutes of Health
Straight, Aaron, Harvard Medical School
Swedlow, Jason, University of Dundee, Scotland

*Students*

An, Seong, Oregon Health Sciences University
Bevan, Cassandra, Dartmouth Medical School
Brown, Christa, Johns Hopkins University
Butler, Peter, University of California, San Diego
Conrad, Jacinta, Harvard University
Delay, Eugene, Regis University
DiBella, Linda, University of Connecticut Health Center
Diegert, Carl, Sandia National Laboratories
Dixon, Wendy, CalPoly, Pomona
DuJardin, Denis, University of Massachusetts Medical School
Edwards, Kathryn, Kenyon College
Gosse, Julie, Cornell University
Jeong, Juhee, Harvard University
Kobayashi, Miya, Nagoya University School of Medicine
Kovacs, Birgit, University of Pennsylvania
Larsen, Melinda, National Institutes of Health/NIDCR
Lim, Kuei-Cheng, University of Rochester
Lingner, Joachim, Swiss Institute for Experimental Cancer Research
Ma, Zhengyu, University of Pennsylvania

Maéda, Yuichiro, RIKEN Harima Institute at SPring-8
Merz, Alexey, Dartmouth Medical School
Mundy, William, U.S. Environmental Protection Agency
Powers, Thomas, Brown University
Ross, Stephen, Nikon Instruments Inc.
Sanchez, Vicente, INAOE
Schroth-Diez, Britta, Max Planck Institute
Shannon, Katie, University of North Carolina, Chapel Hill
Soriano, Sulpicio, Children's Hospital
Stanton, Susan, University of Cincinnati
Watters, Christopher, Middlebury College
Yu, Hongtao, University of Texas Southwestern Medical Center, Dallas
Zhou, Zheng, Massachusetts Institute of Technology

## *Frontiers in Reproduction: Molecular and Cellular Concepts and Applications*

*(May 20–June 30, 2001)*

### *Directors*

Hunt, Joan, University of Kansas Medical Center
Mayo, Kelly, Northwestern University
Schatten, Gerald, Oregon Health Sciences University

### *Faculty*

Ascoli, Mario, University of Iowa College of Medicine
Berard, Mark, University of Michigan Medical School
Campbell, Keith, University of Nottingham, United Kingdom
Camper, Sally, University of Michigan Medical School
Croy, Barbara Anne, University of Guelph, Canada
Dominko, Tanja, Advanced Cell Technology
Fazleabas, Asgerally, University of Illinois at Chicago
Hunt, Patricia A., Case Western Reserve University
Jaffe, Laurinda, University of Connecticut Health Center
Moore, Karen, University of Florida
Page, Ray, Advanced Cell Technology
Rainey, Hilary, Northwestern University
Santiago, Jose, Northwestern University
Shupnik, Margaret, University of Virginia Medical Center
St. John, Justin, University of Birmingham, United Kingdom
Suszko, Magdalena, Northwestern University
Terasaki, Mark, University of Connecticut Health Center
Wakayama, Teruhiko, Rockefeller University
Weck, Jennifer, Northwestern University
Weigel, Nancy, Baylor College of Medicine
Woodruff, Teresa, Northwestern University

### *Lecturers*

Albrecht, Eugene, University of Maryland Medical School
Behringer, Richard, University of Texas
Corbould, Anne, Brigham and Women's Hospital
Crowley, William, Massachusetts General Hospital
Guillette, Louis J., University of Florida
Hennighausen, Lothar, National Institutes of Health
Lessey, Bruce, University of North Carolina, Chapel Hill
Lockwood, Charles, New York University School of Medicine
Myles, Diana, University of California, Davis
Nilson, John, Case Western Reserve Medical School
Ober, Carole, University of Chicago
Patrizio, Pasquale, Hospital University of Pennsylvania
Richards, Jo-Anne, Baylor College of Medicine
Sarras, Michael, University of Kansas Medical Center
Thomas, Peter
Thornburg, Kent, Oregon Health Sciences University
Tilly, Jonathan L., Massachusetts General Hospital
Wessel, Gary, Brown University

### *Pioneer Awardees*

Eicher, Eva, Jackson Laboratory
Handyside, Alan, University of Leeds

### *Teaching Assistants*

Betts, Dean, Case Western Reserve Medical School
Butterbrodt, Julie, University of Iowa
Carroll, David, Florida Institute of Technology
Hewitson, Laura, Oregon Health Sciences University
Hodges, Craig, Case Western Reserve University
Jacoby, Ethan, Oregon Health Sciences University
Kalinowski, Rebecca, University of Connecticut Health Center
Kim, Julie, University of Illinois College of Medicine
Malik, Nusrat, Baylor College of Medicine
Payne, Christopher, Oregon Health Sciences University
Runft, Linda, University of Connecticut Health Center
Saunders, Thomas, University of Michigan
Takahashi, Diana, Oregon Health Sciences University

### *Course Coordinators*

Aldrich, Carrie, University of Chicago
Petroff, Margaret, University of Kansas Medical Center
Simerly, Calvin, Oregon Health Sciences University

### *Students*

Arenas, Lidia, Inst Par el Estudio
Cameo, Paula, Instituto de Biologia y Medicina Experimental
Chohan, Kazim, College of Veterinary Sciences, Lahore
Del Priore, Giuseppe, New York University Medical Center
Esplin, Michael, University of Utah Medical Center
Grace, Kristen, State University of New York at Stony Brook
Lee, Men-Jean, New York University School of Medicine
Mahale, Smita, Institute for Research in Reproduction, India
McGee, Elizabeth, Magee Women's Research Institute
Paduch, Darius, Oregon Health Sciences University
Palomino, Alberto, University of Chile
Petroff, Brian, University of Kansas Medical Center
Rawe, Vanesa, Center of Studies in Gynecology and Reproduction
Sinclair, Kevin, Scottish Agricultural College
Songsasen, Nucharin, Audubon Center for Research of Endangered Species
Tung, Joyce, University of California San Francisco

## *Medical Informatics I (May 27–June 3, 2001)*

### *Director*

Cimino, James, Columbia-Presbyterian Medical Center

### *Faculty*

Ackerman, Michael, National Library of Medicine
Bakken, Suzanne, Columbia University
Canese, Kathi, National Library of Medicine
Cimino, Chris, Albert Einstein College of Medicine
Friedman, Charles, University of Pittsburgh
Hammond, William, Duke University Medical Center
Kingsland, Lawrence, National Library of Medicine

Kohane, Isaac, Children's Hospital
Lindberg, Donald D. A. B., National Library of Medicine
Masys, Daniel, University of California, San Diego
McCray, Alexa, National Library of Medicine
Starren, Justin, Columbia University

*Students*

Assar, Karen, Charles R. Drew University Library
Bain, Paul, Countway Library of Medicine
Baker, Kathleen, Hawaii Department of Health
Barrett, James, University of Virginia
Bergstrom, Mary Linn, University of California, San Diego
Boston, Brian, Georgetown University
Calderon, Alfredo, Universidad Central del Caribe
Carroll, Lisa, University of California, Los Angeles
Ching, Carolyn, Hawaii Medical Library
Cuenco, Marlene, Hawaii Medical Library
Dalrymple, Prudence, Dominican University
Darling, Robert, U.S. Army Medical Research Institute
Engram, Barbara, Halifax Medical Center
Freedman, Kenneth, Connecticut Valley Hospital
Friedman, Patricia, University of Pittsburgh
Haaland, Ardis, University of Mississippi Medical Center
Hanson, Douglas, The Forsyth Institute
Hawkins, Diane, SUNY Upstate Medical University
Hile, Deborah, University of Utah
Jenkins, Melinda, University of Pennsylvania
Lawrence, Valerie, Kaiser Permanente
Lindstrom, Richard, Charles R. Drew University
Montes, Myrtho, St. Vincent's Hospital and Medical Center
Pineiro, Nilsa, University of Puerto Rico
Ruhlen, Michael, Toledo Children's Hospital
Seifried, Steven, University of Hawaii
Soliz, Tricia, University Medical Center
Springston, Lorna, Ball Memorial Hospital
Vance, Lyle, North Lake Community Library
Williamson, Ann, University of California, San Francisco Medical Center

## *Medical Informatics II (Sept. 30–Oct. 7, 2001)*

*Director*

Masys, Daniel, University of California, San Diego

*Faculty*

Cimino, James, Columbia University
Friedman, Charles, University of Pittsburgh
Giuse, Nunzia, Vanderbilt University Medical Center
Hightower, Allen, Centers for Disease Control and Prevention
Jenders, Robert, Columbia-Presbyterian Medical Center
Kingsland, Lawrence, National Library of Medicine
Lindberg, Donald D. A. B., National Library of Medicine
McDonald, Clement, Regenstrief Institute
Miller, Randolph, Vanderbilt University Medical Center
Nahin, Annette, National Library of Medicine
Ozbolt, Judy, Vanderbilt University Medical Center
Perednia, Douglas, Association of Telehealth Service Providers
Stead, William, Vanderbilt University Medical Center
Wheeler, David, National Library of Medicine

*Students*

Adams, Carolyn, Legacy Health System
Alpino, Robert, Eastern Virginia Medical School
Ascher, Marie, The New York Academy of Medicine
Bansal, Mohanlal, ENT Hospital
Barrett, Laura, UMDNJ-Smith Library
Benzoni, Thomas, Mercy Medical Center
Bunnett, Brian, University of Texas Southwestern Medical Center Library
Deeney, Kay, University of California, Los Angeles
Garcia, John, St. John's Mercy Medical Center
Gaskell, Stephanie, Visiting Nurse Association of Southeastern Massachusetts
Gilbert, Carole, Providence Hospital and Medical Centers
Givens, Nancy, Commonwealth Health Corporation
Habetler, Anna, Children's Hospital and Health Center
Herreño, Diógenes, University of Puerto Rico School of Medicine
Jacobs, Joshua, University of Hawaii
Jerome, Rebecca, Vanderbilt University Medical Center
Lucas, Brian, Cook County Hospital
Markinson, Andrea, State University of New York
McCann, Mary, University of Pennsylvania Health System
Milrod, Lewis, Seton Hall University
Poole, Connie, Southern Illinois University
Potter, Ann, HQ, U.S. Army Medical Command
Pryor, Jan, Fiji School of Medicine
Roos, Joel, Naval Medical Center, San Diego
Rosendale, Douglas, Grand Junction Veterans Affairs Medical Center
Ross, Stephen, University of Colorado Health Sciences Center
Schulman, Joseph, Albany Medical College
Smith, Rita, U.S. Air Force Medical Center
Tayrien, Richard, St. Joseph's Hospital and Medical Center
Varner, Douglas, California Pacific Medical Center

## *Methods in Computational Neuroscience (July 29–August 26, 2001)*

*Directors*

Bialek, William, NEC Research Institute
de Ruyter, Rob, NEC Research Institute

*Faculty*

Abbott, Lawrence, Brandeis University
Delaney, Kerry, Simon Fraser University, Canada
Ermentrout, Bard, University of Pittsburgh

Gelperin, Alan, Bell Laboratories
Hopfield, John, Princeton University
Johnston, Daniel, Baylor College of Medicine
Kelley, Darcy, Columbia University
Marder, Eve, Brandeis University
Nemenman, Ilya, NEC Research Institute
Rieke, Fred, University of Washington
Seung, H., Sebastian, Massachusetts Institute of Technology
Solla, Sara A., Northwestern University Medical School
Sompolinsky, Haim, The Hebrew University of Jerusalem, Israel
Tank, David, Bell Laboratories
Tishby, Naftali, The Hebrew University of Jerusalem, Israel
Zucker, Steven, Yale University

*Lab Instructor*

Jensen, Roderick, Wesleyan University

*Lecturers*

Koberle, Roland, Universidade de São Paulo, Brasil
Logothetis, Nikos, Max-Planck-Institute for Biological Cybernetics, Germany
Srinivasan, Mandyam V., Australian National University, Australia

*Teaching Assistants*

Aguera y Arcas, B.
Lewen, Geoffrey David, NEC Research Institute
White, John, Boston University

*Course Assistant*

Jensen, Kate, Marine Biological Laboratory

*Students*

Anderson, Britt, Brown University
Corrado, Greg, Stanford University
Dorval, Alan, Boston University
Escalada, Artur, University of Barcelona
Faisal, Ahmed, Emmanuel College
Fourcaud, Nicolas, Université Paris 5 René Descartes
Goldberg, Jesse, Columbia University
Goldberg, Joshua, The Hebrew University
Gollisch, Tim, Humboldt-Universität zu Berlin
Gordon, Michael, Albert Einstein College of Medicine
Gregor, Thomas, Princeton University
Grove, Charlotte, Einstein College of Medicine
Haas, Julie, Boston University
Hasenstaub, Andrea, Yale University
Loewenstein, Yonatan, Hebrew University
Neimark, Maria, Princeton University
Osan, Remus, University of Pittsburgh
Oviedo, Hysell, New York University
Puchalla, Jason, Princeton University
Rust, Nicole, New York University
Schenk, Ana Katrin, University of California, San Francisco
Sharpee, Tatyana, Michigan State University
Sripati, Arun, Johns Hopkins University
Stepanyants, Armen, Cold Spring Harbor Laboratory

## *Microinjection Techniques in Cell Biology*
### *(May 22–29, 2001)*

*Director*

Silver, Robert, Marine Biological Laboratory

*Faculty*

Klaessig, Suzanne, Cornell University
Kline, Douglas, Kent State University
Shelden, Eric, University of Michigan

*Teaching Assistant*

Miller, Roy Andrew, Kent State University

*Students*

Agarwal, Madhavi, Clark University
Ali, Zulfiqar, State University of New York
Chen, Mei Ling, University of Illinois, Chicago
Cohen, David, Dyson Institute for Vision Research
Day, Eric Yuan-Ji, University of Virginia
Domozych, David, Skidmore College
Findlay, Kirk, Mayo Clinic Jacksonville
Gilthorpe, Jonathan, King's College London
Henry, Stephen, University of Texas, Houston
LaFountain, James, University of Buffalo
Pollenz, Richard, University of South Florida
Quaderi, Nandita, King's College London
Stanton, Susan, University of Cincinnati
Wilde, Andrew, Carnegie Institution of Washington
Yaroslavskiy, Beatrice, University of Pittsburgh

## *Molecular Biology of Aging*
### *(July 30–August 18, 2001)*

*Directors*

Guarente, Leonard P., Massachusetts Institute of Technology
Wallace, Douglas, Emory University School of Medicine

*Faculty*

Bohr, Vilhelm, National Institutes of Health
Campisi, Judith, Lawrence Berkeley National Laboratory
Culotta, Valeria L., Johns Hopkins University
de Lange, Titia, The Rockefeller University
Goldberg, Fred, Harvard Medical School
Hanawalt, Philip, Stanford University
Harley, Calvin, Geron Corporation
Hekimi, Siegfried, McGill University
Helfand, Stephen, University of Connecticut Health Center
Jones, Dean P., Emory University
Kim, Stuart, Stanford University School of Medicine
Kirkwood, Tom, University of Manchester
Lambeth, J. David, Emory University
Martin, George, University of Washington School of Medicine
Partridge, Linda, University College London
Price, Donald, Johns Hopkins University
Richardson, Arlan, University of Texas Health Science Center, San Antonio
Ruvkun, Gary, Massachusetts General Hospital
Tanzi, Rudolph E., Harvard Medical School
Tower, John, University of Southern California
Valentine, Joan S., University of California, Los Angeles
Weindruch, Richard H., Veterans Administration Hospital
Wright, Woodring E., University of Texas Southwestern Medical Center
Yuan, Junying, Harvard Medical School

### *Teaching Assistants*

Bordone, Laura, University of Minnesota
Coskun, Elif Pinar, Emory University School of Medicine
Cottrell, Barbara, Emory University
Kaeberlein, Matt, Massachusetts Institute of Technology
Kerstann, Keith, Emory University School of Medicine
Kokoszka, Jason, Emory University
Viswanathan, Mohan, Massachusetts Institute of Technology

### *Course Coordinator*

Burke, Rhonda E., Emory University School of Medicine

### *Students*

Agbas, Abdulbaki, University of Kansas
Arum, Oge, University of Colorado, Boulder
Falcon, Alaric, University of Florida
Fisher, Tim, Albert Einstein College of Medicine
Gallo-Cromie, Gloria, New York University
Haq, Rizwan, University of Toronto
Kumar, Siva, Centre for Cellular and Molecular Biology
Lambert, Adrian, University of Liverpool
Lee, Jaewon, NIH/NIA/GRC
Lewis, Marc, University of Texas at Austin
Lopez, Norma, UAM-Iztapalapa
Mele, James, UT Health Science Center, San Antonio
Michán, Shaday, UNAM
Park, Jeong-Soo, Seoul National University
Poole, Jason, University of Illinois, Chicago
Pritsker, Moshe, Princeton University
Renault, Valerie, CNRS UMR 7000
Rodier, Francis, University of Montreal Hospital Research Center
Sharrow, Keith, University of Kentucky
Shea, Molly, University of Minnesota, Twin Cities

## *Molecular Mycology: Current Approaches to Fungal Pathogenesis (August 6–24, 2001)*

### *Directors*

Edwards, John Jr., Harbor-UCLA Medical Center
Magee, Paul T., University of Minnesota
Mitchell, Aaron P., Columbia University

### *Faculty*

Buchanan, Kent L., Tulane University Health Science Center
Doering, Tamara L., Washington University School of Medicine
Filler, Scott, Harbor-UCLA Medical Center
Gow, Neil A., University of Aberdeen
Heitman, Joseph, Duke University Medical Center
May, Gregory S., University of Texas
Rhodes, Judith, University of Cincinnati Medical Center
Sil, Anita, University of California, San Francisco
Sundstrom, Paula, Ohio State University
White, Ted, Seattle Biomedical Research Institute

### *Lecturer*

Newman, Simon, University of Cincinnati College of Medicine

### *Teaching Assistants*

Breeding, Connie, Duke University Medical Center
Johnston, Douglas, Harbor-UCLA Medical Center
Lephart, Paul, University of Minnesota
Xu, Wenjie, Columbia University

### *Course Coordinator*

Rafkin, Wendy, Harbor-UCLA Medical Center

### *Students*

Barelle, Caroline, University of Aberdeen
Bruno, Vincent, Columbia University
Feldmesser, Marta, Albert Einstein College of Medicine
Forche, Anja, University of Minnesota
Fox, Deborah, Duke University Medical Center
Fraser, James, University of Melbourne
Izumikawa, Koichi, National Institutes of Health
Jackson, Lydgia, University of Oklahoma Health Science Center
Knight, Simon, University of Pennsylvania
Lee, Nancy, University of British Columbia
Mansour, Michael, Boston University School of Medicine
McBride, Anne, Dana-Farber Cancer Institute
Mootien, Sarapadee, Yale University School of Medicine
Peltroche-Llacsahuanga, Heidrun, University Hospital RWTH Aachen
Sinha, Himanshu, Duke University Medical Center
Snyder, Wiliam, MicroGenomics, Inc.
Uicker, William, Tulane University Health Sciences Center
Young, Timothy, Pfizer GRD

## *Neural Development and Genetics of Zebrafish (August 12–25, 2001)*

### *Directors*

Dowling, John E., Harvard University
Talbot, William S., Stanford University School of Medicine

### *Faculty*

Chien, Chi-Bin, University of Utah Medical Center
Collazo, Andres, House Ear Institute
Eisen, Judith S., University of Oregon
Fetcho, Joseph, State University of New York, Stony Brook
Hanlon, Roger, Marine Biological Laboratory
Hopkins, Nancy, Massachusetts Institute of Technology
Houart, Corrine, King's College London
Kimmel, Charles, University of Oregon
Lin, Shuo, Medical College of Georgia
Moens, Cecilia, Fred Hutchinson Cancer Research Center
Neuhauss, Stephan, Universität Zurich
Raible, David, University of Washington
Wilson, Stephen, University College London, United Kingdom

### *Lecturers*

Astrofsky, Keith, Massachusetts Institute of Technology
Fraser, Scott, California Institute of Technology

### *Teaching Assistants*

Clarke, Jon, University College London, United Kingdom
Fadool, James, Florida State University
Granato, Michael, University of Pennsylvania School of Medicine
Lawrence, Christian, Harvard University
Mazanec, April, University of Oregon
Mullins, Mary, University of Pennsylvania
Perkins, Brian, Harvard University
Rhodes, Sean

Rikhof, Holly, Fred Hutchinson Cancer Research Center
Schneider, Valerie, University of Pennsylvania
Walker-Durchanck, Charline, University of Oregon

### *Course Coordinator*

Schmitt, Ellen, Harvard University

### *Course Assistant*

Dugan, Maureen, Nashoba Regional High School

### *Technician*

Wilson, Carole, University College London, United Kingdom

### *Students*

Breithaupt, Thomas, University of Konstanz
Bricaud, Olivier, House Ear Institute
Conway, Gregory, NASA Ames Research Center
Corwin, Jeffrey, University of Virginia School of Medicine
Diez Del Corral, Ruth, University of Dundee
Gillette-Ferguson, Ilona, Case Western Reserve University
Hua, Yuanyuan, Stanford University
Luo, Wenqin, Johns Hopkins Medical Institution
Mazanec, April, Zebrafish International
McDermott, Brian, Rockefeller University
Mumm, Jeffrey, Washington University
Prior, Heather, The King's University College
Psychoyos, Delphine, The Salk Institute
Sagasti, Alvaro, University of California, San Francisco
Wang, Jian, Dana-Farber Cancer Institute
Wood, Elizabeth, Boston University
Wright, Gavin, Imperial Cancer Research Fund

## *Optical Microscopy and Imaging in the Biomedical Sciences (October 10–19, 2001)*

### *Director*

Izzard, Colin, State University of New York, Albany

### *Faculty*

DePasquale, Joseph, New York State Department of Health
Hard, Robert, State University of New York, Buffalo
Inoué, Shinya, Marine Biological Laboratory
Maxfield, Frederick, Cornell University Medical College
Murray, John, University of Pennsylvania School of Medicine
Piston, David M., Vanderbilt University
Scott, Martin
Spring, Kenneth, National Institutes of Health
Swedlow, Jason, University of Dundee, United Kingdom

### *Lecturers*

Hinsch, Jan, Leica, Inc.
Keller, Ernst, Zeiss Optical Systems
Oldenbourg, Rudolf, Marine Biological Laboratory

### *Course Associates*

Pierini, Lynda, Weill Medical College of Cornell University
Sigurdson, Wade, State University of New York, Buffalo
Snyder, Kenneth, State University of New York, Buffalo
Wuestner, Daniel, Cornell University Medical College

### *Students*

Arnesen, Solfrid, The Royal Vet and Agricultural University
Brown, Michael, SUNY Upstate Medical University
Corson, Laura, Mt. Sinai Hospital
Courvoisier, Hélène, The Rockefeller University
Cushman, Samuel, National Institutes of Health/NIDDK
Duggal, Rajat, Rice University
Harvey, Robert, Case Western Reserve University
Kemmer, Danielle, Karolinska Institute
Kremyanskaya, Marina, University of Pennsylvania
Monks, Jenifer, National Jewish Medical and Research Center
Nydegger, Sascha, University of Vermont
Patel, Kamala, University of Calgary
Praetorius, Helle, National Institutes of Health
Rubina, Kseniya, Moscow State University
Sagot, Isabelle, Dana-Farber Cancer Institute
Schweitzer, Jill, University of Notre Dame
Shaw, Michael, University of Pennsylvania
Siegrist, Sarah, University of Oregon
Trogadis, Judy, St. Michael's Hospital
Vallejo, Johana, University of Missouri, Columbia
Wang, Exing, Indiana University
Weaver, Alissa, Washington University School of Medicine
Wibrand, Karin, SARS International Centre for Marine Biology
Wolthuis, Rob, Wellcome/CRC Institute

## *Pathogenesis of Neuroimmunologic Diseases (August 12–August 25, 2001)*

### *Directors*

Brosnan, Celia F., Albert Einstein College of Medicine
Rosenbluth, Jack, New York University School of Medicine
Waksman, Byron, Foundation of Microbiology

### *Faculty*

Berman, Joan, Albert Einstein College of Medicine
Chao, Moses, New York University Medical Center
Coyle, Patricia, State University of New York, Stony Brook
Darnell, Robert, Rockefeller University
Drachman, Daniel, Johns Hopkins University School of Medicine
Kaplan, Gilla, Rockefeller University
Kuchroo, Vijay, Brigham and Women's Hospital
Martiney, James
Popko, Brian, University of North Carolina, Chapel Hill
Price, Donald, Johns Hopkins University

Reder, Anthony, University of Chicago
Saper, Clifford, Beth Israel Deaconess Medical Center
Scherer, Steven, University of Pennsylvania
Shrager, Peter, University of Rochester Medical Center
Solimena, Michele, Yale University
Sontheimer, Harald, University of Alabama, Birmingham
Sternberg, Esther, National Institutes of Health
Wiley, Clayton, University of Pittsburgh

*Lecturers*
Benveniste, Etty, University of Alabama, Birmingham
Brightman, Milton, National Institutes of Health
Dalakas, Marinos, National Institutes of Health
Griffin, Diane, Johns Hopkins University School of Medicine
Griffin, John, Johns Hopkins University School of Medicine
Hickey, William, Dartmouth-Hitchcock Medical Center
Knopf, Paul, Brown University
Lipton, Stuart, University of California, San Diego
Ransohoff, Richard, Cleveland Clinic Foundation
Salzer, James, New York University School of Medicine
Shin, Moon, University of Maryland School of Medicine

*Students*
Brand-Schieber, Elimor, Albert Einstein College of Medicine
Clerval, Cliff, Mercy College
Conant, Stephanie, Wayne State University
Cosenza, Melissa, Albert Einstein College of Medicine
Davis, Julie, Genzyme Corporation
Korvatska, Elena, University of California, Davis
Masterman, Thomas, Karolinska Institutet
McKee, Mary Ann, Henry Ford Hospital
Murphy, Tanya, University of Florida
Ringger, Clair, University of Florida
Rivieccio, Mark, Albert Einstein College of Medicine
Rose, Rosalind, Genzyme Corporation
Sakic, Boris, McMaster University
Souayah, Nizar, Temple School of Medicine
Sundararajan, Sophia, University Hospitals of Cleveland
Trebst, Corinna, Cleveland Clinic Foundation
Vasic, Rada, University of Connecticut Health Center
Vehmas, Anne, Johns Hopkins University
Weerth, Susanna, Albert Einstein College of Medicine
Weimer, Jill, Univ of Rochester School of Medicine and Dentistry

## Summer Program in Neuroscience, Ethics, and Survival (SPINES) *(June 9–July 7, 2001)*

*Directors*
Martinez, Joe, University of Texas, San Antonio
Townsel, James G., Meharry Medical College

*Faculty*
Augustine, George, Duke University
Berger-Sweeney, Joanne E., Wellesley College
Escalona de Motta, Gladys, University of Puerto Rico
Etgen, Anne, Albert Einstein College of Medicine
Fox, Thomas O., Harvard Medical School
Gonzalez-Lima, Francisco, University of Texas
Zakon, Harold, University of Texas, Austin

*Lecturers*
Castaneda, Edward, Arizona State University
Gale, Karen, Georgetown University Medical Center
Johnston, Dan, Baylor College of Medicine
Jones, James, American Psychological Association
Kravitz, Edward, Harvard Medical School
Mensinger, Allen, University of Minnesota
Nickerson, Kim, American Psychological Association
Wyche, James, Brown University
Zayas, Ricardo, Tufts University
Messinger, Alan, U., of Minnesota

*Teaching Assistants*
Gonzalez-Lima, Erika
Gray, Paul, University of California, Los Angeles
Heinrichs, Stephen
Herness, Scott

*Course Coordinator*
Orfila, James, University of Texas, San Antonio

*Students*
Avila, Irene, Arizona State University
Brewster, Kiyona, Bennett College
Cola, Monique, Tulane University Medical School
Doyon, William, The University of Texas at Austin
Foster, Katrina, Indiana University-Purdue University
Guerrero Berroa, Elizabeth, Herbert H., Lehman College
Hill, Nicole, University of California, Los Angeles
Hudson, Jeffrey, New York State Psychiatric Institute
Johnson, Latoya, Tulane University
Jones, Clayton, Florida A&M University
Jordan, Kenneth, Ohio State University
Kudwa, Andrea, University of Virginia
Maldonado, Jaime, University of Puerto Rico
Medina, David, University of Illinois, Chicago
Moore, Kraig, Rutgers University
Soto, Ileana, University of Puerto Rico
Whittlesey, Kevin, Northwestern University

## Workshop on Molecular Evolution *(July 29–August 10, 2001)*

*Director*
Cummings, Michael, Marine Biological Laboratory

*Faculty*
Beerli, Peter, University of Washington
Edwards, Scott, University of Washington
Eisen, Jonathan, Institute for Genomic Research
Felsenstein, Joseph, University of Washington
Fraser, Claire M., The Institute for Genomic Research
Kuhner, Mary, University of Washington
Lewis, Paul O., University of Connecticut
Martins, Emilia, University of Oregon
Meyer, Axel, University of Konstanz, Germany
Pearson, William, University of Virginia Health Sciences Center
Rand, David, Brown University
Rice, Ken, Glaxo-Smith-Kline Pharmaceuticals
Swofford, David, Smithsonian Institution
Thompson, Steven, BioInfo 4U

Voytas, Daniel F., Iowa State University
Yang, Ziheng, University College London
Yokoyama, Shozo, Syracuse University

#### *Lecturer*

Yoder, Anne D., Northwestern University Medical School

#### *Teaching Assistants*

Bahin, Josephine, Louisiana State University
Church, Sheri A., University of Virginia
Handley, Scott, Washington University
McArthur, Andrew, Marine Biological Laboratory
Pritham, Ellen, University of Massachusetts
Reed, David, University of Utah
Rokas, Antonis, University of Edinburgh
Thompson-Maaloum, Julie, Inst. de Genetique et de Biologie Moleculaire et Cellulaire
Winka, Katarina, Umea University

#### *Students*

Adams, Keith, Indiana University
Anderson, Iain, Integrated Genomics, Inc.
Anderson, Jennifer, University of California, Davis
Anisimova, Maria, University College London
Arkhipova, Irina, Harvard University
Bacci, Mauricio, Universidade Estadual Paulista
Beer, Brigitte, National Institutes of Health
Bell, Charles, Yale University
Bench, Shellie, Molecular Dynamics
Bowie, Rauri, University of Cape Town
Brito, Patricia, American Museum of Natural History
Brunstein, Adriana, Universidade Federal de São Paulo
Bryant, Juliet, University of Texas Medical Branch
Davids, Wagied, Stockholm Bionformatics Ctr.
de Koning, Jason, University at Albany, SUNY
de Oliveira, Tulio, Africa Centre
Dean, Matthew, University of Illinois, Chicago
Durbin, Mary, University of California
Edwards, Katrina, Woods Hole Oceanographic Institution
Fahey, Shireen, University of Queensland
Feil, Edward, University of Bath
Frias-Lopez, Jorge, University of Illinois, Urbana-Champaign
Gilchrist, George, Clarkson University
Goldberg, Tony, University of Illinois
Haddock, Steven, Monterey Bay Aquarium Research Institute
Hankeln, Thomas, Universität Mainz
Hildebrand, Terri, University of Kansas
Ingvarsson, Par, University of Virginia
Kopp, Artyom, University of Wisconsin
Labate, Joanne, Cornell University
Lavrov, Dennis, Université de Montreal
Lercher, Martin, University of Bath
Li, Li, University of Pennsylvania
Louie, Kristina, University of California
Malik, Shehre-Banoo, Emory University
Maloof, Julin, The Salk Institute for Biological Studies
Masta, Susan, San Francisco State University
Miadlikowska, Jolanta, The Field Museum
Morando, Mariana, Brigham Young University
Murphy, Edward, University of California, San Francisco
NesbØ, Camilla, Dalhousie University
Nielsen, Lene Rostgaard, University of Copenhagen
Pagan, Moraima, University of North Carolina, Chapel Hill

Palacios, Carmen, Marine Biological Laboratory
Peijnenburg, Katja, University of Amsterdam
Preston, Joanne, University of Southampton
Ribas de Pouplana, Lluis, The Scripps Research Institute
Rodriguez, Luis, Plum Island Animal Disease Center
Samaan, Magdi, U.S. Naval Medical Research
Sap, Jan, New York University School of Medicine
Schulmeister, Susanne, Institute of Zoology and Anthropology and Zoological Museum
Schwarzbach, Andrea, Kent State University
Shufran, Kevin, USDA-ARS
Simmons, Sheri, Woods Hole Oceanographic Institution
Sischo, William, University of California, Davis
Summers, Kyle, East Carolina University
Tilley, Aimee, University of Salford
Vernesi, Cristiano, University of Ferrara
Ybazeta, Gustavo, University of Toronto
Zoller, Stefan, The Field Museum

## *Other Programs*

### *Marine Models in Biological Research Undergraduate Program*

### *(June 13–August 10, 2001)*

#### *Directors*

Browne, Carole, Wake Forest University
Tytell, Michael, Wake Forest University School of Medicine

#### *Faculty*

Barlow, Robert, SUNY Health Science Center
Browne, Carole L., Wake Forest University
Eckberg, William, Howard University
Furie, Barbara, Harvard University
Furie, Bruce, Harvard University
Gould, Robert, New York State Institute for Basic Research
Hanlon, Roger, Marine Biological Laboratory
Heck, Diane, Rutgers University
Jonas, Elizabeth, Yale University
Kuzirian, Alan, Marine Biological Laboratory

Laufer, Hans, University of Connecticut
Mensinger, Allen, University of Minnesota
Rome, Larry, University of PA
Silver, Robert, Marine Biological Laboratory
Tytell, Michael, Wake Forest University
Wainwright, Norman, Marine Biological Laboratory

*Students*

Bartman, Marc, Fairfield University
Burgents, Joseph, College of NJ
Byam, Keisha, Howard University
Byfield, Victoria, Clark University
Carroll, Ian, Brown University
Fulton, Matthew, Wake Forest University
Griffiths, Shylise, North Carolina A&T University
Hull, Princelli, Duke University
Johnson, Michael, University of Connecticut
Knowles, James, Colgate University
Louis, Lydia, Rutgers University
McCarthy, Erin, Wake Forest University
Meadors, Stephan, University of South Carolina
Pollema, Sarah, University of Minnesota
Shipwith, Aurelia, Howard University
Rubright, James, Wake Forest University
Smith, Ryan, Wake Forest University
Stephenson, Katherine, University of Minnesota

## *NASA Planetary Biology Internship*
### *(June–September 2001)*

*Directors*

Margulis, Lynn, University of Massachusetts, Amherst
Dolan, Michael F., University of Massachusetts, Amherst

*Interns*

Gunnard, Jessie, University of Massachusetts, Amherst
Hunter, Ryan, University of Guelph
Kovalyora, Irina V., Queen's University, Ontario
Lam, Phyllis, University of Hawaii, Manoa
Lancaster, Venessa L., Arizona State University
Noël, Christophe, Institut Pasteur Lille
Roig, Xavier, University of Barcelona

*Sponsors*

Margulis, Lynn, University of MA, Amherst
Nealson, Kenneth, NASA Jet Propulsion Laboratory
Rothschild, Lynn, NASA Ames Research Center
Sogin, Mitch, Marine Biological Laboratory
Stolz, John, Duquesne University
Teske, Andreas, Woods Hole Oceanographic Institution

## *Semester in Environmental Science*
### *(September 3–December 17, 2001)*

*Administration*

Hobbie, John E., Director
Foreman, Kenneth H., Associate Director
Johnson-Horman, Frances, Administrative Assistant

*Faculty*

Deegan, Linda A.
Foreman, Kenneth H.
Giblin, Anne E.
Hobbie, John E.
Hopkinson, Charles S., Jr.
Hughes, Jeffrey
Liles, George
Melillo, Jerry M.
Neill, Christopher
Nadelhoffer, Knute J.
Peterson, Bruce J.
Rastetter, Edward B.
Shaver, Gaius R.
Vallino, Joseph J.
Williams, Mathew

*Research and Teaching Assistants*

Bowen, Jennifer
Gay, Marcus
Kwiatkowski, Bonnie
Micks, Patricia
Tholke, Kris
Ziemann, Tori

*Students*

Baldauf, J. Nicholas, Allegheny College
Burrows, Elizabeth H., Mount Holyoke College
Charkoudian, Louise K., Haverford College
Fertig, Benjamin M., Brandeis University
Forbes, Andrew A., Colgate University
Hartmann, Megan C., Lawrence University
Levine, Uri Y., Kenyon College
McCalley, Carmody K., Middlebury College
Murphy, Meaghan T., Mount Holyoke College
O'Connor, Catherine L., Lafayette College
Reardon, Matthew, Gettysburg College
Whittinghill, Kyle A., Middlebury College
Yum, Man-yu, Mount Holyoke College

## *Teachers' Workshop: Living in the Microbial World (August 12–18, 2001)*

*Directors*

Olendzenski, Lorraine, University of Connecticut, Storrs
Dugas, Jeff, University of Connecticut, Storrs

*Faculty*

DeMars, Abby, University of Connecticut
Dorritie, Barbara, Cambridge Rindge and Latin School, Cambridge, MA

*Presenters*

Bermudes, David, Vion Pharmaceuticals, New Haven, CT
Edgcomb, Virginia, Marine Biological Laboratory
Edwards, Katrina, Woods Hole Oceanographic Institute
Guerrero, Ricardo, University of Barcelona, Spain
Margulis, Lynn, University of Massachusetts, Amherst
Patterson, David, University of Sydney, Australia

*Teacher Participants*

Aquino, Sandra, Tappan Middle School, Ann Arbor, MI
Boyd, Valeria, George Washington Carver High School, Memphis, TN
Brock, David, Roland Park Country School, Baltimore, MD
Burke, Elisa, Stonington High School, Stonington, CT
DeRemer, Roy, Warwick School District, Lititz, PA
Gray, Pamela, Stetson Middle School, West Chester, PA
Idoine, Karen, Rhode Island School of Design, Providence, RI
Markovich, Paul, Nauset Regional High School, N. Eastham, MA
Meister, Laurie, Roland Park Country School, Baltimore, MD
Pumplin, Susan, Roland Park Country School, Baltimore, MD
Reardon, Anne Marie, The Dwight Englewood School, Englewood, NJ
Reppard, Donna, Antioch College, Keene, NH
Schwendau, Jean, George Washington Carver High School, Memphis, TN
Weinrich, Roseann, Tamaqua Area High School, Tamaqua, PA
Whiting, Rosa, MacDuffie School, Springfield, MA
Wilkinson, Dee, Stetson Middle School, West Chester, PA
Wright, David, Booker T., Washington High School, Memphis, TN

# Summer Research Programs

## *Principal Investigators*

Allen, Nina, North Carolina State University
Armstrong, Clay, University of Pennsylvania
Armstrong, Peter B., University of California, Davis
Augustine, George J., Duke University Medical Center

Baker, Robert, New York University Medical Center
Barlow, Robert B., Jr., State University of New York Upstate Medical University
Beaugé, Luis, Instituto de Investigacion Medica "Mercedes y Martin Ferreyra," Argentina
Bennett, Michael V. L., Albert Einstein College of Medicine
Bodznick, David, Wesleyan University
Boyer, Barbara, Union College
Boyle, Richard, NASA
Brady, Scott T., The University of Texas Southwestern Medical Center, Dallas
Brown, Joel, Albert Einstein College of Medicine
Browne, Carole, Wake Forest University School of Medicine
Burbach, Peter, Rudolf Magnus Institute for Neurosciences, The Netherlands
Burger, Max M., Friedrich Miescher Institut, Switzerland
Burgess, David, Boston College

Cameron, Chris, The University of Texas, Austin
Canessa, Cecilia, Yale University
Chang, Fred, Columbia University
Chappell, Richard L., Hunter College, City University of New York
Clay, John, National Institutes of Health
Cohen, Lawrence B., Yale University School of Medicine
Cohen, William D., Hunter College, City University of New York
Costello, John, Providence College
Crawford, Karen, St. Mary's College of Maryland

De Weer, Paul, University of Pennsylvania School of Medicine
Denton, Jerod S., Dartmouth Medical School
Devlin, C. Leah, Penn State University
DiPolo, Reinaldo, Instituto Venezolano Investigaciones Cientificas, Venezuela
Dodge, Frederick, State University of New York Upstate Medical University

Eckberg, William, Howard University
Edds-Walton, Peggy, University of California, Riverside

Fay, Richard, Loyola University of Chicago
Field, Christine, Harvard University Medical School
Fields, Douglas, National Institutes of Health
Fishman, Harvey M., University of Texas Medical Branch, Galveston

Gadsby, David, The Rockefeller University
Galione, Antony, Oxford University, United Kingdom
Garcia-Blanco, Mariano, Duke University Medical Center
Gelman, Benjamin, University of Texas Medical Branch, Galveston
Gerhart, John, University of California, Berkeley
Giuditta, Antonio, Universita di Napoli "Federico II," Italy
Goldman, Robert D., Northwestern University Medical School
Gould, Robert, New York State Institute for Basic Research
Gray, Paul, University of California, Los Angeles
Groden, Joanna, University of Cincinnati
Gruenbaum, Yosef, The Hebrew University of Jerusalem, Israel

Haimo, Leah, University of California, Riverside
Hall, Benjamin, Simon Fraser University, Canada
Han, Zhiyoung, Brown University
Heck, Diane, Rutgers University
Hershko, Avram, Technion-Israel Institute of Technology, Israel
Highstein, Steven M., Washington University School of Medicine
Hill, Susan Douglas, Michigan State University
Hines, Michael, Yale University School of Medicine
Hoke, Kim L., Stanford University
Holmgren, Miguel, Harvard University Medical School

Jena, Bhanu, Wayne State University School of Medicine
Johnston, Daniel, Baylor College of Medicine
Jonas, Elizabeth, Yale University School of Medicine
Jovanovic, Jasmina, University of College London, United Kingdom

Kaczmarek, Leonard, Yale University School of Medicine
Kaminer, Benjamin, Boston University School of Medicine
Kaplan, Barry, National Institutes of Mental Health
Kaplan, Ilene M., Union College
Kapoor, Tarun, The Rockefeller University
Kaupp, U.B., Institut für Biologische Informationsverarbeitung, Germany
Khan, Shahid, State University of New York Upstate Medical University
Khodakhah, Kamran, University of Colorado School of Medicine
Khodjakov, Alexey, Wadsworth Center
Kirschner, Marc, Harvard University Medical School
Kuhns, William, The Hospital for Sick Children, Canada

Lafer, Eileen M., University of Texas Health Science Center, San Antonio
Landowne, David, University of Miami School of Medicine
Langford, George, Dartmouth College

Laskin, Jeffrey, University of Medicine and Dentistry of New Jersey
Laufer, Hans, University of Connecticut
LeBaron, Richard, University of Texas, San Antonio
Link, Brian, Harvard University
Lipicky, Raymond J., Food and Drug Administration
Llinás, Rodolfo R., New York University Medical Center
Luthi, Theres, *Neue Zürcher Zeitung*, Switzerland

Magee, Jeff, Louisiana State University Medical Center
Malchow, Robert Paul, University of Illinois, Chicago
Marom, Shimon, Technion-Israel Institute of Technology, Israel
Martinez, Joe, University of Texas, San Antonio
Matus, Andrew, Friedrich Miescher Institute, Switzerland
McNeil, Paul, Medical College of Georgia
Mensinger, Allen, University of Minnesota, Duluth
Mitchison, Timothy, Harvard University Medical School
Miyake, Katsuya, Medical College of Georgia
Moore, John W., Duke University Medical Center
Mooseker, Mark, Yale University
Murray, Andrew, Harvard University

Nasi, Enrico, Boston University School of Medicine

Ogden, David, National Institute for Medical Research

Palazzo, Robert, University of Kansas
Pant, Harish, National Institutes of Health
Pantazis, Panayotis, Brown University
Parysek, Linda, University of Cincinnati
Ponka, Prem, McGill University, Canada

Quigley, James, Scripps Research Institute

Rakowski, Robert F., Ohio University
Ratner, Nancy, University of Cincinnati
Reese, Thomas S., National Institutes of Health
Richards, Kathryn, Emory University
Rieder, Conly, Wadsworth Center
Ripps, Harris, University of Illinois College of Medicine
Rome, Larry, University of Pennsylvania
Rosenbaum, Joel, Yale University
Ruderman, Joan, Harvard University Medical School
Russell, James, National Institutes of Health
Russell, John M., Syracuse University

Salmon, Edward, University of North Carolina, Chapel Hill
Sauve, Kevin, New York University School of Medicine
Schwartz, Lawrence, University of Massachusetts
Shashar, Nadav, Interuniverity Institute of Eilat, Israel
Silver, Robert, Marine Biological Laboratory
Sloboda, Roger D., Dartmouth College
Soares, Daphne, University of Maryland
Spiegel, Evelyn, Dartmouth College
Spiegel, Melvin, Dartmouth College
Steinacker, Antoinette, University of Puerto Rico
Stockbridge, Norman, Federal Department of Agriculture
Sugimori, Mutsuyuki, New York University Medical Center

Telzer, Bruce, Pomona College
Tilney, Lewis, University of Pennsylvania
Twig, Gilad, Technion-Israel Institute of Technology, Israel
Tytell, Michael, Wake Forest University School of Medicine

Vollrath, Melissa Ann, Baylor College of Medicine

Weidner, Earl, Louisiana State University
Wyche, James, Brown University

Young, Iain, University of Pennsylvania
Yu, Lei, University of Cincinnati

Zecevic, Dejan P., Yale University School of Medicine
Zimmerberg, Joshua, National Institutes of Health
Zochowski, Michal, Yale University School of Medicine
Zottoli, Steven, Williams College
Zukin-Bennett, R. Suzanne, Albert Einstein College of Medicine

## *Other Research Personnel*

Altamirano, Anibal, Instituto de Investigacion Medica "Mercedes y Martin Ferreyra," Argentina
Alverez, Rita, Hunter College
Arnolds, David, Williams College
Asomoah, Nikiya, Williams College
Avila, Irene, Arizona State University

Babu, Nina, Syracuse University
Baubet, Valerie, Institut Pasteur, France
Bearer, Elaine, Brown University
Berridge, Georgina, University of Oxford, United Kingdom
Bertetto, Lisa, Wesleyan University
Boal, Jean, Millersville University
Brown, Hannah, Barnard College
Brown, Jeremiah, Dartmouth College
Bucior, Iwona, Friedrich Miescher Institut, Switzerland

Cala, David, New York University School of Medicine
Canman, Julie, University of North Carolina
Cardell, Robert, University of Cincinnati
Carroll, Ian, Brown University
Case, Andrew, University of Maryland
Chen, Xiaobing, National Institutes of Health
Cheng, Chong Nam, Hong Kong University of Science and Technology, Hong Kong
Chevez, Carolyn, Williams College
Conrad, Mara, Hunter College
Cook, Erik, Baylor College of Medicine
Crawford, Karen, St. Mary's College of Maryland
Curtis, Jessica, Gladstone Institute of Neurological Disease

DeBose, Jennifer, Flower Garden Banks NMS
Deonauth, Kamla, Howard University
DiClerico, John, New York State Institute for Basic Research
Djurisic, Maja, Yale University School of Medicine
Dunham, Philip, Syracuse University

Evans, Louise, Harvard Medical School
Eyman, Maria, Universita di Napoli "Federico II," Italy

Fernholz, Brian, New York University
Ferrara, Eugenia, Universita di Napoli "Federico II," Italy
Flaumenhaft, Robert, Harvard University
Forger, Daniel, Courant Institute
Frick, Andreas, Baylor College of Medicine
Fuller, Shakierah, Williams College
Fulton, Matthew, Wake Forest University

Gainer, Harold, National Institutes of Health
Galbraith, Jim, National Institutes of Health
Gallant, Paul, National Institutes of Health
Galloway, University of Virginia
Ginsberg, Zachary, Brown University
Gioio, Anthony, National Institutes of Health
Glushakova, Svetlana, National Institutes of Health
Goldman, Anne, Northwestern University Medical School
Gomez, Maria del Pilar, Boston University School of Medicine
Grant, Philip, National Institutes of Health
Gyoeva, Fatima, Institute of Protein Research, Russia

Harrington, John, University of California, Davis
Harwood, Claire, University of Pennsylvania
Helfand, Brian, Northwestern University Medical School
Hellemons, Anita, University of Utrecht, The Netherlands
Helm, Jessica, Yale University School of Medicine
Hernandez, Carlos, New York University School of Medicine
Hernandez, Ruben, University of Texas
Hinton, Shanta, Howard University
Hitt, James, State University of New York Upstate Medical University
Hiza, Nick, Williams College
Hoffman, Mathew, Boston College
Holtz, Scott, Northwestern University Medical School
Holz, George, New York University School of Medicine
Hrabetova, Sabine, New York University School of Medicine
Hull, Pincelli, Duke University

Imani, Farzin, University of Colorado School of Medicine

Johnson, Michael, University of Connecticut
Jurkovicova, Dana, National Institutes of Health

Kavanagh, Emma, New York State Institute for Basic Research
Khorgami, Pouyeh, University of Colorado School of Medicine
King, Curtis, University of Utah
Kumar, Mukesh, National Institutes of Health

Lam, Phillis, University of Hawaii
Lambert, Nevin, Medical College of Georgia
LaVail, Jennifer, University of California, San Francisco
Lee, Kyeng-Gea, Hunter College
Lee, Vivian, California Institute of Technology
Lenart, Peter, European Molecular Biology Laboratory, Germany
Llinas, Alexander, New York University School of Medicine
Louis, Lydia, Rutgers, the State University of New Jersey
Lowe, Chris, University of California, Berkeley
Lukyanetz, Elena, Bogomoletz Institute of Physiology, Ukraine

Maddox, Paul, University of North Carolina
Martindale, Mark, University of Hawaii
Masgrau, Roser, Oxford University, United Kingdom
McGuinnes, Carrie, Syracuse University
Meadors, Stephan, University of South Carolina
Miledi, Richard, University of California, Irvine
Miller, Todd, Hunter College
Mittmann, Beate, Humboldt-Universität, Germany
Molloy, Christopher, UMDNJ-Robert Wood Johnson Medical School
Morgan, Anthony, University of Oxford, United Kingdom

Navarro, Paula, Women and Infants Hospital
Ng, Michelle, Boston College
Nguyen, Michael, University of Texas Medical Branch
Nichols, Amy, Millersville University
Nierman, Jennifer, Williams College
Noel, Christophe, Institut Pasteur, France

Olsen, Gary, University of Illinois

Pappas, George, University of Illinois
Patten, Manus, Syracuse University
Paydarfar, David, University of Massachusetts
Payne, John, University of California, Davis
Prasad, Kondury, University of Texas Health Science Center

Reigada, David, University of Barcelona, Spain
Remick, Katherine, University of Texas Medical Branch
Rengifo, Juliana, Yale University
Rhodes, Paul, New York University Medical School
Rigby, Alan, Beth Israel Deaconess Medical Center
Rubright, James, Wake Forest University

Sayles, Suzanne, Boston College
Schaak, Sarah, University of Minnesota
Scheraga, David, Syracuse University
Schneider, Eric, Brown University
Sheftel, Alexander, McGill University, Canada
Shuster, Charles, Boston College
Silva, Diana, Hunter College
Simonetta, Kyle, Dartmouth College
Simpson, Tracy, University of Hartford
Solzin, Johannes, Institut für Biologische Informationsverarbeitung, Germany
Squillace, Angela, University of Rome, Italy

Taboada, Luis, Williams College
Tanner, Geoffrey, Wesleyan University
Tauscher, Andrew, University of California, San Francisco
Thai, Ngee Foong, Hunter College
Thrower, Edwin, Yale University
Tokumaru, Hiroshi, Duke University Medical Center
Tokumaru, Keiko, Duke University Medical Center
Tran, Phong, Columbia University

Wachowiak, Matt, Yale University
Wassersug, Richard, Dalhousie University, Canada
Weyand, Ingo, Institut für Biologische Informationsverarbeitung, Germany
Wharton, Kristi, Brown University
Williams, Jeff, University of California, Davis
Womack, Mary, University of Colorado School of Medicine

Yang, Dazhi, Howard University
Yu, Ming-Jium, Cornell University
Yu, Xin, Yale University

Zakevicius, Jane, University of Illinois College of Medicine
Zhang, Ping, Yale University School of Medicine
Zochowski, Michal, Yale University School of Medicine

## *Library Readers*

Abbott, Jayne, Marine Research
Ahmadjiian, Vernon, Clark University
Allen, Garland, Washington University
Alliegro, Mark, LSU Health Center
Anderson, Everett, Harvard University

Baccetti, Baccio, University of Siena
Benjamin, Thomas, Harvard Medical School
Borgese, Thomas, Lehman College
Boyer, John, Union College
Burke, Donald, Johns Hopkins School of Medicine

Cariello, Lucio, Stazione, Zoologica "A. Dohrn"
Candelas, Graciela, University of Puerto Rico
Child, Frank, Trinity College
Clark, Eloise, Bowling Green State University
Clarkson, Kenneth, Lucent Technologies
Cobb, Jewel, California State University
Cohen, Leonard, American Health Institute
Cohen, Seymour, American Cancer Society
Cohen, William, Hunter College
Corwin, Jeffrey, University of Virginia
Couch, Ernest, Texas Christian University

D'Alessio, Giuseppe, University of Naples
Dodge, Frederick, SUNY
Duncan, Thomas, Nichols College

Epstein, Herman, Brandeis University

Fischback, Gerald, National Institute of Mental Health
Fraenkel, Dan, Harvard University Medical School
Frantz, John, Carnegie Institute of Washington
Fujita, Rodney, Environmental Defense Organization

Galatzer-Levy, Robert, University of Chicago
German, James, Cornell University
Goldstein, Moise, Johns Hopkins University
Gore, John, Yale University
Grossman, Albert, NYU Medical Center
Gruner, John, Cephalon

Halvorson, Harlyn, University of Massachusetts
Harrington, John, SUNY New Paltz
Heisler, Kenneth, Falmouth, MA
Hernandez-Nicaise, Mari-Luz, University of Nice
Herskovits, Theodore, Fordham University
Hines, Michael, Yale University
Hunter, Robert, Gartnaval Royal Hospital

Inoue, Sadayuki, McGill University
Iribane, Oscar, University of Argentina

Jacobson, Allan, University of Massachusetts Medical Center
Jaye, Robert, Soloman Schechter
Jones, Teresa, National Institutes of Health
Josephson, Robert, University of California

Kaltenbach, Jane, Mt. Holyoke College
Karlin, Arthur, Columbia University
Kelly, Robert, Northwestern University
Keynan, Alex, Israel Academy of Science and Humanity
King, Kenneth, Woods Hole, MA
Kornberg, Hans, Boston University

Laderman, Aimlee, Yale University School of Forestry
Lee, John, CUNY
Lesser, Carolyn, University of Wisconsin, Oshkosh
Lisman, John, Brandeis University
Loewenstein, Werner, *Journal of Membrane Biology*, N. Falmouth, MA

Lorand, Laszlo, Northwestern University
Luckenbill, Louise, Ohio University

Milkman, Roger, University of Iowa
Minini, Ann, Marine Biological Laboratory
Mitchell, Ralph, Harvard University
Moore, John, Duke University Medical Center
Morfini, Gerardo, Southwestern Medical
Morrell, Leyla, Rush University

Nagel, Ronald, Albert Einstein University
Narahashi, Toshio, Northwestern University Medical School
Naugle, John, National Aeronautics and Space Administration
Nicaise, Ghislain, University of Nice
Nickerson, Peter, SUNY Buffalo

Prendergast, Robert, Johns Hopkins University

Rabinowitz, Michael, Marine Biological Laboratory
Rafferty, Nancy, Marine Biological Laboratory
Reynolds, George, Princeton University
Rome, Larry, University of Pennsylvania

Schippers, Jay, Resource Foundation
Schwartz, Lawrence, University of Massachusetts at Amherst
Selby, Cecily, Falmouth, MA
Shanklin, Douglas R, University of Tennessee Health Science Center
Shepro, David, Boston University
Spector, Abraham, Columbia University
Spotte, Stephen, Longboat Key
Stuart, Ann, University of North Carolina
Sundquist, Eric, USGS
Sweet, Frederick, Washington University
Sydlik, Mary Ann, Hope College

Torre, Vincent, Marine Biological Laboratory
Traver, Timothy, Sustainability Institute, Hartland, VT
Tweedell, Kenyon, University of Notre Dame

Van Holde, Kensal, Oregon State University

Walton, Alan, Cavandish Lab, Cambridge, UK
Warren, Leonard, University of Pennsylvania
Weissmann, Gerald, NYU School of Medicine

Zimmerberg, Joshua, National Institutes of Health

# *Domestic Institutions Represented*

Alabama, University of, Birmingham
Albany Medical College
Albert Einstein College of Medicine
American Museum of Natural History
Arizona State University
Arizona, University of
Audubon Center for Research of Endangered Species

Ball Memorial Hospital
Barnard College
Baylor College of Medicine
Bell Laboratories, Lucent Technologies
Beth Israel Deaconess Medical Center
Boston College
Boston University
Boston University School of Medicine
Bowling Green State University
Brigham Young University
Brookhaven National Laboratory
Brown University
Buffalo, University of

California Academy of Sciences
California Institute of Technology
California Pacific Medical Center
California, University of, Berkeley
California, University of, Davis
California, University of, Irvine
California, University of, Los Angeles
California, University of, Riverside
California, University of, San Diego
California, University of, San Francisco
California, University of, San Francisco Medical Center
CalPoly-Pomona
Carnegie Institution of Washington
Case Western Reserve University
Center for Cellular and Molecular Biology
Center of Studies in Gynecology and Reproduction
Charles R. Drew University
Chicago Medical School
Chicago, University of
Children's Hospital, Boston
Children's Hospital of Philadelphia
Cincinnati, University of
Clark University
Clarkson University
Cleveland Clinic Foundation
Cold Spring Harbor Laboratory
Colorado School of Medicine, University of
Colorado, University of, Health Sciences Center
Colorado, University of, Boulder
Columbia University
Commonwealth Health Corporation
Connecticut Valley Hospital
Connecticut, University of
Connecticut, University of, Health Center
Cook County Hospital
Cornell University
Cornell University Medical College
Countway Library of Medicine
Courant Institute

Dana-Farber Cancer Institute
Dartmouth College
Dartmouth Medical School
Dominican University
Duke University
Duke University Medical Center
Dyson Institute for Vision Research

East Carolina University
Eastern Virginia Medical School
Emmanuel College
Emory University
Emory University School of Medicine
ENT Hospital

Federal Department of Agriculture
Field Museum of Natural History
Florida A&M University
Florida, University of
Flower Garden Banks NMS
Food and Drug Administration
Forsyth Institute

Genzyme Corporation
George Mason University
Georgetown University
Gladstone Institute of Neurological Disease
Grand Junction Veterans Affairs Medical Center

Hartford, University of
Harvard University
Harvard University Medical School
Hawaii Department of Health
Hawaii Medical Library
Hawaii, University of
Henry Ford Hospital
Herbert H. Lehman College
House Ear Institute
Howard University
HQ, U.S. Army Medical Command
Hunter College

Illinois, University of
Illinois, University of, Chicago
Illinois, University of, Urbana-Champaign
INAOE
Indiana University
Institute for Research in Reproduction
Institute of Neurology
Institute of Zoology and Anthropology and Zoological Museum
Integrated Genomics, Inc.
Iowa State University
Iowa, University of

Johns Hopkins University School of Medicine

Kaiser Permanente
Kansas, University of
Kansas, University of, Medical Center
Kent State University
Kentucky, University of
Kenyon College

Legacy Health System
Louisiana State University
Loyola University of Chicago

Magee Women's Research Institute
Marine Biological Laboratory
Maryland, University of
Massachusetts Institute of Technology
Massachusetts, University of
Massachusetts, University of, Medical School
Mayo Clinic Jacksonville
McLean Hospital
Medical College of Georgia
Mercy College
Mercy Medical Center
Miami, University of, School of Medicine
Michigan State University
MicroGenomics, Inc.
Middlebury College
Millersville University
Minnesota, University of
Minnesota, University of, Twin Cities
Mississippi, University of, Medical Center
Missouri, University of
Missouri, University of, Columbia
Molecular Dynamics
Montana State University
Monterey Bay Aquarium Research Institute
Mt. Sinai Hospital

NASA Ames Research Center
National Aeronautics and Space Administration Headquarters
National Center for Biological Sciences
National Institute of Mental Health
National Institutes of Health
National Institutes of Health/NIDCR
National Institutes of Health/NIDDK
National Jewish Medical and Research Center
Naval Medical Center, San Diego
New York Academy of Medicine
New York State Institute for Basic Research
New York State Psychiatric Institute
New York University
New York University Medical Center
New York University School of Medicine
NIH/NIA/GRC
Nikon Instruments Inc.
North Carolina State University
North Carolina, University of
North Carolina, University of, Chapel Hill
North Lake Community Library
Northern Arizona University
Northwestern University
Northwestern University Medical School
Notre Dame, University of

Ohio State University
Ohio University
Oklahoma, University of, Health Science Center
Oregon Health and Science University
Oregon, University of

Penn State University
Pennsylvania, University of
Pennsylvania, University of, Health System
Pennsylvania, University of, School of Medicine
Pfizer GRD
Pittsburgh, University of
Plum Island Animal Disease Center
Pomona College
Princeton University
Providence College
Providence Hospital and Medical Centers
Puerto Rico, University of
Puerto Rico, University of, School of Medicine
Purdue University

Regis University
Rice University
Riley Hospital for Children, Indiana
Rochester, University of
Rochester, University of, School of Medicine and Dentistry
Rockefeller University
Rutgers University

Salk Institute for Biological Studies
San Francisco State University
Sandia National Laboratories
Scripps Institution of Oceanography
Scripps Research Institute
Seton Hall University
Shippensburg University
Skidmore College
South Carolina, University of
South Florida, University of
Southern California, University of
Southern Illinois University
St. John's Mercy Medical Center
St. Joseph's Hospital and Medical Center
St. Mary's College of Maryland
St. Michael's Hospital
St. Vincent's Hospital and Medical Center
Stanford University
State University of New York at Albany
State University of New York at Stony Brook
SUNY Upstate Medical University
Syracuse University

Temple School of Medicine
Texas A&M University
Texas Health Science Center, University of
Texas Southwestern Medical Center, University of
Texas, University of, Medical Branch
Texas, University of, Southwestern Medical Center
Texas, University of, Austin
Texas, University of, Houston
Texas, University of, San Antonio
Toledo Children's Hospital
Tulane University
Tulane University Health Sciences Center
Tulane University Medical School

U.S. Air Force Medical Center
U.S. Army Medical Research Institute
U.S. Environmental Protection Agency
U.S. Naval Medical Research
UMDNJ-New Jersey Medical School
UMDNJ-Smith Library
Union College
Universidad Central del Caribe, Puerto Rico
University Hospitals of Cleveland
USDA-ARS

UT Health Science Center, San Antonio
Utah, University of
Utah, University of, Medical Center

Vanderbilt University Medical Center
Vermont, University of
Virginia, University of
Virginia, University of, School of Medicine
Visiting Nurse Association of Southeastern Massachusetts

Wadsworth Center
Wake Forest University
Washington, University of
Washington, University of, School of Medicine
Wayne State University
Wayne State University School of Medicine
Wesleyan University
Williams College
Wisconsin, University of
Women and Infants Hospital
Woods Hole Oceanographic Institution

Yale University
Yale University School of Medicine

Zebrafish International Resource Center, University of Oregon

## *Foreign Institutions Represented*

Aberdeen, University of, Scotland
Africa Centre
Amsterdam, University of, The Netherlands

Barcelona, University of, Spain
Bath, University of, United Kingdom
Ben Gurion University, Israel
Biozentrum, University of Basel, Switzerland
Bogomoletz Institute of Physiology, Ukraine
British Columbia, University of, Canada

Calgary, University of, Canada
Cambridge, University of, United Kingdom
Cape Town, University of, South Africa
Centre National de la Recherche Scientifique—CNRS, France
Chile, University of
College of Veterinary Sciences, Lahore, Pakistan
Copenhagen, University of, Denmark

Dalhousie University, Canada
Dundee, University of, Scotland
Edinburgh, University of, Scotland
European Molecular Biology Laboratory, Germany

Ferrara, University of
Fiji School of Medicine
Friedrich Miescher Institute, Switzerland

Halifax Medical Center, Canada
Hebrew University of Jerusalem, Israel
Hong Kong University of Science and Technology
Hospital for Sick Children, Canada
Humboldt-Universität, Germany

Ibadan, University of, Nigeria
IMP
Imperial Cancer Research Fund, United Kingdom
Inst. para el Estudio
Institut für Biologische Informationsverarbeitung, Germany
Institut Pasteur, France
Institut Pasteur de Lille, France
Institute of Animal Pathology
Institute of Protein Research, Russia
Instituto de Biologia y Medicina Experimental, Argentina
Instituto de Investigacion Medica "Mercedes y Martin Ferreyra," Argentina
Instituto Venezolano Investigaciones Cientificas, Venezuela
Interuniversity Institute of Eilat, Israel

Karolinska Institutet, Sweden
King's College, London, United Kingdom
Konstanz, University of, Germany
La Sapienza University of Rome, Italy
Liverpool, University of, United Kingdom

Max-Planck-Institut für Biophysikalische, Germany
Max-Planck-Institute for Marine Microbiology, Germany
McGill University, Canada
McMaster University, Canada
Melbourne, University of, Australia
Moscow State University, Russia

Nagoya University School of Medicine, Japan
Napoli "Federico II," Universita di, Italy
National Institute for Medical Research, United Kingdom
National University of Mexico
*Neue Zürcher Zeitung*, Switzerland

Oxford University, United Kingdom

Philippines, University of the, Diliman
Pretoria, University of, South Africa

Queensland, University of, Australia

RIKEN Harima Institute, Japan
Rome, University of, Italy
Rudolf Magnus Institute for Neuroscience, The Netherlands

Salford, University of, United Kingdom
SARS International Centre for Marine Biology, Norway
Scottish Agricultural College
Seoul National University, Korea
Sheffield, University of, United Kingdom
Simon Fraser University, Canada
SISSA-ISAS International School for Advanced Studies, Italy
Southampton, University of, United Kingdom
Swiss Institute for Experimental Cancer Research, Switzerland

Tata Institute of Fundamental Research, India
Technical University of Denmark
Technion-Israel Institute of Technology, Israel
Tel Aviv University, Israel
The King's University College, Canada
The Royal Veterinary and Agricultural University, Denmark
Tokyo University Pharmacy and Life Science, Japan
Toronto, University of, Canada

UAM-Iztapalapa, Mexico
UNAM, Mexico
Universidade Estadual Paulista, Brazil
Universidade Federal de Minas Gerais, Brazil
Universidade Federal de São Paulo, Brazil
Universität Mainz, Germany
Universität zu Köln, Germany
Université de Montreal, Canada
Université Paris 5 René Descartes, France
University College London, United Kingdom
University Hospital RWTH, Aachen, Germany
University of Montreal Hospital Research Center, Canada
Utrecht University of, The Netherlands

Wellcome/CRC Institute, United Kingdom

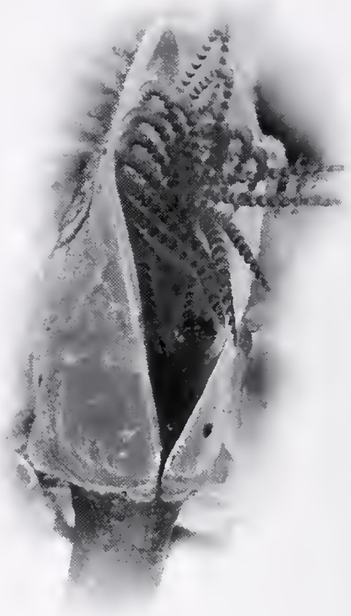

# Resident Research Programs

## *Architectural Dynamics in Living Cells Program*

Established in 1992, this program focuses on architectural dynamics in living cells—the timely and coordinated assembly and disassembly of macromolecular structures essential for the proper functioning, division, motility, and differentiation of cells; the spatial and temporal organization of these structures; and their physiological and genetic control. The program is also devoted to the development and application of powerful new imaging and manipulation devices that permit such studies directly in living cells and functional cell-free extracts. The Architectural Dynamics in Living Cells Program promotes interdisciplinary research carried out by resident core and visiting investigators.

### *Resident Core Investigators*

Inoué, Shinya, Distinguished Scientist
Oldenbourg, Rudolf, Associate Scientist
Shribak, Michael, Staff Scientist

### *Staff*

Knudson, Robert, Instrumental Development Engineer
Baraby, Diane, Laboratory Assistant
MacNeil, Jane, Executive Assistant

### *Visiting Investigators*

Burgos, Mario, IHEM Medical School, Mendoza, Argentina
Goda, Makoto, Japan Biological Information Research Center, Tokyo, Japan
Inoué, Theodore D., Universal Imaging Corporation
Mitchison, Timothy J., Harvard Medical School
Salmon, Edward D., University of North Carolina, Chapel Hill
Tran, Phong, Columbia University

## *The Josephine Bay Paul Center for Comparative Molecular Biology and Evolution*

This Center employs the latest advances in phylogenetic theory, computational biology, and high-throughput genome sciences to study evolutionary processes that trace back to the first life forms on earth. Through the application of high-powered statistical techniques, scientists in the Josephine Bay Paul Center investigate how the evolution of genes and genomes has driven phenotypic change at all levels of biological organization. This holistic approach provides tools to quantify and assess biodiversity and to identify genes and genetic mechanisms of biomedical and environmental importance. We study all kinds of microbes, their evolutionary history, their interactions with each other and macroscopic forms of life, and how members of diverse microbial communities contribute and respond to environmental change. Examples of current research include: 1) a project supported by the National Science Foundation to study the co-evolution of genomes for symbiotic bacteria and their hosts; 2) investigations supported by the National Institutes of Health to study expression and the complete genome sequence of *Giardia lamblia,* a water-borne human pathogen that attacks the intestinal tract and exacts a terrible toll on public health worldwide; 3) a computational biology program funded by the NIH, NASA, and private corporations to integrate evolutionary theory with the functional annotation of protein coding regions in bacterial genomes; and 4) an interdisciplinary study supported by NASA and NSF to study life in extreme environments on the planet earth in search of general principles that can guide the quest for living forms elsewhere in the universe. The Center encourages studies of genotypic diversity across all phyla and promotes the use of modem molecular genetics and phylogeny to gain insights into the evolution of molecular structure and function.

Our research activities are complemented by an active education program. In addition to training postdoctoral fellows, the Josephine Bay Paul Center offers the internationally recognized Workshop in Molecular Evolution at the Marine Biological Laboratory, a workshop for secondary educators titled Living in the Molecular World, and several comprehensive web sites: 1) a description of research and education associated with our membership in the Astrobiology Institute at the Marine Biological Laboratory; 2) the interactive EcoCyc Project (an interactive program that describes the metabolism of *E. coli* as well as the identity and location of functional genes in the *E. coli* genome); 3) the *Giardia lamblia* genome page (which provides annotated analyses and current progress summaries from the MBL's *Giardia lamblia* genome project); and 4) the Workshop in Molecular Evolution site (which offers descriptions, information, and advice about sophisticated software packages for phylogenetic inferences and analyses of population biology data).

A generous gift from the Bay Paul Foundation and continuing annual support from the G. Unger Vettlesen Foundation provided initial funding in 1997 to form The Josephine Bay Paul Center for Comparative Molecular Biology and Evolution. The Center has excellent resources for studies of molecular biology and evolution, including well-equipped research laboratories and a powerful computational facility. With a grant from the W. M. Keck Foundation in 2000, the Center established a technology-rich Ecological and Evolutionary Genetics Facility. This advanced laboratory provides a full range of high-throughput, DNA-sequencing equipment, a DNA microarray facility and high-performance computers. Several adjunct appointments and collaborative projects strengthen research activities in the center. These activities include interdisciplinary investigations of microbial diversity with scientists at the Woods Hole Oceanographic Institution, molecular ecology studies at the MBL Ecosystem Center's Plum Island LTER site, physiology studies of acidophilic protists with the MBL BioCurrents Research Center, and collaborative efforts to study mechanisms and patterns of evolution with faculty of Harvard University, the Harvard School of Public Health, and the University of Sydney, Australia.

Future expansion in the Josephine Bay Paul Center will focus upon molecular evolution of global infectious disease and genome sciences. The Ellison Medical Foundation has provided funding for this new initiative, which over the course of the next two years will add at least three new research groups to the Josephine Bay Paul Center in Comparative Molecular Biology and Evolution.

### *Resident Core Investigators*

Sogin, Mitchell, Director and Senior Scientist
Amaral Zettler, Linda, Staff Scientist I
Cummings, Michael, Assistant Scientist
Edgcomb, Virginia, Staff Scientist I
McArthur, Andrew, Staff Scientist II
Morrison, Hilary, Staff Scientist II
Riley, Monica, Senior Scientist
Wernegreen, Jennifer, Assistant Scientist

### *Adjunct Scientists*

Halanych, Ken, Woods Hole Oceanographic Institution
Meselson, Matthew, Harvard University
Patterson, David, University of Sydney
Teske, Andreas, Woods Hole Oceanographic Institution

### *Visiting Scientists*

Mark Welch, David, Harvard University
Mark Welch, Jessica, Harvard University

### *Executive Assistants*

Lim, Pauline
Nihill, Tara

## *Laboratory of Michael P. Cummings*

Our research is in the area of molecular evolution and genetics and includes examination of patterns and processes of sequence evolution. We use methods from molecular biology, population genetics, systematics, statistics, and computer science. The basis for much of the research is comparative; it includes several levels of biological organization, and involves both computer-based and empirical studies. A major research focus is analysis genotype-phenotype relationships using tree-based statistical models (decision trees) and extension of this methodology. Current investigations in this area examine how gene sequence data can be used to understand and predict drug resistance in tuberculosis, variation in color vision, and basic immune system functions at the molecular level. For example, using drug resistance in *Mycobacterium tuberculosis* as a model system, we are investigating how well phenotype (level of drug resistance) can be predicted with genotype information (DNA sequence data). Understanding evolution of drug resistance, and developing accurate methods for its prediction using DNA sequence data, can help in assessing potential resistance in a more timely fashion and circumvent the need for culturing bacteria. More generally, the relationship of genotype to phenotype is a fundamental problem in genetics, and through these investigations we hope to gain insight. The primary empirical work in the laboratory involves examination of opsins, proteins involved in color vision, from local species of Odonata (dragonflies and damselflies). Other projects include a review of genetic diversity in plants using coalescence-based analyses and the genetic consequences of reserve designs in conservation.

### *Staff*

Cummings, Michael P., Assistant Scientist
McInerney, Laura A., Research Assistant II

### *Visiting Investigator*

Neel, Maile C., University of California, Riverside

### *Visiting Graduate Student*

Winka, Katarina, Umeå University, Sweden

### *Undergraduates*

Chang, Annie, Harvey Mudd College
Harley, Eric T., Harvey Mudd College
Myers, Daniel S., Pomona College

### *High School Student*

Cohen, Alissa, Sturgis Charter School

## *Laboratory of Monica Riley*

The genome of the bacterium *Escherichia coli* contains all of the information required for a free-living chemoautotrophic organism to live, adapt, and multiply. The information content of the genome can be dissected from the point of view of understanding the role of each gene and gene product in achieving these ends. The many functions of *E. coli* have been organized in a hierarchical system representing the complex physiology and structure of the cell. In collaboration with Dr. Peter Karp of SRI International, an electronic encyclopedia of information has been constructed on the genes, enzymes, metabolism, transport processes, regulation, and cell structure of *E. coli*. The interactive EcoCyc program has graphical hypertext displays, including literature citations, on nearly all of *E. coli* metabolism, all genes and their locations, a hierarchical system of cell functions and some regulation and transport processes. The data developed in the work has proven to be valuable to the community of scientists sequencing other genomes. *E. coli* data serve as needed reference points for many genomic projects.

In addition, the *E. coli* genome contains valuable information on molecular evolution. We are analyzing the sequences of proteins of *E. coli* and 49 other organisms in terms of their evolutionary origins. By grouping like sequences and tracing back to their common ancestors, we learn not only about the paths of evolution for all contemporary proteins, but we extend even further back before the last common ancestor, traversing millennia to the earliest evolutionary times when a relatively few ancestral proteins served as ancestors to all contemporary proteins of all living organisms.

### *Staff*

Riley, Monica, Senior Scientist
Goswami, Sulip, Research Assistant II
Murray, Maria, Research Assistant I
Nahum, Laila, Postdoctoral Scientist
Serres, Margerethe, Staff Scientist I

## *Laboratory of Mitchell L. Sogin*

This laboratory employs comparative phylogenetic studies of genes and genomes to define patterns of evolution that gave rise to contemporary biodiversity on the planet earth. The laboratory is especially interested in discerning how the eukaryotic cell was invented as well as the identity of microbial groups that were ancestral to animals, plants, and fungi. The laboratory takes advantage of the extraordinary conservation of ribosomal RNAs to define phylogenetic relationships that span the largest of evolutionary distances. These studies have overhauled traditional eukaryotic microbial classifications systems. The laboratory has discovered new evolutionary assemblages that are as genetically diverse and complex as plants, fungi, and animals. The nearly simultaneous separation of these eukaryotic groups (described as the eukaryotic "Crown") occurred approximately one billion years ago and was preceded by a succession of earlier diverging protist lineages, some as ancient as the separation of the prokaryotic domains. Many of these early branching life forms are represented by parasitic protists including *Giardia lamblia,* which is a significant human parasite. Because of its medical importance and relevance to understanding the evolutionary history of eukaryotes, we have initiated a project to determine the entire genome sequence of *Giardia lamblia.* In addition to identifying other genes that will be of value for unraveling sudden evolutionary radiations that cannot be resolved by rRNA comparisons, this project will provide insights into the presence or absence of important biochemical properties in the earliest ancestors common to all eukaryotic species. Finally, this project has revealed important features of genome architecture that require a reconsideration of available mechanisms for controlling gene expression in eukaryotes.

A second research theme is the study of microbial life in extreme environments and molecular-based investigations of diversity and gene expression in microbial communities. Using the ribosomal RNA database and nucleic acid-based probe technology, it is possible to detect and monitor microorganisms, including those that cannot be cultivated in the laboratory. This strategy has uncovered new habitats and major revelations about geographical distribution of microorganisms. We are particularly interested in protists that thrive in acid mine drainages and the characterization of physiological mechanisms that allow their growth at extraordinarily low ($<2.0$) pH levels. Our investigations of gene expression in microbial communities is based upon the premise that microorganisms are the primary engines of our biosphere. They orchestrate all key processes in geochemical cycling, biodegradation, and in the protection of entire ecosystems from environmental insults. They are responsible for most of the primary production in the oceans. Microbial creatures of untold diversity have complex chemistries, physiologies, developmental cycles, and behaviors. With the powerful tools of high-throughput DNA sequencing and DNA microarrays for massive parallel expression studies, we can directly measure how microbial gene expression patterns in an entire ecosystem respond to changing chemical and physical parameters. We will employ an experimental paradigm that links biogeochemical processes with ever-changing temporal and spatial distributions of microbial populations and their metabolic properties. The concurrent measurement of biogeochemical parameters, community-wide gene expression patterns, and spatial descriptions of microbial populations offers a means to understand the structure and function of biogeochemical machinery at different levels of biological organization. We seek to discover the links between biological diversity and the resilience and stability of biogeochemical transformations.

### *Staff*

Sogin, Mitchell L., Director and Senior Scientist
Amaral Zettler, Linda, Staff Scientist I
Beaudoin, David, Research Assistant
Crump, Amy, Research Assistant
Dhillon, Ashita, Postdoctoral Scientist
Edgcomb, Virginia, Staff Scientist I
Kim, Ulandt, Research Assistant
Kysela, David, Research Assistant
Laatsch, Abby, Research Assistant
Luders, Bruce, Research Assistant
McArthur, Andrew, Staff Scientist II
Morrison, Hilary G., Staff Scientist II
Pacocha, Sarah, Research Assistant
Palacios, Carmen, Postdoctoral Scientist
Shakir, Muhammed Afaq, Postdoctoral Scientist
Ward, Jillian, Research Assistant

### *Consultants*

Olendzenski, Lorraine, University of Connecticut, Storrs
Shulman, Laura

### *Visiting Investigators*

Atkins, Michael, NSF Postdoctoral Scientist
Bahr, Michele, The Ecosystems Center
Campbell, Robert, Serono Laboratories, Inc.
Crump, Byron, The Ecosystems Center
Messerli, Mark, Postdoctoral Scientist

### *High School Student*

Papa, Alexandria, Falmouth High School, Falmouth, MA

## *Laboratory of Jennifer Wernegreen*

The work in this lab focuses on the evolution of bacteria that complete their life cycles within or closely related with eukaryotic host cells. These symbiotic prokaryotes include well-known parasites as well as obligately mutualistic bacteria that provide nutritional or other benefits to their hosts. By virtue of their host associations, endosymbionts may have smaller population sizes and experience different selective forces than their free-living bacterial relatives. These changes in population size and selection may each contribute to the features shared by many endosymbiont genomes, such as low genomic G + C (guanine + cytosine) contents, small genome sizes, and elevated rates of DNA sequence evolution. Our research explores the molecular and evolutionary mechanisms that shape these characteristics of endosymbiont genomes, with a focus on mutualistic endosymbionts of insects and obligate pathogens of animals.

One aim of this lab is to differentiate the effects of genetic drift, directional mutation pressure, and natural selection on molecular evolution of symbiotic and free-living bacteria. Our primary approach has been to compare patterns of DNA sequence divergence at homologous loci across symbiotic and related free-living bacterial species. These comparisons have revealed a strong effect of genetic drift and directional mutational pressure on sequence evolution in *Buchnera aphidicola*, the vertically transmitted endosymbiont of aphids, compared to its close free-living relative, *Escherichia coli*. Recently, our molecular phylogenetic analyses have shown that *Buchnera* lacks horizontal gene transfer that is typical of many free-living bacterial groups. On-going and future work will explore the molecular evolution of other insect endosymbionts in the gamma-3 Proteobacteria, including the obligate bacterial associates of carpenter ants (*Camponotus*). We also employ full genome comparisons to identify genes that have been lost in small endosymbiont genomes, and to compare patterns of genome reduction in mutualistic and pathogenic lineages. Of particular interest is the substantial loss of proof-reading and DNA repair loci from several symbiont genomes, which may elevate mutational rates and biases in these species.

*Staff*

Wernegreen, Jennifer, Assistant Scientist
Degnan, Patrick, Research Assistant
Lazarus, Adam, Research Assistant

## *BioCurrents Research Center*

The current structure of the BioCurrents Research Center (BRC) comprises the core support facility and three independent laboratories, as well as a number of affiliate endeavors where the members of the Center work closely with colleagues in the MBL and regional medical schools. In particular, we have strong links with the MBL program in Architectural Dynamics in Living Cells, the Laboratory for Reproductive Medicine and the Bay Paul Center. Our involvement with regional hospitals includes Boston Medical Center (diabetes), Massachusetts General Hospital (protein trafficking), and Women and Infants (reproductive biology). The core in-house research emphasis is on biophysics of ionic calcium regulation (S. I. McDonough), the molecular biology of ABC-transporters (O. Shirihai), as well as the biophysics and function of transport mechanisms (P. J. S. Smith).

The activities of the BRC are focused on the study of transport mechanisms across the membranes at the molecular, cellular and systemic level. The biological themes studied lie in secretory events along with vesicle transport and docking, channel biophysics, the characterization, molecular biology, and pharmacology of pumps and porters, cellular metabolism, and messenger molecules. Physiological studies have been undertaken on diverse systems, frequently in collaboration with visiting scientists. Notably, hydrogen ion gradients surrounding transporting epithelia have been described in several preparations and the underlying mechanisms studied with the aid of pharmacological and immuno-histochemical tools. Of particular interest has been the physiology of the vacuolar-type proton ATPases and associated transporters. Oxygen gradients surrounding neurons and single cells have been described, as has the release of nitric oxide. Work is also in progress on the adaptations of extremophiles to acidic environments, and we are developing new approaches to study the biophysics of the multi-drug resistant pathway. The latter is part of an infectious disease initiative.

An important component of these studies is the development of new micro-sensor technologies which operate in a self-referencing mode and biomedical application of techniques for the detection of specific molecules, in particular those designed to measure flux of calcium, potassium, chloride, hydrogen, oxygen, nitric oxide, and ascorbate. We offer access to non-invasive ion-selective, electrochemical, and biosensor devices, coupled to advanced imaging techniques and electro-physiological approaches—combinations unique to the BRC. Overall, our emphasis remains on biomedical studies utilizing the specialized micro-sensors available. To meet these objectives the BRC is funded as a resource center through the NIH National Center for Research Resources. The BRC, in addition to its involvement with regional hospitals and medical schools, supports an extensive outreach program to regional and national universities, and publishes extensively.

To further the understanding of the patho-physiology of metabolic disorders, we have recently published the first report of our new generation of self-referencing sensors based on the incorporation of an enzyme, glucose oxidase, with *in vitro* measurements of glucose flux into pancreatic islets. This research offers insight into the mechanisms underlying insulin secretion. Also, a self-referencing micro-sensor was used to detect $H_2O_2$ changes in the nano-molar range near the surface of a single micro-glia cell (macrophages resident in the brain), which can enhance neuro-toxicity of the surrounding tissue. This assay will be useful for quantifying the potential contribution of endogenous micro-glial-induced activators in neurodegenerative diseases.

The BRC has also launched a database on handling and specificity of pharmaceutical compounds targeting transport mechanisms. Public access is available through the BRC web pages at www.mbl.edu/BioCurrents.

In 2001 the BRC hosted 40 short-term visiting scientists at both the national and international level. The majority of the studies were biomedical, with strong collaborative components from regional and national medical schools and hospitals.

*Staff*

Smith, Peter J. S., Director and Senior Scientist
Graf, Solomon, Research Assistant I
Hammar, Kasia, Research Assistant III
Lewis, Robert, Electronic Support
McDonough, Stefan I., Assistant Scientist
McLaughlin, Jane A., Research Assistant III
Moore, Laurel, Research Assistant II
Sanger, Richard, H., Research Assistant III
Shirihai, Orian, Assistant Scientist

### *Post-doctoral Investigators and Graduate Student*

Diarra, Abdoullah, Post-doctoral Scientist
Hengstenberg, Andreas, Post-doctoral Scientist
Jung, Sung-Kwon, Post-doctoral Scientist
Katzman, Shana, Post-doctoral Scientist
Messerli, Mark, NRC Research Fellow

### *Adjunct and Visiting Investigators*

Holz, George, Adjunct Scientist
Khawaled, Radwan, Adjunct Scientist & Visiting Investigator
Liu, Lin, Adjunct Scientist
Trimarchi, James, Adjunct Scientist

### *MBL Research Fellows*

Twig, Gilad, Grass Fellow
Ponka, Prem, Research Fellow
Marom, Shimon, Lipper Research Fellow

## *Laboratory of Stefan McDonough*

Calcium ions trigger many cellular functions including neurotransmission, muscle contraction, regulation of cell membrane excitability, and the activation of enzymatic cascades. A major route of calcium entry into a cell is through voltage-gated calcium ion channels, proteins found in the plasma membrane of every excitable cell and many nonexcitable cells. These proteins form channels that open to allow a selective influx of calcium ions into the cell when the cell fires an electrical spike. Calcium channels are current or potential targets for clinical drugs treating cardiac arrhythmia, epilepsy, hypertension, pain, diabetes, and brain damage after stroke.

Research in this laboratory focuses on the channels that conduct calcium entry, the mechanisms controlling calcium levels within the cell, and the tools to distinguish among different types of calcium channels. Experiments are carried out using patch-clamp electrophysiology on mammalian neurons, mammalian cardiac myocytes, or cloned calcium channels expressed in nonexcitable cells. One effort, in collaboration with the laboratories of Bruce and Barbara Furie and of Alan Rigby, is to identify and characterize conotoxins that target voltage-gated ion channels. Other experiments use the self-referencing ion-selective and oxygen sensors of the BioCurrents Center, in collaboration with the laboratory of Peter Smith. Current areas of research include the effects of zinc ions on calcium channels, a possible cause of ischemic neuronal damage; calcium channel biophysics during the cardiac ventricular action potential; the metabolic cost to the heart of maintaining calcium homeostasis during resting and excited states; and, in collaboration with the lab of Diane Lipscombe, the mechanisms of activation of alternatively spliced forms of neuronal N-type calcium channels.

## *Laboratory of Orian Shirihai*

This lab is applying imaging, biochemical, and proteomics approaches to the study of mitochondrial physiology in differentiating blood cells and in insulin-secreting beta cells. Collaborators include the labs of Stuart Orkin at Harvard Medical School, Prem Ponka at McGill University, and the Interdisciplinary Center for Functional Cellomics at Bar Ilan University. A long-term and fruitful collaboration with Pharmacia Upjohn is allowing the incorporation of proteomics and high throughput technologies into our research. Medically applicable aspects of our research assist drug discovery through this collaboration.

Our Research is focused on important functions carried out by mitochondria in these cells and the consequences of their malfunctioning:

- In differentiating red blood cells, mitochondria are involved with extensive production heme for hemoglobin. Production of heme requires the import of a large amount of iron and the synthesis and transport of heme precursors. Conditions such as sideroblastic anemia, porphyria and myelodysplastic syndrome are all characterized by abnormal heme synthesis and accumulation of heme intermediates and iron. However, the mechanisms of export or import of iron, heme products, and intermediates are as yet unknown. In the past two years we have reported on and investigated the first mitochondrial transporter involved in hemoglobin synthesis. In this project, Solomon Graf is employing protein biochemistry techniques in the study of the transporter structure in the intact mitochondria and its function when reconstituted in artificial proteoliposomes. Alex Sheftel and Prof. Prem Ponka are focusing on the mechanism of iron trafficking to mitochondria. By applying time-lapse fluorescence microscopy, Alex has shown that iron-containing endosomes migrate from the plasma membrane and interact with mitochondria.
- In pancreatic beta cells, mitochondria serve as the fuel processors, incorporating variables such as nutrients and hormonal signaling into insulin secretion. Using confocal microscopy, Shana Katzman and Jakob Wikstrom are looking at mitochondrial activity of individual beta cells in the intact islet and studying the role of various endocrine modulators on fuel processing and insulin secretion. By applying this approach, Shana has demonstrated that diabetic animals show distinctive abnormalities in mitochondrial activity of cells in the intact islet.

Orian Shirihai and the BRC have had an ongoing collaboration since 1996 with the Grass lab to study microglia. The current anti-inflammatory therapeutics used in Alzheimer's disease, such as non-steroidal anti-inflammatory drugs (NSAIDs), only partially suppress microglial activation. We are investigating microglial ion channels in search of new therapeutic modes. Our goal is to reveal the effects on ionic currents of beta amyloid and CGA, the major microglial activators, which are components of the Alzheimer plaque. Gilad Twig, a Grass fellow, used the BRC self-referencing probe and ELISA to monitor the secretion of reactive oxygen radicals and cytokines by microglia, comparing the potency of different activators and inhibitors.

## *Laboratory of Peter J. S. Smith*

The activities of this laboratory center on instrument development, providing new insights into cellular transport mechanisms, and applying these devices to biomedical problems. Much of the biological work is done in collaboration with visiting investigators to the BRC. An increasing body of work has been undertaken using the new amperometric micro-sensors capable of measuring single cell movement of gases such as oxygen and nitric oxide. We continue to investigate the metabolic cost of ion regulation in single cultured neurons and have started a new initiative on the biophysics of the ABC-transporter family in collaboration with Orian Shirihai.

In collaboration with Mitch Sogin of the Bay Paul Center, work is also in progress on the physiological and molecular adaptations of extremophiles to acidic environments. The emphasis is on understanding how membrane-borne transport proteins continue to regulate a near neutral cytosol while being exposed to acidic conditions of pH 1 or 2. This project is funded through the NSF LEXEN program, with researcher Mark Messerli funded by a NRC Fellowship.

In sensor design, we have published the first report on the new generation of amperometric sensors, incorporating an immobilized enzyme. Our attempts have focused on glucose and, with Sung-Kwon Jung, our first single cell glucose flux measurements have been achieved and recently published. Hybrid, electro-optical sensors also have been a focus and, with visiting fellow Andreas Hengstenberg, we have

successfully built a micro-oxygen sensor on the surface of a single mode fiber optic capable of stimulating a preloaded cellular reporter molecule. In collaboration with Stefan McDonough, this technology has been successful in imaging calcium activity while recording oxygen uptake from a single cardiac myocyte.

## *Boston University Marine Program*

*Faculty*

Atema, Jelle, Professor of Biology, Director
Dionne, Vincent, Professor of Biology
Golubic, Stjepko, Professor of Biology
Grasso, Frank, Research Assistant Professor
Kaufman, Les, Associate Professor of Biology
Lobel, Phillip, Associate Professor of Biology
Valiela, Ivan, Professor of Biology
Voigt, Rainer, Research Associate Professor
Ward, Nathalie, Lecturer

*Adjunct Faculty*

Hanlon, Roger, Marine Biological Laboratory
Giblin, Anne, Marine Biological Laboratory
Wainwright, Norman, Marine Biological Laboratory

*Staff*

Gilbert, Niki, Program Coordinator, Boston
Hall, Sheri, Program Manager
Mazzilli, Stefano, Research Assistant, Valiela Lab
McCafferty, Michelle, Program Coordinator
Morano, Janelle, Research Technician, Lobel Lab
Portnoy, David, Research Technician, Lobel Lab
Ripley, Jennifer, Senior Staff Coordinator

*Postdoctoral Investigator*

Kaatz, Ingrid, Lobel Laboratory

*Visiting Faculty*

Hecker, Barbara, Hecker Consulting
Simmons, Bill, Sandia National Laboratory

*Graduate Students*

*PhD Students*

*Existing*
Carmichael, Ruth
Cole, Marci
Kroeger, Kevin
Miller, Carolyn
Oliver, Steven
Skomal, Gregory
Stieve, Erica
Tomasky, Gabrielle
York, Joanna
Zettler, Erik

*New*
Annett, Brendan
Bowen, Jennifer
Grady, Sara
Teichberg, Mirta

*Masters Students*

*Existing*
Atkinson, Abby
Bogomolni, Andrea
Bonacci, Lisa
Casper, Brandon
deHart, Pieter
Errigo, Michael
Estrada, James
Grebner, Dawn
Lever, Mark
Malley, Vanessa
Martel, David
Ojwang, William Oweke
Perez, Edmundo
Pugh, Tracy
Rice, Aaron
Ripley, Jennifer
Rutecki, Deborah
Shriver, Andrea
Stueckle, Todd
Summers, Erin
Sweeny, Melissa
Weiss, Erica
Wittenmyer, Robert

*New*
Florio, Christopher
Hsu, Andrea Chia-Chien
Morschauser, Karen

*Undergraduate Students*

*Spring 01*
Mattei, Bethany
McKay, Breda

*Fall 01*
Al-Qatami, Heba
Balderas, Andrea
Brooke, Samantha
Burdick, Stacy
Cermak, Michael
Colamussi, Lauralea

Dalton, Deborah
Defilippi, Julie
Doty, Alice
Doverspike, Sarah
Dutkiewicz, Laura
Ellis, Karyn
Feldman, Lindsey
Foley, Heather
Fox, Catherine
Gallo, Sarah
Gerwitzman, Aron
Jekielek, Phoebe
Johnson, Margaret
Jordan, Katherine
Marshall, Kristin
Preisner, Karolina
Ramsey, Sara
Smith, Miranda
Smith-Gillen, Jasmine
Solari, Alysa
Szleper, Kathleen
West, Katharine
Wilensky, Chai
Zuck, Michelle

### *Laboratory of Jelle Atema*

Many organisms and cellular processes use chemical signals as their main channel of information about the environment. All environments are noisy and require some form of filtering to detect important signals. Chemical signals are transported by turbulent currents, viscous flow, and molecular diffusion. Receptor cells extract chemical signals from the environment through various filtering processes. In our laboratory, fish, marine snails, and crustacea have been investigated for their ability to use chemical signals under water. Currently, we use the lobster and its exquisite senses of smell and taste as our major model to study the signal-filtering capabilities of the whole animal and its narrowly tuned chemoreceptor cells.

Research in our laboratory focuses on amino acids, which represent important food signals for the lobster, and on the function and chemistry of pheromones used in lobster courtship. We examine animal behavior in the sea and in the lab. This includes social interactions and chemotaxis. To understand the role of chemical signals in the sea, we use real lobsters and untethered small robots. Our research includes measuring and computer modeling odor plumes and the water currents lobsters generate to send and receive chemical signals. Other research interests include neurophysiology of receptor cells and anatomical studies of receptor organs and pheromone glands.

### *Laboratory of Vincent Dionne*

Odors are powerful stimuli. They can focus the attention, elicit behaviors (or misbehaviors), and even resurrect forgotten memories. These actions are directed by the central nervous system, but they depend upon the initial transduction of chemical signals by olfactory receptor neurons in the nasal passages. More than just a single process appears to underlie odor transduction, and the intracellular pathways that are used are far more diverse than once thought. Hundreds of putative odor receptor molecules have been identified that work through several different second messengers to modulate the activity of various types of membrane ion channels.

Our studies are being conducted with aquatic salamanders using amino acids and other soluble chemical stimuli that these animals perceive as odors. Using electrophysiological and molecular approaches, the research examines how these cellular components produce odor detection, and how odors are identified and discriminated.

### *Laboratory of Les Kaufman*

Current research projects in the laboratory deal with speciation and extinction dynamics of haplochromine fishes in Lake Victoria. We are studying the systematics, evolution, and conservation genetics of a species flock encompassing approximately 700 very recently evolved taxa in the dynamic and heavily impacted landscape of northern East Africa. In the lab we are studying evolutionary morphology, behavior, and systematics of these small, brightly colored cichlid fishes.

Another area of study is developmental and skeletal plasticity in fishes. We are studying the diversity of bone tissue types in fishes, differential response to mineral and mechanical challenge, and matrophic *versus* environmental effects in the development of coral reef fishes.

We also study the biological basis for marine reserves in the New England fisheries. We are involved in collaborative research with NURC, NMFS, and others studying the relative impact on groundfish stocks of juvenile habitat destruction *versus* fishing pressure.

### *Laboratory of Phillip Lobel*

Fishes are the most diverse vertebrate group and provide opportunities to study many aspects of behavior, ecology and evolution. We primarily study how fish are adapted to different habitats and behavioral ecology of species interactions. Current research focuses on fish acoustic communications.

We are also conducting a long-term study of the marine biology of Johnston Atoll, Central Pacific Ocean. Johnston Atoll has been occupied continuously by the military since the 1930s and has proven to be a unique opportunity for assessing the biological impacts of island industrialization and its effects on reefs. Johnston Atoll is the site of the U.S. Army's chemical weapons demilitarization facility, JACADS.

### *Laboratory of Ivan Valiela*

A focus of our work is the link between land use on watersheds and consequences in the receiving estuarine ecosystems. The work examines how landscape use and urbanization increase nutrient loading to groundwater and streams. Nutrients in groundwater are transported to the sea, and, after biogeochemical transformation, enter coastal waters. There, increased nutrients bring about a series of changes on the ecological components. To understand the coupling of land use and consequences to receiving waters, we study the processes involved, assess ecological consequences, and define opportunities for coastal management.

A second long-term research topic is the structure and function of salt marsh ecosystems, including the processes of predation, herbivory, decomposition and nutrient cycles.

## *Center for Advanced Studies in the Space Life Sciences*

In 1995, the NASA Life Sciences Division and the Marine Biological Laboratory established a cooperative agreement with the formation of the Center for Advanced Studies in the Space Life Sciences (CASSLS at MBL). The Center's overall goals are to increase awareness of the NASA Life Sciences Program within the basic science community.

The Center sponsored and organized the workshop "The Limits to Self-organization in Biological Systems" in 2001. This workshop was chaired by Scott Camazine, Ph.D., of Pennsylvania State University. At this workshop, leading scientists from social biology and self-organization gathered to discuss key issues in their fields. Peer-reviewed proceedings will be published in *The Biological Bulletin* in June 2002.

CASSLS staff partnered with BUMP and the Marine Resources Center to organize the well-attended Marine Behavior Series at the MBL.

During the summer of 2001, Dr. Richard Wassersug joined us as scholar-in-residence. His projects were related to exploring and promoting public interest in the space life sciences.

Outreach activities included partnering with other institutions to support a statewide middle school science fair offered in Worcester in June 2001. We also worked with Lorraine Olendzenski of the Astrobiology group to offer a successful teacher enhancement workshop, "Life and Living in Space," for 24 high school and community college students.

### *Staff*

Blazis, Diana E. J., Director
Farrell, Heather, Administrative Assistant
Wassersug, Richard, Scholar-in-Residence

## *The Ecosystems Center*

The Ecosystems Center carries out research and education in ecosystems ecology. Terrestrial and aquatic scientists work in a wide variety of ecosystems ranging from the streams, lakes and tundra of the Alaskan Arctic (limits on plant primary production) to sediments of Massachusetts Bay (controls of nitrogen cycling), to forests in New England (effects of soil warming on carbon and nitrogen cycling), and South America (effects on greenhouse gas fluxes of conversion of rain forest to pasture) and to large estuaries in the Gulf of Maine (effects on plankton and benthos of nutrients and organic matter in stream runoff). Many projects, such as those dealing with carbon and nitrogen cycling in forests, streams, and estuaries, use the stable isotopes $^{13}C$ and $^{15}N$ to investigate natural processes. A mass spectrometer facility is available. Data from field and laboratory research are used to construct mathematical models of whole-system responses to change. Some of these models are combined with geographically referenced data to produce estimates of how environmental changes affect key ecosystem indexes, such as net primary productivity and carbon storage, throughout the world's terrestrial biosphere.

The results of the Center's research are applied, wherever possible, to the questions of the successful management of the natural resources of the earth. In addition, the ecological expertise of the staff is made available to public affairs groups and governmental agencies who deal with problems such as acid rain, coastal eutrophication, and possible carbon dioxide-caused climate change.

The Semester in Environmental Science was offered again in Fall 2001. Thirteen students from ten colleges participated in the program. The Center also offers opportunities for postdoctoral fellows.

### *Administrative Staff*

Hobbie, John E., Co-Director
Melillo, Jerry M., Co-Director
Foreman, Kenneth H., Associate Director, Semester in Environmental Science
Berthel, Dorothy J., Administrative Assistant
Donovan, Suzanne J., Executive Assistant
Johnson-Horman, Frances, Administrative Assistant, Semester in Environmental Science
Moniz, Priscilla C., Administrative Assistant, Semester in Environmental Science
Nuñez, Guillermo, Research Administrator
Scanlon, Deborah G., Executive Assistant
Seifert, Mary Ann, Administrative Assistant

### *Scientific Staff*

Hobbie, John E., Senior Scientist
Melillo, Jerry M., Senior Scientist
Felzer, Benjamin, Research Associate
Garcia-Montiel, Diana, Staff Scientist
Deegan, Linda A., Associate Scientist
Giblin, Anne E., Associate Scientist
Herbert, Darrell A., Staff Scientist
Holmes, Robert M., Staff Scientist
Hopkinson, Charles S., Senior Scientist
Hughes, Jeffrey E., Staff Scientist
Kicklighter, David, Research Associate
Marino, Roxanne, Staff Scientist
Nadelhoffer, Knute J., Senior Scientist
Neill, Christopher, Assistant Scientist
Peterson, Bruce J., Senior Scientist
Rastetter, Edward B., Associate Scientist
Shaver, Gaius R., Senior Scientist
Steudler, Paul A., Senior Research Specialist
Tian, Hanqin, Staff Scientist
Vallino, Joseph J., Assistant Scientist

### *Educational Staff Appointments*

Booth, Mary, Postdoctoral Scientist
Broughton, Laura, Postdoctoral Scientist
Buzby, Karen, Postdoctoral Scientist
Crump, Byron, Postdoctoral Scientist
Filoso, Solange, Postdoctoral Scientist
LeDizès-Maurel, Séverine, Postdoctoral Scientist
McClelland, James, Postdoctoral Scientist
Raymond, Peter, Postdoctoral Scientist
Rueth, Heather, Postdoctoral Scientist
Sanzone, Diane, Postdoctoral Scientist
Sommerkorn, Martin, Postdoctoral Scientist
Tobias, Craig R., Postdoctoral Scientist
Williams, Michael R., Postdoctoral Scientist
Zhuang, Qianlai, Postdoctoral Scientist

*Technical Staff*

Ahrens, Toby, Research Assistant
Bahr, Michele P., Research Assistant
Bettez, Neil D., Research Assistant
Burnette, Donald W., Research Assistant
Colman, Benjamin P., Research Assistant
Evans, Jeffrey, Research Assistant
Fox, MaryKay, Research Assistant
Garritt, Robert H., Senior Research Assistant
Gay, Marcus O., Research Assistant
Goldstein, Joshua H., Research Assistant
Hu, Shaomin, Research Assistant
Kelsey, Samuel, Research Assistant
Kicklighter, David W., Senior Research Assistant
Kwiatkowski, Bonnie L., Research Assistant
Laundre, James A., Senior Research Assistant
Lezberg, Ann, Research Assistant
Logan, John, Research Assistant
Lux, Heidi, Research Assistant
Micks, Patricia, Research Assistant
Morriseau, Sara, Research Assistant
O'Brien, Katherine A., Research Assistant
Otter, Marshall L., Research Assistant
Pan, Shufen, Research Assistant
Peterson, G. Gregory, Research Assistant
Randazzo, Suzanne, Research Assistant
Schwamb, Carol, Laboratory Assistant
Slavik, Karie A., Research Assistant
Stieve, Erica, Research Assistant
Thieler, Kama K., Research Assistant
Tholke, Kristin S., Research Assistant
Thomas, Suzanne M., Research Assistant
Tucker, Jane, Senior Research Assistant
Vasiliou, David S., Research Assistant

*Consultants*

Bowles, Francis P., Research Systems Consultant
Bowles, Margaret C., Administrative Consultant

*Visiting Scientists and Scholars*

Galloway, James, University of Virginia
Howarth, Robert, Cornell University
Naiman, Robert, University of Washington
Sheldon, Sallie, SES Faculty Fellow, Middlebury College

## Laboratory of Aquatic Biomedicine

Our laboratory has developed the *Spisula solidissima* embryo model to study mechanisms of neurotoxicology. We have shown that polychlorinated biphenyls (PCBs) selectively target the nervous system during development. We are now linking up and down regulation of the p53 family of genes with neuronal cell development using new probes developed by this laboratory.

In the second line of research, we are using the clam leukemia model to investigate how environmental chemicals influence the progression of leukemia. Further, we are studying whether mutations in p53 alter the pathogenesis of leukemia in populations of *Mya arenaria*. Field work to Nova Scotia showed that leukemia in *Mya* was also detected in Sydney, N.S., which is heavily polluted with a variety of industrial chemicals.

*Staff*

Reinisch, Carol L., Senior Scientist
Cox, Rachel, Postdoctoral Scientist
Kreiling, Jill, Postdoctoral Scientist
Stephens, Ray, Adjunct Scientist

*Visiting Scientists*

Shohet, Stephen, University of California, San Francisco
Walker, Charles, University of New Hampshire

*Students*

Kabat, Daniel, Bronx High School of Science
Miller, Jessica, Boston University

## Laboratory of Paul Colinvaux

With our collaborators in Germany and Finland we brought to a synthesis our reconstruction of the climatic history of Amazonia, an undertaking of nearly two decades that was transferred to the MBL with the founding of this laboratory in 1998. By the year 2000 we had published the conclusion from our pollen analyses of sediments of ancient lakes, showing that forests occupied the Amazon lowlands throughout glacial cycles—contrary to the widespread belief that the forest had been fragmented by aridity in glacial maxima. Based on this reconstruction of a permanently forested Amazon, we concluded that various claims for the existence of fossil dune fields of the Pleistocene age were either mistaken, wrongly dated, or both. These conclusions were tested by G. Irion, of the Senckenberg Institute in Wilhelmshaven, with a ground-truth survey of critical Amazonian sites in February 2001. Dr. Irion reported that our inferences of the non-existence of the proposed Pantanal dune fields, together with the wrong attribution of dunes on Amazon white sands to glacial periods, were correct. With the matter of the dunes resolved, with the available pollen histories largely augmented by our long transglacial pollen history from Maicuru completed in 2000, and with the dating of low-water periods in Amazon lakes firmly correlated to dry season severities triggered by Milankovitch forcing, as shown by our 170,000-year record of sediment chemistry from Lake Pata, it was appropriate to write a new synthesis of Amazon climate and vegetation history. Accordingly, we worked with G. Irion, M. Rasanen of Turku University in Finland, and M. Bush of the Florida Institute of Technology to review all the available data on the paleoecology, paleopedology, geomorphology, and paleoclimatology of Amazonia. The resulting synthesis was published in *Amazoniana* in December 2001.

In a related project we are working with the Lawrence Livermore AMS laboratory and Lamont-Doherty Earth Observatory to test whether tree rings in the widespread neotropical leguminous tree *Hymenaea courbaril* can be reliably correlated with climatic factors. While tree-ring studies from temperate latitudes have proven immensely useful in extending climate records beyond the instrument records, no equivalent records are yet available from tropical America. This laboratory has supplied test samples from Panama and has organized the collecting effort in both Panama and Brazil. The project is still exploratory but, if it proves practical, would hold promise of a significant extension of the instrumental record, of great value to climate modelling.

*Staff*

Colinvaux, Paul, Adjunct Scientist

## Laboratory of Ayse Dosemeci

The laboratory investigates molecular processes that underlie synaptic modification. The main project aims to clarify how the frequency of

activation at a synapse can determine whether the synapse will be potentiated (strengthened) or depressed (weakened) through the participation of an enzyme called CaM kinase II. This enzyme is regulated by autophosphorylation on distinct sites in the presence and absence of calcium. During 2001, studies were continued to test the hypothesis that the temporal pattern of calcium is an important determinant of the phosphorylation state and activity level of CaM Kinase II.

A related project, in collaboration with Dr. T. Reese (NINDS/NIH), concerns the molecular architecture and activity-dependent modification of the postsynaptic density, a multi-protein complex that anchors and organizes neurotransmitter receptors and signal transduction molecules at the receiving end of the synapse. To identify the proteins that make up the complex, a highly pure postsynaptic density fraction was obtained using an affinity-based strategy. Analysis of this fraction indicated the presence of AMPA receptors and one of their anchoring proteins (SAP-97) within the PSD-95-containing complex. Experiments with cultured hippocampal neurons were conducted to characterize activity-induced modifications in the postsynaptic density. These studies indicated that thickening of the postsynaptic density under excitatory conditions is accompanied by increased phosphorylation of CaM Kinase II and that inhibition of phosphatase activity prolongs the observed changes in the structure.

*Staff*

Dosemeci, Ayse, Adjunct Scientist

*Visiting Investigators*

Pozzo-Miller, Lucas, University of Alabama
Lucia Vinade, NIH

## Laboratory of Barbara Furie and Bruce Furie

γ-Carboxyglutamic acid is a calcium-binding amino acid that is found in the conopeptides of the predatory marine cone snail, *Conus*. This laboratory has been investigating the biosynthesis of this amino acid in *Conus* and the structural role of γ-carboxyglutamic acid in the conopeptides. This satellite laboratory relates closely to the main laboratory, the Center for Hemostasis and Thrombosis Research, on the Harvard Medical School campus in Boston; the main focus of the primary laboratory is the synthesis and function of γ-carboxyglutamic acid in blood clotting proteins and the role of vitamin K.

Cone snails are obtained from the South Pacific and maintained in the Marine Resources Center. Until recently, the marine cone snail had been the sole invertebrate known to synthesize γ-carboxyglutamic acid (Gla). The venomous cone snail produces neurotoxic conopeptides, some rich in Gla, which it injects into its prey to immobilize it. To examine the biosynthetic pathway for Gla, we have studied the *Conus* carboxylase which converts glutamic acid to γ-carboxyglutamic acid. This activity has an absolute requirement for vitamin K. The *Conus* carboxylase substrates contain a carboxylation recognition site on the conotoxin precursor. Given the functional similarity of mammalian vitamin K-dependent carboxylases and the vitamin K-dependent carboxylase from *Conus textile*, we hypothesized that structurally conserved regions would identify sequences critical to this common functionality.

Furthermore, we examined the diversity of animal species that maintain vitamin K-dependent carboxylation to generate γ-carboxyglutamic acid. We have cloned full-length carboxylase homologs from the beluga whale (*Delphinapterus leucas*), the toadfish (*Opsanus tau*), and cone snail (*Conus textile*) in order to compare these structures to the known bovine, human, rat, and mouse cDNA sequences. In addition, we have partially cloned the carboxylase gene from chicken (*Gallus gallus*), hagfish (*Myxine glutinosa*), and horseshoe crab (*Limulus polyphemus*). Comparison of the predicted amino acid sequences identified a highly conserved 32-amino acid residue region in all of these putative carboxylases. In addition, this amino acid motif is also present in the *Drosophila* genome and identified a *Drosophila* homolog of the γ-carboxylase. Assay of hagfish liver and *Drosophila* demonstrated carboxylase activity in these non-vertebrates. The predicted amino acid sequence of the carboxylase cDNA from *Conus textile* shows some regions are nearly identical to the mammalian sequence, and that there is about 40% sequence identity overall. This protein has been expressed, and the recombinant enzyme identified as a carboxylase and epoxidase. These results demonstrate the broad distribution of the vitamin K-dependent carboxylase gene, including a highly conserved motif that is likely critical for enzyme function. The vitamin K-dependent biosynthesis of γ-carboxyglutamic acid appears to be a highly conserved function in the animal kingdom.

*Staff*

Furie, Barbara C., Adjunct Scientist
Furie, Bruce, Adjunct Scientist
Begley, Gail, Visiting Scientist
Czerwiec, Eva, Scientist I
Rigby, Alan, Adjunct Scientist
Stenflo, Johan, Visiting Scientist

## Laboratory of Shinya Inoué

Scientists in this laboratory study the molecular mechanism and control of mitosis, cell division, cell motility, and cell morphogenesis, with emphasis on biophysical studies made directly on single living cells, especially developing eggs in marine invertebrates. Development of biophysical instrumentation and methodology, such as the centrifuge polarizing microscope, high-extinction polarization optical and video microscopy, digital image processing techniques including dynamic stereoscopic imaging, and exploration of their underlying optical theory are an integral part of the laboratory's efforts.

*Staff*

Inoué, Shinya, Distinguished Scientist
Baraby, Diane, Research Assistant
Knudson, Robert, Instrument Development Engineer
MacNeil, Jane, Executive Assistant

## *Laboratory of Rudolf Oldenbourg*

We develop microscope instrumentation for investigating the architectural dynamics of living cells and of biological model systems. For non-invasive imaging of biological material, we have developed a new polarized light microscope called the Pol-Scope, which combines microscope optics with electro-optic components, electronic imaging, and digital image processing. The Pol-Scope provides polarization optical measurements, such as birefringence retardation, at unprecedented speed, sensitivity, and resolution over the entire field of view. We use the Pol-Scope to analyze the structural basis of cell motility as it is displayed, for example, in the architectural dynamics of mitotic spindles in dividing cells and of f-actin networks in neuronal growth cones.

### *Staff*

Oldenbourg, Rudolf, Associate Scientist
Shribak, Michael, Staff Scientist I
Knudson, Robert, Instrument Development Engineer
Baraby, Diane, Research Assistant

## *Laboratory of Michael Rabinowitz*

This laboratory investigates environmental geochemistry and epidemiology. Areas of recent activity include modeling lead bioavailability, writing a history of lead biokinetic models, performing a case control survey of tea drinking and oral cancer in Taiwan, quantifying the transport and fate of various sources of residential lead exposure, and serving on several advisory boards of Superfund research projects in Boston and New York.

Current activity focuses on characterizing lead paints and pigments. Hundreds of lead poisoning lawsuits are filed every year against landlords, but no compensation has ever been paid by the half dozen companies that made lead pigments, because it has not been possible to identify the specific manufacturer. This research has been funded by the Eagle Picher Trust. Other activity, sponsored by HUD, involves using stable isotopes of lead to determine the relative importance of various household surfaces (doors, floors, windows, walls) as sources of indoor dust lead levels. Dust lead is the major predictor of childhood lead exposure and poisoning. This would allow for more focused deleading.

Another effort has been using historical fire insurance maps to locate and identify unrecognized hazardous waste sites.

### *Staff*

Rabinowitz, Michael, Associate Scientist

## *Laboratory for Reproductive Medicine, Brown University and Women and Infants Hospital, Providence*

Work in this laboratory centers on investigating cellular mechanisms underlying female infertility. Particular emphasis is placed on the physiology, morphology, and genetics of the oocyte and early embryo, with the aim of assessing the effects of maternal aging and of environmental toxicants on oocyte and embryo developmental potential. Studies taking place at the MBL branch of the Brown/Women and Infants Hospital Laboratory for Reproductive Medicine apply some of the unique instrumentation available through the resident programs directed by Rudolf Oldenbourg and Peter J. S. Smith, including non-invasive methods to analyze dynamic birefringence of meiotic spindles (Pol-Scope) and to study transmembrane ion and gas transport (self-referencing electro-physiological techniques). Specifically, both approaches are yielding new insights into the pathophysiology of apoptotic cell death in oocytes and embryos, which occurs during maternal aging and after exposure to some environmental toxicants.

Our laboratory also studies the role of telomeres on developmental competence of oocytes and embryos. Using a transgenic mouse model, which is null for the enzyme telomerase, and quantitative FISH to measure telomere length, we have demonstrated telomere shortening, aneuploidy, apoptosis, and cell cycle arrest after exposure to reactive oxygen species, generated pharmacologically or by some environmental toxicants with effects on mitochondria. Our laboratory makes extensive use of micromanipulation, including nuclear transfer technology.

Ultimately, the Brown/Women and Infants Hospital Laboratory for Reproductive Medicine aims to translate studies on the pathophysiology of embryo development to produce clinical methods for assessing preimplantation embryo viability, an advance that will significantly contribute to the health of women and children.

### *Staff*

Keefe, David, Director, Adjunct Scientist
Liu, Lin, Adjunct Scientist
Trimarchi, James, Adjunct Scientist

## *Laboratory of Osamu Shimomura*

Aequorin, from the jellyfish *Aequorea aequorea,* was the first calcium-sensitive photoprotein discovered by us in 1961. Because of its high sensitivity to $Ca^{2+}$ and biological harmlessness, the protein has been widely used as a probe to monitor intracellular free calcium levels. Aequorin is a unique protein that contains a high level of energy for light emission in the molecule, and its structure has been the target of many studies in the past. The complete 3-dimensional structure of aequorin was finally obtained by X-ray crystallography 38 years after its discovery, in collaboration with three other laboratories. Aequorin is found to be a globular molecule having four helix-loop-helix "EF-hand" domains, of which three can bind $Ca^{2+}$. The molecule contains coelenterazine-2-hydroperoxide in its hydrophobic core cavity, as the chromophoric ligand which decomposes into coelenteramide and carbon dioxide accompanied by the emission of blue light.

*Staff*

Shimomura, Osamu, Senior Scientist, MBL, and Boston University School of Medicine
Shimomura, Akemi, Research Assistant

## *Laboratory of Robert B. Silver*

The members of this laboratory study how living cells make decisions. The focus of the research, typically using marine models, is on two main areas: the role of calcium in the regulation of mitotic cell division (sea urchins, sand dollars, etc.) and structure and function relationships of hair cell stereociliary movements in vestibular physiology (oyster toadfish). Other related areas of study, *i.e.*, synaptic transmission (squid), are also, at times, pursued. Tools include video light microscopy, multispectral, subwavelength, and very high-speed (sub-millisecond frame rate) photon counting video light microscopy, telemanipulation of living cells and tissues, and modeling of decision processes. A cornerstone of the laboratory's analytical efforts is high performance computational processing and analysis of video light microscopy images and modeling. With luminescent, fluorescent, and absorptive probes, both empirical observation and computational modeling of cellular, biochemical, and biophysical processes permit interpretation and mapping of space-time patterns of intracellular chemical reactions and calcium signaling in living cells. A variety of *in vitro* biochemical, biophysical, and immunological methods are used. In addition to fundamental biological studies, the staff designs and fabricates optical hardware, and designs software for large video image data processing, analysis, and modeling.

*Staff*

Silver, Robert, Associate Scientist

*Visiting Investigators*

Bartman, Marc, Fairfield University
Hummel, John, Argonne National Laboratory
Keller, Bruce, SUNY Upstate Medical University
Kriebel, Mahlon, SUNY Upstate Medical University
Pappas, George, University of Illinois School of Medicine
Rubright, James, Wake Forest University

## *Laboratory of Norman Wainwright*

The mission of the laboratory is to understand the molecular defense mechanisms exhibited by marine invertebrates in response to invasion by bacteria, fungi, and viruses. The primitive immune systems demonstrate unique and powerful strategies for survival in diverse marine environments. The key model has been the horseshoe crab, *Limulus polyphemus. Limulus* hemocytes exhibit a very sensitive LPS-triggered protease cascade which results in blood coagulation. Several proteins found in the hemocyte and hemolymph display microbial binding proteins that contribute to antimicrobial defense. Application of these enzymatic amplification cascades is being applied to life detection goals of NASA in programs of Astrobiology and Planetary Protection. Commensal or symbiotic microorganisms may also augment the antimicrobial mechanisms of macroscopic marine species. Secondary metabolites are being isolated from diverse marine microbial strains in an attempt to understand their role.

*Staff*

Wainwright, Norman, Senior Scientist
Child, Alice, Research Assistant
Williams, Kendra, Research Assistant

*Visiting Investigator*

Anderson, Porter, University of Rochester

## *The Marine Resources Center*

The Marine Resources Center (MRC) is a highly advanced facility for maintaining, culturing, and providing aquatic organisms essential to advanced biological, biomedical, and ecological research. Research is partitioned into two programs: the Program in Sensory Biology and Neuroethology; and the Program in Scientific Aquaculture.

Service and education also play important and complementary roles in this 32,000-square-foot, state-of-the-art facility. The MRC and its life support systems have increased the ability of MBL scientists to conduct research and have inspired new concepts in scientific experiments. The MRC provides a variety of services to the MBL community through its Aquatic Resources Division, its Aquaculture and Engineering Division, and its administrative division.

Research and educational opportunities at the facility are available to established investigators, to postdoctoral fellows, and to graduate and undergraduate students. Investigators and students find that the MRC's unique life support and seawater engineering systems make this a favorable environment in which to conduct masters and doctoral theses and independent research using a variety of aquatic organisms and flexible tank space for customized experimentation on live animals.

The MRC also has a colony of freshwater zebrafish (*Danio rerio*) to serve the MBL community.

*Staff*

Hanlon, Roger, Director and Senior Scientist
Carroll, James, Life Support Technical Assistant
Enos, Edward, Aquatic Resources Division Superintendent
Gilland, Edwin, Research Associate
Grossman, William, Marine Specimen Collector/Diving Safety Officer
Hanley, Janice, Water Quality and Animal Health Technician
Klimm, William, Licensed Boat Captain—R/V *Gemma*
Kuzirian, Alan, Associate Scientist
Linnon, Beth, Special Projects Coordinator
Mebane, William, Aquaculture and Engineering Division Superintendent
Santore, Gabrielle, Executive Assistant
Sexton, Andrew, Marine Organism Shipper
Smolowitz, Roxanna, MBL Veterinarian
Sullivan, Daniel, Boat Captain
Tassinari, Eugene, Senior Biological Collector
Whelan, Sean, Diver/Marine Specimen Collector

*Seasonal Employees and Volunteers*

Carroll, Amanda, Volunteer
Colamussi, Lauralea, Intern, Boston University
Dimond, Jay, Diver/Collector
Dutkiewicz, Laura, Intern, Boston University
Follett, Chris, Pre-intern, Acton Boxboro Regional High School
Gannon, George, Intern, Massachusetts Bay Community College
Henderson, Tracy, Intern, Cape Cod Community College
Lemieux, Joan, AmeriCorps Senior Member

Liszewski, Ted, AmeriCorps Senior Member
Kosky, Pat, AmeriCorps Senior Member
Lewis, Chloe, Pre-intern, Phillips Academy
Magliozzi, Amanda, Intern, University of Massachusetts at Dartmouth
McAuley, Casey, Pre-intern, Marshfield High School
Nelson, Birgit, AmeriCorps Senior Member
Olliver, Carl, AmeriCorps Senior Member
Potter, Ben, Diver/Collector
Ramsey, Sara, Intern, Boston University
Reynolds, Justin, Diver/Collector
Sterling, Christian, Diver/Collector

### *Laboratory of Roger Hanlon*

This laboratory investigates the behavior of cephalopods and other marine organisms, with an integrative biology approach focused at the organismal level. Molecular, cellular, and ecological approaches are used to complement this organismal approach, and there is emphasis on sensory biology and behavioral ecology.

Laboratory studies on the mechanisms and functions of polarized light sensitivity in cephalopods are underway. Olfactory sensing by *Nautilus* (which functions in food detection and location as well as mate choice) is being studied in the laboratory. Visual features that octopuses and cuttlefish use for maze learning are also being investigated. Lab experiments in large indoor seawater tanks are being conducted to determine how male squids, *Loligo pealeii*, use visual, then contact chemical cues in egg capsules to initiate highly robust agonistic behavior.

The functional morphology and neurobiology of the chromatophore system of cephalopods are studied on a variety of cephalopod species, and image analysis techniques are being developed to study crypsis and the mechanisms that enable cryptic body patterns to be neurally regulated by visual input. Various aspects of predation, antipredator defenses, and reproduction are conducted in field sites worldwide.

Sexual selection theory is being tested using squid and cuttlefish. Field and laboratory studies focus on mechanisms of agonistic behavior, female mate choice, and sperm competition. The latter studies involve DNA fingerprinting to determine paternity and help assess alternative mating tactics.

Population structure and reproductive success in several highly valuable squid fisheries (*Loligo vulgaris reynaudii* in South Africa, *Loligo pealeii* in the NE United States, *Loligo opalescens* in California) are being assessed for fishery management and conservation. We also culture species of commercial and biomedical importance in the sophisticated seawater systems of the Marine Resources Center. For example, the toadfish *Opsanus tau* is used in vestibular research related to human medicine, yet the species is difficult to obtain from nature. Thus, we are performing the first mariculture experiments to culture toadfish through the life cycle to provide the biomedical community with high-quality experimental animals. Such an approach lightens the impact of collecting toadfish from the natural environment.

#### *Staff*

Hanlon, Roger, Senior Scientist
Boal, Jean, Adjunct Scientist
Buresch, Kendra, Research Assistant
Gilles, Nicole, Research Assistant
Richmond, Hazel, Research Assistant
Shashar, Nadav, Adjunct Scientist
Sussman, Raquel, Associate Scientist
Tubbs, Mollie, Research Assistant

#### *Visiting Investigators*

Baker, Robert, New York University
Chiao, Chuan-Chin, Postdoc, Howard Hughes Medical Institute
DeBose, Jennifer, Flower Garden Banks National Marine Sanctuary
Grable, Melissa, Graduate Student, Boston University Marine Program
Kangas, Nuutti, Postdoc, Academy of Finland
Karson, Miranda, Graduate Student, Michigan State University
Mensinger, Allen, University of Minnesota at Duluth
Saidel, William, Rutgers University

#### *Interns*

Abendroth, Angie, Intern, Ripon College
Erwin, Alexis, Intern, Brown University
Knowles, James, REU Intern, Colgate University
Nichols, Amy, Intern, Millersville University of Pennsylvania
Rostron, Amy, Intern, Richard Stockton College of New Jersey
Roy, Becka, Pre-intern, Cape Cod Academy
Sit, Stephanie, Intern, University of California at Santa Cruz
Tungate, Katherine, Intern, Mount Holyoke College

### *Laboratory of Alan Kuzirian*

Research in the laboratory explores the functional morphology and ultrastructure of various organ systems in molluscs. The program includes mariculture of the nudibranch, *Hermissenda crassicornis*, with emphasis on developing reliable culture methods for rearing and maintaining the animal as a research resource. The process of metamorphic induction by natural and artificial inducers is also being explored. Morphologic studies stress the ontogeny of neural and sensory structures associated with the photic and vestibular systems that have been the focus of learning and memory studies. Concurrent studies include behavioral and cytochemical investigations of the $Ca^{2+}$/GTP binding protein, calexcitin, and its modulation with learning and lead exposure, as well as its role in short- and long-term memory.

Active research also includes population genetic studies using RAPD-PCR DNA fingerprinting techniques to assess the standing stocks and population structure of bay scallops (*Argopecten irradians*), sea scallops (*Placopecten magellanicus*), Atlantic goosefish (*Lophius americanus*) and yellowtail flounder (*Limanda ferruginea*) in the Northeast Fisheries Region.

Collaborative research focuses on histochemical investigations of strontium's role in initiating calcification in molluscan embryos (shell and statoliths), immuno-cytochemical labeling of cell-surface antigens, neurosecretory products, second messenger proteins involved with learning and memory, as well as intracellular transport vesicles in squid (*Loligo pealeii*) giant axons and *Hermissenda* sensory and neurosecretory neurons. Additional collaborations involve studying neuronal development of myelin, myelination defects, and nerve regeneration and repair in phylogenetically-conserved vertebrate nervous systems.

Systematic and taxonomic studies—including molecular phylogenetics—of nudibranch molluscs are also of interest.

#### *Staff*

Kuzirian, Alan, Associate Scientist
Chikarmane, Hemant, Investigator
Dengler, Robbin, Research Assistant

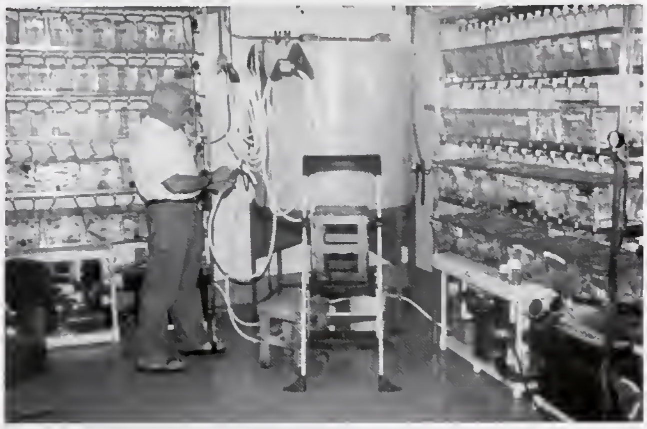

*Visiting Investigators*

Child, Frank, Trinity College
Clay, John, National Institutes of Health
Epstein, Herman
Gould, Robert, New York State Institute for Basic Research

*Interns*

Bechtel, Deanna, Intern, Massachusetts Maritime Academy
Carroll, Ian, REU Intern, Brown University
Honsberger, Sarah, AmeriCorps Member
Kalowski, Lee, Intern, Union College
McGrath, Sarah, Intern, University of Massachusetts at Dartmouth
Terry, Eleanor, Pre-intern, Maret School

### *Laboratory of Roxanna Smolowitz*

This laboratory investigated the pathogenesis of aquatic animal diseases using traditional pathological methods combined with *in situ* molecular methods. Research conducted during 2001 included 1) examination of hard clam strains susceptibility to a protistan disease agent named Quahog Parasite Unknown and the methods of transmission of that organism between infected and uninfected animals; 2) detection of disease-causing, protozoan organisms (MSX and SSO) in eastern oysters using PCR and *in situ* staining techniques; 3) evaluation of inbred strains of oyster for resistance to the above diseases *vs.* productivity as commercial aquaculture stock; and 4) investigation into the causes of lobster shell disease.

*Staff*

Smolowitz, Roxanna, MBL Veterinarian
Balderas, Andrea, Work-study Student, Boston University
Ehlen, Jill, Research Assistant
Hsieh, Jen, AmeriCorps Member
Hsu, Andrea, Work-study Student, Boston University
Stukey, Jetly, Research Assistant
Summers, Erin, Work-study Student, Boston University
Tirrell, Kerri-Ann, AmeriCorps Member

*Interns*

Bahrawy, Dina, Intern, Cornell University College of Veterinary Medicine
Hunt, Kyle, Pre-intern, Mashpee High School
Reynolds, Taylor, Veterinary Intern, North Carolina State University College of Veterinary Medicine

# Honors

## *Friday Evening Lectures*

| | |
|---|---|
| June 15 | Judah Folkman, Children's Hospital, Harvard Medical School<br>"Angiogenesis Research: From Laboratory to Clinic" |
| June 22 | Keith Campbell, University of Nottingham, United Kingdom<br>"Cloning Dolly: How and Why?" |
| June 29 | Keith Gull, University of Manchester, United Kingdom<br>"Genomes and Gene Function in Parasites: New Hope for Understanding and Intervention" |
| July 6 | Randolf Menzel, Freie Universität Berlin<br>"A Mini Brain with Mega Power: The Honeybee" |
| July 13 | Elaine Fuchs, University of Chicago<br>"Cell Adhesion, the Cytoskeleton, and Morphogenesis in Skin" |
| July 20 | Colleen Cavanaugh, Harvard University<br>"Exploration in the Deep Sea: Sulfur Springs, Symbiosis, and Microbial Diversity" |
| July 26, 27 | Bert Sakmann, Max Planck Institute, Germany<br>I. "The Eloquent Cerebral Cortex"<br>II. "$Ca^{2+}$ Dynamics at the Two Business Ends of CNS Neurons" |
| August 3 | Avram Hershko, The Technion, Israel<br>"How and Why Cells Destroy Their Proteins" |
| August 10 | Paul Greengard, The Rockefeller University<br>"Signal Transduction in the Brain" |
| August 17 | J. Craig Venter, Celera Genomics<br>"Sequencing the Human Genome" |

## *Fellowships and Scholarships*

*In 2001, the MBL awarded research fellowships to 15 scientists from around the world. The MBL awarded scholarships to 80 students in the MBL's summer courses as well as 5 post-course research awards. Donors provided gifts for endowed and expendable funds amounting to $2,577,854 in support of the research fellowships program and an additional $440,749 to provide scholarships to students in MBL courses. Those funds that received donations in 2001 are listed below. The individuals who received fellowships and scholarships are listed beginning on p. R60.*

### The Bruce and Betty Alberts Endowed Scholarship in Physiology

Dr. and Mrs. Bruce M. Alberts

### Robert Day Allen Fellowship Fund

Drs. Joseph and Jean Sanger

### Frederik B. Bang Fellowship Fund

Mrs. Betsy G. Bang

### Max Burger Endowed Scholarship for the Embryology Course

Dr. Max M. Burger

### John and Elisabeth Buck Endowed Scholarship

Dr. and Mrs. David Hibbitt

### Laura and Arthur Colwin Fellowships

Drs. Arthur L. and Laura H. Colwin

### Charles R. Crane Fellowship Fund

Thomas S. Crane and Friendship Fund, Inc.

### John O. Crane Fellowship Fund

Thomas S. Crane and Friendship Fund, Inc.

### Jean and Katsuma Dan Fellowship Fund

Mrs. Eleanor Steinbach
Drs. Joseph and Jean Sanger

### Bernard Davis Fellowship Fund

Mrs. Elizabeth M. Davis

### The Mac V. Edds, Jr. Endowed Scholarship Fund

Dr. Louise M. Luckenbill-Edds

### Daniel S. and Edith T. Grosch Scholarship Fund

Ms. Laura Grosch and Mr. Herb Jackson

### Aline D. Gross Scholarship Fund

Dr. and Mrs. Paul R. Gross
Dr. and Mrs. Lewis P. Rowland
Technic, Inc.

### The Gruss Lipper Fund

The Gruss Lipper Foundation

### E. E. Just Endowed Research Fellowship Fund

The Cole Memorial Family Fund
Mr. and Mrs. Jonathan Conrad
Fiduciary Trust Company
William Townsend Porter Foundation
Georgia-Pacific Corporation

### Fred Karush Endowed Library Readership

Mrs. Sally Karush
Dr. and Mrs. Laszlo Lorand
Dr. and Mrs. Arthur M. Silverstein

### Keffer Hartline Fellowship Fund

Dr. Earl Weidner

### William Randolph Hearst Foundation Scholarship

William R. Hearst Foundation

### S. O. Mast Founders' Scholarship Fund

Dr. and Mrs. David Hibbitt

### MBL Associates Endowed Scholarship Fund

MBL Associates
Mrs. Nawrie Meigs-Brown

### Charles Baker Metz and Charles William Metz Scholarship Fund in Reproductive Biology

Mrs. Grace S. Metz

### James A. and Faith Miller Fellowship Fund

Drs. David and Virginia Miller

### Mountain Memorial Fund

Dr. and Mrs. Dean C. Allard, Jr.
Ms. Brenda J. Bodian
Mr. and Mrs. Thomas H. Roberts

### Emily Hartshorne Mudd Scholarship Fund

World Academy of Art and Science

### Neural Systems and Behavior Scholarship Fund

Mr. Srdjan D. Antic
Dr. Elizabeth Debski
Dr. and Mrs. Alan Gelperin
Dr. Warren M. Grill
Drs. William Kristan and Kathleen French
Dr. Mark W. Miller
Drs. Janis C. Weeks and William M. Roberts
Ms. M. Jade Zee

### Nikon Fellowship

Nikon Instruments Inc.

### The Plum Foundation John E. Dowling Fellowship Fund

The Plum Foundation

### William Townsend Porter Scholarship Fund for Minority Students

William Townsend Porter Foundation

### Phillip H. Presley Scholarship Fund

Carl Zeiss, Inc.

### Florence C. Rose and S. Meryl Rose Endowed Scholarship Fund

Dr. Gwynn Akin Bowers
Dr. Elizabeth D. Hay
Dr. B. Elizabeth Horner
Dr. and Mrs. Anthony Liuzzi
Dr. and Mrs. Merle Mizell
Drs. Betty C. and John A. Moore
Mr. and Mrs. John Oberpriller
Dr. Christina and Mr. Lawrence Richards
Mrs. Florence C. Rose
Mrs. Elizabeth H. Rose-Corrington
Drs. Priscilla and John Roslansky
Mr. and Mrs. Marc Shulman
Mr. Matthew Shulman
Dr. and Mrs. Stephen D. Smith
Dr. John B. Stanbury
Dr. and Mrs. Robert A. Weinberg

### The Catherine Filene Shouse SES Scholarship Fund

The Catherine Filene Shouse Foundation

### The Catherine Filene Shouse Scholarship Fund

The Catherine Filene Shouse Foundation

### The Catherine Filene Shouse Fellowship Fund

The Catherine Filene Shouse Foundation

### Science Writing Fellowships Program

American Society for Biochemistry & Molecular Biology
The American Society for Cell Biology
American Society for Photobiology
Federation of American Societies for Experimental Biology
The New York Times Company Foundation
NASA Astrobiology Institute
NIH National Cancer Institute
NIH Office of Science Education
NSF Office of Polar Programs
The Times Mirror Foundation
Waksman Foundation for Microbiology

### The Evelyn and Melvin Spiegel Fellowship Fund

The Sprague Foundation
Drs. Joseph and Jean Sanger

### H. B. Steinbach Fellowship Fund

Mrs. Eleanor Steinbach

### Horace W. Stunkard Scholarship Fund

Drs. Albert Stunkard and Margaret Maurin

### Eva Szent-Gyorgyi Scholarship Fund

Dr. and Mrs. Laszlo Lorand
Dr. Vivianne Nachmias
Drs. Joseph and Jean Sanger
Dr. Andrew and Ms. Ursula Szent-Gyorgyi

### Universal Imaging Fellowship Fund

Universal Imaging Corporation

### Walter L. Wilson Endowed Scholarship

Dr. Paul N. Chervin
Dr. Jean R. Wilson
Mr. and Mrs. Wayne V. Wilson

### Young Scholars/Fellows Program

Dr. and Mrs. David E. Adelberg
Drs. James and Helene Anderson
Dr. and Mrs. Thomas L. Benjamin
Rev. and Mrs. Worthington Campbell, Jr.
Mr. and Mrs. James M. Cleary
Dr. and Mrs. Maynard M. Cohen
Drs. Harry Conner and Carol Scott-Conner
Dr. and Mrs. Sherwin J. Cooperstein
Mr. and Mrs. Thomas Crane
Dr. and Mrs. John M. Cummings
Ms. Dorothy L. Drummey
Dr. and Mrs. Albert Grossman
Mr. and Mrs. Gary G. Hayward
Mr. and Mrs. Paul W. Knaplund
Dr. M. Lynne McAnelly
Mr. and Mrs. Archie T. Morrison
Dr. and Mrs. Harris Ripps
Drs. Dorothy Skinner and John Cook
Dr. and Mrs. Edward A. Spiegel
Mr. and Mrs. David Stone
Dr. and Mrs. Edwin W. Taylor
Dr. and Mrs. Kensal E. Van Holde
Ms. Sylvia Vatuk and Mr. George Rosen
Mr. and Mrs. Henry Wheeler
Drs. Jonathan and Beatrice Wittenberg

## *Fellowships Awarded*

### MBL Summer Research Fellows

- Peter Burbach, Ph.D., is Director of Research at the Department of Medical Pharmacology and Anatomy, Rudolf Magnus Institute for Neurosciences, University Medical Center Utrecht, The Netherlands. His research project was titled, "Homeobox Codes in the Stellate and Optic Ganglia of the Squid." His recent research has focused on homeobox cascades in the developmental specification of neuronal systems, particularly in establishing transmitter identity and neuronal connectivity, using the mouse as a model. He wants to exploit the unique morphological and functional properties of the stellate and optic neurons of the squid to define such homeobox codes for two classes of homeobox subfamilies. Adult squid as well as squid in various embryonic and posthatching developmental stages will be used. The results of this study will help direct research in mammalian and fly systems. Dr. Burbach was funded by the *MBL Associates, Baxter Postdoctoral Fellowship Fund, H. Burr Steinbach Memorial Fellowship Fund,* and the *James A. and Faith Miller Fellowship Fund.*

- David Burgess, Ph.D., is a Professor of Biology at Boston College, Chestnut Hill, Massachusetts. The title of his research project was "Control of Cytokinesis." He is interested in how cells change shape or form and how that is precisely regulated using the cytoskeleton. Specifically, he studies how timing and placement of the contractile ring is coupled to mitotic controls in cell division. Investigations are underway on the timing of cytokinesis as a function of the delivery of a positive cleavage stimulus to the cortical cytoskeleton and on the response system orchestrating the assembly and dynamics of the contractile ring. He followed up on work begun last summer by focussing on the source of new plasma membrane needed to increase the surface area of the cells during cytokinesis. His primary research organisms are sea urchins and sand dollars. Dr. Burgess was funded by the *Josiah Macy, Jr. Foundation.*

- Chris Cameron, Ph.D., is currently a Research Associate in the Department of Marine Science, The University of Texas at Austin, Marine Science Institute, Port Aransas, Texas. His research focussed on "Cell Lineage Studies of Hemichordate Worms: Clues to the Ancestral Developmental Patterning of Deuterostomes and the Origin of the Chordates." He proposed to construct a fate map by marking defined regions of the egg and early cleavage stage embryo in the hemichordate worms *Schizocardium* and *Saccoglossus.* These fate maps will establish where gastrulation is initiated, follow morphogenetic movements during early development, find out if the principal body axes are correlated with certain planes of cleavage, and establish which cells of the early cleavage stage embryo normally become the different components of the larvae. His research will also compare developmental patterning between these species that represent two superfamilies, and between echinoderms and chordates. Dr. Cameron was funded by the *Evelyn and Melvin Spiegel Fellowship Fund* and the *MBL Associates.*

- Cecilia Canessa, M.D., is an Associate Professor in the Department of Cellular and Molecular Physiology and Medicine, Yale University, New Haven, Connecticut. The title of her research project is "Activation of ASIC1 Channels by Synaptic Transmission in the Giant Synapse from Squid." The purpose of this research project is to test the hypothesis that protons released during synaptic transmission can activate the acid-sensitive channel 1 (ASIC1). She used the giant synapse of the stellate ganglion from squid (*Loligo pealei*) as the experimental model. The main focus of this research is the characterization of the structure-function and regulation of channels from the EnaC/Degenerin family. The recent cloning of new members of this family, the mammalian ASIC channels, has opened new avenues of research to define the functional role(s) of these channels in the nervous system. Dr. Canessa was funded by The *Catherine Filene Shouse Foundation.*

- Fred Chang, M.D., Ph.D., is Assistant Professor in the Department of Microbiology, Columbia University, New York, New York. His research was titled "Spatial Regulation of Cellular Architecture: Development of Multi-wavelength, 3D, Time-lapse Microscopic Imaging and Photo-ablation in Living Yeast Cells." He studies the molecular mechanisms of spatial organization using genetics and microscopy approaches in fission yeast, *Schizosaccharomyces pombe.* Dr. Chang set up microscopy stations for high speed, time-lapse, Z-series, multiple wave-length fluorescence digital acquisition and for blue-green laser-mediated photo-ablation (GFP-assisted CALI) in living cells. The research explored mechanisms of nuclear positioning and intracellular motility of cell polarity and cytokineses factors and shed light on how fusion proteins to GFP and other fluorescent proteins can be used to probe the function of sub-cellular structures to establish spatial architecture in cells. Dr. Chang was funded by *Nikon Instruments Inc.*

- Mariano A. Garcia-Blanco, M.D., Ph.D., is an Associate Professor of Genetics, Microbiology and Medicine, Duke University Medical Center, Durham, North Carolina. He has been named a Raymond and Beverly Sackler Scholar and is a member of the Biochemistry Study Section of the National Institutes of Health. The title of his research project was "Elongation Dynamics of DNA Dependent RNA Polymerases." His research focuses on RNA transport in the nucleus and between the nucleus and the cytoplasm as well as the proteins responsible for this transport mechanism. He also studies the enzymes that are functionally relevant to transactivation of the HIV promoter. In his previous work at the MBL, he and his colleagues built an evanescent wave microscope that allows scientists to visualize single molecule enzymology and mechanics. Dr. Garcia-Blanco was funded by *The Josiah Macy, Jr. Foundation.*

- Yosef Gruenbaum, Ph.D., is a Professor in the Department of Genetics, The Institute of Life Sciences, The Hebrew University of Jerusalem, Jerusalem, Israel. The title of his research project was "The Molecular Basis of Lamina Activity in *Spisula solidissima.*" The lamina is involved in nuclear organization, cell cycle regulation, transcriptional repression, cell differentiation and apoptosis. Mutations in protein components of the lamina and the lamin-associated protein, emerin, give rise to a range of inherited life threatening diseases, including various dystrophies and cardiomyopathies. The proposed research will address fundamental questions about the function of the nuclear lamina, by identifying evolutionarily conserved residues in lamin and emerin and testing the role of these residues in lamin-emerin interactions. Dr. Gruenbaum was funded by the *Gruss Lipper Foundation.*

- George Langford, Ph.D., is the Ernest Everett Just Professor of Natural Sciences and Professor of Biological Sciences at Dartmouth College, Hanover, New Hampshire. His research project was titled, "Actin-based Vesicle Transport in the Squid Giant Axon." It has been shown recently that vesicles contain multiple types of motors including actin-based and microtubule-based as well as plus-end and minus-end directed motors. In addition to the finding that multiple types of motors are present, current studies show that different types of motors interact with each other on the vesicle to produce a "hetero-motor" complex. He studied the mechanism by which vesicle transport on microtubules and actin filaments is coordinated and regulated. He tested the hypothesis that myosin V and kinesin form a complex on vesicles through tail-tail interactions and that feedback between the two proteins facilitates the transition of vesicles from microtubules to actin filaments. This work has a bearing on the regeneration of nerve cells after spinal injury. Dr. Langford was funded by the *Josiah Macy, Jr. Foundation.*

- Shimon Marom, M.D., Ph.D., is an Associate Professor in the Department of Physiology and Biophysics, Technion-Israel Institute of Technology, Haifa, Israel. The title of his research was "Learning in Networks of Cortical Neurons: Rewarding by Stimulus Removal." In the process of learning, "appropriate" stimulus-response associations are selected over many other "inappropriate" ones. The principles underlying this selection are usually thought of in terms of a reward system, realized in the form of a neuromodulator that is released from a unique set of neurons after the occurrence of a salient event. The results of his recent research challenge this view by demonstrating selective learning in a cortical network without a neural rewarding entity. His research explored the hypothesis that the learning network involves clear changes in calcium dynamics. In addition, he explored the possibility that using voltage sensitive dyes will enhance the spatial resolution of the neural activity groups involved in the "learning" process. Dr. Marom was funded by the *Gruss Lipper Foundation.*

- Katsuya Miyake, Ph.D., is a Research Fellow in the Department of Cellular Biology and Anatomy, Institute for Molecular Medicine and Genetics, The Medical College of Georgia, Augusta, Georgia. The title of his research was "Resealing of Plasma Membrane Disruption in Sea Urchin Eggs," which investigates how cells repair tears in their surface covering. Rapid resealing of the disrupted plasma membrane is a crucial first step in repair, since otherwise cell death rapidly ensues. He plans to develop a quantitative assay for the wound-induced endocytotic response, and use this assay to define its time course, and its basic characteristics, including: 1) dependence, if any, on external $Ca^{2+}$ and $Ca^{2+}$ channels; 2) dependence, if any, on actin and/or microtubule-based cytoskeleton; 3) dependence, if any, on phosphoinositide 3-kinase activity. Dr. Miyake was funded by *The Frederik B. Bang Fellowship Fund.*

- Prem Ponka, M.D., Ph.D., is Professor of Physiology and Medicine at McGill University, Montreal, Canada. The title of his research project was "Endosome-Mitochondria Interaction in Erythroid Cells: Role in Efficient Iron Trafficking for Heme Synthesis." Iron plays a fundamental role in vital processes such as oxygen transport, electron transfer and DNA synthesis. His research will focus on the mechanisms involved in the acquisition and intracellular transport of iron in immature red blood cells. Defects either in iron acquisition by red blood cells or in its translocation within the cells lead to anemias. He conducted time-lapse fluorescence microscopy studies to investigate the mechanism and regulation of endosome-mitochondria interactions and investigated the unique mechanism that protects cells from iron overload. This research will be important for understanding some of the anemias occurring in humans. Dr. Ponka was funded by *The Universal Imaging Corporation Fellowship Fund.*

- Lawrence Schwartz, Ph.D., is a Professor in the Department of Biology, University of Massachusetts, Amherst, Massachusetts. Dr. Schwartz is planning to write a book that introduces the topic of cell death to general audiences. While he has been active in the field of programmed cell death for the past 25 years, he notes there has been an explosive interest since the mid-90's. It is now known that all cells "know" how to commit suicide and mis-regulation of this process is the basis for the majority of human diseases, *e.g.*, inappropriate suicide by valuable cells results in the loss of neurons in Alzheimer's Disease or CD4+T cells in HIV infection. He believes that the field has matured sufficiently and is ready for a book covering the history, biology, and clinical relevance of cell death for non-scientists. Dr. Schwartz was funded *by The Erik B. Fries Endowed Fellowship, The Frank A. Brown Memorial Readership,* and the *Fred Karush Endowed Library Readership.*

- Nadav Shashar, Ph.D., is an Assistant Professor at the Hebrew University of Jerusalem and the H. Steinitz Interuniversity Institute, Eilat, Israel. The title of his research was "Predator-Prey Interactions in the Visual Domain-Polarization Vision in Squid and their Planktonic Prey." The research addressed four specific issues in the context of interactions between squid and their prey: 1) Field measurements of the polarization of ambient light at night; 2) examining potential human impact; 3) electrophysiological examination of partial polarization limitations to polarization sensitivity of squid; and 4) examining polarization sensitivity (PS) in planktonic crustaceans. His research evaluated the actual ambient conditions and physiological limitations in which polarization vision operates. It will further provide information as to whether PS is uniquely available only to the predator, or to both predator and prey acting on the same playing field. Dr. Shashar was funded by the *H. Keffer Hartline Fellowship Fund,* the *Lucy B. Lemann Fellowship Fund,* and the *Plum Foundation John E. Dowling Fellowship Fund.*

- Iain Stuart Young, Ph.D., is a Research Associate in the Department of Biology at the University of Pennsylvania, Philadelphia, Pennsylvania. The title of Dr. Young's summer research was "Molecular Mechanism of Relaxation and Contraction in Toadfish (*Opsanus tau*) Superfast Muscle." He studied muscle fiber design and function to understand how a given system is fine-tuned to provide optimal performance under a variety of conditions. He researched the toadfish swimbladder, as it is the fastest muscle found in any vertebrate (vibrating at 200 times a second). This study examined the molecular processes of activation and relaxation using calcium-sensitive fluorescent dyes to determine the definitive $Ca^{2+}$ stored in the sarcoplasmic reticulum (SR). He also determined the rate of ATP use by the $Ca^{2+}$ pumps. Dr. Young's research will assist in the explanation of myopathies that include increased fatigability of muscle. Dr. Young was funded by the *Frederik B. Bang Fellowship Fund, The Charles R. Crane Fellowship Fund, The John O. Crane Fellowship Fund,* and the *MBL Associates.*

- Michael Zochowski, Ph.D., is a Postdoctoral Fellow in the Department of Molecular and Cellular Physiology, Yale University School of Medicine, New Haven, Connecticut. The title of his research was "Characterization of Spatio-Temporal Changes in Oscillatory Response to Multiple Odor Stimulation in Turtle Olfactory Bulb." The aim of the proposed research was to understand the mechanisms underlying formation of odor evoked oscillations in the turtle olfactory bulb. Specifically, he characterized how the rostral, middle, and caudal oscillations change their character dramatically when additional odor pulses are applied within a short time period (1–20 s). The olfactory bulb responds differently to the second and third presentation of odors and the two mechanisms that may produce this effect are lateral inhibition induced by the first odor presentation and/or habituation effects. The experimental data was used to construct a dynamical model of odor-evoked activity in the olfactory bulb. This research has the potential of being applied to the discovery of mechanisms of odor processing in the brain. Dr. Zochowski was funded by *The Stephen W. Kuffler Fellowship Fund, MBL Associates,* and the *M.G.F. Fuortes Memorial Fellowship Fund.*

## Grass Fellows

- Jerod S. Denton, Dartmouth Medical Center. Project: "Regulation of intrinsic $CO_2/H^+$ chemosensitivity and intracellular pH in *Helix aspersa* neurons *in situ.*"
- Paul Gray, Ph.D., UCLA School of Medicine. Project: "Identification and respiratory rhythm generating neurons in non-mammalian species."
- Benjamin Hall, Simon Fraser University. Project: "Spatio-temporal parameters of non-stimulated and odor-evoked oscillatory activity in an intact frog olfactory bulb assessed by simultaneous dual whole-cell recordings of intrinsic interneurons."
- Kim L. Hoke, Stanford University. Project: "Mechanism of cone mosaic rearrangement during metamorphosis in the winter flounder."
- Sabrina Hrabetova, M.D., Ph.D., New York University Medical School. Project: "Diffusion in the synaptic cleft of giant synapse calyx of Held."
- Jasmina N. Jovanovic, Ph.D., University College of London. Project: "Functional analysis of conserved domains and phosphorylation sites in squid synapsins."
- Kathryn Richards, Ph.D., Emory University. Project: "The role of seratonin in developing networks."
- Kevin Sauve, Ph.D., New York University School of Medicine. Project: "The temporal properties of tropical flounder camouflage."
- Daphne Soares, University of Maryland. Project: "The role of facial receptors in underwater sensory behavior of the *Alligator mississipiensis.*"
- Gilad Twig, Technion-Israel Institute of Technology. Project: "Cellular mechanisms involved in the pathophysiology of microglial response to CGA, an active component found in Alzheimer plaques."
- Melissa Ann Vollrath, Baylor College of Medicine. Project: "Transduction currents and sensory processing in hair cells in the statocyst of the squid, *Loligo pealei.*"

## MBL Science Writing Fellowships Program

### *Fellows*

Anderson, Christopher, *San Antonio Express-News*
Bonner, Hannah, Freelance Illustrator
Devins, Dorian, Freelance
Fitzgerald, Kevin, Freelance
Henderson, Diedtra, Freelance
Jensen, Mari, *Tucson Citizen*
Keck, Aries, Freelance
Kestenbaum, David, National Public Radio
Menon, Subhadra, Freelance
Mertl, Melissa, BioMedNet
Mirsky, Steve, *Scientific American*
Osterberg, Kerstin, *Ny Teknik*
Reed, Christina, *Geotimes*
Regalado, Antonio, *Wall Street Journal*
Romano-Lax, Andromeda, Freelance
Soares, Christine, Freelance
Steger, Volker, Freelance photographer
Lori Valigra, Freelance

### *Program Staff*

Goldman, Robert D., Northwestern University, Co-Director
Rensberger, Boyce, Knight Science Journalism Program, Co-Director
Hinkle, Pamela Clapp, Marine Biological Laboratory, Administrative Director

### *Biomedical Hands-On Laboratory Faculty*

Bloom, Kerry, University of North Carolina at Chapel Hill, Co-Director
Palazzo, Robert, University of Kansas, Co-Director
Beach, Dale, University of North Carolina at Chapel Hill
Pearson, Chad, University of North Carolina at Chapel Hill
Schnackenberg, Bradley J., University of North Carolina at Chapel Hill
Vogel, Jackie, Yale University

### *Environment Hands-On Laboratory Faculty*

Foreman, Ken, Marine Biological Laboratory, Co-Director
Neill, Christopher, Marine Biological Laboratory, Co-Director
Tholke, Kris, Marine Biological Laboratory

# *Scholarships Awarded*

### The Bruce and Betty Alberts Endowed Scholarship in Physiology

Labunskiy, Dmitriy, Institute of Neurology, Moscow, Russia
Maritz, Christine, University of Pretoria

### American Society for Cell Biology

Barreto, Ernest, George Mason University
Garza, Annette, University of Texas, San Antonio
Moore, Timothy, Clark Atlanta University
Robidart, Julie, Scripps Institution of Oceanography

### Biology Club of the College of the City of New York

Nader, Karim, New York University

### C. Lalor-Burdick Scholarship

Grace, Kristen, State University of New York at Stony Brook
Liu, Feng, University of Southern California
Petroff, Brian, University of Kansas Medical Center
Songsasen, Nucharin, Audubon Center for Research of Endangered Species
Tung, Joyce, University of California San Francisco
Yu, Jr-Kai, Scripps Institution of Oceanography

## Burroughs Wellcome Fund
## Biology of Parasitism Course

Adoro, Stanley, University of Ibadan
Barak, Efrat, Technion-Israel Institute of Technology
Boscardin, Silvia, Universidade Federal de São Paulo
Echeverria, Pablo, ANLIS "Dr. Carlos G. Malbran"
Frischknecht, Friedrich, Institut Pasteur
Kriek, Neline, University of Oxford
Rottenberg, Sven, Institute of Animal Pathology
Silva, Neide, Universidade Federal de Minas Gerais
Uzureau, Pierrick, Institut Pasteur

## Burroughs Wellcome Fund
## Frontiers in Reproduction Course

Arenas, Lidia, Inst para el Estudio
Cameo, Paula, Instituto de Biologia y Medicina Experimental
Chohan, Kazim, College of Veterinary Sciences, Lahore
Mahale, Smita, Institute for Research in Reproduction
Paduch, Darius, Oregon Health Sciences University
Petroff, Brian, University of Kansas Medical Center
Rawe, Vanesa, Center of Studies in Gynecology and Reproduction

## Burroughs Wellcome Fund
## Molecular Mycology Course

Bruno, Vincent, Columbia University
Feldmesser, Marta, Albert Einstein College of Medicine
Forche, Anja, University of Minnesota
Fraser, James, University of Melbourne
Jackson, Lydgia, University of Oklahoma Health Science Center
Knight, Simon, University of Pennsylvania
Mansour, Michael, Boston University School of Medicine
Sinha, Himanshu, Duke University Medical Center
Uicker, William, Tulane University Health Sciences Center

## Gary N. Calkins Memorial Scholarship Fund

Alexander, Tara, University of Houston
Sousa Nunes, Rita, National Institute for Medical Research

## Edwin Grant Conklin Memorial Fund

Bachler, Monika, IMP
Sousa Nunes, Rita, National Institute for Medical Research

## William F. and Irene C. Diller
## Memorial Scholarship Fund

Kulisz, Andre, Iowa State University
Vidaltamayo, Roman, National University of Mexico

## The Ellison Medical Foundation
## Biology of Parasitism Course

Arastu, Shirin, Oregon Health Sciences University
Blair, Peter, University of Notre Dame
Brown, Mark, Brookhaven National Laboratory
Foth, Bernardo, University of Melbourne
Motyka, Shawn, Johns Hopkins University School of Medicine
Sherrer, Rita, University of Alabama, Birmingham
Westwood, Nick, Harvard Medical School

## The Ellison Medical Foundation
## Molecular Biology of Aging Course

Agbas, Abdulbaki, University of Kansas
Arum, Oge, University of Colorado, Boulder
Falcon, Alaric, University of Florida
Fisher, Tim, Albert Einstein College of Medicine
Gallo-Cromie, Gloria, New York University
Haq, Rizwan, University of Toronto
Kumar, Siva, Center for Cell and Molecular Biology, Hyderabad, India
Lambert, Adrian, University of Liverpool, United Kingdom
Lee, Jaewon, NIH/NIA/GRC
Lewis, Marc, University of Texas at Austin
Lopez, Norma, UAM-Iztapalapa, Mexico
Mele, James, UT Health Science Center, San Antonio
Michán, Shaday, UNAM, Mexico
Park, Jeong-Soo, Seoul National University
Poole, Jason, University of Illinois, Chicago
Pritsker, Moshe, Princeton University
Renault, Valerie, CNRS UMR 7000, France
Rodier, Francis, University of Montreal Hospital Research Center
Sharrow, Keith, University of Kentucky
Shea, Molly, University of Minnesota, Twin Cities

## Caswell Grave Scholarship Fund

Alexander, Tara, University of Houston
Dowell, Joshua, Riley Hospital for Children, Indiana
Herve, Maxime, Institut Pasteur de Lille
Maritz, Christine, University of Pretoria
Ricci, Giulia, La Sapienza University of Rome
Sousa Nunes, Rita, National Institute for Medical Research
Vidaltamayo, Roman, National University of Mexico
Yu, Jr-Kai, Scripps Institution of Oceanography

## Daniel S. Grosch Scholarship Fund

Gerlach, Robin, Montana State University

## Aline D. Gross Scholarship Fund

Kulisz, Andre, Iowa State University
Nakauchi, Sakura, Tokyo University Pharmacy and Life Science

## William Randolph Hearst Foundation

Dowell, Joshua, Riley Hospital for Children, Indiana
Griffis, Eric, Emory University School of Medicine
Kalinowski, Rebecca, University of Connecticut Health Center
Lutton, Bram, Boston University
Marshall, Shannon, California Institute of Technology
Melnick, Richard, University of Vermont
Moore, Jamie, University of California San Francisco
Ramsey, David, University of Illinois at Chicago
Sigal, Irina, UMDNJ-New Jersey Medical School
Silverstein, Robert, University of Washington, Seattle
Yanochko, Gina, University of Arizona

## Howard Hughes Medical Institute

Bachler, Monika, IMP
Behrens, Sebastian, Max-Planck-Institute for Marine Microbiology
Datta, Debkanya, National Centre for Biological Sciences
de Hoz, Livia, University of Edinburgh

Dowell, Joshua, Riley Hospital for Children, Indiana
Fourcaud, Nicolas, Université Paris 5 René Descartes
Garcia de Polavieja, Gonzalo, University of Cambridge
Gerlach, Robin, Montana State University
Halabisky, Brian, Case Western Reserve University
Haspel, Gal, Ben Gurion University
Karpova, Alla, Harvard Medical School
Kulisz, Andre, Iowa State University
Lim, Grace, Scripps Institution of Oceanography
Loewenstein, Yonatan, Hebrew University
Ludwar, Bjoern, Universität zu Köln
Lupp, Claudia, University of Hawaii
Martiny, Adam, Technical University of Denmark
Melnick, Richard, University of Vermont
Nader, Karim, New York University
Patten, Iain, University of Sheffield
Prince, Frédéric, University of Basel Biocenter
Ramsey, David, University of Illinois at Chicago
Riemann, Lasse, Scripps Institution of Oceanography
Rust, Nicole, New York University
Schenk, Ana Katrin, University of California, San Francisco
Sen, Anindya, Tata Institute of Fundamental Research
Sharpee, Tatyana, Michigan State University
Yu, Jr-Kai, Scripps Institution of Oceanography

### Arthur Klorfein Scholarship and Fellowship Fund

Liu, Feng, University of Southern California
Luria, Victor, Columbia University
Medina, Mónica, California Academy of Sciences
Prince, Frédéric, University of Basel Biocenter
Sousa Nunes, Rita, National Institute for Medical Research
Van Raay, Terrence, University of Utah
Yu, Jr-Kai, Scripps Institution of Oceanography

### Frank R. Lillie Fellowship and Scholarship Fund

Dhingra, Anuradha, University of Pennsylvania
Herve, Maxime, Institut Pasteur de Lille
Karres, Janina, University of Massachusetts
Labunskiy, Dmitriy, Institute of Neurology
Lutton, Bram, Boston University
Maritz, Christine, University of Pretoria
Sell, Anne, Woods Hole Oceanographic Institution
Vidaltamayo, Roman, National University of Mexico

### The Gruss Lipper Foundation Scholarship

Haspel, Gal, Ben Gurion University, Israel
Sumbre, German, Hebrew University of Jerusalem, Israel

### Jacques Loeb Founders' Scholarship Fund

Kalinowski, Rebecca, University of Connecticut Health Center
Selak, Sanya, University of Calgary
Sell, Anne, Woods Hole Oceanographic Institution

### S.O. Mast Memorial Fund

Datta, Debkanya, National Centre for Biological Sciences
Zuo, Yi, Northwestern University Medical School

### MBL Associates Endowed Scholarship Fund

Griffis, Eric, Emory University School of Medicine

### MBL Pioneers Scholarship Fund

Alexander, Tara, University of Houston
Liu, Feng, University of Southern California
Luria, Victor, Columbia University
Medina, Monica, California Academy of Sciences
Patten, Iain, University of Sheffield
Ricci, Giulia, La Sapienza University of Rome
Sen, Anindya, Tata Institute of Fundamental Research
Van Raay, Terrence, University of Utah

### Merck Research Laboratories Scholarships

Adoro, Stanley, University of Ibadan
Barak, Efrat, Technion-Israel Institute of Technology
Boscardin, Silvia, Universidade Federal de São Paulo
Echeverria, Pablo, ANLIS "Dr. Carlos G. Malbran"
Frischknecht, Friedrich, Institut Pasteur
Kriek, Neline, University of Oxford
Rottenberg, Sven, Institute of Animal Pathology
Silva, Neide, Universidade Federal de Minas Gerais
Uzureau, Pierrick, Institut Pasteur

### Charles Baker Metz and William Metz Scholarship Fund in Reproductive Biology

Chohan, Kazim, College of Veterinary Sciences, Lahore
Grace, Kristen, State University of New York at Stony Brook
Rawe, Vanesa, Center of Studies in Gynecology & Reproduction
Songsasen, Nucharin, Audubon Center for Research of Endangered Species
Tung, Joyce, University of California San Francisco

### Frank Morrell Endowed Memorial Scholarship

Rasse, Tobias, Max-Planck-Institut für Biophysikalische

### Mountain Memorial Fund Scholarship

Griffis, Eric, Emory University School of Medicine
Melnick, Richard, University of Vermont
Moore, Jamie, University of California San Francisco
Ramsey, David, University of Illinois at Chicago
Sell, Anne, Woods Hole Oceanographic Institution
Silverstein, Robert, University of Washington, Seattle
Yanochko, Gina, University of Arizona

### Pfizer Inc Endowed Scholarship

Lutton, Bram, Boston University
Selak, Sanya, University of Calgary
Silverstein, Robert, University of Washington, Seattle

### Planetary Biology Internship Scholarships

Behrens, Sebastian, Max-Planck-Institute for Marine Microbiology
Riemann, Lasse, Scripps Institution of Oceanography
Schuster, Martin, University of Iowa

### William Townsend Porter Fellowship and Scholarship Fund

Barreto, Ernest, George Mason University
Garza, Annette, University of Texas, San Antonio
Moore, Timothy, Clark Atlanta University

Oviedo, Hysell, New York University
Robidart, Julie, Scripps Institution of Oceanography

### Herbert W. Rand Fellowship and Scholarship Fund

Escalada, Artur, University of Barcelona
Faisal, Ahmed, Emmanuel College
Gollisch, Tim, Humboldt-Universität zu Berlin
Gregor, Thomas, Princeton University
Griffis, Eric, Emory University School of Medicine
Labunskiy, Dmitriy, Institute of Neurology, Moscow, Russia
Marshall, Shannon, California Institute of Technology
Neimark, Maria, Princeton University
Osan, Remus, University of Pittsburgh
Silverstein, Robert, University of Washington, Seattle
Yanochko, Gina, University of Arizona

### Ruth Sager Memorial Scholarship

Selak, Sanya, University of Calgary
Sell, Anne, Woods Hole Oceanographic Institution

### Society of General Physiologists' Scholarship

Babbitt, Courtney, University of Chicago
Karpova, Alla, Harvard Medical School
Labunskiy, Dmitriy, Fumio Mekata Scholar, Institute of Neurology, Moscow, Russia
Rasse, Tobias, Max-Planck-Institut für Biophysikalische

### Howard A. Schneiderman Endowed Scholarship

Datta, Debkanya, National Centre for Biological Sciences
Halabisky, Brian, Case Western Reserve University

### Milton L. Shifman Endowed Scholarship

Elliott, Taffeta, Columbia University
Kelly, Kristie, Cornell University Medical College
Luria, Victor, Columbia University

### Moshe Shilo Memorial Scholarship Fund

Kelman, Dovi, Tel Aviv University

### Catherine Filene Shouse Scholarship

Kelly, Kristie, Cornell University Medical College
Neill, Anna, Scripps Institution of Oceanography
Sigal, Irina, UMDNJ-New Jersey Medical School

### Marjorie W. Stetten Scholarship Fund

Kalinowski, Rebecca, University of Connecticut Health Center
Nakauchi, Sakura, Tokyo University Pharmacy and Life Science

### Massachusetts Space Grant Consortium

Bryant, Juliet, University of Texas Medical Branch at Galveston
Fahey, Shireen, University of Queensland, Brisbane, Australia
Hildebrand, Terri, University of Kansas
Louie, Kristina, UCLA

### Horace W. Stunkard Scholarship Fund

Arenas, Lidia, Inst para el Estudio
Tung, Joyce, University of California San Francisco

### Surdna Foundation Scholarship

Datta, Debkanya, National Centre for Biological Sciences
de Hoz, Livia, University of Edinburgh
Dhingra, Anuradha, University of Pennsylvania
Garcia de Polavieja, Gonzalo, University of Cambridge
Herve, Maxime, Institut Pasteur de Lille
Karpova, Alla, Harvard Medical School
Karres, Janina, University of Massachusetts
Nakauchi, Sakura, Tokyo University Pharmacy and Life Science
Rasse, Tobias, Max-Planck-Institut für Biophysikalische
Zuo, Yi, Northwestern University Medical School

### Irving Weinstein Endowed Scholarship

Alexander, Tara, University of Houston

### William Morton Wheeler Family Founders' Scholarship

Zuo, Yi, Northwestern University Medical School

### Selman A. Waksman Endowed Scholarship in Microbial Diversity

Lim, Grace, Scripps Institution of Oceanography

### Walter L. Wilson Endowed Scholarship Fund

Kalinowski, Rebecca, University of Connecticut Health Center
Karres, Janina, University of Massachusetts

### World Academy of Arts and Sciences Emily Mudd Scholarship

Chohan, Kazim, College of Veterinary Sciences, Lahore
Grace, Kristen, State University of New York at Stony Brook
Paduch, Darius, Oregon Health Sciences University
Petroff, Brian, University of Kansas Medical Center
Songsasen, Nucharin, Audubon Center for Research of Endangered Species

### World Health Organization

Cameo, Paula, Instituto de Biologia y Medicina Experimental
Palomino, Alberto, University of Chile

## *Post-Course Research Awards*

Dowell, Joshua, Riley Hospital for Children, Indiana (Physiology)
Kulisz, Andre, Iowa State University (Physiology)
Labunskiy, Dmitriy, Institute of Neurology, Moscow (Physiology)
Ramsey, David, University of Illinois at Chicago (Physiology)
Selak, Sanya, University of Calgary (Physiology)

# Board of Trustees and Committees

## *Corporation Officers and Trustees*

Chairman of the Board of Trustees, Sheldon J. Segal, The Population Council
Vice Chair of the Board of Trustees, Alfred M. Zeien, The Gillette Company
President of the Corporation, John E. Dowling, Harvard University
Director and Chief Executive Officer, William T. Speck, Marine Biological Laboratory*
Treasurer of the Corporation, Mary B. Conrad, Fiduciary Trust International*
Clerk of the Corporation, Thomas S. Crane, Mintz, Levin, Cohn, Ferris, Glovsky & Popeo, PC*
Chair of the Science Council, Robert B. Barlow, SUNY Upstate Medical University*

## *Class of 2002*

Lakian, John R., The Fort Hill Group, Inc.
Ruderman, Joan V., Harvard Medical School
Segal, Sheldon J., The Population Council
Zeien, Alfred M., The Gillette Company

## *Class of 2003*

Kelley, Darcy Brisbane, Columbia University
Landeau, Laurie J., Marinetics, Inc.
Lee, Burton J. III, Vero Beach, FL
O'Hanley, Ronald P., Mellon Institutional Asset Mgt.
Pierce, Jean, Boca Grande, FL
Ryan, Vincent J., Schooner Capital LLC

## *Class of 2004*

Jacobson, M. Howard, Bankers Trust
Langford, George M., Dartmouth College
Miller, G. William, G. William Miller & Co., Inc.
Press, Frank, The Washington Advisory Group
Weld, Christopher M., Sullivan and Worcester, Boston
Wiesel, Torsten N., Rockefeller University

**Ex officio*

## *Class of 2005*

Anderson, Porter W., Key Largo, FL
Fraser, Claire M., The Institute for Genomic Research
Logan, George W., Salem, VA
Prendergast, Robert, Falmouth, MA
Rowe, John W., Aetna U.S. Healthcare

## *Ex Officio Trustees*

Barlow, Robert B., Chair of the Science Council
Conrad, Mary B., Treasurer of the Corporation
Crane, Thomas S., Clerk of the Corporation
Speck, William T., Director and Chief Executive Officer

## *Honorary Trustees*

Ebert, James D., Baltimore, MD (deceased 2001)
Golden, William T., New York, NY
Grass, Ellen R., The Grass Foundation (deceased 2001)
Mainer, Robert E., Wayland, MA

## *Trustees Emeriti*

Adelberg, Edward A., Yale University, New Haven, CT
Buck, John B., Sykesville, MD
Cohen, Seymour S., Woods Hole, MA
Colwin, Arthur L., Key Biscayne, FL
Colwin, Laura Hunter, Key Biscayne, FL
Copeland, Donald Eugene, Woods Hole, MA
Crowell, Sears Jr., Indiana University, Bloomington, IN (deceased 2002)
Hayashi, Teru, Woods Hole, MA
Hubbard, Ruth, Cambridge, MA
Kleinholz, Lewis, Reed College, Portland, OR
Krahl, Maurice, Tucson, AZ
Prosser, C. Ladd, University of Illinois, Urbana, IL (deceased 2002)
Russell-Hunter, W.D., Syracuse University, Syracuse, NY
Saunders, John W., Waquoit, MA
Shepro, David, Boston, MA
Trigg, D. Thomas, Wellesley, MA
Vincent, Walter S., Woods Hole, MA

## *Directors Emeriti*

Ebert, James D., Baltimore, MD (deceased 2001)
Gross, Paul, Falmouth, MA
Halvorson, Harlyn O., Woods Hole, MA

## *Executive Committee of the Board of Trustees*

Segal, Sheldon J., Chair
Zeien, Alfred M., Vice-Chair
Conrad, Mary B., Treasurer
Anderson, Porter W.
Barlow, Robert B.
O'Hanley, Ronald P.
Palazzo, Robert E.

## *Science Council*

Barlow, Robert B., Chair (2001)
Armstrong, Clay M. (2002)
Armstrong, Peter (2002)
Atema, Jelle (2003)
Fraser, Scott (2003)
Haimo, Leah (2003)
Hopkinson, Charles (2002)
Jaffe, Laurinda (2001)
Palazzo, Robert E. (2003)
Smith, Peter J. S. (2003)
Sogin, Mitchell (2002)
Weeks, Janis C. (2002)
Dawidowicz, E. A.*
Speck, William T.*

## *Standing Committees of the Board of Trustees*

### *Development*

Weld, Christopher, Chair
Anderson, Porter W.
Armstrong, Peter
Barlow, Robert
Conrad, Mary B.
Cox, Martha
Dowling, John
Fraser, Claire
Lakian, John
Langford, George
Lee, Burton
Miller, G. William
Pierce, Jean
Prendergast, Robert
Rowe, John W.
Wiesel, Torsten

### *Facilities and Capital Equipment*

Anderson, Porter, Chair
Langford, George
Press, Frank
Ruderman, Joan
Weld, Christopher

### *Investment*

Conrad, Mary B., Chair
Crane, Thomas S.
Jacobson, M. Howard
Lakian, John R.
Logan, George W.
Miller, G. William
O'Hanley, Ronald
Prendergast, Robert A.
Ryan, Vincent J.
Segal, Sheldon
Zeien, Alfred

### *Finance*

O'Hanley, Ronald P., Chair
Conrad, Mary B.
Crane, Thomas S.
Goldman, Maynard
Jacobson, M. Howard
Kelley, Darcy
Lakian, John R.
Landeau, Laurie
Logan, George W.
Miller, G. William
Zeien, Alfred

### *Nominating*

Segal, Sheldon, Chair Protem
Palazzo, Robert
Fraser, Claire
Pierce, Jean
Rowe, John W.
Ryan, Vincent J.
Speck, William
Wiesel, Torsten

## *Standing Committees of the Corporation and Science Council*

### *Buildings and Grounds*

Boyer, Barbara C., Chair
Cohen, Lawrence
Eckberg, Bill
McArthur, Andrew
Tweedell, Kenyon
Valiela, Ivan
Abbott, Thomas*
Cutler, Richard*
Fleet, Barry*
Hayes, Joe*

**Ex officio*

## Education Committee

Dionne, Vincent, Chair
Dunlap, Paul
Fink, Rachel
Hanlon, Roger
Kiehart, Dan
Madison, Dan
Palazzo, Robert
Venuti, Judith
Wadsworth, Patricia
Waterbury, John
Dawidowicz, E. A.*
Holzworth, Kelly*

## Fellowships

Pederson, Thoru, Chair
Deegan, Linda
Ehrlich, Barbara
Lipscombe, Diane
Sluder, Greenfield
Smith, Peter J. S.
Dawidowicz, E. A.*
Kaufmann, Sandra*

## Housing, Food Service and Child Care

Browne, Carole, Chair
Augustine, George
Malchow, Robert P.
McAnnelly, Lynne
McDonough, Stefan
Mensinger, Alan
Rastetter, Edward
Stuart, Ann E.
Beckwith, Mary*
Cutler, Richard*

## MBL/WHOI Library Joint Advisory Committee

Shepro, David, Chair, MBL
Dow, David, NMFS
Harbison, G. Richard, WHOI
Hobbie, John, MBL
Robb, James, USGS
Smith, Peter J. S., MBL
Smolowitz, Roxanna, MBL
Tucholke, Brian, WHOI
Warren, Bruce, WHOI
Hurter, Colleen, WHOI*
Norton, Cathy, MBL*
Uhlinger, Eleanor, MBL*

## Research Services and Space

Laufer, Hans, Chair
Allen, Nina
Armstrong, Peter B.
Foreman, Kenneth
Landowne, David
Melillo, Jerry
Mizell, Merle
Smith, Peter J. S.
Steudler, Paul
Valiela, Ivan
Cutler, Richard*
Dawidowicz, E. A.*
Kerr, Louis M.*
Mattox, Andrew*

## Council of Visitors

Norman B. Asher, Esq., Hale and Dorr, Counsellors at Law, Boston, MA
Mr. Robert W. Ashton, Bay Foundation, New York, NY

Mr. Donald J. Bainton, Continental Can Co., Boca Raton, FL
Mr. David Bakalar, Chestnut Hill, MA
Mr. Charles A. Baker, The Liposome Company, Inc., Princeton, NJ
Dr. George P. Baker, Massachusetts General Hospital, Boston, MA
Dr. Sumner A. Barenberg, Bernard Technologies, Chicago, IL
Mr. Mel Barkan, The Barkan Companies, Boston, MA
Mr. Frederick Bay, Josephine Bay Paul and C. Michael Paul Foundation, Inc., New York, NY
Mr. Bruce A. Beal, The Beal Companies, Boston, MA
Mr. Robert P. Beech, Component Software International, Inc., Mason, OH
Mr. George Berkowitz, Legal Sea Foods, Allston, MA
Jewelle and Nathaniel Bickford, New York, NY
Dr. Elkan R. Blout, Harvard Medical School, Boston, MA
Mr. and Mrs. Philip Bogdanovitch, Lake Clear, NY
Mr. Malcolm K. Brachman, Northwest Oil Company, Dallas, TX
Dr. Goodwin M. Breinin, New York University Medical Center, New York, NY
Mr. Murray H. Bring, New York, NY

Mr. John Callahan, Carpenter, Sheperd & Warden, New London, NH
Mrs. Elizabeth Campanella, West Falmouth, MA
Dr. Stephen D. Crocker, Bethesda, MD
Mr. Michael J. Cronin, President/CEO, Cognition Corporation, Bedford, MA
Mrs. Lynn W. Piasecki Cunningham, Film and Videomaker, Piasecki Productions, New York, NY
Dr. Anthony J. Cutaia, Anheuser-Busch, Inc., St. Louis, MO

Dr. Georges de Ménil, DM Foundation, New York, NY
Dr. Lorenzo DiCarlo and Mrs. Sally Stegeman DiCarlo, Ann Arbor, MI
Mr. D. H. Douglas-Hamilton, Hamilton Thorne Research, Beverly, MA
Mr. Benjamin F. du Pont, Du Pont Company, Deepwater, NJ

Dr. Sylvia A. Earle, Founder, Deep Ocean Engineering, Oakland, CA
Mr. and Mrs. Hoyt Ecker, Vero Beach, FL
Mr. Anthony B. Evnin, Venrock Associates, New York, NY

Stuart Feiner, Esq., Inco Limited, Toronto, Ontario, Canada
Judah Folkman, M.D., Children's Hospital, Boston, MA
Mrs. Hadley Mack French, Edsel and Eleanor Ford House, Grosse Pointe Farms, MI

Mr. and Mrs. Huib Geerlings, Boston, MA
Mr. William J. Gilbane, Jr., Gilbane Building Company, Providence, RI
Dr. Michael J. Goldblatt, Defense Sciences Office, Arlington, VI
Mr. Maynard Goldman, Maynard Goldman & Associates, Boston, MA

*Ex officio*

Ms. Charlotte I. Hall, Edgartown, MA
Mrs. Elizabeth Heald, West Falmouth, MA
Dr. Thomas R. Hedges, Jr., Neurological Institute, Pennsylvania Hospital, Philadelphia, PA
Drs. Linda Hirshman and David Forkosh, Brandeis University & FMH Foundation, Waltham, MA
Mrs. Barbara W. Hostetter, Barr Foundation, Boston, MA
Mr. Chuck Hunter, Kessinger Hunter & Co., Kansas City, MO
Mr. Thomas J. Hynes, Jr., Meredith & Grew, Inc., Boston, MA

Mrs. Elizabeth Ford Kontulis, New Canaan, CT
Ms. Ellyn V. Korzun, Goldman, Sachs & Co., New York, NY

Mr. and Mrs. Robert Lambrecht, Boca Grande, FL
Dr. Catherine C. Lastavica, Tufts University School of Medicine, Boston, MA
Mr. Joel A. Leavitt, Boston, MA
Mr. Stephen W. Leibholz, TechLabs, Inc., Huntingdon, PA
Mrs. Margaret Lilly, West Falmouth, MA
Mr. Richard Lipkin, Laird & Co., LLC, New York, NY

Mr. Michael T. Martin, SportsMark, Inc., New York, NY
Mrs. Christy Swift Maxwell, Grosse Pointe Farms, MI
Mr. Ambrose Monell, G. Unger Vetlesen Foundation, Palm Beach, FL

Dr. Mark Novitch, Washington, DC

Mr. David R. Palmer, David Ross Palmer & Associates, Waquoit, MA
Dr. Roderic B. Park, Richmond, CA
Mr. Santo P. Pasqualucci, Falmouth Co-operative Bank, Falmouth, MA
Mr. Robert Pierce, Jr., Pierce Aluminum Co., Franklin, MA

Mr. Richard Reston, Vineyard Gazette, Edgartown, MA
Mr. Marius A. Robinson, Fundamental Investors Ltd., Key Biscayne, FL
Mr. Edward Rowland, Tucker, Anthony, Inc., Boston, MA

Mr. Gregory A. Sandomirsky, Mintz Levin Cohen Ferris Glovsky & Popeo, PC, Boston, MA
Mrs. Mary Schmidek, Marion, MA
Dr. Cecily C. Selby, New York, NY
Mr. Robert S. Shifman, St. Simon's Island, GA
Mr. and Mrs. Gregory Skau, Grosse Pointe Farms, MI
Mr. Malcolm B. Smith, General American Investors Co., New York, NY
Mr. John C. Stegeman, Campus Rentals, Ann Arbor, MI
Mr. Joseph T. Stewart, Jr., Skillman, NJ
Mr. Gerard L. Swope, Washington, DC
Mr. John F. Swope, Concord, NH

Mr. and Mrs. Stephen E. Taylor, Milton, MA
Mr. Samuel Thorne, Thorne Trading Company, LLC, Manchester, MA

Mrs. Donna Vanden Bosch-Flynn, Spring Lake, NJ
Mrs. Carolyn W. Verbeck, Vineyard Haven, MA

Mr. Benjamin S. Warren III, Grosse Pointe Farms, MI
Nancy B. Weinstein, R.N., The Hospice, Inc., Glen Ridge, NJ
Stephen S. Weinstein, Esq., Morristown, NJ
Mr. Frederick J. Weyerhaeuser, Beverly, MA
Mrs. Robin Wheeler, West Falmouth, MA
Mr. Tony L. White, The Perkin Elmer Corporation, Norwalk, CT
Ms. Rosalind C. Whitehead, New York, NY

# Administrative Support Staff[1]

## *Biological Bulletin*

Greenberg, Michael J., Editor-in-Chief
Hinkle, Pamela Clapp, Managing Editor
  Child, Wendy
  Gibson, Victoria R.
  Marrama, Carol
  Schachinger, Carol H.

## *Director's Office*

Speck, William T., Interim Director and Chief Executive Officer
  Donovan, Marcia H.

*Equal Employment Opportunity*
  MacNeil, Jane L.

*Veterinarian Services*
  Smolowitz, Roxanna, Campus Veterinarian
  Avtges, Suzanne[2]
  Cavanaugh, Joseph[2]
  Ehlen, Jill[2]
  Hunt, Kyle[2]
  Mulroy, Richard[2]
  O'Shea, Erin[2]
  Reynolds, Taylor[2]
  Summers, Erin[2]
  Stukey, Jetley
  Tirrell, Kerri-Ann[2]

## *Ecosystems Center Administrative Staff*

Nunez, Guillermo, Center Research Administrator
  Berthel, Dorothy J.
  Donovan, Suzanne J.
  Seifert, Mary Ann

## *External Affairs*

Carotenuto, Frank C., Director
  Butcher, Valerie
  Faxon, Wendy P.
  Johnson, A. Kristine
  Martin, Theresa H.
  Patch-Wing, Dolores
  Quigley, Barbara A.
  Shaw, Kathleen L.

*Associates Program*
  Joslin, Susan
  Bean, Maureen[2]
  Sgarzi, Dorothy J.

*Communications Office*
  Hinkle, Pamela Clapp, Director
  Adinolfi, Nancy[2]
  Brown, Lily[2]
  Hartmann, Kelley[2]
  Joslin, Susan
  Langill, Christine[2]
  Liles, Beth R.
  Rullo, Gina
  Sloboda, Lara N.[2]
  Sullivan, Beth

## *Financial Services Office*

Lane, Jr., Homer W., Chief Financial Officer
Bowman, Richard, Controller
McLean, David, Controller
Mullen, Richard J., Manager, Research Administration
  Adams, Taryn
  Afonso, Janis
  Aguiar, Deborah
  Bliss, Casey M.
  Crosby, Kenneth
  Griffin, Bonnie Jean
  Lancaster, Cindy
  Livingstone, Suzanne
  Newman, Melissa
  Ranzinger, Laura
  Stellrecht, Lynette
  White, Laurie

*Stock Room*
  Schorer, Timothy M., Supervisor
  Olive, Jr., Charles W.
  Frederickson, Trevor[2]

---

[1] Including persons who joined or left the staff during 2001.

[2] Summer or temporary.

*Purchasing*
Hall Jr., Lionel E., Supervisor
Diggs, Tanisha[2]
Hunt, Lisa M.

## Housing and Conferences

Beckwith, Mary M., Director
Ament, Elinor[2]
Campbell, Anne T.
Fuglister, Charles K.
Grasso, Deborah
Inzirillo, Wendi
Johnson-Horman, Frances N.
Kruger, Sally J.
Oldham, Pamela
Perito, Diana
Wagner, Carol[2]

*Housekeeping*
Bailey, Jeffrey Jr.[2]
Barnes, Susan M.
Berrios, Jessica
Chen, Zhi Xin
Christianson, Derek[2]
Clark, Daniel[2]
Cohen, Alex[2]
Doherty, Bryant[2]
Gaylord, David[2]
Johnston, David[2]
Hannigan, Catherine
MacDonald, Cynthia C.
McNamara, Noreen M.
Santiago, Crystal
Shum, Mei Wah
Wagner, Paul[2]
Ware, Lynn
Waterbury, Matthew[2]

## Human Resources

Goux, Susan P., Director
Houser, Carmen
Snow, Linda

## Josephine Bay Paul Center for Comparative Molecular Biology and Evolution Administrative Staff

Lim, Pauline
Nihill, Tara
Schlichter, Mimi

## Marine Resources Center

Hanlon, Roger T., Director
Santore, Gabrielle

*Aquatic Resources Department*
Enos, Jr., Edward G., Superintendent
DeGiorgis, Joseph[2]
Dimond, James L.[2]
Grossman, William M.
Gudas, Christopher N.[2]
Klimm III, Henry W.
Potter, Benjamin[2]
Reynolds, Justin M.[2]
Sexton, Andrew W.
Sterling, Christian[2]
Sullivan, Daniel A.
Tassinari, Eugene
Whelan, Sean P.

*MRC Life Support System*
Mebane, William N., Systems Operator
Carroll, James
Hanley, Janice S.
Kuzirian, Alan

## MBL/WHOI Library

Norton, Catherine N., Director
Ashmore, Judith A.
Deveer, Joseph M.
Monahan, A. Jean
Nelson, Heidi
Person, Matthew
Reuter, Laura
Riley, Jacqueline
Stafford, Nancy
Stout, Amy
Uhlinger, Eleanor
Walton, Jennifer

*Copy Center*
Mountford, Rebecca J., Supervisor
Campbell, Anne
Clark, Sarah
Hadway (Cosgrove), Nancy
Eldridge, Myles[2]
Reuter, Laura
Westburg, Joanne

*Information Systems Division*
Inzina, Barbara, Network Manager
Callahan, Michael[2]
Campbell, Jr., David J.
Cohen, Alex[2]
Fournier, Pamela
Jones, Patricia L.
Leary, Patrick[2]
Lowell, Gregory
Mazzilli, Stefano[2]
Mountford, Rebecca J.
Remsen, David P.
Renna, Denis J.
Space, David B.

## NASA Center for Advanced Studies in the Space Life Sciences

Blazis, Diana, Administrator
Farrell, Heather
Oldham, Pamela

## Research Administration & Educational Programs

Dawidowicz, Eliezar A., Director
Brooks, Marilyn[2]

Hamel, Carol C.
Holzworth, Kelly
Kaufmann, Sandra J.

*Central Microscopy Facility and General Use Rooms*
Kerr, Louis M., Supervisor
Luther, Herbert
Parmenter, Marjorie[2]
Peterson, Martha B.
Scanlon, John[2]

## Safety Services

Mattox, Andrew H., Environmental, Health, and Safety Manager
Normand, Danielle[2]
Elder, Kristopher[2]

## Satellite/Periwinkle Children's Programs

Robinson, Paulina H.[2]
Camire, Aaron[2]
Creedon, Kellen[2]
DeGroof, Emily[2]
Fitzelle, Annie[2]
Guiffrida, Beth[2]
Halter, Sarah[2]
Houser, Clarissa[2]
Karalekas, Nina[2]
Noonan, Patrick[2]
O'Connor, Padraic[2]
Paradise, Kristin[2]
Plourde, Anna[2]
Shwartz, Cortney[2]
Urciuoli, Karen[2]

## Service, Projects and Facilities

Cutler, Richard D., Director
Enos, Joyce B.
Boudreau, Trinity[2]
Guarente, Jeffrey[2]

*Apparatus*
Baptiste, Michael G.
Barnes, Franklin D.
Haskins, William A.
Pratt, Barry

*Transportation Services and Grounds*
Hayes, Joseph H., Supervisor
Bast, Paul C.[2]
Boucher, Richard L.
Bradley, Sean[2]
Brereton, Richard S.[2]
Cabral, Jameason[2]
Cameron, Lawrence M.[2]
Clayton, Daniel
Collins, Paul J.
Illgen, Robert F.
Kanellopoulos, Paul[2]
Lawson, Joshua[2]
Mendoza, Guy[2]
Santoro, John[2]
Sherwin, Jason[2]
Walsh, Matthew[2]

*Plant Operations and Maintenance*
Abbott, Thomas E., Supervisor
Anderson, Lewis B.
Atwood, Paul R.
Bailey, Jeffrey B.
Barnes, John S.
Berthel, Frederick
Blunt, Hugh F.
Bourgoin, Lee E.
Cadose, James W.
Callahan, John J.
Coppinger, John
Elias, Michael
Ficher, Jason
Gibbons, Roberto
Goehl, George
Gonsalves, Jr., Walter W.
Hathaway, Peter J.
Henderson, Jon R.
Howell, Robert
Langill, Richard
Laurino, Frank
McAdams III, Herbert M.
McHugh, Michael O.
McQuillan, Jeffrey[2]
Mendoza, Duke
Mills, Stephen A.
Pratt, Barry
Rattacasa, Frank[2]
Santiago, Kody[2]
Settlemire, Donald
Shepherd, Denise M.
Toner, Michael
Ware, Lynn M.

*Security and Projects*
Fleet, Barry M., Manager
Fish Jr., David L.
Kelley, Kevin
Lochhead, William M.
Rozum, John
Scanlan, Melanie

# Members of the Corporation

## *Life Members*

**Adelberg, Edward A.,** 204 Prospect Street, New Haven, CT 06511-2107
**Afzelius, Bjorn,** University of Stockholm, Wenner-Gven Institute, Department of Ultrastructure Research, Stockholm, SWEDEN
**Amatniek, Ernest,** (address unknown)
**Arnold, John M.,** 329 Sippewissett Road, Falmouth, MA 02540
**Arnold, William A.,** Oak Ridge National Laboratory, Biology Division, 102 Balsalm Road, Oak Ridge, TN 37830 (deceased 2001)

**Bang, Betsy G.,** 76 F. R. Lillie Road, Woods Hole, MA 02543
**Berne, Robert M.,** 19 Gardiner Road, Woods Hole, MA 02543 (deceased 2001)
**Bernheimer, Alan W.,** New York University Medical Center, Department of Microbiology, 550 First Avenue, New York, NY 10016
**Bertholf, Lloyd M.,** Westminster Village, #2114, 2025 East Lincoln Street, Bloomington, IL 61701-5995
**Bosch, Herman F.,** 163 Elm Road, Falmouth, MA 02540-2430
**Brinley, F. J.,** National Institutes of Health, NINCDS, Neurological Disorders Program, Room 812 Federal Building, Bethesda, MD 20892
**Buck, John B.,** Fairhaven C-020, 7200 Third Avenue, Sykesville, MD 21784
**Burbanck, Madeline P.,** P.O. Box 15134, Atlanta, GA 30333
**Burbanck, William D.,** P.O. Box 15134, Atlanta, GA 30333

**Chaet, Alfred B.,** University of West Florida, Department of Cellular and Molecular Biology, 11000 University Parkway, Pensacola, FL 32514
**Clark, Arnold M.,** 53 Wilson Road, Woods Hole, MA 02543
**Clark, James M.,** 258 Wells Road, Palm Beach, FL 33480-3625
**Cohen, Seymour S.,** 10 Carrot Hill Road, Woods Hole, MA 02543-1206
**Collier, Jack R.,** P.O. Box 139, Effie, LA 71331
**Collier, Marjorie McCann,** P.O. Box 139, Effie, LA 71331
**Colwin, Arthur L.,** 320 Woodcrest Road, Key Biscayne, FL 33149-1322
**Colwin, Laura Hunter,** 320 Woodcrest Road, Key Biscayne, FL 33149-1322
**Cooperstein, Sherwin J.,** University of Connecticut, School of Medicine, Department of Anatomy, Farmington, CT 06030-3405
**Copeland, D. Eugene,** Marine Biological Laboratory, Woods Hole, MA 02543
**Corliss, John O.,** P.O. Box 2729, Bala Cynwyd, PA 19004-2116
**Costello, Helen M.,** 137 Carolina Meadows, Chapel Hill, NC 27514-8512
**Crouse, Helen,** 231 Geiskey Creek Road, Hayesville, NC 28904
**Crowell, Sears,** Indiana University, Department of Biology, Bloomington, IN 47405 (deceased 2002)

**DeHaan, Robert L.,** Emory University School of Medicine, Department of Anatomy & Cell Biology, 1648 Pierce Drive, Room 108, Atlanta, GA 30322
**Dudley, Patricia L.,** 3200 Alki Avenue SW, #401, Seattle, WA 98116

**Edwards, Charles,** 3429 Winding Oaks Drive, Longboat Key, FL 34228
**Elliott, Gerald F.,** The Open University Research Unit, Foxcombe Hall, Berkeley Road, Boars Hill, Oxford OX1 5HR, UK

**Failla, Patricia M.,** 2149 Loblolly Lane, Johns Island, SC 29455
**Frazier, Donald T.,** University of Kentucky Medical Center, Department of Physiology and Biophysics, MS501 Chandler Medical Center, Lexington, KY 40536

**Gabriel, Mordecai L.,** Brooklyn College, Department of Biology, 2900 Bedford Avenue, Brooklyn, NY 11210
**Glusman, Murray,** New York State Psychiatric Institute, 722 W. 168th St., Unit #70, New York, NY 10032
**Graham, Herbert,** 36 Wilson Road, Woods Hole, MA 02543

**Hamburger, Viktor,** Washington University, Department of Biology, 740 Trinity Avenue, St. Louis, MO 63130
**Hamilton, Howard L.,** University of Virginia, Department of Biology, 238 Gilmer Hall, Charlottesville, VA 22901
**Harding, Jr., Clifford V.,** 100 Saconesset Road, Falmouth, MA 02540
**Haschemeyer, Audrey E. V.,** 21 Glendon Road, Woods Hole, MA 02543-1406
**Hayashi, Teru,** 15 Gardiner Road, Woods Hole, MA 02543-1113
**Hisaw, Frederick L.,** Oregon State University, Zoology Department, Corvallis, OR 97731
**Hoskin, Francis C. G.,** c/o Dr. John E. Walker, U.S. Army Natick RD&E Center, SAT NC-YSM, Kansas Street, Natick, MA 01760-5020
**Hubbard, Ruth,** Harvard University, Biological Laboratories, Cambridge, MA 02138
**Hunter, W. Bruce,** 305 Old Sharon Road, Peterborough, NH 03458-1736
**Hurwitz, Charles,** Stratton VA Medical Center, Research Service, Albany, NY 12208

**Katz, George,** 1636 Brookhouse Drive, Apt. BR131, Sarasota, FL 34731
**Kingsbury, John M.,** Cornell University, Department of Plant Biology, Plant Science Building, Ithaca, NY 14853
**Kleinholz, Lewis,** Reed College, Department of Biology, 3203 SE Woodstock Boulevard, Portland, OR 97202

**Kusano, Kiyoshi,** National Institutes of Health, Building 36, Room 4D-20, Bethesda, MD 20892

**Laderman, Ezra,** Yale University, New Haven, CT 06520
**LaMarche, Paul H.,** Eastern Maine Medical Center, 489 State Street, Bangor, ME 04401
**Lauffer, Max A.,** Penn State University Medical Center, Department of Biophysics & Physiology, Hershey, PA 17033
**Levitan, Herbert,** National Science Foundation, 4201 Wilson Boulevard, Room 835, Arlington, VA 22230
**Lochhead, John H.,** 49 Woodlawn Road, London SW6 6PS, UK
**Loewus, Frank A.,** Washington State University, Institute of Biological Chemistry, Pullman, WA 99164
**Loftfield, Robert B.,** University of New Mexico, School of Medicine, 915 Stanford Drive, Albuquerque, NM 87131
**Lorand, Laszlo,** Northwestern University Medical School, CMS Biology, Searle 4-555, 303 East Chicago Avenue, Chicago, IL 60611-3008

**Mainer, Robert E.,** The Boston Company, Inc., One Boston Place, OBP-15-D, Boston, MA 02108
**Malkiel, Saul,** 174 Queen Street, #9A, Falmouth, MA 02540
**Marsh, Julian B.,** 9 Eliot Street, Chestnut Hill, MA 02467-1407
**Martin, Lowell V.,** 10 Buzzards Bay Avenue, Woods Hole, MA 02543
**Mathews, Rita W.,** East Hill Road, P.O. Box 237, Southfield, MA 01259-0237
**Metuzals, Janis,** University of Ottawa Faculty of Medicine, Department of Pathology, 451 Smyth Road, Ottawa, ON K1H 8M5, Canada
**Moore, John A.,** University of California, Department of Biology, Riverside, CA 92521
**Moore, John W.,** Duke University Medical Center, Department of Neurobiology, Box 3209, Durham, NC 27710
**Moscona, Aron A.,** 221 West 82nd Street, #8C, New York, NY 10024
**Musacchia, X. J.,** P.O. Box 5054, Bella Vista, AR 72714-0054

**Nasatir, Maimon,** P.O. Box 379, Ojai, CA 93024

**Passano, Leonard M.,** University of Wisconsin, Department of Zoology, Birge Hall, Madison, WI 53706
**Potts, William T. W.,** University of Lancaster, Department of Biology, 524 Burrill Hall, Urbana, IL 61801
**Price, Carl A.,** 20 Maker Lane, Falmouth, MA 02540
**Prosser, C. Ladd,** University of Illinois, Department of Physiology, 524 Burrill Hall, Urbana, IL 61801 (deceased 2002)
**Prytz, Margaret McDonald,** (Address unknown)

**Renn, Charles E.,** (Address unknown)
**Reynolds, George T.,** Princeton University, Department of Physics, Jadwin Hall, Princeton, NJ 08544
**Rice, Robert V.,** 30 Burnham Drive, Falmouth, MA 02540
**Rockstein, Morris,** 600 Biltmore Way, Apt. 805, Coral Gables, FL 33134
**Roth, Jay S.,** 26 Huettner Road, P.O. Box 692, Woods Hole, MA 02543-0692
**Ronkin, Raphael R.,** 3212 McKinley Street, NW, Washington, DC 20015-1635
**Roslansky, John D.,** 57 Buzzards Bay Avenue, Woods Hole, MA 02543
**Roslansky, Priscilla F.,** Associates of Cape Cod, Inc., P.O. Box 224, Woods Hole, MA 02543-0224

**Sanders, Howard L.,** Woods Hole Oceanographic Institution, Woods Hole, MA 02543 (deceased 2001)
**Sato, Hidemi,** Nagoya University, 3-24-101, Oakinishi Machi, Toba Mie 517-0023, JAPAN
**Schlesinger, R. Walter,** P.O. Box 1424, North Falmouth, MA 02556
**Scott, Allan C.,** Colby College, Waterville, ME 04901
**Silverstein, Arthur M.,** Johns Hopkins University, Institute of the History of Medicine, 1900 E. Monument Street, Baltimore, MD 21205
**Sjodin, Raymond A.,** 3900 N. Charles Street, Apt. #1301, Baltimore, MD 21218-1719
**Smith, Paul F.,** P.O. Box 264, Woods Hole, MA 02543-0264
**Speer, John W.,** 293 West Main Road, Portsmouth, RI 02871
**Sperelakis, Nicholas,** University of Cincinnati, Department of Physiology/Biophysics, 231 Bethesda Avenue, Cincinnati, OH 45267-0576
**Spiegel, Evelyn,** Dartmouth College, Department of Biological Sciences, 204 Gilman, Hanover, NH 03755
**Spiegel, Melvin,** Dartmouth College, Department of Biological Sciences, 204 Gilman, Hanover, NH 03755
**Stephens, Grover C.,** University of California, School of Biological Sciences, Department of Ecology and Evolution/Biology, Irvine, CA 92717
**Stetten, Jane Lazarow,** 4701 Willard Avenue, #1413, Chevy Chase, MD 20815-4627
**Strehler, Bernard L.,** 31561 Crystal Sands Drive, Laguna Niguel, CA 92677
**Sussman, Maurice,** 72 Carey Lane, Falmouth, MA 02540
**Sussman, Raquel B.,** Marine Biological Laboratory, Woods Hole, MA 02543
**Szent-Gyorgyi, Gwen P.,** 45 Nobska Road, Woods Hole, MA 02543

**Thorndike, W. Nicholas,** Wellington Management Company, 200 State Street, Boston, MA 02109
**Trager, William,** The Rockefeller University, 1230 York Avenue, New York, NY 10021-6399
**Trinkaus, J. Philip,** Yale University, Department of Molecular, Cellular and Developmental Biology, Osborne Memorial Laboratory, New Haven, CT 06520

**Villee, Jr., Claude A.,** Harvard Medical School, Carrel L. Countway Library, 10 Shattuck Street, Boston, MA 02115
**Vincent, Walter S.,** 16 F.R. Lillie Road, Woods Hole, MA 02543

**Waterman, Talbot H.,** Yale University, Box 208103, 912 KBT Biology Department, New Haven, CT 06520-8103
**Wigley, Roland L.,** 35 Wilson Road, Woods Hole, MA 02543
**Wilkens, Lon A.,** University of Missouri, Department of Biology, 8001 Natural Bridge Road, St. Louis, MO 63121-4499
**Witkovsky, Paul,** NYU Medical Center, Department of Ophthalmology, 550 First Avenue, New York, NY 10016

## *Members*

**Aht, Donald A.,** Aquavet, University of Pennsylvania, School of Veterinary Medicine, 230 Main Street, Falmouth, MA 02540
**Adams, James A.,** 3481 Paces Ferry Road, Tallahassee, FL 32308
**Adelman, William J.,** 160 Locust Street, Falmouth, MA 02540
**Alkon, Daniel L.,** National Institutes of Health, Laboratory of Adaptive Systems, 36 Convent Drive, MSC 4124, 36/4A21, Bethesda, MD 20892-4124
**Allen, Garland E.,** Washington University, Department of Biology, Box 1137, One Brookings Drive, St. Louis, MO 63130-4899
**Allen, Nina S.,** North Carolina State University, Department of Botany, Box 7612, Raleigh, NC 27695
**Alliegro, Mark C.,** Louisiana State University Medical Center,

Department of Cell Biology and Anatomy, 1901 Perdido Street, New Orleans, LA 70112
**Anderson, Everett,** Harvard Medical School, Department of Cell Biology, 240 Longwood Avenue, Boston, MA 02115-6092
**Anderson, John M.,** 110 Roat Street, Ithaca, NY 14850
**Anderson, Porter W.,** 914 Grande Avenue, Key Largo, FL 33037
**Arnett-Kibel, Christine,** University of Massachusetts, Dean of Science Faculty, Boston, MA 02125
**Armstrong, Clay M.,** University of Pennsylvania School of Medicine, B701 Richards Building, Department of Physiology, 38th and Hamilton Walk, Philadelphia, PA 19104-6085
**Armstrong, Ellen Prosser,** 57 Millfield Street, Woods Hole, MA 02543
**Armstrong, Peter B.,** University of California, Section of Molecular and Cell Biology, One Shields Avenue, Davis, CA 95616-8755
**Ashton, Robert W.,** Bay Foundation, 17 West 94th Street, New York, NY 10025
**Atema, Jelle,** Boston University Marine Program, Marine Biological Laboratory, Woods Hole, MA 02543

**Baccetti, Baccio,** University of Sienna, Institute of Zoology, 53100 Siena, Italy
**Baker, Robert G.,** New York University Medical Center, Department Physiology and Biophysics, 550 First Avenue, New York, NY 10016
**Baldwin, Thomas O.,** University of Arizona, Department of Biochemistry, P.O. Box 210088, Tucson, AZ 85721-0088
**Baltimore, David,** California Institute of Technology, 1200 East California Boulevard, Pasadena, CA 91125
**Barlow, Robert B.,** SUNY Upstate Medical University, Center for Vision Research, 750 East Adams Street, Syracuse, NY 13210
**Barry, Daniel T.,** National Aeronautics and Space Administration, Lyn B. Johnson Space Center, 2101 NASA Road 1, Houston, TX 77058
**Barry, Susan R.,** Mount Holyoke College, Department of Biological Sciences, South Hadley, MA 01075
**Bass, Andrew H.,** Cornell University, Department of Neurobiology and Behavior, Seely Mudd Hall, Ithaca, NY 14853
**Battelle, Barbara-Anne,** University of Florida, Whitney Laboratory, 9505 Ocean Shore Boulevard, St. Augustine, FL 32086
**Bay, Frederick,** Bay Foundation, 17 W. 94th Street, First Floor, New York, NY 10025-7116
**Baylor, Martha B.,** P.O. Box 93, Woods Hole, MA 02543
**Bearer, Elaine L.,** Brown University, Division of Biology and Medicine, Department of Pathology, BMC 518, Providence, RI 02912
**Beatty, John M.,** University of Minnesota, Department of Ecology and Behavioral Biology, 1987 Gortner, St. Paul, MN 55108
**Beaugè, Luis Alberto,** Instituto de Investigacion Medica, Department of Biophysics, Casilla de Correo 389, Cordoba 5000, Argentina
**Begenisich, Ted,** University of Rochester, Medical Center, Box 642, 601 Elmwood Avenue, Rochester, NY 14642
**Begg, David A.,** University of Alberta, Faculty of Medicine, Department of Cell Biology and Anatomy, Edmonton, Alberta T6G 2H7, Canada
**Bell, Eugene,** 305 Commonwealth Avenue, Boston, MA 02115
**Benjamin, Thomas L.,** Harvard Medical School, Pathology, D2-230, 200 Longwood Avenue, Boston, MA 02115
**Bennett, Michael V. L.,** Albert Einstein College of Medicine, Department of Neuroscience, 1300 Morris Park Avenue, Bronx, NY 10461
**Bennett, Miriam F.,** Colby College, Department of Biology, Waterville, ME 04901
**Bennett, R. Suzanne,** Albert Einstein College of Medicine, Department of Neuroscience, 1410 Pelham Parkway South, Bronx, NY 10461
**Berg, Jr., Carl J.,** P.O. Box 681, Kilauea, Kauai, HI 96754-0681
**Berlin, Suzanne T.,** 87 Payneton Hill Road, York, ME 03909-5401
**Bernstein, Norman,** Columbia Realty Venture, 5301 Wisconsin Avenue, NW, #600, Washington, DC 20015-2015
**Bezanilla, Francisco,** Health Science Center, Department of Physiology, 405 Hilgard Avenue, Los Angeles, CA 90024
**Biggers, John D.,** Harvard Medical School, Department of Physiology, Boston, MA 02115
**Bishop, Stephen H.,** 2609 Eisenhower, Ames, IA 50010
**Blaustein, Mordecai P.,** University of Maryland, School of Medicine, Department of Physiology, Baltimore, MD 21201
**Blazis, Diana E. J.,** Marine Biological Laboratory, Center for Advanced Studies in the Space Life Sciences, Woods Hole, MA 02543
**Blennemann, Dieter,** 1117 East Putnam Avenue, Apt. #174, Riverside, CT 06878-1333
**Bloom, George S.,** The University of Texas Southwestern Medical Center, Department of Cell Biology and Neuroscience, 5323 Harry Hines Boulevard, Dallas, TX 75235-9039
**Bloom, Kerry S.,** University of North Carolina, Department of Biology, 623 Fordham Hall CB#3280, Chapel Hill, NC 27599-3280
**Bodznick, David A.,** Wesleyan University, Department of Biology, Lawn Avenue, Middletown, CT 06497-0170
**Boettiger, Edward G.,** P.O. Box 48, Rochester, VT 05767-0048
**Boolootian, Richard A.,** (address unknown)
**Borgese, Thomas A.,** Lehman College, CUNY, Department of Biology, Bedford Park Boulevard, West, Bronx, NY 10468
**Borst, Jr., David W.,** Illinois State University, Department of Biological Sciences, Normal, IL 61790-4120
**Bowles, Francis P.,** Marine Biological Laboratory, Ecosystems Center, Woods Hole, MA 02543
**Boyer, Barbara C.,** Union College, Biology Department, Schenectady, NY 12308
**Brandhorst, Bruce P.,** Simon Fraser University, Institute of Molecular Biology/Biochemistry, Barnaby, B.C. V5A 1S6, Canada
**Bronner-Fraser, Marianne,** California Institute of Technology, Beckman Institute Division of Biology, 139-74, Pasadena, CA 91125
**Brown, Stephen C.,** SUNY, Department of Biological Sciences, Albany, NY 12222
**Brown, William L.,** 80 Black Oak Road, Weston, MA 02193
**Browne, Carole L.,** Wake Forest University, Department of Biology, Box 7325 Reynolda Station, Winston-Salem, NC 27109
**Browne, Robert A.,** Wake Forest University, Department of Biology, Box 7325, Winston-Salem, NC 27109
**Bucklin, Anne C.,** University of New Hampshire, Ocean Process Analysis Laboratory, 142 Morse Hall, Durham, NH 03824
**Bullis, Robert A.,** Oceanic Institute of Applied Aquaculture, 41-202 Kalanianaole Highway, Waimanalo, HI 96795
**Burger, Max M.,** Friedrich Miescher-Institute, P.O. Box 2543, CH-4002 Basel, Switzerland
**Burgess, David R.,** Boston College, Department of Biology, Higgins Hall, 140 Commonwealth Avenue, Chestnut Hill, MA 02167
**Burgos, Mario H.,** IHEM Medical School, UNC Conicet, Casilla de Correo 56, 5500 Mendoza, Argentina
**Burky, Albert,** University of Dayton, Department of Biology, Dayton, OH 45469
**Burris, John E.,** Beloit College, 700 College Street, Beloit, WI 53511
**Burstyn, Harold Lewis,** Syracuse University, L. C. Smith College of Engineering and Computer Science, Link Hall 237, Syracuse, NY 13244
**Bursztajn, Sherry,** (address unknown)

**Calabrese, Ronald L.,** Emory University, Department of Biology, 1510 Clifton Road, Atlanta, GA 30322
**Cameron, R. Andrew,** California Institute of Technology, Division of Biology 156-29, Pasadena, CA 91125
**Campbell, Richard H.,** Bang-Campbell Associates, Eel Pond Place, Box 402, Woods Hole, MA 02543
**Candelas, Graciela C.,** University of Puerto Rico, Department of Biology, P.O. Box 23360, UPR Station, San Juan, PR 00931-3360

**Cariello, Lucio,** Stazione Zoologica "A. Dohrn," Villa Comunale, 80121 Naples, Italy
**Case, James F.,** University of California, Marine Science Institute, Santa Barbara, CA 93106
**Cassidy, Father Joseph D.,** Providence College, Priory of St. Thomas Aquinas, Providence, RI 02918-0001
**Cavanaugh, Colleen M.,** Harvard University, Biological Laboratories, 16 Divinity Avenue, Cambridge, MA 02138
**Chambers, Edward L.,** University of Miami School of Medicine, Department of Physiology and Biophysics, P.O. Box 016430, Miami, FL 33101
**Chang, Donald C.,** Hong Kong University, Science and Technology, Department of Biology, Clear Water Bay, Kowloon, Hong Kong
**Chappell, Richard L.,** Hunter College, CUNY, Department of Biological Sciences, 695 Park Avenue, New York, NY 10021
**Child, Frank M.,** 28 Lawrence Farm Road, Woods Hole, MA 02543-1416
**Chisholm, Rex Leslie,** Northwestern University, Medical School, Department of Cell Biology, Chicago, IL 60611
**Citkowitz, Elena,** Hospital of St. Raphael, Lipid Disorders Clinic, 1450 Chapel Street, New Haven, CT 06511
**Clapham, David E.,** Children's Hospital, Enders 1309, 320 Longwood Avenue, Boston, MA 02115
**Clark, Eloise E.,** Bowling Green State University, Biological Sciences Department, Bowling Green, OH 43403
**Clark, Hays,** 150 Gomez Road, Hobe Sound, FL 33455
**Clark, Jr., Wallis H.,** RR1 Box 916, Madison, ME 32615
**Claude, Philippa,** University of Wisconsin, Department of Zoology, Zoology Research Building 125, 1117 W Johnson Street, Madison, WI 53706
**Clay, John R.,** National Institutes of Health, NINDS, Building 36, Room 2-CO2, Bethesda, MD 20892
**Clowes, Alexander W.,** University of Washington, School of Medicine, Department of Surgery, Box 356410, Seattle, WA 98195-6410
**Cobb, Jewel Plummer,** California State University, 5151 University Drive, Health Center 205, Los Angeles, CA 90032-8500
**Cohen, Carolyn,** Brandeis University, Rosenstiel Basic Medical, Sciences Research Center, Waltham, MA 02254
**Cohen, Lawrence B.,** Yale University School of Medicine, Department of Physiology, 333 Cedar Street, New Haven, CT 06520
**Cohen, Maynard M.,** Rush Medical College, Department of Neurological Sciences, 600 South Paulina, Chicago, IL 60612
**Cohen, William D.,** Hunter College, Department Biological Sciences, 695 Park Avenue, New York, NY 10021
**Coleman, Annette W.,** Brown University, Division of Biology and Medicine, Providence, RI 02912
**Colinvaux, Paul,** Marine Biological Laboratory, Woods Hole, MA 02543
**Collier, R. John,** Harvard Medical School, Department of Microbiology and Molecular Genetics, 200 Longwood Avenue, Room 356, Boston, MA 02115
**Collins, James P.,** Arizona State University, College of Liberal Arts and Sciences, Department of Biology, P.O. Box 871501, Tempe, AZ 85287-1501
**Cook, Joseph A.,** Edna McConnell Clark Foundation, 250 Park Avenue, New York, NY 10177-0026
**Cornwall, Jr., Melvin C.,** Boston University School of Medicine, Department of Physiology L714, Boston, MA 02118
**Corson, Jr., D. Wesley,** Storm Eye Institute, Room 537, 171 Ashley Avenue, Charleston, SC 29425
**Corwin, Jeffrey T.,** University of Virginia, School of Medicine, Department Otolaryngology and Neuroscience, Box 396, Charlottesville, VA 22908
**Couch, Ernest F.,** Texas Christian University, Department of Biology, TCU Box 298930, Fort Worth, TX 76129
**Cox, Rachel Llanelly,** Marine Biological Laboratory, Woods Hole, MA 02543
**Crane, Sylvia E.,** c/o Mr. Thomas Crane, 40 Chestnut Street, Weston, MA 02493 (deceased 2002)
**Cremer-Bartels, Gertrud,** Horstmarer Landweg 142, 48149 Muenster, Germany
**Crow, Terry J.,** University of Texas Medical School, Department of Neurobiology and Anatomy, Houston, TX 77225
**Crowther, Robert J.,** Shriners Hospitals for Children, 51 Blossom Street, Boston, MA 02114
**Cummings, Michael P.,** Marine Biological Laboratory, Bay Paul Center, Woods Hole, MA 02543
**Cutler, Richard D.,** Marine Biological Laboratory, Woods Hole, MA 02543

**Davidson, Eric H.,** California Institute of Technology, Division of Biology 156-29, 391 South Holliston, Pasadena, CA 91125
**Davison, Daniel B.,** Bristol-Myers Squibb PRI, Bioinformatics Department, 5 Research Parkway, Wallingford, CT 06492
**Daw, Nigel W.,** 5 Old Pawson Road, Branford, CT 06405
**Dawidowicz, Eliezar A.,** Marine Biological Laboratory, Office of Research Administration and Education, Woods Hole, MA 02543
**De Weer, Paul J.,** University of Pennsylvania, B400 Richards Building, Department of Physiology, 3700 Hamilton Walk, Philadelphia, PA 19104-6085
**Deegan, Linda A.,** Marine Biological Laboratory, The Ecosystems Center, Woods Hole, MA 02543
**DeGroof, Robert C.,** 145 Water Crest Drive, Doylestown, PA 18901-3267
**Denckla, Martha Bridge,** Johns Hopkins University, School of Medicine, Kennedy-Krieger Institute, 707 North Broadway, Baltimore, MD 21205
**DePhillips, Henry A.,** Trinity College, Department of Chemistry, 300 Summit Street, Hartford, CT 06106
**DeSimone, Douglas W.,** University of Virginia, Department of Cell Biology, Box 800732, Charlottesville, VA 22908
**Dettbarn, Wolf-Dietrich,** 4422 Wayland Drive, Nashville, TN 37215
**Dionne, Vincent E.,** Boston University, Biology Department, 5 Cummington Street, Boston, MA 02215-2406
**Dowling, John E.,** Harvard University, Biological Laboratories, 16 Divinity Street, Cambridge, MA 02138
**DuBois, Arthur Brooks,** John B. Pierce Foundation Laboratory, 290 Congress Avenue, New Haven, CT 06519
**Duncan, Thomas K.,** Nichols College, Environmental Sciences Department, Dudley, MA 01571
**Dunham, Philip B.,** Syracuse University, Department of Biology, 130 College Place, Syracuse, NY 13244-1220
**Dunlap, Paul V.,** University of Michigan, Department of Biology, 830 North University Avenue, Ann Arbor, MI 48109-1048

**Eckberg, William R.,** Howard University, Department of Biology, P.O. Box 887, Administration Building, Washington, DC 20059
**Edds, Kenneth T.,** Bayer Diagnostics, 511 Benedict Avenue, Tarrytown, NY 10591
**Eder, Howard A.,** Albert Einstein College of Medicine, 1300 Morris Park Avenue, Bronx, NY 10461
**Edstrom, Joan,** 53 Two Ponds Road, Falmouth, MA 02540
**Egyud, Laszlo G.,** Cell Research Corporation, P.O. Box 67209, Chestnut Hill, MA 02167-0209
**Ehrlich, Barbara E.,** Yale University Medical School, Department of Pharmacology, Box 208066, 333 Cedar Street, New Haven, CT 06520-8066
**Eisen, Arthur Z.,** Washington University, Division of Dermatology, St. Louis, MO 63110

**Eisen, Herman N.,** Massachusetts Institute of Technology, Center for Cancer Research, E17-128, 77 Massachusetts Avenue, Cambridge, MA 02139-4307
**Elder, Hugh Young,** University of Glasgow, Institute of Physiology, West Medical Building, Glasgow G12 8QQ, Scotland
**Englund, Paul T.,** Johns Hopkins Medical School, Department of Biological Chemistry, 725 North Wolfe Street, Baltimore, MD 21205
**Epel, David,** Stanford University, Hopkins Marine Station, Ocean View Boulevard, Pacific Grove, CA 93950
**Epstein, Herman T.,** 18 Lawrence Farm Road, Woods Hole, MA 02543
**Epstein, Ray L.,** 701 Winthrop Street, #311, Taunton, MA 02780-2187

**Farb, David H.,** Boston University School of Medicine, Department of Pharmacology L603, 80 East Concord Street, Boston, MA 02118
**Farmanfarmaian, A. Verdi,** Rutgers University, Department of Biological Sciences, Nelson Biology Laboratory POB 1059, Piscataway, NJ 08855
**Feldman, Susan C.,** University of Medicine and Dentistry, New Jersey Medical School, 100 Bergen Street, Newark, NJ 07103
**Festoff, Barry William,** VA Medical Center, Neurology Service (151), 4801 Linwood Boulevard, Kansas City, MO 64128
**Fink, Rachel D.,** Mount Holyoke College, Department of Biological Sciences, Clapp Laboratories, Room 215, South Hadley, MA 01075
**Finkelstein, Alan,** Albert Einstein College of Medicine, 1300 Morris Park Avenue, Bronx, NY 10461
**Fischbach, Gerald D.,** Columbia College of Physicians and Surgeons, 630 West 168th Street, R 2-401, New York, NY 10032
**Fishman, Harvey M.,** University of Texas Medical Branch, Department of Physiology and Biophysics, 301 University Boulevard, Galveston, TX 77555-0641
**Flanagan, Dennis,** 12 Gay Street, New York, NY 10014
**Fluck, Richard Allen,** Franklin and Marshall College, Department of Biology, Box 3003, Lancaster, PA 17604-3003
**Foreman, Kenneth H.,** Marine Biological Laboratory, Woods Hole, MA 02543
**Fox, Thomas Oren,** Harvard Medical School, Division of Medical Sciences, MEC 435, 260 Longwood Avenue, Boston, MA 02115
**Franzini-Armstrong, Clara,** University of Pennsylvania, School of Medicine, 330 South 46th Street, Philadelphia, PA 19143
**Fraser, Scott,** California Institute of Technology, Beckman Institute 139-74, 1201 East California Boulevard, Pasadena, CA 91125
**French, Robert J.,** University of Calgary, Health Sciences Centre, Alberta, T2N 4N1, CANADA
**Fulton, Chandler M.,** Brandeis University, Department of Biology, MS 008, Waltham, MA 02454-9110
**Furie, Barbara C.,** Beth Israel Deaconess Medical Center, BIDMC Cancer Center, Kirstein 1, 330 Brookline Avenue, Boston, MA 02215
**Furie, Bruce,** Beth Israel Deaconess Medical Center, BIDMC Cancer Center, Kirstein 1, 330 Brookline Avenue, Boston, MA 02215
**Furshpan, Edwin J.,** Harvard Medical School, Department of Neurobiology, 220 Longwood Avenue, Boston, MA 02115
**Futrelle, Robert P.,** Northeastern University, College of Computer Science, 360 Huntington Avenue, Boston, MA 02115

**Gabr, Howaida,** Suez Canal University, Department of Marine Science, Faculty of Science, Ismailia, Egypt
**Gadsby, David C.,** The Rockefeller University, Laboratory of Cardiac Physiology, 1230 York Avenue, New York, NY 10021-6399
**Gainer, Harold,** National Institutes of Health, NINDS,BNP,DIR, Neurochemistry, Building 36, Room 4D20, Bethesda, MD 20892-4130
**Galatzer-Levy, Robert M.,** 534 Judson Avenue, Evanston, IL 60202
**Gall, Joseph G.,** Carnegie Institution, 115 West University Parkway, Baltimore, MD 21210
**Gallo, Michael A.,** UMDNJ-Robert Wood Johnson Medical School, EOHSI, Room 408, 170 Frelinghuysen Road, Piscataway, NJ 08854-8020
**Garber, Sarah S.,** Allegheny University of the Health Sciences, Department of Physiology, 2900 Queen Lane, Philadelphia, PA 19129
**Gelperin, Alan,** Bell Labs Lucent, Department Biology Comp., Rm 1C464, 600 Mountain Avenue, Murray Hill, NJ 07974
**German, III, James L.,** Weill Medical College of Cornell University, 1300 York Avenue, New York, NY 10021
**Gibbs, Martin,** Brandeis University, Institute for Photobiology of Cells and Organelles, Waltham, MA 02254
**Giblin, Anne E.,** Marine Biological Laboratory, The Ecosystems Center, Woods Hole, MA 02543
**Gibson, A. Jane,** Cornell University, Department of Biochemistry, Biotech Building, Ithaca, NY 14850
**Gifford, Prosser,** Library of Congress, Madison Building LM605, Washington, DC 20540
**Giudice, Giovanni,** Universita di Palermo, Dipartimento di Biologia, Cellulare e Dello Sviluppo, 1-90123 Palermo, Italy
**Giuditta, Antonio,** University of Naples, Department of General Physiology, Via Mezzocannone 8, Naples, 80134, Italy
**Glynn, Paul,** P.O. Box 6104, Cooks Corner, Brunswick, ME 04011
**Golden, William T.,** Chairman Emeritus, American Museum of Natural History, 500 Fifth Avenue, 50th Floor, New York, NY 10110
**Goldman, Robert D.,** Northwestern University Medical School, Department of Cell and Molecular Biology, 303 E. Chicago Avenue, Chicago, IL 60611-3008
**Goldsmith, Paul K.,** National Institutes of Health, 9000 Rockville Pike, Building 10, Room 8C206, Bethesda, MD 20892
**Goldsmith, Timothy H.,** Yale University, Department of Biology, New Haven, CT 06510
**Goldstein, Jr., Moise H.,** The Johns Hopkins University, ECE Department, Barton Hall, Baltimore, MD 21218
**Gould, Robert Michael,** NYS Institute of Basic Research, Department of Pharmacology, 1050 Forest Hill Road, Staten Island, NY 10314-6399
**Govind, C. K.,** Scarborough College, Life Sciences Division, 1265 Military Trail, West Hill, Ontario M1C 1A4, Canada
**Grace, Dick,** Doreen Grace Fund, The Brain Center, Promontory Point, New Seabury, MA 02649
**Graf, Werner M.,** College of France, 11 Place Marcelin Berthelot, 75231 Paris Cedex 05, France
**Grant, Philip,** National Institutes of Health, NINDS\BN\DIR-Neurochemistry, Building 36, Room 4D20, Bethesda, MD 20892-4130
**Grassle, Judith P.,** Rutgers University, Institute of Marine and Coastal Studies, 71 Dudley Road, New Brunswick, NJ 08901-8521
**Graubard, Katherine G.,** University of Washington, Department of Zoology, NJ-15, Box 351800, Seattle, WA 98195-1800
**Greenberg, Everett Peter,** University of Iowa, College of Medicine, Department of Microbiology, Iowa City, IA 52242
**Greenberg, Michael J.,** University of Florida, The Whitney Laboratory, 9505 Ocean Shore Boulevard, St. Augustine, FL 32086-8623
**Greer, Mary J.,** 176 West 87th Street, #12A, New York, NY 10024-2902
**Griffin, Donald R.,** Harvard University, Concord Field Station, Old Causeway Road, Bedford, MA 01730
**Gross, Paul R.,** 123 Perkins Street, Jamaica Plain, MA 02130
**Grossman, Albert,** New York University Medical Center, 550 First Avenue, New York, NY 10016
**Grossman, Lawrence,** The Johns Hopkins University, Hygiene Building, Room W8306, Baltimore, MD 21205
**Gruner, John A.,** Cephalon, Inc., 145 Brandywine Parkway, West Chester, PA 19380-4245
**Gunning, A. Robert,** P.O. Box 165, Falmouth, MA 02541
**Gwilliam, G. Francis,** Reed College, Department of Biology, Portland, OR 97202

**Haimo, Leah T.,** University of California, Department of Biology, Riverside, CA 92521
**Hajduk, Stephen L.,** University of Alabama, School of Medicine/Dentistry, Department of Biochemistry/Molecular Genetics, University Station, Birmingham, AL 35294
**Hall, Linda M.,** Shriners Hospital for Children, 2425 Stockton Boulevard, Sacramento, CA 95817
**Halvorson, Harlyn O.,** University of Massachusetts, Policy Center for Marine Biosciences and Technology, 100 Morrissey Boulevard, Boston, MA 02125-3393
**Haneji, Tatsuji,** The University of Tokushima, Department of Histology & Oral Histology, School of Dentistry, 18-15, 3 Kuramoto-cho, Tokushima 770-8504, Japan
**Hanlon, Roger T.,** Marine Biological Laboratory, Woods Hole, MA 02543
**Harosi, Ferenc,** New College of the USF, Division of Natural Sciences, 5700 North Tamiami Trail, Sarasota, FL 34243-2197
**Harrigan, June F.,** 2311 Bingham Street, Honolulu, HI 96825
**Harrington, Glenn W.,** Weber State University, Department of Microbiology, Ogden, UT 84408
**Harrington, John P.,** SUNY-New Paltz, Physical Sciences & Engineering, REH-114, New Paltz, NY 12561
**Harrison, Stephen C.,** Harvard University, Department of Molecular and Cell Biology, 7 Divinity Avenue, Cambridge, MA 02138
**Haselkorn, Robert,** University of Chicago, Department of Molecular Genetics and Cell Biology, Chicago, IL 60637
**Hastings, J. Woodland,** Harvard University, The Biological Laboratories, 16 Divinity Avenue, Cambridge, MA 02138-2020
**Hayes, Jr., Raymond L.,** Howard University, College of Medicine, 520 W Street, NW, Washington, DC 20059
**Heck, Diane E.,** Rutgers University, Department of Pharmacology/Toxicology, 681 Frelinghuysen Road, Piscataway, NJ 08855
**Henry, Jonathan Joseph,** University of Illinois, Department of Cell and Structural Biology, 601 South Goodwin Avenue #B107, Urbana, IL 61801-3709
**Hepler, Peter K.,** University of Massachusetts, Department of Biology, Morrill III, Amherst, MA 01003
**Herndon, Walter R.,** University of Tennessee, Department of Botany, Knoxville, TN 37996-1100
**Hershko, Avram,** Technion-Israel Institute of Technology, Unit of Biochemistry, The Bruce Rappaport Faculty of Medicine, Haifa 31096, Israel
**Herskovits, Theodore T.,** Fordham University, Department of Chemistry, John Mulcahy Hall, Room 638, Bronx, NY 10458
**Hiatt, Howard H.,** Brigham and Women's Hospital, Department of Medicine, 75 Francis Street, Boston, MA 02115
**Highstein, Stephen M.,** Washington University, Department of Otolaryngology, 517 S Euclid, Box 8115, St. Louis, MO 63110
**Hildebrand, John G.,** University of Arizona, ARL Division of Neurobiology, P.O. Box 210077, Tucson, AZ 85721-0077
**Hill, Richard W.,** Michigan State University, Department of Zoology, East Lansing, MI 48824
**Hill, Robert B.,** University of Rhode Island, Department of Biological Sciences, 100 Flagg Road, Kingston, RI 02881
**Hill, Susan D.,** Michigan State University, Department of Zoology, East Lansing, MI 48824
**Hillis, Llewellya W.,** Marine Biological Laboratory, Woods Hole, MA 02543
**Hinchcliffe, Edward H.,** University of Massachusetts Medical School, Department of Cell Biology, 377 Plantation Street, Worcester, MA 01605
**Hinkle, Gregory J.,** Bioinformatics Group, Cereon Genomics, 45 Sidney Street, Cambridge, MA 02139
**Hinsch, Gertrude W.,** University of South Florida, Department of Biology, Tampa, FL 33620
**Hinsch, Jan,** Leica, Inc., 110 Commerce Drive, Allendale, NJ 07401
**Hobbie, John E.,** Marine Biological Laboratory, The Ecosystems Center, Woods Hole, MA 02543
**Hodge, Alan J.,** 3843 Mount Blackburn Avenue, San Diego, CA 92111
**Hoffman, Joseph F.,** Yale University School of Medicine, Cellular and Molecular Physiology, 333 Cedar Street, New Haven, CT 06520-8026
**Hollyfield, Joe G.,** The Cleveland Clinic, Opthalmic Research, 9500 Euclid Avenue, Cleveland, OH 44195
**Holz IV, George G.,** New York University Medical Center, Department of Physiology and Neuroscience, Medical Sciences Building, Room 442, 550 First Avenue, New York, NY 10016
**Hopkinson, Jr., Charles S.,** Marine Biological Laboratory, Woods Hole, MA 02543
**Houk, James C.,** Northwestern University Medical School, 303 East Chicago Avenue, Ward 5-315, Chicago, IL 60611-3008
**Hoy, Ronald R.,** Cornell University, Section of Neurobiology and Behavior, 215 Mudd Hall, Ithaca, NY 14853
**Huang, Alice S.,** California Institute of Technology, Mail Code 1-9, Pasadena, CA 91125
**Hufnagel-Zackroff, Linda A.,** University of Rhode Island, Department of Microbiology, Kingston, RI 02881
**Hummon, William D.,** Ohio University, Department of Biological Sciences, Athens, OH 45701
**Humphreys, Susie H.,** Food and Drug Administration, HFS-308, 200 C Street, SW, Washington, DC 20204-0001
**Humphreys, Tom,** University of Hawaii, Kewalo Marine Laboratory, 41 Ahui Street, Honolulu, HI 96813
**Hunt, Tim,** ICRF, Clare Hall Laboratories, South Mimms Potter's Bar, Herts EN6-3LD, England
**Hunter, Robert D.,** Oakland University, Department of Biological Sciences, Rochester, MI 48309-4401
**Huxley, Hugh E.,** Brandeis University, Rosenstiel Center, Biology Department, Waltham, MA 02154

**Ilan, Joseph,** Case Western Reserve University, School of Medicine, Department of Anatomy, Cleveland, OH 44106
**Ingoglia, Nicholas A.,** New Jersey Medical School, Department of Pharmacology/Physiology, 185 South Orange Avenue, Newark, NJ 07103
**Inoué, Saduyki,** McGill University, Department of Anatomy, 3640 University Street, Montreal, PQ H3A 2B2, Canada
**Inoué, Shinya,** Marine Biological Laboratory, Woods Hole, MA 02543
**Isselbacher, Kurt J.,** Massachusetts General Hospital Cancer Center, Charlestown, MA 02129
**Issidorides, Marietta Radovic,** (address unknown)
**Izzard, Colin S.,** SUNY-Albany, Department of Biological Sciences, 1400 Washington Avenue, Albany, NY 12222

**Jacobs, Neil,** Hale and Dorr, 60 State Street, Boston, MA 02109
**Jaffe, Laurinda A.,** University of Connecticut Health Center, Department of Physiology, Farmington Avenue, Farmington, CT 06032
**Jaffe, Lionel,** Marine Biological Laboratory, Woods Hole, MA 02543
**Jeffery, William R.,** University of Maryland, Department of Biology, College Park, MD 20742
**Johnston, Daniel,** Baylor College of Medicine, Division of Neuroscience, One Baylor Plaza, Room S740, Houston, TX 77030
**Josephson, Robert K.,** University of California, School of Biological Science, Department of Psychobiology, Irvine, CA 92697

**Kaczmarek, Leonard K.,** Yale University School of Medicine, Department of Pharmacology, 333 Cedar Street, New Haven, CT 06520
**Kaley, Gabor,** New York Medical College, Department of Physiology, Basic Sciences Building, Valhalla, NY 10595

**Kaltenbach, Jane,** Mount Holyoke College, Department Biological Sciences, South Hadley, MA 01075

**Kaminer, Benjamin,** Boston University Medical School, Physiology Department, 715 Albany Street, Boston, MA 02118

**Kaneshiro, Edna S.,** University of Cincinnati, Biological Sciences Department, JL 006, Cincinnati, OH 45221-0006

**Kaplan, Ehud,** Mount Sinai School of Medicine, 1 Gustave Levy Place, Box 1183, New York, NY 10029

**Karakashian, Stephen J.,** Apartment 16-F, 165 West 91st Street, New York, NY 10024

**Karlin, Arthur,** Columbia University, Center for Molecular Recognition, 630 West 168th Street, Room 11-401, New York, NY 10032

**Karnovsky, Morris John,** Harvard Medical School, Department of Pathology, 200 Longwood Avenue, Building D2, Room 430, Boston, MA 02115

**Keller, Hartmut Ernst,** Carl Zeiss, Inc., One Zeiss Drive, Thornwood, NY 10594

**Kelley, Darcy B.,** Columbia University, Department of Biological Sciences, 911 Fairchild, Mailcode 2432, New York, NY 10027

**Kelly, Robert E.,** 5 Little Harbor Road, Woods Hole, MA 02543

**Kemp, Norman E.,** University of Michigan, Department of Biology, Ann Arbor, MI 48109

**Kendall, John P.,** Faneuil Hall Associates, 176 Federal Street, 2nd Floor, Boston, MA 02110

**Kerr, Louis M.,** Marine Biological Laboratory, Woods Hole, MA 02543

**Keynan, Alexander,** Israel Academy of Science and Humanity, P.O. Box 4040, Jerusalem, Israel

**Khan, Shahid M. M.,** SUNY Upstate Medical University, Biochemistry and Molecular Biology, 4295 Weiskotten Hall Addition, 7 East Adams Street, Syracuse, NY 13210

**Khodakhah, Kamran,** University of Colorado School of Medicine, Department of Physiology and Biophysics, 4200 East 9th Avenue, C-240, Denver, CO 80262

**Kiehart, Daniel P.,** Duke University Medical Center, Department of Cell Biology, Box 3709, 308 Nanaline Duke Building, Durham, NC 27710

**Kleinfeld, David,** University of California, Department of Physics, 0319 9500 Gilman Drive, La Jolla, CA 92093

**Klessen, Rainer,** (address unknown)

**Klotz, Irving M.,** Northwestern University, Department of Chemistry, Evanston, IL 60201

**Knudson, Robert A.,** Marine Biological Laboratory, Woods Hole, MA 02543

**Koide, Samuel S.,** The Rockefeller University, The Population Council, 1230 York Avenue, New York, NY 10021

**Kornberg, Hans,** Boston University, The University Professors, 745 Commonwealth Avenue, Boston, MA 02215

**Kosower, Edward M.,** Tel-Aviv University, Department of Chemistry, Ramat-Aviv, Tel Aviv, 69978, Israel

**Krane, Stephen M.,** Massachusetts General Hospital, 55 Fruit Street, Bulf-165, Boston, MA 02114

**Krauss, Robert,** P.O. Box 291, Denton, MD 21629

**Kravitz, Edward A.,** Harvard Medical School, Department of Neurobiology, 220 Longwood Avenue, Boston, MA 02115

**Kriebel, Mahlon E.,** SUNY Health Science Center, Department of Physiology, Syracuse, NY 13210

**Kristan Jr., William B.,** University of California, Department of Biology 0357, 9500 Gilman Drive, La Jolla, CA 92093-0357

**Kropinski, Andrew M.,** Queen's University, Department of Microbiology/Immunology, Botterell Hall, Room 74, Kingston, Ontario K7L 3N6, Canada

**Kuffler, Damien P.,** Institute of Neurobiology, 201 Boulevard del Valle, San Juan 00901, PR

**Kuhns, William J.,** Hospital for Sick Children, Biochemistry Research, 555 University Avenue, Toronto, Ontario M5G 1X8, Canada

**Kunkel, Joseph G.,** University of Massachusetts, Department of Biology, Amherst, MA 01003

**Kuzirian, Alan M.,** Marine Biological Laboratory, Woods Hole, MA 02543-1015

**Laderman, Aimlee D.,** Yale University, School of Forestry and Environmental Studies, 370 Prospect Street, New Haven, CT 06511

**Landeau, Laurie J.,** Listowel, Inc., 2 Park Avenue, Suite 1525, New York, NY 10016

**Landis, Dennis M. D.,** University Hospital of Cleveland, Department Neurology, 11100 Euclid Avenue, Cleveland, OH 44106

**Landis, Story C.,** National Institutes of Health, Building 36, Room 5A05, 36 Convent Drive, Bethesda, MD 20892-4150

**Landowne, David,** University of Miami Medical School, Department of Physiology and Biophysics, PO Box 016430, Miami, FL 33101

**Langford, George M.,** Dartmouth College, Department of Biological Sciences, 6044 Gilman Laboratory, Hanover, NH 03755

**Laskin, Jeffrey,** University of Medical and Dentistry of New Jersey, Robert Wood Johnson Medical School, 675 Hoes Lane, Piscataway, NJ 08854

**Lasser-Ross, Nechama,** New York Medical College, Department of Physiology, Valhalla, NY 10595

**Laster, Leonard,** University of Massachusetts Medical School, 55 Lake Avenue, North, Worcester, MA 01655

**Laties, Alan,** Scheie Eye Institute, Myrin Circle, 51 North 39th Street, Philadelphia, PA 19104

**Laufer, Hans,** University of Connecticut, Department of Molecular and Cell Biology, U-125, 75 North Eagleville Road, Storrs, CT 06269-3125

**Lazarow, Paul B.,** Mount Sinai School of Medicine, Department of Cell Biology and Anatomy, 1190 Fifth Avenue, Box 1007, New York, NY 10029-6574

**Lazarus, Maurice,** Federated Department Stores, Sears Crescent, City Hall Plaza, Boston, MA 02108

**Leadbetter, Edward R.,** University of Connecticut, Department of Molecular and Cell Biology, U-131, Beach Hall, Room 249, 354 Mansfield Road, Storrs, CT 06269-2131

**Lederberg, Joshua,** The Rockefeller University, Suite 400 (Founders Hall), 1230 York Avenue, New York, NY 10021

**Lee, John J.,** City College of CUNY, Department of Biology, Convent Avenue and 138th Street, New York, NY 10031

**Lehy, Donald B.,** 35 Willow Field Drive, North Falmouth, MA 02556

**Leighton, Stephen B.,** Beecher Instruments, P.O. Box 8704, Silver Spring, MD 20910

**Lerner, Aaron B.,** Yale University School of Medicine, Department of Dermatology, P.O. Box 3333, New Haven, CT 06510

**Levin, Jack,** Veterans Administration, Medical Center, 111 H2, 4150 Clement Street, San Francisco, CA 94121

**Levine, Michael,** University of California, Department MCB, 401 Barker Hall, Berkeley, CA 94720

**Levine, Richard B.,** University of Arizona, Division of Neurobiology, Room 611, Gould Simpson Building, P.O. Box 210077, Tucson, AZ 85721-0077

**Levinthal, Francoise,** Columbia University, Department of Biological Sciences, Broadway and 116th Street, New York, NY 10026

**Levitan, Irwin B.,** University of Pennsylvania, School of Medicine, 218 Stemmler Hall, 3450 Hamilton Walk, Philadelphia, PA 19104-6074

**Linck, Richard W.,** University of Minnesota School of Medicine, Cell Biology and Neuroanatomy Department, 4-135 Jackson Hall, 321 Church Street, Minneapolis, MN 55455

**Lipicky, Raymond J.,** Food and Drug Administration, CDER/ODEI/HFD-110, 5600 Fishers Lane, Rockville, MD 20857

**Lisman, John E.,** Brandeis University, Molecular and Cell Biology, 415 South Street, Waltham, MA 02454-9110

**Liuzzi, Anthony,** 180 Beacon Street, #8G, Boston, MA 02116
**Llinas, Rodolfo R.,** New York University Medical Center, Department of Physiology/Biophysics, 550 First Avenue, Room 442, New York, NY 10016
**Lobel, Phillip S.,** Boston University Marine Program, Marine Biological Laboratory, Woods Hole, MA 02543
**Loew, Franklin M.,** Becker College, 61 Sever Street, Worcester, MA 01615-0071
**Loewenstein, Birgit Rose,** 102 Ransom Road, Falmouth, MA 02540
**Loewenstein, Werner R.,** 102 Ransom Road, Falmouth, MA 02540
**London, Irving M.,** Harvard-MIT, Division, E-25-551, Cambridge, MA 02139
**Longo, Frank J.,** University of Iowa, Department of Anatomy, Iowa City, IA 52442
**Luckenbill, Louise M.,** 430 Sippiwissett Road, Falmouth, MA 02540

**Macagno, Eduardo R.,** University of California, Division of Biology, 9500 Gilman Drive, MC-0346, La Jolla, CA 92093-0346
**MacNichol Jr., Edward F.,** Boston University School of Medicine, Department of Physiology, 80 East Concord Street, Boston, MA 02118
**Maglott-Duffield, Donna R.,** American Type Culture Collection, 12301 Parklawn Drive, Rockville, MD 20852-1776
**Maienschein, Jane Ann,** Arizona State University, Department of Philosophy, P.O. Box 872004, Tempe, AZ 85287-2004
**Malbon, Craig C.,** SUNY, University Medical Center, Pharmacology-HSC, Stony Brook, NY 11794-8651
**Malchow, Robert P.,** University of Illinois, Department of Biology, M/C 066, 845 West Taylor Street, Chicago, IL 60607
**Manalis, Richard S.,** Indiana-Purdue University, Department of Biological Science, 2101 Coliseum Boulevard East, Fort Wayne, IN 46805
**Manz, Robert D.,** (address unknown)
**Margulis, Lynn,** University of Massachusetts, Department of Geosciences, Morrill Science Center, Box 35820, Amherst, MA 01003-5820
**Marinucci, Andrew C.,** 102 Nancy Drive, Mercerville, NJ 08619
**Martinez, Jr., Joe L.,** The University of Texas, Division of Life Sciences, 6900 North Loop 1604 West, San Antonio, TX 78249-0662
**Martinez-Palomo, Adolfo,** CINVESTAV-IPN, Sec. de Patologia Experimental, 07000 Mexico, D.F.A.P.140740, Mexico
**Mastroianni, Jr., Luigi,** Hospital of University of Pennsylvania, 106 Dulles, 3400 Spruce Street, Philadelphia, PA 19104-4283
**Mauzerall, David,** Rockefeller University, 1230 York Avenue, New York, NY 10021
**McAnelly, M. Lynne,** University of Texas, Section of Neurobiology, School of Life Sciences, Austin, TX 78712
**McArthur, Andrew G.,** Marine Biological Laboratory, Josephine Bay Paul Center, Woods Hole, MA 02543
**McCann Murray, Frances V.,** Dartmouth Medical School, Department of Physiology, Lebanon, NH 03756
**McLaughlin, Jane A.,** Marine Biological Laboratory, Woods Hole, MA 02543
**McMahon, Robert F.,** University of Texas, Arlington, Department of Biology, Box 19498, Arlington, TX 76019
**Meedel, Thomas,** Rhode Island College, Biology Department, 600 Mount Pleasant Avenue, Providence, RI 02908
**Meinertzhagen, Ian A.,** Dalhousie University, Department of Psychology, Halifax, NS B3H 4J1, Canada
**Meiss, Dennis E.,** Immunodiagnostic Laboratories, 488 McCormick Street, San Leandro, CA 94577
**Melillo, Jerry M.,** Marine Biological Laboratory, Ecosystems Center, Woods Hole, MA 02543
**Mellon, Jr., DeForest,** University of Virginia, Department of Biology, Gilmer Hall, Charlottesville, VA 22903
**Mellon, Richard P.,** P.O. Box 187, Laughlintown, PA 15655-0187
**Mendelsohn, Michael E.,** New England Medical Center, Molecular Cardiology Laboratory, NEMC Box 80, 750 Washington Street, Boston, MA 02111
**Mensinger, Allen F.,** University of Minnesota, Biology Department, LSCI 211, Duluth, MN 55812
**Merriman, Melanie Pratt,** Touchstone Consulting, 7511 Beach View Drive, North Bay Village, FL 33141
**Meselson, Matthew,** Harvard University, Fairchild Biochemistry Building, 7 Divinity Avenue, Cambridge, MA 02138
**Miledi, Ricardo,** University of California, Irvine, Department of Psychobiology, 2205 Biology Science II, Irvine, CA 92697-4550
**Milkman, Roger D.,** University of Iowa, Department of Biological Sciences, Biology Building, Room 318, Iowa City, IA 52242-1324
**Miller, Andrew L.,** Hong Kong University of Science & Technology, HKUST Calcium-Aequorin Imaging Laboratory, Department of Biology, Clearwater Bay, Kowloon, Hong Kong, People's Republic of China
**Miller, Thomas J.,** Analogic, 8 Centennial Drive, Peabody, MA 01960
**Misevic, Gradimir,** University Hospital of Basel, Department of Research, Mebelstr. 20, CH-4031 Basel, Switzerland
**Mitchell, Ralph,** Harvard University, Division of Applied Sciences, 29 Oxford Street, Cambridge, MA 02138
**Miyakawa, Hiroyoshi,** Tokyo College of Pharmacy, Laboratory of Cellular Neurobiology, 1432-1 Horinouchi, Hachiouji, Tokyo 192-03, Japan
**Miyamoto, David M.,** Drew University, Department of Biology, Madison, NJ 07940
**Mizell, Merle,** Tulane University, Department of Cell and Molecular Biology, New Orleans, LA 70118
**Moreira, Jorge E.,** National Institutes of Health, NICHD, Department of Cell and Molecular Biol., Bethesda, MD 20852
**Morin, James G.,** Cornell University, Department of Ecology and Evolutionary Biology, G14 Stimson Hall, Ithaca, NY 14853-2801
**Morrell, Leyla deToledo,** Rush-Presbyterian-St. Lukes, Medical Center, 1653 West Congress Parkway, Chicago, IL 60612
**Morse, Stephen S.,** 275 Central Park West, New York, NY 10024
**Mote, Michael I.,** Temple University, Department of Biology, Philadelphia, PA 19122
**Muller, Kenneth J.,** University of Miami School of Medicine, Department of Physiology and Biophysics, 1600 NW 10th Avenue, R-430, Miami, FL 33136
**Murray, Andrew W.,** Harvard University, Department of Molecular & Cellular Biology, 16 Divinity Avenue, Room 3000, Cambridge, MA 02138

**Nabrit, Samuel M.,** 686 Beckwith Street, SW, Atlanta, GA 30314
**Nadelhoffer, Knute J.,** Marine Biological Laboratory, 7 MBL Street, Woods Hole, MA 02543
**Nagel, Ronald L.,** Albert Einstein College of Medicine, 1300 Morris Park Avenue, Bronx, NY 10461
**Naka, Ken-ichi,** 2-9-2 Tatumi Higashi, Okazaki, 444, Japan
**Nakajima, Yasuko,** University of Illinois, College of Medicine, Anatomy and Cell Biology Department, M/C 512, Chicago, IL 60612
**Narahashi, Toshio,** Northwestern University Medical School, Department of Pharmacology, 303 East Chicago Avenue, Chicago, IL 60611
**Nasi, Enrico,** Boston University School of Medical, Department of Physiology, R-406, 80 East Concord Street, Boston, MA 02118
**Neill, Christopher,** Marine Biological Laboratory, 7 MBL Street, Woods Hole, MA 02543
**Nelson, Margaret C.,** Cornell University, Section of Neurobiology and Behavior, Ithaca, NY 14850
**Nickerson, Peter A.,** SUNY at Buffalo, Department of Pathology, Buffalo, NY 14214
**Nicosia, Santo V.,** University of South Florida, College of Medicine, Box 11, Department of Pathology, Tampa, FL 33612

**Noe, Bryan D.,** Emory University School of Medicine, Department of Anatomy and Cell Biology, Atlanta, GA 30322
**Norton, Catherine N.,** Marine Biological Laboratory, 7 MBL Street, Woods Hole, MA 02543
**Nusbaum, Michael P.,** University of Pennsylvania School of Medicine, Department of Neuroscience, 215 Stemmler Hall, Philadelphia, PA 19104-6074

**O'Herron, Jonathan,** Lazard Freres and Company, 30 Rockefeller Plaza, 59th Floor, New York, NY 10020-1900
**Obaid, Ana Lia,** University of Pennsylvania School of Medicine, Neuroscience Department, 234 Stemmler Hall, Philadelphia, PA 19104-6074
**Ohki, Shinpei,** SUNY at Buffalo, Department of Biophysical Sciences, 224 Cary Hall, Buffalo, NY 14214
**Oldenbourg, Rudolf,** Marine Biological Laboratory, 7 MBL Street, Woods Hole, MA 02543
**Olds, James L.,** George Mason University, Krasnow Institute for Advanced Studies, Mail Stop 2A1, Fairfax, VA 22030-4444
**Olins, Ada L.,** Foundation for Blood, 69 U.S. Route One, P.O. Box 190, Scarborough, ME 04070-0190
**Olins, Donald E.,** Foundation for Blood, 69 U.S. Route One, P.O. Box 190, Scarborough, ME 04070-0190
**Oschman, James L.,** 827 Central Avenue, Dover, NH 03820

**Palazzo, Robert E.,** University of Kansas, Department of Physiology and Cell Biology, Lawrence, KS 66045
**Palmer, John D.,** University of Massachusetts, Department of Zoology, 221 Morrill Science Center, Amherst, MA 01003
**Pant, Harish C.,** National Institutes of Health, NINCDS, Laboratory of Neurochemistry, Building 36, Room 4D20, Bethesda, MD 20892
**Pappas, George D.,** University of Illinois, Psychiatric Institute, 1601 W. Taylor Street, MC 912, Chicago, IL 60612
**Pardee, Arthur B.,** Dana-Farber Cancer Institute, D810, 44 Binney Street, Boston, MA 02115
**Pardy, Rosevelt L.,** University of Nebraska, School of Life Sciences, Lincoln, NE 68588
**Parmentier, James L.,** Massachusetts General Hospital, Partners/Fenway/Shattuck Center for Aids Research, 149 13th Street, Room 5219, Charlestown, MA 02129
**Pederson, Thoru,** University of Massachusetts Medical Center, Biochemistry & Molecular Biology, 377 Plantation Street, Worcester, MA 01605
**Perkins, Courtland D.,** 400 Hilltop Terrace, Alexandria, VA 22301
**Person, Philip,** 137-87 75th Road, Flushing, NY 11367
**Peterson, Bruce J.,** Marine Biological Laboratory, 7 MBL Street, Woods Hole, MA 02543
**Pethig, Ronald,** University College of North Wales, School of Electronic Engineering, Bangor, Gwynedd, LL 57 1UT, United Kingdom
**Pfohl, Ronald J.,** Miami University, Department of Zoology, Oxford, OH 45056
**Pierce, Jr., Sidney K.,** University of South Florida, Department of Biology, SCA 110, 4202 East Fowler Avenue, Tampa, FL 33620
**Pleasure, David E.,** Children's Hospital, Neurology Research, 5th Floor, Ambramson Building, Philadelphia, PA 19104
**Poindexter, Jeanne S.,** Barnard College, Columbia University, 3009 Broadway, New York, NY 10027-6598
**Pollard, Harvey B.,** U.S.U.H.S., 4301 Jones Bridge Road, Bethesda, MD 20814
**Pollard, Thomas D.,** Yale University, Molecular, Cellular & Developmental Biology, New Haven, CT 06520
**Porter, Beverly H.,** 5542 Windysun Court, Columbia, MD 21045
**Porter, Mary E.,** University of Minnesota, Department of Cell Biology and Neuroanatomy, 4-135 Jackson Hall, 321 Church Street SE, Minneapolis, MN 55455
**Potter, David D.,** Harvard Medical School, Department of Neurobiology, 25 Shattuck Street, Boston, MA 02115
**Powers, Maureen K.,** 2771 Sargent Avenue, San Pablo, CA 94806
**Prendergast, Robert A.,** 29 Pondlet Place, Falmouth, MA 02540
**Prior, David J.,** Northern Arizona University, Arts and Sciences Dean's Office, Box 5621, Flagstaff, AZ 86011
**Prusch, Robert D.,** Gonzaga University, Department of Life Sciences, Spokane, WA 99258
**Purves, Dale,** Duke University Medical Center, Department of Neurobiology, Box 3209, 101-1 Bryan Research Building, Durham, NC 27710

**Quigley, James P.,** The Scripps Research Institute, Department of Vascular Biology, 10550 N. Torrey Pines Road VB-1, La Jolla, CA 92037

**Rabb, Irving W.,** 1010 Memorial Drive, #20A, Cambridge, MA 02138
**Rabin, Harvey,** 1102 Ralston Road, Rockville, MD 20852
**Rabinowitz, Michael B.,** Marine Biological Laboratory, 7 MBL Street, Woods Hole, MA 02543
**Rafferty, Nancy S.,** Marine Biological Laboratory, 7 MBL Street, Woods Hole, MA 02543
**Rakowski, Robert F.,** Ohio University, Biological Sciences, 106 Irvine Hall, Athens, OH 45701
**Ramon, Fidel,** Universidad Nacional Autonoma de Mexico, Division EStreet Posgrado E Invest., Facultad de Medicina, 04510, D.F., Mexico
**Rastetter, Edward B.,** Marine Biological Laboratory, The Ecosystems Center, Woods Hole, MA 02543
**Rebhun, Lionel I.,** University of Virginia, Department of Biology, Gilmer Hall 45, Charlottesville, VA 22901
**Reddan, John R.,** Oakland University, Department of Biological Sciences, Rochester, MI 48309-4401
**Reese, Thomas S.,** National Institutes of Health, NINDS, Department of Neurobiology, Building 36, Room 2A-21, 36 Convent Drive, Bethesda, MD 20892
**Reinisch, Carol L.,** Marine Biological Laboratory, 7 MBL Street, Woods Hole, MA 02543
**Rickles, Frederick R.,** 3910 Highwood Court, N.W., Washington, DC 20007
**Rieder, Conly L.,** Wadsworth Center, Division of Molecular Medicine, P.O. Box 509, Albany, NY 12201-0509
**Riley, Monica,** Marine Biological Laboratory, 7 MBL Street, Woods Hole, MA 02543
**Ripps, Harris,** University of Illinois at Chicago, Department of Ophthalmology/Visual Sciences, 1855 West Taylor Street, Chicago, IL 60612
**Ritchie, J. Murdoch,** Yale University School of Medicine, Department of Pharmacology, 333 Cedar Street, New Haven, CT 06510
**Rome, Lawrence C.,** University of Pennsylvania, Department of Biology, Leidy Labs, Philadelphia, PA 19104
**Rosenbluth, Jack,** New York University School of Medical, Department of Physiology and Biophysics, RR 714, 400 East 34th Street, New York, NY 10016
**Rosenbluth, Raja,** Simon Fraser University, Institute of Molecular Biology and Biochemistry, Burnaby, BC V5A 1S6, Canada
**Rosenfield, Allan,** Columbia University School of Public Health, 600 West 168th Street, New York, NY 10032-3702
**Rosenkranz, Herbert S.,** 130 Desoto Street, Pittsburgh, PA 15213-2535
**Ross, William N.,** New York Medical College, Department of Physiology, Valhalla, NY 10595

**Rottenfusser, Rudi,** Marine Biological Laboratory, 7 MBL Street, Woods Hole, MA 02543

**Rowland, Lewis P.,** Neurological Institute, 710 West 168th Street, New York, NY 10032

**Ruderman, Joan V.,** Harvard Medical School, Department of Cell Biology, C2-428, 240 Longwood Avenue, Boston, MA 02115

**Rummel, John D.,** NASA Headquarters, Office of Space Science, Washington, DC 20546

**Rushforth, Norman B.,** Case Western Reserve University, Department of Biology, Cleveland, OH 44106

**Russell-Hunter, William D.,** 711 Howard Street, Easton, MD 21601-3934

**Saffo, Mary Beth,** Harvard University, MCZ Labs 408, 26 Oxford Street, Cambridge, MA 02138

**Salama, Guy,** University of Pittsburgh, Department of Physiology, Pittsburgh, PA 15261

**Salmon, Edward D.,** University of North Carolina, Department of Biology, CB 3280, Chapel Hill, NC 27514

**Salyers, Abigail,** University of Illinois, Department of Microbiology, B-103, 601 South Goodwin Avenue, Urbana, IL 61801

**Salzberg, Brian M.,** University of Pennsylvania School of Medicine, Department of Neuroscience, 215 Stemmler Hall, Philadelphia, PA 19104-6074

**Sanger, Jean M.,** University of Pennsylvania School of Medicine, Department of Anatomy, 36th and Hamilton Walk, Philadelphia, PA 19104

**Sanger, Joseph W.,** University of Pennsylvania Medical Center, Department of Cell and Developmental Biology, 36th and Hamilton Walk, Philadelphia, PA 19104-6058

**Saunders, Jr., John W.,** 118 Metoxit Road, P.O. Box 3381, Waquoit, MA 02536

**Schachman, Howard K.,** University of California, Molecular and Cell Biology Department, 229 Stanley Hall, #3206, Berkeley, CA 94720-3206

**Schatten, Gerald P.,** Oregon Health Sciences University, Oregon Regional Primate Research Center, 505 N.W. 185th Avenue, Beaverton, OR 97006

**Schmeer, Arlene C.,** Mercenene Cancer Research Institute, 790 Prospect Street, New Haven, CT 06511

**Schuel, Herbert,** SUNY at Buffalo, Department of Anatomy/Cell Biology, Buffalo, NY 14214

**Schwartz, Lawrence,** University of Massachusetts, Department of Biology, Morrill Science Center, Amherst, MA 01003

**Schweitzer, A. Nicola,** Brigham and Women's Hospital, Immunology Division, Department of Pathology, 221 Longwood Avenue, LMRC 521, Boston, MA 02115

**Segal, Sheldon J.,** The Population Council, One Dag Hammarskjold Plaza, New York, NY 10036

**Senft, Stephen Lamont,** Yale University, Neuroengineering/Neuroscience Center, P.O. Box 208205, New Haven, CT 06520-8205

**Shanklin, Douglas R.,** University of Tennessee, Department of Pathology, Room 576, 800 Madison Avenue, Memphis, TN 38117

**Shashar, Nadav,** The Interuniversity Institute of Eilat, P.O. Box 469, Eilat 88103, Israel

**Shashoua, Victor E.,** Harvard Medical School, Ralph Lowell Labs, McLean Hospital, 115 Mill Street, Belmont, MA 02178

**Shaver, Gaius R.,** Marine Biological Laboratory, The Ecosystems Center, Woods Hole, MA 02543

**Shaver, John R.,** Michigan State University, Department of Zoology, East Lansing, MI 48824

**Sheetz, Michael P.,** Columbia University, Department of Biological Sciences, New York, NY 10027

**Shepro, David,** Boston University, CAS Biology, 5 Cummington Street, Boston, MA 02215

**Shimomura, Osamu,** Marine Biological Laboratory, 7 MBL Street, Woods Hole, MA 02543

**Shipley, Alan M.,** P.O. Box 943, Forestdale, MA 02644

**Silver, Robert B.,** Wayne State University, Department of Pharmacology, Physiology & Radiology, 540 East Canfield Avenue, Detroit, MI 48201

**Siwicki, Kathleen K.,** Swarthmore College, Biology Department, 500 College Avenue, Swarthmore, PA 19081-1397

**Skinner, Dorothy M.,** 24 Gray Lane, Falmouth, MA 02540

**Sloboda, Roger D.,** Dartmouth College, Department of Biological Science, 6044 Gilman, Hanover, NH 03755-1893

**Sluder, Greenfield,** University of Massachusetts Medical School, Room 324, 377 Plantation Street, Worcester, MA 01605

**Smith, Peter J. S.,** Marine Biological Laboratory, 7 MBL Street, Woods Hole, MA 02543

**Smith, Stephen J.,** Stanford University School of Medicine, Department of Molecular and Cellular Physiology, Beckman Center, Stanford, CA 94305

**Smolowitz, Roxanna S.,** Marine Biological Laboratory, 7 MBL Street, Woods Hole, MA 02543

**Sogin, Mitchell L.,** Marine Biological Laboratory, 7 MBL Street, Woods Hole, MA 02543

**Sorenson, Martha M.,** Cidade Universitaria-UFRJ, Department Bioquimica Medica-ICB, 21941-590 Rio de Janerio, Brazil

**Speck, William T.,** Marine Biological Laboratory, 7 MBL Street, Woods Hole, MA 02543

**Spector, Abraham,** Columbia University, Department of Ophthalmology, 630 West 168th Street, New York, NY 10032

**Speksnijder, Johanna E.,** DeMeent 12, 3984JJ Odijk, The Netherlands

**Spray, David C.,** Albert Einstein College of Medicine, Department of Neuroscience, 1300 Morris Park Avenue, Bronx, NY 10461

**Spring, Kenneth R.,** National Institutes of Health, 10 Center Drive, MSC 1598, Building 10, Room 6N260, Bethesda, MD 20892-1603

**Steele, John H.,** Woods Hole Oceanographic Institution, Woods Hole, MA 02543

**Steinacker, Antoinette,** University of Puerto Rico, Institute of Neurobiology, 201 Boulevard Del Valle, San Jan, PR 00901

**Steinberg, Malcolm,** Princeton University, Department of Molecular Biology, M-18 Moffett Laboratory, Princeton, NJ 08544-1014

**Stemmer, Andreas C.,** Institut für Robotik, ETH-Sentrum, 8092 Zurich, Switzerland

**Stenflo, Johan,** University of Lund, Department of Clinical Chemistry, Malmo General Hospital, S-205 02 Malmo, Sweden

**Steudler, Paul A.,** Marine Biological Laboratory, The Ecosystems Center, Woods Hole, MA 02543

**Stokes, Darrell R.,** Emory University, Department of Biology, 1510 Clifton Road NE, Atlanta, GA 30322-1100

**Stommel, Elijah W.,** Darmouth Hitchcock Medical Center, Neurology Department, 1 Medical Drive, Lebanon, NH 03756

**Stracher, Alfred,** SUNY Health Science Center, Department of Biochemistry, 450 Clarkson Avenue, Brooklyn, NY 11203

**Strumwasser, Felix,** P.O. Box 923, East Falmouth, MA 02536-2278

**Stuart, Ann E.,** University of North Carolina at Chapel Hill, Cellular & Molecular Physiology, 254 Medical Science Research Building, Campus Box 7545, Chapel Hill, NC 27599

**Sugimori, Mutsuyuki,** New York University Medical Center, Department of Physiology and Neuroscience, Room 442, 550 First Avenue, New York, NY 10016

**Summers, William C.,** Western Washington University, Huxley College of Environmental Studies, Bellingham, WA 98225-9181

**Suprenant, Kathy A.,** University of Kansas, Department of Physiology and Cell Biology, 4010 Haworth Hall, Lawrence, KS 66045

**Sydlik, Mary Anne,** Hope College, Peale Science Center, 35 East 12th St./P.O. Box 9000, Holland, MI 49422

**Szent-Gyorgyi, Andrew G.,** Brandeis University, Molecular and Cell Biology, 415 South Street, Waltham, MA 02454-9110

**Tamm, Sidney L.,** Boston University, CAS Biology, 5 Cummington Street, Boston, MA 02215
**Tanzer, Marvin L.,** University of Connecticut School of Dental Medicine, Department of Biostructure and Function, Farmington, CT 06030-3705
**Tasaki, Ichiji,** National Institutes of Health, NIMH, Laboratory of Neurobiology, Building 36, Room 2B-16, Bethesda, MD 20892
**Taylor, D. Lansing,** Cellomics, Inc., 635 William Pitt Way, Pittsburgh, PA 15238
**Taylor, Edwin W.,** University of Chicago, Department of Molecular Genetics, 920 E. 58th Street, Chicago, IL 60637
**Telfer, William H.,** University of Pennsylvania, Department of Biology, Philadelphia, PA 19104
**Telzer, Bruce,** Pomona College, Department of Biology, Thille Building, 175 West 6th Street, Claremont, CA 91711
**Terasaki, Mark,** University of Connecticut Health Center, Department of Physiology, 263 Farmington Avenue, Farmington, CT 06032
**Townsel, James G.,** Meharry Medical College, Department of Anatomy and Physiology, 1005 DB Todd Boulevard, Nashville, TN 37208
**Travis, David M.,** 19 High Street, Woods Hole, MA 02543-1221
**Treistman, Steven N.,** University of Massachusetts Medical Center, Department of Pharmacology, 55 Lake Avenue North, Worcester, MA 01655
**Trigg, D. Thomas,** One Federal Street, 9th Floor, Boston, MA 02211
**Troll, Walter,** NYU Medical Center, Department of Environmental Medicine, 550 First Avenue, New York, NY 10016
**Troxler, Robert F.,** Boston University School of Medicine, Department of Biochemistry, 80 East Concord Street, Boston, MA 02118
**Tucker, Edward B.,** Baruch College, CUNY, Department of Natural Sciences, 17 Lexington Avenue, New York, NY 10010
**Tweedell, Kenyon S.,** University of Notre Dame, Department of Biological Sciences, Notre Dame, IN 46556-0369
**Tykocinski, Mark L.,** Case Western Reserve University, Institute of Pathology, 2085 Adelbert Road, Cleveland, OH 44106
**Tytell, Michael,** Wake Forest University, Bowman Gray School of Medicine, Department of Anatomy and Neurobiology, Winston-Salem, NC 27157

**Ueno, Hiroshi,** Kyoto University, AGR Chemistry, Faculty of Agriculture, Sakyo, Kyoto 606-8502, Japan

**Valiela, Ivan,** Boston University Marine Program, Marine Biological Laboratory, Woods Hole, MA 02543
**Vallee, Richard,** University of Massachusetts Medical Center, Worcester Foundation Campus, 222 Maple Avenue, Shrewsbury, MA 01545
**Valois, John J.,** 420 Woods Hole Road, Woods Hole, MA 02543
**Van Dover, Cindy Lee,** The College of William and Mary, Biology Department, 328 Millington Hall, Williamsburg, VA 23187
**Van Holde, Kensal E.,** Oregon State University, Biochemistry and Biophysics Department, Corvallis, OR 97331-7503
**Vogl, Thomas P.,** Environmental Research Institute of Michigan, 1101 Wilson Boulevard, Arlington, VA 22209

**Wadsworth, Patricia,** University of Massachusetts, Department of Biology, C.B. 35810, Amherst, MA 01003
**Wainwright, Norman R.,** Marine Biological Laboratory, 7 MBL Street, Woods Hole, MA 02543
**Waksman, Byron H.,** New York University Medical Center, Department of Pathology, 550 First Avenue, New York, NY 10016
**Wall, Betty,** 9 George Street, Woods Hole, MA 02543
**Wangh, Lawrence J.,** Brandeis University, Department of Biology, 415 South Street, Waltham, MA 02254
**Warner, Robert C.,** 1609 Temple Hills Drive, Laguna Beach, CA 92651
**Warren, Leonard,** Wistar Institute, 36th and Spruce Streets, Philadelphia, PA 19104
**Waterbury, John B.,** Woods Hole Oceanographic Institution, Department of Biology, Woods Hole, MA 02543
**Waxman, Stephen G.,** Yale Medical School, Neurology Department, 333 Cedar Street, P.O. Box 208018, New Haven, CT 06510
**Weber, Annemarie,** University of Pennsylvania School of Medicine, Department of Biochemistry and Biophysics, Philadelphia, PA 19066
**Weeks, Janis C.,** University of Oregon, Institute of Neuroscience, Eugene, OR 97403-1254
**Weidner, Earl,** Louisiana State University, Department of Biological Sciences, 502 Life Sciences Building, Baton Rouge, LA 70803
**Weiss, Alice Sara,** 105 University Boulevard West, Silver Spring, MD 20901
**Weiss, Dieter G.,** University of Rostock, Institute of Zoology, D-18051 Rostock, Germany
**Weiss, Leon P.,** University of Pennsylvania School of Veterinary Medicine, Department of Animal Biology, Philadelphia, PA 19104
**Weiss, Marisa C.,** Paoli Memorial Hospital, Department of Radiation Oncology, 255 W. Lancaster Avenue, Paoli, PA 19301
**Weissmann, Gerald,** New York University Medical Center, Department of Medicine/Division Rheumatology, 550 First Avenue, New York, NY 10016
**Westerfield, Monte,** University of Oregon, Institute of Neuroscience, Eugene, OR 97403
**Whittaker, J. Richard,** University of New Brunswick, Department of Biology, BS 4511, Fredericton, NB E3B 6E1, Canada
**Wiesel, Torsten N.,** Rockefeller University, 1230 York Avenue, New York, NY 10021
**Wilson, Darcy B.,** Torrey Pines Institute, 3550 General Atomics Court, Building 2, Room 138, San Diego, CA 92121
**Wilson, T. Hastings,** Harvard Medical School, Department of Physiology, 25 Shattuck Street, Boston, MA 02115
**Wittenberg, Beatrice,** Albert Einstein College of Medicine, Department of Physiology and Biophysics, Bronx, NY 10461
**Wittenberg, Jonathan B.,** Albert Einstein College of Medicine, Department of Physiology and Biophysics, Bronx, NY 10461
**Wonderlin, William F.,** West Virginia University, Pharmacology and Toxicology Department, Morgantown, WV 26506
**Worden, Mary Kate,** University of Virginia, Department of Neuroscience, McKim Hall Box 230, Charlottesville, VA 22908
**Worgul, Basil V.,** Columbia University, Department of Ophthalmology, 630 West 168 Street, New York, NY 10032
**Wu, Chau Hsiung,** Northwestern University Medical School, Department of Pharmacology (S215), 303 East Chicago Avenue, Chicago, IL 60611-3008
**Wyttenbach, Charles R.,** University of Kansas, Biological Sciences Department, 2045 Haworth Hall, Lawrence, KS 66045-2106

**Zakon, Harold H.,** University of Texas, Section of Neurobiology, School of Life Science, Austin, TX 78712
**Zigman, Seymour,** Marine Park Condominiums, 174 Queen Street, Unit 10-F, Falmouth, MA 02540
**Zigmond, Michael J.,** University of Pittsburgh, S-526 Biomedical Science Tower, 3500 Terrace Street, Pittsburgh, PA 15213
**Zimmerberg, Joshua J.,** National Institutes of Health, LCMB, NICHD, Building 10, Room 10D14, 10 Center Drive, Bethesda, MD 20892
**Zottoli, Steven J.,** Williams College, Department of Biology, Williamstown, MA 01267
**Zucker, Robert S.,** University of California, Neurobiology Division, Molecular and Cellular Biology Department, Berkeley, CA 94720

# MBL Associates

## *Executive Board*

Ruth Ann Laster, President
Jack Pearce, Vice President
Kitty Brown, Treasurer
Molly N. Cornell, Secretary
Duncan Aspinwall, Membership Chair
Tammy Smith Amon
Elizabeth Farnham
Barbara Atwood
Julie Child
Seymour Cohen
Michael Fenlon
Pat Ferguson
Sallie A. Giffen
Alice Knowles
Rebecca Lash
Cornelia Hanna McMurtrie
Joan Pearlman
Virginia Reynolds
Volker Ulbrich

## *Associates Administrator*

Susan Joslin

## *Patron*

Mr. and Mrs. Norman Bernstein
Judge and Mrs. John S. Langford
Dr. and Mrs. Edward F. MacNichol, Jr.
Mr. and Mrs. William Niles

## *Sustaining Associate*

Mr. and Mrs. David Bakalar
Bufftree Building Co., Inc.
Mr. and Mrs. G. Nathan Calkins, Jr.
Mrs. Sally Cross
Mrs. James Ferguson
Drs. David Forkosh and Linda Hirshman
Mrs. James R. Glazebrook

## *Supporting Associate*

Dr. and Mrs. Samuel C. Armstrong
Mr. and Mrs. Malcolm Campbell
Mr. and Mrs. Thomas Claflin
Mrs. George H. A. Clowes
Ms. Anne R. DuBois
Mr. Mike Fenlon and Ms. Linda Sallop
Mrs. Mary L. Goldman
Mr. and Mrs. Gary G. Hayward
Mr. and Mrs. Lon Hocker
Mr. and Mrs. Arthur King
Dr. and Mrs. Leonard Laster
Dr. and Mrs. Berton J. Leach
Dr. and Mrs. William M. McDermott
Mr. and Mrs. James McSherry
Mr. and Mrs. William J. Pechilis
Mr. and Mrs. Walter J. Salmon
Mrs. Anne W. Sawyer
Dr. John Tochko and Mrs. Christina Myles-Tochko
Mr. and Mrs. Leslie J. Wilson

## *Family Membership*

Dr. and Mrs. Edward A. Adelberg
Mr. and Mrs. David C. Ahearn
Dr. and Mrs. Dean C. Allard, Jr.
Drs. James and Helene Anderson
Mr. and Mrs. Duncan P. Aspinwall
Mr. and Mrs. Donald R. Aukamp
Mr. and Mrs. John M. Baitsell
Dr. and Mrs. Robert B. Barlow, Jr.
Mr. and Mrs. John E. Barnes
Mrs. Beth Berne
Drs. Harriet and Alan Bernheimer
Mr. and Mrs. Robert O. Bigelow
Dr. and Mrs. Edward G. Boettiger
Mr. and Mrs. Kendall B. Bohr
Dr. and Mrs. Thomas A. Borgese
Dr. and Mrs. Francis P. Bowles
Dr. and Mrs. John B. Buck
Dr. and Mrs. John E. Burris
Mr. and Mrs. William O. Burwell
Mr. and Mrs. D. Bret Carlson
Dr. and Mrs. Richard L. Chappell
Dr. and Mrs. Frank M. Child
Dr. and Mrs. Arnold M. Clark
Mr. and Mrs. James M. Cleary
Dr. and Mrs. Laurence P. Cloud
Drs. Harry Conner and Carol Scott-Conner
Mr. and Mrs. Donald B. Cook
Mr. and Mrs. Theron S. Curtis, Jr.
Mr. and Mrs. Joel P. Davis
Mr. and Mrs. F. Gerald Douglass
Dr. and Mrs. John E. Dowling
Dr. and Mrs. Arthur Brooks DuBois
Mr. and Mrs. Jerome Fanger
Dr. and Mrs. Michael J. Fishbein
Mr. and Mrs. Howard G. Freeman
Dr. and Mrs. Robert A. Frosch
Dr. and Mrs. John J. Funkhouser
Dr. and Mrs. Mordecai L. Gabriel
Miss Eleanor Garfield
Dr. and Mrs. James L. German, III
Dr. and Mrs. Harold S. Ginsberg
Dr. and Mrs. Murray Glusman
Drs. Alfred and Joan Goldberg
Mr. Michael P. Goldring
Dr. and Mrs. Moise H. Goldstein, Jr.
Mrs. Ann Goodman and Dr. Arthur Pardee
Mr. and Mrs. Charles Goodwin, III
Dr. and Mrs. Thomas C. Gregg
Dr. and Mrs. Newton H. Gresser
Mr. and Mrs. Peter A. Hall
Dr. and Mrs. Harlyn O. Halvorson
Mrs. Penelope Hare
Dr. and Mrs. Richard Bennet Harvey
Dr. and Mrs. J. Woodland Hastings
Dr. Robert R. Haubrich
Mr. and Mrs. Edward S. Heard
Dr. and Mrs. Howard H. Hiatt
Mr. and Mrs. David Hibbitt
Dr. Llewellya Hillis and Dr. Paul Colinvaux
Dr. and Mrs. John E. Hobbie
Dr. Peter A. Hoenig
Mr. and Mrs. Gerald J. Holtz
Drs. Francis Hoskin and Elizabeth Farnham
Mrs. Carmela J. Huettner and Ms. Susan Huettner
Dr. and Mrs. Shinya Inoue
Dr. and Mrs. Kurt J. Isselbacher
Mrs. Mary D. Janney
Mr. and Mrs. DeWitt C. Jones
Dr. and Mrs. Benjamin Kaminer
Dr. Morris John Karnovsky
Dr. and Mrs. George Katz
Mr. and Mrs. Paul W. Knaplund
Mr. and Mrs. A. Sidney Knowles, Jr.
Mr. and Mrs. Walter E. Knox
Sir and Lady Hans Kornberg
Dr. and Mrs. S. Andrew Kulin
Dr. and Mrs. George M. Langford
Dr. Hans Laufer
Mr. William Lawrence and Mrs. Barbara Buchanan
Dr. and Mrs. John J. Lee
Mr. and Mrs. Robert Livingstone, Jr.
Dr. and Mrs. Laszlo Lorand
Mr. Richard C. Lovering
Mr. and Mrs. Francis C. Lowell, Jr.
Mr. and Mrs. Joseph C. Martyna
Drs. Luigi and Elaine Mastroianni
Dr. and Mrs. Robert T. McCluskey
Dr. and Mrs. Jerry M. Melillo
Dr. Martin Mendelson
Mr. and Mrs. Richard Meyers
Mr. and Mrs. Charles A. Mitchell
Dr. and Mrs. Merle Mizell
Dr. and Mrs. Charles H. Montgomery
Mr. and Mrs. Stephen A. Moore
Mr. James V. Moynihan
Mr. and Mrs. Lewis Nassikas
Dr. and Mrs. John E. Naugle
Dr. Pamela Nelson and Mr. Christopher Olmsted
Mr. and Mrs. Frank L. Nickerson
Dr. and Mrs. Clifford T. O'Connell
Mr. and Mrs. James J. O'Connor
Mr. David and Ms. Anastasia Palmer
Dr. Arthur Pardee and Mrs. Ann Goodman
Mr. and Mrs. Robert Parkinson
Mr. and Mrs. Richard M. Paulson, Jr.
Dr. and Mrs. John B. Pearce
Mrs. Nancy Pendleton
Mr. and Mrs. John B. Peri
Dr. and Mrs. Courtland D. Perkins
Dr. and Mrs. Philip Person
Mr. and Mrs. Frederick S. Peters
Mr. and Mrs. Frederick S. Peters
Mr. and Mrs. E. Joel Peterson
Mr. and Mrs. Harold Pilskaln
Mr. and Mrs. George H. Plough

Dr. and Mrs. Aubrey Pothier, Jr.
Mr. and Mrs. Allan Putnam
Dr. and Mrs. Lionel I. Rebhun
Dr. and Mrs. George T. Reynolds
Dr. and Mrs. Harris Ripps
Dr. Paul B. Rizzoli
Ms. Jean Roberts
Drs. Priscilla and John Roslansky
Mr. and Mrs. John D. Ross
Dr. and Mrs. John W. Saunders, Jr.
Dr. and Mrs. R. Walter Schlesinger
Mr. and Mrs. Harold H. Sears
Dr. and Mrs. Sheldon J. Segal
Dr. and Mrs. Robert Seidler
Mr. and Mrs. Daniel Shearer
Dr. and Mrs. David Sheprow
Mr. and Mrs. Bertram R. Silver
Mr. and Mrs. Jonathan O. Simonds
Mr. and Mrs. John A. Simourian
Mr. Brian Braginton Smith
Drs. Frederick and Marguerite Smith
Dr. and Mrs. Alan B. Steinbach
Dr. and Mrs. Malcolm S. Steinberg
Dr. and Mrs. William K. Stephenson
Dr. and Mrs. Thomas R. Stetson
Mr. and Mrs. E. Kent Swift, Jr.
Mr. and Mrs. Gerard L. Swope
Mr. and Mrs. Emil D. Tietje, Jr.
Mr. D. Thomas Trigg
Dr. and Mrs. Walter Troll
Prof. and Mrs. Michael Tytell
Mr. and Mrs. Volker Ulbrich
Mr. and Mrs. John J. Valois
Dr. John Waterbury and Ms. Vicky Cullen
Mr. and Mrs. John T. Weeks
Dr. and Mrs. Gerald Weissmann
Dr. and Mrs. Paul S. Wheeler
Ms. Mabel Whelpley and Mr. George Rollins
Dr. and Mrs. Martin Keister White
Mr. and Mrs. Geoffrey G. Whitney, Jr.
Mr. and Mrs. Lynn H. Wilke
Mr. and Mrs. Leonard M. Wilson
Dr. and Mrs. T. Hastings Wilson
Mrs. Marilyn G. Zacks
Mr. and Mrs. Bruce Zimmerli

### *Individual Membership*

Mrs. Frederica Z. Alpert
Dr. Peggy Alsup
Mrs. Tammy Smith Amon
Mr. Dean N. Arden
Mrs. Ellen Prosser Armstrong
Mr. Garfield M. Arthur
Mrs. Kimball C. Atwood, III
Mr. Everett E. Bagley
Dr. Millicent Bell
Mr. C. John Berg
Ms. Olive C. Beverly
Mrs. Ellen F. Binda
Dr. Thomas P. Bleck
Ms. Avis Blomberg
Mr. James V. Bracchitta
Mrs. Jennie P. Brown
Mrs. M. Kathryn S. Brown
Dr. Robert H. Broyles
Mrs. Barbara Gates Burwell
J. G. Butch
Mr. Bruce E. Buxton
Dr. Graciela C. Candelas
Mr. Frank C. Carotenuto
Dr. Robert H. Carrier
Dr. Sallie Chisholm
Ms. Paula Ciara
Mrs. Octavia C. Clement
Dr. Jewel Plummer Cobb
Mrs. Margaret H. Coburn
Dr. Seymour S. Cohen
Dr. Alan Robert Cole
Ms. Genevieve Coleman
Ms. Anne S. Concannon
Ms. Margaret S. Cooper
Dr. D. Eugene Copeland
Mrs. Neal Cornell
Dr. Vincent Cowling
Mrs. Marilyn E. Crandall
Ms. Cathleen Creedon
Ms. Dorothy Crossley
Ms. Helen M. Crossley
Mrs. Villa B. Crowell
Mrs. Doris M. Curran
Mrs. Alexander T. Daignault
Mrs. Elizabeth M. Davis
Ms. Maureen Davis
Ms. Carol Reimann DeYoung
Ms. Shirley Dierolf
Mrs. Juliette G. Dively
Mr. David L. Donovan
Ms. Suzanne Droban
Mr. Roy A. Duffus
Ms. Maureen J. Dugan
Mrs. Frances E. Eastman
Dr. Frank Egloff
Mr. Robert Elias
Dr. Stephen L. Estabrooks
Mrs. Eleanor B. Faithorn
Mrs. Ruth Alice Fitz
Ms. Sylvia M. Flanagan
Mr. John W. Folino, Jr.
Mrs. Kathryn W. Foster
Dr. Krystyna Frenkel
Mr. Paul J. Freyheit
Mrs. Ruth E. Fye
Mr. Joseph C. Gallagher
Mrs. Lois E. Galvin
Mrs. Ruth H. Garland
Mrs. Matilda L. Gellis
Mrs. Doris D. Gerace
Ms. Sallie A. Giffen
Mrs. Janet F. Gillette
Ms. Muriel Gould
Ms. Janet M. Gregg
Mrs. Jeanne B. Griffith
Mrs. Barbara Grossman
Mrs. Valerie A. Hall
Ms. Mary Elizabeth Hamstrom
Dr. Carol W. Hannenberg
Mrs. Elizabeth Heald
Mrs. Jane M. Heald
Mrs. Betsy Honey
Mr. Roger W. Hubbell
Miss Elizabeth B. Jackson
Ms. Barbara W. Jones
Mrs. Sally S. Joslin
Mrs. Joan T. Kanwisher
Mrs. Sally Karush
Ms. Patricia E. Keoughan
Dr. Peter N. Kivy
Ms. Kathryn M. Kleekamp
Mr. Ezra Laderman
Ms. Margaret D. Lakis
Mrs. Janet W. Larcom
Ms. Rebecca Lash
Dr. Marian E. LeFevre
Mr. Edwin M. Libbin
Mr. Lennart Lindberg
Mrs. Barbara C. Little
Mrs. Sarah J. Loessel
Ms. Susan Loucks
Dr. Zella Luria
Ms. Sallie G. Lyon
Mrs. Margaret M. MacLeish
Mrs. Annemarie E. Mahler
Mrs. Nancy R. Malkiel
Mr. Brett Mandel
Mrs. Diane B. Maranchie
Mrs. Marjorie Marshall
Dr. Miriam Jacob Mauzerall
Mrs. Mary Hartwell Mavor
Mr. Bill McGoey
Mr. Paul McGonigle
Dr. Susan Gerbi McIlwain
Ms. Mary W. McKoan
Ms. Jane A. McLaughlin
Ms. Louise McManus
Ms. Cornelia Hanna McMurtrie
Mrs. Nawrie Meigs-Brown
Ms. Carmen Merryman
Ms. Vivagean V. Merz
Mrs. Polly Miles
Mrs. Marianne F. Milkman
Mrs. Florence E. Mixer
Mr. Lawrence A. Monte
Ms. Cynthia Moor
Mrs. Carol Murray
Mrs. Eleanor M. Nace
Mrs. Anne Nelson
Ms. C. Marie Newman
Dr. Eliot H. Nierman
Mr. Edmund F. Nolan
Ms. Catherine N. Norton
Dr. Renee Bennett O'Sullivan
Ms. Carolyn L. Parmenter
Ms. Joan Pearlman
Ms. Dianne Purves
Mrs. Julia S. Rankin
Dr. Margaret M. Rappaport
Mrs. Carol V. Rasic
Mr. Fred J. Ravens, Jr.
Ms. Mary W. Rianhard
Dr. Mary Elizabeth Rice
Dr. Monica Riley

Mrs. Lola E. Robertson
Dr. Steven R. Rodermel
Mrs. Arlene Rogers
Ms. Jean Rogers
Mrs. Wendy E. Rose
Mrs. Atholie K. Rosett
Dr. Virginia F. Ross
Dr. John D. Rummel
Mrs. Rosalind Russell
Mr. Raymond A. Sanborn
Dr. Thomas Sbarra
Ms. Mary M. Scanlan
Mr. Claude Schoepf
Ms. Emily Schwartz-Clark
Mr. Samuel C. Schon
Mrs. Elsie M. Scott
Dr. Cecily C. Selby
Mrs. Deborah G. Senft
Ms. Dorothy Sgarzi
Mrs. Charlotte Shemin
Mrs. Ruth Shephard
Ms. Dorothy Shiebler
Ms. Enid K. Sichel
Dr. Jeffrey D. Silberman
Mrs. Cynthia C. Smith
Mr. Sean W. Smith
Mrs. Louise M. Specht
Dr. Guy L. Steele, Sr.
Dr. Robert E. Steele
Mrs. Eleanor Steinbach
Ms. Eleanor Sterling
Mrs. Jane Lazarow Stetten
Mrs. Elizabeth Stommel
Ms. Maren Studlien
Mr. Albert H. Swain
Mr. Dorman J. Swartz
Mrs. Belle K. Taylor
Mr. James K. Taylor
Mrs. Alice Todd
Mr. Arthur D. Traub
Ms. Natalie Trousof
Ms. Eleanor S. Uhlinger
Ms. Ciona Ulbrich
Ms. Sylvia Vatuk
Ms. Dawn Vaughn
Ms. Susan Veeder
Mr. Lee D. Vincent
Mr. Arthur D. Voorhis
Mrs. Eve Warren
Mr. Michael S. Weinstein
Ms. Lillian Wendorff
Mr. George R. Wezniak
Ms. Mabel Y. Whelpley
Mr. Gerry White
Mrs. Barbara Whitehead
Mrs. Ava Whittemore
Mrs. Clare M. Wilber
Mrs. Helen Wilson
Ms. Nancy Woitkoski
Mr. Dale Wolfgram
Mrs. Dorothy M. York
Dr. Linda Amaral Zettler
Mrs. Bunnie Rose Zigman
Mrs. Margery P. Zinn

## *MBL Gift Shop Volunteers*

Marion Adelberg
Barbara Atwood
Harriet Bernheimer
Avis Blomberg
Gloria Borgese
Elisabeth Buck
Julie Child
Vera Clark
Jewel Cobb
Janet Daniels
Carol DeYoung
Fran Eastman
Pat Ferguson
Muriel Gould
Barbara Grossman
Jean Halvorson
Hanna Hastings
Sally Karush
Marcella Katz
Alice Knowles
Donna Kornberg
Meryl Langbort
Barbara Little
Winnie Mackey
Diane Maranchie
Mary Mavor
Louise McManus
Polly Miles
Florence Mixer
Helen Murphy
Bertha Person
Margareta Pothier
Julie Rankin
Arlene Rogers
Atholie Rosett
Cynthia Smith
Peggy Smith
Jane Stetten
Barbara Thomson
Alice Todd
Natalie Trousof
Barbara Van Holde
Susan Veeder
Carol Ann Wagner
Mabel Whelpley
Clare Wilber
Betty Wilson
Grace Witzell
Bunnie Rose Zigman

## *MBL Summer Tour Guides*

Gloria Borgese
Frank Child
Julie Child
Nancy Fraser
Sallie Giffen
Barbara Little
Charles Mahoney
Julie Rankin
Howard Redpath
Pucky Roslansky
Margery Zinn

# Certificate of Organization
# Articles of Amendment
# Bylaws

## *Certificate of Organization*

(On File in the Office of the Secretary of the Commonwealth)

No. 3170

We, Alpheus Hyatt, President, William Stanford Stevens, Treasurer, and William T. Sedgwick, Edward G. Gardiner, Susan Mims and Charles Sedgwick Minot being a majority of the Trustees of the Marine Biological Laboratory in compliance with the requirements of the fourth section of chapter one hundred and fifteen of the Public Statutes do hereby certify that the following is a true copy of the agreement of association to constitute said Corporation, with the names of the subscribers thereto.

We, whose names are hereto subscribed, do, by this agreement, associate ourselves with the intention to constitute a Corporation according to the provisions of the one hundred and fifteenth chapter of the Public Statutes of the Commonwealth of Massachusetts, and the Acts in amendment thereof and in addition thereto.

The name by which the Corporation shall be known is
THE MARINE BIOLOGICAL LABORATORY.

The purpose for which the Corporation is constituted is to establish and maintain a laboratory or station for scientific study and investigations, and a school for instruction in biology and natural history.
The place within which the Corporation is established or located is the city of Boston within said Commonwealth.
The amount of its capital stock is none.
In Witness Whereof, we have hereunto set our hands, this twenty seventh day of February in the year eighteen hundred and eighty-eight, Alpheus Hyatt, Samuel Mills, William T. Sedgwick, Edward G. Gardiner, Charles Sedgwick Minot, William G. Farlow, William Stanford Stevens, Anna D. Phillips, Susan Mims, B. H. Van Vleck.
That the first meeting of the subscribers to said agreement was held on the thirteenth day of March in the year eighteen hundred and eighty-eight.
In Witness Whereof, we have hereunto signed our names, this thirteenth day of March in the year eighteen hundred and eighty-eight, Alpheus Hyatt, President, William Stanford Stevens, Treasurer, Edward G. Gardiner, William T. Sedgwick, Susan Mims, Charles Sedgwick Minot.
(Approved on March 20, 1888 as follows:
I hereby certify that it appears upon an examination of the within written certificate and the records of the corporation duly submitted to my inspection, that the requirements of sections one, two and three of chapter one hundred and fifteen, and sections eighteen, twenty and twenty-one of chapter one hundred and six, of the Public Statutes, have been complied with and I hereby approve said certificate this twentieth day of March A.D. eighteen hundred and eighty-eight.

Charles Endicott
Commissioner of Corporations)

## *Articles of Amendment*

(On File in the Office of the Secretary of the Commonwealth)

We, James D. Ebert, President, and David Shepro, Clerk of the Marine Biological Laboratory, located at Woods Hole, Massachusetts 02543, do hereby certify that the following amendment to the Articles of Organization of the Corporation was duly adopted at a meeting held on August 15, 1975, as adjourned to August 29, 1975, by vote of 444 members, being at least two-thirds of its members legally qualified to vote in the meeting of the corporation:

Voted: That the Certificate of Organization of this corporation be and it hereby is amended by the addition of the following provisions:
"No Officer, Trustee or Corporate Member of the corporation shall be personally liable for the payment or satisfaction of any obligation or liabilities incurred as a result of, or otherwise in connection with, any commitments, agreements, activities or affairs of the corporation.
"Except as otherwise specifically provided by the Bylaws of the corporation, meetings of the Corporate Members of the corporation may be held anywhere in the United States.
"The Trustees of the corporation may make, amend or repeal the Bylaws of the corporation in whole or in part, except with respect to any provisions thereof which shall by law, this Certificate or the bylaws of the corporation, require action by the Corporate Members."

The foregoing amendment will become effective when these articles of amendment are filed in accordance with Chapter 180, Section 7 of the General Laws unless these articles specify, in accordance with the vote adopting the amendment, a later effective date not more than thirty days after such filing, in which event the amendment will become effective on such later date.

In Witness whereof and Under the Penalties of Perjury, we have hereto signed our names this 2nd day of September, in the year 1975, James D. Ebert, President; David Shepro, Clerk.
(Approved on October 24, 1975, as follows:
I hereby approve the within articles of amendment and, the filing fee in the amount of $10 having been paid, said articles are deemed to have been filed with me this 24th day of October, 1975.

Paul Guzzi
Secretary of the Commonwealth)

## *Bylaws*

(Revised August 7, 1992, December 10, 1992, and November 10, 2001)

ARTICLE I—THE CORPORATION

A. *Name and Purpose.* The name of the Corporation shall be The Marine Biological Laboratory. The Corporation's purpose shall be to establish and maintain a laboratory or station for scientific study and investigation and a school for instruction in biology and natural history.

B. *Nondiscrimination.* The Corporation shall not discriminate on the basis of age, religion, color, race, national or ethnic origin, sex or sexual preference in its policies on employment and administration or in its educational and other programs.

## ARTICLE II—MEMBERSHIP

A. *Members.* The Members of the Corporation ("Members") shall consist of persons elected by the Board of Trustees (the "Board"), upon such terms and conditions and in accordance with such procedures, not inconsistent with law or these Bylaws, as may be determined by the Board. At any regular or special meeting of the Board, the Board may elect new Members. Members shall have no voting or other rights with respect to the Corporation or its activities except as specified in these Bylaws, and any Member may vote at any meeting of the Members in person only and not by proxy. Members shall serve until their death or resignation unless earlier removed with or without cause by the affirmative vote of two-thirds of the Trustees then in office. Any Member who has retired from his or her home institution may, upon written request to the Corporation, be designated a Life Member. Life Members shall not have the right to vote and shall not be assessed for dues.

B. *Meetings.* The annual meeting of the Members shall be held on the Friday following the first Tuesday in August of each year, at the Laboratory of the Corporation in Woods Hole, Massachusetts, at 9:30 a.m. The Chairperson of the Board shall preside at meetings of the Corporation. If no annual meeting is held in accordance with the foregoing provision, a special meeting may be held in lieu thereof with the same effect as the annual meeting, and in such case all references in these Bylaws, except in this Article II.B., to the annual meeting of the Members shall be deemed to refer to such special meeting. Members shall transact business as may properly come before the meeting. Special meetings of the Members may be called by the Chairperson or the Trustees, and shall be called by the Clerk, or in the case of the death, absence, incapacity or refusal by the Clerk, by any other officer, upon written application of Members representing at least ten percent of the smallest quorum of Members required for a vote upon any matter at the annual meeting of the Members, to be held at such time and place as may be designated.

C. *Quorum.* One hundred (100) Members shall constitute a quorum at any meeting. Except as otherwise required by law or these Bylaws, the affirmative vote of a majority of the Members voting in person at a meeting attended by a quorum shall constitute action on behalf of the Members.

D. *Notice of Meetings.* Notice of any annual meeting or special meeting of Members, if necessary, shall be given by the Clerk by mailing notice of the time and place and purpose of such meeting at least 15 days before such meeting to each Member at his or her address as shown on the records of the Corporation.

E. *Waiver of Notice.* Whenever notice of a meeting is required to be given a Member, under any provision of the Articles or Organization or Bylaws of the Corporation, a written waiver thereof, executed before or after the Meeting by such Member, or his or her duly authorized attorney, shall be deemed equivalent to such notice.

F. *Adjournments.* Any meeting of the Members may be adjourned to any other time and place by the vote of a majority of those Members present at the meeting, whether or not such Members constitute a quorum, or by any officer entitled to preside at or to act as Clerk of such meeting, if no Member is present or represented. It shall not be necessary to notify any Members of any adjournment unless no Member is present or represented at the meeting which is adjourned, in which case, notice of the adjournment shall be given in accordance with Article II.D. Any business which could have been transacted at any meeting of the Members as originally called may be transacted at an adjournment thereof.

## ARTICLE III—ASSOCIATES OF THE CORPORATION

*Associates of the Corporation.* The Associates of the Marine Biological Laboratory shall be an unincorporated group of persons (including associations and corporations) interested in the Laboratory and shall be organized and operated under the general supervision and authority of the Trustees. The Associates of the Marine Biological Laboratory shall have no voting rights.

## ARTICLE IV—BOARD OF TRUSTEES

A. *Powers.* The Board of Trustees shall have the control and management of the affairs of the Corporation. The Trustees shall elect a Chairperson of the Board who shall serve until his or her successor is elected and qualified. They shall annually elect a President of the Corporation. They shall annually elect a Vice Chairperson of the Board who shall be Vice Chairperson of the meetings of the Corporation. They shall annually elect a Treasurer. They shall annually elect a Clerk, who shall be a resident of Massachusetts. They shall elect Trustees-at-Large as specified in this Article IV. They shall appoint a Director of the Laboratory for a term not to exceed five years, provided the term shall not exceed one year if the candidate has attained the age of 65 years prior to the date of the appointment. They shall choose such other officers and agents as they shall think best. They may fix the compensation of all officers and agents of the Corporation and may remove them at any time. They may fill vacancies occurring in any of the offices. The Board shall have the power to choose an Executive Committee from their own number as provided in Article V, and to delegate to such Committee such of their own powers as they may deem expedient in addition to those powers conferred by Article V. They shall, from time to time, elect Members to the Corporation upon such terms and conditions as they shall have determined, not inconsistent with law or these Bylaws.

B. *Composition and Election.*

(1) The Board shall include 24 Trustees elected by the Board as provided below:

(a) At least six Trustees ("Corporate Trustees") shall be Members who are scientists, and the other Trustees ("Trustees-at-Large") shall be individuals who need not be Members or otherwise affiliated with the Corporation.

(b) The 24 elected Trustees shall be divided into four classes of six Trustees each, with one class to be elected each year to serve for a term of four years, and with each such class to include at least one Corporate Trustee. Such classes of Trustees shall be designated by the year of expiration of their respective terms.

(c) At the end of a second four-year term, the term of a Trustee who is serving as Chairperson may be extended by the Board for a term of one year, in which event, there shall be 25 Trustees for that year with one class of Trustees having seven Trustees.

(2) The Board shall also include the Chief Executive Officer, Treasurer and the Chairperson of the Science Council, who shall be *ex officio* voting members of the Board.

(3) Although Members or Trustees may recommend individuals for nomination as Trustees, nominations for Trustee elections shall be made by the Nominating Committee in its sole discretion. The Board may also elect Trustees who have not been nominated by the Nominating Committee.

C. *Eligibility.* A Corporate Trustee or a Trustee-at-Large who has been elected to an initial four-year term or remaining portion thereof, of which he/she has served at least two years, shall be eligible for re-election to a second four-year term, and, if the Trustee is serving as Chairperson, at the end of the second four-year term, the Trustee shall be eligible for a one year term extension, but shall be ineligible for re-election to any subsequent term until one year has elapsed after he/she has last served as a Trustee.

D. *Removal.* Any Trustee may be removed from office at any time with or without cause, by vote of a majority of the Members entitled to vote in the election of Trustees; or for cause, by vote of two-thirds of the Trustees then in office. A Trustee may be removed for cause only if notice of such action shall have been given to all of the Trustees or Members entitled to vote, as the case may be, prior to the meeting at which such action is to be taken and if the Trustee to be so removed shall have been given reasonable notice and opportunity to be heard before the body proposing to remove him or her

E. *Vacancies.* Any vacancy in the Board may be filled by vote of a majority of the remaining Trustees present at a meeting of Trustees at which a quorum is present. Any vacancy in the Board resulting from the resignation or removal of a Corporate Trustee shall be filled by a Member who is a scientist.

F. *Meetings.* Meetings of the Board shall be held from time to time, not less frequently than twice annually, as determined by the Board. Special meetings of Trustees may be called by the Chairperson, or by any seven Trustees, to be held at such time and place as may be designated. The Chairperson of the Board, when present, shall preside over all meetings of the Trustees. Written notice shall be sent to a Trustee's usual or last known place of residence at least two weeks before the meeting. Notice of a meeting need not be given to any Trustee if a written waiver of notice executed by such Trustee before or after the meeting is filed with the records of the meeting, or if such Trustee shall attend the meeting without protesting prior thereto or at its commencement the lack of notice given to him or her.

G. *Quorum and Action by Trustees.* A majority of all Trustees then in office shall constitute a quorum. Any meeting of Trustees may be adjourned by vote of a majority of Trustees present, whether or not a quorum is present, and the meeting may be held as adjourned without further notice. When a quorum is present at any meeting of the Trustees, a majority of the Trustees present and voting (excluding abstentions) shall decide any question, including the election of officers, unless otherwise required by law, the Articles of Organization or these Bylaws.

H. *Transfers of Interests in Land.* There shall be no transfer of title nor long-term lease of real property held by the Corporation without prior approval of not less than two-thirds of the Trustees. Such real property transactions shall be finally acted upon at a meeting of the Board only if presented and discussed at a prior meeting of the Board. Either meeting may be a special meeting and no less than four weeks shall elapse between the two meetings. Any property acquired by the Corporation after December 1, 1989 may be sold, any mortgage or pledge of real property (regardless of when acquired) to secure borrowings by the Corporation may be granted, and any transfer of title or interest in real property pursuant to the foreclosure or endorsement of any such mortgage or pledge of real property may be effected by any holder of a mortgage or pledge of real property of the Corporation, with the prior approval of not less than two-thirds of the Trustees (other than any Trustee or Trustees with a direct or indirect financial interest in the transaction being considered for approval) who are present at a regular or special meeting of the Board at which there is a quorum.

## ARTICLE V—COMMITTEES

A. *Executive Committee.* There shall be an Executive Committee of the Board of Trustees which shall consist of not more than eleven (11) Trustees, including *ex officio* Trustees, elected by the Board.

The Chairperson of the Board shall act as Chairperson of the Executive Committee and the Vice Chairperson as Vice Chairperson. The Executive Committee shall meet at such times and places and upon such notice and appoint such subcommittees as the Committee shall determine.

The Executive Committee shall have and may exercise all the powers of the Board during the intervals between meetings of the Board except those powers specifically withheld, from time to time, by vote of the Board or by law. The Executive Committee may also appoint such committees, including persons who are not Trustees, as it may, from time to time, approve to make recommendations with respect to matters to be acted upon by the Executive Committee or the Board.

The Executive Committee shall keep appropriate minutes of its meetings, which shall be reported to the Board. Any actions taken by the Executive Committee shall also be reported to the Board

B. *Nominating Committee.* There shall be a Nominating Committee which shall consist of not fewer than four nor more than six Trustees appointed by the Board in a manner which shall reflect the balance between Corporate Trustees and Trustees-at-Large on the Board. The Nominating Committee shall nominate persons for election as Corporate Trustees and Trustees-at-Large, Chairperson of the Board, Vice Chairperson of the Board, President, Treasurer, Clerk, Director of the Laboratory and such other officers, if any, as needed, in accordance with the requirements of these Bylaws. The Nominating Committee shall also be responsible for overseeing the training of new Trustees. The Chairperson of the Board of Trustees shall appoint the Chairperson of the Nominating Committee. The Chairperson of the Science Council shall be an *ex officio* voting member of the Nominating Committee.

C. *Science Council.* There shall be a Science Council (the "Council") which shall consist of Members of the Corporation elected to the Council by vote of the Members of the Corporation, and which shall advise the Board with respect to matters concerning the Corporation's mission, its scientific and instructional endeavors, and the appointment and promotions of persons or committees with responsibility for matters requiring scientific expertise. Unless otherwise approved by a majority of the members of the Council, the Chairperson of the Council shall be elected annually by the Council. The chief executive officer of the Corporation shall be an *ex officio* voting member of the Council.

D. *Board of Overseers.* There shall be a Board of Overseers which shall consist of not fewer than five nor more than eight scientists who have expertise concerning matters with which the Corporation is involved. Members of the Board of Overseers may or may not be Members of the Corporation and may be appointed by the Board of Trustees on the basis of recommendations submitted from scientists and scientific organizations or societies. The Board of Overseers shall be available to review and offer recommendations to the officers, Trustees and Science Council regarding scientific activities conducted or proposed by the Corporation and shall meet from time to time, not less frequently than annually, as determined by the Board of Trustees.

E. *Board Committees Generally.* The Trustees may elect or appoint one or more other committees (including, but not limited to, an Investment Committee, a Development Committee, an Audit Committee, a Facilities and Capital Equipment Committee and a Long-Range Planning Committee) and may delegate to any such committee or committees any or all of their powers, except those which by law, the Articles of Organization or these Bylaws the Trustees are prohibited from delegating; provided that any committee to which the powers of the Trustees are delegated shall consist solely of Trustees. The members of any such committee shall have such tenure and duties as the Trustees shall determine. The Investment Committee, which shall oversee the management of the Corporation's endowment funds and marketable securities shall include as *ex officio* members, the Chairperson of the Board, the Treasurer and the Chairperson of the Audit Committee, together with such Trustees as may be required for not less than two-thirds of the Investment Committee to consist of Trustees. Except as otherwise provided by these Bylaws or determined by the Trustees, any such committee may make rules for the conduct of its business, but, unless otherwise provided by the Trustees or in such rules, its business shall be conducted as nearly as possible in the same manner as is provided by these Bylaws for the Trustees.

F. *Actions Without a Meeting.* Any action required or permitted to be taken at any meeting of the Executive Committee or any other committee elected by the Trustees may be taken without a meeting if all members of such committees consent to the action in writing and such written consents are filed with the records of meetings. Members of the Executive Committee or any other committee elected by the Trustees may also participate in any meeting by means of a telephone conference call, or otherwise take action in such a manner as may, from time to time, be permitted by law.

G. *Manual of Procedures.* The Board of Trustees, on the recommendation of the Executive Committee, shall establish guidelines and modifications thereof to be recorded in a Manual of Procedures. Guidelines shall establish procedures for: (1) Nomination and election of members of the Corporation, Board of Trustees and Executive Committee; (2) Election of Officers; (3) Formation and Function of Standing Committees.

## ARTICLE VI—OFFICERS

A. *Enumeration.* The officers of the Corporation shall consist of a President, a Treasurer and a Clerk, and such other officers having the powers of President, Treasurer and Clerk as the Board may determine, and a Director of the Laboratory. The Corporation may have such other officers and assistant officers as the Board may determine, including (without limitation) a Chairperson of the Board, Vice Chairperson and one or more Vice Presidents, Assistant Treasurers or Assistant Clerks. Any two or more offices may be held by the same person. The Chairperson and Vice Chairperson of the Board shall be elected by and from the Trustees, but other officers of the Corporation need not be Trustees or Members. If required by the Trustees, any officer shall give the Corporation a bond for the faithful performance of his or her duties in such amount and with such surety or sureties as shall be satisfactory to the Trustees.

B. *Tenure.* Except as otherwise provided by law, by the Articles of Organization or by these Bylaws, the President, Treasurer, and all other officers shall hold office until the first meeting of the Board following the annual meeting of Members and thereafter, until his or her successor is chosen and qualified.

C. *Resignation.* Any officer may resign by delivering his or her written resignation to the Corporation at its principal office or to the President or Clerk and such resignation shall be effective upon receipt unless it is specified to be effective at some other time or upon the happening of some other event.

D. *Removal.* The Board may remove any officer with or without cause by a vote of a majority of the entire number of Trustees then in office, at a meeting of the Board called for that purpose and for which notice of the purpose thereof has been given, provided that an officer may be removed for cause only after having an opportunity to be heard by the Board at a meeting of the Board at which a quorum is personally present and voting.

E. *Vacancy.* A vacancy in any office may be filled for the unexpired balance of the term by vote of a majority of the Trustees present at any meeting of Trustees at which a quorum is present or by written consent of all of the Trustees, if less than a quorum of Trustees shall remain in office.

F. *Chairperson.* The Chairperson shall have such powers and duties as may be determined by the Board and, unless otherwise determined by the Board, shall serve in that capacity for a term coterminous with his or her term as Trustee.

G. *Vice Chairperson.* The Vice Chairperson shall perform the duties and exercise the powers of the Chairperson in the absence or disability of the Chairperson, and shall perform such other duties and possess such other powers as may be determined by the Board. Unless otherwise determined by the Board, the Vice Chairperson shall serve for a one-year term.

H *Director.* The Director shall be the chief operating officer and, unless otherwise voted by the Trustees, the chief executive officer of the Corporation. The Director shall, subject to the direction of the Trustees, have general supervision of the Laboratory and control of the business of the Corporation. At the annual meeting, the Director shall submit a report of the operations of the Corporation for such year and a statement of its affairs, and shall, from time to time, report to the Board all matters within his or her knowledge which the interests of the Corporation may require to be brought to its notice.

I *Deputy Director.* The Deputy Director, if any, or if there shall be more than one, the Deputy Directors in the order determined by the Trustees, shall, in the absence or disability of the Director, perform the duties and exercise the powers of the Director and shall perform such other duties and shall have such other powers as the Trustees may, from time to time, prescribe.

J. *President.* The President shall have the powers and duties as may be vested in him or her by the Board.

K. *Treasurer and Assistant Treasurer.* The Treasurer shall, subject to the direction of the Trustees, have general charge of the financial affairs of the Corporation, including its long-range financial planning, and shall cause to be kept accurate books of account. The Treasurer shall prepare a yearly report on the financial status of the Corporation to be delivered at the annual meeting. The Treasurer shall also prepare or oversee all filings required by the Commonwealth of Massachusetts, the Internal Revenue Service, or other Federal and State Agencies. The account of the Treasurer shall be audited annually by a certified public accountant.

The Assistant Treasurer, if any, or if there shall be more than one, the Assistant Treasurers in the order determined by the Trustees, shall, in the absence or disability of the Treasurer, perform the duties and exercise the powers of the Treasurer, shall perform such other duties and shall have such other powers as the Trustees may, from time to time, prescribe.

L. *Clerk and Assistant Clerk.* The Clerk shall be a resident of the Commonwealth of Massachusetts, unless the Corporation has designated a resident agent in the manner provided by law. The minutes or records of all meetings of the Trustees and Members shall be kept by the Clerk who shall record, upon the record books of the Corporation, minutes of the proceedings at such meetings. He or she shall have custody of the record books of the Corporation and shall have such other powers and shall perform such other duties as the Trustees may, from time to time, prescribe.

The Assistant Clerk, if any, or if there shall be more than one, the Assistant Clerks in the order determined by the Trustees, shall, in the absence or disability of the Clerk, perform the duties and exercise the powers of the Clerk and shall perform such other duties and shall have such other powers as the Trustees may, from time to time, prescribe.

In the absence of the Clerk and an Assistant Clerk from any meeting, a temporary Clerk shall be appointed at the meeting.

M. *Other Powers and Duties.* Each officer shall have in addition to the duties and powers specifically set forth in these Bylaws, such duties and powers as are customarily incident to his or her office, and such duties and powers as the Trustees may, from time to time, designate.

## ARTICLE VII—AMENDMENTS

These Bylaws may be amended by the affirmative vote of the Members at any meeting, provided that notice of the substance of the proposed amendment is stated in the notice of such meeting. As authorized by the Articles of Organization, the Trustees, by a majority of their number then in office, may also make, amend or repeal these Bylaws, in whole or in part, except with respect to (a) the provisions of these Bylaws governing (i) the removal of Trustees and (ii) the amendment of these Bylaws and (b) any provisions of these Bylaws which by law, the Articles of Organization or these Bylaws, requires action by the Members.

No later than the time of giving notice of meeting of Members next following the making, amending or repealing by the Trustees of any Bylaw, notice thereof stating the substance of such change shall be given to all Members entitled to vote on amending the Bylaws.

Any Bylaw adopted by the Trustees may be amended or repealed by the Members entitled to vote on amending the Bylaws.

## ARTICLE VIII—INDEMNITY

Except as otherwise provided below, the Corporation shall, to the extent legally permissible, indemnify each person who is, or shall have been, a Trustee, director or officer of the Corporation or who is serving, or shall have served at the request of the Corporation as a Trustee, director or officer of another organization in which the Corporation directly or indirectly has any interest as a shareholder, creditor or otherwise, against all liabilities and expenses (including judgments, fines, penalties, and reasonable attorneys' fees and all amounts paid, other than to the Corporation or such other organization, in compromise or settlement) imposed upon or incurred by any such person in connection with, or arising out of, the defense or disposition of any action, suit or other proceeding, whether civil or criminal, in which he or she may be a defendant or with which he or she may be threatened or otherwise involved, directly or indirectly, by reason of his or her being or having been such a Trustee, director or officer.

The Corporation shall provide no indemnification with respect to any matter as to which any such Trustee, director or officer shall be finally adjudicated in such action, suit or proceeding not to have acted in good faith in the reasonable belief that his or her action was in the best interests of the Corporation. The Corporation shall provide no indemnification with respect to any matter settled or comprised unless such matter shall have been approved as in the best interests of the Corporation, after notice that indemnification is involved, by (i) a disinterested majority of the Board of the Executive Committee, or (ii) a majority of the Members.

Indemnification may include payment by the Corporation of expenses in defending a civil or criminal action or proceeding in advance of the final disposition of such action or proceeding upon receipt of an undertaking by the person indemnified to repay such payment if it is ultimately determined that such person is not entitled to indemnification under the provisions of this Article VIII, or under any applicable law.

As used in the Article VIII, the terms "Trustee," "director," and "officer" include their respective heirs, executors, administrators and legal representatives, and an "interested" Trustee, director or officer is one against whom in such capacity the proceeding in question or another proceeding on the same or similar grounds is then pending.

To assure indemnification under this Article VIII of all persons who are determined by the Corporation or otherwise to be or to have been "fiduciaries" of any employee benefits plan of the Corporation which may exist, from time to time, this Article VIII shall be interpreted as follows: (i) "another organization" shall be deemed to include such an employee benefit plan, including without limitation, any plan of the Corporation which is governed by the Act of Congress entitled "Employee Retirement Income Security Act of 1974," as amended, from time to time, ("ERISA"); (ii) "Trustee" shall be deemed to include any person requested by the Corporation to serve as such for an employee benefit plan where the performance by such person of his or her duties to the Corporation also imposes duties on, or otherwise involves services by, such person to the plan or participants or beneficiaries of the plan; (iii) "fines" shall be deemed to include any excise tax plan pursuant to ERISA; and (iv) actions taken or omitted by a person with respect to an employee benefit plan in the performance of such person's duties for a purpose reasonably believed by such person to be in the interest of the participants and beneficiaries of the plan shall be deemed to be for a purpose which is in the best interests of the Corporation.

The right of indemnification provided in this Article VIII shall not be exclusive of or affect any other rights to which any Trustee, director or officer may be entitled under any agreement, statute, vote of Members or otherwise. The Corporation's obligation to provide indemnification under this Article VIII shall be offset to the extent of any other source of indemnification of any otherwise applicable insurance coverage under a policy maintained by the Corporation or any other person. Nothing contained in the Article shall affect any rights to which employees and corporate personnel other than Trustees, directors or officers may be entitled by contract, by vote of the Board or of the Executive Committee or otherwise.

## ARTICLE IX—DISSOLUTION

The consent of every Trustee shall be necessary to effect a dissolution of the Marine Biological Laboratory. In case of dissolution, the property shall be disposed of in such a manner and upon such terms as shall be determined by the affirmative vote of two-thirds of the Trustees then in office in accordance with the laws of the Commonwealth of Massachusetts.

## ARTICLE X—MISCELLANEOUS PROVISIONS

A. *Fiscal Year.* Except as otherwise determined by the Trustees, the fiscal year of the Corporation shall end on December 31st of each year.

B. *Seal.* Unless otherwise determined by the Trustees, the Corporation may have a seal in such form as the Trustees may determine, from time to time.

C. *Execution of Instruments.* All checks, deeds, leases, transfers, contracts, bonds, notes and other obligations authorized to be executed by an officer of the Corporation in its behalf shall be signed by the Director or the Treasurer except as the Trustees may generally or in particular cases otherwise determine. A certificate by the Clerk or an Assistant Clerk, or a temporary Clerk, as to any action taken by the Members, Board of Trustees or any officer or representative of the Corporation shall as to all persons who rely thereon in good faith be conclusive evidence of such action.

D. *Corporate Records.* The original, or attested copies, of the Articles of Organization, Bylaws and records of all meetings of the Members shall be kept in Massachusetts at the principal office of the Corporation, or at an office of the Corporation's Clerk or resident agent. Said copies and records need not all be kept in the same office. They shall be available at all reasonable times for inspection by any Member for any proper purpose, but not to secure a list of Members for a purpose other than in the interest of the applicant, as a Member, relative to the affairs of the Corporation.

E. *Articles of Organization.* All references in these Bylaws to the Articles of Organization shall be deemed to refer to the Articles of Organization of the Corporation, as amended and in effect, from time to time.

F. *Transactions with Interested Parties.* In the absence of fraud, no contract or other transaction between this Corporation and any other corporation or any firm, association, partnership or person shall be affected or invalidated by the fact that any Trustee or officer of this Corporation is pecuniarily or otherwise interested in or is a director, member or officer of such other corporation or of such firm, association or partnership or in a party to or is pecuniarily or otherwise interested in such contract or other transaction or is in any way connected with any person or person, firm, association, partnership, or corporation pecuniarily or otherwise interested therein; provided that the fact that he or she individually or as a director, member or officer of such corporation, firm, association or partnership in such a party or is so interested shall be disclosed to or shall have been known by the Board of Trustees or a majority of such Members thereof as shall be present at a meeting of the Board of Trustees at which action upon any such contract or transaction shall be taken; any Trustee may be counted in determining the existence of a quorum and may vote at any meeting of the Board of Trustees for the purpose of authorizing any such contract or transaction with like force and effect as if he/she were not so interested, or were not a director, member or officer of such other corporation, firm, association or partnership, provided that any vote with respect to such contract or transaction must be adopted by a majority of the Trustees then in office who have no interest in such contract or transaction.

# Publications

**Amaral Zettler, L. A., T. A. Nerad, C. J. O'Kelly, and M. L. Sogin. 2001.** The nucleariid amoebae: more protists at the animal-fungal boundary. *J. Eukaryot. Microbiol.* **48:** 293–297.

**Arkhipova, I. R., and H. G. Morrison. 2001.** Three retrotransposon families in the genome of *Giardia lamblia:* two telomeric, one dead. *Proc. Natl. Acad. Sci. USA* **98:** 14,497–14,502.

**Armstrong, P. B. 2001.** The contribution of proteinase inhibitors to immune defense. *Trends Immunol.* **22:** 47–52.

**Asteggiano, C., G. Berberián, and L. Beaugé. 2001.** Phosphatidylinositol-4,5-biphosphate bound to bovine cardiac Na/Ca exchanger displays a MgATP regulation similar to that of the exchange fluxes. *Eur. J. Biochem.* **268:** 437–442.

**Augustine, G. J. 2001.** How does calcium trigger neurotransmitter release? *Curr. Opin. Neurobiol.* **11:** 320–326.

**Barbieri, E., B. J. Paster, D. Hughes, L. Zurek, D. P. Moser, A. Teske, and M. L. Sogin. 2001.** Phylogenetic characterization of epibiotic bacteria in the accessory nidamental gland and egg capsules of the squid *Loligo pealei* (Cephalopoda:Loliginidae). *Environ. Microbiol.* **3:** 151–167.

**Barlow, R. B. 2001.** Efferent and circadian modulation of visual sensitivity. Pp. 487–503 in *Concepts and Challenges in Retinal Biology: Tribute to John E. Dowling*, H. Kolb, H. Ripps, and S. Wu, eds. Series: Progress in Brain Research, 131. Elsevier Press, New York.

**Barlow, R. B., J. M. Hitt, and F. A. Dodge. 2001.** *Limulus* vision in the marine environment. *Biol. Bull.* **200:** 169–176.

**Basanez, G., and J. Zimmerberg. 2001.** HIV and apoptosis. Death and the mitochondrion. *J. Exp. Med.* **193:** F11–F14.

**Berntson, E. A., F. M. Bayer, A. G. McArthur, and S. C. France. 2001.** Phylogenetic relationships within the Octocorallia (Cnidaria: Anthozoa), based on nuclear 18S rRNA sequences. *Mar. Biol.* **138:** 235–246.

**Billack, B., D. E. Heck, D. M. Porterfield, R. P. Malchow, P. J. S. Smith, C. R. Gardner, D. L. Laskin, and J. D. Laskin. 2001.** Minimal amidine structure for inhibition of nitric oxide biosynthesis. *Biochem. Pharmacol.* **61:** 1581–1586.

**Blank, P., S. Vogel, J. Malley, and J. Zimmerberg. 2001.** A kinetic analysis of calcium-triggered exocytosis. *J. Gen. Physiol.* **118:** 145–155.

**Boudko, D. Y., L. L. Moroz, W. R. Harvey, and P. J. Linser. 2001.** Alkalinization by chloride/bicarbonate pathway in larval mosquito midgut. *Proc. Natl. Acad. Sci.* **98:** 15,354–15,359.

**Boudko, D. Y., L. L. Moroz, P. J. Linser, J. R. Trimarchi, P. J. S. Smith, and W. R. Harvey. 2001.** *In situ* analysis of pH gradients in mosquito larvae using non-invasive, self-referencing, pH-sensitive microelectrodes. *J. Exp. Biol.* **204:** 691–699.

**Bowen, J. L., and I. Valiela. 2001.** The ecological effects of urbanization of coastal watersheds: historical increases in nitrogen loads and eutrophication of Waquoit Bay estuaries. *Can. J. Fish. Aquat. Sci.* **58:** 1489–1500.

**Bowen, J. L., and I. Valiela. 2001.** Historical changes in atmospheric nitrogen deposition to Cape Cod, Massachusetts. *Atmos. Environ.* **35:** 1039–1051.

**Boyle, Richard, Allen F. Mensinger, Kaoru Yoshida, Shiro Usui, Anthony Intravaia, Timothy Tricas, and Stephen M. Highstein. 2001.** Neural readaptation to earth's gravity following return from space. *J. Neurophysiol.* **86:** 2118–2122.

**Bret-Harte, M. S., G. R. Shaver, J. P. Zoerner, J. F. Johnstone, J. L. Wagner, A. S. Chavez, R. F. Gunkelman, S. C. Lippert, and J. A. Laundre. 2001.** Developmental plasticity allows *Betula nana* to dominate tundra subjected to an altered environment. *Ecology* **82:** 18–32.

**Brown, Jeremiah R., Kyle R. Simonetta, Leslie A. Sandberg, Phillip Stafford, and George M. Langford. 2001.** Recombinant globular tail fragment of myosin-V blocks vesicle transport in squid nerve cell extracts. *Biol. Bull.* **201:** 240–241.

**Bucior, I., and M. M. Burger. 2001.** Carbohydrate-carbohydrate interactions = cell-cell recognition? *Glycobiology* **11:** 896.

**Burbach, J. Peter H., Anita J. C. G. M. Hellemons, Marco Hoekman, Philip Grant, and Harish C. Pant. 2001.** The stellate ganglion of the squid *Loligo pealeii* as a model for neuronal development: expression of a POU Class VI homeodomain gene, *Rpf-1*. *Biol. Bull.* **201:** 252–254.

**Buresch, K. M., Roger T. Hanlon, M. R. Maxwell, and S. Ring. 2001.** Microsatellite DNA markers indicate a high frequency of multiple paternity within individual field-collected egg capsules of the squid *Loligo pealeii*. *Mar. Ecol. Prog. Ser.* **210:** 161–165.

**Bush, M. B., E. Moreno, P. E. De Oliveira, E. Asanza, and P. A. Colinvaux. 2001.** The influence of biogeographic and ecological heterogeneity on Amazonian pollen spectra. *J. Trop. Ecol.* **17:** 729–744.

**Bush, M. B., M. Stute, M.-P. Ledru, H. Behling, P. A. Colinvaux, P. E. De Oliveira, E. C. Grimm, H. Hooghiemstra, S. Haberle, B. W. Leyden, M.-L. Salgado-Labouriau, and R. Webb. 2001.** Paleotemperature estimates for the lowland Americas between 30°S and 30°N at the last glacial maximum. Pp. 293–306 in *Interhemispheric Climate Linkages: Present and Past Interhemispheric Climatic Linkages in the Americas and Their Societal Effects*. V. Markgraf, ed. Academic Press, New York.

**Calzone, W. L., C. Silva, D. L. Keefe, and N. S. Stachenfeld. 2001.** Progesterone does not alter osmotic regulation of AVP. *Am. J. Physiol. Regulatory Integrative Comp. Physiol.* **281:** R2011–R2020.

**Canonne-Hergaux, F., A.-S. Zhang, P. Ponka, and P. Gros. 2001.** Characterization of iron transporter DMT1 (NRAMP2/DCT1) in red blood cells of normal and anemic mk/mk mice. *Blood* **98:** 3823–3830.

**Chappell, R. L. 2001.** Retinal information processing and ambient illumination. Pp. 177–184 in *Concepts and Challenges in Retinal Biology: Tribute to John E. Dowling,* H. Kolb, H. Ripps, and S. Wu, eds. Series: Progress in Brain Research, 131. Elsevier Press, New York.

**Chappell, Richard L., and Stephen Redenti. 2001.** Endogenous zinc as a neuromodulator in vertebrate retina: evidence from the retinal slice. *Biol. Bull.* **201:** 265–267.

**Chiao, Chuan-Chin, and Roger T. Hanlon. 2001.** Cuttlefish camouflage: visual perception of size, contrast and number of white squares on artificial checkerboard substrata initiates disruptive coloration. *J. Exp. Biol.* **204:** 2119–2125.

**Chiao, Chuan-Chin, and Roger T. Hanlon. 2001.** Cuttlefish cue visually on area—not shape or aspect ratio—of light objects in the substrate to produce disruptive body patterns for camouflage. *Biol. Bull.* **201:** 269–270.

**Chikarmane, Hemant M., Alan M. Kuzirian, Ian Carroll, and Robbin Dengler. 2001.** Development of genetically tagged bay scallops for evaluation of seeding programs. *Biol. Bull.* **201:** 285–286.

**Clark, D. A., S. Brown, D. W. Kicklighter, J. Q. Chambers, J. R. Thomlinson, and J. Ni. 2001.** Measuring net primary production in forests: concepts and field methods. *Ecol. Appl.* **11:** 356–370.

**Clay, John R., and Alan M. Kuzirian. 2001.** A novel, kinesin-rich preparation derived from squid giant axons. *Biol. Bull.* **201:** 243–245.

**Clay, J. R., and Alan M. Kuzirian. 2001.** Trafficking of axonal $K^+$ channels: potential role of Hsc70. *J. Neurosci. Res.* **67:** 745–752.

**Clay, J. R., and A. Shrier. 2001.** Action potentials occur spontaneously in squid giant axons with moderately alkaline intracellular pH. *Biol. Bull.* **201:** 186–192.

**Cohen, A. L., G. D. Layne, S. R. Hart, and P. S. Lobel. 2001.** Kinetic control of skeletal Sr/Ca in a symbiotic coral. *Paleoceanography* **16:** 20–26.

**Cohen, M., Y. Gruenbaum, K. K. Lee, and K. L. Wilson. 2001.** Transcriptional repression, apoptosis, human disease and the functional evolution of the nuclear lamina. *Trends Biochem. Sci.* **26:** 41–47.

**Cohen, M., K. L. Wilson, and Y. Gruenbaum. 2001.** Membrane proteins of the nuclear pore complex: Gp210 is conserved in *Drosophila, C. elegans* and *Arabidopsis. Gene Ther. Mol. Biol.* **6:** 47–55.

**Colinvaux, P. A. 2001.** Paradigm lost: Pleistocene environments of the Amazon basin (continued forest cover in perpetual flux, Part 2). *Review of Archaeology* **22:** 20–31.

**Colinvaux, P. A., and P. E. De Oliveira. 2001.** Amazon history on a Cenozoic timescale. *Palaeogeogr. Palaeoclimatol. Palaeoecol.* **166:** 51–63.

**Colinvaux, P. A., G. Irion, M. E. Rasanen, M. B. Bush, and J. De Mello. 2001.** A paradigm to be discarded: geological and paleoecological data falsify the Haffer & Prance refuge hypothesis of Amazonian speciation. *Amazoniana* **16:** 609–646.

**Conrad, Mara L., R. L. Pardy, and Peter B. Armstrong. 2001.** Response of the blood cell of the American horseshoe crab, *Limulus polyphemus,* to a lipopolysaccharide-like molecule from the green alga *Chlorella. Biol. Bull.* **201:** 246–247.

**Contreras, D., and R. Llinas. 2001.** Voltage-sensitive dye imaging of neocortical spatiotemporal dynamics to afferent activation frequencies. *J. Neurosci.* **21:** 9403–9413.

**Cornelissen, J. H. C., T. V. Callaghan, J. M. Alatalo, A. Michelsen, E. Graglia, A. E. Hartley, D. S. Hik, S. E. Hobbie, M. C. Press, C. H. Robinson, G. H. R. Henry, G. R. Shaver, G. K. Phoenix, D. Gwynn Jones, S. Jonasson, F. S. Chapin III, U. Molau, C. Neill, J. A. Lee, J. M. Melillo, B. Sveinbjörnsson and R. Aerts. 2001.** Global change and arctic ecosystems: is lichen decline a function of increases in vascular plant biomass? *J. Ecol.* **89:** 984–994.

**Cox, R. L., T. M. Mariano, D. E. Heck, J. D. Laskin, and J. J. Stegeman. 2001.** Nitric oxide synthase sequences in the marine fish *Stenotomus chrysops* and the sea urchin *Arbacia punctulata,* and phylogenetic analysis of nitric oxide synthase calmodulin-binding domains. *Comp. Biochem. Physiol. B* **131:** 479–491.

**Crawford, Karen. 2001.** Ooplasm segregation in the squid embryo, *Loligo pealeii. Biol. Bull.* **201:** 251–252.

**Créton, R., and L. F. Jaffe. 2001.** Chemiluminescence microscopy as a tool in biomedical research. *BioTechniques* **31:** 1098–1105.

**Cronin, T. W., and N. Shashar. 2001.** The linearly polarized light field in clear tropical marine waters: spatial and temporal variation of light intensity, degree of polarization, and e-vector angle. *J. Exp. Biol.* **204:** 2461–2467.

**De Weer, P., D. C. Gadsby, and R. F. Rakowski. 2001.** Voltage dependence of the apparent affinity for external $Na^+$ of the backward-running sodium pump. *J. Gen. Physiol.* **117:** 315–328.

**Deegan, L. A., J. Kremer, T. Webler, and J. Brawley. 2001.** The use of models in integrated resource management in the coastal zone. Pp. 295–306 in *Science and Integrated Coastal Management,* B. Von Bodungen and R. K. Turner, eds. Dahlem University Press, Berlin.

**Devlin, C. L. 2001.** 5-Hydroxytryptamine stimulates net $Ca^{2+}$ flux in the ventricular muscle of a mollusc (*Busycon canaliculatum*) during cardioexcitation. *Biol. Bull.* **200:** 344–350.

**Dosemeci, A., J.-H. Tao-Cheng, L. Vinade, C. A. Winters, L. Pozzo-Miller, and T. S. Reese. 2001.** Glutamate-induced transient modification of the postsynaptic density. *Proc. Natl. Acad. Sci. USA* **98:** 10,428–10,432.

**Doughty, J. M., and P. D. Langton. 2001.** Measurement of chloride flux associated with the myogenic response in rat cerebral arteries. *J. Physiol.* **534:** 753–761.

**Eckel, W., M. Rabinowitz, and G. Foster. 2001.** Discovering unrecognized lead smelting sites by historical methods. *Am. J. Public Health* **91:** 625–627.

**Edgcomb, V. P., A. J. Roger, A. G. Simpson, D. T. Kysela, and M. L. Sogin. 2001.** Evolutionary relationships among "jakobid" flagellates as indicated by alpha- and beta-tubulin phylogenies. *Mol. Biol. Evol.* **18:** 514–522.

**Emeis, K.-C., J. R. Benoit, L. Deegan, A. J. Gilbert, V. Lee, J. M. Glade, M. Meybeck, S. B. Olsen, and B. von Bodungen. 2001.** Group 4: Unifying concepts for integrated coastal management. Pp. 341–364 in *Science and Integrated Coastal Management,* B. Von Bodungen and R. K. Turner, eds. Dahlem University Press, Berlin.

**Errigo, M., C. McGuiness, S. Meadors, B. Mittmann, F. Dodge, and R. Barlow. 2001.** Visually guided behavior of juvenile horseshoe crabs. *Biol. Bull.* **201:** 271–272.

**Fay, R. R. 2001.** Stream segregation in goldfish: auditory scene analysis. Pp. 485–491 in *Physiological and Psychophysical Bases of Auditory Function: Proceedings of the XIIth Symposium on Hearing,* D. J. Breebaart, A. J. M. Houtsma, A. Kohlrausch, V. F. Prijs, and R. Schoonhoven, eds. Shaker Publishing, Maastricht, The Netherlands.

**Fay, R. R., and P. L. Edds-Walton. 2001.** Bimodal units in the torus semicircularis of the toadfish (*Opsanus tau*). *Biol. Bull.* **201:** 280–281.

**Feierbach, B., and F. Chang. 2001.** Cytokinesis and the contractile ring in fission yeast. *Curr. Opin. Microbiol.* **4:** 713–719.

**Fila, Laurie, Ruth Herrold Carmichael, Andrea Shriver, and Ivan Valiela. 2001.** Stable N isotopic signatures in bay scallop tissue, feces, and pseudofeces in Cape Cod estuaries subject to different N loads. *Biol. Bull.* **201:** 294–296.

**Fukuda, M., T. Yamamoto, and R. Llinas. 2001.** The isochronic band hypothesis and the climbing fiber regulation of motricity. An experimental study. *Eur. J. Neurosci.* **13:** 315–326.

**Funk, D. J., J. J. Wernegreen, and N. A. Moran. 2001.** Intraspecific variation in symbiont genomes: bottlenecks and the aphid-Buchnera association. *Genetics* **157:** 477–489.

**Garcia-Montiel, D. C., P. A. Steudler, M. C. Piccolo, J. M. Melillo, C. Neill, and C. C. Cerri. 2001.** Controls of soil nitrogen oxide emissions from forest and pastures in the Brazilian Amazon. *Global Biogeochem. Cycles* **15:** 1021–1030.

**Gerbod, D., V. P. Edgcomb, C. Noel, S. Vanacova, R. Wintjens, J. Tachezy, M. L. Sogin, and E. Viscogliosi. 2001.** Phylogenetic relationships of class II fumarase genes from trichomonad species. *Mol. Biol. Evol.* **18:** 1574–1584.

**Gerbod, D., V. P. Edgcomb, C. Noel, L. Zenner, R. Wintjens, P. Delgado-Viscogliosi, M. E. Holder, M. L. Sogin, and E. Viscogliosi. 2001.** Phylogenetic position of the trichomonad parasite of turkeys, *Histomonas meleagridis* (Smith) Tyzzer, inferred from small subunit rRNA sequence. *J. Eukaryot. Microbiol.* **48:** 498–504.

**Gioio, A. E., M. Eyman, H. Zhang, Z. Scotto Lavina, A. Giuditta, and B. B. Kaplan. 2001.** Local synthesis of nuclear-encoded mitochondrial proteins in the presynaptic nerve terminal. *J. Neurosci. Res.* **64:** 447–453.

**Goldstrohm, A. C., T. Albrecht, C. Sune, M. Bedford, and M. A. Garcia-Blanco. 2001.** The transcription elongation factor CA150 interacts with RNA polymerase II and the pre-mRNA splicing factor SF1 to repress transcription. *Mol. Cell. Biol.* **21:** 7617–7628.

**Goldstrohm, A. C., A. Greenleaf, and M. A. Garcia-Blanco. 2001.** Co-transcriptional splicing of pre-messenger RNAs: considerations for the mechanism of alternative splicing. *Gene* **277:** 31–47.

**Gordeev, V. V., A. V. Zhullidov, R. M. Holmes, and B. J. Peterson. 2001.** River input of nutrients to the Russian Arctic: achievements and problems. Pp. 108–113 in *Ecology of Siberian Arctic Rivers*, Tomsk, Russia. (in Russian).

**Grady, Sara P., Deborah Rutecki, Ruth Carmichael, and Ivan Valiela. 2001.** Age structure of the Pleasant Bay population of *Crepidula fornicata:* a possible tool for estimating horseshoe crab age. *Biol. Bull.* **201:** 296–297.

**Graf, W., H. Baker, R. F. Spencer, and R. Baker. 2001.** The vestibulo-ocular reflex of the adult flatfish: III. A species-specific reciprocal pattern of excitation and inhibition. *J. Neurophysiol.* **86:** 1376–1388.

**Graglia, E., R. Julkunen-Tiitto, G. R. Shaver, I. K. Schmidt, S. Jonasson, and A. Michelsen. 2001.** Changes in birch phenolic compounds in long term manipulations of temperature, nutrients and light in Alaska and N. Sweden. *New Phytol.* **151:** 227–236.

**Gray, P. A., W. A. Janczewski, N. Mellen, D. R. McCrimmon, and J. L. Feldman. 2001.** Normal breathing requires preBötzinger complex neurokinin-1 receptor-expressing neurons. *Nat. Neurosci.* **4:** 927–930.

**Gray, P. M., B. Krause, J. Atema, R. Payne, C. Krumhansl, and L. Baptista. 2001.** BioMusic: the music of nature and the nature of music. *Science* **291:** 52–54.

**Griffin, M. P. A., and I. Valiela. 2001.** The use of d15N signatures in studies of life history and trophic position of fish (*Fundulus heteroclitus* and *Menidia menidia*). *Mar. Ecol. Prog. Ser.* **214:** 299–305.

**Hall, Benjamin, and Kerry Delaney. 2001.** Cholinergic modulation of odor-evoked oscillations in the frog olfactory bulb. *Biol. Bull.* **201:** 276–277.

**Hamilton, S. K., J. L. Tank, D. F. Raiknow, W. F. Wollheim, B. J. Peterson, and J. R. Webster. 2001.** Nitrogen uptake and transformation in a midwestern U.S. stream: a stable isotope enrichment study. *Biogeochemistry* **54:** 297–340.

**Hatfield, E. M. C., Roger T. Hanlon, J. W. Forsythe, and E. P. M. Grist. 2001.** Laboratory testing of a growth hypothesis for juvenile squid *Loligo pealeii* (*Cephalopoda: Loliginidae*). *Can. J. Fish. Aquat. Sci.* **58:** 845–857.

**Hauxwell, Alyson M., Christopher Neill, Ivan Valiela, and Kevin D. Kroeger. 2001.** Small-scale heterogeneity of nitrogen concentrations in groundwater at the seepage face of Edgartown Great Pond. *Biol. Bull.* **201:** 290–292.

**Hauxwell, J., J. Cebrián, C. Furlong, and I. Valiela. 2001.** Macroalgal canopies associated with increased anthropogenic nitrogen supply contribute to eelgrass (*Zostera marina*) decline in temperate estuarine ecosystems. *Ecology* **82:** 1007–1022.

**Havens, K. E., J. Hauxwell, A. C. Tyler, S. Thomas, K. J. McGlathery, J. Cebrian, I. Valiela, A. D. Steinman, and S. Hwang. 2001.** Complex interactions between autotrophs in shallow marine and freshwater ecosystems: implications for community responses to nutrient stress. *Environ. Pollut.* **113:** 95–107.

**Hernandez, R. V., J. M. Garza, M. E. Graves, J. L. Martinez, Jr., and R. G. LeBaron. 2001.** The process of reducing CA1 long-term potentiation by the integrin peptide, GRGDSP, occurs within the first few minutes following theta-burst stimulation. *Biol. Bull.* **201:** 236–237.

**Hilfiker, S., A. J. Czernik, P. Greengard, and G. J. Augustine. 2001.** Tonically active protein kinase A regulates neurotransmitter release at the squid giant synapse. *J. Physiol.* **531:** 141–146.

**Hill, Susan D., and Barbara C. Boyer. 2001.** Phalloidin labeling of developing muscle in embryos of the polychaete *Capitella* sp. I. *Biol. Bull.* **201:** 257–258.

**Hinckley, Eve-Lyn S., Christopher Neill, Richard McHorney, and Ann Lezberg. 2001.** Dissolved nitrogen dynamics in groundwater under a coastal Massachusetts forest. *Biol. Bull.* **201:** 288–290.

**Hobbie, J. E., A. E. Hershey, P. W. Lienesch, M. E. McDonald, G. W. Kling, and W. J. O'Brien. 2001.** Studies of fresh waters on the North Slope. Pp. 123–128 in *Fifty More Years Below Zero: Tributes and Meditations for the Naval Arctic Research Laboratory's First Half Century at Barrow, Alaska*, D. Norton, ed. University of Alaska Press, Fairbanks, Alaska.

**Hoit, D., J. A. Hickman, J. Zhang, I. Ivanovska, J. M. Hardwick, L. K. Kaczmarek, and E. A. Jonas. 2001.** Modulation of mitochondrial conductance and synaptic transmission by Bcl-xL. *Biophys. J.* **80:** 239a.

**Holmes, R. M., B. J. Peterson, A. V. Zhulidov, V. V. Gordeev, P. N. Makkaveev, P. A. Stunzas, L. S. Kosmenko, G. H. Kohler, and A. I. Shiklomanov. 2001.** Nutrient chemistry of the Ob' and Yenisey rivers, Siberia: results from June 2000 expedition and evaluation of long-term data sets. *Mar. Chem.* **75:** 219–227.

**Hopkinson, C. S., A. E. Giblin, and J. Tucker. 2001.** Benthic metabolism and nutrient regeneration on the continental shelf of eastern Massachusetts, USA. *Mar. Ecol. Prog. Ser.* **224:** 1–19.

**Inoué, S. 2001.** Digitally enhanced, polarization-based microscopy: Reality and dreams. *Microsc. Microanal.* **7:** 2–3.

**Inoué, S., and M. Goda. 2001.** Fluorescence polarization and crystal structure of native GFP. *Mol. Biol. Cell* **12:** 259a.

**Inoué, S., and M. Goda. 2001.** Fluorescence polarization of GFP crystals. *Biol. Bull.* **201:** 231–233.

**Jonasson, S., F. S. Chapin, and G. R. Shaver. 2001.** Biogeochemistry in the Arctic: patterns, processes and controls. Pp. 139–150 in *Global Biogeochemical Cycles in the Climate System*, E.-D. Schulze, S. P. Harrison, M. Heimann, E. A. Holland, J. J. Lloyd, I. C. Prentice, and D. Schimel, eds. Academic Press, San Diego, CA.

**Jung, S.-K., J. R. Trimarchi, R. H. Sanger, and P. J. S. Smith. 2001.** Development and application of a self-referencing glucose microsensor for the measurement of glucose consumption by pancreatic cells. *Anal. Chem.* **73:** 3759–3767.

**Kaatz, Ingrid M., and Phillip S. Lobel. 2001.** A comparison of sounds recorded from a catfish (*Orinocodoras eigenmanni*, Doradidae) in an aquarium and in the field. *Biol. Bull.* **201:** 278–280.

**Kakhlon, O., Y. Gruenbaum, and Z. Y. Cabantchik. 2001.** Repression of ferritin expression increases the labile iron pool, oxidative stress and short term growth of human erythroleukemia cells. *Blood* **97:** 2863–2871.

**Kakhlon, O., Y. Gruenbaum, and Z. Y. Cabantchik. 2001.** Repression of the heavy ferritin chain increases the labile iron pool of human K562 cells. *Biochem. J.* **356:** 311–316.

**Kálmán, M., and R. M. Gould. 2001.** GFAP-immunopositive structures in spiny dogfish, *Squalus acanthias*, and in little skate, *Raia erinacea*, brains: differences have evolutionary implications. *Anat. Embryol.* **204:** 59–80.

**Kapoor, T. M., and T. J. Mitchison. 2001.** Eg5 is static in bipolar spindle relative to tubulin: evidence for a static spindle matrix. *J. Cell Biol.* **154:** 1125–1133.

**Kaufman, L. S. 2001.** Most excellent of fishes. *Nat. Hist.* **110:** 84–85. (Book Review).

**Kelley, M., P. Winge, J. Heaney, R. Stephens, J. Farell, R. Van Beneden, C. L. Reinisch, M. Lesser, and C. Walker. 2001.** Expression of homologues for p53 and p73 in the softshell clam (*Mya arenaria*), a naturally occurring model for human leukemia. *Oncogene* **20:** 748–758.

**Kim, K. M., C. D. Giedt, G. Basanez, J. W. O'Neill, J. J. Hill, Y. H. Han, S. P. Tzung, J. Zimmerberg, D. M. Hockenbery, and K. Y. Zhang. 2001.** Biophysical characterization of recombinant human Bcl-2 and its interactions with an inhibitory ligand, Antimycin A. *Biochemistry* **40:** 4911–4922.

**Knudson, Robert A., Shinya Inoué, and Makoto Goda. 2001.** Centrifuge polarizing microscope with dual specimen chambers and injection ports. *Biol. Bull.* **201:** 234.

**Kozlowski, Corinne, Kara Yopak, Rainer Voigt, and Jelle Atema. 2001.** An initial study on the effects of signal intermittency on the odor plume tracking behavior of the American lobster, *Homarus americanus*. *Biol. Bull.* **201:** 274–276.

**Kreiling, J., K. Jessen-Eller, J. Miller, R. Seegal, and C. L. Reinisch. 2001.** Development of the serotonergic nervous system in the *Spisula solidissima* (surf clam) veliger. *Comp. Biochem. Physiol. A* **130:** 341–351.

**Kriebel, M., B. Keller, R. B. Silver, G. Q. Fox, and G. D. Pappas. 2001.** Porocytosis: quantal synaptic secretion by an array of pores. *Brain Res.* **38:** 20–32.

**Kuhns, William J., Dario Rusciano, Jane Kaltenbach, Michael Ho, Max Burger, and Xavier Fernandez-Busquets. 2001.** Up-regulation of integrins $\alpha_3 \beta_1$ in sulfate-starved marine sponge cells: functional correlates. *Biol. Bull.* **201:** 238–239.

**Kumar, S. M., D. M. Porterfield, K. J. Muller, P. J. S. Smith, and C. L. Sahley. 2001.** Nerve injury induces a rapid efflux of nitric oxide (NO) detected with a novel microsensor. *J. Neurosci.* **21:** 215–220.

**Kuzirian, Alan M., Eleanor C. S. Terry, Deanna L. Bechtel, and Patrick L. James. 2001.** Hydrogen peroxide: an effective treatment for ballast water. *Biol. Bull.* **201:** 297–299.

**LaFountain, J. R., R. Oldenbourg, R. W. Cole, and C. L. Rieder. 2001.** Microtubule flux mediates poleward motion of acentric chromosome fragments during meiosis in insect spermatocytes. *Mol. Biol. Cell* **12:** 4054–4065.

**Lammers, R. B., A. I. Shiklomanov, C. J. Vorosmarty, B. M. Fekete, and B. J. Peterson. 2001.** Assessment of contemporary arctic river runoff based on observational discharge records. *J. Geophys. Res.* **106:** 3321–3334.

**Land, S. C., and A. Collett. 2001.** Detection of Cl$^-$ flux in the apical microenvironment of cultured foetal distal lung epithelial cells. *J. Exp. Biol.* **204:** 785–795.

**Laufer, Hans, and William J. Biggers. 2001.** Unifying concepts learned from methyl farnesoate for invertebrate reproduction and post-embryonic development. *Am. Zool.* **41:** 442–457.

**Lezberg, A., C. B. Halpern, and J. A. Antos. 2001.** Clonal development of *Maianthemum dilatatum* in forests of differing age and structure. *Can. J. Bot.* **79:** 1028–1038.

**Li, Q., D. Hansen, H. C. Joshi, R. E. Palazzo, and R. D. Balczon. 2001.** Pericentrin B, a centrosome protein with homology to pericentrin that forms a complex with PCM-1. *J. Cell Sci.* **114:** 797–809.

**Liu, L., K. Hammar, P. J. S. Smith, S. Inoué, and D. Keefe. 2001.** Mitochondrial modulation of calcium signaling at the initiation of development. *Cell Calcium* **30:** 423–433.

**Lindholm, J. B., P. J. Auster, M. Ruth, and L. S. Kaufman. 2001.** Modeling the effects of fishing, and implications for the design of marine protected areas: juvenile fish responses to variations in seafloor habitat. *Conserv. Biol.* **15:** 424–437.

**Link, Brian A. 2001.** Evidence for directed mitotic cleavage plane reorientations during retinal development within the zebrafish. *Biol. Bull.* **201:** 254–255.

**Llinas, R., and U. Ribary. 2001.** Consciousness and the brain. The thalamocortical dialogue in health and disease. *Ann. NY Acad. Sci.* **929:** 166–175.

**Lobel, P. S. 2001.** Acoustic behavior of cichlid fishes. *J. Aquaric. Aquat. Sci.* **9:** 167–186.

**Lobel, P. S. 2001.** Fish bioacoustics and behavior: passive acoustic detection and the application of a closed-circuit rebreather for field study. *Mar. Technol. Soc. J.* **35:** 19–28.

**Makkaveev, P. N., P. A. Stunzhas, P. V. Khlebopashev, V. V. Gordeev, R. M. Holmes, B. J. Peterson, and A. I. Shiklomanov. 2001.** Flux of nutrients from Ob' and Yenisey rivers to the Arctic Ocean: results from June 2000 expeditions. Pp. 97–106 in *Changes in the Atmosphere-Land-Sea System in the Amerasian Arctic: Proceedings of the Arctic Regional Centre,* Vol. 3, Igor P. Semiletov, ed. Dalnauka, Vladivostok.

**McArthur, A. G., L. Knodler, J. D. Silberman, B. Davids, F. D. Gillin, and M. L. Sogin. 2001.** The evolutionary origins of eukaryotic protein disulfide isomerase domains: new evidence from the amitochondriate protist *Giardia lamblia*. *Mol. Biol. Evol.* **18:** 1455–1463.

**McGladdery, S., C. Reinisch, S. MacCallum, R. Stephens, C. Walker, and J. Davidson. 2001.** Haemic neoplasia in soft-shell clams (*Mya arenaria*): recent outbreaks in Atlantic Canada and discovery of a p53 gene homologue associated with the condition. *Bull. Aquac. Assoc. Canada* **2001:** 101–103.

**McGuire, A. D., S. Sitch, J. S. Clein, R. Dargaville, G. Esser, J. Foley, M. Heimann, F. Joos, J. Kaplan, D. W. Kicklighter, R. A. Meier, J. M. Melillo, B. Moore III, I. C. Prentice, N. Ramankutty, T. Reichenau, A. Schloss, H. Tian, L. J. Williams, and U. Wittenberg. 2001.** Carbon balance of the terrestrial biosphere in the twentieth century: analyses of CO$_2$, climate and land-use effects with four process-based ecosystem models. *Global Biogeochem. Cycles* **15:** 183–206.

**McLaughlin, J. A. 2001.** Albert Szent-Gyorgyi and the nature of life. Pp. 1–4 in *Ascorbic Acid in Aquatic Organisms,* Konrad Dabrowski, ed. CRC Press, Boca Raton, FL.

**Meadors, S., C. McGuiness, F. A. Dodge, and R. B. Barlow. 2001.** Growth, visual field, and resolution in the juvenile *Limulus* lateral eye. *Biol. Bull.* **201:** 272–274.

**Medina, M., A. G. Collins, J. D. Silberman, and M. L. Sogin. 2001.** Evaluating hypotheses of basal animal phylogeny using complete sequences of large and small subunit rRNA. *Proc. Natl. Acad. Sci. USA* **98:** 9707–9712.

**Melillo, J. M., P. A. Steudler, B. J. Fiedl, C. Neill, D. Garcia, M. C. Piccolo, C. C. Cerri, and H. Tian. 2001.** Nitrous oxide emissions from forests and pastures of various ages in the Brazilian Amazon. *J. Geophys. Res.* **106:** 34,179–34,188.

**Mensinger, Allen F., Katherine A. Stephenson, Sarah L. Pollema, Hazel E. Richmond, Nichole Price, and Roger T. Hanlon. 2001.** Mariculture of the toadfish *Opsanus tau*. *Biol. Bull.* **201:** 282–283.

**Mitchison, T. J., and E. D. Salmon. 2001.** Mitosis: a history of division. *Nat. Cell. Biol.* **3:** E17–E21.

**Miyake, K., P. L. McNeil, K. Suzuki, R. Tsunoda, and N. Sugai. 2001.**

An actin barrier to membrane resealing. *J. Cell Sci.* **114:** 3487–3494.

**Morfini, G., G. Szebenyi, B. Richards, and S. T. Brady. 2001.** Regulation of kinesin: implications for neuronal development. *Dev. Neurosci.* **23:** 364–376.

**Morgan, J. R., E. Lafer, and G. J. Augustine. 2001.** Rapid-fire synaptic vesicle exocytosis. *Neuron* **30:** 5–7.

**Morgan, J. R., K. Prasad, S. Jin, G. J. Augustine, and E. M. Lafer. 2001.** Uncoating of clathrin-coated vesicles in presynaptic terminals: roles for Hsc70 and auxilin. *Neuron* **32:** 289–300.

**Morrison, H. G., A. J. Roger, T. G. Nystul, F. D. Gillin, and M. L. Sogin. 2001.** *Giardia lamblia* expresses a proteobacterial-like DnaK homolog. *Mol. Biol. Evol.* **18:** 530–541.

**Mwanja, W. W., A. S. Armoudlian, S. B. Wandera, L. Kaufman, L. Wu, G. C. Booton, and P. A. Fuerst. 2001.** The bounty of minor lakes: the role of small satellite water bodies in evolution and conservation of fishes. *Hydrobiologia* **458:** 55–62.

**Nadelhoffer, K. J. 2001.** The impacts of nitrogen deposition on forest ecosystems. Pp. 311–331 in *Nitrogen in the Environment: Sources, Problems, and Management,* R. F. Follett and J. L. Hatfield, eds. Elsevier Science, Amsterdam.

**National Assessment Synthesis Team. 2001.** *Climate Change Impacts on the United States: The Potential Consequences of Climate Variability and Change, Report for the US Global Change Research Program,* J. M. Melillo, A. C. Janetos and T. R. Karl, eds. Cambridge University Press, Cambridge, UK.

**Neill, C., L. A. Deegan, S. M. Thomas, and C. C. Cerri. 2001.** Deforestation for pasture alters nitrogen and phosphorus in small Amazonian streams. *Ecol. Appl.* **11:** 1800–1816.

**Nillson, H., W. Steffen, and R. E. Palazzo. 2001.** *In vitro* reconstitution of fish melanophore pigment aggregation. *Cell Motil. Cytoskelet.* **48:** 1–10.

**Novak, Melissa, Mark Lever, and Ivan Valiela. 2001.** Top-down *vs.* bottom-up controls of microphytobenthic standing crop: role of mud snails and nitrogen supply in the littoral of Waquoit Bay estuaries. *Biol. Bull.* **201:** 292–294.

**Pabich, W. J., I. Valiela, and H. F. Hemond. 2001.** The effect of vadose zone thickness and depth below the water table on DOC concentrations in groundwater on Cape Cod. *Biogeochemistry* **55:** 247–268.

**Pan, Y., J. M. Melillo, D. W. Kicklighter, X. Xiao, and A. D. McGuire. 2001.** Modeling structural and functional responses of terrestrial ecosystems in China to changes in climate and atmospheric CO$_2$. *Acta Phytoecologica Sin.* **25:** 175–189.

**Pearson, C. G., P. S. Maddox, E. D. Salmon, and K. Bloom. 2001.** Budding yeast chromosome structure and dynamics during mitosis. *J. Cell Biol.* **152:** 1255–1266.

**Pedroarena, C. M., and R. Llinas. 2001.** Interaction of synaptic and intrinsic electroresponsiveness determine corticothalamic activation dynamics. *Thalamus and Related Systems* **1:** 3–13.

**Peterson, B. J., W. M. Wollheim, P. J. Mulholland, J. R. Webster, J. L. Meyer, J. L. Tank, E. Martí, W. B. Bowden, H. M. Valett, A. E. Hershey, W. H. McDowell, W. K. Dodds, S. K. Hamilton, S. Gregory, and D. D. Morrall. 2001.** Control of nitrogen export from watersheds by headwater streams. *Science* **292:** 86–90.

**Podar, M., S. H. Haddock, M. L. Sogin, and G. R. Harbison. 2001.** A molecular phylogenetic framework for the phylum *Ctenophora* using 18S rRNA genes. *Mol. Phylogenet. Evol.* **21:** 218–230.

**Ponka, P. 2001.** Iron deficiency. Pp. 369–376 in *Conn's Current Therapy,* R. E. Rakel and E. T. Bope, eds. W. B. Saunders, Philadelphia.

**Ponka, P. 2001.** Transferrin receptor (CD71). Pp. 3211–3216 in *Encyclopedia of Molecular Medicine,* T. Creighton, ed. John Wiley, New York.

**Porterfield, D. M., J. D. Laskin, S.-K. Jung, R. P. Malchow, B. Billack, P. J. S. Smith, and D. E. Heck. 2001.** Proteins and lipids define the diffusional field of nitric oxide. *Am. J. Physiol. Lung Cell Mol. Physiol.* **281:** L904–L912.

**Powell, H. K., D. Jin, and I. M. Kaplan. 2001.** Commercial fishing vessel safety and fisheries management. *Journal of Safety at Sea* **58:** 2.

**Puttaraju, M., J. DiPasquale, C. C. Baker, L. Mitchell, and M. A. Garcia-Blanco. 2001.** Messenger RNA repair and restoration of protein function by spliceosome-mediated RNA trans-splicing. *Mol. Ther.* **4:** 105–114.

**Qian, H., and H. Ripps. 2001.** The GABAc receptors of retinal neurons. Pp. 295–308 in *Concepts and Challenges in Retinal Biology: Tribute to John E. Dowling,* H. Kolb, H. Ripps, and S. Wu, eds. Series: Progress in Brain Research, 131. Elsevier Press, New York.

**Qian, H., H. Ripps, E. Schuette, and R. L. Chappell. 2001.** Responses of small- and large-field bipolar cells to GABA and glycine. *Brain Res.* **893:** 273–277.

**Rastetter, E. B., P. M. Vitousek, C. Field, G. R. Shaver, D. Herbert, and G. I. Ågren. 2001.** Resource optimization and symbiotic N fixation. *Ecosystems* **4:** 369–388.

**Raymond, P. A., and J. E. Bauer. 2001.** DOC cycling in a temperate estuary: A mass balance approach using natural $^{14}$C and $^{13}$C isotopes. *Limnol. Oceanograph.* **46:** 655–667.

**Raymond, P. A., and J. E. Bauer. 2001.** Riverine export of aged terrestrial organic matter to the North Atlantic Ocean. *Nature* **409:** 497–500.

**Raymond, P. A., and J. E. Bauer. 2001.** Use of $^{14}$C and $^{13}$C natural abundances for evaluating riverine, estuarine, and coastal DOC and POC sources and cycling: review and Synthesis. *Org. Geochem.* **32:** 469–485.

**Raymond, P. A., and J. J. Cole. 2001.** Gas exchange in rivers and estuaries: choosing a gas transfer velocity. *Estuaries* **24:** 312–217.

**Rhodes, P., and R. Llinas. 2001.** Efficacy of input to the apical tuft of layer 5 cells. *J. Physiol.* **536:** 167–187.

**Rice, Aaron N., David S. Portnoy, Ingrid M. Kaatz, and Phillip S. Lobel. 2001.** Differentiation of pharyngeal muscles on the basis of enzyme activities in the cichlid *Tramitichromis intermedius. Biol. Bull.* **201:** 258–260.

**Richardson, D. R., C. Mouralian, P. Ponka, and E. Becker. 2001.** Development of potential iron chelators for the treatment of Friedreich's ataxia: ligands that mobilize mitochondrial iron. *Biochim. Biophys. Acta* **1536:** 133–140.

**Richey, J. E., A. Krusche, L. A. Deegan, V. Ballester, T. Biggs, and R. Victoria. 2001.** Land use changes and the biogeochemistry of river corridors in the Amazon. *IGBP Global Change Newsletter* **45:** 19–22.

**Rieder, C. L., S. Faruki, and A. Khodjakov. 2001.** The centrosome in vertebrates: more than a microtubule organizing center. *Trends Cell Biol.* **11:** 413–419.

**Rieder, Leila E., and Allen F. Mensinger. 2001.** Strategies for increasing growth of juvenile toadfish. *Biol. Bull.* **201:** 283–285.

**Rinkwitz, S., E. Bober, and R. Baker. 2001.** Development of the vertebrate inner ear. *Ann. NY Acad. Sci.* **942:** 1–14.

**Ripps, H. 2001.** The rhodopsin cycle: a twist in the tale. Pp. 335–350 in *Concepts and Challenges in Retinal Biology: Tribute to John E. Dowling,* H. Kolb, H. Ripps, and S. Wu, eds. Series: Progress in Brain Research, 131. Elsevier Press, New York.

**Rome, L. C., and D. M. Swank. 2001.** The Influence of thermal acclimation on power production during swimming I: Acclimation of the scup nervous systems. *J. Exp. Biol.* **204:** 409–418.

**Schnackenberg, B. J., and R. E. Palazzo. 2001.** Reconstitution of centrosome microtubule nucleation potential in *Spisula* oocyte extracts. *Methods Cell Biol.* **67:** 149–164.

**Shahaf, G., and S. Marom. 2001.** Learning in networks of cortical neurons. *J. Neurosci.* **21:** 8782–8788.

**Shashar, Nadav, Douglas T. Borst, Seth A. Ament, William M. Saidel, Roxanna M. Smolowitz, and Roger T. Hanlon. 2001.** Polarization reflecting iridophores in the arms of the squid *Loligo pealeii*. *Biol. Bull.* **201:** 267–268.

**Shaver, G. R., M. S. Bret-Harte, M. H. Jones, J. Johnstone, L. Gough, J. Laundre, and F. S. Chapin, III. 2001.** Species composition interacts with fertilizer to control long-term change in tundra productivity. *Ecology* **82:** 3163–3181.

**Shaver, G. R., and S. Jonasson. 2001.** Productivity of Arctic ecosystems. Pp. 189–210 in *Terrestrial Global Productivity*, H. Mooney, J. Roy, and B. Saugier, eds. Academic Press, New York.

**Silver, Robert B. 2001.** LtB4 evokes the calcium signal that initiates nuclear envelope breakdown through a multi-enzyme network in sand dollar (*Echinaracnius parma*) cells. *Biol. Bull.* **201:** 248–250.

**Silver, Robert B., Mahlon E. Kriebel, Bruce Keller, and George D. Pappas. 2001.** Porocytosis: quantal synaptic secretion of neurotransmitter at the neuromuscular junction through arrayed vesicles. *Biol. Bull.* **201:** 263–264.

**Smith, P. J. S., P. G. Haydon, A. Hengstenberg, and S.-K. Jung. 2001.** Analysis of cellular boundary layers: application of electrochemical microsensors. *Electrochimica Acta* **47:** 283–292.

**Smith, P. J. S., A. Hengstenberg, and S.-K. Jung. 2001.** Measuring molecular flux in the diffusionary boundary layer of cells and tissues. *Radiat. Res.* **156:** 436–437.

**Smith, P. J. S., and J. R. Trimarchi. 2001.** Non-invasive measurement of hydrogen and potassium ion flux from single cells and epithelial structures. *Am. J. Physiol. Cell Physiol.* **280:** C1–C11.

**Smith, Ryan, Emma Kavanagh, Hilary G. Morrison, and Robert M. Gould. 2001.** Messenger RNAs located in spiny dogfish oligodendrocyte processes. *Biol. Bull.* **201:** 255–256.

**Smolowitz, R., D. Leavitt, B. Lancaster, E. Marks, R. Hanselmann, and C. Brothers. 2001.** Laboratory based transmission studies of quahog parasite unknown (QPX) in *Mercenaria mercenaria*. P. 599 in *Aquaculture 2001: Book of Abstracts, World Aquaculture Society*, Louisiana State University, Baton Rouge, LA.

**Stachenfeld, N. S., S. Palter, and D. L. Keefe. 2001.** Estrogen and progesterone effects on transcapillary fluid dynamics. *Am. J. Physiol. Regulatory Integrative Comp. Physiol.* **281:** R1319–R1329.

**Stachenfeld, N. S., A. Splenser, W. L. Calzone, M. P. Taylor, and D. L. Keefe. 2001.** Genome and hormones: Gender differences in physiology. Selected contribution: Sex differences in osmotic regulation of AVP and renal sodium handling. *J. Appl. Physiol.* **91:** 1893–1901.

**Stephens, R., C. Walker, and C. L. Reinisch. 2001.** Multiple protein differences distinguish clam leukemia cells from normal hemocytes: evidence for the involvement of p53 homologs. *Comp. Biochem. Physiol. C* **129:** 329–338.

**Stokes, N. A., L. M. R. Calvo, K. Apakupakul, E. M. Burreson, I. Sunila, and R. Smolowitz. 2001.** Validation of DNA-based molecular diagnostics for the hard clam parasite QPX (Quahog Parasite Unknown) and the oyster parasite SSO (*Haplosporidium costale*). P. 613 in *Aquaculture 2001: Book of Abstracts, World Aquaculture Society*, Louisiana State University, Baton Rouge, LA.

**Straka, H., E. Gilland, and R. Baker.** Rhombomeric organization of vestibular pathways in larval frogs. *J. Comp. Neurol.* **437:** 42–55.

**Surguchov, A., R. E. Palazzo, and I. Surgucheva. 2001.** Gamma synucleins: subcellular localization in neuronal and non-neuronal cells and effect on signal transduction. *Cell Motil. Cytoskel.* **49:** 218–228.

**Swank, D. M., and L. C. Rome. 2001.** The influence of thermal acclimation on power production during swimming. II: Acclimation of scup red muscle. *J. Exp. Biol.* **204:** 419–430.

**Tal, Dror, Eyal Jacobson, Vladimir Lyakhov, and Shimon Marom. 2001.** Frequency tuning of input-output relation in a rat cortical neuron *in vitro*. *Neurosci. Lett.* **300:** 21–24.

**Tao-Cheng, J.-H., L. Vinade, C. Smith, C. A. Winters, R. Ward, M. W. Brightman, T. S. Reese, and A. Dosemeci. 2001.** Sustained elevation of calcium induces transient Ca$^{2+}$/calmodulin-dependent protein kinase II clusters in neurons. *Neuroscience* **106:** 69–78.

**Telzer, B. R., and L. T. Haimo. 2001.** Chromatophores as tools for the study of organelle transport. Pp. 201–214 in *Methods in Molecular Biology, Vol. 161, Cytoskeleton Methods and Protocols*, R. Gavin, ed. Humana Press, Totowa, NJ.

**Tilman, D., J. Fargione, B. Wolff, C. D'Antonio, A. Dobson, R. W. Howarth, D. Schindler, W. Schlesinger, D. Simberloff, and D. Swackhamer. 2001.** Forecasting agriculturally driven global environmental change. *Science* **292:** 281–284.

**Tobias, C. R., I. C. Anderson, E. A. Canuel, and S. A. Macko. 2001.** Nitrogen cycling through a fringing marsh-aquifer ecotone. *Mar. Ecol. Prog. Ser.* **210:** 25–39.

**Tobias, C. R., J. W. Harvey, and I. C. Anderson. 2001.** Quantifying groundwater discharge through fringing wetlands to estuaries: seasonal variability, methods comparison, and implications for wetland-estuary exchange. *Limnol. Oceanogr.* **46:** 604–615.

**Tobias, C. R., S. A. Macko, I. C. Anderson, E. A. Canuel, and J. W. Harvey. 2001.** Tracking the fate of a high concentration groundwater nitrate plume through a fringing marsh: a combined groundwater tracer and *in situ* isotope enrichment study. *Limnol. Oceanogr.* **46:** 1977–1989.

**Tokumaru, H., L. L. Pelligrini, T. Ishizuka, K. Umayahara, H. Saisu, H. Betz, G. J. Augustine, and T. Abe. 2001.** SNARE complex oligomerization by synaphin/complexin is essential for synaptic vesicle exocytosis. *Cell* **104:** 421–432.

**Tran, P. T., and Fred Chang. 2001.** Transmitted light fluorescence microscopy revisited. *Biol. Bull.* **201:** 235–236.

**Tran, P. T., L. Marsh, V. Doye, S. Inoué, and F. Chang. 2001.** A mechanism for nuclear positioning in fission yeast based on microtubule pushing. *J. Cell Biol.* **153:** 397–411.

**Twig, Gilad, Sung-Kwon Jung, Mark A. Messerli, Peter J. S. Smith, and Orian S. Shirihai. 2001.** Real-time detection of reactive oxygen intermediates from single microglial cells. *Biol. Bull.* **201:** 261–262.

**Tzyung, P. S., K. M. Kim, G. Basanez, C. D. Giedt, J. Simon, J. Zimmerberg, K. Y. J. Zhang, and D. M. Hockenbery. 2001.** Antimycin A mimics a pro-apoptotic BH3 domain and selectively induces apoptosis in cell lines overexpressing Bcl-XL. *Nat. Cell Biol.* **3:** 163–191.

**Valiela, I., J. L. Bowen, and J. K. York. 2001.** Mangrove forests: one of the world's threatened major tropical environments. *BioScience* **51:** 807–815.

**Valiela, I., J. L. Bowen, M. L. Cole, K. D. Kroeger, D. Lawrence, W. J. Pabich, G. Tomasky, and G. S. Mazzilli.** Following up on a Margalevian concept: interactions and exchanges among adjacent parcels of coastal landscapes. *Sci. Mar.* **65:** 271–231.

**Valiela, I., M. L. Cole, J. McClelland, J. Hauxwell, J. Cebrian, and S. Joye.** Role of salt marshes as part of coastal landscapes. Pp. 23–38 in *Concepts and Controversies in Tidal Marsh Ecology*, M. P. Weinstein and D. A. Kreeger, eds. Kluwer Academic Publishers, Dordrecht, The Netherlands.

**Vinade, L., J. D. Petersen, K. Do, A. Dosemeci, and T. S. Reese. 2001.** Activation of calpain may alter the postsynaptic density structure and modulate anchoring of NMDA receptors. *Synapse* **40:** 302–309.

**Vörösmarty, C. J., L. D. Hinzman, B. J. Peterson, D. H. Bromwich, L. C. Hamilton, J. Morison, V. E. Romanovsky, M. Sturm, and R. S. Webb. 2001.** *The Hydrologic Cycle and its Role in Arctic and Global Environmental Change: A Rationale and Strategy for Synthesis Study*. Arctic Research Consortium of the U.S., Fairbanks, Alaska. 84 pp.

**Wachowiak, M., and L. B. Cohen. 2001.** Representation of odorants by receptor neuron input to the mouse olfactory bulb. *Neuron* **32:** 725–737.

**Wachowiak, M., Y-W. Lam, L. B. Cohen, and M. R. Zochowski. 2001.**

Voltage-sensitive and calcium sensitive dye imaging of activity in the olfactory bulb: presynaptic inhibition, maps of receptor input, and oscillations. Pp. 91–15 in *Methods in Chemosensory Research*. S. A. Simon and M. Nicolelis, eds. CRC Press, Boca Raton, FL.

**Wagner, E. J., and M. A. Garcia-Blanco. 2001.** Polypyrimidine tract binding protein antagonizes exon definition. *Mol. Cell. Biol.* **21:** 3281–3288.

**Wang, W. H., L. Meng, R. J. Hackett, and D. L. Keefe. 2001.** Developmental ability of human oocytes with or without birefringent spindles imaged by polscope before insemination. *Hum. Reprod.* **16:** 1464–1468.

**Wang, W. H., L. Meng, R. J. Hackett, R. Oldenhourg, and D. L. Keefe. 2001.** Limited recovery of meiotic spindles in human eggs after cooling—rewarming observed in living eggs using polarized light microscope. *Hum. Reprod.* **16:** 2374–2378.

**Wang, W. H., L. Meng, R. J. Hackett, R. Oldenbourg, and D. L. Keefe.** The spindle observation and its relationship with fertilization after intracytoplasmic sperm injection in living human oocytes. *Fertil. Steril.* **75:** 348–353.

**Weidner, Earl. 2001.** Microsporidian spore/sporoplasm dynactin in *Spraguea*. *Biol. Bull.* **201:** 245–246.

**Wernegreen, J. J., and N. A. Moran. 2001.** Vertical transmission of biosynthetic plasmids in aphid endosymbionts (Buchnera). *J. Bacteriol.* **183:** 785–790.

**Wernegreen, J. J., A. O. Richardson, and N. A. Moran. 2001.** Parallel acceleration of evolutionary rates in symbiont genes underlying host nutrition. *Mol. Phylogenet. Evol.* **19:** 479–485.

**Williams, Libby, G. Carl Noblitt IV, and Robert Buchsbaum. 2001.** The effects of salt marsh haying on benthic algal biomass. *Biol. Bull.* **201:** 287–288.

**Williams, M., E. B. Rastetter, G. R. Shaver, J. E. Hobbie, E. Carpino, and B. L. Kwiatkowski. 2001.** Primary production of an arctic watershed: an uncertainty analysis. *Ecol. Appl.* **11:** 1800–1816.

**Wilson, K. L., R. Benavente, B. Burke, R. Craigie, R. Foisner, K. Furukawa, L. Gerace, R. D. Goldman, Y. Gruenbaum, C. Harris, C. J. Hutchison, G. Krohne, G. E. Morris, H. Otto, A. J. Simon, and H. J. Worman.** Problems with LAP nomenclature. *Nat. Cell Biol.* **3:** E90.

**Wöllert, Torsten, Ana S. DePina, Leslie A. Sandberg, and George M. Langford. 2001.** Reconstitution of active pseudo-contractile rings and myosin-II-mediated vesicle transport in extracts of clam oocytes. *Biol. Bull.* **201:** 241–243.

**Wollheim, W. M., B. J. Peterson, L. A. Deegan, J. E. Hobbie, B. Hooker, W. B. Bowden, K. J. Edwardson, D. B. Arscott, and A. E. Hershey. 2001.** Influence of stream size on ammonium and suspended particulate nitrogen processing. *Limnol. Oceanogr.* **46:** 1–13.

**Yamaguchi, A., L. K. Kaczmarek, and D. B. Kelley. 2001.** Intrinsic membrane properties of laryngeal motoneurons that generate sexually distinct vocalizations in African clawed frogs *Xenopus Laevis*. *Soc. Neurosci. Abstr.* **27:** 241.

**Yamamoto, T., M. Fukuda, and R. Llinas. 2001.** Bilaterally synchronous complex spike Purkinje cell activity in the mammalian cerebellum. *Eur. J. Neurosci.* **13:** 327–339.

**Yamauchi, A., R. D. Rabbitt, R. Boyle, and S. M. Highstein.** Relationship between inner-ear fluid pressure and semicircular canal afferent nerve discharge. *JARO* **03:** 26–44.

**Young, I. S., and L. C. Rome. 2001.** Mutually exclusive muscle designs: the power output of the locomotory and sonic muscles of the oyster toadfish (*Opsanus tau*). *Proc. R. Soc. Lond. B Biol. Sci.* **268:** 1965–1970.

**Zago, C., A. E. Giblin, and A. Bergamasco. 2001.** Changes in metal content of surficial sediments of Boston Harbor since the cessation of sludge discharge. *Mar. Environ. Res.* **51:** 359–415.

**Zand, R. S.-y. Jin, J.-K. Kim, D. B. Wall, R. Gould, and D. M. Lubman. 2001.** Studies of posttranslational modifications in spiny dogfish myelin basic protein. *Neurochem. Res.* **26:** 539–547.

**Zottoli, S. J., D. E. W. Arnolds, N. O. Asamoah, C. Chevez, S. N. Fuller, N. A. Hiza, J. E. Nierman, and L. A. Taboada. 2001.** Dye coupling evidence for gap junctions between supramedullary/dorsal neurons of the cunner, *Tautogolabrus adspersus*. *Biol. Bull.* **201:** 277–278.

# MARINE RESOURCES CENTER

MARINE BIOLOGICAL LABORATORY • WOODS HOLE, MA 02543 • (508)289-7700
WWW.MBL.EDU/SERVICES/MRC/INDEX.HTML

zebrafish facilities

## Animal and Tissue Supply for Education & Research

- 150 aquatic species available for shipment via online catalog: <http://www.mbl.edu/animals/index.html>; phone: (508)289-7375; or e-mail: specimens@mbl.edu
- zebrafish colony containing limited mutant strains
- custom dissection and furnishing of specific organ and tissue samples

## MRC Services Available

- basic water quality analysis
- veterinary services (clinical, histopathologic, microbial services, health certificates, etc.)
- aquatic systems design (mechanical, biological, engineering, etc.)
- educational tours and collecting trips aboard the R/V Gemma

## Using the MRC for Your Research

- capability for advanced animal husbandry (temperature, light control, etc.)
- availability of year-round, developmental life stages
- adaptability of tank system design for live marine animal experimentation

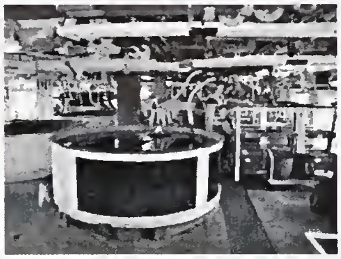

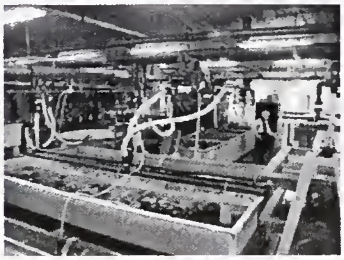

It's Worth A Closer Look.
ZEISS
40x/1.0 Oil Iris
44 07 56
0,5 1,0

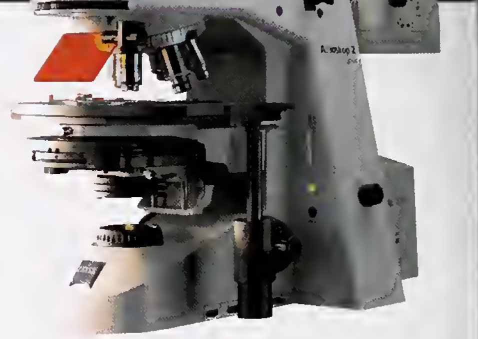

*New Axioskop 2 Plus.*
*The Ultimate Microscope For Life Science.*

**Brilliant and easy.**

Supporting all fluorescence techniques, producing brilliant images with outstanding documentation and digital image processing, the **Axioskop 2 Plus** and motorized **Axioskop 2 MOT** offer new levels of comfort and productivity in biomedical research.

**Ergonomics made to order.**

The Axioskop 2 Plus effortlessly adjusts to your individual viewing posture. Move the eyepiece tubes up or down, or change the angle for optimum comfort. With low-positioned focusing knobs, you can simply rest your elbows on the table for hours of fatigue free observation. An adjustable height stop gets you back to focus fast after a specimen change. Rotating stage with click-stops retrieves your initial stage position quickly.

**Fluorescence. Quick and quintuple.**

New reflector turret holds up to 5 different filter combinations for fast, easy and vibration free exchange. Pre-adjusted filter sets are mounted in cubes and can be quickly exchanged using new Push & Click mechanism. And with the smart condenser, switching between DIC, BF, DF, or Phase is easy. Illumination/condenser settings will adjust automatically. Streamlined beam path ensures high UV range transmission, maximum brightness, and homogeneous illumination.

*For more information call 800.233.2343 or email micro@zeiss.com.*

Carl Zeiss MicroImaging, Inc.
Thornwood, NY 10594
800.233.2343

Fax 914.681.7446
micro@zeiss.com
zeiss.com/micro

ZEISS

Volume 203

Number 2

# THE BIOLOGICAL BULLETIN

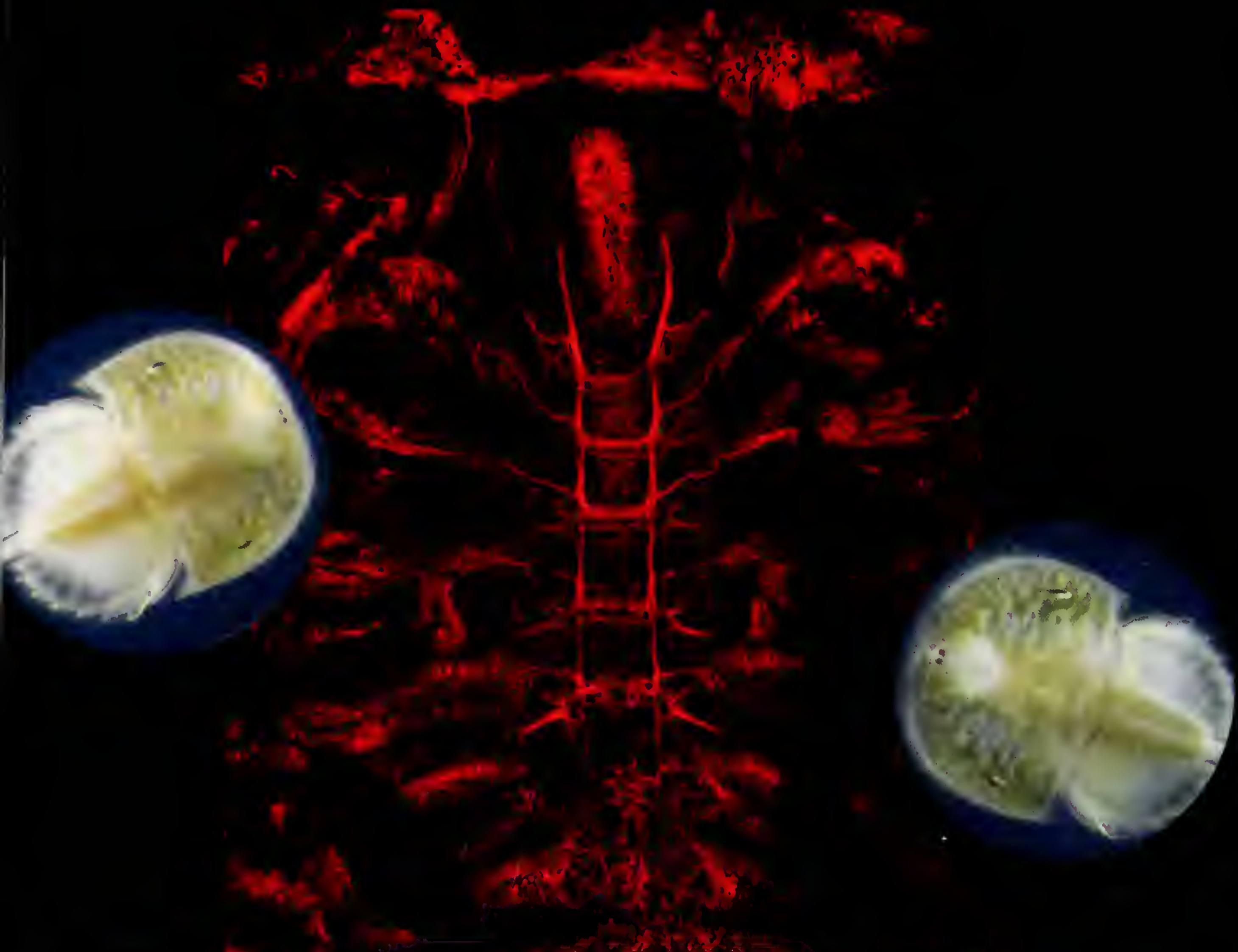

OCTOBER 2002

Published by the Marine Biological Laboratory

http://www.biolbull.org

# INVERTED MICROSCOPES

# DRAWN FROM EXPERIENCE

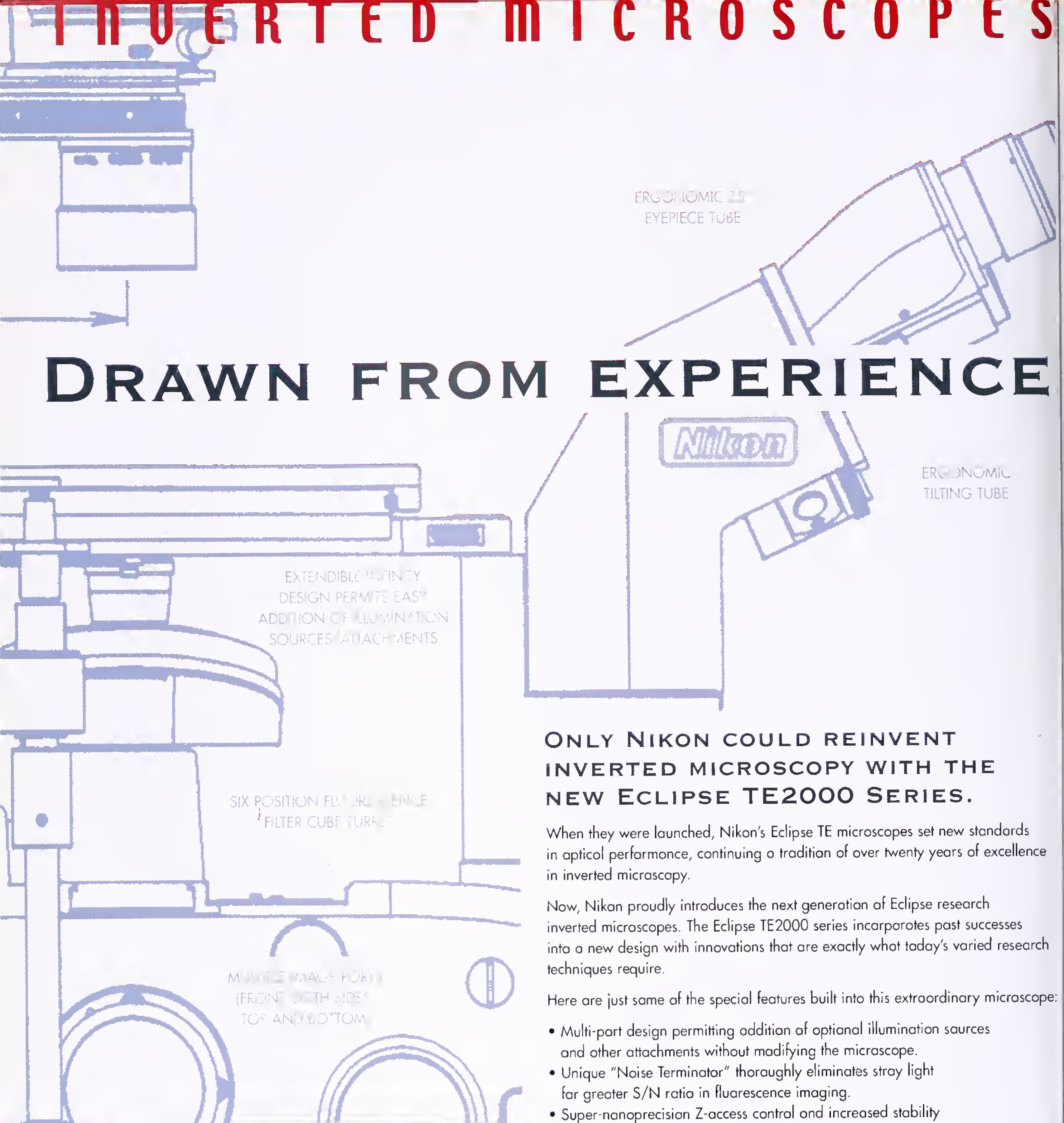
ERGONOMIC 25°
EYEPIECE TUBE
Nikon
ERGONOMIC
TILTING TUBE
EXTENDIBLE INFINITY
DESIGN PERMITS EASY
ADDITION OF ILLUMINATION
SOURCES/ATTACHMENTS
SIX POSITION FLUORESCENCE
FILTER CUBE TURRET
MULTIPLE IMAGE PORTS
(FRONT, BOTH SIDES,
TOP AND BOTTOM)

## ONLY NIKON COULD REINVENT INVERTED MICROSCOPY WITH THE NEW ECLIPSE TE2000 SERIES.

When they were launched, Nikon's Eclipse TE microscopes set new standards in optical performance, continuing a tradition of over twenty years of excellence in inverted microscopy.

Now, Nikon proudly introduces the next generation of Eclipse research inverted microscopes. The Eclipse TE2000 series incorporates past successes into a new design with innovations that are exactly what today's varied research techniques require.

Here are just some of the special features built into this extraordinary microscope:

- Multi-port design permitting addition of optional illumination sources and other attachments without modifying the microscope.
- Unique "Noise Terminator" thoroughly eliminates stray light for greater S/N ratio in fluorescence imaging.
- Super-nanoprecision Z-access control and increased stability for superior 3D imaging.
- Modular motorized components for automated control.
- Exclusive CFI60™ infinity optical system for excellent resolution with high numerical apertures and longer working distances.

The Eclipse TE2000 is available in three models, each configured to meet your research needs. Draw on Nikon's experience.
For more information, call 1-800-52-NIKON, ext. 392
or visit www.nikonusa.com
In Canada, call 1-866-99-NIKON.

Visit MicroscopyU at
www.nikonusa.com to learn more
about inverted microscopy.

CFI60
ECLIPSE

Nikon

©2002 Nikon Instruments Inc.

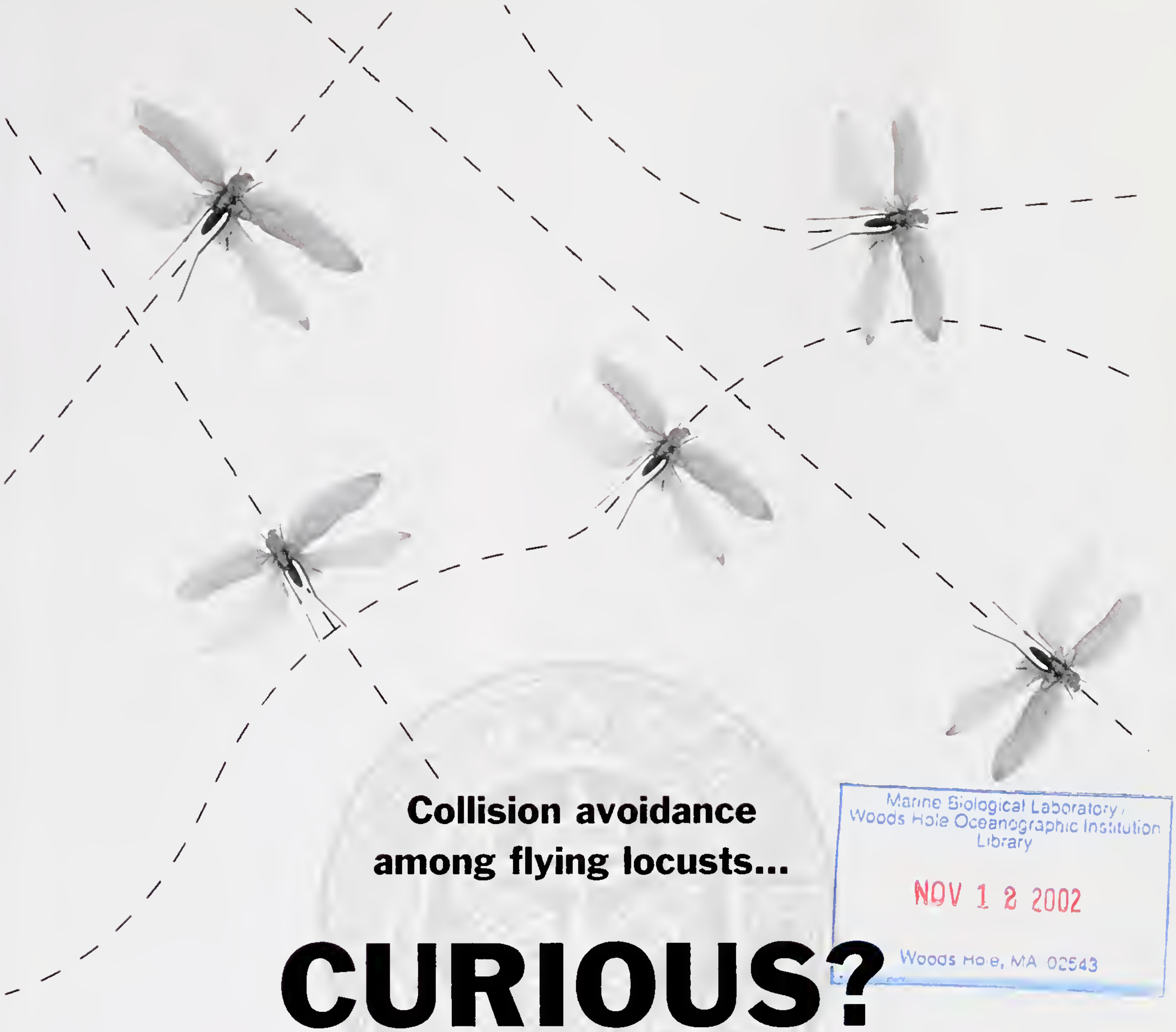

**Collision avoidance among flying locusts...**

**CURIOUS?**

- More than 12 million searchable journal articles
- World's largest collection of free full-text articles
- 4 different search tools to locate what you need
- Online archives of *The Biological Bulletin* plus more than 330 other journals covering the sciences and medicine

Find what you need at Stanford University's
www.highwire.org

HighWire LIBRARY OF THE SCIENCES AND MEDICINE

Marine Biological Laboratory /
Woods Hole Oceanographic Institution
Library
NOV 1 2 2002
Woods Hole, MA 02543

# THE BIOLOGICAL BULLETIN
# ONLINE

The Marine Biological Laboratory is pleased to announce that the full text of *The Biological Bulletin* is available online at

## http://www.biolbull.org

*The Biological Bulletin* publishes outstanding experimental research on the full range of biological topics and organisms, from the fields of Neurobiology, Behavior, Physiology, Ecology, Evolution, Development and Reproduction, Cell Biology, Biomechanics, Symbiosis, and Systematics.

Published since 1897 by the Marine Biological Laboratory (MBL) in Woods Hole, Massachusetts, *The Biological Bulletin* is one of America's oldest peer-reviewed scientific journals.

The journal is aimed at a general readership, and especially invites articles about those novel phenomena and contexts characteristic of intersecting fields.

*The Biological Bulletin Online* contains the full content of each issue of the journal, including all figures and tables, beginning with the February 2001 issue (Volume 200, Number 1). The full text is searchable by keyword, and the cited references include hyperlinks to Medline. PDF files are available beginning in February 1990 (Volume 178, Number 1), some abstracts are available beginning with the October 1976 issue (Volume 151, Number 2), and some Tables of Contents are online beginning with the October 1965 issue (Volume 129, Number 2).

Each issue will be placed online approximately on the date it is mailed to subscribers; therefore the online site will be available prior to receipt of your paper copy. Online readers may want to sign up for the eTOC (electronic Table of Contents) service, which will deliver each new issue's table of contents *via* e-mail. The web site also provides access to information about the journal (such as Instructions to Authors, the Editorial Board, and subscription information), as well as access to the Marine Biological Laboratory's web site and other *Biological Bulletin* electronic publications.

The free trial period for access to *The Biological Bulletin* online has ended. Individuals and institutions who are subscribers to the journal in print or are members of the Marine Biological Laboratory Corporation may now activate their online subscriptions. All other access (*e.g.*, to Abstracts, eTOCs, searching, Instructions to Authors) remains freely available. Online access is included in the print subscription price.

For more information about subscribing or activating your online subscription, visit <www.biolbull.org/subscriptions>.

---

## http://www.biolbull.org

OLYMPUS
XLUMPlanFl
20x/0.95 W
∞/0
The objective is not to touch the objective.

**The BX51WI.** A single 20x water immersion objective. A high N.A. of 0.95. A W.D. of 2.0mm. An intermediate magnification changer. Switch between low and high magnifications. Objective is untouched. Vibrations eliminated. Electrodes unmoved. It's a new movement in microscopy. **How Original. How Olympus.** Visit us at olympusamerica.com or call 1-800-446-5967.

OLYMPUS®
FOCUS ON LIFE

## *Cover*

The horseshoe crabs are among the oldest living chelicerates, and they show many ancestral characters during embryogenesis. Therefore, Beate Mittmann (Humboldt-Universität, Berlin) has been examining early neurogenesis in *Limulus polyphemus* and using the results to shed new light on our understanding of phylogenetic relationships among the arthropods.

In this issue of *The Biological Bulletin* (p. 186, p. 221), Mittmann—using immunocytochemical techniques—describes the formation of neurons and ganglia from the ventral neuroectoderm of *Limulus* embryos that have been developing for about 10 to 12 days since fertilization. The mode of gangliogenesis is similar to that reported for other chelicerates (especially spiders), but is distinct from that in crustaceans and insects.

The central image on the cover of this issue shows an embryo (about 1.5 mm long) that has been developing for an additional 5 to 8 days. The yolk mass has been excised from this embryo, and the parallel ventral nerve cords, joined ladder-like by connectives, are clearly visible. Nerve cords in this location and of this structure are a feature among many protostome invertebrates. The areas containing the limb buds, and their innervation by a thick bundle of nerve fibers, are also obvious in this image, as is the stomodeum, which is near the anterior end of the embryo. Embryos of this stage will be ready to hatch in about 10 days. Two such hatchlings (3-5 mm long) also appear on the cover; they are called trilobite larvae because of their similarity to the trilobites—an ancient group of arthropods, now extinct and known only from fossils.

The cover images were made by Beate Mittmann. The embryo was treated with a fluorescent antibody to $\alpha$-tubulin and examined with a Pascal confocal microscope (Zeiss), which produced a projection of a stack of 64 images. This picture was the winner, in Scientific Imaging, of the 2002 Marine Biological Laboratory Photography and Photomicrography Contest. The cover design is by Beth Liles, MBL.

# THE
# BIOLOGICAL BULLETIN
## OCTOBER 2002

| | | |
|---|---|---|
| **Editor** | Michael J. Greenberg | The Whitney Laboratory, University of Florida |
| **Associate Editors** | Louis E. Burnett | Grice Marine Laboratory, College of Charleston |
| | R. Andrew Cameron | California Institute of Technology |
| | Charles D. Derby | Georgia State University |
| | Michael LaBarbera | University of Chicago |
| **Section Editor** | Shinya Inoué, *Imaging and Microscopy* | Marine Biological Laboratory |
| **Online Editors** | James A. Blake, *Keys to Marine Invertebrates of the Woods Hole Region* | ENSR Marine & Coastal Center, Woods Hole |
| | William D. Cohen, *Marine Models Electronic Record and Compendia* | Hunter College, City University of New York |
| **Editorial Board** | Peter B. Armstrong | University of California, Davis |
| | Joan Cerdá | Center of Aquaculture-IRTA, Spain |
| | Ernest S. Chang | Bodega Marine Lab., University of California, Davis |
| | Thomas H. Dietz | Louisiana State University |
| | Richard B. Emlet | Oregon Institute of Marine Biology, Univ. of Oregon |
| | David Epel | Hopkins Marine Station, Stanford University |
| | Kenneth M. Halanych | Woods Hole Oceanographic Institution |
| | Gregory Hinkle | Millennium Pharmaceuticals, Cambridge, Massachusetts |
| | Nancy Knowlton | Scripps Inst. Oceanography & Smithsonian Tropical Res. Inst. |
| | Makoto Kobayashi | Hiroshima University of Economics, Japan |
| | Esther M. Leise | University of North Carolina Greensboro |
| | Donal T. Manahan | University of Southern California |
| | Margaret McFall-Ngai | Kewalo Marine Laboratory, University of Hawaii |
| | Mark W. Miller | Institute of Neurobiology, University of Puerto Rico |
| | Tatsuo Motokawa | Tokyo Institute of Technology, Japan |
| | Yoshitaka Nagahama | National Institute for Basic Biology, Japan |
| | Sherry D. Painter | Marine Biomed. Inst., Univ. of Texas Medical Branch |
| | J. Herbert Waite | University of California, Santa Barbara |
| | Richard K. Zimmer | University of California, Los Angeles |
| **Editorial Office** | Pamela Clapp Hinkle | Managing Editor |
| | Victoria R. Gibson | Staff Editor |
| | Carol Schachinger | Editorial Associate |
| | Wendy Child | Subscription & Advertising Administrator |

Published by
Marine Biological Laboratory
Woods Hole, Massachusetts

http://www.biolbull.org

**Microway transforms state-of-the-art processors into fully-integrated clusters for real-world applications, including gene sequencing, jet engine design and galaxy mapping . . .**

**Microway's magic is already working for hundreds of leading universities, Cessna, Exxon, GE, J&J, LANL, LION Bioscience, MBL, Millennium Pharmaceuticals, Myricom, NASA, NIH, NOAA, Raytheon, Seagate, the U.S. Air Force, Army and Navy, and thousands more.**

**The value is magical too. Microway's GigaClusters™ are not just fast. They run cool and perform reliably for years, resulting in low total lifetime cost.**

**MicrowayMagic℠**

**Scientists have been counting on it for 20 years.**

## The latest magic...

- GigaBlade™ technology—four Intel® Xeons™ per 1U chassis
- NodeWatch™ remote cluster monitoring and management
- Across the Board™ cooling in Microway 1U and 2U chassis
- CW Series, powered by Platform™ Clusterware™

# You could win a $50,000 research grant

It's been 20 years since scientists and engineers first started counting on Microway to put the magic into their HPC systems. To celebrate, we're offering an opportunity for you to make magic too: Now you can turn your purchase of a 16-node or larger Microway cluster into a $50,000 research grant for your choice of Microway products.* At least one in every 150 buyers who enter the contest will win!

## To enter:

1. Call Microway now. Talk to one of our technical sales people. Order or take delivery of your Microway cluster during our anniversary celebration (9/1/02–8/31/03).
2. Use it for three months. Then tell us about your application and how Microway made the difference. Your entry must be received within 6 months of receipt of your cluster or no later than 3/1/04, whichever is earlier.
3. One prize will be awarded for every 150 eligible entries (or portion thereof) received. Judges will select the best submissions based on criteria listed on our website. You must visit our website for complete eligibility requirements and rules.

* Winners may select any combination of the following Microway products and/or services valued at a total of up to $50,000: (a) a new cluster or additional nodes, (b) workstations, or (c) other Microway computer equipment and/or software. Open to U.S. residents, at least 21, including employees of universities, private labs, for-profit and not-for-profit organizations, except government employees and their immediate families or the Sponsor, its suppliers and agencies. Contest is void where prohibited.

**800 Gigaflops in 44U!**

Microway CoolRak™ cabinet with
48 1U Quadputer®–Xeons™
featuring GigaBlade™ technology

**Talk to us now. Let the magic begin.**
**on the web: www.microway.com**
**or by phone: 508.746.7341**

Microway®

# CONTENTS

Volume 203, No. 2: October 2002

## DEVELOPMENT AND REPRODUCTION

**Vickery, Minako, Michael C.L. Vickery, and James B. McClintock**
Morphogenesis and organogenesis in the regenerating planktotrophic larvae of asteroids and echinoids . . . . . . . . . . 121

**Eckelbarger, Kevin J., and Craig M. Young**
Spermiogenesis and modified sperm morphology in the "seepworm" *Methanoaricia dendrobranchiata* (Polychaeta: Orbiniidae) from a methane seep environment in the Gulf of Mexico: implications for fertilization biology . . . . . . . . . . 134

## NEUROBIOLOGY AND BEHAVIOR

**Lawrence, K.A., and W.H. Watson III**
Swimming behavior of the nudibranch *Melibe leonina* . . . . . . . . . . 144

**Watson, Winsor H. III, James M. Newcomb, and Stuart Thompson**
Neural correlates of swimming behavior in *Melibe leonina* . . . . . . . . . . 152

## ECOLOGY AND EVOLUTION

**Barnes, David K.A.**
Clade perseverance from Mesozoic to present: a multidisciplinary approach to interpretation of pattern and process . . . . . . . . . . 161

**Lohse, David P.**
Relative strengths of competition for space and food in a sessile filter feeder . . . . . . . . . . 173

## SHORT REPORTS FROM THE 2002 GENERAL SCIENTIFIC MEETINGS OF THE MARINE BIOLOGICAL LABORATORY

**The Editor**
Introduction to the featured reports: The MBL awards for 2002 . . . . . . . . . . 185

### *Neurobiology*

**Arnolds, D. E. W., S. J. Zottoli, C. E. Adams, S. M. Dineen, S. Fevrier, Y. Guo, and A. J. Pascal**
Physiological effects of tricaine on the supramedullary/dorsal neurons of the cunner, *Tautogolabrus adspersus* . . . . . . . . . . 188

**Giuditta, Antonio, Maria Eyman, and Barry B. Kaplan**
Gene expression in the squid giant axon: neurotransmitter modulation of RNA transfer from periaxonal glia to the axon . . . . . . . . . . 189

**Landowne, David**
Perchlorate prevents sodium channel gating and sodium protects in the squid giant axon . . . . . . . . . . 190

**Ripps, Harris, Haohua Qian, and Jane Zakevicius**
Blockade of an inward sodium current facilitates pharmacological study of hemi-gap-junctional currents in *Xenopus* oocytes . . . . . . . . . . 192

**Garber, Sarah S., and Mary M. Hoffman**
Cl⁻ and glutamate⁻ competition for a volume-regulated anion channel . . . . . . . . . . 194

**Fay, Richard R., and Peggy L. Edds-Walton**
Preliminary evidence for interpulse interval selectivity of cells in the torus semicircularis of the oyster toadfish *(Opsanus tau)* . . . . . . . . . . 195

**Borley, Kimberly A., Herman T. Epstein, and Alan M. Kuzirian**
Effects of a sensory block on calexcitin levels in the photoreceptors of *Hermissenda crassicornis* . . . . . . . . . . 197

**Twig, Gilad, Robert Paul Malchow, Katherine Hammar, Peter J. S. Smith, Hanna Levy, and Ido Perlman**
A novel turtle retinal preparation for simultaneously measuring light-induced electrical activity and changes in metabolite levels . . . . . . . . . . 198

**Redenti, Stephen, and Richard L. Chappell**
Zinc chelation enhances the zebrafish retinal ERG b-wave . . . . . . . . . . 200

### *Cell Biology*

**Armstrong, Peter B., Margaret T. Armstrong, R. L. Pardy, Alice Child, and Norman Wainwright**
Immunohistochemical demonstration of a lipopolysaccharide in the cell wall of a eukaryote, the green alga *Chlorella* . . . . . . . . . . 203

**Lee, K.-G., A. Braun, I. Chaikhoutdinov, J. DeNobile, M. Conrad, and W. Cohen**
Rapid visualization of microtubules in blood cells and other cell types in marine model organisms . . . 204

**Wöllert, Torsten, Ana S. DePina, Reid F. Thompson, and George M. Langford**
$Ca^{2+}$ effects on myosin-II-mediated contraction of pseudo-contractile rings and transport of vesicles in extracts of clam oocytes. . . . . . . . . . . . . . . . . . . . . . 206

**Wöllert, Torsten, Ana S. DePina, Reid F. Thompson, and George M. Langford**
GTPase Rho is involved in myosin-II-mediated contraction of pseudo-contractile rings and transport of vesicles in extracts of clam oocytes . . . . . . . . . . . . . . 208

**Brown, Jeremiah R., Elizabeth M. Peacock-Villada, and George M. Langford**
Globular tail fragment of myosin-V displaces vesicle-associated motor and blocks vesicle transport in squid nerve cell extracts . . . . . . . . . . . . . . . . . . . . . 210

**Weidner, Earl, and Ann Findley**
Peroxisomal catalase in extrusion apparatus posterior vacuole of microsporidian spores. . . . . . . . . . . . 212

**Silver, Robert B., and Marc Bartman**
A metronome-like control of the calcium signal leading to nuclear envelope breakdown and mitosis in sand dollar *(Echinaracnius parma)* cells . . . . . . . . . . . 213

### Developmental Biology

**Crawford, Karen**
Culture method for *in vitro* fertilization to hatching of the squid, *Loligo pealeii* . . . . . . . . . . . . . . . . . . . . . 216

**Pahl, Nicholas, Sara Homsi, Hilary G. Morrison, and Robert M. Gould**
mRNAs located in *Squalus acanthias* (spiny dogfish) oligodendrocyte processes. . . . . . . . . . . . . . . . . . . . . 217

**Eddleman, Christopher S., George D. Bittner, and Harvey M. Fishman**
SEM comparison of severed ends of giant axons isolated from squid *(Loligo pealeii)* and crayfish *(Procambarus clarkii)*. . . . . . . . . . . . . . . . . . . . . . . . . . . . . . . 219

### Studia Limulorum

**Mittmann, Beate**
Early neurogenesis in the horseshoe crab *Limulus polyphemus* and its implication for arthropod relationships. . . . . . . . . . . . . . . . . . . . . . . . . . . . . . . . . . . . . 221

**Smith, K., C. Ridings, F. A. Dodge, and R. B. Barlow**
Development of the lateral eye of juvenile *Limulus*. . . 222

**Ridings, C., D. Borst, K. Smith, F. Dodge, and R. Barlow**
Visual behavior of juvenile *Limulus* in their natural habitat and in captivity . . . . . . . . . . . . . . . . . . . . . . . . 224

**Suggs, Dianne N., Ruth H. Carmichael, Sara P. Grady, and Ivan Valiela**
Effects of individual size on pairing in horseshoe crabs . . . . . . . . . . . . . . . . . . . . . . . . . . . . . . . . . . . . . . 225

**Borst, Douglas, and Robert Barlow**
Circadian rhythms in locomotor activity of juvenile horseshoe crabs. . . . . . . . . . . . . . . . . . . . . . . . . . . 227

**Gaines, Emily F., Ruth H. Carmichael, Sara P. Grady, and Ivan Valiela**
Stable isotopic evidence for changing nutritional sources of juvenile horseshoe crabs . . . . . . . . . . . . 228

### Comparative Physiology

**Smotherman, Michael**
Acetylcholine mediates excitatory input to chromatophore motoneurons in the squid, *Loligo pealeii*. . . . . 231

**Grable, Melissa M., Nadav Shashar, Nicole L. Gilles, Chuan-Chin Chiao, and Roger T. Hanlon**
Cuttlefish body patterns as a behavioral assay to determine polarization perception . . . . . . . . . . . . . . . . 232

**Rohrkasse, Sarah M., and Jelle Atema**
Tracking behavior of Busyconinae whelks . . . . . . . . 235

**Graf, Werner, Edwin Gilland, Matt McFarlane, Laura Knott, and Robert Baker**
Central pathways mediating oculomotor reflexes in an elasmobranch, *Scyliorhinus canicula*. . . . . . . . . . . . 236

**Montgomery, John, Guy Carton, and David Bodznick**
Error-driven motor learning in fish . . . . . . . . . . . . . 238

**Delaney, Martha, Christopher Follet, Nick Ryan, Nick Hanney, Jenny Lusk-Yablick, and Gabriele Gerlach**
Social interaction and distribution of female zebrafish *(Danio rerio)* in a large aquarium. . . . . . . . . . 240

**Cermak, Michael J.**
*Caranx latus* (Carangidae) chooses dock pilings to attack silverside schools: A tactic to interfere with stereotyped escape behavior of prey? . . . . . . . . . . . . 241

### Ecology and Population Biology

**La Du, Jane, Deana Erdner, Sonya Dyhrman, and Don Anderson**
Molecular approaches to understanding population dynamics of the toxic dinoflagellate *Alexandrium fundyense* . . . . . . . . . . . . . . . . . . . . . . . . . . . . . . . . . 244

**Philibotte, Jason**
Pelagic larval duration of the Caribbean wrasse, *Thalassoma bifasciatum* . . . . . . . . . . . . . . . . . . . . . . . . 245

**Hunter-Thomson, Kristin, Jeffrey Hughes, and Bradley Williams**
Estuarine–open-water comparison of fish community structure in eelgrass (*Zostera marina* L.) habitats of Cape Cod. . . . . . . . . . . . . . . . . . . . . . . . . . . . . . . . . . . 247

**Williams, Bradley S., Jeffrey E. Hughes, and Kristin Hunter-Thomson**
Influence of epiphytic algal coverage on fish predation rates in simulated eelgrass habitats . . . . . . . . . . 248

**Ludlam, John P., David H. Shull, and Robert Buchsbaum**
Effects of haying on salt-marsh surface invertebrates . . . . . . . . . . 250

**Levine, Uri Y., and Byron C. Crump**
Bacterioplankton community composition in flowing waters of the Ipswich River watershed . . . . . . . . . . 251

**Huffaker, Diana, and R. Gil Pontius, Jr.**
Reconstruction of historical land cover in the Ipswich watershed . . . . . . . . . . 253

*Estuarine and Freshwater Biogeochemistry*

**Testa, Jeremy M., Matthew A. Charette, Edward R. Sholkovitz, Matt C. Allen, Adam Rago, and Craig W. Herbold**
Dissolved iron cycling in the subterranean estuary of a coastal bay: Waquoit Bay, Massachusetts . . . . . . . . 255

**Twichell, Sarah, Sallie Sheldon, Linda Deegan, and Robert Garritt**
Nutrient and freshwater inputs from sewage effluent discharge alter benthic algal and infaunal communities in a tidal salt marsh creek . . . . . . . . . . 256

**Koop-Jakobsen, Ketil, and Anne Giblin**
Tidal flushing of ammonium from intertidal salt marsh sediments: the relative importance of adsorbed ammonium . . . . . . . . . . 258

**Barron, Stacy, Carolyn Weber, Roxanne Marino, Eric Davidson, Gabrielle Tomasky, and Robert Howarth**
Effects of varying salinity on phytoplankton growth in a low-salinity coastal pond under two nutrient conditions . . . . . . . . . . 260

**Weber, Carolyn F., Stacy Barron, Roxanne Marino, Robert W. Howarth, Gabrielle Tomasky, and Eric A. Davidson**
Nutrient limitation of phytoplankton growth in Vineyard Sound and Oyster Pond, Falmouth, Massachusetts . . . . . . . . . . 261

**Millman, Melissa, Mirta Teichberg, Paulina Martinetto, and Ivan Valiela**
Response of shrimp populations to land-derived nitrogen in Waquoit Bay, Massachusetts . . . . . . . . . . 263

*Laboratory Animal Health*

**Smolowitz, Roxanna, Janice Hanley, and Hazel Richmond**
A three-year retrospective study of abdominal tumors in zebrafish maintained in an aquatic laboratory animal facility . . . . . . . . . . 265

**Hsieh, Jennifer L., Hemant M. Chikarmane, Roxanna Smolowitz, Kevin R. Uhlinger, W. Mebane, and Alan M. Kuzirian**
Microbial analysis of ozone disinfection in a recirculating seawater system . . . . . . . . . . 266

*Oral Presentations*

Published by title only . . . . . . . . . . 268

**Notice to Subscribers**

2003 Subscription Rates for *The Biological Bulletin*
Prices include print and electronic versions

| | Libraries | Individuals |
|---|---|---|
| Per year (six issues, two volumes): | $280.00 | $105.00 |
| Per volume (three issues): | $140.00 | $52.50 |
| Back and single issues (subject to availability): | $50.00 | $20.00 |

For additional information, please contact our subscription administrator at the Maine Biological Laboratory, 7 MBL Street, Woods Hole, MA 02543; tel: (508) 289-7402; e-mail: wchild@mbl.edu. Visit our new website at www.biolbull.org

THE BIOLOGICAL BULLETIN

THE BIOLOGICAL BULLETIN is published six times a year by the Marine Biological Laboratory, 7 MBL Street, Woods Hole, Massachusetts 02543

Subscriptions and similar matter should be addressed to Subscription Administrator, THE BIOLOGICAL BULLETIN, Marine Biological Laboratory, 7 MBL Street, Woods Hole, Massachusetts 02543. Subscription includes both print and online journals. Subscription per year (six issues, two volumes): $260 for libraries; $105 for individuals. Subscription per volume (three issues): $130 for libraries; $52.50 for individuals. Back and single issues (subject to availability): $45 for libraries; $20 for individuals.

Communications relative to manuscripts should be sent to Michael J. Greenberg, Editor-in-Chief, or Pamela Clapp Hinkle, Managing Editor, at the Marine Biological Laboratory, 7 MBL Street, Woods Hole, Massachusetts 02543. Telephone: (508) 289-7428. FAX: 508-289-7922. E-mail: pclapp@mbl.edu.

http://www.biolbull.org

THE BIOLOGICAL BULLETIN is indexed in bibliographic services including *Index Medicus* and MEDLINE, *Chemical Abstracts, Current Contents, Elsevier BIOBASE/Current Awareness in Biological Sciences,* and *Geo Abstracts.*

Printed on acid free paper,
effective with Volume 180, Issue 1, 1991.

POSTMASTER: Send address changes to THE BIOLOGICAL BULLETIN, Marine Biological Laboratory,
7 MBL Street, Woods Hole, MA 02543.

Copyright © 2002, by the Marine Biological Laboratory

Periodicals postage paid at Woods Hole, MA, and additional mailing offices.
ISSN 0006-3185

# INSTRUCTIONS TO AUTHORS

*The Biological Bulletin* accepts outstanding original research reports of general interest to biologists throughout the world. Papers are usually of intermediate length (10–40 manuscript pages). A limited number of solicited review papers may be accepted after formal review. A paper will usually appear within four months after its acceptance.

Very short, especially topical papers (less than 9 manuscript pages including tables, figures, and bibliography) will be published in a separate section entitled "Research Notes." A Research Note in *The Biological Bulletin* follows the format of similar notes in *Nature.* It should open with a summary paragraph of 150 to 200 words comprising the introduction and the conclusions. The rest of the text should continue on without subheadings, and there should be no more than 30 references. References should be referred to in the text by number, and listed in the Literature Cited section in the order that they appear in the text. Unlike references in *Nature,* references in the Research Notes section should conform in punctuation and arrangement to the style of recent issues of *The Biological Bulletin.* Materials and Methods should be incorporated into appropriate figure legends. See the article by Lohmann *et al.* (October 1990, Vol. **179:** 214–218) for sample style. A Research Note will usually appear within two months after its acceptance.

The Editorial Board requests that regular manuscripts conform to the requirements set below; those manuscripts that do not conform will be returned to authors for correction before review.

1. ***Manuscripts.*** Manuscripts, including figures, should be submitted in quadruplicate, with the originals clearly marked. (Xerox copies of photographs are not acceptable for review purposes.) If possible, please include an electronic copy of the text of the manuscript. Label the disk with the name of the first author and the name and version of the wordprocessing software used to create the file. If the file was not created in some version of Microsoft Word, save the text in rich text format (rtf). The submission letter accompanying the manuscript should include a telephone number, a FAX number, and (if possible) an E-mail address for the corresponding author. The original manuscript must be typed in no smaller than 12 pitch or 10 point, using double spacing (*including* figure legends, footnotes, bibliography, etc.) on one side of 16- or 20-lb. bond paper, 8 by 11 inches. Please, no right justification. Manuscripts should be proofread carefully and errors corrected legibly in black ink. Pages should be numbered consecutively. Margins on all sides should be at least 1 inch (2.5 cm). Manuscripts should conform to the *Council of Biology Editors Style Manual,* 5th Edition (Council of Biology Editors, 1983) and to American spelling. Unusual abbreviations should be kept to a minimum and should be spelled out on first reference as well as defined in a footnote on the title page. Manuscripts should be divided into the following components: Title page, Abstract (of no more than 200 words), Introduction, Materials and Methods, Results, Discussion, Acknowledgments, Literature Cited, Tables, and Figure Legends. In addition, authors should supply a list of words and phrases under which the article should be indexed.

2. ***Title page.*** The title page consists of a condensed title or running head of no more than 35 letters and spaces, the manuscript title, authors' names and appropriate addresses, and footnotes listing present addresses, acknowledgments or contribution numbers, and explanation of unusual abbreviations.

3. ***Figures.*** The dimensions of the printed page, 7 by 9 inches, should be kept in mind in preparing figures for publication. We recommend that figures be about 1 times the linear dimensions of the final printing desired, and that the ratio of the largest to the smallest letter or number and of the thickest to the thinnest line not exceed 1:1.5. Explanatory matter generally should be included in legends, although axes should always be identified on the illustration itself. Figures should be prepared for reproduction as either line cuts or halftones. Figures to be reproduced as line cuts should be unmounted glossy photographic reproductions or drawn in black ink on white paper, good-quality tracing cloth or plastic, or blue-lined coordinate paper. Those to be reproduced as halftones should be mounted on board, with both designating numbers or letters and scale bars affixed directly to the figures. All figures should be numbered in consecutive order, with no distinction between text and plate figures and cited, in order, in the text. The author's name and an arrow indicating orientation should appear on the reverse side of all figures.

*Digital art: The Biological Bulletin* will accept figures submitted in electronic form; however, digital art must conform to the following guidelines. Authors who create digital images are wholly responsible for the quality of their material, including color and halftone accuracy.

*Format.* Acceptable graphic formats are TIFF and EPS. Color submissions must be in EPS format, saved in CMKY mode.

*Software.* Preferred software is Adobe Illustrator or Adobe Photoshop for the Mac and Adobe Photoshop for Windows. Specific instructions for artwork created with various software programs are available on the Web at the Digital Art Information Site maintained by Cadmus Professional Communications at http://cpc.cadmus.com/da/

*Resolution.* The minimum requirements for resolution are 1200 DPI for line art and 300 for halftones.

*Size.* All digital artwork must be submitted at its actual printed size so that no scaling is necessary.

*Multipanel figures.* Figures consisting of individual parts (*e.g.*, panels A, B, C) must be assembled into final format and submitted as one file.

*Hard copy.* Files must be accompanied by hard copy for use in case the electronic version is unusable.

*Disk identification.* Disks must be clearly labeled with the following information: author name and manuscript number; format (PC or Macintosh); name and version of software used.

*Color: The Biological Bulletin* will publish color figures and plates, but must bill authors for the actual additional cost of printing in color. The process is expensive, so authors with more than one color image should—consistent with editorial concerns, especially citation of figures in order—combine them into a single plate to reduce the expense. On request, when supplied with a copy of a color illustration, the editorial staff will provide a pre-publication estimate of the printing cost.

4. ***Tables, footnotes, figure legends, etc.*** Authors should follow the style in a recent issue of *The Biological Bulletin* in preparing table headings, figure legends, and the like. Because of the high cost of setting tabular material in type, authors are asked to limit such material as much as possible. Tables, with their headings and footnotes, should be typed on separate sheets, numbered with consecutive Roman numerals, and placed after the Literature Cited. Figure legends should contain enough information to make the figure intelligible separate from the text. Legends should be typed double spaced, with consecutive Arabic numbers, on a separate sheet at the end of the paper. Footnotes should be limited to authors' current addresses, acknowledgments or contribution numbers, and explanation of unusual abbreviations. All such footnotes should appear on the title page. Footnotes are not normally permitted in the body of the text.

5. ***Literature cited.*** In the text, literature should be cited by the Harvard system, with papers by more than two authors cited as Jones *et al.*, 1980. Personal communications and material in preparation or in press should be cited in the text only, with author's initials and institutions, unless the material has been formally accepted and a volume number can be supplied. The list of references following the text should be headed Literature Cited, and must be typed double spaced on separate pages, conforming in punctuation and arrangement to the style of recent issues of *The Biological Bulletin*. Citations should include complete titles and inclusive pagination. Journal abbreviations should normally follow those of the U. S. A. Standards Institute (USASI), as adopted by BIOLOGICAL ABSTRACTS and CHEMICAL ABSTRACTS, with the minor differences set out below. The most generally useful list of biological journal titles is that published each year by BIOLOGICAL ABSTRACTS (BIOSIS List of Serials; the most recent issue). Foreign authors, and others who are accustomed to using THE WORLD LIST OF SCIENTIFIC PERIODICALS, may find a booklet published by the Biological Council of the U.K. (obtainable from the Institute of Biology, 41 Queen's Gate, London, S.W.7, England, U.K.) useful, since it sets out the WORLD LIST abbreviations for most biological journals with notes of the USASI abbreviations where these differ. CHEMICAL ABSTRACTS publishes quarterly supplements of additional abbreviations. The following points of reference style for THE BIOLOGICAL BULLETIN differ from USASI (or modified WORLD LIST) usage:

A. Journal abbreviations, and book titles, all underlined (for *italics*)

B. All components of abbreviations with initial capitals (not as European usage in WORLD LIST *e.g., J. Cell. Comp. Physiol.* NOT *J. cell. comp. Physiol.*)

C. *All* abbreviated components must be followed by a period, whole word components *must not* (*i.e., J. Cancer Res.*)

D. Space between all components (*e.g., J. Cell. Comp. Physiol.*, not *J.Cell.Comp.Physiol.*)

E. Unusual words in journal titles should be spelled out in full, rather than employing new abbreviations invented by the author. For example, use *Rit Vísindafjélags Islendinga* without abbreviation.

F. All single word journal titles in full (*e.g., Veliger, Ecology, Brain*).

G. The order of abbreviated components should be the same as the word order of the complete title (*i.e., Proc.* and *Trans.* placed where they appear, not transposed as in some BIOLOGICAL ABSTRACTS listings).

H. A few well-known international journals in their preferred forms rather than WORLD LIST or USASI usage (*e.g., Nature, Science, Evolution* NOT *Nature, Lond., Science, N.Y.; Evolution, Lancaster, Pa.*)

6. ***Reprints, page proofs, and charges.*** Authors may purchase reprints in lots of 100. Forms for placing reprint orders are sent with page proofs. Reprints normally will be delivered about 2 to 3 months after the issue date. Authors (or delegates for foreign authors) will receive page proofs of articles shortly before publication. They will be charged the current cost of printers' time for corrections to these (other than corrections of printers' or editors' errors). Other than these charges for authors' alterations, *The Biological Bulletin* does not have page charges.

Reference: *Biol. Bull.* **203:** 121–133. (October 2002)

# Morphogenesis and Organogenesis in the Regenerating Planktotrophic Larvae of Asteroids and Echinoids

MINAKO S. VICKERY*, MICHAEL C. L. VICKERY, AND JAMES B. McCLINTOCK

*Department of Biology, University of Alabama at Birmingham, 1300 University Boulevard,
Birmingham, Alabama 35294-1170*

**Abstract.** In a previous study, we described complete body regeneration (with organogenesis) following surgical bisection in the planktotrophic larvae of the asteroids *Luidia foliolata* and *Pisaster ochraceus*. Here we present further detailed observations of these unique regenerative processes not presented in the previous paper. Furthermore, we describe for the first time complete regeneration following surgical bisection of planktotrophic larvae of the regular echinoid *Lytechinus variegatus* and the irregular echinoid *Dendraster excentricus*. Larvae of both asteroids and echinoids displayed a capacity for rapid regeneration regardless of their developmental stage. Within 48 h after bisection, aggregations of mesenchyme cells with pseudopodia were observed at the site of surgical bisection. These cellular aggregations were similar in appearance to the mesenchymal blastemas that form in adult echinoderms prior to their arm regeneration, and to those described in other deuterostomes that undergo regeneration. When asteroid larvae were surgically bisected in the early stages of their development, clusters of mesenchyme cells developed into completely new pairs of coelomic pouches located anterior to the newly regenerated digestive tract. This indicates that cell fate in regenerating asteroid larvae remains indeterminate during early development. In the larvae of *P. ochraceus*, regardless of the developmental stage at the time of bisection, both the anterior and posterior portions regenerated all their missing organs and tissues. However, the larvae of *L. foliolata* displayed differential regenerative capacity in bisected larval halves at the late bipinnaria stage. The differences observed may be due to differences in larval development (*L. foliolata* has no brachiolaria stage), and may have evolutionary implications. In the regular echinoid *L. variegatus*, both larval portions regenerated into morphologically and functionally normal larvae that were indistinguishable from non-bisected control larvae. The regenerative processes were similar to those we observed in planktotrophic asteroid larvae. Regenerating larvae readily metamorphosed into normal juveniles. In the irregular echinoid *D. excentricus*, posterior portions of larvae completed regeneration and metamorphosis, but anterior portions regenerated only partially during the 2-week study. Our observations confirm that asteroid and echinoid larvae provide excellent models for studies of regeneration in deuterostomes.

## Introduction

Regeneration has been described at both the cellular and the tissue level in many animals including planarians, crustaceans, reptiles, and amphibians (Goss, 1969; Mattson, 1976; Baguñà *et al.*, 1989; Martin, 1997; Hopkins, 2001). Many adult echinoderms, including asteroids, ophiuroids, and holothuroids, are known to possess considerable regenerative capacities as well as the ability to reproduce by clonal division (Emson and Wilkie, 1980; Mladenov and Burke, 1994). The occurrence of cloning in planktotrophic larvae of asteroids and ophiuroids has also been reported (Bosch, 1988; Bosch *et al.*, 1989; Rao *et al.*, 1993; Jaeckle, 1994; Balser, 1998). However, complete regeneration in echinoderm larvae after surgical bisection has only recently been documented. Bipinnaria and brachiolaria larvae of the asteroids *Luidia foliolata* and *Pisaster ochraceus* were surgically bisected into anterior and posterior portions, and the regeneration process was followed for 2 weeks (Vickery and McClintock, 1998). Both portions of the larvae in both species completely regenerated all missing organs and tissues.

The discovery of regeneration in planktotrophic asteroid

---

Received 4 March 2002; accepted 16 July 2002.

* To whom correspondence should be addressed. E-mail: vickerym@uab.edu

larvae provided a previously unknown model system for the molecular study of regeneration in deuterostomes (Vickery, 2001; Vickery *et al.*, 2001a, b). This model offers several advantages. For example, echinoderms share many developmental traits with other deuterostomes, including vertebrates (Halanych and Passamaneck, 2001; Nielsen, 2001). Also, asteroid larvae possess simple body structures compared to adults, and their transparent bodies make it possible to observe the regeneration process not only externally, but also internally.

In the present study we used larvae of the asteroids *L. foliolata* and *P. ochraceus* to gain detailed information about the regeneration process at the cellular and organ levels. We examined the regenerative capacity and organogenesis of larvae of both asteroid species throughout all developmental stages. This study provides the first assessment of the ability of discrete stages of larvae to regenerate. We also report on the regenerative capacity of surgically removed portions of the larval body in *Pisaster ochraceus.*

Although early studies examined the ability of echinoid larvae to regenerate specific missing tissues (reviewed in Hörstadius, 1973, and Vickery *et al.*, 2001b), few studies similar to those we have outlined above for planktotrophic asteroid larvae have examined regenerative characteristics in planktotrophic echinoid larvae (Mortensen, 1921, 1938; Czihak, 1965). Given our immense knowledge of aspects of echinoid molecular genetics and cellular development, echinoid larvae could become a model system for studies of deuterostome regeneration. In the present study we examine the regenerative capacity of both the planktotrophic pluteus larvae of the regular echinoid *Lytechinus variegatus* and the irregular echinoid *Dendraster excentricus.*

## Materials and Methods

### *Asteroids*

*Larval cultures.* Sexually mature individuals of *Luidia foliolata* and *Pisaster ochraceus* were collected near San Juan Island, Washington, in the late spring to early summer of 1998. Artificial fertilizations were conducted by intracoelomic injection of 1-methyladenine (Kanatani, 1969), and ambient seawater temperature (12–15 °C) was maintained during the experiments. After the embryos established functional digestive systems, larvae were fed a quantitatively equal mixture of the single-celled algae *Chaetocerous calcitrans, Dunaliella tertiolecta,* and *Isocrysis galbana.* Standard protocols for larval culturing were followed (Strathmann, 1987).

First we investigated larval regenerative capacities in three representative stages of larval development, chosen on the basis of larval anatomy. Early-stage larvae were defined, for both species, as embryos (Fig. 1A) that had developed into early bipinnaria larvae with a functional digestive system and a pair of non-connected coelomic pouches (Fig. 1B). Mid-stage larvae were defined as fully grown bipinnaria larvae in *L. foliolata* (Fig. 1C), and as either fully developed bipinnaria (Fig. 1D) or brachiolaria (Fig. 1E) larvae in *P. ochraceus.* All mid-stage larvae possessed long larval arms, and *P. ochraceus* brachiolaria larvae had a brachiolar apparatus in the anterior region. Internally, the left and right coelomic pouches were connected at the anterior ends of the larvae; in brachiolaria larvae, the brachiolar apparatus possessed an underlying coelom. Late-stage larvae were defined as either bipinnaria or brachiolaria larvae with an adult rudiment on the posterior portion. The coelom had developed hydrocoelic lobes that would eventually form the water vascular system in the juvenile (Fig. 1F). Moreover, spicules were present that would eventually form the juvenile skeletal system.

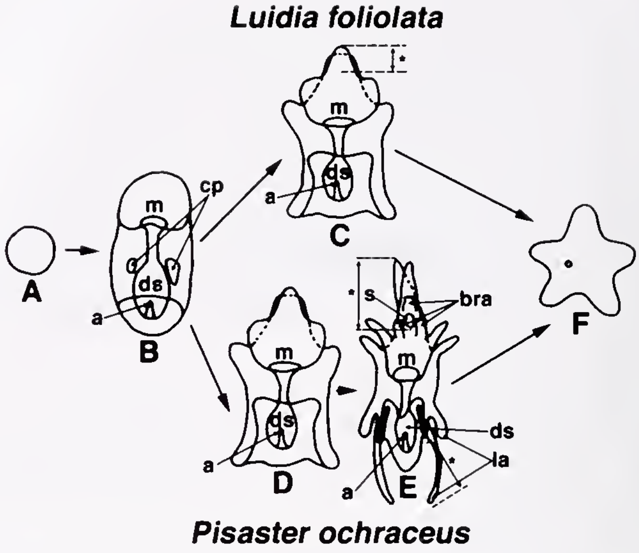

**Figure 1.** Diagram of two types of planktotrophic larval asteroid development. The embryo (A) develops into a planktotrophic bipinnaria larva (B). Bipinnaria larvae of *Luidia foliolata* develop into a late bipinnaria (C), and complete metamorphosis to become juvenile asteroids (F) while swimming in the water column. Bipinnaria larvae of *Pisaster ochraceus* (D) develop into brachiolaria (E), after which they complete metamorphosis to the juvenile stage (F). Arrows with * in (C) and (E) show area of larva removed to examine regeneration of partial body parts. a, anus; bra, brachiolar apparatus; cp, coelomic pouches; ds, digestive system; la, larval arms; m, mouth; s, sucker.

*Surgical bisection.* At each discrete larval stage, subsamples of larvae ($n = 20$) of both species were first measured, then surgically bisected with a scalpel across the horizontal larval axis, at a point equidistant between the anterior and posterior poles (Vickery and McClintock, 1998). Bisected anterior and posterior portions and non-bisected control larvae ($n = 20$) for each stage were maintained separately for 2 weeks in fingerbowls placed in a water table with a circulating seawater system. The seawater in each fingerbowl was changed every 3 days (Strathmann, 1987). Using dissecting and compound light microscopy, we examined and measured the specimens daily. Growth was determined by their increase in length. A Nikon Optiphoto-2 compound microscope was used to photograph larvae. All measurements were analyzed statistically, and a value of $P < 0.05$ was employed to assess statistical significance.

To further assess larval regenerative capacity, we examined *P. ochraceus* because this species possesses both bipinnaria and brachiolaria larval stages. The anterior tip containing the axocoel was removed from both mid-stage bipinnaria ($n = 20$) and brachiolaria ($n = 20$) larvae (including the brachiolar apparatus) (Fig. 1C, D). Moreover, sets of posterior larval arms were removed from brachiolaria larvae ($n = 20$) (Fig. 1C, D). The dissected fragments and the larvae from which they were removed were maintained separately and observed for 2 weeks as described above.

### *Echinoids*

*Larval cultures.* Adult specimens of *Lytechinus variegatus* were collected from shallow waters (about 0.3–2 m depth) from the Gulf of Mexico near Port Saint Joseph, Florida, during late spring of 1999. Individuals were maintained in aerated, 160-l recirculating aquaria containing artificial seawater (ASW) (Instant Ocean, Aquarium Systems, Mentor, OH) and held at about 20–25 °C. Larvae were obtained from a single male-female pair by artificial fertilization using gametes from spawn triggered *via* intracoelomic injection of 0.5 *M* KCl. Embryological and larval development were monitored and photographed using an Olympus CO-11 binocular dissecting microsope and an Olympus CH binocular compound light microscope equipped with a camera. Cultures were maintained with gentle stirring at about 20–23 °C at a density of no greater than 0.8 larvae/ml, and the culture water was changed every 3 days. Larvae were fed approximately $5 \times 10^4$ cells/ml of a diet composed of equal amounts of the single-celled algae *Chaetocerous calcitrans, Dunaliella tertiolecta,* and *Isocrysis galbana* (Strathmann, 1987). Thirteen days after fertilization, the larvae had developed into early 8-armed pluteii. These larvae were cultured for an additional 2 days to allow them to attain the late 8-armed pluteus stage for use in the present experiment.

The 8-armed pluteus larvae of the irregular echinoid *Dendraster excentricus* were cultured at Friday Harbor Laboratories, University of Washington, during the summer of 1998. These larvae, which were obtained by artificial fertilization using methods similar to those described above, were cultured in natural seawater in glass fingerbowls (250 ml). The fingerbowls were held in a circulating seawater system at 12–15 °C. Larvae were fed the single-celled algae *Rhodomonas* sp. (Strathmann, 1987). Larval regeneration was monitored and photographed using a Nikon Wild M-5 dissecting microscope and a Nikon Optiphoto-2 microscope equipped with a camera system. Only 15-day-old larvae were used in the present experiment.

*Surgical bisection.* Pluteus larvae of the regular echinoid *L. variegatus* were surgically bisected into anterior and posterior sections at a point about equidistant between the anterior and posterior poles (Figs. 9A, 10A) (Vickery and McClintock, 1998; Vickery *et al.*, 2001b; Vickery, 2002). Before bisection, the larvae ranged from about 600 to 1100 μm in length (along the anterior to posterior larval axis), possessed a larval skeleton (Fig. 9A), and were actively swimming and feeding. The same procedure was used to surgically bisect pluteus larvae of the irregular echinoid *D. excentricus*. Larvae ranged from about 700 to 1000 μm in length (along the anterior to posterior larval axis) and like the larvae of *L. variegatus,* possessed a larval skeleton before they were bisected (Fig. 10A). All anterior and posterior portions of larvae were maintained in 250-ml glass fingerbowls under the culture conditions described above for each species. Non-bisected control larvae were simultaneously cultured under identical conditions for comparison. Anterior and posterior larval portions of both species were observed and photographed daily for 14 days.

## Results

### *Regeneration in larval asteroids*

*Regeneration in early-stage larvae.* Early-stage larvae of *Luidia foliolata* were surgically bisected 21 days after fertilization. Before bisection the bipinnaria larvae measured 710 ± 80 μm in length ($n = 20$, Fig. 2A). After bisection, both the anterior and the posterior portions of the larvae continued utilizing their ciliary bands to swim and collected phytoplankton to feed. Even though the anterior portions had lost the gut due to surgical bisection, phytoplankton was still accumulating in the oral cavity. The posterior portions of the larvae collected phytoplankton directly through the esophagus. Within 24 h, rough edges of tissues originally seen at the site of bisection in both the anterior and posterior portions of the larvae had become smooth. Within 48 h of bisection, mesenchyme cells with pseudopodia appeared at the site of bisection (Fig. 2B, E) in both the anterior and posterior larval portions. In the anterior portions, a thickening of the former upper esophagus/lower mouth region became evident (Fig. 2B); and aggregations of mesenchyme cells around this thickened area became more prominent. Eventually this thickened wall invaginated into the body cavity, forming a tube (Fig. 2C). Similar aggregations of mesenchyme cells were observed in the bisected posterior portions at various locations throughout the regenerating larval body, most notably at the site of bisection.

The anterior portions of bisected larvae gradually decreased in size after bisection (immediately after bisection = 306 ± 47 μm in length; 11 days later = 233 ± 29

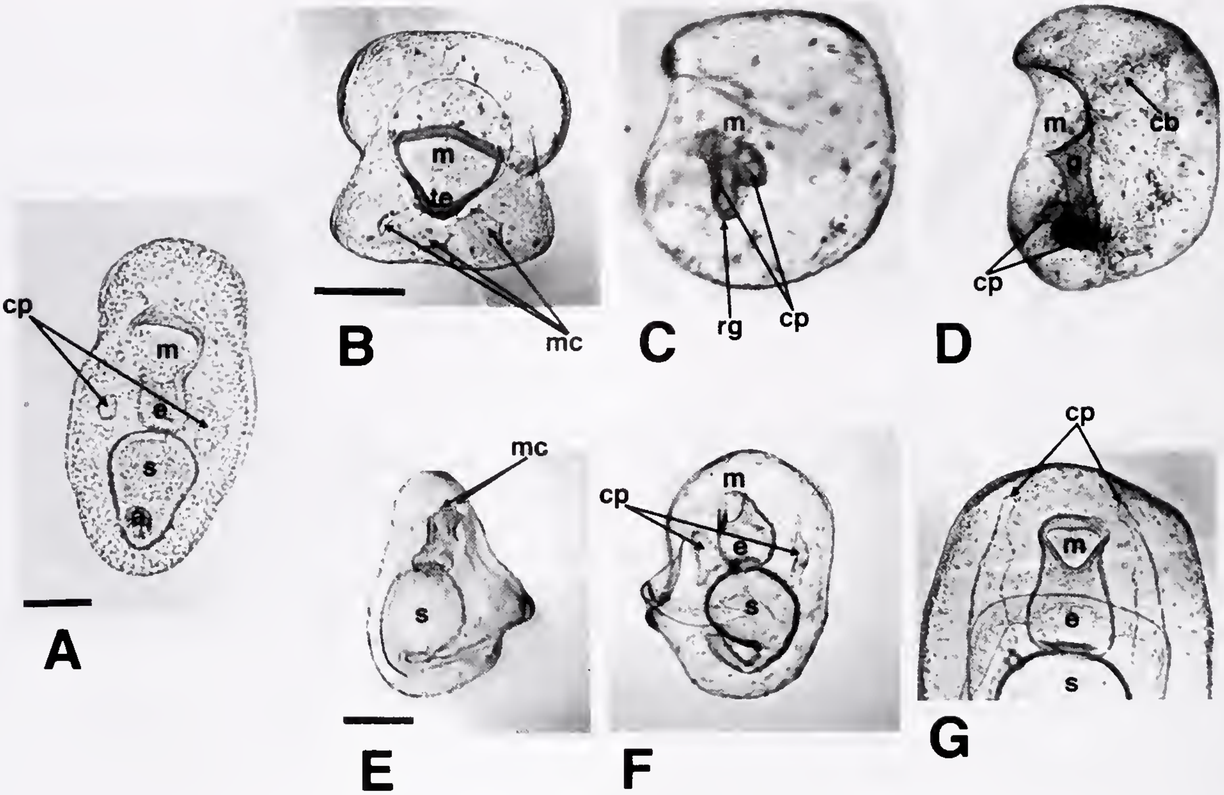

**Figure 2.** Light photomicrographs of regenerating early-stage bipinnaria larvae of *Luidia foliolata*. (A) A 21-day-old bipinnaria larva with a pair of coelomic pouches located on the sides of the larval esophagus. Two days after bisection, mesenchyme cells are apparent at the surgical plane in the anterior (B) and posterior (E) portions. Note that the anterior portion (B) does not possess any coelomic components following surgical bisection and that a thickening of the epidermis is evident at the rear part of the former mouth. Three days after bisection, the larval epidermis invaginates into the body cavity and forms a new pair of coeloms evaginating from the upper portion of the newly formed rudimental gut in the anterior portion (C). The posterior portion (F) increases in size, and regeneration of the missing mouth and elongation of the right and left coeloms are evident (F). Seven days after bisection, the newly formed coeloms are clearly separated from the newly formed gut in the anterior portion (D), further extension of the right and left coelomic pouches is evident, and the lost mouth has completely regenerated (G). Scale bars = 200 $\mu$m in (A), 100 $\mu$m in (B)–(D), 100 $\mu$m in (E)–(F). a, anus; cb, ciliary band; cp, coelomic pouches; e, esophagus; g, gut; m, mouth; mc, mesenchyme cell; rg, rudimental gut; s, stomach.

$\mu$m in length; $n$ = 20 ± 1 SD). However, the posterior portions of the bisected larvae, which retained a functional digestive system and continued feeding throughout the regeneration process, continued to grow (immediately after bisection = 378 ± 31 $\mu$m in length; 11 days later = 495 ± 136 $\mu$m in length; $n$ = 20 ± 1 SD). Seven days after bisection (28 days after fertilization), the aggregation of mesenchyme cells (described above) seen in the anterior portions of the larvae appeared to be involved in development of a new pair of coelomic pouches that evaginated from the anterior portion of the newly formed "digestive tube" (Fig. 2C). The digestive tube then elongated towards the posterior and reconnected to the posterior portion of the larval wall, forming an opening that eventually became a new anus (Fig. 2D). By 7 days after bisection, the posterior portions of the bisected larvae had almost completely regenerated the mouth (Fig. 2F, G), and an elongation of the coelomic pouches was prominent. Once the anterior portions of the bisected larvae had reformed a complete digestive tube, actual feeding and digestion of phytoplankton began; differentiation of the digestive tube into a new esophagus, stomach, and intestine was observed by day 10 (Fig. 2D). After about 12–14 days, both the anterior and posterior portions of the bisected larvae had completely regenerated all missing body structures, including all internal organs.

From our observations, we constructed a schematic diagram of regeneration and organogenesis of the anterior portion of bisected asteroid larvae (Fig. 3). Immediately after bisection, the anterior portion is left with no coelom components (Fig. 3Aa), but it retains one complete preoral ciliary band and one incomplete postoral ciliary band. To

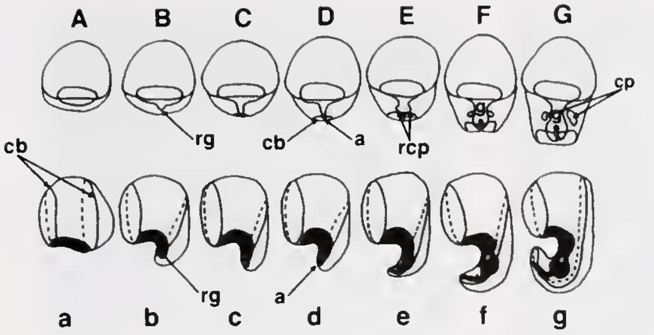

**Figure 3.** Diagrams of organogenesis in early-stage anterior portions of surgically bisected regenerating bipinnaria larvae. (A) through (G) represent a frontal view, (a) through (g) represent a lateral view. (A) and (a) represent the anterior portion immediately after surgical bisection. (B) and (b) through (D) and (d) represent the formation of a new gut described in Fig. 2(B) and (C). (E) and (e) through (G) and (g) represent the formation of a new set of coeloms and differentiation of the newly formed gut into esophagus, stomach, and intestine described in Fig. 2 (D). a, anus; cb, ciliary band; cp, coelomic pouch; g, gut; rcp, rudiment of coelomic pouch; rg, regenerating gut.

regenerate the missing digestive system, the body wall begins to invaginate (Fig. 3Bb, Cc), eventually forming a new anus (Fig. 3Dd). During this time, the postoral ciliary band extends toward the posterior. Meanwhile, from the anterior portion of the new gut, an entirely new set of coeloms is formed by lateral evagination of the newly formed digestive system (Fig. 3Ee), which then separate from the gut and elongate anteriorly and posteriorly alongside the newly formed digestive system (Fig. 3Ff).

Afterwards, complete differentiation of the newly formed digestive system, completion of regeneration of the lost components of the postoral ciliary band, and further development of both coeloms are observed (Fig. 3Gg). Our observations of the regeneration process in early-stage bipinaria larva of *P. ochraceus* were virtually identical to those described above for *L. foliolata*.

*Regeneration in mid-stage larvae.* Regenerative processes in bisected mid-stage larvae of both *L. foliolata* and *P. ochraceus* were virtually identical to those described above for early bipinnaria larva of *L. foliolata* (as previously reported by Vickery and McClintock, 1998). The only difference was that the anterior portions of mid-stage bisected larvae contained an axocoel, and therefore did not have to regenerate the coelomic pouches as they were already present. Bisected anterior portions continued to swim and collect phytoplankton in the oral cavity (Fig. 4A). An invagination of the body wall occurred after the appearance of mesenchyme cells, and the coelomic pouches elongated toward the posterior (Fig. 4B). A new digestive system completed regeneration about one week after bisection (Fig. 4C). The posterior portions, which retained a functional gut, continued to digest phytoplankton (Fig. 4D). During the process of regeneration of the lost anterior portions, mesenchyme cells with pseudopodia were evident (Fig. 4E).

*Regeneration in late-stage larvae.* In *L. foliolata*, the anterior portions of bisected larvae underwent regeneration as described above for mid-stage bipinnaria larva ($n = 30$, Fig. 5A). However, the posterior portions of bisected larvae, each possessing a juvenile rudiment, invariably metamorphosed into juveniles within 3 days ($n = 30$, Fig. 5B) (Vickery and McClintock, 1998). The resulting juveniles measured about 500 $\mu$m in diameter, which was not statistically different ($P > 0.05$) than the size of control juveniles ($n = 20$) from non-bisected larvae.

In contrast, both the anterior and posterior portions of late-stage larvae of *P. ochraceus* underwent complete regeneration, without exception, and with no mortality ($n = 350$, Fig. 5C, D), in a process similar to that described above for mid-stage larvae. However, formation of a new juvenile (adult rudiment, including the spicules and hydrolobes) in association with the anterior portions of bisected larvae occurred at an accelerated rate (within only 7 days). In comparison, the control larvae required an additional 7–10 days (14–21 days total) to form an equivalent adult rudiment on the posterior portions of the larvae. Within 7 days of late-stage bisection, the anterior portions of bisected larvae were morphologically and functionally indistinguishable from control larvae, and later metamorphosed into juveniles that were indistinguishable both morphologically and functionally from juveniles obtained from non-bisected control larvae.

During the regeneration process of the posterior portions of bisected larvae, a new larval body formed in each posterior portion (Fig. 5E). The newly formed secondary larval body first developed into a bipinnaria (Fig. 5F), and later formed a brachiolar apparatus, without exception (Fig. 5G). After completing regeneration of the brachiolar apparatus, the posterior portions metamorphosed into juveniles that were morphologically and functionally indistinguishable from juveniles resulting from non-bisected control larvae. The juveniles resulting from metamorphosis of regenerated larvae (both anterior and posterior portions) measured about 500 $\mu$m in diameter ($n > 20$), a size not statistically different ($P > 0.05$) than that seen in control juveniles ($n = 20$) from non-bisected larvae.

*Regeneration of partial larval body parts in* Pisaster ochraceus. The far ends of the anterior tips were removed from both bipinnaria and brachiolaria larvae of *P. ochraceus* ($n = 10$ each). Immediately after removal from bipinnaria larvae, the anterior tips, which contained both the axocoel and portions of the preoral and postoral ciliary bands, continued to swim (Fig. 6A). After 2 weeks the anterior tips showed no signs of regeneration; but they retained their ability to swim, and they displayed muscle contractions (Fig. 6B). In contrast, the posterior portions of the larvae partially regenerated (Fig. 6C) and proceeded to become

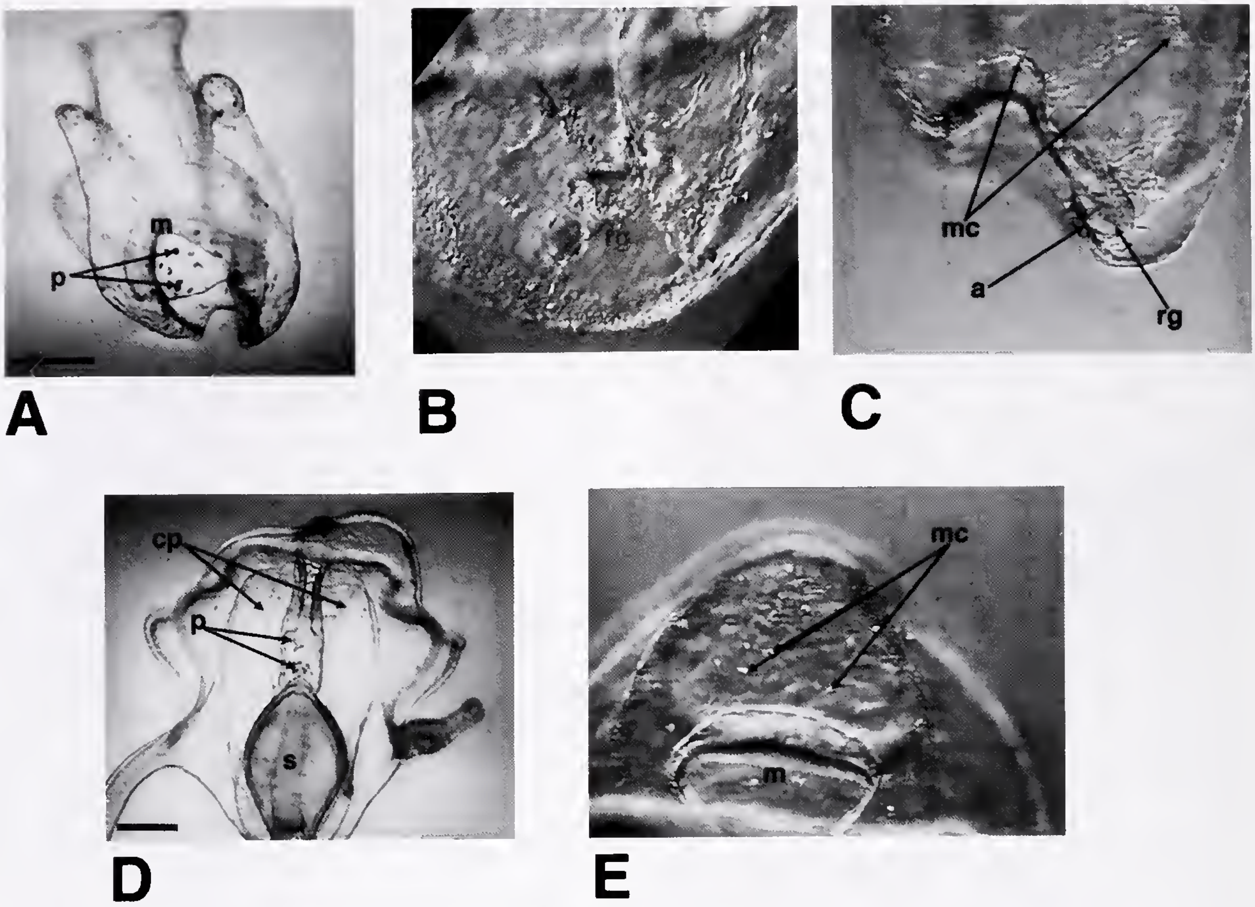

**Figure 4.** Light photomicrographs of regenerating mid-stage larva of *Pisaster ochraceus.* (A) through (C) represent an anterior larval portion and (D) and (E) represent a posterior larval portion. The anterior portion continues to swim in a fashion similar to the non-bisected control larvae, and collects phytoplankton into the oral cavity using the ciliary bands (A), even though it lost its digestive system during the surgical bisection. (B) shows invagination of the thickened rear part of the former mouth into the body cavity to form a rudimental digestive tube, which later becomes a new digestive system. A lateral view of the anterior portion (C) shows how the rudimental gut forms an external opening, forming a new anus. Note that many mesenchyme cells with pseudopodia are present. The posterior portion (D) continues to swim and feed, and increases in size even during regeneration. (E) shows the newly-regenerated anterior portion containing mesenchyme cells with pseudopodia. Scale bars = 200 $\mu$m in (A) and (D). a, anus; cp, coelomic pouches; m, mouth; mc, mesenchyme cell; p, phytoplankton; rg, rudimental gut.

brachiolaria larvae. When the tips were removed from brachiolaria larvae, the tips, which retained the brachiolar apparatus, continued to swim using cilia (Fig. 7A), but no signs of regeneration of the larval body were evident after 2 weeks (Fig. 7B). However, the posterior portions regenerated the lost brachiolar apparatus within 7 days, as shown in Figure 7C.

Regeneration of short, stubby arm buds was observed in many brachiolaria larvae when the larval arms were surgically removed (Fig. 8A). In most cases, larval arms regenerated but never reached the same length as before. Sometimes no regeneration of the larval arms occurred at all. The severed larval arms continued to swim in a spiral fashion (Fig. 8B), and muscular contractions could still be observed in the still-swimming severed arms after one week (Fig. 8C). After 2 weeks, no regeneration was observed in the severed arms; however, the arms themselves continued to swim actively with no mortality (Fig. 8D).

### *Regeneration in larval echinoids*

Within 5 days, anterior and posterior portions of pluteus larvae of the regular echinoid *L. variegatus* regenerated missing body components including a digestive system and a larval mouth, respectively (Fig. 9 A-E). The morphogenetic and organogenic processes appeared to be similar to

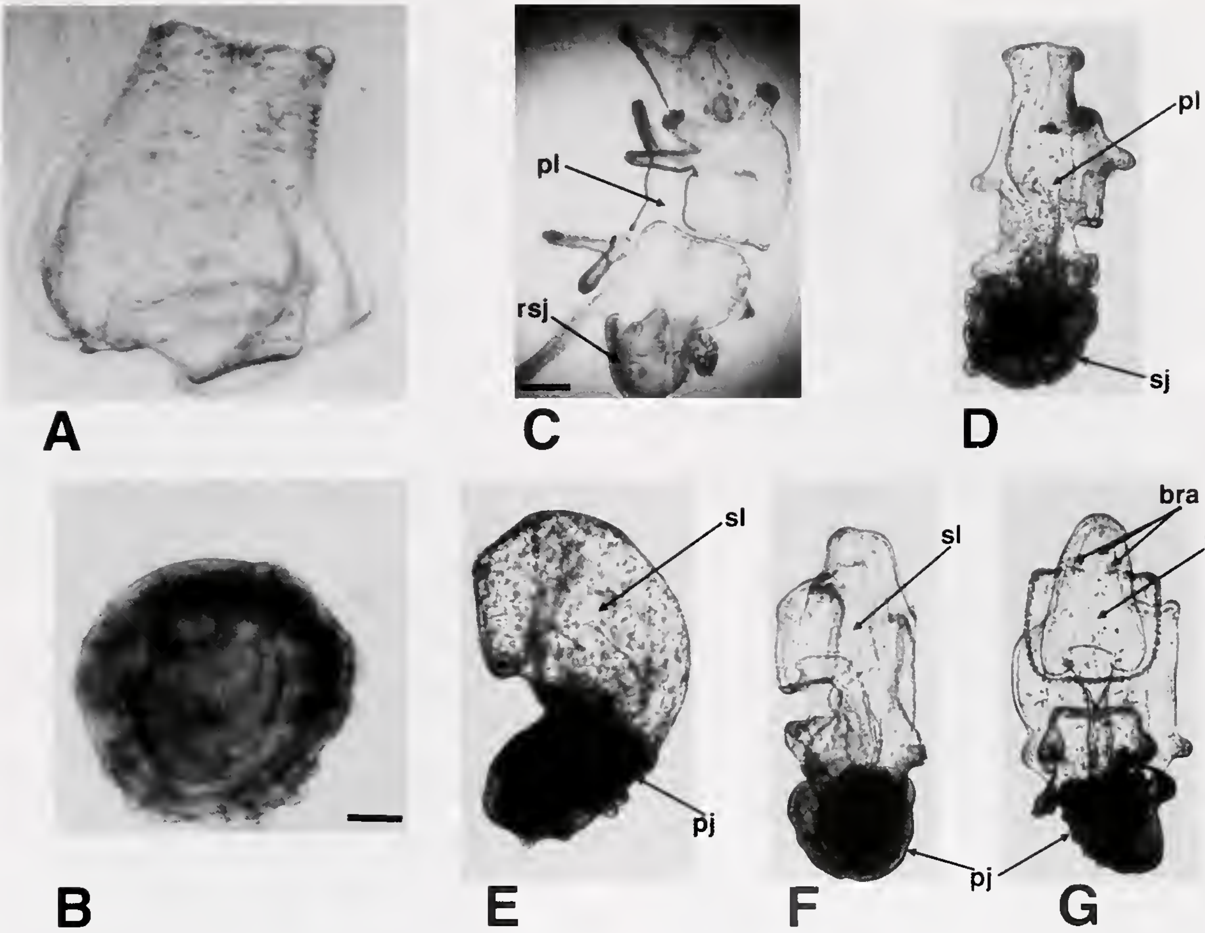

**Figure 5.** Three days after bisection of a late-stage larva of *Luidia foliolata*, the anterior portion is shown in the process of regeneration (A). In contrast, the posterior portion completes metamorphosis and becomes a juvenile (adult) (B), as we previously reported (Vickery and McClintock, 1998). After 3 days, in late-stage larvae of *Pisaster ochraceus*, the anterior portion has partially regenerated the lost primary juvenile (adult) rudiment, forming a secondary juvenile (adult) rudiment on the posterior portion (C). About 7 days after bisection, a lateral view of the anterior larva (D) shows complete regeneration of a secondary juvenile (adult) rudiment, during which the larval arms are absorbed, suggesting a progression of the process of metamorphosis. Three days after bisection, a secondary larval body is in the process of regenerating from the bisected primary juvenile (adult) rudiment (E). The secondary larval body then becomes a seemingly normal late-stage bipinnaria larva (with juvenile rudiment) after 7 days (F). By about 9 days after bisection, the secondary larval body (with juvenile rudiment) has regenerated the lost brachiolar apparatus (G). Scale bars = 200 $\mu$m in (A)–(B), 100 $\mu$m in (C)–(G). bra, brachiolar apparatus; pl, primary larval body; pj, primary juvenile (adult) rudiment; rsj, rudiment of secondary juvenile (adult); sl, secondary larval body; sj, secondary juvenile (adult).

those we observed in regenerating asteroid larvae, with aggregations of mesenchyme cells with pseudopodia evident at the site of bisection (Vickery, 2002). Elongation of the larval skeleton resulted in replacement of the larval arms (Fig. 9E). Eight days after bisection, both larval portions had completely regenerated missing larval structures (Fig. 9F, G). Two weeks after bisection, regenerated larvae were morphologically and functionally indistinguishable from non-bisected control larvae. They displayed normal swimming and feeding behaviors. Eighteen days after bisection, regenerated larvae developed adult rudiments on the posterior and metamorphosed into normal juveniles.

In larvae of the irregular echinoid *D. excentricus*, the regeneration processes were almost identical to those in larvae of *L. variegatus*. Six days after bisection, the digestive system of anterior portions of larvae had almost completed regeneration, although the anus had yet to form (Fig. 10A, B). Elongation of the larval skeleton was observed in the regenerating posterior larval portion, while the exposed larval skeleton was surrounded by newly regenerated epidermis and ciliary bands (Fig. 10A, C). Although posterior portions of larvae were capable of complete regeneration, the anterior portions regenerated only partially during the course of the study (about 2 weeks).

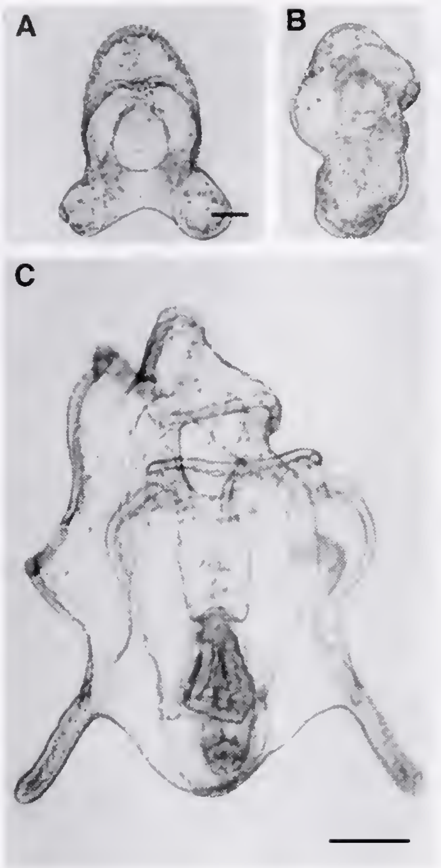

**Figure 6.** Two weeks after surgical removal of the far anterior tips of the bipinnariae of *Pisaster ochraceus*, the anterior tips showed no signs of regeneration of the larval body but continued to actively swim, while the posterior portions had partially regenerated the missing tips. (A) Anterior tip (including axocoel) immediately after bisection. (B) Anterior tip 2 weeks after bisection. (C) Posterior portion approximately 1 week after bisection. Scale bars = 50 $\mu$m in (A)–(B), 200 $\mu$m in (C).

## Discussion

The present study demonstrates that planktotrophic larvae of the asteroids *Luidia foliolata* and *Pisaster ochraceus* possess extensive regenerative capacities regardless of their developmental stage. In early and mid-stage surgically bisected larvae, both species regenerated missing body components within 2 weeks; and no mortality occurred due to bisection, a result similar to our previous observations (Vickery and McClintock, 1998). Mesenchyme cells possessing pseudopodia played a regenerative role in the formation of an entirely new digestive system. In early-stage larvae, a new pair of coelomic pouches was formed by evagination of the anterior portion of the newly formed digestive system in association with aggregations of mesenchyme cells (possessing pseudopodia). A similar type of coelom formation was documented in echinoid larvae that had been surgically manipulated (reviewed in Hörstadius, 1973, and Vickery *et al.*, 2001b). The resultant coelomic structures are essential body components that eventually form the body cavity in adult organisms, ultimately surrounding the digestive and reproductive organs. Coelomocytes (located within the coelom) have been reported to participate in regenerative processes in adult echinoderms (Thorndyke *et al.*, 1999). In contrast, we found that bisected larvae, lacking coelomic pouches in their anterior regions, completed regeneration. Thus, coelomocytes apparently do not play a critical role in larval regeneration.

In adult asteroids, regeneration is initiated by a proliferation of epidermal cells forming a mesenchymatous blastema, which later gives rise to the missing body structures (Candia Carnevali and Bonasoro, 1994; Bonasoro *et al.*, 1998; Thorndyke *et al.*, 1999). Our observations demonstrate that regenerative processes occur in a similar fashion in planktotrophic asteroid larvae. Our microscopic exami-

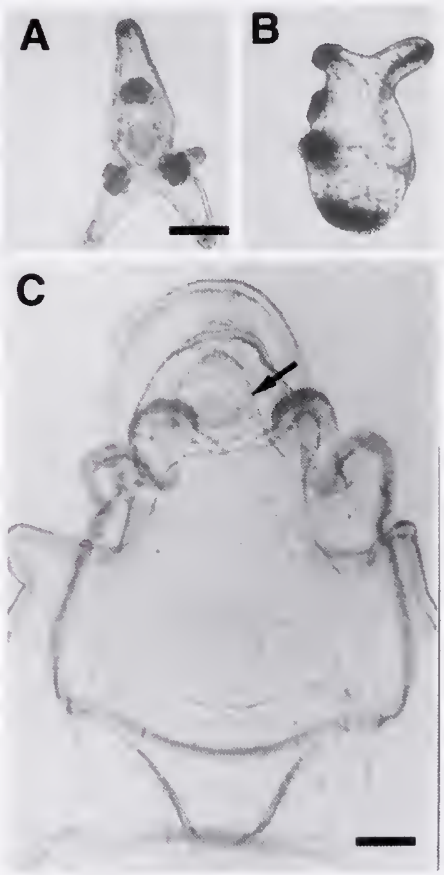

**Figure 7.** No regeneration of the larval body from the surgically removed brachiolar apparatus was observed in *Pisaster ochraceus*, but the larval posterior portion regenerated the brachiolar apparatus within 7 days, and within 2 weeks the larva was morphologically and functionally indistinguishable from non-bisected control larvae. (A) A swimming brachiolar apparatus with axocoel immediately after surgical removal. (B) A swimming brachiolar apparatus (lateral view) 2 weeks after surgical removal. Morphological changes are evident. (C) Larval posterior portion with regenerating brachiolar apparatus (arrow) about 5 days after surgical bisection. Scale bars = 50 $\mu$m in (A)–(B), 200 $\mu$m in (C).

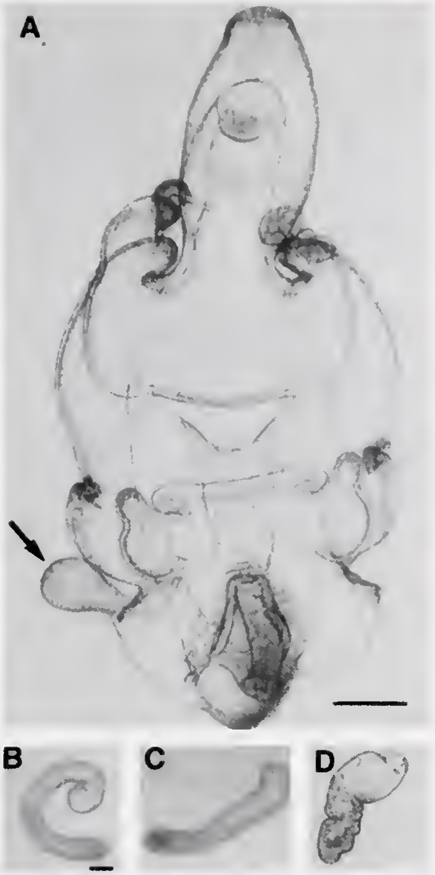

**Figure 8.** When posterolateral arms were removed from *Pisaster ochraceus* brachiolaria larvae, the formation of (arm) buds was often observed at the site of amputation, while the severed arms continued to swim (with no sign of regeneration) for over 2 weeks. In most cases, regenerated posterolateral arms never reached the same length as before. (A) Regenerating (arm) bud (arrow). (B) Severed posterolateral arm immediately after bisection. After 2 weeks the severed arm still continued to actively swim (C), and muscle contractions were evident (D). Scale bars = 200 $\mu$m in (A), 50 $\mu$m in (B)–(D).

nations revealed that a proliferation of cells was initiated at the larval epithelium (ectoderm) near the surgical plane. During the process of regeneration, these cells appeared to dedifferentiate into mesenchymal-like cells and then to redifferentiate into new types of cells that later gave rise to the regenerated structures (Thorndyke *et al.*, 1999). However, further confirmation is necessary.

Cell fate in echinoderm larvae has previously been considered by some researchers to be determinate and irreversible once embryos or larvae attain discrete developmental stages (Cameron *et al.*, 1987; Cameron and Davidson, 1991; Davidson *et al.*, 1995; Thorndyke *et al.*, 1999). Nonetheless, the flexibility of developmental pathways and morphogenesis has been questioned lately (Balser, 1998). Our results demonstrate that fully differentiated larval body tissues are capable of additional proliferation and apparent dedifferentiation and redifferentiation in order to reconstruct missing body parts, including the larval epidermis and coelomic pouches, suggesting organogenesis from previously differentiated cells. Moreover, our observations are supported by those of Balser (1998) in asexually cloning ophiuroid larvae, in which cloning apparently required both development and growth of new tissues as well as a reorganization of some existing tissues. Thus, many cells apparently remain omnipotent or pluripotent (capable of differentiation into any type of cell) in the larval stages, at least in the planktotrophic echinoderm species examined to date. However, since our studies and those of Balser (1998) have primarily relied upon morphological observations, future work using cell marking or other methods to follow the fate of individual larval cells is required to absolutely determine whether dedifferentiation/redifferentiation and organogenesis from previously differentiated cells occurs during larval regeneration.

Peterson *et al.* (1997), discussing larval forms (including planktotrophic echinoderm larvae) with what they termed "maximal indirect development" (Davidson *et al.*, 1995), suggested that larva-specific embryonic cell lineages with a fixed fate and a limited capacity for division give rise to the larval structures, whereas pluripotent "set-aside" cells, capable of relatively unlimited cell division, give rise to the adult form. The results of the present study and others (Jaeckle, 1994; Balser, 1998; Vickery and McClintock, 1998) suggest that in planktotrophic echinoderm larvae the fate of larval-specific cells is not fixed, and their division capacity is not limited to only a few division cycles as was suggested by Peterson *et al.* (1997). Since it has been demonstrated that omnipotent or pluripotent larval cells, which remain versatile even after differentiation into specific larval tissues, are capable of replacing missing larval structures, it is questionable whether pluripotent set-aside cells are required to give rise to the adult structures as was suggested by Peterson *et al.* (1997). Further studies should shed more light on this subject.

In both asteroid species we examined, the anterior portions of bisected larvae lost their functional gut as a result of surgical bisection, retaining only the upper part of the mouth and oral cavity. Therefore, these larval anterior portions could not feed on phytoplankton until they had regenerated a functional digestive system; they decreased in size for 7 days until the digestive system had regenerated, restoring their capacity to feed. It is possible that they obtained some nutrients directly through the larval epidermis (ectoderm) in the form of dissolved organic matter from the surrounding seawater (Stephens, 1972, 1981; Manahan, 1990; Jaeckle and Manahan, 1989, 1992). Also, the bisected, regenerating anterior portions apparently reabsorbed some larval body parts as a nutrient source during regeneration of the digestive system (this would partly explain their decrease in body size). Absorption and utilization of the larval body during regeneration was suggested by Chia and Burke (1978). In

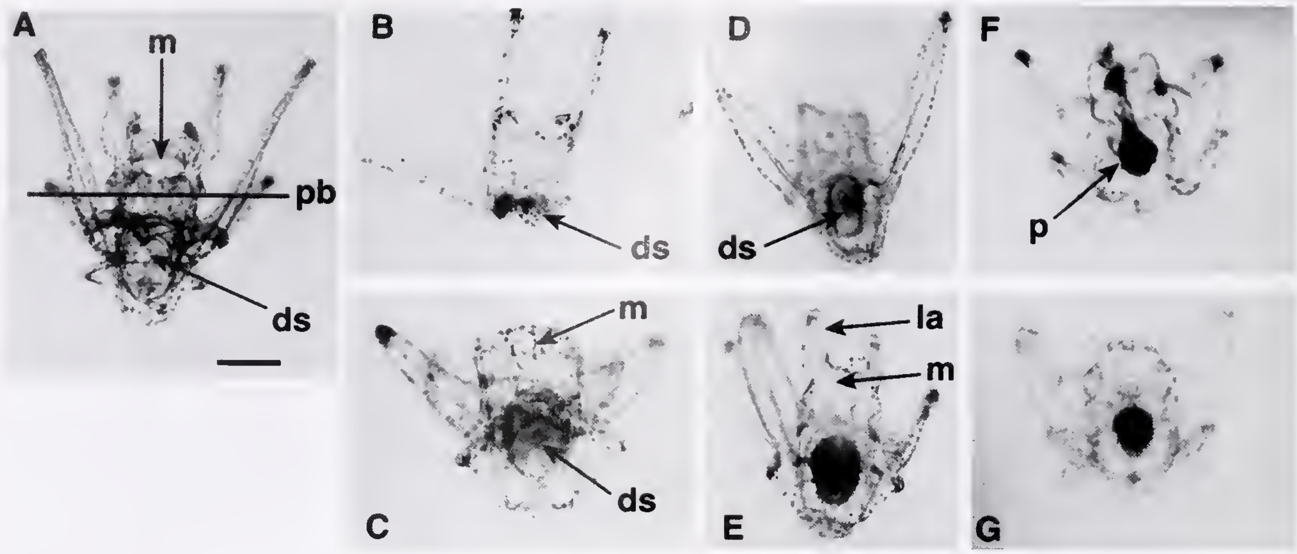

**Figure 9.** Surgically bisected pluteus larva of the regular echinoid *Lytechinus variegatus*. (A) Non-bisected echinopluteus larva. (B) Regenerating anterior portion of larva immediately after bisection. (C) Regenerating posterior portion of larva immediately after bisection. (D) Regenerating anterior portion of larva 5 days after bisection. (E) Regenerating posterior portion of larva 5 days after bisection. Missing structures from both the anterior and posterior larval halves (including the larval digestive system) are seen undergoing regeneration. (F) Regenerated anterior portion of larva 8 days after bisection. (G) Regenerated posterior portion of larva eight days after bisection. ds, digestive system; la, larval arm; m, mouth; p, phytoplankton; pb, plane of bisection. Scale bars = 200 $\mu$m (A), and 100 $\mu$m (B-G, shown in B).

contrast, the posterior portions of bisected larvae, which retained functional digestive systems from the esophagus to the anus (and therefore continued to actively feed) increased in size over a 2-week period. Both anterior and posterior portions of bisected larvae of both species somehow obtained the required energy or nutrition to support regeneration of their missing structures, either through active feeding, absorption of dissolved organic matter, or absorption of larval body tissues. Future investigations are necessary to evaluate the energetics of the regeneration process in planktotrophic asteroid larvae. In the present study we used size (larval length) as an indicator for growth during regeneration. In future studies it also would be valuable to examine larval body mass, the thickness of larval tissues, or both in addition to body length during regeneration at various larval stages. Under certain conditions tissues could become thinner to accommodate an overall increase in body length.

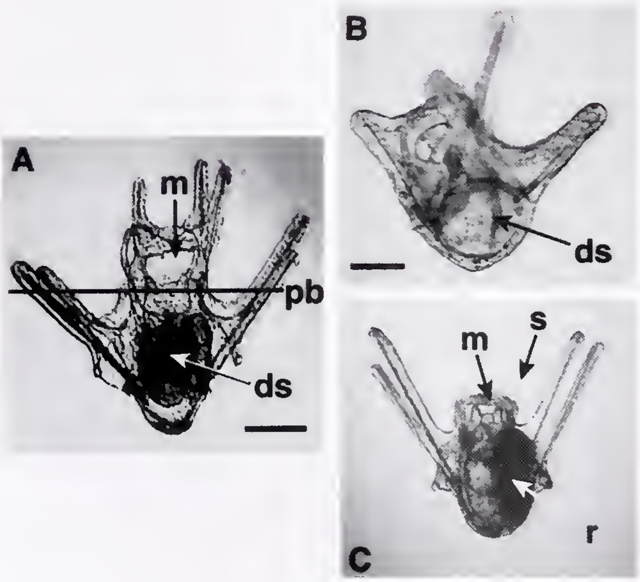

**Figure 10.** Surgically bisected pluteus larva of the irregular echinoid *Dendraster excentricus*. (A) Non-bisected echinopluteus larva. (B) Regenerating anterior portion of larva 6 days after bisection. (C) Regenerating posterior portion of larva 6 days after bisection. ds, digestive system; m, mouth; r, rudiment; pb, plane of bisection. Scale bars = 200 $\mu$m (A), and 100 $\mu$m (B-C, shown in B).

In late-stage larvae, the anterior portions of both species regenerated in a process identical to that described for the early and mid-stage larvae. The posterior portions (with adult rudiment) of *L. foliolata*, however, instead of regenerating their missing anterior larval components, rapidly completed metamorphosis into juvenile asteroids within 3 days of bisection (Vickery and McClintock, 1998). Apparently surgical bisection either initiated or dramatically accelerated the process of metamorphosis. This suggests that incorporation of the entire larval body mass into the juvenile is not required during the metamorphic process, contradicting the report of Chia and Burke (1978) for larvae of the sand dollar *Dendraster excentricus*. Future studies examining the energetics of larval regeneration and metamorphosis, and comparing the internal anatomy and survival and fate of juveniles resulting from bisected larvae to the internal anatomy and survival and fate of juveniles resulting from non-bisected controls, will be of great interest.

In contrast, the posterior portions of *P. ochraceus* larvae (which lacked the brachiolar apparatus) did not readily complete metamorphosis following surgical bisection. Instead they regenerated their missing larval anterior components, including the brachiolar apparatus, prior to metamorphosis. The brachiolar apparatus is considered to be important for metamorphosis (Baker, 1978). These observations are probably due to developmental differences (described below) that characterize *L. foliolata* and *P. ochraceus*. *L. foliolata* is a member of the family Luidiidae, which lacks a brachiolaria larval stage in its ontogeny (Chia *et al.*, 1993). These larvae complete metamorphosis while swimming in the water column (Chia *et al.*, 1993). In contrast, *P. ochraceus* is a member of Asteriidae family and possesses a brachiolaria larval stage. Larvae of this species require attachment of the brachiolar apparatus to a favorable substrata in order to complete metamorphosis (Baker, 1978; Chia *et al.*, 1993). Therefore, it is possible that metamorphically competent posterior portions of bisected larvae of *L. foliolata*, which do not require a brachiolar apparatus for substrata attachment to trigger metamorphosis, rapidly complete metamorphosis following surgical bisection to avoid unnecessary feeding and growth to reform anterior tissues that are not required for metamorphosis. The remaining portion of the larval body is absorbed into the adult rudiment during metamorphosis. *P. ochraceus*, on the other hand, requires the brachiolar apparatus for attachment and metamorphosis; thus it is reasonable that this structure would have to be regenerated before metamorphosis.

A number of theories about the evolution of developmental modes in asteroids and marine invertebrate larvae in general have been proposed (reviewed by McEdward and Janies, 1993; Wray and Raff, 1991). Within planktotrophic modes of development in Asteroidea, the Luidiidae are often considered to possess more primitive development than the Asteriidae (Downey, 1973; Clark and Downey, 1992; McEdward and Janies, 1993). Others argue exactly the opposite (Blake, 1988). Our observations do not clearly support either hypothesis; however, they do demonstrate that a brachiolar apparatus is necessary for development in the Asteriidae and that there are clearly regenerative differences between Luidiidae and Asteriidae.

When small portions of the larval body were removed from *P. ochraceus*, the missing portion of the larval body usually regenerated. Some of these surgical procedures produced anterior larval body fragments almost identical to those Jaeckle (1994) observed in larva from plankton tow samples. Jaeckle reported that these fragments, which were produced by autotomization of the far anterior portion of the larval preoral lobe, developed into bipinnaria larvae in 1–2 days. We did not consistently observe regeneration of the entire larval body from our surgically removed anterior portions of the preoral lobe over the 2 weeks they were followed. However, Jaeckle's larval fragments were maintained at higher seawater temperatures than ours, and their developmental processes might have been accelerated.

One exception to this pattern was in brachiolaria larvae that had lost their larval arms. In mid-stage larvae, missing portions were regenerated even as development progressed (the adult rudiment was forming). No mortality of small larval fragments was observed during the 2-week studies. Subsequent observations indicated that these small larval pieces continued to swim in the water column for up to 4 weeks, suggesting they may obtain energy or nutrients for maintenance through the uptake of dissolved organic matter from the surrounding seawater (Stephens, 1972, 1981; Manahan, 1990; Jaeckle and Manahan, 1989, 1992).

Our studies further demonstrate that the planktotrophic larvae of regular and irregular echinoids are capable of complete regeneration following surgical bisection. Additional studies are needed to determine whether bisected anterior portions of larvae of *D. excentricus* can fully regenerate and metamorphose into juveniles. The inability of the anterior larval portion of *D. excentricus* to fully regenerate over a 2-week period may be related to the comparatively low ambient seawater temperatures at which these larvae were reared (12–15 °C for *D. excentricus* compared to 20–23 °C for *L. variegatus*). Lower temperature can suppress metabolic rates in developing marine invertebrate larvae (Pearse *et al.*, 1991; Boidron-Metairon, 1995; Marsh *et al.*, 2001).

The planktotrophic larvae of asteroids are morphologically similar to those of holothuroids (Smiley, 1986), whereas the planktotrophic larvae of echinoids are similar to those of ophiuroids (Levin and Bridges, 1995). Ophiuroid larvae, like asteroid larvae, undergo asexual clonal reproduction (involving regeneration of a complete new larval body) (Balser, 1998). Therefore, it is likely that planktotrophic larvae of most if not all echinoderms have the capacity for regeneration. This capacity may help offset their presumably high mortality rates in the plankton (Menge, 1975; Vickery and McClintock, 1998).

Research in the area of regeneration of echinoderm larvae has only begun (Balser, 1998; Vickery and McClintock, 1998; Vickery, 2001, 2002; Vickery *et al.*, 2001a, 2001b). Because echinoderms share many developmental traits with other deuterostomes, an understanding of the processes of regeneration in echinoderm larvae may lead to a better understanding of regeneration in many higher animals, including vertebrates.

## Acknowledgments

We thank Drs. Dennis Willows and Richard Strathmann of Friday Harbor Laboratories, University of Washington, for the use of laboratory facilities and for staff technical support. We thank Dr. Stephen Watts and his students for collection of *Lytechinus variegatus*. We also thank Drs. Charles Amsler, Asim Bej, Stephen Watts, and Thane Wibbels for the use of their laboratory facilities. Finally, we thank Dr. Daniel Jones, Chair Emeritus of the Department of Biology at the University of Alabama at Birmingham, and The University of Alabama at Birmingham for partial financial support of this study. Also, the manuscript was improved based upon the comments of two anonymous reviewers. We dedicate this paper to the memory of Dr. Larry McEdward, a true visionary in the field of marine invertebrate larval ecology.

## Literature Cited

**Baguñà, J., E. Saló, and C. Auladell. 1989.** Regeneration and pattern formation in planarians. III. Evidence that neoblasts are totipotent stem cells and the source of blastema cells. *Development* **107:** 77–86.

**Baker, M. F. 1978.** Structure of the organs of attachment of brachiolaria larvae of *Stichaster australis* (Verrill) and *Coscinasterias calamaria* (Gray) (Echinodermata: Asteroidea). *J. Exp. Mar. Biol. Ecol.* **33:** 1–36.

**Balser, E. J. 1998.** Cloning by ophiuroid echinoderm larvae. *Biol. Bull.* **194:** 187–193.

**Blake, D. B. 1988.** Paxillosidans are not primitive asteroids: a hypothesis based on functional considerations. Pp. 309–314 in *Echinoderm Biology*, R. D. Burke, P. V. Mladenov, P. Lambert, and R. L. Parsley, eds. Balkema, Rotterdam.

**Boidron-Métairon, I. F. 1995.** Larval Nutrition. Pp. 223–248 in *Ecology of Marine Invertebrate Larvae*, L. R. McEdward, ed. CRC Press, Boca Raton, FL.

**Bonasoro, F., M. D. Candia Carnevali, C. Moss, and M. C. Thorndyke. 1998.** Epimorphic versus morphalactic mechanisms in arm regeneration of crinoids and asteroids: pattern of cell proliferation and lineage. Pp. 13–18 in *Echinoderms*, R. Mooi and M. Telford, eds. Balkema, Rotterdam.

**Bosch, I. 1988.** Replication by budding in natural populations of bipinnaria larvae of the sea star genus *Luidia*. P. 728 in *Echinoderm Biology*, R. D. Burke, P. V. Mladenov, P. Lambert, and R. L. Parsley, eds. Balkema, Rotterdam.

**Bosch, I., R. B. Rivkin, and S. P. Alexander. 1989.** Asexual reproduction by oceanic planktotrophic echinoderm larvae. *Nature* **337:** 169–170.

**Cameron, R. A., and E. H. Davidson. 1991.** Cell type specification during sea urchin development. *Trends Genet.* **7:** 212–218.

**Cameron, R. A., B. R. Hough-Evans, R. J. Britten, and E. H. Davidson. 1987.** Lineage and fate of each blastomere of the sea urchin embryo. *Genes Dev.* **1:** 75–84.

**Candia Carnevali, M. D., and F. Bonasoro. 1994.** Mechanisms of arm regeneration in *Antedon mediterranea* (Echinodermata, Crinoidea). *Anim. Biol.* **3:** 83–88.

**Chia, F. S., and R. B. Burke. 1978.** Echinoderm metamorphosis: fate of larval structures. Pp. 219–234 in *Settlement and Metamorphosis of Marine Invertebrate Larvae*, F. S. Chia, ed. Elsevier, New York.

**Chia, F. S., C. Oguro, and M. Komatsu. 1993.** Sea-star (asteroid) development. *Oceanogr. Mar. Biol. Ann. Rev.* **31:**223–257.

**Clark, A. M., and M. E. Downey. 1992.** *Starfishes of the Atlantic.* Chapman and Hall, New York.

**Czihak, G. 1965.** Entwicklungsphysiologische Untersuchungen an Echiniden (Experimentelle Analyse der Coelomentwicklung). *Wilhelm Roux' Arch. Entwicklungsmech. Org.* **155:** 709–729.

**Davidson, E. H., K. Peterson, and R. A. Cameron. 1995.** Origin of the adult bilaterian body plans: developmental regulatory mechanisms. *Science* **270:** 1319–1325.

**Downey, M. E. 1973.** Starfishes from the Caribbean and the Gulf of Mexico. *Smithson. Contrib. Zool.* **126:** 1–158.

**Emson, R. H., and I. C. Wilkie. 1980.** Fission and autotomy in echinoderms. *Oceanogr. Mar. Biol. Ann. Rev.* **18:** 169–183.

**Goss, R. J. 1969.** *Principles of Regeneration.* Academic Press, London.

**Halanych, K. M., and Y. Passamaneck. 2001.** A brief review of metazoan phylogeny and future prospects in hox-research. *Am. Zool.* **41:** 629–639.

**Hopkins, P. M. 2001.** Limb regeneration in the fiddler crab, *Uca pugilator:* hormonal and growth factor control. *Am. Zool.* **41:** 389–398.

**Hörstadius, S. 1973.** *Experimental Embryology of Echinoderms.* Clarendon, Oxford.

**Jaeckle, W. B. 1994.** Multiple modes of asexual reproduction by tropical and subtropical sea star larvae: an unusual adaptation for genet dispersal and survival. *Biol. Bull.* **186:** 62–71.

**Jaeckle, W. B., and D. T. Manahan. 1989.** Growth and energy imbalance during the development of a lecithotrophic molluscan larva (*Haliotis rufescens*). *Biol. Bull.* **177:** 237–246.

**Jaeckle, W. B., and D. T. Manahan. 1992.** Experimental manipulations of the organic chemistry of seawater: implications for studies of energy budgets in marine invertebrate larvae. *J. Exp. Mar. Biol. Ecol.* **156:** 273–284.

**Kanatani, H. 1969.** Inducing of spawning and oocyte maturation by 1-methyladenine in starfishes. *Exp. Cell. Res.* **57:** 333–337.

**Levin, L. A., and T. S. Bridges. 1995.** Pattern and diversity in reproduction and development. Pp. 1–48 in *Ecology of Marine Invertebrate Larvae*, L. R. McEdward, ed. CRC Press, Boca Raton, FL.

**Manahan, D. T. 1990.** Adaptations by invertebrate larvae for nutrient acquisition from seawater. *Am. Zool.* **30:** 147–160.

**Marsh, A. G., R. Maxson, and D. T. Manahan. 2001.** High macromolecular synthesis with low metabolic cost in Antarctic sea urchin embryos. *Science* **291:** 1950–1952.

**Martin, P. 1997.** Wound healing—aiming for perfect skin regeneration. *Science* **276:** 75–81.

**Mattson, P. 1976.** *Regeneration.* Bobbs-Merrill, Indianapolis, IN.

**Menge, B. 1975.** Brood or broadcast? The adaptive significance of different reproductive strategies in two intertidal sea stars *Leptasterias hexactis* and *Pisaster ochraceus. Mar. Biol.* **31:** 87–110.

**McEdward, L. R., and D. A. Janies. 1993.** Life cycle evolution in asteroids: what is a larva? *Biol. Bull.* **184:** 255–268.

**Mladenov, P. V., and R. D. Burke. 1994.** Echinodermata: asexual propagation. Pp. 339–383 in *Reproductive Biology of Invertebrates*, K. G. Adiyodi and R. G. Adiyodi, eds. Oxford and IBH, New Delhi.

**Mortensen, T. H. 1921.** *Studies of the Development and Larval Forms of Echinoderms*, G. E. C. Gad, Copenhagen, Denmark.

**Mortensen, T. H. 1938.** Contributions to the study of the development and larval forms of echinoderms VI. *K. Dan. Vidensk. Selsk. Skr. Naturvid. Math. Afd.*, **Series 9:** 1–59.

**Nielsen, C. 2001.** *Animal Evolution: Interrelationships of the Living Phyla.* 2nd ed. Oxford University Press, Oxford.

**Pearse, J. S., J. B. McClintock, and I. Bosch. 1991.** Reproduction of Antarctic benthic marine invertebrates: tempos, modes, and timing. *Am. Zool.* **31:** 65–80.

**Peterson, K. J., R. A. Cameron, and E. H. Davidson. 1997.** Set-aside cells in maximal indirect development: evolutionary and developmental significance. *BioEssays* **19:** 623–631.

**Rao, P. S., K. H. Rao, and K. Shyamasundari. 1993.** A rare condition of budding in bipinnaria larva (Asteroidea). *Curr. Sci.* **65:** 792–793.

**Smiley, S. 1986.** Metamorphosis of *Stichopus californicus* (Echinodermata: Holothuroidea) and its phylogenetic implications. *Biol. Bull.* **171:** 611–631.

**Stephens, G. C. 1972.** Amino acid accumulation and assimilation in marine organisms. Pp. 155–184 in *Nitrogen Metabolism and the Environment.* J. W. Campbell and L. Goldstein, eds. Academic Press, New York.

**Stephens, G. C. 1981.** The trophic role of dissolved organic material. Pp. 271–291 in *Analysis of Marine Ecosystems,* A. L. Longhurst, ed. Academic Press, New York.

**Strathmann, M. F. 1987.** *Reproduction and Development of Marine Invertebrates of the Northern Pacific Coast.* University of Washington Press, Seattle, WA.

**Thorndyke, M. C., C.-W. Chen, C. Moss, M. D. Candi Carnevali, and F. Bonasoro. 1999.** Regeneration in echinoderms: cellular and molecular aspects. Pp. 159–164 in *Echinoderm Research,* M. D. Candi Carnevali and F. Bonasoro, eds. Balkema, Rotterdam.

**Vickery, M. C. L. 2001.** Development and utilization of a novel deuterostome model employing larval echinoderms for the study of regeneration genetics. Ph.D. Dissertation. The University of Alabama at Birmingham, Birmingham, AL.

**Vickery, M. S. 2002.** Comparative studies of regeneration and cloning in the planktotrophic larvae of echinoderms. Ph.D. Dissertation. The University of Alabama at Birmingham, Birmingham, AL.

**Vickery, M. S., and J. B. McClintock. 1998.** Regeneration in metazoan larvae. *Nature* **394:** 140.

**Vickery, M. C. L., M. S. Vickery, J. B. McClintock, and C. D. Amsler. 2001a.** Utilization of a novel deuterostome model for the study of regeneration genetics: molecular cloning of genes that are differentially expressed during early stages of larval asteroid regeneration. *Gene* **262:** 73–80.

**Vickery, M. C. L., M. S. Vickery, J. B. McClintock, and C. D. Amsler. 2001b.** Regeneration in echinoderm larvae. *Microsc. Res. Tech.* **55:** 464–473.

**Wray, G. A., and R. A. Raff. 1991.** The evolution of developmental strategy in marine invertebrates. *Tree* **6:** 45–54.

Reference: *Biol. Bull.* **203:** 134–143. (October 2002)

# Spermiogenesis and Modified Sperm Morphology in the "Seepworm" *Methanoaricia dendrobranchiata* (Polychaeta: Orbiniidae) From a Methane Seep Environment in the Gulf of Mexico: Implications for Fertilization Biology

KEVIN J. ECKELBARGER[1] AND CRAIG M. YOUNG[2]

[1]*Darling Marine Center, 193 Clark's Cove Road, Walpole, Maine 04573; and* [2]*Division of Marine Sciences, Harbor Branch Oceanographic Institution, 5600 U.S. 1 North, Ft. Pierce, Florida 34946*

**Abstract.** Spermatogenesis and mature sperm morphology have been described along with limited observations of the ovary in *Methanoaricia dendrobranchiata*, an orbiniid polychaete associated with dense populations of the mussel *Bathymodiolus childressi* at brine pools on the Louisiana slope, Gulf of Mexico. The species is gonochoric with gonads serially repeated in numerous segments and each associated with a nexus of blood vessels at the base of the parapodia. In the female, synchronous, intraovarian egg development occurs with the release from the ovary of large, yolky eggs into the coelom at first meiotic metaphase. Sperm develop in the coelom as free-floating, plasmodial clones interconnected *via* an anuclear cytophore. At the end of spermiogenesis, mature spermatozoa float freely in the coelom. The mature spermatozoon differs significantly from that of shallow-water orbiniid species by possessing an elongated nucleus and a greatly elongated and curved acrosome reaching 19.5 μm in length. The spermatozoon resembles an ent-aquasperm and may not fertilize the eggs directly in seawater in the classical manner. We hypothesize that the unusual spermatozoon morphology in this species has evolved due to the hypoxic environment in which the adults live and that fertilization biology is likely modified in some way to minimize sperm exposure to high levels of hydrogen sulfide. An analysis of life-history features in shallow-water orbiniids is used to infer reproductive features in *M. dendrobranchiata* that could not be directly documented.

Received 16 April 2002, accepted 10 July 2002.

## Introduction

The reproductive biology of invertebrates from deep-sea hydrothermal vents and cold methane seeps continues to receive a great deal of attention (Tyler and Young, 1999). Hydrothermal vents and cold-water methane seep habitats show significant ecological differences, and the two kinds of communities have few species in common (Tunnicliffe, 1991). There are, however, strong taxonomic affinities between seeps and vents, suggesting that divergent life-history features could evolve in closely related species. Studies on deep-sea polychaetes have been almost exclusively directed at hydrothermal vent species (reviewed in Eckelbarger *et al.*, 2001) and have included only 3 of 80 polychaete families. Polychaetes show a remarkable diversity of reproductive attributes and life-history features (Schroeder and Hermans, 1975; Wilson, 1991) and offer abundant opportunities to study the evolution of reproductive mechanisms. Despite the ecological importance of this group, the entire life history is known for only about 3% of known species (Giangrande, 1997). Recently, Eckelbarger *et al.* (2001) described the reproductive biology of the hesionid polychaete *Hesiocaeca methanicola*, the first such description for any methane-seep polychaete. A recent series of papers describes the reproductive biology of other methane-seep invertebrates from the Gulf of Mexico, including oogenesis (Eckelbarger and Young, 1997) and spermatogenesis (Hodgson *et al.*, 1998) in the neritid gastropod *Bathynerita naticoidea*, and gametogenesis in the seep mussel *Bathymodiolus childressi* (Eckelbarger and Young, 1999).

In contrast to studies of shallow-water invertebrates, studies of the reproductive biology of deep-sea species can be challenging, especially direct observations of spawning and fertilization. However, sperm ultrastructure can have predictive value in indirectly assessing possible fertilization mechanisms, because sperm morphology is highly correlated with the biology of fertilization (Franzen, 1956). Sperm structure is also widely used in the analysis of phylogenetic relationships within the Polychaeta (Rouse, 1995). It has been specifically noted that sperm ultrastructure from species occupying deep-sea reducing environments can be particularly revealing when compared to spermatozoa of related taxa from more conventional habitats (Beninger and Le Pennec, 1997).

During several submersible dives to the brine-pool methane seep at 650 m in the Gulf of Mexico, we encountered dense populations of a robust, unidentified polychaete living among individuals of *Bathymodiolus childressi,* a chemosynthetic mytilid bivalve, ringing a pool of hypersaline brine. The worms were observed extending the anterior portions of their bodies above the surrounding mussels into the overlying water, an unusual behavior in polychaetes. Low oxygen and high sulfide levels have been reported in this habitat (Smith *et al.*, 2000) and it is believed that the worms are subject to respiratory stress (Hourdez *et al.*, 2001). This specific hydrocarbon seep site was described previously by MacDonald *et al.* (1990) and MacDonald (1998). MacDonald *et al.* (1990) noted the presence of an "unidentified paranoid [*sic*] polychaete". Blake (2000) later described it as a new genus and species of orbiniid polychaete, *Methanoaricia dendrobranchiata* Blake 2000, and suggested that its unusual adult morphology may reflect adaptations to a hypoxic environment. A recent study concluded that this species differs from other orbiniids in several ways, including the presence of anterior hypertrophied gills (Hourdez *et al.*, 2001) that may be required in its oxygen-limited habitat. In our preliminary examination of the sperm of *M. dendrobranchiata,* we noted that the sperm heads were extremely long and sickle-shaped, an uncommon sperm morphology for any polychaete. In this paper, we describe the ultrastructural features of spermatogenesis and mature sperm morphology in *M. dendrobranchiata* and speculate on the phylogenetic and life-history significance of its occurrence in this unusual marine habitat.

## Materials and Methods

Living specimens of *Methanoaricia dendrobranchiata* were collected in August 1997 by the *Johnson-Sea-Link II* submersible from the "brine pool" at Green Canyon, MMS Block 232, in the Gulf of Mexico (MacDonald *et al.*, 1990) at 650-m depth (27°43.327′N, 91°16.606′W). The worms were found in dense mussel beds (*Bathymodiolus childressi*) within 1 m of the pool perimeter. Specimens were brought to the surface in carousel buckets on the submersible and immediately transferred to glass containers containing cold (8°C) filtered (45 $\mu$m) seawater in the walk-in cold room of the ship. The sex of specimens was determined by puncturing the body wall with a fine needle and examining the extruded coelomic contents under a compound microscope for the presence of sperm or eggs. Four females and ten males of varying lengths (10–15 cm) were selected for fixation. A razor blade was used to cut cross sections of 2–4 body segments containing coelomic sperm or ovaries. The tissue samples were immersed for 1.5 h in cold (4°C) primary fixative (2.5% glutaraldehyde buffered with 0.2 *M* sodium phosphate), and post-fixed for 1.5 h in room temperature 1% osmium textroxide buffered with 1.25% sodium bicarbonate. Tissue was then dehydrated in ascending concentrations of ethanol to 100%, followed by two changes with propylene oxide (3 min each), and embedded in Epon. Only thick sections were cut of females, but thin sections of males were cut with a diamond knife on a Porter-Blum MT2-B ultramicrotome, stained with uranyl acetate and lead citrate, and examined with a Zeiss EM 10A transmission electron microscope.

## Results

### *Female*

*Methanoaricia dendrobranchiata* is a gonochoric species, but the sexes cannot be distinguished externally. Although sperm development is the primary subject of this paper, we also made preliminary observations on female specimens, examining thick sections with a light microscope. Pairs of serially repeated ovaries are found in most segments and are associated with a nexus of blind-ending genital blood vessels at the base of the parapodia. Individual oocytes lie close to the blood vessels (Fig. 1), and thin follicle cells surround each oocyte. Oogenesis is intraovarian; developing oocytes remain within the ovary until at least the late stages of vitellogenesis, when they are released into the coelom. Sexually mature females were so packed with eggs that the coelomic spaces were nearly obliterated. In the specimens we examined, oogenesis was synchronous; the majority of oocytes were in late stages of vitellogenesis, although a few previtellogenic oocytes were observed. Most intraovarian oocytes contained a prominent germinal vesicle with a single eccentric nucleolus and relatively large amounts of lipid-type yolk stores (Fig. 2). Coelomic eggs measured about 280 $\mu$m, and all female specimens we examined showed evidence of germinal vesicle breakdown (Figs. 3, 4) indicating that prematuration has occurred and the primary oocytes have proceeded to first meiotic metaphase.

### *Male*

Germ cells enter the coelom in the early stages of spermatogenesis, and in all specimens examined, the coelomic

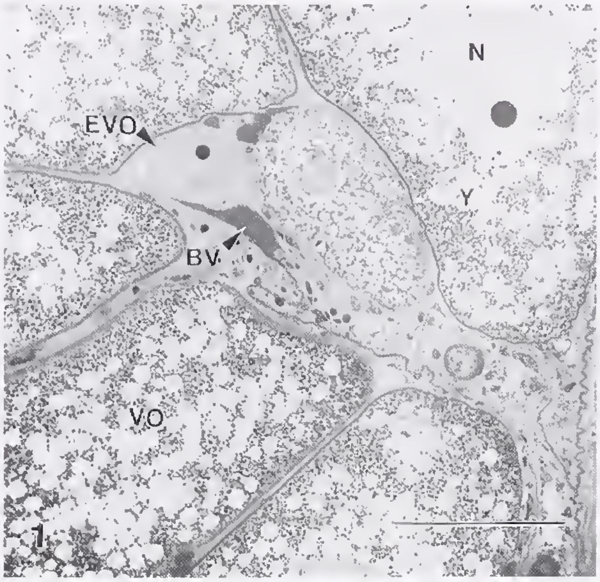

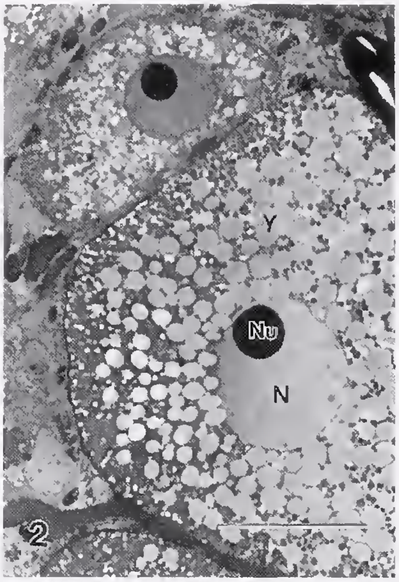

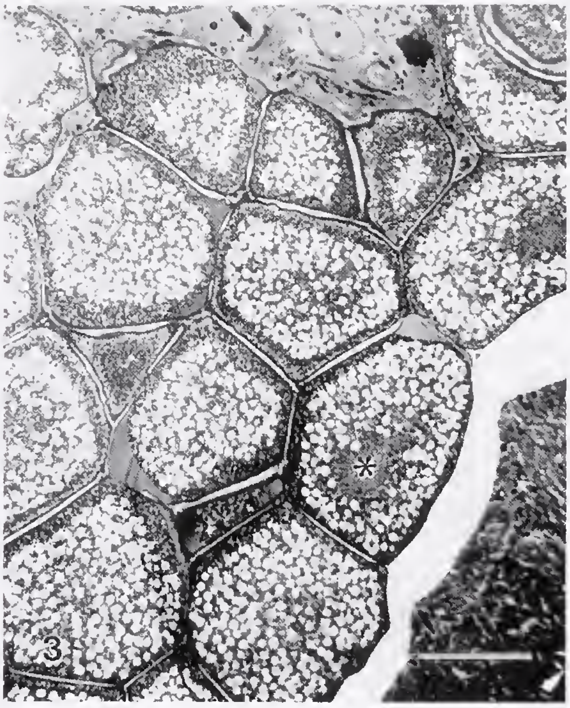

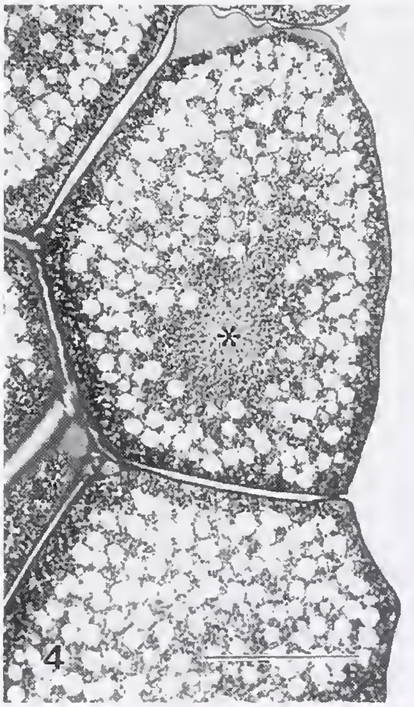

**Figure 1.** Light micrograph of ovary showing blood vessel (BV) surrounded by early vitellogenic oocyte (EVO) and large, vitellogenic oocytes (VO). N = nucleus; Y = yolk granule. Scale = 100 μm.

**Figure 2.** Close-up of oocyte containing nucleus (N), nucleolus (Nu), and yolk granules (Y). Scale = 75 μm.

**Figure 3.** Coelomic oocytes showing apparent germinal vesicle breakdown (*). Scale = 140 μm.

**Figure 4.** Close-up of coelomic oocyte showing germinal vesicle breakdown (*). Scale = 120 μm.

cavity was tightly packed with gametes in all stages of development (Fig. 5), including single, free-floating mature sperm (Figs. 5, 6). Sperm develop as disc-shaped, plasmodial clones (=sperm morulae) 30–40 μm in diameter consisting of 50–70 cells interconnected to a central, anucleate cytophore whose origin is unknown (Fig. 8). Gametogenic stages undergo synchronous development and remain associated with the morulae until late spermiogenesis, when mature sperm apparently detach and float individually in the coelomic fluid. Mitotic and meiotic cell divisions are readily apparent in histological section.

Spermatocytes are spherical cells about 8.0 μm in

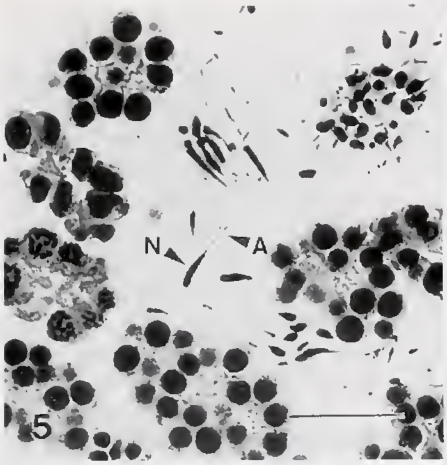

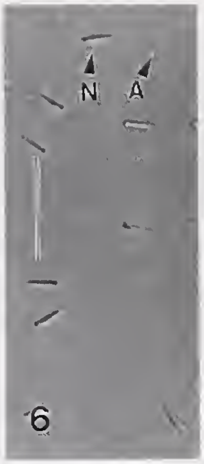

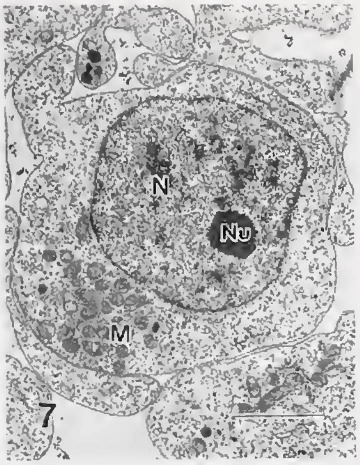

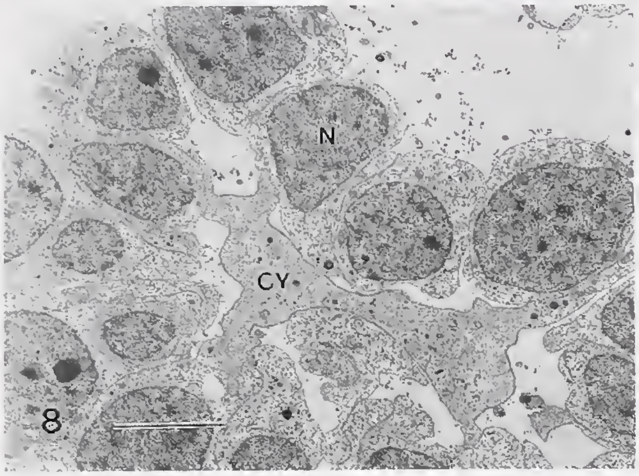

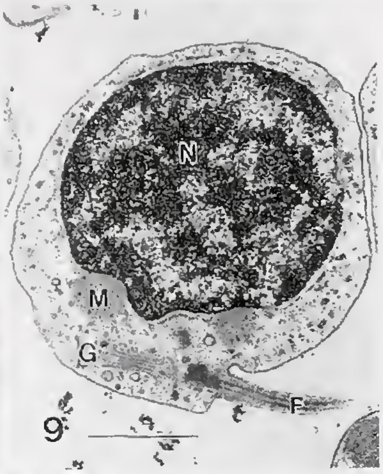

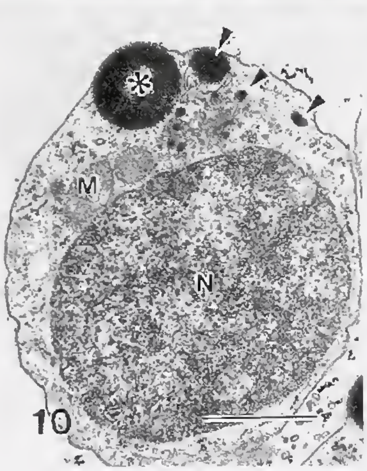

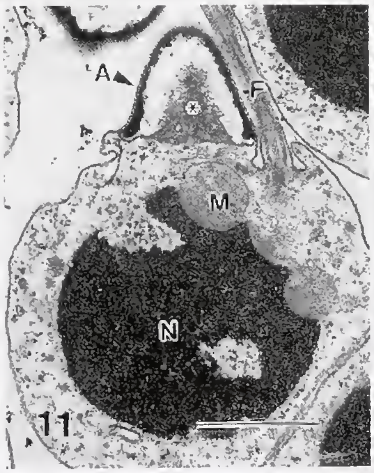

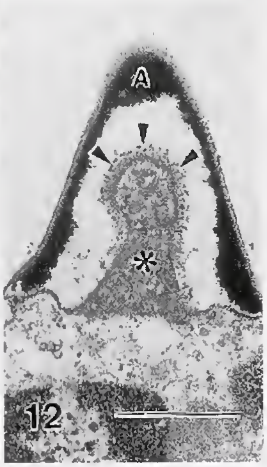

**Figure 5.** Light micrograph showing sperm and sperm morulae floating in coelom. The nucleus (N) and acrosome (A) of the coelomic sperm are evident. Scale = 20 $\mu$m.

**Figure 6.** Light micrograph of living sperm showing elongated nucleus (N) and acrosome (A). Scale = 20 $\mu$m.

**Figure 7.** Spermatocyte containing nucleus (N), nucleolus (Nu), and clustered mitochondria (M). Scale = 2.0 $\mu$m.

**Figure 8.** Sperm morula with central cytophore (CY) and attached spermatocytes with large nuclei (N). Scale = 4.0 $\mu$m.

**Figure 9.** Spermatid containing nucleus (N), mitochondria (M), Golgi complex (G), and flagellum (F). Scale = 2.0 $\mu$m.

**Figure 10.** Spermatid showing large (*) proacrosomal granule and adjacent smaller ones (arrowheads), mitochondria (M), and nucleus (N). Scale = 2.2 $\mu$m.

**Figure 11.** Spermatid showing acrosomal vesicle (A) with subacrosomal material (*). N, nucleus; M, mitochondrion; F, flagellum. Scale = 2.0 $\mu$m.

**Figure 12.** Spermatid acrosomal vesicle (A) with growing subacrosomal region consisting of an electron-dense outer region (arrowheads) and flocullent interior (*). Scale = 1.0 $\mu$m.

diameter containing large nuclei (dia. 5.5 μm) with finely diffuse heterochromatin and a single nucleolus (Figs. 7, 8). Their cytoplasm is devoid of organelles except for clusters of small perinuclear mitochondria (Fig. 7). Early spermatids have spherical nuclei (6.5 μm dia.) with lightly staining heterochromatin and small mitochondria positioned in shallow nuclear fossae at the future posterior pole of the cell (Fig. 9). A single Golgi complex is associated with a developing flagellum that projects at a 90° angle from the future anterior-posterior axis. The cytoplasm of early spermatids often contains a number of proacrosomal granules (Fig. 10) that later coalesce into a single organelle. As spermiogenesis progresses, chromatin condensation results in moderately dense, spherical nuclei (4.5 μm dia). A small cone-shaped acrosomal vesicle projects from the cell surface in close association with the flagellum and associated distal centriole (Fig. 11). As the acrosomal vesicle elongates, it tapers to a blunt tip and retains an electron dense appearance for approximately the anterior two-thirds of its length while the basal region contains a light staining flocculent subacrosomal material (Fig. 12). The elongating acrosomal vesicle remains at the posterior end of the cell until the late stages of spermiogenesis (Figs. 13–15), when it abruptly appears in the anterior region (Fig. 16). As it elongates, the subacrosomal component is clearly visible in the posterior region as a digitate, central projection that appears hollow in the anterior portion (Fig. 17). The flagellum still projects from the posterior region of the cell nearly 90° from the longitudinal axis (Fig. 18).

The mature spermatozoon has a small midpiece, an elongate, bullet-shaped nucleus 6.5 μm in length with a bulbous base and a gently curved anterior surface, and a gently curved, sickle-shaped acrosome about 19.5 μm in length, giving the sperm head a total length of about 26 μm (Figs. 19, 20). The acrosomal vesicle flares gently at its base (Fig. 21) and gradually tapers to a relatively blunt tip. Internally, the posterior region of the acrosome contains a solid cone-shaped mass of flocculent subacrosomal material that extends anteriorly within the acrosomal vesicle (Figs. 21–24). The subacrosomal material contains a centrally positioned rod-like structure that is more electron dense than the surrounding material and that projects anteriorly about 0.5 μm (Fig. 23). In the more anterior region of the acrosome, the subacrosomal material has a more filament-like substructure (Fig. 24). The midpiece contains six mitochondria positioned within shallow nuclear fossae (Fig. 28), and a centriolar complex and associated flagellum. In cross section, the distal centriole possesses radiating, satellite rays that extend to the adjacent cell plasmalemma and trifurcate to form a dense ring (Fig. 26). Whereas the distal centriole lies parallel with the longitudinal axis of the cell, the proximal centriole is laterally positioned at a 30° angle (Fig. 25). The two centrioles are joined by a flocculent satellite connector (Fig. 27).

We saw no evidence that mature sperm are concentrated in a particular region of the body prior to spawning (as, for example, in a nephridium), and we did not observe a seminal vesicle in any male specimen.

## Discussion

Orbiniid polychaetes are common infaunal residents of bays and estuaries throughout the world (Hartman, 1957) but are also represented in deep-sea hydrothermal vent communities (Tunnicliffe *et al.*, 1998). Limited information is available on the reproductive biology of shallow-water species (Anderson, 1961; Blake, 1980; Giangrande, 1997) (Table 1) and nothing is known about those from deep-water habitats. Orbiniids show a high degree of conservatism with respect to life-history features including annual, iteroparous breeding patterns; deposition of relatively large eggs in jelly masses or cocoons; lecithotrophic or nonpelagic development (Chapman, 1965; Anderson, 1961; Blake, 1980; Giangrande, 1997); and ect-aquasperm (*sensu* Rouse and Jamieson, 1987). On the basis of a study of *Nainereis laevigata* (Giangrande and Petraroli, 1991), our observations of *Methanoaricia dendrobranchiata* (present study), and previous studies of *Leitoscoloplos fragilis* (Eckelbarger, pers. obs.), we conclude that intraovarian oogenesis and ovaries associated with blood vessels are probably additional family traits.

Little is known about orbiniid spermatogenesis and sperm morphology except for a light microscopic study on *Nainereis laevigata* by Giangrande and Petraroli (1991), in which they reported developing coelomic sperm "platelets." Rice (1992) made some ultrastructural observations of mature sperm morphology for *Leitoscoloplos pugettensis* (=*Leitoscoloplos elongatus*). Both species have sperm of the ect-aquasperm type found in broadcast-spawning species; characteristics include a rounded head with a simple cap-like acrosome, four or five spherical mitochondria in the midpiece, and a tail with 9 + 2 arrangement of microtubules (Franzen, 1956). Rice (1992) noted that *Leitoscoloplos pugettensis* also possesses an eccentric flagellum, but we could not confirm this in *M. dendrobranchiata*. Ect-aquasperm are the most common sperm in the Polychaeta and are considered plesiomorphic for the group (Jamieson and Rouse, 1989). The presence of intracoelomic sperm morulae in both *M. dendrobranchiata* and *N. laevigata* suggests that this form of sperm differentiation is also a plesiomorphic feature. The shape of sperm morulae and the number of sperm they contain have proven useful characters for phylogenetic analysis (Rouse and Fitzhugh, 1994; Rouse, 1995).

The sperm head (nucleus plus acrosome) of *Methanoaricia dendrobranchiata* is curved, needle-like, and extraordinarily long, with the acrosome accounting for about two-thirds of the head length. The acrosome is among the

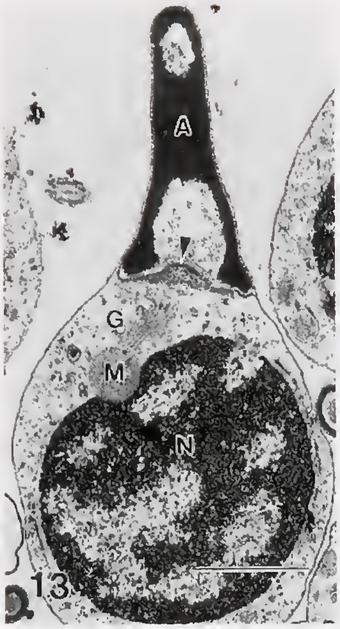

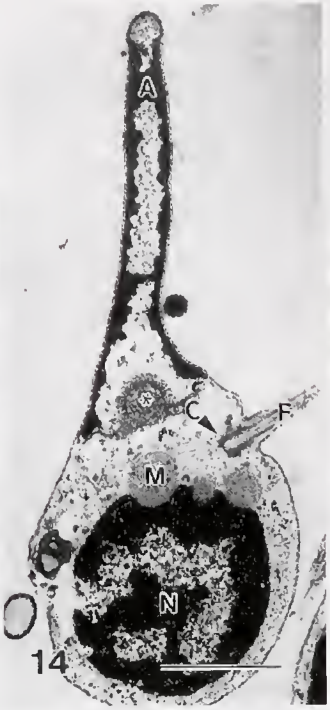

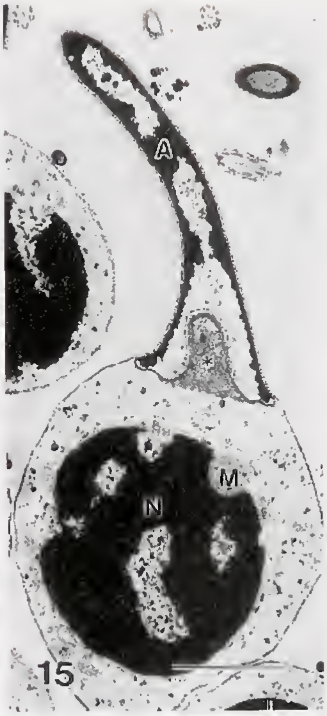

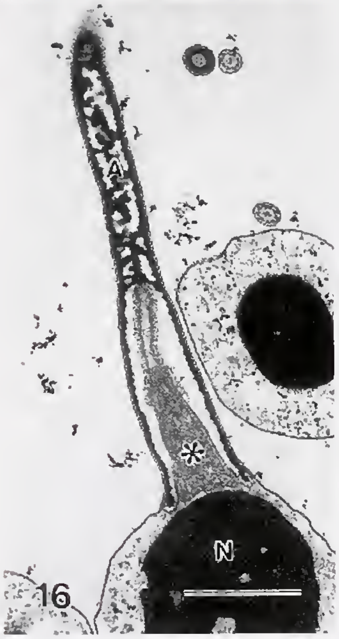

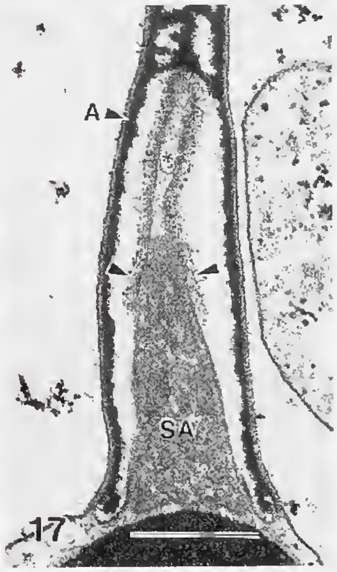

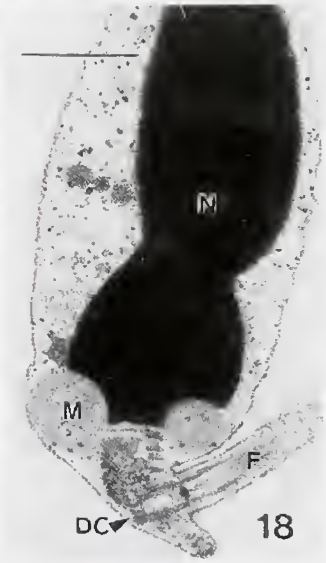

**Figure 13.** Spermatid with elongating acrosomal vesicle (A) and small subacrosomal material (arrowhead). N, nucleus; M, mitochondrion; G, Golgi complex. Scale = 2.0 μm.

**Figure 14.** Spermatid with acrosomal vesicle (A), subacrosomal material (*), flagellum (F) with associated centriole (C), mitochondrion (M), and nucleus (N). Scale = 2.0 μm.

**Figure 15.** Spermatid with acrosomal vesicle (A) and subacrosomal material (*). N, nucleus; M, mitochondrion. Scale = 2.0 μm.

**Figure 16.** Spermatid with acrosomal vesicle (A) and elongated subacrosomal material (*). N, nucleus. Scale = 2.0 μm.

**Figure 17.** Closeup of Fig. 16 showing features of subacrosomal (SA) region of acrosomal vesicle (A). Arrowheads indicate fuzzy external layer; note hollow anterior region (*). Scale = 1.0 μm.

**Figure 18.** Middlepiece region of sperm showing nucleus (N), mitochondria (M), and flagellum (F) and associated distal centriole (DC) that projects at a 90° angle. Scale = 2.0 μm.

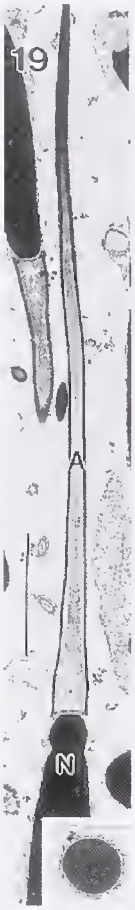

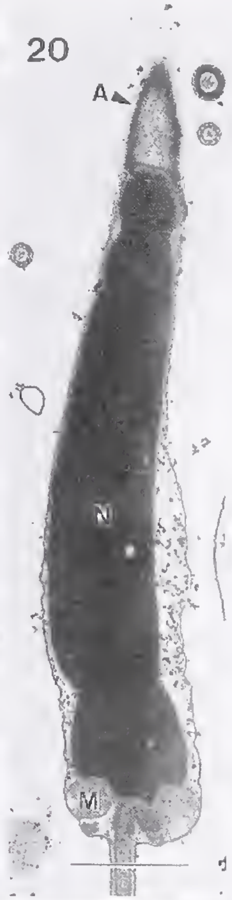

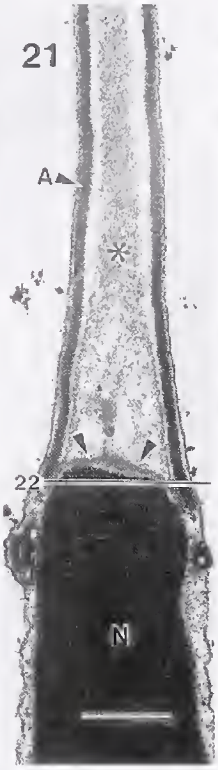

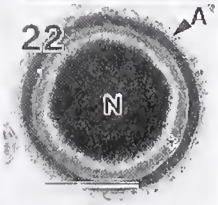

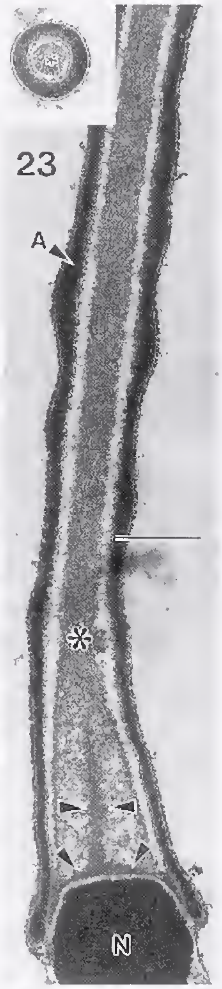

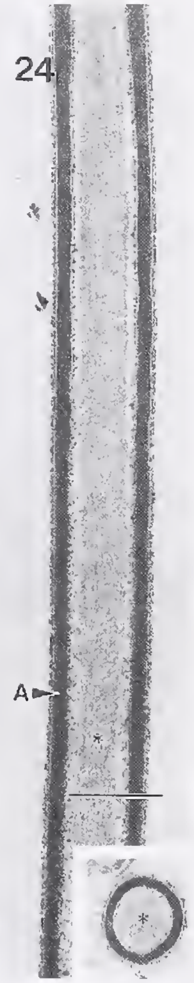

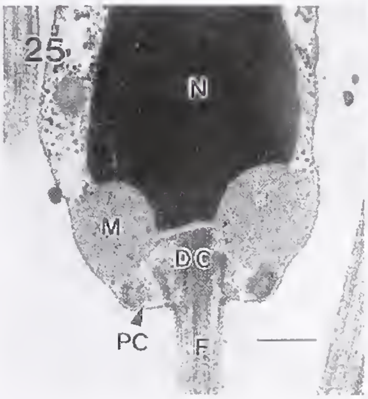

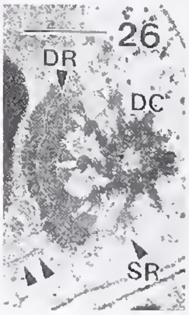

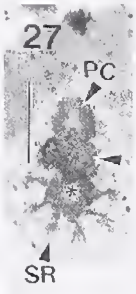

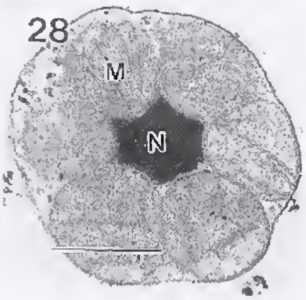

**Figure 19.** Mature spermatozoon showing elongated acrosome (A) and nucleus (N). Insert shows transverse section through anterior region of acrosome. Scale = 3.0 μm.

**Figure 20.** Nuclear (N) region of spermatozoon showing grazing section of anterior acrosomal vesicle (A). M, mitochondrion. Scale = 2.0 μm.

**Figure 21.** Posterior region of acrosomal vesicle (A) showing subacrosomal space consisting of dense basal plate (arrowheads) and flocculent interior (*). Scale = 1.5 μm.

**Figure 22.** Transverse section through region where acrosomal vesicle (A) meets the anterior nucleus (N) (see Fig. 21). Scale = 1.5 μm.

**Figure 23.** Posterior region of acrosomal vesicle (A) showing details of subacrosomal area including dense basal plate and digitate process in posterior region (arrowheads), and flocculent central region further anteriorly (*). N, nucleus. Insert shows transverse section through anterior acrosomal vesicle. Scale = 1.5 μm.

**Figure 24.** Anterior region of acrosomal vesicle (A) showing filamentous interior (*). Insert shows transverse section through vesicle. Scale = 1.5 μm.

**Table 1**

*Life-history traits of the Orbiniidae*

| Species | Periodicity | Egg Dia. | Pelagic Phase | Egg Mass | Citation |
|---|---|---|---|---|---|
| *Leitoscoloplos robustus* | ? | 160 | 3.5 days | No | Horn & Bookhout (1950) |
| *Leitoscoloplos kerguelensis* | ? | 200 | 3 days | Yes | Okuda (1946) |
| *Leitoscoloplos pugettensis* | ? | 210 | omitted or 1–9 days | Yes | Blake (1980) |
| *Scoloplos armiger* Type I | ? annual | 250 | omitted | Yes | Anderson (1959), Gibbs (1968), Thorson (1946) |
| *Scoloplos armiger* Type II | ? | 230 | ~10 days | Yes | Sveshnikov (1960) |
| *Scoloplos simplex* | ? | 150 | 5 days | Yes | Anderson (1961) |
| *Scoloplos acmeceps* | ? | 188–210 | ~20 days | No | Blake (1980) |
| *Phylo foetida foetida* | ? | ? | omitted | Yes | Salensky (1883) |
| *Phylo foetida atlantica* | ? | 200 | 9 days | No | Cazaux (1972) |
| *Naineris laevigata* | ? | 250 | 1.5 days | Yes | Okuda (1946), Strathmann (1987) |
| " " | annual | 240 | ? | Yes | Giangrande & Petraroli (1991) |
| *Microrbinia linea* | continuous? | 200–364 × 75–152 | ? | ? | Blake (1993) |
| *Methanoaricia dendrobranchiata* | ? | ~280 | ? | ? | Present study |

longest recorded for any polychaete spermatozoon and is certainly the longest for any large-bodied species. Of the 138 polychaete species for which Rice (1992) lists sperm dimensions, only 5% have acrosomes exceeding 10.0 μm—all of them from small-bodied, interstitial species in the family Protodrilidae. Protodrilid species in which fertilization occurs in the coelom of the female often transfer sperm *via* spermatophores, and they frequently have highly modified filiform introsperm (Jamieson and Rouse, 1989), one of which has an acrosome reaching 50.0 μm in length. The presence of such an unusually modified spermatozoon in *M. dendrobranchiata* is unexpected because orbiniids are traditionally considered to be broadcast spawners with simple ect-aquasperm. Ect-aquasperm have been described from three shallow-water orbiniids—*Nainereis laevigata* (Giangrande and Petraroli, 1991), *Leitoscoloplos pugettensis* (Rice, 1992), and *L. fragilis* (Eckelbarger, pers. obs.)—none of which has a modified acrosome. Blake (1993) described sperm with elongated heads measuring 8–10 μm in length from the continental slope orbiniid *Microrbinia linea*, although no details of acrosome length were noted. Large acrosomes have been reported in other polychaetes with introsperm as well as some ent-aquasperm and have been attributed to features of the egg (Jamieson and Rouse, 1989). In oligochaetes, Jamieson *et al.* (1983) clearly demonstrated a statistical correlation between sperm acrosome length and thickness of the vitelline envelope. However, Jamieson and Rouse (1989), using data from Eckelbarger and Grassle (1987a, b), found a high negative correlation between sperm acrosome length and egg dimensions in capitellid polychaetes. Franzen (1983) suggests that, in bivalves, the type of nuclear elongation seen in *M. dendrobranchiata* is correlated with egg size and lecithotrophic development.

We do not believe that acrosome elongation in *Methanoaricia dendrobranchiata* sperm is correlated with attributes of the egg, because the egg closely resembles that observed in two shallow-water orbiniids, *Leitoscoloplos pugettensis* (Rice, 1992) and *L. fragilis* (Eckelbarger, pers. obs.), both of which have ect-aquasperm with a simple cap-like acrosome. *M. dendrobranchiata* is an aerobic organism that thrives in a microhabitat that is both hypoxic and highly sulfidic (Smith *et al.*, 2000; Nix *et al.*, 1995). Its anterior gills are hypertrophied, apparently to facilitate gas exchange, and its gill cells contain many mitochondria and electron-dense organelles that may play a role in sulfide detoxification (Hourdez *et al.*, 2001). We suggest that the unusual sperm morphology observed in this species is an indication that fertilization does not occur through simple broadcast spawning into seawater, but rather by some mech-

**Figure 25.** Midpiece of spermatozoon showing nucleus (N), mitochondria (M), distal (DC) and proximal (PC) centrioles and associated flagellum (F). Scale = 1.0 μm.

**Figure 26.** Pericentriolar complex of spermatozoon showing distal centriole (DC) with satellite rays (SR) attaching to dense ring-like structure (DR) and microtubules extending to the nucleus (arrowheads). Scale = 0.8 μm.

**Figure 27.** Proximal centriole (PC) attached to distal centriole (*) *via* a satellite connector (arrowhead). Note satellite rays (SR) projecting from distal centriole. Scale = 1.0 μm.

**Figure 28.** Transverse section through spermatozoon midpiece showing mitochondria (M) encircling the basal region of the nucleus (N). Scale = 1.0 μm.

anism that limits exposure of gametes to high sulfide levels. Roughly half of the orbiniid species studied to date release their eggs into jelly-coated egg masses or cocoons (reviewed by Blake, 1996), so it is possible that *M. dendrobranchiata* also protects its eggs from the sulfide environment with a jelly mass. This would probably require that the sperm penetrate a matrix in the egg mass to achieve fertilization. It is also conceivable that the jelly used to form the cocoon is chemically distinct from that used by related species in nonsulfide environments. To our knowledge, Blake (1980) is the only worker to have observed spawning in any orbiniid. He described egg release and cocoon formation in *Leitoscoloplos pugettensis* but did not observe sperm release. Although copulation (De Groot, 1907) and pseudocopulation (Anderson, 1959) have been proposed for other orbiniids, Chapman (1965) suggested that males and females come into close association during spawning and that eggs are fertilized as they emerge along with the jelly secretions. We view this as a likely scenario for *M. dendrobranchiata*. We also noted that all of the coelomic eggs in the females of *M. dendrobranchiata* that we examined had undergone germinal vesicle breakdown, indicating that the eggs had proceeded to first meiotic metaphase and were ready for fertilization. Polychaete eggs undergo fertilization either before or after germinal vesicle breakdown, and this "prematuration" event can occur before or after spawning (reviewed in Schroeder and Hermans, 1975). Intracoelomic germinal vesicle breakdown may indicate that fertilization occurs quickly after egg release as a way to minimize egg exposure to sulfides.

Until more is known about spawning behavior, we would categorize the sperm of *M. dendrobranchiata* as a putative ent-aquasperm (*sensu* Jamieson and Rouse, 1989), unlike the ect-aquasperm of other orbiniids previously described. Ent-aquasperm may swim freely in seawater at some stage or they may be stored by the female or reach the female *via* spermatozeugmata or spermatophores prior to fertilization (Rouse and Fitzhugh, 1994). They may be significantly modified from the basic plesiosperm type, and they appear in species with poorly motile females that produce large, yolky eggs (Jamieson and Rouse, 1989). For example, the sperm of the sabellid *Perkinsiana rubra* has a round nucleus but an extremely long acrosome (Chughtai, 1986). Knight-Jones and Bowden (1984) reported specimens of *P. antarctica* brooding embryos in the branchial crown. The spermatozoon of this species has been classified as an ent-aquasperm on the basis of ultrastructural criteria and the fact that it likely encounters the eggs in a jelly mass in the crown (Rouse, 1992; Rouse and Fitzhugh, 1994). We are certain that spermatozeugmata are not employed in *M. dendrobranchiata*, because mature sperm are free in the coelom prior to spawning. Sperm storage, spermatophores, or both might be employed, but we have no direct evidence of this.

Reproductive studies of deep-sea species are often difficult because seasonal sampling and direct observation of spawning behavior and fertilization may be impossible. For this reason, an analysis of reproductive and life-history features of shallow-water relatives can be useful as a means of inferring these features in related deep-sea species. In a recent paper describing gametogenesis, spawning behavior, and early development in another methane-seep polychaete, *Hesiocaeca methanicola* (Eckelbarger *et al.*, 2001), we applied "phylogenetic inference" as a means of predicting life-history features that are difficult to document directly. In his description of *Methanoaricia dendrobranchiata*, Blake (2000) stated that this species is difficult to place in any known polychaete family, but it has more affinities to the Orbiniidae than any other. The present study documents several reproductive features of *M. dendrobranchiata* that are shared with other orbiniids: (1) repeated ovaries in a large number of segments, (2) an ovary associated with a blood vessel nexus, (3) intraovarian oogenesis, (4) large, yolky eggs, (5) sperm developing as coelomic clones, and (6) mature spermatozoa with a similar centriolar satellite complex and subacrosomal material. On the basis of the life histories of other orbiniids (summarized in Table 1), we predict that *M. dendrobranchiata* is an annual, iteroparous breeder that produces an egg mass or cocoon.

## Acknowledgments

We thank the crews of the research vessel *Edwin Link* and the *JSL II* submersible of Harbor Branch Oceanographic Institution. This work was supported by grant no. 9539 from the NOAA National Underwater Research Program at the Univ. of North Carolina at Wilmington and grant no. OCE-9619606 from the National Science Foundation.

## Literature Cited

**Anderson, D. T. 1959.** The embryology of the polychaete *Scoloplos armiger*. *Q. J. Microsc. Sci.* **100:** 89–166.

**Anderson, D. T. 1961.** The development of the polychaete *Haploscoloplos fragilis*. *Q. J. Microsc. Sci* **102:** 257–272.

**Beninger, P. G., and M. Le Pennec. 1997.** Reproductive characteristics of a primitive bivalve from a deep-sea reducing environment: giant gametes and their significance in *Acharx alinae* (Cryptodonta: Solemyidae). *Mar. Ecol. Prog. Ser.* **157:** 195–206.

**Blake, J. A. 1980.** The larval development of polychaeta from the northern California coast. IV. *Leitoscoloplos pugettensis* and *Scoloplos acmeceps* (Family Orbiniidae). *Ophelia* **19:** 1–18.

**Blake, J. A. 1993.** Life history analysis of five dominant infaunal polychaete species from the continental shelf off North Carolina. *J. Mar. Biol. Assoc. UK* **73:** 123–141.

**Blake, J. A. 1996.** Family Orbiniidae Hartman, 1942. Pp. 1–26 in *Taxonomic Atlas of the Benthic Fauna of the Santa Maria Basin and Western Santa Barbara Channel*. J.A. Blake, J.A. Hilbig, and P.H. Scott, eds. Santa Barbara Museum of Natural History, Santa Barbara, CA.

**Blake, J. A. 2000.** A new genus and species of polychaete worm (Family Orbiniidae) from methane seeps in the Gulf of Mexico. With a review of the systematics and phylogenetic interrelationships of the genera of Orbiniidae. *Cah. Biol. Mar.* **41:** 435–449.

**Cazaux, C. 1972.** Développment larvaire d'annélides polychaètes (Bassin d'Arcachon). *Archs. Zool. Exp. Gén.* **113:** 71–108.

**Chapman, G. 1965.** The egg cocoons of *Scoloplos armiger* O.F. Müller. *Biol. Bull.* **128:** 189–197.

**Chughtai, I. 1986.** Fine structure of spermatozoa in *Perkinsiana rubra* and *Pseudopotamilla reniformis* (Sabellidae: Polychaeta). *Acta Zool.* **67:** 165–171.

**De Groot, G. J. 1907.** Aanteekeningen over de ontwikkeling van *Scoloplos armiger*. Dissertation. Leiden. 74 pp.

**Eckelbarger, K. J., and J. P. Grassle. 1987a.** Spermatogenesis, sperm storage and comparative sperm morphology in nine species of *Capitella, Capitomastus* and *Capitellides* (Polychaeta: Capitellidae). *Mar. Biol.* **95:** 415–429.

**Eckelbarger, K. J., and J. P. Grassle. 1987b.** Interspecific variation in genital spine, sperm, and larval morphology in six sibling species of *Capitella*. *Bull. Biol. Soc. Wash.* **7:** 62–76.

**Eckelbarger, K. J., and C. M. Young. 1997.** Ultrastructure of the ovary and oogenesis in the methane-seep mollusc, *Bathynerita naticoidea* (Gastropoda: Neritidae) from the Louisiana slope. *Invertebr. Biol.* **116:** 299–312.

**Eckelbarger, K. J., and C. M. Young. 1999.** Ultrastructure of gametogenesis in a chemosynthetic mytilid bivalve (*Bathymodiolus childressi*) from a bathyal, methane seep environment (northern Gulf of Mexico). *Mar. Biol.* **135:** 635–646.

**Eckelbarger, K. J., C. M. Young, E. Ramirez Llodra, S. Brooke, and P. A. Tyler. 2001.** Gametogenesis, spawning behavior, and early development in the "iceworm" *Hesiocaeca methanicola* (Polychaeta: Hesionidae) from methane hydrates in the Gulf of Mexico. *Mar. Biol.* **138:** 761–775.

**Franzen, A. 1956.** On spermiogenesis, morphology of the spermatozoon, and biology of fertilization among invertebrates. *Zool. Bidr. Upps.* **31:** 355–482.

**Franzen, A. 1983.** Ultrastructural studies of spermatozoa in three bivalve species with notes on evolution of elongated sperm nucleus in primitive spermatozoa. *Gamete Res.* **7:** 199–214.

**Giangrande, A. 1997.** Polychaete reproductive patterns, life cycles and life histories: an overview. *Ocean. Mar. Biol. Ann. Rev.* **35:** 323–386.

**Giangrande, A., and A. Petraroli. 1991.** Reproduction, larval development and post-larval growth of *Naineris laevigata* (Polychaeta, Orbiniidae) in the Mediterranean Sea. *Mar. Biol.* **111:** 129–137.

**Gibbs, P. E. 1968.** Observations on the populations of *Scoloplos armiger* at Whitstable. *J. Mar. Biol. Assoc. UK* **48:** 225–254.

**Hartman, O. 1957.** Orbiniidae, Apistobranchidae, Paraonidae and Longosomidae. *Allan Hancock Pacific Expeditions* 15 (3): 211–393. University of Southern California Press, Los Angeles.

**Hodgson, A. N., K. J. Eckelbarger, and C. M. Young. 1998.** Sperm morphology and spermiogenesis in the methane-seep mollusc *Bathynerita naticoidea* (Gastropoda: Neritacea) from the Louisiana slope. *Invertebr. Biol.* **117:** 199–207.

**Horn, E. C., and C. G. Bookhout. 1950.** The early development of *Haploscoloplos robustus* (Eisig). *J. Elisha Mitchell Sci. Soc.* **66:** 1–66.

**Hourdez, S., L.-A. Frederick, A. Schernecke, and C. R. Fisher. 2001.** Functional respiratory anatomy of a deep-sea orbiniid polychaete from the Brine Pool NR-1 in the Gulf of Mexico. *Invertebr. Biol.* **120:** 29–40.

**Jamieson, B. G. M., and G. W. Rouse. 1989.** The spermatozoa of the Polychaeta (Annelida): an ultrastructural review. *Biol. Rev. Camb. Philos. Soc.* **64:** 93–157.

**Jamieson, B. G. M., K. S. Richards, T. P. Fleming, and C. Erséus. 1983.** Comparative morphometrics of oligochaete spermatozoa and egg-acrosome correlations. *Gamete. Res.* **8:** 149–169;

**Knight-Jones, P., and N. Bowden. 1984.** Incubation and scissiparity in Sabellidae (Polychaeta). *J. Mar. Biol. Assoc. UK* **64:** 809–818.

**MacDonald, I. R. 1998.** Habitat formation in the Gulf of Mexico hydrocarbon seeps. *Cah. Biol. Mar.* **39:** 337–340.

**MacDonald, I. R., J. F. Reilly II, N. L. Guinasso, J. M. Brooke, R. S. Carney, W. A. Bryant, and T. J. Bright. 1990.** Chemosynthetic mussels at a brine-filled pockmark in the Northern Gulf of Mexico. *Science* **248:** 1096–1098.

**Nix, E. E., C. R. Fisher, J. Vodenichar, and K. M. Scott. 1995.** Physiological ecology of a mussel with methanotrophic endosymbionts at three hydrocarbon seep sites in the Gulf of Mexico. *Mar. Biol.* **122:** 605–617.

**Okuda, S. 1946.** Studies on the development of the Annelida Polychaeta. *J. Fac. Sci. Hokkaido Univ.* **9:** 115–219.

**Rice, S. A. 1992.** Polychaeta: Spermatogenesis and spermiogenesis. Pp. 129–151 in *Microscopic Anatomy of Invertebrates, Vol. 7, Annelida*, F.W Harrison and S.L Gardner eds. Wiley-Liss, New York.

**Rouse, G. W. 1992.** Ultrastructure of spermiogenesis and spermatozoa of four *Oriopsis* species (Sabellinae, Sabellidae, Polychaeta). *Zool. Scr.* **21:** 363–379.

**Rouse G. W. 1995.** Is sperm ultrastructure useful in polychaete systematics? An example using 20 species of the Fabriciinae (Polychaeta: Sabellidae). *Acta Zool.* **76:** 57–74.

**Rouse, G. W., and K. Fitzhugh. 1994.** Broadcasting fables: is external fertilization really primitive? Sex, size, and larvae in sabellid polychaetes. *Zool. Scr.* **23:** 271–312.

**Rouse, G. W., and B. G. M. Jamieson. 1987.** An ultrastructural study of the spermatozoa of the polychaetes *Eurythoe complanata* (Amphinomidae), *Clymenella laseroni* and *Micromaldane laseroni* (Maldanidea) with definition of sperm types in relation to reproductive biology. *J. Submicrosc. Cytol.* **19:** 573–584.

**Salensky, W. 1883.** Etude sur le développement des Annélides. Premiere partie. III *Pileolaria, Aricia, Terebella. Arch. Biol. Paris* **4:** 188–220.

**Schroeder, P. C., and C. O. Hermans. 1975.** Annelida: Polychaeta. Pp. 1–213 in *Reproduction of Marine Invertebrates*, Vol. 3., A.C. Giese and J.S. Pearse, eds. Academic Press, New York.

**Smith, E. B., K. M. Scott, E. R. Nix, C. Korte, and C. R. Fisher. 2000.** Growth and condition of seep mussels (*Bathymodiolus childressi*) at a Gulf of Mexico brine pool. *Ecology* **81:** 2392–2403.

**Strathmann, M. F. 1987.** *Reproduction and Development of Marine Invertebrates of the Northern Pacific Coast.* University of Washington Press, Seattle.

**Sveshikov, V. A. 1960.** Pelagic larvae of some Polychaeta in the White Sea. *Zool. Zh.* **39:** 345–355. (in Russian)

**Thorson, G. 1946.** Reproduction and larval development of Danish marine bottom invertebrates, with special reference to the planktonic larvae in the South (Øresund). *Medd. Komm. Dan. Fisk. Havund. Serie Plankton* **4:** 1–523.

**Tunnicliffe, V. 1991.** The biology of hydrothermal vents: ecology and evolution. *Oceanogr. Mar. Biol. Ann. Rev.* **29:** 319–407.

**Tunnicliffe, V., A. G. McArthur, and D. McHugh. 1998.** A biogeographical perspective of the deep-sea hydrothermal vent fauna. *Adv. Mar. Biol.* **34:** 355–46.

**Tyler, P. A., and C. M. Young. 1999.** Reproduction and dispersal at vents and cold seeps. *J. Mar. Biol. Assoc. UK* **79:** 193–208.

**Wilson, W. H. 1991.** Sexual reproductive modes in polychaetes: classification and diversity. *Bull. Mar. Sci.* **48:** 500–516.

Reference: *Biol. Bull.* **203:** 144–151. (October 2002)

# Swimming Behavior of the Nudibranch *Melibe leonina*

K. A. LAWRENCE* AND W. H. WATSON III‡

*Zoology Department & Center for Marine Biology, University of New Hampshire, Durham, New Hampshire 03824; and Friday Harbor Laboratories, University of Washington, Friday Harbor, Washington 98250*

**Abstract.** Swimming in the nudibranch *Melibe leonina* consists of five types of movements that occur in the following sequence: (1) withdrawal, (2) lateral flattening, (3) a series of lateral flexions, (4) unrolling and swinging, and (5) termination. *Melibe* swims spontaneously, as well as in response to different types of aversive stimuli. In this study, swimming was elicited by contact with the tube feet of the predatory sea star *Pycnopodia helianthoides*, pinching with forceps, or application of a 1 *M* KCl solution. During an episode of swimming, the duration of swim cycles (2.7 ± 0.2 s [mean ± SEM], $n = 29$) and the amplitude of lateral flexions remained relatively constant. However, the latency between the application of a stimulus and initiation of swimming was more variable, as was the duration of an episode of swimming. For example, when touched with a single tube foot from a sea star ($n = 32$), the latency to swim was 7.0 ± 2.4 s, and swimming continued for 53.7 ± 9.4 s, whereas application of KCl resulted in a longer latency to swim (22.3 ± 4.5 s) and more prolonged swimming episodes (174.9 ± 32.1 s). Swimming individuals tended to move in a direction perpendicular to the long axis of the foot, which propelled them laterally when they were oriented with the oral hood toward the surface of the water. The results of this study indicate that swimming in *Melibe*, like that in several other molluscs, is a stereotyped fixed action pattern that can be reliably elicited in the laboratory. These characteristics, along with the large identifiable neurons typical of many molluscs, make swimming in this nudibranch amenable to neuroethological analyses.

## Introduction

Swimming is a common form of locomotion in marine gastropods. It has been described for at least 47 species (reviewed by Farmer, 1970), and the neural mechanisms underlying swimming have been investigated in detail in four of these: *Pleurobranchaea californica* (Jing and Gillette, 1995, 1999), *Tritonia diomedea* (Willows *et al.*, 1973; Hume *et al.*, 1982; Getting, 1983), *Clione limacina* (Arshavsky *et al.*, 1985; Satterlie, 1985, 1991; Satterlie and Spencer, 1985; Satterlie *et al.*, 1985; Satterlie and Norekian, 1996), and *Aplysia brasiliana* (von der Porten *et al.*, 1982; McPherson and Blankenship, 1991a,b). In general, both rhythmic swimming and fictive swimming in molluscs are highly stereotyped and reliably expressed in intact and semi-intact preparations, as well as in isolated ganglia. These characteristics of molluscan swimming, combined with the suitability of their nervous systems for neurophysiological experimentation (Willows, 1965), have allowed scientists to elucidate some of the fundamental neural mechanisms responsible for producing swimming and other rhythmic behaviors (reviewed in Audesirk and Audesirk, 1985; Getting, 1989).

In opisthobranchs, five general types of swimming have been described, but only three types are common (Farmer, 1970): (1) parapodial or mantle flapping (as in *Gasteropteron*, *Hexabranchus*, and *Aplysia*); (2) dorsoventral undulation (as in *Tritonia* and *Pleurobranchaea*); and (3) lateral bending (as in *Dendronotus*). Of the 47 swimming species listed by Farmer (1970), 21 swim by flapping either the mantle or some part of the foot, 5 swim using dorsoventral undulation, and 18 swim using lateral flexions. The latter is the most common type used by aeolidaceans and dendronotaceans. Lateral-bending swimming in these animals does not seem to propel them in a particular direction; rather, it appears as if swimming moves these animals into the water

---

Received 7 November 2001; accepted 28 June 2002.

* Current address: Highline Community College, 2400 S. 240th Street, P.O. Box 98000, Des Moines, WA 98198-9800.

‡ To whom correspondence should be addressed. E-mail: win@unh.edu

column where the current may carry them away from potential predators.

Thompson (1976) hypothesized that swimming in opisthobranchs evolved as a means of escape. For most of the species studied, this seems to be a feasible explanation, since swimming can be elicited by noxious stimuli such as strong tactile stimulation or contact with a potential predator (Mauzey *et al.*, 1968; Edmunds, 1968; Farmer, 1970; Willows *et al.*, 1973; Page, 1993). Some animals, such as *T. diomedea*, apparently swim solely as a means of escape (Willows *et al.*, 1973). In others, such as *A. brasiliana*, which has no known predators, swimming is fairly directional and may serve a migratory role (Hamilton and Ambrose, 1975).

Studies of the opisthobranch *Melibe leonina* offer conflicting hypotheses as to the function and general characteristics of swimming behavior in this species. In one of the earliest papers on the subject, Agersborg (1921) states that the position of animals during a swimming episode may vary from dorsal aspect up to ventral aspect up. He further notes that swimming seems to be correlated with copulating masses of animals, suggesting that it may be a voluntary method for finding mates. In the same paper, Agersborg also refers to a method of "falling" through the water column, by completely relaxing the body musculature, which looks like "a feigned death." Hurst (1968) briefly describes the swimming behavior of this species as occurring only dorsal aspect up, and does not mention the ecological significance of the behavior. Farmer (1970) concluded that *Melibe* uses swimming to move from one kelp blade to the next. Most recently, Bickell-Page (1991; Page, 1993) suggested that swimming is an escape response. However, it is unclear which organisms in the natural habitat of *Melibe* might elicit escape swimming. Mauzey *et al.* (1968) and Bickell-Page (1991) have observed the sea star *Crossaster papposus* eating *Melibe*, and Ajeska and Nybakken (1976), Mauzey *et al.* (1968), and Bickell-Page (1991) have reported that several crab species, including *Pugettia producta*, will capture and eat *Melibe*. In contrast, it has also been reported that several species of sea stars avoid *Melibe*, presumably because they find the secretions of its repugnatorial gland repulsive (Ajeska and Nybakken, 1976; Bickell-Page, 1991). One goal of this study was to determine if *Melibe* would swim in response to these potential predators, which would indicate that one function of swimming in this species is escape.

In this paper we present results from three types of experiments concerned with swimming behavior in *M. leonina*. First, we analyzed swimming in 29 animals to enhance our understanding of the behavior and to quantify the various components of the swim. Second, we sought to determine the types of stimuli and potential predators that elicit swimming. Third, we assessed the movement of animals through the water column to determine whether swimming propels animals in random directions or predictable ones. We found that swimming in *Melibe* is a stereotyped rhythmic behavior that is most readily elicited in the laboratory by touching animals with the tube feet of the predatory sea star *Pycnopodia helianthoides*. Furthermore, what appears to be random motion during swimming has a fairly predictable directional component, with an animal typically moving in a path perpendicular to the long axis of its foot. These studies clarify some controversial issues concerning the swimming behavior of *M. leonina* and lay the framework for the neurophysiological studies presented in the subsequent paper (Watson *et al.*, 2002).

## Materials and Methods

### *Animals*

Specimens of the nudibranch *Melibe leonina* (Gould, 1852) were collected during May and June of 1994 and January through June of 1995 in sheltered bays throughout the San Juan Archipelago, Washington. Collections were made by scuba divers and the animals were maintained in flow-through seawater tables, typically between 10 and 12° C, at the University of Washington's Friday Harbor Laboratories. Animals were provided with blades of eelgrass (*Zostera marina*) to crawl upon, and they fed on planktonic crustaceans from the unfiltered water supply, supplemented with *Artemia* nauplii twice weekly.

### *Analysis of normal swimming*

We analyzed the progression of a complete bout of swimming (from initiation to termination) in 29 animals. Each animal was placed in a 50-l aquarium with a small amount of eelgrass. Swimming was initiated by using a 3-ml syringe without a needle to apply 1 ml of 1 *M* KCl to the skin of either the oral hood or body wall. Not every animal responded to the salt stimulus. Our analyses are based on the 29 animals that swam. The following parameters were then measured: (1) latency between application of the stimulus and initiation of the swim; (2) swim duration; (3) number of complete swim cycles in each swimming episode; (4) average swim cycle duration (duration of an episode divided by the number of swim cycles); and (5) direction (right or left) of the first and last flexions. Finally, for one animal, we measured the duration of each individual swim cycle from a videotape of a complete swim episode. All averages are presented as the mean ± SEM.

To assess the magnitude of lateral flexions throughout the course of a swim, three animals were videotaped while they swam in place and the tapes were digitized for measurement of flexion angles. Two loops of 4-0 surgical silk were attached to the middle of the body wall of each animal, one on either side, at the point where their body pivots during swimming. After one day of recovery, animals were individually suspended by these loops, ventral aspect up, in an acrylic plastic chamber. The chamber was supplied with a continuous flow of natural seawater so that it remained at 10–12° C. A video camera was mounted above the chamber, and the output of the camera was recorded onto videotape. Swimming was induced by dislodging the foot of the animal from its attachment to the surface tension of the water in the chamber. The video recordings were digitized, one frame/second, and version 1.55 of the public domain NIH Image software program (developed at the U.S. National Institutes of Health and available on the Internet at ⟨http://rsb.info.nih.gov/nih-image/⟩) was used to measure changes in the angle of the portion of the body anterior to the pivot point, relative to the region of the body posterior to that point.

### *Stimuli that elicit swimming*

Different stimuli were applied to animals to determine their effectiveness in eliciting swimming behavior. The stimuli included (1) pinching of the cerata with self-closing forceps; (2) prodding of the foot with a glass rod; (3) application of a 1 *M* KCl solution to the oral hood or body wall; and (4) presence of, or contact with, potential natural predators (sea stars—*Pycnopodia helianthoides, Henricia leviuscula, Pisaster* spp; crabs—*Cancer magister, Scyra acutifrons, Oregonia gracilis, Cancer productus;* and an anemone found on eelgrass—*Epiactus prolifera*). In each experiment, the stimulus was given at time zero, and the latency to swim and the duration of any ensuing swim episodes were recorded. In the sea star contact experiments, a single tube foot was excised from a live sea star, held in self-closing forceps, and brought into contact with the back of the oral hood of a specimen of *Melibe*.

To determine if certain animals commonly found in the natural habitat (eelgrass beds) of *Melibe* were potential predators, we performed a series of predation experiments. Individual *Pycnopodia, Epiactus,* or crabs were placed in a 50-l aquarium with flow-through seawater. Then one specimen of *Melibe* was placed in the tank, which also contained a small amount of eelgrass, and left there for 24 h. Every 6–8 h the nudibranch was examined for evidence of an attack. Three trials were carried out with each potential predator.

### *Direction of swimming*

The movement of *Melibe* through the water column during a swimming episode was determined for seven animals. The goal of this study was to test the hypothesis that this species moves ventrally, in a direction roughly perpendicular to the long axis of the foot. Individual nudibranchs were induced to swim in a 50-l aquarium that had $x$-$y$ coordinates drawn on a clear plastic cover placed over the top and on one side. Each animal was placed on a blade of eelgrass that was located in the center of the tank and secured to the bottom, then induced to swim using a brief touch on the back of the oral hood with a single sea star tube foot. The tube foot had been excised from a live *Pycnopodia* with fine scissors and was held with a pair of self-closing forceps. A line representing the orientation of the foot was marked on the $x$-$y$ grids at 5-s intervals. These lines were then plotted in two dimensions and used to calculate the predicted position of the midpoint of the foot at successive time intervals. The "variance angle" (the angle between the actual and predicted position of the foot at the next time point) was then calculated for each 5-s time interval, averaged, plotted using polar coordinates, and compared to the predicted path.

## Results

### *Analysis of normal swimming*

Although *Melibe* is occasionally observed swimming near the ocean surface (Mills, 1994; pers. obs.), typically it is found attached to eelgrass or kelp blades. *Melibe* swims spontaneously, as well as when forced off the substrate or exposed to a noxious stimulus. Its swimming behavior is characterized by slow, rhythmic, lateral flexions that last for 1–2 s (2–4 s for a full swim cycle). During each flexion, the body bends laterally into a shape resembling the letter C, with the oral hood approaching the tip of the tail (Fig. 1). A digitized video of swimming can be viewed at the following web site: http://zoology.unh.edu/faculty/win/Melibe/melibeswimming.htm.

The overall organization of a swim episode can be broken down into five basic components, some of which are illustrated in Figure 1. When not swimming, *Melibe* is often found attached, by means of its flattened foot, to a vertical substrate, such as a blade of eelgrass, with oral hood open and cerata extended (Fig. 1, top). A spontaneous swimming episode begins with closure of the oral hood and release of the foot, usually starting with the anterior portion, from the substrate (component 1—withdrawal). Once in the water column, the bottom of the foot is rolled medially, the body is compressed laterally, and the cerata are extended dorsally (2—lateral flattening). Swimming movements consist of an alternating lateral-bending, or flexion, of the body that brings the closed oral hood in close proximity to the tail (3—flexions). These rhythmic flexions may continue for a period of a few seconds to over an hour. The conclusion of a swim episode is preceded by the anterior tip of the foot unrolling and "probing" for an appropriate substrate on which to settle (4—unrolling and swinging). A swim episode is terminated (5—termination) when the anterior foot comes in contact with a suitable substrate and the animal uses its flattened foot to attach to it. Termination does not necessarily occur during the first encounter of the foot with a substrate; often the animal will make multiple contacts before ceasing to swim. Moreover, animals will occasion-

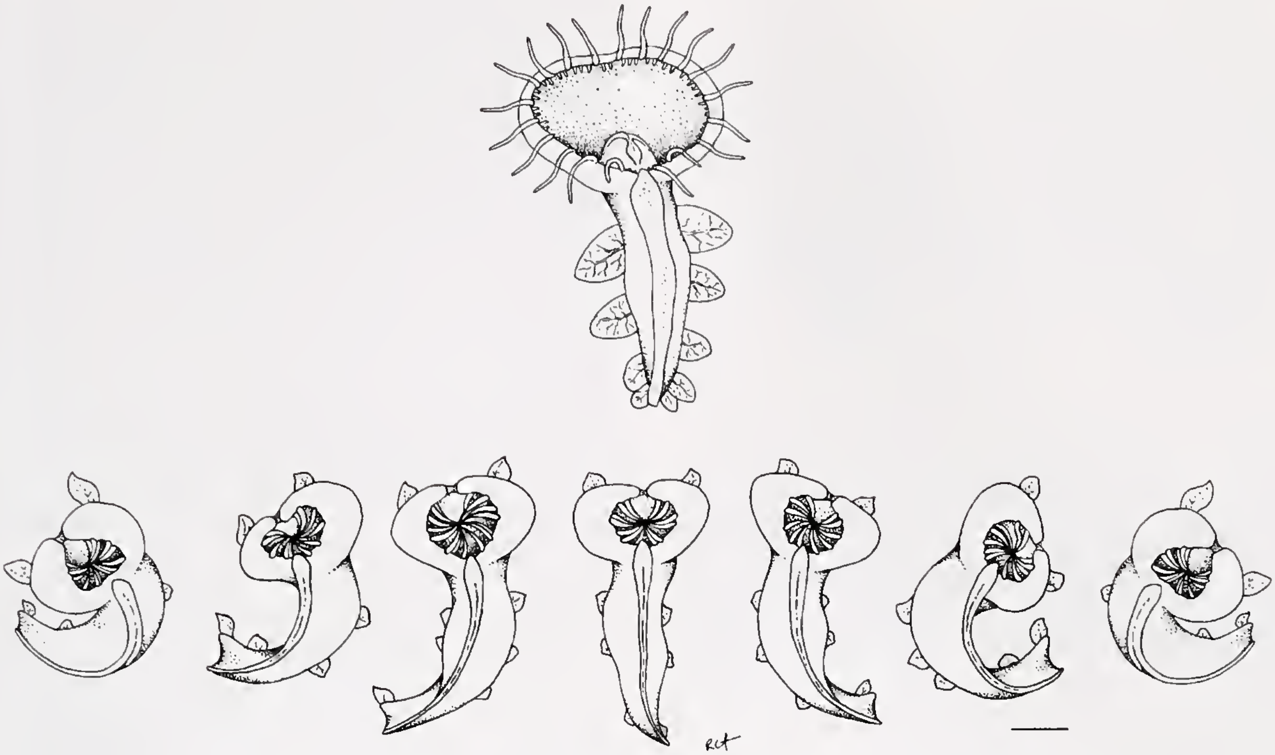

**Figure 1.** Illustrations of *Melibe leonina* at rest (top) and swimming (all ventral views). The sequence of drawings on the bottom show 50% of a swim cycle, as the nudibranch goes from being fully flexed to the right, to fully flexed to the left. Note the slight twisting of the posterior portion of the foot, which creates a sculling motion that propels animals in the ventral direction. Scale bar = 1 cm.

ally stop swimming in the water column, without contact of the foot with a substrate.

The flexions involved in the swim are not equivalent along the entire length of the body. In addition to the lateral flexions, there is also a concurrent twisting of the posterior part of the body, so that the foot becomes the leading edge during each lateral flexion (Fig. 1). This "sculling" motion provides a propulsive force that pushes water dorsally and moves the animal in a ventral direction, much as the sculling movements of the wings of the pteropod *Clione* cause it to move in the anterior direction (Satterlie *et al.*, 1985). This sculling movement was originally described by Hurst (1968), but no further mention of it has appeared in the literature on *Melibe*. The combination of lateral bending of the entire body and dorsal twisting of the foot typically propels the animal in the ventral direction. If the animal is oriented with its oral hood toward the surface, swimming will propel it in a lateral direction.

Although some aspects of swimming are quite variable in *Melibe*, the duration of each swim cycle, the magnitude of rhythmic lateral flexions, and the instantaneous swimming velocity are all very consistent during a swim episode. For example, in a single swim episode lasting 58 s, the average duration of each swim cycle was 2.03 ± 0.03 s, with no appreciable variation throughout the course of the swim. In 29 different animals, the average duration of a swim cycle was 2.7 ± 0.2 s. The magnitude of the lateral flexions was also quite consistent throughout a swim episode (Fig. 2). Other than the first and last few flexions in the swim episode, the contractions of the body in both directions were similar in amplitude for most of the episode.

In contrast to the stereotyped swimming escape response of *Tritonia*, where the duration of the swim and the direction of the first and last swimming flexion can be reasonably predicted (Willows *et al.*, 1973; Hume *et al.*, 1982), the swims of *Melibe* show little consistency in those parameters. Fifty-eight percent of the animals tested began with a left flexion ($n = 29$), and 53% of the animals finished a swimming episode with a flexion to left. The variation in the duration of swim episodes was also quite large. The mean swim duration in response to a salt stimulus was 174.9 ± 32.1 s ($n = 11$; data were taken from the 11 animals that swam, out of the 49 tested with a salt stimulus); some animals swam for only 33 s, but others continued for as long as 1546 s (25.7 min).

One of the unique features of swimming in *Melibe* is the motionless floating behavior which Agersborg (1921) referred to as "feigned death." During these floating events the animals lie in one place, dorsal aspect up, with the cerata inflated and spread parallel to the surface of the water; they

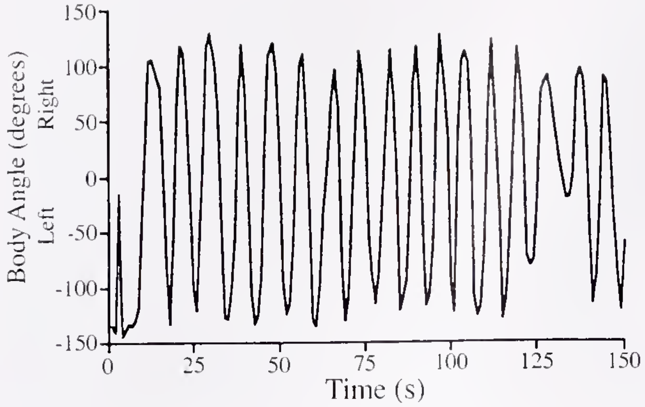

**Figure 2.** Swimming in *Melibe* is characterized by vigorous lateral flexions of the body. These motions are repeated without significant variation in timing or amplitude throughout the duration of the swim episode. This graph is a plot of the angle of the body of a single tethered individual, as viewed from the ventral side, during slightly more than 2 min of swimming. Animals were induced to swim by dislodging them from their attachment to the surface tension of the water. In the example shown in this figure, the animal was slightly flexed to the left when the stimulus was applied, and also remained slightly flexed to the left when it stopped swimming.

will occasionally remain in this position for several minutes. During a separate set of long-term swimming experiments (60–90 min), during which the animals were not allowed to attach to any substrate, these pauses occurred every 10–20 min.

### *Stimuli that elicit swimming*

To determine what external factor probably causes *Melibe* to swim in its natural habitat, and how to reliably stimulate swimming in the laboratory, we screened a number of possible noxious stimuli, including pinches with forceps, salt (KCl), and contact with several different putative predators. There was a significant effect of these treatments on the tendency of *Melibe* to swim, with some treatments being more effective than others ($P < 0.001$, $G$-test for independence). Of the three stimuli, the touch of the predatory sea star *Pycnopodia* yielded the most reliable response (Fig. 3A; 62% of the 32 animals that were touched swam, $P < 0.0001$ Fisher's exact test, comparing sea star responses to pooled KCl and pinch responses). In fact, a very brief (<1 s) touch with an individual *Pycnopodia* tube foot was usually sufficient to elicit a swim. This finding contrasts with an earlier report that "*M. leonina* rarely swim following sea star contact" (Page, 1993). Single pinches to a cerata, as well as trains of pinches, caused rapid escape crawling but rarely swimming (5% swam, $n = 20$). A salt solution (1 ml of 1 $M$ KCl) applied to the skin of the head elicited swimming in 22% of the trials ($n = 49$).

Of the three stimuli that were found to be most effective, contact with sea stars elicited a rapid escape response that occurred significantly faster than the response to a salt stimulus, but not significantly faster than the response to a pinch (Fig. 3B; $P < 0.05$ Kruskal-Wallis nonparametric ANOVA, Dunn's multiple comparison post-test). The three stimuli also elicited swims with variable durations (Fig. 3B). Swims in response to contact with a sea star tube foot lasted an average of 53.7 ± 9.4 s ($n = 20$) and were significantly shorter than swims elicited by salt (174.9 ± 32.1 s, $n = 11$, $P < 0.01$, Kruskal-Wallis nonparametric ANOVA, Dunn's multiple comparison post-test), but not significantly different in duration from swims triggered by a pinch (91.0 ± 76.9 s, $n = 6$, $P > 0.05$). There was no significant difference between the duration of swims elicited by salt and swims triggered by a pinch with forceps ($P > 0.05$). Finally, there was no correlation between the latency to respond to a particular stimulus and the duration of the subsequent swim episode ($r^2 = 0.05$). However, animals

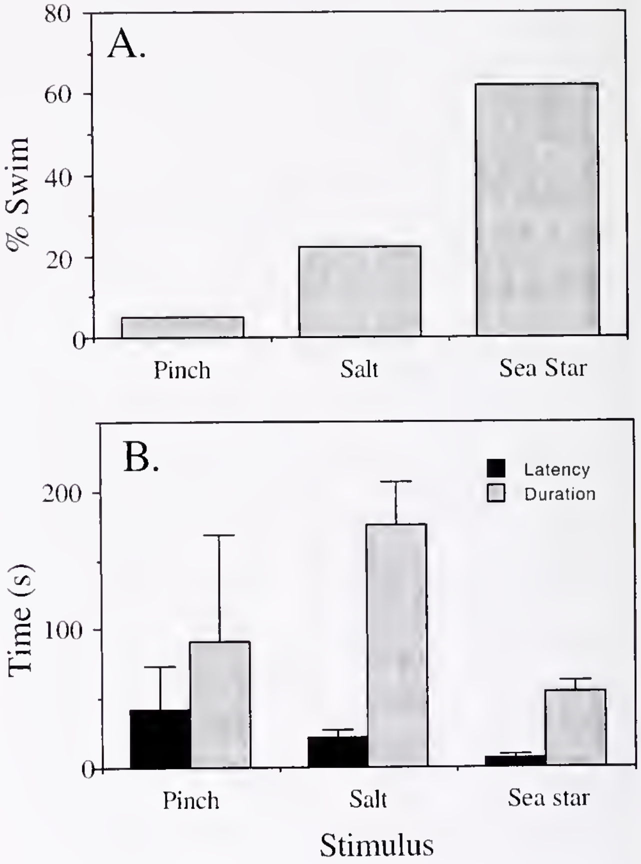

**Figure 3.** The influence of various stimuli on swimming behavior in *Melibe*. Animals were exposed to three different stimuli (pinch, $n = 20$; salt, $n = 49$; tube foot of the sea star *Pycnopodia*, $n = 32$) and their tendency to swim (panel A, % that swam), latency to swim (Panel B, time from stimulus to initiation of swim), and duration of the swim episode (Panel B) were measured. The sea star stimulus was significantly more effective than the other stimuli. Animals touched with sea star tube feet responded very rapidly and consistently in comparison to those given the other stimuli.

often swam multiple times in response to a single sea star contact. If these multiple swims are viewed as one long swim episode, then in general, "stronger" stimuli (sea star>salt>pinch) caused animals to respond more quickly and swim longer compared to "weaker" stimuli.

All the crabs and anemones tested, as well as the sea stars other than *Pycnopodia,* elicited no responses at all in *Melibe.* Neither animal seemed to take any notice of the other's presence. When contact between crabs and nudibranchs occurred, the nudibranch would often simply crawl over the carapace of the crab without incident. No contact between the anemone and the nudibranch was ever observed. Some nudibranchs were left with crab and sea star predators for up to 48 h, with no signs of predation. Finally, in a number of cases, nudibranchs were placed on the oral surface of potential sea star predators, and no ingestion occurred. However, we did not control for the state of hunger of the test predators, and on other occasions we have observed both *Pycnopodia* and anemones eating small specimens of *Melibe* in the laboratory. In addition, Ajeska and Nybakken (1976) have reported that *Pugettia,* a crab found in California kelp beds, is a predator of *Melibe.*

*Direction of swim*

Preliminary observations indicated that, when swimming, *Melibe* moved in a ventral direction, perpendicular to the long axis of the foot. To test this hypothesis, we analyzed the instantaneous swimming direction of seven animals, in 5-s intervals, as described in the Materials and Methods. Five of these animals moved, on average, in a direction that varied less than one standard deviation (14°) from the predicted direction (90° from the long axis of the foot). The variance angles of the other two animals were only slightly different than predicted (Fig. 4). These data support the hypothesis that the general direction of movement, from one swimming flexion of *Melibe* to the next, can be predicted if the orientation of the foot is known. This prediction is most accurate after the first two swimming flexions, which tend to propel the animal upward. Subsequently, most movement generated by an individual flexion is in a plane that is perpendicular to the long axis of the foot. Therefore, if an animal is positioned vertically in the water column, with its oral hood toward the surface, as it is often found on blades of eelgrass (pers. obs.), swimming would most likely move it in a lateral direction.

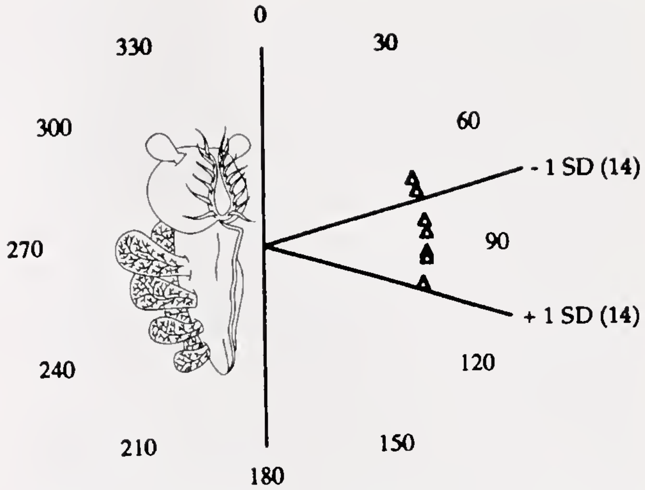

**Figure 4.** A comparison of the swimming direction of a specimen of *Melibe* with a predicted path (perpendicular to the foot). Seven animals were observed for the duration of an induced swim, and the angle of travel, relative to the long-axis of the foot, was measured at 5-s intervals. An angle of 90 degrees represents movement in a direction perpendicular to the long axis of the foot. The average angles were calculated and plotted for each animal. The average angle traveled by five of seven animals fell within one standard deviation of the prediction (=14 degrees).

## Discussion

In this study we examined the swimming behavior of *Melibe leonina,* from initiation, elicited by a variety of stimuli, to termination, marked by reattachment to a suitable substrate. As in other lateral-bending swimmers (Agersborg, 1922), and many other swimming molluscs (Thompson, 1976), the behavior is elicited most reliably by noxious stimuli, such as contact with the tube feet of the predatory sea star *Pycnopodia.* It is also very stereotyped in terms of the consistent rhythmic flexions used to propel the animals through the water.

*Melibe* is rarely observed swimming in its natural eelgrass and kelp habitats, even though potential predators such as *Pycnopodia,* anemones, and crabs are present (Ajeska and Nybakken, 1976; unpubl. obs.). One explanation for this apparent low frequency of swimming might be that *Melibe* rarely encounters predators. This nudibranch tends to situate itself near the distal portions of eelgrass and kelp blades, where large sea stars and crabs are rarely found. *Melibe* may also have less of a tendency to swim where currents are strong, because swimming animals have a high probability of being carried away from their preferred habitat, and potential mates, by these currents. The high density of swimming and floating individuals observed intermittently at considerable distances from local eelgrass beds suggests that other factors, besides predators, may also trigger swimming in *Melibe* (Mills, 1994). Farmer (1970) suggested that these animals might use voluntary swimming episodes to move from one kelp blade to another, and we have observed spontaneous bouts of swimming on many occasions in the laboratory. Voluntary swimming may also be a means of dispersal, which would allow mixing of the gene pools from spatially isolated populations inhabiting eelgrass beds located several kilometers from each other (Mills, 1994).

A unique feature of swimming in *Melibe,* in comparison with other swimming molluscs, is motionless floating behavior. These pauses may represent an energy-saving strategy that allows the animals to "rest" and remain in the water column for a time, at a relatively low energy cost. An alternative hypothesis is that floating may enable this nudibranch to periodically open its oral hood to sample the water column for prey. It cannot feed and swim at the same time, so this sampling activity would allow it to "forage" while floating. When it encountered a high density of food, it could stop, seek a suitable substrate, and feed (Trimarchi and Watson, 1992; Watson and Chester, 1993). Preliminary studies in our laboratory indicate that prey (*Artemia*) reduce both the rate of crawling and the frequency of spontaneous swimming episodes in *Melibe*.

The most effective stimulus for eliciting swimming in *Melibe* is contact with the tube feet of *Pycnopodia*. This stimulus is probably effective due to the surfactants found on the tube feet of certain predatory sea stars (Mauzey *et al.*, 1968; Mackie, 1970). Oddly enough, we rarely observe sea stars attacking an adult *Melibe*. Page (1993) suggests that sea stars avoid *Melibe* because its repugnatorial glands, located throughout the epidermis, release a chemical that renders it repulsive to predators. These glands do not mature until the animals are 4–7 weeks old, and sea stars do attack and consume younger individuals. It is interesting that even though their repugnatorial glands help deter potential predators, mature specimens retain their tendency to escape when they sense the presence of certain sea stars.

The direction that *Melibe* travels during a swim appears to be random, upon casual observation. However, certain features of the path taken during a swim episode are fairly predictable. When this nudibranch starts to swim, it first releases the anterior part of its foot from the substrate. Then, no matter what the initial orientation of the animal is, its head moves toward the surface and the first few lateral flexions tend to move its body in the anterior direction. Once an individual has "pushed off" and is in the water column, the combination of lateral flexions and twisting of the posterior portions of the foot and tail region creates a "sculling" motion that reliably propels it along a plane perpendicular to the long axis of the foot (Fig. 4). Thus, although its swimming behavior has less of a directional component than seen in some molluscs that use parapodial flapping, such as *Aplysia brasiliana* and *Clione*, *Melibe* appears to have more control than the animals that use dorsal-ventral flexions, like *Tritonia* and *Pleurobranchaea*. This raises the question of whether *Melibe* has the ability to seek out its preferred habitats or potential mates, or whether it attempts to move laterally from one eelgrass or kelp blade to another. Certainly, in the laboratory, it swims spontaneously, especially during the night (Watson and Newcomb, unpubl. obs.), and our working hypothesis is that it uses swimming both as a response to predators and as a means of intermittent locomotion.

According to Audesirk and Audesirk (1985), three criteria must be fulfilled for a behavior to be useful in neuroethological studies: reliability, robustness, and stereotypy. All of these criteria are characteristic of the swimming behavior of *Melibe leonina*. It can be reliably initiated in the laboratory with natural stimuli or a salt solution. The robustness and stereotypy are illustrated in Figure 2, which shows that over the time course of a swim, the flexion amplitude and frequency do not change significantly. Furthermore, *Melibe* is amenable to electrophysiological investigations, as are many other opisthobranch species, because it has large, identifiable neurons, and impulses from these neurons can be recorded both in swimming, semi-intact animals and in isolated brains (see companion paper, Watson *et al.*, 2002). Finally, in *Melibe*, relatively few higher order interneurons constitute the swim central pattern generator, so a very thorough neuroethological understanding of the behavior is possible (Watson *et al.*, 2001).

## Acknowledgments

We thank A. O. Dennis Willows and Glen Brown for their advice during the experimental phases of this study and for providing critical comments on this paper, Eric Abrahamson and Jen Wishinski for their help with several behavioral experiments, Jim Newcomb and Stuart Thompson for constructive comments on the manuscript, and the entire staff of FHL for their continuous support and assistance with all phases of the work. This study was supported by Center for Marine Biology grants and Summer Teaching fellowships to K.A.L. through the University of New Hampshire and an NIH grant to W.H.W. It is contribution number 386 of the Center for Marine Biology/Jackson Estuarine Laboratory series.

## Literature Cited

**Agersborg, H. P. v. W. K. 1921.** Contributions to the knowledge of the nudibranchiate mollusk, *Melibe leonina* (Gould). *Am. Nat.* **55:** 222–253.

**Agersborg, H. P. v. W. K. 1922.** Notes on the locomotion of the nudibranchiate mollusk, *Dendronotus giganteus* O'Donoghue. *Biol. Bull.* **42:** 257–266.

**Ajeska, R. A., and J. Nybakken. 1976.** Contributions to the biology of *Melibe leonina* (Gould, 1852) (Mollusca: Opisthobranchia). *Veliger* **19:** 19–26.

**Arshavsky, Yu. I., I. N. Beloozerova, G. N. Orlovsky, Yu. V. Panchin, and G. A. Pavlova. 1985.** Control of locomotion in marine mollusc *Clione limacina*. II. Rhythmic neurons of pedal ganglia. *Exp. Brain Res.* **58:** 263–272.

**Audesirk, T., and G. Audesirk. 1985.** Behavior of gastropod molluscs. Pp. 1–94 in *Neurobiology and Behavior*, Vol. 8, A.O.D. Willows, ed. Academic Press, New York.

**Bickell-Page, L. R. 1991.** Repugnatorial glands with associated striated muscle and sensory cells in *Melibe leonina* (Mollusca: Nudibranchia). *Zoomorphology* **110:** 281–291.

**Edmunds, M. 1968.** On the swimming and defensive response of *Hexabranchus marginatus* (Mollusca: Nudibranchia). *J. Linn. Soc. Lond.* **47:** 425–429.

**Farmer, W. M. 1970.** Swimming gastropods (Opisthobranchia and Prosobranchia). *Veliger* **13:** 73–89.

**Getting, P. A. 1983.** Neural control of swimming in *Tritonia*. Pp. 89–128 in *Neural Origin of Rhythmic Movements*, A. Roberts and B. L. Roberts, eds. Cambridge University Press, New York.

**Getting, P. A. 1989.** Emerging principles governing the operation of neural networks. *Annu. Rev. Neurosci.* **12:** 185–204.

**Hamilton, P. V., and H. W. Ambrose. 1975.** Swimming and orientation in *Aplysia brasiliana* (Mollusca: Gastropoda). *Mar. Behav. Physiol.* **3:** 131–144.

**Hume, R. I., P. A. Getting, and M. A. Del Beccaro. 1982.** Motor organization of *Tritonia* swimming. I. Quantitative analysis of swim behavior and flexion neuron firing patterns. *J. Neurophysiol.* **47:** 60–74.

**Hurst, A. 1968.** The feeding mechanism and behaviour of the opisthobranch *Melibe leonina*. *Symp. Zool. Soc. Lond.* **22:** 151–166.

**Jing, J., and R. Gillette. 1995.** Neuronal elements that mediate escape swimming and suppress feeding behavior in the predatory sea slug *Pleurobranchaea*. *J. Neurophysiol.* **74:** 1900–1910.

**Jing, J., and R. Gillette. 1999.** Central pattern generator for escape swimming in the notaspid sea slug *Pleurobranchaea californica*. *J. Neurophysiol.* **81:** 654–667.

**Mackie, A. M. 1970.** Avoidance reactions of marine invertebrates to either steroid glycosides of starfish or synthetic surface-active agents. *J. Exp. Mar. Biol. Ecol.* **5:** 63–69.

**Mauzey, K. P., C. Birkeland, and P. K. Dayton. 1968.** Feeding behavior of asteroids and escape responses of their prey in the Puget Sound Region. *Ecology* **49:** 603–619.

**McPherson, D. R., and J. E. Blankenship. 1991a.** Neural control of swimming in *Aplysia brasiliana*. I. Innervation of parapodial muscles by pedal ganglion motorneurons. *J. Neurophysiol.* **66:** 1338–1351.

**McPherson, D. R., and J. E. Blankenship. 1991b.** Neural control of swimming in *Aplysia brasiliana*. II. Organization of pedal motorneurons and parapodial motor fields. *J. Neurophysiol.* **66:** 1352–1365.

**Mills, C. E. 1994.** Seasonal swimming of sexually mature benthic opisthobranch molluscs (*Melibe leonina* and *Gasteropteron pacificum*) may augment population dispersal. Pp. 313–319 in *Reproduction and Development of Marine Invertebrates*, W. H. Wilson, S. A. Stricker, and G. L. Shinn, eds. The Johns Hopkins University Press, Baltimore.

**Page, L. R. 1993.** Development of behavior in juveniles of *Melibe leonina* (Gastropoda: Nudibranchia). *Mar. Behav. Physiol.* **22:** 141–161.

**Satterlie, R. A. 1985.** Reciprocal inhibition and postinhibitory rebound produce reverberation in a locomotor pattern generator. *Science* **229:** 402–404.

**Satterlie, R. A. 1991.** Neural control of speed changes in an opisthobranch locomotory system. *Biol. Bull.* **180:** 228–233.

**Satterlie, R. A., and T. P. Norekian. 1996.** Modulation of swimming speed in the pteropod mollusc, *Clione limacina:* role of a compartmental serotonergic system. *Invertebr. Neurosci.* **2:** 157–165.

**Satterlie, R. A., and A. N. Spencer. 1985.** Swimming in the pteropod mollusc, *Clione limacina*. II. Physiology. *J. Exp. Biol.* **116:** 205–222.

**Satterlie, R. A., M. LaBarbera, and A. N. Spencer. 1985.** Swimming in the pteropod mollusc, *Clione limacina*. I. Behavior and morphology. *J. Exp. Biol.* **116:** 189–204.

**Thompson, T. E. 1976.** *Biology of Opisthobranch Molluscs*, Vol. 1. The Ray Society, London. 206 pp.

**Trimarchi, J., and W. H. Watson. 1992.** The role of *Melibe* buccal ganglia in feeding behavior. *Mar. Behav. Physiol.* **19:** 195–209.

**von der Porten, K., D. W. Parsons, B. S. Rothman, and H. Pinsker. 1982.** Swimming in *Aplysia brasiliana:* analysis of behavior and neuronal pathways. *Behav. Neural. Biol.* **36:** 1–23.

**Watson, W. H. III, and C. M. Chester. 1993.** The influence of olfactory and tactile stimuli on the feeding behavior of *Melibe leonina* (Gould 1852) (Opisthobranchia: Dendronotacea). *Veliger* **36:** 311–316.

**Watson, W. H. III, K. D. Lawrence, and J. M. Newcomb. 2001.** Neuroethology of *Melibe leonina* swimming behavior. *Am. Zool.* **41:** 1026–1035.

**Watson, W. H. III, J. M. Newcomb, and S. Thompson. 2002.** Neural correlates of swimming behavior in *Melibe leonina*. *Biol. Bull.* **203:** 152–160.

**Willows, A. O. D. 1965.** Giant nerve cells in the ganglia of nudibranch molluscs. *Comp. Biochem. Physiol.* **14:** 707–710.

**Willows, A. O. D., Dorsett, D. A., and G. Hoyle. 1973.** The neuronal basis of behavior in *Tritonia*. III. Neuronal mechanism of a fixed action pattern. *J. Neurobiol.* **4:** 255–285.

Reference: *Biol. Bull.* **203:** 152–160. (October 2002)

# Neural Correlates of Swimming Behavior in *Melibe leonina*

WINSOR H. WATSON III[1,2,*], JAMES M. NEWCOMB[1,2,‡], AND STUART THOMPSON[2,3]

[1]*Zoology Department and Center for Marine Biology, University of New Hampshire, Durham, New Hampshire 03824;* [2]*Friday Harbor Laboratories of the University of Washington, Friday Harbor, Washington 98250; and* [3]*Hopkins Marine Station, Stanford University, Pacific Grove, California 93950*

**Abstract.** The nudibranch *Melibe leonina* swims by rhythmically bending from side to side at a frequency of 1 cycle every 2–4 s. The objective of this study was to locate putative swim motoneurons (pSMNs) that drive these lateral flexions and determine if swimming in this species is produced by a swim central pattern generator (sCPG). In the first set of experiments, intracellular recordings were obtained from pSMNs in semi-intact, swimming animals. About 10–14 pSMNs were identified on the dorsal surface of each pedal ganglion and 4–7 on the ventral side. In general, the pSMNs in a given pedal ganglion fired synchronously and caused the animal to flex in that direction, whereas the pSMNs in the opposite pedal ganglion fired in anti-phase. When swimming stopped, so did rhythmic pSMN bursting; when swimming commenced, pSMNs resumed bursting. In the second series of experiments, intracellular recordings were obtained from pSMNs in isolated brains that spontaneously expressed the swim motor program. The pattern of activity recorded from pSMNs in isolated brains was very similar to the bursting pattern obtained from the same pSMNs in semi-intact animals, indicating that the sCPG can produce the swim rhythm in the absence of sensory feedback. Exposing the brain to light or cutting the pedal-pedal connectives inhibited fictive swimming in the isolated brain. The pSMNs do not appear to participate in the sCPG. Rather, they received rhythmic excitatory and inhibitory synaptic input from interneurons that probably comprise the sCPG circuit.

## Introduction

Investigations of rhythmic behaviors, such as feeding, swimming, and walking, have significantly contributed to our understanding of the neural mechanisms underlying stereotyped behaviors (Grillner and Wallen, 1985; Getting, 1989; Pearson, 1993; Marder and Calabrese, 1996). Invertebrate preparations have been particularly useful because they often have large, identifiable neurons that are accessible to intracellular investigation in both isolated ganglia and in semi-intact preparations (Lukowiak, 1991; Calabrese and De Schutter, 1992). The general view that has emerged from these studies is that rhythmic fixed-action patterns are produced by central pattern generators (CPGs) that are modulated and controlled by sensory inputs and neurohormones (Delcomyn, 1980; McCrohan, 1988; Getting, 1989; Harris-Warrick and Marder, 1991; Pearson, 1993; Marder and Calabrese, 1996).

The rhythmic swimming behavior of marine molluscs has been studied extensively since the classic investigations of Willows, Getting, Hoyle, Dorsett, and their colleagues on the nudibranch *Tritonia diomedea* (Willows, 1967; Willows and Hoyle, 1969; Willows *et al.*, 1973; Dorsett *et al.*, 1973; Getting *et al.*, 1980; Hume *et al.*, 1982). By developing a method for recording from identifiable neurons in swimming animals, they were able to identify the motoneurons and the network of interneurons responsible for generating the dorsal-ventral swimming movements. Subsequent work yielded many additional features of the swim CPG and showed that the rhythm depended on complex synaptic interactions between neurons, as well as on the intrinsic properties of a subset of the CPG neurons (Getting, 1983a, b). More recently, Katz and Frost identified cells that trigger swimming, and neuromodulators, such as serotonin, that

---

Received 7 November 2001; accepted 28 June 2002.

* To whom correspondence should be addressed. E-mail: win@unh.edu

‡ Current address: Department of Biology, Georgia State University, PO Box 4010, Atlanta, GA 30302-4010.

*Abbreviations:* IBI, interburst interval; pSMN, putative swim motoneuron; sCPC, swim central pattern generator; STG, stomatogastric ganglion.

alter the pattern produced by the swim CPG (Katz and Frost, 1995, 1996).

Whereas *Tritonia* swims using dorsal-ventral flexions of its entire body, *Clione limacina*, a pteropod mollusc, swims almost continuously by beating two "wings." The swim CPG consists of two groups of about 10 interneurons that reciprocally inhibit each other (Satterlie, 1985). Although the basic neural mechanisms underlying swimming appear to be simple, the actual swimming behavior of *Clione* is quite complex, and during the last decade Satterlie, Norekian, Arshavsky, and their colleagues have contributed a great deal to our understanding of pattern generator reconfiguration, the neural basis of behavioral switching, and modulation of neural networks (Arshavsky *et al.*, 1985a, b; Huang and Satterlie, 1990; Satterlie, 1991; Satterlie and Norekian, 1996).

In comparison to our knowledge about *Tritonia* and *Clione*, our understanding of the neural basis of swimming in many other marine molluscs is more limited. Of the 47 swimming molluscs identified by Farmer (1970), electrophysiological investigations have been conducted on only three species in addition to *Tritonia* and *Clione: Pleurobranchaea* (Jing and Gillette, 1995, 1999); *Aplysia brasiliana* (von der Porten *et al.*, 1982; McPherson and Blankenship, 1991a, b); and *Melibe leonina* (Watson *et al.*, 2001). In these species, although the swim motoneurons and some critical elements of the CPG have been investigated, the neural circuits underlying swimming have not been elucidated in the detail that exists for both *Tritonia* and *Clione*.

The swimming behavior of the nudibranch *Melibe leonina* has been described in several publications (Agersborg, 1921; Hurst, 1968; Ajeska and Nybakken, 1976; Page, 1993; Watson *et al.*, 2001), most recently in the accompanying manuscript (Lawrence and Watson, 2002). *Melibe* uses slow, rhythmic lateral flexions of its body wall to propel itself through the water. Although *Melibe* often swims spontaneously, a bout of swimming can also be elicited by contact with a predatory sea star (*Pycnopodia*). Behavioral analyses and preliminary intracellular recordings from semi-intact specimens of *Melibe* (Hurst, 1968; Thompson, unpubl. data), indicate that swimming is probably produced by a CPG. To expand upon our current knowledge of the neural basis of swimming in marine molluscs, and perhaps reveal certain common principles of neural organization through comparison with other well-studied species, we undertook a neurophysiological investigation of swimming behavior in *Melibe*. In this paper, we characterize the activity of putative swim motoneurons (pSMNs) that give rise to swimming movements in semi-intact specimens and to fictive swimming in isolated brains (fused cerebral-pleural-pedal ganglia). These studies demonstrate that swimming in *Melibe* is a highly stereotyped fixed-action pattern that is likely produced by a sCPG that rhythmically drives the pSMNs responsible for causing the alternating lateral flexions characteristic of the behavior.

## Materials and Methods

### *Animals*

Specimens of *Melibe leonina* (Gould, 1852) were collected by scuba in eelgrass beds near the University of Washington's Friday Harbor Laboratories, Friday Harbor, Washington. Specimens were maintained in flow-through seawater tables at 11–15 °C. Some animals were shipped to the Zoology Department, University of New Hampshire, Durham, New Hampshire, and held at 11–15 °C in a recirculating seawater aquarium. In general, animals held at Friday Harbor ate small zooplankton that were not filtered out of the seawater system, as well as organisms associated with eelgrass blades in the sea tables. The diet of specimens in the New Hampshire laboratory aquariums was similar and was supplemented with cultured *Artemia* once each week.

### *Lucifer yellow injections of pSMNs*

Lucifer yellow (5% solution in 0.15 *M* lithium chloride) was injected into putative swim motoneurons by passing 0.5-s, 10-nA hyperpolarizing current pulses, at a 50% duty cycle, for 20 min. Brains with injected cells were fixed overnight in 0.1 *M* phosphate-buffered saline (PBS) with 4% paraformaldehyde at 4 °C. Preparations were rinsed with PBS (four changes in 1 h), dehydrated, cleared in xylene and methyl salicylate, and mounted in DPX (Fluka). They were then viewed and photographed using either a Nikon or Zeiss epifluorescent microscope or a BioRad confocal microscope.

### *Cobalt chloride backfilling*

Pedal nerves were backfilled with 500 m*M* $CoCl_2$, using a procedure modified from Croll (1986). Brains were removed, leaving the nerve that was to be backfilled as long as possible and cutting all other nerve roots close to the brain. The brain was placed inside a small petroleum jelly well filled with seawater, and the nerve to be filled was placed across one of the walls of the well, into a pool of 500 m*M* $CoCl_2$. After incubating in the refrigerator for 24 h, the brain was removed and washed four times, for 5 min each, in seawater. The cobalt was then precipitated by adding a few drops of ammonium sulfide to the seawater and incubating the brain in that solution for 5 min. The brain was then fixed for 1 h with Carnoy's fixative, cleared, dehydrated, and mounted in Permount for viewing.

### *Intact animal preparations*

A semi-intact, whole-animal preparation similar to that developed by Willows (1967) for investigating swimming in *Tritonia* was modified for use with *Melibe*. After a small slit was made in the dorsal integument just over the brain, animals were suspended in a recording chamber by threads attached to the integument with small pins. Pins were inserted around the border of the slit to hold it open, while at the same time stabilizing that portion of the specimen. A small platform coated with wax and attached to a metal rod was slipped under the brain and held in place with a micromanipulator. The thick sheath covering the brain was opened and pinned to the wax platform to stabilize the brain, but the very thin sheath holding the neuronal cell bodies in place was left intact. The entire chamber was continuously perfused with natural seawater at 11–15 °C.

Swimming movements were monitored by two methods. In one, a silk suture was tied to the posterior tip of the animal's body and connected to a lever arm bearing a flag. Swimming caused the flag to move and partially shield a photocell that was illuminated from above. This yielded a voltage output from the photocell that was maximal at peak right flexion and minimal at peak left flexion. The other approach was to direct a small Photonic sensor at the posterior region of the animal. This sensor transmitted light and recorded the reflected light, yielding a maximal signal when the body bent towards it and minimal output during flexion in the other direction. Although neither measured the strength and magnitude of movements with complete accuracy, these methods were adequate for recording the relative amplitude and frequency of swimming contractions.

### *Isolated brain preparations*

The brain, which consists of the fused cerebral, pleural, and pedal ganglia, was removed by cutting all nerve roots except the three connectives that pass around the esophagus. The esophagus was then removed, taking care not to cut the pedal-pedal and para-pedal connectives that run parallel to the buccal-buccal connectives (Trimarchi and Watson, 1992). The isolated brain was pinned in a small (2–5 ml) Sylgard-lined acrylic plastic chamber that was maintained at 11–15 °C by circulating ambient seawater or antifreeze, from a temperature-controlled water bath, through an aluminum cooling jacket surrounding the chamber. The brain was continuously perfused with cool seawater or with artificial saline containing (in m*M*): 470 NaCl, 10 KCl, 10 $CaCl_2$, 50 $MgCl_2$, 10 HEPES (pH 8).

### *Electrophysiology*

A focal extracellular recording method was used to identify neurons that might participate in swimming. An extracellular electrode consisting of a pair of pipets with 20–50 μm diameter tips was positioned over the soma of a neuron of interest, and the somatic currents associated with action potentials were measured by pressing one pipet tip against the sheath just over the cell body. A systematic survey of the dorsal and ventral surfaces of more than 30 preparations made it possible to tentatively map the position of neurons whose firing was correlated with swimming activity.

Intracellular recordings were obtained using 20–40 megohm electrodes filled with 3 *M* KCl or 2 *M* potassium acetate. Current was injected using bridge-circuits to reduce stimulus artifacts. Permanent records were produced with Gould/Brush or Astro-Med chart recorders. In some experiments, a digital oscilloscope was used to generate averages or to produce interval histograms.

## Results

### *Overview of* Melibe *brain anatomy and location of putative swim motoneurons*

The brain of *Melibe leonina* has been described and illustrated by Hurst (1968), Trimarchi and Watson (1992), and most recently Watson *et al.* (2001) and Newcomb and Watson (2001). It consists of fused cerebral-pleural ganglia connected to a pair of lateral pedal ganglia (Fig. 1A). A pair of pedal-pedal connectives encircle the esophagus and link the two pedal ganglia. Finally, the eyes and statocysts are prominent features on the dorsal surface of the brain.

Two methods were used to establish the approximate locations of neurons involved in the swimming behavior of *Melibe*. First, an extracellular electrode was used to scan the surface of the brain in a swimming animal and identify those neurons whose bursting pattern correlated with swimming movements. In five preparations, it was estimated that between 10 and 14 pSMNs exist on the dorsal surface of each pedal ganglion and from 4 to 7 on the ventral surface. A few additional neurons that fired with the same basic pattern as the pSMNs in the pedal ganglia were found in the cerebral-pleural ganglia. The second approach was to backfill pedal nerves with $CoCl_2$. Although this was successful in revealing pSMNs, many non-pSMN cell bodies also stained; thus this method did not help focus subsequent intracellular investigations on a specific area of the pedal ganglia.

The anatomical properties of swim motoneurons were characterized in more than 20 neurons that were filled with Lucifer yellow after their electrophysiological properties were characterized. In all cases, these cells sent processes out one or more of the pedal nerves, typically PD4 and PD5 (Fig. 1B). They never projected to the cerebral-pleural ganglia or through the pedal-pedal connectives to the opposite pedal ganglia. Although we were unable to trace pSMN axons to their targets, we could determine the general area innervated by these nerves. Nerve PD4 bifurcated into an anterior branch and a posterior branch. The anterior branch

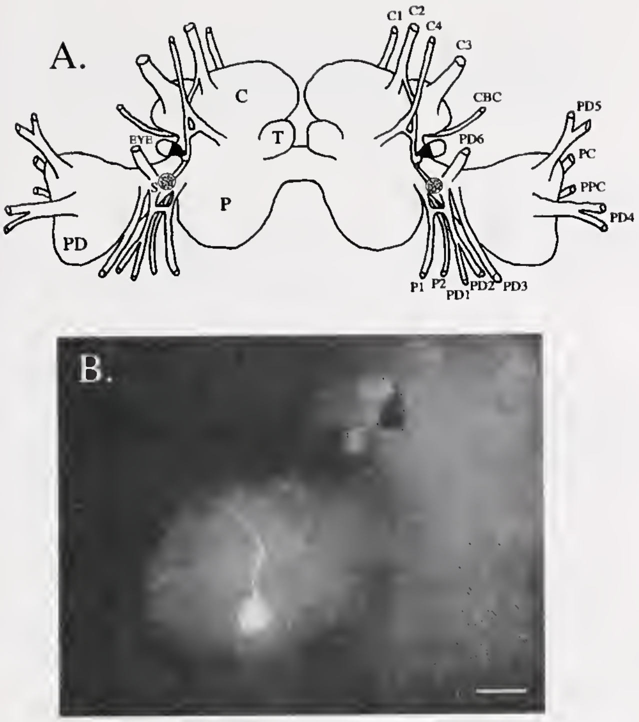

**Figure 1.** Anatomy of the brain and putative swim motoneurons in *Melibe leonina*. (A) Drawing of the brain. The two fused ganglia that constitute most of the brain are the cerebral (C) and pleural (P) ganglia (also referred to jointly as the cerebro-pleural ganglia). Near the large commissure that connects both halves of the brain are the paired tentacular lobes (T). The left and right pedal ganglia (PD) are lateral to the cerebro-pleural ganglia. Note that the eyes are located close to the brain, as are the statocysts (S), which are nestled between the pleural and pedal ganglia. The abbreviations for all the nerves are as follows: C1 = cerebral nerve, C2 = cerebral nerve 2, C3 = cerebral nerve 3, C4 = cerebral nerve 4, CBC = cerebro-buccal connective, P1 = pleural nerve 1, P2 = pleural nerve 2, PC = pedal connective, PD1 = pedal nerve 1, PD2 = pedal nerve 2, PD3 = pedal nerve 3, PD4 = pedal nerve 4, PD5 = pedal nerve 5, PD6 = pedal nerve 6, PPC = parapedal connective. (B) Photomicrograph of a swim motoneuron in the left pedal ganglion that was injected with Lucifer yellow. It projects out nerve PD5, which innervates portions of the foot and body wall. Scale bar = 100 $\mu$m.

innervated the anterior region of the foot and body wall, and the posterior branch projected to the middle region of the foot and body wall, as well as the ovotestes. Pedal nerve 5 projected to the neck region (anterior branch) and the most anterior 1 cm of the foot. The remainder of the pedal nerves (1–3) projected to portions of the gut and body wall.

### *Activity of putative swim motoneurons in intact animals*

When semi-intact specimens of *Melibe* were swimming, the pSMNs in each pedal ganglia expressed a strong, rhythmic firing pattern (Fig. 2). Each burst preceded a bending of the body wall, with activity of neurons in a given pedal ganglion correlated with bending of the body in the ipsilateral direction (Fig. 2). The pattern of rhythmic bursting that characterized swimming was observed only during swimming behavior, and swimming was always closely coupled to rhythmic bursting of certain pedal neurons. When animals paused, with the body bent in one direction, the ipsilateral pSMNs were tonically active, while those on the opposite side were inhibited (Fig. 2). Stimulation of these same neurons in quiescent animals gave rise to small contractions in discrete body wall muscles and movements similar to the ones observed during portions of swimming activity. These observations, taken together with the anatomy of these neurons, suggest that they are swim motoneurons. However, until more definitive anatomical studies are carried out to determine if they directly innervate body wall musculature, we will continue to refer to them as putative SMNs.

### *Recordings from isolated brains*

Isolated brains spontaneously expressed a swim motor pattern that was nearly identical to the pattern recorded from pSMNs in intact swimming individuals (Fig. 3). Putative SMNs fired in strong bursts, triggered by periodic waves of depolarization that alternated with periods of intense hyperpolarization. In an examination of recordings from 10 brains, the average cycle period, from the beginning of one burst to the beginning of the next, was 3.26 ± 0.18 s, while the average burst duration was 1.54 ± 0.14 s and the interburst interval (IBI) was 1.72 ± 0.13 s. These figures correlate very well with similar parameters recorded from five semi-intact preparations (cycle = 3.40 ± 0.20, burst = 1.84 ± 0.16 s, IBI = 1.57 ± 0.11 s; $n = 5$) and to a lesser extent with data from freely swimming animals (mean swim cycle = 2.7 ± 0.2 s; see Lawrence and Watson, 2002).

Isolated brains spontaneously expressed the swim motor program as soon as they were excised from the animal. Preparations with both the pedal-pedal connectives cut were unable to generate a swim pattern, suggesting that critical components of the swim CPG interact through this pathway. In general, preparations were more likely to express the swim pattern in the dark, or in dim light, than during bright illumination. The eyes of *Melibe* are located on the brain, and it is likely that the inhibitory effect of light is mediated by the eyes (Lawrence, 1997).

As demonstrated in semi-intact animals, pSMNs in the same pedal ganglion are synergistic, whereas those in opposite pedal ganglia are out of phase with each other (Fig. 3A). However, within the same ganglion, the pSMNs do not all fire simultaneously. Rather, different cells fire during slightly different phases of the cycle. At least one cell in each pedal ganglion fires out of phase with the rest of the cells in the ganglion (Fig. 3B) and in phase with cells in the opposite pedal ganglion (Fig. 3C). The exact role of this cell is not fully understood, although in semi-intact preparations direct stimulation of these cells causes the anterior of the

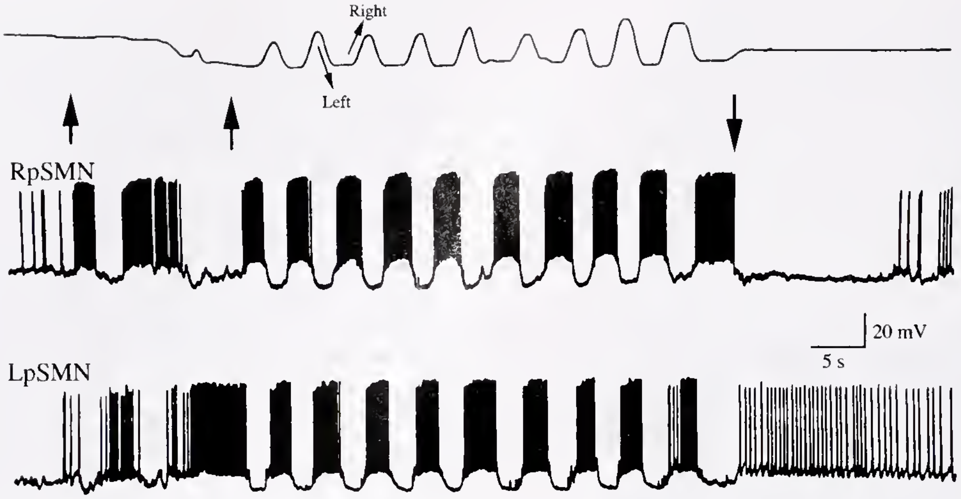

**Figure 2.** Relationship between putative swim motoneuron activity and swimming movements in *Melibe*. Swimming and associated left pedal and right pedal pSMN bursting activity were initiated by dislodging the foot of the animal from the substrate and terminated when the substrate was brought back in contact with the foot. The two up arrows indicate the beginning and end of the time during which the animal was slowly withdrawing from the substate, and the down arrow indicates when swimming stopped and the animal reattached to the substrate. The upper trace illustrates the output of a photocell that was used to monitor swimming movements. Output of the photocell was maximal when the animals were flexed to the right. Bursting of the pSMNs occurred before slow bending in the ipsilateral direction. When swimming stopped, the left pSMN remained tonically active, at a frequency that was too low to cause much flexion, while the right SMN stopped firing.

foot to be pulled to the ipsilateral side, a movement that is recognized as one of the early events in contralateral bending.

### *Interneurons drive the putative swim motoneurons*

The swim pattern appears to be imposed on the pSMNs by the interneurons that generate the pattern (Watson *et al.*, 2001; Thompson and Watson, unpubl. data). When individual pSMNs are either hyperpolarized below threshold or depolarized to elicit continuous spiking, the overall swimming pattern is not altered in either intact animals or in isolated brains (Fig. 4). Furthermore, no evidence for synaptic interactions between pSMNs was obtained during several different types of experiments. In the first, >70 pairs of pSMNs were impaled in quiescent, non-swimming preparations, and action potentials were elicited in one while searching for constant latency PSPs in the other. In the second series of experiments, one cell in a pair was slightly depolarized so that it fired tonically at a frequency of between 0.25 and 1 Hz, and then the other neuron was depolarized so that it produced 5 s bursts. No change was observed in the firing frequency of the tonically firing neuron in any of the 48 experiments performed in this manner, using both antagonistic and synergistic pairs of pSMNs. Finally, no evidence of electrical coupling was observed in >20 pairs of pSMNs. Thus, based on these results, it is very unlikely that the pSMNs influence each other or participate in production of the swim motor program.

### *The role of putative swim motoneurons in other behaviors*

Many of the pSMNs that normally produce bursts of spikes during swimming are active in a different pattern, with variable frequencies, during the movements associated with other behaviors. For example, during crawling, pSMNs are weakly activated while the animal is moving directly forward, and during turning they are active irregularly at frequencies correlated with the direction and vigor of the right or left turning. Figure 5 shows activity recorded from two pSMNs in the right pedal ganglion during a turn to the right that was elicited with a touch to the left body wall. Following the touch, the cells received excitatory synaptic drive, which gave rise to bursts of spikes and subsequent turning of the animal to the right. In contrast, during the crumpling response, when animals undergo bilateral contraction of the body wall, left and right pedal pSMNs fire at the same time. Thus, it appears as if the pSMNs are involved in a number of different behaviors that involve movements of the lateral body wall, and their pattern of activity during these different behaviors is primarily dictated by their synaptic input and not by connections between the pSMNs.

## Discussion

The results of this study suggest that the swimming behavior of *Melibe leonina* is produced by a central pattern generator (CPG) capable of expressing a swimming motor

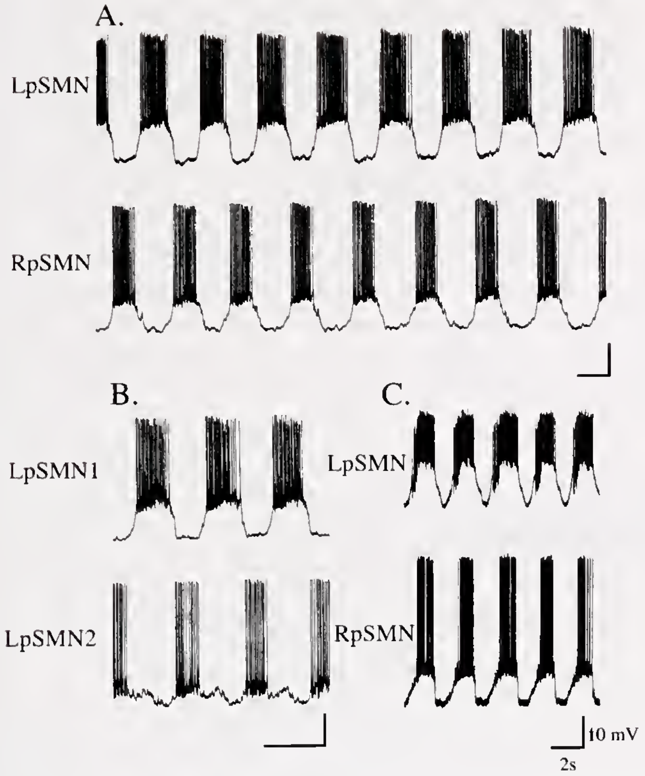

**Figure 3.** Swim motor program recorded from spontaneously active pedal motoneurons in the isolated *Melibe* brain. (A) Most putative swim motoneurons in the left (LpSMN, top) and right (RpSMN, bottom) pedal ganglia fire out of phase with each other, and thus produce the rhythmic lateral bending movements that characterize swimming. (B, C) All pSMNs on a given side do not fire with the same pattern. (B) Recordings from two pSMNs (1, 2) in the same pedal ganglia, in an isolated brain, that fire out of phase. (C) Recordings in a different isolated brain, obtained from two pSMNs in opposite pedal ganglia that fired in phase with each other. The right pSMN (RpSMN) is out of phase with the rest of the pSMNs in the right pedal ganglion. Scale markers = 2 s and 10 mV for all panels.

program in the absence of sensory feedback. When recording intracellularly from putative swim motoneurons (pSMNs) in the pedal ganglia of semi-intact animals, we found that swimming behavior was very closely correlated with pSMN bursting. When swimming started, bursting commenced; when swimming stopped, bursting stopped. Stimulation of these same pSMNs caused bending of the animal in the ipsilateral direction, and Lucifer yellow injections of these neurons revealed axons projecting out pedal nerves toward the lateral body musculature. Furthermore, it was possible to record from these same pSMNs in isolated brains spontaneously expressing the swim motor program, and they produced bursts in a pattern that was nearly identical to the activity they expressed during swimming in semi-intact animals. In intact animals, contact of the foot with a substrate, such as an eelgrass blade, normally suppressed swimming. When the brain was excised, this inhibitory input was apparently eliminated, causing spontaneous expression of the swim motor program. In fact, isolated brains that were still attached to a piece of the anterior foot did not swim spontaneously. These data, taken together, suggest that swimming in *Melibe* is a rhythmic fixed-action pattern produced by a CPG.

Our study suggests the existence of sCPG that drives appropriate sets of pSMNs that, in turn, activate the body wall muscles that move this nudibranch in a series of lateral flexions. These pSMNs have very little influence on each other or the sCPG. Hyperpolarizing and depolarizing individual pSMNs does not influence the swimming behavior of semi-intact animals and has little impact on the fictive swim pattern produced by the isolated brain. Furthermore, there is no evidence of synaptic interactions, either chemical or electrical, between antagonistic or synergistic pairs of pSMNs (although on occasion we observed the type of subtle influence shown in Fig. 4B). This type of organization allows for the pedal motoneurons to fire in different patterns and thus participate in a wide variety of behaviors. For example, during an aversive crumpling response, both right

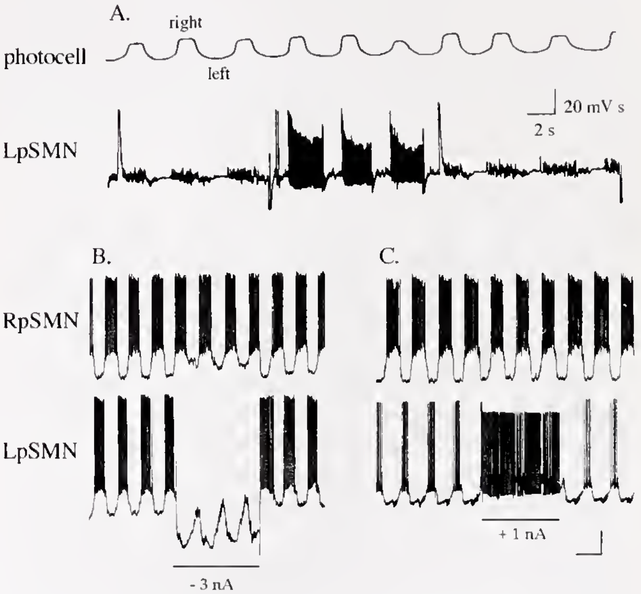

**Figure 4.** Depolarization and hyperpolarization of individual putative swim motoneurons have little influence on the swim motor program in intact animals (A) or in isolated brains (B, C). The records in panel A show the animal's movements (upper trace) and the activity recorded from a left pSMN during swimming (lower trace, AC coupled). At the beginning of the record, the neuron was strongly hyperpolarized for three cycles to prevent spiking despite excitatory input from the swim interneurons. It was then depolarized for three cycles to cause prolonged bursting, and hyperpolarized again. These alterations in the firing pattern had no effect on the ongoing swimming rhythm. The records shown in B and C are from two different isolated brains. Hyperpolarization (B) or depolarization (C) of a left pSMN (bottom) did not influence the swim pattern recorded from a RpSMN (top). However, in this example, strong hyperpolarization of the LpSMN did cause a slight depolarization of the RpSMN in the opposite pedal ganglion. This was not typical, and we do not know what pathways mediate this interaction.

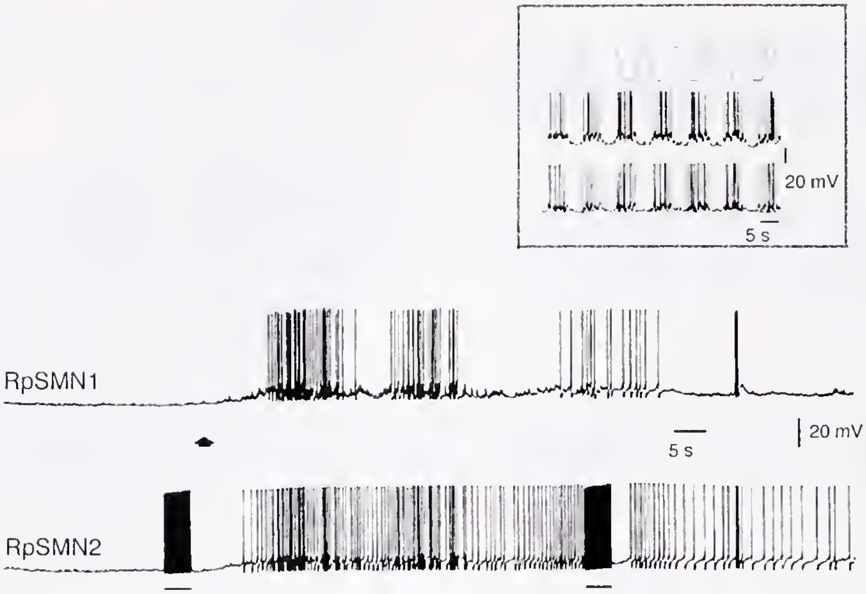

**Figure 5.** Activity of two putative swim motoneurons in the right pedal ganglion during a spontaneous turning movement to the right while the animal was crawling on a substrate. The turning movement was initiated by touching the contralateral body wall with a probe at the time marked by the arrow. The lower cell was depolarized with applied current so that it fired a burst of spikes before initiation of the turning movement and again during the movement (time of stimulation marked by bars). The stimulation had no effect on the activity recorded in the other pSMN. The insert shows bursting activity in the same two cells during swimming. The top trace is a monitor of movement, as in Figure 2, with movements to the right indicated by the trace going in the upward direction. In both figures the scale bars are 5 s and 20 mV.

and left pSMNs fire together rather than out of phase with each other (Thompson, unpubl. data); and during turning, ipsilateral motoneurons fire prolonged bursts together (Fig. 5). This type of sharing of motoneurons by different circuits is a common organizational theme that has been demonstrated in other swimming molluscs (*Tritonia,* Getting, 1989; *Clione,* Satterlie, 1991) as well as in many other species. However, it is not the only way that neural circuits driving rhythmic behaviors are organized. For example, in the stomatogastric ganglia (STG) of crustaceans, motoneurons have extensive synaptic interactions with each other and with interneurons (Miller and Selverston, 1985; Marder and Calabrese, 1996). Yet, they can participate in different motor outputs because a variety of neuroactive substances are capable of modulating the synaptic interactions between STG neurons, as well as the electrical properties of individual cells, thus pharmacologically creating transiently coherent neural networks (Harris-Warrick and Marder, 1991).

It is difficult to compare the neural basis of swimming in *Melibe* with the mechanisms underlying swimming in other opisthobranchs. In part, this is because, although the dominant form of swimming in opisthobranchs involves lateral-bending movements (Farmer, 1970), little is known about the neural basis of this form of swimming. Of the species most thoroughly investigated in terms of neuroethology, *Tritonia* (both *T. diomedea* and *T. hombergi*) and *Pleurobranchaea* swim using doral-ventral flexions, *Clione* flaps its wings, and *Aplysia brasiliana* flaps its parapodia. In *Tritonia* and *Pleurobranchaea* the sCPGs are located in the cerebral-pleural ganglia, and the sCPG drives motoneurons in the pedal ganglia (Willows, 1967; Getting *et al.,* 1980; Satterlie, 1985; see Lukowiak, 1991; McPherson and Blankenship, 1991a, b; Jing and Gillette, 1995, 1999). In contrast, in *Clione* and *Aplysia brasiliana,* the swim CPG and swim motoneurons are both located in the pedal ganglia (von der Porten *et al.,* 1982; Arshavsky *et al.,* 1985a, b; Satterlie, 1985; Satterlie and Norekian, 1996). Interestingly, the sCPG in *Melibe* appears to be a hybrid of these two organizational schemes, with critical elements of the sCPG located in both the cerebral-pleural ganglia and the pedal ganglion, and motoneurons concentrated in the pedal ganglia (Watson *et al.,* 2001; Thompson and Watson, unpubl. data). *Melibe* also differs from the aforementioned species in the way the pSMNs are arranged within the pedal ganglia. In *Melibe,* the right and left pSMNs are well segregated between the left and right pedal ganglia, with most pSMNs located on the dorsal surface of each ganglion. In contrast, in *Tritonia,* a dorsal-ventral swimmer, the dorsal and ventral swim motoneurons are located together in both pedal ganglia (Hume *et al.,* 1982); and in *Clione* and *Aplysia,* which move their wings and parapodia in the dorsal-ventral direction, the motoneurons are also mixed in each pedal ganglia.

Further investigations of the neural basis of swimming in molluscs, especially other lateral-bending species, are likely to reveal additional organizational principles that are common to a wide range of neural circuits underlying rhythmic behaviors such as swimming.

## Acknowledgments

We thank all the people at the Friday Harbor Laboratories, particularly Dennis Willows, David Duggins, and Craig Staude, for being wonderful hosts and providing a great atmosphere for research. We also appreciate all the FHL and UNH students who contributed insights throughout the years. We greatly appreciate the efforts of Cy, Sooz, Celia, Janis, Peter, David, and Cathy in collecting *Melibe*. This study was supported by Center for Marine Biology grants through the University of New Hampshire, a SICB Grant-in-Aid of Research to J.M.N., an NIH grant (R15NSOD3641101) to W.H.W., and an NSF grant (#IBN-9514421) to S.T. It is contribution number 385 of the Center for Marine Biology/Jackson Estuarine Laboratory series.

## Literature Cited

**Agersborg, H. P. v. W. K. 1921.** Contributions to the knowledge of the nudibranchiate mollusk, *Melibe leonina* (Gould). *Am. Nat.* **55:** 222–253.

**Ajeska, R. A., and J. Nybakken. 1976.** Contributions to the biology of *Melibe leonina* (Gould, 1852) (Mollusca: Opisthobranchia). *Veliger* **19:** 19–26.

**Arshavsky, Yu. I., I. N. Beloozerova, G. N. Orlovsky, Yu. V. Panchin, and G. A. Pavlova. 1985a.** Control of locomotion in marine mollusc *Clione limacina*. II. Rhythmic neurons of pedal ganglia. *Exp. Brain Res.* **58:** 263–272.

**Arshavsky, Yu. I., N. Beloozerova, G. N. Orlovsky, Yu. V. Panchin, and G. A. Pavlova. 1985b.** Control of locomotion in marine mollusc *Clione limacina*. III. On the origin of locomotory rhythm. *Exp. Brain Res.* **58:** 273–284.

**Calabrese, R. L., and E. De Schutter. 1992.** Motor-pattern-generating networks in invertebrates: modeling our way toward understanding. *Trends Neurosci.* **15:** 439–444.

**Croll, R. P. 1986.** Modified cobalt staining and silver intensification techniques for use with whole-mount gastropod ganglion preparations. *J. Neurobiol.* **17:** 569–576.

**Delcomyn, F. 1980.** Neural basis of rhythmic behavior in animals. *Science* **210:** 492–498.

**Dorsett, D. A., A. O. D. Willows, and G. Hoyle. 1973.** The neuronal basis of behaviour in *Tritonia*. IV. The central origin of a fixed action pattern demonstrated in an isolated brain. *J. Neurobiol.* **4:** 287–300.

**Farmer, W. M. 1970.** Swimming gastropods (Opisthobranchia and Prosobranchia). *Veliger* **13:** 73–89.

**Getting, P. A. 1983a.** Central pattern generator mediating swimming in *Tritonia*. III. Intrinsic and synaptic mechanisms for delayed excitation. *J. Neurophysiol.* **49:** 1036–1050.

**Getting, P. A. 1983b.** Neural control of swimming in *Tritonia*. Pp. 89–128 in *Neural Origin of Rhythmic Movements. Symposia of the Society for Experimental Biology 37*, A. Roberts and B. L. Roberts, eds. Cambridge University Press, New York.

**Getting, P. A. 1989.** Emerging principles governing the operation of neural networks. *Annu. Rev. Neurosci.* **12:** 185–204.

**Getting, P. A., P. R. Lennard, and R. I. Hume. 1980.** Central pattern generator mediating swimming in *Tritonia*. I. Identification and synaptic interactions. *J. Neurophysiol.* **44:** 151–164.

**Grillner, S., and P. Wallen. 1985.** Central pattern generators for locomotion, with special reference to vertebrates. *Annu Rev. Neurosci.* **8:** 233–261.

**Harris-Warrick, R. M., and E. Marder. 1991.** Modulation of neural networks for behavior. *Annu. Rev. Neurosci.* **14:** 39–57.

**Huang, Z., and R. A. Satterlie. 1990.** Neuronal mechanisms underlying behavioral switching in a pteropod mollusc. *J. Comp. Physiol. A* **166:** 875–887.

**Hume, R. I., P. A. Getting, and M. A. Del Beccaro. 1982.** Motor organization of *Tritonia* swimming. I. Quantitative analysis of swim behavior and flexion neuron firing patterns. *J. Neurophysiol.* **47:** 60–74.

**Hurst, A. 1968.** The feeding mechanism and behaviour of the opisthobranch *Melibe leonina*. *Symp. Zool. Soc. Lond.* **22:** 151–166.

**Jing, J., and R. Gillette. 1995.** Neuronal elements that mediate escape swimming and suppress feeding behavior in the predatory sea slug *Pleurobranchaea*. *J. Neurophysiol.* **74:** 1900–1910.

**Jing, J., and R. Gillette. 1999.** Central pattern generator for escape swimming in the notaspid sea slug *Pleurobranchaea californica*. *J. Neurophysiol.* **81:** 654–667.

**Katz, P. S., and W. N. Frost. 1995.** Intrinsic neuromodulation in the *Tritonia* swim CPG: serotonin mediates both neuromodulation and neurotransmission by the dorsal swim interneurons. *J. Neurophysiol.* **74:** 2281–2294.

**Katz, P. S., and W. N. Frost. 1996.** Intrinsic neuromodulation: altering neuronal circuits from within. *Trends in Neurosci.* **19:** 54–61.

**Lawrence, K. A. 1997.** Neuroethology of the swimming behavior of the Pacific nudibranch, *Melibe leonina*. Ph. D. dissertation, University of New Hampshire, Durham. 78 pp.

**Lawrence, K. A., and W. H. Watson III. 2002.** The swimming behavior of the nudibranch *Melibe leonina*. *Biol. Bull.* **203:** 144–151.

**Lukowiak, K. 1991.** Central pattern generators: some principles learned from invertebrate model systems. *J. Physiol.* **85:** 63–70.

**Marder, E., and R. L. Calabrese. 1996.** Principles of rhythmic motor pattern generation. *Physiol. Rev.* **76:** 687–717.

**McCrohan, C. R. 1988.** Modification of central pattern generation in invertebrates. *Comp. Biochem. Physiol.* **90A:** 17–22.

**McPherson, D. R., and J. E. Blankenship. 1991a.** Neural control of swimming in *Aplysia brasiliana*. I. Innervation of parapodial muscles by pedal ganglion motorneurons. *J. Neurophysiol.* **66:** 1338–1351.

**McPherson, D. R., and J. E. Blankenship. 1991b.** Neural control of swimming in *Aplysia brasiliana*. II. Organization of pedal motorneurons and parapodial motor fields. *J. Neurophysiol.* **66:** 1352–1365.

**Miller, J. P., and A. I. Selverston. 1985.** Neural mechanisms for the production of the lobster pyloric motor pattern. Pp. 37–48 in *Model Neural Networks and Behavior*, A. I. Selverston, ed. Plenum Press, New York.

**Newcomb, J. M., and W. H. Watson III. 2001.** Identifiable nitrergic neurons in the central nervous system of the nudibranch *Melibe leonina*, localized with NADPH-diaphorase histochemistry and nitric oxide synthase immunoreactivity. *J. Comp. Neurol.* **437:** 70–78.

**Page, L. R. 1993.** Development of behavior in juveniles of *Melibe leonina* (Gastropoda: Nudibranchia). *Mar. Behav. Physiol.* **22:** 141–161.

**Pearson, K. G. 1993.** Common principles of motor control in vertebrates and invertebrates. *Annu. Rev. Neurosci.* **16:** 265–297.

**Satterlie, R. A. 1985.** Reciprocal inhibition and postinhibitory rebound produce reverberation in a locomotor pattern generator. *Science* **229:** 402–404.

**Satterlie, R. A. 1991.** Neural control of speed changes in an opisthobranch locomotory system. *Biol. Bull.* **180:** 228–233.

**Satterlie, R. A., and T. P. Norekian. 1996.** Modulation of swimming speed in the pteropod mollusc, *Clione limacina*: role of a compartmental serotonergic system. *Invertebr. Neurosci.* **2:** 157–165.

**Trimarchi, J., and W. H. Watson. 1992.** The role of *Melibe* buccal ganglia in feeding behavior. *Mar. Behav. Physiol.* **19:** 195–209.

**von der Porten, K., D. W. Parsons, B. S. Rothman, and H. Pinsker. 1982.** Swimming in *Aplysia brasiliana*: analysis of behavior and neuronal pathways. *Behav. Neural Biol.* **36:** 1–23.

**Watson, W. H., K. D. Lawrence, and J. M. Newcomb. 2001.** Neuroethology of *Melibe leonina* swimming behavior. *Am. Zool.* **41:** 1026–1035.

**Willows, A. O. D. 1967.** Behavioral acts elicited by stimulation of single, identifiable brain cells. *Science* **157:** 570–574.

**Willows, A. O. D., and G. Hoyle. 1969.** Neuronal network triggering a fixed action pattern. *Science* **166:** 1549–1551.

**Willows, A. O. D., D. A. Dorsett, and G. Hoyle. 1973.** The neuronal basis of behavior in *Tritonia*. III. Neuronal mechanism of a fixed action pattern. *J. Neurobiol.* **4:** 255–285.

Reference: *Biol. Bull.* **203:** 161–172. (October 2002)

# Clade Perseverance From Mesozoic to Present: a Multidisciplinary Approach to Interpretation of Pattern and Process

DAVID K. A. BARNES

*British Antarctic Survey, Natural Environment Research Council, High Cross, Madingley Road, Cambridge, CB3 OET, United Kingdom*

**Abstract.** Two clades of marine bryozoans, cyclostomes and cheilostomes, exemplify the benefits of applying a multidisciplinary approach to the interpretation of long-term evolutionary patterns. The cyclostome bryozoans were dominant in the Mesozoic; since that era, they have decreased in absolute terms and the cheilostomes have come to exceed them in both abundance and diversity. Many studies of living assemblages of the encrusting members of these two clades indicate that cheilostomes are superior space competitors, but paleontological studies suggest that competition between the two taxa has not been escalating over geological time. Both clades occur throughout the world's oceans and seas, and recent work in the geographical extremes has shown that the relative success of the clades varies markedly from place to place. In this study, the importance of differential patterns of recruitment and cumulative space occupation in the two clades was evaluated over four years and in two environments, one temperate and one polar. In both of these environments, peaks of recruitment and space occupation by the two clades were out of phase. The different strategies and outcomes of spatial competition are examined, largely using data from the literature. Only recently has it been realized that tied outcomes of competition are stable alternative results and not simply transitory phases. Many competitive encounters involving cyclostomes result in ties, implying that their strategy is based on persistence rather than dominance. When different indices and models are used to analyze competition data from the two clades, the interpretation varies markedly with methodology. The differences in patterns of recruitment, space occupation, and spatial competition have influenced both our understanding of how the two clades have persisted alongside each other and our perception of cheilostome superiority. Analysis of fluid dynamics has shown that small differences in the mechanical structure of typical members of each clade lead to fundamental differences in water movement. For animals that rely on water motion for transport of nutritional and excretory elements (suspension feeders), small changes in current velocity and direction can have a major impact. Preliminary chemical analysis of the excurrent stream leaving cheilostome colonies has shown it to be laden with excretory products, which can interfere and mix with a neighbor's feeding currents. Clearly, spatial competition involves more than a simple mechanical "showdown."

## Introduction

During the past two decades, taxon perseverance through geological time has been the center of much paleontological study, which has usually been focused on mass extinctions and radiations. Although the underlying causes of discrete taxon (clade) perseverance may be stochastic, other factors, such as competition, may contribute; but these factors are difficult to assess. Typically, taxonomic richness per unit time has been taken to reflect the scale and pattern of clade survival, whereas the processes involved in clade persistence have been deduced from limited paleontological evidence and inferred from processes that occur in Recent times but are assumed to be equivalent to ones that functioned in the past. However, temporal snapshots of processes such as interference competition can be obtained from the fossilized remains of certain fauna, particularly

Received 19 September 2001; accepted 18 July 2002.

E-mail: dkab@bas.ac.uk

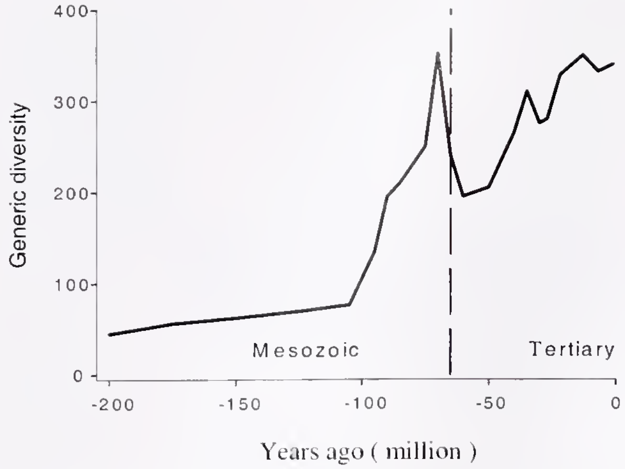

**Figure 1.** Global generic diversity of cyclostome and cheilostome bryozoans (combined clades) from late Triassic to Holocene times. Data from Taylor (1993) and McKinney *et al.* (1998) based on boundaries designated by Harland *et al.* (1990). The K-T boundary is shown as a vertical dashed line.

those with a high skeletal investment—sedentary lithophyllic encrusters (*e.g.*, bryozoans) foremost among them. Clades that are preserved in this way—that are diverse, abundant, extensive in the fossil record, and extant—offer us the opportunity to apply geological, biological, mathematical, fluid dynamic, and chemical (*i.e.*, multidisciplinary) approaches to understanding the processes underlying persistence.

Cyclostome and cheilostome marine bryozoans, two clades with such attributes, have co-occurred in similar environments for 150 million years. After a long period of gradual taxonomic increase, they underwent a rapid but punctuated increase in diversity during the Late Cretaceous (Fig. 1). Paleontologists and ecologists have studied these bryozoans extensively, and recent information has clarified the interpretation of scale, pattern, and process in their comparative ecology and evolution. In this manuscript, I examine how two competitor clades have managed to persist alongside one another for more than 100 million years. As background, I first describe the historical patterns of abundance and taxon richness in these bryozoan clades.

## Geological Scale and Pattern of Persistence

Cyclostome and cheilostome bryozoans occur together in most benthic lithophyllic assemblages, across latitudinal and longitudinal spectra, and frequently in direct competition for space and food (*e.g.*, Sebens, 1986; Lopez Gappa, 1989; Barnes and Dick, 2000). The older of the two clades, the cyclostomes, are the sole survivors of the class Stenolaemata; they were the dominant bryozoans for 100 million years, throughout most of the Mesozoic (Lidgard *et al.*, 1993) and are still locally important (*e.g.*, Harmelin, 1976). Other clades and paraphyletic or diphyletic groups (see Taylor, 2000) of the class Stenolaemata perished in the mass extinctions that began and ended the Triassic. The explosive radiation of bryozoans 100 million years ago (Fig. 1), comparable in its size to the more familiar success of the euteleost fish and neogastropods (Sepkoski and Hulver, 1985), was largely due to the cheilostome families (Fig. 2). The switch from cyclostomes to cheilostomes, in both species dominance and abundance of individuals, has been drastic, although abundance is slightly decoupled from taxonomic richness (Fig. 3).

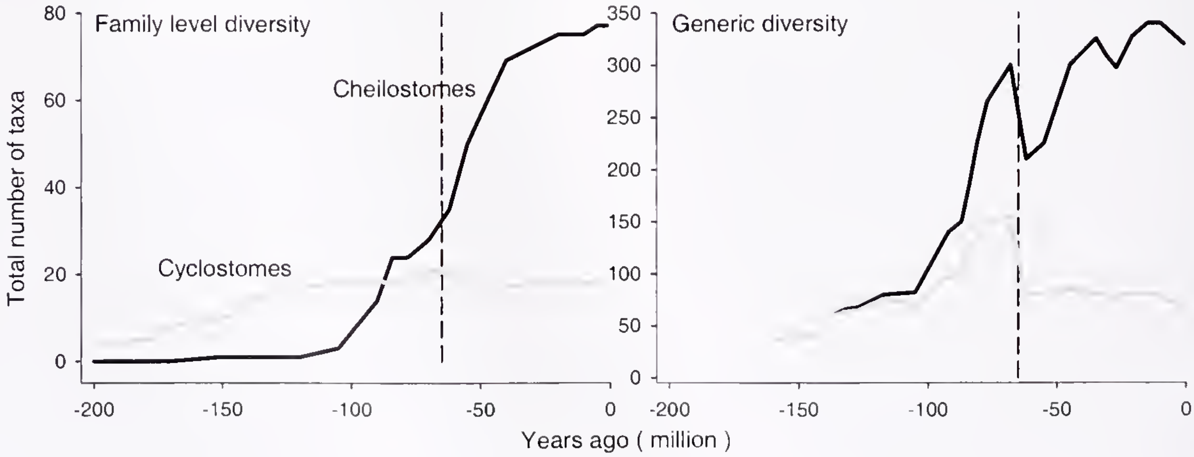

**Figure 2.** Family- and genus-level diversity of cyclostome and cheilostome bryozoans from Triassic to Recent times. Diversity values are from Taylor (1993) and Sepkoski *et al.* (2000). Family diversity levels (from Jablonski *et al.*, 1997) are absolute for each clade, whereas the generic plot (Sepkoski *et al.*, 2000) shows cyclostomes (lower line) and total (upper line); cheilostome generic diversity is thus equivalent to the divergence of the two lines. The K-T boundary is shown as a vertical dashed line.

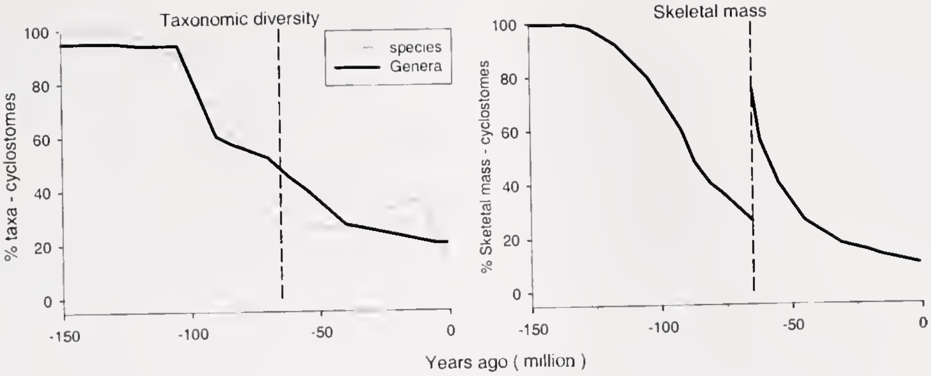

**Figure 3.** Relative species richness and a measure of abundance (skeletal mass) of cyclostomes and cheilostomes from the Cretaceous to the Cenozoic (from McKinney *et al.*, 1998). Data are trend lines plotted as moving average curves, which are fitted by the distance-weighted least-squares method (see McKinney *et al.*, 1998). The proportion of cyclostomes as a percentage of the total for the two study clades) is shown in the legend. The K-T boundary is shown as a vertical dashed line.

Following the end-Cretaceous mass extinctions, the ecological recovery of cheilostome abundance (measured as % skeletal mass) was slower than that of cyclostomes, taking more than 5 million years, and perhaps 25 million years, to return to Late Cretaceous levels. The competition between the two clades has, however, been stable over the last 100 million years (McKinney, 1995a); that is, cheilostomes have consistently overgrown cyclostomes in two-thirds of their encounters (mean 0.66 ± SE 0.11, $n$ = 24, range 0.55–0.75), so this cheilostome superiority has not increased. Cheilostomes in modern assemblages also overgrow cyclostomes, but with significantly more variability than is evident in the fossil record (Barnes and Dick, 2000). Competition is complicated, not only by the conditions of preservation, but also by the ways in which the outcomes are measured (*e.g.*, as a ratio of wins to losses, or wins to total interactions), and by the way that competition data are analyzed (see Petraitis, 1979; Rubin, 1982; Tanaka and Nandakumar, 1994).

Examination of recruitment (*i.e.*, establishment of adult colonies) is another crucial approach to interpreting clade success, as spatial competition occurs only after colonies have formed. This is particularly true with the two bryozoan clades, which generate larvae by different methods and at different times, disparities that might explain the persistence or differential advantages gained by each clade.

In this study, temporal patterns of cyclostome and cheilostome recruitment and persistence were assessed over 4 years and in two very different environments: Lough Hyne (Ireland) and Signy Island (Antarctica). These environments represent extremes in disturbance: the habitat at Lough Hyne has very low energy and relatively warm water, whereas that at Signy Island has cold water that is highly disturbed periodically. The performance of the two clades in overgrowth competition is compared by applying various computations to a model data set (from Barnes and Dick, 2000). I have used both the original data and that from Barnes and Dick (2000) to address three questions: (1) What characteristics of cyclostomes allow them to persist alongside cheilostomes? (2) What attributes have made cheilostomes superior to cyclostomes in their competition for space? (3) And what are the bases for the proportional and absolute decline of cyclostomes since the K-T boundary?

## Materials and Methods

### *Recruitment and community development at Signy Island, Antarctica*

Recruitment of cheilostome and cyclostome bryozoans was measured from 1991 to 1994 at Powell Rock, Signy Island, Antarctica. This is a rocky site that is exposed to ice scour and currents varying from 1 m $s^{-1}$ to <5 cm $s^{-1}$. The ecology, composition, and seasonality of the recruit community have been described by Stanwell-Smith and Barnes (1997). The experimental protocol followed that of Todd and Turner (1986). Machined slate panels (15 cm × 15 cm × 1 cm) were attached, in sets of three, to weighted rods. Two of these triplicate panels were positioned horizontally 1 cm above hard substratum at 25 m depth. Each month, in alternation, one of these two triplicate panels was replaced, and all colonists were counted and identified. Only the central area (10 cm × 10 cm) of the undersurfaces of the panels was thus analyzed. The mean numbers of cyclostomes and cheilostomes were standardized to recruits per 30-day period, and these values were graphed against time; standard error bars were generated with data from the monthly, three-panel replicates.

### *Recruitment and community development at Lough Hyne*

Recruitment of cheilostome and cyclostome bryozoans was measured from 1997 to 2001 at Lough Hyne Marine Nature Reserve, County Cork, West Ireland. An overview of the hydrology and marine biology of the site, Labhra Cliff, is given in Kitching (1987). Many environmental parameters at the site are the converse of those at Signy Island. Ambient currents, when measured, did not exceed 5 cm $s^{-1}$ (Maughan, 2000), surface waves were rarely higher than 10 cm, and the maximum water temperature may be more than 20 °C (Barnes *et al.*, 2001). Experimental protocol followed Todd and Turner (1986), Stanwell-Smith and Barnes (1997), and that at Lough Hyne (Maughan and Barnes, 2000).

The machined slate panels were set up as at Signy Island, but at two sites, and with two sets of triplicate panels, at 3 m, 6 m, and 12 m depth, at each site. One set of triplicate panels at each site and each depth was replaced (by scuba) each month between October 1997 and May 2001. As with the data generated from the study at Signy Island, the number of recruits from the cyclostome and cheilostome clades was plotted monthly as the mean and standard error. The remaining set of panels was photographed and inspected monthly, and the colonists were identified: the relative amount of space occupied by each clade (% cover) was calculated. After 2 years, these panels were retrieved, analyzed, scraped clean, and repositioned; they were then photographed and inspected monthly for another 18 months. The data on relative space occupation generated from these panels left *in situ* at each depth for 2 years, and then for an additional 18 months, were also graphed.

### *Interference competition*

The outcomes of interference competition between cyclostomes and cheilostomes were recorded on panels at three sites at Lough Hyne and at various depths: Rapids, 3 m; Rapids, 6 m; Whirlpool, 6 m; Whirlpool, 12 m; Labhra, 6 m; and Labhra, 12 m. These study sites constitute an energy gradient with the following, respective, typical current velocities: 3 m $s^{-1}$, 2.5 m $s^{-1}$, 1 m $s^{-1}$, 0.8 m $s^{-1}$, 0.1 m $s^{-1}$, and 0.05 m $s^{-1}$. To boost sample size, cheilostomes were categorized into functional groups (so the interaction outcomes for all species within a functional group were pooled into win, tie, and loss totals), as described in Maughan and Barnes (2000). Functional groups are essentially a set of organisms with similar modes of life and, in the context of interference competition (here), of growth form. The following functional groups were used here: each of the two study clades (cheilostomes and cyclostomes), polychaete worms (phylum Annelida), ascidians (phylum Chordata, subphylum Urochordata), and sponges (phylum Porifera). Outcomes of interference competition were scored as wins, losses, or ties. In accordance with interpretations in the wider literature, a colony that occluded more than 5% of the active zooids of another was awarded a win, whereas its competitor was assigned a loss. Interactions were scored as ties if mutual overgrowth occurred, or if growth was redirected such that a clear "impasse" line was formed. Any tied interaction between representatives of the two clades was monitored further by repeated underwater photographs of interactions, to ascertain the permanency of the outcome.

### *Treatment of data*

Competitive interactions upon the panels at Signy Island and Lough Hyne were used to generate performance scores for site comparisons. These data sets, however, involved too few cheilostome-cyclostome interactions for strong comparisons of different mathematical statistical techniques. Therefore, a data set from the recent literature was selected to illustrate variability in interference competition in a subarctic assemblage (Barnes and Dick, 2000). Competitive "performance scores" of representatives of the two clades were assessed by various methods. The first of these was to calculate, from raw data, the proportion of wins to interactions, and then to rank these values. These "initial rankings" may differ from those of populations because each species participated in a different number of interactions, no species met any of the others on the same number of occasions, and some species never met each other at all. To rectify this problem, the data were standardized: pairwise interactions involving each species were appropriately multiplied such that each totaled 100; total wins, losses, and ties for each competitor identity were then multiplied by the same factor. Several computations were then applied to the standardized values to investigate how the method of assessment would affect the rankings, and thus the apparent success of each species in competition. (1) A scoring system was applied, where a win = 3, a tied outcome = 1, and a loss = 0; wins were rated much higher than ties because ties often prevent further growth and development of colonies; see Barnes and Clarke (1998). (2) The number of wins was divided by the total number of interactions for that competitor. (3) The number of losses was divided by the total number of interactions for that competitor. (4) The number of wins divided by the number of losses for that competitor. (5) In addition, two novel methods from recent literature (see de Vries, 1998; Jameson *et al.*, 1999) were included in this analysis, as they were specifically designed to reduce sources of bias and error in estimating competitor success. These methods are linear ordering procedures based on iterative algorithms (de Vries, 1998) and on mathematical models of paired comparisons involving fairly simple estimations (Jameson *et al.*, 1999); both methods assume that the data form a near-linear hierarchy.

## Results

### *Recruitment at Signy Island, Antarctica*

The scale of recruitment of both cheilostome and cyclostome clades was generally comparable throughout the

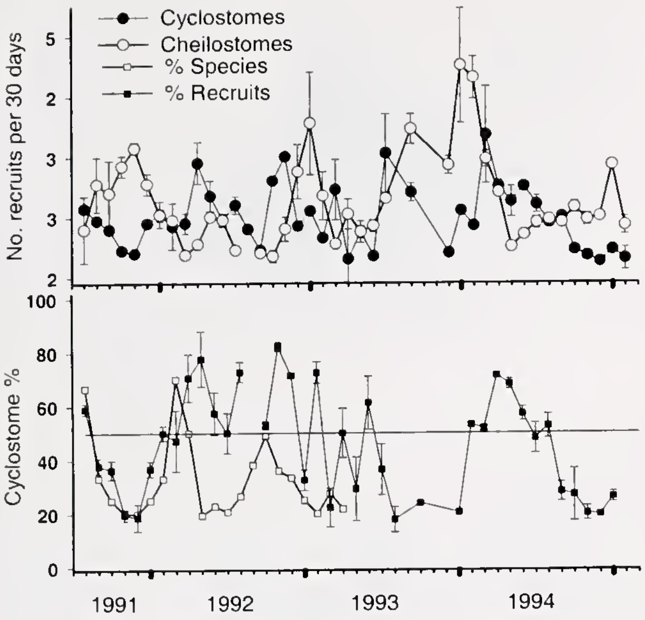

**Figure 4.** Number and proportion of cyclostome and cheilostome species and recruited colonies, identified at Signy Island, Antarctica, and plotted as a function of time. Data are shown as the mean (from three replicate panels) and standard error. Clade recruitment data were not separated into species after March 1993.

study period (1991–1994) in Antarctic waters (Fig. 4). Monthly, seasonal, and annual variabilities were high in both the timing and magnitude of recruitment in both clades. Between-panel variability was generally low except at peak settlement. But some cheilostome and cyclostome recruits were recorded in every month of the study. Of most note was the aphasic alignment of peak settlement for the two clades. Cheilostomes recruited in peak numbers at the start of the austral summer (December), and cyclostome recruitment usually occurred just before or after peak cheilostome recruitment (*i.e.*, spring and autumn). The proportion of species constituted by cyclostome recruits typically varied between 20% and 40%, but on three occasions was 50% or more. The proportion of recruits that were cyclostomes was, in contrast, considerably higher (especially outside summer periods) and more variable. Only on two occasions was the proportion of recruits smaller than that of the species. Variability in the proportion of recruits was higher than that in the proportion of species, both in space (between panels) and time (between months). Therefore, the phases of recruitment of the two clades were not coincident, but scales were; and abundance of species (taxonomic richness) was decoupled from abundance of individuals (ecological dominance).

### *Recruitment and community development at Lough Hyne*

As at Signy Island, both clades recruited at similar levels during the 4-year study (Fig. 5). Moreover the scale of recruitment at Lough Hyne was also of a similar magnitude to that at Signy Island, although there were months when there were no recruits of either clade. In contrast to the polar results, most of the variability in recruit numbers was seasonal, but peak recruitment was much greater in 1998 than in any other year in both clades. Between panel variability was very low. Peak recruitment of the two clades was, as at Signy Island, out of phase but in a regular manner: cyclostomes peaked just before cheilostomes in each study year. Peak cheilostome recruit numbers occurred in midsummer (July), and the corresponding cyclostome peak was in May. By species, cyclostomes formed about 20% of recruits in summer but increased to about 70% over each winter. Measured in absolute numbers of recruits, cyclostomes nearly always represented a higher proportion, but this difference varied with season from <30% to >90%. So at Lough Hyne, as at Signy Island, peaks of clade recruitment were similar in scale, but separated in time. The clear distinction between the proportion of recruits and the proportion of their species indicates that, for these two clades, taxonomic richness does not mirror ecological dominance. Patterns in the data collected at 6 m (not shown) were essentially similar to those collected at 12 m (Fig. 5), differing only in the magnitude of the peaks.

Both clades were major components of the cumulative faunal buildup on panels at 6 m and 12 m (Fig. 6), but not on the intertidal panels (not shown). As with the serially replaced panels (Figs. 4 and 5), temporal variability was primarily seasonal, but also annual. Variability changed with depth: seasonal patterns were more distinct at 12 m,

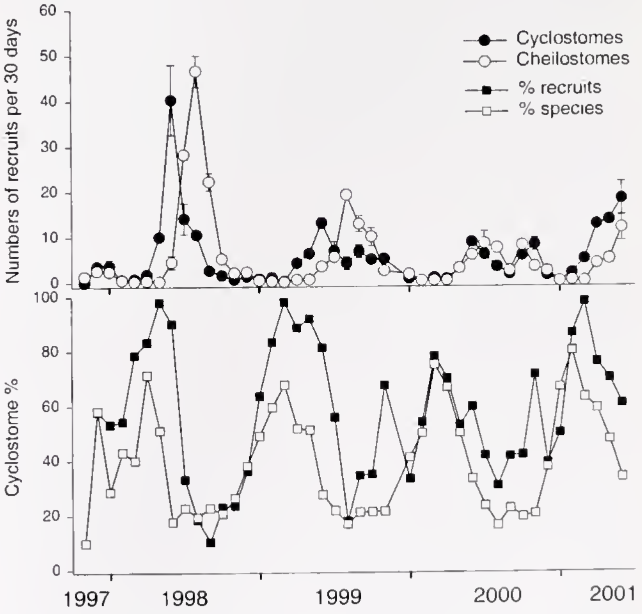

**Figure 5.** Number and proportion of cyclostome and cheilostome species and recruited colonies collected and identified at Lough Hyne, Ireland, and plotted as a function of time. Data presentation as in Figure 4.

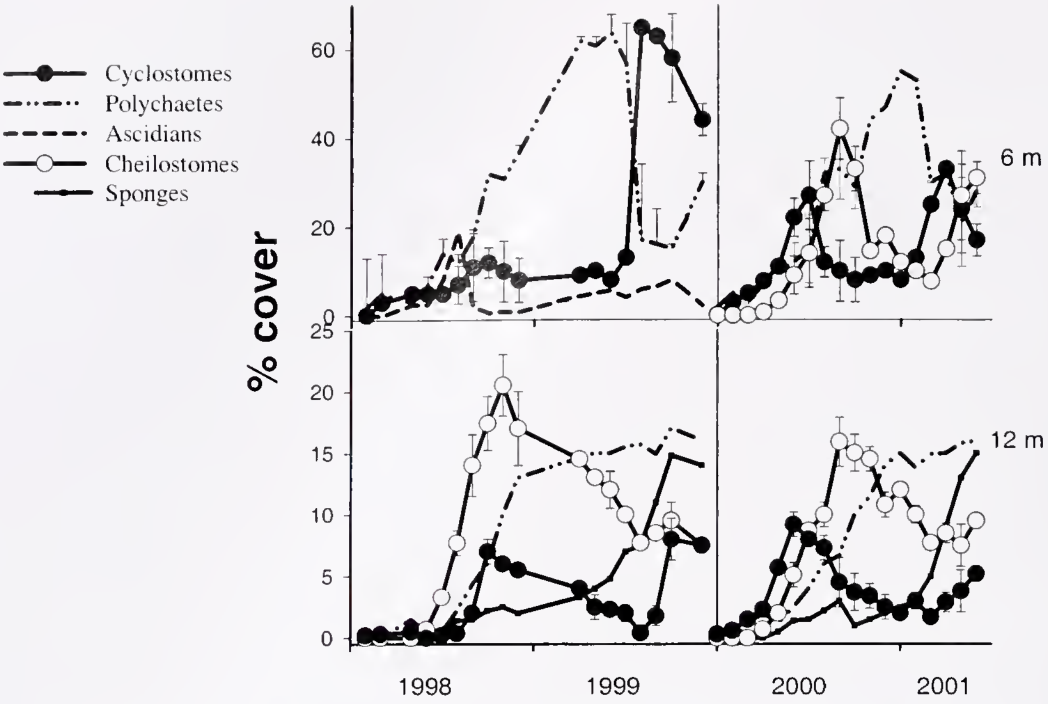

**Figure 6.** Cumulative space occupation, with time, by marine benthic taxa at Lough Hyne, Ireland. Data are shown as the mean (from three replicate panels) and standard error. The symbols for taxon identity are shown on the figure. Two upper plots represent data from Labhra, 6 m; and the data for Labhra, 12 m, is shown in the two lower plots. Cheilostomes formed a negligible component of the fauna at Labhra, 6 m, in 1998–1999 and are thus not illustrated.

while annual patterns were more distinct at 6 m. The clades peaked at similar year-points at both depths and in the two cumulative runs (1998–1999 and 2000–2001). In contrast to the monthly recruitment patterns, clades differed with respect to scale: cheilostomes typically occupying more space than cyclostomes (despite the similarity in recruitment). At 6 m in 1998–1999, however, the cheilostome buildup was minor despite normal recruitment patterns (pattern as in Fig. 5).

All of the major faunal groups that colonized the panels peaked at different points during the study. Cyclostome space occupation, as with recruitment, peaked both in summer and just before the greatest cheilostome coverage. A clear succession was apparent at 12 m; the cyclostomes were the initial major space occupiers but were replaced sequentially by cheilostomes, polychaetes, and sponges. At 6 m, however, no such succession was apparent in either 1998–1999 or 2000–2001. Faunal groups were sequentially replaced (at 6 m) in 2000 in a pattern similar to that at 12 m, but this pattern appeared to break down in 2001. Curiously, when the experiment was terminated in 1998–1999, cyclostomes were the dominant space occupiers. As for space on the intertidal panels, it was monopolized throughout the study period by barnacles (not shown).

### *Interference competition and performance assessment*

Cyclostomes were poor spatial competitors at Lough Hyne, being overgrown by most other encrusting faunal groups. Against cheilostomes, their performance was average, with a combined win/total interactions score (win index) of 0.44, indicating that cyclostomes win slightly less than half of the encounters. Cyclostome performance varied, however, both with the functional group of cheilostomes with which they competed and with site energy (current velocity) (Fig. 7). With increasing site energy, cyclostomes clearly lost fewer interactions against most of the different functional groups; nevertheless, the improvement in performance increase against some groups was only minor. With a win index of just 0.1, Antarctic cyclostomes at Signy Island were much less effective than those at Lough Hyne at overcoming cheilostomes. When the local performance of cyclostomes (against cheilostomes) was graphed against their local species richness, performance was seen to increase with richness (Fig. 8). Although significant, this correlation must be treated with caution, as it is almost certainly due to the relationship of both parameters with yet other factors.

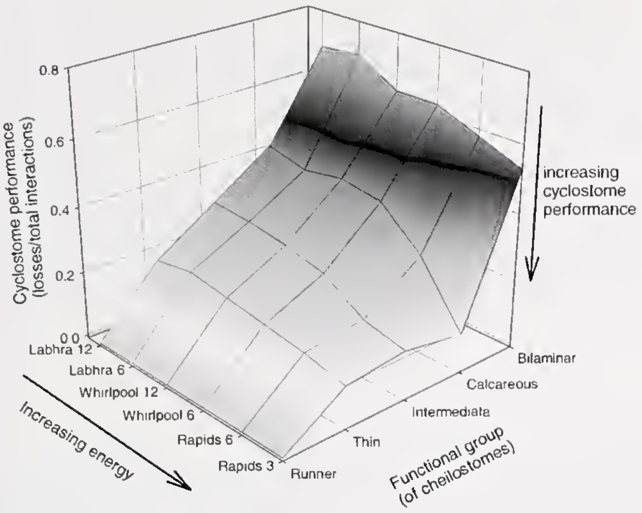

**Figure 7.** Cyclostome performance in interference competition against functional groups of cheilostomes, plotted as a function of site energy. Performance was measured as proportion of losses in competitive interactions. The cheilostome clade incorporates many colony forms, which are categorized here into the functional groups bilaminar (foliaceous sheets), calcareous (heavily calcified sheets), intermediate, thin (membranous sheets) and runner (stolons). The sites (at Lough Hyne, Ireland) are organized along an energy gradient as shown. For more information on sites, functional groups, or species, see Maughan and Barnes (2000). Performance is measured as L/T, so performance increases as L/T declines.

The highest measured performance of cyclostomes against cheilostomes was in Alaska (data from Barnes and Dick, 2000), but further analysis suggests that the assessment depends on the method of measurement. Initial (non-standardized) and standardized win-tie scored ranking showed cyclostomes to be medium to poor performers against cheilostomes (Table 1). The low proportion of wins to total encounters suggested that *Patinella* (a model cyclostome genus) is a very poor competitor. However, most of the interactions were tied, with the number of wins and losses roughly balancing out. Indeed, the very low proportion of losses was second only to that of the cheilostome *Tegella aquilostris*. Taken together, these observations indicate that although *Patinella* neither won nor lost many encounters, it persisted as a member of the assemblage. This emphasizes that overgrowth performance is not the only mechanism by which a bryozoan can maintain itself in the community. Data were also subjected to two recognized techniques that reduce bias in mathematical comparisons of competitor performance from accumulated pairwise interactions (de Vries, 1998; Jameson *et al.*, 1999). Both measures ranked *Patinella* differently from each other and from previous measures (Table 1), but both suggested approximately medium rankings for the cyclostome genus.

## Discussion

*What are the implications of differences in recruitment, space occupation, and competition on inter-clade dynamics?*

Although the cyclostome and cheilostome clades are similar and occur together on marine hard substrata from the poles to the tropics and from the Mesozoic to present day, their life strategies differ subtly but importantly. Cyclostomes occupy less space and have lower species richness in the temperate and polar study localities, but the intensity of their recruitment is similar to that of cheilostomes (Figs. 4 and 5). More important perhaps, peak levels of recruitment for the two clades are out of phase; cyclostome recruits are typically a month or more ahead of cheilostomes. The reproductive strategy of cyclostomes—which is termed polyembryony and involves repeated cleavage of blastomeres to give large numbers of genetically identical embryos (Harmer, 1893)—may help explain both the high and early recruitment observed in the present study. That peak cyclostome recruitment precedes that of cheilostomes is important for two reasons. First, it maximizes the potential of the clade to occupy temporarily available space. Second, most cyclostomes have grown for a month longer than the same cohort of cheilostomes and thus have the potential advantages of size both in spatial competition and in achieving reproductive activity. The early cyclostome recruitment explains the initial dominance of space by cyclostomes in both Ireland and Antarctica. Six months later, however, cheilostomes occupy more space and are overgrowing cyclostomes. In conclusion, although competitive performance varies with the functional group of cheilostome competitors (Fig. 7), methods of mathematical analysis (Table 1), local cyclostome species richness (Fig. 8), and energy of the environment (in roughly descending order), cheilostomes are overall superior space competitors.

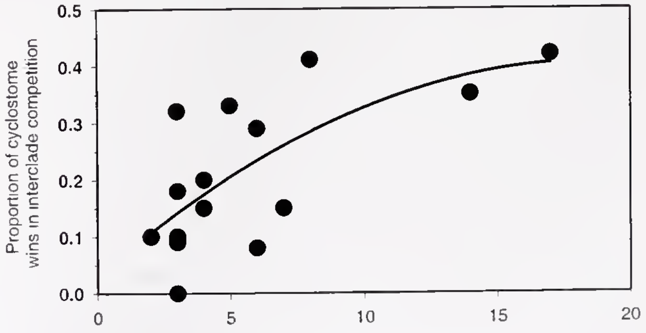

**Figure 8.** Competitive performance of cyclostomes (against cheilostomes) plotted against local cyclostome species richness. Observations made at Signy Island, Antarctica; data from Barnes and Dick (2000).

**Table 1**

*Alaskan cheilostome and cyclostome bryozoans ranked according to their performance in interference competition*

| | Initial | Win-Tie score | Win/Total | Loss/Total | Win/Loss | De Vries (1998) | Jameson *et al.* (1999) |
|---|---|---|---|---|---|---|---|
| 1 | Ta | Tq | Tq | Tq | Ta | Ta | Ta |
| 2 | Tq | Ta | Ta | **P** | Tq | Tq | Mp |
| 3 | Mp | Mp | Mp | Ta | Mp | Mp | Tq |
| 4 | Ca | Ca | Tr | Mp | Ca | Ca | **P** |
| 5 | Mc | Tr | Ca | Ca | **P** | Tr | Mc |
| 6 | Tr | Mc | Mc | A | Tr | A | Tr |
| 7 | **P** | **P** | M | Tr | Mc | **P** | Ca |
| 8 | M | M | Cn | Mc | A | Mc | A |
| 9 | Cn | A | **P** | Cn | M | Cn= | Cn |
| 10 | Pa | Cn | A | Pa | Cn | Pa= | Pa |
| 11 | A | Pa | Pa | M | Pa | M= | M |

Data from Barnes and Dick (2000) were variously manipulated, and the resulting values are ranked. The rankings, in descending order (1 = best, 11 = worst) can be initial (number of wins/total number of interactions) or standardized (multiplied so every competitor meets the others with the same frequency). The standardized ranking are win-tie scored (wins score 3, ties score 1, so a species with 10 wins, 2 ties, and 88 losses scores [10 × 3] + [2 × 1] + [88 × 0] = 32, while a species with 4 wins, 30 ties, and 66 losses scores [4 × 3] + [30 × 1] + [66 × 0] = 42, which gives a better ranking); W/T (proportion of wins over total number of interactions); L/T (proportion of losses over total number of interactions—rank 1 here is the smallest number, [*i.e.*, a winning performance] and rank 11 is the largest number [*i.e.*, a poor performance] and W/L (proportion of wins over losses). Two novel methods were also applied; they are described in recent literature (De Vries, 1998; Jameson *et al.*, 1999). Abbreviations of taxa are *Tegella armifera* (Ta), *Tegella aquilostris* (Tq), *Myriozoella plana* (Mp), *Caulorhamphus* sp. (Ca), *Microporella californica* (Mc), *Tegella arctica* (Tr), *Patinella* sp. (P), *Microporella* sp. (M), *Cribrilina annulata* (Cn), *Porella alba* (Pa) and *Alcyonidium* sp. (A). The genus *Lichenopora* was revised by Gordon and Taylor (1997) and Recent species were reassigned to the genus *Patinella*. Cyclostome taxa are in shaded cells and printed in bold. Equals signs (=) signify that the taxa have equal ranking.

### *How do cyclostomes persist alongside superior space competitors?*

Since the Mesozoic, cheilostomes have not only dramatically increased at various taxonomic levels (family, genus and species), but also maintained their historical competitive dominance over the cyclostomes (see Taylor, 1993; McKinney, 1995a; Jablonski *et al.*, 1997; McKinney *et al.*, 1998). Marine ecological studies of modern assemblages (such as those of Ireland and Antarctica in the present study) have revealed a variable but a distinct competitive edge of cheilostomes over cyclostomes (McKinney, 1992; Barnes and Dick, 2000). Despite the evolutionary and ecological increase of cheilostomes over the past 100 million years, cyclostomes have maintained global and local diversity (Lidgard *et al.*, 1993). The inevitable increased frequency of cheilostome-cyclostome meetings resulting from the proliferation of cheilostomes might be expected to bring about a progressive displacement of cyclostomes. This may have contributed to the decline in ecological success and species richness of cyclostomes from the end of the Cretaceous to the Recent (Lidgard *et al.*, 1993; McKinney *et al.*, 1998; Sepkoski *et al.*, 2000). The effect seems better explained, however, as merely adding to total bryozoan diversity rather than as displacement (Sepkoski *et al.*, 2000).

The comparative lack of effect on cyclostomes of the K-T boundary event (McKinney *et al.*, 1998) suggests that this clade has been very resilient in the face of major changes with time. Recruitment patterns revealed in the present study show that cyclostomes are best positioned, not just amongst the bryozoans, but also throughout encrusting macrobiota, to exploit newly available habitats. Cyclostome recruits peaked high and early (Figs. 4 and 5) and were initially the dominant component developing subtidal assemblages at Lough Hyne (Fig. 6). Thus, on ephemeral substrata they gain advantage. In highly disturbed environments, such as the nearshore polar environment, cyclostomes should (and do), therefore, constitute a major portion of the lithophyllic biota (Barnes *et al.*, 1996; Barnes and Dick, 2000). The advantage of early colonization and establishment (Fig. 6) is maintained by a strategy that prevents overgrowth (Table 1). Thus persistence, rather than winning competitive encounters outright, is a feature of cyclostomes.

The evolutionary success (species richness) and ecological success (biomass) of the cyclostomes have been decoupled over geological time (McKinney *et al.*, 1998) and, during Recent times, in geographical space, as well. Localities where cyclostomes have their highest inter-clade performance levels are not linked with areas of greatest numerical abundance. Cyclostomes perform well against cheilostomes in Alaska and Ireland, but compete poorly on Antarctic rocks. Yet, of these localities, it is in Antarctica that they occupy most space (see Barnes and Dick, 2000; Barnes and Maughan, 2002). Cyclostomes are poorly represented at low latitudes (Taylor, 2001) and around some small island groups (Banta and Redden, 1990; Hayward and Winston, 1994). Between 45 °S and 75 °S, the relationship between latitude and the ratio of extant cheilostome species to cyclostome species seems to be parabolic (Barnes and DeGrave, 2000). Cheilostomes constitute more than 70% of species (of the two clades) between 55 °S and 65 °S, and cyclostomes are nearly 50% at 50 °S and at 70 °S (Barnes and DeGrave, 2000). Causes of the differences in cheilostome and cyclostome species richness in the Southern Ocean may be linked to historical diversity centers and events in the Tertiary (*e.g.*, see Moyano, 1983; Winston, 1983) when Antarctica became isolated and ultimately polar (Lawver *et al.*, 1992).

### *How superior are cheilostomes to cyclostomes?*

Determination of superiority in ecology is relatively straightforward, if only one aspect is considered. In fossil assemblages, an asymmetric performance relationship between cyclostomes and cheilostomes is clear-cut (McKinney, 1995a). The demonstration that Recent variability in performance is more than twice that in the fossil record (Barnes and Dick, 2000) casts doubt on the meaningfulness of mean performance scores for the two clades on large spatial or temporal scales. Only a weak relationship between site energy and performance is shown here (Fig. 7). In Ireland, the performance of cyclostomes against each functional group of cheilostomes increased slightly with currents of increasing energy, but this increase in performance was much less in the very high energy Antarctic waters. A further relationship, between local cyclostome performance and species richness (Fig. 8), suggests that further factors are yet to be determined. The variation in competitive performance with the particular index chosen to measure it (Table 1) complicates any overall assessment. Essentially, cyclostomes are fairly poor at gaining space from a competitor by physical contact. They are much more adept at avoiding being overgrown.

Depending upon the degree of crowding and competition, cheilostomes often initiate or increase their formation of brood chambers (reproductive activity) on contact with competitors (Barnes and Clarke, 1998). There is some evidence that fossil cyclostomes also initiated brood chamber construction when crowded by competitors. There is, indeed, even evidence that sexual reproductive activity may have been exclusively or nearly exclusively initiated by fossil cyclostomes coming into contact with competitors (McKinney and Taylor, 1997). When examining certain fossil cyclostomes, McKinney and Taylor (1997) found reproductive activity only in colonies that abutted other colonies. Certainly the peaks of cyclostome larvae appear just after an increase in cheilostome abundance at Lough Hyne (Fig. 5), though no distinct pattern is evident in the Antarctic data set (Fig. 6). Although cyclostomes appeared able to hold off most cheilostomes for the duration of the temperate and polar studies reported here, ultimately both clades were easily overgrown by sponges and ascidians (Maughan and Barnes, 2000), as has been found elsewhere (Russ, 1982; Sebens, 1986). At Lough Hyne and Signy Island, more than 90% of spatial competitive encounters by cyclostomes were against cheilostomes. The cyclostome survival strategy is to hold off their most common competitor, cheilostomes, until larvae can be produced; and this may be an effective plan. Whether the high proportion of stalemates between representatives of the two clades is permanent may be irrelevant, for both clades may then be overgrown by other superior space competitors.

Comparable densities of recruits (Figs. 4 and 5) indicate that the reproductive output of the two clades is similar at the two very different study sites. However, when recruitment and space occupation at the same locality are considered, cheilostomes must grow considerably faster. At Signy Island, the absolute number of cheilostome species recruiting was considerably greater than the number of cyclostomes, with the mean number of species recruiting per unit time oscillating around 50%. Furthermore, in the two study assemblages, as established for the fossil record (McKinney *et al.*, 1998), taxonomic richness patterns did not reflect ecological dominance. In summary, the extent of superiority of cheilostomes is highly variable; it depends both on attribute (reproduction, growth, or spatial competition) and, as shown by Table 1, on how superiority is measured.

### *What makes cheilostomes superior to cyclostomes—better by design?*

Evolution of cheilostome and cyclostome skeletal structure has followed similar and often convergent paths. The sequence of origin of structural novelties was similar between the two clades, but the timing and speed of acquisition (Fig. 9) was not (Jablonski *et al.*, 1997). Because most structural novelties of cyclostomes originated more than 50 million years earlier than those of cheilostomes, the ecological context of their design innovations are different: that is, cyclostome novelties evolved during a period of relatively low and stable familial and generic diversity, whereas those of cheilostomes appeared during a phase of high and rapid increase of diversity (Fig. 2). The design of cheilostomes made them certain to be superior competitors to cyclostomes, although chance has probably played a major role in survival of many groups of organisms. Cheilostomes possess many superior attributes focused at the colony margin, where (1) zooidal skeletons and feeding structures are full-sized because of rapid ontogenetic development; (2) labile morphogenetic responses (such as raising growing edges, frontal budding, and stolon production) are possible; and (3) excurrents are produced (McKinney, 1992; 1993; 1995a, b). The latter discovery, along with others from studies of fluid dynamics, has important ramifications for inter-clade competition. Cyclostome incurrents emanate

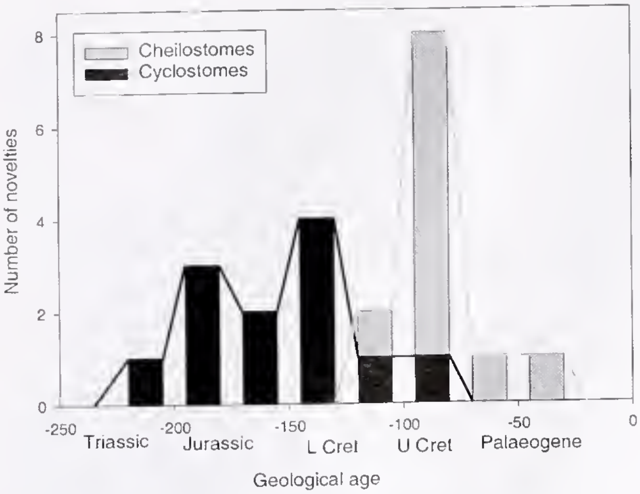

**Figure 9.** Evolution of morphological novelties in the cyclostome and cheilostome clades plotted against geological age. Figure adapted from Jablonski *et al.*, (1997).

from the periphery; therefore, in competition with a cheilostome neighbor, cyclostome incurrents are potentially the excurrents of cheilostomes. Cheilostome incurrents, in contrast, are drawn down from the water above a colony and are thus separated from the excurrents of a neighbor. Fisher (1989) has suggested that an element of chemical warfare exists, whereby feces can be passed from one competitor into the feeding current of its neighbor (though this study featured only cheilostomes). The combination of these features, combined with higher growth rates, larger colonies, and feeding structure novelties—and possibly the acquisition of non-planktotrophic (lecithotrophic) larvae, have made possible the great radiation of the cheilostomes since the mid-Cretaceous period (Taylor, 1988; Lidgard *et al.*, 1993). Despite the generalities of inter-clade differences (discussed above), the design and structure of bryozoans are characterized by significant intra-clade variability and inter-clade overlap. The cheilostome clade incorporates a huge range of colony forms, including spot, runner (stolon), membranous sheets, bilaminar foliaceous sheets, and a variety of erect forms of flexible or rigid structure. Some of these forms strongly resemble those of certain cyclostomes. Spot colonies, such as those of the cheilostome *Cribrilina* (Bishop, 1989), are similar in shape, structure, and even performance in spatial competition to the cyclostome *Patinella* (Table 1). Although cheilostomes can generally be considered to have a superior design, the range of colony form effectively incorporates most cyclostome structures.

### *Why have the cyclostomes declined ecologically over the last 100 million years?*

Despite the revival of ecological dominance for at least 5 million years after the K-T extinctions (Fig. 3, and see McKinney *et al.*, 1998), cyclostomes have, for the last 90 million years, constituted only a minor proportion of bryozoan taxa and of skeletal mass, aside from the early Cenozoic excursion. Although cyclostomes have maintained family diversity levels, neither generic richness nor species richness has recovered from the end-Cretaceous crashes.

The lower rate (post K-T) of origination of cyclostome genera has mostly accounted for their decline relative to cheilostomes (McKinney and Taylor, 2001). But erect, rather than encrusting, species are mainly responsible for this pattern (P. D. Taylor, Natural History Museum, London, unpub. data), which highlights a major problem with inter-clade comparisons based on existing knowledge. Although most evidence and discussion concerns encrusting species, as in this study, some changes may have little to do with this colony form. Interpretation of comparative historical records of a clade is difficult for many reasons, including increase of species diversity along nonlinear paths over macro-evolutionary time (Fig. 2; Sepkoski, 1979, 1991) and differential rates of evolution between clades. Specific diversification of clades seems to be controlled by a number of factors, such as the resolution of resource division (Bambach, 1983, 1985), presence and identity of other competing clades (Kitchell and Carr, 1985), and clade-specific speciation and extinction rates (Sepkoski, 1996). Cyclostome displacement may have largely occurred through increased meetings with typically superior competitors (cheilostomes) from end-Cretaceous to Recent time (Lidgard *et al.*, 1993; McKinney, 1995a; Sepkoski *et al.*, 2000). Such a displacement may have been merely geographic. As with species niche shifts, cyclostome species and abundance centers may have shifted to occupation of a "realized niche" at higher latitudes. Although niche shifts have been much discussed at the species or genus level, the same process could theoretically occur at higher taxonomic levels.

Recent assessments of the consistently asymmetric performance in interference competition between the two clades, carried out in living and fossil assemblages (McKinney, 1992 and 1995a, respectively), were important pieces of evidence supporting competition as an explanation for absolute clade displacement. Although this conclusion may be true for the types of environments ideal for fossilization (shallow, warm, low-energy seas), it is clearly not applicable to all geographic regions (Barnes and Dick, 2000). In high-energy environments, performance and space occupation by cyclostomes may differ considerably. Thus, rather than necessarily having diversity and abundance depressed by cheilostome competition, cyclostomes could have undergone a clade niche shift to higher energy conditions—a shift that may be unrepresented in the fossil record because of differences in the likelihood of environmental preservation. Whether competition has been entirely responsible for such a shift is debatable. The competitive performance of cyclostomes increases with increased energy conditions (Fig. 7), and their increased occupation of space in high-energy conditions provides some supporting evidence for a shift along an energy gradient. In contrast, other data from the northern Adriatic Sea shows decreasing cyclostome richness and diversity with increasing site energy (F. K. McKinney, Appalachian State University, North Carolina, unpubl. data).

### *Conclusions*

Despite fluid dynamic, ultrastructural, and morphogenetic evidence of cheilostome design superiority, cyclostomes persist through differential recruitment strategy, rapid colonization, and maintenance of space. Some of the multiple methods of survival have only recently begun to be recognized by biologists. Rather than being a rare or temporary event, tied outcomes may be a regular outcome in competition between certain taxa (Stebbing, 1973; Russ, 1982; Sebens, 1986; McKinney, 1992; Barnes and Dick, 2000), and may represent a temporally stable state (Tanaka and Nandakumar, 1994). Only with understanding of these concepts is cyclostome strategy becoming apparent. Therefore, cheilostome expansion may have indeed added to bryozoan diversity, and cyclostomes may have undergone some geographical displacement possibly mediated by inter-clade competition. Ecological and evolutionary success is clearly decoupled in cyclostomes at global and local levels. Domination in early community development or after disturbance is possible at varying geographical and temporal scales despite the prolific expansion of a competitively superior and co-occurring clade (cheilostomes).

## Acknowledgments

The author thanks all members of the Lough Hyne research group and the British Antarctic Survey inshore marine diving team for help in data collection; F. K. McKinney and three anonymous reviewers for comments that greatly improved the manuscript; Declan O'Donnell for the Lough Hyne research permit; and John Bohane for consistent caretaking of the Lough Hyne environment.

## Literature Cited

**Bambach, R. K. 1983.** Ecospace utilization and guilds in marine communities through the Phanerozoic. Pp. 719–746 in *Biotic Interactions in Recent and Fossil Benthic Communities*, M. J. S. Tevesz and P. L. McCall, eds. Plenum, New York.

**Bambach, R. K. 1985.** Classes and adaptive variety: the ecology of diversification in marine faunas through the Phanerozoic. Pp. 191–253 in *Phanerozoic Diversity Patterns: Profiles in Macroevolution*, J. W. Valentine, ed. Princeton University Press, Princeton, NJ.

**Banta, W. C., and J. Redden. 1990.** A checklist of the Bryozoa of the Galápagos. *Proc. Biol. Soc. Wash* **103:** 789–802.

**Barnes, D. K. A., and A. Clarke. 1998.** The ecology of an assemblage dominant: the encrusting bryozoan *Fenestrulina rugula*. *Invertebr. Biol.* **117:** 331–340.

**Barnes, D. K. A., and S. De Grave. 2000.** Biogeography of southern polar bryozoans. *Vie Milieu* **50:** 261–274.

**Barnes, D. K. A., and M. H. Dick. 2000.** Overgrowth competition between clades: implications for interpretation of the fossil record and overgrowth indices. *Biol. Bull.* **199:** 85–94.

**Barnes, D. K. A., and B. Maughan. 2002.** Seasonality and inter-annual variability in recruitment patterns of temperate encrusting fauna. Pp. 19–27 in *Proceedings of the International Bryozoology Association 12th Conference*, Balkema, Trinity College, Dublin, Ireland.

**Barnes, D. K. A., P. J. Rothery, and A. Clarke. 1996.** Colonisation and development in encrusting communities from the Antarctic intertidal and sublittoral. *J. Exp. Mar. Biol. Ecol.* **196:** 251–265.

**Barnes, D. K. A., A. C. Crook, M. O'Mahoney, S. Steele, and D. Maguire. 2001.** Sea temperature variability and *Paracentrotus lividus* (Echinoidea) population fluctuations. *J. Mar. Biol. Assoc. UK* **81:** 359–360.

**Bishop, J. D. D. 1989.** Colony form and the exploitation of spatial refuges by encrusting Bryozoa. *Biol. Rev.* **64:** 197–218.

**Fisher, E. 1989.** Competition for food in the Bryozoa. Ph.D. thesis, University of Liverpool, Liverpool, United Kingdom.

**Gordon, D. P., and P. D. Taylor. 1997.** The Cretaceous-Miocene genus *Lichenopora* (Bryozoa), with a description of a new species from New Zealand. *Bull. Nat. Hist. Mus., Lond. (Geol. Ser.)* **53:** 71–78.

**Harland, W. B., R. Armstrong, A. V. Cox, L. E. Craig, A. G. Smith, and D. G. Smith. 1990.** *A Geologic Time Scale 1989*. Cambridge University Press, Cambridge.

**Harmelin, J. G. 1976.** Le sous-order de Tubuliporina (Bryozoaires Cyclostomes) en Mediteranée, écologie et systématique. *Mém. Inst. Océanogr. Monaco* **10:** 1–326.

**Harmer, S. F. 1893.** On the occurrence of embryonic fission in cyclostomatous Polyzoa. *Q. J. Microsc. Sci.* **34:** 199–241.

**Hayward, P. J., and J. E. Winston. 1994.** New species of cheilostomate Bryozoa collected by the U.S. Antarctic Research Program. *J. Nat. Hist.* **28:** 237–246.

**Jablonski, D., S. Lidgard, and P. D. Taylor. 1997.** Comparative ecology of bryozoan radiations: origin of novelties in cyclostomes and cheilostomes. *Palaios* **12:** 505–523.

**Jameson, K. A., M. C. Appleby, and L. C. Freeman. 1999.** Finding an appropriate order for a hierarchy based on probabilistic dominance. *Anim. Behav.* **57:** 991–998.

**Kitchell, J. A., and T. R. Carr. 1985.** Nonequilibrium model of diversification: faunal turnover dynamics. Pp. 227–310 in *Phanerozoic Diversity Patterns: Profiles in Macroevolution*, J. W. Valentine, ed. Princeton University Press, Princeton, NJ.

**Kitching, J. A. 1987.** Ecological studies at Lough Hyne. *Adv. Ecol. Res.* **17:** 115–186.

**Lawver, L. A., L. M. Gahagan, and M. F. Coffin. 1992.** The development of paleoseaways around Antarctica. *Antarct. Res. Ser.* **56:** 7–30.

**Lidgard, S., F. K. McKinney, and P. D. Taylor. 1993.** Competition, clade replacement, and a history of cyclostome and cheilostome bryozoan diversity. *Paleobiology* **19:** 352–371.

**Lopez Gappa, J. J. 1989.** Overgrowth competition in an assemblage of encrusting bryozoans settled on artificial substrata. *Mar. Ecol. Prog. Ser.* **51:** 121–130.

**Maughan, B. 2000.** The influence of environmental parameters of encrusting community dynamics. Ph.D. thesis, University College Cork, Cork, Ireland.

**Maughan, B., and D. K. A. Barnes. 2000.** Seasonality of competition in early development of subtidal encrusting communities. *Pubbl. Stn. Zool. Napoli Mar. Ecol.* **21:** 205–220.

**McKinney, F. K. 1992.** Competitive interactions between related clades: evolutionary implications of overgrowth interactions between encrusting cyclostome and cheilostome bryozoans. *Mar. Biol.* **114:** 645–652.

**McKinney, F. K. 1993.** A faster paced world?: contrasts in biovolume and life process rates in cyclostome (Class Stenolaemata) and cheilostome (Class Gymnolaemata) bryozoans. *Paleobiology* **19:** 335–351.

**McKinney, F. K. 1995a.** One hundred million years of competitive interactions between bryozoan clades: asymmetrical but not escalating. *Biol. J. Linn. Soc.* **56:** 465–481.

**McKinney, F. K. 1995b.** Taphonomic effects and preserved overgrowth relationships among encrusting marine organisms. *Palaios* **10:** 279–282.

**McKinney, F. K., and P. D. Taylor. 1997.** Life histories of some Mesozoic encrusting cyclostome bryozoans. *Palaeontology* **40:** 515–556.

**McKinney, F. K., and P. D. Taylor. 2001.** Bryozoan generic extinctions and originations during the last one hundred million years. *Palaeontol. Electron.* **4:** 26 pp.

**McKinney, F. K., S. Lidgard, J. J. Sepkoski, and P. D. Taylor. 1998.** Decoupled temporal patterns of evolution and ecology in two post-Paleozoic clades. *Science* **281:** 807–809.

**Moyano, G. H. I. 1983.** Southern Pacific Bryozoa: a general emphasis on Chilean species. *Gayana Zool.* **46:** 1–45.

**Petraitis, P. S. 1979.** Competitive networks and measures of intransivity. *Am. Nat.* **114:** 921–925.

**Rubin, J. A. 1982.** The degree of intransivity and its measurement in an assemblage of encrusting cheilostome Bryozoa. *J. Exp. Mar. Biol. Ecol.* **60:** 119–128.

**Russ, G. R. 1982.** Overgrowth in a marine epifaunal community: competitive hierarchies and competitive networks. *Oecologia* **53:** 12–19.

**Sebens, K. P. 1986.** Spatial relationships among encrusting marine organisms in the New England subtidal zone. *Ecol. Monogr.* **56:** 73–96.

**Sepkoski, J. J. 1979.** A kinetic model of Phanerozoic taxonomic diversity. II. Early Phanerozoic families and multiple equilibria. *Paleobiology* **5:** 222–251.

**Sepkoski, J. J. 1991.** Population biology models in macroevolution. Pp. 136–156 in *Analytical Paleontology. Short Courses in Paleontology 4. N. L. Gilinsky and P. W. Signor, eds. Paleontological Society, Knoxville, TN.*

**Sepkoski, J. J. 1996.** Competition in macroevolution: the double wedge revisited. Pp. 211–255 in *Evolutionary Paleobiology*, D. Jablonski, D. H. Erwin, and J. H. Lipps, eds. University of Chicago Press, Chicago, IL.

**Sepkoski, J. J., and M. L. Hulver. 1985.** An atlas of Phanerozoic clade diversity diagrams. Pp. 11–39 in *Phanerozoic Diversity Patterns: Profiles in Macroevolution*, J. W. Valentine, ed. Princeton University Press, Princeton, NJ.

**Sepkoski, J. J., F. K. McKinney, and S. Lidgard. 2000.** Competitive displacement among post-Paleozoic cyclostome and cheilostome bryozoans. *Paleobiology* **26:** 7–18.

**Stanwell-Smith, D., and D. K. A. Barnes. 1997.** Benthic community development in Antarctica: recruitment and growth on settlement panels at Signy Island. *J. Exp. Mar. Biol. Ecol.* **212:** 61–79.

**Stebbing, A. R. D. 1973.** Competition for space between the epiphytes of *Fucus serratus*. L. *J. Mar. Biol. Assoc. UK* **53:** 247–261.

**Tanaka, M., and K. Nandakumar. 1994.** Measurement of the degree of intransitivity in a community of sessile organisms. *J. Exp. Mar. Biol. Ecol.* **182:** 85–95.

**Taylor, P. D. 1988.** Major radiation of cheilostome bryozoans: triggered by the evolution of a new larval type? *Hist. Biol.* **1:** 45–64.

**Taylor, P. D. 1993.** Bryozoa. Pp. 465–489 in *The Fossil Record 2*, M. J. Benton, ed. Chapman & Hall, London.

**Taylor, P. D. 2000.** Cyclostome systematics: phylogeny, suborders and the problem of skeletal organisation. Pp. 87–103 in *Proceedings of the 11th International Bryozoology Association Conference*, A. Herrera Cubilla and J. B. C. Jackson, eds. Smithsonian Tropical Research Institute, Panama.

**Taylor, P. D. 2001.** Preliminary systematics and diversity patterns of cyclostome bryozoans from the Neogene of the Central American Isthmus. *J. Paleontol.* **75:** 578–589.

**Todd, C. D., and S. J. Turner. 1986.** Ecology of intertidal and sublittoral cryptic epifaunal assemblages. I. Experimental rationale and analysis of larval settlement. *J. Exp. Mar. Biol. Ecol.* **99:** 199–231.

**de Vries, H. 1998.** Finding a dominance order most consistent with a linear hierarchy: a new procedure and review. *Anim. Behav.* **55:** 827–843.

**Winston, J. E. 1983.** Patterns of growth, reproduction and mortality in bryozoans from the Ross Sea, Antarctica. *Bull. Mar. Sci.* **33:** 688–702.

Reference: *Biol. Bull.* **203:** 173–180. (October 2002)

# Relative Strengths of Competition for Space and Food in a Sessile Filter Feeder

DAVID P. LOHSE

*Virginia Institute of Marine Science, Gloucester Point, Virginia 23062; and *Department of Ecology and Evolutionary Biology, Long Marine Laboratory, University of California, Santa Cruz, 100 Shaffer Road, Santa Cruz, California 95060*

**Abstract.** Previous workers have demonstrated that sessile filter feeders compete for food and space, but little is known about the relative strengths of these two processes. To determine this, the density and position of barnacles (*Balanus improvisus*) in a unidirectional current were manipulated to alter the amount of competition for space and food, respectively. Results indicated that competition for space significantly reduced growth, and marginally reduced survivorship. Competition for food was also detected, but only among uncrowded individuals; thus, it appears to be the weaker of the two interactions. However, under crowded conditions, downstream individuals actually grew more than those upstream. The most likely explanation for this result is that downstream individuals fed more efficiently because they were not exposed to the full force of the current. The results also suggest that since natural densities started high but continually decreased throughout the study, barnacles undergo an ontogenetic shift in the relative importance of these processes.

## Introduction

Because all organisms need a place to live, it is not unreasonable for ecologists to consider competition for space a potentially important interaction. However, for some organisms access to space is inherently linked with access to other resources. For example, for terrestrial plants, access to space also involves access to water, light, and nutrients (Grime, 1979). Similarly, Buss (1979) argued that for sessile filter feeders, access to food depends, in part, on access to space. Although much is known about the role of competition for space on rocky shores (*e.g.*, Connell, 1961a, b; Menge, 1976; Wu, 1980; Bertness, 1989), little is known about the importance of competition for food. At one time it was even suggested that filter feeders do not compete for food (Levinton, 1972), but an established and growing body of evidence indicates that they in fact do (Crisp and Davies, 1955; Crisp, 1964; Glynn, 1973; Buss, 1979; Jorgensen, 1980; Buss and Jackson, 1981; Peterson, 1982; Peterson, 1983; Frechette and Bourget, 1985; Okamura, 1986; Page and Hubbard, 1987; Peterson and Black, 1987; Newell, 1990; Prins *et al.*, 1995).

For sessile filter feeders, competition for space and competition for food are mechanistically different. Competition for space, where neighbors overgrow or undercut each other, is interference competition. Competition for food, which occurs when upstream individuals take food away from those downstream, is exploitation competition. Therefore, a logical question is, What are the relative strengths of these two processes? Few studies have dealt with both competition for space and food, so little information is available to answer this question. Frechette and Lefaivre (1990) concluded that the relative importance of these processes varies seasonally. Frechette and Despland (1999), however, concluded that, for small mussels at low densities, competition for food was more important. Cote *et al.* (1994) reached a similar conclusion for scallops, but a problem with their statistical analysis raises questions about this result. Best and Thorpe (1986) and Frechette *et al.* (1992) considered both processes, but did not assess their relative strengths.

This study assesses the relative strengths of exploitation and interference competition for a sessile filter feeder. Specifically, the question addressed was, Do immediate neighbors compete more for space or food? To answer this question, barnacles were induced to settle in rows on rectangular panels, and densities on half of the panels were

Received 8 June 2001; accepted 3 July 2002.

* Current address. E-mail: lohse@biology.ucsc.edu

reduced to test for competition for space. The panels were then deployed in a unidirectional current, and the growth and survivorship of upstream and downstream individuals were compared to test for competition for food. Food availability was not directly manipulated, but half of the panels were rotated weekly to change the position of the upstream and downstream individuals. By altering the barnacles' position in the current, this change potentially altered their food supply.

## Materials and Methods

This study was conducted from May to July 1993 at the Virginia Institute of Marine Science, located at the mouth of the York River, Virginia. Because the York River is a tributary of the Chesapeake Bay, there are twice daily reversals in the direction of the water flow coincident with the tidal cycle. The tides here are semidiurnal, and the tidal range is about −0.2 to 0.9 m (mean low water). Maximum current speed is about 50 cm/s in the center of the river, but is lower near the shore. During the study the water temperature ranged from 25 to 27 °C, and the salinity from 15 to 21 ppt.

The common rocky shore organisms in the intertidal region at this site are the barnacles *Balanus improvisus*, *B. eberneus*, and *Chthamalus fragilis*, and the oyster *Crassostrea virginica*. Only *B. improvisus* was used in this experiment. Midway through the study the hydroid *Hydractinia* spp. appeared and overgrew everything, making it necessary to scrub the panels used (see below) every week to keep them free of this organism. The predatory flatworm *Stylochus* spp. was also consistently found on the panels and probably contributed to the mortality observed during the study.

### *Experimental setup*

In early May 1993, 6 × 20 cm settlement panels were constructed of 4-mm acrylic plastic. Because barnacles preferentially settle in depressions (Crisp and Barnes, 1954), five shallow grooves, 1–2 mm deep and 1 cm apart, were cut down the length of each panel to induce settlement. The edges of the panels were beveled to minimize problems with boundary-layer detachment (see Mullineaux and Butman, 1991; Mullineaux and Garland, 1993). Plastic cable ties were used to attach the panels to wooden blocks that were also beveled at one end (Fig. 1), and the blocks were deployed at two locations on a pier owned by the institute. To suspend the panels from the pier, a rope was passed through a hole drilled through the top of each block (Fig. 1). Twelve panels (six wooden blocks) were placed about 150 m offshore (site A), and ten panels (five wooden blocks) were deployed about 50 m offshore (site B) where the current was slower (unpubl. data). All the panels were placed at about −0.1 m (mean low water).

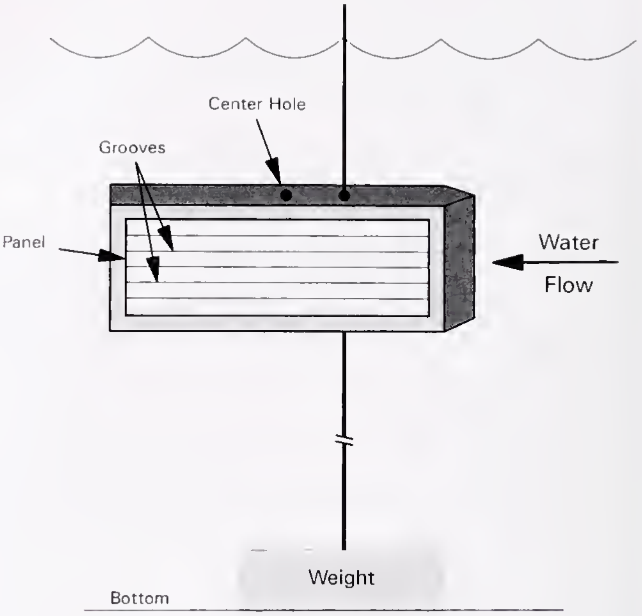

**Figure 1.** The experimental setup. The panels were attached to wooden blocks that had two holes drilled through their tops, one midway down the block and the other several centimeters towards the front. Initially, when the panels were deployed to collect recruits, the ropes used to suspend the blocks from the pier were passed through the center hole. This allowed the blocks to rotate freely with the current. During the experiment, however, the rope was placed through the forward-most hole. Just like a weather vane, this kept the front (beveled end) of the blocks always pointed upstream. To prevent the ropes from swaying with the current, the bottoms of the ropes were attached to concrete blocks. These blocks rested on the bottom so the ropes could be pulled taut.

The panels were checked weekly for recruitment, and any barnacles that settled outside of the grooves were removed. Once the grooves were filled with barnacles, all the panels were removed from the blocks and randomly assigned to one of two treatments, uncrowded or crowded. The barnacles on the uncrowded panels were thinned (mean = 1.2 barnacles per linear cm, SE = 0.02, $n$ = 56) so they could grow without touching. Nothing was done to the crowded panels, so densities started out higher (mean = 4.4 barnacles per linear cm, SE = 0.08, $n$ = 56), and adjacent barnacles touched one another. Any new barnacles settling on the panels after this point were removed.

After designating one end of each panel as the front, 4 (uncrowded) to 7 (crowded) barnacles in each groove at the front, middle, and back of the panels (for a total of 12–21 individuals per row) were "marked" by mapping their positions onto sheets of clear acetate. The opercular diameter of these individuals was measured to the nearest 0.1 mm, using a dissecting scope with an ocular micrometer. The panels were then reattached to the wooden blocks with the front of the panels at the front (the beveled end) of the block, and the blocks were deployed as before, with one exception. This time the ropes used to suspend the blocks

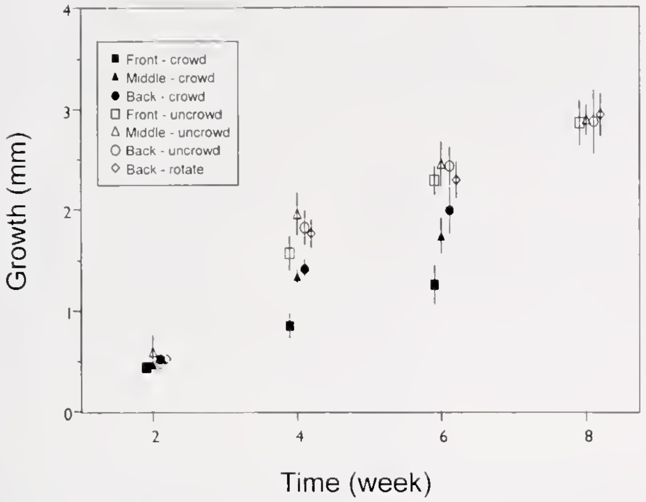

**Figure 2.** Mean growth (±1 SE) of the barnacles in the different treatments on the panels. In some cases error bars are smaller than the symbol.

were placed in a hole that was closer to the front of the block (Fig. 1). This caused the block to act like a weather vane, with its front always pointing upstream. Therefore, barnacles at the front had first access to food, while those at the back fed in water that had passed over all the individuals upstream of them. Thus, those at the back should grow more slowly if there is competition for food. Meanwhile, those on the crowded panels should grow more slowly if there is competition for space. Four crowded and eight uncrowded panels were deployed at site A, and three crowded and six uncrowded panels were deployed at site B.

As an additional test for food competition, half of the panels in the low-density treatment were rotated every week so that the front and back of the panels switched places on the blocks. "Back" individuals on these panels spent half their time at the front of the blocks, with no barnacles upstream of them, and half the time at the back, with many barnacles upstream of them. In contrast, back individuals on the nonrotated panels had barnacles upstream of them all of the time. Therefore, back individuals on the rotated panels had, on average, fewer barnacles upstream of them and, thus, potentially more food available to them than those on the non-rotated panels. Since rotating the panels also altered the position of the rows, every week the non-rotated panels were removed and reattached to the opposite sides of the blocks. This altered the position of the rows, but not the location of the front and back of the panels.

Every 2 weeks, individuals were remeasured and maps were made of all the living barnacles on each panel. These maps were used to determine how many barnacles were upstream of each measured individual during each 2-week interval. The experiment was terminated after week 8.

### *Analyses*

Two *a priori* expectations dictated how the data were analyzed. First, because they were thinned out, the barnacles on the uncrowded panels could not compete for space. Therefore, the effects of competition for space were examined by comparing crowded and uncrowded individuals at the front of the non-rotated panels. Second, since barnacles feed by trapping particles in their cirral net as water passes over them, there is no way for downstream individuals to take food from upstream individuals. Thus, barnacles at the front of the panels could not experience competition for food. Therefore, the effects of competition for food were examined by comparing individuals at the front and back of the uncrowded, non-rotated panels. Rotation, which placed back individuals at the front of the blocks for half of the time, was expected to increase growth compared to back individuals on the nonrotated panels.

Two-way ANCOVA was used to look for the effects of competition for space on growth. Treatment (crowded *vs.* uncrowded) and site (higher *vs.* lower current) were fixed factors, and initial size of the barnacle was used as the covariate. Only those at the front of the non-rotated panels were used, to avoid any confounding problems with competition for food. Separate analyses were performed for the first three periods (weeks 0–2, 0–4, 0–6), but none was done for the last (week 0–8) because virtually all barnacles had become uncrowded by week 6. Although several individuals within each row were measured, it was the panels that were considered replicates. Therefore, prior to analysis a single growth measurement was determined for each panel as follows. First, the average growth for each row was calculated, then a weighted average was taken of the five row means on each panel, using the number of individuals in each row as a weighting factor. The same was done to determine the value of the covariate (initial size) for each panel. As necessary, crowded barnacles (defined as those that, within a row, touched their neighbors on both sides) that became uncrowded were eliminated from the analyses.

Since growth at the back of the panels was potentially dependent upon how much growth took place at the front, ANCOVA was not used to test for competition for food because an underlying assumption of this test is that treatments are independent. Instead, two different analyses were used. First, a paired $t$ test was used to compare the difference in growth measured at the front and back of the panels against a value of zero. Only the non-rotated panels were used for this analysis, and separate analyses were done for each interval (weeks 0–2, 0–4, 0–6, 0–8). Since the initial size of the barnacles was similar among the locations (for crowded panels $F = 1.42$, df = 2,18, $P = 0.27$, for uncrowded panels $F = 2.12$, df = 2,18, $P = 0.15$), no correction for initial size was deemed necessary for this analysis. As with the previous analysis, differences were

**Table 1**

*Results of ANCOVA comparing effects of crowding among "front" individuals on the crowded and uncrowded, non-rotated panels*

| | Weeks 0–2 | | | Weeks 0–4 | | | Weeks 0–6 | | |
|---|---|---|---|---|---|---|---|---|---|
| Variable | df | MS | *F* | df | MS | *F* | df | MS | *F* |
| Crowding (A) | 1 | 0.24 | 0.33 | 1 | 209.6 | 30.9*** | 1 | 192.9 | 11.3** |
| Site (B) | 1 | 8.52 | 11.9** | 1 | 21.5 | 3.17 | 1 | 1.9 | 0.11 |
| Initial size | 1 | 0.11 | 0.15 | 1 | 73.9 | 10.9** | 1 | 15.9 | 0.93 |
| A × B | 1 | 0.37 | 0.52 | 1 | 31.4 | 4.62 | 1 | 8.13 | 0.48 |
| Error | 9 | 0.72 | | 8 | 6.8 | | 7 | 17.02 | |

Presented here is the reduced model; the interaction terms involving the covariate (initial size) were not significant, so they were eliminated. ** = $P < 0.01$, *** = $P < 0.001$.

calculated after first obtaining a single value for growth for each location on each panel.

The second analysis determined whether growth was a function of the number of upstream barnacles. Using the non-rotated panels, the individual farthest back in each row was identified, and the number of barnacles upstream of it was determined. This was done at the start and end of each 2-week interval, and the average was taken. (Note: for the first interval [week 0–2] only the number present at week 2 was used because, unfortunately, the appropriate data were not collected at week 0). This number was then compared against growth by using regression analysis. Separate analyses were done for the crowded and uncrowded panels for the first three intervals (weeks 0–2, 2–4, 4–6), but they were combined for the last interval (week 6–8) because by then all barnacles had become uncrowded.

The effects of rotation were examined using two-way ANCOVA. This analysis was essentially the same as that used to test for competition for space. Treatment (rotated *vs.* non-rotated) and site (higher *vs.* lower current) were fixed factors, and initial size of the barnacle was used as the covariate. Comparisons were made for all four intervals (weeks 0–2, 0–4, 0–6, 0–8), and means per panel were calculated as previously described.

Chi-square analysis was used to look for differences in survivorship. As above, the effects of crowding were examined using the barnacles at the front of the crowded and uncrowded panels. The effects of competition for food were examined using those at the front and back of the uncrowded panels. Again, only the non-rotated panels were used.

## Results

The comparison of growth at the front of the panels found that crowded individuals grew significantly less than uncrowded ones (Fig. 2, Table 1). On the uncrowded, non-rotated panels there were no significant differences in growth among locations (Fig. 2, Table 2), but there were significant, negative relationships between growth and the number of upstream barnacles (Fig. 3). In contrast, on the crowded, non-rotated panels there were significant differences in growth among locations (Fig. 2, Table 2), but there were no significant relationships between growth and the number of upstream barnacles (Fig. 3). There was no difference in growth between rotated and non-rotated individuals (Table 3).

Although crowded individuals had lower survivorship, the difference was only marginally significant (Fig. 4, $\chi^2 = 3.04$, df = 1, $P = 0.08$). Survivorship was similar at the front and back of the uncrowded, non-rotated panels (Fig. 4, $\chi^2 = 0.04$, df = 1, $P = 0.85$).

## Discussion

### *Comparing competion for food and competion for space*

Although the idea that filter feeders compete for food is not new (*e.g.*, Moore, 1935; Barnes and Powell, 1950), more is known about the role of competition for space on rocky shores than about competition for food. This study was designed to decouple the effects of these two processes. Since the uncrowded barnacles could not compete for space, they were expected to grow more than the crowded indi-

**Table 2**

*Difference in mean growth ± 1 SE between front and back of the uncrowded, non-rotated panels*

| Interval | Difference (Front-Back) | *t* | df | *P* |
|---|---|---|---|---|
| Uncrowded | | | | |
| 0–2 | −0.04 ± 0.05 | −0.8 | 6 | 0.42 |
| 0–4 | −0.25 ± 0.19 | −1.3 | 5 | 0.24 |
| 0–6 | −0.13 ± 0.20 | −0.7 | 5 | 0.52 |
| 0–8 | −0.12 ± 0.38 | −0.3 | 4 | 0.76 |
| Crowded | | | | |
| 0–2 | −0.09 ± 0.04 | −2.2 | 6 | 0.07 |
| 0–4 | −0.56 ± 0.06 | −9.7 | 6 | <0.001 |
| 0–6 | −0.68 ± 0.20 | −3.5 | 4 | 0.03 |

Results were compared against an expected value of 0 using paired *t* test.

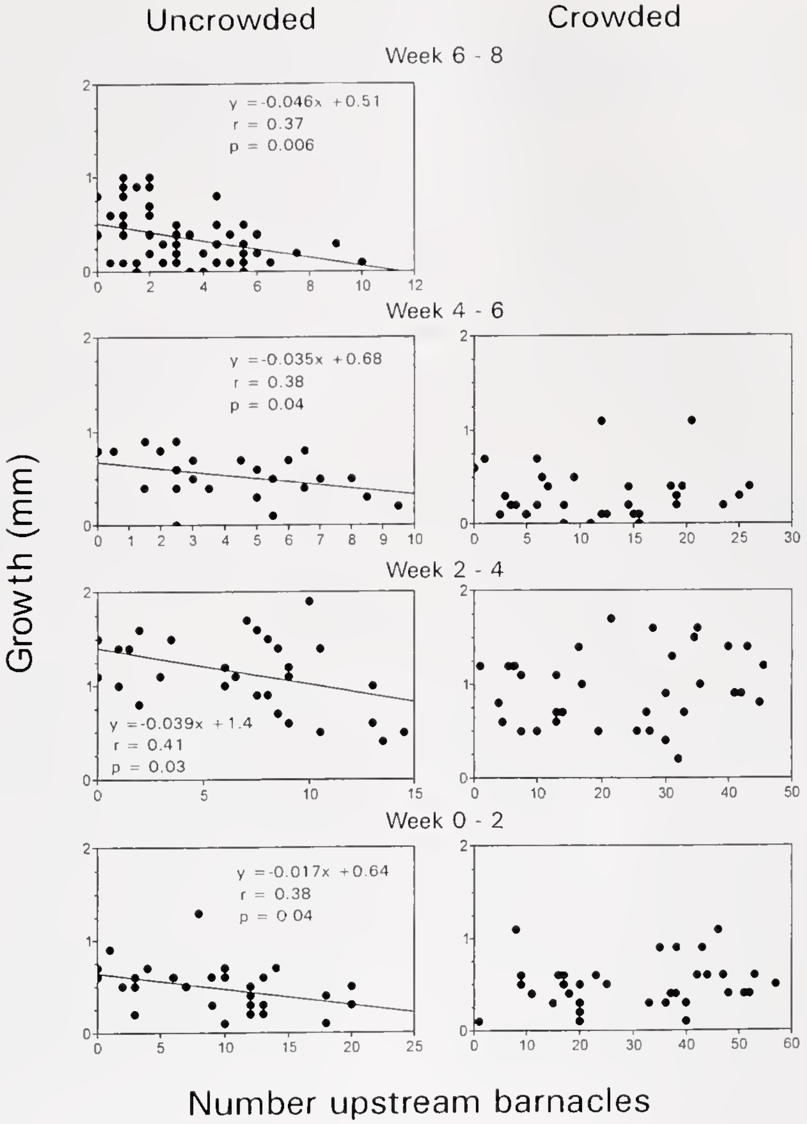

**Figure 3.** Relationship between growth and the number of upstream barnacles on the non-rotated panels.

viduals. Similarly, because the front of the wooden blocks always pointed upstream, the barnacles at the back of the blocks were expected to experience competition for food.

Overall, these predictions are supported by the results. For example, the crowded barnacles grew less than the uncrowded ones, a result found by many others (*e.g.*, Connell, 1961a, b; Wu, 1980; Bertness, 1989). Furthermore, growth at the back of the panels was a function of the number of upstream barnacles, which is evidence of competition for food. However, this negative relationship was observed only on the uncrowded panels. Thus, competition for food was measurable only in the absence of competition for space, which suggests that it is the weaker of the two processes. This is further illustrated by the fact that the slopes of the regression lines were all quite shallow (Fig. 3). In fact, if the mean of the four slopes (mean = −0.034 mm growth per upstream barnacle per interval) is used as an estimate of the strength of the effect, after 6 weeks an upstream barnacle would reduce the growth of its downstream neighbor by about 0.1 mm. In comparison, after 6 weeks, crowding reduced growth by 1.1 mm (Fig. 2).

However, this does not mean that competition for food is unimportant. Since growth requires access to food, and adult barnacles compete for space only when they are growing, anything that affects the supply of food will ultimately affect the amount of competition for space. Although an individual's growth is apparently not much affected by the feeding of its immediate neighbors, competition for food is exploitation competition, unlike competition for space, which is interference competition. This means that individuals can be far apart and still interact, which makes competition for food a larger scale phenomenon than competi-

**Table 3**

*Results of ANCOVA testing the effects of rotation on growth at the back of the uncrowded panels*

| | Weeks 0–2 | | | Weeks 0–4 | | | Weeks 0–6 | | | Weeks 0–8 | | |
|---|---|---|---|---|---|---|---|---|---|---|---|---|
| Source | df | MS | *F* | df | MS | *F* | df | MS | *F* | df | MS | *F* |
| Rotate (A) | 1 | 0.14 | 0.11 | 1 | 5.35 | 1.3 | 1 | 10.5 | 1.38 | 1 | 19.2 | 0.96 |
| Site (B) | 1 | 3.14 | 2.4 | 1 | 3.44 | 0.81 | 1 | 0.56 | 0.074 | 1 | 0.01 | 0.000 |
| Initial | 1 | 2.08 | 1.6 | 1 | 89.6 | 21.1** | 1 | 172.7 | 22.7*** | 1 | 186.3 | 9.27* |
| A × B | 1 | 0.80 | 0.61 | 1 | 0.34 | 0.08 | 1 | 0.747 | 0.098 | 1 | 0.81 | 0.04 |
| Error | 9 | 1.31 | | 8 | 4.24 | | 8 | 7.62 | | 6 | 20.1 | |

Presented here is the reduced model; the interaction terms involving the covariate (initial size) were not significant, so they were eliminated from the analyses. * = $P < 0.05$, ** = $P < 0.01$, *** = $P < 0.001$.

tion for space. In fact, the results of the regression analyses suggest that with the addition of each upstream barnacle should come a small reduction in growth for those downstream. Thus, the cumulative effect of many upstream individuals could have important consequences for those downstream.

Despite the fact that upstream individuals take food from their downstream neighbors, growth on the crowded panels was greater at the back than at the front. Thus crowded individuals did better downstream, where they competed for both space and food, than upstream, where they only competed for space. There are three possible explanations for this result. First, previous studies have shown that when competition for space is severe, barnacles alter their morphology and grow taller instead of wider (Barnes and Powell, 1950; Bertness *et al.*, 1998). Thus it is possible that, since growth is dependent upon food, those at the front of the panels experienced more intense competition for space than those at the back because more food was available at the front. If true, then most of the growth at the front of the panels would have been upwards, rather than outwards, resulting in barnacles that, for a given diameter, would be taller than those at the back. However, measurements of barnacles at both locations found little difference in their morphologies (Fig. 5). Therefore, this explanation seems unlikely.

It is also possible that growth was greater at the back of the panels because of the way the experiment was set up. Studies have shown that if the leading edge of the panel is not streamlined, a recirculating eddy can form at the front of the panel (Mullineaux and Butman, 1991; Mullineaux and Garland, 1993), which could cause individuals there to receive less food than those farther back. However, there are two reasons why this does not seem to be the correct explanation. First, the panels and blocks were beveled to minimize the chances of eddy formation. And second, if these recirculating eddies were indeed present, there should have also been a difference in growth among locations on

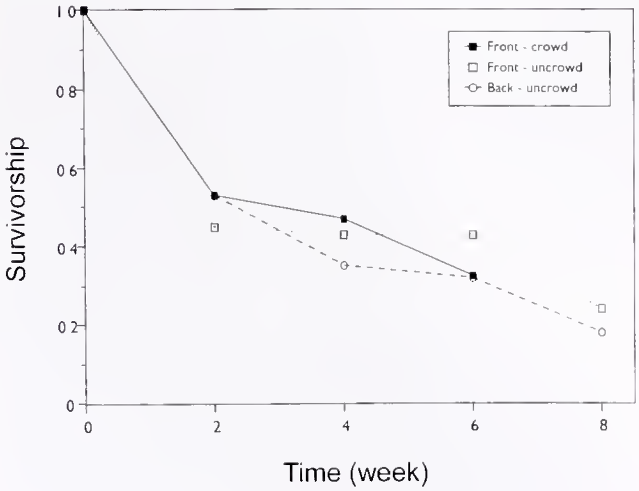

**Figure 4.** Survivorship of barnacles in the different treatments.

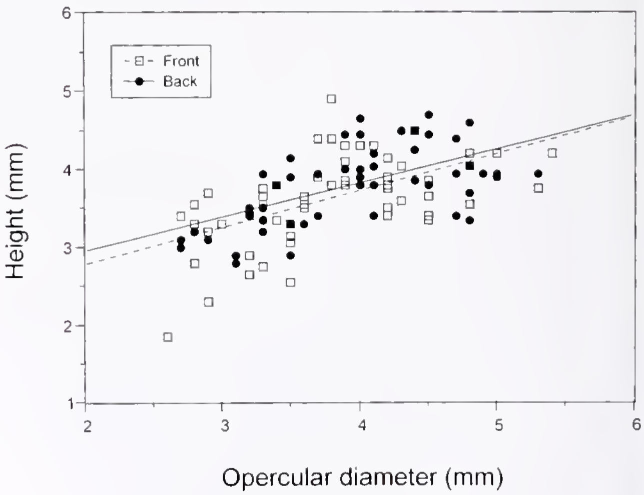

**Figure 5.** Relationship between the height and opercular diameter of barnacles at the front and back of the crowded panels measured at the end of the study.

the uncrowded panels. Since there was not, this explanation also seems unlikely.

The third, and perhaps most likely, explanation for growth being greater at the back of the crowded panels is that those at the front were unable to feed efficiently because they were exposed to the full force of the current. This has been observed in bryozoans (Okamura, 1984, 1987; Eckman and Duggins, 1993) and in barnacles in currents as low as 10 cm/s (Trager *et al.*, 1994; however, see Eckman and Duggins, 1993). During the present study, current speeds as high as 35 cm/s were measured (unpubl. data). As the current travels down the panel, drag would cause it to slow down, so barnacles farther downstream should feed more efficiently. The fact that growth in the middle of the panels was greater than at the front, but less than at the back, supports this idea (Fig. 1). That this was not observed on the uncrowded panels may be due to the fact that there were fewer barnacles on them to slow the current.

### *Temporal changes in competition*

Over the course of the study, the barnacles on the crowded panels grew from about 2 mm basal diameter to 1–1.5 cm. Since adjacent barnacles started out touching, this means that many more barnacles were initially present on the panels than could be supported as adults. Therefore, it is not surprising that competition for space was intense on these panels during the first few weeks. However, by week 6, densities had been reduced so much by competition and predation that all crowded individuals had become uncrowded. Therefore, competition for space was no longer important, and for the first time competition for food became detectable on the crowded panels (Fig. 3, week 6–8).

This suggests that the type of competition barnacles like *Balanus improvisus* experience changes over the course of their life. During settlement, when cyprids cannot settle on occupied substrate, they may compete exploitatively for space (= preemption competition). Although the barnacles in this study did not experience this, several times during the study the panels became totally covered with new recruits. Thus, during the height of the settlement season, this type of competition may be severe. After settlement, interference competition for space is important. Eventually, as densities decrease, the effects of competition for space decline and the relative importance of competition for food increases.

Unless these ontogenetic changes were known, it would be possible to make erroneous conclusions about the importance of competition in structuring this community. For example, a study that used older individuals would probably conclude that competition for space was not important. However, this would underestimate the true importance of space competition, because this process is intense among young barnacles. Since similar ontogenetic changes undoubtedly take place for other species, this suggests that conclusions based on short-term experiments, which often focus on only one segment of an organism's life cycle, should be interpreted with caution.

## Conclusions

Important resources for sessile filter feeders like barnacles include space and food. This study has shown how a barnacle's ability to utilize these resources is influenced by its neighbors. Immediate neighbors had little measurable impact on each other's food supply, but when crowded reduced each other's growth and survivorship through competition for space. In contrast, though distant neighbors cannot directly affect each other's access to space, they did so indirectly by affecting food availability. When uncrowded, upstream individuals reduced the growth of their downstream neighbors *via* competition for food. When crowded, however, they increased the growth of those downstream by increasing their feeding efficiency. Both such effects were not as great as those caused by competition for space with their immediate neighbors. Thus, the number (crowded *vs.* uncrowded), proximity (immediate *vs.* distant), and location (upstream *vs.* downstream) of an individual's neighbors have important consequences for its performance.

## Acknowledgments

This study was conducted while I was a post-doctoral researcher at the Virginia Institute of Marine Science. Thanks go to Anthony Boxshall, Joe Connell, Amanda Maximchuk-Daly, Bob Diaz, Pete Raimondi, Eric Sanford, Sue Swarbrick, and Michelle Thompson for their help and comments.

## Literature Cited

**Barnes, H., and H. T. Powell. 1950.** The development, general morphology, and subsequent elimination of barnacle populations, *Balanus crenatus* and *B. balanoides*, after a heavy initial settlement. *J. Anim. Ecol.* **19:** 175–179.

**Bertness, M. D. 1989.** Intraspecific competition and facilitation in a northern acorn barnacle population. *Ecology* **70:** 257–268.

**Bertness, M. D., S. D. Gaines, and Su Ming Yeh. 1998.** Making mountains out of barnacles: the dynamics of acorn barnacle hummocking. *Ecology* **79:** 1382–1394.

**Best, M. A., and J. P. Thorpe. 1986.** Feeding-current interactions and competition for food among the bryozoan epiphytes of *Fucus serratus*. *Mar. Biol.* **93:** 371–375.

**Buss, L. W. 1979.** Bryozoan overgrowth interactions—the interdependence of competition for space and food. *Nature* **281:** 475–477.

**Buss, L. W., and J. B. C. Jackson. 1981.** Planktonic food availability and suspension-feeder abundance: evidence of *in situ* depletion. *J. Exp. Mar. Biol. Ecol.* **49:** 151–161.

**Connell, J. H. 1961a.** Effects of competition, predation by *Thais lapillus*, and other factors on natural populations of the barnacle *Balanus balanoides*. *Ecol. Monogr.* **31:** 61–104.

**Connell, J. H. 1961b.** The influence of interspecific competition and other factors on the distribution of the barnacle *Chthamalus stellatus*. *Ecology* **42:** 710–723.

**Cote, J., J. H. Himmelman, and M. R. Claereboudt. 1994.** Separating effects of limited food and space on growth of the scallop *Placopecten magellanicus* in suspended culture. *Mar. Ecol. Prog. Ser.* **106:** 85–91.

**Crisp, D. J. 1964.** An assessment of plankton grazing by barnacles. Pp. 251–264 in *Grazing in Terrestrial and Marine Environments*, D. J. Crisp, ed. Blackwell, Oxford.

**Crisp, D. J., and H. Barnes. 1954.** The orientation and distribution of barnacles at settlement with particular reference to surface contour. *J. Anim. Ecol.* **23:** 142–162.

**Crisp, D. J., and P. A. Davies. 1955.** Observations *in vivo* on the breeding of *Elminius modestus* grown on glass slides. *J. Mar. Biol. Assoc. UK* **34:** 357–380.

**Eckman, J. E., and D. O. Duggins. 1993.** Effects of flow speed on growth of benthic suspension feeders. *Biol. Bull.* **185:** 28–41.

**Frechette, M., and E. Bourget. 1985.** Food-limited growth of *Mytilus edulis* in relation to the benthic boundary layer. *Can. J. Fish. Aquat. Sci.* **42:** 1166–1170.

**Frechette, M., and E. Despland. 1999.** Impaired shell gaping and food depletion as mechanisms of asymmetric competition in mussels. *Ecoscience* **6:** 1–11.

**Frechette, M., and D. Lefaivre. 1990.** Discriminating between food and space limitation in benthic suspension feeders using self-thinning relationships. *Mar. Ecol. Prog. Ser.* **65:** 15–23.

**Frechette, M., A. E. Aitken, and L. Page. 1992.** Interdependence of food and space limitation of a benthic suspension feeder: consequences for self-thinning relationships. *Mar. Ecol. Prog. Ser.* **83:** 55–62.

**Glynn, P. W. 1973.** Ecology of a Caribbean coral reef. The *Porites* reef-flat biotype: Part II. Plankton community with evidence for depletion. *Mar. Biol.* **22:** 1–21.

**Grime, J. P. 1979.** *Plant Strategies and Vegetation Processes*. Wiley, Chichester.

**Jorgensen, B. B. 1980.** Seasonal oxygen depletion in the bottom waters of a Danish fjord and its effect on the benthic community. *Oikos* **34:** 68–76.

**Levinton, J. 1972.** Stability and trophic structure in deposit-feeding and suspension-feeding communities. *Am. Nat.* **106:** 472–486.

**Menge, B. A. 1976.** Organization of New England rocky intertidal community—role of predation, competition, and environmental heterogeneity. *Ecol. Monogr.* **46:** 355–393.

**Moore, H. B. 1935.** The biology of *Balanus balanoides*. IV. Relation to environmental factors. *J. Mar. Biol. Assoc. U.K.* **20:** 279–307.

**Mullineaux, L. S., and C. A. Butman. 1991.** Initial contact, exploration and attachment of barnacle (*Balanus amphitrite*) cyprids settling in flow. *Mar. Biol.* **110:** 93–103.

**Mullineaux, L. S., and E. D. Garland. 1993.** Larval recruitment in response to manipulated field flows. *Mar. Biol.* **116:** 667–683.

**Newell, C. R. 1990.** The effects of mussel (*Mytilus edulis*, Linnaeus, 1758) position in seeded bottom patches on growth at subtidal lease sites in Maine. *J. Shellfish Res.* **8:** 113–118.

**Okamura, B. 1984.** The effects of ambient flow velocity, colony size, and upstream colonies on the feeding success of Bryozoa. I. *Bugula stolonifera* Ryland, an arborescent species. *J. Exp. Mar. Biol. Ecol.* **83:** 179–193.

**Okamura, B. 1986.** Group living and the effects of spatial position in aggregations of *Mytilus edulis*. *Oecologia* **69:** 341–347.

**Okamura, B. 1987.** The effects of ambient flow velocity, colony size, and upstream colonies on the feeding success of Bryozoa. II. *Conopeum reticulum* (Linnaeus), an encrusting species. *J. Exp. Mar. Biol. Ecol.* **89:** 69–80.

**Page, H. M., and D. M. Hubbard. 1987.** Temporal and spatial patterns of growth in mussels *Mytilus edulis* on an offshore platform: relationships to water temperature and food availability. *J. Exp. Mar. Biol. Ecol.* **111:** 159–179.

**Peterson, C. H. 1982.** The importance of predation and intra- and interspecific competition in the population biology of two infaunal suspension-feeding bivalves, *Protothaca staminea* and *Chione undatella*. *Ecol. Monogr.* **52:** 437–475.

**Peterson, C. H. 1983.** Interactions between two infaunal bivalves, *Chione undatella* (Sowerby) and *Protothaca staminea* (Conrad), and two potential enemies, *Crepidula onyx* Sowerby and *Cancer anthonyi* (Rathbun) *J. Exp. Mar. Biol. Ecol.* **68:** 145–158.

**Peterson, C. H., and R. Black. 1987.** Resource depletion by active suspension feeders on tidal flats: influence of local density and tidal elevation. *Limnol. Oceanogr.* **32:** 143–166.

**Prins, T. C., V. Escaravage, A. C. Smaal, and J. C. H. Peeters. 1995.** Nutrient cycling and phytoplankton dynamics in relation to mussel grazing in a mesocosm experiment. *Ophelia* **41:** 289–315.

**Trager, G., Y. Achituv, and A. Genin. 1994.** Effects of prey escape ability, flow speed, and predator feeding mode on zooplankton capture by barnacles. *Mar. Biol.* **120:** 251–259.

**Wu, R. S. S. 1980.** Effects of crowding on the energetics of the barnacle *Balanus glandula* Darwin. *Can. J. Zool.* **58:** 559–566.

# *Reports of Papers Presented at* THE GENERAL SCIENTIFIC MEETINGS OF THE MARINE BIOLOGICAL LABORATORY, Woods Hole, Massachusetts

## 12 to 14 August 2002

*Program Chairs:*
KAREN CRAWFORD, St. Mary's College of Maryland
ROBERT GOULD, New York State Institute for Basic Research
EDWARD RASTETTER, The Ecosystems Center, MBL
ROBERT PAUL MALCHOW, University of Illinois at Chicago

---

Each of these reports was reviewed by two members of a special editorial board
drawn from the research community of Woods Hole, Massachusetts.
Reviewers included scientists from
THE MARINE BIOLOGICAL LABORATORY,
THE WOODS HOLE OCEANOGRAPHIC INSTITUTION,
AND THE NATIONAL MARINE FISHERIES SERVICE.

# SHORT REPORTS FROM THE 2002 GENERAL SCIENTIFIC MEETINGS OF THE MARINE BIOLOGICAL LABORATORY

**The Editor**
Introduction to the featured reports: The MBL awards for 2002 . . . . . . . . . . 185

*Neurobiology*

**Arnolds, D. E. W., S. J. Zottoli, C. E. Adams, S. M. Dineen, S. Fevrier, Y. Guo, and A. J. Pascal**
Physiological effects of tricaine on the supramedullary/dorsal neurons of the cunner, *Tautogolabrus adspersus* . . . . . . . . . . 188
**Giuditta, Antonio, Maria Eyman, and Barry B. Kaplan**
Gene expression in the squid giant axon: neurotransmitter modulation of RNA transfer from periaxonal glia to the axon . . . . . . . . . . 189
**Landowne, David**
Perchlorate prevents sodium channel gating and sodium protects in the squid giant axon . . . . . . . . . . 190
**Ripps, Harris, Haohua Qian, and Jane Zakevicius**
Blockade of an inward sodium current facilitates pharmacological study of hemi-gap-junctional currents in *Xenopus* oocytes . . . . . . . . . . 192
**Garber, Sarah S., and Mary M. Hoffman**
$Cl^-$ and glutamate$^-$ competition for a volume-regulated anion channel . . . . . . . . . . 194
**Fay, Richard R., and Peggy L. Edds-Walton**
Preliminary evidence for interpulse interval selectivity of cells in the torus semicircularis of the oyster toadfish *(Opsanus tau)* . . . . . . . . . . 195
**Borley, Kimberly A., Herman T. Epstein, and Alan M. Kuzirian**
Effects of a sensory block on calexcitin levels in the photoreceptors of *Hermissenda crassicornis* . . . . . . . . . . 197
**Twig, Gilad, Robert Paul Malchow, Katherine Hammar, Peter J. S. Smith, Hanna Levy, and Ido Perlman**
A novel turtle retinal preparation for simultaneously measuring light-induced electrical activity and changes in metabolite levels . . . . . . . . . . 198
**Redenti, Stephen, and Richard L. Chappell**
Zinc chelation enhances the zebrafish retinal ERG b-wave . . . . . . . . . . 200

*Cell Biology*

**Armstrong, Peter B., Margaret T. Armstrong, R. L. Pardy, Alice Child, and Norman Wainwright**
Immunohistochemical demonstration of a lipopolysaccharide in the cell wall of a eukaryote, the green alga *Chlorella* . . . . . . . . . . 203
**Lee, K.-G., A. Braun, I. Chaikhoutdinov, J. DeNobile, M. Conrad, and W. Cohen**
Rapid visualization of microtubules in blood cells and other cell types in marine model organisms . . . 204
**Wöllert, Torsten, Ana S. DePina, Reid F. Thompson, and George M. Langford**
Ca$^{2+}$ effects on myosin-II-mediated contraction of pseudo-contractile rings and transport of vesicles in extracts of clam oocytes . . . . . . . . . . 206
**Wöllert, Torsten, Ana S. DePina, Reid F. Thompson, and George M. Langford**
GTPase Rho is involved in myosin-II-mediated contraction of pseudo-contractile rings and transport of vesicles in extracts of clam oocytes . . . . . . . . . . 208
**Brown, Jeremiah R., Elizabeth M. Peacock-Villada, and George M. Langford**
Globular tail fragment of myosin-V displaces vesicle-associated motor and blocks vesicle transport in squid nerve cell extracts . . . . . . . . . . 210
**Weidner, Earl, and Ann Findley**
Peroxisomal catalase in extrusion apparatus posterior vacuole of microsporidian spores . . . . . . . . . . 212
**Silver, Robert B., and Marc Bartman**
A metronome-like control of the calcium signal leading to nuclear envelope breakdown and mitosis in sand dollar *(Echinaracnius parma)* cells . . . . . . . . . . 213

*Developmental Biology*

**Crawford, Karen**
Culture method for *in vitro* fertilization to hatching of the squid, *Loligo pealeii* . . . . . . . . . . 216
**Pahl, Nicholas, Sara Homsi, Hilary G. Morrison, and Robert M. Gould**
mRNAs located in *Squalus acanthias* (spiny dogfish) oligodendrocyte processes . . . . . . . . . . 217
**Eddleman, Christopher S., George D. Bittner, and Harvey M. Fishman**
SEM comparison of severed ends of giant axons isolated from squid *(Loligo pealeii)* and crayfish *(Procambarus clarkii)* . . . . . . . . . . 219

*Studia Limulorum*

**Mittmann, Beate**
Early neurogenesis in the horseshoe crab *Limulus polyphemus* and its implication for arthropod relationships . . . . . . . . . . 221
**Smith, K., C. Ridings, F. A. Dodge, and R. B. Barlow**
Development of the lateral eye of juvenile *Limulus* . . . 222

**Ridings, C., D. Borst, K. Smith, F. Dodge, and R. Barlow**
Visual behavior of juvenile *Limulus* in their natural habitat and in captivity . . . . . . . . . . . . . . . . . . . . . . . 224
**Suggs, Dianne N., Ruth H. Carmichael, Sara P. Grady, and Ivan Valiela**
Effects of individual size on pairing in horseshoe crabs . . . . . . . . . . . . . . . . . . . . . . . . . . . . . . . . . . . . 225
**Borst, Douglas, and Robert Barlow**
Circadian rhythms in locomotor activity of juvenile horseshoe crabs . . . . . . . . . . . . . . . . . . . . . . . . . . . 227
**Gaines, Emily F., Ruth H. Carmichael, Sara P. Grady, and Ivan Valiela**
Stable isotopic evidence for changing nutritional sources of juvenile horseshoe crabs . . . . . . . . . . . . . 228

*Comparative Physiology*

**Smotherman, Michael**
Acetylcholine mediates excitatory input to chromatophore motoneurons in the squid, *Loligo pealeii*. . . . . 231
**Grable, Melissa M., Nadav Shashar, Nicole L. Gilles, Chuan-Chin Chiao, and Roger T. Hanlon**
Cuttlefish body patterns as a behavioral assay to determine polarization perception . . . . . . . . . . . . . . . . 232
**Rohrkasse, Sarah M., and Jelle Atema**
Tracking behavior of Busyconinae whelks . . . . . . . . 235
**Graf, Werner, Edwin Gilland, Matt McFarlane, Laura Knott, and Robert Baker**
Central pathways mediating oculomotor reflexes in an elasmobranch, *Scyliorhinus canicula*. . . . . . . . . . . . 236
**Montgomery, John, Guy Carton, and David Bodznick**
Error-driven motor learning in fish . . . . . . . . . . . . . 238
**Delaney, Martha, Christopher Follet, Nick Ryan, Nick Hanney, Jenny Lusk-Yahlick, and Gabriele Gerlach**
Social interaction and distribution of female zebrafish *(Danio rerio)* in a large aquarium . . . . . . . . . . 240
**Cermak, Michael J.**
*Caranx latus* (Carangidae) chooses dock pilings to attack silverside schools: A tactic to interfere with stereotyped escape behavior of prey? . . . . . . . . . . . . 241

*Ecology and Population Biology*

**La Du, Jane, Deana Erdner, Sonya Dyhrman, and Don Anderson**
Molecular approaches to understanding population dynamics of the toxic dinoflagellate *Alexandrium fundyense* . . . . . . . . . . . . . . . . . . . . . . . . . . . . . . . . . 244
**Philibotte, Jason**
Pelagic larval duration of the Caribbean wrasse, *Thalassoma bifasciatum* . . . . . . . . . . . . . . . . . . . . . . . . 245
**Hunter-Thomson, Kristin, Jeffrey Hughes, and Bradley Williams**
Estuarine–open-water comparison of fish community structure in eelgrass (*Zostera marina* L.) habitats of Cape Cod. . . . . . . . . . . . . . . . . . . . . . . . . . . . . . . . . . . 247
**Williams, Bradley S., Jeffrey E. Hughes, and Kristin Hunter-Thomson**
Influence of epiphytic algal coverage on fish predation rates in simulated eelgrass habitats . . . . . . . . . . 248
**Ludlam, John P., David H. Shull, and Robert Buchsbaum**
Effects of haying on salt-marsh surface invertebrates. . . . . . . . . . . . . . . . . . . . . . . . . . . . . . . . . . . . . . 250
**Levine, Uri Y., and Byron C. Crump**
Bacterioplankton community composition in flowing waters of the Ipswich River watershed. . . . . . . . . . . . 251
**Huffaker, Diana, and R. Gil Pontius, Jr.**
Reconstruction of historical land cover in the Ipswich watershed. . . . . . . . . . . . . . . . . . . . . . . . . . . . . . . . . 253

*Estuarine and Freshwater Biogeochemistry*

**Testa, Jeremy M., Matthew A. Charette, Edward R. Sholkovitz, Matt C. Allen, Adam Rago, and Craig W. Herbold**
Dissolved iron cycling in the subterranean estuary of a coastal bay: Waquoit Bay, Massachusetts . . . . . . . . 255
**Twichell, Sarah, Sallie Sheldon, Linda Deegan, and Robert Garritt**
Nutrient and freshwater inputs from sewage effluent discharge alter benthic algal and infaunal communities in a tidal salt marsh creek. . . . . . . . . . . . . . . . . . 256
**Koop-Jakobsen, Ketil, and Anne Giblin**
Tidal flushing of ammonium from intertidal salt marsh sediments: the relative importance of adsorbed ammonium . . . . . . . . . . . . . . . . . . . . . . . . . 258
**Barron, Stacy, Carolyn Weber, Roxanne Marino, Eric Davidson, Gabrielle Tomasky, and Robert Howarth**
Effects of varying salinity on phytoplankton growth in a low-salinity coastal pond under two nutrient conditions. . . . . . . . . . . . . . . . . . . . . . . . . . . . . . . . . . . . 260
**Weber, Carolyn F., Stacy Barron, Roxanne Marino, Robert W. Howarth, Gabrielle Tomasky, and Eric A. Davidson**
Nutrient limitation of phytoplankton growth in Vineyard Sound and Oyster Pond, Falmouth, Massachusetts . . . . . . . . . . . . . . . . . . . . . . . . . . . . . . . . . . . . 261
**Millman, Melissa, Mirta Teichberg, Paulina Martinetto, and Ivan Valiela**
Response of shrimp populations to land-derived nitrogen in Waquoit Bay, Massachusetts . . . . . . . . . . . 263

*Laboratory Animal Health*

**Smolowitz, Roxanna, Janice Hanley, and Hazel Richmond**
A three-year retrospective study of abdominal tumors in zebrafish maintained in an aquatic laboratory animal facility . . . . . . . . . . . . . . . . . . . . . . . . . . . . . . . 265
**Hsieh, Jennifer L., Hemant M. Chikarmane, Roxanna Smolowitz, Kevin R. Uhlinger, W. Mebane, and Alan M. Kuzirian**
Microbial analysis of ozone disinfection in a recirculating seawater system . . . . . . . . . . . . . . . . . . . . . . . 266

*Oral Presentations*

Published by title only. . . . . . . . . . . . . . . . . . . . . . . . 268

Reference: *Biol. Bull.* **203:** 185–187. (October 2002)

# *Introduction to the Featured Reports*
# The MBL Awards for 2002

In 1928, to foster communication among summer investigators with similar interests, a series of scientific meetings (one or two evenings per week) were instituted at the Marine Biological Laboratory (MBL). Three or four short papers on related subjects were presented at each meeting, and informality and free discussion were encouraged. In 1931, the character of the final evening meeting of the summer was altered: it became an all-day affair devoted to talks about work that had been completed at the Laboratory during that season. These end-of-summer meetings continued and were well-attended; the modern label "General Scientific Meeting" (GSM) was applied in 1936.

Abstracts of the summer presentations were first published in *The Biological Bulletin* in its October 1933 issue and, excepting the World War II period (1942–1945), the proceedings of the General Scientific Meetings have been so published for 55 years. In 1991, the editors of the *Bulletin* replaced the abstracts with peer-reviewed short reports, which are more substantial and more credible. This year's meeting included 56 presentations, and 47 reports are published in this issue.

To encourage greater participation in the General Scientific Meetings, the MBL's Science Council recently instituted the MBL Awards for the best paper presented at the GSMs by a senior investigator, a junior faculty member or postdoctoral fellow, a graduate student, and an undergraduate. The awards—based on both the presentation and the short report—are made by the Editor of *The Biological Bulletin* with recommendations from meeting organizers, session chairs, and participants. This year, the Editor also selected two student presentations for Honorable Mention.

The four presentations selected for MBL Awards this year reflect the broad scope of MBL science and the interconnectedness of comparative biology. We find, among these reports, a special feature of one animal used to analyze characteristics of organisms in another kingdom; the neural control of unique organs effecting camouflage and communication; a mode of neurogenesis described and then used as a phylogenetic character; and molecular assays as potential prognosticators of algal blooms. This year's awardees are listed below together with the title of their presentation and a brief summary of each project. The page on which the full report begins is also indicated.

*—The Editor*
*August 2002*

---

### Senior Award

*Peter B. Armstrong (University of California, Davis)*
*(with Margaret T. Armstong, R. L. Pardy, Alice Child, and Norman Wainwright)*
Immunohistochemical demonstration of lipopolysaccharide in the cell wall of a eukaryote, the green alga *Chlorella* (p. 203)

Lipopolysaccharides (LPS) are components of the outer cell membrane of gram-negative bacteria; they are supposedly restricted to prokaryotes but have recently been detected in *Chlorella*. A protein, *Limulus* anti-LPS factor (LALF), is secreted by horseshoe crab blood cells, binds to bacterial endotoxin and neutralizes it. An immunohistochemical test based on this reaction and on a tagged antiserum raised to LALF was used to localize an LPS-like molecule to the cell surface of *Chlorella*, a eukaryote. Thus, in addition to its presence in some prokaryotes, LPS appears also to be present at the cell surface of certain eukaryotes.

## Junior Award

*MICHAEL SMOTHERMAN (University of California, Los Angeles)*

### Acetylcholine mediates excitatory input to chromatophore motoneurons in the squid, *Loligo pealeii* (p. 231)

Thousands of chromatophores distributed throughout the skin of all decapod cephalopods function in camouflage and communication. The size (and thus visibility) of each of the pigment-filled chromatophoric sacs is controlled by a set of muscles, which are innervated from the central nervous system by motoneurons that project from the anterior and posterior chromatophore lobes (PCL). Acetylcholine (ACh) and nicotine applied directly to cell bodies in the PCL expanded a specific population of chromatophores on the surface of the ipsilateral mantle. Thus, the excitatory input to the chromatophoric motoneurons is, at least in part, cholinergic.

## Graduate Student Award

*BEATE MITTMANN (Humboldt-Universität, Berlin)*

### Early neurogenesis in the horseshoe crab *Limulus polyphemus* and its implication for arthropod relationships (p. 221)

Within the neuroectoderm on the ventral surface of *Limulus* embryos, clusters of bottle-shaped cells invaginate dorsally, probably never divide again, and form the ventral ganglia. This mode of gangliogenesis in *Limulus*—the most primitive chelicerate extant—is similar to that in all of the terrestrial arachnids (*e.g.*, spiders) that have been investigated to date. Thus it is likely to be the ancestral mode of ganglion formation in the chelicerates. In contrast, gangliogenesis in insects and crustaceans occurs through the formation of neuroblasts; so this process, distinct from that in chelicerates, is probably derived and can be seen as an apomorphic character for a monophyletic crustacean-insect unit.

## Undergraduate Award

*JANE LA DU (Oregon State University)*

*(with Deana Erdner, Sonya Dyhrman, and Don Anderson)*

### Molecular approaches to understanding population dynamics of the toxic dinoflagellate *Alexandrium fundyense* (p. 244)

Some dinoflagellates in the genus *Alexandrium* produce neurotoxins; and when the algae bloom, these toxins accumulate sufficiently in shellfish that consumers are poisoned. To monitor the development of such a harmful algal bloom (HAB), predict its effects, and thus mount credible public warnings, a pair of assays for *Alexandrium fundyense* are being developed that would rapidly and reliably measure cell density and growth rate. These assays are based on two algal gene fragments. One encodes a part of ribulose-1,5-bisphosphate carboxylase, a Calvin-Benson enzyme; so its expression is a likely marker for growth rate. The second fragment—a candidate for quantifying cell density—is species specific and encodes for large subunit ribosomal RNA. Specific primers for both fragments have been designed and tested in quantitative PCR, and show promise for use in the field.

### Student Honorable Mention

*Jeremy M. Testa (SUNY, Syracuse)*
*(with Matthew A. Charette, Edward R. Sholkovitz, Matt C. Allen, Adam Rago, and Craig W. Herbold)*
Dissolved iron cycling in the subterranean estuary of a coastal bay:
Waquoit Bay, Massachusetts (p. 255)

*D. E. Arnolds (Williams College)*
*(with S. J. Zottoli, C.E. Adams, S. M. Dineen, S. Fevrier, Y. Guo, and A. J. Pascal)*
Physiological effects of tricaine on the supramedullary/dorsal neurons
of the cunner, *Tautogolabrus adspersus* (p. 188)

**Reference:** *Biol. Bull.* **203:** 188–189. (October 2002)

# Physiological Effects of Tricaine on the Supramedullary/Dorsal Neurons of the Cunner, *Tautogolabrus adspersus*

*D. E. W. Arnolds, S. J. Zottoli, C. E. Adams, S. M. Dineen, S. Fevrier, Y. Guo, and A. J. Pascal*
*(Department of Biology, Williams College, Williamstown, Massachusetts 01267)*

Ethyl-*m*-aminobenzoate, known as tricaine, metacaine, or MS-222, is a commonly used general anesthetic for fish and amphibia. This anesthetic depresses neuronal activity in both the peripheral (1) and central nervous systems (2) of fish, but its effects on the basic physiological properties of individual neurons are unknown. Clearly, the action of tricaine must be determined, if neurophysiological data obtained during its use are to be correctly interpreted. We have therefore studied the effect of tricaine on the level of current necessary to elicit an action potential and spike height of supramedullary/dorsal neurons of the cunner *Tautogolabrus adspersus* (3, 4).

Responses of supramedullary/dorsal cells to depolarizing current pulses were recorded from cunner, 8–13.9 cm in body length; the fish were either under general or local anesthesia. In the first condition (general anesthesia), eight fish were initially anesthetized in tricaine (300 mg/l, Sigma) in seawater with sodium bicarbonate (450 mg/l) added. When respiration ceased, the fish were transferred to an operating chamber where tricaine (100 mg/l) in chilled seawater with sodium bicarbonate (450 mg/l; pH = 7.2) was recirculated through the mouth and over the gills for the duration of the experiment. In the second condition (local anesthesia), 10 fish were injected with pancuronium bromide (0.1 mg/kg; Sigma) to block neuromuscular transmission and were then placed in an operating chamber, where a respiratory current of chilled seawater was applied through the mouth and over the gills. Local anesthetic (20% benzocaine gel, Ultradent) was applied to the skin overlying the rostral spinal cord. After 5 min, the skin was removed and local anesthetic was applied to the underlying muscle. After 5 min, the rostral spinal cord was exposed. Single microelectrode recordings (3 *M* KCl filled, 5–15 MΩ) were then made from supramedullary/dorsal cell somata.

Under general anesthesia, action potentials 77 ± 8 mV (mean ± SD, $n = 12$) in amplitude could be evoked by 7 ± 2 nA of current. Under local anesthesia, spike height (91 ± 6 mV, $n = 12$) was significantly higher ($P < 0.001$; unpaired *t* test) and the current needed to evoke the spike was significantly lower (3 ± 2 nA; $P < 0.001$; unpaired *t* test) than values obtained under general anesthesia. These changes occurred without significant shifts in resting membrane potential (general anesthesia = −68 ± 5 mV; local anesthesia = −66 ± 5 mV).

Recordings were made in the supramedullary/dorsal cell soma, a location that is believed to be distant from the spike initiating zone (5). If the position of the microelectrode varied in its proximity to the spike initiating zone between experiments, then one might expect anesthetic-independent variation in spike height and current needed to elicit the spike. We controlled for this possibility in three experiments by continuously monitoring supramedullary/dorsal cells without moving the microelectode while the levels of tricaine were changed. The spike height decreased and current needed to elicit the spike increased upon the addition of tricaine (100 mg/l) to the water (Fig. 1). When the tricaine was removed by running anesthetic-free seawater over the gills, the current needed returned close to pre-anesthetic levels, and the spike height began to recover.

Supramedullary/dorsal cells are known to respond to touch (3, 6). Displacement of the tail usually resulted in the generation of

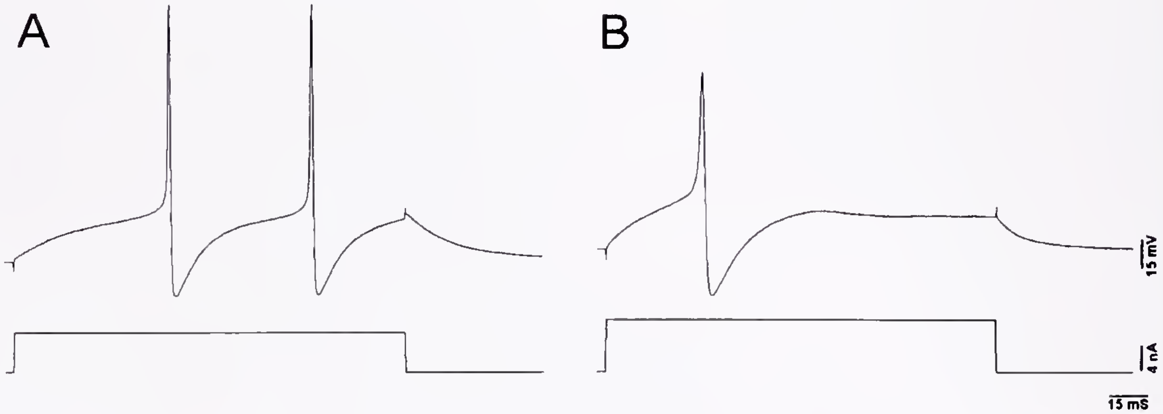

**Figure 1.** *Comparison of action potential amplitude and current needed to elicit an action potential in a single supramedullary/dorsal cell before and after addition of tricaine (100 mg/l; general anesthesia) to seawater passing over the gills. (A) Action potential elicited by a depolarizing current pulse of 6.5 nA. (B) Fifteen minutes after the addition of tricaine, 8.5 nA of depolarizing current was needed to elicit a spike which is notably smaller than that in (A). The current pulse is 150 ms in duration.*

multiple action potentials in supramedullary/dorsal cells of fish that were locally anesthetized. Under general anesthesia, action potentials could not be elicited, although underlying postsynaptic potentials were still apparent. These results support studies in which tricaine decreased afferent activity from other receptor types, such as the lateral line organs and ampullae of Lorenzini (1).

The physiological effects of tricaine on individual supramedullary/dorsal neurons support previous findings that this anesthetic is blocking sodium channels. Specifically, voltage clamp studies on the squid giant axon have shown that the internal application of tricaine caused a major reduction of the peak sodium currents and a smaller reduction of potassium currents; these effects were reversible (7).

This study indicates that tricaine significantly alters afferent input, spike height, and current needed to elicit an action potential of supramedullary/dorsal cells. Consequently, physiological measurements must be viewed with caution if tricaine is used as a general anesthetic. The physiological effects of tricaine on supramedullary/dorsal cells are partially reversible, but the possibility that this anesthetic has long-term residual effects remains to be determined.

This work was supported in part by Howard Hughes Medical Institute and Essel Foundation grants to Williams College.

### Literature Cited

1. **Hensel, H., R. Bromm, and K. Nier. 1975.** *Experientia* **31:** 958–960.
2. **Walsh, R. R., and R. T. Schopp. 1966.** *Am. J. Physiol.* **211:** 1–5.
3. **Zottoli, S. J., F. R. Akanki, N. A. Hiza, D. A. Ho-Sang, M. Motta, X. Tan, and K. M. Watts. 1999.** *Biol. Bull.* **197:** 239–240.
4. **Zottoli, S. J., D. E. W. Arnolds, N. O. Asamoah, C. Chevez, S. N. Fuller, N. A. Hiza, J. E. Nierman, and L. A. Taboada. 2001.** *Biol. Bull.* **201:** 277–278.
5. **Bennett, M. V. L., S. M. Crain, and H. Grundfest. 1959.** *J. Gen. Physiol.* **43:** 221–250.
6. **Bennett, M. V. L., Y. Nakajima, and G. D. Pappas. 1967.** *J. Neurophysiol.* **30:** 161–179.
7. **Frazier, D. T., and T. Narahashi. 1975.** *Eur. J. Pharmacol.* **33:** 313–317.

---

**Reference:** *Biol. Bull.* **203:** 189–190. (October 2002)

## Gene Expression in the Squid Giant Axon: Neurotransmitter Modulation of RNA Transfer From Periaxonal Glia to the Axon

*Antonio Giuditta, Maria Eyman (Università "Federico II," Naples, Italy), and Barry B. Kaplan*[1]

The presence of RNA in axons has been known for nearly 40 years (1). In large model axons, such as the goldfish Mauthner axon and the squid giant axon, axoplasmic RNA includes the main cytoplasmic species, that is, tRNA, rRNA, and mRNA. These findings have significantly contributed to the demonstration of an active protein synthetic system in axons (for reviews, see 2–4). In the squid, protein synthesis also occurs in the presynaptic terminals of the retinal photoreceptor neurons (5).

The above data have led us to question the cellular origin of axonal and presynaptic RNAs, often located at considerable distances from the neuronal soma. Evidence that axonal RNAs may not exclusively derive from cell bodies, but may also be synthesized locally, has been reported in several systems, including the isolated squid giant axon (6; for reviews, see 3, 4). Indeed, when the giant axon was incubated with [$^3$H]uridine, all axoplasmic RNA species were labeled (6).

To further investigate this process, we have been using the perfused squid giant axon—a cannulated axon still embedded in the stellate nerve but lacking the nerve cell bodies. The axon is placed in a sealed chamber containing artificial seawater (ASW), and perfusion is routinely continued for about 2 h, at which time EM analyses show the lack of axonal damage.

Upon addition of [$^3$H]uridine to the chamber, [$^3$H]RNA appears in the perfusate after a brief lag period, and continues to accumulate at a linear rate for at least 2 h. The perfusate [$^3$H]RNA is transcribed from a nuclear DNA template, as shown by its reproducible inhibition by actinomycin D added to the external medium (20–50 $\mu$g/ml), and by electrophoretic analyses indicating tRNA and eukaryotic rRNA as its main components. As noted for axoplasmic [$^3$H]RNA (6), these observations suggest that the perfusate [$^3$H]RNA is synthesized by periaxonal glial cells, thus opening the way to investigations of the mechanisms modulating RNA transfer from glia to axon.

In initial studies, we assessed the effect of raising the concentration of $K^+$ ions to 100 m*M* in the ASW bathing the perfused axon. Under this depolarizing condition, the rate at which [$^3$H]RNA appeared in the perfusate increased markedly, often in more than one episode. Similar effects were obtained when the concentration of $K^+$ ions in the axon perfusate was drastically reduced, thereby inducing depolarization of the axon but not of the glia. These results suggested that the increased rate of synthesis, delivery, or both, of [$^3$H]RNA to the axon perfusate was mediated by the release of one or more neurotransmitters from the depolarized axon that activated receptors in the glial plasma membrane.

These receptors include two glutamate receptors (NMDA and metabotropic of class II), and a nicotinic ACh autoreceptor, identified on the basis of voltage changes induced in periaxonal glia by

---

[1] NIMH, NIH, Bethesda, MD.

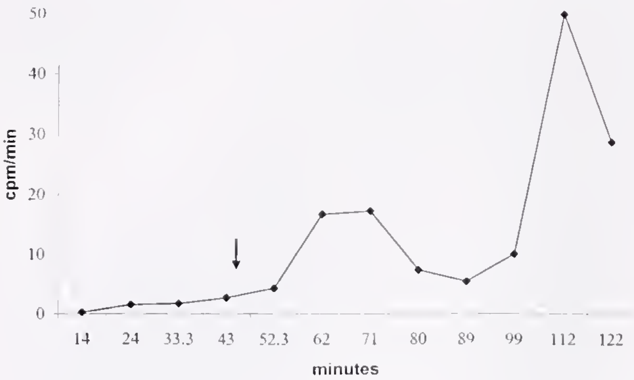

**Figure 1.** *Effect of 1 μM N-acetylaspartylglutamate (NAAG; arrow) on the rate of appearance of [$^3$H]RNA in the axon perfusate (cpm/min). The perfused axon was incubated at 19° with 400 μl artificial seawater containing 125 μCi/ml [$^3$H]uridine. Comparable data were obtained in 4 experiments with NAAG, 6 with glutamate, 4 with NMDA, and 3 with carbachol.*

neurophysiological stimulation of squid or crayfish giant axons, or by addition of agonists or antagonists of these receptors (7, 8). None of these receptors is present on the axonal membrane. While glutamate was initially considered the candidate neurotransmitter released by the axon, recent studies have shown that the true neurotransmitter is the dipeptide N-acetylaspartylglutamate (NAAG), which specifically binds to the metabotropic glutamate receptor, and is rapidly degraded to N-acetylaspartate and glutamate by a glial ectocarboxypeptidase (9).

In our most recent experiments, we have used several agonists of the glutamate and ACh glial receptors, singly or in association with specific antagonists, to examine their effects on the rate of appearance of [$^3$H]RNA in the perfusate. Our data indicate that NAAG, glutamate, NMDA, or carbachol markedly increase the delivery of glial [$^3$H]RNA to the perfusate, generally in more than one wave (Fig. 1). Activation of either glutamate receptor in the presence of the specific antagonist of the other (MK801 for the NMDA receptor, EGLU for the metabotropic II receptor) elicits comparable effects.

These results suggest that, in the squid giant axon, the complex system of neurotransmitter-mediated axon to glia signaling modulates the synthesis, the delivery, or both, of newly synthesized RNA from periaxonal glial cells to the axon. Further work is required to determine whether the same signaling system modulates the transfer of newly synthesized proteins and other glial components to the axon. The data are consistent with the view that, in addition to proteins and RNAs delivered by the neuronal soma, the axonal domain is endowed with a local system of gene expression based on a cooperative glia-axon interaction.

We gratefully acknowledge friendly support from the MBL staff, grants from the University of Naples "Federico II" and MUIR to AG, and NIH support to BBK. We thank R. De Stefano, C. Cefaliello, and D. De Martino for the [$^3$H]RNA analyses.

## Literature Cited

1. **Edström, A., *et al.* 1969.** *J. Neurochem.* **16:** 53–66.
2. **Koenig, E., and A. Giuditta. 1999.** *Neuroscience* **89:** 5–151.
3. **Alvarez, J., A. Giuditta, and E. Koenig. 2000.** *Prog. Neurobiol.* **62:** 1–62.
4. **Giuditta, A., B. B. Kaplan, J. van Minnen, J. Alvarez, and E. Koenig. 2002.** *TINS (Trends Neurosci.)* **25:** 400–404.
5. **Crispino, M., B. B. Kaplan, R. Martin, J. Alvarez, J. T. Chun, and A. Giuditta. 1997.** *J. Neurosci.* **17:** 7694–7702.
6. **Rapallino, M. V., A. Cupello, and A. Giuditta. 1988.** *Neurochem. Res.* **13:** 625–631.
7. **Villegas, J. 1984.** *Curr. Top. Membr. Transp.* **22:** 547–571.
8. **Lieberman, E. M., P. T. Hargittai, and R. M. Grossfeld. 1994.** *Prog. Neurobiol.* **44:** 333–376.
9. **Gafurov, B., A. K. Urazaev, R. M. Grossfeld, and E. M. Lieberman. 2001.** *Neuroscience* **106:** 227–235.

---

**Reference:** *Biol. Bull.* **203:** 190–191. (October 2002)

## Perchlorate Prevents Sodium Channel Gating and Sodium Protects in the Squid Giant Axon

*David Landowne (University of Miami, Miami, Florida 33101)*

Depolarization of nerve axon membranes induces conformational changes in sodium channel molecules which then open, allowing the flow of inward current that underlies the propagated nerve impulse. One sign of these conformational changes is the outward gating current that precedes the ionic current. The conformational changes are independent of the sodium concentration (1, 2). Therefore, the gating current—which can be obscured by the larger ionic currents present in full sodium—is best studied in low or zero sodium.

Water and small solutes in the bathing medium have access to the working parts of sodium channel molecules, including the S4 transmembrane segments with their distinctive arrangement of positively charged amino acids (3–5). Looking for possible effects of counterions, I selected perchlorate as a chloride substitute because it is near the end of the Hofmeister series, which ranks ion effects on soluble proteins (6).

Segments of squid axons were superfused with an artificial seawater (asw) containing, in millimoles, $x$ Na, 442-$x$ tetramethylammonium (TMA), 50 Ca, $y$ $ClO_4$, 540-$y$ Cl and 2 HEPES, pH 7.4. That is, the sum of Na and TMA was 442 and the sum of Cl and

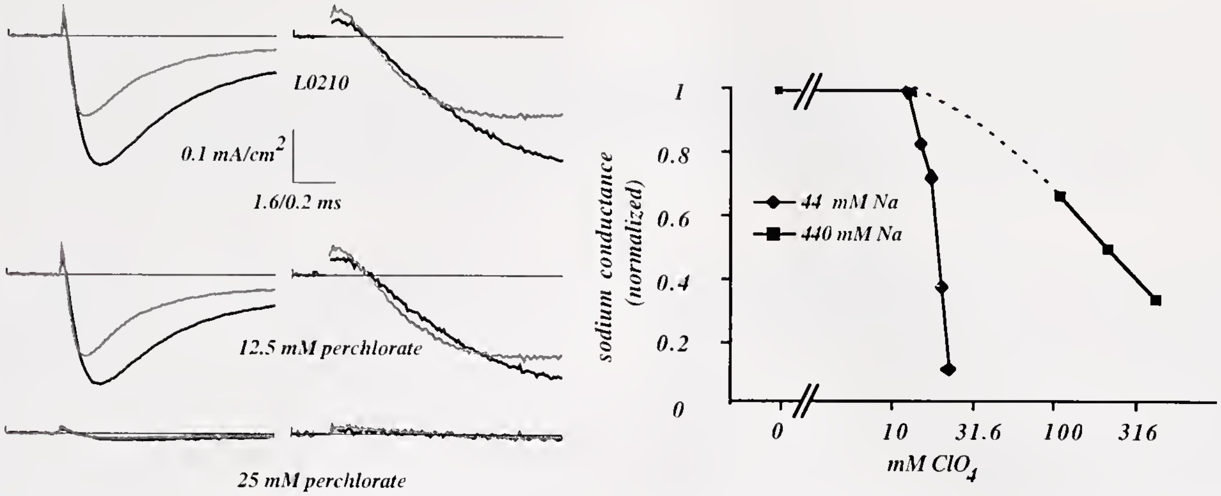

**Figure 1.** *Perchlorate reduces gating and ionic currents. The records are for steps from a −80 mV holding potential. The gray records are to +20 mV; the black, to −5 mV. The records on the right are shown at the expanded timebase. The graph shows the maximum Na conductance, normalized to the value obtained in Cl artificial seawater, as a function of $ClO_4$ concentration for two different Na concentrations.*

$ClO_4$ was 540. They were internally perfused with either a Cs perfusion fluid (pf) containing 240 Cs, 150 glutamate, 50 F, 750 sucrose, and 40 HEPES, pH 7.4; or a K pf containing 200 K, 80 Na, 190 glutamate, 50 F, 550 glycine, and 40 HEPES, pH 7.4. Experiments were performed at 3–4°C. The axons were voltage-clamped at a −80 mV holding potential. Currents were recorded with a p/4 protocol (7), filtered at 40 kHz and sampled at 100 kHz. The records presented are averaged over 64 cycles.

The tracings at the left of the figure were made in 44 m*M* Na asw, with Cs pf inside. Current traces for pulses to −5 mV (black) and +20 mV (gray) are shown on two different time bases. The top set of records is in Cl asw. Replacing 25 m*M* of Cl in the asw with $ClO_4$ almost eliminated both the inward ionic current and the early outward gating current, and 12.5 m*M* $ClO_4$ had hardly any effect. Intermediate concentrations of $ClO_4$ partially reduced both ionic and gating currents proportionally (not shown), with reduction of the sodium conductance to one half at about 16 m*M*. The preparation recovered partially when returned to $ClO_4$-free solutions; but the recovery was less at higher $ClO_4$ concentrations or after longer exposure times.

The effects of $ClO_4$ on the maximum sodium conductance are summarized in the graph at the right of the figure. In full Na asw, with K pf internally, 25 m*M* $ClO_4$ had no effect, and reduction of the sodium conductance to one half occurred at about 200 m*M*. About 25% of the sodium conductance remained with 440 m*M* $ClO_4$. In full Na asw, increasing $ClO_4$ altered the time course of the remaining sodium current, first reducing sodium inactivation and then replacing it with a slowly rising conductance. At 300 n*M*, tetrodotoxin blocked more than 90% of the current remaining in 440 m*M* $ClO_4$.

Potassium currents were more sensitive to $ClO_4$ than Na currents and were also protected by external Na. In 44 m*M* Na asw, 15 m*M* $ClO_4$ eliminated the K currents; in 440 m*M* Na asw, between 220 and 440 m*M* $ClO_4$ was required.

These results in squid axons are quite different from those reported in frog skeletal muscle, where $ClO_4$ shifts sodium channels excitability (8), excitation-contraction coupling, and intramembranous charge movement to more negative potentials (9). In squid axons, Na permeability was reduced 35% by 110 m*M* $ClO_4$ in the presence of 440 m*M* Na, compared with an 8% reduction by 115 m*M* $ClO_4$ in the presence of 115 m*M* Na in frog muscle (8).

In conclusion, in squid axons, anions can have large effects on ion channels. A log-log (Hill) plot of the concentration dependence of $ClO_4$ on sodium conductance in 44 m*M* Na asw has a slope of about −4. It seems unlikely that this indicates cooperativity between the four domains of the protein (5) because gating current decreased with about the same concentration dependence, and most current models (3) involve all four domains in the gating current. There are four or more positively charged amino acids on each S4 segment that could support a cooperative effect on each domain, but this possibility does not explain the lack of cooperativity seen in 440 m*M* Na.

I thank Dr. R.J. Lipicky and the Howard Gilman Foundation for encouragement and support.

## Literature Cited

1. **Armstrong, C. M., and F. Bezanilla. 1973.** *Nature* **242:** 459–461.
2. **Landowne, D. 1985.** *J. Membr. Biol.* **88:** 173–185.
3. **Bezanilla, F. 2000.** *Physiol. Rev.* **80:** 555–592.
4. **Landowne, D. 2000.** *Biol. Bull.* **199:** 164–165.
5. **Sato C., and G. Matsumoto. 1995.** *J. Membr. Biol.* **147:** 45–70.
6. **Hofmeister, F. 1888.** *Arch. Exp. Pathol. Pharmakol.* (Leipzig) **24:** 247–260.
7. **Bezanilla F., and C. M. Armstrong. 1975.** *Philos. Trans. R. Soc. Lond. B. Biol. Sci.* **270:** 449–458.
8. **Dani J. A., J. A. Sanchez, and B. Hille. 1983.** *J. Gen. Physiol.* **81:** 255–281.
9. **Luttgau, H. C., G. Gottschalk, L. Kovacs, and M. Fuxreiter. 1983.** *Biophys. J.* **43:** 247–249.

**Reference:** *Biol. Bull.* **203:** 192–194. (October 2002)

# Blockade of an Inward Sodium Current Facilitates Pharmacological Study of Hemi-Gap-Junctional Currents in *Xenopus* Oocytes

*Harris Ripps (Lions of Illinois Eye Research Institute, Department of Ophthalmology and Visual Sciences, UIC College of Medicine, Chicago, Illinois 60612), Haohua Qian, and Jane Zakevicius*

Signal transmission through gap-junctional channels serves to synchronize and regulate a broad range of cellular activities in tissues throughout the body (1). The structural proteins that constitute gap-junctional channels are the connexins, a multigene family of homologous proteins, whose members are identified by their predicted molecular mass in kilodaltons (*e.g.*, Cx35). Six connexin polypeptides oligomerize to form a membrane hemichannel, or *connexon*, which can dock with the connexons from adjacent cells to form an aqueous pore (d ≈ 16 Å) which allows the cell-to-cell diffusion of ions, second-messenger molecules, and metabolites having a molecular mass ≤ 1 kDa. The delivery and insertion of connexin subunits in the plasma membrane and their assembly into connexons represent important stages in the formation of gap junctions. It is not surprising, therefore, that the gap-junctional channels of electrically coupled cells and the hemichannels formed by their connexon precursors often exhibit similar regulatory mechanisms and gating properties (2).

Because the *Xenopus* oocyte has the capacity to efficiently translate foreign genetic information and to assemble and insert oligomeric channel complexes into its plasma membrane, it has become a widely used expression system for the functional analysis of gap-junctional proteins. Oocytes expressing connexin subunits, and brought into contact after removal of the follicular and vitelline membranes, typically form gap-junction channels, affording the opportunity for electrophysiological and pharmacological study. In addition, there is growing interest in the functional properties of the hemichannels formed in isolated neurons (3, 4) and in single oocytes (5) expressing various gap-junctional proteins. The presence of non-junctional hemichannels is readily demonstrated electrophysiologically. Prolonged membrane depolarization results in the development of a time- and voltage-dependent outward current attributable to the opening of hemi-gap-junctional channels. However, the same voltage protocol brings into play a $Na^+$-dependent current of similar time course, but opposite polarity (6). Although this slow inward current is clearly different from the transient $Na^+$ current of neurons and muscle cells, which inactivates rapidly during depolarization and is abolished by tetrodotoxin at concentrations about 1000 times lower than that required to block the sustained inward current (7), it tends to reduce the apparent amplitude of the hemichannel current or greatly restrict the voltage range over which it can be reliably recorded. The interaction between these two currents can be particularly troublesome when attempting a quantitative pharmacological analysis of hemichannel activity. Most agents that modulate gap-junctional communication produce a reduction in channel conductance, and thus low-amplitude hemichannel currents are not suitable for obtaining dose-response data over a significant concentration range.

In the present study, we used the two-electrode voltage-clamp technique to examine the interaction between the sodium current and the hemichannel currents mediated by the endogenous connexin (Cx38) of *Xenopus* oocytes. As illustrated in Figure 1, the large inward sodium currents elicited in the normal modified Barth's (MB) solution (Fig. 1A) obscured the weaker hemichannel currents. However, when we removed extracellular sodium (choline substitution) the presence of the underlying hemichannel currents was revealed (Fig. 1B). Although the small hemicurrents recorded from some oocytes may be attributable to a low level of Cx38 expression, in most cases the sodium current either completely masked hemichannel activity (as in Fig. 1A) or reduced its magnitude to such an extent as to preclude pharmacological studies.

The cinchona alkaloid quinine also effectively blocked the inward current (Fig. 1C) and, in addition, enhanced significantly the endogenous Cx38 hemichannel currents in a dose-dependent fashion (Fig. 1D); the Hill coefficient of 1.9 suggests that the binding of at least two molecules of quinine are required to produce the effect. Both the dose-response curve and the Hill coefficient are remarkably similar to results reported previously for hemichannel currents recorded from horizontal cells isolated from skate (8) and catfish (9) retinas. In contrast, 400 $\mu M$ intracellular quinine failed to affect hemichannel currents in the oocyte preparation. A similar result was obtained in isolated retinal neurons (8), and suggests that the potentiating effect of quinine probably results from binding to a site accessible from the extracellular side of the membrane near or within the mouth of the open hemichannel.

With the full magnitude of the hemichannel currents exposed, either by replacing sodium with choline in the MB solution or by the addition of quinine, we could conduct pharmacological studies of agents that are known to modulate gap-junctional conductances in coupled neurons and other cell types. All-*trans* retinoic acid (RA), a metabolite of vitamin A, acting through a plasma membrane retinoic acid-binding protein, has been shown to reduce electrical coupling between horizontal cells both *in situ* and between cell pairs in culture (10). A similar action was observed in our recordings of Cx38-mediated hemichannel recordings from *Xenopus* oocytes superfused with a Na-free solution supplemented with various concentrations of RA (Fig. 1E); the $IC_{50}$ of approximately 2 $\mu M$ is comparable to that obtained with coupled horizontal cells in culture (10). Figure 1F illustrates the results obtained with carbenoxolone, applied to an MB solution containing 200 $\mu M$ quinine. Carbenoxolone is one of the many derivatives of glycyrrhetinic acid, a saponin obtained from the licorice root *Glycyrrhizia glabra*, that has been shown to be a potent inhibitor of gap-junctional communication in various cell types (11). Figure 1F shows that the drug blocked Cx38 hemichannel activity with an $IC_{50}$ of approximately 34 $\mu M$.

In sum, our study describes some of the membrane properties of

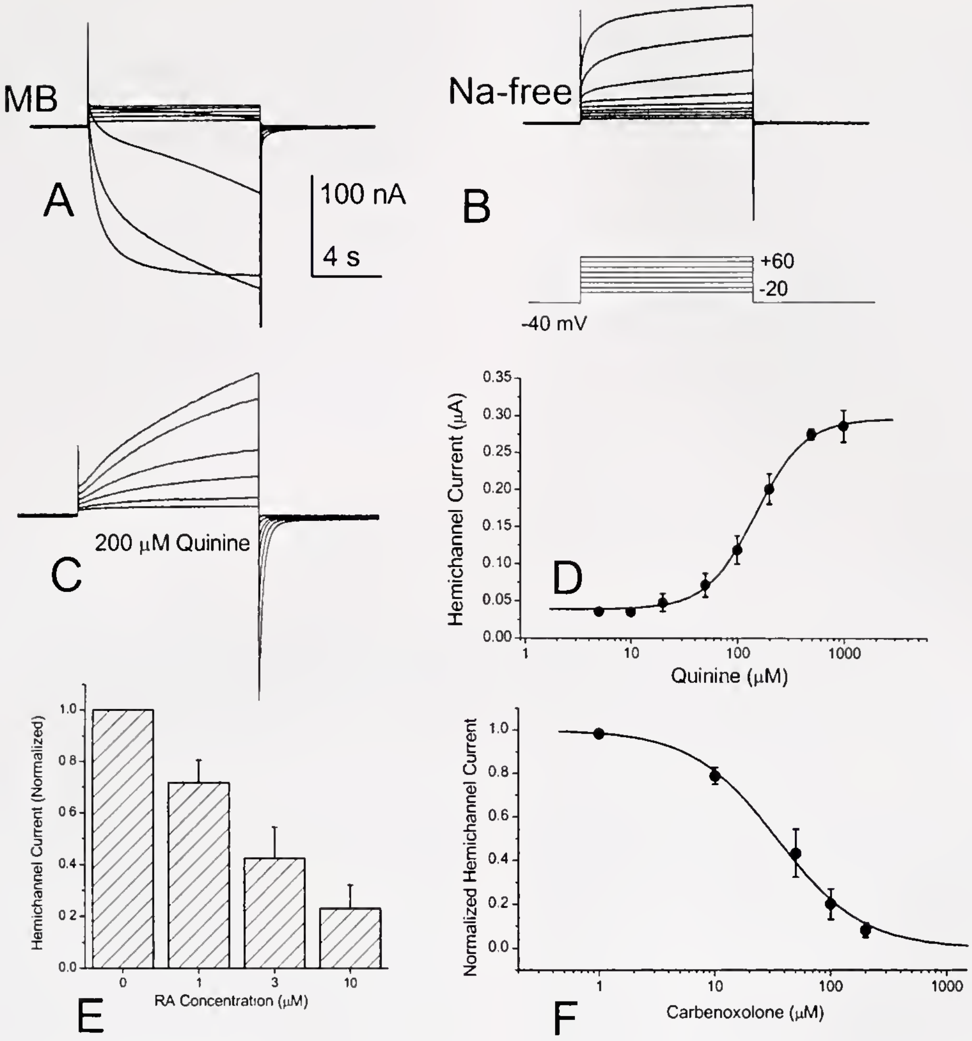

**Figure 1.** *(A) Depolarizing voltage steps from* $-40$ *mV to* $+60$ *mV (inset) fail to reveal hemichannel currents in a* Xenopus *oocyte expressing Cx38. With the cell bathed in modified Barth's (MB) solution, passive outward currents are elicited with voltages up to* $+20$ *mV; with further depolarization* ($\geq +30$ *mV) only inward currents are seen. The MB solution contained [in* mM*]: NaCl [88], KCl [1], NaHCO*$_3$ *[2.4], N-2-hydroxyethylpiperazine-N'-2-ethanesulfonic acid (HEPES) [15], Ca(NO*$_3$*)*$_2$ *[0.33], CaCl*$_2$ *[0.41], and MgSO*$_4$ *[0.82]; 10 mg/liter gentamycin was added, and the solution titrated with NaOH to pH7.4. (B) After replacing the bath solution with Na*$^+$*-free (choline substitution) MB solution, voltage steps* $\gtrsim 20$ *mV evoke voltage- and time-dependent hemichannel currents of increasing magnitude. (C) Hemicurrents enhanced by 200* μM *quinine show no voltage-activated Na*$^+$ *current. (D) The dose-response data for the full range of concentrations tested (5–1000* μM*) are plotted on log-linear coordinates and fit by the Hill equation with an EC*$_{50}$ *of 150* μM *and a Hill coefficient of 1.9. Error bars =* $\pm$ *SEM* (n = 4)*. (E) Hemichannel currents were recorded in Na*$^+$*-free MB with a single step protocol (depolarization from* $-40$ *mV to* $+40$ *mV) in response to various concentrations of retinoic acid (RA). The bar graph shows the averaged results from four cells in which currents were normalized to the maximum obtained in Na*$^+$*-free MB. Error bars =* $+$*SEM. Over this limited range of concentrations, there is a dose-dependent block of hemichannel activity with half-maximal effect at approximately 2* μM *RA. (F) Log-linear plot of the dose-dependent blockage of hemichannel activity by carbenoxolone. The hemichannel currents in carbenoxolone were normalized to the mean current obtained in 200* μM *quinine with a depolarizing voltage step to* $+50$ *mV. The data were fit by the Hill equation with an IC*$_{50}$ *of 34* μM *and a Hill coefficient of 1.2. Error bars =* $\pm$ *SEM* (n = 4)*.*

*Xenopus* oocytes in response to prolonged depolarizing voltage steps, and illustrates the interaction between an inward sodium current and the hemichannel current mediated by the endogenous gap-junctional protein, Cx38. Blocking the Na$^+$ current enhanced the recorded hemichannel currents, and enabled us to show that the chemical gating of Cx38 hemichannels corresponds in many respects to that observed with fully formed gap-junctional channels in other systems. The use of this "modified" oocyte hemichannel preparation should prove useful for developing response profiles or "signatures" with which to distinguish the properties of one connexin from another, and for determining the modulatory effects of pharmacological agents that affect the gating of gap-junctional channels.

These studies were conducted at the Marine Biological Labora-

tory, Woods Hole, Massachusetts, and supported in part by grants from the National Eye Institute (EY-06516, EY- 12028, and EY-01792); an unrestricted award to the Department of Ophthalmology and Visual Sciences from Research to Prevent Blindness, Inc.; a Career Development Award from RPB (HQ); and an Award from the Alcon Research Institute (HR).

## Literature Cited

1. **Bennett, M. V. L., L. C. Barrio, T. A. Bargiello, D. C. Spray, E. Hertzberg, and J. C. Saez. 1991.** *Neuron* **6:** 305–320.
2. **Ebihara, L., V. M. Berthoud, and E. C. Beyer. 1995.** *Biophys. J.* **68:** 1796–1803.
3. **DeVries, S. H., and E. A. Schwartz. 1992.** *J. Physiol.* **445:** 201–230.
4. **Malchow, R. P., H. Qian, and H. Ripps. 1993.** *J. Neurosci. Res.* **35:** 237–245.
5. **White, T. W., M. R. Deans, J. O'Brien, M. R. Al-Uhaidi, D. A. Goodenough, H. Ripps, and R. Bruzzone. 1999.** *Eur. J. Neurosci.* **11:** 1883–1890.
6. **Baud, C., R. T. Kado, and K. Marcher. 1982.** *Proc. Natl. Acad. Sci. USA* **79:** 188–192.
7. **Parker, I., and R. Miledi. 1987.** *Proc. R. Soc. Lond. B* **232:** 289–296.
8. **Malchow, R. P., H. Qian, and H. Ripps. 1994.** *J. Gen. Physiol.* **104:** 1039–1055.
9. **Dixon, D. B., K.-I. Takahashi, M. Bieda, and D. R. Copenhagen. 1996.** *Vision Res.* **36:** 3925–3931.
10. **Zhang, D.-Q., and D. G. McMahon. 2000.** *Proc. Natl. Acad. Sci. USA* **97:** 14754–14759.
11. **Davidson, J. S., and I. M. Baumgarten. 1988.** *J. Pharmacol. Exp. Thera.* **246:** 1104–1107.

---

**Reference:** *Biol. Bull.* **203:** 194–195. (October 2002)

# $Cl^-$ and Glutamate$^-$ Competition for a Volume-Regulated Anion Channel

*Sarah S. Garber (Department of Physiology and Biophysics, Finch University of the Health Sciences/*
*The Chicago Medical School, North Chicago, Illinois) and Mary M. Hoffman*[1]

Volume-regulated anion currents are ubiquitous and contribute to volume recovery in response to cell swelling under hypotonic conditions. Glutamate (Glut$^-$) and other amino acids are involved in volume regulatory processes (*e.g.*, 1–5), and one pathway for volume-regulated amino acid release is through a volume-regulated anion conductance (6, 7). Glut$^-$, unlike many other volume-sensitive amino acids, is negatively charged at physiological pH; and Glut$^-$ current may therefore be measured using whole cell patch clamp recording (3). This study addresses the relative permeability of Glut$^-$ and $Cl^-$ through a volume-regulated anion conductance in the presence and absence of an ionic strength gradient.

Human embryonic kidney cells (tsA201a) were maintained as previously described (8, 9). Extracellular solutions contained (in m*M*): 1 EGTA, 2 $CaCl_2$, 10 HEPES, adjusted to pH 7.2 with 1*M* HCl or N-methyl D-glutamine. High ionic strength external solutions contained 150 $Cl^-$ or Glut$^-$; low ionic strength solutions contained 50 $Cl^-$ or Glut$^-$. Intracellular solutions contained (in m*M*): 1.1 EGTA, 0.1 $CaCl_2$, 10 HEPES, 4 ATP, pH 7.2 and molar fractions (MF = [Glut$^-$]/{[Glut$^-$] + [$Cl^-$]}) of $Cl^-$ and Glut$^-$ ranging from 0.0 to 1.0 at high (150 m*M*) or low (50 m*M*) ionic strength. At least 0.2 m*M* $Cl^-$ was present in all solutions for electrode stability. Solution osmolality was measured with a vapor pressure osmometer (Wescor, Logan, Utah) and adjusted such that the intracellular osmolarity was 100 ± 5 mOsm greater than the external osmolarity. Isotonic osmolarity = 313 ± 5 m*M*. In some experiments, a transmembrane ionic strength gradient was established with high extracellular and low intracellular ionic strength solutions. The difference between high and low ionic strength solutions was 100 m*M*, as determined by $\Delta\Gamma = \Gamma_o - \Gamma_{in} = 0.5(\Sigma c_i z_i^2)_o - 0.5(\Sigma c_i z_i^2)_{in}$, where $\Gamma$ = ionic strength, $c_i$ = concentration of $ion_i$ and $z_i$ = valance of $ion_i$.

Whole cell recording and analysis was performed as described in (3). Swelling activated anion currents were elicited by a voltage ramp from −60 to +100 mV. Reversal potentials ($V_r$) were measured when the maximal current amplitude was no longer changing and were corrected for liquid junction potentials using JPCalc (Cell MicroControls, Virginia Beach, VA). Corrected $V_r$s were substituted into a standard form of the Goldman-Hodgkin-Katz equation, rearranged to solve for the permeability ratio:

$$\frac{P_{Glut^-}}{P_{Cl^-}} = \frac{e^{V_r(zF/RT)}[Cl^-]_{out} - [Cl^-]_{in}}{[Glut^-]_{in} - e^{V_r(zF/RT)}[Glut^-]_{out}}$$

Where $P_{Glut}/P_{Cl}$ is the relative permeabilities of Glut$^-$ and $Cl^-$, and *z*, *F*, *R*, and *T* have their usual meanings.

Figure 1A shows that $P_{Glut}/P_{Cl}$ was always less than 1.0, indicating a greater relative chloride permeability when the intra- and extracellular ionic strength was the same on both sides of the membrane. The $P_{Glut}/P_{Cl}$, however, varied as the intracellular molar fraction of Glut$^-$ moved from 0 toward 1.0, indicating that the anions compete for the permeation pathway of the anion channel and interact within the pore (10).

The effect of intracellular anion composition on the relative permeability of $Cl^-$ and Glut$^-$ reversal potentials was again measured in the presence of a transmembrane ionic strength gradient, at different intracellular MFs, and in the presence of either extracellular $Cl^-$ or Glut$^-$ (Fig. 1B). $P_{Glut}/P_{Cl}$ was dependent on the

---

[1] Dept. of Pharmacology and Physiology, MCP Hahnemann School of Medicine, Philadelphia, PA.

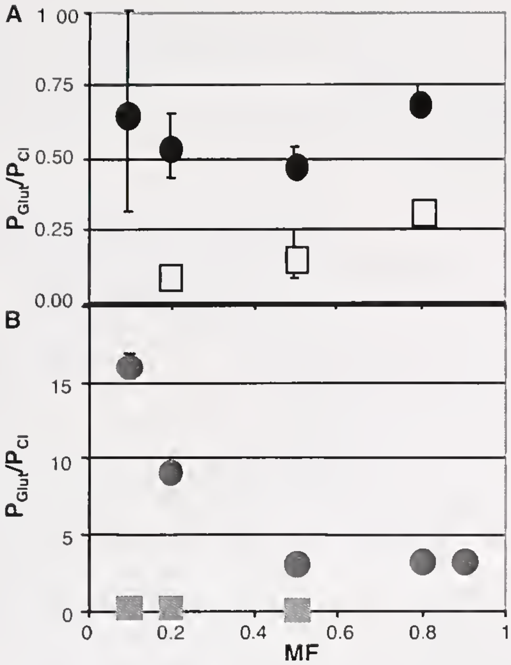

**Figure 1.** *(A)* $P_{Glut}/P_{Cl}$ *varies with intracellular MF with either high (●) or low (□) ionic strength on both sides of the membrane and was less than 1.0 over the range of MFs tested. (B)* $P_{Glut}/P_{Cl}$ *also varies with intracellular MF but was greater than 1.0 over the range of MFs tested when determined in the presence of a transmembrane ionic-strength gradient and extracellular* $Cl^-$ *containing solutions (●).* $P_{Glut}/P_{Cl}$ *was always less than 1.0 in the presence of a transmembrane ionic strength gradient and extracellular* $Glut^-$ *containing solutions (■). Intracellular MF was varied as indicated.* n $\geq$ *5, ± SEM.*

intracellular MF and the extracellular anion in the presence of a transmembrane ionic strength gradient of 100 m*M*. $P_{Glut}/P_{Cl}$ showed a strong dependence on the intracellular anion composition in the presence of extracellular $Cl^-$, and $P_{Glut}/P_{Cl}$ was greater than 1.0 for all MFs tested, indicating greater permeability of $Glut^-$. In contrast, $P_{Glut}/P_{Cl}$ was less than 1.0 for all MFs tested with extracellular $Glut^-$. $Cl^-$ was always more permeable than $Glut^-$, even in the presence of an ionic strength gradient.

The major finding of this study was that the anion permeability associated with the volume-regulated anion conductance is dependent on both extra- and intracellular ionic composition and on a transmembrane ionic strength gradient. These results are consistent with an ion conductive pathway that can be occupied simultaneously by more than one permeant species, and with interactions between the permeant anions within this pathway.

The combined effect of an ionic strength gradient and extracellular $Cl^-$ results in a switch in the relative permeability of the volume-regulated anion current, from preferring $Cl^-$, to $Glut^-$. Our hypothesis is that this effect is due to a change in the ion channel protein underlying the current, as our results indicate ion-ion interaction. It is possible that an additional glutamate transport pathway is activated under these conditions. A change in the intracellular ion composition as a result of swelling may alter the volume-regulated anion conductance so that $Glut^-$ passes more easily than $Cl^-$ during volume recovery. This may increase the $Glut^-$-induced excitotoxicity found in neuronal and glial cell populations.

Supported by NIDDK46672 and AHA94002340.

## Literature Cited

1. **Lang, F., G. L. Busch, and H. Volkl. 1998.** *Cell. Physiol. Biochem.* **8:** 1–45.
2. **Lang, F., G. L. Busch, M. Ritter, H. Volkl, S. Waldegger, E. Gulbins, and D. Haussinger. 1998.** *Physiol. Rev.* **78:** 247–306.
3. **Levitan, I., and S. S. Garber. 1998.** *Biophys. J.* **75:** 226–235.
4. **Pasantes-Morales, H., R. Franco, M. E. Torres-Marquez, K. Hernandez-Fonseca, and A. Ortega. 2000.** *Cell. Physiol. Biochem.* **10:** 361–370.
5. **Jackson, P. S., and K. Strange. 1993.** *Am. J. Physiol.* **265:** C1489–C1500.
6. **Song, D., M. H. O'Regan, and J. W. Phillis. 1998.** *Eur. J. Pharmacol.* **341:** 273–280.
7. **Strange, K., and P. S. Jackson. 1995.** *Kidney Int.* **48:** 994–1003.
8. **Margolskee, R. F., B. McHendry-Rinde, and R. Horn. 1993.** *Biotechniques* **15:** 906–911.
9. **Hubert, M. D., I. Levitan, M. M. Hoffman, M. Zgraggen, M. E. Hofreiter, and S. S. Garber. 2000.** *Biochim. Biophys. Acta* **1466:** 105–114.
10. **Hille, B. 1992.** *Ionic Channels of Excitable Membranes.* Sinauer Associates, Sunderland, MA.

---

**Reference:** *Biol. Bull.* **203:** 195–196. (October 2002)

# Preliminary Evidence for Interpulse Interval Selectivity of Cells in the Torus Semicircularis of the Oyster Toadfish (*Opsanus tau*)

*Richard R. Fay and Peggy L. Edds-Walton (Marine Biological Laboratory, Woods Hole, Massachusetts 02543 and Loyola University Chicago, Chicago, Illinois 60626)*

Both the grunt and the boatwhistle sounds of toadfish are a series of rapidly produced sound pulses. These sounds can therefore be described, not only by their spectral components, but also by the pulse repetition rate (pulses/s) or interval between the beginning of consecutive pulses (interpulse interval, IPI). Indeed, some of the information conveyed in these communication sounds may be encoded in the pulse repetition rate or in the IPI (1). As part of our investigation on auditory processing in the toadfish (*e.g.*, 2), we have evaluated the sensitivity of the auditory midbrain (torus semicircularis, TS) to sound pulses produced at several periodic rates. The stimuli for our previous experiments have been various frequencies of sinusoidal particle motion (described in 3). Here, we have used sound pulses to determine whether cells in the TS are selective for IPI or pulse rate.

Fish were anesthetized with 3 aminobenzoic acid (1:1000, Sigma), immobilized with an injection of pancuronium bromide (0.05 mg/kg); and lidocaine was applied to the skin prior to surgery. After its left midbrain region was exposed, the fish was secured to a seawater-filled dish in the stimulus shaker system (3). Glass micropipettes were broken to obtain low impedance electrodes (5–20 megohms) when filled with 4% neurobiotin in 2 *M* NaCl for determining electrode tip locations. All recordings were made in the left torus semicircularis.

The stimulus pulse was a 150-Hz sinusoid multiplied by the first half-cycle (10 ms duration) of a 50-Hz cosine. This produced a pulse as brief as possible, but still having frequency components low enough to stimulate the toadfish auditory system. Pulse trains were produced at 13 repetition rates between 10 and 83 pulses/s, or IPIs of 12–100 ms. The shortest IPI was dictated by the pulse duration (10 ms), because higher rates would have resulted in pulse coincidence. The pulse trains (500-ms duration) were presented 8 times each, in random order, at several levels (peak-peak displacement in dB with respect to 1 nm) within a cell's dynamic range. The total number of spikes produced for each set of 8 pulse-train repetitions was measured at each level.

Responses were classified as selective or nonselective. A selective unit was defined as one for which the number of spikes evoked by the most effective IPI was at least 2.5 standard deviation units above the average number of spikes for all pulsed stimuli, and for which the most effective IPI was independent of sound intensity. Of 71 units evaluated, 43 (61%) were selective and the rest non-selective. Of the selective units, 56% responded best at the shortest IPI (12 ms, or 84 pulses/s). The remaining selective units responded best to IPIs between 16 and 50 ms, with a secondary mode at 20 ms.

Figure 1 shows the pulse response functions for three selective units (panels A–C). Panel A shows the data for one unit that responded best to the shortest IPI (12 ms). Panel B shows a unit that is clearly most selective to a 20-ms IPI, and panel C shows a unit responding best to a 40-ms IPI.

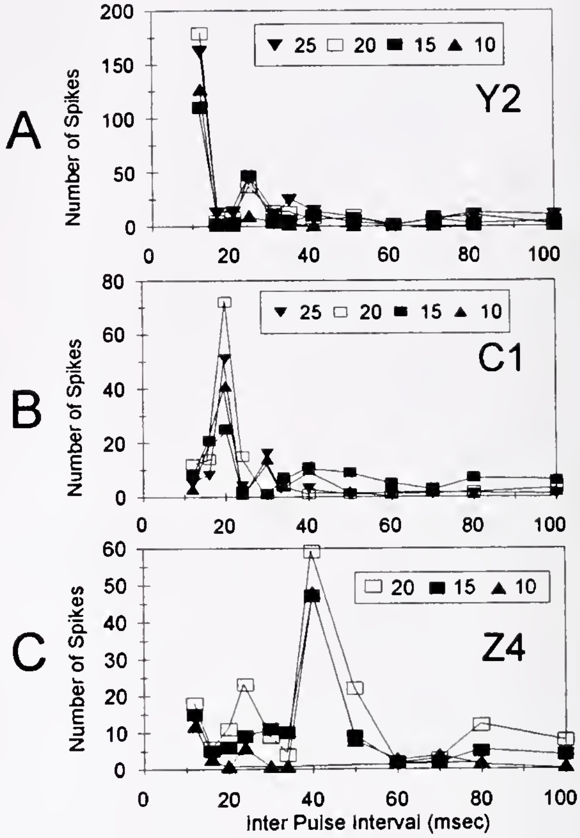

**Figure 1.** *Representative responses to pulses with varying IPIs (or pulse repetition rates). (A) Four stimulus levels for cell Y2 are represented by different symbols. The cell preferred an IPI of 12 ms (84 pulses/s). This was the most common response that was observed. The best frequency for this cell was 84 Hz, and the background activity (in the absence of a stimulus) was 1.8 spikes/s. (B) Cell C1 was nonmonotonic in that fewer spikes were produced at the highest level of stimulation (25 dB) than at the lower level (20 dB). This cell preferred an IPI of 20 ms (50 pulses/s). It had a best frequency of 141 Hz, and background activity of 4.8 spikes/s. (C) A rare cell (Z4) that responded best to a low pulse repetition rate, at three stimulus levels. This cell exhibited a preference for a 40-ms IPI (25 pulses/s). It had a best frequency of 65 Hz and background activity of 1 spike/s.*

Selectivity of brain units to the pulse rate or IPI of sounds has been demonstrated in other fishes (1) and in vertebrates generally (*e.g.*, 4). Pulse repetition rates for boatwhistle sounds produced by male toadfish (100–200 pulses/s) are higher than those that we could generate in this study. However, our data indicate that most cells in the midbrain that exhibit pulse selectivity respond best to the highest pulse repetition rate (84 pulses/s) used. Thus, these units might respond to pulse rates well above 84 pulses/s. Additional research on pulse selectivity by cells in the toadfish TS is warranted, particularly at higher repetition rates. Because temporally selective units occur widely in vertebrate auditory systems (1, 4), it is not yet clear whether this selectivity is a primitive (*i.e.*, widely shared) vertebrate character generally useful in sound source determination, or is a special adaptation for processing communication sounds.

Research funded by an NIH, NIDCD R01 grant to R. Fay (1 R01 DC 03666-4), and by an NIH, NIDCD Program Project Grant (1 P01 DC 00293-11) to the Parmly Hearing Institute.

## Literature Cited

1. **Crawford, J. D. 1997.** *J. Comp. Physiol. A* **180:** 439–450.
2. **Edds-Walton, P., R. Fay, and S. Highstein. 1999.** *J. Comp. Neurol.* **411:** 212–238.
3. **Fay, R. R., and P. L. Edds-Walton. 1997.** *Hear. Res.* **111:** 1–21.
4. **Langner, G. 1992.** *Hear. Res.* **60:** 115–142.

**Reference:** *Biol. Bull.* **203**: 197–198. (October 2002)

# Effects of a Sensory Block on Calexcitin Levels in the Photoreceptors of *Hermissenda crassicornis*

*Kimberly A. Borley*[1]*, Herman T. Epstein, and Alan M. Kuzirian (Marine Biological Laboratory, Woods Hole, Massachusetts 02543)*

The nudibranch mollusc *Hermissenda crassicornis* can be trained through classical Pavlovian conditioning to contract its foot (the conditioned response) when presented with light alone. If, between 5 and 55 min after conditioning, a sensory block (SB) is induced by inverting and re-righting animals, the expression of the conditioned response, when tested 90 min after training, will be inhibited. A similar inhibitory effect also will occur when the SB is given between 70 and 85 min after training (1). However, animals that receive the SB at 60 min post-training will demonstrate recall of the conditioned response when tested at 90 min. Thus, 60 min after training must be a key time in the formation of long-term memory in *Hermissenda*. To investigate the nature of this inhibitory effect further, animals that had a SB administered at 50, 60, or 65 min after conditioning were chemically fixed, and their central nervous systems were examined immunocytochemically for the protein calexcitin, a known mediator of learning.

Calexcitin is a GTP/$Ca^{2+}$ binding protein that is present in the visual cells of *Hermissenda* (2) as well as in other specific but restricted areas of the brain (3). After calexcitin is phosphorylated by protein kinase C, it binds to the ryanodine receptors of the ER, triggering the release of internal $Ca^{2+}$ stores. Concomitantly, calexcitin blocks the voltage-dependent outward $K^+$ currents ($I_A$; $I_{Ca\text{-}K}$). The release of $Ca^{2+}$ from the ER into the cytosol and the blockade of $K^+$ currents are believed to cause the enhanced long-lasting depolarization (LLD) that has been observed in photoreceptors of *Hermissenda* and shown to be necessary for learning and memory to occur in this animal (4). The intensity of calexcitin immunostaining has not only been shown to be higher in trained *Hermissenda*, but also appears to be positively correlated with the strength of the memory (3, 5).

Specimens of *Hermissenda* were purchased from Sea Life Supply (Sand City, California) and adapted to laboratory conditions for 3 days. Previous research had shown that nine training events of classical Pavlovian conditioning are sufficient to initiate long-term memory (LTM) in *Hermissenda* when tested 90 min later (1). After 10 min of dark adaptation, the animals were conditioned with nine training events (TEs), in which they were exposed to 6 s of bright light (700 lux; conditioned stimulus, CS), paired, after a 2-s delay, with 4 s of horizontal orbital rotation (unconditioned stimulus, US). The inter-trial interval was 1 min. The animals reacted to the US by contracting their foot (unconditioned response; UR). Animals were tested with the light (CS) alone, and a positive learning response was indicated by a contraction of the animal's foot (*i.e.*, shortening of body length) with the CS alone; no change in length or elongation as in normal locomotory movement (6) meant that no learning had occurred.

For this study, four to six animals per group were given nine TEs as described above. A sensory block was applied to three groups of animals at 50, 60, and 65 min following training; the procedure was to turn the tray containing the animals upside down for 5 s and then to re-right it. As mentioned above, this additional

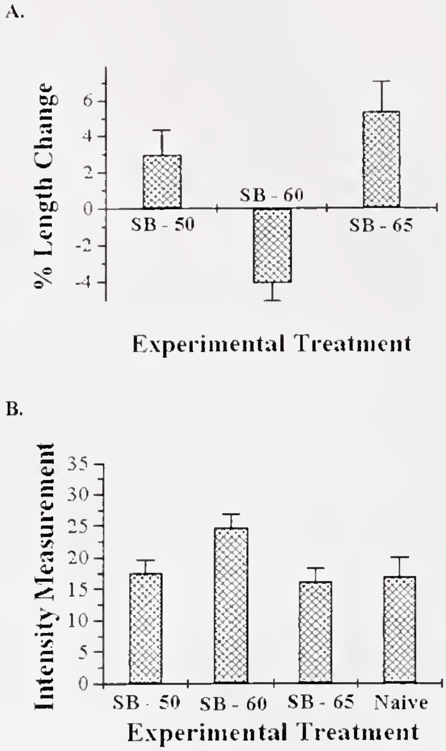

**Figure 1.** *(A) The behavioral responses of* Hermissenda *to a sensory block (SB) applied at either 50, 60, or 65 min following 9 training events (TE) of Pavlovian conditioning; 6 s of light (conditioned stimulus, CS) paired to co-terminate after a 2-s delay with 4 s of agitation (unconditioned stimulus, US) applied at 1-min intervals. Testing after 90 min with the CS alone produced a shortening of the animal's body length (positive conditioned response [CR], negative change in body length). The sensory block consisted of rotating the tray containing the animals upside down for 5 s, re-righting it, and then testing as usual. SBs applied at 50 and 65 min inhibited the CR (positive change or elongation of body length), while its application at 60 min did not impede memory recall of the CR (body shortening). The 60-min time point, in* Hermissenda, *defines long-term memory (error bars = S.E.M.;* n *= 12–14 behavioral measures per condition from 4 animals each, 50, 65 min; 6 animals, 60 min). (B) The staining intensity of immunolabeling with the calexcitin antibody, 25U2, from the photoreceptors of the same animals trained, sensory blocked, and tested for Figure 1A. Animals demonstrating positive memory recall at 60 min despite the applied SB had the highest intensity levels for calexcitin. ANOVA and paired Student* t *values between SBs at 50, 65 min and naive, and 60 min indicated significant statistical differences* ($F = 3.34$; $t = 2.44, 2.91, 2.1$; $P < 0.05$; $n = 8\text{–}24$ *intensity measures per condition from 4, 4, 6, and 6 animals respectively).*

---

[1] Ohio University, Athens, OH.

vestibular stimulus had been demonstrated to interfere with the formation or completion of LTM in *Hermissenda* (1). After testing at 90 min, all animals were immediately removed from the training tray and submerged in 4% paraformaldehyde in Tris-buffered artificial seawater (Tris-ASW; pH 8.0). The animals' brains were subsequently removed and fixed overnight in 4% paraformaldehyde/0.2% glutaraldehyde in Tris-ASW. The brains were then washed, dehydrated in a series of increasing alcohol concentrations to 95% ethanol, embedded in polyethylene glycol-400-distearate, and sectioned (5 $\mu$m). Following de-waxing and rehydration, sections containing photoreceptors were immunolabeled for calexcitin using a polyclonal antibody (25U2; cloned from squid optic lobe and raised in rabbit; 1:1000 dil.) (3, 5). A biotinylated horse anti-rabbit secondary antibody and avidin-bound microperoxidase (ABC method, Vector) were applied, followed by staining with the chromogen, 3-amino-9-ethylcarbazole (AEC). The negative control used was normal horse serum (NHS at 2%). NIH Image software was used to measure grayscale intensities from digital images of the original sections. Intensity levels were taken from areas of interest drawn around the cytoplasm of the B-photoreceptors of the eyes. That same perimeter was then transferred to an unstained area of the central neuropile to obtain background levels. The background readings were then subtracted from the photoreceptor values and the difference data analyzed statistically (ANOVA, Student's *t* test).

The behavioral data (Fig. 1A) show that animals experiencing SBs at 50 and 65 min did not contract when tested with the CS alone at 90 min; they demonstrated no memory recall. However, when the SB was applied at 60 min and the animals tested at 90 min, these animals exhibited a positive learning response (memory recall); the SB was ineffective. From the previous study (1) and from experiments currently being conducted using transcription and translation inhibitors, this 60-min time point appears to define the establishment of LTM in *Hermissenda*. Thus, SBs applied before 60 min interfere with LTM formation, while SBs after 65 min interfere with the more permanent cellular changes of consolidated long-term memory (CLTM; work in progress).

This study revealed a significant difference between the intensity level of calexcitin immunostaining in animals that exhibited memory recall (SB 60 min) and those experiencing interference with recall (SB 50 min and SB 65 min) (Fig. 1B). These intensity results directly parallel the behavioral data of this and previous studies (1). These data showed that the intensity of immunostaining for calexcitin (*i.e.*, intracellular concentration) was higher in trained animals that expressed positive associative conditioning (where long-term memory had been established). Thus, these data add to the body of evidence (3, 4, 5) suggesting that calexcitin is actively involved in the formation of various memory stages in *Hermissenda* as well as in some mammals (4), and that its intracellular concentration may directly modulate the process. The study further demonstrates that sensory blocks can be used to explore and define the temporal stages in memory development, especially from an evolutionary standpoint, in an animal, *Hermissenda*, that carries out sensory processing and memory formation within a well-defined and simple neural network.

The authors acknowledge Drs. Daniel Alkon and Tom Nelson, Blanchette Rockefeller Institute, Johns Hopkins University, Rockville, Maryland, for their support and for providing *Hermissenda* and calexcitin antibodies for this study. This work was supported in part by a NSF-REU Site Grant (9912287) to the Marine Biological Laboratory, Woods Hole, Massachusetts.

### Literature Cited

1. **Epstein, D. A., H. T. Epstein, F. M. Child, and A. M. Kuzirian. 2000.** *Biol. Bull.* **199:** 182–183.
2. **Nelson, T. J., S. Cavallaro, C.-L. Yi, D. McPhie, B. G. Schreurs, P. A. Gusev, A. Favit, O. Zohar, J. Kim, S. Beushausen, G. Ascoli, J. Olds, R. Neve, and D. L. Alkon. 1996.** *Proc. Natl. Acad. Sci.* **93:** 13,808–13,813.
3. **Kuzirian, A. M., H. T. Epstein, T. J. Nelson, N. S. Rafferty, and D. L. Alkon. 1998.** *Biol. Bull.* **195:** 198–201.
4. **Alkon, D. L., T. J. Nelson, W. Zhao, and S. Cavallaro. 1998.** *Trends Neurosci.* **21:** 529–537.
5. **Kuzirian, A. M., H. T. Epstein, D. Buck, F. M. Child, T. J. Nelson, and D. L. Alkon.** *J. Neurocytol.* (accepted, in revision).
6. **Epstein, H. T. 1997.** *Biol. Bull.* **193:** 255–257.

---

**Reference:** *Biol. Bull.* **203:** 198–200. (October 2002)

## A Novel Turtle Retinal Preparation for Simultaneously Measuring Light-Induced Electrical Activity and Changes in Metabolite Levels

*Gilad Twig (Technion-Israel Institute of Technology, Haifa, Israel), Robert Paul Malchow*[1], *Katherine Hammar*[2], *Peter J. S. Smith*[2], *Hanna Levy*[3], *and Ido Perlman*[3]

The vertebrate retina has been the focus of extensive anatomical, biochemical and physiological research for the past 50 years due, not only to its inherent importance for the process of vision, but also to its excellence as a model of information processing in the central nervous system (1). In general, two different approaches have been adopted by researchers examining retinal physiology. First, electrophysiological recordings of retinal activity (the electroretinogram) or of single cells have been used to analyze information processing; and second, biochemical techniques have been employed to study metabolic pathways within the retina. If these two techniques were combined, we would have the advantage of correlating information processing with metabolism.

The retina of the turtle *Pseudemys scripta elegans* has long been

---

[1] University of Illinois at Chicago, Chicago, IL.

[2] Marine Biological Laboratory, Woods Hole, MA.

[3] Technion-Israel Institute of Technology, Haifa, Israel.

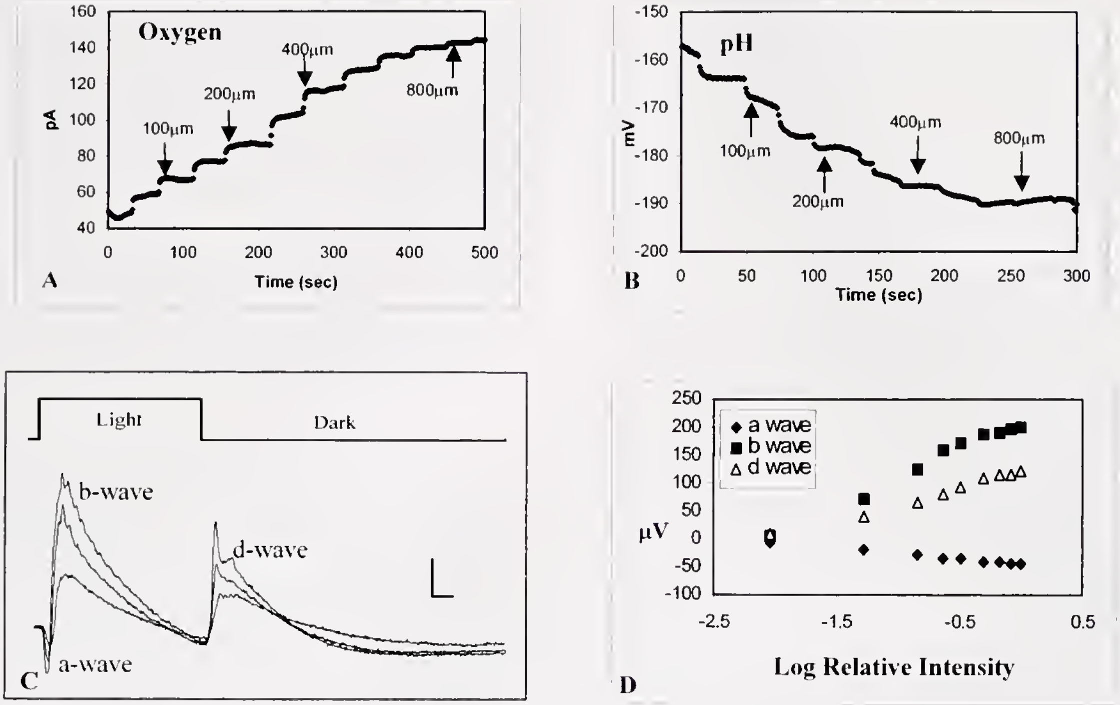

**Figure 1.** *Measurements of oxygen, pH, and the electroretinogram from the everted turtle eyecup preparation. (A) Response from an oxygen-selective microelectrode as it was withdrawn with time in a stepwise manner from the surface of the retina. The first four steps were 50 µm each; thereafter, the electrode was moved in 100-µm steps until the last two, which were 200 µm. For ease of interpretation, arrows indicate the distances from the retina at steps 2, 4, 6, and 10. (B) pH gradient measured from a second eyecup as a function of distance from the retinal surface. The first four steps were 50 µm, the next four 100 µm, and the last two 200 µm. Arrows indicate the distances from the retina at steps 2, 4, 6, and 10. (C) Representative ERG responses that were elicited by light stimuli of three different intensities (log relative intensity of −1.3, −0.5, and 0.0). Calibration: vertical scale, 50 µV, horizontal scale, 100 ms. The upper trace indicates stimulus timing. (D) Intensity-response curves for the ERG a-wave, b-wave, and d-wave. The amplitudes of these waves in µV are plotted as a function of log relative intensity.*

used as a model preparation for examining retinal function (2, 3, 4). Here we have developed a new variation of the turtle eyecup preparation, which permits us to examine metabolic parameters, including oxygen consumption and changes in extracellular hydrogen ion concentration, while simultaneously assessing the physiological state of retinal function from the electroretinogram.

Turtles were placed in ice for 20 min and then decapitated and pithed, in accordance with NIH guidelines and as approved by the institutional animal care committee of the MBL. The eyes were enucleated and the anterior portion of the eye was removed. The remaining eyecup was then carefully everted atop a conical mound of wax and fastened to the wax with minuten pins. The wax, with the eyecup attached, was firmly anchored to the bottom of a 140-mm glass petri dish. The Ringer solution contained (in m*M*): NaCl, 110; KCl, 2.6; $CaCl_2$, 2.0; $MgCl_2$, 2.0; $NaHCO_3$, 22; glucose, 10; it had been bubbled with a mixture of 95% air/5% $CO_2$ to reach a pH of 7.4. A polyethelene tube attached to the cover of the petri dish (but not touching the fluid) was used to supply an environment of 95% air/5% $CO_2$, which maintained the bath solution at a pH of 7.4. The electroretinogram was recorded between two electrodes: an Ag-AgCl wire that had previously been inserted into the wax (resting firmly against the back of the sclera); and an Ag-AgCl reference electrode placed in the bath solution. Oxygen-sensitive or pH-selective microelectrodes were placed within 5–10 µm of the retinal surface; the placement was guided visually through an upright microscope. Oxygen was measured with amperometric microelectrodes held at a constant voltage of −0.6 volts (5). The response of these electrodes was calibrated in Ringer solutions bubbled with air or with 100% nitrogen. Hydrogen ion activity was monitored with voltametric microelectrodes, whose response varied as a function of the log of the hydrogen ion concentration (6). Electrode responses were calibrated using turtle Ringer solutions adjusted to pH-6, 7, and 8. A white LED placed 1.5 inches from the retinal surface was used to generate light stimuli of varying intensity; at its brightest setting, this LED produced a light of 440 lux at the surface of the retina, as measured with an Extech Instruments light meter. The intensity of the light was controlled by varying the voltage supplied to the LED.

Figure 1A illustrates the oxygen gradient obtained from one eyecup as a function of the distance of the electrode from the retinal surface. A reading of approximately 50 pA was measured with the electrode within 10 µm of the retina, a value significantly less than that obtained in the bulk solution. As the electrode was withdrawn from the retina in a stepwise manner, the current reading increased until a maximum value of 145 pA was obtained with the electrode 1.4 mm away from the eyecup. This value corresponds to an oxygen concentration of about 250 µ*M*. From the linear characteristics of the oxygen electrode, we estimated the oxygen concentration in the layer close to the retina in this example to be approximately 40 $\mu M$. Thus, the solution in contact with the retinal surface was significantly lower in oxygen content, indicating a high rate of oxygen consumption, as has been observed in other species (7). The turtle eyecup preparation also exhibited a significant pH gradient from the retinal surface to the bulk solution (Fig. 1B). In this example, the surface of the retina was approximately 0.6 pH units more acidic than the bulk solution, indicating retinal production of hydrogen ions, and again replicating similar findings from several other species (8). Note that our results reflect the summed total response of the entire retina.

Figure 1C shows representative dark-adapted ERG responses that were obtained from an eyecup preparation (Fig. 1A) that was being used simultaneously to measure an oxygen gradient. Long duration (900 ms) light stimuli allowed us to separate the a- and b-wave complex that developed after stimulus onset, from the d-wave that reflected stimulus offset. We measured the amplitude of the a-wave, from the baseline to its trough; the amplitude of the b-wave, from the trough of the a-wave to the peak of the b-wave; and the amplitude of the d-wave, from the potential level recorded just prior to light offset, to its peak. Intensity-response curves for these three ERG waves are shown in Figure 1D. In preliminary experiments, we could also demonstrate light/dark modulation of the oxygen signal near the retina, indicating higher metabolic activity under dark-adapted conditions compared to background illumination. In these experiments, the ERG responses were used to monitor the adaptation status of the retina.

In summary, we have demonstrated that metabolite gradients can be readily recorded outside the retina in parallel with the electroretinogram, thus enhancing our assessment of the physiological responses to light. Moreover, these measurements are possible from the vitreal side, using the eyecup preparation, and from the photoreceptor side, using the isolated retina. These preparations, coupled with self-referencing probes, make possible a detailed and comprehensive analysis of the relationships between retinal biochemistry (including production of messenger molecules) and signal processing.

This project was supported by a Gruss Lipper Foundation Fellowship (I.P.), a Grass Foundation Fellowship (G.T.), NSF grant 009-1240 (R.P.M), and NCRR grant P41-RRO1395 (P.J.S.S.). We are grateful to Mr. Richard Sanger for expert electronic assistance during the course of this research.

## Literature Cited

1. **Dowling, J. E. 1987.** *The Retina: An Approachable Part of the Brain.* Belknap Press, Cambridge, MA.
2. **Baylor D. A., A. L. Hodgkin, and T. D. Lamb. 1974.** *J. Physiol.* **242:** 685–727.
3. **Fuortes, M. G., and E. J. Simon. 1974.** *J. Physiol.* **240:** 177–98.
4. **Adolph, A. R. 1985.** *Vision Res.* **25:** 483–492.
5. **Malchow, R. P., M. P. Verzi, and P. J. S. Smith. 1998.** *Biol. Bull.* **195:** 203–204.
6. **Malchow, R. P., S. C. Land, L. S. Patel, and P. J. S. Smith. 1997.** *Biol. Bull.* **193:** 231–232.
7. **Haugh-Scheidt, L. M., R. A. Linsenmeier, and E. R. Griff. 1995.** *Exp. Eye Res.* **61:** 63–72.
8. **Dmitriev, A. V., and S. C. Mangel. 2000.** *J. Physiol.* **522:** 77–82.

---

**Reference:** *Biol. Bull.* **203:** 200–202. (October 2002)

# Zinc Chelation Enhances the Zebrafish Retinal ERG b-Wave

*Stephen Redenti, (Ph.D. Program in Biology, The Graduate Center, CUNY, 365 Fifth Avenue, New York, NY 10016) and Richard L. Chappell*[1]

Zinc is an important trace element found in relatively high concentration in the pigment epithelium and visual cells of the vertebrate retina (1). Zinc deficiency has been associated with night blindness and age-related macular degeneration (AMD) (2). Dietary zinc supplementation is now commonly prescribed for AMD on the basis of the benefits recently reported from the Age-Related Eye Disease Study (3). Nevertheless, the role zinc plays in the processing of visual information or in retinal disease is not well understood (2). We believe the possible role of zinc in the processing of visual information is an important consideration in the diagnosis and treatment of retinal disorders. Abnormalities involving light or dark adaptation, contrast sensitivity, or glutamate toxicity in the outer retina should be investigated from this perspective.

Studies in the all-rod retina of the skate (*Raja erinacea*) support the notion of a role for endogenous zinc as a neuromodulator in the outer retina of vertebrates. Application of the zinc chelator histidine (100 $\mu M$) in the presence of the GABA-blocker picrotoxin (200 $\mu M$) doubled the amplitude of the skate electroretinogram (ERG) b-wave recorded in the skate eyecup preparation (4). Consistent with this observation, we found that application of histidine to the skate retinal slice preparation resulted in a reversible increase in inward current from identified horizontal cells recorded in voltage clamp mode (5). Here we report results from an ERG study that is similar to the one in skate but uses the *in situ* eyecup preparation of the zebrafish, a vertebrate whose retina has both rods and cones.

Adult zebrafish (*Danio rerio*) obtained from a colony maintained at the Marine Biological Laboratory, Woods Hole, Massachusetts, were anesthetized using 0.02% tricaine, immobilized with a 2-$\mu$l injection of 1% gallamine triethiodide (Flaxidil), and placed on their sides on a small sponge over a silver chloride pellet reference electrode. Their gills were irrigated with an oxygenated oral solution containing 2 g Instant Ocean per gallon distilled water (6). The cornea and lens were carefully removed to allow superfusion of the retina using a glass capillary manifold that could be switched from zebrafish Ringer (116 m$M$ NaCl, 2.9 m$M$ KCl,

---

[1] Department of Biological Sciences, Hunter College, CUNY, 695 Park Avenue, New York, NY 10021.

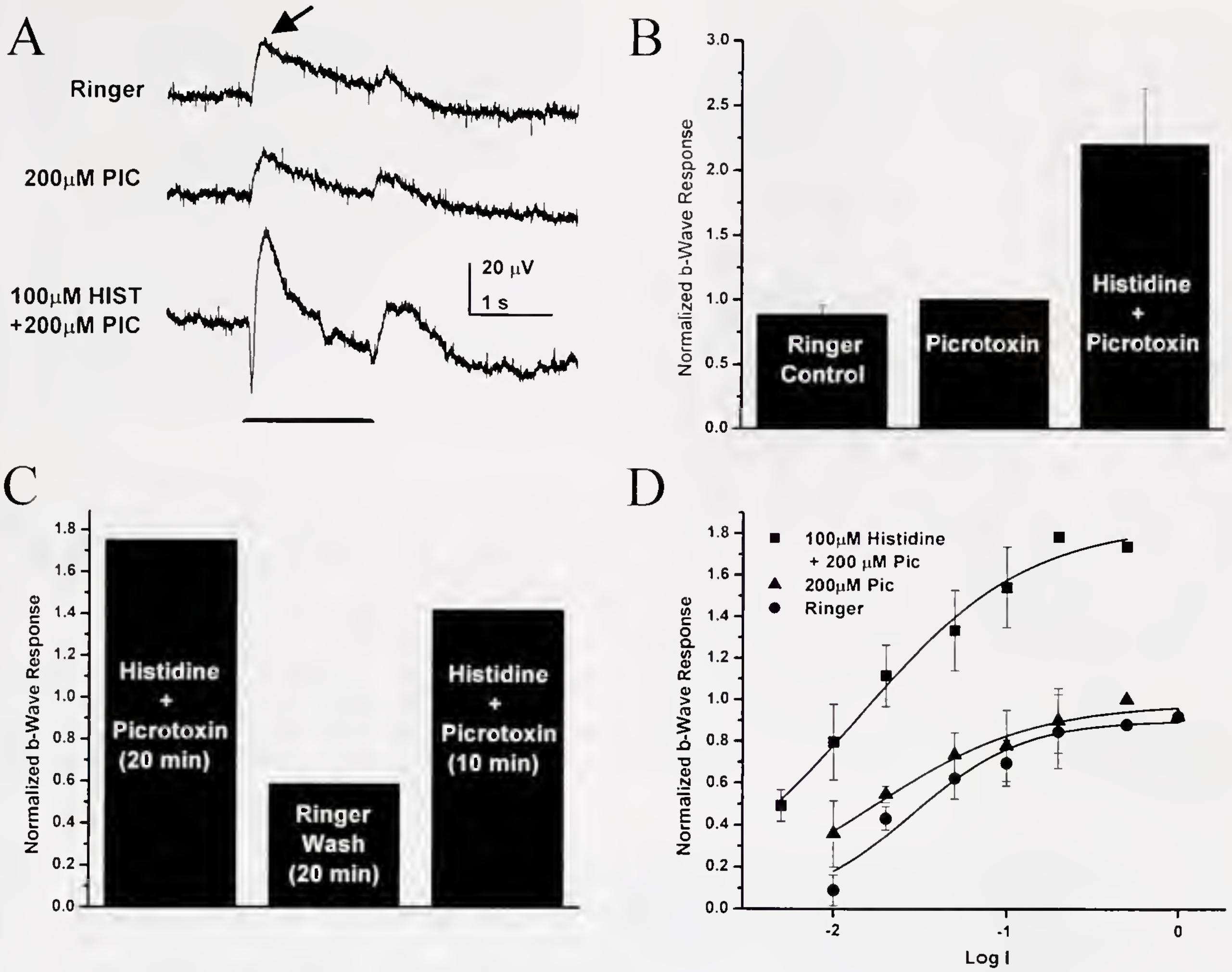

**Figure 1.** *The zinc chelator histidine enhances the zebrafish ERG b-wave amplitude. (A) Adding histidine (HIST) nearly doubles b-wave amplitude of light response (bar = light ON, log I = −0.7) compared to Ringer with or without picrotoxin (PIC). (B) Normalized data at log I = −1 from five preparations. (C) Histidine-induced b-wave increment can be reversed and repeated by Ringer wash and reapplication of histidine-containing solution. (D) Intensity-response data from five preparations fitted by Naka-Rushton curves. Concentrations: 100 μM histidine, 200 μM picrotoxin. See text for details.*

1.8 m$M$ $CaCl_2$, and 5 m$M$ HEPES) (6) to Ringer containing 200 $\mu M$ picrotoxin alone or 200 $\mu M$ picrotoxin plus 100 $\mu M$ histidine. All solutions were adjusted to pH 7.2. A glass capillary agar bridge to another silver chloride pellet was placed in the eyecup as the recording electrode. Experiments were conducted in a darkened room in the presence of dim ambient illumination. ERG responses were recorded using a low-noise differential preamplifier (PAR 113) having a bandpass of 0.03 Hz to 1 kHz, and stored with a DigiData 1200 acquisition system and pClamp6 software. The intensity of the unattenuated beam (log I = 0) from a 100-W tungsten-halogen lamp operated at 8 amps from a dc-regulated power supply was 30 $\mu W/cm^2$ at the retina. ERG responses recorded from the zebrafish eyecup preparation following removal of the cornea and lens were generally smaller than those recorded using a corneal electrode on the intact eye, possibly due to trauma caused during the microsurgery. Thereafter, responses remained stable for up to an hour.

Figure 1A shows ERG records obtained from one preparation in response to 1.1-s flashes of intensity log I = −0.7. The b-wave component of the response (arrow) recorded during superfusion with Ringer (upper trace) was not significantly changed after 10 min in picrotoxin (middle trace). This suggests that GABAergic mechanisms do not have a large impact on the magnitude of the ERG b-wave in the zebrafish retina. The amplitude of the b-wave nearly doubled, however, within 30 min after the superfusate was switched to Ringer containing both histidine and picrotoxin (Fig. 1A, lower trace). Note also the large apparent increase in the a-wave (photoreceptor potential), which is due probably to delayed onset of the b-wave as suggested by a 40% delay (50 ms ± 13, $n$ = 5) in b-wave time to peak in the histidine solution.

Results obtained in response to 1.1-s flashes of intensity log I = −1 from five zebrafish eyecup preparations, normalized to the response in picrotoxin, are illustrated in Figure 1B. After addition of histidine, b-wave amplitudes doubled (2.2 ± 0.4; mean ± SEM), while the average picrotoxin response was only slightly larger (by 0.12 ± 0.07) than the response in the control Ringer solution. Reversibility of the histidine enhancement of the b-wave response (log I = −1.7, normalized to the picrotoxin response at that intensity) is shown in Figure 1C. Note that a 20-min wash in Ringer reversed the b-wave enhancement induced by 20 min in the histidine-containing test solution. The b-wave increased again when the histidine plus picrotoxin solution was reapplied for 10 min.

Intensity-response data (mean ± SEM) from the five preparations, normalized to the picrotoxin response at log I = −0.3, are shown in Figure 1D. The curves represent the best fit of each data set to the Naka-Rushton equation (7) obtained using the Origin analysis package. The maximum responses determined for the fitted curves were, respectively, $R_{\max} = 0.96$, 0.97, and 1.80 for Ringer, picrotoxin, and histidine plus picrotoxin. In the histidine solution, the value of $\sigma$, the intensity eliciting a response of ½ $R_{\max}$ (8), was shifted to the left by 0.4 log units. Thus, saturating responses ($R_{\max}$) were essentially the same for Ringer alone or with the addition of picrotoxin. However, when histidine was added to the superfusate, the maximum response increased by a factor of about 1.9, consistent with the near-doubling observed in responses at lower intensities.

On the basis of the results of this study, we conclude that the effects of the zinc chelator histidine on the zebrafish retina, which contains both rods and cones, is similar to that observed in the all-rod retina of the skate. It appears, therefore, that zinc may be acting as a neuromodulator in the outer retina. In addition to any direct effect zinc may have on the sensitivity of glutamate receptors on second-order cells or to other possible neuromodulatory effects of zinc, an interesting possibility of negative feedback of zinc co-released with glutamate from photoreceptor terminals to reduce calcium entry into these terminals has been proposed by Wu and his colleagues (9). Since calcium is a cofactor in synaptic vesicle release, they suggest that this feedback will reduce the release of photoreceptor transmitter, including zinc, until an equilibrium is reached. The zinc neuromodulatory hypothesis is also consistent with histological evidence of a band of free zinc in the region of photoreceptor terminals in salamander (9) and skate (10) retinas and with a recent report that the relative concentration of free zinc in that region changes with the state of light adaptation in a mammalian retina (1).

The authors express their appreciation to Dr. Alan Adolph and Kwoon Wong for their assistance concerning the zebrafish eyecup preparation. Supported by NIH Grant EY00777, PSC/CUNY Grants 62245-0031 and 64225-0033, as well as by an NIH/RISE (Research Institute for Scientific Enhancement) GM60665 award to Hunter College. Research Centers in Minority Institutions Award RR-03037 from the National Center for Research Resources of the NIH, which supports the infrastructure of the Biological Sciences Department at Hunter College, is also acknowledged. The contents are solely the responsibility of the authors and do not necessarily represent the official views of the NCRR/NIH.

## Literature Cited

1. **Ugarte, M., and N. N. Osborne. 1999.** *Exp. Eye Res.* **69:** 459–461.
2. **Ugarte, M., and N. N. Osborne. 2001.** *Prog. Neurobiol.* **64:** 219–249.
3. **Age-Related Eye Disease Study Research Group. 2001.** *Arch. Ophthalmol.* **119:** 1417–1436.
4. **Rosenstein, F. J., R. W. Miller, and R. L. Chappell. 2001.** *Investig. Opthalmol. Vis. Sci.* **42:** S668.
5. **Chappell, R. L., and S. Redenti. 2001.** *Biol. Bull.* **201:** 265–267.
6. **Westerfield, M. 2000.** *The Zebrafish Book. A Guide for the Laboratory Use of Zebrafish* (Danio rerio). 4th ed., Univ. of Oregon Press, Eugene.
7. **Naka, K. I., and W. A. H. Rushton. 1966.** *J. Physiol.* **185:** 587–599.
8. **Chappell, R. L., and K.-I. Naka. 1991.** *Visual Neurosci.* **6:** 371–374.
9. **Wu, S. M., X. Qiao, J. L. Noebels, and X. L. Yang. 1993.** *Vision Res.* **33:** 2611–2616.
10. **Qian, H., L. Li, R. L. Chappell, and H. Ripps. 1997.** *J. Neurophysiol.* **78:** 2402–2412.

**Reference:** *Biol. Bull.* **203:** 203–204. (October 2002)

# Immunohistochemical Demonstration of a Lipopolysaccharide in the Cell Wall of a Eukaryote, the Green Alga, *Chlorella*

*Peter B. Armstrong (Department of Molecular and Cellular Biology, University of California, Davis, California), Margaret T. Armstrong*[1], *R. L. Pardy*[2], *Alice Child*[3], *and Norman Wainwright*[3]

The lipopolysaccharides (LPS) are ubiquitous components of the outer leaflet of the outer membrane of all gram-negative bacteria and are the principal toxic products of these organisms (1). The membrane anchor of LPS is lipid A, a central phosphodisaccharide unit that is attached to multiple $\beta$-hydroxy fatty acid chains. LPS also contains the novel sugar, 3-deoxy-D-manno-octulosonic acid (KDO). Although generally believed to be restricted to prokaryotes, specifically the gram-negative eubacteria and the cyanobacteria (2), an LPS-like molecule has recently been reported from a eukaryote, the green alga *Chlorella* sp., strain NC64A. The algal molecule includes KDO, lipid A, and $\beta$-hydroxy fatty acids and is thus chemically similar to bacterial LPS (3). The subject of this study is the localization of the LPS-like molecule in the algal cell.

One of the defenses raised against LPS by the horseshoe crab, *Limulus*, is a small, 101-amino acid, cationic protein—*Limulus* anti-LPS factor (LALF) (4)—which is released from the secretory granules of the blood cells during their exocytosis response to LPS challenge (5). LALF binds and neutralizes bacterial LPS (6). In the present study, we use the specific LPS-binding activity of LALF to localize the LPS-like molecule in eukaryotic and prokaryote cells.

The reactivity of LALF is apparently specific for LPS, with an amphipathic loop of LALF serving as the LPS-binding motif (7). A standard assay for bacterial LPS is the *Limulus* amebocyte lysate (LAL) test. This test (Charles River Endosafe, used according to accompanying instructions) reported 7.3 U/ml for 50 $\mu$g/ml of algal LPS. This activity was diminished to 0.08 U/ml in the presence of 50 $\mu$g/ml of LALF.

For immunohistochemical investigation, *Chlorella* cells, strain NC64A, were grown under bacteria-free conditions, then were freeze-dried and fixed in freshly-prepared 4% paraformaldehyde

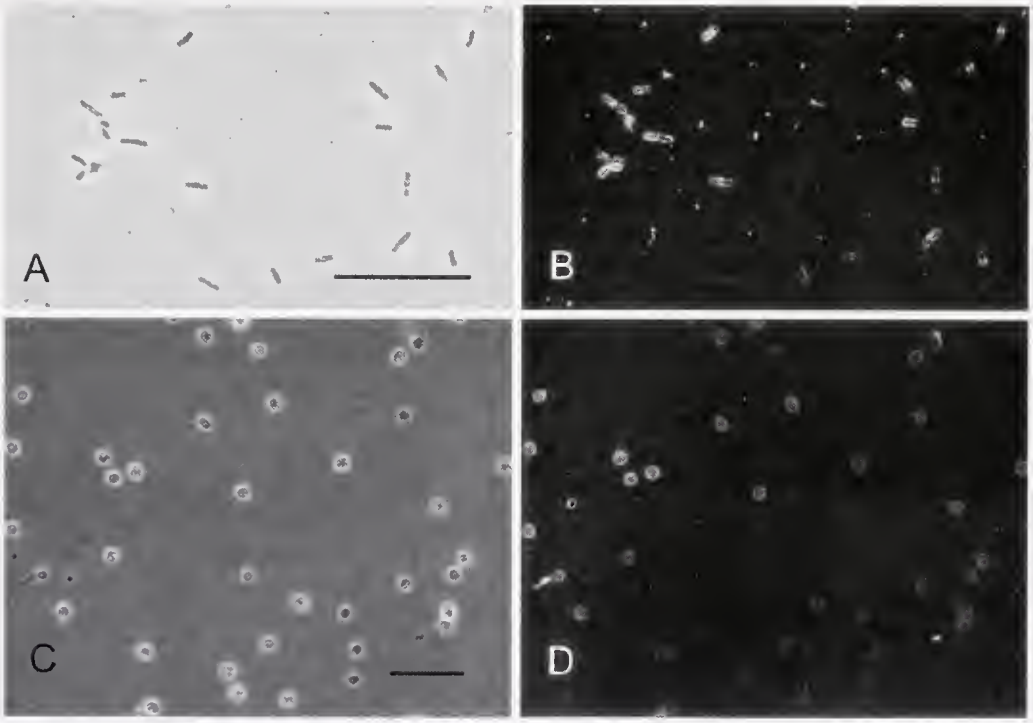

**Figure 1.** *Immunohistochemical demonstration of LPS at the surfaces of the Gram-negative bacterium,* Escherichia coli *(Fig. 1A, B), and the green alga,* Chlorella *strain NC64A (Fig. 1C, D). Cells were exposed to the LPS-binding protein, LALF, then immunostained with a rabbit anti-LALF antibody and a FITC-labeled second antibody. Fluorescence in Figure 1B and 1D shows the location of binding of LALF and, thus, the localization of highest concentrations of LPS. Figures 1A and 1C are phase contrast views of the fields shown in Figures 1B and 1D, respectively. Scale: 20 μm.*

---

[1] Department of Molecular and Cellular Biology, University of California, Davis, CA 95616.

[2] School of Biological Sciences, University of Nebraska, Lincoln, NE 68583.

[3] Marine Biological Laboratory, Woods Hole, MA 02543.

dissolved in phosphate-buffered saline for 10 min, then blocked successively with 0.1 *M* glycine in Tris-buffered saline (TBS) and with 5 mg/ml bovine serum albumin (BSA) in the same buffer. The cells were then exposed to 0.1 mg/ml LALF in TBS, then were treated with an anti-LALF antiserum (rabbit) in TBS + BSA, followed by exposure to a fluorescein-labeled goat anti-rabbit IgG second antibody in the same buffer. Finally, the cells were examined with a Zeiss Axiophot 2 fluorescence microscope.

The LALF labeling procedure stained the outer surface of aldehyde-fixed *Escherichia coli* cells, which served as our positive control for the method (Fig. 1A, 1B). Cells of the alga *Chlorella* showed a similar staining pattern, with LALF staining the outer surface of the cell, the cell wall (Fig. 1C, 1D). The cells failed to stain when LALF was omitted from the reaction scheme. This observation indicates that the LPS-like molecule of *Chlorella* is positioned at the appropriate location for a true lipopolysaccharide and adds substance to the still controversial claim that LPS is not confined to the prokaryotes, but is also present in certain eukaryotes.

This research was supported by NSF Grant No. MCB 26771.

## Literature Cited

1. **Levin, J. 1988.** Pp. 3–15 in *The Horseshoe Crab: A Model for Gram-Negative Sepsis in Marine Organisms and Humans,* J. Levin, H. R. Buller, J. W. Ten Cate, S. J. H. VanDeventer, and A. Sturk, eds. Alan R. Liss, New York.
2. **Mikheyskaya, L. V., R. G. Ovodova, and Y. S. Ovodov. 1977.** *J. Bacteriol.* **130:** 1–3.
3. **Royce, C. L., and R. L. Pardy, 1996.** *J. Endotoxin Res.* **3:** 437–444.
4. **Aketagawa, J., T. Miyata, S. Ohtsubo, T. Nakamura, T. Morita, H. Hayashida, S. Iwanaga, T. Takao, and Y. Shimonishi. 1986.** *J. Biol. Chem.* **261:** 7357–7365.
5. **Armstrong, P. B., and F. R. Rickles. 1982.** *Exp. Cell Res.* **140:** 15–24.
6. **Wainwright, N. R., R. J. Miller, E. Paus, T. J. Novitsky, M. A. Fletcher, T. M. McKenna, and T. Williams. 1990.** Pp. 315–325 in *Cellular and Molecular Aspects of Endotoxin Reactions,* A. Nowotmy, J. J. Spitzer, and E. J. Ziegler, eds. Elsevier Science Publishers B.V., New York.
7. **Hoess, A., S. Watson, G. R. Siber, and R. Liddington. 1993.** *EMBO J.* **12:** 3351–3356.

---

**Reference:** *Biol. Bull.* **203:** 204–206. (October 2002)

# Rapid Visualization of Microtubules in Blood Cells and Other Cell Types in Marine Model Organisms

*K-G. Lee (CUNY Graduate Center, New York), A. Braun*[1]*, I. Chaikhoutdinov*[1]*, J. DeNobile*[1]*,*
*M. Conrad*[1]*, and W. Cohen*[1]

Although specific proteins in living cells can now be labeled routinely with Green Fluorescent Protein, indirect immunofluorescence (IIF) methods for fixed material remain in widespread use (*e.g.*, 1). While relatively easy to apply, the standard IIF procedure is lengthy and, for blood cells and other cell types in suspension, the required attachment of the material to a glass substrate can result in differential adhesion or losses. In addition, the nonmammalian erythrocytes and clotting cells (2–5) studied in our laboratory undergo a variety of naturally occurring or experimentally induced alterations to cell morphology. For these cell types, the fixation and permeabilization methods that have produced our best IIF cytoskeletal labeling to date have not preserved the morphology of the living cells very well.

This work had three initial objectives: (a) developing improved methods for morphological preservation and permeabilization of non-mammalian erythrocytes and clotting cells prior to IIF; (b) combining such methods with rapid fluorescence pre-labeling of a mouse primary antibody (use of Zenon™; 6) to eliminate steps including substrate attachment; and (c) testing the combined approach on cells studied by others, or previously unstudied. For objectives (a) and (b) we employed dogfish erythrocytes and thrombocytes (*Mustelus canis*), blood ark erythrocytes (*Anadara ovalis*), and horseshoe crab amebocytes (*Limulus polyphemus*), all of which contain a marginal band (MB) of microtubules. For (c) we tested sea urchin sperm (*Arbacia punctulata*) and dividing zygotes (*Lytechinus pictus*) with known microtubule organization, plus spider crab hemocytes (*Libinia emarginata*) not studied previously.

Dogfish erythrocytes were first employed in an experimental survey of variables to develop both sequential and simultaneous methods of rapid fixation and permeabilization (objective a). Standard aldehyde or methanol fixation had produced cross-linked hemoglobin (Hb) that blocked antibody access in our earlier studies, and complete detergent lysis prior to fixation distorted cell morphology. Our experiments produced a major advance: brief formaldehyde prefixation (1%, < 7 min) and detergent extraction (0.4% Triton X-100, 10 min) yielded partial Hb retention and superior preservation of erythrocyte morphology, yet also allowed IIF labeling. Similar results were obtained with erythrocytes treated simultaneously with 4% formaldehyde and 0.6% Brij 58 (10 min). The slow extraction rate observed with Brij (compared with Triton) minimized morphological distortion when cells were not pre-fixed.

These methods were then tested on erythrocytes, other blood cells, and additional cell types in combination with Zenon™ labeling (objectives b and c). Thrombocytes were pre-fixed in 1% formaldehyde in 3% non-pyrogenic NaCl ("saline," ~7 min), then extracted with 0.4% Triton X-100 in PEM (100 m*M* PIPES, 5 m*M* EGTA, 1 m*M* $MgCl_2$, pH 6.8, 10 min). Other cell types were permeabilized and fixed simultaneously in PEM containing 4% formaldehyde, 0.6% Brij 58, plus precautionary protease inhibitors (Sigma P8340 cocktail + 10 m*M* TAME; amebocytes: TAME only). All preparations were washed in phosphate buffered saline,

---

[1] Hunter College of the City University of New York.

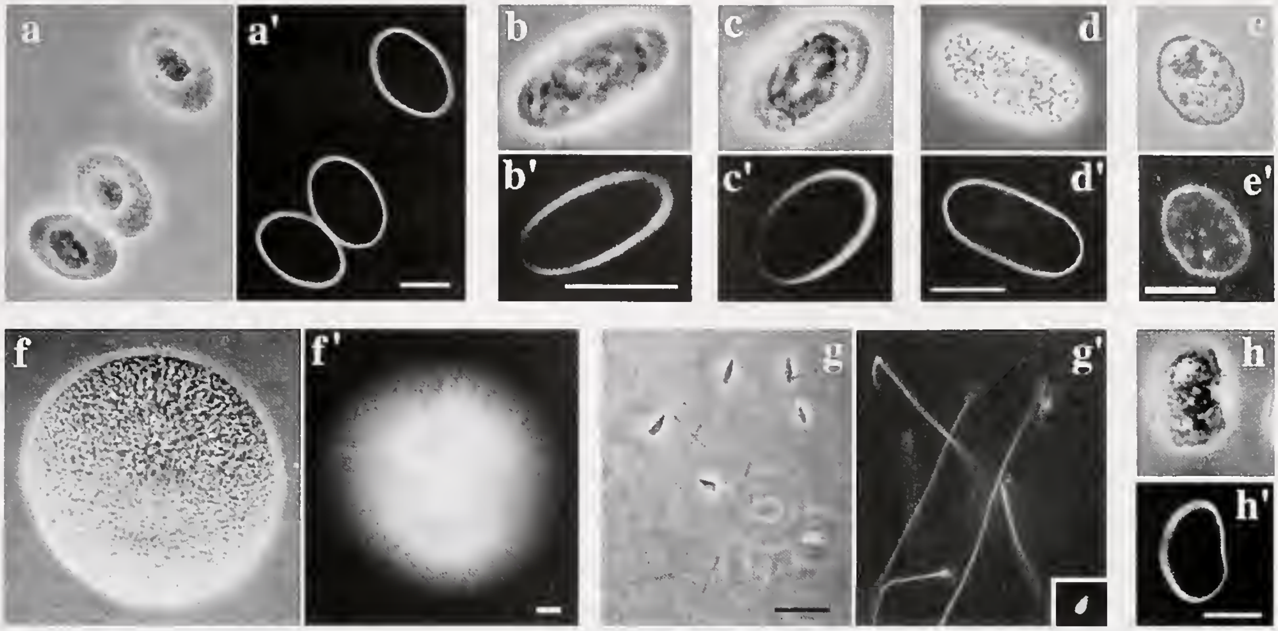

**Figure 1.** *Microtubules in various model cell types visualized by rapid fixation and detergent permeabilization followed by Zenon™ immunolabeling. The images are phase contrast-fluorescence pairs, with ′ indicating fluorescence. Marginal bands (MBs) are visible in dogfish erythrocytes (a, a′); unactivated dogfish thrombocytes (b, b′; c, c′);* Limulus *amebocytes (d, d′); and blood ark erythrocytes (e, e′). Sea urchin zygote mitotic apparatus* (Lytechinus pictus; *f, f′; fertilization membrane removed by Nitex filtration) and sea urchin sperm flagella* (Arbacia punctulata; *g, g′) are also readily labeled. (g′, inset): a DAPI-stained sperm nucleus. Also, an unknown type of spider crab hemocyte exhibits distinct MB labeling (h, h′). The thrombocyte MB in c, c′ was labeled by on-slide perfusion of the pre-selected fixed cell. Bars = 10 μm.*

(PBS, pH 7.2), then incubated in PBS containing mouse monoclonal anti-$\alpha$ and anti-$\beta$ tubulins (Sigma T9026, T-4026, 1:1 mass mixture) pre-bound with Zenon™ Alexa Fluor 488 $F_{ab}$ (Z-25002, 1:1 by mass; Molecular Probes). Representative results using a Zeiss standard epifluorescence microscope and Nikon 950 digital camera are shown in Figure 1.

MBs were readily visible in dogfish erythrocytes (Fig. 1 a, a′), unactivated dogfish thrombocytes (Fig. 1b, b′; c, c′), unactivated *Limulus* amebocytes (granulocytes; Fig. 1d, d′), and blood ark erythrocytes (Fig. 1e, e′); moreover, the preservation of blood cell morphology was the best obtained to date. Sea urchin zygote mitotic apparatus was well labeled (Fig. 1f, f′), including such details as crossing astral rays in the equatorial periphery. Sea urchin sperm flagellar microtubules were brightly labeled (Fig. 1g, g′), as were MBs discovered in unknown types of spider crab hemocytes (Fig. 1 h, h′). In all cases, microtubules were observed in only 30 min or less after antibody application. Precautionary pre-antibody blocking (PBS-1% bovine serum albumin, 60 min) was performed in some cases, but even without it there was little background. No labeling was observed when fluorescent $F_{ab}$ was used without anti-tubulin.

How rapidly were microtubules labeled? Perfusion chambers were made on slides scratched so as to enhance flow while retarding cell movement. Fixed dogfish leucocytes were loaded into the chamber and individual identified thrombocytes were viewed during successive perfusion with 0.4% Triton X-100 in PEM (10 min), and PBS (wash). Upon subsequent perfusion with Zenon™-labeled anti-tubulin, the thrombocyte MB became visible almost immediately (< 30 s; Fig. 1c, c′).

The rapidity of the procedure led us to ask whether all steps might be readily performed by perfusion, while individual preselected cells were being continually observed. This possibility was tested with dogfish thrombocytes, which can be activated to initiate clotting functions, adhesion, and shape transformation in saline containing 25U/ml bovine thrombin and 20 m*M* $CaCl_2$. Living, unactivated thrombocytes were loaded into the chamber and activated. Then all steps of pre-fixation and extraction, postfixation (4% formaldehyde in PEM, 10 min), wash (PBS), and immunolabeling were performed by perfusion. Microtubule labeling was again rapid and comparable in intensity to that in Figure 1 (c, c′), confirming feasibility.

These new methods constitute a major practical advance. They now enable us to monitor morphological preservation and examine the cytoskeleton of preselected, activating blood cells at specific stages by perfusion. This process is much more rapid and convenient than was previously possible working with these cells. In addition, for cell populations naturally existing in suspension, all steps can be performed while maintaining them in suspension, bypassing glass adhesion (Fig. 1). Other important advantages for non-mammalian blood cells are (a) greatly improved preservation of erythrocyte morphology; (b) little non-specific labeling without blocking; (c) sufficient signal intensity even against the labeling antibody background; and (d) reduction of processing time from ~4 h to ~1 h. The same rapid methods are effective with other cell types (Fig. 1, f, f′; g, g′) and with multiple labeling (*e.g.*, DAPI; Fig. 1g′ inset), indicating that they will be useful to other researchers. As a by-product, they may also be of considerable value in designing time-constrained laboratory exercises for courses.

We thank David Burgess and Michelle Ng for sea urchin samples, and HHMI Undergraduate Biosciences Education Program 2002679, PSC-CUNY64249, and NSF9726771 for support.

### Literature Cited

1. **Bikoue, A., G. Janossy, and D. Barnett. 2002.** *J. Immunol. Methods* **266:** 19–32.
2. **Mainwaring, G., and A. F. Rowley. 1985.** *Cell Tissue Res.* **241:** 283–290.
3. **Conrad, M. L., R. L. Pardy, and P. B. Armstrong. 2001.** *Biol. Bull.* **201:** 246–247.
4. **Lema-Foley, C., K. G. Lee, T. Parris, Z. Koroleva, N. Mohan, P. Noailles, and W. D. Cohen. 1999.** *Biol. Bull.* **197:** 395–405.
5. **Cohen, W. D., and I. Nemhauser. 1985.** Pp. 3–49 in *Blood Cells of Marine Invertebrates*, W. D. Cohen, ed. Alan R. Liss, New York.
6. **Filanoski, B. 2002.** *Zenon™ Technology Bulletin*. Molecular Probes, Inc., Eugene, OR.

---

**Reference:** *Biol. Bull.* **203:** 206–208. (October 2002)

# Ca$^{2+}$ Effects on Myosin-II-Mediated Contraction of Pseudo-Contractile Rings and Transport of Vesicles in Extracts of Clam Oocytes

*Torsten Wöllert[1], Ana S. DePina, Reid F. Thompson, and George M. Langford (Department of Biological Sciences, Dartmouth College, Hanover, NH 03755)*

Ca$^{2+}$ is a key regulator of cytokinesis, the process by which the contractile ring constricts the cell to form the cleavage furrow. BAPTA (1,2-bis (aminophenoxy)-ethane-N,N,N′,N′-tetraacetic acid) has been used to investigate the role of Ca$^{2+}$ in this process. Several studies have shown that buffering cytosolic Ca$^{2+}$ with BAPTA blocks cytokinesis in a variety of cultured cells and fertilized eggs (1, 2). These results support a model of cytokinesis in which a local rise in free Ca$^{2+}$ is part of the signaling pathway that regulates assembly of the cytokinetic ring of actin filaments. In addition, Ca$^{2+}$ is required for Ca$^{2+}$-calmodulin (CaM)-stimulated phosphorylation of the regulatory light chain of myosin-II by myosin light chain kinase (MLCK). Therefore, Ca$^{2+}$ serves both as a signal for cytokinesis and as a regulator of myosin-II activity.

We studied cytokinesis *in vitro* by reconstituting pseudo-contractile rings in M-phase extracts made from clam oocytes. In these extracts, actin filaments spontaneously organized into a cooperative, 3-D network of interconnected filaments. We refer to this self-organized network of actin filaments as a pseudo-contractile ring because it shares the following two fundamental properties with the contractile ring: (i) it exhibits myosin-II-mediated, antiparallel sliding of actin filaments; and (ii) it assembles during the M-phase of the cell cycle. Fortuitously, actin filaments within the pseudo-contractile ring co-aligned to form bundles (10–20 parallel filaments) that were thick enough to be visualized by Allen Video Enhanced Contrast (AVEC) - Differential Interference Contrast (DIC) microscopy. Therefore, sliding of actin filaments could be monitored and studied in networks reconstituted *in vitro*. The term "contraction" refers to the myosin-II-mediated sliding of actin filaments in the network; the network itself does not shorten.

In a previous study, we used a function-blocking myosin-II-specific antibody to establish that the sliding of actin bundles observed in these pseudo-contractile rings is mediated by myosin-II (3). Using the same antibody, we showed that vesicle transport on actin filaments observed in these extracts is also mediated by myosin-II. In this report, we determined the effects of Ca$^{2+}$ buffering by BAPTA on actin filament sliding and vesicle transport in M-phase extracts of clam oocytes.

Extracts were prepared from mature oocytes obtained from gravid female clams. The cytoplasmic extracts were diluted 2-fold to a final protein concentration of about 15 mg/ml and clarified to remove large membrane aggregates. Nocodazole (30 $\mu M$) was added to the extracts to block microtubule assembly, an ATP regenerating system was added to maintain ATP levels, and the preparation was incubated for 45 min at 18 °C. Rhodamine-phalloidin (0.5 $\mu M$) was added to stain the actin filaments that assembled during the 45-min incubation. The myosin-II motor activity was monitored by AVEC-DIC and fluorescence microscopy.

In control extracts, actin filaments organized spontaneously into a 3-D network, or pseudo-contractile ring (Fig. 1C; control). The actin filaments in the network moved by sliding relative to each other. An average of 2 sliding actin bundles/field/min was observed (Fig 1B; control). The advancing tips of the sliding filaments were tracked at an average speed of 0.2 $\mu$m/s and for distances greater than 25 $\mu$m. In addition, the movement of vesicles on actin filaments was observed. In a given video field that measured 25 $\mu$m$^2$, the motile activity on actin filaments was 46 ± 2 vesicles/field/min (v/f/m). The average speed of vesicle movement was 1.0 $\mu$m/s (Fig. 1A; control). The difference in the speed of vesicle movement and filament sliding provided evidence that vesicle movement was not due to the passive attachment of vesicles to sliding filaments. In addition, vesicle movement was observed on stationary actin filaments that were tightly bound to the glass coverslip.

The effects of buffering free Ca$^{2+}$ levels on myosin-II-mediated filament sliding and vesicle transport were determined. We incubated extracts with BAPTA at 2 m$M$ (4) and 10 m$M$ (5) final concentrations. The addition of 2 m$M$ BAPTA increased motile activity by 1.4-fold (66 v/f/m), and sliding of actin filaments by 1.2-fold (Fig. 1A, B). The number of actin bundles in the network was similar to that of the control (Fig. 1C; 2 m$M$). However, at 10 m$M$ BAPTA, the results were significantly different. Although motile activity increased 1.7-fold (77 v/f/m; Fig. 1A; 10 m$M$), the

---

[1] Rostock University, Germany.

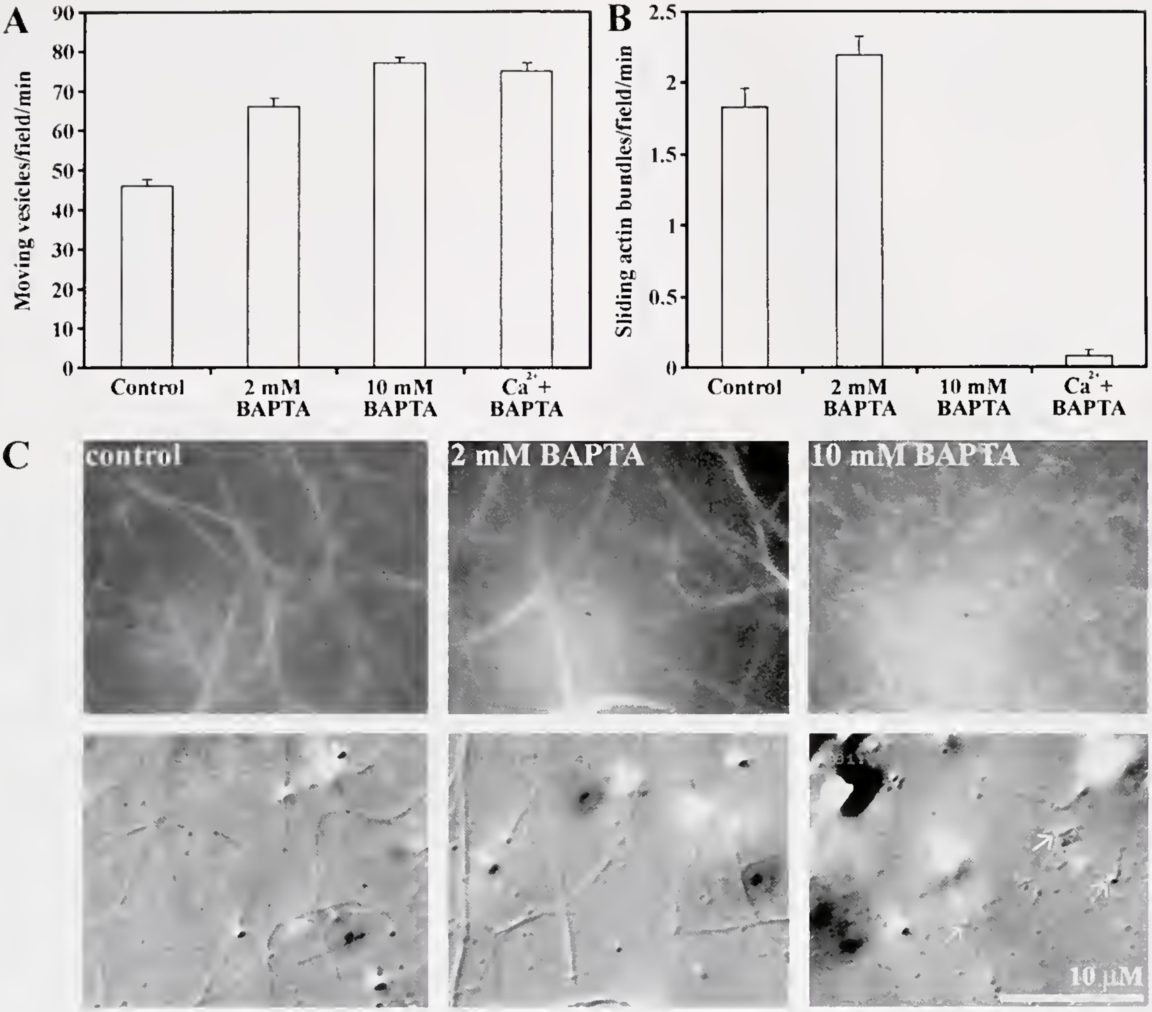

**Figure 1.** *(A) The motile activities (moving vesicles/field/min) in control extracts, extracts treated with 2 mM and 10 mM BAPTA, and extracts in the presence of 1 mM $Ca^{2+}$ plus 10 mM BAPTA are shown. BAPTA stimulated motile activity at both concentrations. (B) The number of sliding actin bundles/field/min is shown. No actin bundles formed in the presence of 10 mM BAPTA. (C) The presence of actin filaments and bundles was verified by fluorescence microscopy (top row) for control extracts and extracts treated with two concentrations of BAPTA (2 mM and 10 mM). The same fields are shown by AVEC-DIC microscopy (bottom row), photographed 3 min earlier than the corresponding fluorescence images. Actin bundles did not form in extracts treated with 10 mM BAPTA, but the vesicles formed large clusters (arrows in DIC micrograph). Extracts treated with 1 mM $Ca^{2+}$ and 10 mM BAPTA were similar to extracts treated with 10 mM BAPTA when viewed by fluorescence and AVEC-DIC microscopy (data not shown).*

cross-linking of actin filaments into bundles was inhibited (Fig. 1C; 10 m*M*), and sliding could not be observed (Fig. 1B; 10 m*M*). These studies showed that, while myosin-II activity as measured by vesicle transport was stimulated by buffering free $Ca^{2+}$ with BAPTA, cross-linking of actin filaments was inhibited. Therefore, actin filaments assembled and served as tracks for vesicle movement, although the cross-linking of actin filaments into visible bundles was blocked by 10 m*M* BAPTA.

In summary, when the calcium concentration in the extract was reduced by the addition of 10 m*M* BAPTA, myosin-II-mediated vesicle transport increased 1.7-fold. Therefore the activation of MLCK by $Ca^{2+}$-CaM was not attenuated by the addition of this calcium chelator. However, actin filament bundling was inhibited, suggesting that actin filament bundling activity involves a calcium-sensitive step.

The stimulation of motile activity in these extracts was due, most likely, to the demonstrated effect of BAPTA on membrane network formation. BAPTA (10 m*M*) has been shown by Drier and Rapoport (6) to stimulate the formation of ER-like networks in extracts of *Xenopus* oocytes. A similar effect was observed in the extracts that we made from clam oocytes. The vesicles in these extracts underwent fusion events, forming large clusters of vesicles connected to each other by thin membrane tubules (Fig. 1C, arrows in DIC micrograph). The clustering of vesicles into large complexes increased the number of vesicles observed moving per unit time. Our results are consistent with the observation that high calcium levels inhibit membrane fusion and the formation of ER-like networks.

These data suggest that calcium fluctuations of about 1 μ*M* may be important for ER-like network formation. BAPTA, a calcium chelator with a binding constant in this range, affects membrane fusion while chelators with either a lower or higher binding constant do not (6). Therefore, the lack of a strong inhibitory effect of BAPTA on MLCK activity suggests that the binding constant for calmodulin lies outside the range of calcium fluctuations reported for BAPTA (1).

The generation of sliding forces between anti-parallel actin filaments is a well-established activity of bipolar filaments of myosin-II. Therefore, the observation that actin filaments self-organized and moved in an anti-parallel fashion in these extracts fits current models of the contractile ring. These data support models in which the bundling of actin filaments involves a calcium-sensitive step. Calcium signaling through Rho G-protein pathways, which modulate the actin cytoskeleton, is the most likely mechanism by which cytosolic $Ca^{2+}$ controls actin bundle formation (7). The involvement of actin bundling activity in the formation of contractile rings has yet to be established, although these data raise such a possibility.

Supported by NSF grant IBN-0131470 and MBL Shifman award to RFT.

## Literature Cited

1. **Miller, A. L., R. A. Fluck, J. A. McLaughlin, and L. F. Jaffe. 1993.** *J. Cell Sci.* **106:** 523–534.
2. **Snow, P., and R. Nuccitelli. 1993.** *J. Cell Biol.* **122:** 387–394.
3. **Wöllert, T., A. S. DePina, L. A. Sandberg, and G. M. Langford. 2001.** *Biol. Bull.* **201:** 241–243.
4. **Matsumoto, Y., and J. L. Maller. 2002.** *Science* **295:** 499–502.
5. **Kolodney, M. S., M. S. Thimgan, H. M. Honda, G. Tsai, and H. F. Yee, Jr. 1999.** *J. Physiol.* **515:** 87–92.
6. **Drier, L., and T. A. Rapoport. 2000.** *J. Cell Biol.* **148:** 883–898.
7. **Matozaki, T., H. Nakanishi, and Y. Takai. 2000.** *Cell. Signal.* **12:** 515–524.

---

**Reference:** *Biol. Bull.* **203:** 208–210. (October 2002)

# GTPase Rho Is Involved in Myosin-II-Mediated Contraction of Pseudo-Contractile Rings and Transport of Vesicles in Extracts of Clam Oocytes

*Torsten Wöllert[1], Ana S. DePina, Reid F. Thompson, and George M. Langford (Department of Biological Sciences, Dartmouth College, Hanover, New Hampshire 03755)*

Small GTP-binding proteins (G-proteins) of the Rho family have been shown to regulate cytoskeleton reorganization, whereas G-proteins of the Rab family have been shown to regulate intracellular trafficking and vesicle transport (1). In mammalian cells, Rho proteins Rho/Rac/Cdc42 regulate the formation of stress fibers, lamellipodia, and filopodia. One of the ways in which Rho proteins mediate effects on the cytoskeleton is *via* the Rho-ROK/Rho kinase-myosin phosphatase pathway (Fig. 1A). In this pathway, myosin light-chain phosphatase (MyoP) is phosphorylated by ROK/Rho kinase and is thereby inhibited (2). The net result is the activation of myosin-II and the sustained contraction of smooth muscle cells, even after the $Ca^{2+}$ concentration is decreased.

To study the role of Rho proteins in cytokinesis *in vitro*, we inhibited Rho GTPases with Rho GDP dissociation inhibitor (GDI) and measured the contraction of pseudo-contractile rings in M-phase extracts, which were obtained from clam oocytes. In these extracts, actin filaments spontaneously organized into a cooperative, 3-D network of interconnected filaments. We refer to this self-organized network of actin filaments as a pseudo-contractile ring because of the following two fundamental properties that it shares with the contractile ring: (i) it exhibits myosin-II-mediated, anti-parallel sliding of actin filaments (3, 4), and (ii) it assembles during the M-phase of the cell cycle.

Fortuitously, actin filaments within the pseudo-contractile ring co-aligned to form bundles (10–20 parallel filaments) that were thick enough to visualize by AVEC-DIC microscopy. Therefore, sliding of actin filaments could be monitored and studied in networks reconstituted *in vitro*. The term contraction is used to refer to the myosin-II-mediated sliding of actin filaments in the network; the network itself does not shorten. In this report, we show that RhoGDI blocked filament sliding and vesicle transport in these extracts.

Extracts were prepared from mature oocytes obtained from gravid female clams. The cytoplasmic extracts were diluted 2-fold to a final protein concentration of about 15 mg/ml and clarified to remove large membrane aggregates. Nocodazole (30 $\mu M$) was added to the extracts to block microtubule assembly, an ATP regenerating system was added to maintain ATP levels, and the preparation was incubated for 45 min at 18 °C to assemble actin filaments and reconstitute motor activity. Rhodamine-phalloidin (0.5 $\mu M$) was added to stain the actin filaments, and the myosin-II motor activity was monitored by AVEC-DIC and fluorescence microscopy.

In control extracts, bundles of actin filaments in the pseudo-contractile ring (Fig. 1C, control) were observed to slide relative to each other. The advancing tips of sliding bundles were tracked at speeds greater than 0.2 $\mu$m/s for distances greater than 25 $\mu$m. An average of 2 sliding actin bundles/field/min were observed (Fig. 1B, control). In addition, movement of vesicles on actin filaments was observed. In a given video field that measured 25 $\mu m^2$, 46 ± 2 vesicles/min ($n = 2$) moved at an average speed of 1.0 $\mu$m/s (Fig. 1B). The difference in speed of vesicle movement and filament sliding provided evidence that vesicle movement was not due to the passive attachment of vesicles to sliding filaments. In addition, vesicle movement was observed on stationary actin filaments tightly bound to the glass coverslip.

To determine the effect of RhoGDI on filament sliding and vesicle transport mediated by myosin-II, we incubated extracts with 200 n$M$ bacterially expressed RhoGDI (gift from S. Kuznetsov). Vesicle transport was measured by counting the num-

---

[1] Rostock University, Germany.

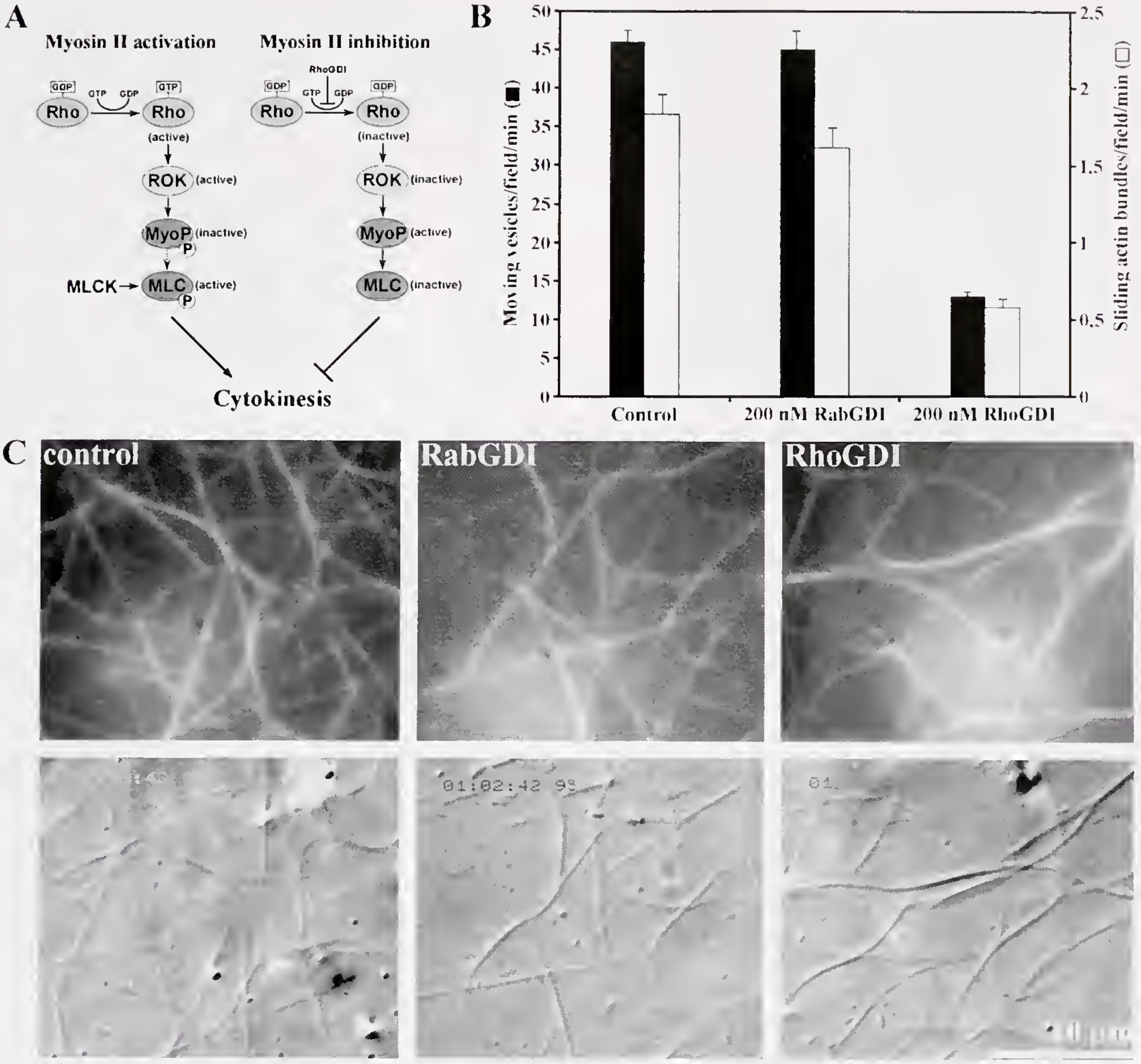

**Figure 1.** *(A) Diagram of signal transduction pathway involved in Rho-induced myosin II activation (left); RhoGDI blocks the exchange of GTP for GDP and blocks RhoGTPase activity (right). (B) The motile activities (moving vesicles/field/min) and the number of sliding actin bundles in control extracts and extracts in the presence of 200 nM RabGDI and 200 nM RhoGDI are shown. (C) The presence of actin filaments and bundles was verified by fluorescence microscopy (top row) for control extracts and extracts treated with RabGDI and RhoGDI. The same fields are shown by AVEC-DIC microscopy photographed 3 min earlier (bottom row).*

ber of vesicles moving/video field/min (v/f/m; motile activity) at 15-min time intervals after GDI addition. RhoGDI inhibited motile activity by 72% (13 ± 1 v/f/m, $n = 3$) and filament sliding by 68% (Fig. 1B). Pseudo-contractile ring formation was similar to the controls (Fig. 1C). On the other hand, 200 n*M* RabGDI affected neither motile activity nor filament sliding: the motile activity and number of sliding filament bundles were similar to the controls (Fig. 1B). In addition, bundles of actin filaments in pseudo-contractile rings were similar to the control extracts (Fig. 1C). These studies showed that blocking Rho proteins with RhoGDI inhibited myosin-II-mediated vesicle transport and filament sliding. We conclude, therefore, that Rho proteins are required for contraction of the contractile ring during cytokinesis.

The generation of sliding forces between actin filaments is a well-established activity of bipolar filaments of myosin-II. Therefore the observation that actin filaments self-organized and moved in an anti-parallel fashion in these extracts fits current models of the contractile ring. These studies provide evidence that the two activities mediated by myosin-II in these extracts are activated by Rho GTPases. The downstream effector of the Rho proteins is most likely myosin light-chain phosphatase (5). Therefore, because inhibition of Rho proteins blocked cytokinesis, the Rho-

ROK/Rho kinase-myosin phosphatase pathway appears to regulate cell division in clam oocytes.

Supported by NSF Grant IBN-0131470 and MBL Shifman award to RFT.

## Literature Cited

1. **Matozaki, T., H. Nakanishi, and Y. Takai. 2000.** *Cell. Signalling* **12:** 515–524.
2. **Kimura, K., M. Ito, M. Amano, K. Chihara, Y. Fukata, M. Nakafuku, B. Yamamori, J. Feng, T. Nakano, K. Okawa, A. Iwamatsu, and K. Kaibuchi. 1996.** *Science* **273:** 245–248.
3. **Wöllert, T., A. S. DePina, L. A. Sandberg, and G. M. Langford. 2001.** *Biol. Bull.* **201:** 241–243.
4. **DePina, A. S., and G. M. Langford. 1999.** *Microsc. Res. Tech.* **47:** 93–106.
5. **Bishop, A. L., and A. Hall. 2000.** *Biochem. J.* **348:** 241–255.

---

**Reference:** *Biol. Bull.* **203:** 210–211. (October 2002)

## Globular Tail Fragment of Myosin-V Displaces Vesicle-Associated Motor and Blocks Vesicle Transport in Squid Nerve Cell Extracts

*Jeremiah R. Brown, Elizabeth M. Peacock-Villada, and George M. Langford (Department of Biological Sciences, Dartmouth College, Hanover, New Hampshire 03755)*

Myosin-V, an actin-based motor that is highly enriched in the brain, mediates the movement of vesicles on cortical actin filaments. Recent evidence suggests that the globular tail of myosin-V interacts with the microtubule-based motor, kinesin (1), to form a "hetero-motor" complex on vesicles. The complex of these two motors, one microtubule-based and the other actin-based, facilitates the movement of vesicular cargo from microtubules to actin filaments. In this study we show that the globular tail fragment of myosin-V displaces native myosin-V from vesicles isolated from squid brain and blocks vesicle transport on actin filaments in axoplasm from the squid giant axon.

Myosin-V recruitment and binding to neuronal vesicles are active areas of investigation. Recent studies suggest that myosin-V is recruited to vesicles by members of the Rab family of proteins (2). Rab proteins are known to regulate intracellular trafficking, and recent studies show that they also regulate vesicle transport. Rab27a is the member of the Rab family that recruits myosin-Va to melanosomes (3, 4). Melanophilin, an activator of Rab27a, has been shown to be required for binding of Rab27a to melanosomes (5). The members of the Rab family of proteins responsible for myosin-V recruitment to neuronal vesicles in the squid nervous system have not been determined, although Rab3a is known to be associated with synaptic vesicles in squid brain (6).

To study the recruitment of the globular tail domain of myosin-V to neuronal vesicles, we used a GST-tagged fragment of the globular tail in motility and vesicle-binding experiments. The mouse GST globular tail domain (MG-GTD) fragment (plasmid was a gift from Dr. Huang) contained the glutathione S-transferase (GST)-labeled mouse AF6/Cno tail-globular-domain (Fig. 1A). The 84 kDa GST-tagged fragments were expressed in *E. coli*, purified on affinity columns, and used in experiments with squid brain extracts and purified vesicles.

The bacterially expressed globular tail domain of myosin-V (Fig. 1B, lane 3) was used in affinity-precipitation experiments to show that it pulled down kinesin. MG-GTD was incubated with squid brain homogenates for 2 h and then recovered as a precipitate with glutathione beads. MG-GTD was detected in the precipitate by the GST antibody (Fig. 1B lane 3), and kinesin was detected with H2, an antibody to the heavy chain of kinesin (Fig. 1B lane 5). GST was used in place of MG-GTD in control affinity-precipitation experiments (Fig. 1B lane 2) to show that kinesin was not pulled down by GST alone (Fig. 1B lane 4).

MG-GTD was then incubated with purified squid brain vesicles to displace native myosin-V, and therefore to block vesicle transport. Vesicles were purified by Nycodenz density gradients from clarified homogenates of squid brain prepared in Tris buffered saline (TBST). The vesicle fractions from the gradient were analyzed by SDS-PAGE and western blots. Both myosin-V and kinesin were present on these vesicles (Fig. 1C). Purified vesicle fractions were incubated for 2 h at 4 °C with the GST-MyoV-tail fragment. After incubation, vesicles were fractionated on a Nycodenz gradient; blots of the vesicle fraction showed a band for the GST-tagged tail fragment, indicating binding of the tail domain to vesicles (Fig. 1D lane 4). Blots of the vesicle pellet showed an absence of myosin-V when incubated with GST-MyoV-tail (Fig. 1D lane 2), indicating displacement of native myosin-V from the vesicles by the recombinant tail fragment. Myosin was detected on the vesicles in the control (Fig. 1D lane 1), and kinesin remained on the vesicles after displacement of myosin-V by the tail fragment (Fig. 1D lane 6).

The recombinant fragment of myosin-V was then used in motility assays to determine its effects on vesicle transport. The GST-MyoV-tail fragment (at 3.12, 6.25, 12.5, 25, and 50 $\mu$g/ml) was added to freshly extruded axoplasm (Fig. 1E) in the presence of 5 m$M$ ATP. Purified GST was used in the control experiment. After extrusion, actin filaments, detected by fluorescence microscopy (Fig. 1F), assembled at the margins of the axoplasm, and vesicle movement on these filaments was observed by AVEC-DIC microscopy (Fig. 1E). Actin-based vesicle transport was quantified by counting the number of vesicles moving/field/min (v/f/m, motile activity) at two time points during a 1-h incubation. Motility was reduced by 39% at 6.25 $\mu$g/ml, and by 80%–90% at the higher concentrations of the globular tail fragment (Fig. 1G). These data show that the

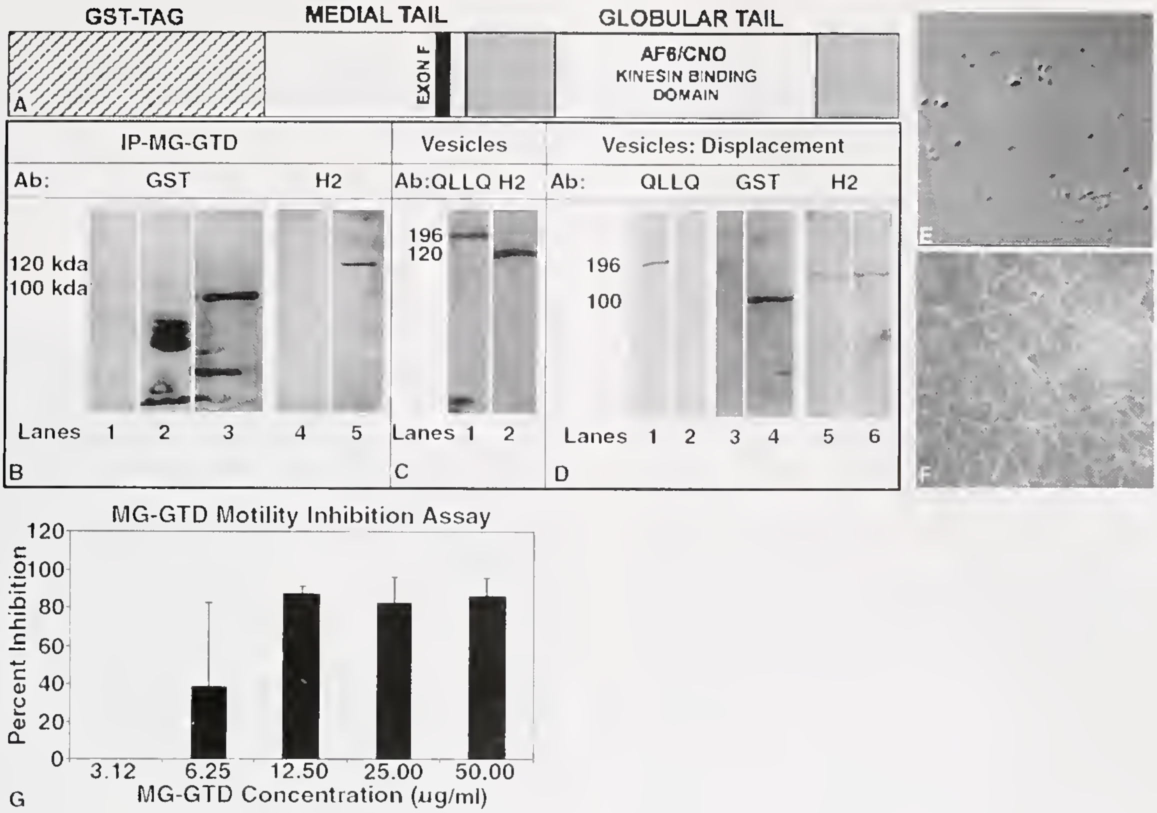

**Figure 1.** *(A) Diagram of the mouse GST-Myosin-V globular tail domain (MG-GTD) construct. The GST-tag is located at the amino-terminus. Myosin-V medial tail domain (including exon F) and the globular-tail domain, including the AF6/Canoe Region (kinesin binding domain), are shown. (B) Western blots of affinity-precipitations with glutathione 4B sepharose beads: bead control (lanes 1 and 4), GST-tag control (lane 2) and MG-GTD (lanes 3 and 5). The MG-GTD affinity-precipitate was probed with α-GST (lanes 1-3) and shows no GST in the affinity control (beads only, lane 1), 25 kDa GST in the GST control (lane 2), and GST-tagged MG-GTD (lane 3) in the experimental. The MG-GTD affinity-precipitate was also probed with α-H2 (lanes 4 and 5), an antibody to kinesin. The blot shows an absence of kinesin in the affinity control (lane 4) and the presence of kinesin in the MG-GTD affinity pull-down (lane 5). (C) Western blot probed with myosin-V antibody α-QLLQ (lane 1) and α-H2 (lane 2) of purified vesicle fractions. Myosin-V (lane 1) and kinesin (lane 2) are present. (D) Western blot with α-QLLQ (lanes 1 and 2), α-GST (lanes 3 and 4), and α-H2 (lanes 5 and 6) of purified vesicle fractions treated with MG-GTD (lanes 2, 4, and 6) and control fractions (1, 3, and 5). α-QLLQ identified myosin-V in the control vesicle fraction (lane 1) and showed an absence of myosin-V in the MG-GTD treated fraction (lane 2); α-GST shows the absence of MG-GTD in the control (lane 3) and the presence of MG-GTD in the treated fraction (lane 4); α-H2 shows kinesin in the control (lane 5) and in the presence of MG-GTD (lane 6). (E) AVEC-DIC microscopy of axoplasm shows the presence of moving vesicles. (F) Fluorescence microscopy shows the presence of actin stained with rhodamine-phalloidin. (G) MG-GTD motility assay shown as percent inhibition (y-axis) of increasing concentrations of MG-GTD (x-axis). The error bars represent standard deviation. Inhibition approaches 90% at concentrations of MG-GTD above 6.25 μg/ml.*

headless myosin-V fragment is an effective inhibitor of vesicle transport in cell extracts and could be used to determine the mechanism of motor recruitment to vesicles.

In summary, the recombinant globular tail fragment of myosin-V pulled down kinesin by affinity-precipitation from squid brain homogenates and displaced native myosin-V from vesicles purified from these homogenates. In addition, the tail fragment blocked vesicle transport on actin filaments that assembled at the margins of axoplasm extruded from the squid giant axon. We conclude, therefore, that inhibition of vesicle transport is due to the displacement of native myosin-V from axoplasmic vesicles. We will use the globular tail domain in future experiments to study the recruitment of myosin-V to neuronal vesicles by Rab-family proteins.

Supported by NSF Grant IBN-0131470 and MBL Shifman Award to EMP-V.

## Literature Cited

1. **Huang, J., S. Brady, B. Richards, D. Stensoien, J. Resau, N. Copeland, and N. Jenkins. 1999.** *Nature* **397:** 267–70.
2. **Hammer, J., and X. Wu. 2002.** *Curr. Opin. Cell Biol.* **14:** 69–75.
3. **Wu, X., F. Wang, K. Rao, J. Sellers, and J. Hammer, III. 2002.** *Mol. Biol. Cell.* **13:** 1735–1749.
4. **Bahadoran, P., E. Aberdam, F. Mantoux, R. Busca, K. Bille, N. Yalman, G. de Saint-Basile, R. Cusaroli-Maranos, J. Ortonne, and R. Ballotti. 2001.** *J. Cell Biol.* **152:** 843–849.
5. **Wu, X., K. Rao, H. Zhang, F. Wang, J. Seller, L. Matesic, N. Copeland, N. Jenkins, and J. Hammer, III. 2002.** *Nat. Cell Biol.* **4:** 271–278.
6. **Chin, G., and S. Goldman. 1992.** *Brain Res.* **571:** 89–96.

**Reference:** *Biol. Bull.* **203:** 212. (October 2002)

# Peroxisomal Catalase in Extrusion Apparatus Posterior Vacuole of Microsporidian Spores

*Earl Weidner and Ann Findley[1] (Biology, Louisiana State University, Baton Rouge, Louisiana 20803)*

A remarkable survival adaptation of microsporidians is the spore extrusion apparatus (EXA), which is equipped to explosively discharge a tube through which the infective sporoplasm is sent into a host cell. The EXA consists of a membrane-associated aperture, polaroplast, polar filament protein, and a posterior vacuole. When the spore activates, the EXA discharges a long, fine tube by an apparent eversion process. When the tube is fully formed, the sporoplasm moves down the tube and ends up in an enveloped compartment thought to be derived from the everted extrusion apparatus membrane. The energy source for spore discharge is believed to reside in the EXA posterior vacuole. In activated spores, the posterior vacuole swells before and during spore extrusion.

We report here the presence of catalase in the posterior vacuole of the spores of a microsporidian, *Spraguea lophii.* This was first made evident when significant levels of molecular oxygen were detected in a medium containing the discharging spores. Clark-style oxygen microelectrodes (Model 7376C, Diamond General, Ann Arbor, Michigan) were used to measure dissolved oxygen in the medium. The oxygen appeared only when low levels of hydrogen peroxide were added to the medium, either before or during spore discharge. In the absence of hydrogen peroxide, no oxygen formed in the medium containing the firing spores. The medium was recovered from the fired spores and was analyzed for catalase enzyme using western blot analysis and using the protocol described earlier (1). The results indicate that catalase was present in the medium, and that the molecular weight corresponded to control catalase (Fig. 1A). This finding supports the old hypothesis that the EXA contents may be released directly into the surrounding medium during tube eversion.

Catalase crystals were successfully isolated using the protocol described by Reinlein (2). The catalase-rich medium was placed in 10% NaCl, containing 2 m$M$ $KH_2PO_4$ at pH 5.5, and after 1 h, this was dialyzed against 1 m$M$ ammonium chloride (pH 5.5). To recrystalize the catalase, there were two cycles of 10-h dialysis. For clean crystals, the entire sample was recycled through the procedure a second time. The crystals tested positive for catalase on the basis of western blots with rabbit anti-bovine catalase (Rockland Immunochemicals, Gilbertsville, Pennsylvania).

To identify the specific location of the catalase, spores of *S. lophii* were subjected to the alkaline-diaminobenzidine (DAB) procedure as reported by Novikoff and Goldfischer (3). The DAB reaction localized to the posterior vacuole before and during spore activation (Fig. 1B). After spore discharge, no detectable DAB activity was found in either the spore ghosts or the extruded sporoplasms.

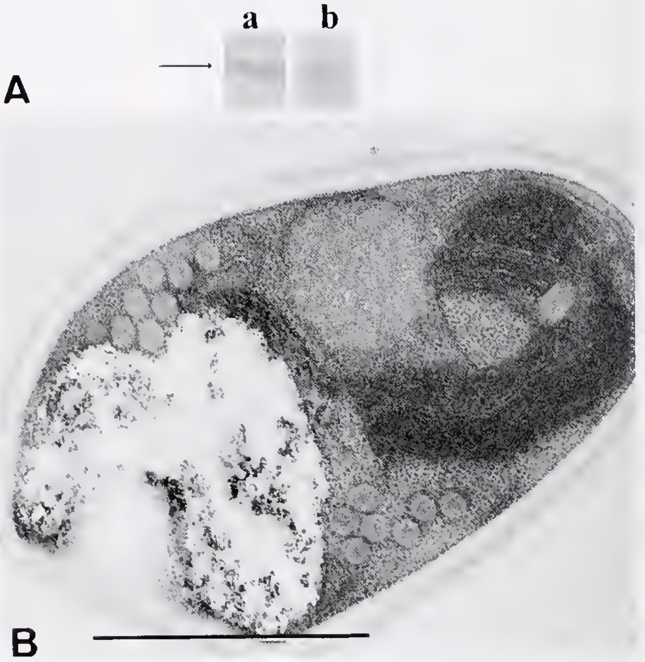

**Figure 1.** Spraguea lophii *catalase. (A) Western blot analysis. In the right panel (b) anti-rabbit serum directed to control catalase (bovine liver), and (a) is the same anti-rabbit serum directed to presumptive catalase from* S. lophii *spores (antibody from Rockland Immunochemicals, Gilbertsville, PA). (B) Electron micrograph of alkaline-DAB reaction confined particularly to the boundary of the posterior vacuole of the spore. Bar scale represents 1 μm.*

Although the mechanism by which catalase works in the posterior vacuole is unclear, it may be associated with the oxidation of long chain fatty acids. Docosahexaenoic acid, commonly associated with peroxisomes, is significantly represented in *S. lophii* spores (4). A function of peroxisomes is to manage the beta-oxidation of long chain fatty acids. Acyl-coA oxidase, an essential enzyme in this process, produces hydrogen peroxide. The catalase in the area can convert the hydrogen peroxide to water and oxygen. The rapid oxidation of the long chain fatty acids may effect the swelling of the posterior vacuole and induce spore discharge.

## Literature Cited

1. **Weidner, E., and S. Halonen. 1993.** *J. Euk. Microbiol.* **40:** 783–788.
2. **Reilein, A. 1998.** Beckan Inst. Advanced Science and Technol. Technical Report 98-009. 1–4.
3. **Novikoff, A., and S. Goldfischer. 1969.** *J. Histochem. Cytochem.* **17:** 675–680.
4. **Hicham, E., J. Bata, D. Bauchart, and C. Vivares. 1997.** *J. Euk. Microbiol.* **44:** 74S.

---

[1] Biology, University of Louisiana, Monroe, LA.

**Reference:** *Biol. Bull.* **203:** 213–215. (October 2002)

# A Metronome-Like Control of the Calcium Signal Leading to Nuclear Envelope Breakdown and Mitosis in Sand Dollar (*Echinaracnius parma*) Cells

*Robert B. Silver (Departments of Pharmacology, Physiology and Radiology, School of Medicine, Department of Biomedical Engineering, College of Engineering, Wayne State University, Detroit, Michigan; Decision and Information Sciences Division, Argonne National Laboratory, Argonne, Illinois; Marine Biological Laboratory, Woods Hole, Massachusetts) and Marc Bartman*[1]

The calcium signal required for nuclear envelope breakdown (NEB) and mitosis arises from a calcium-regulatory subset of the perinuclear endoplasmic reticulum (pn-ER) (1–4); further, this pre-NEB calcium signal is encoded in space-time and evoked by leukotriene $B_4$ ($LtB_4$) (4, 5), a downstream product of phospholipase $A_2$ ($PLA_2$). In fact, a calcium-independent phospholipase $A_2$ ($iPLA_2$) activity (6, 7), revealed by *in vivo* imaging with a confocal microscope (5), is also associated with the pn-ER and occurs just before the pre-NEB calcium signal (3, 5). If this $iPLA_2$ activity is blocked, both the pre-NEB calcium signal and NEB itself are inhibited (5). We have also reported that phosphofructokinase (PFK) is present on that same calcium-regulatory subfraction of pn-ER (which we designated as subfraction B; 2, 5). PFK activity is known to be modulated by its downstream metabolic products; thus, this activity is up-regulated by AMP and ADP, and is down-regulated by ATP in excess over ADP, by ATP analogues with a $\beta$-$\gamma$ phosphodiester bond that cannot be hydrolyzed (*e.g.*, AMP-PCP), and by citrate. Finally, we previously demonstrated that the pn-ER subfraction that exhibits ATP-dependent calcium uptake activity (*e.g.*, 2) has a non-mitochondrial creatine kinase activity that rapidly established and maintained an excess of ATP over ADP under conditions used in that study (8).

This set of related activities, all associated with the pn-ER, are reminiscent of various mechanisms involving a rapid and reversible co-regulatory interaction between $iPLA_2$ and PFK, mediated by glycolytic products. Such mechanisms have been observed in cardiac muscle (9, 10), rat parotid secretory cells (11), pancreatic islet cells and pancreatic tumor cells (12, 13), and control of radiation repair (14). We therefore hypothesized that a reversible interaction between $iPLA_2$ and PFK, modulated by the metabolic products of PFK activity, would also provide a metronome-like mechanism that would, in turn, control the series of biochemical events (3, 4, 5) leading to the pre-NEB calcium signal, NEB, and mitosis. To test this hypothesis, we have used, as a model system, pn-ER subfractions isolated from first and second cell cycle prophase cells obtained from the sand dollar (*Echinaracnius parma*). First, we assayed these subfractions for the effects of calcium levels on $PLA_2$, and then we determined the effect of metabolic products of PFK on $iPLA_2$ activity.

The pn-ER subfractions were isolated from prophase mitotic apparatus (MA) from first and second cell cycle cells, as previously described (2, 3, 6). Briefly, the prophase MA-associated pn-ER subfractions were resolved using ultracentrifugation at 140,000 × *g* on sucrose density gradients. Four pn-ER subfractions were collected at the interfaces between 0.25 *M* and 1.0 *M* sucrose, 1.0 *M* and 1.3 *M* sucrose, 1.3 *M* and 1.5 *M* sucrose, and 1.5 *M* and 2.0 *M* sucrose; these subfractions are designated A, B, C and D, respectively. The sucrose solutions were buffered with 100 m*M* KCl, 10 m*M* NaCl, 30 m*M* imidazole, 5 m*M* $MgCl_2$; and pH was adjusted to 7.20.

The assay for $PLA_2$ activity was significantly modified from that described previously (7). The reactions were performed in 100 m*M* KCl, 10 m*M* NaCl, 30 m*M* imidazole, 5 m*M* $MgCl_2$, 4 m*M* CHAPS, 30% (v/v) glycerol, pH 7.20, with a reaction volume of 500 $\mu$l; the substrate stock solution was 100 m*M* 1-hexadecyl-2-arachidonylthio-2-deoxy-*sn*-glycero-3-phosphorylcholine (arachidonyl-thio-PC) at 12° C. The reactions were stopped by the addition of 10 $\mu$l of a solution containing 1.0 mg/ml bromoenol lactone, 25 m*M* 5,5′-dithio-bis(2-nitrobenzoic acid, 500 m*M* EGTA, pH 7.20. A minimum of triplicate assays was performed on eight different pn-ER preparations; the mean values are presented. The standard deviations from the mean of $PLA_2$ activity, measured for each subfraction at each calcium concentration, did not exceed 4.5% of the mean values. The effect of calcium was assessed by including $CaCl_2$ in the reaction solutions to make a series of final reaction concentrations between 0 and 500 m*M* $CaCl_2$ (Fig. 1A). The data for each pn-ER subfraction were expressed as specific activity per milligram protein as a function of calcium concentration in the reaction milieu (Fig. 1A).

The effects of PFK activity modulators on $iPLA_2$ activity were assessed under the calcium-free reaction conditions described above. The PFK modulators were added in concentrations of 1 m*M*. Duplicate or triplicate assays were performed on pn-ER that had been prepared on three different dates, drop-frozen in liquid $N_2$, and stored at −85°C. Protein concentrations were determined as described earlier (2). Phospholipase $A_2$ activity was calibrated with commercially obtained purified $PLA_2$, under assay conditions described above. Data were analyzed as described earlier (*e.g.*, 3, 4).

When no calcium was added, all pn-ER subfractions exhibited nearly identical levels of specific activity for $PLA_2$ (Fig. 1A). Therefore, this $PLA_2$ activity, which is independent of added calcium, is defined as an $iPLA_2$ activity (8). Addition of 10 n*M* calcium to the reaction milieu decreased the $PLA_2$ activity in each pn-ER subfraction, relative to $iPLA_2$. In 30 n*M* calcium, the $PLA_2$ activity in subfraction B was stimulated 3.5-fold relative to $iPLA_2$ activity, but was reduced in subfractions A and C and only slightly elevated in D relative to the level of $iPLA_2$. In the presence of 50 n*M* calcium, the $PLA_2$ activity in all subfractions was again lower than that for $iPLA_2$. In 100 n*M* calcium, $PLA_2$ activities in subfraction B and D were stimulated 1.7-fold and 2-fold, respectively;

---

[1] Marine Biological Laboratory, Woods Hole, MA.

A

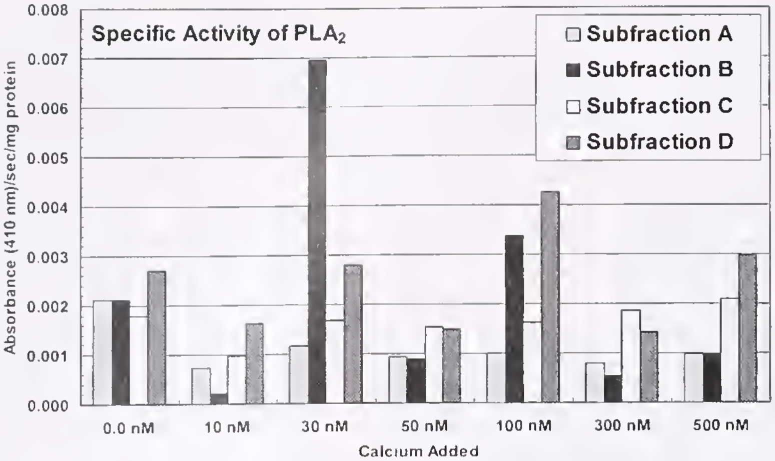

B

**$iPLA_2$ Activity is Effected by Modulators of PFK Activity**

| Condition Tested | Control | Citrate | AMP | ADP | ADP + Creatine Phosphate | AMP-PCP |
|---|---|---|---|---|---|---|
| Mean | 100.0% | 168.7% | 10.0% | 84.9% | 139.1% | 195.4% |
| Std Dev % of Mean | 0.3% | 3.0% | 4.4% | 1.0% | 0.1% | 0.7% |

C

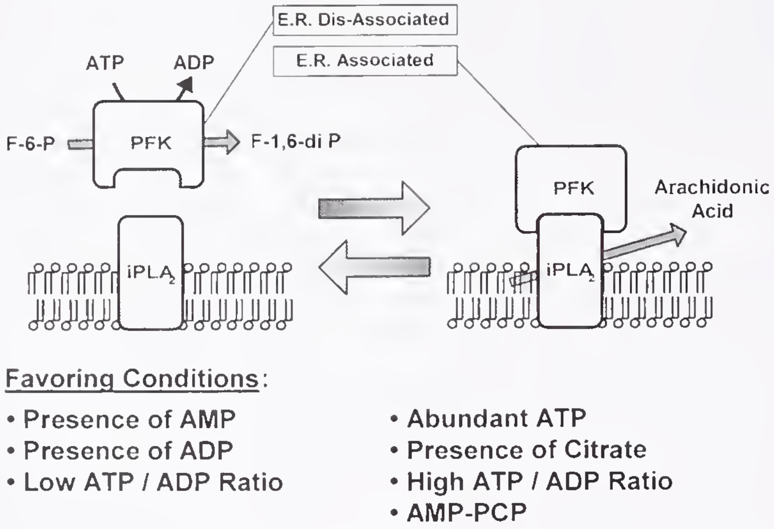

**Figure 1.** *(A) A histogram showing the calcium dependence of the specific activities (absorbance/second/milligram protein) of phospholipase $A_2$ ($PLA_2$) associated with each of four membrane subfractions. Membrane subfractions A, B, C, and D sediment onto 1.0, 1.3, 1.5, and 2.0* M *sucrose, respectively. Note the calcium-independent phospholipase $A_2$ ($iPLA_2$) activities (0 nM calcium), and the peaks of calcium-dependent phospholipase $A_2$ ($cPLA_2$) activity at 30 and 100 nM calcium. A minimum of triplicate assays was performed on eight different pn-ER preparations; the mean values are presented. The standard deviations from the mean of $PLA_2$ activity, measured for each subfraction at each calcium concentration, did not exceed 4.5% of the mean values. A key to bars in the histogram bar is within the figure. (B) The effect upon $iPLA_2$ of modulators of phosphofructokinase (PFK) activity. Modulators of PFK were present at a final concentration of 1 mM. The data presented represent the mean values for those assays; the standard deviations were between 0.1% and 4.4% of those values. (C) A schematic of the "metronome" model for reversible co-regulation of the $iPLA_2$ and PFK activities on the pn-ER of the prophase mitotic apparatus.*

but the activity was again lower in subfractions A and C. In 300 n*M* calcium, $PLA_2$ activity declined in each subfraction relative to values for $iPLA_2$ activity. Finally, in 500 n*M* calcium, activities for subfractions A and B were roughly one-third that of $iPLA_2$, while values for subfractions C and D were similar to those observed for $iPLA_2$ activities in those subfractions. In summary, clear increases in calcium-dependent $PLA_2$ ($cPLA_2$) activities, relative to $iPLA_2$ activities, were observed in subfraction B in 30 n*M* and 100 n*M* calcium, and in D in 100 n*M* calcium. As for the other fractions, substantial reductions in $cPLA_2$ activity relative to $iPLA_2$ activities in all subfractions, were observed at 10 n$M$, 50 n$M$ and 300 n$M$ calcium.

Among downstream metabolic products of PFK, citrate increased iPLA$_2$ activity nearly 1.7-fold over control values (Fig. 1B). In contrast, AMP and ADP, known up-regulators of PFK activity, decreased iPLA$_2$ activity to 10% and 84.9% of control values, respectively. In addition, we observed that addition of ADP and creatine phosphate (and thus ATP), and AMP-PCP resulted in marked elevations of iPLA$_2$ activity. The iPLA$_2$ activity for ADP + creatine phosphate was about 1.4-fold greater than controls; the iPLA$_2$ activity for AMP-PCP was about 2-fold greater than controls (Fig. 1B).

We have found, in this study, that the pn-ER of prophase MA contains both calcium-independent (iPLA$_2$), and calcium-dependent PLA$_2$ (cPLA$_2$) activities (Fig. 1A). Addition of calcium to 30 n$M$ or 100 n$M$ appears to stimulate PLA$_2$ activity in pn-ER subfraction B. Addition of calcium to 100 n$M$ also appears to stimulate PLA$_2$ activity in pn-ER subfraction D. Our discovery of a 30 n$M$ cPLA$_2$ activity in pn-ER subfraction B may indicate a type of calcium-modulated PLA$_2$ activity not previously reported. Our finding of a 100 n$M$ cPLA$_2$ activity is consistent with the requirement for 80 to 100 n$M$ calcium for cPLA$_2$ in other systems (7).

The reciprocal modulation of iPLA$_2$ by metabolic by-products of PFK supports our notion that an interaction between iPLA$_2$ and PFK could regulate perinuclear iPLA$_2$. The reduction of iPLA$_2$ activities upon exposure to AMP or ADP may represent a modulator-induced disassociation of iPLA$_2$ and PFK that had remained associated during the isolation of the MA and the preparation of the pn-ER. The pattern of responses is consistent with a transient regulatory interaction of PFK and iPLA$_2$ (Fig. 1C).

These results confirm and extend our earlier observations that the pn-ER exhibits an iPLA$_2$ activity that is necessary for the pre-NEB calcium signal and NEB. These results, taken together with our earlier modeling efforts (4, 5) further suggest that a potential regulatory interaction between iPLA$_2$ and PFK may be used to coordinately regulate iPLA$_2$ activity, the production of arachidonic acid, LtB$_4$ and thus calcium signals, and glycolysis (4, 5). Moreover, this interaction would also impact the pentose phosphate pathway, and control of glutathione red/ox state (4, 5). This would provide an essential level of feedback regulation both within and among the metabolic pathways that have been described as the integrated metabolic network present on the calcium regulatory subfraction of the pn-ER (4, 5).

At a whole cell scale, such a mechanism would involve rapid and extensive changes in metabolite levels, which are not observed. However, evidence for this regulatory mechanism has been observed to operate on vesicles within microdomains (very restricted spaces), where levels of calcium and other metabolites can vary over several orders of magnitude of concentration in a millisecond timescale (*e.g.*, 3, 15, 16, 17). Conditions that favor PFK activity would contribute to the disassociation of PFK from iPLA$_2$ (Fig. 1C, left), while increases in local levels of downstream products of PFK activity that exert feedback inhibition on PFK would promote reassociation of PFK with iPLA$_2$, thereby activating iPLA$_2$ activity, and thus leading to a calcium signal. Localized decrease in ATP levels, due to calcium pump or calcium-dependent kinase activities, would deplete local ATP levels, and thus activate PFK, which in turn, would inhibit iPLA$_2$ activity (Fig. 1C, right).

The metabolically modulated interaction between iPLA$_2$ and PFK would also provide a limit oscillator on individual vesicles within microdomains that would coordinately control calcium signals and glucose-6-phosphate metabolism. Such a mechanism would be switched by localized changes in levels of ATP or citrate or other modulators of PFK activity. Thus, a coded localized calcium signal could be evoked and terminated by changes in the level of metabolites within an individual microdomain. The combination of iPLA$_2$, 30 n$M$ cPLA$_2$, and 100 n$M$ cPLA$_2$ activities may provide the mitotic cell with an amplitude-selective notch filter mechanism for producing arachidonic acid, LtB$_4$ and a space-time coded calcium signal. Such a mechanism would provide a "metronome" type switch, dependent upon local metabolic conditions, that would regulate localized space-time encoded calcium signals during a brief, defined period in the cell cycle, as exemplified by the pre-NEB calcium signal (1–5).

Research grant support by NSF (MCB-99082680) and Wayne State University is gratefully acknowledged. Thanks are extended to Drs. John R. Hummel, George D. Pappas, Howard Rasmussen, Raoul F. Reiser, and Stephen M. Wolniak for their helpful comments and advice during these studies. We also thank the anonymous reviewers for their helpful suggestions in the refinement of the manuscript.

## Literature Cited

1. **Silver, R. B. 1989.** *Dev. Biol.* **131:** 11–26.
2. **Silver, R. B. 1986.** *Proc. Nat. Acad. Sci. USA* **83:** 4302–4306.
3. **Silver, R. B. 1996.** *Cell Calcium* **20:** 161–179.
4. **Silver, R. B. 1999.** *FASEB J.* **13:** S209–S215.
5. **Silver, R. B. 2001.** *Biol. Bull.* **201:** 248–250.
6. **Silver, R. B., M. S. Saft, A. R. Taylor, and R. D. Cole. 1983.** *J. Biol. Chem.* **258:** 13,287–13,291.
7. **Dennis, E. A. 1994.** *J. Biol. Chem.* **269:** 13,057–13,060.
8. **Yang, H.-C., M. Mosior, C. A. Johnson, Y. Chen, and E. A. Dennis. 1999.** *Anal. Biochem.* **269:** 278–288.
9. **Mizuno Kamiya, M., Y. Kamayama, and A. Fujita. 1998.** *J. Biochem (Tokyo).* **123:** 205–212.
10. **Hazen, S. L., and R. W. Gross. 1991.** *J. Biol. Chem.* **266:** 14,528–14,534.
11. **Hazen, S. L., and R. W. Gross. 1991.** *Biochem. J.* **280:** 581–587.
12. **Hazen, S. L., and R. W. Gross. 1993.** *J. Biol. Chem.* **268:** 9892–9900.
13. **Hazen, S. L., M. J. Wolf, D. A. Ford, and R. W. Gross. 1994.** *FEBS Lett.* **339:** 213–216.
14. **Zhang, Y. M., T. Y. Wong, L. Y. Chen, C. S. Lin, and J. K. Liu. 2000.** *Appl. Environ. Microbiol.* **66:** 105–112.
15. **Llinás, R., M. Sugimori, and R. B. Silver. 1992.** *Science* **256:** 677–679.
16. **Silver, R. B., M. Sugimori, E. J. Lang, and R. Llinás. 1994.** *Biol. Bull.* **187:** 293–299.
17. **Sugimori, M., E. J. Lang, R. B. Silver, and R. Llinás. 1994.** *Biol. Bull.* **187:** 300–303.

**Reference:** *Biol. Bull.* **203:** 216–217. (October 2002)

# Culture Method for *in vitro* Fertilization to Hatching of the Squid, *Loligo pealeii*

*Karen Crawford (Department of Biology, St. Mary's College of Maryland, St. Mary's City, Maryland 20686, and Marine Biological Laboratory, Woods Hole, Massachusetts 02543)*

Much of what we know about cephalopod development is drawn from observing embryos in, or dissected from, naturally laid jelly strings or egg capsules (1, 2). Although embryos extracted from jelly strings survive in culture for short periods (3), reliable *in vitro* fertilization and culture would greatly enhance our ability to study the molecular and cellular events of fertilization and development, including pronuclear migration (4), cleavage (5), cytoplasmic movements (6), differentiation, and organogenesis. When *in vitro* fertilized embryos are cultured in glassware or plastic petri dishes, their development is typically arrested at the early blastoderm stage (<48 h). Embryos fertilized *in vitro* may be successfully cultured on cushions of 0.2% agarose in Millipore (0.22 $\mu$m) filtered seawater (MFSW) (Sigma, Type II) (7), but their chorions do not reliably swell to permit complete development or hatching.

Recently, a considerable advancement in culture methodology was reported for *in vitro* fertilized embryos of the argentine short-fin squid, *Illex argentinus* (8). In this study, embryos cultured in plastic petri dishes filled with seawater alone died after 3 days, while those cultured in seawater supplemented with fresh or freeze-dried oviductal gland jelly underwent sufficient chorion expansion to support normal development and hatching. It is worth mentioning that for this to occur, the culture medium was changed at 3-h intervals throughout the 6–7-day culture period (15 °C). In comparison, *Loligo pealeii* embryos require 20–21 days to develop at 17 °C, and therefore the goal of this study was to develop an alternative culture method for routinely obtaining *in vitro* fertilized cephalopod hatchlings. This report describes an *in vitro* fertilization method, in addition to the effects of a commercially available sera and serum protein on chorion expansion and embryonic development. Embryos from some of these cultures undergo significant chorion expansion, develop normally, and after 20–21 days in culture (17 °C) hatch independently.

In vitro *fertilization.* Clear mature eggs from the oviduct of a cold-anesthetized dissected female were collected and washed several times with well-aerated MFSW. Next, spermatophores (20–30) from the spermatophore duct of a dissected, anesthetized male were placed in 15 ml MFSW in a syracuse dish and the sperm were discharged with slight pressure. To this sperm suspension, approximately 1500–2000 eggs were added in concentrated drops (~100 embryos/drop). After 15 min, the fertilized eggs were washed several times in MFSW to remove sperm and spermatophore casings. Rate of fertilization (typically 85%–95%) was determined following first and second polar body formation (20 min and 1.5 h, respectively) and first cleavage (3.5 h).

*Embryo culture.* To enhance embryonic development, either horse serum (HS) (Sigma) or bovine serum albumin (BSA) (ICN) was added to the MFSW culture. In each case, 20–40 embryos per dish were cultured in 60-mm plastic petri dishes (Falcon) lined with a cushion of 0.2% agarose (Type II-A, Sigma) in MFSW. Dishes and solutions were changed every other day, and dead or damaged embryos were removed. Control embryos cultured in MFSW alone, although alive, do not undergo chorion expansion and fail to develop normally or hatch. Adding 0.2% or 0.5% HS to the culture resulted in the reduction or loss of the perivitelline space (the area between the embryo and inner chorion surface), possibly due to osmosis. Embryos cultured in lower concentrations of HS/MFSW (0.01%, 0.05%, and 0.1%), grew well initially, underwent some chorion expansion, but failed to complete development or hatch. In striking contrast, embryos from six independent trials cultured in BSA (0.1%, 0.2%, or 0.5% dissolved into MFSW and refiltered) developed normally and underwent gradual chorion expansion from 1600 $\mu$m (egg chorion length at fertilization) to measure an average of 1800, 2000, and 3000 $\mu$m (100 embryos/concentration), respectively, after 21 days in culture (Fig. 1a, b). Moreover, embryos cultured in 0.5% BSA/MFSW nearly always completed development to hatch independently after 20–21 days in culture (Fig. 1c). Although the majority of embryos (53%–91% from 100 embryos/trial × 6 trials) cultured in 0.5% BSA/MFSW develop normally in a synchronous fashion, and proceed through similar or identical developmental stages when compared to embryos in naturally laid jelly strings, it is important to note that there was variability among these cultures. Perhaps, when the method of Sakai and Brunetti (8) is considered, increasing the frequency of embryo transfer to fresh culture dishes and media might improve the overall percentage of normal embryos observed in BSA/MFSW cultures.

*Possible mechanisms for chorion expansion.* Since chorion expansion is concentration dependent, with embryos developing best in 0.5% BSA/MFSW, simple osmosis does not appear to be responsible for this response. Interestingly, the chorions of unfertilized eggs cultured in the presence of 0.5% BSA/MFSW do not change, suggesting that an actively developing embryo is required for chorion expansion. Moreover, embryos cultured in 0.5% BSA/MFSW in plastic petri dishes unlined by an agarose cushion fail to undergo chorion expansion and die after 3 or 4 days. These observations suggest that it is the mixture of protein and carbohydrate present in the BSA and agarose that best mimics the environment of the egg jelly string and thus promotes normal development and hatching.

Recently, homeobox gene clusters were identified from tissues of adult cephalopods (9), and the role of these genes in early neurogenesis is being explored using embryos harvested from jelly strings (10). Culturing squid embryos *in vitro* creates new opportunities to study and understand cephalopod development. While *in vitro* fertilization enables one to control parentage, culturing embryos away from their tenacious jelly allows for the study of individual embryos, simplifies stage-specific embryo collection for immunohistochemistry and *in situ* hybridization analysis, and permits the embryo to be microinjected with lineage-tracing dyes or factors designed to inhibit or enhance development. Moreover,

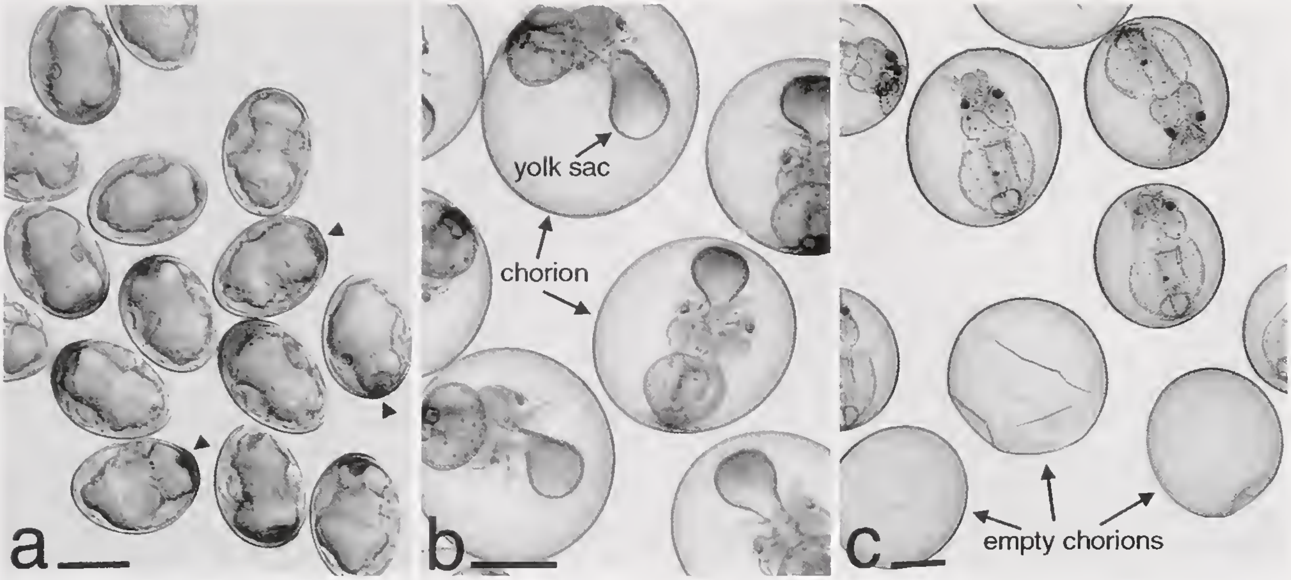

**Figure 1.** *Bovine serum albumin enhances chorion expansion to permit normal development and hatching of* in vitro *fertilized squid embryos. (a) Eighteen-day-old embryos cultured in MFSW alone. Note: the chorion has not expanded to permit normal development. Arrowheads indicate deteriorating yolk sac tissue. (b) Eighteen-day embryos cultured in 0.5% BSA/MFSW permits chorion expansion and normal development. (c) Twenty-one-day embryos, hatchling stage, cultured in 0.5% BSA/MFSW. Arrows indicate three empty chorions recently discarded by hatchlings. Scale bars = 1000 μm.*

embryo culture enables us to treat cephalopod embryos with chemical agents, such as lithium chloride (11) or retinoids (12), that have been shown to predictably alter development in other organisms, thereby enhancing our ability to work with and understand the embryos of this evolutionarily old and successful group of organisms.

This work was supported by the Marine Biological Laboratory Associates Fellowships, The James A. and Faith Miller Memorial fund, and The Evelyn and Melvin Spiegel Fellowship Fund to Karen Crawford.

## Literature Cited

1. **Brooks, W. K. 1880.** *Anniv. Mem. Boston Soc. Nat. Hist.* 1–22.
2. **Arnold, J. 1965.** *Biol. Bull.* **128:** 24–32.
3. **Arnold, J. M., and L. D. Williams-Arnold. 1974.** *J. Embryol. Exp. Morphol.* **31:** 1–25.
4. **Crawford, K. 1985.** *Biol. Bull.* **169:** 540.
5. **Crawford, K. 2000.** *Biol. Bull.* **199:** 207–208.
6. **Crawford, K. 2001.** *Biol. Bull.* **201:** 251–252.
7. **Klein, K., and L. A. Jaffe. 1984.** *Biol. Bull.* **167:** 518.
8. **Sakai, M., and N. E. Brunetti. 1997.** *Fish. Sci.* **63**(5): 664–667.
9. **Callaerts, P., P. N. Lee, B. Hartmann, C. Farfan, D. W. Y. Choy, K. Ikeo, K-F. Fischbach, W. J. Gehring, and H. Gert de Couet. 2002.** *Proc. Natl. Acad. Sci. USA* **99:** 2088–2093.
10. **Burbach, J. P. H., A. J. C. G. M. Hellemons, M. Hoekman, P. Grant, and H. C. Pant. 2001.** *Biol. Bull.* **201:** 252–254.
11. **Kao, K. R., Y. Masui, and R. P. Elinson. 1986.** *Nature* **322:** 371–373.
12. **Marshall, H., S. Nonchev, M. H. Sham, I. Muchamore, A. Lumsden, and R. Krumlauf. 1992.** *Nature* **360:** 737–741.

---

**Reference:** *Biol. Bull.* **203:** 217–218. (October 2002)

# mRNAs Located in *Squalus acanthias* (Spiny Dogfish) Oligodendrocyte Processes

*Nicholas Pahl*[1], *Sara Homsi*[2], *Hilary G. Morrison*[3], *and Robert M. Gould*
*(IBR, Staten Island, New York 10314)*

This study identifies mRNAs located in oligodendrocyte (OL) processes of spiny dogfish and compares them with mRNAs that were previously identified in rat OL processes (1, 2). Because these two species have independent evolutionary histories covering hundreds of millions of years, mRNAs common to OL processes in both species likely represent proteins recruited to form the original myelin sheaths in the common gnathostome ancestor. Of the mRNAs present in rat OL processes, myelin basic protein (MBP) and myelin-associated oligodendrocytic basic protein (MOBP) mRNAs dominate (1, 2). Surprisingly, however, MBP mRNA is not located in spiny dogfish OL processes; rather it is restricted to OL soma as measured in both *in situ* hybridization and subcellular fractionation experiments (Gould, unpubl.). Thus, MBP synthesis must have moved from the OL soma to its processes sometime after the mammalian line diverged from elasmobranches.

---

[1] Florida Institute of Technology, Melbourne, FL 32901.

[2] Marine Models for Biomedical Research, Marine Biological Laboratory, Woods Hole, MA 02543.

[3] Josephine Bay Paul Center for Comparative Molecular Biology and Evolution, Marine Biological Laboratory, Woods Hole, MA 02543.

To identify mRNAs in spiny dogfish OL processes, we applied the method we developed to identify mRNAs in rat OL processes. This method takes advantage of the finding that mRNAs located in OL processes are selectively trapped in myelin vesicles during homogenization of brain tissue (1–3). As starting material for subtractive hybridization, RNA was obtained from low-speed supernatant, myelin, and pellet fractions prepared from adult (4) and fetal (20–22 cm) spiny dogfish brains. Fetal spiny dogfish brains were used because they have a greater ratio of OL process cytoplasm to myelin sheaths than adult brains. In initial studies, we obtained results suggesting that adult spiny dogfish myelin was contaminated with non-OL process mRNAs (see below). Brains were removed, homogenized in 0.85 *M* (adult) or 1 *M* (fetal) sucrose with 10 m*M* HEPES, pH 7.4, 3 m*M* dithiothreitol (DTT) (5). The homogenate was centrifuged at 4000 rpm for 10 min at 4 °C to pellet nuclei and cell debris. LSS was transferred to an ultracentrifuge tube, overlaid with 0.25 *M* sucrose in HEPES/DTT, and centrifuged at 26,000 rpm for 3.5 h at 4 °C in a SW28 rotor. Myelin (white material accumulated at the 0.25 *M* sucrose/0.85 or 1 *M* sucrose interface) and pellet were transferred to separate tubes, diluted with 10 m*M* $MgCl_2$, and centrifuged at 12,000 rpm for 10 min at 4 °C. Total RNA was extracted from LSS, myelin, and pellet samples with Tri Reagent (Molecular Research Center, Inc., Cincinnati, OH) according to the manufacturer's instructions. For studies with adult tissue, low-speed supernatant (LSS) was used to prepare driver for subtractive hybridization. For studies with fetal tissue, the 1 *M* sucrose pellet was used to prepare driver. Poly A RNA was prepared (MicroPolyA Pure™ kit, Ambion, Austin, TX) and used for suppression subtractive hybridization (PCR-Select™ Subtractive Hybridization kit, BD Clontech, Palo Alto, CA) according to the manufacturer's instructions. PCR products were subcloned into pGEM T-easy vector (Promega, Madison, WI) and sequenced on Li-Cor and ABI 3700 sequencing machines in the Josephine Bay Paul Center. Sequences that matched GenBank non-redundant (NR) nucleotide entries were identified using the Basic Local Alignment Search Tool (BLASTN) (http://www.ncbi.nlm.nih.gov) (6).

For the adult studies, over 150 sequences were analyzed (4). Twenty-five that had matches in the GenBank non-redundant database were analyzed by Northern blot for enrichment of mRNA in myelin *versus* LSS. None of the cDNAs identified mRNAs that were enriched in myelin, probably because the abundant myelin in adult brain caused non-specific trapping of mRNAs present at other neural locations. With the fetal brain subtraction, 280 sequences were analyzed. Over half (148, 53%) were derived from the *Squalus acanthias* mitochondrial genome. Another 73 (26%) did not match any sequence in the GenBank non-redundant database. We will determine if any of these sequences match entries in GenBank using BLASTN (EST database) and BLASTX (NR database) as well as the pufferfish (http://fugu.hgmp.mrc.ac.uk/) and the zebrafish (http://www.ensembl.org/Danio_rerio/blastview) databases. The remaining 59 (21%) sequences matched entries in the GenBank NR database. Fifteen different ribosomal protein mRNAs were identified as well as three elongation factors ($1\alpha$, 2 and $5\alpha$); all are important for translational control of OL process protein synthesis. We previously identified four different ribosomal protein mRNAs and two different elongation factor mRNAs in rat OL processes (2, 7). Together, these results suggest that local regulation of OL process protein synthesis was an original property. Some of these were larger than known ribosomal protein and elongation factor mRNAs (Gould, unpubl.), indicating that they either code for different proteins or contain untranslated regions that target them to OL processes. In an independent study, the mRNA for ribosomal protein L4 was identified in PC12 neurites (8), a finding consistent with local translational control being a property of process-based protein synthesis. As in rat myelin, spiny dogfish myelin contains ferritin heavy chain mRNA. This result suggests that iron storage in OL processes was locally regulated early in evolutionary time. None of the other 18 known mRNAs identified here matched mRNAs identified in rat OL processes. Among the mRNAs of particular interest are homologues of sec61 (accession number BC019158), proteosome protein (BC003197), calmodulin-2 (NM_001743) and epsilon-coatamer (AB042117), all proteins with potential function in membrane biogenesis. We will use both Northern blot and subtractive hybridization efficiency analysis to confirm that these cDNAs represent mRNAs located in spiny dogfish OL processes. As neither MBP or MOBP mRNAs were identified in these studies, our results indicate that these proteins were targeted to OL processes after mammalian ancestors diverged from elasmobranches.

Because numerous mitochondrial genes and limited numbers of other genes were identified in this study, we are conducting additional studies with myelin and pellet fractions prepared by subjecting fetal spiny dogfish brains to hyperosmotic conditions (1.4 *M* sucrose) during homogenization and hypotonic conditions (0.85 *M* sucrose) just prior to density gradient centrifugation. We already know that when rat brain is homogenized in hyperosmotic sucrose the variety of cDNAs obtained by subtractive hybridization is increased in comparison with homogenization in iso-osmotic sucrose (2, 7). In ongoing studies, we lowered the sucrose interface to 0.85 *M* sucrose. Future studies are planned to determine which of the mRNAs identified in rat OL process mRNAs are expressed in spiny dogfish OL processes and *vice versa*.

This work was funded by grants from the National Multiple Sclerosis Society (RG-2944) and the National Science Foundation (IBN9986132).

## Literature Cited

1. **Gould, R. M., C. Freund, and E. Barbarese. 1999.** *J. Neurochem.* **73:** 1913–1924.
2. **Gould, R. M., C. M. Freund, F. Palmer, and D. L. Feinstein. 2000.** *J. Neurochem.* **74:** 1834–1844.
3. **Colman, D. R., G. Kreibich, A. B. Frey, and D. D. Sabatini. 1982.** *J. Cell Biol.* **95:** 598–608.
4. **Smith, R., E. Kavanagh, H. G. Morrison, and R. M. Gould. 2001.** *Biol. Bull.* **201:** 255–256.
5. **Gillespie, C. S., L. Bernier, P. J. Brophy, and D. R. Colman. 1990.** *J. Neurochem.* **54:** 656–661.
6. **Altschul, S. F., T. L. Madden, A. A. Schäffer, J. Zhang, Z. Zhang, W. Miller, and D. J. Lipman. 1997.** *Nucleic Acids Res.* **25:** 3389–3402.
7. **Gould, R. M., C. M. Freund, J. Engler, and H. G. Morrison. 2000.** *Biol. Bull.* **199:** 215–217.
8. **Twiss, J. L., and E. M. Shooter. 1995.** *J. Neurochem.* **64:** 550–557.

**Reference:** *Biol. Bull.* **203:** 219–220. (October 2002)

# SEM Comparison of Severed Ends of Giant Axons Isolated From Squid (*Loligo pealeii*) and Crayfish (*Procambarus clarkii*)

*Christopher S. Eddleman*[1], *George D. Bittner*[2], *and Harvey M. Fishman*
*(University of Texas Medical Branch, Galveston, Texas 77555-0641)*

The identification and characterization of processes and proteins involved in restoring a plasma membrane seal after axonal injury have been advanced by studies of invertebrate giant axons (GAs) with techniques inapplicable to smaller cells (1–7). These studies showed that $Ca^{2+}$-induced endocytotic vesicles mediate sealing by protein-facilitated interactions and fusions (2–5) among themselves and with the plasma membrane, which enabled restoration of electrical function (6). In contrast to GAs isolated from squid, which vesiculate but do *not* form a seal 1–2 h after severance (7), transected crayfish medial GAs vesiculate and do seal within 1 h after severance (2–4). We thought that structural manifestations of sealing might be evident in scanning electron microscope (SEM) images of severed GAs isolated from the two invertebrates and fixed at times posttransection (PT) that are relevant to the previous assessments of sealing. Here we compare such micrographs, which show unorganized vesicles at an open, cut end of a squid GA, but a plug-like aggregation of vesicles at the closed, cut end of a crayfish GA. These structural comparisons at axonal cut ends are consistent with previous electrical (3, 6, 7) and dye exclusion (2–4) assessments of sealing in these two preparations.

Axons were prepared for SEM (JEOL model JSM840) as follows. GAs dissected from live squid (*Loligo pealeii*) were placed in artificial seawater (ASW) consisting of (in m*M*): 430 NaCl, 5 KCl, 10 $CaCl_2$, 50 $MgCl_2$, 5 TrisCl, pH 7.4 at 22 °C. GAs were transected in ASW with fine, spring microscissors. At 1 h PT, fixative (2% glutaraldehyde in ASW) was added; the GAs remained in fixative for 1–4 h, after which they were washed 3 times for 20 min each with ASW without fixative. The samples were placed in 1% osmium tetroxide in ASW for 1 h on ice and then washed 3 times in ASW. Next, the samples were dehydrated on ice in an ethanol (EtOH) series: 50%, 70%, 85%, and 95% for 10 min each, and lastly in 100% EtOH, 3 times for 15 min each. To dry the samples without surface tension changes, we placed them in a critical point dryer and then glued them to an SEM stub. Finally, the samples were sputter-coated with Au/Pd. Medial GAs were dissected from the ventral nerve cord of live crayfish (*Procambarus clarkii*) as described previously (2). The crayfish GAs were prepared like those of squid, except that medial GAs were placed in van Harreveld's (vanH) solution (22 °C) consisting of (in m*M*): 205 NaCl, 5.4 KCl, 13.5 $CaCl_2$, 2.6 $MgCl_2$, 10 HEPES pH 7.4, and fixative was added at 30 min PT. In $Ca^{2+}$-free vanH solution, $CaCl_2$ was omitted, and 1 m*M* EGTA added.

The cut end of a squid GA (Fig. 1A) after transection in ASW and fixation at 1 h PT was slightly constricted, but open, with the glial sheath folded back on itself. At higher magnifications (Fig. 1B and C), the axoplasmic core appeared layered and surrounded by a large collection of vesicles on its periphery (axoplasmic cortex). The highest magnification of the vesicles (Fig. 1C) showed a vesicle size distribution ranging from submicrometer to several micrometers in diameter. Structures that would constitute a barrier to the movement of ions or molecules into or out of the cut end were not evident. In contrast, the cut end of a crayfish medial GA (Fig. 1D)—after transection in vanH solution and fixation at 30 min PT—was closed, as indicated by a seam made by the close apposition of the flattened boundary at the severed end. Furthermore, a prominent vesicular mass filled and protruded from an apparent residual opening at the constricted cut end. Higher magnification (Fig. 1E) showed that this vesicular mass was very densely packed and had a distribution of vesicle sizes similar to that in the squid GA. To confirm the essential role of $Ca^{2+}$ in vesiculation and in the restoration of an ionic seal (structural barrier) after transection (2–5), the cut end of another crayfish GA (Fig. 1F) was transected in $Ca^{2+}$-free vanH solution and fixed at 30 min PT. The cut end was open, and vesicles were absent.

These structural data at the cut end of isolated squid and crayfish axons are consistent with previous ultrastructural data (2, 4, 7, 8) and physical assessments of the restoration of a seal (2–7). That is, 1) the open, cut end of a squid GA and the closed, cut end of a crayfish medial GA match their respective sealing properties, and 2) vesiculation and sealing in crayfish medial GAs require $Ca^{2+}$. Furthermore, the structure of the apparently restored seal at the cut end of a crayfish GA suggests a vesicular plug-like seal rather than the restoration of an intact, continuous, axolemmal membrane sheet.

We thank Mr. Louis Kerr for assistance. This work was supported by NIH grant NS31256 and a Texas, Advanced Technology Program grant.

## Literature Cited

1. **Bittner G. D., and H. M. Fishman. 2000.** Pp. 337–370 in *Nerve Regeneration*, N. Ingoglia and M. Murray, eds. Marcel Dekker, New York.
2. **Eddleman, C. S., M. L. Ballinger, C. M. Godell, M. S. Smyers, H. M. Fishman, and G. D. Bittner. 1997.** *Proc. Natl. Acad. Sci. USA* **94:** 4759–4764.
3. **Godell, C. M., M. S. Smyers, C. S. Eddleman, M. L. Ballinger, H. M. Fishman, and G. D. Bittner. 1997.** *Proc. Natl. Acad. Sci. USA* **94:** 4765–4770.
4. **Eddleman, C. S., M. L. Ballinger, M. S. Smyers, H. M. Fishman, and G. D. Bittner. 1998.** *J. Neurosci.* **18:** 4029–4041.
5. **Detrait, E. R., C. S. Eddleman, S. Yoo, M. Fukuda, M. P. Nguyen, G. D. Bittner, and H. M. Fishman. 2000.** *J. Neurobiol.* **44:** 382–391.
6. **Eddleman, C. S., G. D. Bittner, and H. M. Fishman. 2000.** *Biophys. J.* **79:** 1883–1890.
7. **Krause, T. L., H. M. Fishman, M. L. Ballinger, and G. D. Bittner. 1994.** *J. Neurosci.* **14**(11 part1): 6638–6651.
8. **Gallant, P. E., K. Hammar, and T. S. Reese. 1995.** *J. Neurocytol.* **24:** 943–954.
9. **Gallant, P. E., and J. A. Galbraith. 1997.** *J. Neurotrauma* **14:** 811–822.

---

[1] Texas Tech Medical School, Lubbock, TX.

[2] The University of Texas, Austin, TX.

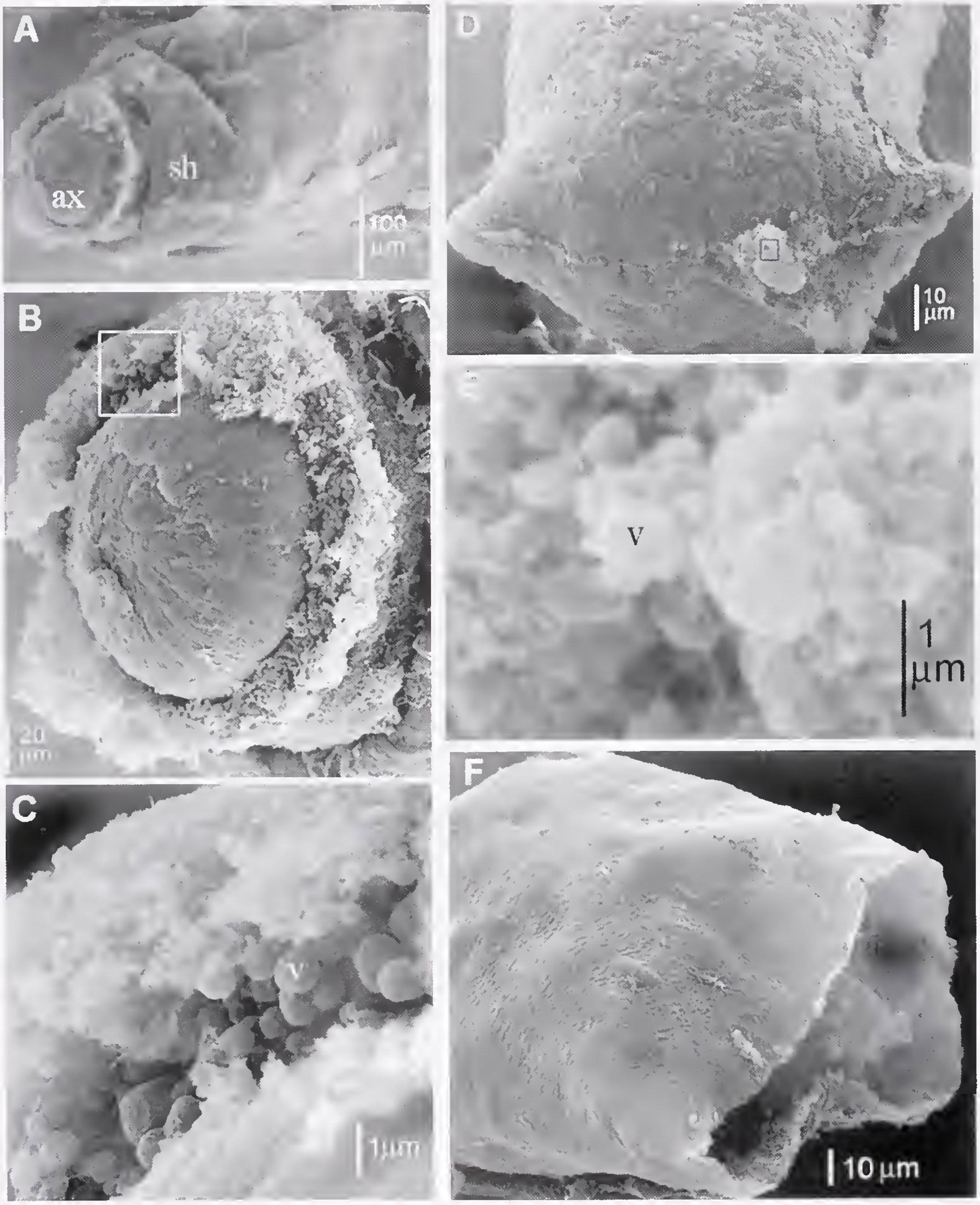

**Figure 1.** *Scanning electron micrographs of a squid GA (A, B, C) severed in ASW and fixed at 1 h PT, and of a crayfish medial GA (D, E, F) severed in vanH solution and fixed at 30 min PT. (A) Low resolution of the open, cut end. ax = axoplasmic core; sh = glial sheath folded back on itself. (B) Magnified cut end showing layered core of axoplasm surrounded by vesicles in the periphery (axoplasmic cortex region). (C) Magnification of boxed region in B in the axoplasmic cortex region showing a large number of vesicles in a wide range of sizes. v = vesicle. (D) Low resolution of the closed, cut end showing a seam at the boundary of the injury and a protruding plug of vesicles. (E) Magnification of boxed region in D showing that the plug consists of a dense aggregation of vesicles. (F) Low resolution of another crayfish medial GA, severed and fixed in $Ca^{2+}$-free vanH solution, showing an open, cut end and the absence of vesicles.*

**Reference:** *Biol. Bull.* **203:** 221–222. (October 2002)

# Early Neurogenesis in the Horseshoe Crab *Limulus polyphemus* and Its Implication for Arthropod Relationships

*Beate Mittmann*[1] *(Marine Biological Laboratory, Woods Hole, Massachusetts 02543)*

The relationships among the four arthropod groups (insects, crustaceans, myriapods, chelicerates) have been a point of controversy for many years. According to the traditional view, the myriapods are most closely related to the insects (common taxon "Tracheata" or Antennata), the crustaceans are the closest relatives of the Antennata (common taxon Mandibulata), and the chelicerates are the sister group of the Mandibulata. However, when the characters that have been used to connect the insects and the myriapods were reviewed, the results suggested that they are either suspected of being convergent (*i.e.,* Malpighian tubules, tracheae) or are not significant in a phylogenetic discussion (loss or absence of characters) (1, 2). Moreover, many characters were found to support a close crustacean-insect relationship, a group that is named "Tetraconata" due to the tetrapartite crystalline cones of the ommatidia (3). In addition, several phylogenetic trees based on molecular data suggested a Crustacea-Insecta unit (4, 5, 6). One of the morphological characters that supports a monophyletic Crustacea-Insecta unit is the mode of development of the central nervous system *via* neuroblasts. Neuroblasts are specific neuroectodermal cells that repeatedly divide unequally, giving rise to a smaller ganglion mother cell that is pushed dorsally into the interior of the embryo and divides once to give rise to neurons or glial cells ("stem cell mode"). The neuroblasts of crustaceans and insects are homologous. In the myriapods so far investigated, ganglia form in a different way and can vary somewhat: clusters of tightly packed cells invaginate into the interior of the embryo. To determine whether the presence of neuroblasts is an apomorphic character for the Tetraconata or a plesiomorphic character introduced earlier in arthropod evolution (and differentiated in myriapods), an outgroup comparison including chelicerates is necessary. If chelicerate ganglia form *via* neuroblasts, they are probably an old arthropod character and therefore invalid for establishing a crustacean-insect sister group relationship. If chelicerates have a different mode of ganglion formation, neuroblasts can be interpreted as an apomorphic character for the Tetraconata.

Examinations of chelicerate neurogenesis are relatively rare. Weygoldt (7) found that several arachnids form ganglia *via* invaginations of multiple cells. A substantial immunocytochemical study of neurogenesis in the spider *Cupiennius salei* recently provided similar results (8). No neuroblasts occur in either case: ganglia are formed through invagination. However, to decide whether an "invagination mode" is an ancestral pattern for chelicerate neurogenesis, it is necessary to study more ancestral species. The horseshoe crab is one of the oldest living chelicerates, showing many ancestral characters during embryogenesis (9). Therefore I examined early neurogenesis in the horseshoe crab *Limulus polyphemus* using immunocytochemical techniques.

Horseshoe crab embryos of different stages (following staging of Brown and Clapper, 10) were fixed in paraformaldehyde (4%). All antibody stainings (anti-horseradish-peroxidase, Sigma, 48 $\mu$g/ml; anti-phopho-histone H3, Upstate Biotech) were performed with slightly changed standard protocols (11). Primarily, I used TRITC-labeled phalloidin (Sigma, 2 $\mu$g/ml, incubation 1.25 h), which labels F-actin filaments of the cytoskeleton and can be used to visualize nervous cells and muscle cells. Staining patterns were investigated with a Pascal confocal laser scanning microscope (Zeiss).

The results in the horseshoe crab show a strong similarity to the data from *Cupiennius* (8). As of stage 14, I found multiple sites of high phalloidin staining (Fig. 1a); the number of these sites increases as development progresses. Both the development and the increase in number of these sites occur in a kind of wave from anterior to posterior, as was described for *Cupiennius* (8). Deep to the fluorescently stained dots were clusters of invaginating bottle-shaped cells slightly larger than those in the surrounding tissue (Fig. 1a). The strongly stained areas were formed by bundled cell processes that extend to the ventral surface (Fig. 1b). At about stage 17, these invaginating cells could be seen to be involved in the differentiation of neurons. This was also shown by labeling with horseradish-peroxidase antibody, which binds to neurons in all arthropods. Furthermore, experiments on cell proliferation, using phospho-histone-H3 antibody to label mitotic cells, suggested that most if not all of the divisions take place in the apical layer of the neuroectoderm. No proliferation of already invaginated cells could be detected. The proliferation pattern and invaginating activity differed from the neurogenetic "stem cell mode" of insects or crustaceans and was more similar to ganglion formation in several myriapods.

In summary, no neuroblasts have been detected in horseshoe crabs or arachnids. Because of the striking accordance in neurogenesis of *Limulus* and *Cupiennius* (8), the similarities with neurogenesis in other arachnids (7), and the fact that *Limulus* is one of the most ancestral chelicerates, I suggest that the "invagination mode" represents the ancestral mode of neurogenesis in chelicerates (Fig. 1c). Further investigations are required to decide whether it represents the ancestral mode of arthropod neurogenesis. The "stem cell mode" of insect and crustacean neurogenesis thus seems to be derived and can therefore be counted as an apomorphic character of the Tetraconata (Fig. 1c).

Supported by the Grass Foundation and the Deutsche Forschungsgemeinschaft (DFG).

## Literature Cited

1. **Dohle, W. 1997a.** *Ent. Scand. Suppl.* **51:** 7–16.
2. **Dohle, W. 1997b.** Pp. 305–315 in *Arthropod Relationships,* R. A. Fortey and R. H. Thomas, eds. Chapman & Hall, London.
3. **Dohle, W. 2001.** *Ann. Soc. Entomol. Fr. (N.S.)* **37**(1–2): 85–103.
4. **Friedrich, M., and D. Tautz. 1995.** *Nature* **376:** 165–167.
5. **Boore, J. L., D. V. Lavrov, and W. M. Brown. 1998.** *Nature* **392:** 667–668.

---

[1] Humboldt-Universität Berlin, Germany.

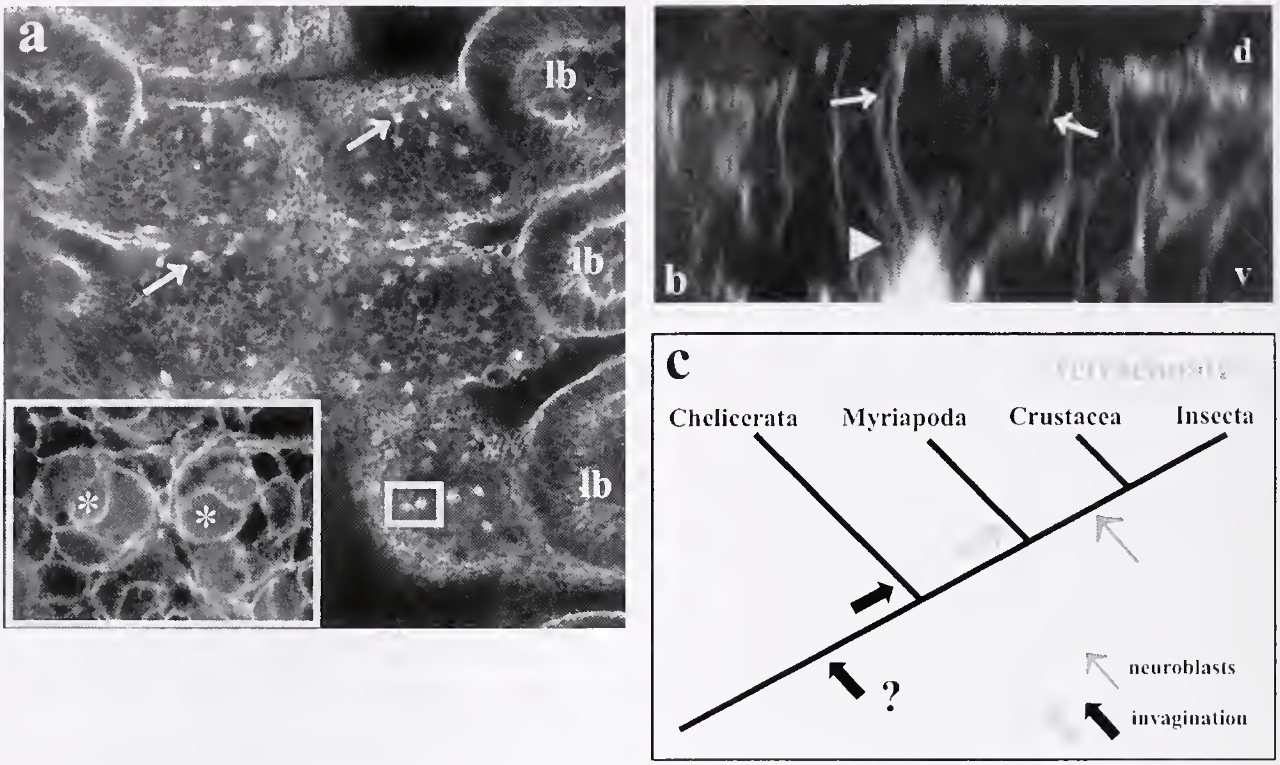

**Figure 1.** *(a) A ventral view of three segments of a phalloidin-labeled horseshoe crab embryo shows numerous fluorescently stained areas, which represent the bundled cell processes of the invagination sites (arrows). The higher magnification inset shows a horizontal section through the bottle-shaped cells of two invagination sites (asterisk). lb = limb bud. (b) One invagination site consisting of a cluster of bottle-shaped cells (arrow). The bundled cell processes extend to the ventral surface (arrowhead). v = ventral, d = dorsal. (c) The probable relationships of the arthropod groups. The "invagination mode" of ganglia formation occurs at least at the base of the chelicerates, whereas the "stem cell mode"* via *neuroblasts is an apomorphic character for the Tetraconata. The myriapods examined to date show a different invagination mode.*

6. **Friedrich, M., and D. Tautz. 2001.** *Ann. Soc. Entomol. Fr. (N.S.)* **37**(1–2): 21–40.
7. **Weygoldt, P. 1985.** Pp. 20–37 in *Neurobiology of Arachnids*, F. G. Barth, ed. Springer, Berlin.
8. **Stollewerk, A., M. Weller, and D. Tautz. 2001.** *Development* **128:** 2673–2688.
9. **Anderson, D. T. 1973.** *Embryology and Phylogeny in Annelids and Arthropods.* Pergamon Press, Oxford.
10. **Brown, G. C., and D. L. Clapper. 1981.** Pp. 268–290 in *Marine Invertebrates.* National Academy Press, Washington, D.C.
11. **Mittmann, B., and G. Scholtz. 2001.** *Dev. Genes Evol.* **211**(5): 232–243.

---

**Reference:** *Biol. Bull.* **203:** 222–223. (October 2002)

# Development of the Lateral Eye of Juvenile *Limulus*

*K. Smith[1], C. Ridings[2], F. A. Dodge[3], and R. B. Barlow[3] (Marine Biological Laboratory, Woods Hole, Massachusetts 02543)*

A horseshoe crab, *Limulus polyphemus*, begins life with approximately 6 ommatidia in each of its lateral eyes. When the animal matures, 15 or 16 molts later, each eye will have close to 1000 ommatidia. New ommatidia are added at each molt (1), and optic nerve fibers must also develop between new ommatidia and the brain if they are to be functional visual units. Therefore, determining the retinal location of all added ommatidia may help us to understand how subunits of the optic nerve (2) develop and how retinotopic maps form in the central visual pathways (lamina and medulla) of the brain (3). We already knew that new ommatidia are added to the anterior edge of the eye (4, 5) but it was not known if they were added elsewhere. In this study we closely examined all regions of the lateral eye before and after the Stage IX molt.

Retinas of two Stage IX specimens of *Limulus*, 3 years of age,

[1] Cornell University.
[2] Occidental College.
[3] SUNY Upstate Medical University.

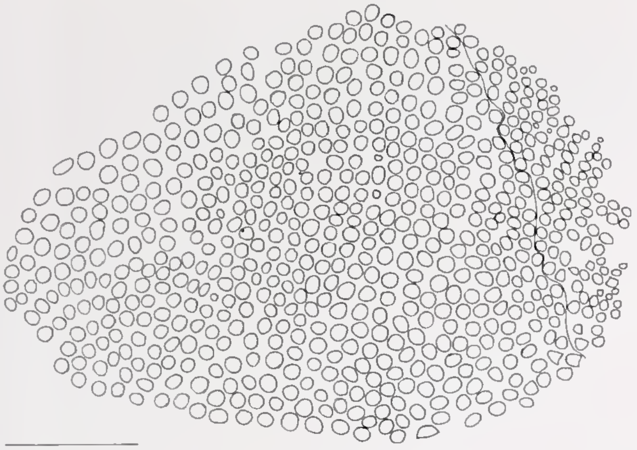

**Figure 1.** *Reconstruction of the retinal mosaic of a Stage X* Limulus *lateral eye. Each circle represents an identified ommatidum. The curved vertical line shows the demarcation between the 529 ommatidia present in the pre-molt Stage IX eye (left of line) and the 116 new ommatida added as the animal molted to Stage X (right of line). The eye measures 2.4 mm in the anterior (right)-posterior (left) direction, and 1.5 mm in the dorsal (top)-ventral (bottom) direction. Scale bar is 500 μm. The overall configuration of the eye is slightly distorted because the curved surface of the eye is projected onto a two-dimensional surface.*

were scarred with a sharp metal needle. The scars, placed along the anterior and ventral edges and at five central locations in August of 2001, would serve as landmarks for assessing the growth of the retina when the animal molted to Stage X. Ommatidia in every scar appeared damaged, and the pigmented tissue often clung to the scarring needle when it was withdrawn. After the scarring, the juveniles were maintained under natural diurnal lighting in a shallow seawater trough (40 cm × 50 cm; 10 cm water depth; 2 cm sand depth) at the Marine Biological Laboratory, Woods Hole, Massachusetts. In May of 2002 both animals molted.

We studied the development of the eyes by viewing the post-molt animals and molted carapaces with a Nikon SMZ-2T dissecting microscope. In spite of the trauma incurred by the deep scarring, the cornea and ommatidial array of the post-molt animal appear normal, as do most of the individual ommatidia. A few ommatidia where we expected scars appear stunted, but we have not investigated these areas anatomically because we do not want to sacrifice the animals.

Although scars were not readily apparent in the post-molt animal, we observed that naturally occurring patterns of ommatidia are retained from the pre-molt animal. Thus we could identify all ommatidia in the post-molt animal that were also present in the molt. We used the patterns, together with fragments of retinal pigments that remained inside the cornea of the molt (a result of scarring), as landmarks to completely reconstruct the right eye of a Stage IX molt (prosomal width, 30 mm). Using this reconstruction of the molt as a base, we added to it every ommatidium in the Stage X post-molt animal (prosomal width, 37 mm) that was not present or distinguishable in the molt (Fig. 1).

A thorough examination of the retinal arrays of the molt and post-molt animal revealed 529 ommatidia in the Stage IX eye (molt) and 645 ommatidia in the Stage X eye (post-molt animal). The 529 ommatidia of the Stage IX eye may be an underestimate because we were conservative in identifying corneal lens facets along the most anterior edge of the molt (Stage IX). Thus 116 new ommatidia, at most, were added in about five vertical columns at the anterior edge of the eye. These new ommatidia are smaller (diameter, 13–35 μm) than older ones (diameter, 65–80 μm), now located in the medial and posterior parts of the eye. A partial reconstruction (not shown) of the lateral eye of the second animal before (Stage IX; prosomal width, 29 mm) and after molting (Stage X; prosomal width, 37 mm) supports these findings. Even though the entire eye of this animal was not reconstructed, all ommatidia near the periphery of the eye and the relative positions of all scars were completely accounted for.

The eye grows asymmetrically. As Waterman (1) noted, the eye grows more in width than in height. We measured a 33% increase in width and a 15% increase in height. The greater increase in width is accounted for by new ommatidia added to the anterior edge together with an increase in ommatidial diameter. The growth of ommatidia is also asymmetric. Ommatidia in medial and posterior regions of the eye of the molt increased 15% in diameter, while those in the anterior portion increased 25% or more. Because no ommatidia are added to the dorsal or ventral parts of the eye, the increase in eye height results only from an increase in ommatidial diameter. Indeed the number of ommatidia in the vertical direction (26 ommatidia) is the same as that of adults (2, 3), indicating that at least after Stage IX changes in view in the vertical direction are complete.

Our reconstructions confirm previous findings that relatively small ommatidia are added at the anterior edge in vertical columns (4, 5). They also show conclusively that ommatidia are added only at the anterior edge. Waterman's (1) original conclusion, that the eye grows by adding ommatidia at the posterior edge, is in error.

Because the lateral eyes of the horseshoe crab grow by adding ommatidia to the anterior edge, the animal's view of the world changes dramatically as it matures from a Stage 1 trilobite (~6 ommatidia) to an adult (~1000 ommatidia). At the Stage IX molt, over 100 small ommatidia are added to the anterior edge, and the existing ommatidia increase in size. After molting, the optic axes of the ommatidia change, and an increasing percentage of ommatidia "look" posteriorly (5). How the brain accommodates optic nerve fibers from new ommatidia, and how soon after addition new ommatidia begin sending visual information to the brain, remain to be determined.

Supported by grants from the National Science Foundation, National Eye Institute, and the National Institute of Mental Health. K. Smith and C. Ridings received REU Fellowships from the National Science Foundation.

## Literature Cited

1. **Waterman, T. H. 1954.** *J. Morphol.* **54:** 125–158.
2. **Snodderly, D. M., and R. B. Barlow. 1970.** *Nature* **227:** 284–286.
3. **Chamberlain, S. C., and R. B. Barlow. 1982.** *J. Neurophysiol.* **48:** 505–520.
4. **Marler, J. J., R. B. Barlow, L. Eisele, and L. Kass. 1983.** *Biol. Bull.* **165:** 541.
5. **Meadors, S., C. McGuiness, F. A. Dodge, and R. B. Barlow. 2001.** *Biol. Bull.* **201:** 272–274.

**Reference:** *Biol. Bull.* **203:** 224–225. (October 2002)

# Visual Behavior of Juvenile *Limulus* in Their Natural Habitat and in Captivity

*C. Ridings*[1], *D. Borst*[2], *K. Smith*[3], *F. Dodge*[4], *and R. Barlow*[4] *(Marine Biological Laboratory, Woods Hole, Massachusetts 02543)*

*Limulus polyphemus,* the common horseshoe crab, inhabits coastal estuaries of North America and the Yucatan peninsula. It has been an admirable model for vision research because its relatively simple visual system has marked functional similarities to those of many species, including humans (1). Adult male horseshoe crabs use their lateral eyes to find mates (2), and their ability to see underwater has been studied in the estuaries where mating occurs (3, 4, 5). However, studies of the visually guided behavior of adults in captivity have not been successful (R.B., pers. obs.). On the other hand, juvenile horseshoe crabs do exhibit visually guided behavior under laboratory conditions (6). Here we report a comprehensive investigation into the visually guided behavior of juveniles, both in their natural habitat and in captivity.

Between May 15 and June 30, 2002, we studied the behavior of juvenile specimens of *Limulus* in Nantucket Sound, along the Western shore of the North Monomoy Island Refuge in Chatham, Massachusetts. The sand bars on the tidal flats of the island are a protected natural habitat for both juveniles and adults; the waters are relatively clear and calm. Juveniles were most active near shore at depths ranging from 30–120 cm, usually during the late afternoon and evening. In testing the visually guided behavior of a juvenile horseshoe crab, we followed the procedure of a previous study of such behavior in adults (4). First we determined its direction of travel along the bottom and then placed a small object directly in front of it at a distance of 20–40 cm. We used three cylindrical acrylic plastic objects (diameter 7.6 cm, height 5.2 cm): one was painted matte black, one matte gray, and one remained unpainted. Because these objects were designed for experiments with adults, their size was reduced proportionally for small juveniles (prosomal width range = 2–14 cm). We filmed 713 trials, defined as an approach of an animal to an object, on a Sony camcorder (model DCR-PC110 NTSC; underwater housing by Gates Underwater Products) and then analyzed the behavior with a computer.

All videotaped trials were analyzed with an eMac computer using iMovie software (copyright 2001–2002 Apple Corporation). We categorized each trial as representing one of three behaviors: "hit," an animal moves directly toward an object and makes direct contact with it; "pass-by," an animal passes by an object without changing direction; and "turn-away," an animal turns away from an object. For turn-away behavior, we measured the distance from the center of the object to the middle of the animal at the point where it turned. For the pass-by behavior, we measured the distance of closest approach to the object. Figure 1 (top) shows percentages for all three behaviors.

We performed a similar set of experiments in the laboratory, where we observed the behavior of 10 juveniles in a large trough (130 × 62 cm; the water 6.5 cm deep). The bottom of the trough was covered with a thin fiberglass mesh screen, giving the crabs traction for walking and righting themselves if overturned. The crabs were maintained in ambient diurnal lighting in a separate trough before being placed in the experimental trough, where we used diffuse overhead illumination to simulate, as closely as possible, an overcast day. The same three objects used in the ocean observations were now placed in the center of the trough and rotated every 15 min. The crab's behavior was filmed and analyzed, as in the ocean trials. We defined a behavioral event as a crab entering the camera's field of view (51 × 74 cm). We filmed 797 trials, mostly in the evening hours when the crabs were most active. Figure 1 (bottom) gives percentages for the laboratory trials.

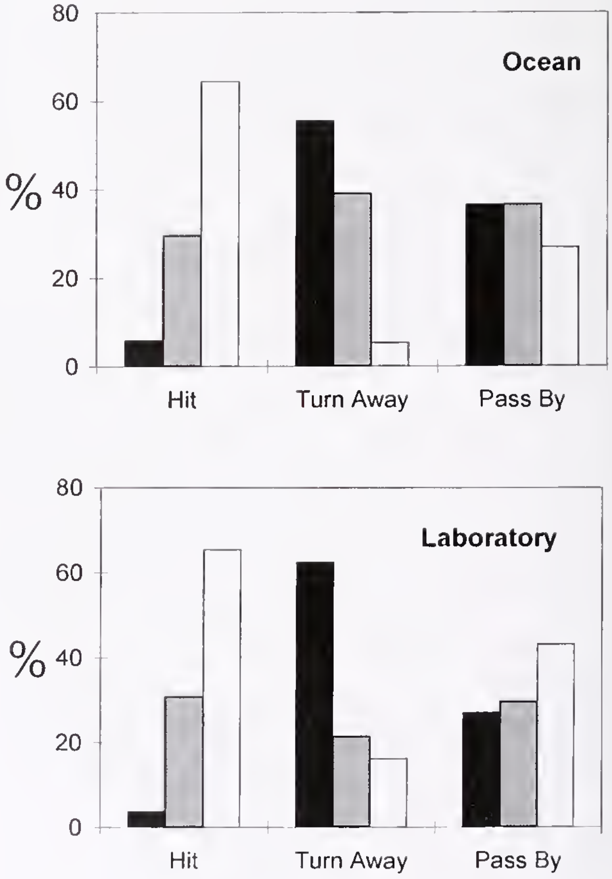

**Figure 1.** *Percentages of behavioral responses to black, gray, and clear objects in the ocean and in the laboratory.*

---

[1] Occidental College.

[2] Reed College.

[3] Cornell University.

[4] SUNY Upstate Medical University.

The animals behaved about the same toward each of the three objects in the ocean and in the laboratory (Fig. 1). In both settings, most animals hit the clear object and turned away from the black and gray objects. The juveniles appear to be avoiding objects with high visual contrast; the higher the contrast, the greater the avoidance. Because juveniles avoided black objects more than the lower contrast gray and clear ones, we conclude that these are visually guided behaviors. In short, juveniles exhibit functional vision.

Averaging the distances of turn-away events and pass-by events reveals the differential effects of contrast on the crab's behavior. For example, crabs in the ocean turned away from the black and gray objects at average distances of 16.2 ± 6.4 (SD) cm and 14.9 ± 6.5 cm, respectively, indicating that the black object can be seen at a greater distance; that is, it is more visible. Likewise, the average distance of closest approach in pass-by events was 15.0 ± 5.7 cm and 11.8 ± 4.1 cm for the black and gray objects respectively, indicating that juveniles will pass closer to the lower contrast gray object without responding to it.

The width of the eyes (~4.0 mm) of the juveniles we tested (prosomal width 4.6 cm) was about 25% of that of an adult eye (15–20 mm), and juvenile eyes have fewer and smaller ommatidia (7). Even though the visual system of juvenile crabs is not fully developed, we show here that they have functional vision. In particular, juvenile crabs have contrast-sensitive vision, as do adult crabs. Adult females avoid objects of high contrast, whereas adult males are attracted to them; thus juveniles behave like adult females. As the animal grows, the eyes mature in parallel with growth of the brain and organization of the brain's map of the visual world. Because *Limulus* juveniles can see and distinguish contrast, they may serve as a useful alternative model for understanding not only how the brain processes visual information, but also how behavior changes during the developmental process.

Supported by grants from the National Science Foundation, National Eye Institute, and the National Institutes of Mental Health. C. Ridings and K. Smith received REU Fellowships from the National Science Foundation. We thank the Monomoy National Wildlife Refuge, Morris Island, Chatham, Massachusetts, and Debbie and Hoyt Ecker for their generosity.

## Literature Cited

1. **Ratliff, F. 1974.** *Studies on Excitation and Inhibition in the Retina.* The Rockefeller University Press, New York.
2. **Barlow, R. B., L. C. Ireland, and L. Kass. 1982.** *Nature* **296:** 65–66.
3. **Powers, M. K., R. B. Barlow, and L. Kass. 1991.** *Visual Neurosci.* **7:** 179–189.
4. **Herzog, E. D., M. K. Powers, and R. B. Barlow. 1996.** *Visual Neurosci.* **13:** 31–41.
5. **Krutky, M. A., J. Atherton, S. Smith, F. Dodge, and R. Barlow. 2000.** *Biol. Bull.* **199:** 178–180.
6. **Errigo, M., C. McGuiness, S. Meadors, B. Mittman, F. Dodge, and R. Barlow. 2001.** *Biol. Bull.* **201:** 271–272.
7. **Smith, K., C. Ridings, F. Dodge, and R. Barlow. 2002.** *Biol. Bull.* **203:** 222–223.

---

**Reference:** *Biol. Bull.* **203:** 225–227. (October 2002)

# Effects of Individual Size on Pairing in Horseshoe Crabs

*Dianne N. Suggs*[1]*, Ruth H. Carmichael, Sara P. Grady, and Ivan Valiela (Boston University Marine Program, Marine Biological Laboratory, Woods Hole, Massachusetts 02543)*

During late spring and early summer, spawning horseshoe crabs (*Limulus polyphemus*) can be readily observed along the beaches of Cape Cod, Massachusetts. Males use specially modified claws to clasp onto the carapace of females (1). This pairing is called amplexus. Amplexed pairs attract unattached males that cluster around them during spawning. These satellite males are frequently successful in fertilizing a portion of the female's eggs (2). What determines which males amplex with females, while others do not, has not been clearly defined. Numerous studies have investigated factors thought to influence pairing in *L. polyphemus*, such as visual (3, 4) and chemical cues (5, 6) and body size. Studies regarding how body size may affect pairing have generated conflicting results—some research suggests size-based pairing is random (7, 8), while other work has found a weak relationship between body size and mate selection (2, 9).

In this study we examined the relationship between male and female body size and its influence on mate selection for amplexus in *L. polyphemus* in field and laboratory studies. To describe the reproductive categories within a horseshoe crab population during the spawning season, we carried out field surveys within a known spawning area along the eastern shore of Pleasant Bay, Cape Cod. Field surveys were conducted 15 May–15 June in 2001 and 25 June–25 July in 2002. The 2001 survey spanned the peak of the spawning season; the 2002 survey spanned only the latter part of the spawning season. We collected data regarding sex, spawning state, and size (prosomal width) from 56 pairs along 125 m of beach in 2001, 84 pairs throughout the bay in 2002, and an additional 761 crabs, including single males and females and satellite males.

To determine whether pairing was mediated by horseshoe crab size, we first compared sizes of paired crabs in the field; and second, we collected animals from the field for laboratory studies on mate selection. Experimental studies were conducted in 140 cm × 90 cm × 40 cm recirculating aquaria, containing 4 cm of native beach sand. Trials were performed by pairing a single male (155–215 mm prosomal width) with 2, 3, 4, or 7 females (190–282 mm). Each male was used in three trials, and trials were allowed to run for 12 h or until amplexus was achieved. We examined the effect of number of individuals in these trials and found that density did not affect success of pairing. Similarly, there was no difference between the trials in which males were used more than once and those in which males were used once. Hence, all data were pooled in Fig. 1C.

---

[1] Brown University, Providence, RI 02912.

The majority of animals surveyed in intertidal areas during the spawning season were single males (79%), followed by amplexed pairs (18%), single females (2%), and satellite males (1%) (Fig. 1A). Most males were unpaired and most females were paired. These results are consistent with observations that unpaired males tend to gather on the beach, while females tend to remain offshore unless approaching the beach to spawn (4, 9, 10). Adult females are larger than adult males, which is characteristic of the species (1). In addition, the mean prosomal width of paired females was larger than that of paired males, suggesting that males may tend to pair with females having a larger prosomal width than their own (Fig. 1A).

To ascertain whether there was size-based mate selection in amplexed pairs in the field, we compared the prosomal widths of paired males and females (Fig. 1B) measured in the field surveys done in the two years. There was no significant difference in size of paired males and females sampled in 2001 and 2002. This finding implies that there were also no differences in pairs observed during the peak of spawning compared to those sampled post-peak (Males: $t = 1.17$, $P = 0.24$; Females: $t = -0.67$, $P = 0.50$). Hence, data were combined in Fig. 1B. The aggregated data indicated no significant size-based selective mating across the full range of sizes observed ($R^2 = 0.01$, df = 83, $P > 0.05$). Pairings did not, however, occur between the smallest [Fig. 1A, B (area to the lower left of ———)] or largest [Fig. 1A, B (area to the lower right of ······)] males and females in the general field population. These results suggest that some of the smallest animals may not have reached sexual maturity and that some size selectivity may occur among larger males. In addition, size reversals among pairs (females having a smaller prosomal width than their male partner) were rarely observed (2%).

To further test the effect of size on mate selection, we compared the size of males to the size of the females chosen for amplexus during laboratory trials (Fig. 1C). In 35 trials, small males (154–170 mm) tended to select the smallest females offered (regardless of the females' absolute size). Intermediate-sized males (171–190 mm) tended to prefer the smallest or intermediate-sized females, and the only large male (215 mm) to accomplish amplexus chose the largest female offered. Males did not amplex with the first female they encountered and took at a minimum 35 min to pair. Overall, small and medium-sized males were more successful in achieving amplexus than large males (Fig. 1C). These results suggest that some size-based mate selection may occur at the largest and smallest sizes only, as observed in the field, and that male size may also affect success of amplexus.

To further examine whether male size affects the likelihood of amplexus in the field, we compared the success of males of different sizes tested in the laboratory to those observed in the field. The percent of amplexus as a function of size was similar for both field and laboratory animals (Fig. 1D), where smaller male crabs (up to 180 mm) were generally more successful than larger crabs.

In sum, for the majority of male and female prosomal widths, size did not appear to affect mate selection. At the largest sizes, however, males tended to prefer larger-sized females and were generally less successful in achieving amplexus. Hence, our results are consistent with previous reports that selection is not size-based

A)

| Sex | Pairing category | N = | Size Range (mm) |
|---|---|---|---|
| M | Paired | 84 | 140-204 |
| M | Single | 737 | 140-250 |
| M | Satellite | 8 | 170-203 |
| F | Paired | 84 | 180-264 |
| F | Single | 18 | 194-282 |

B)

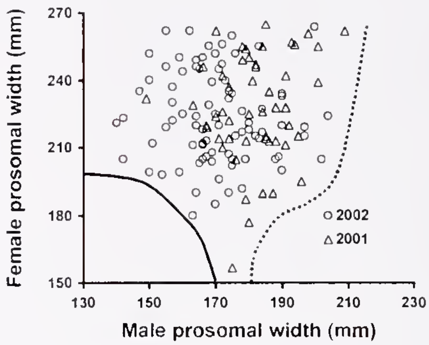

C)

| | Size selection | | | Success | |
|---|---|---|---|---|---|
| | Female size | | | | |
| Male size (mm) | Small | Medium | Large | No. of trials | % ending in amplexus |
| Small (154-170) | 6 | 1 | 1 | 15 | 53 |
| Medium (171-190) | 2 | 2 | 1 | 9 | 56 |
| Large (191-215) | 0 | 0 | 1 | 11 | 9 |

D)

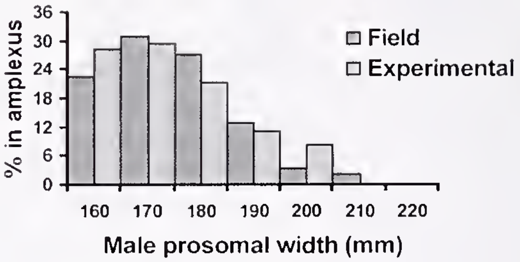

**Figure 1.** *(A) Sex (M = male, F = female), pairing category, number, and size range of sexually-mature horseshoe crabs observed during the spawning season in Pleasant Bay. (B) Prosomal widths of male and female crabs in amplexus measured in two years. Solid line indicates approximate size boundary below which most crabs are not sexually mature. Dashed line indicates upper size boundary of paired males. (C) Number of females of three sizes selected by males of three sizes for amplexus in laboratory trials, number of trials, and success rate of amplexus for the three sizes of males. (D) Size distribution of males in amplexus among experimental and field observations.*

(7, 8) and also with reports that some size-based selection may occur (2, 9). Size selectivity and apparent random pairing can both occur, but do so within different size ranges.

This research was supported by NSF Research Experience for Undergraduates (OCE-0097498) and by the Friends of Pleasant Bay. Special thanks to Emily Gaines for her assistance in the field and to Jason Norberg for his technical assistance.

## Literature Cited

1. **Sekiguchi, K. H. 1988.** *Biology of Horseshoe Crabs*. Tokyo, Science House Press.
2. **Brockmann, H. J. 1990.** *Behaviour* **114:** 206–220.
3. **Barlow, R. B., L. C. Ireland, and L. Kass. 1982.** *Nature* **296:** 65–66.
4. **Barlow, R. B. Jr., M. K. Powers, H. Howard, and L. Kass. 1986.** *Biol. Bull.* **171:** 310–329.
5. **Brockmann, J. H. 1996.** *Ethology* **102:** 1–21.
6. **Hassler, C., and H. J. Brockmann. 2001.** *J. Chem. Ecol.* **27:** 2319–2335.
7. **Pomerat, C. M. 1933.** *Biol. Bull.* **64:** 243–252.
8. **Loveland, R. E., and M. L. Botton. 1992.** *Anim. Behav.* **44:** 907–916.
9. **Cohen, J. A., and H. J. Brockmann. 1983.** *Bull. Mar. Sci.* **33:** 274–281.
10. **Rudloe, A. 1980.** *Estuaries* **3:** 177–183.

---

**Reference:** *Biol. Bull.* **203:** 227–228. (October 2002)

# Circadian Rhythms in Locomotor Activity of Juvenile Horseshoe Crabs

*Douglas Borst*[1] *and Robert Barlow*[2] *(Marine Biological Laboratory,
Woods Hole, Massachusetts 02543)*

The American horseshoe crab, *Limulus polyphemus*, is a classic model for vision research. Not only are the lateral eyes of *Limulus* relatively simple, but they share many processes with the eyes of more advanced animals, including humans (1). The eyes of *Limulus* also exhibit a remarkable circadian rhythm: they become nearly 1,000,000-fold more sensitive at night, accommodating for the roughly 1,000,000-fold decrease in ambient light (2). Is visual sensitivity the only process controlled by a circadian oscillator in *Limulus*? Other marine animals have been shown to possess circadian as well as circatidal rhythms in locomotor activity (3). Does *Limulus* exhibit a rhythm in locomotor activity? Past attempts in this laboratory to determine the locomotor activity cycle of adult horseshoe crabs were largely unsuccessful, with only one of more than 100 crabs tested exhibiting circadian activity in darkness. Here we report a study to determine the locomotor activity rhythm of juvenile crabs. We found that most juveniles were nocturnally active under natural cyclic lighting, and that some maintain rhythmic activity in constant darkness.

We assessed the locomotor activity of 10 juveniles maintained in isolation. The animals were collected in the environs of Woods Hole, Massachusetts, and were placed in a 39 × 49-cm tank (water depth: 8 cm) filled with about 2 cm of sand. The tank was placed in a lightproof box with a porthole pressed directly against a laboratory window to provide natural light. The tank was continuously illuminated with infrared light sources (Sony: Model HVL-IRC) so that we could observe the activities of the animals day and night with a video camera (SeaView Video Technology, Inc.) sensitive to infrared light. Using Snappy Video Snapshot (Play, Inc.) hardware and SnapRecorder (SB Software) software, we took one picture per minute and measured activity with the following algorithm: if an animal moved onto an imaginary line drawn across the tank, it scored a point; if the animal turned approximately 120° or moved along the line at least one-half body length, it scored a point; if an animal remained in the same place on the line, crossed it without being caught on camera, or moved less than one-half body length along the line, no points were awarded. When collected in 30-min bins, activity scores ranged from 0 to 36. We considered scores of 9 or more to represent significant locomotor activity. When kept in constant darkness, the group was cyclically active with 77% of their daily activity occurring during their subjective night (data not shown). The period of the endogenous rhythm was about 23.5 h, which is less than 24 h, indicative of a circadian rather than a circatidal clock.

Did the circadian oscillators of all 10 crabs have the same period? Frame-by-frame inspection indicated that after a prolonged period of inactivity, one crab would become active first and was soon followed by the rest. We could not differentiate between crabs, so we do not know if an individual crab possessed the short period of 23.5 h and thus was an "early riser" who "woke up" all the rest. To answer this question we monitored the locomotor activity of five crabs separated into individual small plastic pens 15 cm in diameter. All five were predominantly active at night under cyclic lighting, but only two exhibited clear rhythmic activity in constant darkness.

Figure 1 plots the locomotor activity of an individual crab during 4 days in diurnal lighting and 9 days in constant darkness. The crab's activity was observed for 1-h periods and analyzed with a different algorithm: active 0–6 min, score = 0; active 6–49 min, score = 1; active 50–69 min, score = 2. Figure 1 shows activity with a score of 2. Under diurnal lighting, the crab was nocturnally active; 91% of its activity occurred during the night. When placed in constant darkness, the crab remained cyclically active; 72% of its activity occurred during its subjective night. The endogenous rhythm appears to be drifting with a period of less than 24 h, but no firm conclusions can be drawn about the length of the period because we analyzed activity in 1-h bins. We conclude that circadian oscillators in *Limulus* modulate both visual sensitivity and locomotor activity. It is not known

---

[1] Reed College, Portland, Oregon.

[2] SUNY Upstate Medical University, Syracuse, New York.

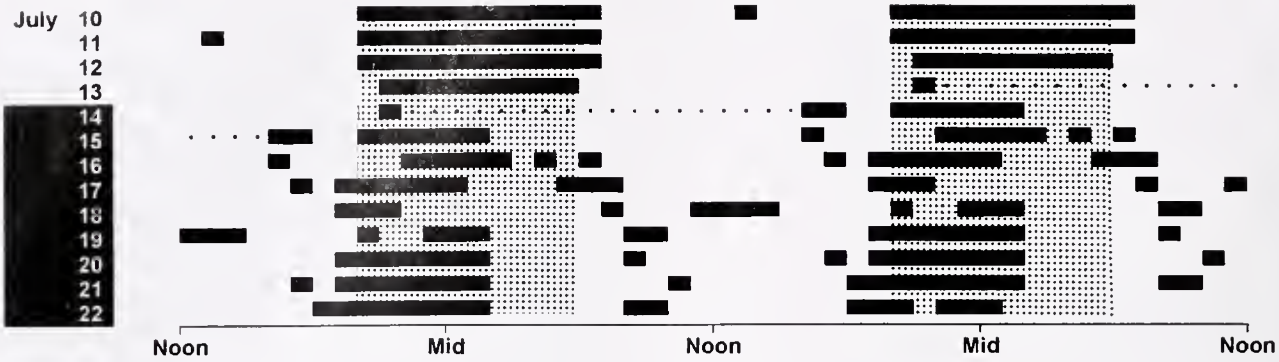

**Figure 1.** *Locomotor activity of a juvenile horseshoe crab maintained first in natural cyclic lighting and then in constant darkness. The data are double-plotted to emphasize periodic events. Black bars indicate periods of activity; large dots indicate no data collection. Stippled regions indicate the solar night (sunset to sunrise). The juvenile was exposed to cyclic lighting from July 10 to July 14, when the porthole was closed to produce constant darkness until July 22.*

whether these processes are modulated by one or more circadian oscillators.

This research was funded by grants from the National Science Foundation and the National Institutes of Health. We would like to thank Rick Sanger for helping us capture still images from video, and Corey Ridings and Kalmia Smith for help in taking care of the animals.

## Literature Cited

1. **Ratliff, F. 1974.** *Studies of Excitation and Inhibition in the Retina.* Rockefeller University Press, New York.
2. **Barlow, R. B. Jr. 1988.** *Invest. Ophthalmol. Visual Sci.* (Suppl.) **29:** 350.
3. **Palmer, J. D. 1995.** *Biological Clocks in Marine Organisms: The Control of Physiological and Behavioral Tidal Rhythms.* John Wiley & Sons, New York.

---

**Reference:** *Biol. Bull.* **203:** 228–230. (October 2002)

## Stable Isotopic Evidence for Changing Nutritional Sources of Juvenile Horseshoe Crabs

*Emily F. Gaines*[1], *Ruth H. Carmichael, Sara P. Grady, and Ivan Valiela (Boston University Marine Program, Marine Biological Laboratory, Woods Hole, Massachusetts 02543)*

Horseshoe crabs, *Limulus polyphemus*, are important predators in shallow environments (1). The feeding habits of adult horseshoe crabs have been examined (2), but the natural diet of juveniles has not. Juvenile crabs grow through 16 to 17 instars (3), and the increases in size during development suggest that nutritional sources may change (4). We identified likely components of juvenile diets using $\delta^{13}C$ and $\delta^{15}N$ stable isotope signatures of juvenile horseshoe crabs and their potential prey species.

To obtain samples for isotope analyses, we collected juvenile crabs from intertidal sand flats at Nauset Beach, Massachusetts, during June and July 2002. Instars of crabs were determined based on data of Carmichael *et al.* (unpublished) on size of juveniles at each instar. To determine the size of juveniles, we measured the widest portion of the crab prosoma to the nearest 0.1 mm using vernier calipers. To assess position of juveniles within food webs, we collected potential prey items by hand and by sieving sediment from 0.3 m × 0.3 m × 0.1 m grabs from intertidal areas.

All specimens were dried at 60 °C, ground, and sent to the University of California—Davis Stable Isotope Facility to measure $\delta^{13}C$ and $\delta^{15}N$ signatures of crabs and potential prey species by mass spectrometry. To estimate maximum possible contributions of different taxa of prey items to the diet, we applied a linear mixing model (5) to the isotope data.

$\delta^{15}N$ and $\delta^{13}C$ of horseshoe crabs changed as crabs grew (Fig. 1a). Signatures of the first instar juveniles are likely inherited from the parent, since first instars live off yolk made by the parent (6). The signatures of first instars were enriched in $\delta^{15}N$ by approximately 0.32‰ and depleted in $\delta^{13}C$ by approximately 2.8‰ relative to the average adult signature. These results extend, to an invertebrate, the range of results from studies on birds, which show yolk to be enriched in $\delta^{15}N$ and depleted in $\delta^{13}C$ relative to the parent signature (7).

Once juvenile crabs reached the second instar, the carbon and nitrogen signatures changed (Fig. 1b). This change in isotope signature coincides with the onset of assimilatory capacity in the digestive tract (3) and with the start of active burrowing behavior (8). Juveniles in instars 2–3 that gained assimilatory capacity may feed on sedimentary organic matter and meiofauna (lower dotted circle, Fig. 1b), and their signature moved steeply to the lower right of Fig. 1b. Eventually, these juveniles became large enough to eat smaller crustaceans and polychaetes on the sediment (right-hand dotted oval, Fig. 1b). As juveniles grew beyond the third instar, their $\delta^{15}N$ signatures became heavier, up to instar 11. The shift in $\delta^{15}N$ after instar 3 confirms the usual finding that, as consumers increase in size, they move up trophic steps because they seek larger prey; and larger prey characteristically show heavier signatures (4). The $\delta^{15}$N signatures of adults remain similar to instar 11, and their offspring then start the isotopic cycle again.

---

[1] University of Virginia, Charlottesville, VA.

As the horseshoe crab juveniles grew, they evidently made use of mixed diets. To roughly quantify the proportion of different items contributing to the mixed diet, we calculated possible maximal contributions to diets of the different instars (Fig. 1c). For instars 2–3, benthic and suspended matter made up the diet. As crabs went through instars 5–11 (Fig. 1b and 1c), the contribution of polychaetes increased markedly; and molluscs contributed less than a quarter of the diet, considerably less than reported for adults (2).

The change in $\delta^{15}$N values according to life cycle of horseshoe crabs depends on the size of the crab and their prey. The changes in $\delta^{13}$C, in contrast, tell us that as horseshoe crabs grow, they make remarkable shifts in food webs. Judging by the $\delta^{13}$C signature, the instar 2 juveniles probably assimilated food from organisms that derived their nutrition in part from phytoplankton and macroalgal food webs, which have $\delta^{13}$C values of about −21‰ and −17‰, respectively (9), and in part from a food web based on *Spartina alterniflora*, the salt marsh cordgrass, which has a $\delta^{13}$C of −13‰ (10) (vertical gray lines in Fig. 1b). By instar 3, the juveniles largely shifted to prey that depended primarily on *Spartina* alone. This dependency on the salt marsh-supported food web continued until instar 11. Adult signatures markedly changed from those of juveniles, again turning to the phytoplankton- and macroalgae-based parts of the food web. This pattern likely exists because juveniles largely eat small benthic polychaetes, amphipods, and isopods, whereas adults consume more bivalves (2), which are suspension feeders assimilating phytoplankton.

The isotopic data showed remarkable shifts in the diet and food web position of juvenile horseshoe crabs as they grow. Juvenile diets changed on the basis of prey size, as well as shifting from a food web based on phytoplankton to one supported by salt marsh producers. The crabs then returned to the phytoplankton-based food web as adults. These shifts in position in the food web reflect the changing array of prey consumed by horseshoe crabs of dif-

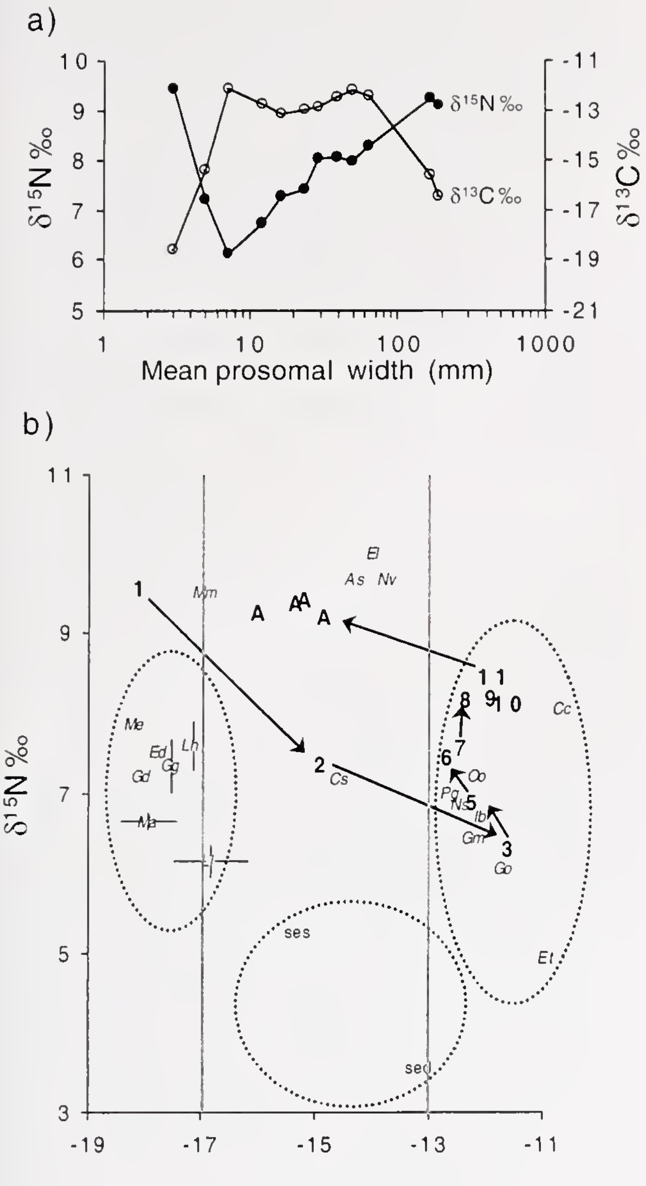

c)

| Prey Category | Instar 2 | 3 | 5 | 6 | 7 | 8 | 9 | 10 | 11 |
|---|---|---|---|---|---|---|---|---|---|
| Bivalves | - | - | 11 | 22 | 20 | 22 | 16 | 11 | 17 |
| Gastropods | - | - | 14 | 27 | 24 | 27 | 20 | 13 | 21 |
| Crustaceans/ Polychaetes | - | - | 44 | 56 | 63 | 79 | 87 | 84 | 95 |
| Benthic POM | 21 | <100 | 100 | 100 | 99 | 74 | 77 | 64 | 70 |
| Suspended POM | 100 | <100 | 23 | 42 | 34 | 31 | 18 | 9 | 16 |

**Figure 1.** *(a) Change in $\delta^{15}$N and $\delta^{13}$C signatures of the horseshoe crab with increasing prosomal width. Data points correspond to the sequence of instars; 1–3, 5–11, and two adult samples, respectively. Where there is no visible standard error for the mean prosomal widths, the error is smaller than the symbol. (b) $\delta^{15}$N and $\delta^{13}$C signatures of horseshoe crabs compared with signatures of potential prey items. Horseshoe crab data points are labeled by instar number until adult. (A) Prey items are labeled by abbreviation: Bivalves*—Mercenaria mercenaria* *(Mm)*, Mytilus edulis *(Me)*, Ensis directus *(Ed)*, Geukensia demissa *(Gd)*, Mya arenaria *(Ma)*, Gemma gemma *(Gg)*; *Gastropods*—Lunatia heros *(Lh)*, Littorina littorea *(Ll)*; *Amphipods*—Caprella *spp.* (Cs)*, Gammarus oceanicus *(Go)*, Gammarus mucronatus *(Gm)*; *Isopods*—Edotea triloba *(Et)*, Chiridotea coeca *(Cc)*, Idotea baltica *(Ib)*; *Polychaetes*—Orbinia ornata *(Oo)*, Neanthes succinia *(Ns)*, Pectinaria gouldii *(Pg)*, Ampharete *spp.* (As)*, Eteone longa* *(El)*, Nereis virens* *(Nv)*; *Benthic particulate organic matter (POM)—sediment (sed); Suspended POM—seston (ses). An asterisk (*) indicates prey items excluded from mixed diet analysis. In cases where multiple samples were pooled, signatures were averaged and error bars are shown. Circles, from left to right, signify dietary groups: molluscs, POM, crustaceans/polychaetes. Grey lines represent expected $\delta^{13}$C values for food webs based on macroalgae (−17‰) and* Spartina *(−13‰). (c) Estimated maximum percentage of potential prey items in the mixed diet of juvenile horseshoe crabs at Nauset Beach, Massachusetts. Percentages were calculated using a linear mixing model (5).*

ferent instars and demonstrate that this species depends on widely different food webs. Conservation of horseshoe crab populations, therefore, depends on suitable management that assures both a phytoplankton and macroalgal source, as well as continued accessibility of salt marsh habitats.

This work was supported by a grant from the Friends of Pleasant Bay and a grant from the National Science Foundation REU (OCE-0097498). Many thanks to Dianne Suggs for field assistance and to the Cape Cod National Seashore for providing access to Nauset Beach. Thanks also to Paulina Martinetto, Mirta Teichberg, and Brad Williams for lab assistance.

## Literature Cited

1. **Botton, M. L. 1984.** *J. Mar. Res.* **42:** 139–161.
2. **Botton, M. L., and J. W. Ropes. 1989.** *Bull. Mar. Sci.* **45:** 637–647.
3. **French, K. A. 1979.** Pp. 61–71 in *Biomedical Application of the Horseshoe Crab* (Limulidae), E. Cohen *et al.*, eds. Alan R. Liss, New York.
4. **Valiela, I. 1995.** *Marine Ecological Processes.* Springer-Verlag, New York.
5. **Phillips, D. L. 2001.** *Oecologia* **127:** 166–170.
6. **Jegla, T. C. 1982.** Pp. 83–101 in *Physiology and Biology of Horseshoe Crabs; Studies on Normal and Environmentally Stressed Animals,* J. Bonaventura, C. Bonaventura, and S. Tesh, eds. Alan R. Liss, New York.
7. **Hobson, K. A. 1995.** *Condor* **97:** 752–762.
8. **Rudloe, A. 1981.** *Bull. Mar. Sci.* **31:** 125–133.
9. **McClelland, J., and I. Valiela. 1998.** *Mar. Ecol. Prog. Ser.* **168:** 259–271.
10. **Peterson, B. J., R. W. Howarth, and R. H. Garritt. 1985.** *Science* **227:** 1361–1363.

**Reference:** *Biol. Bull.* **203:** 231–232. (October 2002)

# Acetylcholine Mediates Excitatory Input to Chromatophore Motoneurons in the Squid, *Loligo pealeii*

*Michael Smotherman (UCLA Department of Physiological Sciences, Los Angeles, California 90095-1606)*

All cephalopods save the Nautilidae possess the ability to rapidly modify their body coloration (1). Cephalopod color patterning probably serves foremost as camouflage, yet many also use species-specific color patterns for communication (1–3). Color patterning in cephalopods is achieved by the synchronized neural manipulation of many thousands of small chromatophore organs distributed throughout the skin (4). These chromatophore organs consist of centrally located, pigment-containing cells surrounded by 6–30 radially-arranged muscle fibers (4, 5). Stimulation of chromatophore nerves causes contraction of muscle fibers and thereby chromatophore expansion (6, 7). Motoneurons project uninterrupted to the chromatophores from brain structures known as the chromatophore lobes (8). Anterior chromatophore lobe motoneurons project to chromatophores on the head, arms, and tentacles, while the posterior chromatophore lobe (PCL) motoneurons innervate ipsilateral chromatophores on the fins and mantle. The chromatophore lobes receive their principal inputs from the lateral basal lobes (LBL) and from the contralateral chromatophore lobes (8, 9). Although the physiological role of the LBL in the control of chromatophore activity has been demonstrated (8), neither the pharmacology nor the complexity of the synaptic inputs to the chromatophore lobes has been investigated. The goal of this project was to identify neurotransmitters that can effectively stimulate chromatophore motoneurons located in the PCL of the squid, *Loligo pealeii*.

Pharmacological agents were applied to cell bodies located peripherally in the right or left PCL of intact, unanesthetized male and female squids (8–10 cm mantle length). All experiments were performed in a 500-ml tank of cold (12–15 °C) flowing seawater with a white background. Under these conditions, a squid remains pale in color. The head was restrained against a plexiglass plate with a small hole positioned over the skull, and a small incision was made just above the site where the esophagus exits from the skull. The esophagus and salivary glands were gently displaced, and care was taken not to damage the cephalic aorta. The PCLs could be localized under a dissecting microscope, allowing micropipettes (2–5 $\mu$m tips) to be lowered into the PCL under visual control. A video camera was positioned to record chromatophore activity on the dorsal side of the mantle and fins. Several transmitters suspected of being active in the PCL (2) were tested. Drugs were applied under pressure (Picospritzer II, General Valve Corp.) in concentrations ranging from $10^{-6}$ to $10^{-3}$ $M$ (10–50 picoliters). Most drugs were dissolved in artificial seawater (ASW), but neither ASW nor distilled water elicited chromatophore expansion when applied to the PCL. In some experiments, to confirm the injection site, the vital dye methylene blue was included in the carrier solution.

Of all the drugs tested, only L-glutamate and acetylcholine (ACh) were observed to cause rapid, localized and reproducible chromatophore expansion (Table 1). However, the effects of glutamate were irregular and were often followed by prolonged deactivation of chromatophores over large areas of the mantle.

**Table 1**

*Pharmacological stimulation of squid posterior chromatophore lobe motoneurons*

| | L-Glutamate | ACh | Nicotine | Octopamine | 5-HT | Dopamine |
|---|---|---|---|---|---|---|
| # animals[1] | 20 | 16 | 6 | 5 | 4 | 3 |
| # injections[2] | 65 | 55 | 10 | 15 | 16 | 10 |
| + responses[3] | 16 | 45 | 9 | 0 | 0 | 0 |

[1] Number of animals tested. [2] Number of drug applications; using multiple electrodes and electrode penetrations. [3] Total number of positive responses resulting from pharmacological injections. A positive response was defined as a rapid ($<5$ s onset) and repeatable elicitation of chromatophore expansion.

Because the effects of ACh were more consistent and reproducible, they were explored in greater detail. When a pipette containing $10^{-6}$ $M$ ACh was pushed through the outer capsule of the PCL and into the cellular layer, it was common to see a flickering of chromatophore activity at a localized position somewhere on the ipsilateral mantle. Then, when ACh was applied, many chromatophores around that site would rapidly expand. In every case, chromatophores of multiple colors were observed to expand in response to the injection. Effects typically lasted 30–60 s. The response location, the total area of the mantle to exhibit chromatophore expansion, the duration of the response, and the spread of the response over time were assessed digitally after each experiment and were found to vary with the quantity of solution delivered and the concentration of the drug. ACh injections repeated at the same pipette position elicited similar responses from the same group of chromatophores. Injections of ACh into the neuropil of the PCL or more caudally into the base of the pallial nerve did not elicit chromatophore activity. The ACh agonist nicotine was also tested and was found to be equally effective in generating chromatophore expansion. ACh antagonists have not yet been investigated.

These experiments suggest that ACh may be an important excitatory input to the chromatophore motoneurons in the squid. This conclusion is supported by histochemical evidence that acetylcholinesterase is present in the PCL (10). Whether nicotinic ACh receptors are present on the motoneurons, and whether ACh represents input derived from the LBL or elsewhere in the squid brain, remains to be determined.

This work was supported by a Grass Fellowship.

## Literature Cited

1. **Hanlon, R. T., and J. B. Messenger. 1996.** *Cephalopod Behavior.* Cambridge University Press, Cambridge.
2. **Messenger, J. B. 2001.** *Biol. Rev.* **76:** 473–528.
3. **Moynihan, M. 1985.** *Communication and Noncommunication in Cephalopods.* Indiana University Press, Bloomington.
4. **Boycott, B. B. 1953.** *Proc. Linn. Soc. Lond.* **164:** 235–240.

5. **Florey, E. 1969.** *Am. Zool.* **9:** 429–442.
6. **Florey, E. 1966.** *Comp. Biochem. Physiol.* **18:** 305–324.
7. **Dubas, F., R. T. Hanlon, G. P. Ferguson, and H. M. Pinsker. 1986.** *J. Exp. Biol.* **121:** 1–25.
8. **Boycott, B. B. 1961.** *Proc. R. Soc. Lond. B* **153:** 503–534.
9. **Young, J. Z. 1976.** *Philos. Trans. R. Soc. Lond. B* **274:** 101–167.
10. **Tansey, E. M. 1980.** *Philos. Trans. R. Soc. Lond. B* **291:** 127–145.

**Reference:** *Biol. Bull.* **203:** 232–234. (October 2002)

# Cuttlefish Body Patterns as a Behavioral Assay to Determine Polarization Perception

*Melissa M. Grable*[1,2], *Nadav Shashar*[1,3], *Nicole L. Gilles*[1], *Chuan-Chin Chiao*[1,4], and *Roger T. Hanlon*[1]
*(Marine Biological Laboratory, Woods Hole, Massachusetts 02543)*

Cuttlefish use body patterns for camouflage on benthic substrata. These body patterns, described by Hanlon and Messenger (1), fall into three broad categories: uniform, in which the whole body of the cuttlefish presents a single design; mottle, in which dark blotches of irregular shapes and sizes cover the body; and disruptive, in which high-contrast features visually disrupt the body outline. The body pattern chosen depends upon the visual input to the cuttlefish and the perception of this input. We can study the animal's visual perception (1–4) by presenting cuttlefish with various artificial substrate backgrounds and examining the body patterns produced in response.

In this study, a similar behavioral assay was developed as a new tool with which to learn about cuttlefish perception of polarization information. Specifically, we wanted to examine whether cuttlefish discriminate between (*i.e.*, respond differently to) intensity and polarization patterns. In cephalopods, polarization sensitivity (PS) arises from the orthogonal arrangement of microvilli in the retina (5). Although most nerve fibers exiting the eye respond maximally to either vertically or horizontally polarized light (6), the integration of the signals arriving from these PS units is not well understood.

Cuttlefish reared at the National Research Center for Cephalopods in Galveston, Texas, were shipped to the Marine Resources Center at the Marine Biological Laboratory in Woods Hole, Massachusetts. Animals were tested from August 2000 through May 2002, and the experimental procedure followed that of Chiao and Hanlon (3, 4). In short, cuttlefish were placed on one of four substrate patterns (illustrated in Fig. 1): (1) black and white checkerboard, (2) polarized checkerboard, (3) digital video image of the polarized checkerboard, or (4) polarized checkerboard but with all filters oriented to polarize the same way. The expected results were to observe disruptive coloration on (1) and (2), and uniform coloration on (3) and (4). In fact, results on the 4th pattern were unexpected, so 5 animals were later examined on a 5th background, a single sheet of continuous linear polarizing filter (Fig. 1, pattern 5). Following Chiao and Hanlon (3), the size of the squares in the checkerboard patterns was determined experimentally for each group of cuttlefish; this was necessary because the size of the checkerboard squares is determined by the size of the "White square" produced on the skin of the cuttlefish (see Fig. 2C). Body pattern definitions follow Hanlon and Messenger (1).

The black and white checkerboard pattern (Fig. 1, pattern 1) was created using MATLAB Software. Intensity contrast levels of this pattern [defined as (max − min)/(max + min)], as recorded by an overhead video camera during trials and digitized into Adobe PhotoShop (TM) software, were no less than 66%. No polarization contrast could be detected in this pattern. The polarized checkerboard pattern (Fig. 1, pattern 2) was constructed of orthogonally set square pieces of linearly polarizing filter with an adhesive backing (Frank Wooley & Co., PA) attached to a depolarizing waterproof paper. Intensity contrasts on this pattern were not correlated with the orientation or type of squares and in any case were lower than 5%. When the pattern was viewed through another piece of linearly polarizing filter set at 0° or 90°, the pattern looked to a human observer like a black-and-white checkerboard (Fig. 2A). Using video recordings through such a linear filter, polarization contrast (as coded into intensity) was approximately 70%. The digital video image of the polarized checkerboard (Fig. 1, pattern 3) was created by taking a digital image and then printing it. The image had little intensity contrast in it (less than 5%, see other intensity contrast experiments in ref. 3) and no polarization contrast. This digital video image was used to control for possible responses of the cuttlefish to whatever small intensity contrast the polarization checkerboard pattern possesses. As an additional control, we used a polarized checkerboard in which all polarizing filters were parallel to each other and, therefore, all polarized the same way (Fig. 1, pattern 4). When this pattern, as well as the continuous polarizing filter, were viewed through another piece of linear polarizing filter, they looked uniformly gray to a human observer (intensity and polarization contrasts less than 5%, typically 3% distributed randomly). Polarization patterns were sealed between two thin sheets of plexiglass for waterproofing (which did not affect polarization as perceived by human observers with a linearly polarized filter). Non-polarization patterns were printed and waterproofed by lamination.

The patterns were placed underwater in a tank with running seawater. A bottomless PVC box (20 cm × 26 cm) that restricted the animal to the boundaries of the pattern was then placed on top of the pattern. The tank was illuminated evenly from above (at a consistent oblique angle of less than 30°) to minimize shadows by the animals. A digital video camera mounted above the tank recorded a 2-s video clip every minute. Once the video camera was

---

[1] Marine Biological Laboratory, 7 MBL Street, Woods Hole, MA 02543.
[2] Boston University Marine Program, 7 MBL Street, Woods Hole, MA 02543.
[3] Hebrew University of Jerusalem, ESE Department, Interuniversity Institute for Marine Sciences, P.O. Box 469, Eilat 88103, Israel.
[4] Department of Life Science, National Tsing-Hua University, 101 Section 2 Kuang Fu Road, Hsinchu 300, Taiwan, R.O.C.

1.

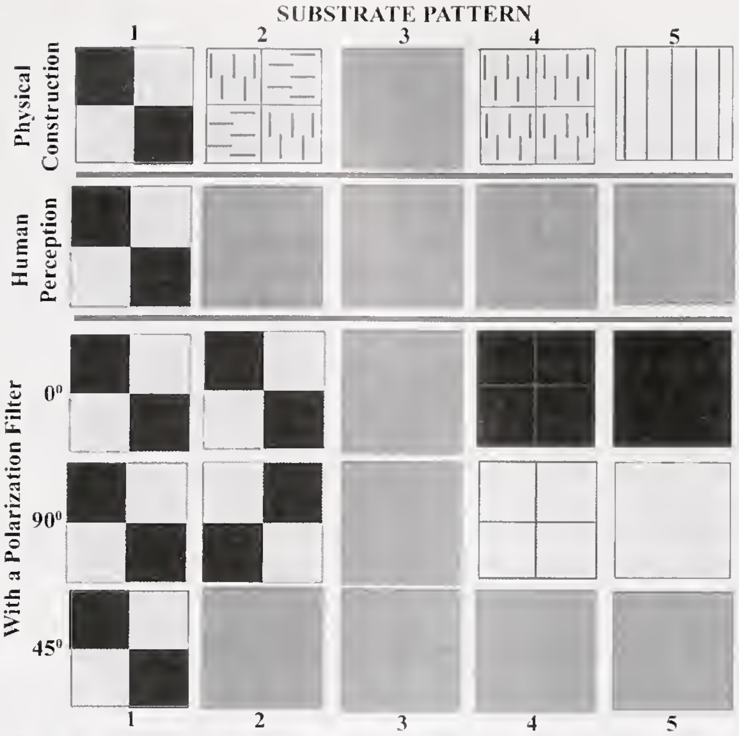

2.

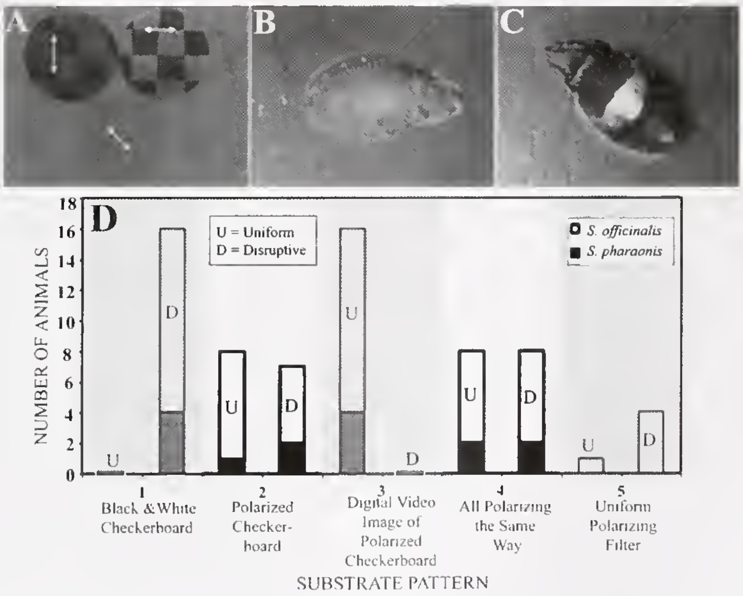

**Figure 1.** *Details of the five experimental substrate patterns, showing how they might appear to humans, either unimpeded or through polarizing filters. The top row represents the physical construction of the patterns. Patterns 1 and 3 were sheets constructed in a computer and then printed. Patterns 2 and 4 were made of cut-out squares of polarizing filter oriented in different directions (indicated by the vertical or horizontal lines in each square). Pattern 5 was a single large sheet of polarizing filter oriented in only one plane. The second row shows what the patterns look like to a human. The bottom three rows indicate how the patterns look to a human when a polarizing filter is placed over the substrate patterns at 0, 90, or 45 degrees. Note that any patterns made of polarizing filter material (i.e., patterns 2, 4, 5) appear uniformly gray to a human observer.*

**Figure 2.** *(A) A checkerboard made of linearly polarizing filters, which were set at orthogonal orientations to each other, served as one background test (Fig. 1, pattern 1). This pattern is visible to humans when a linearly polarizing filter is placed in front of the pattern (upper circles; orientation of polarization of filter is indicated by arrows) except when the front filter is positioned at an exact 45° orientation to the axis of the pattern (bottom circle). When placed on a polarized checkerboard, cuttlefish showed either a uniform body pattern (B) or a disruptive body pattern (C). (D) Responses to the five substrate patterns described in the text and Figure 1.*

turned on, each session lasted for 30 min, with a total of 60 s recorded. At the beginning of each session, the animal was placed within the PVC box on top of the test substrate pattern and allowed to settle for at least 5 min before recording began. Videotapes were evaluated by assigning a grade (either uniform or disruptive) to each of the 30 two-second video clips. This scoring technique is similar to that used by Chiao and Hanlon (3, 4). If the animal was showing a uniform or stipple pattern, it was given a grade of uniform (Fig. 2B). However, if a White square or a White mantle bar was conspicuous, the animal was given a grade of disruptive (Fig. 2C), as were cases in which another conspicuous transverse or bold patterning component was present (see details in ref. 1). Because cuttlefish will only camouflage themselves if they are settled, scores were rejected if the animal was swimming or appeared restless. The grades were used to determine whether an animal showed a uniform or a disruptive body pattern most of the time (Fig. 2D).

Only animals that showed a disruptive body pattern on the black and white checkerboard pattern and a uniform body pattern on the digital video image of the polarized checkerboard were tested. These 16 animals (4 *Sepia pharaonis* and 12 *S. officinalis*) did not show a consistent body pattern on any of the polarizing patterns (polarized checkerboard, and all polarized the same way; Fig. 2D). Indeed, of the five animals tested on the uniform polarizing filter, one animal showed a uniform body pattern and four showed a disruptive pattern. Time and other logistical restrictions prevented us from testing more animals on this pattern; this should be a priority in future experimentation.

It is clear from these results that animals showed mixed body patterns (both uniform and disruptive) on all substrates made of polarizing materials (Fig. 2D; Fig. 1, patterns 2, 4, 5). Assuming that intensity and polarization provide equivalent visual information, or that polarization is coded into a type of a gray scale (cuttlefish are color blind, ref. 2), one would predict that cuttlefish would show either a uniform or a disruptive pattern based upon the overall contrast of the backgrounds. The mixed body patterns shown by cuttlefish only on polarized backgrounds indicates that these backgrounds were distinguished from non-polarized ones.

The underwater light environment is partially linearly polarized (7), and polarization underwater also occurs when light hits particles suspended in the water. Cuttlefish use polarization information in predation (8) and could, hypothetically, use polarization sensitivity for navigation because the orientation of partial polarization changes throughout the day. Cuttlefish are also able to produce distinct polarization patterns on their bodies, and these may be used in communication (9). However, despite numerous observations with different types of polarization imaging devices, we detected no evidence that cuttlefish produce polarization body patterns that match or even resemble the polarization of their background. Therefore, cuttlefish probably do not use polarized body patterning for camouflage.

How are polarized backgrounds perceived by cuttlefish, and how is the polarization information linked to body patterning? The animals may have two visual channels, one for polarization information and the other for non-polarization information (such as intensity), and these two channels may interact in higher-order processing. Alternatively, cuttlefish may use opponency processes to extract polarization information (10) by subtracting the responses of units sensitive to vertical e-vectors from ones sensitive to horizontal e-vectors. Since each portion of the animal's eye has a different field of view, the opponency processing might sometimes enhance the polarization patterns (*e.g.*, subtracting two orthogonal intensities as in the upper circles of Fig. 2A) and at other times reduce the polarization signals (*e.g.*, subtracting two similar intensities as in lower circle of Fig. 2A). Our results do not distinguish these possibilities, yet they do suggest different ways to study how cephalopods perceive polarization signals.

Perception of polarization signals by animals is difficult to study or conceptualize for human investigators, who are mostly polarization insensitive. Body patterning used for camouflage by cuttlefish provides a robust behavioral assay with which to assess visual perception and information processing (2, 3, 4). The unexpected findings in the report warrant future studies aimed at the interaction between the PS and non-PS channels, and the processing of polarization information.

We thank Janice Hanley and Bill Mebane for help with cuttlefish maintenance, Gabrielle Santore for manuscript preparation, and Bill Saidel and Jean Boal for stimulating discussions. Part of this work was in fulfillment of a Masters Thesis by MMG for Boston University Marine Program. This study was supported by NSF Grant IBN 9729598 to RTH and BSF Grant 1999040 to NS.

## Literature Cited

1. **Hanlon, R. T., and J. B. Messenger. 1988.** *Philos. Trans. R. Soc. Lond. B* **320:** 437–487.
2. **Marshall, N. J., and J. B. Messenger. 1996.** *Nature* **382:** 408–409.
3. **Chiao, C.-C., and R. T. Hanlon. 2001.** *J. Exp. Biol.* **204:** 2119–2125.
4. **Chiao, C.-C., and R. T. Hanlon. 2001.** *Biol. Bull.* **201:** 269–270.
5. **Moody, M. F. 1962.** *J. Exp. Biol.* **39:** 21–30.
6. **Saidel, W. M., J. Y. Lettvin, and E. F. McNichol, Jr. 1983.** *Nature* **304:** 534–536.
7. **Waterman, T. H. 1988.** *SPIE* **925:** 431–437.
8. **Shashar, N., R. Hagan, J. G. Boal, and R. T. Hanlon. 2000.** *Vision Res.* **40:** 71–75.
9. **Shashar, N., P. S. Rutledge, and T. W. Cronin. 1996.** *J. Exp. Biol.* **199:** 2077–2084
10. **Bernard, G. D., and R. Wehner. 1977.** *Vision Res.* **17:** 1019–1028.

**Reference:** *Biol. Bull.* **203:** 235–236. (October 2002)

# Tracking Behavior of Busyconinae Whelks

*Sarah M. Rohrkasse*[1] *and Jelle Atema (Boston University Marine Program, Marine Biological Laboratory, Woods Hole, Massachusetts 02543)*

Odor plume tracking behavior has been studied mostly in animals with bilateral chemoreceptor organs, which permit spatial comparison, a mechanism basic to locating an odor source (1). Marine snails have a single olfactory organ that samples water entering through the siphon (2). We expected that the siphon of such animals would swing from side to side, effecting bilateral sampling. We were interested in seeing if this animal could become a beneficial model for the study of spatial odor sampling.

Whelks (subfamily Busyconinae) are large marine neogastropod snails that prey upon live bivalve molluscs but will scavenge when carrion is available. We tested two sympatric species of the Busyconinae: the channeled whelk *Busycotypus canaliculatus* tends to be nocturnal, whereas the knobbed whelk *Busycon carica* does not show a preferred active time (3). *Busycotypus* also moves at a faster rate and preys upon more active bivalves (4).

Whelks have several sensory organs. Bilateral tentacles contain mechanoreceptors and chemoreceptors; eyes are located at their base (5). The siphon supplies water and its chemical contents to gills and the osphradium, the major chemoreceptor organ. Whelks can detect waterborne odors from potential prey, predators, and conspecifics (5, 2). Because odor travels *via* water currents, whelks depend on hydrodynamic factors, especially currents and turbulence, which influence their ability to orient (2, 5, 6).

Although whelks have a wide range of prey, pieces of horseshoe crab (*Limulus polyphemus*) have been overwhelmingly successful as a bait in whelk traps (7). Research is in progress to determine the compounds responsible for the whelk's attraction to female *Limulus* and to produce an artificial bait (Nancy Targett, pers. comm.). In addition to our basic scientific goals, we were also interested in contributing to bait development. Therefore, we measured the responses of channeled and knobbed whelks in a flume to various target sources introduced upstream. The target sources were dead *Limulus* bodies, *Limulus* hemolymph, dark-painted cement casts of *Limulus*, 5% mussel juice (from *Geukensia demissa*, a food source readily consumed in the laboratory), seawater, and the non-flowing tubing, nozzle, and lead weight of the liquid stimulus introduction system. The flume was large (dimensions: 10 m × 2 m × 0.5 m) and had a constant background flow of 7 cm $s^{-1}$. Target sources were used individually and in combinations; the liquid stimuli were introduced onto the bottom of the flume, *via* gravity flow, through a 5-mm-diameter nozzle (flow velocity 40 ml/min, Reynolds number = 100). In each trial, five whelks were placed 1 m downstream from the target sources, and responses were recorded on videotape for at least 45 min. Paths of both the siphon tip and the center of the shell were digitized at 1 Hz. From these data, crawling velocity, heading angles, and turn angles were determined. "Orientation" was defined as a path ending or passing within one body length from the source. "Non-orienting" whelks responded by moving from their starting position but did not pass close by the source. "Zigzag" was defined as locomotion with turn angles greater than 45° over more than 50% of the path; all other tracks were "smooth."

In general, responsiveness to any source was low (range 0.00%–19.23%) when compared to that of *Illyanassa obsoleta* responding to *Mytilus edulis* (range 60%–100%) (8). Over the course of the summer, the activity of all the whelks tended to decrease (ANOVA, $F = 3.17$, $P = .058$). This trend may have been due to increasing temperature (20 to 23.5 °C) or to the natural decrease in feeding that occurs May to September during the mating season (9). Whelks may show stronger feeding attraction and activity in their natural environment, during the winter, or at night.

Channeled whelks responded and oriented more often than knobbed whelks (ANOVA, $F = 6.48$, $P = .018$) (Fig. 1A). Knobbed whelks zigzagged more than channeled whelk. Because channeled whelks oriented more often ($\chi^2 = 7.5$, $P = .0062$), but zigzagged less ($\chi^2 = 6.29$, $P = .012$), zigzag may not be characteristic of orientation behavior (Fig. 1A). Zigzag was not an individual characteristic, because zigzagging whelks also exhibited smooth behavior. We limited further analysis to the responses of orienting channeled whelks. When these whelks approached a target source, half of them exhibited no change in velocity, and the other half decreased their speed or (in rare cases) stopped near the source. Only two zigzagged, and these stopped or decreased in speed near the source. Zigzagging occurred in similar proportions in response to control conditions, food, and combination targets; this behavior, to our surprise, is thus unlikely to be a response to chemical stimuli.

Among all target sources, the channeled whelks responded most often to dead *Limulus* bodies, followed in order by seawater, no flow, mussel juice, hemolymph, and *Limulus* cast (Fig. 1B). Compared with *Limulus* bodies, mussel juice ($\chi^2 = 12.76$, $P = .0004$) and hemolymph ($\chi^2 = 10.40$, $P = .0013$)—but, to our surprise, not seawater ($\chi^2 = 2.14$, $P = .14$)—elicited significantly fewer responses. In fact, the flowing seawater control elicited more responses than mussel juice ($\chi^2 = 4.72$, $P = .03$) and hemolymph ($\chi^2 = 5.81$, $P = .016$) (Fig. 1B). *Limulus* cast elicited no responses (Fig. 1B), showing that attraction to *Limulus* bodies was not due to their hydrodynamic (wake-producing) properties. Lower responses to chemical sources (hemolymph and mussel juice) than to controls (seawater and no flow) suggest, if anything, that these presumed attractants were actually repellents.

In conclusion, the evidence indicates behavioral differences between channeled and knobbed whelks. It also demonstrates that *Limulus* bodies are an attractive target for channeled whelks, whereas *Limulus* hemolymph and the hydrodynamic wake are not attractive. Because orienting paths most often showed a smooth character, the use of bilateral chemoreceptive organs, such as the tentacles, should be considered.

---

[1] Xavier University, Cincinnati, OH 45207.

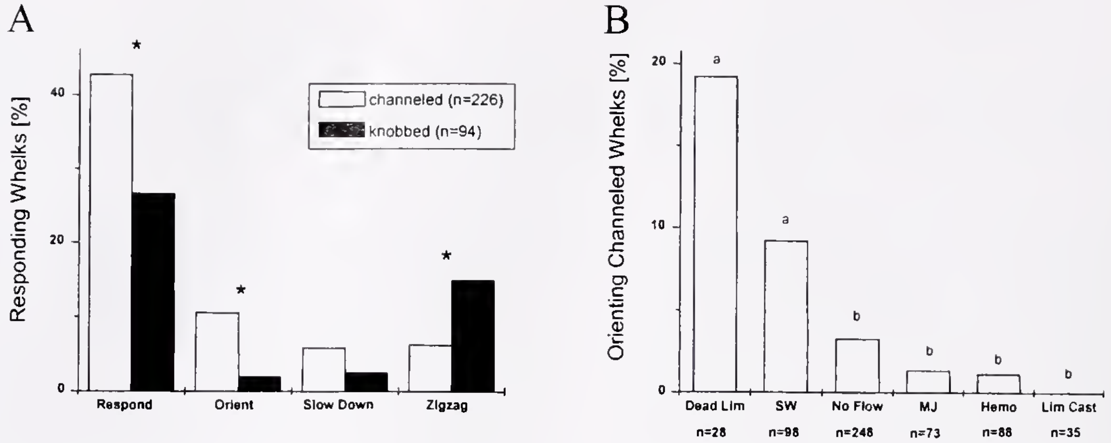

**Figure 1.** *(A) Responses of channeled and knobbed whelks to all targets. Orientation: defined in text. Slow down: a reduction in crawling speed near the source, where speed within 10 cm from the source was less than 80% of the speed over the prior 90 cm distance. Zigzag: defined in text. *Significant difference ($\chi^2$, $\alpha = .01$). (B) Responses of orienting channeled whelks* (Busycotypus) *to control and experimental sources, presented in order of responsiveness. Dead Lim, dead, punctured and bleeding* Limulus *body; SW, seawater control; No Flow, fluid source nozzle and lead weight only; MJ, mussel juice; Hemo,* Limulus *hemolymph; Lim cast, dark painted cement cast of* Limulus. *"a" and "b" denote significant differences ($\chi^2$, $\alpha = .01$).*

Supported by the National Science Foundation Research Experience for Undergraduates at the Boston University Marine Program (OCE 0097498). We thank Gabriele Gerlach for statistical advice and the laboratory of Robert Barlow, Jr. for the loan of the *Limulus* cast.

## Literature Cited

1. **Moore, P. A., N. Scholz, and J. Atema. 1991.** *J. Chem. Ecol.* **17:** 1293–1307.
2. **Croll, R. P. 1983.** *Biol. Rev.* **58:** 293–319.
3. **Edwards, A. L., and M. G. Harasewych. 1988.** *J. Shellfish Res.* **7:** 467–472.
4. **Davis, J. P. 1981.** *Biol. Bull.* **161:** 338–339.
5. **Smith, C. R. 1977.** *Veliger* **19:** 331–340.
6. **Weissburg, M. J., and R. K. Zimmer-Faust. 1993.** *Ecology* **74:** 1428–1443.
7. **Alternative Bait-Trap Design Workshop for Horseshoe Crabs.** 5 Oct. 1999, Atlantic States Marine Fisheries Commissions Horseshoe Crab Technical Committee, Essington, PA.
8. **Stenzler, D., and J. Atema. 1977.** *J. Chem. Ecol.* **3:** 159–171.
9. **Himmelman, J. H. 1988.** *Mar. Biol.* **97:** 521–531.

---

**Reference:** *Biol. Bull.* **203:** 236–238. (October 2002)

# Central Pathways Mediating Oculomotor Reflexes in an Elasmobranch, *Scyliorhinus canicula*

*Werner Graf (Marine Biological Laboratory, Woods Hole, Massachusetts 02543), Edwin Gilland,*
*Matt McFarlane, Laura Knott, and Robert Baker*

In vertebrates, primary vestibular afferents from the semicircular canals are linked to extraocular motoneurons by second-order vestibular neurons, which reflect a functional compartmentalization and topographic organization of hindbrain segments during development (1–4). Since the overall patterning of hindbrain segments is specified by the expression of particular genes (5), segmental segregation of second-order vestibular neurons suggests evolutionary relationships between specific oculomotor behaviors and the expression of particular genetic regulatory elements (*e.g.,* a particular Hox gene (6)). Accordingly, neurons arising from the same hindbrain segment should always be correlated with a given oculomotor behavior regardless of species (3). However, the neurons subservient to horizontal eye movements in cartilaginous fishes (sharks, skates, and rays) are asserted, by some, to be organized quite differently from those of other vertebrates (7–9).

Anatomical studies of extraocular motoneurons in the adults of elasmobranch species have uniformly demonstrated that medial rectus (MR) muscle innervation is contralateral, as compared with ipsilateral in all other vertebrates (7, 10, 11), including an eye muscle similarly located in the lamprey orbit (9). On the other hand, innervation of the lateral rectus (LR) muscle is ipsilateral in elasmobranches, just as it is in all other vertebrates (Fig. 1). The contralateral innervation of the MR, taken with the ipsilateral innervation of the LR, has suggested that vertical axis second-order vestibuloocular reflex (VOR) pathways in elasmobranchs must be realized in another way than shown for most vertebrates in Figure 1 (7). In addition, labeling of the oculomotor nucleus with

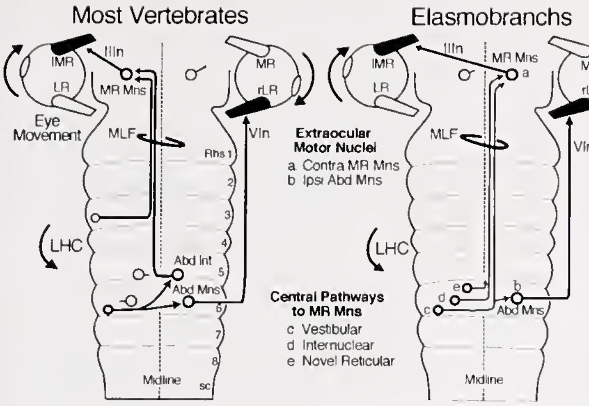

**Figure 1.** *Schematic illustration of hindbrain excitatory pathways to the abducens and medial rectus motor nuclei in most vertebrates and elasmobranchs. The central pathways to MR Mns (3–5) were based on the results illustrated in Figure 2. Abbreviations: Abd Mns, abducens motoneurons; Abd Int, abducens internuclear neurons; IIIn and VIn, oculomotor and abducens nerve, respectively; LHC, left horizontal canal; MR Mns, medial rectus motoneurons; Rhs, rhombomeric segment; MLF, medial longitudinal fasciculus.*

horseradish peroxidase conjugates failed to demonstrate the existence of other afferent projections from the hindbrain (8), such as the excitatory abducens internuclear neurons (Abd Int) and prepositus neurons, both of which are essential for achieving symmetric conjugate horizontal motion of both eyes during saccades, fixation, and visual tracking (12–15).

Developmental differences between elasmobranchs and other vertebrates also hinted that the horizontal oculomotor system might have followed a divergent evolutionary pathway since the origin of jawed fishes (9). MR muscles stem embryonically from the dorsal part of the premandibular head cavity in elasmobranchs, but from the ventral part in other vertebrates (Gilland, unpubl.), thus possibly offering an explanation for the contralateral *versus* ipsilateral positioning of MR motoneurons. Developmental differences also exist for Abd motoneurons, as the abducens nucleus originates from embryonic rhombomeres (Rhs) 5 and 6 for most vertebrates, including lampreys, teleosts, birds, and reptiles (1), and exclusively from Rhs 5 in frogs (16) and mammals (1). The elasmobranch developmental pattern is different yet, as Abd motoneurons appear to be derived only from Rhs 6 (17). Thus, elasmobranchs provide a valuable living case study, in which the interplay of genetic and behavioral determinants of neuronal identity can be evaluated during divergent evolution. These differences allow the evolutionary validity of proposed relationships between Hox gene expression, neuronal identity, and behavior to be tested; they also allow us to determine whether the anatomical divergence of elasmobranchs reflects only relatively slight differences in a common vertebrate morphogenetic plan, or a more radical reorganization undertaken specifically by elasmobranchs, but masked by similarities in oculomotor behaviors.

First, however, the precise anatomical configuration of the central horizontal oculomotor system in elasmobranchs must be analyzed in rigorous structure/function experimental paradigms. This study was meant to locate the neurons projecting to the oculomotor nucleus of the lesser spotted dogfish, *Scyliorhinus canicula*, by applying biocytin to either the oculomotor nuclei or the medial longitudinal fasciculus (MLF). Animals were anesthetized with 0.05% ethyl-aminobenzoate until respiration ceased. After cartilage removal, the rostral cerebellum was aspirated to visualize the

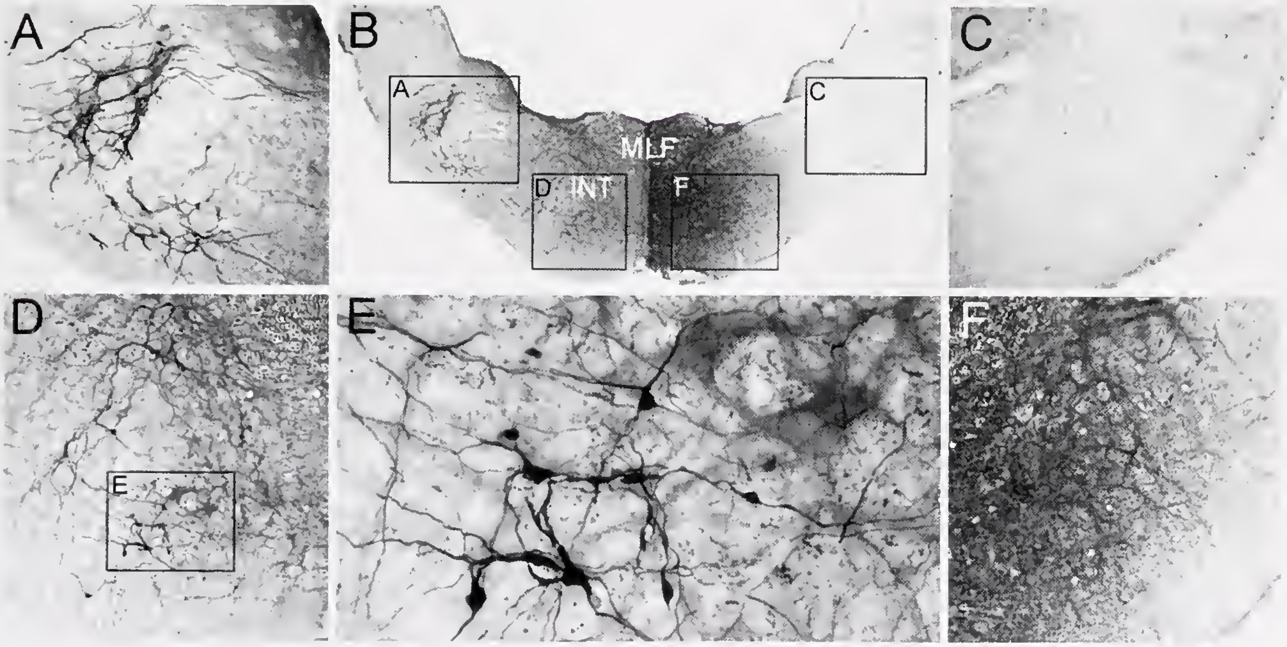

**Figure 2.** *Location and distribution of hindbrain neurons projecting through the contralateral MLF (A–F). The low-magnification coronal section was photographed at the level of the abducens nucleus (22). Each inset in B is labeled and illustrated at higher magnification in A, C, D, and F. Abbreviations: INT, internuclear neurons; MLF, medial longitudinal fasciculus; VES, vestibular nucleus.*

hindbrain at the level of the anterior medullary velum. Either the right MLF or caudal oculomotor nucleus was cut ($n$ = 6 and 4, respectively), and biocytin crystals were applied for 20 min. Cartilage was replaced, the skin was tightly sutured, and the animals were resuscitated. They were again anesthetized after 48–72 h and perfused with 4% formaldehyde and 0.5% glutaraldehyde. The midbrain and hindbrain were dissected out, gelatin embedded, and sectioned at 75 $\mu$m. The sections were processed with the use of the avidin-biotin peroxidase complex including NiCo intensification (18).

In all cases, many heavily labeled vestibular neurons were found in the contralateral descending/posterior octaval subnucleus (Fig. 2A) and ipsilateral anterior octaval subnucleus (not illustrated). However, in all experiments, neurons were distributed throughout the contralateral hindbrain from the dorsal to ventral surface (Fig. 2B, D). In particular, a distinct subgroup of neurons largely ventrolateral to the abducens nucleus (Fig. 2E) was reminiscent of the contralateral abducens internuclear neurons described in all other vertebrates (Fig. 1). Neurons were also distributed dorsally up to, and surrounding, the MLF; these neurons could be envisioned as analogous to the prepositus nucleus described in mammals. Clearly, neurons ipsilateral to either the oculomotor or MLF biocytin label were either sparse or absent (Fig. 2C, F). Significant terminal arborization appeared throughout the ipsilateral Abd nucleus (Fig. 2F) that conceivably derived from axon collaterals of ascending vestibular neurons. If so, then individual vestibular neurons might contact a pair of synergistic horizontal extraocular motoneurons (see Fig. 1). Neurons were also found in the pretectum, midbrain, and cerebellar nuclei that are, in all probability, correlated primarily with vertical eye movements and gaze (not illustrated). Overall, the distribution pattern of neurons throughout the brainstem of the elasmobranchs was surprisingly more extensive than expected and only different in anatomical detail from that observed in other vertebrates (6, 19–21).

In conclusion, the evolutionary significance of a proposed divergence in elasmobranch oculomotor organization remains uncertain. It is parsimonious to conclude that elasmobranchs have used the same genes located in conserved hindbrain segments to generate novel neurons and connections contributing to conjugate horizontal eye movements (1, 3, 4, 18) (see Fig. 1). Single-cell experiments that correlate structure with function will precisely delineate the uniqueness of of these brainstem neurons. In association with the study of developmental gene expression, elucidation of oculomotor circuitry in elasmobranchs will ultimately provide a unique view of how specific neuronal architecture underlying specified behaviors can take alternative evolutionary pathways.

This work was supported by the Grass Foundation (W. Graf, M. McFarlane, and E. Gilland) and NIH Research Grants (R. Baker).

## Literature Cited

1. **Gilland, E., and R. Baker. 1993.** *Acta Anat.* **148:** 110–123.
2. **Graf, W. 1988.** *Ann. NY Acad. Sci.* **545:** 154–169.
3. **Baker, R. 1998.** *Otolaryngol. Head Neck Surg.* **119:** 263–275.
4. **Suwa, H., E. Gilland, and R. Baker. 1996.** *Biol. Bull.* **191:** 257–259.
5. **Krumlauf, R. 1994.** *Cell* **78:** 191–201.
6. **Glover, J. C. 2000.** *Prog. Brain Res.* **124:** 3–21.
7. **Graf, W., and W. J. Brunken. 1984.** *J. Comp. Neurol.* **227:** 569–581.
8. **Puzdrowski, R. L., and R. B. Leonard. 1994.** *J. Comp. Neurol.* **339:** 587–597.
9. **Fritzsch, B. 1998.** *Otolaryngol. Head Neck Surg.* **119:** 182–192.
10. **Rosiles, J. R., and R. B. Leonard. 1980.** *J. Comp. Neurol.* **193:** 677–687.
11. **Puzdrowski, R. L. 1998.** *J. Comp. Neurol.* **400:** 571–579.
12. **Evinger, C. 1988.** *Rev. Oculomot. Res.* **2:** 81–117.
13. **Highstein, S. M., A. Karabelas, R. Baker, and R. A. McCrea. 1982.** *J. Comp. Neurol.* **208:** 369–381.
14. **Aksay, E., R. Baker, H. S. Seung, and D. W. Tank. 2000.** *J. Neurophysiol.* **84:** 1035–1049.
15. **Harris, A. J. 1965.** *J. Exp. Biol.* **43:** 107–138.
16. **Straka, H., E. Gilland, and R. Baker. 1998.** *Biol. Bull.* **195:** 220–222.
17. **Gilland, E., and R. Baker. 1992.** *Biol. Bull.* **183:** 356–358.
18. **Graf, W., R. Spencer, H. Baker, and R. Baker. 1997.** *J. Neurophysiol.* **77:** 2765–2779.
19. **Straka, H., E. Gilland, and R. Baker. 2001.** *J. Comp. Neurol.* **437:** 42–55.
20. **Diaz, C., and J. C. Glover. 2002.** *Brain Res. Bull.* **57:** 307–312.
21. **Gonzalez, M. J., M. A. Pombal, M. C. Rodicio, and R. Anadon. 1998.** *J. Comp. Neurol.* **401:** 1–15.
22. **Ballard, W. W., J. Mellinger, and H. Lechenault. 1993.** *J. Comp. Neurol.* **225:** 581–590.

---

**Reference:** *Biol. Bull.* **203:** 238–239. (October 2002)

# Error-Driven Motor Learning in Fish

*John Montgomery (Leigh Marine Laboratory, University of Auckland, Auckland, New Zealand), Guy Carton, and David Bodznick*[1]

The cerebellum is considered a motor control structure, yet it shares strong anatomical similarities with the cerebellar-like nuclei of the fish hindbrain, which are clearly sensory and process electrosensory and lateral line information. Can these contrasting roles be brought together in a single framework, providing insight into cerebellar function?

The striking anatomical similarity between the cerebellum and the cerebellar-like sensory nuclei is that they share a molecular layer organization in which the apical dendrites of the projection neurons receive input from many thousands of parallel fibers (1, 2). Our hypothesis is that, in both systems, plasticity of the synapses between the parallel fibers and the projection neurons allows the formation of a parallel fiber composite that can subtract unwanted activity in the projection neurons and their downstream targets. In cerebellar-like structures, this subtraction can be directly observed as a negative sensory image (1). Here we report a motor learning paradigm in fish that exhibits an analogous negative motor image.

---

[1] Department of Biology, Wesleyan University, Middletown, CT.

The cerebellar-like sensory nuclei receive primary afferent input from octavolateralis sensory systems, and relay that activity to midbrain levels. In these nuclei, spike activity of a projection neuron reduces the synaptic strength of concurrently active parallel fibers (3, 4, 5), a learning rule termed anti-Hebbian plasticity. The composite signal thus formed subtracts re-afferent noise generated on the sensory system by the animal's own movements. Experiments show that the projection neurons learn to cancel an external stimulus that is paired with the animal's own activity; and a defining feature of these adaptive filters is the negative sensory image, or cancellation signal, that is revealed when the stimulus is withheld (6). One way of describing cerebellar-like function is that the ongoing activity of the projection neurons themselves is, in effect, the error that selects the parallel fiber composite that forms the required negative sensory image. External signals are inherently unpredictable and are not cancelled by this mechanism because they are not represented in the parallel fiber system.

In the cerebellum, the projection neurons are called Purkinje cells. Like the principal cells in cerebellar-like nuclei, Purkinje cells receive many thousands of parallel fiber inputs. In addition, however, Purkinje cells receive a unique, strong synaptic input from climbing fibers. In many current models of cerebellar function, climbing fibers signal error in motor control (7, 8), and their activity drives learning at the parallel fiber to Purkinje cell synapses in such a way as to reduce that error in a manner not unlike the learning that takes place in cerebellar-like sensory structures. However, learning in this case has become uncoupled from the ongoing activity of the Purkinje cell and only occurs in response to "instruction" from the climbing fiber. Can error-driven motor learning and the adaptive sensory filters be drawn into a single functional framework? We have sought to do this by developing a motor-learning paradigm that we predicted would exhibit an explicit negative motor image comparable to the negative sensory image of the adaptive filter.

From first principles, it should be possible to perturb almost any motor control system, provide a cue to allow the animal to anticipate and hence to reduce the impact of the perturbation, and thence reveal the negative motor image by providing the cue but withholding the perturbation. We have chosen to work with the postural control system of fish. Fish swimming in an upright position maintain their posture with a classical feedback control system. The vestibular system detects roll-error, which is then corrected by the fins. To provide a repeatable perturbation we attached magnets to the dorsal and ventral edge of the fish with their poles facing in opposite directions. These fish then swam in a small flume, outside of which were situated magnetic coils. Switching the coils on provided a rotational perturbation to the fish. Light-emitting diodes situated within the fish's visual field provided the learning cue. The roll of the fish was quantified by processing the images from a digital video camera positioned above the flume. In these experiments, the cue and the field were on simultaneously for a period of 1 s, and were repeated at 10- to 20-s intervals. A minimum of 5 records were taken at the beginning and the end of the learning period, which lasted for a minimum of 1 h. The magnetic stimulus was then turned off, and a comparable number of records were taken of the learning cue presented alone. The peak roll at the end of the 1-s stimulus was quantified in each case. Experiments were performed on four rainbow fish (*Glossolepis incisus*) and three scup (*Stenotomus chrysops*). With rainbow fish, the learning period reduced the normalized roll from 62% ± 3.3 (mean ± standard error of the mean) to 46.2% ± 3.8, and the size of the negative roll on the presentation of the learning cue alone was $-8.3\% \pm 2.1$, which is significantly less than zero ($z = 2.02$, $P < 0.05$). In preliminary experiments with scup, a similar pattern was seen in two out of three fish.

These experiments provide an example of error-driven motor learning that demonstrates an explicit negative motor image comparable to the negative sensory image of cerebellar-like adaptive filters. Although we have no direct evidence that the site of learning in this paradigm is cerebellar, these experiments do suggest how cerebellum (at least in its simplest form) and cerebellar-like sensory structures can be considered within a single conceptual framework. In both systems, synaptic plasticity between the parallel fibers and the projection neurons may generate a parallel fiber composite that subtracts unwanted activity in the respective projection neurons. On this view, the essence of the molecular layer organization is that it provides a vast array of potential information from which to generate a cancellation signal, or error correction signal, *via* the anti-Hebbian learning mechanism.

Funded in part by an NSF grant to DB.

## Literature Cited

1. **Montgomery, J. C., S. Coombs, R. A. Conley, and D. Bodznick. 1995.** *Auditory Neurosci.* **1:** 207–231.
2. **Devor, A. 2000.** *Brain Res. Rev.* **34:** 149–156.
3. **Bastian, J. 1999.** *J. Exp. Biol.* **202:** 1327–1337.
4. **Bell, C. C., V. Z. Han, Y. Sugawara, and K. Grant. 1999.** *J. Exp. Biol.* **202:** 1339–1347.
5. **Bodznick, D., J. C. Montgomery, and M. Carey. 1999.** *J. Exp. Biol.* **202:** 1357–1364.
6. **Montgomery, J. C., and D. Bodznick. 1994.** *Neurosci. Lett.* **174:** 145–148.
7. **Ito, M. 2001.** *Physiol. Rev.* **81:** 1143–1195.
8. **Mauk, M. D., K. S. Garcia, J. F. Medina, and P. M. Steele. 1998.** *Neuron* **20:** 359–362.

**Reference:** *Biol. Bull.* **203:** 240–241. (October 2002)

# Social Interaction and Distribution of Female Zebrafish (*Danio rerio*) in a Large Aquarium

*Martha Delaney, Christopher Follet, Nick Ryan, Nick Hanney, Jenny Lusk-Yablick, and Gabriele Gerlach*
*(Marine Biological Laboratory, Woods Hole, Massachusetts 02543)*

The zebrafish (*Danio rerio*) is native to freshwater streams and rice paddies in the Ganges River of East India, Bangladesh, and Burma. Although this species is widely used as a genetic model and for developmental research, little is known about its natural behavior (*e.g.*, spatial distribution and social interactions). In the laboratory, zebrafish are usually kept in small aquaria under high densities.

The mating behavior of the zebrafish seems to be influenced by the exposure of mating partners to one another several to 24 h before spawning begins at sunrise; female gonadal hormones apparently stimulate males to perform courtship behavior (1, 2). Our preliminary experiments (unpubl. data) showed reproductive suppression of female zebrafish kept together for 4 days before they were separated and mated with a single male overnight. On average, each of these females ($n$ = 52) laid only 45 ± 12 (SE) eggs, in comparison to 200 ± 12 (SE) eggs of a female kept isolated for 4 days and then mated with one male ($n$ = 15; 150 ± 12 (SE) eggs) or two males ($n$ = 30; 180 ± 12 (SE) eggs) overnight. Females kept together in a aquarium behaved aggressively toward each other and developed a dominance hierarchy. These results led us to assume that females would avoid other females if they could. The aim of this study was to investigate spatial and social distribution of female zebrafish in a large aquarium where they could choose between different localities and partners.

We observed wild-type zebrafish, aged 10 months, which were kept in 30-l aquaria under a day/night cycle of 14/10 h with light on at 9:00 am before the experiments were started. Four males and four females were selected for each experiment. The eight fish were tagged individually behind the dorsal fin with Floy fish tags, all bearing a different color. These tags did not seem to affect the behavior of the fish.

The fish were placed in a large 195-cm × 195-cm aquarium filled with 600 l (water height: 16 cm) of formulated freshwater. A grid system of 16 equal squares was drawn on the bottom of the aquarium. In 7 of the 16 squares, artificial plants were placed in order to imitate zebrafish habitat. The fish were left to adjust to their new environment for about 3 h. Each of the five experiments lasted for 5 days. Half-hour observations were made twice daily, with at least 1 h between observation sessions. The observation sessions were split into 1-min intervals (31 intervals per observation), and the location of each fish was noted at every time interval.

Newly released fish showed a strong tendency for shoaling, but after about 2–3 h they dispersed to different parts of the aquarium. Thereafter, they spent 99% of their time in one of the seven squares containing artificial plants.

We evaluated how often each female was seen either alone or in the presence of only males (1 or 2 males) or with other females without any males (Fig. 1). In addition, we calculated how often females were expected to be found either alone or in these groups, assuming a random distribution (expected values). The comparison of observed and expected values showed that females avoided staying alone ($\chi^2 = 4.8$, df = 1, $P < 0.05$), but they preferred to stay with a single male ($\chi^2 = 3.9$, df = 1, $P < 0.05$) or with two males ($\chi^2 = 142$, df = 1, $P < 0.001$) when no other females were around. They spent only 5% of the observation time with female-only groups ($\chi^2 = 5.7$, df = 1, $P < 0.05$). Females showed no pairing with specific males. On average, each female was observed with 1.6 males per observation period.

Our study indicates that under more normal conditions female zebrafish might live with one or two males but separated from other females. Males seemed to change female partners on a daily basis. We assume that they were probably attracted by female pheromones indicating female reproductive stage. Bloom and Perlmutter (3) showed that zebrafish, when placed in a T-maze, demonstrated either a preference for or an avoidance of donor water produced when specified numbers of conspecifics of either sex were kept in holding systems for set lengths of time. Their results and ours are consistent with the higher egg production we observed in females kept with one or two males. The conditions under which zebrafish are often kept in laboratories seem to conflict with their natural preferences. Egg production could be increased by considering these observed behavioral patterns.

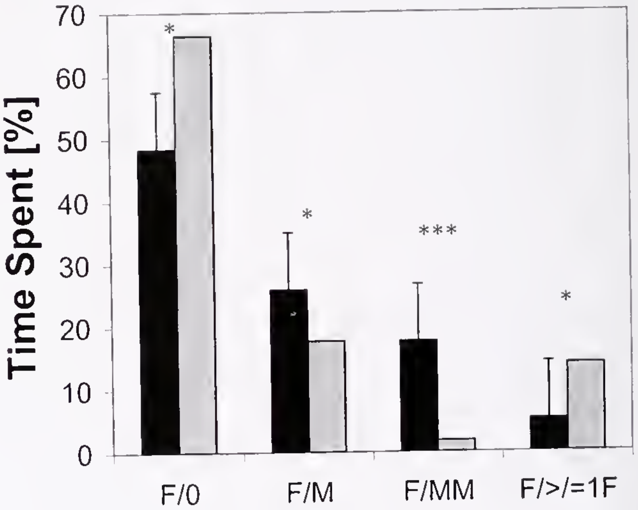

**Figure 1.** *Time females spent in groups of different size and sex. Black bars indicate mean values of the observed time (%) ± SE a female spent in different social groups; grey bars indicate the expected values based on a random distribution. Number of experiments = 5. Groups: F/0, single female; F/M, 1 female and 1 male; F/MM, 1 female and 2 males; F/>/=1F, 1 female with 1 or more females without males:* * $P < 0.05$, *** $P < 0.001$.

## Literature Cited

1. **van den Hurk, R., W. G. E. J. Schoonenen, G. A. v. Zoelen, and J. G. D. Lambert. 1987.** *Gen. Comp. Endocrinol.* **68:** 179–188.
2. **van den Hurk, R., and J. G. D. Lambert. 1983.** *Can. J. Zool.* **61:** 2381–2387.
3. **Bloom, H. D., and A. Perlmutter. 1977.** *J. Exp. Zool.* **199:** 215–226.

---

**Reference:** *Biol. Bull.* **203:** 241–243. (October 2002)

# *Caranx latus* (Carangidae) Chooses Dock Pilings to Attack Silverside Schools: A Tactic to Interfere With Stereotyped Escape Behavior of Prey?

*Michael J. Cermak (Boston University Marine Program, Marine Biological Laboratory, Woods Hole, Massachusetts 02543)*

In predator-prey dynamics, structural complexity of the habitat is traditionally considered to convey benefits to prey (1, 2, 3). Alternatively, Flynn and Ritz (4) have proposed that habitat structures may interfere with escape behavior in tightly aggregated formations of prey. Field observations of horse-eye jack, *Caranx latus,* suggest that this fish predator may exploit habitat structure to interrupt stereotyped prey defense. The jacks were observed attacking mixed schools of silversides (Engraulidae, Clupeidae, Atherinidae) near Wee Wee Caye, a mangrove island in Belize. Attacks were observed exclusively under a dock where silversides routinely gathered. In this paper I describe the jack hunting patterns, and develop a spatial model based on the argument that dock pilings interfere with prey escape and have therefore become the driving factor for the predator to attack only under the dock.

Holding on to a dock piling, I recorded predator presence, absence, and attack events continuously for 90-minute sessions three times per day spaced evenly from 0550 to 1800. Attacks were evident from the sudden accelerations of the predator group, the scattering behavior of the prey, and the remains of the prey that were often visible in the aftermath. Subsequently, I tracked the predator schools in their excursions beyond the dock. The path of the school was constructed by swimming behind it and recording my positions with reference to a grid of shore points and submerged landmarks.

While under the dock I observed 31 attacks in 3 days. Through tracking observations, groups of *C. latus* comprising 4–25 individuals were identified; these predators traveled in loops up to 70 m in length, and each time returned to the dock to attack (Fig. 1A). During the 5-day sampling period, every attack recorded during 15 observation sessions ($n = 40$; 8 stationary sessions, $n = 31$; 7 tracking sessions, $n = 9$) was between the pilings under the dock, although the predators would calmly cruise through the same dense aggregation of silversides just outside the dock.

Thirty-seven of the forty observed attacks were completed across an identical set of dock pilings, dubbed "hot spots." The predators, attacking at high velocity in a straight trajectory, would cause a stereotyped avoidance response by the prey. As the silversides could not outrun the jacks in a straight line, they dashed sideways, out of the path of the attacking predators, and immediately filled in the space left in the predators' wake. Computer modeling studies of the defensive formations of related prey (Clupeidae) have demonstrated that this observed "vacuole" formation is a stereotyped response to a predator attack and results from individual lateral movement (5). Placed in the context of the hotspots, this lateral escape path is, in specific places, blocked by the pilings (Fig. 1B). Some prey will not be able to make the necessary lateral move and will therefore be forced to remain in the path of the predators for a longer time.

The avoidance formation, although observed at the school level, is a product of individual prey maximizing distance from the predator, and using conspecifics as shields (6). Prey may aggregate in a high density because the number of surrounding conspecifics is more effective as a shield against attack. However, under these conditions, prey-to-prey interference with escape is also greatest and exacerbates the blocking effect of the pilings.

The silversides, however, were not always present in high density. Due to their diel patterns of migration, they occupied the area under the dock only in the daylight hours. During dock observations, prey accumulation at dawn was quantified from "time at first prey sighting" until "time at homogenous distribution" (400 individuals/$m^3$) (Fig. 1C). The predators visited the dock before and during prey accumulation. The first attack did not occur until 2 min after the highest density was attained (Fig. 1D). This predator behavior is consistent with maximizing the proposed blocking effect of the pilings.

In sum, the behavioral observations clearly indicate that the predators are choosing the dock habitat for attack. The spatial model demonstrates that dock pilings can interrupt stereotyped prey defense. Finally, the temporal attack pattern shows that these predators hunt under the dock only when the high density of the prey causes further limits on their escape. The predator thus uses both spatial and timing constraints in its hunting attacks. From these observations, I could not determine if the dock pilings and prey densities actually improved hunting efficiency since the jacks never attacked at other locations or at low prey densities. The Pacific bluefin trevally, *Caranx melampygus,* has been shown to use natural habitat structure to allow ambush attack behavior (7). Here, I show that the Caribbean *Caranx latus* selects an anthropogenic structure for its daily hunting attacks. These findings add to the repertoire of known fish hunting tactics and support the developing theory that habitat structure is not solely beneficial for prey.

This research was conducted as part of a Boston University Marine Program field Ichthyology course. Thanks to Dr. P. S. Lobel and Dr. J. Atema for outstanding support.

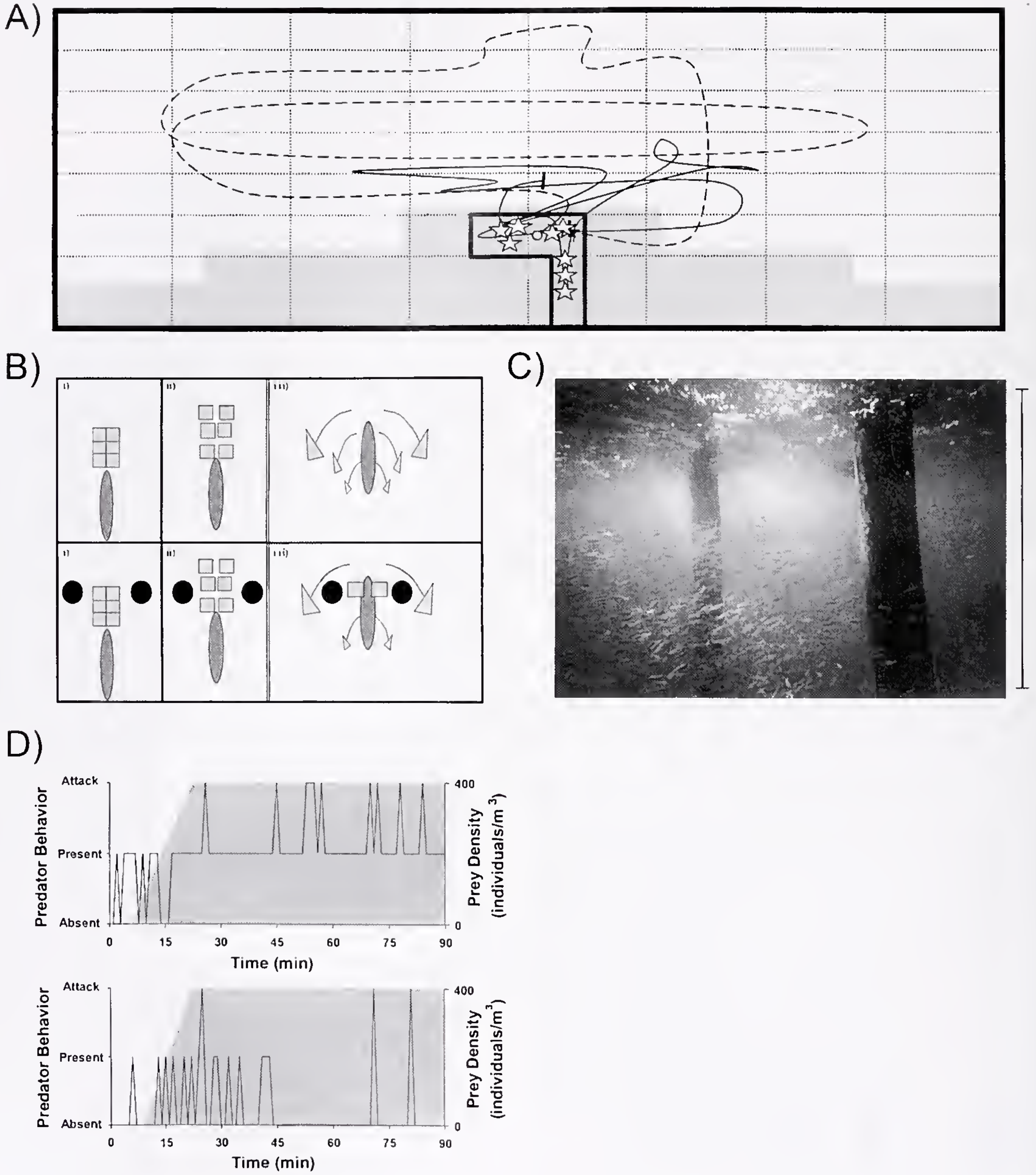

**Figure 1.** *(A) Maps of* Caranx latus *path on 12-09-01 (0555–0640; dashed line), and 12-10-01 (0601–0630; solid line). Grid is 5 m × 10 m beyond the nearshore area. Gray area is the approximate daytime prey distribution. ☆ = attack; ○ = tracking start; | = tracking end. (B) Two-dimensional model of a silverside school splitting in an open habitat (top row); compare with a hotspot, with pilings positioned along the sides of the linear predator attack run (bottom row). Path of the prey school is adapted from the "vacuole" formation of Vabo and Nottestad (5). The oval represents the predator group of average size 10, in 2 rows of 5 fish each (observation). The rectangles each represent a group of prey (5–10 fish). For clarity, the rest of the aggregation is omitted; the focus is only on those silverside groups in the most immediate danger when the velocity of the predators increases. In the observed habitat, the prey would permeate the entire area shown. (i) The initial increase in velocity by the predator group. Split point (ii), and time of lateral movement (iii). (C) Photograph of maximum prey density (400 individuals/m$^3$). Scale bar is 1 m. (D) Graphs of predator behavior on two mornings (12-07-01 and 12-08-01; 0550–0720) under the dock with prey accumulation data (gray).*

## Literature Cited

1. **Gotceitas, V., and P. Colgan. 1989.** *Oecologia* **80:** 158–166.
2. **Eklov, P. 1997.** *Can. J. Fish. Aquat. Sci.* **54:** 1520–1531.
3. **Bartholomew, A., R. J. Diaz, and G. Ciccheti. 2000.** *Mar. Ecol. Prog. Ser.* **206:** 45–58.
4. **Flynn, A. J., and D. A. Ritz. 1999.** *J. Mar. Biol. Assoc. UK* **79:** 487–494.
5. **Vabo, R., and L. Nottestad. 1997.** *Fish. Oceanogr.* **6:** 155–171.
6. **Axelsen, B., T. Anker-Nilssen, P. Fossum, C. Kvamme, and L. Nottestad. 2001.** *Can. J. Zool.* **79:** 1586–1596.
7. **Sancho, G. 2000.** *Bull. Mar. Sci.* **66:** 487–496.

**Reference:** *Biol. Bull.* **203:** 244–245. (October 2002)

# Molecular Approaches to Understanding Population Dynamics of the Toxic Dinoflagellate *Alexandrium fundyense*

*Jane La Du*[1], *Deana Erdner, Sonya Dyhrman, and Don Anderson (Biology Department, Woods Hole Oceanographic Institution, Woods Hole, Massachusetts 02543)*

Toxic dinoflagellates of the genus *Alexandrium* are the primary organisms responsible for seasonal harmful algal blooms (HABs) in coastal New England waters. Members of the genus *Alexandrium* can produce powerful neurotoxins that accumulate in filter-feeding shellfish, causing debilitating or lethal paralytic shellfish poisoning (PSP) in humans and other higher trophic consumers (1).

To better understand the formation and persistence of HABs, it is important to have accurate measures of population dynamics, specifically growth rate and abundance of toxic cells. Recently, molecular assays have been used to quantify the abundance of the HAB organism *Pfiesteria piscicida* (2), and similar assays may be useful for efficient analysis of field samples and for prediction of potential *A. fundyense* HABs. Analogous molecular tools could be used to assess growth rate of *A. fundyense* populations.

This project employed gene sequencing and specific primer design targeting two *Alexandrium fundyense* (CA28) gene fragments: one encoding for ribulose-1,5-bisphosphate carboxylase (RubisCO, *rbcL*); the other encoding for large subunit ribosomal RNA (LSU). This research also explored the use of quantitative polymerase chain reaction (QPCR) to assess growth rate through *rbcL* gene expression and to quantify cell density through LSU gene abundance. QPCR is highly sensitive, enabling users to monitor increases in PCR product formation during amplification (3). By using an appropriate standard, the starting quantity of the specific mRNA or DNA target in a sample can be calculated.

The *rbcL* gene was chosen because dinoflagellates, unlike other photosynthetic eukaryotes, express only a Form II RubisCO (4). RubisCO is the key enzyme for fixing $CO_2$ into organic cellular components during the Calvin-Benson cycle. Measurement of *rbcL* gene expression may be a useful marker for determining changes in cellular growth rate. The LSU gene has a high copy number and is species-specific, making it a good candidate for quantifying CA28 cell density through QPCR.

Degenerate *rbcL* primers, based on three published dinoflagellate *rbcL* sequences (GenBank as of June 2002) were used to PCR amplify a weak 320 base pair product (5). This product was sequenced, and the resulting sequences were aligned and used to design specific *rbcL* primers (forward primer 5′-CACTTTGCAGCTGAGTCTTCCA-3′, reverse primer 5′-CAACGCATCCACGGTTTTTGTG-3′) that target an 81 base pair fragment of the *rbcL* gene.

The LSU forward primer (5′-GGAATGCAAAGTGGGTGG-3′) was designed from published *Alexandrium* strain sequences (6). A previously designed oligonucleotide (NA1) was used as a reverse primer. The NA1 oligonucleotide is specific to toxic North American ribotypes of the *Alexandrium fundyense/tamarense/catenella* species complex (7). These primers targeted a 174 base pair sequence.

Gradient PCR with an annealing temperature range of 50–70 °C was used to determine the highest annealing temperature possible for optimal product formation and primer specificity. Optimal annealing temperatures for the specific rbcL and LSU primers were 63.5 °C and 58 °C respectively.

The specific *rbcL* primers produced robust amplification of the *rbcL* gene fragment as compared to the degenerate primers (Fig.

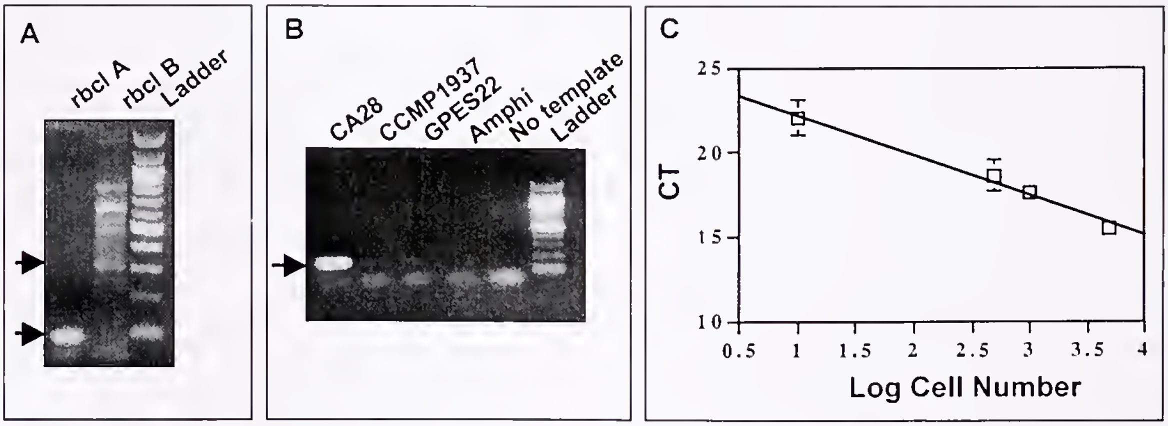

**Figure 1.** *PCR amplification comparisons of designed rbcL and LSU primers, and QPCR standard curve of LSU amplification from known cell densities. (A) Arrows indicate new rbcL primers (A) vs. old primers (B). (B) Specificity and amplifiction robustness of new CA28 LSU primers. (C) QPCR standard curve comparing* $C_t$ *vs. cell number from LSU amplification.*

---

[1] Oregon State University, Corvallis, OR.

1A). The LSU primer pair also produced strong amplification and was highly specific to *Alexandrium* when tested against members of three other dinoflagellate genera, *Gymnodinium* sp. (CCMP1937), *Lingulodinium polyedra* (GPES22), and *Amphidinium carterae* (Amphi) (Fig. 1B).

The LSU primers were tested on *A. fundyense* clonal culture DNA, extracted from a range of known cell quantities. QPCR was performed using SYBR green fluorescent dye with amplification conditions established previously from gradient PCR. Successful amplification resulted in a standard curve (Fig. 1C) that compares the PCR cycle number that crosses a designated fluorescence threshold ($C_T$) to cell density ($R^2 = 0.98$).

The specific *rbcL* primers designed and tested during this project may be used for further research on *rbcL* expression to determine if there is a correlation between growth rate and *rbcL* message abundance. This could be a valuable tool for rapid analysis of *Alexandrium* growth rate in field populations.

The LSU primers described here may be useful for analysis of *Alexandrium* cell densities within mixed field samples, augmenting our abilities to monitor *Alexandrium fundyense* population density in the field. Future work is needed to optimize conditions for DNA extraction from mixed samples containing known *A. fundyense* cell densities. If successful, *A. fundyense* cell numbers in field samples could be quantified by QPCR determination of LSU abundance through comparison to a standard curve.

This work was supported by NSF-REU site grant (OCE-0097498), Boston University Marine Program and Woods Hole Oceanographic Institution.

## Literature Cited

1. **Anderson, D. M. 1997.** *Limnol. Oceanogr.* **42**(5, part 2): 1009–1022.
2. **Bowers, H., T. Tengs, H. Glasgow, J. Burkholder, P. Rublee, and D. Oldach. 2000.** *Appl. Environ. Microbiol.* **66:** 4641–4648.
3. **Wawrik, J., J. H. Paul, and F. R. Tabita. 2002.** *Appl. Environ. Microbiol.* **68:** 3771–3779.
4. **Morse, D., P. Salois, P. Markovic, and J. W. Hastings. 1995.** *Science* **268:** 1622–1624.
5. **Reece, K., M. Siddall, E. Burreson, and J. Graves. 1997.** *J. Parasitol.* **83:** 417–423.
6. **Sholin, C. A. 1993.** Pp. 93–100 in Doctoral dissertation, Woods Hole Oceanographic Institution and Massachusetts Institute of Technology Joint Program.
7. **Sholin, C. A., M. Herzog, M. Sogin, and D. M. Anderson. 1994.** *J. Phycol.* **30:** 999–1011.

---

**Reference:** *Biol. Bull.* **203:** 245–246. (October 2002)

# Pelagic Larval Duration of the Caribbean Wrasse, *Thalassoma bifasciatum*

*Jason Philibotte (Boston University Marine Program, Marine Biological Laboratory,*
*Woods Hole, Massachusetts 02543)*

Most coral reef fishes have a pelagic larval life stage that varies in length from a few days to several months (1). It has been suggested that reef fish developed a larval life stage for one or more of the following reasons: increased food availability, reduced threats of predation over reefs, or improved dispersal (2). The pelagic stage can also be instrumental in determining reef diversity, biogeographic range, and population dynamics of coral reef fish (1, 3, 4). The optimal method for determining pelagic larval duration (PLD) in reef fish is the otolith aging technique. Microincrement formation (daily growth rings) can help determine the primary factors that influence the recruitment patterns (spawning patterns, lunar cycles, oceanographic processes, etc.) of larval fish. In this study, PLD of the bluehead wrasse, *Thalassoma bifasciatum,* from Glover's Atoll, Belize, was determined using the otolith aging technique. These results, along with results from previous studies conducted throughout the Caribbean, were used to determine variability in the mean PLD and the overall range of PLD for *T. bifasciatum.* Sampling seasons within studies were used as separate data sets to calculate the variability in the mean PLD.

Fifty-eight specimens of *T. bifasciatum* were captured with a dip net from reefs around Glover's Atoll. Samples were collected on December 12 to 15, 1994. The fish were measured to the nearest 1 mm and preserved in 95% ethanol. The sagittae and the lapilli, the two largest of the three pairs of otoliths, were used in this study. The sagittae were removed from the semicircular canal at the base of the cranium, and the lapilli were removed from the lateral wall above the sagittae. Otoliths were cleaned in xylene for 24 h and then placed on a slide in immersion oil. Otoliths were examined using a compound microscope with magnifications between 100× and 1000×. Victor (1) validated the presence of daily growth rings and discovered a settlement mark on the otoliths of *T. bifasciatum.* The settlement mark is a series of closely set rings that forms when the larva makes the transition from the plankton to the benthos. PLD was determined by counting the number of increments from the focus to the settlement mark and adding 2 days, in order to account for the time delay in otolith formation after fertilization.

This study found PLD of *T. bifasciatum* to range from 38 to 54 days, with a mean of 45 days. The spawning dates of the larvae collected ranged from October 6 to 27, 1994. The larvae subsequently settled out of the plankton from November 21, 1994, to December 15, 1994, a period of 25 days.

The mean and range of PLD varies considerably among and within species (3, 4). Larvae with longer PLD will potentially have higher levels of dispersal (1) and more variance around the mean PLD (2) due to longer exposure to oceanographic processes. For example, Pomacentrids have a short and consistent PLD: Wellington and Robertson (5) showed that 12 species from Panama had PLDs ranging from 17 to 37 days; the largest range within a species was 14 days. Comparatively, Labrids have a longer PLD with greater variability. For 100 species of Labrids in the Pacific and Caribbean, Victor (6) determined PLDs ranging from 15 to 121 days; the largest range within species was 56 days. Of these 100 species, 20 had a mean PLD greater than *T. bifasciatum* (49.3

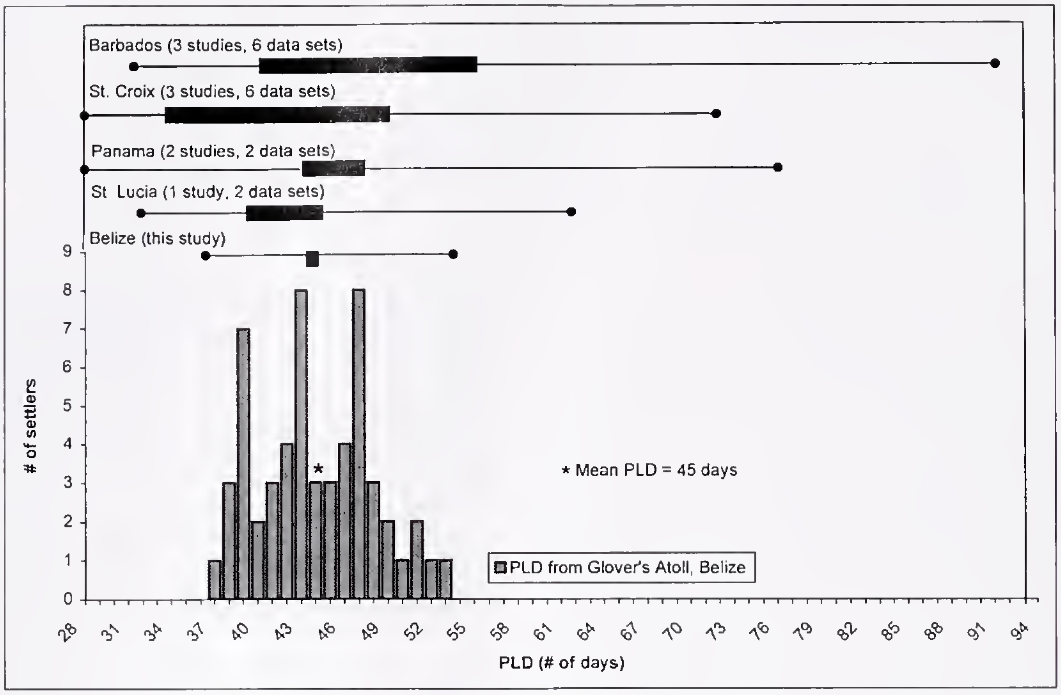

**Figure 1.** *Frequency distribution of pelagic larval duration of* Thalassoma bifasciatum. *Black boxes indicate the minimum to maximum values of mean pelagic larval duration (PLD) obtained in separate data sets. A data set is defined as a sampling season within a study. Lines indicate overall range of PLD from that site.*

days), but only 5 had a higher maximum age at settlement. This discrepancy could be due to Victor's small sample sizes.

Many studies have used the mean PLD to assess the recruitment dynamics of *T. bifasciatum* (2, 3, 4, 7, 8, 9). A review of these studies and the current study shows that PLD varies not only within species but also within sites at different seasons (Fig. 1). The overall range of PLD was 29 to 94 days. This span of 65 days was larger than the range for any individual species in Victor's study (6); this could be due to the very large sample size created by combining these studies. The mean PLDs ranged from 37 to 56.8 days, with Barbados and St. Croix having the greatest variability (Fig. 1). The minimum age at settlement was typically 29 to 34 days. This may represent the competent stage, defined as the age at which metamorphosis may occur given the right environmental cue (2). Larvae at this stage have developed the ability to swim, allowing for a more active role in finding a suitable habitat. The maximum age at settlement was slightly variable; most larvae settled out within 9 to 10 weeks of spawning, with a maximum at 94 days. The large difference between minimum and maximum age at settlement may be due to the larvae's ability to delay metamorphosis until a suitable habitat is encountered (6).

Individuals of *T. bifasciatum* spend, on average, 6 to 7 weeks as pelagic larvae. During this time, they are subject to oceanic processes such as tides, currents, and ocean eddies (10). To what extent the destinies of the larvae are affected by these processes is still unknown. One can hypothesize that, if larvae could settle out when they reach the competent stage, there would be little variance around the mean PLD, without further effects from oceanic processes. One can also hypothesize that the greater the variation around the mean PLD, the more the larvae were subject to oceanic processes. The range in PLD of 29–94 days, and variation in mean PLD of 37 to 56.8 days, would suggest that in different areas throughout the Caribbean, the *T. bifasciatum* are affected by oceanic processes to varying degrees. This would account for the variability in age at settlement between seasons and sites.

## Literature Cited

1. **Victor, B. C. 1991.** Pp. 231–260 in *The Ecology of Coral Reefs*, P. F. Sale, ed. Academic Press, San Diego.
2. **Cowen, R. K. 1991.** *Mar. Ecol. Prog. Ser.* **69:** 9–15.
3. **Sponaugle, S., and R. K. Cowen. 1997.** *Ecol. Monogr.* **67:** 177–202.
4. **Robertson, D. R., S. E. Swearer, K. Kaufman, and E. B. Brothers. 1999.** *Ecol. Monogr.* **69:** 195–218.
5. **Wellington, G. M., and D. R. Robertson. 2001.** *Mar. Biol.* **138:** 11–22.
6. **Victor, B. C. 1986.** *Mar. Biol.* **90:** 317–326.
7. **Hunte von Herbing, I., and W. Hunte. 1991.** *Mar. Ecol. Prog. Ser.* **72:** 49–58.
8. **Masterson, C. F., B. S. Danilowicz, and P. F. Sale. 1997.** *J. Exp. Mar. Biol. Ecol.* **214:** 149–166.
9. **Searcy, S. P., and S. Sponaugle. 2000.** *Mar. Ecol. Prog. Ser.* **206:** 213–226.
10. **Lobel, P. S. 1997.** *Biol. Bull.* **193:** 281–283.

**Reference:** *Biol. Bull.* **203:** 247–248. (October 2002)

# Estuarine–Open-Water Comparison of Fish Community Structure in Eelgrass (*Zostera marina* L.) Habitats of Cape Cod

*Kristin Hunter-Thomson (Williams College, Williamstown, Massachusetts 01267), Jeffrey Hughes*[1], *and Bradley Williams*[2]

While it is generally accepted that eelgrass habitats support diverse and productive fish communities, most of our information about the ecological function of eelgrass habitats comes from estuarine environments. Research demonstrates a high correlation between estuarine eelgrass biomass and fish diversity, abundance, and biomass (1, 2). The few studies that have compared estuarine and open-water eelgrass habitats demonstrate that these habitats support similar species at different abundances (3, 4). Estuarine eelgrass habitats function as a nursery and feeding ground for many marine transient species (5, 6), and recent information suggests that open-water eelgrass habitats can support similar functions (7, 8). Our study tested whether estuarine and open-water eelgrass habitats support similar fish community structure (abundance, biomass, and number and type of species) and also contrasted these fish communities to those of nearby non-eelgrass habitats.

Life-history patterns of many fish species vary with geographical location (1, 9). We identified four major categories of life history patterns for nearshore fish species in southern New England, based on the literature (1, 9): estuarine resident (entire life history occurs primarily in-estuary; *e.g.*, northern pipefish [*Syngnathus fuscus*]), estuarine spawner (juveniles spawned in-estuary, adults occur in open waters; *e.g.*, Atlantic silverside [*Menidia menidia*]), marine spawner (adults spawn juveniles in open waters, development occurs in-estuary; *e.g.*, tautog [*Tautoga onitis*]), and marine species (spawning and juvenile development occurs primarily in open water, and juveniles and adults are estuarine "visitors"; *e.g.*, scup [*Stenotomus chrysops*]). Our study tested whether these life-history classifications were true for the nearshore species we collected.

We sampled five sites in estuarine and open-water environments in Cape Cod: West Falmouth Harbor (estuarine eelgrass habitat); Nobska Point and Falmouth Heights (open-water eelgrass habitats); South Cape Beach and Popponessett Beach (open-water non-eelgrass habitats). To complement our sampling, we randomly chose five sites sampled and analyzed by Hughes *et al.* (1) in the summer of 1998. At least three 1–2 min otter trawls (0.3-cm cod-end mesh aperture) were conducted at each site, and distance trawled was determined by GPS technology. We sorted, identified, and measured (wet weight and standard length) each specimen in the catch. Most fish caught were juveniles.

Our analyses compared location (estuarine, open-water) and habitat type (with and without eelgrass). Two-way ANOVAs (location × habitat type, with sampling sites nested within location and habitat) were used to test differences among means. Number of species was expressed per trawl sample because area trawled explained <3% of species variation. Abundance and biomass data (scaled to 100 $m^{-2}$) were ln-transformed to homogenize variances, and back-transformed means were reported. Probabilities were adjusted by the sequential Bonferroni method (10), and Tukey-Kramer tests ($\alpha = 0.05$) were used for multiple comparisons of means.

Estuarine eelgrass habitats supported significantly more species than did open-water eelgrass habitats (Fig. 1A), although both contained similar fish abundance and biomass (Fig. 1B, C). Eelgrass appears to provide similar ecological benefits (*e.g.*, food, protection) at estuarine and open-water locations.

Non-eelgrass habitats maintained significantly higher fish abundance and biomass in open water than in comparable estuarine locations, suggesting that these environments better accommodate living requirements of fish (Fig. 1B, C). Estuarine non-eelgrass habitats are often eutrophic and hypoxic (1), whereas open-water habitats are better flushed and continually replenished with oxygen, which could produce these more beneficial conditions.

As found in previous research (1, 2), estuarine sites with eelgrass harbored significantly higher numbers of species, abundance, and biomass than estuarine sites without eelgrass (Fig. 1A, B, C). Yet surprisingly, open-water eelgrass and non-eelgrass habitats contained relatively similar numbers of species, numbers of individuals, or biomass (Fig. 1A, B, C).

Some of our life-history classifications were supported by differential abundances by habitat type (Fig. 1D). As expected, estuarine resident and estuarine spawner species existed predominantly in estuarine eelgrass sites. Marine species were significantly more abundant in open water than estuarine locations. Marine species showed no apparent preference for eelgrass in open-water habitats, implying that eelgrass presence does not greatly affect their habitat selection in the open-water habitats. However, marine spawner species displayed an affiliation primarily with eelgrass, suggesting that their abundance depended more on habitat type than on location. The habitat use by this species group needs to be reconsidered in light of these findings.

The difference in community structure between open-water and estuarine locations indicates that fish populations obtain different ecological benefits from each location. However, more extensive research will be necessary to ascertain the ecological function of open-water eelgrass habitats.

A Research Experience for Undergraduates NSF grant (OCE-0097498) supported this research. Thanks to Sasha Clifton, Emily Gaines, and Malin Pinsky for their help in the field.

---

[1] Marine Biological Laboratory, Woods Hole, MA 02543.

[2] University of Central Arkansas, Conway, AK 72035.

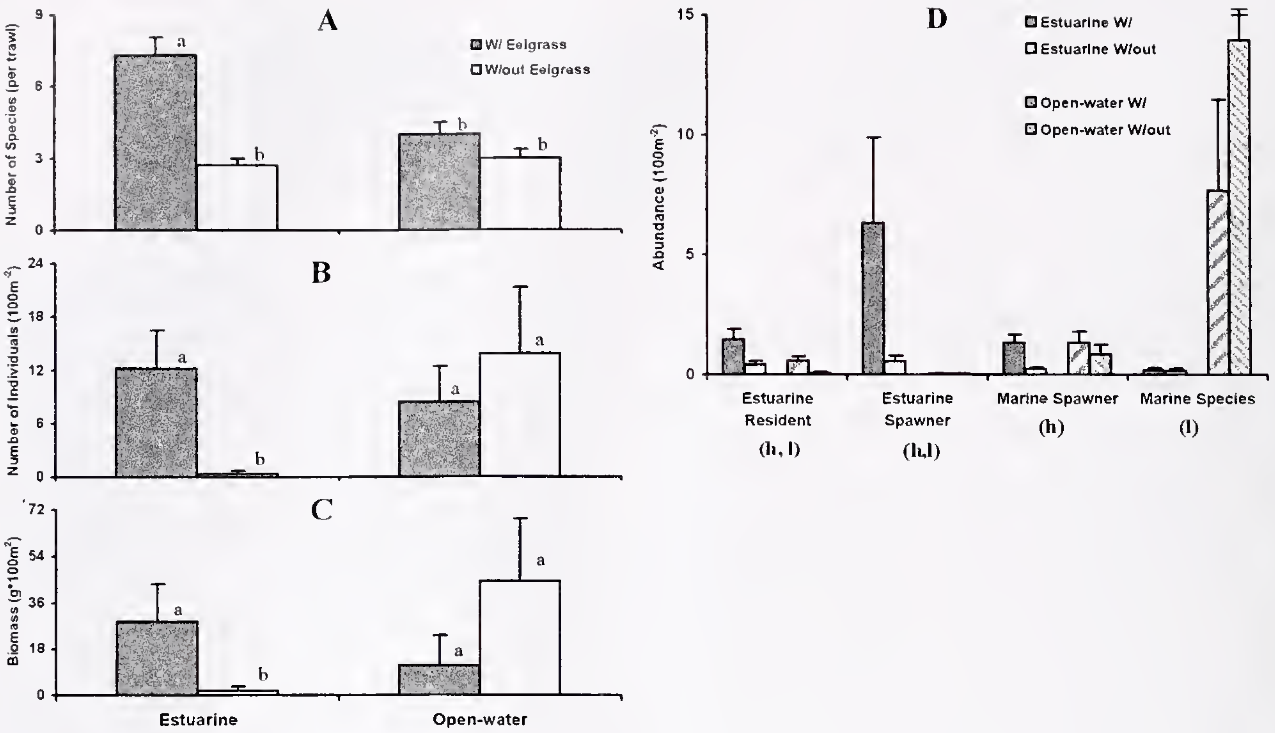

**Figure 1.** *Mean number (+ SE, n = 6–17) of species (A), abundance (B), and biomass (C) in habitats with eelgrass and without eelgrass at estuarine and open-water locations. Different letters represent statistically different (P < 0.05) means. (D) Abundance (+ SE, n = 6–17) by life-history classifications. h, significantly (P < 0.05) habitat-dependent. l, location-dependent.*

## Literature Cited

1. **Hughes, J. E., L. A. Deegan, J. C. Wyda, M. J. Weaver, and A. Wright. 2002.** *Estuaries* **25:** 235–249.
2. **Wyda, J. C., L. A. Deegan, J. E. Hughes, and M. J. Weaver. 2002.** *Estuaries* **25:** 86–100.
3. **Raposa, K. B., and C. A. Oviatt. 2000.** *Estuaries* **23:** 46–55.
4. **Zacharias, M. A., and J. C. Roff. 2001.** *J. Biogeogr.* **28:** 471–483.
5. **Heck, K. L. Jr., K. W. Able, M. P. Fahay, and C. T. Roman. 1989.** *Estuaries* **12:** 59–65.
6. **Nagelkerken, I., G. van der Velde, M. W. Gorissen, G. J. Meijer, T. van't Hof, and C. den Hartog. 2000.** *Estuar. Coast. Shelf Sci.* **51:** 31–44.
7. **Lenanton, R. C., and I. C. Potter. 1987.** *Estuaries* **10:** 28–35.
8. **Lenanton, R. C. 1982.** *Aust. J. Mar. Freshw. Res.* **33:** 881–900.
9. **Able, K. W., and M. P. Fahay. 1988.** Pp. 38–246 in *The First Year in the Life of Estuarine Fishes in the Middle Atlantic Bight.* Rutgers University Press, New Brunswick, NJ.
10. **Sokal, R. R., and F. J. Rohlf. 1995.** Pp. 241-42 in *Biometry.* WH Freeman, New York.

---

**Reference:** *Biol. Bull.* **203:** 248–249. (October 2002)

# Influence of Epiphytic Algal Coverage on Fish Predation Rates in Simulated Eelgrass Habitats

*Bradley S. Williams (University of Central Arkansas, Conway, Arkansas 72035),*
*Jeffrey E. Hughes[1], and Kristin Hunter-Thomson[2]*

The effects of ever-increasing anthropogenic nitrogen loads on marine ecosystems have been well documented (1, 2, 3). Nitrogen from fossil-fuel emissions, fertilizer application, and wastewater discharge increases the total nitrogen load to local bays and estuaries, leading to the accelerated growth of macroalgae and epiphytic algae (2, 3). Epiphytic algae grow on a variety of surfaces such as rocks, eelgrass, and other algae. These fast-growing algae can out-compete eelgrass (*Zostera marina*) for light (2, 3). However, the effects of epiphytic algal proliferation on estuarine communities are not well known (2). One consequence could be increased canopy structure in eelgrass beds, which could decrease foraging efficiency of fish and decrease the rate of predation on small invertebrates. Our study focused on how increased canopy structure due to epiphytic algal growth in eelgrass beds affected fish predation rates on invertebrates in a simulated eelgrass environment.

---

[1] Marine Biological Laboratory, Woods Hole, MA 02543.
[2] Williams College, Williamstown, MA 01267.

The mummichog *Fundulus heteroclitus* was used as the predator because it is commonly found in nearshore eelgrass habitats and is a hardy experimental animal. The fish were maintained in 38-l glass aquaria flushed with flowing seawater, and were given 4 days to acclimate to the laboratory conditions. Fish used in this experiment averaged 6.5 (± 0.3) cm in total length. The amphipod *Gammarus mucronatus*, also found in eelgrass habitats, was used as the prey species. All the amphipods averaged 6 (± 2) mm in total length.

The eelgrass blades, with and without epiphytic alga *Desmarestia aculeata*, were obtained from waters of Vineyard Sound adjacent to the Marine Biological Laboratory pier in Woods Hole, Massachusetts. These blades were qualitatively separated into three categories of epiphytic coverage—zero (0%), low (about 20%), and high (about 80%)—by adapting the methods used for field assessment of percent coverage of eelgrass wasting disease (4). The blades were cut to a standard length of 25 cm. The epiphytic cover was then quantified by taking a random sample of 20 blades from each coverage category and measuring the wet biomass of the epiphytic algae. The low epiphytic cover group had a biomass of 0.11 g/blade (± 0.02 g) and the high epiphytic cover group had a biomass of 0.98 g/blade (± 0.10 g).

Predation experiments were conducted in 38-l aquaria. Ambient temperature (15° C) and salinity (29.9 ppt) were maintained. Three hundred blades that had been sorted by epiphytic coverage category were placed together in clusters of 10. The clusters were evenly distributed in the sand at the bottom of the aquaria. The overall density of the blades was 2307.7 $m^{-2}$. The control group consisted of aquaria with no vegetative cover (*i.e.*, no eelgrass). Eight replicates of the control and experimental treatments were conducted and were interspersed over time.

*F. heteroclitus* individuals selected for experimental trials were denied food for 24 h before the predation experiment. Two fish and 100 amphipods were used for each trial. Individuals introduced into treatments had 1 h to acclimate to the surrounding environment. The predators and the prey were kept in separate sections of the tank by a solid barrier. The trial began as soon as the barrier was removed and the fish were free to forage. One hour of foraging was allowed, and then the predation rate (pr)—the number of *G. mucronatus* consumed/fish/h—was calculated as an indicator of foraging efficiency. The amphipods were recovered by filtering the water and the sand through a 149-μm-aperture screen. The sand, eelgrass, eelgrass with epiphytes, and aquaria were thoroughly flushed with seawater after each experiment to ensure that no amphipods remained.

The predation rate was the highest in the control group (Fig. 1), in which the amphipods had no refuge from the mummichogs, and lowest in the high epiphytic cover treatment (Fig. 1). The high algal biomass formed a thick canopy, which acted as a refuge for amphipods from their predators. Canopy structure had a highly significant effect on the predation rate (one-way ANOVA: $F_s$ = 65.11, d.f. = 3.28, $P$ = 0.0001). All means were statistically different from one another (Scheffe's multiple-comparison method: $P < 0.001$), except for the eelgrass *vs.* eelgrass + low epiphytic algal biomass treatments ($P \approx 0.28$) (Fig. 1).

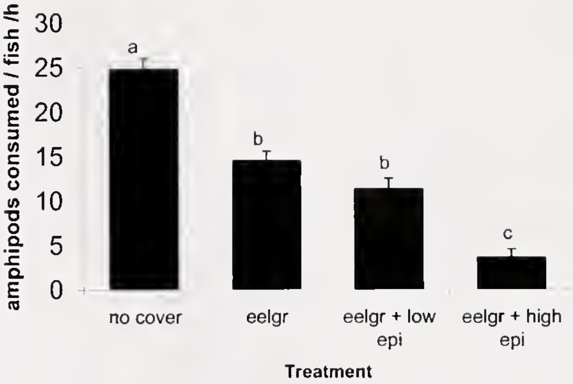

**Figure 1.** *The predation rate (mean number of amphipods consumed/fish/h, ± standard error,* n = *8) of* Fundulus heteroclitus *on* Gammarus mucronatus *in no vegetative cover, 300 blades of eelgrass, 300 blades of eelgrass + low epiphytic biomass, 300 blades of eelgrass + high epiphytic biomass. Different letters above bars indicate significantly different means* (P < *0.001).*

Increased canopy complexity due to high epiphytic algal biomass resulted in a significant decline in predation rate in relation to the predation rate in eelgrass alone. Heightened epiphytic cover could be beneficial to invertebrates in these habitats by providing protection from predation. This benefit would likely occur early in the process of eutrophication before the algae out-competed eelgrass for light, therefore decreasing eelgrass density and making predation more likely. Anoxic or hypoxic conditions caused by algal respiration could also moderate the benefits of increased epiphytic cover.

This research was funded by a NSF Research Experience for Undergraduates site Grant (OCE-0097498). Special thanks are given to Sarah Twichell and Hies Vigo for their assistance and support.

## Literature Cited

1. **Bowen, J. L., and I. Valiela. 2001.** *Can. J. Fish Aquat. Sci.* **58:** 1489–1500.
2. **Deegan, L. A., A. Wright, S. G. Ayvazian, J. T. Finn, H. Golden, R. Rand Merson, and J. Harrison. 2002.** *Aquat. Conserv. Mar. Freshw. Ecosyst.* **12:** 193–212.
3. **Valiela, I., J. McClelland, J. Hauxwell, P. J. Beher, D. Hersh, and K. Foreman. 1997.** *Limnol. Oceanogr.* **42:** 1105–1118.
4. **Burdick, D. M., F. T. Short, and J. Wolf. 1993.** *Mar. Ecol. Prog. Ser.* **94:** 83–90.

**Reference:** *Biol. Bull.* **203:** 250–251. (October 2002)

# Effects of Haying on Salt-Marsh Surface Invertebrates

*John P. Ludlam (Gordon College, Wenham, Massachusetts 01984), David H. Shull*[1], *and Robert Buchsbaum*[2]

Marsh plants may affect the structure of epibenthic communities in a variety of ways. They might reduce temperature stress on organisms by shading, provide refuge from predators, increase the rate of organic matter accumulation at the sediment surface, and serve as a food source. Thus, salt marsh plants might control the spatial distributions of epibenthic invertebrates within the marsh. An ongoing "experiment" on the impact of the periodic removal of plants has been carried out by New England farmers who have been haying some salt marshes for over 300 years. Earlier research by the Plum Island Estuary Long-Term Ecological Research project (PIE-LTER) has shown that haying causes a short-term increase in the growth of benthic algae (1), causes a shift in the diet of some marsh invertebrates to a greater percentage of algae (2), and results in a change in plant species composition (PIE-LTER, unpubl. results).

To determine the short- and long-term effects of haying on the epibenthic community and to identify the principal variables controlling the distribution of epibenthic invertebrates, we carried out two sets of experiments: a marsh-grass-removal experiment to mimic the effects of haying and a survey of invertebrates in areas of the marsh subjected to different haying schedules. Our work was conducted in the Plum Island Sound estuary in Rowley, Massachusetts, from June to August 2002.

For our marsh-grass-removal experiment, we clipped and removed the vegetation from three randomly selected circular sites of 3-m radius along a 50-m transect in a marsh that is hayed roughly every other year. Before clipping we counted organisms in four 0.25-$m^2$ sampling areas, located 1.5 m from the center of the circle and equidistant from each other, within each of the three sites. We sampled the same four areas within each site immediately before clipping, and 1 and 4 days after clipping. Differences in abundances of organisms before and after clipping were evaluated by the Kruskal-Wallis test with time of sampling as treatment. Because differences among circular hayed sites were not significantly different, we pooled replicates from each site before our analysis.

For our surveys of invertebrates in areas subjected to different intensities of haying, we examined randomly selected sites in recently hayed and reference marshes along 12 previously established transects for which GPS elevation data were available. We sampled 40 sites between 1 and 3 July, and 40 more between 16 and 18 July. At each site, we visually estimated percent cover of different plant species. A count of organisms was made after clipping all vegetation from 0.25-$m^2$ plots. A 177-$cm^2$ plant sample was collected, live biomass was separated from standing dead biomass and weighed separately to determine above-ground biomass. Commonly encountered plants included *Spartina patens, Spartina alterniflora, Distichlis spicata, Salicornia europaea,* and *Juncus gerardi.* To evaluate the effect of plant cover on predation rate, we tethered amphipods, *Orchestia grillus,* to thin-diameter line and deployed 5 per site at most sites for 24 h before clipping. We used stepwise multiple regression to describe the relationship between measured environmental variables and abundance of epifauna for the 16–18 July sampling period (criteria $P = 0.1$ to accept, $P = 0.25$ to reject). Environmental variables used in stepwise multiple regression were haying frequency, elevation, temperature, humidity, dried live plant biomass, dried standing dead, total dried weight, percent live, percent dead, percent bare, percent *S. alterniflora,* percent *S. patens,* percent *D. spicata,* percent *S. europaea,* percent *Atriplex patula,* percent *Triglochin maritima,* percent *Iva frutescens,* proportion tethered live amphipods, and proportion eaten tethered amphipods. Collinearity among environmental variables was assessed by examining the variance inflation factor for each included variable. All variance inflation factors were less than 2, which indicated that collinearity among independent variables did not significantly affect our results. A few sampling sites were omitted from the regression analysis due to missing data. Analyses were performed using SPSS software.

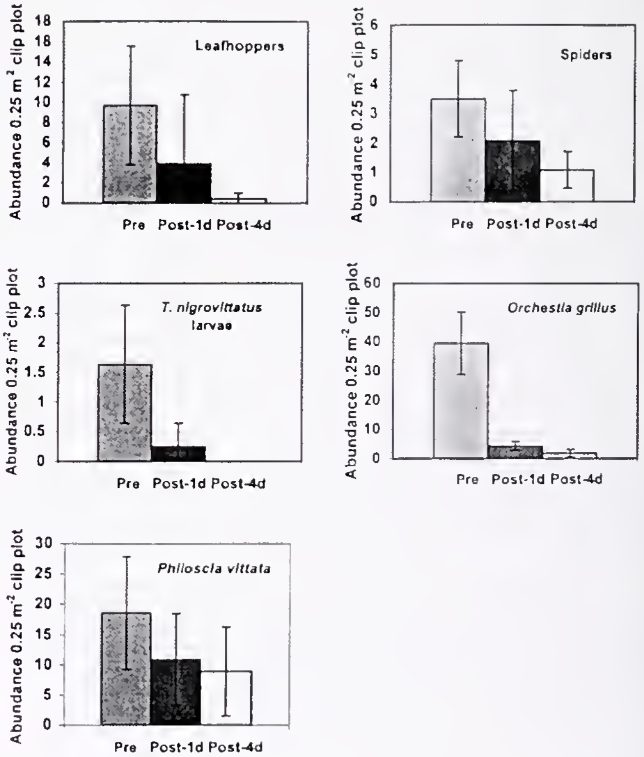

**Figure 1.** *Mean abundances of organisms in the marsh-grass-removal experiment prior to marsh grass removal (Pre), and at 1 day and 4 days following removal (Post-1d and Post-4d). Error bars represent 95% confidence limits.*

---

[1] Department of Biology, Gordon College, Wenham, MA.

[2] Massachusetts Audubon Society, Wenham, MA.

The amphipod *Orchestia grillus*, leafhoppers (Order Homoptera), and the isopod *Philoscia vittata* were the most common invertebrates encountered in the marsh. In the marsh-grass-removal experiment we found a significant decrease in abundance of leafhoppers ($\chi^2_{[2]} = 26.9$, $P < 0.0001$), as well as spiders (Order Araneae) ($\chi^2_{[2]} = 8.72$, $P = 0.013$), greenhead fly larvae (*Tabanus nigrovittatus*) ($\chi^2_{[2]} = 14.23$, $P = 0.001$), and *O. grillus* ($\chi^2_{[2]} = 26.9$, $P < 0.0001$) after clipping (Fig. 1). *P. vittata* was not significantly affected ($\chi^2_{[2]} = 3.32$, $P = 0.19$, Fig. 1).

The stepwise multiple regression indicated that percent *S. alterniflora*, percent bare space, percent *Salicornia europaea*, and temperature were correlated with patterns of leafhopper abundance ($F_{[4,32]} = 40.02$, $P < 0.0001$). The positive correlation between leafhoppers and *S. alterniflora* cover is consistent since leafhoppers often feed on *S. alterniflora* (3).

Spiders were positively related to dead above-ground biomass, and percent bare space ($F_{[2,34]} = 8.25$, $P = 0.001$), which is consistent with their reduced abundance in our experimental marsh-grass-removal treatments. The measured environmental variables related to the abundance of *T. nigrovittatus* larvae were percent *Juncus gerardi*, sediment surface temperature, and proportion of tethered amphipods eaten ($F_{[3,33]} = 8.04$, $P < 0.0001$). The abundance of *T. nigrovittatus* larvae was negatively correlated with sediment surface temperature. It is likely that temperatures in the newly clipped patches were higher than in the unclipped marsh. Abundances of *T. nigrovittatus* larvae were also positively correlated with the proportion of tethered amphipods eaten, which is consistent with our observations of predation by *T. nigrovittatus* larvae on tethered *O. grillus* specimens.

*O. grillus* abundance was not significantly correlated with any variables, and the amphipod was widely distributed throughout the marsh. The lack of a significant correlation with aboveground biomass or haying frequency is noteworthy since the amphipods experienced a strong drop in abundance in the marsh-grass haying experiment. This finding suggests that the long-term effects of haying on *O. grillus* abundances are much less severe than the immediate response. Many invertebrate species may experience a strong reduction in abundance just after haying; however, many environmental variables in addition to haying had an effect on patterns of invertebrate abundance in the long-term.

We thank Carl Noblitt, our research assistant. This research was supported by an REU fellowship through the Plum Island Sound LTER program to JPL.

## Literature Cited

1. **Williams, L., G. C. Noblitt, and R. Buchsbaum. 2001.** *Biol. Bull.* **201:** 287–288.
2. **Horowitz, J., L. Deegan, and R. Garritt. 2000.** Abstract for MBL General Scientific Meetings, August 2001. Available from the Library, Marine Biological Laboratory, Woods Hole, MA.
3. **Vince, S., I. Valiela, and J. M. Teal. 1981.** *Ecology* **62:** 1662–1678.

---

**Reference:** *Biol. Bull.* **203:** 251–252. (October 2002)

# Bacterioplankton Community Composition in Flowing Waters of the Ipswich River Watershed

*Uri Y. Levine*[1] *and Byron C. Crump (Ecosystems Center, Marine Biological Laboratory,*
*Woods Hole, Massachusetts 02543)*

The Ipswich River (Massachusetts) watershed is the largest (404 km$^2$), and most developed watershed of the three that compose the Plum Island Sound Long-Term Ecological Research (LTER) site. Twenty-five percent of the watershed has been set aside for conservation, but development is rapidly occurring in the southern portion of the watershed, because the area is attractive to Boston commuters (1). The effects of development upon a watershed are pronounced because land use is the most important factor dictating water quality, runoff, and productivity, and also contributes to other environmental problems (2). Past watershed studies have not characterized the natural bacterial community, focusing instead on overall microbial processes or the presence of enteric bacteria (3).

We hypothesized that land use would change the bacterioplankton community composition in the first-order streams (the smallest permanently flowing streams) of the watershed; so, for example, streams with predominantly urban land use would yield a unique microbial community. We also hypothesized that the communities of the first-order streams were likely to affect the population of the main stem of the river.

To investigate these hypotheses, we sampled first-order streams from within the watershed representing different land-use areas: urban streams 102 (78% urban land use) (labeling is consistent with that of the Ipswich-Parker Suburban Watershed Channel [IPSWATCH] [4]), 103 (90%), 104 (69%), and 161 (73%); forested streams 143 (81%) and 167 (56% forest and 27% urban); and agricultural streams 170 (28% agriculture, 37% forest, 13% urban) and 172 (28% agriculture, 15% forest, and 35% urban). Unfortunately, other primarily agricultural and forested sites could not be sampled, because the streams were either dry or not flowing as a result of the dry weather. The main stem of the river was also sampled at five points: at its intersection with Woburn St., Boston St. Bridge, Route 97, Winthrop St., and at the mouth of the river at the Ipswich River Dam (IRD, Sylvania Dam). The sites are visually represented in Figure 1A.

Base-flow water samples were collected on June 27 and July 11, 2002, in two acid-washed 1-l Nalgene bottles and kept on ice until further processing within 4 h of collection. Bacterioplankton were preserved for DNA extraction by passing as much as 1 l through 0.2-$\mu$m pore-size Sterivex filter capsules (Millipore) and flooding with DNA extraction buffer. Once concentrated on the filter, the samples were immediately frozen. The DNA extraction procedure was adapted from Zhou *et al.* (5). Polymerase chain reaction (PCR) products for denaturing gradient gel electrophoresis analy-

---

[1] Department of Biology, Kenyon College, Gambier, OH 43022.

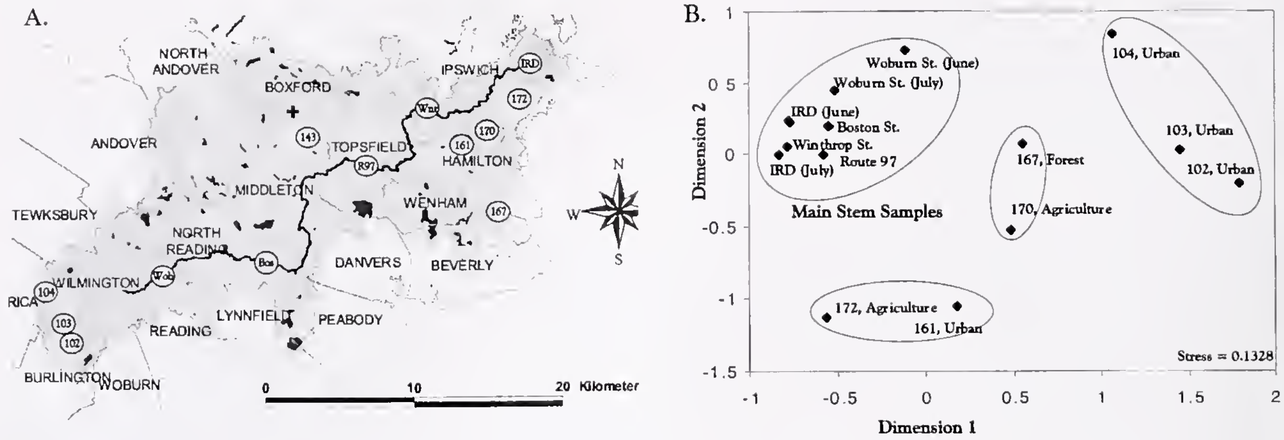

**Figure 1.** *(A) Map of the Ipswich watershed (modified from (4)) with the approximate location of sample sites. Sites along the main stem are labeled as Wob (Woburn St.), Bos (Boston St.), R97 (Route 97), Wnt (Winthrop St.), and IRD (Ipswich River Dam). (B) Multi-dimensional scaling diagram representing a pairwise similarity matrix (Dice) based on the presence or absence of DGGE bands (each band is assumed to represent an individual bacteria population) of bacterioplankton 16S rRNA genes taken from water samples collected during base flow conditions. Samples were collected on June 27, 2002, with the exception of I.S. 103, I.S. 104, Woburn St. (July), Boston St., Winthrop St., and IRD (July) which were collected on July 11, 2002. Circled populations represent waters either from similar land-use areas or from the main stem of the river that clustered together.*

sis (DGGE) were produced using 50 ng of each of the general bacterial primers 357f(g + c) (5′-CGCCCGCCGCGCGCCCCGCGCCCGGCCCGCCGCCCCCGCCCC-CCTACGGGAGGCAGCAG-3′) (6) and 519r (ACCGCGGCTGCTGGCAC), and conditions adapted from Muyzer *et al.* (6). Approximately 50 μl of product, with 6× loading dye, was run on an 8% polyacrylamide gradient gel (30%–50% denaturant, 0.5× TAE) at 70 V for 17 h. Images were analyzed using GelCompar II and Statistica software package (StatSoft, Inc., Tulsa, OK).

With the exception of 161, all of the urban sites had relatively similar bacterial populations (Fig. 1B). Two streams with predominantly forested land-use percentages (167 and 170) clustered together despite 170 being classified as an agricultural site. Streams 161 and 172 also clustered together, presumably because 172 has more urban than agricultural land use. Stream 143, the other forested site, did not cluster with any other sites (data not shown). It is also notable that the sites which clustered together are from similar areas of watershed—102, 103, and 104 are all sites in Burlington, while 170, 167, 161, and 172 are located in the northeast part of the watershed.

The final grouping was that of the main stem of the river. Samples collected the previous summer from the Ipswich River Dam as well as a sample from the nearby Parker River Dam were analyzed with the current samples (data not shown), and it was found that the data from this summer are consistent with previously observed seasonal variations in bacterial community composition (Crump, unpubl. data). Interestingly, the Woburn St. samples had the most unique community compositions of the main stem samples, presumably because this site had more in common with the sites that are immediately upstream (102, 103, and 104).

In addition to indicating that different land-use areas produce distinct communities, the banding patterns also suggest that the bacterioplankton population of the river is established in the first-order catchments and is maintained throughout the course of the river. Of the 38 DGGE bands in the July Ipswich River Dam sample near the mouth of the river, 30 were found in first-order streams throughout the watershed.

In conclusion, we found evidence that microbial communities of first-order streams correlate with land-use type and control the composition of the bacterioplankton of the river.

The work was supported through the NSF grant OCE 976921.

## Literature Cited

1. PIE LTER website (http://ecosystems.mbl.edu/pie/data/wat/WATDescription.htm). Accessed 14 August 2002.
2. **Schneider, L. C., and R. G. Pontius. 2001.** *Agric. Ecosyst. Environ.* **85:** 83–94.
3. **Mallin, M. A., K. E. Williams, E. C. Esham, and R. P. Lowe. 2000.** *Ecol. Appl.* **10:** 1047–1056.
4. IPSWATCH website (http://www.ipswatch.sr.unh.edu/). Accessed 14 August 2002.
5. **Zhou, J., M. A. Burns, and J. M. Tiedje. 1996.** *Appl. Environ. Microbiol.* **62:** 316–322.
6. **Muyzer, G., E. C de Waal., and A. G. Uitterlinden. 1993.** *Appl. Environ. Microbiol.* **59:** 695–700.

**Reference:** *Biol. Bull.* **203:** 253–254. (October 2002)

# Reconstruction of Historical Land Cover in the Ipswich Watershed

*Diana Huffaker and R. Gil Pontius, Jr. (Clark University, Worcester, Massachusetts 01610)*

This paper presents the latest results of a multi-year research effort to examine land-use change in the Ipswich River watershed. Located in northeastern Massachusetts, the watershed covers 404 $km^2$ and is a major component of the Plum Island Estuary-Long-Term Ecological Research site. Researchers at Clark University have been collaborating with scientists at the Marine Biological Laboratory in Woods Hole, Massachusetts, to examine the relationship between land cover and various ecological phenomena (1, 2). To determine how the land-use legacy may influence present ecological phenomena, we must first create a digital map of historical land cover. This paper uses a land-use change model; town-level tabular data from 1951; and maps of land cover at the 30-m by 30-m resolution for 1971, 1991, and 1999 to reconstruct the 1951 landscape (3, 4, 5). This method is applicable to any landscape for which the necessary maps and tabular data are available. Therefore, the method provides a link between ecological scientists and geographers working on multidisciplinary projects where land use is crucial.

Our method uses the land-use change model GEOMOD2, which reads tabular data by town of two exclusive categories, forest and non-forest, and then predicts the category of each 30-m by 30-m grid cell. The model requires a map for the starting time, tabular information at the town level for the ending time, a towns map, and calibration maps. We perform two runs of GEOMOD2; the first, beginning in 1991 and ending in 1971, is a validation run to establish the model's accuracy. The second run, beginning in 1971 and ending in 1951, is the extrapolation.

Forest in the Ipswich watershed has given way to residential development over the past 50 years. Therefore, we calibrate GEOMOD2 to first return forest on cells that are predominantly residential and have relatively young housing stock. To do this, we use land-cover maps of 1999 and 1991 to identify categories of land use that are likely to be the product of recent deforestation, and census information on the age of housing stock to separate old developments from new (6). GEOMOD2 reconstructs the 1971 landscape with 90% of the grid cells classified correctly. This high overall accuracy is a combination of the model's (a) correct knowledge of the proportion of forest and non-forest in each town and (b) ability to locate the forested cells within each town. To determine the spatial accuracy at the 30-m resolution, we use Kappa for Location. This shows that the grid-cell-level prediction of location within the towns is 80% of the way between random and perfect (7).

For the run from 1971 to 1951, we recalibrate the model using land-use maps from 1971 and 1999, and census data from 1990. This will likely improve the model's accuracy because the calibration is based on a strong signal of land change over 28 years. Ultimately, GEOMOD2 produces a map at the 30-m resolution,

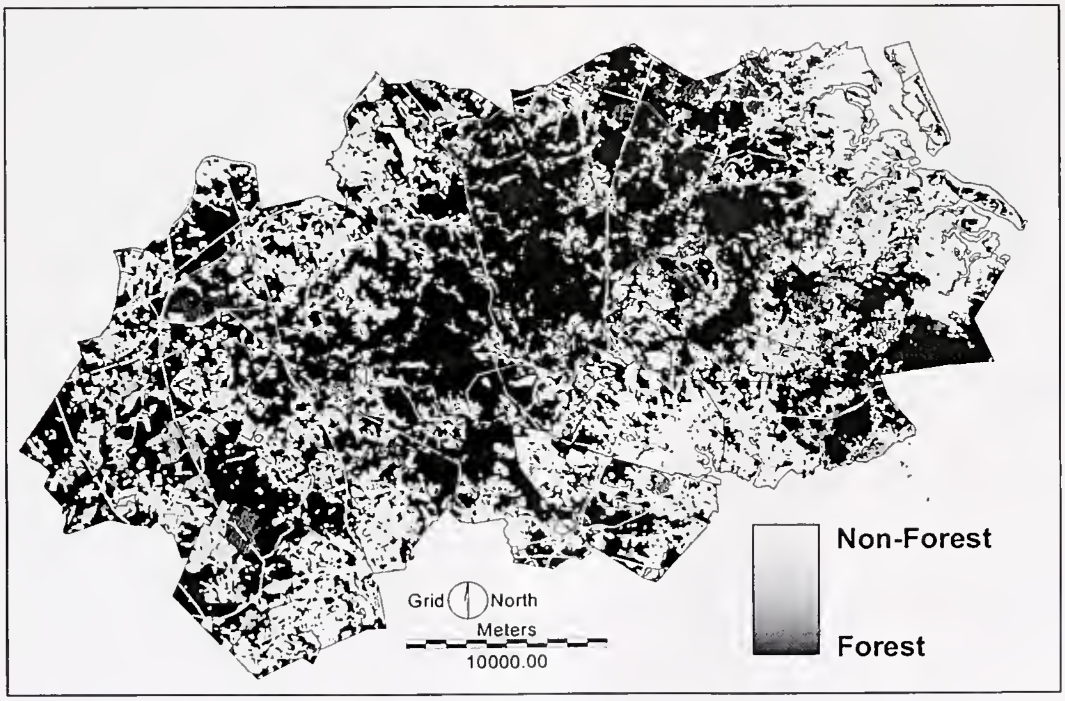

**Figure 1.** *GEOMOD2's best simulation of forest coverage on the 1951 landscape, where shading indicates the level of certainty: black means high certainty of forest; white means high certainty of non-forest; gray means low certainty of cover type.*

where the proportion of forest in each town matches the tabular data for 1951.

Based on the validation of the 1991–1971 run and the simulation of 1971–1951, we estimate that the simulated map of 1951 has 91% of the grid cells classified correctly at the 30-m resolution. At the discrete town level the accuracy ranges from 90% to 93%. When GEOMOD2 simulates a grid cell as forest, we are between 86% and 96% certain that it is truly forest; and when GEOMOD2 simulates a grid cell as non-forest, we are between 84% and 94% certain that it is truly non-forest. The range of certainty in both cases reflects the model's greater accuracy at extremes. When the proportion of forest in a town is close to 0 or 1, the certainty of all individual cells within that town is higher. Figure 1 shows GEOMOD2's best simulation of the 1951 landscape, where the shade of gray indicates the level of certainty of forest. Future steps include incorporating additional census data to detect which residential areas have certain characteristics, such as septic tanks, which influence ecological phenomena.

The National Science Foundation supported this work through the Research Experience for Undergraduates Summer Fellowship Program with the Marine Biological Laboratory (MBL) at Wood's Hole, and NSF's Long-Term Ecological Research program OCE-9726921. Chuck Hopkinson served as advisor from the MBL. Hao Chen of Clark Labs programmed GEOMOD2 into the GIS software IDRISI.

## Literature Cited

1. **Pontius, R. G., Jr., L. Claessens, C. Hopkinson, Jr., A. Marzouk, E. Rastetter, L. Schneider, and J. Vallino. 2000.** *Proceedings of the 4th International Conference on Integrating GIS and Environmental Modeling. CIRES, University of Colorado, Boulder.* (http://www.colorado.edu/research/cires/banff/pubpapers/165/). Accessed 22 Aug. 2002.
2. **Schneider L., and R. G. Pontius, Jr. 2001.** *Agric. Ecosyst. Environ.* 85: 83–94.
3. **Massachusetts Geographic Information System. 2000.** (http://www.state.ma.us/mgis/lus.htm). Accessed 18 July 2002.
4. **MacConnell, W. P., and M. Cobb. 1974.** *Remote Sensing 20 Years of Change in Middlesex County 1951–1971.* Massachusetts Agricultural Experiment Station, Amherst, MA.
5. **MacConnell, W., W. Cunningham, and R. Blanchard. 1974.** *Remote Sensing 20 Years of Change in Essex County 1951–1971.* Cooperative Extension Service, University of Massachusetts, Amherst, MA.
6. **United States Bureau of the Census.** *Census of Population and Housing 1990.* (CD-ROM) Summary File 3, Questions H0260002–8. U.S. Department of Commerce, Washington, D.C.
7. **Pontius, R. G., Jr. 2000.** *Photogrammetric Engineering and Remote Sensing* **66:** 1011–1016.

**Reference:** *Biol. Bull.* **203:** 255–256. (October 2002)

# Dissolved Iron Cycling in the Subterranean Estuary of a Coastal Bay: Waquoit Bay, Massachusetts

*Jeremy M. Testa*[1], *Matthew A. Charette, Edward R. Sholkovitz, Matt C. Allen, Adam Rago, and Craig W. Herbold (Department of Marine Chemistry and Geochemistry, Woods Hole Oceanographic Institution, Woods Hole, Massachusetts, 02543)*

Iron oxides have a strong affinity for dissolved phosphates and certain trace metals (1). Charette and Sholkovitz (2) observed iron oxide-coated sands in sediment cores extracted from the intertidal zone of Waquoit Bay, Massachusetts, and determined that the iron oxides were intercepting phosphates entering the bay in groundwater. They subsequently hypothesized the formation of an "iron curtain," following the oxidation of dissolved ferrous iron to various iron oxides when iron-rich groundwater mixes with intruding saltwater in the subterranean estuary (3). Although the iron oxide-rich sands proved the formation of iron precipitates, more information was needed about the aqueous phase of iron and the conditions surrounding its oxidation. In this study, we have mapped the distribution and concentration of dissolved iron in the subterranean estuary of Waquoit Bay.

Water samples were collected from two transects on the north shore of Waquoit Bay. A map of Waquoit Bay is included in Charette *et al.* (4). One transect spanned 178 m and was orientated parallel to the beach; the second transect, which we examine in this paper, was placed perpendicular to the beach. This 17-m transect extended from the berm of the beach to the intertidal zone. Water samples were collected at 0.5-m intervals to depths of up to 8 m using retract-a-tip, well-point piezometers and a peristaltic pump. At each depth, water was pumped from the ground and immediately filtered to remove particulates, using 10% HCl-cleaned 0.22-$\mu$m filters. We measured dissolved ferrous iron, total dissolved iron, salinity, dissolved oxygen, phosphate, nitrate, ammonium, and silicate in each sample. Ferrous iron and total dissolved iron concentrations were determined using the ferrozine method (5). An automated Winkler titration system was used to determine dissolved oxygen concentrations, and a salinometer was used to measure salinity (6). Concentrations of phosphate, nitrate, ammonium, and silicate were measured colorimetrically, using a Lachat nutrient auto-analyzer (Zellweger Analytics, Quickchem© 8000 Series).

Using a 2D-cross-sectional view, we identified three distinct regions of high ferrous iron in groundwater and pore water profiles (Fig. 1). Region 1 was located in upland groundwater between 2.5 and 4.5 m below sea level, and from 15 to 6 m from the shoreline. Region 2 was found below 4.5 m in the high-salinity subterranean estuary, and region 3 was located between depths of 0.15 to 1 m in the bay sediments.

Region 1 contained the highest measured concentrations of ferrous iron (21.9 $\mu M$) and was located in completely freshwater (Fig. 1B). Dissolved ferrous iron concentrations in this plume decreased close to the shoreline (Fig. 1A). Dissolved oxygen did not exceed 1 mg/l in this region. We identify this region to be a plume of terrestrially derived ferrous iron, given the absence of saltwater and the fact that the pocket of high iron appeared to shoal as it neared the shoreline (Fig. 1A). Basic hydrology suggests that groundwater will discharge into coastal waters after travelling upward at the seepage face, in order to pass over heavier, saline waters that are encroaching into the aquifer. This path permits the mixing of ferrous iron-rich groundwater with shallower aquifer

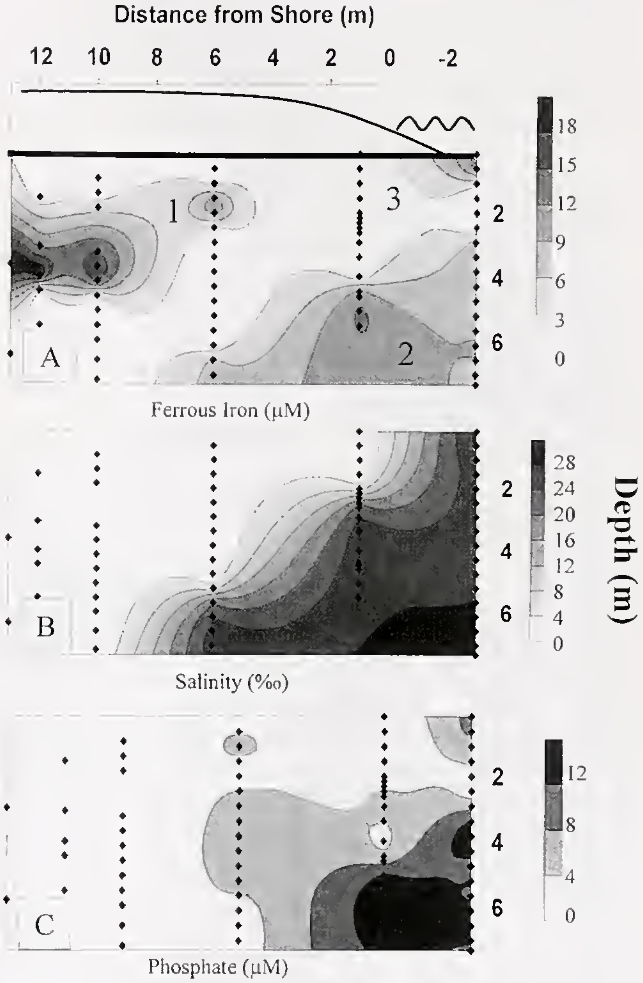

**Figure 1.** *Contour plots showing a 2D cross-sectional view of dissolved ferrous iron (A, contour line interval 3 $\mu$M), salinity (B, contour line interval 4‰), and dissolved phosphate (C, contour-line interval 4 $\mu$M) in water samples from the perpendicular transect. Diamonds (◆) represent where individual samples were extracted. Contours were generated using kriging in SURFER software (version 6.01), which statistically estimates the values of unknown data, based on actual data.*

---

[1] The State University of New York College of Environmental Science and Forestry, Syracuse, NY.

waters that contain higher concentrations of dissolved oxygen. In fact, we recorded a plume of oxygen-rich groundwater (~5 mg/l) at 1.5–2 m in all profiles in our transect parallel with the beach. Ferrous iron appears to oxidize when interacting with this plume. It should be noted that iron-oxidizing bacteria have been recognized to potentially occur in neutral pH groundwater at the oxic/anoxic boundary and could be contributing to iron oxidation (7).

Region 2 was associated with salinity values of 16 to 28‰ and also contained high concentrations of ferrous iron (Fig. 1A, B). This region is located where saltwater is encroaching into the aquifer. Given the hypoxic nature of the groundwater in this region (0.5–1 mg/l), iron-reducing bacteria may be active, utilizing iron oxides as an alternative electron acceptor to oxidize organic material (8). Hypoxia may prevail in the stagnant waters of this region, where fresh groundwater is passing over the saline waters. Encroaching saltwater may also deliver organic substrates from bay sediments that contribute to bacterial activity.

Region 3 contains high levels of ferrous iron in the first meter of sediment, where a black precipitate of iron sulfide exists just beneath the sediment surface. Organic matter deposition in this region results in the utilization of oxygen in decay processes that contribute to reducing conditions. In addition, peak temperatures in summer months increase respiration in benthic communities occupying these sediments, which reduce oxygen concentrations (9).

If we assume that a given concentration of iron oxides will scavenge a proportional amount of dissolved phosphate, then proportional concentrations of dissolved ferrous iron and dissolved phosphate should be released in regions where iron oxide deposits are dissolved. We did not, however, find a strong linear relationship between dissolved ferrous iron and dissolved phosphate in region 1 ($r^2 = 0.32$) (see Fig. 1A, C). This supports the idea that the ferrous iron is not released from previously oxidized iron, but is being transported to Waquoit Bay *via* groundwater. The correlation between ferrous iron and phosphate in region 2 is positive, but not strong ($r^2 = 0.24$). We did, however, find a strong linear correlation between ferrous iron and dissolved phosphate in region 3 ($r^2 = 0.89$), suggesting the reduction of iron oxides (see Fig. 1A, C) and the release of dissolved phosphate. In region 2, processes aside from iron oxide dissolution must be controlling the concentration of phosphate (see Fig. 1A, C), and these factors are probably present in region 3 as well. Likely processes are the mineralization of organic matter to release phosphate and the formation of iron-phosphorus minerals.

Charette and Sholkovitz (2) suggested that dissolved ferrous iron in the subterranean estuary was removed from solution *via* precipitation to iron oxides following mixing with oxygen-rich seawater. It appears the mechanisms responsible for groundwater iron oxidation are more complex. In fact, this study shows that the conversion of ferrous iron to various iron oxides occurred in almost completely salt-free water and that the oxidation and dissolution of iron is also a dynamic process.

We thank staff members of the Waquoit Bay National Estuarine Research Reserve for their support in our field efforts in June/July 2002 and for allowing us to utilize their facilities. This research was funded by a NSF-Research Experience for Undergraduates grant (OCE-0097498), a National Science Foundation grant (OCE-0095384) to M.A.C. and E.R.S., and a fellowship to M.A.C. from the Coastal Ocean Institute at WHOI.

## Literature Cited

1. **Griffioen, J. 1994.** *Environ. Sci. Tech.* **28:** 675–681.
2. **Charette, M. A., and E. R. Sholkovitz. 2002.** *Geophys. Res. Lett.* **29:** 2001GL014512.
3. **Moore, W. S. 1999.** *Mar. Chem.* **65:** 111–125.
4. **Charette, M. A., K. O. Buesseler, and J. E. Andrews. 2001.** *Limnol. Oceanogr.* **46:** 465–470.
5. **Stookey, L. L. 1970.** *Anal. Chem.* **42:** 779–781.
6. **Knapp, G. P., M. C. Stalcup, and R. J. Stanley. 1990.** *Technical Report WHOI-90-35,* Woods Hole Oceanographic Institution. 25 pp.
7. **Emerson, D., and C. Moyer. 1997.** *Appl. Environ. Microbiol.* **63:** 4784–4792.
8. **Lovely, D. R., and E. J. P. Phillips. 1986.** *Appl. Environ. Microbiol.* **51:** 683–689.
9. **D'Avanzo, C., and J. N. Kremer. 1994.** *Estuaries* **17:** 131–139.

---

**Reference:** *Biol. Bull.* **203:** 256–258. (October 2002)

# Nutrient and Freshwater Inputs From Sewage Effluent Discharge Alter Benthic Algal and Infaunal Communities in a Tidal Salt Marsh Creek

*Sarah Twichell (Middlebury College, Middlebury, Vermont 05753), Sallie Sheldon[1], Linda Deegan[2], and Robert Garritt[2]*

Nutrient loading of coastal aquatic ecosystems is becoming a globally important issue. Elevated nitrogen, such as near sewage discharge pipes, has been found to be responsible for algal blooms in coastal areas (1). Raising nitrogen and phosphorus concentrations results in increased algal productivity and standing stock and has been shown to favor filamentous algae and diatom communities (2). Other studies demonstrated a decline in algal species diversity with nutrient inputs, although species richness was unaffected (3). Although a number of studies have linked nutrient loading with algal growth, the response of animal communities to nutrient inputs has been less well studied, especially in salt marsh estuaries (4).

Greenwood Creek, a tidal salt marsh creek in the Plum Island Sound estuarine system of northern Massachusetts, has been the site of sewage effluent input from the secondary wastewater treatment facility for the town of Ipswich, Massachusetts, for over 40 years. Recent measurements of nitrogen inputs from the treatment plant indicate that the predominant form is nitrate ($NO_3 > 80\%$, dissolved organic nitrogen 10%–15%, $NH_4$ 5%–10% [Deegan, unpubl. data]). Current inputs are 3500 $m^3$ of effluent per day and are oxygen (> 6.0 mg/l) regulated. We examined algal standing stock and the abundance of benthic invertebrates in Greenwood Creek and a nearby reference creek (Club Head Creek) to address the impact of sewage effluent (nutrients and freshwater) on benthic communities.

---

[1] Middlebury College, Middlebury, VT.

[2] The Ecosystems Center, Marine Biological Laboratory, Woods Hole, MA.

Two-kilometer transects along the stream were established, with sites spaced every 10 m for the first 30 m downstream of the point source of effluent (where we presumed the greatest sewage influence to be), and more widely spaced (about every 500 m) farther downstream. Sites in the reference creek were chosen to be similar in geomorphology to the sites in the sewage creek. All parameters were measured in late June or mid-July when the effects of sewage are expected to be fully developed. Nitrate ($\mu M$), temperature, and salinity were measured ($n = 1$) at high and low tide at each station ($n = 9$ stations). Mudflat algae samples were taken using a 2-cm-diameter syringe ($n = 3$ for each of 5 sites), and the uppermost 2 cm was analyzed for chlorophyll *a* (5). Infaunal mudflat invertebrates were collected using a 0.25 × 0.25 m quadrat ($n = 3$ for each site) dug to a depth of 0.05 m and sieved through a 500-$\mu$m sieve. Invertebrates were sorted, identified, and preserved in 70% ethanol. The snail *Ilyanassa obsoleta* was sampled by counting all snails in a 1-m-wide transect starting from the edge of the *Spartina patens* down into the creek channel. Two-way analyses of variance were used to test if ln-corrected concentration of chlorophyll *a*, abundance of the polychaete *Nereis*, or abundance of oligochaetes differed between creeks or among sites within a creek.

The sewage effluent input had elevated nitrate levels and lowered salinity. At low tide, nitrate was over 300 times that of the reference creek near the effluent source in the sewage creek, and declined downstream until it was 50 times that of the reference creek when it emptied into Plum Island Sound (Fig. 1A). Salinity was lowest (close to zero) near the effluent source and increased to 30 ppt downstream in the sewage creek. Salinity was high (32 ppt) and constant along the length of the reference creek (Fig. 1B). Temperature was similar between the two creeks (range of 19–21 °C). Chlorophyll *a* was lower at the upper sites of the sewage creek than in the reference creek, but farther downstream levels of chlorophyll *a* between the two streams were similar. The depressed chlorophyll levels in the sewage creek may be linked to the low salinity near the sewage input. Future studies could relate sediment $NO_3^-$ levels to algal growth. As salinity increased, chlorophyll *a* concentration was similar to that of the reference creek (Fig. 1C).

Benthic invertebrate populations also differed between the two creeks. The infaunal samples were dominated by an oligochaete (f. *Enchytraeidae*), and a polychaete (*Nereis virens*). Oligochaetes were most abundant at the three sites closest to the sewage effluent input and declined in the downstream sites of the sewage creek to abundances similar to those in the reference creek (Fig. 1D). *Nereis* was only found in low numbers upstream in the sewage creek, and increased farther downstream as salinity increased. These polychaetes were less abundant in the reference creek and remained fairly constant along the transect (Fig. 1E). *Nereis* is typically found in more saline conditions (6), and, therefore, could be less able to survive upstream in the sewage creek, where salinity is lower and fluctuates more. *Ilyanassa* was very abundant in the downstream sites of the reference creek but was not present in the sewage creek (Fig. 1F). We do not yet understand why *Ilyanassa* was completely missing from the sewage creek.

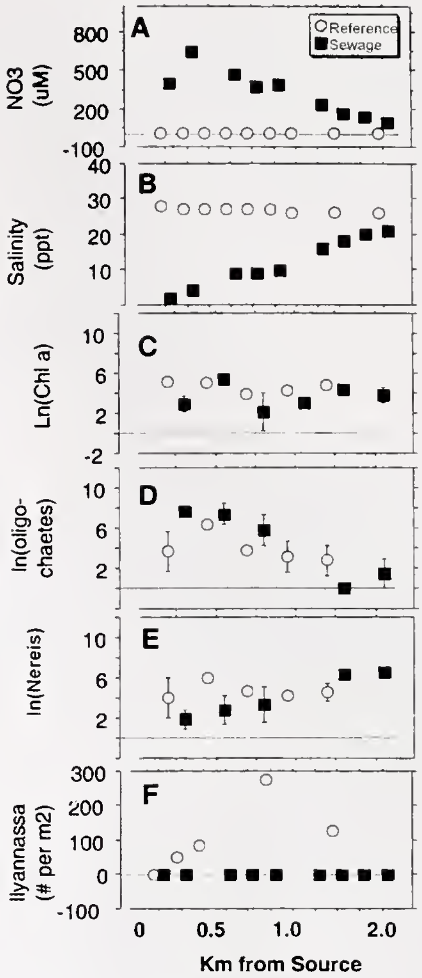

**Figure 1.** *Chemical and biological responses (mean ± 1 standard error) to sewage effluent input into a tidal salt marsh creek. The bottom was too rocky at station 1.1 in the sewage creek for the benthic invertebrate sampling technique to work. Two-way ANOVA* P-*values on ln-transformed values: Ln(chl a): Creek 0.02, Km 0.04, Creek*km 0.43; ln(Oligochaetes): Creek 0.21, Km 0.001, Creek*km 0.06; ln(Nereis): Creek 0.09, Km 0.33, Creek*km 0.0042. ANOVA was not run on* Ilyanassa, *$NO_3^-$, or salinity.*

We found differences in both the algal and benthic invertebrate communities in a tidal salt marsh creek influenced by sewage effluent compared to a reference creek with no sewage input. These differences are most apparent near the outfall and rapidly disappear downstream. They are probably linked to both freshwater input and nutrients, although the relative importance of these factors is not yet clear.

This project was supported by the Research Experience for Undergraduates program through NSF (OCE-972694). We thank Kyle Whittinghill, Molly Yazwinski, Dalton Cox, Carl Noblitt, John Ludlam, and John Logan for their field assistance.

## Literature Cited

1. **Ryther, J. H., and W. M. Dunstan. 1971.** *Science* **171:** 1008–1013.
2. **Sundbäck, K., and P. Snoejs. 1991.** *Bot. Mar.* **34:** 341–358.
3. **Hillebrand, H., and U. Sommer. 2000.** *Aquat. Bot.* **67:** 221–231.
4. **Deegan, L. A. 2002.** *Estuaries* **25:** 585–600.
5. **Lorenzen, G. L. 1967.** *Limnol. Oceanogr.* **12:** 343–346.
6. **Weiss, H. M. 1995.** 8.14 in *Marine Animals of Southern New England and New York—Identification Keys to Common Nearshore and Shallow Water Macrofauna.* State Geological and Natural History Survey of Connecticut Department of Environmental Protection, Connecticut.

---

**Reference:** *Biol. Bull.* **203:** 258–259. (October 2002)

# Tidal Flushing of Ammonium From Intertidal Salt Marsh Sediments: The Relative Importance of Adsorbed Ammonium

*Ketil Koop-Jakobsen (Roskilde University, Denmark) and Anne Giblin*[1]

Intertidal sediments are areas of high nutrient processing. During low tides, air exposure of the sediment increases the rate of degradation of organic matter, causing the ammonium concentration in the sediment to increase between tidal inundations (1). At high tide, when the flooding water inundates the lower part of the salt marsh, ammonium is often released from the sediment to the water column by diffusion and convection (1, 2, 3). However, temporary seasonal import of ammonium from the water column to the sediment has also been observed (4).

In the sediment, a dynamic equilibrium exists between ammonium dissolved in the pore water and that adsorbed onto either inorganic particles or organic matter (5). The ratio between dissolved and adsorbed ammonium can be expressed by the unitless equilibrium constant $K_D$ (6). Since ammonium adsorption to sediment particles and organic matter is a rapid and reversible process (5), not only does pore water ammonium have the potential of being flushed out of the sediment, but the ammonium adsorbed also has the potential of being released to the inundating water, due to a rapid shift in the equilibrium. This study investigates the importance of adsorbed ammonium during tidal flushing.

In the field, tidal flushing of ammonium was studied in late July 2002 in a salt marsh area in the Plum Island Sound, Massachusetts. The study area was dominated by *Spartina alterniflora* and was regularly flooded. Tidal flushing was studied during one tidal cycle in late July at temperatures of 20.9 °C, 22.2 °C, and 23.5 °C for sediment, inundating water, and air, respectively. The amount of ammonium flushed from the sediment was determined as the difference in sediment ammonium concentration before and after inundation. Sediment cores were collected in 6.5-cm diameter acrylic plastic cylinders 1 h before and 1 h after inundation. The cores were sliced in 1-cm sections immediately after sampling. From depths of 1, 2, 3, 5, 7, and 10 cm, subsamples of 3–8 g were collected and placed on ice until further analysis. Total pore water and exchangeable ammonium was extracted from the sediment using $2M$ KCl (5), and the ammonium concentration was determined by the phenol hypochlorite method (7).

In the laboratory, a K-value depth profile was measured under comparable conditions. Sediment cores were collected in the same sampling area during high tide when the sediment was inundated. The cores were placed in a lighted growth chamber at 25 °C and left inundated overnight to equilibrate core temperature. Subsequently, the water column was removed, and the sediment surface was left exposed to air for 12 h, after which the cores were sliced using the same method as in the field. Subsamples were collected for the determination of total ammonium concentration, pore water ammonium concentration, and sediment density. Pore waters were separated from sediments by centrifugation, and the concentration of adsorbed ammonium was determined as the difference between total- and pore-water ammonium. The $K_D$-value is determined as

$$K_D = \frac{[\mathrm{NH}_4^+]_{\mathrm{adsorbed}}(\mu mol/g.ww.sed.)}{[\mathrm{NH}_4^+]_{\mathrm{porewater}}(\mu mol/g.ww.sed.)}$$

and measured at the same depths as the ammonium concentration profiles.

The difference between the total ammonium profiles before and after inundation indicates that a substantial amount of ammonium is released from sediment at this location during inundation at high tides (Fig. 1A). The effect of flushing was greatest in the top 0–1-cm sediment layer, where 50% of the available ammonium was lost. The effect steadily decreased with depth, and at 10-cm depth only 10% of the available ammonium was released (Fig. 1B). In the upper 0–5 cm, more than 50% of the ammonium flushed from each sediment layer originated from the adsorbed pool; in the upper 0–1 cm, this value was as high as 95%. Hence the pool of adsorbed ammonium can account for a significant part of the ammonium released by tidal flushing.

Ammonium adsorbed onto sediment particles and organic matter is by far the largest ammonium pool in the sediment (Fig. 1C). In the upper 0–1-cm sediment layer, this pool can be up to 50 times larger than the pool of ammonium dissolved in the pore water. Farther down in the sediment, from the depths 2 cm to 10 cm, the pool of adsorbed ammonium is still dominant, but is here only about 10 times larger than the dissolved pool.

Since the proportion of ammonium released from the sediment exceeds the proportion of ammonium dissolved in the pore water, the flushing of ammonium from the sediment during inundation is not only a result of ammonium being released from the pore water by diffusive and convective forces, but much more a result of a change in the conditions determining the ammonium adsorption

---

[1] Ecosystems Center, Marine Biological Laboratory, Woods Hole, MA.

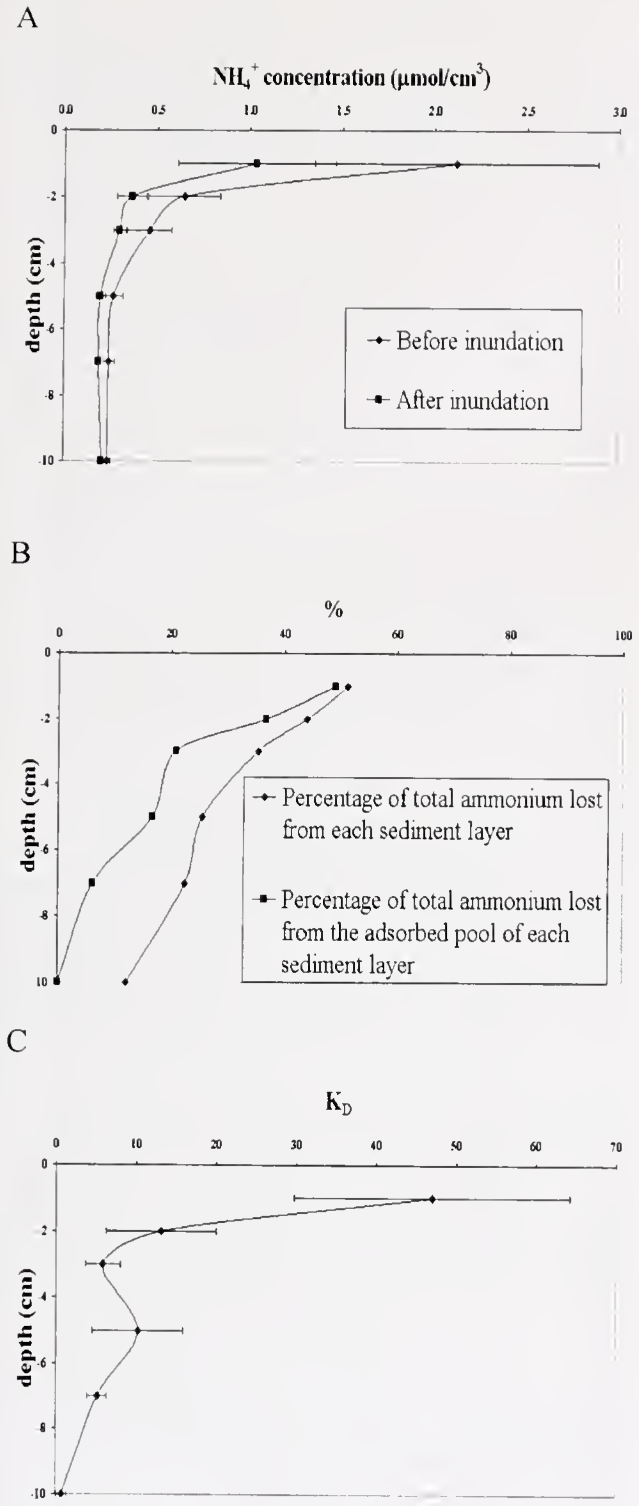

**Figure 1.** *(A) Ammonium concentration profiles before and after inundation. (B) Percentage of total ammonium removed from each sediment layer due to tidal flushing, and percentage of total ammonium lost from the adsorbed ammonium pool. (C) $K_d$-profile after 12 h of air exposure.*

equilibrium. Based on the difference in the ammonium concentration in the sediment before and after inundation, the release of ammonium from the sediment over a tidal cycle was calculated to be 18.6 mmol/m$^2$. That accounts for as much as 37% of the total ammonium in the upper 10-cm sediment layers, of which 80% originated from the adsorbed ammonium pool. These values are in accordance with other data for ammonium flushing (1, 2), and indicate that studies examining the loss of ammonium in sediments need to consider the adsorbed pools as well as the dissolved pools.

This research was supported by a grant from NOAA Sea Grant.

## Literature Cited

1. **Rocha, C. 1998.** *Limnol. Oceanogr.* **43:** 823–831.
2. **Cabrita, M. T., F. Catarino, and C. Vale. 1999.** *Oceanol. Acta* **22:** 291–302.
3. **Caetano, M., M. Falcao, C. Vale, and M. J. Bebianno. 1997.** *Mar. Chem.* **58:** 203–211.
4. **Wolaver, T. G., G. J. Whiting, R. F. Dame, T. M. Williams, and J. D. Spurrier. 1988.** *Mar. Ecol. Prog. Ser.* **49:** 107–116.
5. **Rosenfeld, J. K. 1979.** *Limnol. Oceanogr.* **24:** 356–364.
6. **Mackin, J. E., and R. C. Aller. 1984.** *Limnol. Oceanogr.* **29:** 250–257.
7. **Solorzano, L. 1969.** *Limnol. Oceanogr.* **14:** 799–801.

**Reference:** *Biol. Bull.* **203:** 260–261. (October 2002)

# Effects of Varying Salinity on Phytoplankton Growth in a Low-Salinity Coastal Pond Under Two Nutrient Conditions

*Stacy Barron*[1], *Carolyn Weber*[2], *Roxanne Marino*[3], *Eric Davidson*[4], *Gabrielle Tomasky*[5], *and Robert Howarth*[6] *(Ecosystems Center, Marine Biological Laboratory, Woods Hole, Massachusetts 02543)*

Coastal ponds are highly susceptible to negative effects from nutrient loading (1). The usual approach for managing such systems is to reduce nutrient input. Another possibility for some low-salinity systems may be to control salinity if salinity has a pronounced influence on phytoplankton growth. Freshwater species generally compose the phytoplankton of low-salinity systems. One might expect growth to slow as salinity increases until the assemblage switches from freshwater to marine. Similarly, phytoplankton native to systems with fairly constant salinity through space and time may not tolerate any change in salinity, as they may be adapted to that specific salinity (Valiela, Boston University, pers. comm.).

Oyster Pond (Falmouth, MA) is a brackish pond connected to Vineyard Sound through a lagoon. The pond is currently mesotrophic to eutrophic (based on chlorophyll levels; 1), perhaps due to nutrient loading from the expanding residential population surrounding the pond. Oyster Pond's salinity has decreased from 32‰ (open to the ocean) to less than 2‰ (road restricting Vineyard Sound inflow) (2). Currently, dredging and a weir maintain the salinity at a fairly constant 2.3‰. Oyster Pond managers have the option of manipulating salinity within the pond *via* the weir. While managers plan to manipulate salinity according to which fish populations they desire in the pond (Barry Norris, Oyster Pond Environmental Trust), we are interested in considering what effects salinity changes might have on resident phytoplankton populations. To determine if the general Oyster Pond phytoplankton population could adapt to changes in salinity, we added excess nutrients (nitrate and phosphate) under three salinity regimes. To determine if cyanobacteria could adapt to changes in salinity under N-depleted conditions, we added excess phosphate.

Water was collected from the northern end of Oyster Pond. Three salinity treatments (0.2‰, 2.3‰, and 5.0‰) under two nutrient conditions were created by mixing sieved Oyster Pond water (150-$\mu$m mesh to remove macrozooplankton), filtered Vineyard Sound water (GF/F), and deionized water in clear polycarbonate bottles. The 0.2‰ treatment contained 200 ml Oyster Pond water and 1800 ml deionized water. The 2.3‰ contained 200 ml Oyster Pond water, 129 ml Vineyard Sound water, and 1671 ml deionized water. The 5.0‰ treatment contained 200 ml Oyster Pond water, 298 ml Vineyard Sound water, and 1502 ml deionized water. Three replicate bottles in each salinity treatment were enriched with $NaNO_3$ and $NaH_2PO_4$ to final concentrations of 50 $\mu M$ and 3 $\mu M$, respectively (N + P), while another three bottles at each salinity were enriched only with $NaH_2PO_4$ to a final concentration of 3 $\mu M$ (P). Ambient nitrate and SRP (surface reactive phosphate) concentrations in the pond were 0.2 $\mu M$ and less than 0.5 $\mu M$, respectively. Since Vineyard Sound water used to set up the 2.3‰ and 5.0‰ salinity treatments contained some nitrate and SRP (0.01 $\mu M$ and less than 0.5 $\mu M$, respectively), nutrient additions were in excess to avoid a systematic bias. Two m$M$ $NaHCO_3$ was added to each salinity treatment to buffer against $CO_2$ depletion and pH changes (3). Bottles were incubated from 24–29 °C with a 15:9 light:dark cycle. Light intensity ranged from ~280 to 350 $\mu E\ m^{-2}s^{-1}$.

For the N + P enrichments, 100 ml of water was taken from each bottle initially and daily over 8 days. Chlorophyll *a* concentration was measured fluorometrically after overnight extraction in acetone (4). P additions were sampled similarly over 10 days; phytoplankton samples were preserved with Lugol's solution initially and at 10 days. Cyanobacterial heterocysts were estimated using an inverted microscope and Sedgwick-Rafter counting chamber.

Phytoplankton grew well at all three salinities in the N + P enrichment over time (Fig. 1). These data suggest that, given ample nutrients, phytoplankton from north Oyster Pond tolerate salinities ranging from 0.2‰ to 5.0‰; they do not appear to be closely adapted to ambient salinity. The short-term physiological response observed in this experiment suggests that controlling pond salinity in the 0.2‰ to 5.0‰ range is not likely to result in large differences in overall phytoplankton growth when both N and P are available at high levels. We note that salinity manipulations can have effects on higher trophic levels, which may affect phytoplankton production and are not addressed by these experiments.

In the P treatment, phytoplankton growth over time was significantly slower, characteristic of a cyanobacteria response, and lower than in the N + P addition. With P addition alone, growth was significantly greater at ambient salinity (2.3‰) than at 5.0‰ (Fig. 1). The 0.2‰ treatment had intermediate rates of growth that were not significantly different from other treatments (Fig. 1). These data indicate that phytoplankton growth under P-enriched and N-depleted conditions may be differentially affected by salinity. Cyanobacterial heterocysts increased during the experiment at all salinities, indicating that nitrogen fixation was probably occurring. The largest increase in heterocyst numbers was in the 2.3‰ treatment (1307 $ml^{-1}$ at 10 days *vs.* 6 $ml^{-1}$ initially), indicating that N-fixing cyanobacteria present in Oyster Pond seem best adapted to ambient salinity. The 0.2‰ and 5.0‰ treatments increased from 6 $ml^{-1}$ initially to 193 and 345 $ml^{-1}$, respectively. Note that only one sample was counted for each treatment at 10 days, so the difference in heterocyst numbers at 0.2‰ and 5.0‰ is

---

[1] Bowdoin College, Brunswick, ME 04011.

[2] Cornell College, Mount Vernon, IA.

[3] Ecosystems Center, Marine Biological Laboratory, Woods Hole, MA 02543.

[4] Woods Hole Research Center, Woods Hole, MA 02543.

[5] Boston University Marine Program, Marine Biological Laboratory, Woods Hole, MA 02543.

[6] Department of Ecology and Evolutionary Biology, Cornell University, Ithaca, NY 14853, and Boston University Marine Program, Marine Biological Laboratory, Woods Hole, MA 02543.

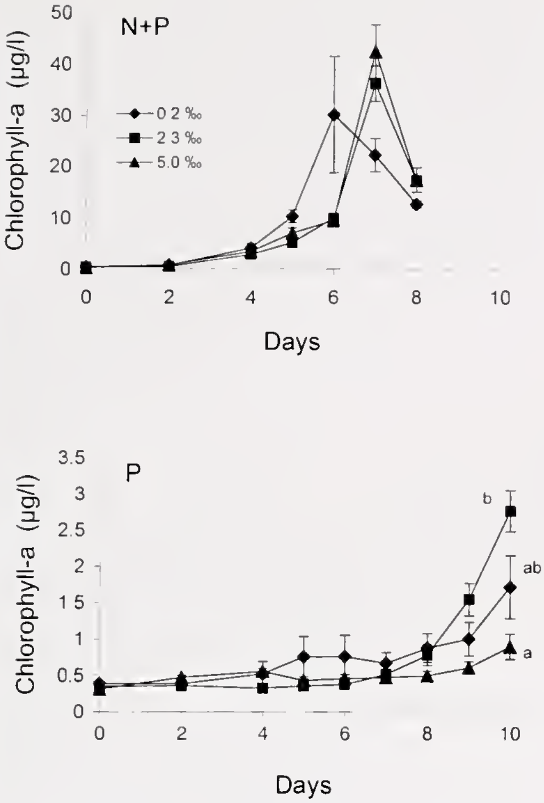

**Figure 1.** *Chlorophyll a (mean ± s.e.) through time in enrichment experiments done with N plus P additions and P additions only for three salinities (0.2‰, 2.3‰, and 5.0‰). Note scale differences on x and y axes. Different letters denote significant differences at the* $P < 0.05$ *level using one-way ANOVA and Tukey's honest significant difference test. Water was collected from the northern end of Oyster Pond and mixed with deionized and Vineyard Sound water to produce the salinities. The experiment was done on July 21, 2002.*

not statistically significant. The large increase in heterocysts in the 2.3‰ treatment may have influenced the final chlorophyll value by adding N to the water, allowing other species to grow.

The stimulation of phytoplankton growth in the P addition treatment contrasts with the finding of a companion study (5) which found that P additions to undiluted Oyster Pond water incubated under the same conditions did not significantly increase phytoplankton biomass. Two differences may explain this. The experiment described here ran for twice as long, allowing more time for the typically slow-growing cyanobacteria, present in the pond water at very low abundances, to respond. Further, our P addition treatment had much lower inorganic N (owing to the 10-fold dilution of Oyster Pond water), which also may have provided conditions more favorable for heterocyst development and N fixation, resulting in enough increase in N availability to increase phytoplankton biomass. This apparent difference between the two experiments bears further experimental investigation.

This short-term experiment should be interpreted with caution because over time cyanobacteria might adapt to a change in salinity. Cyanobacteria can grow and fix N up to 32‰ salinity, although they do so more slowly at higher salinities (3). Also, heterocyst abundance in Oyster Pond is low compared to lakes with high rates of N-fixation (6). Thus N-fixing cyanobacteria may not be present in great enough numbers in Oyster Pond at this time of year to alleviate N-limitation. Nonetheless, these experiments suggest that there may be a potential in Oyster Pond for eutrophication in response to both P enrichment alone as well as to N + P enrichment. Thus, managers should consider the sources of and possible controls on both N and P inputs to the pond. Further, it does not appear that manipulating salinity within the range tested here (0.2‰–5‰) will substantially affect phytoplankton growth directly.

We thank Justin Minihane for help in the field and laboratory, the Ecosystems Center, BUMP, the Valiela lab, and OPET for the use of their facilities. This work was funded by a NSF Research Experience for Undergraduates grant (OCE-0097498).

## Literature Cited

1. **National Research Council. 2000.** *Managing Waste-water in Coastal Urban Areas.* National Academy, Washington, DC.
2. **Emery, K. O. 1997.** P. 111 in *A Coastal Pond Studied by Oceanographic Methods*. Oyster Pond Environmental Trust, Falmouth, Massachusetts.
3. **Marino, R., F. Chan, R. Howarth, M. Pace, and G. E. Likens. 2002.** *Ecosystems* (In press).
4. **Clesceri, L., A. E. Greenberg, and A. Eaton. 1998.** Pp. 10-20–10-21 *in Standard Methods for the Examination of Water and Wastewater, 20th ed.* United Book Press, Baltimore.
5. **Weber, C. F., S. Barron, R. Marino, R. W. Howarth, G. Tomasky, and E. A. Davidson. 2002.** *Biol. Bull.* **203:** 261–263.
6. **Howarth, R., T. Butler, K. Lunde, D. Swaney, and C. Ren Chu. 1993.** *Limnol. Oceanogr.* **38:** 1696–1711.

---

**Reference:** *Biol. Bull.* **203:** 261–263. (October 2002)

# Nutrient Limitation of Phytoplankton Growth in Vineyard Sound and Oyster Pond, Falmouth, Massachusetts

*Carolyn F. Weber (Cornell College, Mount Vernon, Iowa 52314), Stacy Barron*[1]*, Roxanne Marino*[2]*, Robert W. Howarth*[3]*, Gabrielle Tomasky*[4]*, and Eric A. Davidson*[5]

Phytoplankton growth requires nitrogen (N) and phosphorus (P) in an approximate molar ratio of 16:1 (the Redfield ratio; 1). N or P limitation in an aquatic system is considered to occur when the availability of N relative to P is well below or above this ratio, respectively (2, 3). Past studies have shown that marine systems of moderate to high productivity are typically N limited, while sim-

[1] Bowdoin College, Brunswick, ME 04011.
[2] Ecosystems Center, Marine Biological Laboratory, Woods Hole, MA 02543.
[3] Department of Ecology and Evolutionary Biology, Cornell University, Ithaca, NY 14853.
[4] Boston University Marine Program, Marine Biological Laboratory, Woods Hole, MA 02543.
[5] Woods Hole Research Center, Woods Hole, MA 02543.

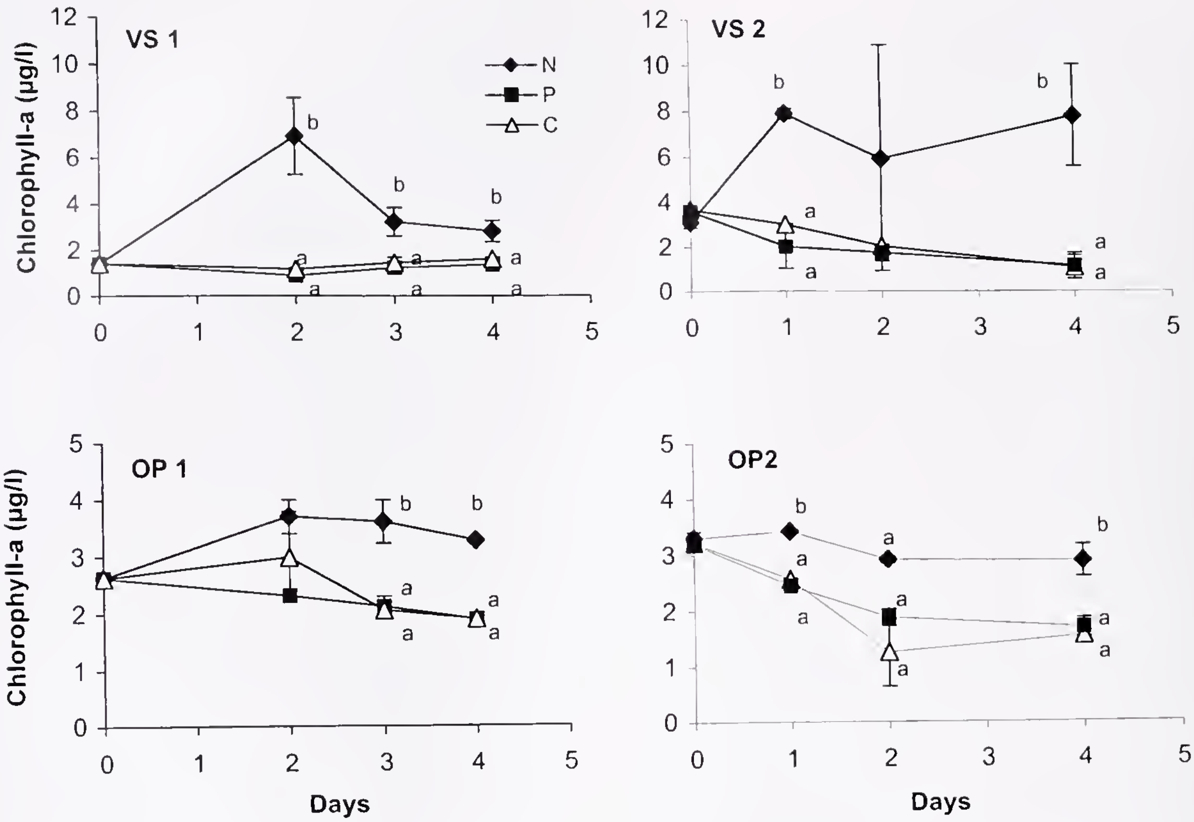

**Figure 1.** *Chlorophyll a concentrations (mean ± 1 s.e.) during experiment 1 and experiment 2 with water collected from Oyster Pond (OP, bottom panels) and Vineyard Sound (VS, top panels). Where standard errors cannot be seen they are smaller than the symbol. Statistical similarities and differences, as denoted by lowercase letters, were determined by a one-way ANOVA followed by Tukey's honest significant difference test ($P < 0.05$).*

ilarly productive freshwater systems are most often P limited (2, 3). However, relatively little is known about low-salinity estuaries. The Baltic Sea is perhaps the best-studied estuary of this type; there, productivity has been shown to be limited by P at salinities lower than 3 to 4‰ and by N at higher salinities (4).

Here, we report the results of a comparative set of nutrient limitation experiments in two coastal systems in Falmouth, Massachusetts, of very different salinities: Vineyard Sound and Oyster Pond (32‰ and 2.3‰, respectively). Previous studies have reported N limitation in Vineyard Sound (5, 6) as would be expected for a high-salinity coastal ecosystem (2, 3). In an October 1986 study, phytoplankton in Oyster Pond did not respond to N or P enrichments (5); Boston University Marine Program students obtained the same result from a similar experiment performed on Oyster Pond in October 2001. However, these experiments were not done during the peak growing season. Oyster Pond is currently considered to be mesotrophic to eutrophic (7), and with the watershed nearing buildout, effective management of nutrient inputs may be important in controlling eutrophication and algal blooms of concern.

We conducted two sets of bottle enrichment experiments, from June 30 to July 5, 2002, and from July 22 to July 26, 2002. For both experiments, we sieved water through a 150-µm mesh to remove large zooplankton. In the first experiment, 12 replicate, 2-l polycarbonate bottles from each system received enrichments of $NaNO_3$ or $NaH_2PO_4$ that increased ambient concentrations of nitrate by about 50 µ*M* (N treatment) or phosphate by about 10 µ*M* (P treatment); 12 control bottles from each system received no nutrient additions (C treatment). As a safeguard against short-term $CO_2$ depletion in the bottles, we added $NaHCO_3$ (2.0 m*M*) to the Oyster Pond samples. At the beginning of the experiment, nine bottles were sampled immediately (three each of controls and three each of the $PO_4$ and $NO_3$ additions) to determine initial chlorophyll *a* concentrations and confirm the effectiveness of the nutrient enrichments. The remaining bottles containing Oyster Pond or Vineyard Sound water were incubated 0.5 m to 1 m below the surface of Oyster Pond on a floating rack, at a light intensity of about 330–560 µE $m^{-2}s^{-1}$ (peak daylight hours). We collected three replicate bottles of each treatment on days 2, 3 and 4. Subsamples were filtered (GF/F) and chlorophyll *a* concentrations were determined fluorometrically (8).

We started our second set of experiments on July 22, 2002. The nutrient treatments were identical to the first experiment, except a treatment was added for Oyster Pond water in which both $NO_3$ and $PO_4$ were added to increase ambient concentrations to 50 µ*M* and 3 µ*M*, respectively, to parallel another concurrent set of experiments done in Oyster Pond (7). We repeatedly removed 100-ml samples from each of twelve 2-l bottles over time for chlorophyll analysis, rather than having replicate bottles for each time point.

We incubated the bottles in a growth chamber on a 15:9 h light: dark cycle at a light intensity of 280–350 $\mu$E m$^{-2}$ s$^{-1}$ and a temperature of 24 to 29 °C. All treatments were sampled initially, and on days 1, 2, and 4.

In the first experiment with Vineyard Sound water, chlorophyll *a* concentrations increased in the N-enriched treatment by day 2, and rapidly declined thereafter (Fig. 1); Concentrations were significantly higher than those of the controls and P-enriched treatment. In the second experiment, chlorophyll concentrations in the N-enriched bottles peaked on day 1 and were always significantly higher than the controls. In contrast, P-enriched treatments were never significantly different from the controls in either experiment (Fig. 1). Both experiments indicate that phytoplankton growth in Vineyard Sound was N limited, as previously reported (5, 6).

In the experiments with Oyster Pond water, chlorophyll *a* concentrations in the N-enriched treatment were significantly higher on two out of the three sampling dates for both experiments (Fig. 1). Chlorophyll *a* concentrations in P-enriched bottles did not differ significantly from controls at any time (Fig. 1). In the second experiment when both N and P were added, the response was far greater, with a final chlorophyll *a* concentration of 23.2 $\mu$g l$^{-1}$ on day 4 (data not shown). This suggests that P can quickly become limiting if enough N is supplied. The significant response in the N-enriched treatment in both our experiments differs from previous studies in Oyster Pond, which found no nutrient limitation (5), and from studies in low-salinity parts of the Baltic Sea (<3 to 4‰) which concluded that P was limiting (4).

Our results contribute to the large body of experimental evidence that finds N limitation in temperate coastal marine ecosystems of moderately high salinity, such as Vineyard Sound. For low-salinity estuaries, there are fewer studies on nutrient limitation, but our finding of N limitation is unusual. The difference between earlier studies in Oyster Pond and our study may reflect seasonal changes in nutrient limitation. Nitrogen may be limiting during the summer (our study) while neither N nor P is limiting in mid-fall (previous studies), either because there is less overall demand for nutrient late in the season or because N fixation over the summer and early fall has helped alleviate N limitation. Further research is needed to better understand nutrient limitation in low-salinity ecosystems, and to evaluate the relative importance of the many biogeochemical processes including N fixation that may regulate limitation in these systems. Nonetheless, our study suggests that N availability, rather than P, currently regulates phytoplankton growth in Oyster Pond during the summer.

We thank the Valiela Laboratory, Ecosystems Center, and the Oyster Pond Environmental Trust. This project was funded by NSF-Research Experience for Undergraduates site grant OCE-0097498.

## Literature Cited

1. **Redfield, A. C. 1958.** *Am. Sci.:* 205–221.
2. **National Research Council. 2000.** Pp. 65–112. Clean Coastal Waters. National Academy Press, Washington, D.C.
3. **Howarth, R. W. 1988.** *Annu. Rev. Ecol.* **19:** 89–110.
4. **Graneli, E., K. Wallstrom, U. Larsson, W. Graneli, and R. Elmgren. 1990.** *Ambio* **19:** 142–151.
5. **Caraco, N., A. Tamse, O. Boutros, and I. Valiela. 1987.** *Can. J. Fish. Aquat. Sci.* **44:** 473–476.
6. **Vince, S., and I. Valiela. 1973.** *Mar. Biol.* **19:** 69–73.
7. **Barron, S., C. Weber, R. Marino, E. Davidson, G. Tomasky, and R. Howarth. 2002.** *Biol. Bull.* **203:** 260–261.
8. **Clesceri, L. S., A. E. Greenberg, and A. D. Eaton. 1998.** *Standard Methods for the Examination of Water and Wastewater.* American Public Health Association, Washington, D.C.

---

**Reference:** *Biol. Bull.* **203:** 263–264. (October 2002)

## Response of Shrimp Populations to Land-Derived Nitrogen in Waquoit Bay, Massachusetts

*Melissa Millman*[1], *Mirta Teichberg, Paulina Martinetto*[2], *and Ivan Valiela (Boston University Marine Program, Marine Biological Laboratory, Woods Hole, Massachusetts 02543)*

Land-derived nitrogen impacts are a major agent of change affecting estuarine populations. Some changes include macroalgae and phytoplankton blooms, which alter food webs and benthic habitats (1). N loads may influence the abundance, species composition, and growth rates of the shrimp species that are common in estuaries of Cape Cod, such as those in the genera *Palaemonetes* and *Crangon* (2). Estuaries of the Waquoit Bay estuarine system offer the opportunity to examine how shrimp of different species respond to different land-derived N loads, because different subestuaries are subject to different land-derived loads. For example, Sage Lot Pond, Quashnet River, and Childs River receive N loads of 15.9, 310.3, and 360 kg N ha$^{-1}$ y$^{-1}$, respectively (3). The estuaries have similar water residence times, about 1–2 days, and range from 0–32 ppt (1).

In this study we assessed the effects of differences in land-derived N loads on shrimp abundance, shrimp species composition, growth rate, and reproduction in estuaries of Waquoit Bay, Massachusetts.

To estimate the abundance and size of shrimp of the different species, we walked a 5-m seine for 10 m in each of five arbitrary locations along the shore, beginning with the most fresh to the most saline of each estuary, during high tide. Shrimp were identified, counted, and measured from the tip of the rostrum to the end of the carapace. To estimate growth rates in *Palaemonetes pugio*, we first identified the modal carapace length of each cohort present, using the software program Mix 3.1.3, and calculated the increment in size per month. In addition, we recorded percent of ovigerous females in each estuary. We used ANOVA to compare species abundance and percent ovigerous females among the

[1] Iowa State University, Ames, IA.

[2] Universidad Nacional de Mar del Plata, Mar del Plata, Argentina.

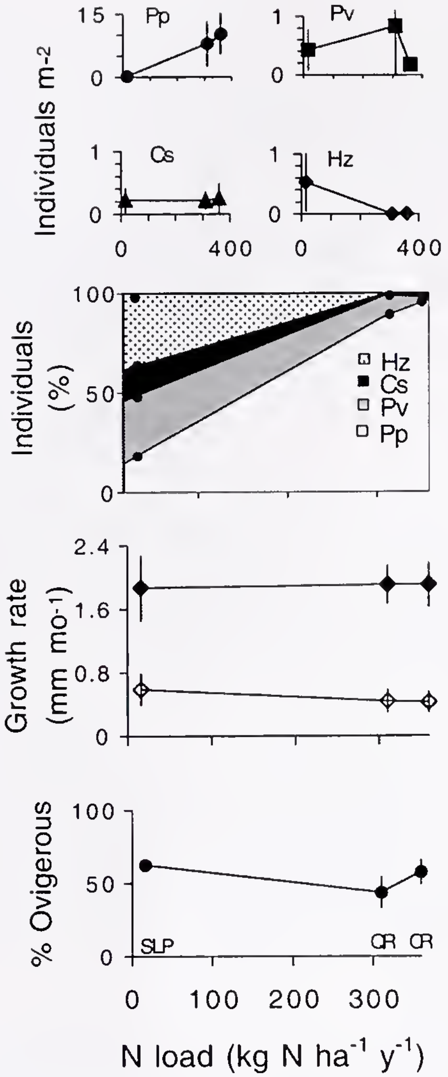

**Figure 1.** *Abundance ± SE of shrimp species (first panel), % species composition (second panel), growth rates of* Palaemonetes pugio *for subadults (◆) and adult cohorts ( ) (third panel), and percent ± SE of ovigerous females of* P. pugio *(fourth panel) in relation to land-derived N loads for the watersheds. Pp =* P. pugio*; Pv =* P. vulgaris*; Cs =* Crangon septemspinosa*; Hz =* Hippolyte zostericola*. CR = Childs River; QR = Quashnet River; SLP = Sage Lot Pond.*

estuaries. A $\log_{10}$ transformation was necessary to meet the ANOVA assumptions to compare abundances. An *a posteriori* Tukey test was used to test differences among estuaries.

We found four species of shrimp in the estuaries: *Palaemonetes pugio, P. vulgaris, Crangon septemspinosa,* and *Hippolyte zostericola* (Fig. 1, first panel). There was no detectable effect of salinity on the abundance of shrimp, so in this paper we pooled data from all stations. Abundance of *P. pugio* was significantly higher in Quashnet River and Childs River than in Sage Lot Pond ($F = 7.83$, df = 2, $P < 0.01$); abundance of *P. vulgaris* and *C. septemspinosa* did not change significantly ($F = 0.073$, df = 2, $P = 0.93$; $F = 0.016$, df = 2, $P = 0.9$). *H. zostericola* was found only in Sage Lot Pond, the estuary with the lowest N load (Fig. 1, first panel).

The differences in abundance of the four species created a clear shift in percent species composition as land-derived N load increased (Fig. 1, second panel). The dominance of *P. pugio* increased in relation to increasing N loading (Fig. 1, second panel); relative abundance of *P. vulgaris* and *C. septemspinosa* did not vary significantly; and *H. zostericola* was only present in the most pristine estuary. *P. pugio* and *H. zostericola* could be useful indicators of level of eutrophication.

We determined growth and reproductive effort for *P. pugio*, the most abundant shrimp species found (Fig. 1, second panel), as also reported in an earlier study (2). Size frequency histograms clearly revealed two cohorts of *P. pugio* in all estuaries. Individuals in cohort 1 had a carapace length of 8–13 mm, and individuals in cohort 2 had lengths of 14–18 mm. Growth rate of cohort 1 was higher than those of adults and was unaffected by N loads (Fig. 1, third panel). Growth rate of adults decreased slightly with increased N loads (Fig. 1, third panel). Egg-bearing females were only found in cohort 2 individuals. There was no effect of level of N loading on the percent of ovigerous females in cohort 2 ($F = 1.7$, df = 2, $P = 0.24$). This suggests that food supply in the estuaries was sufficient to support reproductive needs (4).

Higher N loads lead to higher populations of plants and algae, and the protein content of these are higher. *P. pugio* may be better at exploiting these resources then the other shrimp species (5, 6), although we lack an explanation for the mechanism underlying the different responses by these four shrimp species. We can say, however, that our results suggest that *P. pugio* may be a useful indicator species for increased N loads, and *H. zostericola* may indicate more pristine conditions.

A grant (OCE-0097498) from the National Science Foundation-Research Experience for Undergraduates supported this research.

## Literature Cited

1. **Valiela, I., J. McClelland, J. Hauxwell, P. Behr, D. Hersh, and K. Foreman. 1997.** *Limnol. Oceanogr.* **42:** 1105–1118.
2. **Fritz, C., E. LaBrecque, J. Tober, P. J. Behr, and I. Valiela. 1996.** *Biol. Bull.* **191:** 326–327.
3. **Brawley, J. W., G. Collins, J. N. Kremer, C. H. Sham, and I. Valiela. 2000.** *J. Environ. Qual.* **29:** 1448–1461.
4. **Alon, N. C., and S. E. Stancyk. 1982.** *Mar. Biol.* **68:** 265–276.
5. **Fleeger, J. W., K. R. Carman, S. Webb, N. Hilbun, and M. C. Pace. 1999.** *J. Crustac. Biol.* **19:** 324–333.
6. **Morgan, M. D. 1980.** *Limnol. Oceanogr.* **25:** 896–902.

**Reference:** *Biol. Bull.* **203:** 265–266. (October 2002)

## A Three-Year Retrospective Study of Abdominal Tumors in Zebrafish Maintained in an Aquatic Laboratory Animal Facility

*Roxanna Smolowitz (Marine Biological Laboratory, Woods Hole, Massachusetts 02543),*
*Janice Hanley*[1]*, and Hazel Richmond*[1]

Zebrafish have become important aquatic laboratory animal models for biomedical research. Identification of the types of tumors that occur in zebrafish, and the strains of zebrafish in which they occur, may allow for tumorous animal models used in the study of carcinogenesis to be developed in zebrafish as they have been in other strains of laboratory animals. Although a few reports have described chemically induced zebrafish tumors (1, 2), naturally occurring tumors in zebrafish have not been identified. Chemically induced tumors include papillomas of the skin, hemangiomas, hemangiosarcomas, leiomyosarcomas, neural sheath tumors, and seminomas. Over the past 3 years, six tumors have been found in zebrafish at the Marine Biological Laboratory in Woods Hole, Massachusetts. All affected zebrafish were greater than one year of age and had been held in the aquatic animal facility in recirculating freshwater systems. Affected animals were examined grossly and necropsied. Fish tissues were fixed in 10% neutral buffered formalin. Paraffin-embedded sections of tissue were cut at 6 $\mu$m, stained with hematoxylin and eosin (3), and examined on a Zeiss photomicroscope. Tumors were identified and described (4).

Animals with abdominal tumors were between one and two years of age. They had enlarged abdomens and were either dead or lethargic. Zebrafish with abdominal tumors showed lumpy, asymmetric enlargement of the abdomen rather than the symmetrical enlargement seen in other diseases such as egg binding and *Mycobacteria* sp. infections. Abdominal skin overlying the tumors was thinned (Fig. 1A) and showed vascular congestion. Internally, the tumors filled the abdomen and caused pressure atrophy of surrounding organs (Fig. 1B).

Tumors of the gonadal germ cells (spermatogonia and oogonia) are named seminomas in males and dysgerminomas in females, and have been identified in numerous species of animals as well as humans (4). In this study, zebrafish with seminomas (three animals) and a dysgerminoma (one animal) originated from a wild-type parent strain aquacultured in Floridian ponds (EKKWill Wildlife Resources, Gibsonton, FL). A seminoma was also found in an inbred line of a genetically modified fish (C24-SWATDZ24, swirled tails). This animal was originally identified as a female. Whether this fish produced eggs before developing the tumor is not certain. The gonadal tumors were firm, white to tan, and nodular. Tumors ranging in size from 1.0 × 0.7 × 0.7 to 1.0 × 7.5 × 1.0 cm and were found in the left gonad in 4 of 5 animals. Smaller tumors, 0.2 × 0.2 × 0.2 cm, of the same type were found on the contralateral gonad in 3 of 5 animals. Microscopically, the seminomas were well-encapsulated and composed of sheets and cords of closely packed large polyhedral cells with large round nuclei and usually one nucleolus (Fig. 1C). Probable normal spermatocytes and spermatids (resulting from meiosis of remaining normal spermatogonia) were occasionally seen in the tumor's gonadal tubules. Lymphocytic inflammation and mitotic figures were rarely present, but multinucleated giant tumor cells were common. One animal contained a tumor similar to a seminoma as described above, but also containing eggs interspersed in the neoplastic gonadal tubules.

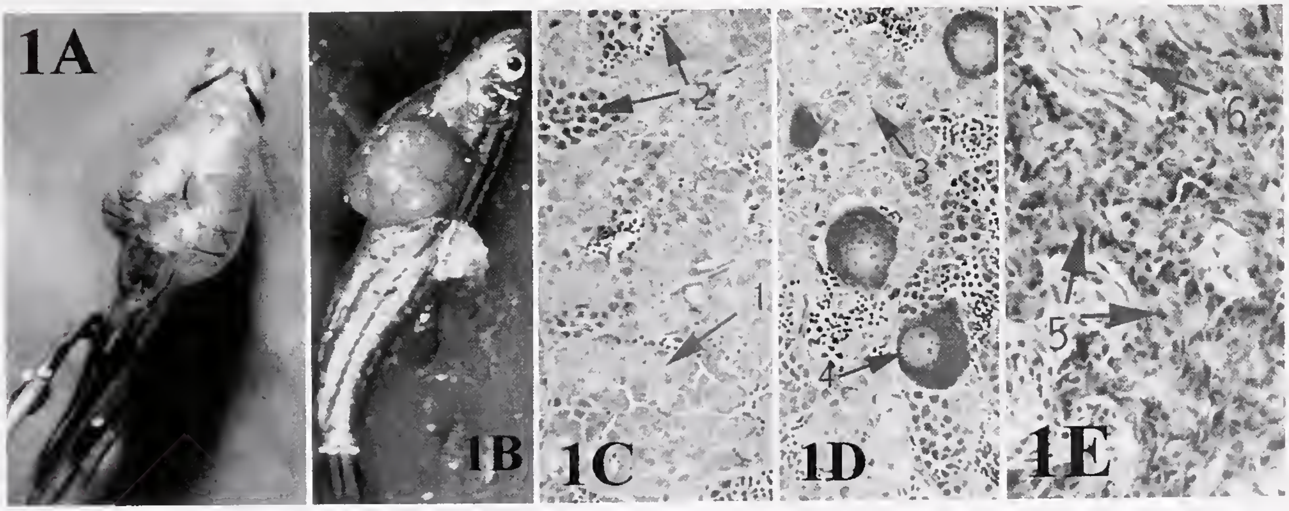

**Figure 1.** *Gross appearance of a seminoma: external (A); internal (B). Histologic appearance (400×) of a seminoma (C), a dysgerminoma (D), and a pancreatic adenocarcinoma (E). 1, seminoma tumor cells; 2, spermatocytes and spermatids; 3, dysgerminoma tumor cells; 4, oocytes; 5, pancreatic carcinoma cells; 6, schirrous reaction.*

---

[1] Marine Biological Laboratory, Woods Hole, MA.

This tumor was named a dysgerminoma, a term that more closely describes its mixed-sex nature (Fig. 1D).

A single pancreatic tumor was identified in a wild-type strain of zebrafish (AB mainline) of greater than one year of age. Externally, the animal had an irregular knobby swelling of the abdomen; internally, a firm, encapsulated white mass was intimately attached to the anterior intestine. The mass was composed of numerous tightly packed clusters, or acini, of well-differentiated pancreatic cells containing variable amounts of secretory granules in the body of the tumor. Mitotic figures were not identified. Small areas of necrosis accompanied by a schirrous reaction (a proliferative fibroblastic response to aggressive carcinomas) were present in some areas of the tumor (Fig. 1E). Less well-differentiated tumor cells accompanied by a moderate schirrous reaction invaded the adjacent mesenteries and extended to the serosal surface where they formed an epithelial border in place of the normal serosal epithelium. Normal pancreatic acini were noted in unaffected mesenteries of the posterior intestine.

Seminomas, dysgerminomas, and pancreatic adenocarcinomas are important and deadly tumors of humans and domestic animals. Once strains and specific lineages of zebrafish with naturally occurring tumors are identified, tumorous animal models using zebrafish could be developed. Such laboratory animal models would be useful in the study of the pathogenesis of tumors at both the molecular and organismal level, and would provide an alternate aquatic animal model for tumor research.

## Literature Cited

1. **Spitsbergen, J. M., H. W. Tsai, A. Reddy, T. Miller, D. Arbogast, J. D. Hendricks, and G. S. Bailey. 2000.** *Toxicol. Pathol.* **28:** 716–725.
2. **Beckwith, L. G., J. L. Moore, G. S. Tsao-Wu, J. C. Harshbarger, and K. C. Cheng. 2000.** *Lab. Investig.* **80:** 379–385.
3. **Humanson, G. L. 1962.** Pp. 3–126 in *Animal Tissue Techniques.* W. H. Freeman, San Francisco.
4. **Jubb, K. V. F., P. C. Kennedy, and N. Palmer. 1985.** Vol. 2, P. 314 and Vol. 3, Pp. 323 and 340 in *Pathology of Domestic Animals.* Academic Press, Orlando, FL.

---

**Reference:** *Biol. Bull.* **203:** 266–267. (October 2002)

# Microbial Analysis of Ozone Disinfection in a Recirculating Seawater System

*Jennifer L. Hsieh*[1], *Hemant M. Chikarmane (Marine Biological Laboratory, Woods Hole, Massachusetts 02543), Roxanna Smolowitz*[2], *Kevin R. Uhlinger*[2], *W. Mebane*[2], *and Alan M. Kuzirian*[2]

The use of ozone to clean and disinfect fresh and seawater life-support systems has become increasingly popular. Many analyses have been performed on their initial setup and design, but as they age and disinfection technology advances, they may require adjustments to function at optimum levels (1). Finding and maintaining the ideal specifications for any given system can be difficult as there are no universally accepted standards (1) and relatively few studies have addressed recirculating seawater systems for fish.

The current efficacy of the ozone disinfection system installed in 1992 at the Marine Resources Center of the Marine Biological Laboratory is unknown. Over the past year, we have linked poor animal health to an increase in bacterial pathogens such as *Vibrio* spp., *Edwardsiella* sp., *Pseudomonas* sp. in the circulating seawater system (Smolowitz, unpublished data), which suggests that the ozone disinfection system is insufficient to reduce fish pathogens to a safe level. To examine the functioning of our current system, we monitored bacterial levels during normal and modified system setups.

One line of the recirculating seawater system was isolated and maintained at a temperature near 15 °C and an ozone dose of 0.52 mg/l ozone, over a period of several months. Three test conditions were set up for a minimum of 3 weeks each. Test 1 was a control period during which no fish were in the system. During Test 2, 30 toadfish (*Opsanus tau*) were maintained in a single tank. Finally in Test 3, a venturi injecting elbow (which increases the ozone gas-water contact) (Ozone Systems model 1584) was added to the disinfection unit at a point prior to the contact chamber. All other parameters were held constant. Feeding and cleaning schedules were controlled. Weekly microbial and chemical analyses were run on samples drawn from four locations in the system: immediately before and after the ozone contact chamber, and immediately before and after the tank. Appropriate dilutions of the water samples were filtered through a sterile 0.45-$\mu$m filter and plated on thiosulfate-citrate-bile salts (TCBS, specific for *Vibrio* spp.) and Levine eosin methylene blue (LEMB, specific for coliforms) agar (Difco). Colonies were counted after 48 ± 2 h incubation at 22–24 °C. To estimate the amount of ozone reaching the water, we monitored the oxidation reduction potential (ORP) using an ORP pinpoint monitor (American Marine).

Bacterial count data (Fig. 1) were analyzed using $t$ tests to compare bacterial levels from different phases and locations. Bacterial levels remained fairly consistent throughout the system during the control phase without toadfish, averaging about 10,700 *Vibrio* and 500 coliform bacteria per 100 ml. Once toadfish were added to the tank, post-tank bacterial levels rose to 535,000 *Vibrio*/100 ml and 17,300 coliforms/100 ml, and average bacterial levels increased to 166,700 *Vibrio*/100 ml and 8,700 coliforms/100 ml.

The difference between bacterial levels before and after ozonation was not significant for any of the three test conditions (dependent pooled-variance $t$ tests: Test 1 *Vibrio* $P = 0.75$, coliform $P = 0.17$; Test 2 *Vibrio* $P = 0.51$, coliform $P = 0.42$). After the venturi injector was added, the bacterial levels following ozonation decreased more than during the other two test conditions, but this difference was still not significant (Test 3 *Vibrio* $P = 0.54$,

---

[1] Barnstable County AmeriCorps Cape Cod, PO Box 427, Barnstable, MA 02630.

[2] Marine Biological Laboratory, Woods Hole, MA 02543.

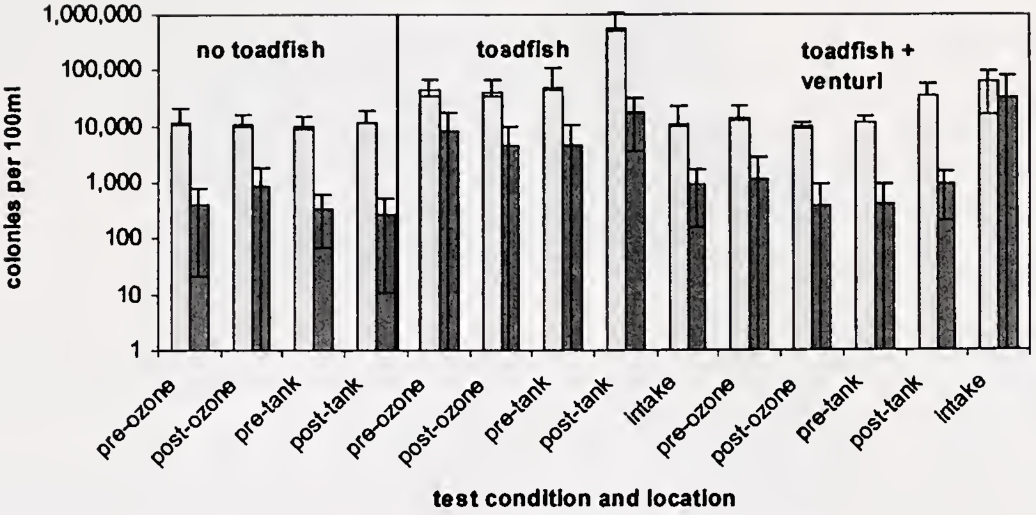

**Figure 1.** *Average* Vibrio *(light grey) and coliform (dark grey) bacteria counts per 100 ml (error bars = ±1 standard deviation) in an ozone-treated recirculating seawater system. Three test conditions are shown: (1) ozone treatment without fish, (2) ozone treatment with 30 toadfish (*Opsanus tau*), and (3) ozone treatment using a venturi injector with 30 toadfish. Microbial analysis was performed weekly for at least 3 weeks during each phase from May 9, 2002, to July 31, 2002. Samples were drawn from four locations within the system and from the system intake water.*

coliform $P = 0.50$). After the venturi injector was added, the average bacterial counts in the system decreased nearly to control levels of 17,400 *Vibrio*/100 ml and 700 coliforms/100 ml.

When compared to standard ozone disinfection, the post-ozone bacterial levels with the venturi were lower, but not significantly so (*Vibrio* $P = 0.21$, coliform $P = 0.23$). When compared to the control phase without toadfish, the post-ozone bacterial levels with a venturi injector were not significantly different (independent pooled-variances $t$ test: *Vibrio* $P = 0.83$, coliform $P = 0.88$). The greatest decrease in bacterial levels occurred between the post-tank sample location and pre-ozone sample location. Coliform bacteria levels were consistently lower than those for *Vibrio* spp. and often more highly variable.

Measurements of the oxidation reduction potential (ORP) averaged 279 mV during Test 1, with a maximum of 288 mV in the post-ozone sample. These values averaged 322 mV during Test 2 (max 329 mV) and 325 mV during Test 3 (max. 349 mV). These ORP values are higher than those of the intake pipe before any treatment, which averaged 299 mV.

At current specifications, the ozone disinfection system does not kill significant numbers of bacteria in the recirculating seawater. The coliform bacteria counts without the venturi injector exceeded the standard set by the Animal and Plant Health Inspection Service for marine mammal aquariums of 1000 coliform bacteria/100 ml (2). Even with the new venturi injector added, bacterial counts were not significantly reduced.

Ozone has been shown to be an effective disinfectant in fresh and seawater systems, but its efficacy depends on system design and specifications (3, 4, 5, 6). In an analysis of multiple disinfection systems for a freshwater hatchery, Wilson (7) found that a venturi injector system using a commercially available source of ozone did not significantly reduce bacterial levels as compared with an air-stone system using onsite ozone production. The best reduction in bacterial counts was achieved by additional filtration followed by UV treatment (7). Preliminary studies at the Marine Resources Center comparing ozone disinfection with UV disinfection have shown similar results.

## Literature Cited

1. **LaBonne, D. 1993.** *Proceedings of the Third International Aquarium Congress* **29:** 347–359. Boston, MA.
2. **Animal and Plant Health Inspection Service, USDA. 1995.** 9CFR3, Subpart E—Specifications for the Humane Handling, Care, Treatment, and Transportation of Marine Mammals (standards).
3. **Liltved, H., H. Hektoen, and H. Efraimsen. 1995.** *Aquac. Eng.* **14:** 107–122.
4. **Sugita, H., T. Asai, K. Hayashi, T. Mitsuya, K. Amanuma, C. Maruyama, and Y. Deguchi. 1992.** *Appl. Environ.* **58:** 4072–4075.
5. **Austin, B. 1983.** *FEMS Microbiol. Lett.* **19:** 211–214.
6. **Kuzirian, A., C. Tamse, and M. Heath. 1990.** *Biol. Bull.* **179:** 227.
7. **Wilson, L. 1990.** *Technical Bulletin: Iowa Dept. of Nat. Res.* **2:** 3–15.

Reference: *Biol. Bull.* **203:** 268. (October 2002)

# Published by Title Only

**Gilland, Edwin, Laura Knott, Robert Baker, and Winfried Denk**
Multiphoton fluorescent imaging of calcium dynamics in embryonic zebrafish

**Hancock, Amy L, and Roxanna Smolowitz**
Investigations into the humane euthanasia of decapod crustaceans using the green crab (*Carcinus maenas*) as a model

**Homsi, Sara, Nicholas Pahl, and Robert M. Gould**
Expression of motor and endocytosis proteins in rat (*Rattus norvegus*) and spiny dogfish (*Squalus acanthias*) brains and squid (*Loligo pealei*) optic lobes

**Jaffe, Lionel**
The propagation speeds of calcium action potentials are remarkably invariant

**Malchow, Robert Paul, Anthony Molina, and Jill Bodily**
Regulation of proton flux from isolated retinal horizontal cells of the skate

**Rice, Aaron N., Janelle L. Morano, and Phillip S. Lobel**
Functional morphology of the pharyngeal jaw muscles of the damselfish *Dascyllus albisella,* based on enzyme activities

**Wikström, Jakob D., Shana S. M. Katzman, and Orian S. Shirihai**
Functional diversity of mitochondria within single pancreatic islet cells demonstrates patterns unique to healthy and diabetic islets

**Yu, Xin, and Barbara Ehrlich**
A model for IP3 induced calcium signals in neurons

**Roberts, Steven, and Rick Goetz**
Characterization of myostatin in fish

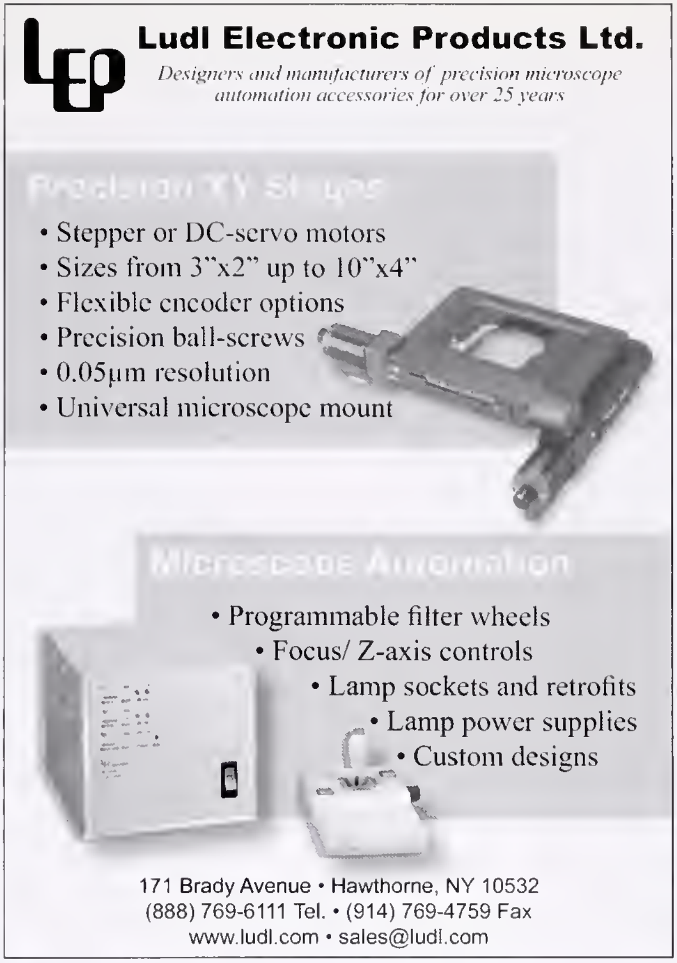

**Ludl Electronic Products Ltd.**

*Designers and manufacturers of precision microscope automation accessories for over 25 years*

Precision XY Stages

- Stepper or DC-servo motors
- Sizes from 3"x2" up to 10"x4"
- Flexible encoder options
- Precision ball-screws
- 0.05μm resolution
- Universal microscope mount

Microscope Automation

- Programmable filter wheels
- Focus/ Z-axis controls
- Lamp sockets and retrofits
- Lamp power supplies
- Custom designs

171 Brady Avenue • Hawthorne, NY 10532
(888) 769-6111 Tel. • (914) 769-4759 Fax
www.ludl.com • sales@ludl.com

---

**2003 SUMMER RESEARCH FELLOWSHIPS**

**FUNDING AVAILABLE FOR SUMMER RESEARCH AT THE MARINE BIOLOGICAL LABORATORY**

The Marine Biological Laboratory is pleased to announce the availability of funding for Summer Research Fellowships in 2003 for junior or senior investigators holding a Ph.D., M.D., or equivalent degree. These prestigious awards provide costs for research and housing, and also enable Fellows to benefit from the rich intellectual and interactive environment of the scientific community at the MBL.

Proposals for Fellowship support will be considered in, but are not limited to, the following fields of investigation:

**Cellular & Molecular Physiology**
**Neurobiology**
**Parasitology**
**Molecular Biology**
**Developmental Biology**
**Ecology**
**Microbiology**

Specific Fellowships in Cell & Developmental Biology are funded by the Laura and Arthur Colwin Fellowship Fund. Additional specific Fellowships also provide state-of-the-art microscopy support.

APPLICATION DEADLINE FOR FELLOWSHIPS IS JANUARY **15, 2003**

Applications are reviewed by the MBL Fellowship Committee. Notification of decisions will be mailed by March 15.

FOR APPLICATION FORMS AND ADDITIONAL INFORMATION, PLEASE CONTACT:
Sandra Kaufmann
Fellowship Coordinator
508-289-7441: skaufman@mbl.edu

*The MBL is an EEO Affirmative Action Institution*

*Applications are encouraged from women and members of underrepresented minorities.*

ADDITIONAL INFORMATION IS AVAILABLE ON OUR WEB-SITE:

**http://www.mbl.edu/fellowships**

**Marine Biological Laboratory, 7 MBL Street, Woods Hole, Massachusetts 02543-1015**

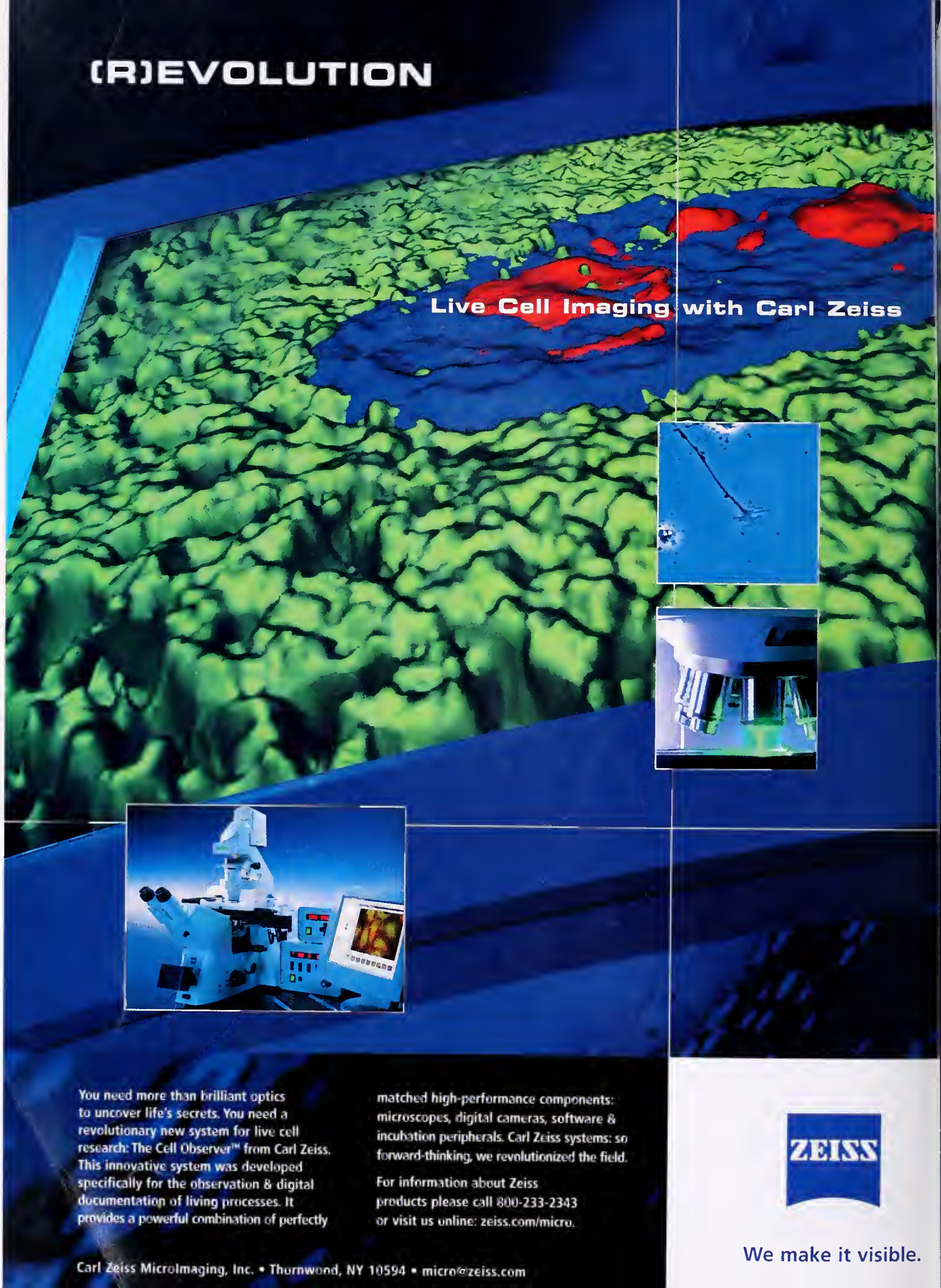

You need more than brilliant optics to uncover life's secrets. You need a revolutionary new system for live cell research: The Cell Observer™ from Carl Zeiss. This innovative system was developed specifically for the observation & digital documentation of living processes. It provides a powerful combination of perfectly matched high-performance components: microscopes, digital cameras, software & incubation peripherals. Carl Zeiss systems: so forward-thinking, we revolutionized the field.

For information about Zeiss products please call 800-233-2343 or visit us online: zeiss.com/micro.

We make it visible.

Carl Zeiss MicroImaging, Inc. • Thornwood, NY 10594 • micro@zeiss.com

December 2002

Volume 203 • Number 3

# THE BIOLOGICAL BULLETIN

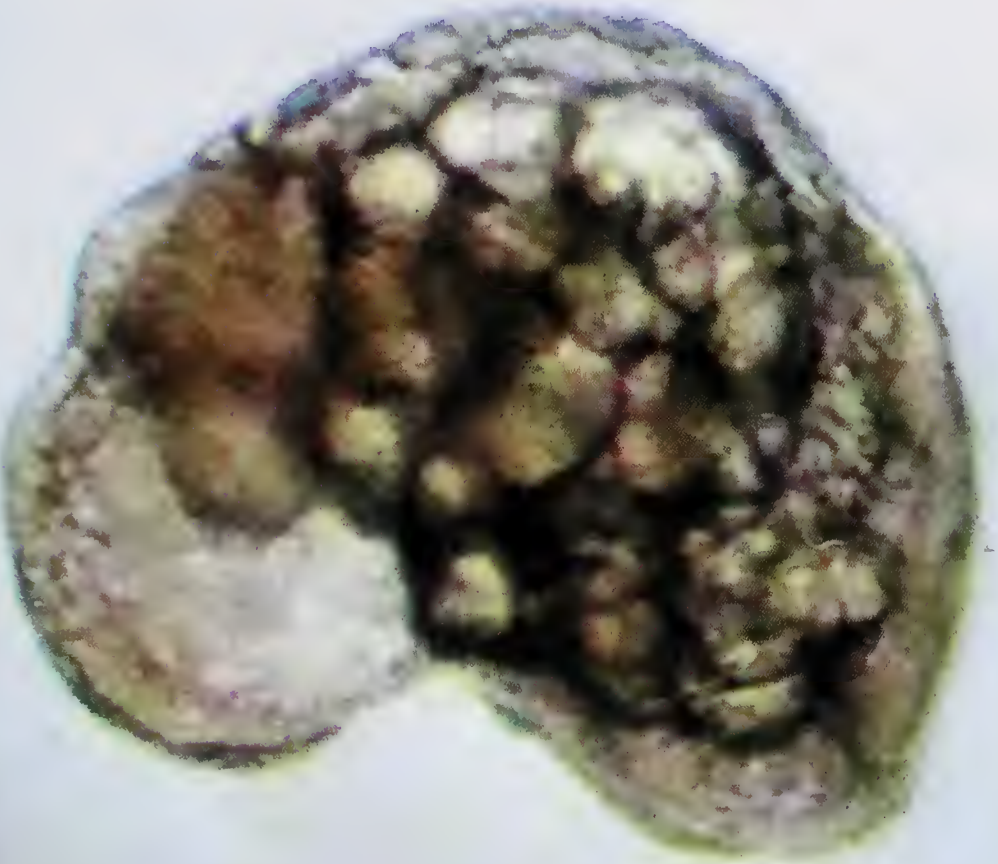

Published by the Marine Biological Laboratory

www.biolbull.org

ERGONOMIC 25° EYEPIECE TUBE
ERGONOMIC TILTING TUBE
EXTENDED INFINITY DESIGN PERMITS EASY ADDITION OF ILLUMINATION SOURCES/ATTACHMENTS
SIX POSITION FLUORESCENCE FILTER CUBE TURRET
MULTIPLE IMAGE PORTS (FRONT, WITH SIDE, TOP AND BOTTOM)
Nikon

INVERTED MICROSCOPES

# DRAWN FROM EXPERIENCE

## ONLY NIKON COULD REINVENT INVERTED MICROSCOPY WITH THE NEW ECLIPSE TE2000 SERIES.

When they were launched, Nikon's Eclipse TE microscopes set new standards in optical performance, continuing a tradition of over twenty years of excellence in inverted microscopy.

Now, Nikon proudly introduces the next generation of Eclipse research inverted microscopes. The Eclipse TE2000 series incorporates past successes into a new design with innovations that are exactly what today's varied research techniques require.

Here are just some of the special features built into this extraordinary microscope

- Multi-port design permitting addition of optional illumination sources and other attachments without modifying the microscope.
- Unique "Noise Terminator" thoroughly eliminates stray light for greater S/N ratio in fluorescence imaging.
- Super-nanoprecision Z-access control and increased stability for superior 3D imaging.
- Modular motorized components for automated control.
- Exclusive CFI60™ infinity optical system for excellent resolution with high numerical apertures and longer working distances.

The Eclipse TE2000 is available in three models, each configured to meet your research needs. Draw on Nikon's experience.
For more information, call 1-800-52-NIKON, ext. 392
or visit www.nikonusa.com
In Canada, call 1-866-99-NIKON.

Visit MicroscopyU at
www.nikonusa.com to learn more
about inverted microscopy.

CFI60
ECLIPSE

Nikon

©2002 Nikon Instruments Inc.

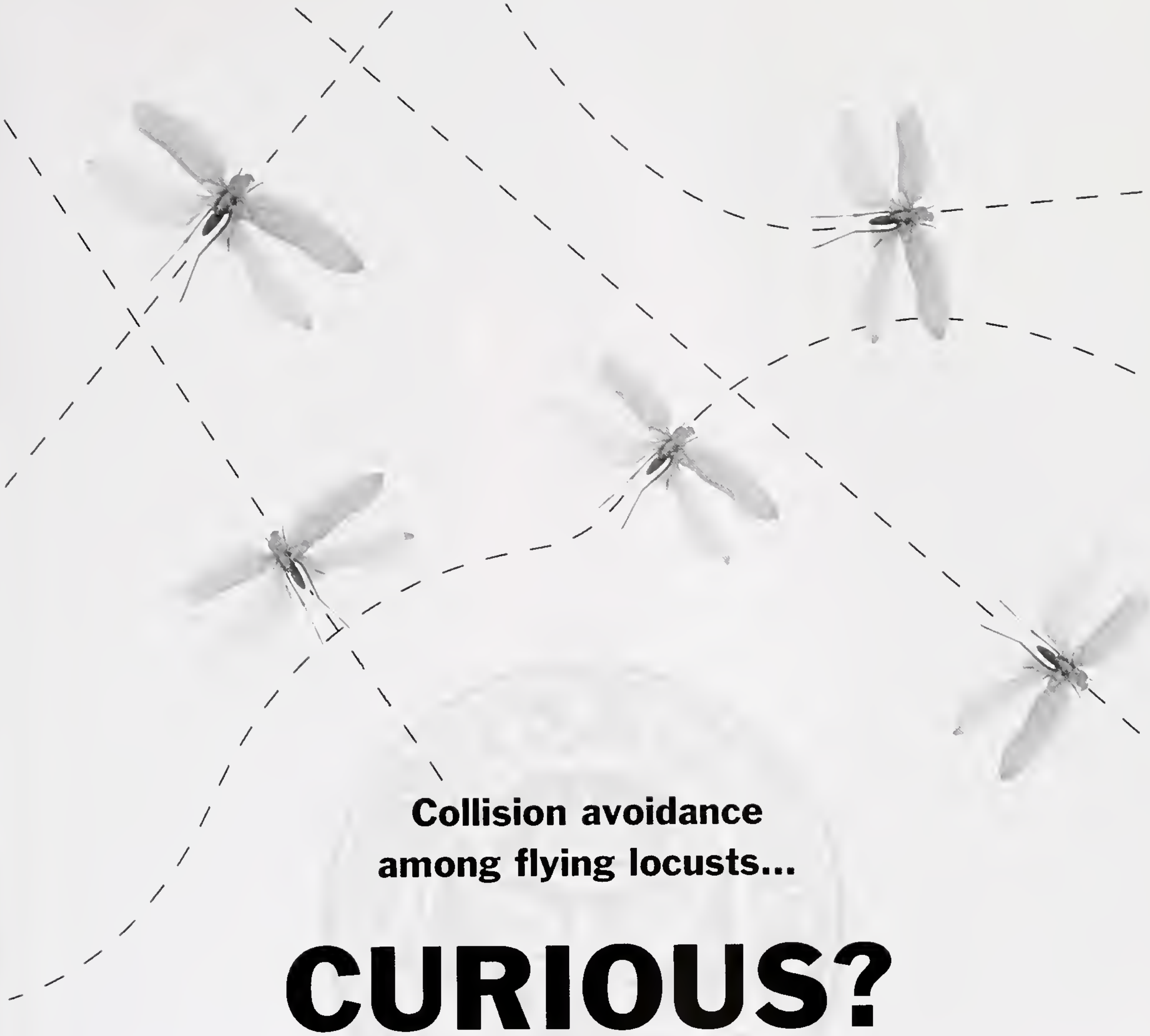

**Collision avoidance among flying locusts...**

**CURIOUS?**

- More than 12 million searchable journal articles
- World's largest collection of free full-text articles
- 4 different search tools to locate what you need
- Online archives of *The Biological Bulletin* plus more than 330 other journals covering the sciences and medicine

Find what you need at Stanford University's
www.highwire.org

HighWire LIBRARY OF THE SCIENCES AND MEDICINE

# THE BIOLOGICAL BULLETIN

# ONLINE

The Marine Biological Laboratory is pleased to announce that the full text of *The Biological Bulletin* is available online at

http://www.biolbull.org

*The Biological Bulletin* publishes outstanding experimental research on the full range of biological topics and organisms, from the fields of Neurobiology, Behavior, Physiology, Ecology, Evolution, Development and Reproduction, Cell Biology, Biomechanics, Symbiosis, and Systematics.

Published since 1897 by the Marine Biological Laboratory (MBL) in Woods Hole, Massachusetts, *The Biological Bulletin* is one of America's oldest peer-reviewed scientific journals.

The journal is aimed at a general readership, and especially invites articles about those novel phenomena and contexts characteristic of intersecting fields.

*The Biological Bulletin Online* contains the full content of each issue of the journal, including all figures and tables, beginning with the February 2001 issue (Volume 200, Number 1). The full text is searchable by keyword, and the cited references include hyperlinks to Medline. PDF files are available beginning in February 1990 (Volume 178, Number 1), some abstracts are available beginning with the October 1976 issue (Volume 151, Number 2), and some Tables of Contents are online beginning with the October 1965 issue (Volume 129, Number 2).

Each issue will be placed online approximately on the date it is mailed to subscribers; therefore the online site will be available prior to receipt of your paper copy. Online readers may want to sign up for the eTOC (electronic Table of Contents) service, which will deliver each new issue's table of contents *via* e-mail. The web site also provides access to information about the journal (such as Instructions to Authors, the Editorial Board, and subscription information), as well as access to the Marine Biological Laboratory's web site and other *Biological Bulletin* electronic publications.

The free trial period for access to *The Biological Bulletin* online has ended. Individuals and institutions who are subscribers to the journal in print or are members of the Marine Biological Laboratory Corporation may now activate their online subscriptions. All other access (*e.g.*, to Abstracts, eTOCs, searching, Instructions to Authors) remains freely available. Online access is included in the print subscription price.

For more information about subscribing or activating your online subscription, visit <www.biolbull.org/subscriptions>.

---

http://www.biolbull.org

OLYMPUS
LUMPlanF
20x/0.95 W
∞/0
The objective is not to touch the objective.

**The BX51WI.** A single 20x water immersion objective. A high N.A. of 0.95. A W.D. of 2.0mm. An intermediate magnification changer. Switch between low and high magnifications. Objective is untouched. Vibrations eliminated. Electrodes unmoved. It's a new movement in microscopy. **How Original. How Olympus.** Visit us at olympusamerica.com or call 1-800-446-5967.

OLYMPUS®
FOCUS ON LIFE

# Announcement

Biological Bulletin Publications announces the addition of a new *Marine Models Electronic Record* at

www.mbl.edu/BiologicalBulletin/mmer.html

Paola Cirino, Alfonso Toscano, Davide Caramiello, Alberto Macina, Valentina Miraglia, and Assunta Monte: Laboratory Culture of the Ascidian *Ciona intestinalis* (L.): A Model System for Molecular Developmental Biology Research.

## *Cover*

Pulmonate snails have unusually large, identifiable neurons, so the central ganglia of these animals have been used for years to study the details of neural physiology, biochemistry, and more recently, molecular genetics. Moreover, because the fertilized eggs of pulmonate gastropods develop directly into juvenile snails, such embryos are particularly well-suited—and have been used—to describe the development of central neurons, neural circuits, and their functions. The full potential of these model systems has, however, never been realized.

The difficulty is captured in essence by the image on the cover—an embryo of the pond snail *Helisoma trivolis.* Freshwater pulmonates develop within a tough egg capsule, which is filled with a nourishing, protective, and regulatory albuminous fluid. This system, though marvelously adaptive to the habitat of these animals, hinders experiments in which embryos are perturbed and then monitored for a time, so that the effect of the treatment on development and function can be determined. Treatment requires only that the embryos be isolated from their capsules and their salubrious medium, but monitoring requires that the exposed embryo develop and grow relatively normally for an experimentally appropriate period—usually hours to days.

In this issue of *The Biological Bulletin* (p. 278), Jeffrey I. Goldberg and his students report that, of various culture media they tested, none could sustain normal embryonic development for more than a short period. But the good news is that, when decapsulated *Helisoma* embryos were transplanted into host capsules, they survived for 13 days (from the 2-cell stage to hatching). Moreover, the development and growth of such transplanted embryos were similar to those of undisturbed controls. This novel methodology was also given a practical test: a pair of serotonergic nerves was laser ablated, the operated embryos were transplanted into host capsules, and a role for the neurons in the regulation of a ciliary rotational behavior was demonstrated the following day. The success of the transplantation technique indicates that a wide range of classic and modern embryological studies can now be performed on important model species with encapsulated eggs.

The *Helisoma* embryo on the cover is in stage E30 (*i.e.*, 30% of development is completed, about four days after egg-laying); the length is about 325 $\mu$m, and the height, 200 $\mu$m. To the right is the domed protoconch being secreted by the underlying shell gland; to the left, the foot points ventrally and the radular sac is visible (see the legend for Fig. 1, p. 281).

The image was provided by Shawn Parries at the University of Alberta, and the cover was designed by Beth Liles, Marine Biological Laboratory, Woods Hole, Massachusetts.

# THE
# BIOLOGICAL BULLETIN
## DECEMBER 2002

| | | |
|---|---|---|
| **Editor** | Michael J. Greenberg | The Whitney Laboratory, University of Florida |
| **Associate Editors** | Louis E. Burnett | Grice Marine Laboratory, College of Charleston |
| | R. Andrew Cameron | California Institute of Technology |
| | Charles D. Derby | Georgia State University |
| | Michael LaBarbera | University of Chicago |
| **Section Editor** | Shinya Inoué, *Imaging and Microscopy* | Marine Biological Laboratory |
| **Online Editors** | James A. Blake, *Keys to Marine Invertebrates of the Woods Hole Region* | ENSR Marine & Coastal Center, Woods Hole |
| | William D. Cohen, *Marine Models Electronic Record and Compendia* | Hunter College, City University of New York |
| **Editorial Board** | Peter B. Armstrong | University of California, Davis |
| | Joan Cerdá | Center of Aquaculture-IRTA, Spain |
| | Ernest S. Chang | Bodega Marine Lab., University of California, Davis |
| | Thomas H. Dietz | Louisiana State University |
| | Richard B. Emlet | Oregon Institute of Marine Biology, Univ. of Oregon |
| | David Epel | Hopkins Marine Station, Stanford University |
| | Kenneth M. Halanych | Auburn University, Alabama |
| | Gregory Hinkle | Millennium Pharmaceuticals, Cambridge, Massachusetts |
| | Nancy Knowlton | Scripps Inst. Oceanography & Smithsonian Tropical Res. Inst. |
| | Makoto Kobayashi | Hiroshima University of Economics, Japan |
| | Esther M. Leise | University of North Carolina Greensboro |
| | Donal T. Manahan | University of Southern California |
| | Margaret McFall-Ngai | Kewalo Marine Laboratory, University of Hawaii |
| | Mark W. Miller | Institute of Neurobiology, University of Puerto Rico |
| | Tatsuo Motokawa | Tokyo Institute of Technology, Japan |
| | Yoshitaka Nagahama | National Institute for Basic Biology, Japan |
| | Sherry D. Painter | Marine Biomed. Inst., Univ. of Texas Medical Branch |
| | J. Herbert Waite | University of California, Santa Barbara |
| | Richard K. Zimmer | University of California, Los Angeles |
| **Editorial Office** | Pamela Clapp Hinkle | Managing Editor |
| | Victoria R. Gibson | Staff Editor |
| | Carol Schachinger | Editorial Associate |
| | Wendy Child | Subscription & Advertising Administrator |

Published by
Marine Biological Laboratory
Woods Hole, Massachusetts

http://www.biolbull.org

Marine Biological Laboratory
Woods Hole Oceanographic Institution
Library

DEC 16 2002

Woods Hole, MA 02543

Microway transforms state-of-the-art processors into fully-integrated clusters for real-world applications, including gene sequencing, jet engine design and galaxy mapping . . .

Microway's magic is already working for hundreds of leading universities, Cessna, Exxon, GE, J&J, LANL, LION Bioscience, MBL, Millennium Pharmaceuticals, Myricom, NASA, NIH, NOAA, Raytheon, Seagate, the U.S. Air Force, Army and Navy, and thousands more.

The value is magical too. Microway's GigaClusters™ are not just fast. They run cool and perform reliably for years, resulting in low total lifetime cost.

MicrowayMagic℠

Scientists have been counting on it for 20 years.

The latest magic...

- GigaBlade™ technology—four Intel® Xeons™ per 1U chassis
- NodeWatch™ remote cluster monitoring and management
- Across the Board™ cooling in Microway 1U and 2U chassis
- CW Series, powered by Platform™ Clusterware™

You could win a $50,000 research grant

It's been 20 years since scientists and engineers first started counting on Microway to put the magic into their HPC systems. To celebrate, we're offering an opportunity for you to make magic too: Now you can turn your purchase of a 16-node or larger Microway cluster into a $50,000 research grant for your choice of Microway products.* At least one in every 150 buyers who enter the contest will win!

To enter:

1. Call Microway now. Talk to one of our technical sales people. Order or take delivery of your Microway cluster during our anniversary celebration (9/1/02–8/31/03).

2. Use it for three months. Then tell us about your application and how Microway made the difference. Your entry must be received within 6 months of receipt of your cluster or no later than 3/1/04, whichever is earlier.

3. One prize will be awarded for every 150 eligible entries (or portion thereof) received. Judges will select the best submissions based on criteria listed on our website. You must visit our website for complete eligibility requirements and rules.

* Winners may select any combination of the following Microway products and/or services valued at a total of up to $50,000: (a) a new cluster or additional nodes, (b) workstations, or (c) other Microway computer equipment and/or software. Open to U.S. residents, at least 21, including employees of universities, private labs, for-profit and not-for-profit organizations, except government employees and their immediate families or the Sponsor, its suppliers and agencies. Contest is void where prohibited.

800 Gigaflops in 44U!

Microway CoolRak™ cabinet with 40 1U Quadputer®–Xeons™ featuring GigaBlade™ technology

Talk to us now. Let the magic begin.
on the web: www.microway.com
or by phone: 508.746.7341

Microway®

# CONTENTS

VOLUME 203, NO. 3: DECEMBER 2002

## RESEARCH NOTES

**Raz, Sefi, Olivier Testeniere, Arnaud Hecker, Steve Weiner, and Gilles Luquet**
Stable amorphous calcium carbonate is the main component of the calcium storage structures of the crustacean *Orchestia cavimana* . . . . . . . . . . . . . . . . . . 269

**Denny, Mark W., Elizabeth K. Nelson, and Kristina S. Mead**
Revised estimates of the effects of turbulence on fertilization in the purple sea urchin, *Strongylocentrotus purpuratus* . . . . . . . . . . . . . . . . . . . . . . . . . . . . . . . . . 275

## DEVELOPMENT AND REPRODUCTION

**Kuang, Shihuan, Marette Regnier, and Jeffrey I. Goldberg**
Long-term culture of decapsulated gastropod embryos: a transplantation study . . . . . . . . . . . . . . . . . . 278

**Saigusa, M., M. Terajima, and M. Yamamoto**
Structure, formation, mechanical properties, and disposal of the embryo attachment system of an estuarine crab, *Sesarma haematocheir*. . . . . . . . . . . . . . . . . . 289

## NEUROBIOLOGY AND BEHAVIOR

**Cohen, Jonathan H., and Richard B. Forward, Jr.**
Spectral sensitivity of vertically migrating marine copepods . . . . . . . . . . . . . . . . . . . . . . . . . . . . . . . . . 307

## PHYSIOLOGY AND BIOMECHANICS

**Shick, J. Malcolm, Walter C. Dunlap, John S. Pearse, and Vicki B. Pearse**
Mycosporine-like amino acid content in four species of sea anemones in the genus *Anthopleura* reflects phylogenetic but not environmental or symbiotic relationships . . . . . . . . . . . . . . . . . . . . . . . . . . . . . . . 315

**Spees, Jeffrey L., Sharon A. Chang, Mark J. Snyder, and Ernest S. Chang**
Osmotic induction of stress-responsive gene expression in the lobster *Homarus americanus* . . . . . . . . . . . 331

**Smith, Andrew M., and Martha C. Morin**
Biochemical differences between trail mucus and adhesive mucus from marsh periwinkle snails . . . . . . . 338

## ECOLOGY AND EVOLUTION

**Bauer, Raymond T.**
Tests of hypotheses on the adaptive value of an extended male phase in the hermaphroditic shrimp *Lysmata wurdemanni* (Caridea: Hippolytidae) . . . . . . 347

* * *

**Index for Volume 203** . . . . . . . . . . . . . . . . . . . . . . . . 358

### Notice to Subscribers

2003 SUBSCRIPTION RATES FOR *THE BIOLOGICAL BULLETIN*
Prices include print and electronic versions

| | Libraries | Individuals |
|---|---|---|
| Per year (six issues, two volumes): | $280.00 | $105.00 |
| Per volume (three issues): | $140.00 | $52.50 |
| Back and single issues (subject to availability): | $50.00 | $20.00 |

For additional information, please contact our subscription administrator at the Maine Biological Laboratory, 7 MBL Street, Woods Hole, MA 02543; tel: (508) 289-7402; e-mail: wchild@mbl.edu. Visit our new website at www.biolbull.org

THE BIOLOGICAL BULLETIN

THE BIOLOGICAL BULLETIN is published six times a year by the Marine Biological Laboratory, 7 MBL Street, Woods Hole, Massachusetts 02543.

Subscriptions and similar matter should be addressed to Subscription Administrator, THE BIOLOGICAL BULLETIN, Marine Biological Laboratory, 7 MBL Street, Woods Hole, Massachusetts 02543. Subscription includes both print and online journals. Subscription per year (six issues, two volumes): $260 for libraries: $105 for individuals. Subscription per volume (three issues): $130 for libraries; $52.50 for individuals. Back and single issues (subject to availability): $45 for libraries; $20 for individuals.

Communications relative to manuscripts should be sent to Michael J. Greenberg, Editor-in-Chief, or Pamela Clapp Hinkle, Managing Editor, at the Marine Biological Laboratory, 7 MBL Street, Woods Hole, Massachusetts 02543. Telephone: (508) 289-7428. FAX: 508-289-7922. E-mail: pclapp@mbl.edu.

http://www.biolbull.org

THE BIOLOGICAL BULLETIN is indexed in bibliographic services including *Index Medicus* and MEDLINE, *Chemical Abstracts, Current Contents, Elsevier BIOBASE/Current Awareness in Biological Sciences,* and *Geo Abstracts.*

Printed on acid free paper,
effective with Volume 180, Issue 1, 1991.

POSTMASTER: Send address changes to THE BIOLOGICAL BULLETIN, Marine Biological Laboratory,
7 MBL Street, Woods Hole, MA 02543.

Copyright © 2002, by the Marine Biological Laboratory

Periodicals postage paid at Woods Hole, MA, and additional mailing offices.
ISSN 0006-3185

# INSTRUCTIONS TO AUTHORS

*The Biological Bulletin* accepts outstanding original research reports of general interest to biologists throughout the world. Papers are usually of intermediate length (10–40 manuscript pages). A limited number of solicited review papers may be accepted after formal review. A paper will usually appear within four months after its acceptance.

Very short, especially topical papers (less than 9 manuscript pages including tables, figures, and bibliography) will be published in a separate section entitled "Research Notes." A Research Note in *The Biological Bulletin* follows the format of similar notes in *Nature.* It should open with a summary paragraph of 150 to 200 words comprising the introduction and the conclusions. The rest of the text should continue on without subheadings, and there should be no more than 30 references. References should be referred to in the text by number, and listed in the Literature Cited section in the order that they appear in the text. Unlike references in *Nature,* references in the Research Notes section should conform in punctuation and arrangement to the style of recent issues of *The Biological Bulletin.* Materials and Methods should be incorporated into appropriate figure legends. See the article by Lohmann *et al.* (October 1990, Vol. **179:** 214–218) for sample style. A Research Note will usually appear within two months after its acceptance.

The Editorial Board requests that regular manuscripts conform to the requirements set below; those manuscripts that do not conform will be returned to authors for correction before review.

1. ***Manuscripts.*** Manuscripts, including figures, should be submitted in quadruplicate, with the originals clearly marked. (Xerox copies of photographs are not acceptable for review purposes.) If possible, please include an electronic copy of the text of the manuscript. Label the disk with the name of the first author and the name and version of the wordprocessing software used to create the file. If the file was not created in some version of Microsoft Word, save the text in rich text format (rtf). The submission letter accompanying the manuscript should include a telephone number, a FAX number, and (if possible) an E-mail address for the corresponding author. The original manuscript must be typed in no smaller than 12 pitch or 10 point, using double spacing (*including* figure legends, footnotes, bibliography, etc.) on one side of 16- or 20-lb. bond paper, 8 by 11 inches. Please, no right justification. Manuscripts should be proofread carefully and errors corrected legibly in black ink. Pages should be numbered consecutively. Margins on all sides should be at least 1 inch (2.5 cm). Manuscripts should conform to the *Council of Biology Editors Style Manual,* 5th Edition (Council of Biology Editors, 1983) and to American spelling. Unusual abbreviations should be kept to a minimum and should be spelled out on first reference as well as defined in a footnote on the title page. Manuscripts should be divided into the following components: Title page, Abstract (of no more than 200 words), Introduction, Materials and Methods, Results, Discussion, Acknowledgments, Literature Cited, Tables, and Figure Legends. In addition, authors should supply a list of words and phrases under which the article should be indexed.

2. ***Title page.*** The title page consists of a condensed title or running head of no more than 35 letters and spaces, the manuscript title, authors' names and appropriate addresses, and footnotes listing present addresses, acknowledgments or contribution numbers, and explanation of unusual abbreviations.

3. ***Figures.*** The dimensions of the printed page, 7 by 9 inches, should be kept in mind in preparing figures for publication. We recommend that figures be about 1 times the linear dimensions of the final printing desired, and that the ratio of the largest to the smallest letter or number and of the thickest to the thinnest line not exceed 1:1.5. Explanatory matter generally should be included in legends, although axes should always be identified on the illustration itself. Figures should be prepared for reproduction as either line cuts or halftones. Figures to be reproduced as line cuts should be unmounted glossy photographic reproductions or drawn in black ink on white paper, good-quality tracing cloth or plastic, or blue-lined coordinate paper. Those to be reproduced as halftones should be mounted on board, with both designating numbers or letters and scale bars affixed directly to the figures. All figures should be numbered in consecutive order, with no distinction between text and plate figures and cited, in order, in the text. The author's name and an arrow indicating orientation should appear on the reverse side of all figures.

*Digital art: The Biological Bulletin* will accept figures submitted in electronic form; however, digital art must conform to the following guidelines. Authors who create digital images are wholly responsible for the quality of their material, including color and halftone accuracy.

*Format.* Acceptable graphic formats are TIFF and EPS. Color submissions must be in EPS format, saved in CMKY mode.

*Software.* Preferred software is Adobe Illustrator or Adobe Photoshop for the Mac and Adobe Photoshop for Windows. Specific instructions for artwork created with various software programs are available on the Web at the Digital Art Information Site maintained by Cadmus Professional Communications at http://cpc.cadmus.com/da/

*Resolution.* The minimum requirements for resolution are 1200 DPI for line art and 300 for halftones.

*Size.* All digital artwork must be submitted at its actual printed size so that no scaling is necessary.

*Multipanel figures.* Figures consisting of individual parts (*e.g.*, panels A, B, C) must be assembled into final format and submitted as one file.

*Hard copy.* Files must be accompanied by hard copy for use in case the electronic version is unusable.

*Disk identification.* Disks must be clearly labeled with the following information: author name and manuscript number; format (PC or Macintosh); name and version of software used.

*Color: The Biological Bulletin* will publish color figures and plates, but must bill authors for the actual additional cost of printing in color. The process is expensive, so authors with more than one color image should—consistent with editorial concerns, especially citation of figures in order—combine them into a single plate to reduce the expense. On request, when supplied with a copy of a color illustration, the editorial staff will provide a pre-publication estimate of the printing cost.

4. ***Tables, footnotes, figure legends, etc.*** Authors should follow the style in a recent issue of *The Biological Bulletin* in preparing table headings, figure legends, and the like. Because of the high cost of setting tabular material in type, authors are asked to limit such material as much as possible. Tables, with their headings and footnotes, should be typed on separate sheets, numbered with consecutive Roman numerals, and placed after the Literature Cited. Figure legends should contain enough information to make the figure intelligible separate from the text. Legends should be typed double spaced, with consecutive Arabic numbers, on a separate sheet at the end of the paper. Footnotes should be limited to authors' current addresses, acknowledgments or contribution numbers, and explanation of unusual abbreviations. All such footnotes should appear on the title page. Footnotes are not normally permitted in the body of the text.

5. ***Literature cited.*** In the text, literature should be cited by the Harvard system, with papers by more than two authors cited as Jones *et al.*, 1980. Personal communications and material in preparation or in press should be cited in the text only, with author's initials and institutions, unless the material has been formally accepted and a volume number can be supplied. The list of references following the text should be headed Literature Cited, and must be typed double spaced on separate pages, conforming in punctuation and arrangement to the style of recent issues of *The Biological Bulletin*. Citations should include complete titles and inclusive pagination. Journal abbreviations should normally follow those of the U. S. A. Standards Institute (USASI), as adopted by BIOLOGICAL ABSTRACTS and CHEMICAL ABSTRACTS, with the minor differences set out below. The most generally useful list of biological journal titles is that published each year by BIOLOGICAL ABSTRACTS (BIOSIS List of Serials; the most recent issue). Foreign authors, and others who are accustomed to using THE WORLD LIST OF SCIENTIFIC PERIODICALS, may find a booklet published by the Biological Council of the U.K. (obtainable from the Institute of Biology, 41 Queen's Gate, London, S.W.7, England, U.K.) useful, since it sets out the WORLD LIST abbreviations for most biological journals with notes of the USASI abbreviations where these differ. CHEMICAL ABSTRACTS publishes quarterly supplements of additional abbreviations. The following points of reference style for THE BIOLOGICAL BULLETIN differ from USASI (or modified WORLD LIST) usage:

A. Journal abbreviations, and book titles, all underlined (for *italics*)

B. All components of abbreviations with initial capitals (not as European usage in WORLD LIST *e.g., J. Cell. Comp. Physiol.* NOT *J. cell. comp. Physiol.*)

C. *All* abbreviated components must be followed by a period, whole word components *must not* (*i.e., J. Cancer Res.*)

D. Space between all components (*e.g., J. Cell. Comp. Physiol.*, not *J.Cell.Comp.Physiol.*)

E. Unusual words in journal titles should be spelled out in full, rather than employing new abbreviations invented by the author. For example, use *Rit Vísindafjélags Islendinga* without abbreviation.

F. All single word journal titles in full (*e.g., Veliger, Ecology, Brain*).

G. The order of abbreviated components should be the same as the word order of the complete title (*i.e., Proc.* and *Trans.* placed where they appear, not transposed as in some BIOLOGICAL ABSTRACTS listings).

H. A few well-known international journals in their preferred forms rather than WORLD LIST or USASI usage (*e.g., Nature, Science, Evolution* NOT *Nature, Lond., Science, N.Y.; Evolution, Lancaster, Pa.*)

6. ***Reprints, page proofs, and charges.*** Authors may purchase reprints in lots of 100. Forms for placing reprint orders are sent with page proofs. Reprints normally will be delivered about 2 to 3 months after the issue date. Authors (or delegates for foreign authors) will receive page proofs of articles shortly before publication. They will be charged the current cost of printers' time for corrections to these (other than corrections of printers' or editors' errors). Other than these charges for authors' alterations, *The Biological Bulletin* does not have page charges.

# CONTENTS
## for Volume 203

No. 1: August 2002

### PHYSIOLOGY AND BIOMECHANICS

**Denny, Mark, and Loretta Roberson**
Blade motion and nutrient flux to the kelp, *Eisenia arborea* . . . . . . . . . . . . 1

**Thompson, Joseph T., and William M. Kier**
Ontogeny of squid mantle function: changes in the mechanics of escape-jet locomotion in the oval squid, *Sepioteuthis lessoniana* Lesson, 1830 . . . . . . . . 14

**Marshall, Jennifer, Wayne P. Kelley, Stanislav S. Rubakhin, Jon-Paul Bingham, Jonathan V. Sweedler, and William F. Gilly**
Anatomical correlates of venom production in *Conus californicus* . . . . . . . . . . 27

**Burnett, Louis, Nora Terwilliger, Amy Carroll, Darwin Jorgensen, and David Scholnick**
Respiratory and acid-base physiology of the purple sea urchin, *Strongylocentrotus purpuratus*, during air exposure: presence and function of a facultative lung . . . . 42

### DEVELOPMENT AND REPRODUCTION

**Farley, Gregory S.**
Helical nature of sperm swimming affects the fit of fertilization-kinetics models to empirical data. . . . . . 51

**Staver, Jennifer M., and Richard R. Strathmann**
Evolution of fast development of planktonic embryos to early swimming . . . . . . . . . . 58

**Brumwell, Gordon B., and Vicki J. Martin**
Immunocytochemically defined populations of neurons progressively increase in size through embryogenesis of *Hydra vulgaris* . . . . . . . . . . 70

**Chaparro, O. R., J. L. Charpentier, and R. Collin**
Embryonic velar structure and function of two sibling species of *Crepidula* with different modes of development . . . . . . . . . . 80

**Okusu, Akiko**
Embryogenesis and development of *Epimenia babai* (Mollusca Neomeniomorpha) . . . . . . . . . . 87

**Martynova, Marina G., and Olga A. Bystrova**
Undifferentiated cells in the snail myocardium are capable of DNA synthesis and myodifferentiation. . . . . 104

### NEUROBIOLOGY AND BEHAVIOR

**Delgado, Gabriel A., Robert A. Glazer, and Nicola J. Stewart**
Predator-induced behavioral and morphological plasticity in the tropical marine gastropod *Strombus gigas*. . . . . . . . . . 112

* * *

**Annual Report of the Marine Biological Laboratory** . . . . R1

No. 2: October 2002

### DEVELOPMENT AND REPRODUCTION

**Vickery, Minako, Michael C.L. Vickery, and James B. McClintock**
Morphogenesis and organogenesis in the regenerating planktotrophic larvae of asteroids and echinoids . . . . . . . . . . 121

**Eckelbarger, Kevin J., and Craig M. Young**
Spermiogenesis and modified sperm morphology in the "seepworm" *Methanoaricia dendrobranchiata* (Polychaeta: Orbiniidae) from a methane seep environment in the Gulf of Mexico: implications for fertilization biology . . . . . . . . . . 134

### NEUROBIOLOGY AND BEHAVIOR

**Lawrence, K.A., and W.H. Watson III**
Swimming behavior of the nudibranch *Melibe leonina* . . . . . . . . . . 144

**Watson, Winsor H. III, James M. Newcomb, and Stuart Thompson**
Neural correlates of swimming behavior in *Melibe leonina* . . . . . . . . . . 152

### ECOLOGY AND EVOLUTION

**Barnes, David K.A.**
Clade perseverance from Mesozoic to present: a multidisciplinary approach to interpretation of pattern and process . . . . . . . . . . 161

**Lohse, David P.**
Relative strengths of competition for space and food in a sessile filter feeder ... 173

## SHORT REPORTS FROM THE 2002 GENERAL SCIENTIFIC MEETINGS OF THE MARINE BIOLOGICAL LABORATORY

**The Editor**
Introduction to the featured reports: The MBL awards for 2002 ... 185

### *Neurobiology*

**Arnolds, D. E. W., S. J. Zottoli, C. E. Adams, S. M. Dineen, S. Fevrier, Y. Guo, and A. J. Pascal**
Physiological effects of tricaine on the supramedullary/dorsal neurons of the cunner, *Tautogolabrus adspersus* ... 188

**Giuditta, Antonio, Maria Eyman, and Barry B. Kaplan**
Gene expression in the squid giant axon: neurotransmitter modulation of RNA transfer from periaxonal glia to the axon ... 189

**Landowne, David**
Perchlorate prevents sodium channel gating and sodium protects in the squid giant axon ... 190

**Ripps, Harris, Haohua Qian, and Jane Zakevicius**
Blockade of an inward sodium current facilitates pharmacological study of hemi-gap-junctional currents in *Xenopus* oocytes ... 192

**Garber, Sarah S., and Mary M. Hoffman**
$Cl^-$ and glutamate$^-$ competition for a volume-regulated anion channel ... 194

**Fay, Richard R., and Peggy L. Edds-Walton**
Preliminary evidence for interpulse interval selectivity of cells in the torus semicircularis of the oyster toadfish (*Opsanus tau*) ... 195

**Borley, Kimberly A., Herman T. Epstein, and Alan M. Kuzirian**
Effects of a sensory block on calexcitin levels in the photoreceptors of *Hermissenda crassicornis* ... 197

**Twig, Gilad, Robert Paul Malchow, Katherine Hammar, Peter J. S. Smith, Hanna Levy, and Ido Perlman**
A novel turtle retinal preparation for simultaneously measuring light-induced electrical activity and changes in metabolite levels ... 198

**Redenti, Stephen, and Richard L. Chappell**
Zinc chelation enhances the zebrafish retinal ERG b-wave ... 200

### *Cell Biology*

**Armstrong, Peter B., Margaret T. Armstrong, R. L. Pardy, Alice Child, and Norman Wainwright**
Immunohistochemical demonstration of a lipopolysaccharide in the cell wall of a eukaryote, the green alga *Chlorella* ... 203

**Lee, K.-G., A. Braun, I. Chaikhoutdinov, J. DeNobile, M. Conrad, and W. Cohen**
Rapid visualization of microtubules in blood cells and other cell types in marine model organisms ... 204

**Wöllert, Torsten, Ana S. DePina, Reid F. Thompson, and George M. Langford**
$Ca^{2+}$ effects on myosin-II-mediated contraction of pseudo-contractile rings and transport of vesicles in extracts of clam oocytes ... 206

**Wöllert, Torsten, Ana S. DePina, Reid F. Thompson, and George M. Langford**
GTPase Rho is involved in myosin-II-mediated contraction of pseudo-contractile rings and transport of vesicles in extracts of clam oocytes ... 208

**Brown, Jeremiah R., Elizabeth M. Peacock-Villada, and George M. Langford**
Globular tail fragment of myosin-V displaces vesicle-associated motor and blocks vesicle transport in squid nerve cell extracts ... 210

**Weidner, Earl, and Ann Findley**
Peroxisomal catalase in extrusion apparatus posterior vacuole of microsporidian spores ... 212

**Silver, Robert B., and Marc Bartman**
A metronome-like control of the calcium signal leading to nuclear envelope breakdown and mitosis in sand dollar (*Echinaracnius parma*) cells ... 213

### *Developmental Biology*

**Crawford, Karen**
Culture method for *in vitro* fertilization to hatching of the squid, *Loligo pealeii* ... 216

**Pahl, Nicholas, Sara Homsi, Hilary G. Morrison, and Robert M. Gould**
mRNAs located in *Squalus acanthias* (spiny dogfish) oligodendrocyte processes ... 217

**Eddleman, Christopher S., George D. Bittner, and Harvey M. Fishman**
SEM comparison of severed ends of giant axons isolated from squid (*Loligo pealeii*) and crayfish (*Procambarus clarkii*) ... 219

### *Studia Limulorum*

**Mittmann, Beate**
Early neurogenesis in the horseshoe crab *Limulus polyphemus* and its implication for arthropod relationships ... 221

**Smith, K., C. Ridings, F. A. Dodge, and R. B. Barlow**
Development of the lateral eye of juvenile *Limulus* ... 222

**Ridings, C., D. Borst, K. Smith, F. Dodge, and R. Barlow**
Visual behavior of juvenile *Limulus* in their natural habitat and in captivity ... 224

**Suggs, Dianne N., Ruth H. Carmichael, Sara P. Grady, and Ivan Valiela**
Effects of individual size on pairing in horseshoe crabs . . . . . . . . 225

**Borst, Douglas, and Robert Barlow**
Circadian rhythms in locomotor activity of juvenile horseshoe crabs . . . . . . . . 227

**Gaines, Emily F., Ruth H. Carmichael, Sara P. Grady, and Ivan Valiela**
Stable isotopic evidence for changing nutritional sources of juvenile horseshoe crabs . . . . . . . . 228

### *Comparative Physiology*

**Smotherman, Michael**
Acetylcholine mediates excitatory input to chromatophore motoneurons in the squid, *Loligo pealeii* . . . . . 231

**Grable, Melissa M., Nadav Shashar, Nicole L. Gilles, Chuan-Chin Chiao, and Roger T. Hanlon**
Cuttlefish body patterns as a behavioral assay to determine polarization perception . . . . . . . . 232

**Rohrkasse, Sarah M., and Jelle Atema**
Tracking behavior of Busyconinae whelks . . . . . . . . 235

**Graf, Werner, Edwin Gilland, Matt McFarlane, Laura Knott, and Robert Baker**
Central pathways mediating oculomotor reflexes in an elasmobranch, *Scyliorhinus canicula* . . . . . . . . 236

**Montgomery, John, Guy Carton, and David Bodznick**
Error-driven motor learning in fish . . . . . . . . 238

**Delaney, Martha, Christopher Follet, Nick Ryan, Nick Hanney, Jenny Lusk-Yablick, and Gabriele Gerlach**
Social interaction and distribution of female zebrafish *(Danio rerio)* in a large aquarium . . . . . . . . 240

**Cermak, Michael J.**
*Caranx latus* (Carangidae) chooses dock pilings to attack silverside schools: A tactic to interfere with stereotyped escape behavior of prey? . . . . . . . . 241

### *Ecology and Population Biology*

**La Du, Jane, Deana Erdner, Sonya Dyhrman, and Don Anderson**
Molecular approaches to understanding population dynamics of the toxic dinoflagellate *Alexandrium fundyense* . . . . . . . . 244

**Philibotte, Jason**
Pelagic larval duration of the Caribbean wrasse, *Thalassoma bifasciatum* . . . . . . . . 245

**Hunter-Thomson, Kristin, Jeffrey Hughes, and Bradley Williams**
Estuarine–open-water comparison of fish community structure in eelgrass (*Zostera marina* L.) habitats of Cape Cod . . . . . . . . 247

**Williams, Bradley S., Jeffrey E. Hughes, and Kristin Hunter-Thomson**
Influence of epiphytic algal coverage on fish predation rates in simulated eelgrass habitats . . . . . . . . 248

**Ludlam, John P., David H. Shull, and Robert Buchsbaum**
Effects of haying on salt-marsh surface invertebrates . . . . . . . . 250

**Levine, Uri Y., and Byron C. Crump**
Bacterioplankton community composition in flowing waters of the Ipswich River watershed . . . . . . . . 251

**Huffaker, Diana, and R. Gil Pontius, Jr.**
Reconstruction of historical land cover in the Ipswich watershed . . . . . . . . 253

### *Estuarine and Freshwater Biogeochemistry*

**Testa, Jeremy M., Matthew A. Charette, Edward R. Sholkovitz, Matt C. Allen, Adam Rago, and Craig W. Herbold**
Dissolved iron cycling in the subterranean estuary of a coastal bay: Waquoit Bay, Massachusetts . . . . . . . . 255

**Twichell, Sarah, Sallie Sheldon, Linda Deegan, and Robert Garritt**
Nutrient and freshwater inputs from sewage effluent discharge alter benthic algal and infaunal communities in a tidal salt marsh creek . . . . . . . . 256

**Koop-Jakobsen, Ketil, and Anne Giblin**
Tidal flushing of ammonium from intertidal salt marsh sediments: the relative importance of adsorbed ammonium . . . . . . . . 258

**Barron, Stacy, Carolyn Weber, Roxanne Marino, Eric Davidson, Gabrielle Tomasky, and Robert Howarth**
Effects of varying salinity on phytoplankton growth in a low-salinity coastal pond under two nutrient conditions . . . . . . . . 260

**Weber, Carolyn F., Stacy Barron, Roxanne Marino, Robert W. Howarth, Gabrielle Tomasky, and Eric A. Davidson**
Nutrient limitation of phytoplankton growth in Vineyard Sound and Oyster Pond, Falmouth, Massachusetts . . . . . . . . 261

**Millman, Melissa, Mirta Teichberg, Paulina Martinetto, and Ivan Valiela**
Response of shrimp populations to land-derived nitrogen in Waquoit Bay, Massachusetts . . . . . . . . 263

### *Laboratory Animal Health*

**Smolowitz, Roxanna, Janice Hanley, and Hazel Richmond**
A three-year retrospective study of abdominal tumors in zebrafish maintained in an aquatic laboratory animal facility . . . . . . . . 265

**Hsieh, Jennifer L., Hemant M. Chikarmane, Roxanna Smolowitz, Kevin R. Uhlinger, W. Mebane, and Alan M. Kuzirian**
Microbial analysis of ozone disinfection in a recirculating seawater system . . . . . . . . 266

### *Oral Presentations*

Published by title only . . . . . . . . 268

CONTENTS: VOLUME 203

No. 3: December 2002

## RESEARCH NOTES

**Raz, Sefi, Olivier Testeniere, Arnaud Hecker, Steve Weiner, and Gilles Luquet**
Stable amorphous calcium carbonate is the main component of the calcium storage structures of the crustacean *Orchestia cavimana* . . . . . . . . . . . . . . . . . . 269

**Denny, Mark W., Elizabeth K. Nelson, and Kristina S. Mead**
Revised estimates of the effects of turbulence on fertilization in the purple sea urchin, *Strongylocentrotus purpuratus* . . . . . . . . . . . . . . . . . . . . . . . . . . . . . . . . . 275

## DEVELOPMENT AND REPRODUCTION

**Kuang, Shihuan, Marette Regnier, and Jeffrey I. Goldberg**
Long-term culture of decapsulated gastropod embryos: a transplantation study . . . . . . . . . . . . . . . . . . 278

**Saigusa, M., M. Terajima, and M. Yamamoto**
Structure, formation, mechanical properties, and disposal of the embryo attachment system of an estuarine crab, *Sesarma haematocheir*. . . . . . . . . . . . . . . . . . 289

## NEUROBIOLOGY AND BEHAVIOR

**Cohen, Jonathan H., and Richard B. Forward, Jr.**
Spectral sensitivity of vertically migrating marine copepods . . . . . . . . . . . . . . . . . . . . . . . . . . . . . . . . . 307

## PHYSIOLOGY AND BIOMECHANICS

**Shick, J. Malcolm, Walter C. Dunlap, John S. Pearse, and Vicki B. Pearse**
Mycosporine-like amino acid content in four species of sea anemones in the genus *Anthopleura* reflects phylogenetic but not environmental or symbiotic relationships . . . . . . . . . . . . . . . . . . . . . . . . . . . . . . . . . 315

**Spees, Jeffrey L., Sharon A. Chang, Mark J. Snyder, and Ernest S. Chang**
Osmotic induction of stress-responsive gene expression in the lobster *Homarus americanus* . . . . . . . . . . . 331

**Smith, Andrew M., and Martha C. Morin**
Biochemical differences between trail mucus and adhesive mucus from marsh periwinkle snails . . . . . . . 338

## ECOLOGY AND EVOLUTION

**Bauer, Raymond T.**
Tests of hypotheses on the adaptive value of an extended male phase in the hermaphroditic shrimp *Lysmata wurdemanni* (Caridea: Hippolytidae) . . . . . . 347

* * *

**Index for Volume 203** . . . . . . . . . . . . . . . . . . . . . . . . 358

Reference: *Biol. Bull.* **203:** 269–274. (December 2002)

# Stable Amorphous Calcium Carbonate Is the Main Component of the Calcium Storage Structures of the Crustacean *Orchestia cavimana*

SEFI RAZ[1,¶], OLIVIER TESTENIERE[2,¶], ARNAUD HECKER[2], STEVE WEINER[1],
AND GILLES LUQUET[2,*]

[1]*UMR Université de Bourgogne/CNRS 5548 "Développement-Communication chimique,"*
*6 Bd Gabriel, 21000-Dijon, France; and* [2]*Department of Structural Biology,*
*Weizmann Institute of Science, Rehovot 76100, Israel*

*Amorphous calcium carbonate (ACC) is the least stable form of the six known phases of calcium carbonate. It is, however, produced and stabilized by a variety of organisms. In this study we examined calcium storage structures from the terrestrial crustacean* Orchestia cavimana, *in order to better understand their formation mode and function. By using X-ray diffraction, infrared and Raman spectroscopy, thermal analysis and elemental analysis, we determined that the mineral comprising these storage structures is amorphous calcium carbonate with small amounts of amorphous calcium phosphate (5%). We suggest that the use of amorphous calcium carbonate might be advantageous for these storage structures, which function as reservoirs of ions during the animal molting period. Its high solubility is beneficial for temporary storage of calcium carbonate ions that are subsequently dissolved and used elsewhere. Stabilization of these amorphous minerals is probably due to macromolecular constituents of the organic matrix, and to the magnesium and phosphate present in the mineral phase.*

Amorphous minerals constitute a little less than a quarter of all known biominerals (1). When formed with no biological control, these minerals are usually metastable in comparison to their crystalline counterparts. They tend to transform into a more stable crystalline form. In contrast, biologically controlled amorphous minerals are, in most cases, stabilized by organisms for their entire lifetime. There are a few examples in which biogenic amorphous minerals are used as precursor phases for crystalline minerals (1), and two of these involve the formation of a transient amorphous calcium carbonate phase (2, 3). Because amorphous minerals are isotropic in polarized light and do not diffract X-rays, their presence in a biological tissue has often been overlooked. It is particularly difficult to identify and characterize them when a crystalline mineral is also present. Biogenic amorphous minerals may thus be much more common than is currently appreciated. Here we identify and characterize the presence of amorphous calcium carbonate and amorphous calcium phosphate (ACP) in one of the more intensively studied biomineralizing systems.

As most amorphous minerals are unstable, they tend to dissolve rather easily. This may be an advantage when frequent replacement of the mineral is required. Most of the crustaceans have mineralized exoskeletons (or cuticles) that are cyclically renewed with exogenous or endogenous calcium carbonate. The use of an amorphous phase as the mineral composing the cuticle, also called carapace, can therefore be advantageous. Indeed, amorphous calcium carbonate has been detected in cuticles, and its presence is associated with large amounts of phosphate (4, 5). Nevertheless, the mineral precipitated in the cuticle of most crustaceans is crystalline calcite, with some vaterite also reported (reviewed in 1, 6, 7).

Frequent renewal of the skeleton requires a reservoir of ions. Crustaceans obtain the calcium they need from their environment, and in addition certain species have developed calcium storage strategies (6, 8). The mineral form in which calcium ions are retained in these storage structures is still enigmatic. Electron diffraction of elaborate calcium storage

---

Received 20 June 2002; accepted 5 September 2002.

[¶] These authors contributed equally to this paper.

[*] To whom correspondence should be addressed. E-mail: gilles.luquet@u-bourgogne.fr

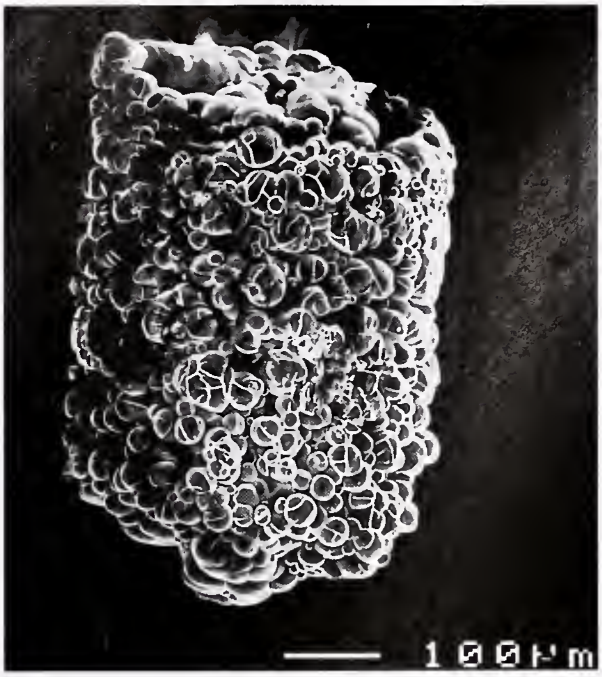

**Figure 1.** Scanning electron micrograph of a compound spherulith of *Orchestia cavimana* elaborated during the premolt period. Terrestrial amphipod crustaceans (*Orchestia cavimana*) were reared in the laboratory in subaquatic terraria and staged as described by Graf (12). Calcareous concretions were extracted from the posterior cæca (the paired storage organs) of animals just before or after ecdysis by microdissection under a binocular magnifying glass. The external bright appearance and the translucent appearance of the concretions as observed by light microscopy ensured that they were completely devoid of any surrounding organic matter. Concretions were stored dessicated at 4°C until use.

structures, also known as sternal plates, of the terrestrial crustacean *Porcellio scaber* showed that they do not diffract and are probably composed of amorphous calcium carbonate (9). In some crayfish, gastroliths are reported to be composed of calcium carbonate in an extremely poorly crystalline state, as they do not diffract X-rays or electrons (10).

The terrestrial crustacean *Orchestia cavimana* stores calcium originating mainly from its old cuticle in diverticula of the midgut (11). The calcium stored in the concretions constitutes about 60% of the cuticle calcium content; the rest originates from the shed cuticle (also known as the exuviae) ingested by the animal just after ecdysis, and from food. Since calcification of this new exoskeleton represents, among other things, a means of defense against environmental pressures, this process must occur as quickly as possible. The calcium is stored for about 15 days in the premolt period (12). After ecdysis, namely the moment when the animal leaves its old cuticle, the calcium is resorbed in less than 48 h to rapidly mineralize the new cuticle in a brief postmolt period (12, 13). The exact mechanism of dissolution is not known. We suspect that carbonic anhydrase may be involved. Carbonic anhydrase activity has been detected histochemically at the apical level of the storage organ epithelial cells (14). This enzyme could be responsible for the rapid release of a large amount of calcium ions that may enter the epithelium *via* $Ca^{2+}$-$2H^+$ antiports or simply down a concentration gradient (15). Calcium then passes through the epithelial cells by a paracellular pathway as calcified spherules. Other transitory mineralized structures are produced in a dilated intercellular membrane network by precipitation of calcium salts within an organic matrix synthesized by the storage organ cells. They are then resorbed at the basal part of the epithelium, and the $Ca^{2+}$ released is discharged into the hemolymph through the basal lamina (13, 15). After complete dissolution of the concretions, the organic matrix is probably removed *via* the midgut to which the storage organs are connected, as indicated by studies of orchestin, a well-characterized component of the organic matrix (16, 17).

The calcified storage structures, called calcareous concretions, are composed of an organic matrix whose proteinaceous components have been analyzed (16, 17). The proteins are synthesized by the storage organ cells within which calcium salts are precipitated. Single spheruliths are firstly elaborated extracellularly in the lumen of the tubular storage organs. The integration of several single spheruliths forms compound spheruliths about 800 μm long and 400 μm in diameter (Fig. 1) in an adult individual. The concretions vary between single spheruliths and compound spheruliths in the 8-mm-long adult storage organs. This facilitates the flexibility required for these jumping animals (18). The concretions were initially considered to be excretion forms.

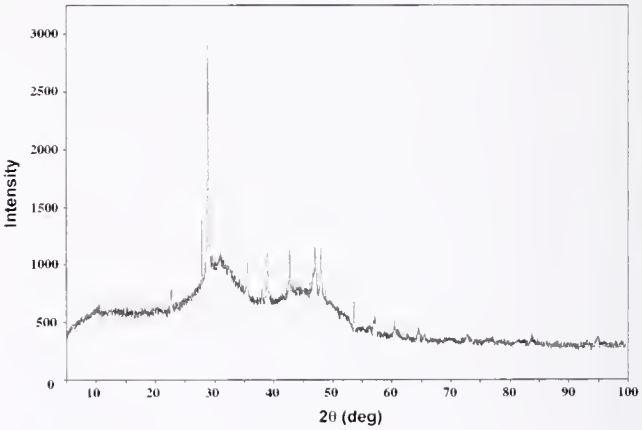

**Figure 2.** X-ray diffraction analysis of the *Orchestia* calcareous concretions. The samples were finely ground and the powder was subjected to an X-ray beam using the Cu Kα radiation at 40 kV and 30 mA. Measurements were performed with a step size of 0.029° and sampling time of 1.0 s/step using a diffractometer fitted out with an INEL CPS 120 localization curved counter. The base-line rise is due to an amorphous phase, whereas the small sharp peaks correspond to calcite.

It is now well established that these mineralized structures are transitory calcium deposits (18, 19).

A previous Debye-Scherrer X-ray diffraction experiment performed by Graf (18) led to the conclusion that the concretions in *Orchestia* are probably poorly crystallized calcite. The nature of the mineralogical form of the calcareous deposits and their characteristics remained, however, unclear. We therefore used X-ray diffraction, thermogravimetric analysis, infrared and Raman spectroscopy, scanning electron microscopy, and energy dispersive spectrometry to characterize the mineral component of these concretions.

Scanning electron microscope observations of the spheruliths that form the concretions (Fig. 1) show that they possess a very smooth surface. Even at high magnification, no sign of crystal structure is evident. This was the first indication that these concretions might be composed of an amorphous phase. We therefore obtained a powder X-ray diffraction analysis of the calcareous concretions (Fig. 2). The pattern reveals a broad peak, consistent with the presence of an amorphous phase, accompanied by sharp peaks, which correspond to calcite. It was, however, noticeable that the intensities of the calcite reflections are very weak, and calcite is therefore not a major component.

To further understand the mineralogy of the concretions, we performed IR and Raman spectroscopic analyses. The IR spectra of the concretions both before and after ecdysis are identical and correspond to amorphous calcium carbonate (Fig. 3a1; 20). When we examined the concretions using a Raman imaging microscope, in 9 out of 12 analyses we obtained a spectrum compatible with amorphous calcium carbonate (Fig. 3b1; 21). In these spectra we also note the peak at about 950 $\mathrm{cm}^{-1}$, which is due to the presence of amorphous calcium phosphate (22). In 3 of the 12 analyses we obtained spectra that correspond to amorphous calcium carbonate, with additional peaks that are assigned to crystalline calcite (280 $\mathrm{cm}^{-1}$ and 712 $\mathrm{cm}^{-1}$). It is noteworthy that the calcite peak intensities are weak enough not to mask the amorphous calcium carbonate peaks. This also indicates that the crystalline part of the sample is small. As we do not detect any calcite peaks in the IR spectra, we conclude that the crystalline part makes up less than about 5% of the overall sample. The occurrence of some crystallinity in the Raman measurements is consistent with the data obtained

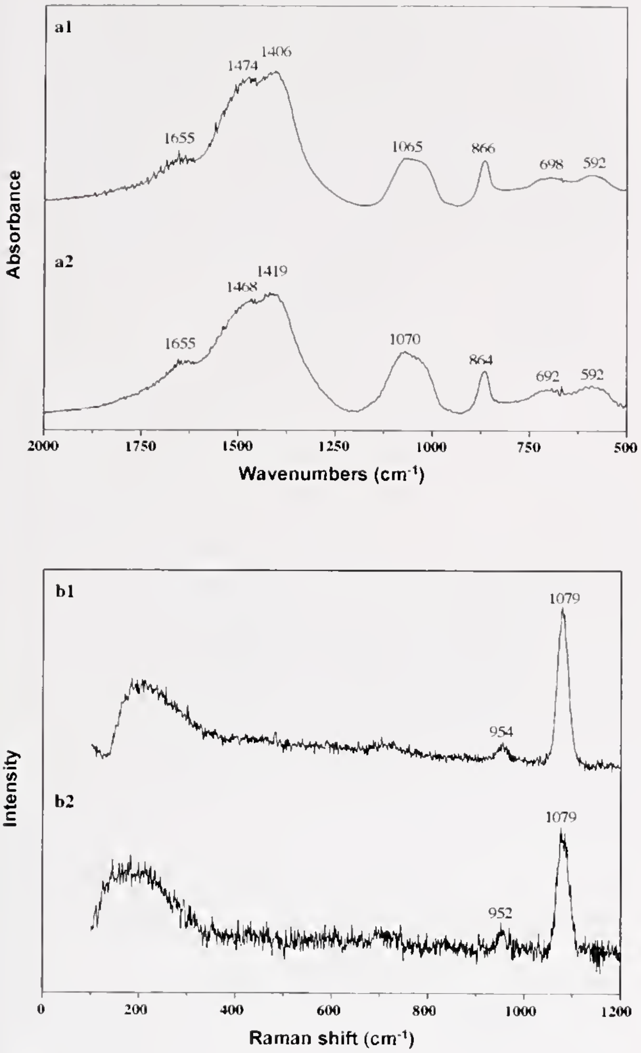

**Figure 3.** (a) Infrared spectra of (a1) the concretions after ecdysis, when the storage structures are being resorbed (the IR spectrum of the concretions before ecdysis was identical and therefore is not shown); and (a2) control antler spicules of *Pyura pachydermatina* composed of stable amorphous calcium carbonate (ACC) (20). The ACC spectrum is characterized by a broad peak of the carbonate bending at 866 $\mathrm{cm}^{-1}$ and a split in the asymmetric stretch of the carbonate ion at 1420 and 1474 $\mathrm{cm}^{-1}$. The additional peak at around 1070 $\mathrm{cm}^{-1}$ is mainly assigned to phosphates. A powdered sample (about 0.1 mg) was mixed with about 10 mg of anhydrous KBr. The mixture was pressed into a 7-mm-diameter pellet. The analysis was performed at 4 $\mathrm{cm}^{-1}$ resolution using a Midac Corporation FTIR spectrometer.

(b) Raman spectra of (b1) one analysis of a concretion before ecdysis, at the end of the storage period; and (b2) control antler spicules of *Pyura pachydermatina* composed of stable amorphous calcium carbonate (21). The spectra are characterized by a broad peak at 150–250 $\mathrm{cm}^{-1}$ and at about 1080 $\mathrm{cm}^{-1}$. Note that both the sample and the control have an additional peak at about 950 $\mathrm{cm}^{-1}$, which corresponds to ACP. Phosphorus was also detected in the concretions by energy dispersive spectrometry (EDS). For Raman spectroscopy, samples were placed on glass slides and were observed with a Leica microscope at a magnification of 50×, using reflected white light. After focusing on the object, the light source of the microscope was transferred to a diode laser (780 nm). The spectra were scanned for 10 s in the range 100–1200 $\mathrm{cm}^{-1}$, using a Renishaw Raman imaging microscope. For EDS, samples were embedded in a mixture of Buehler ultra-mount powder and liquid. The embedded sample was polished, using a Buehler MINIMET polisher, to obtain a flat sample surface and mounted on an aluminum stub with double-sided carbon tape. The conductivity was further increased using conductive carbon paste between the embedded sample and the aluminum stub, and the sample was carbon coated for scanning electron microscopy (JSM-6400) and EDS (Oxford-ISIS). The analysis was performed using SEMQuant with standards of magnesium oxide for magnesium analysis, wollastonite for calcium analysis, and GaP for phosphorus analysis.

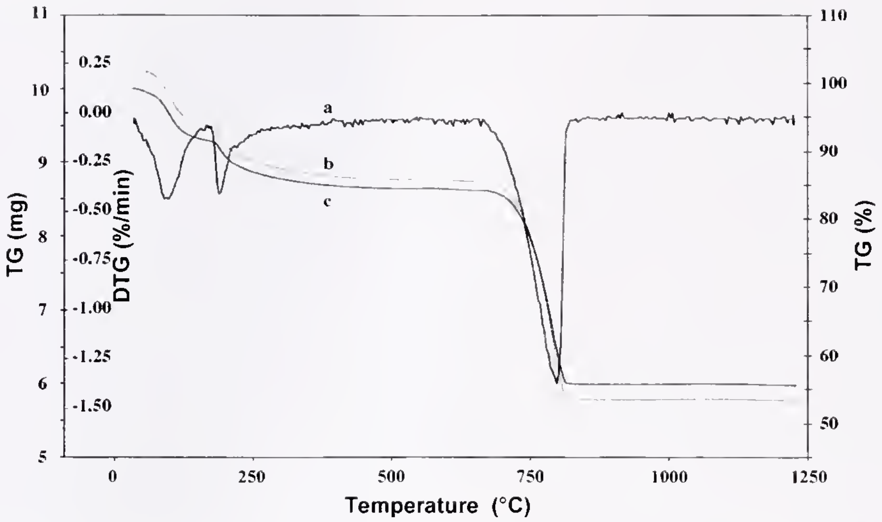

**Figure 4.** Thermogravimetric (TGA/DTA) analysis of the concretions. Variations of (a) differential thermogravimetry (DTG, %/min); (b) thermogravimetry (TG, mg); and (c) thermogravimetry (TG, %), as a function of the temperature (°C). After extraction, calcareous concretions were quickly rinsed in absolute ethanol and air-dried. Experiments were performed using a SETARAM TG-DTA92 thermobalance with a rising temperature of 3°C/min under compressed air. Curve b) shows the loss of weight of the sample as temperature increases. Curve c) corresponds to the same loss of weight but expressed as a percentage of the initial weight of the sample. Curve a) corresponds to the percentage of weight loss with time during the increase of temperature. We note three main variations: two small ones (15%) corresponding to the loss of water and organic matter at around 100 and 200°C and a more important one (30%) corresponding to the transformation of calcium carbonate to calcium oxide.

from the X-ray diffraction measurements. As the calcite is present in small amounts and not always present in the samples analyzed, we suspect that it is an artifact caused by the extraction procedure, which involves some dehydration of the sample. This could cause some of the amorphous phase to crystallize. Travis (10) came to the same conclusion.

We also performed thermogravimetric analysis (TGA) combined with differential thermal analysis (DTA) of the concretions before and after ecdysis (Fig. 4). The curves show water loss of about 15% (w/w), which is similar to other biogenic samples of amorphous calcium carbonate (23), and approximately 30% weight loss at about 780°C, which corresponds to the decomposition of the calcium carbonate to calcium oxide (24).

A previous X-ray microanalysis detected the presence of phosphorus in the calcareous concretions of *Orchestia* (15). To determine the elemental composition of the concretions, we performed energy dispersive spectrometry (EDS; for methods see legend Fig. 3). The elemental composition of the concretions was found to be rather uniform. In addition to the expected elements (calcium and oxygen), the concretions contain 3%–6% phosphorus. The phosphorus is most likely in the form of inorganic phosphate, which is probably a component of the amorphous calcium phosphate (as seen in the Raman and IR spectra). Nevertheless we cannot exclude the possibility that some of the phosphorus corresponds to phosphate groups linked to proteinaceous components of the organic matrix. Indeed, we have evidence for one such phosphorylated protein, orchestin (unpubl. results). Small amounts of magnesium (<1%) were also detected in the elemental analyses of the concretions.

We conclude that the concretions from *Orchestia cavimana* are composed of stable amorphous calcium carbonate together with about 5% amorphous calcium phosphate. The presence of phosphate associated with the amorphous calcium carbonate is widespread (5). Here we show that in *Orchestia*, at least part of this phosphate is associated with a separate amorphous calcium phosphate phase. The benefit of the amorphous phase is probably its relatively high solubility, so that it can be easily dissolved and transported to the newly formed cuticle.

It is interesting that the amorphous phase of the concretion is stable and does not change during the lifetime of the animal into a more stable crystalline form. Amorphous calcium carbonate, which forms *in vitro* only in a supersaturated solution, is usually metastable and transforms rapidly into a crystalline stable phase (25). When amorphous phases are stabilized by organisms, components of the organic matrix, such as macromolecules (1, 20, 26) or ions such as phosphate or magnesium (21, 26–29), are thought to be involved in this stabilization. Both magnesium and phosphate are known to inhibit crystal growth, thus raising the supersaturation levels and allowing the formation of metastable phases such as amorphous calcium carbonate. Several proteins extracted from the cuticle of the blue crab illustrate the importance of macromolecules in similar systems. These proteins were shown to inhibit nucleation of calcium carbonate until about 1 h after ecdysis, when they undergo certain alterations to allow the precipitation of the mineral (30). Interestingly, the macromolecules from the concretions of *Orchestia* are not transported along with the calcium and carbonate ions to the cuticle, but are preserved in the vicinity of the concretions. Understanding the mineralization function of well-characterized matrix proteins such as gastrolith matrix protein (GAMP) from crayfish gastroliths (31) or orchestin from the calcareous concretions of *Orchestia* (17) might contribute to a better understanding of how the amorphous calcium carbonate in the concretions forms and is stabilized.

We show here that amorphous calcium carbonate is the main component of the storage structures of a terrestrial crustacean, with amorphous calcium phosphate as a minor component. Identification and characterization of the mineral phase is essential for understanding the processes of biomineralization of the storage structures of *Orchestia*. These observations support the notion that amorphous calcium carbonate is an important phase in biomineralization, and clarifying how it is formed and stabilized may have broader implications to materials and medical science.

## Acknowledgments

Authors are greatly indebted to Marie Mesnier and Denis Chaumont from the "Laboratoire de Réactivité des Solides," Université de Dijon, France, for skillful assistance in X-ray diffraction and TG experiments. We also thank Prof. Lia Addadi for her advice. This work was supported by a United States-Israel Binational Science Foundation grant and by the Minerva Foundation.

## Literature Cited

1. **Lowenstam, H. A., and S. Weiner, eds. 1989.** *On Biomineralization.* Oxford University Press, New York.
2. **Beniash, E., J. Aizenberg, L. Addadi, and S. Weiner. 1997.** Amorphous calcium carbonate transforms into calcite during sea urchin larval spicule growth. *Proc. R. Soc. Lond.* **264B:** 461–465.
3. **Weiss, I. M., N. Tuross, L. Addadi, and S. Weiner. 2002.** Mollusc larval shell formation: Amorphous calcium carbonate is a precursor phase for aragonite. *J. Exp. Zool.* **293:** 478–491.
4. **Prenant, M. 1928.** L'étude cytologique du calcaire. IV. La vatérite chez les animaux. *Bull. Biol.* **62:** 21–47.
5. **Vinogradov, A. 1953.** *The Elementary Chemical Composition of Marine Organisms.* Sears Foundation for Marine Research, New Haven, CT. 647 pp.
6. **Greenaway, P. 1985.** Calcium balance and moulting in the crustacea. *Biol. Rev.* **60:** 425–454.
7. **Simkiss, K., and K. M. Wilbur. 1989.** Crustacea—The dynamics of epithelial movements. Pp. 205–229 in *Biomineralization: Cell Biology and Mineral Deposition,* K. Simkiss and K. M. Wilbur, eds. Academic Press, San Diego, CA.
8. **Graf, F. 1978.** Les sources de calcium pour les Crustacés venant de muer. *Arch. Zool. Exp. Gen.* **119:** 143–161.
9. **Ziegler, A. 1994.** Ultrastructure and electron spectroscopic diffraction analysis of the sternal calcium deposits of *Porcellio scaber* Latr. (Isopoda, Crustacea). *J. Struct. Biol.* **112:** 110–116.
10. **Travis, D. F. 1963.** Structural features of mineralization from tissue to macromolecular levels of organization in the decapod crustacea. *Ann. N. Y. Acad. Sci.* **109:** 177–245.
11. **Graf, F., and J. C. Meyran. 1983.** Premolt calcium secretion in the midgut posterior cæca of the crustacean *Orchestia:* ultrastructure of the epithelium. *J. Morphol.* **177:** 1–23.
12. **Graf, F. 1986.** Fine determination of the molt cycle stages in *Orchestia cavimana* Heller (Crustacea: Amphipoda). *J. Crustac. Biol.* **6:** 666–678.
13. **Graf, F., and J. C. Meyran. 1985.** Calcium reabsorption in the posterior cæca of the midgut in a terrestrial crustacean, *Orchestia cavimana. Cell Tissue Res.* **242:** 83–95.
14. **Meyran, J. C., F. Graf, and J. Fournié. 1987.** Carbonic anhydrase activity in a calcium-mobilizing epithelium of the crustacean *Orchestia cavimana* during molting. *Histochemistry* **87:** 419–429.
15. **Meyran, J. C., F. Graf, and G. Nicaise. 1986.** Pulse discharge of calcium through a demineralizing epithelium in the crustacean *Orchestia:* ultrastructural cytochemistry and X-ray microanalysis. *Tissue Cell* **18:** 267–283.
16. **Luquet, G., O. Testenière, and F. Graf. 1996.** Characterization and N-terminal sequencing of a calcium binding protein from the calcareous concretion organic matrix of the terrestrial crustacean *Orchestia cavimana. Biochim. Biophys. Acta* **1293:** 272–276.
17. **Testenière, O., A. Hecker, S. Le Gurun, B. Quennedey, F. Graf, and G. Luquet. 2002.** Characterization and spatiotemporal expression of *orchestin,* a gene encoding an ecdysone-inducible protein from a crustacean organic matrix. *Biochem. J.* **361:** 327–335.
18. **Graf, F. 1969.** Le stockage de calcium avant la mue chez les crustacés amphipodes *Orchestia* (Talitridé) et *Niphargus* (Gammaridé hypogé). Thèse Doc. Sci. Nat. Dijon, Impr. Berthier, Arch. Orig. Cent. Document. CNRS N° 2690.
19. **Graf, F. 1962.** Mise en réserve de calcaire avant la mue chez les crustacés amphipodes. *C.R. Acad. Sci.* **255:** 2191–2193.
20. **Aizenberg, J., G. Lambert, L. Addadi, and S. Weiner. 1996.** Stabilization of amorphous calcium carbonate by specialized macromolecules in biological and synthetic precipitates. *Adv. Mater.* **8:** 222–226.
21. **Raz, S., S. Weiner, and L. Addadi. 2000.** Formation of high-magnesian calcites via an amorphous precursor phase: possible biological implications. *Adv. Mater.* **12:** 38–42.
22. **Sauer, G. R., W. B. Zunic, J. R. Durig, and R. E. Wuthier. 1994.** Fourier transform Raman spectroscopy of synthetic and biological calcium phosphates. *Calcif. Tissue Int.* **54:** 414–420.
23. **Levi-Kalisman, Y., S. Raz, S. Weiner, L. Addadi, and I. Sagi. 2000.** X-ray absorption spectroscopy studies on the structure of a biogenic "amorphous" calcium carbonate. *J. Chem. Soc. Dalton Trans.* **21:** 3977–3982.
24. **Kojima, Y., A. Kawanobe, T. Yasue, and Y. Arai. 1993.** Synthesis of amorphous calcium carbonate and its crystallization. *J. Ceram. Soc. Jpn.* **101:** 1145–1152.
25. **Brecevic, L., and A. E. Nielsen. 1989.** Solubility of amorphous calcium carbonate. *J. Cryst. Growth* **98:** 504–510.
26. **Aizenberg, J., G. Lambert, S. Weiner, and L. Addadi. 2002.** Factors involved in the formation of amorphous and crystalline calcium

carbonate: A study of an ascidian skeleton. *J. Am. Chem. Soc.* **124:** 32–39.

27. **Taylor, M. G., and K. Simkiss. 1989.** Structural and analytical studies on metal-ion containing granules. Pp. 427–460 in *Biomineralization, Chemical and Biochemical Perspectives*, S. Mann, J. Webb, and R. J. P. Williams, eds. VCH, Weinheim.
28. **Taylor, M. G., K. Simkiss, G. N. Greaves, M. Okasaki, and S. Mann. 1993.** An X-ray absorption spectroscopy study of the structure and transformation of amorphous calcium carbonate from plant cystoliths. *Proc. R. Soc. Lond.* **252B:** 75–80.
29. **Sawada, K. 1997.** The mechanisms of crystallization and transformation of calcium carbonates. *Pure Appl. Chem.* **69:** 921–928.
30. **Coblentz, F. E., T. H. Shafer, and R. D. Roer. 1998.** Cuticular proteins from the blue crab alter *in vitro* calcium carbonate mineralization. *Comp. Biochem. Physiol. B.* **121:** 349–360.
31. **Tsutsui, N., K. Ishii, Y. Takagi, T. Watanabe, and H. Nagasawa. 1999.** Cloning and expression of a cDNA encoding an insoluble matrix protein in the gastroliths of a crayfish, *Procambarus clarkii. Zool. Sci.* **16:** 619–628.

Reference: *Biol. Bull.* **203:** 275–277. (December 2002)

# Revised Estimates of the Effects of Turbulence on Fertilization in the Purple Sea Urchin, *Strongylocentrotus purpuratus*

MARK W. DENNY*, ELIZABETH K. NELSON, AND KRISTINA S. MEAD[1]

*Hopkins Marine Station of Stanford University, Pacific Grove, California 93950*

*Turbulent water motion can either aid or hinder external fertilization in aquatic organisms. On one hand, turbulence provides the mixing necessary to bring eggs and sperm together; on the other, the forces imposed by turbulent eddies may interfere with the attachment of sperm to eggs and may even damage zygotes. Mead and Denny (1) explored this dichotomy by measuring the efficacy of fertilization in the purple sea urchin* (Strongylocentrotus purpuratus) *while gametes were subjected to sheared flow in a Couette cell. When calculated rates of turbulent energy dissipation exceeded 100 W/m$^3$, fertilization and early development were severely affected. Dissipation rates of this magnitude are common in breaking waves, and Mead and Denny therefore concluded that turbulent flow could be a substantial environmental hindrance to sexual reproduction in nearshore urchins. However, the rates of energy dissipation calculated by Mead and Denny for the Couette cell were erroneously small. Here we use direct measurements of energy dissipation rates to show that fertilization success can exceed 80% even when dissipation is as high as 2200 W/m$^3$, higher than the dissipation likely to be found in breaking waves. Thus, many energetic flow environments that were previously thought to be detrimental to external fertilization may instead be benign or advantageous.*

The majority of benthic marine invertebrates reproduce sexually *via* external fertilization. The effectiveness of this strategy has been the subject of much recent research, and the roles of water motion in "fertilization ecology" have been debated (for a review, see (2)). Given the limited swimming capabilities of sperm, if adults are separated by more than a few centimeters some water motion is required to bring sperm and eggs together. To this end, turbulence (and the bulk mixing that it causes) are advantageous. However, this mixing can occur only if water is sheared, and as a result, turbulence inevitably imposes viscous forces on gametes (3). If these forces inhibit the attachment of sperm to eggs or damage the gametes or zygote, the advantages of mixing can be negated. Whether turbulence is an aid to fertilization or a hindrance thus depends in part on where the line is drawn between effective mixing and shear-induced damage.

Mead and Denny (1) and Mead (4) examined this issue by measuring the ability of sea urchin gametes to fertilize under the controlled imposition of turbulent flow. Eggs of *S. purpuratus* were introduced into a volume of water contained in the space between two coaxial cylinders (a Couette cell, Fig. 1A). When the outer cylinder was rotated, the water was sheared, and, by varying the rate of rotation, the shear stress imposed on gametes could be controlled. Once the apparatus was up to speed, sperm were introduced at a concentration sufficient to result in 80%–90% fertilization in still water, and fertilization was allowed to proceed for 2 min. A volume of KCl solution was then introduced into the cell to prohibit further fertilization, and the percentage of eggs fertilized was determined.

With these results in hand, the turbulence intensity in the Couette cell was compared to the intensity characteristic of the wave-swept habitat in which *S. purpuratus* is found. The translation from laboratory to field conditions was made *via* the turbulent dissipation rate $\varepsilon$ (measured in W/m$^3$), the rate at which turbulence-induced shear stress in the water converts the energy of the moving fluid into heat (1, 5):

---

Received 25 July 2002; accepted 16 October 2002.

* To whom correspondence should be addressed. E-mail: mwdenny@leland.stanford.edu

[1] Present address: Department of Integrative Biology, University of California, Berkeley, California 94720.

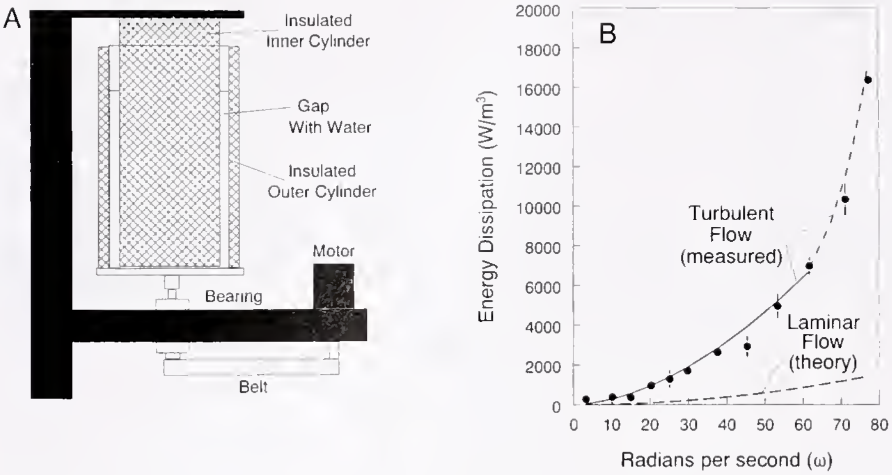

**Figure 1.** (A) The Couette cell of Mead and Denny (1) was modified to measure the rate at which water was heated by turbulent energy dissipation. The water bath was removed from the stainless steel inner cylinder, and a temperature-sensing device (Analog Devices AD590) and resistive heating element (Watlow Columbia K010030C5-0009B) were affixed separately to its inner surface. To minimize heat loss, the inner cylinder was then filled with insulating foam and the outer cylinder wrapped in a layer of closed-cell foam. Enough deionized water (100 ml) was added to the gap between the inner and outer cylinders to rise above the top of the heating element. The instrument was calibrated by passing a known current through the known resistance of the heating element (thereby determining the rate at which heat was injected into the system), and noting the rate at which temperature increased. An Agilent E3630A power supply was used to measure the current passing through the heating element, and an Agilent 34401 6-digit multimeter was used to monitor the voltage output from the temperature sensor and to interface with a computer. During calibration, the outer cylinder was rotated at a rate just sufficient to ensure that heat was well mixed throughout the water, but not so rapidly as to cause measurable heating *via* viscous dissipation. After an initial nonlinear temperature fluctuation associated with the thermal mass of the apparatus, temperature increased linearly at a rate proportional to the heat produced by the resistive element. In this fashion, the rate of temperature increase in the device could be interpreted in terms of the watts of heat energy injected for each cubic meter of water in the cell, in effect giving a measure of the specific heat capacity of the apparatus. The heating element was then turned off, and the apparatus was allowed to return to room temperature. Subsequently, the outer cylinder was rotated at a series of constant angular velocities; in each case the rate at which the water was heated was noted. By comparing these rates to the calibrated rates obtained with the heating element, we were able to measure total energy dissipation as a function of the angular velocity of the outer cylinder. The results shown here (B, filled circles ± 95% CL) indicate that energy dissipation in the cell is much larger than would be predicted by Eq. 2 if only dynamic viscosity, $\mu$, were present. The solid line is a power curve fit to the data, excluding the two points at highest $\omega$ ($\varepsilon = 4.918\omega^{1.751 \pm 0.134\ (\mathrm{SEM})}$, $r^2 = 0.961$). The remaining two points are better fit with a 5th-order polynomial calculated using all of the data ($\varepsilon = -46.903 + 112.22\omega - 10.337\omega^2 + 0.494\omega^3 - 0.00875\omega^4 + 0.000056\omega^5$, $r^2 = 0.998$). The dashed line depicting dissipation in laminar flow is taken from Eq. 2 with $\nu$ set to zero and a small correction for the effect of shear beneath the end of the inner cylinder: $\varepsilon = 0.276\omega^2$.

$$\varepsilon = \frac{\tau^2}{\mu} \tag{1}$$

Here $\tau$ is the shear stress (Pa) and $\mu$ is the dynamic viscosity of the water ($1.24 \times 10^{-3}$ N s m$^{-2}$ at 12 °C, the temperature at which the experiments were carried out). Shear stress can be related in turn to the motion of the Couette cell,

$$\tau = A\frac{\omega r}{h} \tag{2}$$

where $\omega$ is the angular velocity of the outer cylinder (in radians/s), $r$ is the inner radius of the outer cylinder (5.4 cm in this case), and $h$ is the radial separation between cylinders (3.5 mm). $A$ is the total viscosity of the fluid (5). Mead and Denny (1) assumed that $A$ was equal to $\mu$, which is true if flow is laminar. However, when flow is turbulent (as it was in the Couette cell),

$$A = \mu + \nu, \tag{3}$$

where $\nu$ is the eddy viscosity (5). Eddy viscosity is typically much larger than $\mu$ (5). Therefore, by neglecting $\nu$, Mead and Denny grossly underestimated the rate at which energy was dissipated during their experiments.

The magnitude of $A$ is difficult to predict with any precision; theoretical estimates vary over a wide range (*e.g.*, 6, 7, 8). To obtain accurate values, we therefore measured energy dissipation rates directly by monitoring the rate at which water was heated in the Couette cell as a function of

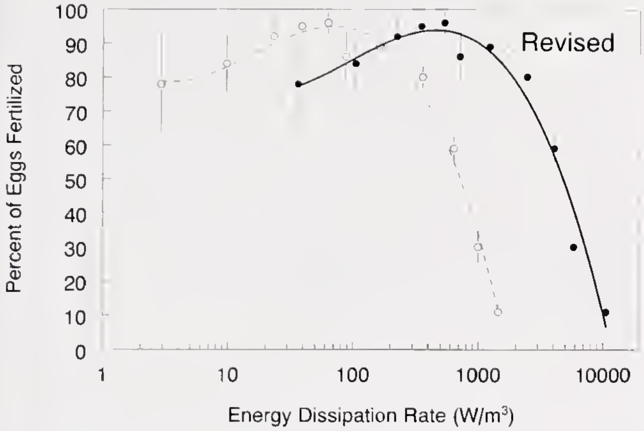

**Figure 2.** Fertilization results of Mead and Denny (1) and Mead (4) replotted using the new, empirical estimates of energy dissipation rate (filled circles). For comparison, the data are also plotted using the previous, erroneous dissipation estimates (open circles).

angular velocity (for the details of the measurements, see the caption to Fig. 1). These measurements were made in the same Couette cell used for the fertilization experiments (Fig. 1A).

Energy dissipation rates in the Couette cell fell within the range predicted by turbulence theory (6, 7, 8), and are indeed far in excess of those calculated by Mead and Denny (Fig. 1B). These empirical results can be used to re-interpret the previous fertilization data (Fig. 2). The percentage of eggs fertilized increases with increasing $\varepsilon$ up to a rate of about 600 W/m$^3$. This dissipation rate is greatly in excess of rates measured in the surf zone for waves 1 m high breaking on a gently sloping beach (10–100 W/m$^3$) (9), and is comparable to the predicted dissipation rate for 1-m-high waves on the steeper slope of a typical rocky shore (1, 10). Indeed, the percentage of eggs fertilized remains above 80% until $\varepsilon$ exceeds 2200 W/m$^3$, a dissipation rate greater than that predicted for the 2-m-high waves that are typical of surf conditions on rocky shores (1, 11). Thus, the high dissipation rates measured in the Couette cell paint a different scenario from that previously presented: the line separating the "good" from the "bad" effects of turbulence-induced shear stress is shifted to much higher turbulence intensities. Only if gametes are subjected to the shear stresses associated with very large breaking waves is fertilization in the purple sea urchin likely to be severely inhibited; under more typical conditions (waves $< 2$ m high), the mixing associated with turbulence may be advantageous in that it brings sperm and eggs into contact. This reinterpretation of laboratory results could help explain why some invertebrates (*e.g.*, gastropods) spawn preferentially when sea conditions are rough (12).

It is important to bear in mind that other free-spawning species may have different sensitivities to intense turbulence. Note, also, that this interpretation of "good" and "bad" ignores at least two potentially detrimental effects of turbulent mixing. Although mixing is commonly required for contact between sperm and eggs, it also can result in the dilution of gametes (13, 14), and the lower the co-occurring concentration of gametes, the lower the probability of fertilization (15). Thus, unless gametes are confined in a manner that reduces dilution (in a surge channel or tide pool, for instance (7)), turbulence may still be disadvantageous for all but the lowest levels needed for effective mixing. Second, in the rare instances when sperm are present in high concentration, an increase in mixing due to turbulence could increase polyspermy, and thereby decrease the fraction of viable zygotes.

## Acknowledgments

Funding was provided by NSF grants OCE 9115688 and 9985946 to MD. EN was supported by an NSF predoctoral fellowship and a stipend from PISCO (Partnership for Interdisciplinary Study of Coastal Oceans). This is contribution 95 of PISCO.

## Literature Cited

1. **Mead, K. S., and M. W. Denny. 1995.** The effects of hydrodynamic shear stress on fertilization and early development in the purple sea urchin, *Strongylocentrotus purpuratus*. *Biol. Bull.* **188:** 46–56.
2. **Levitan, D. R. 1995.** The ecology of fertilization in free-spawning invertebrates. Pp. 123–156 in *Ecology of Marine Invertebrate Larvae*, L. McEdward, ed. CRC Press, Boca Raton, FL.
3. **Denny, M. W. 1993.** *Air and Water.* Princeton University Press, Princeton, NJ.
4. **Mead, K. S. 1997.** The effects of hydrodynamic shear stress on fertilization and early development in free-spawning invertebrates. Ph.D. thesis, Stanford University, Stanford, CA.
5. **Schichting, H., and K. Gersten. 2000.** *Boundary Layer Theory*, 8th ed. Springer-Verlag, Berlin.
6. **Doering, C. R., and P. Constantin. 1992.** Energy dissipation in shear driven turbulence. *Phys. Rev. Letters* **69:** 1648–1652.
7. **Lewis, G. S., and H. L. Swinney. 1999.** Velocity structure functions, scaling, and transitions in high-Reynolds-number Couette-Taylor flow. *Phys. Rev. E.* **59:** 5457–5467.
8. **Balonishnikov, A. M. 2000.** Extended local balance model of turbulence and Couette-Taylor flow. *Phys. Rev. E.* **61:** 1390–1394.
9. **George, R., R. E. Flick, and R. T. Guza. 1994.** Observations of turbulence in the surf zone. *J. Geophys. Res.* **99:** 801–810.
10. **Denny, M., J. Dairiki, and S. Distefano. 1992.** Biological consequences of topography on wave-swept rocky shores: I. Enhancement of external fertilization. *Biol. Bull.* **183:** 220–232.
11. **Denny, M. W. 1995.** Predicting physical disturbance: mechanistic approaches to the study of survivorship on wave-swept shores. *Ecol. Monogr.* **65:** 371–418.
12. **Shanks, A. L. 1998.** Apparent oceanographic triggers to the spawning of the limpet *Lottia digitalis* (Rathke). *J. Exp. Mar. Biol. Ecol.* **222:** 31–41.
13. **Denny, M. W. 1998.** *Biology and the Mechanics of the Wave-Swept Environment.* Princeton University Press, Princeton, NJ.
14. **Denny, M., and M. Shibata. 1989.** Consequences of surf-zone turbulence for settlement and external fertilization. *Am. Nat.* **143:** 859–889.
15. **Vogel, H., G. Chizak, P. Chang, and P. Wolf. 1982.** Fertilization kinetics of sea urchin eggs. *Math. Biosci.* **58:** 189–216.

Reference: *Biol. Bull.* **203:** 278–288. (December 2002)

# Long-Term Culture of Decapsulated Gastropod Embryos: A Transplantation Study

SHIHUAN KUANG, MARETTE REGNIER, AND JEFFREY I. GOLDBERG*

*Department of Biological Sciences, University of Alberta, Edmonton, Alberta, Canada T6G 2E9*

**Abstract.** Encapsulated embryos of the pond snail *Helisoma trivolvis* have been useful for examining neural development and neural circuit function during development. However, their full potential in developmental studies is limited by the lack of an effective method for long-term culture of decapsulated embryos. In the present study, decapsulated early embryos were either cultivated *ex ovo* in various media under different environmental conditions or transplanted into host egg capsules. Although diluted capsular fluid, 30% M199, and albumen-gland-conditioned medium were partially effective in promoting embryonic growth for a short time, none of the media promoted normal embryonic development in long-term tests. In contrast, after previously decapsulated and experimentally manipulated embryos were transplanted into host capsules, their growth and development were similar to their intact siblings. In combination with laser ablation, this transplantation technique was used to demonstrate the role played by a pair of serotonergic neurons in regulating an embryonic rotational behavior. These results suggest that embryonic transplantation is an extremely effective technique for achieving long-term growth and development of previously decapsulated embryos and therefore can be instrumental in investigating cell lineage, function, and development in encapsulated embryos.

## Introduction

Embryos of pulmonate gastropods undergo direct development from fertilized egg to juvenile snail inside egg capsules filled with albuminous perivitelline fluid, also known as capsular fluid (CF). The nutrition required for normal development of embryos is provided by the CF, which is a secretory product of the albumen gland (Raven, 1958; Morrill *et al.*, 1964; Beadle, 1969; Goudsmit, 1976; Morrill, 1982; Stockmann-Bosback and Althoff, 1989; Heras *et al.*, 1998). Early studies identified carbohydrates such as galactogen and proteins as two major categories of nutrition in CF, which together make up more than 94% of its dry weight in the freshwater pond snail *Lymnaea stagnalis* (Horstmann, 1956; Morrill *et al.*, 1964; Wijsman and van Wijck-Batenburg, 1987). However, the specific key nutritive components for the growth and development of early embryos are yet unknown. In addition, several other unique features of the microenvironment of egg capsules can hardly be mimicked *in vitro*. Among such features are a positive hydrostatic pressure (2.1 atmospheres) and negative equilibrium potential (−23 mV) inside newly laid egg capsules of *Lymnaea* (Raven, 1958; Taylor, 1973; Morrill, 1982; Pechenik *et al.*, 1984); antibacterial factors in the CF of the sea slug *Aplysia kurodi* (Kamiya *et al.*, 1984); and an epidermal growth factor (EGF) and various enzymes such as phosphatases and trypsin inhibitors in the CF of several species (Stockmann-Bosback and Althoff, 1989; Hermann *et al.*, 2000; Nagle *et al.*, 2001). These complex structural and compositional features of egg capsules appear to be critical for embryonic development, as attempts to achieve normal development of early stage embryos *ex ovo* have been largely unsuccessful in many species (Morrill, 1982; Pechenik *et al.*, 1984; Stockmann-Bosback and Althoff, 1989; Meshcheryakov, 1990).

In experiments that involve perturbation of embryonic development and function, embryos must be isolated from their egg capsules for experimental treatments and then monitored as they continue to develop. For example, embryos of several encapsulated gastropods display a cilia-driven rotational behavior early in their development (Mor-

---

Received 10 May 2002; accepted 4 September 2002.

* To whom correspondence should be addressed. E-mail: jeff.goldberg@ualberta.ca

*Abbreviations:* AHS, antibiotic *Helisoma* saline; APW, artificial pond water; CF, capsular fluid; EGF, epidermal growth factor; HDM, *Helisoma* defined medium.

rill, 1982; Diefenbach *et al.*, 1991; Voronezhskaya *et al.*, 1999). In *Helisoma trivolvis*, the occurrence of this rotation is accompanied by the differentiation of a pair of embryonic serotonergic neurons identified as ENC1s (Goldberg and Kater, 1989; Diefenbach *et al.*, 1998; Koss *et al.*, 2002). In acute experiments on isolated embryos, ENC1s have been shown to be cilioexcitatory motor neurons that accelerate embryonic rotation in response to hypoxia (Kuang and Goldberg, 2001; Kuang *et al.*, 2002). To assess whether this response is an adaptation that affects embryonic viability and recruitment success, and to examine the mechanisms regulating development of the ENC1-ciliary neural circuit, we need methods that promote normal embryonic development after embryos have been decapsulated and treated.

The goal of this study was to generate a method for long-term culture of decapsulated *Helisoma* embryos. We first tested the effects of pH, epidermal growth factor, and various culture media on the *ex ovo* growth and development of decapsulated embryos. We then tested the feasibility of transplanting previously decapsulated embryos into egg capsules containing host embryos for long-term culture. Our results indicate that transplantation is an effective method for continued growth and development of previously decapsulated embryos. This transplantation technique will facilitate studies of embryonic cell function, lineage, and development of encapsulated species.

## Materials and Methods

### *Animals*

Adult individuals of *Helisoma trivolvis* were maintained in flow-through aquaria containing dechlorinated water (25 °C) and were fed with lettuce and Trout Chow (Unifeed). Since the pond snails usually lay eggs on a smooth surface, plastic petri dishes (diameter 150 mm) were placed in the aquaria to facilitate egg-laying. Egg masses were collected from the petri dishes with a razor blade and transferred into artificial pond water (APW: 0.025% Instant Ocean, pH 7.2–7.3, Aquarium Systems) for experimental use. Embryos were staged as the percentage of the whole intracapsular development, with E0 corresponding to the zygote at 0% development and E100 corresponding to hatching at 100% development (Goldberg *et al.*, 1988; Goldberg, 1995; Diefenbach *et al.*, 1998). In this study, egg masses containing stage E0 to E25 embryos were used.

### Ex ovo *culture of isolated embryos*

Clean and intact egg masses containing embryos of appropriate stages were washed three times, for 30 min each time, in antibiotic APW (150 $\mu$g/ml Gentamicin) to disinfect the surface of the egg mass. Embryos were then isolated in antibiotic *Helisoma* saline (AHS: 51.3 m*M* NaCl, 1.7 m*M* KCl, 4.1 m*M* $CaCl_2$, 1.5 m*M* $MgCl_2$, 5.0 m*M* HEPES, 150 $\mu$g/ml Gentamicin, pH 7.30–7.35, 115–119 mOsm) under sterile conditions. The egg mass and capsular membranes were ruptured with a 30-gauge surgical needle, and the embryos were gently blown or sucked out with a refined and heat-polished Pasteur pipette.

The isolated embryos were then cultured at 23 °C in 2 ml of various media in 35-mm petri dishes (Falcon 3001). The media tested included AHS; antibiotic APW; *Helisoma* defined medium (HDM: 50% Leibovitz-15 (Gibco), 40.0 m*M* NaCl, 1.7 m*M* KCl, 4.1 m*M* $CaCl_2$, 1.5 m*M* $MgCl_2$, 5.0 m*M* HEPES, 50 $\mu$g/ml Gentamicin, 150 $\mu$g/ml l-glutamine, pH 7.30–7.40, 143 mOsm); 30% M199 (Gibco, pH 7.20–7.30, 91 mOsm); 5% galactose in AHS; 1.5% CF in AHS; and albumen-gland-conditioned AHS. The 1.5% CF was harvested by releasing all intracapsular contents from 60 egg capsules into 2 ml AHS with a pipette and subsequently removing the embryos. The average volume of egg capsules was estimated to be 0.47 $\mu$l on the basis of their nearly oval shape and maximal height (916 ± 49 $\mu$m, $n = 7$) and length (1066 ± 16 $\mu$m, $n = 26$). The albumen-gland-conditioned medium was made by incubating isolated albumen glands in AHS (2 glands/ml, 2–12 h at 23 °C) in the presence of 100 $\mu$*M* forskolin, a cyclic AMP activator previously shown to stimulate release of proteins and polysaccharides from the albumen gland (Morishita *et al.*, 1998).

To mimic the capsular environment, isolated embryos were cultured separately in hanging droplets of culture media and in culture media with increased viscosity (1% gelatin). To test the effect of pH on growth and development, isolated embryos were cultured in HDM of different pH (6.4, 7.4, and 8.4). To test the effect of epidermal growth factors (EGF) on growth and development, isolated embryos were cultured in HDM plus 0.1 $\mu$g/ml human recombinant EGF (h-EGF, Sigma), or in a novel EGF purified from the CF of *Lymnaea* (l-EGF, a generous gift from Dr. A. Bulloch, Univ. of Calgary).

The cultured embryos were viewed with an inverted microscope (Zeiss Axiovert) and the digital images were captured by a CCD video camera (Paultek Imaging). The length (maximal dimension) of the embryos was analyzed with NIH image (http://rsb.info.nih.gov/nih-image/).

### *Transplantation of early embryos*

Before they were transplanted into new host capsules, isolated embryos were washed twice in AHS and then either placed in AHS for at least 1 h or experimentally manipulated. Embryos removed from their egg capsules for as long as 2 h before transplantation developed normally after transplantation, allowing sufficient time to perform experimental manipulations. Longer times were not tested. In transplantation of stage E15–E25 embryos, the host egg capsules contained younger embryos (≤stage E10) so that host and transplanted embryos could easily be distinguished. For transplantation of embryos at the 2-cell to 8-cell stages (E1–E2), isolated embryos were transplanted into capsules whose host embryos had been killed by heat shock (water bath at 48 °C for 25 min).

Prior to transplantation, the host egg mass was stabilized at the center of a 35-mm petri dish (Falcon 1008) by surrounding the mass with a strip of dental wax. The host egg mass was then immersed in filtered APW. Transplantation was performed through a 150–300 μm incision made near the edge of each host capsule. In each donor egg mass, half of the embryos were isolated for transplantation; the remaining embryos were kept as *in ovo* controls. A Sigmacote (Sigma)-coated, heat-polished glass micropipette (tip diameter: 120–250 μm depending on the stage of embryos to be transplanted) was used to transfer the embryos. The micropipette was operated by hand and pressure control was exerted with a 0.2-ml calibrated micrometer syringe (Gilmont). The transplanted and control embryos were viewed with an inverted microscope (Nikon Eclipse TE300), and digital images were captured by a CCD camera (Cooke SensiCam). The maximal length of the embryos was analyzed with image analysis software (Slidebook, Intelligent Imaging Innovations, Inc., Denver, CO).

### *Laser ablation of embryonic cells*

The standard procedures for laser ablation are described elsewhere (Kuang and Goldberg, 2001). Briefly, embryos were isolated, mounted on slides, and viewed with differential interference contrast (DIC) optics. Only those with both ENC1s clearly visible were used (about 10% of stage E25 embryos). Pulsed laser beams (pulse length: 3 ns) generated by a VSL-337 nitrogen laser (Laser Science, Inc.) were delivered to the targeted cells *via* a coupling unit (Photonic Instruments, Inc.) and the optical path through a compound microscope (Zeiss, Axioskop). The coupling unit contained a dye laser module (5 m*M* coumarin 440), emitting at a wavelength of 420–475 nm. Laser beams, which theoretically had a diameter equal to the wavelength, were attenuated to a strength that was just able to scratch glass coverslips and were applied at a frequency of 8–10 Hz onto the nucleolus and perinucleolar region of the nuclei. To kill a cell, 200–300 pulses were applied until visible scars or blebs were apparent on the nucleolus, the nuclear boundary became obscure, and the cell started to swell. This procedure induced a gradual cell death that was complete by 6–24 h after laser treatment (Kuang and Goldberg, 2001).

### *Measurement of embryonic rotation*

To test the role of ENC1s in regulating embryonic rotation, stage E25 embryos with ENC1s ablated were transplanted into new egg capsules and embryonic rotation was monitored the following day with a CCD video camera (JVC, TK860U) mounted on a dissecting microscope (Zeiss, StemiSR). Rotation was recorded at 2.5 fields/s with a time-lapse videocassette recorder (VCR; Panasonic, AG-6720) and replayed at 60 fields/s to facilitate quantification. The average rate of rotation in each 10-min interval was analyzed by counting the total number of complete revolutions in 6–8 min. The total number of rotational surges (Diefenbach *et al.*, 1991) was similarly counted at 10-min intervals.

## Results

### Ex ovo *culture of decapsulated embryos*

Initial attempts to achieve sustained development *ex ovo* were made with stage E15, E20, and E25 embryos, corresponding to the period of development of the rotational behavior and underlying ENC1-ciliary neural circuits (Diefenbach *et al.*, 1991, 1998; Koss *et al.*, 2002). A variety of culture media were tested, including AHS, APW, HDM, 30% M199, 5% galactose, 1.5% CF, and albumen-gland-conditioned medium. Although short-term growth and development was observed in all the media tested, none of them supported sustained growth, probably due to the absence of crucial nutritive components or growth-promoting factors. Of all the media tested, 30% M199, 1.5% CF, and albumen-gland-conditioned medium produced the best development, with stage E15, E20, and E25 embryos sometimes reaching stages that display features of normal stage E25, E30, and E40 embryos, respectively, after 3 d of culture (Fig. 1). At the same time point, the control embryos developing *in ovo* consistently reached stages E35, E45, and E50, respectively, when egg masses were immersed in APW (Fig. 1). Similarly, *in ovo* development proceeded normally when egg masses were incubated in HS.

Generally, embryos cultured *ex ovo* displayed abnormal features (Fig. 1) and slower development (Fig. 2) in comparison to *in ovo* controls. In particular, shell formation was either stunted or absent in the *ex ovo* embryos (Fig. 1). Furthermore, accumulation of particles was always found in the canaliculus of the protonephridia (arrows in Fig. 1). Finally, embryos were often hydropic after 72 h of culture *ex ovo*. Although embryos often survived in culture for more than 30 days, no significant development was observed after the first 5 days of *ex ovo* cultivation (Fig. 2). The average increases in the length of embryos over this time period were 54 ± 13 (SE) μm ($n$ = 7) and 69 ± 11 μm ($n$ = 7) for the stage E15 and E20 groups, respectively. In contrast, control embryos exhibited significantly greater increases in length over the same time periods (Fig. 2).

To test whether the high viscosity or other physical properties within egg capsules are important factors promoting embryonic development, embryos were cultured in AHS containing 1% gelatin or in hanging droplets of AHS. Neither of these conditions improved *ex ovo* embryonic development (data not shown).

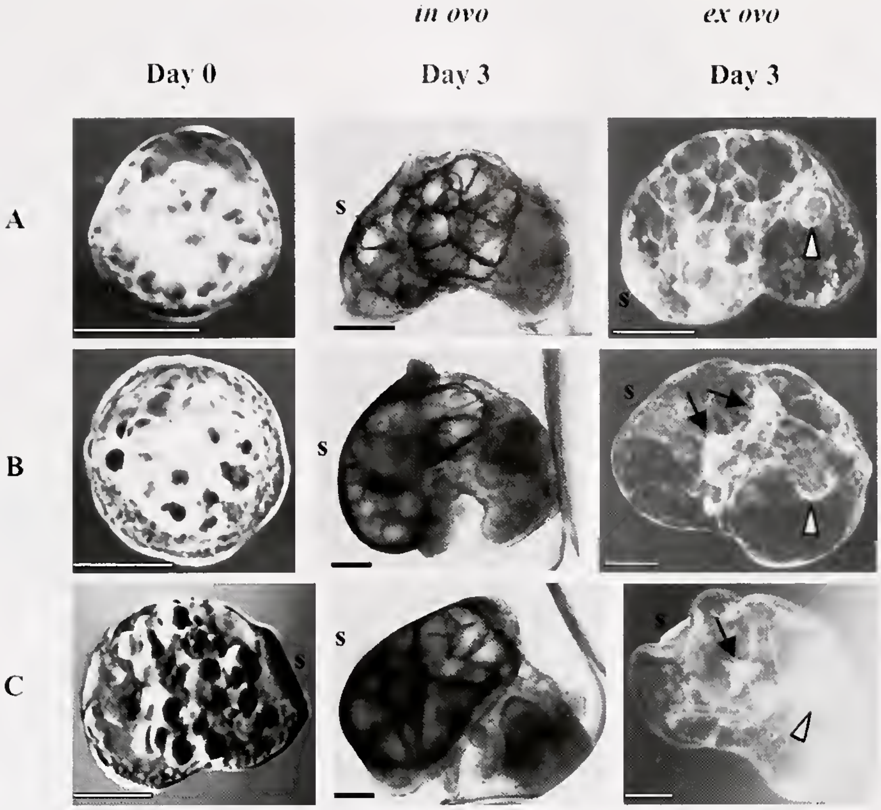

**Figure 1.** Embryonic development of *Helisoma* embryos after 3 days of culture *in ovo* and *ex ovo* at 23 °C. Examples of stage E15 (A), E20 (B), and E25 (C) embryos before culture (Day 0), after 3 days of culture in host egg capsules (*in ovo*), and in *Helisoma* saline plus 1.5% CF (*ex ovo*). Embryos cultured *in ovo* reached stages E40 (A), E45 (B), and E50 (C), whereas embryos cultured *ex ovo* only developed to stage E30 (A and B) or E35 (C). s: shell gland; arrowheads: radular sac; arrows: granular deposition in the protonephridium. Scale bars: 100 $\mu$m.

We next tested the effect of pH on the growth of isolated embryos. Egg mass matrix and CF had a pH of 6.6 ± 0.1 ($n = 4$), suggesting that low pH may promote embryonic development. The growth and development of stage E20 embryos were assessed after 3 days of culture in HDM adjusted to pH 6.4, 7.4, or 8.4. Although none of these groups exhibited significantly improved embryonic development as compared to the previous treatments, embryo development improved inversely with pH, both in terms of embryo length (Fig. 3A) and percent of embryos displaying stage E30 features, including larval kidney formation, muscle contraction of the body wall, and a shell (Fig. 3B). This effect of pH was not observed when embryos were cultured in 30% M199 (data not shown), a medium that generally promoted greater embryonic development than HDM, as described above.

Because a novel EGF has recently been identified in the CF-secreting albumen gland of *Lymnaea stagnalis* (Hermann *et al.*, 2000), we also tested whether EGF can promote the growth and development of *Helisoma* embryos *ex ovo*. Stage E20 embryos cultured for 3 days in HDM at pH 6.4 developed similarly, in both stage and body length, in the presence or absence of human recombinant EGF (450 ng/ml) or *Lymnaea* EGF (100 ng/ml) (data not shown). Although EGF may still be an important factor, other key components are clearly required to sustain normal growth and development of embryos *ex ovo*.

### *Transplantation of decapsulated embryos into host egg capsules*

As an alternative to *ex ovo* culture of embryos, we tested the feasibility of transplanting decapsulated embryos into egg capsules already containing host *Helisoma* embryos. Stage E15 and E20 embryos were transplanted into host egg capsules containing much younger embryos (≤stage E10) to minimize mechanical interactions between host and transplant, and to ensure that they could be easily distinguished. Furthermore, younger egg capsules provide greater nutrition, since the nutritive components of CF become

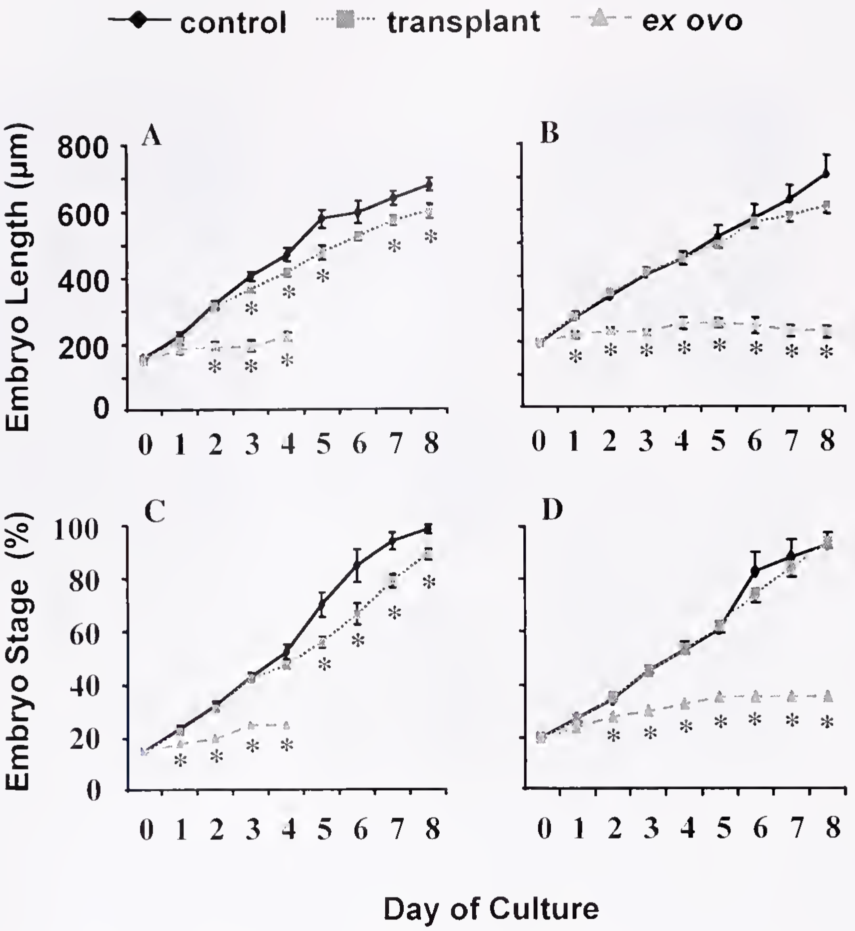

**Figure 2.** Growth and development of *in ovo* control embryos, transplanted embryos, and *ex ovo* (1.5% capsular fluid, pH 7.3–7.4) cultured embryos at 23 °C. The growth (length of embryos) of stage E15 (A) and E20 (B) embryos cultured *ex ovo* was significantly slower than that of control embryos (Student's *t* test, $P < 0.05$ at time points marked by asterisks, $n = 7$ for each of the *ex ovo* culture trials [10–15 embryos in each trial], $n = 6$ and 5 for control stage E15 and E20 embryos, respectively). In contrast, growth of transplanted stage E15 and E20 embryos was very similar to their control counterparts. Slight differences were seen only at later stages of culture in transplanted E15 embryos (marked by asterisks; *t* test, $P < 0.05$, $n = 6$). There was no significant difference in the growth of control and transplanted stage E20 embryos at any time points (*t* test, $P > 0.05$, $n = 6$). The development of the same stage E15 (C) and E20 (D) embryos cultured *ex ovo* was much slower than that of control embryos (asterisks; *t* test, $P < 0.05$). In transplanted stage E15 and E20 embryos, however, the development was very similar to their control counterparts. Small differences were only seen at later stages of culture in transplanted E15 embryos (asterisks; *t* test, $P < 0.05$). There was no significant difference in the development of control and transplanted stage E20 embryos at any time point (*t* test, $P > 0.05$).

depleted as embryonic development proceeds (Morrill, 1982; Stockmann-Bosbach and Althoff, 1989). In most cases, the incision in the capsule membrane re-sealed within 12 h after transplantation.

In striking contrast to the *ex ovo* trials, the growth and development of transplanted embryos was very similar to that displayed by control embryos within intact egg capsules (Fig. 2). At 23 °C, the growth and development of transplanted stage E15 embryos were identical to the controls in the first 3–4 days but slightly slower thereafter (Fig. 2A, C). When transplanted at stage E20 or older, however, the lengths (Fig. 2B) and embryonic stages (Fig. 2D) reached by transplanted embryos at various days were identical to controls (Student's *t* test, $P > 0.05$ at any time point, $n = 7$). Although embryos transplanted at stage E15 had a marginally lower survival rate 8 days after transplantation (Fig. 4A, chi square test, $P < 0.05$), the survival rate of embryos transplanted at stage E20 was not different from that of control (Fig. 4A, chi square test, $P > 0.05$). However, transplantation caused a slight decrease in the

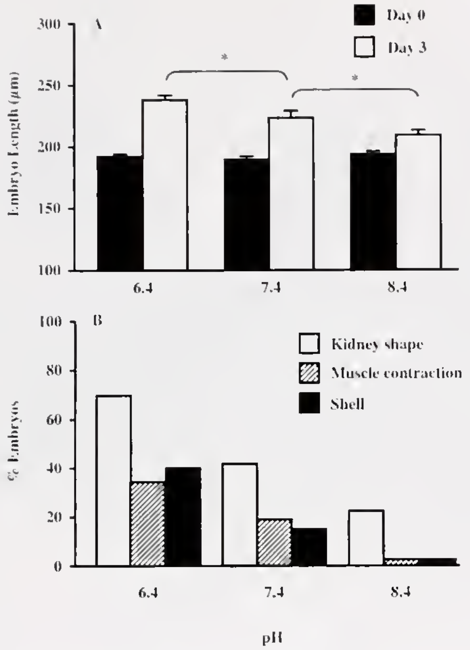

**Figure 3.** Effect of pH on growth and development of embryos cultured *ex ovo* in *Helisoma* defined medium at 23 °C. (A) Embryonic length before and after 3-day culture of stage E20 embryos. At each pH, there was a significant difference in the average embryonic length between Day 0 and Day 3 (Student's $t$ test, $P < 0.05$, $n = 44$–$66$ embryos in 3 replicates). Whereas there were no differences in embryonic length at different pH at Day 0, there were significant differences in embryonic length at Day 3 (asterisks; $t$ test, $P < 0.05$). (B) Percent of embryos expressing specific features of control stage E30 embryos, including larval kidney shape, muscle contraction of the body wall, and presence of a shell, at different pHs. The percentage expression of each feature was significantly different at these three pHs ($G$ test, $P < 0.01$, $n = 51$–$68$ embryos from 3 replicates).

percentage of embryos hatched at 8 days post-transplantation (Fig. 4B); 91% stage E15 ($n = 23$) and 89% stage E20 ($n = 18$) control embryos hatched by this time, as compared to 70% stage E15 ($n = 28$) and 62% stage E20 ($n = 29$) transplanted embryos, respectively (chi square test, $P < 0.05$ for both stages). Nonetheless, transplanted embryos grew normally in APW after hatching (data not shown). These data suggest that transplantation into host egg capsules is an extremely effective technique for achieving a normal course of embryonic development for previously decapsulated stage E15 or older embryos.

To test whether this transplantation technique can be applied to embryos at cleavage stages, we transplanted 2-cell to 8-cell stage embryos (stage E1–E2) into capsules whose hosts were killed previously with heat shock (48 °C for 25 min). About two-thirds of the successfully transplanted embryos died at about stage E10, the time of gastrulation. However, the remaining third survived and displayed normal embryonic growth and development (Figs. 5 and 6).

### *An application of the embryo transplantation technique*

Prior to development of the transplantation technique, we established the motor function of ENC1 by stimulating its release of serotonin with a laser treatment and recording the activity of postsynaptic ciliary cells (Kuang and Goldberg, 2001). It has been hypothesized that ENC1 regulates embryonic rotation through periodic release of serotonin to generate surges of embryonic rotation (Diefenbach *et al.*, 1991). Through transplantation, we can now provide further evidence in support of this hypothesis. Stage E25 embryos were removed from their egg capsules, subjected to bilateral laser ablation of ENC1s or neighboring control cells (Kuang and Goldberg, 2001), and transplanted into host egg capsules for behavioral analysis (Fig. 7A). After an overnight recovery period, the embryonic rotational rate and frequency of rotational surges were measured. In comparison to the control-ablated embryos, embryos with ENC1s ablated displayed a significant reduction in rotational rate (Fig. 7B, $t$ test, $P < 0.05$, $n = 9$ for control and 7 for ENC1 ablation) and almost a total absence of rotational surges (Fig. 7C, $t$ test, $P < 0.01$, $n = 11$ for control and 9 for ENC1 ablation). Therefore, the embryo transplantation technique can be instrumental in investigating cellular function in encapsulated embryos.

## Discussion

An embryonic transplantation technique for long-term sustained growth and development of previously decapsulated embryos was reported in the present study. The *ex ovo* culture conditions that were also tested in this study were effective in the short-term maintenance of embryonic

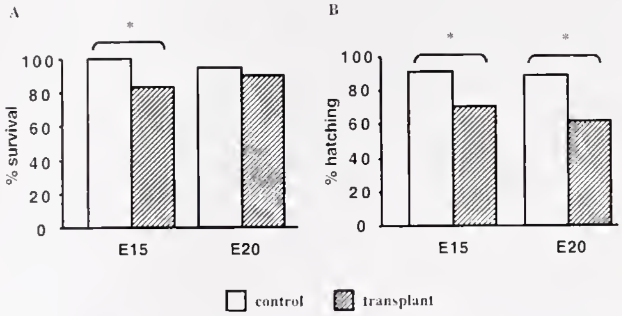

**Figure 4.** Survival and hatching rates of transplanted and control embryos at 23 °C. The survival rate was calculated as the total number of embryos alive at Day 8 as a percentage of total embryos at the beginning of the experiment. The hatching rate was calculated as the total number of embryos hatched as a percentage of the total embryos alive at Day 8. (A) Survival rate of control and transplanted stages E15 and E20 embryos. $n = 23$ (control E15), 30 (transplant E15), 19 (control E20), and 30 (transplant E20). Asterisk: $P < 0.05$, chi square test. (B) Hatching rate of control and transplanted stages E15 and E20 embryos. $n = 23$ (control E15), 28 (transplant E15), 18 (control E20), and 29 (transplant E20). Asterisks: $P < 0.05$, chi square test.

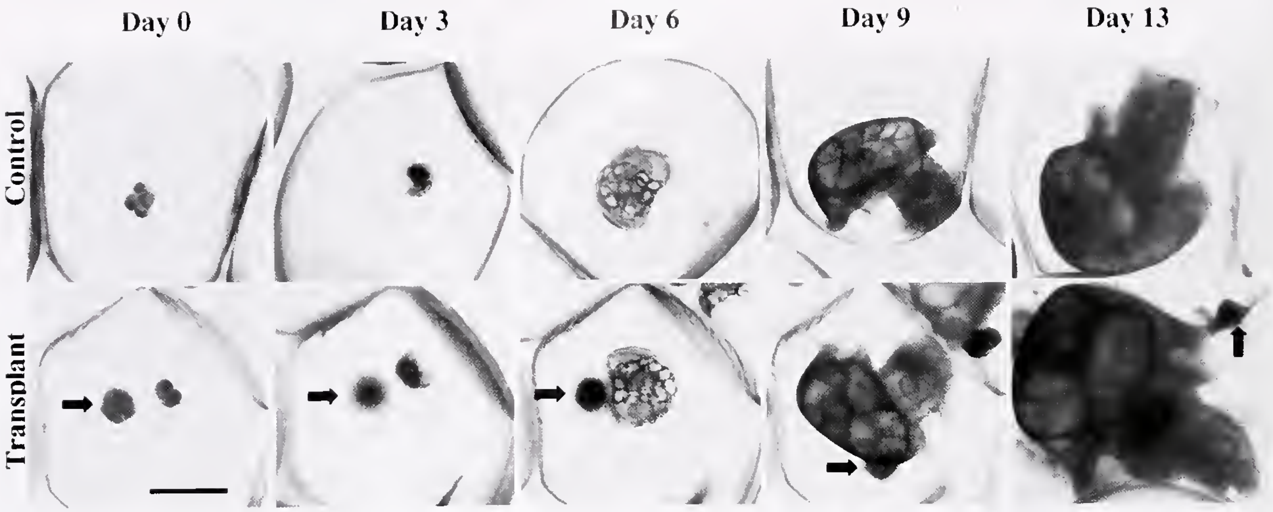

**Figure 5.** Morphological development of control and transplanted stage E1–E2 (2–4 cell stages) embryos at 20.5 °C. A control embryo developed from the 4-cell stage to hatching in 13 days. Similarly, a transplanted embryo developed from the 2-cell stage to hatching at the same rate. The transplanted embryo was isolated from the same egg mass as the control embryo. The transplanted embryos lagged behind the control embryo by 1 cleavage division at Day 0 because of the isolation and the 1-h incubation in saline prior to transplantation. The host embryo (arrows) in the transplantation group was killed by heat shock (45 °C, 25 min) prior to transplantation. Scale bar: 300 $\mu$m.

growth and survival, but failed to promote normal development over the long term.

That embryos at early stages (pre-shell stages) fail to develop normally under various *ex ovo* conditions suggests that some key growth-promoting factors or certain environmental conditions are missing in *ex ovo* culture. It has been reported in several species that encapsulated embryos cannot develop normally if they are removed from the egg capsules at early stages of development (Morrill, 1982; Pechenik *et al.*, 1984; Stockmann-Bosbach and Althoff, 1989; Meshcheryakov, 1990). This is probably because the environment in the capsular matrix is extremely complex and can hardly be mimicked *in vitro*. The situation is further complicated by the substantial variation in the composition of CF among species (Morrill *et al.*, 1964; Morrill, 1982; Heras *et al.*, 1998). Even less is known about the physical properties of the CF and the membranes surrounding it, such as viscosity, electrical charge, pressure, osmolarity, and pH (Beadle, 1969; Taylor, 1973; Morrill, 1982). For instance, this study indicates that *Helisoma* embryos naturally develop in a slightly acidic environment. Furthermore, acidic pH promoted growth and development of early embryos cultured *ex ovo* in *Helisoma* defined medium (HDM) (Fig. 3). Likewise, hamster embryonic cells exhibit optimal clonal proliferation when cultured in medium with a pH of 6.70 (Leboeuf *et al.*, 1989). We do not know why embryonic growth was not promoted by acidic pH when cultured in 30% M199. Intracapsular hydrostatic pressure may also be an important factor for normal embryonic growth and development. In *Lymnaea palustris*, early stage embryos

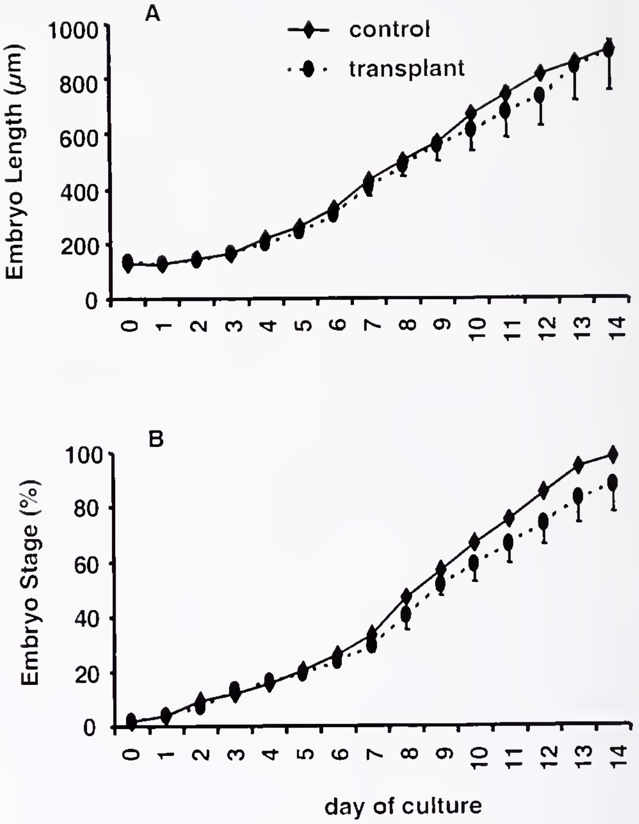

**Figure 6.** Growth (A) and development (B) of control and transplanted stage E1–E2 (2–8 cell stage) embryos at 20.5 °C. No difference in growth or development was found between control and transplanted embryos ($P > 0.05$ on each day, $n = 22$ and 4 for control and transplanted embryos, respectively).

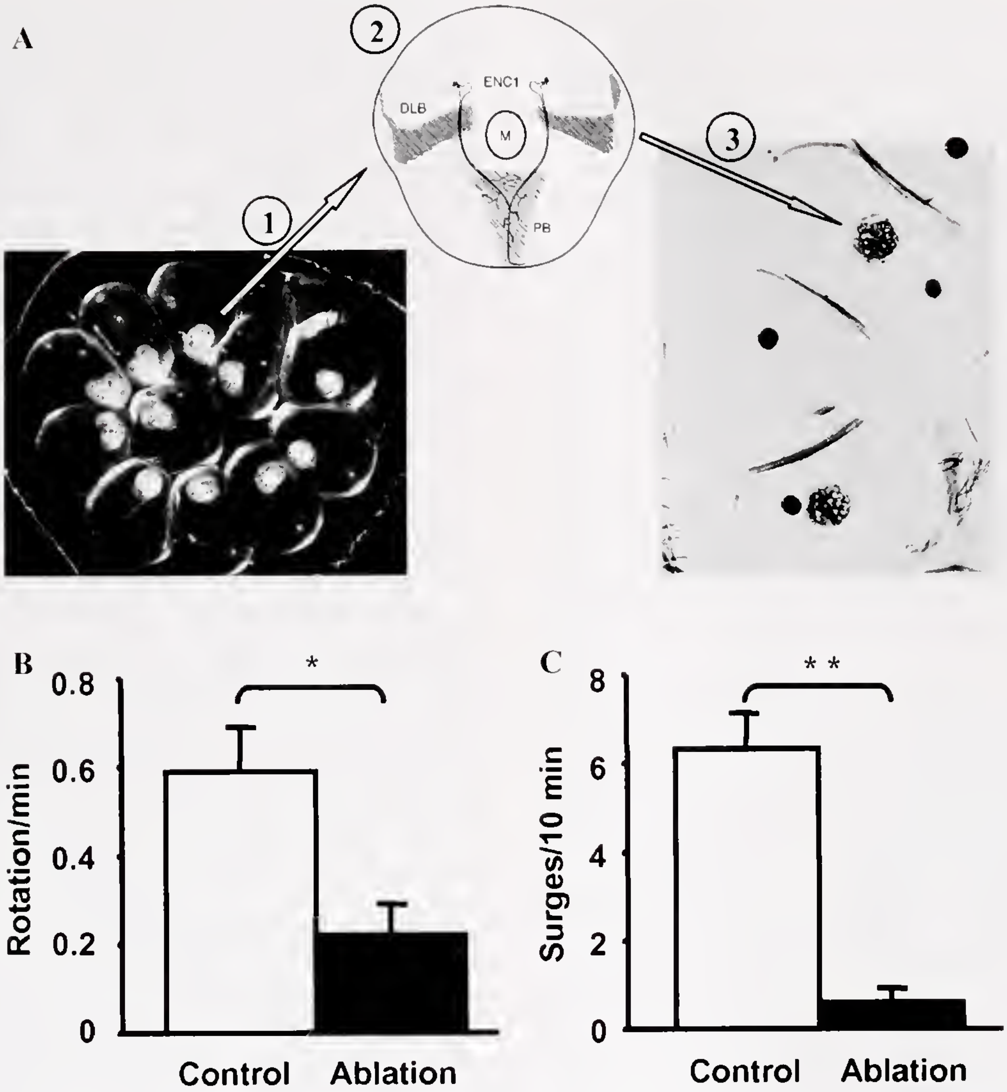

**Figure 7.** An application of embryo transplantation in studying embryonic cell function. (A) Diagram showing the experimental design. Stage E25 embryos were isolated from egg capsules① and a pair of embryonic neurons (ENC1s) or control cells were ablated with laser beams under a compound microscope②. The laser-operated embryos were transplanted into host egg capsules that contain much younger embryos③. The embryonic rotational behavior was subsequently examined after overnight recovery. DLB: dorsolateral ciliary band; M: mouth; PB: pedal ciliary band. (B) The average rate of rotation was reduced in embryos with both ENC1s ablated (*: *t* test, $P < 0.05$, $n = 9$ and 7 for control and ENC1 ablated embryos, respectively). (C) The occurrence of rotational surges was almost abolished in embryos with both ENC1s ablated (**: *t* test, $P < 0.01$, $n = 11$ and 7 for control and ENC1 ablated embryos, respectively).

fail to develop normally if their egg capsules are punctured at 2–4 h intervals to relieve the intracapsular hydrostatic pressure (Morrill, 1982). Pechenik *et al.* (1984) reported increased survival when decapsulated prosobranch embryos were cultured in a pressurized syringe, yet they all failed to develop normally.

Various kinds of abnormal development were observed when embryos were cultured *ex ovo*. In our study, embryos incubated in culture media always accumulated a large number of particles in the canaliculus of the protonephridia, suggesting either a malfunction of these embryonic kidneys or a precocious development of nitrogen catabolism (Morrill, 1982). In addition, all embryos in culture failed to grow a shell and a mantle, indicating incomplete development of the shell gland or lack of $CaCO_3$ in the media. Taylor (1973) reported that a considerable amount of $Ca^{2+}$ in CF is bound to calcium buffer. Given the reasonably high $Ca^{2+}$ concentration in the culture medium, the bound $Ca^{2+}$ that normally exists in the CF may be important for shell formation and development in general. Finally, *ex ovo* cultured embryos were sometimes hydropic after 72 h, suggesting that the osmoregulatory and extracellular fluid control machineries are impaired in these embryos, or that the osmolarity of the media is outside the range that embryos can handle.

Although *Helisoma* and other encapsulated pulmonates undergo direct development, they may still rely on chemical cues similar to those used by indirect developers to trigger settlement and metamorphosis (Morse, 1990). CF may contain cues that allow development to proceed from E30–E50, the stages resembling the transition from veliger to juvenile in metamorphosing gastropods (Raven, 1958; Morrill, 1982). That embryos develop normally when cultured after this transition lends support to this hypothesis (Pechenik *et al.*, 1984). Our preliminary trials also indicate that isolated stage E45 or later embryos grow and develop normally in artificial pond water (APW). Considering that epidermal growth factor (EGF) has recently been identified as a major component in the albumen gland and CF in *Lymnaea* and has been implicated in development of the nervous system (Hermann *et al.*, 2000), it may serve as a metamorphic factor in CF. *Lymnaea* EGF shares 35% of the amino sequence with the well-conserved mammalian EGFs, but lacks a transmembrane domain (Hermann *et al.*, 2000). However, neither human nor *Lymnaea* EGF promoted growth and development of *Helisoma* embryos. It is likely that EGF alone is not sufficient to compensate for other crucial factors that are missing in the culture media, or that the EGFs used in this study are highly species-specific.

If we ignore the physical properties of the intracapsular environment for the moment, CF intuitively seems to be the best medium for cultivation of decapsulated embryos. However, harvest of large quantities of concentrated CF is technically difficult because each capsule contains only 0.47 $\mu$l of the fluid. Moreover, when extracted from egg capsules, the highly viscous CF often clogged the micropipette or solidified in air. We have also tried to culture decapsulated embryos in the liquid fraction of egg mass homogenates, with no apparent improvement in embryonic development. The degradation of certain essential components by enzymes released from homogenized embryonic cells or the inability to mimic the physical environment of the intact egg capsule likely contributed to the poor development. Since the CF is secreted by albumen gland *in vivo*, a recent study showing that cAMP stimulates albumen gland secretion (Morishita *et al.*, 1998) provides a convenient way to produce CF *in vitro*. In future studies, albumen-gland-conditioned medium in combination with physical manipulations such as positive hydrostatic pressures should be attempted.

Transplantation of previously decapsulated gastrulated embryos yields a survival and growth rate similar to that of control embryos, suggesting that experimental manipulations and decapsulation of gastrulated embryos do not permanently hinder embryonic development. We observed that the ruptured openings on the capsular membranes of most egg capsules were self-sealed by 12 h after transplantation. Rich disulfide bonds previously reported in the egg covering of *Littorina saxatilis* (Losse and Greven, 1993) may have played a role in the self-sealing process. Alternatively, the phenomenon might result from the solidification of CF along the suture. In addition, certain physical or chemical properties of the gelatinous matrix surrounding the exterior of the egg capsule membranes may facilitate the sealing process. The layer of polyanionic acid mucopolysaccharide on the surface of capsular membrane (Plesch *et al.*, 1971) might be repelled by APW and therefore keep the ruptured membrane at a closely apposing state. The self-sealing of the ruptured capsular membrane is important in maintaining the physical, chemical, and electrical properties of the intracapsular environment that are essential for normal growth and development of embryos.

Roughly two-thirds of the embryos transplanted at the 2- or 4-cell stages died during gastrulation. Since the heat-treated host capsules resealed equally as well as normal capsules after transplantation, the high mortality of transplanted early stage embryos cannot be attributed to a loss of hydrostatic pressure within the host egg capsules. Instead, this high mortality indicates either that embryos are especially vulnerable to experimental manipulation at early cleavage stages, or that gastrulation is a crucial process during embryonic development. Early in development, each embryo is surrounded by a vitelline membrane that is cast off during gastrulation (Morrill, 1982). The vitelline membrane is very sticky, so that it tends to attach to petri dishes and glass pipettes during isolation and transplantation of embryos. Although we used Sigmacote-coated petri dishes and glass pipettes to prevent adhesion, it is still possible that the vitelline membranes of many embryos were ruptured during experimental manipulation. In *Lymnaea,* fertilized eggs whose vitelline membrane have been chemically removed can develop into embryos (Morrill, 1982); however, the long-term viability of these embryos is unknown. If the integrity of the vitelline membrane is crucial for survival of *Helisoma* embryos, its disruption may explain the high mortality of transplanted cleavage-stage embryos. Alternatively, it is possible that certain key "gastrulation factors" in the host CF are denatured or inactivated during the heat-shock treatment used to kill the host embryos before transplantation. Our preliminary experiments indicated that more cleavage-stage embryos survived gastrulation (80%, $n = 10$) when they were transplanted into host egg capsules that had not been heat shocked. It remains to be determined, however, whether egg capsules contain heat-labile gastrulation factors.

The transplantation technique developed in this study provides a unique opportunity to assess the long-term effects of experimental manipulations on encapsulated embryos. For example, the loss of rotational surges after laser ablation of both ENC1s confirms that these cells function as cilioexcitatory motor neurons (Kuang and Goldberg, 2001). Through transplantation of ENC1-ablated embryos, we have recently demonstrated that ENC1s mediate oxygen sensing and an adaptive response to hypoxia (Kuang *et al.*, 2002). It is now possible to examine the long-term effect of ENC1 ablation on the survival of embryos, as well as on respiratory function after hatching. The embryonic transplantation technique will also be useful in examining cell interactions during neuronal differentiation, neurite outgrowth, and synaptogenesis *in vivo*. Given the organizational simplicity of the ENC1-cilia circuit in *Helisoma* embryos, it is feasible to look into the interaction between ENC1 and its target ciliary cells by ablating either of them and examining the developmental consequences. Finally, studies involving cell lineage tracing or genetic manipulations are now possible, since molecular markers or genetic materials can be injected into early embryos and these embryos can be transplanted into host egg capsules for further development. With the recent molecular cloning of serotonin receptors in *Helisoma* (Mapara *et al.*, 2001), it is possible to look at the developmental and physiological consequences of over- or under-expression of these receptors. These are a few examples of how the transplantation technique can facilitate the investigation of physiological and developmental events in embryos of *Helisoma* and other encapsulated species.

## Acknowledgments

This study was supported by the Natural Science and Engineering Research Council of Canada. We thank Dr. A. G. Bullock for providing the *Lymnaea* epidermal growth factor.

## Literature Cited

**Beadle, L. C. 1969.** Salt and water regulation in the embryos of freshwater pulmonate molluscs. I. The embryonic environment of *Biomphalaria sudanica* and *Lymnaea stagnalis*. *J. Exp. Biol.* **50:** 473–479.

**Diefenbach, T. J., N. K. Koehncke, and J. I. Goldberg. 1991.** Characterization and development of rotational behavior in *Helisoma* embryos: role of endogenous serotonin. *J. Neurobiol.* **22:** 922–934.

**Diefenbach, T. J., R. Koss, and J. I. Goldberg. 1998.** Early development of an identified serotonergic neuron in *Helisomo trivolvis* embryos: serotonin expression, de-expression, and uptake. *J. Neurobiol.* **34:** 361–376.

**Goldberg, J. I. 1995.** Neuronal development in embryos of the mollusk, *Helisoma trivolvis:* multiple roles of serotonin. *Adv. Neural Sci.* **2:** 67–87.

**Goldberg, J. I., and S. B. Kater. 1989.** Expression and function of the neurotransmitter serotonin during development of the *Helisoma* nervous system. *Dev. Biol.* **131:** 483–495.

**Goldberg, J. I., D. P. McCobb, P. B. Guthrie, R. A. Lawton, R. E. Lee, and S. B. Kater. 1988.** Characterization of cultured embryonic neurons from the snail *Helisoma*. Pp. 85–108 in *Cell Culture Approaches to Invertebrate Neuroscience*, D. Beadle, G. Less, and S. B. Kater, eds. Academic Press, London.

**Goudsmit, E. M. 1976.** Galactogen catabolism by embryos of the freshwater snails, *Bulinmaea megasoma* and *Lymnaea stagnalis*. *Comp. Biochem. Physiol.* **53:** 439–442.

**Heras, H., C. F. Garin, and R. J. Pollero. 1998.** Biochemical composition and energy sources during embryo development and in early juveniles of the snail *Pomacea canaliculata* (Mollusca: Gastropoda). *J. Exp. Zool.* **280:** 375–383.

**Hermann, P. M., R. E. van Kesteren, W. C. Wildering, S. D. Painter, J. M. Reno, J. S. Smith, S. B. Kumar, W. P. Geraerts, L. H. Ericsson, A. B. Smit, A. G. Bulloch, and G. T. Nagle. 2000.** Neurotrophic actions of a novel molluscan epidermal growth factor. *J. Neurosci.* **20:** 6355–6364.

**Horstmann, H. J. 1956.** Der Galaktogengehalt der Eier von *Lymnaea stagnalis* L. während der Embryonalentwicklung. *Biochem. Z.* **328:** 342–347.

**Kamiya, H., K. Muramoto, and K. Ogata. 1984.** Antibacterial activity in the egg mass of a sea hare. *Experientia* **40:** 947–949.

**Koss, R., T. J. Diefenbach, S. Kuang, S. A. Doran, and J. I. Goldberg. 2002.** Coordinated development of identified serotonergic neurons and their target ciliary cells in *Helisoma trivolvis* embryos. *J. Comp. Neurol.* (In press).

**Kuang, S., and J. I. Goldberg. 2001.** Laser ablation reveals regulation of ciliary activity by serotonergic neurons in molluscan embryos. *J. Neurobiol.* **47:** 1–15.

**Kuang, S., S. A. Doran, R. J. A. Wilson, G. G. Goss, and J. I. Goldberg. 2002.** Serotonergic sensory-motor neurons mediate a behavioral response to hypoxia in pond snail embryos. *J. Neurobiol.* **52:** 73–83.

**LeBoeuf, R. A., G. A. Kerckaert, J. A. Poiley, and R. Raineri. 1989.** An interlaboratory comparison of enhanced morphological transformation of Syrian hamster embryo cells cultured under conditions of reduced bicarbonate concentration and pH. *Mutat. Res.* **222:** 205–218.

**Losse, G., and H. Greven. 1993.** Structure, composition and permeability of the egg covering in the viviparous prosobranch gastropod *Littorina saxatilis*. *Invertebr. Reprod. Dev.* **24:** 225–236.

**Mapara, S., J. I. Goldberg, and W. J. Gallin. 2001.** Cloning, phylogenetic analysis and localization of two serotonin receptors from the pond snail *Helisoma trivolvis*. *Soc. Neurosci. Abstr.* **786.4.**

**Meshcheryakov, V. N. 1990.** The common pond snail *Lymnaea stagnalis*. Pp. 69–132 in *Animal Species for Developmental Studies, Vol. 1. Invertebrates*, T. A. Dettlaff and S. G. Vassetzky, eds. Consultants Bureau, New York.

**Morishita, F., S. T. Mukai, and A. S. M. Saleuddin. 1998.** Release of proteins and polysaccharides from the albumen gland of the freshwater snail *Helisoma duryi:* effect of cAMP and brain extracts. *J. Comp. Physiol.* **182A:** 817–825.

**Morrill, J. B. 1982.** Development of the pulmonate gastropod, *Lymnaea*. Pp. 399–483 in *Developmental Biology of Freshwater Invertebrates*, W. Harrison and R. F. Cowdon, eds. Alan R. Liss, New York.

**Morrill, J. B., E. Norris, and S. D. Smith. 1964.** Electro- and immunoelectrophoretic patterns of the egg albumen of the pond snail *Limnaea palustris*. *Acta Embryol. Morphol. Exp.* **7:** 155–166.

**Morse, D. E. 1990.** Recent progress in larval settlement and metamorphosis: closing the gaps between molecular biology and ecology. *Bull. Mar. Sci.* **46:** 465–483.

**Nagle, G. T., M. de Jong-Brink, S. D. Painter, and K. W. Li. 2001.** Structure, localization and potential role of a novel molluscan trypsin inhibitor in *Lymnaea*. *Eur. J. Biochem.* **268:** 1213–1221

**Pechenik, J. A., S. C. Chang, and A. Lord. 1984.** Encapsulated development of the marine prosobranch gastropod *Nucella lapillus*. *Mar. Biol.* **78:** 223–229.

**Plesch, B., M. de Jong-Brink, and H. H. Boer. 1971.** Histological and histochemical observations on the reproductive tract of the hermaphrodite pond snail *Lymnaea stagnalis* (L.). *Neth. J. Zool.* **21:** 180–201.

**Raven, C. P. 1958.** *Morphogenesis: The Analysis of Molluscan Development.* Pergamon Press, New York. 311 pp.

**Stockmann-Bosbach, R., and J. Althoff. 1989.** A correlated morphological and biochemical study of capsular fluid of *Nucella lapillus* (Gastropoda: Prosobranchia: Muricidae). *Mar. Biol.* **102:** 283–289.

**Taylor, H. H. 1973.** The ionic properties of the capsular fluid bathing embryos of *Lymnaea stagnalis* and *Biomphalaria sudanica* (Mollusca: Pulmonata). *J. Exp. Biol.* **59:** 543–564.

**Voronezhskaya, E. E., L. Hiripi, K. Elekes, and R. P. Croll. 1999.** Development of catecholaminergic neurons in the pond snail, *Lymnaea stagnalis.* I. Embryonic development of dopamine-containing neurons and dopamine-dependent behaviors. *J. Comp. Neurol.* **404:** 285–296.

**Wijsman, T. C. M., and H. van Wijck-Batenburg. 1987.** Biochemical composition of the eggs of the freshwater snail *Lymnaea stagnalis* and oviposition-induced restoration of albumen gland secretion. *Int. J. Invertebr. Reprod. Dev.* **12:** 199–212.

Reference: *Biol. Bull.* **203:** 289–306. (December 2002)

# Structure, Formation, Mechanical Properties, and Disposal of the Embryo Attachment System of an Estuarine Crab, *Sesarma haematocheir*

M. SAIGUSA[1,*], M. TERAJIMA[1], AND M. YAMAMOTO[2]

[1]*Laboratory of Animal Behavior and Evolution, Graduate School of Natural Science and Technology, Okayama University, Tsushima 3-1-1, Okayama 700-8530, Japan; and* [2]*Ushimado Marine Laboratory, Okayama University, Oku-Ushimado, Okayama 701-43, Japan*

**Abstract.** In most decapod crustaceans, fertilized eggs extruded from the gonopore attach to ovigerous hairs within the incubation chamber of the female. The attachment is effected by an "embryo attachment system." The three continuous components of this system are the egg envelope, the funiculus, and the investment coat, which wraps around an ovigerous hair. Transmission electron microscopy (TEM) revealed that the embryo of *Sesarma haematocheir* is enfolded by three distinct envelopes (E1, E2, and E3), whereas the embryo attachment system is composed of only the outermost, single envelope (E1) with two sublayers (E1a and E1b). This envelope (E1) originates from the outer layer of the vitelline membrane (envelope of the ovum) with two sublayers (E1a′ and E1b′). The sequence and timing of events in the formation of the embryo attachment system was determined on the basis of observations of female behavior, ultrastructure, and mechanical properties of the membranes. The egg envelope (E1a′ + E1b′) is not adhesive immediately after extrusion from the gonopore; but 5 min after egg-laying, it becomes adhesive—a change associated with "fusion" of the two sublayers (E1)—and attaches the eggs to the ovigerous hairs from 5 to 30 min after egg-laying. The layer E1a′ always binds to an ovigerous hair at specific, electron-dense attachment sites that are distributed longitudinally on the surface of each hair. Plasticity of the egg envelope changes, and the female kneads her eggs by the movement of ovigerous setae; this movement forms the investment coat on the ovigerous hair (10–40 min after egg-laying). Thirty minutes after egg-laying, the egg envelope again divides into two sublayers (E1a and E1b), and the adhesiveness rapidly decreases. The plasticity of the envelope remains, and the funiculus is formed, accompanied by kneading of the eggs (40–90 min after egg-laying). The embryos hatch one month after incubation, and the attachment systems all slip off their ovigerous hairs by the actions of the ovigerous-hair slipping substance (OHSS). This substance appears to act specifically at the attachment sites on the hair, lysing the bond with layer E1a, and thereby disposing of the embryonic attachment system and preparing the hairs for the next clutch of embryos.

## Introduction

The oocytes of some decapod crustaceans are fertilized when they pass through the seminal receptacles where sperms are stored (Hartnoll, 1968). Fertilization is followed by egg-laying; that is, the eggs are extruded through two gonopores on the ventral side of the thorax of the female. The number of eggs extruded at once varies with species and the duration of incubation; for example, an estuarine semi-terrestrial crab, *Sesarma haematocheir*, laid 10,000–50,000 eggs in one batch. After laying, the eggs attach to ovigerous hairs borne on the maternal ovigerous seta; the attachment is through a stalk called the funiculus (Herrick, 1895; Yonge, 1937, 1946, 1955; Cheung, 1966; Fisher and Clark, 1983; Goudeau and Lachaise, 1983). The mechanism by which the funiculus forms and attaches to the ovigerous hairs, as well as the process by which the embryonic envelope forms, have been subjects of controversy for many years.

Yonge (1937) reported that many secretory glands occur on the pleopods of the female of the lobster *Homarus*

Received 5 June 1998; accepted 12 September 2002.

* To whom correspondence should be sent.

*vulgaris*. These glands are identical in structure to the tegumental glands that occur everywhere beneath the epithelium, and Yonge speculated that the fertilized eggs are attached by a "cement" secreted by these glands at the time of egg-laying. Observations by Andrews (1906), Stephens (1952), and Aiken and Waddy (1982) supported Yonge's hypothesis. Moreover, Fisher and Clark (1983) reported that the fertilized eggs of an estuarine shrimp, *Palaemon macrodactylus*, are attached to each other, or to the ovigerous hairs of the maternal pleopods, by materials that are produced by the pleopods and form the outer layer of the embryonic envelope.

In contrast, a study of embryonic envelope formation and egg attachment in the shore crab, *Carcinus maenas*, indicated that the funiculus forms from the outermost layer of the "trichromatic membranes," all of which are produced by mature eggs after fertilization (Cheung, 1966). Cheung found no "cement glands" on the pleopod of this crab. Cheung's hypothesis was also supported by the ultrastructural studies of Goudeau and coworkers, who showed that the funiculus of *Carcinus maenas* is an extension of the two vitelline layers of the mature egg. These two layers are altered structurally and stretched by the vigorous beating of the maternal pleopods; by this action the material in the layers wraps around the ovigerous hairs without involving any adhesive substance (Goudeau and Lachaise, 1980, 1983; Goudeau *et al.*, 1987; reviewed by Hinsch, 1990).

The embryo attachment system of many intertidal and estuarine crabs includes, not only the embryonic envelope and the funiculus, but also a clear "coat" that invests the whole hair (Saigusa, 1994). If the newly extruded eggs are attached to the ovigerous hairs by a "cement" or similar substance that is secreted from the female, we should observe two kinds of material on the ovigerous hair: that is, a layer secreted by the maternal pleopods, and another layer originating from the egg envelope. On the other hand, if the egg envelope has only been stretched and wrapped around the ovigerous hairs, the coat should consist only of layers originating from the egg envelope. To solve this problem, the modification of the egg envelope of *Sesarma haematocheir*—an estuarine terrestrial crab—was investigated morphologically, and physiological changes in the properties of the envelope are described in terms of adhesion and plasticity. On the basis of these results, we present a schedule for an egg attachment for this crab.

Another purpose of this study was to investigate the disassociation of the embryo attachment system from the ovigerous hair. When embryonic development is complete, hatching occurs in synchrony with the times of high tide (Saigusa, 1992, 1993; Saigusa and Terajima, 2000). An active factor that we call OHSS (ovigerous-hair stripping substance) is released by the embryos at the time of hatching, causing the investment coat and the rest of the embryo attachment system to slip off the ovigerous hairs several hours after larval release. This process prepares the hairs for the attachment of the next clutch of the embryos (for further details, see Saigusa, 1994, 1995, 1996). But the mechanism by which the investment coat slips off the hairs is not yet known. OHSS might cause morphological changes to the coat. Thus, we have examined ultrastructural changes to investment coats that were treated with OHSS solution and were subsequently stripped off their hairs.

## Materials and Methods

### *Animals and strategy for experiment*

The animal used for this study was *Sesarma haematocheir* (red-handed crab; akate-gani) inhabiting thickets along estuaries in western Japan. The females of this species incubate two to three successive clutches of developing embryos between June and September. After one month of incubation, the embryos hatch, and the zoea larvae are released in the water (Saigusa, 1982). The number of females releasing larvae increases at about the time of full and new moons and decreases at the half moons—a semilunar rhythm.

The most important procedure for this study was to collect females that had just begun to lay their eggs. Egg-laying occurs primarily in the morning, from 0600 to 1200, but it begins with no visual sign, so in the field we cannot specify precisely any particular female that has just started laying eggs. Therefore, these investigations were carried out in the laboratory. We maintained a few hundred females in the laboratory, which enhanced the chance that we could observe females that were starting egg-laying. We also took advantage of the fact that, in *S. haematocheir*, most females incubate their next clutch within a few days after a larval release. Therefore if females that had released zoea larvae during any night were placed in different containers, we could expect that many of them would start egg-laying again a few days later. Thus, this species was well suited for the present study.

### *Maintenance of crabs and observations of egg-laying*

Females used in this study were collected at Kasaoka, Okayama prefecture, Japan (Saigusa, 1982). Ovigerous females on the way to water would cross a road along the seacoast just after sunset, so each evening at this spot, 50–200 females were collected and transported to the laboratory. After the females released their larvae, they were washed repeatedly with a large quantity of tap water to remove adherent hatch water and any zoeas still attached. The females were then kept in plastic containers (70 cm long, 50 cm wide, and 30 cm in depth), each containing a small quantity of seawater diluted less than 5‰. Females that had released larvae each night were moved to different containers. The containers were exposed to the natural day–

night cycle in the laboratory (sunset at 1830–1920 and sunrise at 0450–0530 in July–August). Within a few days, most females began to incubate their new clutch of fertilized eggs. A board in the container, providing shelter for the crabs (see Saigusa, 1980), was gently removed at times, and any female that had just started egg-laying was very carefully isolated to a transparent vessel so that egg-laying and subsequent behaviors could be observed, and the eggs were retrieved.

### *Transmission electron microscopy*

Fertilized eggs for microscopy were obtained from the abdomen after egg-laying (Fig. 1A and 1B), whereas mature, but unfertilized (unextruded) eggs were obtained directly from the ovary. These eggs and embryos were fixed for 1.5 h at room temperature in 2.5% glutaraldehyde dissolved in a cacodylate buffer (400 m*M* NaCl, 100 m*M* Na-cacodylate, pH 7.4), and then washed. These egg samples were further post-fixed for 1 h, at 4 °C, with 1% $OsO_4$ dissolved in the cacodylate buffer. After post-fixation, the specimens were dehydrated through a graded series of ethanol solutions and embedded in a low-viscosity epoxy resin (TAAB). Ultrathin sections were cut with a Porter-Blum MT2-B ultramicrotome and collected on copper grids. These sections were further stained with 1% uranyl acetate dissolved in 50% ethanol, and with 0.1% lead citrate, and were then examined with a Hitachi H500H electron microscope operated at 75 kV.

### *Assaying the adherence and plasticity of the egg envelope*

With a fine forceps, 5–20 fertilized eggs were removed every 10 min from a female just after egg-laying (Fig. 1B). These eggs were placed in a polystyrene petri dish (Falcon 1007; Becton Dickinson Labware, NJ) with seawater diluted to one-third (10‰). Characteristically, when an egg adhered to the bottom of the petri dish it would not roll, even if the dish were slowly shaken by hand (Fig. 1C). The strength of envelope adherence was estimated as the percentage of eggs that adhered to the bottom of a dish. If these adherent eggs were gently rolled with a forceps, the envelope elongated (Fig. 1D). While one end of the elongated envelope (*a*) remained attached to the bottom of the dish, the opposite end (*a'*) still enclosed the egg. If the egg was rolled sufficiently, either the envelope or the egg would break. At this point, the length of the envelope (*a–a'*) was taken as a rough estimate of its plasticity. A new petri dish was used for each test of eggs removed from a female.

### *Action of OHSS on the embryo attachment system: fine structure*

The embryo attachment system slips off of the ovigerous hair after hatching. This is due to an active factor released from the embryo at the time of hatching. This factor, which we call OHSS (ovigerous-hair stripping substance), is contained in the hatch water of crabs (Saigusa, 1994, 1995, 1996). In this study, ovigerous seta with premature embryos attached were separated from a few ovigerous females and cut into three pieces each. The tip of the seta was discarded, and each cluster of embryos was placed in a well of a plastic culture dish and incubated with 0.5 ml of concentrated hatch water (see Saigusa and Iwasaki, 1999). Control embryo clusters were immersed in 0.5 ml of 20 m*M* Tris-HCl buffer (pH 8.5). Each segment of embryo cluster was removed from the hatch water, or the control buffer, after 2 min, 4 min, 6 min, 8 min, 10 min, 20 min, 60 min, and 120 min, and each was fixed for transmission electron microscopy. The fixation and ultrathin sectioning were carried out as described above.

## Results

### *Ultrastructure of the embryo attachment system in the incubating female*

*Egg envelope.* The female of *Sesarma haematocheir* has four pairs of abdominal appendages; each bears one plumose and one non-plumose ovigerous seta (see Saigusa, 1994). Embryos attach to the ovigerous hairs by a stalk, the funiculus, and rarely to each other (Fig. 2A). The funiculus never is attached directly to an ovigerous hair, but rather to a coat that invests the hair. Figure 2B shows the fine structure of the egg envelope. The envelope consists of three layers: the outermost (E1), the thick middle (E2), and the innermost thin (E3) layers. The outermost layer further consists of two distinguishable sublayers designated E1a and E1b.

*Funiculus.* Figure 3A shows the base of the funiculus at its junction with the embryo. The funiculus consists of a single layer, 0.3–0.4 $\mu$m thick, which is continuous with the outermost layer (E1) investing the embryo. Moreover, the two sublayers (E1a and E1b) are also present in the funiculus (Fig. 3B). In contrast, no component of E2 or E3 was ever found in the funiculus. The proximal end of the funiculus is folded onto and wrapped around the ovigerous hair to produce the stratified investment coat (Fig. 3C). The coat usually invests only one hair, but a few hairs are sometimes included in the wrapping. The thickness of the coat differs from one hair to the next; for example, in Figure 3C, the coat is only 2–3 $\mu$m at its thinnest, but 25 $\mu$m at its thickest. In every part, the investment coat, like the funiculus, includes only the E1 layer and its components (E1a and E1b). Thus, the investment coat wrapping the ovigerous hair consists morphologically of the same materials as are present in the funiculus and the outermost layer of the egg envelope. The investment coat is tightly connected to the ovigerous

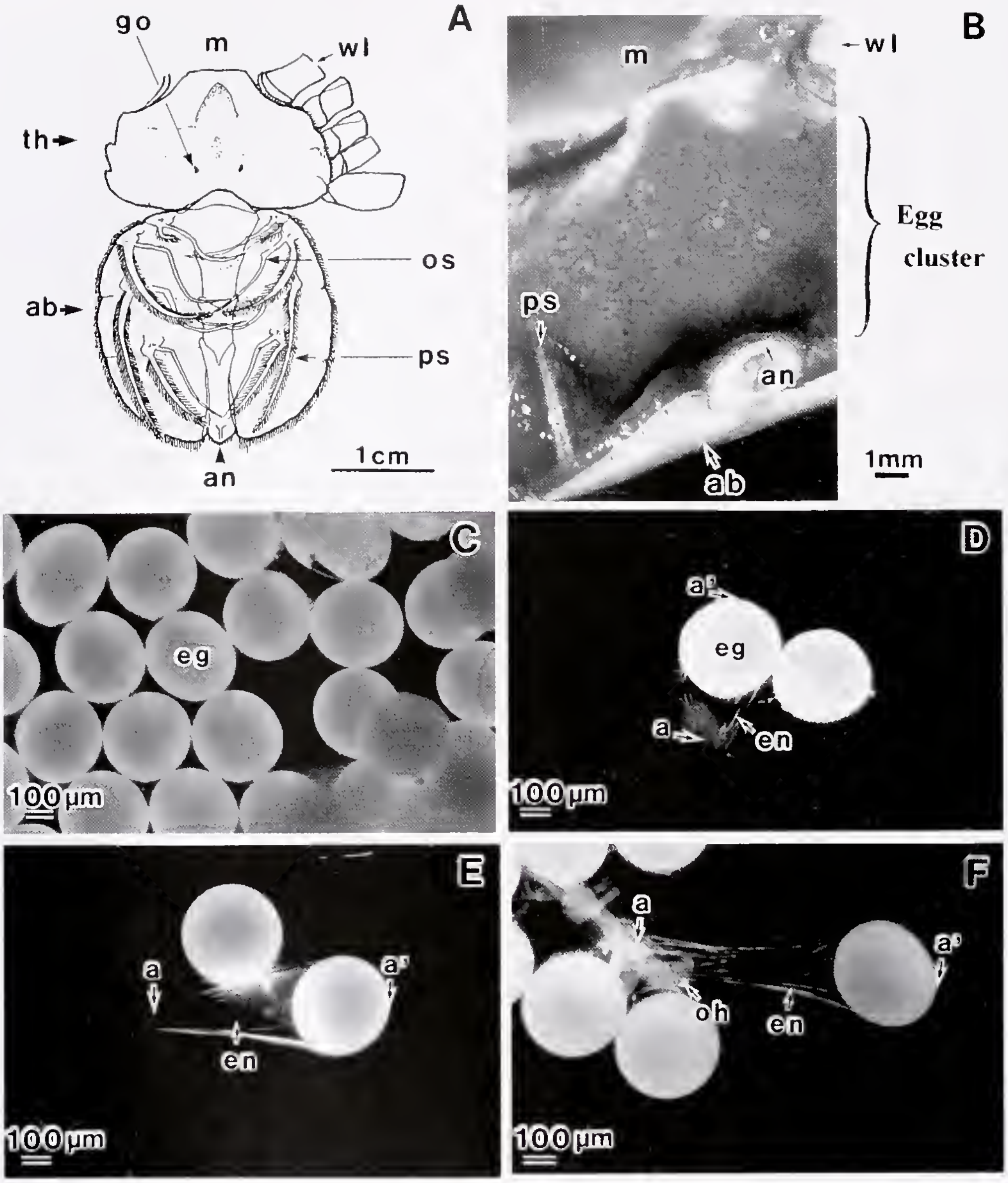

**Figure 1.** Egg-laying in *Sesarma haematocheir* and a method of measuring the adhesiveness and plasticity of the egg envelope. (A) Morphology of the thorax (th) and abdomen (ab) of a female. Eggs just extruded from the gonopore (go) attach to many ovigerous hairs (see Fig. 6A) arranged on the ovigerous seta (os). No eggs adhere to the plumose setae (ps). m: mouth parts. wl: walking leg. an: anus. (B) The incubation chamber, and an egg cluster newly extruded from the gonopore. The extruded eggs lie between thorax and abdomen (*i.e.*, incubation chamber), protected by the folded abdomen, and are incubated for nearly a month. The whole egg cluster is immersed in a transparent incubation fluid. Abbreviations are the same as in (A). (C) Eggs (eg) within 5 min after egg-laying. The egg envelope is not yet adhesive. (D) The eggs 20–30 min after egg-laying. The egg envelope (en) is adhering to the bottom of a petri dish. At this time, if an egg is gently rolled with a fine forceps, it moves a little, then it is slipped (or crushed) out of the envelope. *a*: one end of the envelope, where it adheres to the bottom of the petri dish (attachment point). *a'*: the other end of the envelope where the egg was rolled or pushed with a forceps. The plasticity of the envelope was measured as the length of *a–a'* at this time. (E) The egg 40 min after egg-laying. The envelope (en) showed both adhesiveness and plasticity. (F) The eggs 90 min after egg-laying. Adhesiveness of the envelope (en) was lost, so the envelope did not adhere to the petri dish. But the envelope attained maximum plasticity.

hairs (Fig. 3C); when clusters of embryos were pulled away from the ovigerous seta with fine forceps, most of the hairs broke away from the seta (not shown; see Saigusa, 1995).

*Investment coat.* When cross and oblique sections of the attachment were examined (Fig. 4A), it was always sublayer E1a that was seen to adhere directly to the

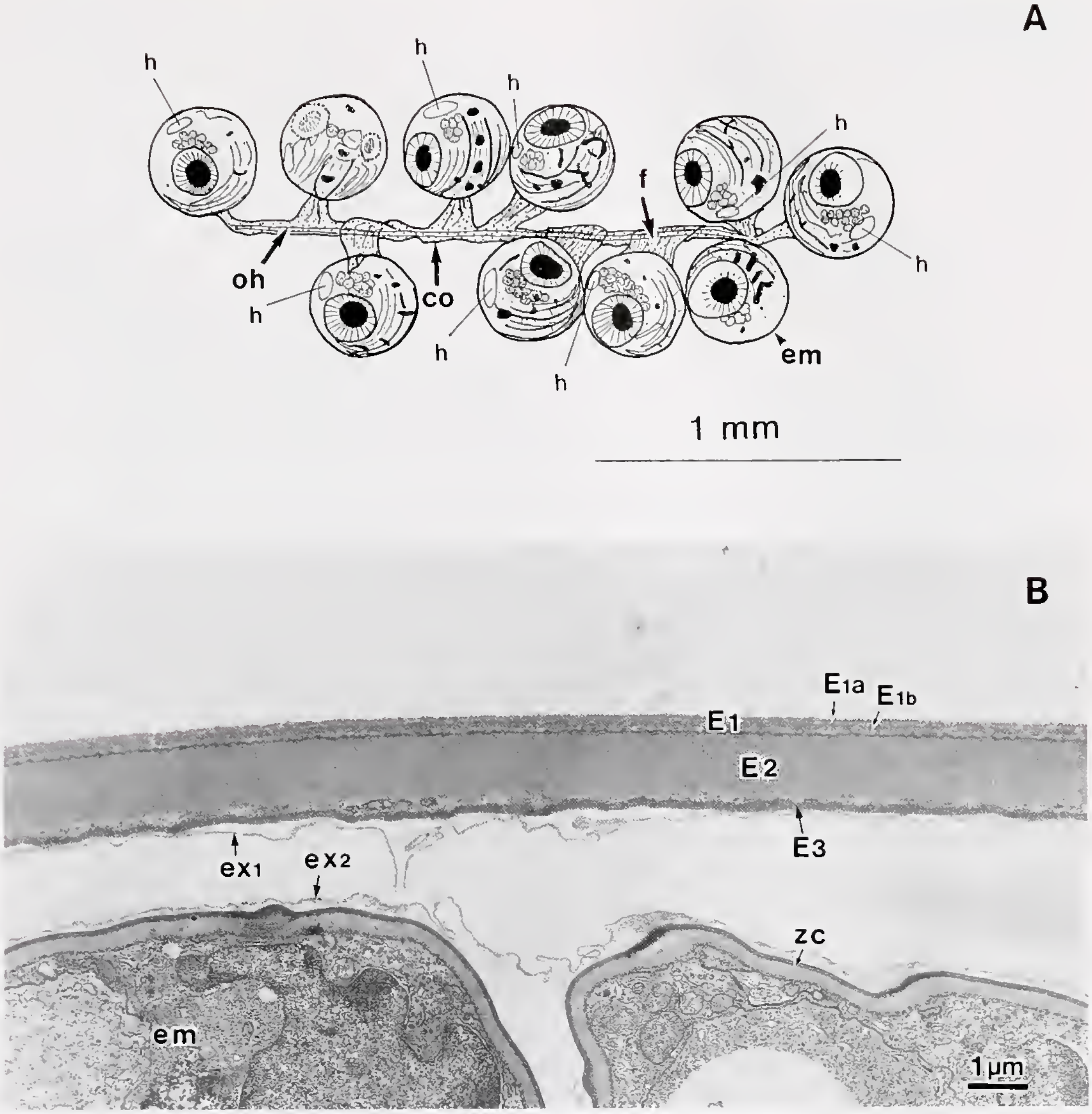

**Figure 2.** Embryo attachment system of *Sesarma haematocheir:* mature embryos that are within hours of hatching. (A) Connection of the embryo (em) to an ovigerous hair (oh). co: investment coat wrapped around the hair. f: funiculus. h: heart of each embryo. Note that the funiculus does not attach at a particular position with respect to the embryo. (B) Fine structure of the embryonic envelope. E1: the outermost layer, which consists of two further sublayers (E1a and E1b). E2: the middle layer. E3: the innermost layer. The embryo (em), close to hatching, is wrapped further in two very thin layers: *i.e.*, exuviae (ex1 and ex2) which are deposited by the embryo. zc: zoeal cuticle. Just after hatching, the zoeas cast off these exuviae and then begin to swim.

ovigerous hair (Fig. 4B, C). A cross section (Fig. 4B) showed the presence of a thin layer 40 nm thick ($\alpha 1$) on the surface of the ovigerous hair. This layer contacts ridges in E1a that are arranged parallel to the hair at intervals of 130–160 nm. Tubular structures, 50–70 nm in diameter, appear at random in the ovigerous hair (small arrows in Figs. 4B, 5A, B).

In oblique, nearly longitudinal section (Figs. 4C, 5A), the ridges on layer E1a in contact with the $\alpha 1$ layer appear as slender electron-dense structures arranged at the same interval as the ridges (130–160 nm) (compare Fig. 5A with Fig. 4B: much the same magnification). In the oblique section, furthermore, the $\alpha 1$ layer is seen to be underlain by a comparatively electron-dense layer ($\alpha 2$). Many tubular structures (25–70 nm in diameter) were observed in this layer and just below it. The remainder of the cuticular wall of the hair has the usual stratified structures. Ovigerous hairs taken from female crabs before egg-laying were also examined (Fig. 5B). Note that iterated electron-dense structures are present on the surface of these hairs, and at the same intervals, although the investment coat, and thus E1a, are absent.

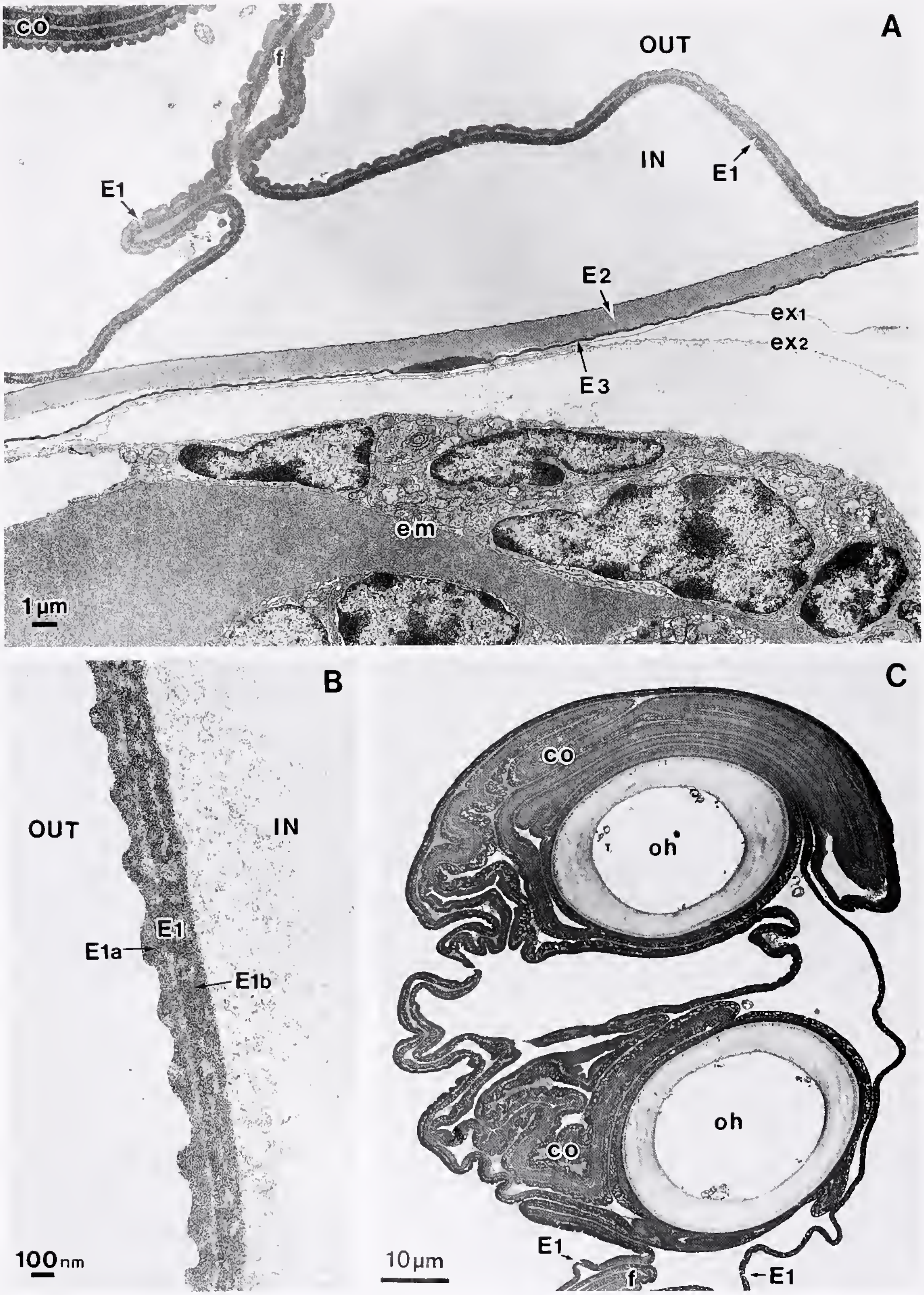
co
f
OUT
A
IN
E1
E1
E2
ex1
ex2
E3
em
1 µm
B
OUT
IN
E1
E1a
E1b
100nm
C
co
oh
oh
co
E1
E1
f
10µm

**Figure 3.** The components of the embryo attachment system: mature embryos that will hatch in a few days. (A) The funiculus (f) is composed of two opposed portions of egg envelope (E1). The funiculus extends toward the coat (co) wrapping one of the female's ovigerous hairs; the ovigerous hair is not shown. IN: inside the funiculus. OUT: outside the funiculus. E2 and E3: middle and innermost layers. em: embryo. ex1 and ex2: exuviae deposited by the embryo. (B) Components of the funiculus. E1a and E1b: two distinguishable sublayers of the outer layer E1. A substance of low electron density is seen inside the funiculus. (C) A continuous coat (co) investing two ovigerous hairs (oh). Symbols are the same as in (A).

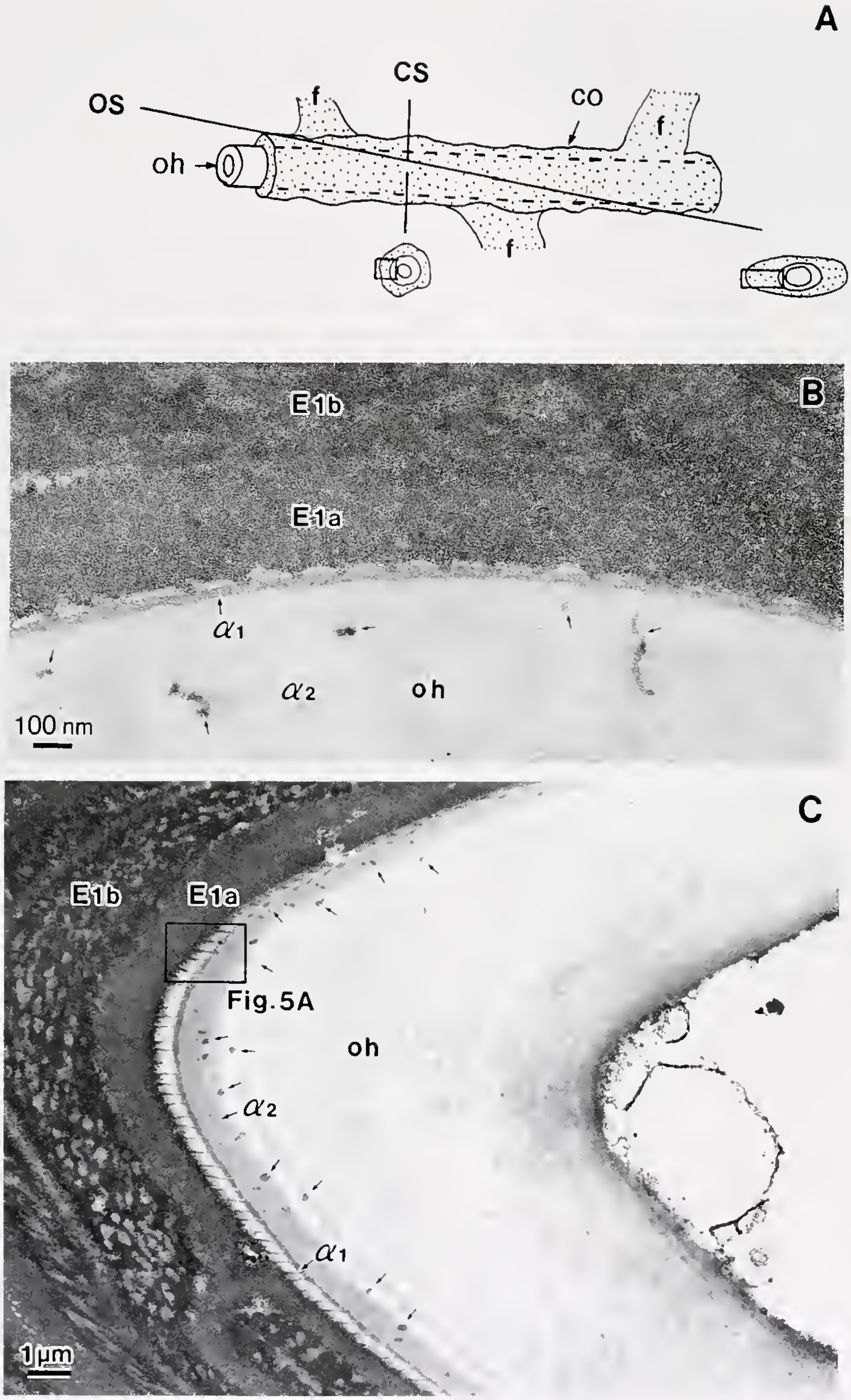

**Figure 4.** Attachment of the investment coat to the ovigerous hair; observed in mature embryos. (A) Sections of an ovigerous hair (oh) invested by the coat (co). CS: cross section. OS: oblique section, nearly longitudinal. f: funiculus. (B) In a cross section, ridge-like extensions of E1a are attached to a layer ($\alpha 1$) on the surface of the ovigerous hair. $\alpha 2$: a layered structure underlying $\alpha 1$. E1a and E1b are the two sublayers of E1. Small arrows indicate tubules in the $\alpha 2$ layer. oh: ovigerous hair. (C) In an oblique section (lower magnification), the ridges appear as slender, evenly spaced structures attached to sublayer E1a. Many tubular structures are seen in the $\alpha 2$ layer and just inside it (some of them are shown by small arrows). Compare with (B).

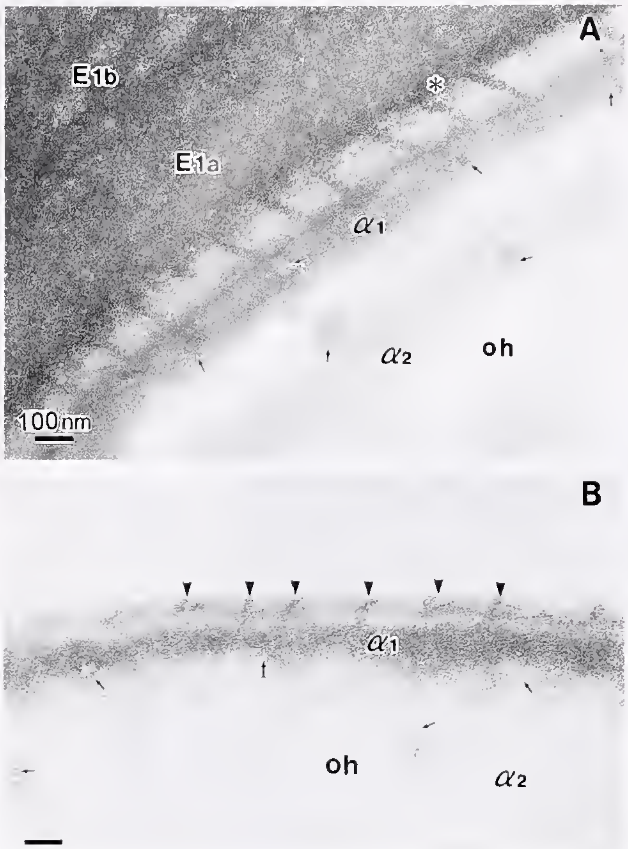

**Figure 5.** Structure of the attachment between the investment coat and an ovigerous hair. (A) An ovigerous hair (oh) wrapped in an investment coat (oblique section, magnified from Fig. 4C; the scale is the same as in Fig. 4B); observed in mature embryos. $\alpha1$: the thin, electron-dense layer to which the slender extensions from layer E1a are regularly arranged. Small arrows show tubules. $\alpha2$: a layered structure underlying $\alpha1$. The thin, electron-dense layer (*) is also observed on the surface of E1a. (B) An ovigerous hair (oh) from a female that is not incubating a clutch of embryos. Thus, this hair is not invested by a coat. Note the electron-dense structures (downward solid arrow heads: ▼) about the same interval as the extensions from E1a (compare with A). Small arrows: tubules seen in both $\alpha1$ and $\alpha2$.

### *Formation of the embryo attachment system after egg-laying*

*Schedule of events.* An examination of behavior in several females revealed the time course of egg-laying, egg attachment, and funiculus formation in *Sesarma*. No visible event signals the start of egg-laying, and it proceeds rapidly, so determining a precise schedule of this process was difficult. In addition, an exact point of transition between successive events could sometimes not be determined. Thus, the timing of each component behavior summarized in Table 1 involves some speculation.

The eggs are extruded from the gonopore and into the incubation chamber (Fig. 1B). Between 10 and 15 min seems to be required for all the eggs to be extruded. When the eggs are laid, the female leaves the water and stands motionless, with her walking legs stretched out and her abdomen half folded. At the same time, however, the pleopods—the ovigerous setae (Fig. 6A)—steadily knead the clutch. The eggs were never adhesive just after laying. Within 5 min, however, the volume of incubation fluid (a transparent liquid appearing in the incubation chamber) increases, and the egg cluster is immersed in this fluid (Fig. 1B). At this time, the egg envelope becomes strongly adherent to the ovigerous hairs (Fig. 6B). The eggs never attach to the plumose hairs (Fig. 6A).

Between 10 and 20 min after egg-laying, the female is still motionless with her abdomen half open, and the egg cluster is still being kneaded by the ovigerous seta. But the number of eggs adhering to the ovigerous hairs is markedly increased. While the eggs are attaching to the hairs, the egg envelope is expanding; its volume becomes 1.5–1.6 times larger than that of the egg itself (Fig. 6C), and it is still strongly adhesive (Fig. 6D). Although the investment coat is complete between 10 and 40 min after egg-laying, the funiculus is not yet formed at this time.

Forty minutes after egg-laying, adherence of the egg envelope seems, actually, to decrease; that is, the eggs still adhere to the bottom of the petri dish (see Fig. 9), but the attachment point (*a* in Fig. 1E) shifts slightly when the egg is gently pushed with a forceps. The incubation fluid immersing the egg cluster is also decreased 40 min after egg-laying. The funiculus begins to form at about this time (Fig. 6E), and is completed between 60 and 120 min after egg-laying. With the funiculus formed, the abdomen of the female begins to move up and down, but this movement stops 2 h after egg-laying. With this behavior, all the eggs would be well folded by the abdomen. This brief period of abdominal fanning is not likely to aerate the eggs; possibly, it serves to fold the clutch into the incubation chamber. At this time, the female becomes mobile again, and can easily escape in response to external stimuli.

Figure 6F shows eggs that were kept in 20 m*M* Tris-HCl buffer in a petri dish for one night after egg-laying. At first, the eggs adhered to the bottom of the dish, or to the other eggs. In the morning, the diameter of the envelope had expanded 3-fold. These eggs could be detached with forceps from the dish or from the other eggs without envelope deformation, but such eggs were never again attached to either a dish or to the other eggs. The plasticity of the envelope was also lost.

*Egg envelope: origin of the outermost layer (E1) and its morphological change after egg-laying.* The fine structure of a mature, unfertilized egg is shown in Figure 7A. The egg is enclosed by a follicle cell (about 1 $\mu$m thick), beneath which is an envelope (vitelline membrane) consisting of two sublayers (E1a′ and E1b′). The sublayer E1b′ is about 0.5 $\mu$m thick in the ovary (Fig. 7A); but within 5–10 min after egg-laying, E1b′ becomes 5-fold thicker (2.5 $\mu$m; Fig. 7B).

**Table 1**

*Time course of egg attachment and formation of the investment coat and funiculus*

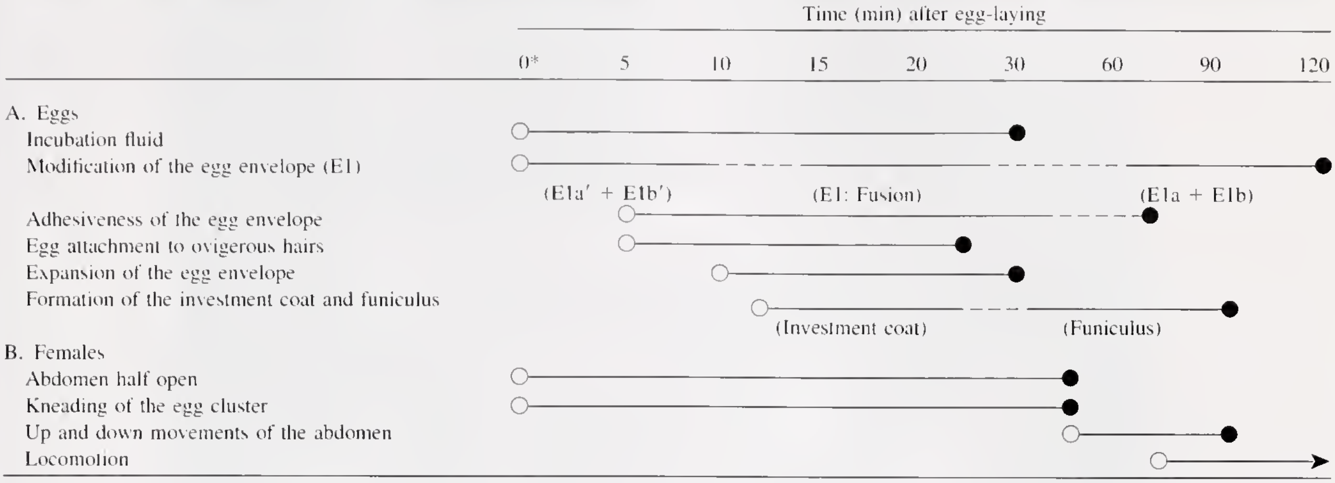

* Zero minutes indicates the estimated end of egg-laying.
Symbols: ○— start, —● end, —➤ continuing, ----- uncertain limits of sequential events.

The sublayer E1b′ is further modified, as its structure comes to resemble that of sublayer E1a′ (Fig. 7C). Soon the distinction between the two sublayers is completely lost, and they fuse to form a homologous envelope (1.2 μm thick); we designate this layer E1 (Fig. 7D). The intermediate stage in the formation of E1 (Fig. 7C) was rarely observed, indicating that the process of fusion progressed very rapidly, possibly within 5 min after the thickening of E1b′. The cause of the rapid modification of sublayer E1b′ is not known, but it could be related to the appearance of clusters of electron-dense granules that seem to be secreted from the egg into the spaces below E1b′ (arrows in Fig. 7B).

After the fast modification of E1b′, the homogenous structure of layer E1 is retained for 10–30 min after egg-laying. By 30–60 min after egg-laying, E1 again divides into two sublayers, E1a and E1b (Fig. 7E); but whether these new sublayers correspond to the original E1a′ and E1b′ (Fig. 7B) is not known. In any event, our morphological findings suggest that the outermost layer enveloping the egg (E1) is produced by the egg itself, rather than being formed by externally secreted materials. Also, formation of the middle layer (E2) begins at 10–15 min after egg-laying (Fig. 7D).

*Formation of subsequent layers of the egg envelope.* In addition to the outermost layer (E1), a thick middle layer (E2) and an innermost thin layer (E3) invest the embryo (Fig. 2B). These two layers are included in neither the funiculus nor the investment coat. The middle layer (E2) appeared at about the time that E1 was becoming homogeneous in structure—possibly 10–15 min after egg-laying (Fig. 7D). The middle layer forms very slowly, and is complete 12–24 h after egg-laying (not shown). This layer may be formed by the secretion from the embryo (see arrows in Fig. 7D, E). The third (E3) layer appears a few days later, possibly secreted by the egg like the middle layer (not shown).

*The egg envelope attaches to ovigerous hairs.* As mentioned earlier, the egg envelope expands just after attaching to the ovigerous hairs (Figs. 6C, 8A). The interaction between the envelope and the ovigerous hair was examined by transmission electron microscope. Attachment of the envelope onto the ovigerous hair occurred about 10 min after egg-laying, when two sublayers (E1a′ and E1b′) began to fuse (Fig. 8B). At higher magnification (Fig. 8D), the egg envelope can clearly be seen to be a homologous layer (E1) (see also Fig. 7D).

The egg envelope at this time (10–15 min after egg-laying: Fig. 8A–D) is strongly adhesive, so it adheres, not only to the hair, but also to other envelopes. For example, Figure 8B shows an envelope (E1) folded on the upper half of the hair. While this envelope is adhering to the ovigerous hair for 14–15 μm (from points a1 to a2), it is also adhering to itself for 20 μm (b1–b2). Note that the envelope in Figure 8B is not attached to the lower part of the hair; this may be due to a weak attachment that was separated during fixation or embedding. The large space between E1 and E2 suggests that the envelope (E1) had started to expand or elongate.

The connection between the newly attached homogenous layer (E1) and the ovigerous hair (Fig. 8C and 8D) is similar to that in a mature coat (Fig. 5A). In Figure 5A, however, the surface of E1a appears as an electron-dense

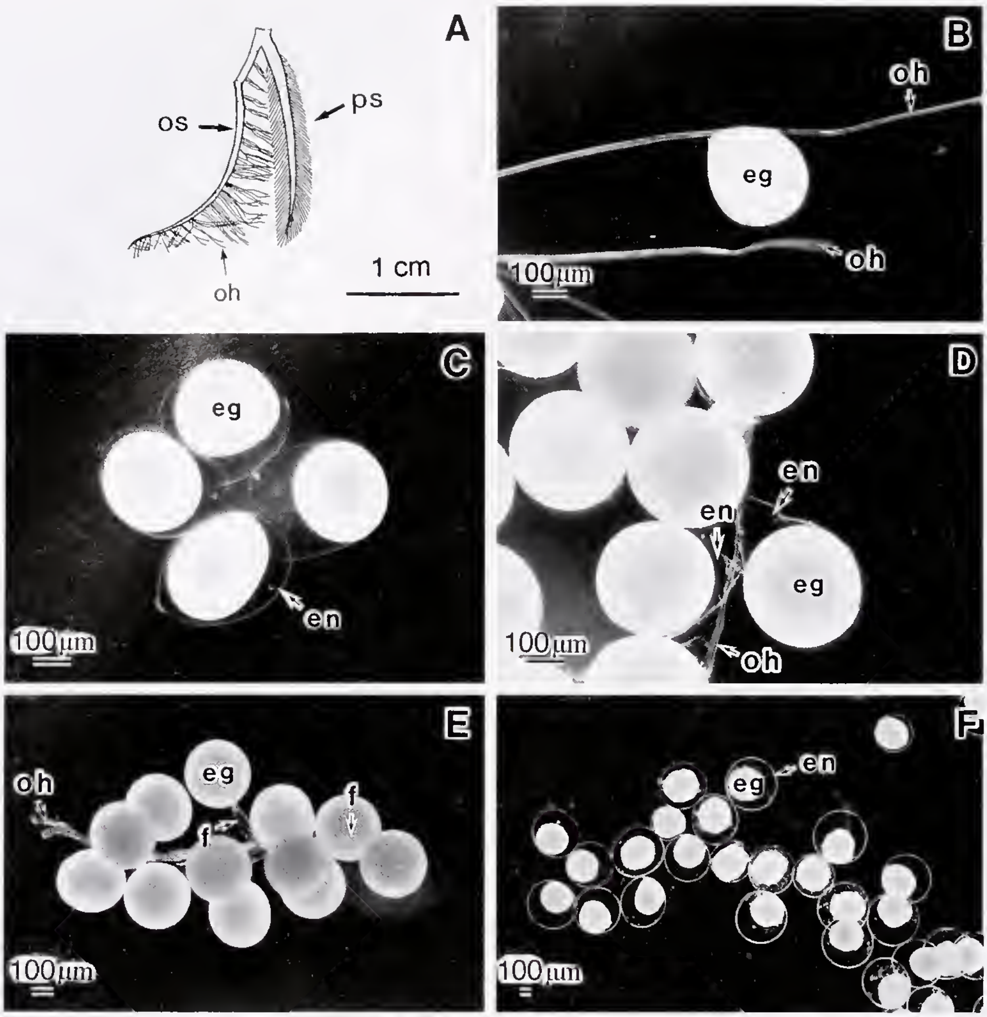

**Figure 6.** Egg attachment and formation of the funiculus after egg-laying: observed with a stereomicroscope. Observations of the eggs that were placed in a petri dish just after laying. (A) A pair of abdominal appendages of a female: ovigerous seta (os) and plumose seta (ps). Ovigerous hairs (oh) are arranged on the ovigerous seta. (B) An egg (eg) adhering to an ovigerous hair (oh): 5–10 min after egg-laying. (C) Expansion of the envelope (en): 10–15 min after egg-laying; the envelope shows strong adhesiveness. (D) Formation of the *investment coat* following attachment to the hair: 15–30 min after egg-laying. (E) Formation of *funiculus* (f): 60 min after egg-laying. Although the adhesiveness of the envelope is lost, the plasticity increases. (F) Eggs placed in a petri dish containing 20 m*M* Tris-HCl buffer overnight. Egg envelope swells in all embryos. Adhesiveness of the envelope has already been lost.

thin layer distinguishable from another sublayer (E1; 40–50 μm thick in oblique section). Such a layer-like structure was never observed in the newly attached envelope. Figure 8E shows the egg envelope about 80 min after egg-laying. The funiculus has already been formed. Moreover, the envelope and funiculus are again divided into two sublayers (E1a and E1b), and the inner layer (E2) has thickened.

*Temporal changes in egg envelope adhesiveness and plasticity.* Newly extruded eggs were removed from the female every 10 min after egg-laying. The eggs were placed in a polystyrene petri dish, and temporal changes in the adherence and plasticity of the envelope were examined with time. Adherence was estimated with 10–20 eggs, and plasticity was measured with 5–10 eggs (Fig. 9). The egg envelope was not adhesive immediately after egg-laying (not shown), but after 5 min, the envelope became strongly attached to the bottom of the dish, and it did elongate as soon as it was gently rolled with a fine forceps.

In Figure 9, adherence of the egg envelope was 100% between 10–50 min after egg-laying. But 40–60 min after egg-laying, the fixed attachment point (*a* in Fig. 1E) became mobile when the eggs were rolled with a forceps. Thus, envelope adhesiveness begins to decrease markedly about 40 min after egg-laying. In contrast, envelope plasticity

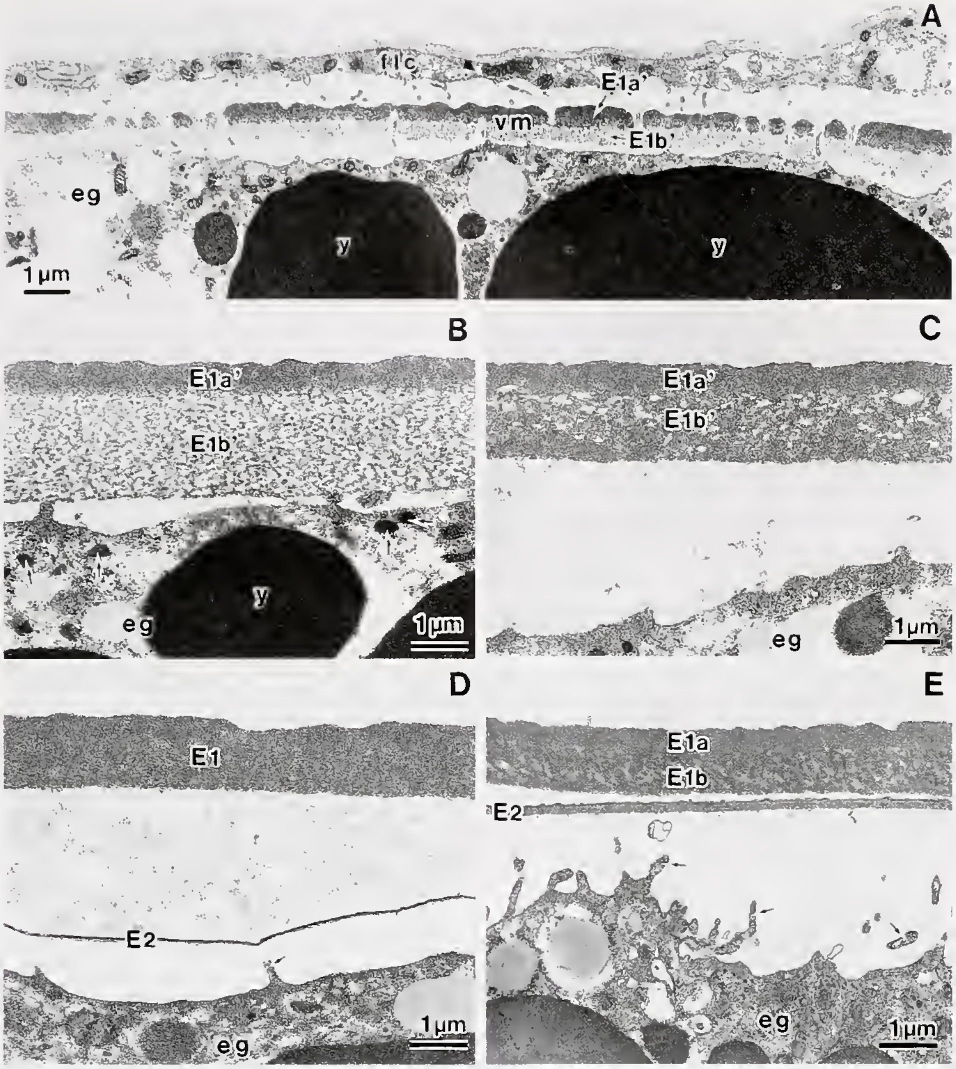

**Figure 7.** Origin of the egg envelope and morphological changes that occur after egg-laying. (A) Surface layers investing a fertilized, mature egg (eg) in the ovary. E1a′ and E1b′: two sublayers of the envelope, *i.e.*, vitelline membrane (vm). flc: follicle cell. y: yolk. (B) The egg envelope 5–10 min after egg-laying. Electron-dense materials seem to be secreted by the embryos (small arrows). (C) The egg envelope about 10 min after egg-laying. Sublayer E1b′ begins to fuse to E1a′. The envelope is adhesive, but plasticity is very weak. (D) The egg envelope 10–30 min after egg-laying. The sublayers of E1 are not distinguishable, and plasticity increases. Small arrows show a possible secretion from the egg. The middle layer (E2) begins to form. (E) The envelope 80 min after egg-laying; sublayers have reappeared. The expanded envelope becomes the funiculus. E2 becomes thicker. Small arrows: possible secretion from the embryo to make E2.

reached a first peak at 40 min after egg-laying and then decreased until 70 min after egg-laying. But at this time, plasticity again increased rapidly, attaining another peak 90 min after egg-laying. After 90 min a stretched envelope (Fig. 1F) regained its form somewhat when the tension was released. Over the next few hours, envelope plasticity gradually decreased again. The size of the eggs did not change through the attachment process.

*Egg attachment to transplanted setae.* Two segments of an ovigerous seta were removed from a non-incubating female and inserted among the egg clusters of another female that had been laying eggs. The donated segments were removed from the host female after 5 min and after 1 h, and examined with a stereomicroscope. The setal segment removed after 5 min had nearly 50 eggs attached to its hairs (Fig. 10A), and the attachment was similar to those of intact females (Figs. 6B and 8A). However, neither the coat nor the funiculus were formed, and the egg envelope was not expanded at this time. The segment removed after 1 h had many eggs attached to its hairs (Fig. 10B). Since adherence of the envelope has already been lost by 1 h (Table 1), the short structure attaching each egg to the hair must be

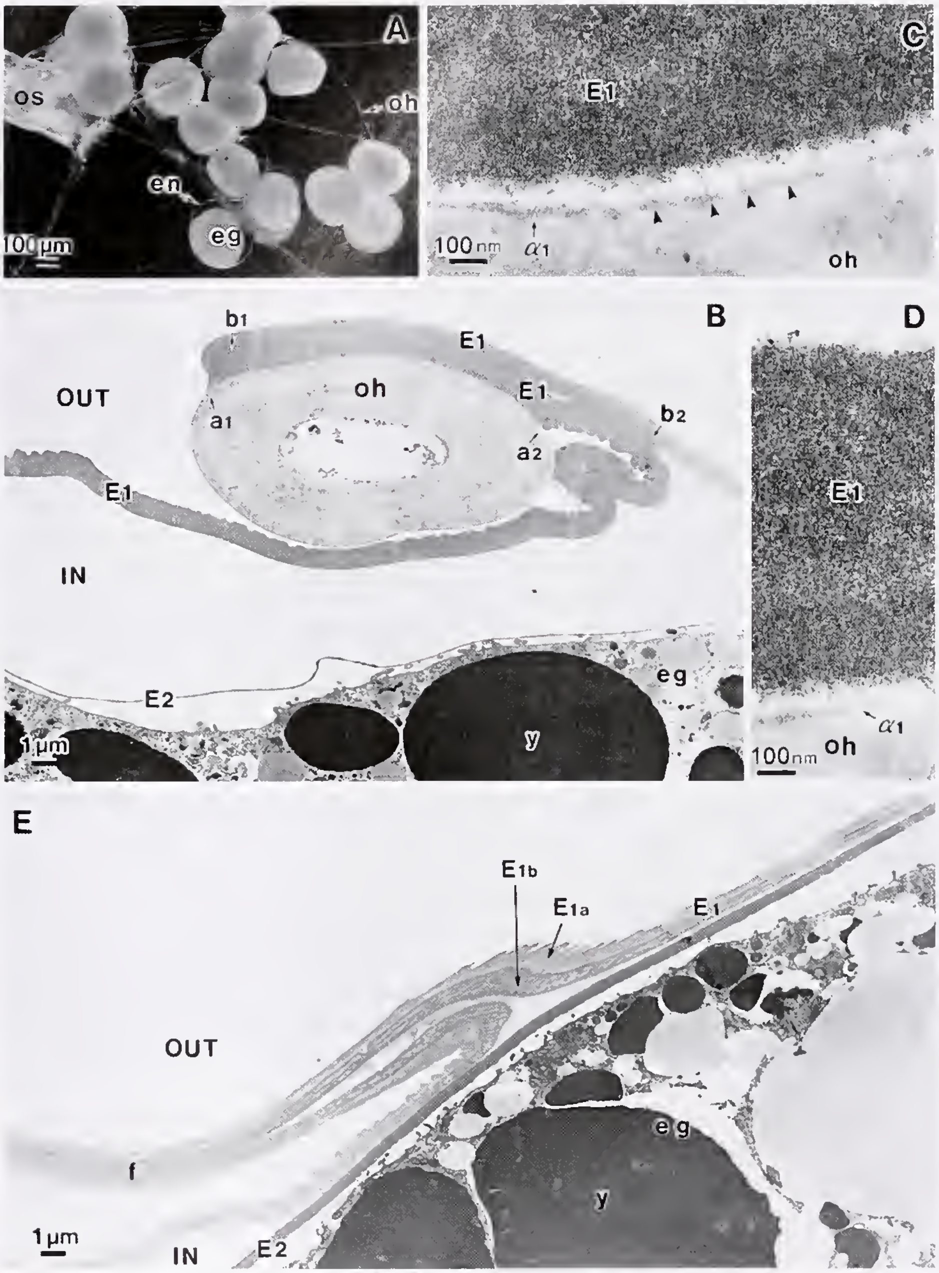

**Figure 8.** Attachment of eggs, and formation of the investment coat and the funiculus. (A) Eggs (eg) 10–15 min after egg-laying. en: envelope. os: ovigerous seta. oh: ovigerous hair. (B) Fine structure of the envelope attaching to the hair: 10–15 min after egg-laying. eg: egg. y: yolk. E1: a homogeneous layer formed by the fusion of E1a and E1b. This layer wraps around the hair or is stratified on the hair (oh), and thus produces the coat. IN: inside E1. OUT: outside E1. a1–a2: envelope-hair adherence. b1–b2: envelope-envelope adherence. E2: the middle layer; its formation has just started. (C) Attachment of fused layer (E1) to the walls of an ovigerous hair (oh): 10–15 min after egg-laying (oblique section). Upward arrowheads show the electron-dense structures about the same interval on the hair. α1: an electron-dense surface layer of the hair. (D) The whole envelope (E1) is homogeneous at this time: oblique section. (But very careful inspection indicates that E1a is still distinguishable from E1b even when the fusion occurs. See also Figures 7D and 8C.) (E) Completion of the funiculus (f): The egg about 80 min after egg-laying. E1 is again divided into two distinguishable sublayers E1a and E1b. E2 becomes thicker, but E2 is not a component of the funiculus. Other symbols are the same as in (B).

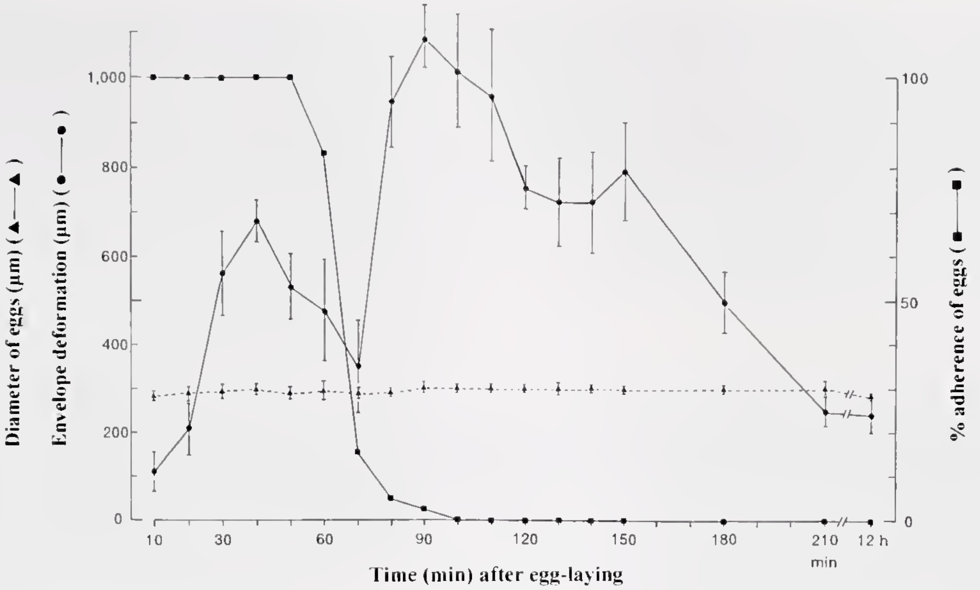

**Figure 9.** Time course of changes in the adhesion and plasticity of the envelope after egg-laying. Envelope adhesion (solid squares: ■), plasticity (solid circles: ●), and diameter of the eggs (solid triangles: ▲) were determined every 10 min. Data points are means with standard deviation (vertical bars).

an immature funiculus (Fig. 10C1–C3). These three examples also show that the hair was incompletely invested by the coat. In summary, the morphology and length of the funiculus were different from those formed in intact females. These funiculi (Fig. 10C1–C3) on the donated setae were shorter and wider than those of intact females (*e.g.*,

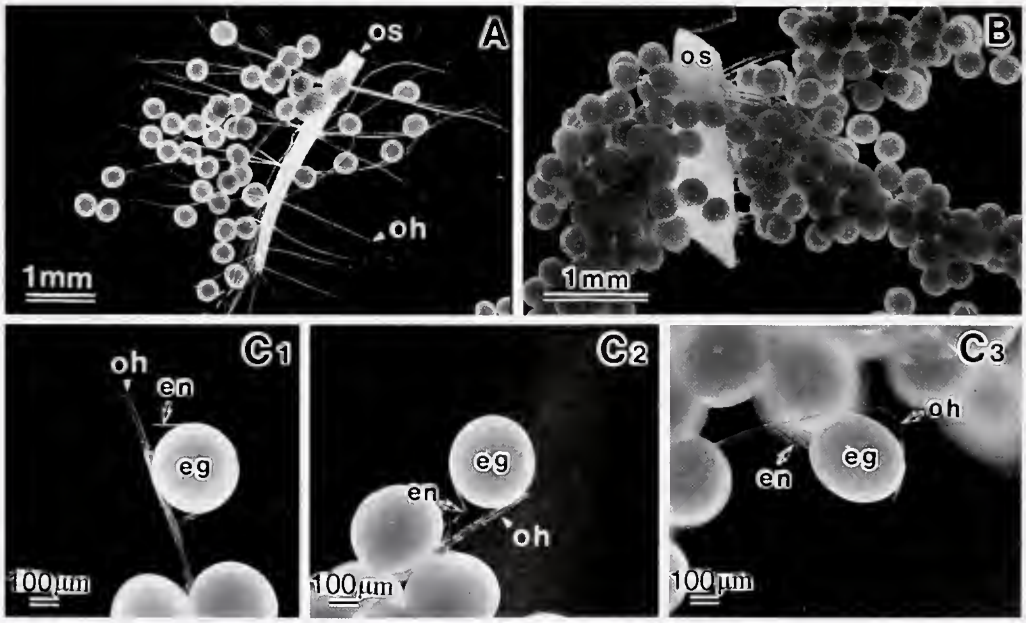

**Figure 10.** Segments of ovigerous setae were removed from non-incubating females and inserted into the egg mass of a female immediately after egg-laying. Effects on egg attachment and funiculus formation were observed. (A) A transplanted segment of an ovigerous seta (os) removed from host female 5 min after egg-laying. oh: ovigerous hair. (B) A transplanted segment removed 60 min after egg-laying. (C) Three examples of the incomplete attachment system formed on the ovigerous hair (oh) in (B). eg: egg. en: an envelope that has already lost adhesiveness.

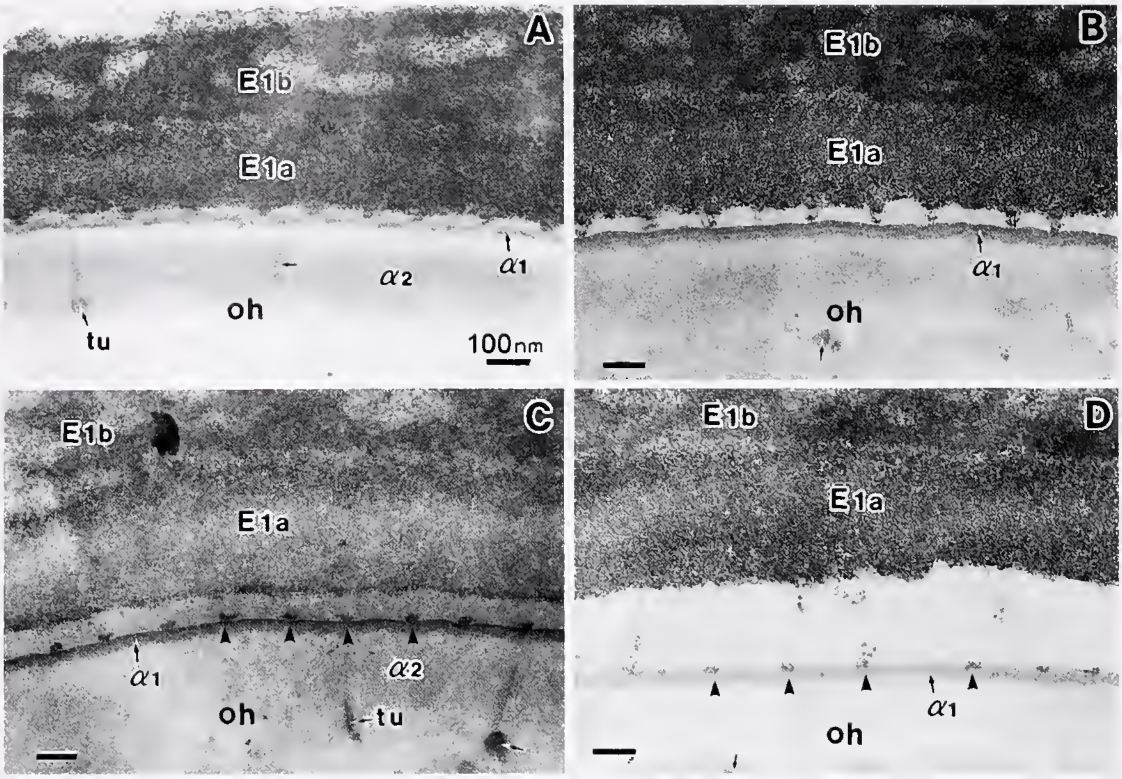

**Figure 11.** Time course of the dissociation of the investment coat from the ovigerous hair. Clusters of embryos were incubated with crude, concentrated hatch water for 2 min (A), 4 min (B), 10 min (C), and 120 min (D). E1a and E1b: sublayers of the investment coat. oh: ovigerous hair. $\alpha1$ and $\alpha2$: surface layers of the hair. Arrows: tubules (tu). Note that the extensions of the sublayer E1a retract, but electron-dense sites remain in the surface of the $\alpha1$ layer of the ovigerous hair (upward arrowheads in C and D). Scales are all 100 nm.

Figs. 2A and 6E). We speculate that the kneading of the egg cluster by the ovigerous setae was not fully transferred to the donated setal segment, so the investment coat and funiculus were incomplete.

### *Disposal of the embryo attachment system after hatching*

The outermost layer of the egg envelope (E1a) attaches to the ovigerous hair (Fig. 4). Moreover, electron-dense, slender structures arranged at intervals of 130–160 nm around the hair seem to be involved in attachment. Figure 11A shows a section of a hair in an investment coat; the hair was treated with crude, concentrated hatch water and fixed 2 min later. The sublayer E1a is still adhering to the ovigerous hair through its ridges. In a section of a hair fixed 4 min after the treatment with hatch water (Fig. 11B), the space between the hair and the envelope has become slightly wider, but the connection between the hair and the ridges of E1a still remain. Note, however, that some of the ridges on E1a seem to be dissociating from a structure that remains on the hair. After 10 min of treatment with hatch water, the envelope was completely detached from the hair, and the dissociation of the ridges of E1a from the structures on the hair has advanced (Fig. 11C). Two hours after treatment (Fig. 11D), the space was widely expanded, and the ovigerous hair easily slipped out of the coat, when the embryos were pulled with a fine forceps. The surface of the stripped hair in Figure 11D is strikingly similar to the hair of a non-incubating female (Fig. 5B). No clear changes were observed in other parts of the investment coat (*e.g.*, compare Fig. 4B with Fig. 11D) or the funiculus (not shown).

## Discussion

The embryo attachment system of the estuarine terrestrial crab *Sesarma haematocheir* consists of (1) the egg envelope, (2) the funiculus, and (3) the investment coat, which wraps around an ovigerous hair. Our observations show that the entire embryo attachment system originates from the vitelline membrane that surrounds an unfertilized egg (ovum) in the ovary. Furthermore, as the adhesiveness and then the plasticity of this envelope change, the sublayers E1a′ and E1b′ fuse and then reappear, and the investment coat and then funiculus are formed. These findings are first compared with the structure and formation of the embryo attachment system in other decapod crustaceans. Then, we propose that orderly production of the egg attachment system—particularly the investment coat and the funiculus—is dependent upon a series of correlated changes in the mechanical properties of the egg envelope. Furthermore, we suggest that, after the larvae have hatched, OHSS acts specifically at the attachment sites, disposing of the embryonic attachment system and preparing the ovigerous hairs for a new clutch of eggs: that is, the ovigerous hair recycling system in these crabs is proposed.

### *Structure and formation of the egg attachment system: comparison with other crustaceans*

Under transmission electron microscopy (TEM), the mature embryonic envelope of *S. haematocheir* consists of three layers (E1, E2, and E3) (Fig. 2). Cheung (1966) observed the mature embryonic envelope of the crab *Carcinus maenas* with a the light microscope (LM), and reported that it consists of three layers which are histochemically distinct (layers 1–3). But it seems that the layers reported by Cheung (1966) do not exactly correspond to the three layers (E1–E3) we have reported here. Envelope formation in *C. maenas*, observed under TEM, was reported by Goudeau and Lachaise (1980). The ultrastructure of the outermost layer (E1) and the thick middle layer (E2) is much the same as that of *S. haematocheir* (Fig. 2). Furthermore, a fertilized egg that has just been extruded into the incubation chamber of the female contains a single envelope (E1) with two sublayers, and the entire embryo attachment system originates from the vitelline membrane that surrounds an unfertilized egg (ovum) in the ovary. This result is also the same as in *C. maenas* reported by Goudeau *et al.* (1987). These findings are contrary to previous notions that a portion or all of the embryo attachment system is formed by extra-ovarian secretions from "cement glands" in the maternal pleopods (see Yonge, 1937, 1955; Stephens, 1952; Aiken and Waddy, 1982; Fisher and Clark, 1983; Saigusa, 1994, 1995).

In the lobsters *Homarus americanus* and *H. gammarus*, the envelope of the newly extruded eggs is also single, and this envelope swells and is adhesive after egg-laying; the envelope is stretched by a vigorous beating of the female pleopods, producing the funiculus (Goudeau *et al.*, 1987). A similar mechanism was also reported for the embryo attachment system of *C. maenas* (Goudeau and Lachaise, 1980). Formation of the embryo attachment system of *S. haematocheir* is also similar to that of other decapods (Cheung, 1966; Goudeau *et al.*, 1987; Talbot and Goudeau, 1988). Thus, the embryo attachment system of most decapod crustaceans may be formed by the same fundamental mechanism.

Newly extruded eggs of *S. haematocheir* are immersed in a transparent incubation fluid until the funiculus starts to form (Fig. 1B). A forceps was put in the incubation chamber, and gently pulled at the surface of the fluid. The viscosity was measured by the distance at which the pulled thread of fluid detached from the bulk fluid in the incubation chamber. Although estimation of this distance could only be rough, this method indicated that the viscosity of this incubation fluid is not different from that of water (unpubl. obs.). Cheung (1966) reported that cement glands are present in *Astacus*, and that a mucous substance may be secreted into the abdomen at egg-laying; but he also noted that such glands are not found in *Carcinus*. We speculate that the incubation fluid may not be a "cement substance," but only water generated by the action of the maxillipeds at the mouth.

### *Formation of the embryo attachment system associated with changes in the mechanical properties of the egg envelope*

Just after fertilization, the vitelline envelope of crustaceans is transformed into the fertilization envelope by the cortical reaction (*e.g.*, Pillai and Clark, 1990; Cuoc *et al.*, 1994). In *Sesarma haematocheir*, the expansion of layer E1b′ may be produced by this reaction, just after egg-laying (Fig. 7B). The expansion of this layer is the first noticeable morphological change (Goudeau and Lachaise, 1980; Talbot and Goudeau, 1988). This envelope then becomes adhesive at the same time.

As shown in Table 1 and Figure 7C, fusion of layers E1a′ and E1b′ begins 5 min after egg-laying, and E1a and E1b appear again 20–30 min after egg-laying. Adhesiveness may be produced by the fusion of these layers, although the mechanism of fusion is not known yet. When the eggs at the bottom of a petri dish were gently pushed with the forceps between 5 and 20 min after egg-laying, the envelope—being strongly pasted on the bottom of the dish—was immediately broken, and the egg was either crushed or it escaped from the envelope. But 20–40 min after egg-laying, the envelope could be easily elongated because its plasticity increased. Thus, we speculate that the adhesiveness of the egg envelope is actually strongest 5–20 min after egg-laying, and that all the eggs attach to the ovigerous hair at this time. The female kneads the egg cluster after egg-laying (Table 1). This behavior would enhance the number of contacts between the egg envelope and the ovigerous hair, and thus help attachment to the hair.

On the other hand, the envelope plasticity increases 20–30 min after egg-laying (Fig. 9). This means that the egg envelopes attached to the ovigerous hairs are elongated by the movement of the maternal ovigerous seta. While the adhesiveness of the envelope still remains strong (20–30 min after egg-laying), an envelope would attach to envelopes at other sites. Movements of the ovigerous seta would

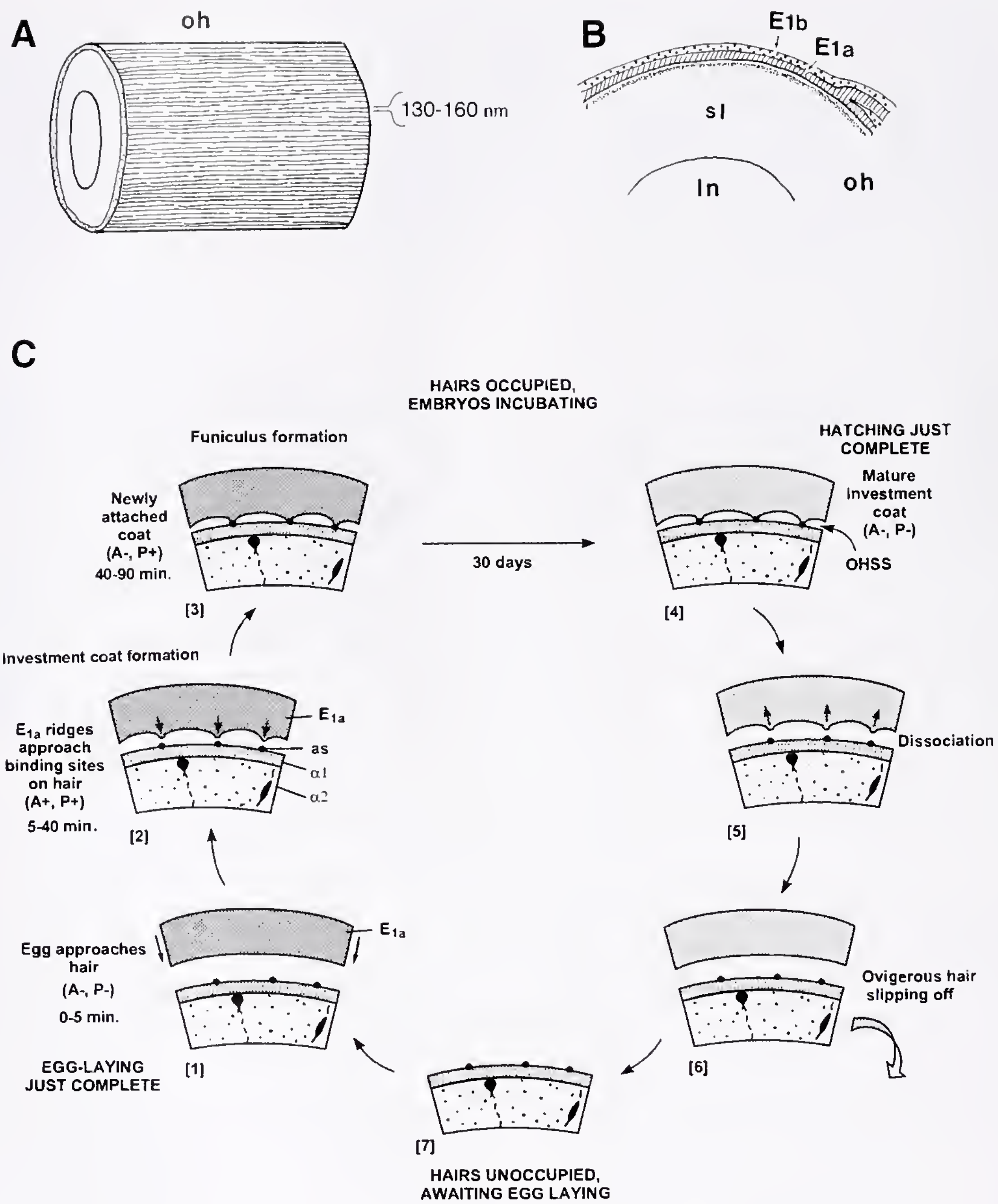
A
oh
130-160 nm
B
E1b
E1a
sl
ln
oh
C
HAIRS OCCUPIED, EMBRYOS INCUBATING
Funiculus formation
Newly attached coat (A-, P+) 40-90 min.
[3]
30 days
HATCHING JUST COMPLETE
Mature investment coat (A-, P-)
OHSS
[4]
Investment coat formation
E1a ridges approach binding sites on hair (A+, P+) 5-40 min.
[2]
E1a
as
α1
α2
Dissociation
[5]
Egg approaches hair (A-, P-) 0-5 min.
E1a
EGG-LAYING JUST COMPLETE
[1]
Ovigerous hair slipping off
[6]
[7]
HAIRS UNOCCUPIED, AWAITING EGG LAYING

**Figure 12.** Attachment structures on the surface of the ovigerous hair and the egg envelope. (A) Diagram of an ovigerous hair (oh) that is not occupied by an investment coat. Proposed linear attachment structures are arranged around the circumference of the hair at intervals of 130–160 nm. (B) An investment coat wrapping around an ovigerous hair (oh). E1a and E1b are two sublayers of the coat. sl: stratified layering of the cuticle. ln: central lumen of the ovigerous hair. (C) Schematic of ovigerous hair recycling. [1] A few minutes after egg-laying: an egg envelope approaches a cleaned ovigerous hair (arrows). But the envelope is not yet adhesive. [2] Five min later the envelope shows adhesiveness. The outer layer of the adhesive envelope E1a develops ridges that extend (small arrows) toward attachment sites (as) on layer $\alpha 1$, which is on the surface of the hair. [3] The E1a ridges bind to the attachment sites and, through the action of the pleopods, an investment coat forms. After the funiculus forms (not shown), the embryos are incubated for nearly 1 month. [4] The embryos hatch, and OHSS (ovigerous-hair stripping substance) attacks the binding of E1a to the attachment sites on the hair. [5] As the investment coat dissociates from the hair, ridges on layer E1a retract, and [6] the investment coat slips off. The female picks remnants of the embryo attachment system off her hairs, and [7] the unoccupied hair is now ready for the next batch of eggs.

wind the elongated egg envelope around the hairs or layer the envelope on the hair. Since the envelope is still strongly adhesive until 40 min after egg-laying, the layers of envelope thus coiled or folded on the hair would adhere to each other, producing the investment coat. While the adhesiveness decreases 40 min after the egg-laying, envelope–envelope adhesion would not persist. In contrast, envelope plasticity remains (Fig. 9). So the envelope 40 min after the egg-laying would form the funiculus.

Embryos of some decapod crustaceans—for example, lobsters in the genus *Homarus* (Yonge, 1937; Talbot and Harper, 1984) and shrimps in the genera *Palaemonetes* (Burkenroad, 1947) and *Palaemon* (Fisher and Clark, 1983)—attach, through the funiculus, not only to ovigerous hairs but also to other embryos. In *S. haematocheir*, however, embryo-to-embryo attachment was only rarely observed. This could be easily explained by changes in adhesiveness and plasticity of the egg envelope after egg-laying. As shown in Figure 8A, when the egg envelope is strongly adhesive, it would attach not only to the ovigerous hairs but also to the other eggs. When the egg cluster is kneaded by the female pleopods, the envelope would become the investment coat. Thereafter, the envelope adhesiveness decreased, whereas the plasticity increased greatly (Fig. 9). At this time, envelopes elongated by the movement of the pleopods would never attach to each other and would thus produce a single funiculus, which would not adhere to the other eggs. In other decapod crustaceans, kneading of the egg cluster may stop while the adhesiveness of the envelope still remains; or the plasticity of the egg envelope may be less than that of *S. haematocheir*. So egg-to-egg adherence may be observed frequently in other crustaceans.

Figure 9 indicates that envelope plasticity decreases at 40–70 min after egg-laying. Up to 40 min after egg-laying, the attachment point of an egg to the bottom of a dish (*a* in Fig. 1D) never moved when the eggs were rolled with a fine forceps. So changes of the plasticity between 10 and 40 min after egg-laying could be measured exactly. For envelopes 40–70 min after egg-laying, however, the attachment point (*a* in Fig. 1E) moved when the eggs were pushed with forceps. This would be due to a decrease of adhesiveness and an increase in the tensile strength of the envelope. Almost all of the eggs were attached to the ovigerous hairs by 80 min (Fig. 1F). From 80–110 min after egg-laying, the egg envelope could easily be fixed by one forceps and elongated by another forceps. So changes of the plasticity at this time could also be measured exactly. Thus, measurement of the envelope plasticity under the conditions where the attachment point was mobile (40–70 min after egg-laying) may not have been correctly estimated. We speculate that the plasticity at this time might increase linearly between 40 min and 90 min after egg-laying.

### *A hypothesis concerning the formation of the egg attachment system and ovigerous hair recycling*

Our TEM examination of mature ovigerous coats shows electron-dense projections from sublayer E1a of the investment coat that extend to the surface of the hair at intervals of 130–160 nm (Fig. 4). These projections are closely apposed to corresponding periodic, ridge-like structures on the surface of the ovigerous hairs. The ridge-like structures are present on the hairs even when the hairs are not occupied by the investment coat (Fig. 5B). Also, if ovigerous hairs are treated with OHSS, and the investment coat slips off the hair, the ridge-like structures are still present (Fig. 11). Therefore, these ridge-like structures on the ovigerous hairs must be attachment sites for the projections from the investment coat. We propose that these evenly-spaced, linear structures are arranged around the circumference of the hair as shown schematically in Figure 12A. Newly extruded eggs always attach to the hairs at the surface of E1a (Fig. 12B).

Ovigerous hair recycling is summarized in Figure 12C ([1]–[7]); the hairs and coats are shown in cross section. Within 5 min after egg-laying, the egg envelope becomes adhesive (Table 1), and the eggs attach to the cleaned ovigerous hairs [1]. The outer layer of the egg envelope (E1a) develops ridges (small arrows) that project toward attachment sites on layer $\alpha 1$ on the surface of the hair [2]; and the E1a ridges bind to the attachment sites when the egg envelope becomes adhesive (5–40 min after egg-laying; Table 1). The plasticity of the egg envelope (E1) increases greatly 10–30 min after egg-laying, when the investment coat is formed through the action of the female's pleopods [3]. The adhesiveness of the egg envelope begins to decrease 40–50 min after egg-laying (Fig. 9), but envelope plasticity is still maintained for more than 1 h (60–150 h after egg-laying). The funiculus is formed during the first half of this period (*i.e.*, 60–90 min after egg-laying). After the funiculus forms, the female incubates the embryos for nearly 1 month. When embryonic development is complete, the embryos hatch. OHSS (ovigerous-hair stripping substance) in the hatch water (see Saigusa, 1995) attacks the binding of E1a to the attachment sites on the ovigerous hair [4]. As the investment coat dissociates from the hair, the ridges on layer E1a retract (Fig. 11B, C) [5], and the ovigerous hair slips out of the layer E1a [6]. As this process ends, the female picks the remnants of the embryo attachment system off her hairs (see Saigusa, 1982), and these unoccupied hairs are now ready for the next batch of eggs [7].

## Acknowledgments

Supported by Grants-in-Aid for Science Research (KAKENHI) (C) (2) to M.S.: No. 08833009 (Marine Biology), No. 10836014 (Natural History), and No. 13839011 (Biodiversity), and KAKENHI on Priority Areas (A) to M.S.: No. 13024253. Also supported by Sumitomo Foundation to M.S. in 1999 (No. 990340). We thank Lynn Milstead (Whitney Laboratory) for help with Figure 12C.

## Literature Cited

**Aiken, D. E., and S. L. Waddy. 1982.** Cement gland development, ovary maturation and reproductive cycles in the American lobster *Homarus americanus. J. Crustac. Biol.* **2:** 315–327.

**Andrews, E. A. 1906.** Egg laying of crayfish. *Am. Nat.* **40:** 343–356.

**Burkenroad, M. D. 1947.** Reproductive activities of decapod Crustacea. *Am. Nat.* **81:** 392–398.

**Cheung, T. S. 1966.** The development of egg-membranes and egg attachment in the shore crab, *Carcinus maenas*, and some related decapods. *J. Mar. Biol. Assoc. UK* **46:** 373–400.

**Cuoc, C., M. Brunet, J. Arnaud, and J. Mazza. 1994.** Formation of egg envelopes in the freshwater calanoid copepod, *Hemidiaptomus ingens. Inv. Rep. Dev.* **26:** 63–78.

**Fisher, W. S., and W. H. Clark, Jr. 1983.** Eggs of *Palaemon macrodactylus:* I. Attachment to the pleopods and formation of the outer investment coat. *Biol. Bull.* **164:** 189–200.

**Goudeau, M., and F. Lachaise. 1980.** Fine structure and secretion of the capsule enclosing the embryo in a crab (*Carcinus maenas* (L.)). *Tissue Cell* **12:** 287–308.

**Goudeau, M., and F. Lachaise. 1983.** Structure of the egg funiculus and deposition of embryonic envelopes in a crab. *Tissue Cell* **15:** 47–62.

**Goudeau, M., P. Talbot, and R. Harper. 1987.** Mechanism of egg attachment stalk formation in the lobster, *Homarus. Gamete Res.* **18:** 279–289.

**Hartnoll, R. G. 1968.** Morphology of the genital ducts in female crabs. *J. Linn. Soc. (Zool.)* **47:** 279–300.

**Herrick, F. H. 1895.** The American lobster—a study of its habits and development. *Bull. U.S. Fish Comm.* **1895:** 1–252, plus 54 plate pages.

**Hinsch, G. W. 1990.** Arthropoda-Crustacea. Pp. 121–155 in *Reproductive Biology of Invertebrates*, Vol. 4, Part B: Fertilization, Development, and Parential Care, K. G. Adiyodi and R. G. Adiyodi, eds. John Wiley, New York.

**Pillai, M. C., and W. H. Clark, Jr. 1990.** Development of cortical vesicles in *Sicyonia ingentis* ova: their heterogeneity and role in elaboration of the hatching envelope. *Mol. Reprod. Dev.* **26:** 78–89.

**Saigusa, M. 1980.** Entrainment of a semilunar rhythm by a simulated moonlight cycle in the terrestrial crab, *Sesarma haematocheir. Oecologia* **46:** 38–44.

**Saigusa, M. 1982.** Larval release rhythm coinciding with solar day and tidal cycles in the terrestrial crab *Sesarma. Biol. Bull.* **162:** 371–386.

**Saigusa, M. 1992.** Control of hatching in an estuarine terrestrial crab. I. Hatching of embryos detached from the female and emergence of mature larvae. *Biol. Bull.* **183:** 401–408.

**Saigusa, M. 1993.** Control of hatching in an estuarine terrestrial crab. II. Exchange of a cluster of embryos between two females. *Biol. Bull.* **184:** 186–202.

**Saigusa, M. 1994.** A substance inducing the loss of premature embryos from ovigerous crabs. *Biol. Bull.* **186:** 81–89.

**Saigusa, M. 1995.** Bioassay and preliminary characterization of ovigerous-hair stripping substance (OHSS) in hatch water of crab larvae. *Biol. Bull.* **189:** 175–184.

**Saigusa, M. 1996.** Two kinds of active factor in crab hatch water: ovigerous-hair stripping substance (OHSS) and protease. *Biol. Bull.* **191:** 234–240.

**Saigusa, M., and H. Iwasaki. 1999.** Ovigerous-hair stripping substance (OHSS) in an estuarine crab: purification, preliminary characterization, and appearance of the activity in the developing embryos. *Biol. Bull.* **197:** 174–187.

**Saigusa, M., and M. Terajima. 2000.** Hatching of an estuarine crab, *Sesarma haematocheir:* from disappearance of the inner (E3) layer to rupture of the egg case. *J. Exp. Zool.* **287:** 510–523.

**Stephens, G. C. 1952.** The control of cement gland development in the crayfish, *Cambarus. Biol. Bull.* **103:** 242–258.

**Talbot, P., and M. Goudeau. 1988.** A complex cortical reaction leads to formation of the fertilization envelope in the lobster, *Homarus. Gamete Res.* **19:** 1–18.

**Talbot, P., and R. Harper. 1984.** Abnormal egg stalk morphology is correlated with clutch attrition in laboratory-maintained lobsters (*Homarus*). *Biol. Bull.* **166:** 349–356.

**Yonge, C. M. 1937.** The nature and significance of the membranes surrounding the developing eggs of *Homarus vulgaris* and other Decapoda. *Proc. Zool. Soc. Lond. (Ser. A).* **107:** 499–517 plus 1 plate page.

**Yonge, C. M. 1946.** Permeability and properties of the membranes surrounding the developing egg of *Homarus vulgaris. J. Mar. Biol. Assoc. UK* **26:** 432–438.

**Yonge, C. M. 1955.** Egg attachment in *Crangon vulgaris* and other Caridia. *Proc. R. Soc. Edin.* **B65:** 369–400.

Reference: *Biol. Bull.* **203:** 307–314. (December 2002)

# Spectral Sensitivity of Vertically Migrating Marine Copepods

JONATHAN H. COHEN* AND RICHARD B. FORWARD, JR.

*Duke University Marine Laboratory, 135 Duke Marine Lab Road, Beaufort, North Carolina 28516; and Biology Department, Duke University, Box 90338, Durham, North Carolina 27708*

**Abstract.** Light is a critical factor in the proximate basis of diel vertical migration (DVM) in zooplankton. A photobehavioral approach was used to examine the spectral sensitivity of four coastal species of calanoid copepod, representing a diversity of DVM patterns, to test whether species that migrate (nocturnal or reverse DVM) have response spectra that differ from non-migratory surface dwellers. The following species were given light stimuli at wavelengths from 350 to 740 nm, and their photoresponses were measured: *Centropages typicus* (nocturnal migrator), *Calanopia americana* (nocturnal migrator), *Anomalocera ornata* (reverse migrator), and *Labidocera aestiva* (non-migrator). *Centropages typicus* and *A. ornata* had peak responses at 500 and 520 nm, respectively, while *Calanopia americana* had maximum responses at 480 and 520 nm. Thus, the species that undergo DVM have peak photobehavioral responses at wavelengths corresponding to those available during twilight in coastal water, although the range of wavelengths to which they respond is variable. Non-migratory surface-dwelling *L. aestiva* had numerous response peaks over a broad spectral range, which may serve to maximize photon capture for vision in their broad-spectrum shallow-water habitat.

## Introduction

Diel vertical migration (DVM) is an extremely common pattern of vertical movement in the water column that occurs in both freshwater and marine zooplankton, particularly the copepods (Haney, 1988; Longhurst and Harrison, 1989). Of the three general DVM patterns that have been recognized, the most common is an ascent in the water column to minimum depth around sunset and descent to maximum depth around sunrise, termed nocturnal, or normal, DVM. Another pattern, reverse DVM, involves an ascent to shallow water at sunrise followed by a descent to deeper water at sunset. The third pattern, twilight DVM, involves an ascent to the surface at sunset, a descent to deeper water around midnight (*i.e.*, the "midnight sink"), followed by a second ascent to the surface and then descent to deeper water at sunrise. There is variability in which pattern is expressed for any given species at a particular place and time (*e.g.*, Bollens and Frost, 1989; Ohman, 1990).

The hypothesis for the ultimate evolutionary advantage of DVM that finds the most support in the literature is that of reduced mortality risk by predator avoidance (*e.g.*, Frost, 1988; Bollens and Frost, 1989; De Robertis *et al.*, 2000). Accordingly, nocturnal and twilight DVM provide both a daytime refuge from visual predation in dim light areas at depth and nighttime access to food-rich surface waters. Reverse DVM provides protection from nocturnally migrating predators (Ohman *et al.*, 1983). The proximate physiological mechanisms thought to control the movement of migrators during DVM involve aspects of the diel light cycle (for reviews of competing hypotheses, see Forward, 1988; Ringelberg, 1999). Some of the strongest evidence for the role of light in DVM comes from field observations that (1) migration usually occurs at twilight, which is the time of day with the greatest relative change in irradiance, and (2) some zooplankton species maintain their depth at distinct levels of irradiance throughout the diel cycle (*e.g.*, Frank and Widder, 2002). Laboratory observations also suggest that many zooplankton species have behavioral responses to relative rates of irradiance change that are consistent with swimming during DVM. Furthermore, photophysiological thresholds for these responses tend to correlate with relative

Received 13 August 2002; accepted 9 October 2002.

* To whom correspondence should be addressed. E-mail: jhc6@duke.edu

rates of irradiance change occurring at twilight at depths inhabited by migrating zooplankton (Forward, 1988; Ringelberg, 1995).

The spectral distribution of light underwater has been well studied and is determined by a combination of the ambient skylight and the optical properties of seawater, with its associated biological materials (*e.g.*, phytoplankton and colored dissolved organic matter). Light becomes increasingly monochromatic with depth; the color is determined by those wavelengths that are attenuated less as they pass into deep water (Jerlov, 1976). Estuarine waters transmit maximally at longer wavelengths (~580 nm), whereas coastal waters transmit better at slightly shorter wavelengths (~500 nm), and clear ocean water transmits best at even shorter wavelengths (~470 nm). Even though UVA (320–400 nm) is attenuated more than blue-green light, a substantial amount is present underwater (Losey *et al.*, 1999). Downwelling irradiance at 380 nm, measured offshore of Beaufort Inlet, North Carolina, at high tide in both spring and fall, was about $10^{15}$ photons $m^{-2}$ $s^{-1}$ at depths of 10 and 13 m, respectively (water column depths 17 and 24 m; NOAA Coastal Remote Sensing Program, http://www.csc.noaa.gov/crs). Given these data for water close to an estuary (Newport River Estuary, NC), there is likely to be adequate long-wavelength UVA light for visual perception over most depths in relatively clearer coastal habitats.

Studies on fish vision have yielded two hypotheses concerning how the spectral sensitivity of visual pigments relates to the spectral quality of light in an organism's habitat. The contrast hypothesis states that wavelength sensitivity is either matched to or offset from ambient wavelengths, depending on depth of habitat and line of sight, in order to maximize contrast between an object and the background (Lythgoe, 1968; McFarland and Munz, 1975). Alternatively, the sensitivity hypothesis suggests that the wavelength sensitivity of visual pigments is matched to the ambient wavelengths present in the environment, in order to maximize photon capture (Munz, 1958; Partridge and Cummings, 1999). Forward (1988) suggested that the spectral sensitivity hypothesis holds for the few species of vertically migrating zooplankton that have been studied; but rather than being adapted to maximize photon capture during the day, these organisms have spectral sensitivities matched to the ambient light during times of vertical migration (*i.e.*, twilight). At twilight, there is a relative reduction in the spectral region of 540–625 nm (yellow) and increases near 500 (blue-green) and 680 nm (red). This phenomenon is termed the Chappuis effect, and is particularly prominent near the surface in coastal regions (Hobson *et al.*, 1981). However, Forward *et al.* (1988) reported that the Chappuis effect was detectable in April near the bottom (2.5 m) of the relatively turbid Newport River Estuary in North Carolina. Given the spectral transmission of estuarine and coastal water, coupled with the Chappuis effect, zooplankton that undergo DVM in these regions will likely be adapted to respond maximally to light at 480–520 nm (Forward, 1988).

The purpose of the present study was to determine whether there are differences in the spectral sensitivities of four coastal species of calanoid copepod (*Centropages typicus, Calanopia americana, Anomalocera ornata,* and *Labidocera aestiva*) that differ in their reported DVM behaviors. Both *Centropages typicus* and *Calanopia americana* undergo nocturnal DVM (Clarke, 1933, 1934; Bowman, 1971; White *et al.*, 1979). *A. ornata* is a reverse migrator (P. Tester, NOAA Coastal Ocean Program, pers. comm.), and *L. aestiva* is a non-migratory surface dweller (Wilson, 1932; Turner *et al.*, 1979). We hypothesized that the non-migratory species that inhabits surface waters during the day (*L. aestiva*) would be responsive to a wide range of wavelengths in order to maximize photon capture for daytime vision in its broad-spectrum habitat. Conversely, vertically migrating species (*Centropages typicus, Calanopia americana,* and *A. ornata*) were predicted to be responsive to a narrow range of wavelengths matched to those occurring at depth in their coastal habitat, particularly at twilight (480–520 nm; Forward *et al.*, 1988). Of the four species tested, the non-migratory surface-dwelling *L. aestiva* responded to the greatest range of wavelengths. The nocturnal migratory species *Centropages typicus* and *Calanopia americana,* as well as the reverse migrator *A. ornata,* were maximally responsive to blue-green light (~500 nm), but the range of wavelengths over which they responded was variable.

## Materials and Methods

*Centropages typicus, Calanopia americana,* and *Labidocera aestiva* were captured using a stationary 0.75-m plankton net with a mesh size of 333 $\mu$m. The net was set prior to maximum current on nighttime flood tides near Beaufort Inlet, North Carolina (34°4′N, 76°41′W). Nets set at this time ensured high densities of these species. *Anomalocera ornata* was captured with the same net during daytime surface tows ~24 km offshore of Beaufort Inlet. Although this species did occur in daytime plankton samples collected inshore, it was more abundant offshore. Salinity in Beaufort Inlet and surrounding areas usually ranges from 30 to 36 ppt. All net samples were diluted with ambient seawater, brought to the laboratory, and allowed to acclimate for at least 4 h to the temperature of all experiments (23 °C).

No longer than 12 h after collection, plankton were sieved twice (3.2 mm and 0.7 mm) to remove macroplankton and macroalgae. Adult female copepods were identified to species and sorted under a dissecting microscope (Fleminger, 1956; Lawson and Grice, 1970; F. Ferrari, Smithsonian Institution, pers. comm.). Groups of copepods were gently pipetted into 40 ml of aged 100-kDa-filtered offshore seawater (36 ppt), in which they remained without food until use in an experiment (no longer than 3 h). Preliminary experiments indicated that photoresponses of unfed copepods remained constant over this time period.

Aged 100-kDa-filtered seawater was prepared by septic filtration (A/G Technology Corp. model UFP-100-C-4X2A) of offshore seawater to remove biologically active molecules larger than 100 kDa, and subsequent aging for at least 1 week. This process produces seawater with a consistent chemical composition that does not alter crustacean photoresponses (Rittschof *et al.*, 1983; Forward and Rittschof, 2000). Since chemical cues from fish predators can alter zooplankton photoresponses involved in DVM (*e.g.*, Forward and Rittschof, 2000), the potential effects of these chemical cues were removed by incubation in the 100-kDa-filtered seawater.

Groups of copepods (90 *Centropages typicus*, 90 *Calanopia americana*, 40 *A. ornata*, and 50 *L. aestiva*) were transferred to a transparent acrylic cuvette (3 × 3 × 5 cm for *Centropages typicus*, *Calanopia americana*, and *L. aestiva;* 5 × 5 × 5 cm for *A. ornata*) filled with 100-kDa-filtered seawater, and dark adapted for at least 1 h prior to spectral sensitivity testing. The number of copepods in a group was inversely proportional to copepod body size. Five replicate groups of each species were tested. Stimuli were presented in increasing order of wavelength, spanning UVA, visible, and far-red light (350–740 nm). Each stimulus lasted 5 s, with 3 min of dark adaptation provided between successive stimuli. A group of copepods received the entire stimulus series, and was then discarded. Preliminary experiments indicated that the order of the stimuli did not alter the response, as repetition of a 500-nm stimulus after the entire stimulus series resulted in a response similar to that observed during the initial 500-nm stimulus for each species. In addition, copepods showed consistent photoresponses upon repeated stimulation at 500 nm with 3 min provided between stimuli, suggesting that the 3-min time interval was sufficient to return the animals to the level of dark adaptation they had prior to the initial stimulus. Copepods resumed pre-stimulus (normal) swimming behavior within 30 s after termination of a stimulus. All experiments were conducted between 0900 and 1700 h to reduce the potential effect of an endogenous rhythm on photobehavior.

A 400-W quartz-tungsten-halogen filament lamp (Oriel housing model 6140-1), fitted with a deionized water filter to remove heat, was used to provide light stimuli. Light from the lamp was focused, using a plano convex lens, onto the 20-nm entrance slit of a grating monochromater (Oriel model 7240). Spectral purity of the monochromater was enhanced by using blocking filters: Corning No. 7–54 for the UVA region, No. 4–96 for the blue-green region, and No. 3–67 for the yellow-red region. Light of a desired waveband emitted from the 12-nm exit slit of the monochromater was collimated and focused through fixed neutral-density filters to control irradiance and onto an electromagnetic shutter (Uniblitz model 300-B) to control stimulus duration. When the shutter was opened, light was allowed to pass through a light-tight shield and into a dark room. Light was reflected off two front-surface mirrors and down into the cuvette containing copepods. All optics were composed of fused silica to transmit UVA.

To control for variation in irradiance among wavelengths due to the emission spectrum of the lamp and transmission from the monochromater/blocking filters, fixed neutral-density filters were used to achieve an equivalent irradiance value at all wavelengths (EG & G model 550 radiometer). In initial experiments examining photoresponse *versus* irradiance at 500 nm, approximate photoresponse thresholds were determined. Experimental irradiance values above this threshold could then be set at levels that were neither too high nor too low for eliciting responses in each species. This procedure helped to account for differences in the absolute photosensitivity among the test species. *Centropages typicus*, *A. ornata*, and *L. aestiva* had photoresponses as low as $1 \times 10^{13}$ photons $m^{-2} s^{-1}$, with distinct responses observed at $1 \times 10^{14}$ photons $m^{-2} s^{-1}$. *Calanopia americana* had greater absolute photosensitivity, with photoresponses as low as $1 \times 10^{12}$ photons $m^{-2} s^{-1}$ and distinct responses observed at $1 \times 10^{13}$ photons $m^{-2} s^{-1}$. Accordingly, for spectral sensitivity experiments, the irradiance level for each test wavelength was controlled arbitrarily at 1 log unit above the apparent threshold for each species. The most recent accounts of vertical distributions of these species (Bowman, 1971; Turner *et al.*, 1979; White *et al.*, 1979; P. Tester, NOAA-COP, pers. comm.) have been studied only to identify DVM pattern and were not related to ambient light levels. Thus, it is likely that the irradiance values used in the experiments are somewhat lower than those the animals would be exposed to during the day in their coastal habitat. PAR (photosynthetically active radiation, 400–700 nm) values of $5 \times 10^{20}$ photons $m^{-2} s^{-1}$ (2-m depth) and $6 \times 10^{19}$ photons $m^{-2} s^{-1}$ (13-m depth) were measured at high tide offshore of Beaufort Inlet, North Carolina, at 1200 h (24-m water column depth, 13 March 1997; NOAA Coastal Remote Sensing Program, http://www.csc.noaa.gov/crs). Accordingly, experimental irradiance levels were probably 5–6 orders of magnitude lower than the daytime levels for the species tested.

Movement of copepods during the experiments was recorded using a closed-circuit video system with near-infrared illumination (maximum transmission = 774 nm), which does not alter or induce crustacean photoresponses (Forward and Cronin, 1979). Aspects of swimming behavior and orientation were later analyzed from video recordings either by hand (*L. aestiva* only) or using a PC-based motion analysis system (CellTrak software, Motion Analysis, Inc.). Swimming behavior was analyzed during the middle 4 s of each 5-s stimulus (response), as well as 10 s prior to each stimulus for the same duration in the dark (control).

The species tested exhibited very different photobehaviors from one another; therefore it was necessary to analyze different aspects of swimming behavior for each species. For *Calaropia americana*, which was strongly phototactic, positive phototaxis was analyzed. The mean angular direction of movement in the *XY*-plane for copepods in the field of view (~25 individuals) was determined from digitized video recordings using CellTrak software. Only animals that oriented in a significant direction were used for analysis (Rayleigh's $z$, $\alpha = 0.01$). The percentage of copepods swimming upward toward the stimulus light ± 30° (positive phototaxis) was determined. An increase in the percentage of copepods exhibiting positive phototaxis relative to the control values indicated increased responsiveness to light, whereas a decrease in responsiveness was indicated by a decreased percentage of positive phototaxis.

*Centropages typicus* was not phototactic, but did exhibit a hop-sink swimming pattern in the dark and a linear swimming pattern with no distinct directional pattern when stimulated with light. Accordingly, an estimate of path linearity, the net-to-gross displacement ratio (NGDR), was analyzed using CellTrak software. NGDR is calculated as the ratio of the net-to-gross displacement of a copepod during the 4-s analysis interval. Net displacement is the distance along a straight line from the starting point of a copepod's path of travel to the ending point. Gross displacement is the distance along the path the copepod traveled over the same time period. NGDRs were calculated for individual copepods in the field of view (~15 individuals) and averaged to obtain stimulus and control NGDR values. An increase in the stimulus NGDR relative to the control value indicated increased responsiveness, whereas a decrease indicated decreased responsiveness.

*A. ornata* was not phototactic. In the dark it exhibited position maintenance with oscillating vertical swimming about a central point; when stimulated with light it responded with linear movement. For this species, the rate of change in direction (RCD) was analyzed. RCD is calculated as the absolute value of the angular velocity measured for every point in the path traveled by a copepod over the 4-s analysis interval and averaged for the path. RCD values for all copepod paths in the field of view (~15 copepod paths) were averaged to obtain stimulus and control RCD values. A decline in stimulus RCD value relative to control values indicated an increase in linear swimming and responsiveness; an increase in the RCD index indicated oscillating swimming and decreased responsiveness.

*L. aestiva* did not exhibit phototaxis, but did demonstrate a dorsal light reflex, which was described by Land (1988). The percentage of copepods in the field of view (~15 individuals) undergoing a dorsal light reflex (frontal axis perpendicular to the stimulus light ± 30°) was analyzed. An increase in the percentage of copepods that displayed this response relative to control values indicated increased responsiveness; decreased responsiveness was indicated by a decreased dorsal light reflex percentage.

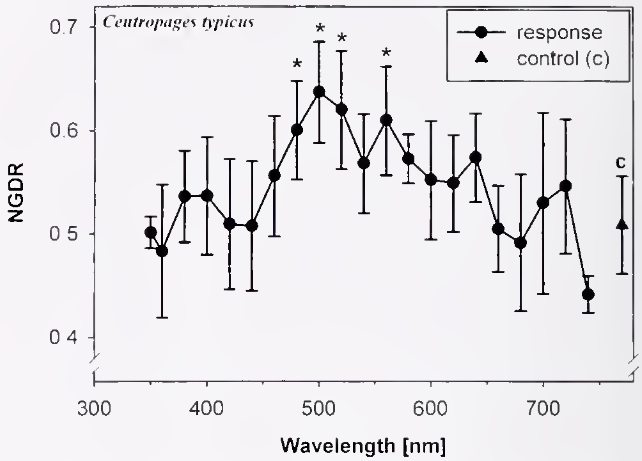

**Figure 1.** Spectral sensitivity of *Centropages typicus*. The ratio of net-to-gross displacement (NGDR) is plotted as a function of wavelength. Circles connected with a solid line represent the mean response value (± SE) for five trials at each wavelength stimulus. The triangle represents the mean control (c) value (± SE) calculated by pooling dark controls for all wavelength stimuli in five trials. Asterisks denote significant differences ($P < 0.05$) between the mean response and the pooled control using a one-factor repeated measures ANOVA with a Dunnett's test for multiple comparisons ($q'_{0.05(1)}$ 84,22, Zar, 1999).

A one-factor repeated measures (RM) ANOVA for each species indicated that there were no differences in the dark control values prior to the stimuli ($P > 0.05$; Zar, 1999). Accordingly, the control values for each wavelength stimulus were pooled, yielding a single mean control and standard error for each species. Response data were then analyzed for each species by using a one-factor repeated measures ANOVA, including the control as an additional treatment. Multiple comparisons were done using a Dunnett's test *versus* the control treatment ($q'_{0.05(1)}$ 84,22; Zar, 1999). A one-tailed statistical test was used because light stimulation was expected to change the response variable in a predictable direction relative to the control (increases for *Centropages typicus*, *Calanopia americana*, and *L. aestiva;* decreases for *A. ornata*).

## Results

The nocturnally migrating *Centropages typicus* responded to few wavelength stimuli (Fig. 1). NGDR values significantly greater than the control value were observed between 480 and 560 nm, with a sensitivity peak at 500 nm (one-factor RM ANOVA, $P = 0.03$; Dunnett's test, $P < 0.05$). Responsiveness was not significant at wavelengths both shorter and longer than this blue-green region (Dunnett's test, $P > 0.05$).

In contrast, the other nocturnally migrating species tested, *Calanopia americana*, responded to many wavelength stimuli

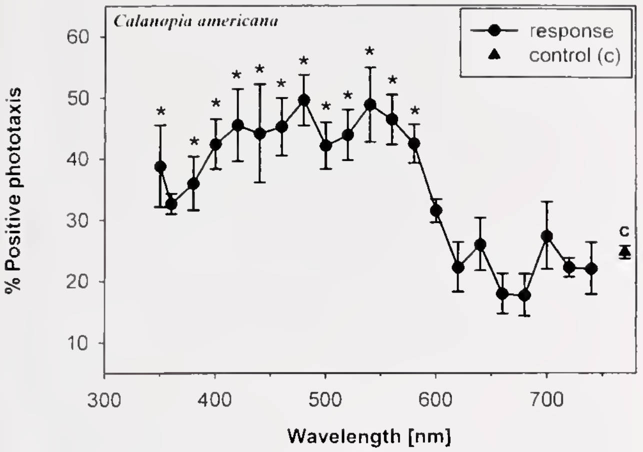

**Figure 2.** Spectral sensitivity of *Calanopia americana*. The percentage of copepods displaying positive phototaxis (upward swimming ± 30°) is plotted as a function of wavelength. All other symbols are as described for Figure 1.

(Fig. 2). Positive phototactic responses significantly greater than the control value were found in the UVA (350, 380, 400 nm), with even greater response values from 420 to 580 nm (one-factor RM ANOVA, $P < 0.001$; Dunnett's test, $P < 0.05$). No significant phototactic response occurred at wavelengths above 580 nm (Dunnett's test, $P > 0.05$).

The reverse migrator, *Anomalocera ornata*, was similar to *Centropages typicus* in that it also responded to few wavelength stimuli (Fig. 3). RCD index values were significantly less than the control value in the spectral region between 460 and 540 nm, with a sensitivity peak at 520 nm (one-factor RM ANOVA, $P < 0.001$; Dunnett's test, $P < 0.05$). Wavelength stimuli outside of this narrow spectral region did not elicit a significant response (Dunnett's test, $P > 0.05$).

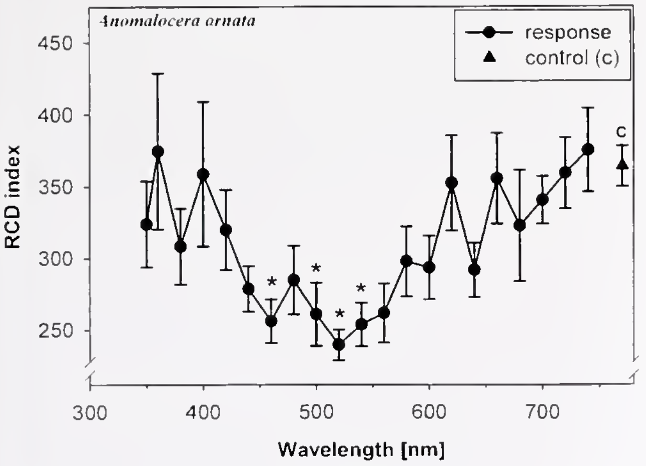

**Figure 3.** Spectral sensitivity of *Anomalocera ornata*. The index of rate of change in direction (RCD) is plotted as a function of wavelength. All other symbols are as described for Figure 1.

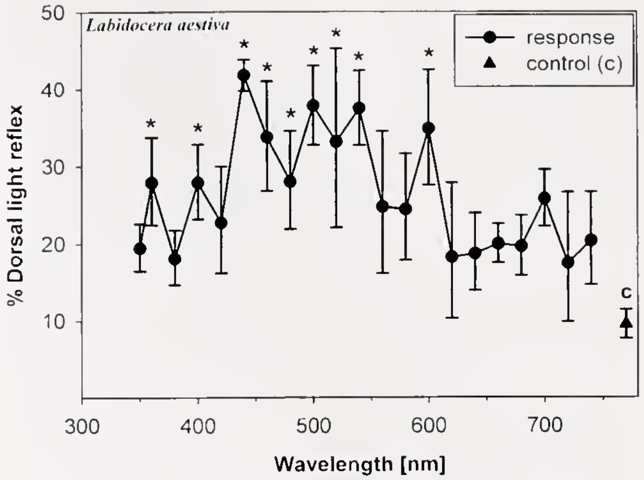

**Figure 4.** Spectral sensitivity of *Labidocera aestiva*. The percentage of copepods displaying the dorsal light reflex (frontal axis perpendicular to the stimulus light ± 30°) is plotted as a function of wavelength. All other symbols are as described for Figure 1.

The surface dwelling *Labidocera aestiva* responded to all wavelength stimuli tested with a higher mean percentage of individuals undergoing a dorsal light reflex than in the dark control (Fig. 4). Peak significant responses occurred at 440–540 and 600 nm in the visible, with minor peaks at 360 and 400 nm in the UVA (one-factor RM ANOVA, $P = 0.005$; Dunnett's test, $P < 0.05$).

## Discussion

We hypothesized that *Labidocera aestiva*, a non-migratory species that inhabits broad-spectrum surface waters during the day, would be responsive to the widest range of wavelengths. We predicted that the nocturnal migrators *Centropages typicus* and *Calanopia americana*, as well as the reverse migrator *Anomalocera ornata*, would have photoresponses over relatively fewer wavelengths, specifically those matched to the ambient wavelengths that occur at twilight in their coastal habitat (480–520 nm). These predictions were verified for all species except *Calanopia americana*, which had photoresponses over a greater range of wavelengths than was expected.

An alternative explanation for the observed interspecific differences in the location and range of spectral sensitivities is that spectral sensitivity relates to the specific behaviors analyzed. While the use of different response variables for each species is not ideal for making interspecific comparisons, the distinctly different behaviors exhibited by each copepod species when exposed to light precluded the use of any one variable to quantify copepod photoresponses. Although no independent direct comparison is available for all the response parameters used here to quantify photobehavior, several studies have analyzed photobehavior with combinations of these parameters or used a single parameter to compare species. Buskey *et al.* (1995) used rate of change in direction (RCD) and the net-to-gross displacement ratio (NGDR) simultaneously as parameters to quantify swarming photobehavior of the copepod *Dioithona oculata* around light shafts that differed in irradiance. Both parameters yielded the same values for the irradiance at which swarming photobehavior occurs. Two studies have used phototaxis as a response variable to examine the spectral sensitivity of marine copepods (*Acartia tonsa*, Stearns and Forward, 1984; *Pleuromamma xiphias* and *P. gracilis*, Buskey *et al.*, 1989). These species all showed phototaxis as a behavioral response to light, but they responded to light stimuli with different orientation directions, and with distinct differences in spectral sensitivity. *A. tonsa* had positive phototactic responses, with sensitivity from 453–620 nm; *P. xiphias* and *P. gracilis* both had negative phototactic responses, with sensitivity from 460–540 nm and 420–620 nm, respectively. These studies demonstrate that copepods vary in their behavioral responses to light stimuli, as was also observed in the present study, and that even when the same behavioral response parameter is used (*e.g.*, phototaxis), there is variability in the observed spectral sensitivity.

*Labidocera aestiva* responded well to wavelengths that transmit best in coastal water (~500 nm); yet it also responded to longer and shorter wavelengths, including those in the UVA. Responsiveness to such a wide range of wavelengths suggests that this surface-dwelling species may be capable of utilizing the broad-spectrum light available at shallow depths to maximize photon capture for daytime vision. *L. aestiva*, like many pontellid copepod species, has highly modified lens eyes and is capable of complex visual behaviors (Vaissière, 1961; Land, 1988). Feeding may represent an important visual task for this species, which is a raptorial predator that relies on its ability to detect and grasp relatively large motile prey items (including copepod nauplii) from the water column rather than exclusively using a suspension-feeding current (Turner, 1984; Conley and Turner, 1985). Aquatic organisms, particularly planktivorous fishes, may utilize UVA wavelengths to visualize opaque and transparent zooplankters (reviewed by Johnsen, 2001). The UVA photoresponses we observed for *L. aestiva* suggest that this surface-dwelling predatory zooplankter could employ a mechanism of UVA-enhanced prey detection.

Of the species we tested that are known to undergo DVM, only *Centropages typicus* (nocturnal migrator) and *A. ornata* (reverse migrator) had spectral sensitivities limited to a narrow range of wavelengths. Their responses peaked between 500–520 nm, so these copepods are well suited for maximizing photon capture in coastal waters, particularly at twilight when—because of the Chappuis effect—blue-green wavelengths dominate the coastal ambient light spectrum. As has been suggested for other zooplankton that undertake vertical migrations at twilight (*e.g.*, Forward, 1988; Forward *et al.*, 1988), their spectral sensitivity matches the ambient wavelengths during a time period when light is a critical environmental cue for orienting and controlling DVM behavior. Interestingly, *A. ornata* has a distinctive blue-green pigmentation (Herring, 1965), and has the highly developed eyes characteristic of the pontellids (*e.g.*, Vaissière, 1961). The coloration presumably confers some protection from predators and photodamage during its daytime residence in surface waters, and the eye may be involved in complex visual behaviors. It is intriguing to speculate that the photoresponsiveness *A. ornata* showed to blue-green wavelengths may relate to the visual detection of pigmented conspecifics, although further study is needed for verification.

Like *Centropages typicus* and *A. ornata*, the nocturnally migrating oceanic species *Pleuromamma xiphias* has photobehaviors limited to blue-green wavelengths (460–540 nm; Buskey *et al.*, 1989). A distinct difference between the coastal species in the present study and the oceanic one is that the sensitivity maximum for the oceanic copepod is shifted to shorter wavelengths. The sensitivity maximum for *P. xiphias* was 480 nm, whereas sensitivity maxima for *Centropages typicus* and *A. ornata* were 500 and 520 nm, respectively. This difference is consistent with the characteristic shift in the spectral transmission of seawater to longer wavelengths in coastal regions relative to oceanic ones; the shift is due to greater amounts of phytoplankton and suspended organic material nearshore.

While the other vertically migrating species we tested, *Calanopia americana*, had maximum responses at 480 and 520 nm, we also observed significant photoresponses at both longer and shorter wavelengths, including the UVA. Instead of being adapted to respond to only a narrow range of ambient twilight wavelengths, this species has a sensitivity maximum in the green spectral region (550 nm), but is equally responsive to shorter wavelengths that would be present at twilight (480 nm). *Calanopia americana* is a very strong nocturnal vertical migrator (Clarke, 1934), and has also been documented to undergo a seasonal shift in distribution off the coast of North Carolina. Bowman (1971) reported that the species was abundant inshore during the summer and fall, but was found mainly at shelf and oceanic stations during winter and spring. The observed spectral sensitivity of *Calanopia americana* suggests that its photobehaviors are well suited for ambient wavelengths offshore, as well as for the relatively longer wavelengths that dominate the inshore light environment. A similarly wide spectral sensitivity (453–620 nm) was previously observed using a similar phototaxis assay for *Acartia tonsa*, a copepod that undergoes nocturnal DVM and is common in both estuarine and shelf waters (Stearns and Forward, 1984).

Knowledge of the spectral absorption characteristics of photopigments for vertically migrating organisms and their relationship to the spectral availability of ambient light is critical to understanding the proximate physiological basis of DVM. Information on the photoresponsiveness of migrators to UV and visible wavelengths is necessary for making appropriate underwater light measurements to be correlated with behavioral movements of migrating organisms (Clarke, 1933; Widder and Frank, 2001). Behavioral observations in this study demonstrate that vertically migrating and non-migrating species of calanoid copepod from the same coastal habitat differ in their spectral sensitivities. Copepods that undertake either nocturnal or reverse vertical migrations are maximally responsive to wavelengths corresponding to those available during twilight, although the range of wavelengths over which they respond is variable. Non-migrating copepods that occur near the surface respond to a greater spectral range that is better suited for maximizing photon capture in broad-spectrum surface waters.

## Acknowledgments

This material is based in part on research supported by the National Science Foundation grant OCE-0095092 to RBF. The manuscript was improved by the helpful comments and suggestions of two anonymous reviewers.

## Literature Cited

**Bollens, S. M., and B. W. Frost. 1989.** Zooplanktivorous fish and variable diel vertical migration in the marine planktonic copepod *Calanus pacificus*. *Limnol. Oceanogr.* **34:** 1072–1083.

**Bowman, T. E. 1971.** The distribution of calanoid copepods off the southeastern United States between Cape Hatteras and southern Florida. *Smithson. Contrib. Zool.* **96:** 1–58.

**Buskey, E. J., K. S. Baker, R. C. Smith, and E. Swift. 1989.** Photosensitivity of the oceanic copepods *Pleuromamma gracilis* and *Pleuromamma xiphias* and its relationship to light penetration and daytime depth distribution. *Mar. Ecol. Prog. Ser.* **55:** 207–216.

**Buskey, E. J., J. O. Peterson, and J. W. Ambler. 1995.** The role of photoreception in the swarming behavior of the copepod *Dioithona oculata*. *Mar. Freshw. Behav. Physiol.* **26:** 273–285.

**Clarke, G. L. 1933.** Diurnal migration of plankton in the Gulf of Maine and its correlation with changes in submarine irradiation. *Biol. Bull.* **65:** 402–436.

**Clarke, G. L. 1934.** The diurnal migration of copepods in St. Georges Harbor, Bermuda. *Biol. Bull.* **67:** 456–460.

**Conley, W. J., and J. T. Turner. 1985.** Omnivory by the coastal marine copepods *Centropages hamatus* and *Labidocera aestiva*. *Mar. Ecol. Prog. Ser.* **21:** 113–120.

**De Robertis, A., J. S. Jaffe, and M. D. Ohman. 2000.** Size-dependent visual predation risk and the timing of vertical migration in zooplankton. *Limnol. Oceanogr.* **45:** 1838–1844.

**Fleminger, A. 1956.** Taxonomic and distributional studies on the epiplankton calanoid copepods (Crustacea) of the Gulf of Mexico. Ph.D. dissertation, Harvard University, Cambridge, MA.

**Forward, R. B., Jr. 1988.** Diel vertical migration: zooplankton photobiology and behavior. *Oceanogr. Mar. Biol. Annu. Rev.* **26:** 361–393.

**Forward, R. B., Jr., and T. W. Cronin. 1979.** Spectral sensitivity of larvae from intertidal crustaceans. *J. Comp. Physiol.* **133:** 311–315.

**Forward, R. B., Jr., and D. Rittschof. 2000.** Alteration of photoresponses involved in diel vertical migration of a crab larva by fish mucus and degradation products of mucopolysaccharides. *J. Exp. Mar. Biol. Ecol.* **245:** 277–292.

**Forward, R. B., Jr., T. W. Cronin, and J. K. Douglass. 1988.** The visual pigments of crabs. II. Environmental adaptations. *J. Comp. Physiol. A* **162:** 479–490.

**Frank, T. M., and E. A. Widder. 2002.** Effects of a decrease in downwelling irradiance on the daytime vertical distribution patterns of zooplankton and micronekton. *Mar. Biol.* **140:** 1181–1193.

**Frost, B. W. 1988.** Variability and possible significance of diel vertical migration in *Calanus pacificus*, a planktonic marine copepod. *Bull. Mar. Sci.* **43:** 675–694.

**Haney, J. F. 1988.** Diel patterns of zooplankton behavior. *Bull. Mar. Sci.* **43:** 583–603.

**Herring, P. J. 1965.** Blue pigment of a surface-living oceanic copepod. *Nature* **205:** 103–104.

**Hobson, E. S., W. N. McFarland, and J. R. Chess. 1981.** Crepuscular and nocturnal activities of California nearshore fish, with consideration of their scotopic visual pigments and the photopic environment. *Fish. Bull.* **79:** 1–30.

**Jerlov, N. G. 1976.** Marine optics. Pp. 127–134 in *Elsevier Oceanography Series*, Vol. 14. Elsevier, Amsterdam.

**Johnsen, S. 2001.** Hidden in plain sight: the ecology and physiology of organismal transparency. *Biol. Bull.* **201:** 301–318.

**Land, M. F. 1988.** The functions of eye and body movements in *Labidocera* and other copepods. *J. Exp. Biol.* **140:** 381–391.

**Lawson, T. J., and G. D. Grice. 1970.** The developmental stages of *Centropages typicus* Kroyer (Copepoda, Calanoida). *Crustaceana* **18:** 187–208.

**Longhurst, A. R., and W. G. Harrison. 1989.** The biological pump: profiles of plankton production and consumption in the upper ocean. *Prog. Oceanogr.* **22:** 47–123.

**Losey, G. S., T. W. Cronin, T. H. Goldsmith, D. Hydes, N. J. Marshall, and W. N. McFarland. 1999.** The UV visual world of fishes: a review. *J. Fish Biol.* **54:** 921–943.

**Lythgoe, J. N. 1968.** Visual pigments and visual range underwater. *Vision Res.* **8:** 997–1012.

**McFarland, W. N., and F. W. Munz. 1975.** Part III: The evolution of photopic visual pigments in fishes. *Vision Res.* **15:** 1071–1080.

**Munz, F. W. 1958.** The photosensitive retinal pigments of fishes from relatively turbid coastal waters. *J. Gen. Physiol.* **42:** 445–459.

**Ohman, M. D. 1990.** The demographic benefits of diel vertical migration by zooplankton. *Ecol. Monogr.* **60:** 257–281.

**Ohman, M. D., B. W. Frost, and E. B. Cohen. 1983.** Reverse diel vertical migration: an escape from invertebrate predators. *Science* **220:** 1404–1407.

**Partridge, J. C., and M. E. Cummings. 1999.** Adaptation of visual pigments to the aquatic environment. Pp. 251–283 in *Adaptive Mechanisms in the Ecology of Vision*, S. N. Archer, M. B. A. Djamgoz, E. R. Loew, and S. Vallerga, eds. Kluwer Academic Publishers, London.

**Ringelberg, J. 1995.** Changes in light intensity and diel vertical migration: a comparison of marine and freshwater environments. *J. Mar. Biol. Assoc. UK* **75:** 15–25.

**Ringelberg, J. 1999.** The photobehavior of *Daphnia* spp. as a model to explain diel vertical migration in zooplankton. *Biol. Rev.* **74:** 397–423.

**Rittschof, D., L. G. Williams, B. Brown, and M. R. Carriker. 1983.** Chemical attraction of newly hatched oyster drills. *Biol. Bull.* **164:** 493–505.

**Stearns, D. E., and R. B. Forward, Jr. 1984.** Photosensitivity of the calanoid copepod *Acartia tonsa*. *Mar. Biol.* **82:** 85–89.

**Turner, J. T. 1984.** Zooplankton feeding ecology: contents of fecal pellets of the copepods *Acartia tonsa* and *Labidocera aestiva* from the continental shelf waters near the mouth of the Mississippi River. *Mar. Ecol.* **5:** 265–282.

**Turner, J. T., S. B. Collard, J. C. Wright, D. V. Mitchell, and P. Steele. 1979.** Summer distribution of pontellid copepods in the neuston of the eastern Gulf of Mexico continental shelf. *Bull. Mar. Sci.* **29:** 287–297.

**Vaissière, R. 1961.** Morphologie et histologie comparées des yeux des crustacés copépodes. *Arch. Zool. Exp. Gen.* **100:** 1–125.

**White, H. H., J. S. Heaton, and K. B. Schmitz. 1979.** Vertical migration of *Centropages typicus* (Copepoda) in Chesapeake Bay, with some thoughts on migration studies. *Estuaries* **2:** 61–63.

**Widder, E. A., and T. M. Frank.** 2001. The speed of an isolume: a shrimp's eye view. *Mar. Biol.* **138:** 669–677.

**Wilson, C. B. 1932.** *The Copepods of the Woods Hole Region, Massachusetts.* Smithsonian Institution, United States National Museum Bulletin, Vol. 158. United States Government Printing Office, Washington D.C.

**Zar, J. H. 1999.** *Biological Statistics.* Prentice Hall, Upper Saddle River, NJ.

Reference: *Biol. Bull.* **203:** 315–330. (December 2002)

# Mycosporine-like Amino Acid Content in Four Species of Sea Anemones in the Genus *Anthopleura* Reflects Phylogenetic but Not Environmental or Symbiotic Relationships

J. MALCOLM SHICK[1,*], WALTER C. DUNLAP[2], JOHN S. PEARSE[3], AND VICKI B. PEARSE[3]

[1]*School of Marine Sciences, University of Maine, 5751 Murray Hall, Orono, Maine 04469-5751;* [2]*Environmental Biochemistry and Marine Biotechnology, Australian Institute of Marine Science, PMB No. 3, Townsville MC, Qld. 4810, Australia; and* [3]*Institute of Marine Sciences, University of California, Santa Cruz, California 95064*

**Abstract.** We examine the occurrence of UV-absorbing, mycosporine-like amino acids (MAAs) in four sympatric species of sea anemones in the genus *Anthopleura*, all collected from intertidal habitats on the Pacific Coast of temperate North America. We compare patterns of MAAs in *A. elegantissima* of several types: specimens having predominately zooxanthellae (dinoflagellates comprising at least two species) or zoochlorellae as symbionts; those containing algal endosymbionts of both kinds, and naturally occurring aposymbiotic specimens that lack the endosymbionts typically found in most specimens. We also compare MAAs in zooxanthellate specimens of *A. sola* and *A. xanthogrammica*, and specimens from the asymbiotic species *A. artemisia*. Our findings indicate that the complements of the four major MAAs in these species of *Anthopleura* (mycosporine-taurine, shinorine, porphyra-334, and mycosporine-2 glycine) broadly reflect phylogenetic differences among the anemones rather than the taxon of endosymbionts, presence or absence of symbionts, or environmental factors. An exception, however, occurs in *A. elegantissima*, where mycosporine-2 glycine increases in concentration with the density of zooxanthellae. Our evidence also shows that *A. elegantissima* can accumulate MAAs from its food, which may explain the occasional occurrence of minor MAAs in some individuals.

## Introduction

Mycosporine-like amino acids (MAAs) are small (244–374 Da), ultraviolet-absorbing ($\lambda_{max}$ = 309–360 nm) molecules that occur in virtually all taxa of marine and freshwater cyanobacteria, algae, and metazoans (reviewed by Bandaranayake, 1998; Dunlap and Shick, 1998; Karentz, 2001; Shick and Dunlap, 2002). Structural diversity among the 20-plus known MAAs and their precursors results from substitutions of various amines, amino acids, and amino alcohols at two conjugated positions of the UV-absorbing chromophore of the MAA base structure (see aforementioned reviews). The often-observed correlation between the exposure of organisms to solar or artificial ultraviolet radiation (UVR) and their concentration of MAAs (see reviews), plus optical considerations (Garcia-Pichel, 1994), suggest a role as UV sunscreens, a contention that has been verified experimentally (Adams and Shick, 1996, 2001; Neale *et al.*, 1998).

As products of the early shikimic acid pathway, MAAs (Shick *et al.*, 1999) and the closely related fungal mycosporines (Favre-Bonvin *et al.*, 1987) are expected to be synthesized by algae, cyanobacteria, fungi, and perhaps bacteria, but not by metazoans. This is because animals lack this biochemical pathway, as inferred from their inability to synthesize shikimate-derived aromatic amino acids (Kishore and Shah, 1988; Bentley, 1990; Haslam, 1993; Herrmann and Weaver, 1999), albeit apparently not from any demonstration that metazoans lack the enzymes of the shikimic acid pathway or the nucleotide sequences coding

Received 3 April 2002; accepted 7 October 2002.

* To whom correspondence should be addressed. E-mail: shick@maine.edu

these enzymes (Shick and Dunlap, 2002). Therefore, the MAAs found in diverse marine microbial-invertebrate phototrophic symbioses were thought at first simply to originate in the algal or cyanobacterial partner (reviewed by Shick and Dunlap, 2002).

Carroll and Shick (1996) first confirmed experimentally the suggestion by Chalker *et al.* (1988) that non-symbiotic metazoans also containing MAAs obtain them from their diet. But the MAA complement in consumers does not always coincide with that in their diet, nor does the MAA complement in symbioses always match that produced by their microbial endosymbionts *in vitro*. Thus, MAAs in the diet may be modified by bacteria in the consumer's digestive tract, and MAAs synthesized by a symbiont could be modified after translocation to the host (see: Dunlap and Shick, 1998; Shick and Dunlap, 2002; and references therein).

Accounting for the MAAs found in a given organism or symbiotic consortium is therefore complicated and requires a detailed knowledge of the diet and the MAAs available therein; the MAAs that the symbionts can produce; and the capacity of the animal to absorb, retain, and modify dietary MAAs and those synthesized by its endosymbionts. These factors may vary spatially (Adams *et al.*, 2001), temporally (including ontogenetically [Adams and Shick, 1996, 2001] and during growth [Sebens, 1981]), and genotypically (Banaszak *et al.*, 2000).

Sea anemones in the genus *Anthopleura* contain taxonomically diverse microalgal endosymbionts that vary with latitude (LaJeunesse and Trench, 2000; Secord and Augustine, 2000), and four species of anemones in this genus overlap in intertidal and shallow subtidal habitats along the Pacific Coast of temperate North America (Fig. 1). From this array, we have selected sympatric populations to test the effects of the foregoing factors (especially the role of exposure to solar radiation, endosymbionts, and diet) on the number, profile, and concentration of MAAs.

We recognized early on that symbiotic and aposymbiotic individuals of *A. elegantissima* present exceptions to the empirically derived paradigms that concentrations of MAAs are determined by exposure to UVR, and that endosymbiotic dinoflagellates (zooxanthellae, *Symbiodinium* spp.) are the source of the MAAs. Exposing both symbiotic and aposymbiotic anemones to natural or artificial UVR does not affect the concentrations or complement of MAAs (Scelfo, 1988; Stochaj *et al.*, 1994; Banaszak and Trench, 1995), nor does *S. californium* isolated from *A. elegantissima* produce MAAs when cultured under UVR (Banaszak and Trench, 1995). A broader study of the MAAs in other species in this genus would provide a comparative context in which to examine these exceptions and clarify the contribution of the several factors involved in the accumulation of the observed complements of MAAs.

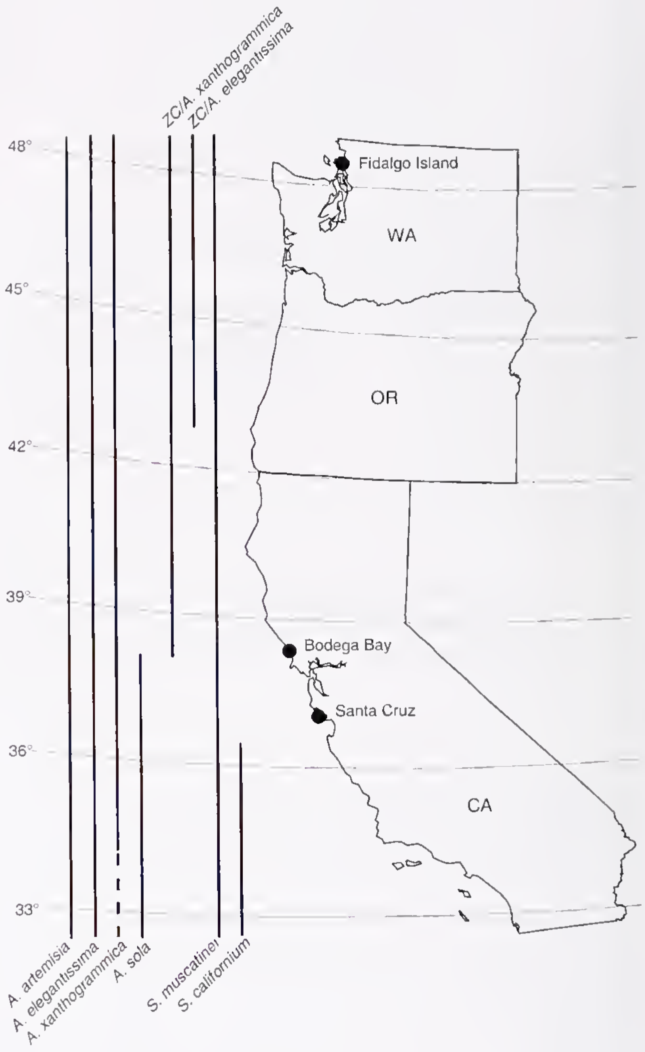

**Figure 1.** Collection sites for the sea anemones used in this study, and the reported ranges of *Anthopleura* species, *Symbiodinium* species, and zoochlorellae (ZC) symbiotic with *A. elegantissima* and *A. xanthogrammica* in Washington, Oregon, and California. Compiled from Hand (1955), Francis (1979), LaJeunesse and Trench (2000), Pearse and Francis (2000), and Secord and Augustine (2000).

Populations of *A. elegantissima* and *A. xanthogrammica* north of Central California host two taxa of phototrophic endosymbionts: zoochlorellae, which are green *Chlorella*-like chlorophytes (Muscatine, 1971), and the dinoflagellate *S. muscatinei* (LaJeunesse and Trench, 2000). An individual anemone may contain exclusively one or the other type of alga, or a combination of both (Muscatine, 1971). The balance between these algae may depend on their differential sensitivity to temperature and sunlight (O'Brien, 1980; O'Brien and Wyttenbach, 1980; Saunders and Muller-Parker, 1997; Secord and Augustine, 2000). Moreover, zoochlorellae translocate, to the host, photosynthetic products that differ qualitatively from zooxanthella photosynthate (Minnick and McCloskey, cited by Verde and McCloskey, 1996), and zooxanthellae contribute more reduced carbon to the host's nutrition than do zoochlorellae (Verde and McCloskey, 1996). Such physiological differences in the algae, and the great evolutionary distance between these algal phyla, might be expected to yield rather different MAA complements in individual sea anemones harboring one or the other endosymbiont—if indeed zoochlorellae (like some other chlorophytes: Karentz, 2001) and *S. muscatinei* can produce MAAs. In addition, populations of *A. elegantissima* in Central and Southern California host only zooxanthellae (Secord and Augustine, 2000), in this case both *S. muscatinei* and *S. californium* (LaJeunesse and Trench, 2000).

In Central California, *A. sola* and *A. xanthogrammica* are sympatric with *A. elegantissima*, often cohabiting the same sites, where all three species harbor only zooxanthellae (Pearse and Francis, 2000). The species of *Symbiodinium* that occur in *A. sola* and *A. xanthogrammica* have not been determined, so these anemones may not host algae capable of synthesizing MAAs.

The asymbiotic species *A. artemisia* rarely (or, more likely, never: see discussion in Pearse and Francis, 2000) contains endosymbiotic algae. Therefore, it should contain only MAAs obtained or modified from its diet. The diet of *A. artemisia* is probably similar to that of *A. elegantissima*, because these two species co-occur at the same sites in Central California and have a similar body size (which would enable them to capture similar prey). Thus, any differences in the MAAs in these two species might arise from secondary modification of dietary MAAs and not from the presence or absence of symbionts. This is suggested by the finding that symbiotic and aposymbiotic specimens of *A. elegantissima* contain an identical complement of MAAs (Stochaj *et al.*, 1994; Banaszak and Trench, 1995). Size-dependent dietary differences between zooxanthellate *A. elegantissima* and *A. xanthogrammica* (Sebens, 1981), and, presumably, between *A. elegantissima* and the larger *A. sola*, may affect the MAAs they ingest in their prey, and result in different MAA complements among the anemones independently of those derived from their endosymbionts. We present the results of a simple experiment to show that *A. elegantissima* can indeed absorb and retain MAAs from its food.

Finally, a phylogeny based on mitochondrial DNA sequences is available for many species in the genus *Anthopleura* (Geller and Walton, 2001). This provides the opportunity to examine the provenance and presumed adaptive role of MAAs in a phylogenetic context (Mangum and Hochachka, 1998). Moreover, MAAs might be useful characters to help resolve the phylogenetic trichotomy of *A. elegantissima, A. sola,* and *A. xanthogrammica,* the interrelationships of which have not yet been clarified by DNA sequencing.

## Materials and Methods

### Collection of sea anemones

Specimens of four species of *Anthopleura* were collected in the summers of 1993 and 1996 in the States of Washington and California. Except as noted, all sea anemones were shipped alive to Orono, Maine, immediately after collection. The anemones were blotted, weighed, minced with a razor blade, and either analyzed immediately for MAAs, or lyophilized. If the material was lyophilized, its dry weight ($_dW$) was first measured, and it was then stored at −79 °C prior to biochemical analysis.

Green, brown, and mixed specimens of *Anthopleura elegantissima* (for descriptions, see Saunders and Muller-Parker, 1997) were taken from a single rock at about +0.6 m (MLLW) tidal height at Anaco Beach, Fidalgo Island, Washington (48°29′N, 122°42′W). We chose this location (Fig. 1) because the anemones there harbor both zooxanthellae and zoochlorellae (Saunders and Muller-Parker, 1997). Differences in their oral disc pigmentation indicated that most of the anemones belonged to different clones, and we used this criterion to select the specimens for analysis, precluding clonemates.

Sea anemones from California were collected in 1996 from Santa Cruz County, a location that is south of the southern limits of zoochlorellae in *A. xanthogrammica* (Bodega Bay area) and *A. elegantissima* (central Oregon) (Fig. 1). Specimens of *A. artemisia, A. elegantissima,* and *A. sola,* and large specimens of *A. xanthogrammica,* were taken from various shore levels at Opal Cliffs near the seaward end of 41st Avenue, Capitola (36°58′N, 121°57′W); small individuals of *A. xanthogrammica* were collected at Scott Creek Beach (37°02′N, 122°13′W). Specimens of *A. elegantissima* came from distinct clonal aggregations of individuals differing in oral disc pattern, and one individual per clone was analyzed. The small specimens of *A. xanthogrammica* were collected in May and held in outdoor tanks without feeding until being shipped to Orono with the other sea anemones collected in August. Aposymbiotic individuals of *A. elegantissima* that had been collected locally and maintained in darkness in the laboratory in flowing seawater at seasonal temperatures for at least a year were also included. They were fed previously frozen adult brine shrimps every week or 2 weeks.

### Determination of algal complement

Several tentacles were snipped from each sea anemone before it was analyzed for MAAs. The tentacles were placed in a drop of artificial seawater on a microscope slide and crushed with a cover slip; the slurry was transferred to a hemacytometer, diluted if necessary, and 500–1000 algal cells were counted. Zoochlorellae and zooxanthellae were readily distinguishable by size and color (Secord and Augustine, 2000). Because the proportions of zoochlorellae and zooxanthellae may vary between the tentacles and column (G. Muller-Parker, Western Washington University, pers. comm.), specimens of *A. elegantissima* from Washington that contained 100% of either algal type in their tentacles were examined further. A section of column wall of such specimens was excised, crushed, and examined for its algal complement to confirm that only one algal taxon was present. As noted above, zoochlorellae do not occur in *Anthopleura* spp. from Santa Cruz. Therefore, to confirm the singular presence of zooxanthellae in specimens from this location, or the lack of algal endosymbionts in *A. artemisia* and aposymbiotic specimens of *A. elegantissima*, only the tentacles were examined.

### *Feeding experiment*

The distinctive complement of MAAs in the ocular lenses of fishes (Dunlap *et al.*, 1989) suggested the use of such lenses as sources of unambiguous dietary markers for a feeding study. The lenses were excised from the lumpfish, *Cyclopterus lumpus*, from Mt. Desert Island, Maine, and their wet weight ($_wW$) was measured. Preliminary analyses by D.S. Mason (University of Maine) indicated the presence of an unknown MAA. Based on its high absorbance at 357 nm and its co-elution with an identically absorbing compound from the red macroalga *Palmaria palmata*, this unknown MAA was tentatively identified as usujirene (Sekikawa *et al.*, 1980; Adams *et al.*, 2001). Because no quantitative standard was available for the presumed usujirene, its concentrations were approximated by matching its extinction coefficient to that of its *trans* isomer palythene (Adams *et al.*, 2001). Because the *cis* isomer will have a lower molar extinction coefficient than the *trans* isomer, this method will slightly overestimate the concentration of usujirene. Preliminary determinations indicated that both lenses from a single fish have the same complement and concentrations of MAAs, so that the amount of MAA available to an anemone ingesting one lens could be estimated from the MAA content of the contralateral lens from the same fish. One lens from each of two fish was frozen at −79 °C for later analysis of MAAs, and the other lens was fed to one of two clonemates of *A. elegantissima*, which were collected from the south jetty at the entrance to Bodega Bay, California (38°19′N, 123°02′W) and held in the laboratory at Orono for 2 weeks at 15 °C, without feeding, prior to the experiment. One anemone was frozen and lyophilized 4 days after feeding, and the second 8 days after feeding. The MAA concentrations in the fed anemones were compared with those in three additional clonemates (controls) that were not fed lenses.

### *Analyses of MAAs*

Fresh, minced sea anemones or frozen lumpfish lenses were extracted in a refrigerator for 1 h in each of three changes of 100% HPLC-grade methanol; the material was sonicated for 30 s during the first extraction. Lyophilized tissues were similarly extracted, but in 80% aqueous methanol. To remove lipids and some lipophilic pigments, extracts of sea anemones were passed through a C18 Sep Pak Plus (Waters Corp., Milford, MA) before being injected onto the HPLC column.

Mycosporine-like amino acids were analyzed using the HPLC method described by Stochaj *et al.* (1994) and using quantitative standards prepared by W.C. Dunlap. The present analyses were carried out on a 250 mm × 4.6 mm Phenosphere 5-$\mu$m C8 column (Phenomenex, Torrance, CA). The mobile phase for methanolic extracts of sea anemones consisted of 55% aqueous methanol with 0.1% acetic acid, this concentration of methanol providing the best separation of mycosporine-2 glycine from porphyra-334 (Stochaj *et al.*, 1994). MAAs from extracts of lumpfish lenses, and of anemones consuming them, were also separated using a mobile phase of 25% aqueous methanol and 0.1% acetic acid to resolve the less polar MAAs. Detection was at 334 and 310 nm for all specimens, and also at 357 nm for lenses and anemones used in the feeding experiment.

### *Taxonomic affinities of MAAs*

Relationships among the four sympatric species of *Anthopleura* from Santa Cruz based on their MAA complements were examined by cluster analysis. Only the four MAAs that occurred in every specimen of all species studied were used in this analysis. Each of the four MAAs common to all species was expressed, for each specimen, as a molar fraction of the total MAA pool, and a matrix of distances was calculated using the average Euclidean distance (Sneath and Sokal, 1973). Distances were clustered using the unweighted pair group method algorithm (UPGMA), and the phenogram was constructed with *Statistica*, release 5.1 (StatSoft, Inc., Tulsa, OK).

## Results

### *MAA and algal complements in* A. elegantissima

In the 1993 collection of *A. elegantissima* from Washington, five MAAs were present in quantifiable amounts: mycosporine-taurine, shinorine, porphyra-334, mycosporine-2 glycine, and palythine, with mycosporine-2 glycine being the most concentrated. When the data for the four predominant MAAs were pooled for all specimens regardless of their algal complement, mycosporine-2 glycine accounted for half of the total concentration of MAAs (Fig. 2A). The highly variable level of palythine was always less than 10% of that of the next-most-concentrated MAA and is

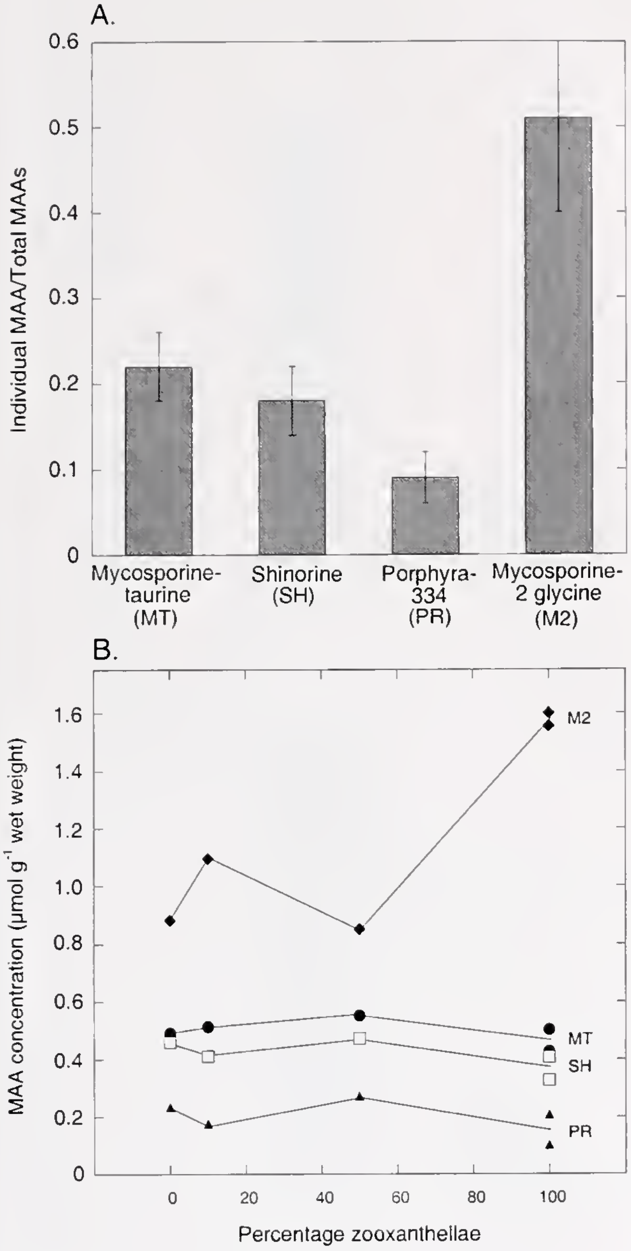

**Figure 2.** Mycosporine-like amino acids (MAAs) in specimens of *Anthopleura elegantissima* from Fidalgo Island, Washington, collected in 1993. (A) Proportion (molar fraction) of the total concentration of the four major MAAs represented by each. Data for 5 specimens were pooled regardless of their algal complement. Vertical bars represent ± 1 standard deviation (SD). (B) Concentration of individual MAAs in relation to the algal complement represented by zooxanthellae (percentage of total number of algae, zoochlorellae plus zooxanthellae). M2 = mycosporine-2 glycine; MT = mycosporine-taurine; SH = shinorine; PR = porphyra-334. Algal complement does not affect the relative concentrations of mycosporine-taurine, shinorine, or porphyra-334; the concentration of mycosporine-2 glycine is positively related to the proportion of zooxanthellae ($r^2$ = 0.816, $P$ = 0.036, $n$ = 5). Assuming a fresh tissue water content of 80% (Shick, 1991), MAA concentrations shown in (B) can be multiplied by 5 to convert to dry weight for comparison with other data on MAA concentrations presented on that basis.

not shown here. There was no obvious trend in the concentration of individual MAAs in anemones having mixed algal complements up to about 50% zooxanthellae: 50% zoochlorellae. However, the concentration of mycosporine-2 glycine in anemones harboring zooxanthellae exclusively was substantially greater than in anemones having mixed symbionts (Fig. 2B). There was a significant, positive relation between the concentration of this MAA and the arcsine-transformed proportion of zooxanthellae in the anemones ($r^2$ = 0.816, $P$ = 0.036, $n$ = 5). No other MAA concentration showed any significant relationship to the proportion of zooxanthellae ($P > 0.05$ in all cases).

In the 1996 collection from the same site, the sea anemones had a more balanced distribution of mycosporine-taurine and mycosporine-2 glycine, and intermediate, similar proportions of shinorine and porphyra-334, regardless of whether they harbored >90% zoochlorellae or >90% zooxanthellae (Fig. 3A and 3B). Of these four MAAs, Student's $t$ tests on arcsine-transformed data indicated that the molar proportions of three of them did not differ significantly between the predominantly zoochlorellate and predominantly zooxanthellate specimens; only shinorine showed a difference, its proportional concentration being marginally greater in the zoochlorellate anemones ($t$ = 2.852, $d.f.$ = 4, $P$ = 0.046).

## *Complements and concentrations of MAAs in sympatric species of* Anthopleura

Microscopic examination of the sea anemones from Santa Cruz confirmed that *A. artemisia* and aposymbiotic specimens of *A. elegantissima* lacked algal endosymbionts, and that *A. elegantissima*, *A. sola*, and *A. xanthogrammica* harbored only zooxanthellae. Collectively, these four species (including zooxanthellate and aposymbiotic individuals of *A. elegantissima* and large and small specimens of *A. xanthogrammica*) contained seven MAAs in quantifiable amounts, but only four of these (mycosporine-taurine, shinorine, porphyra-334, and mycosporine-2 glycine) occurred in all individuals of all species (Fig. 4). Palythine and palythene occurred in some specimens of all species except for *A. artemisia*, which never contained these MAAs but uniquely contained mycosporine-glycine:valine. The total concentration of the four common MAAs (Fig. 5) varied interspecifically [ANOVA, $F_{(5,\ 12)} = 11.923$, $P < 0.001$] among the anemones from Santa Cruz. Both zoochlorellate and zooxanthellate specimens of *A. elegantissima* from Washington (1996 collection) had the same apparent concentration of these MAAs as their zooxanthellate conspecifics from Santa Cruz. (Data for the Washington specimens were included in Fig. 5 for heuristic reasons, but were excluded from the statistical analysis of the sympatric populations from California. Zooxanthellate and zoochlorellate specimens from Washington did not differ in their total

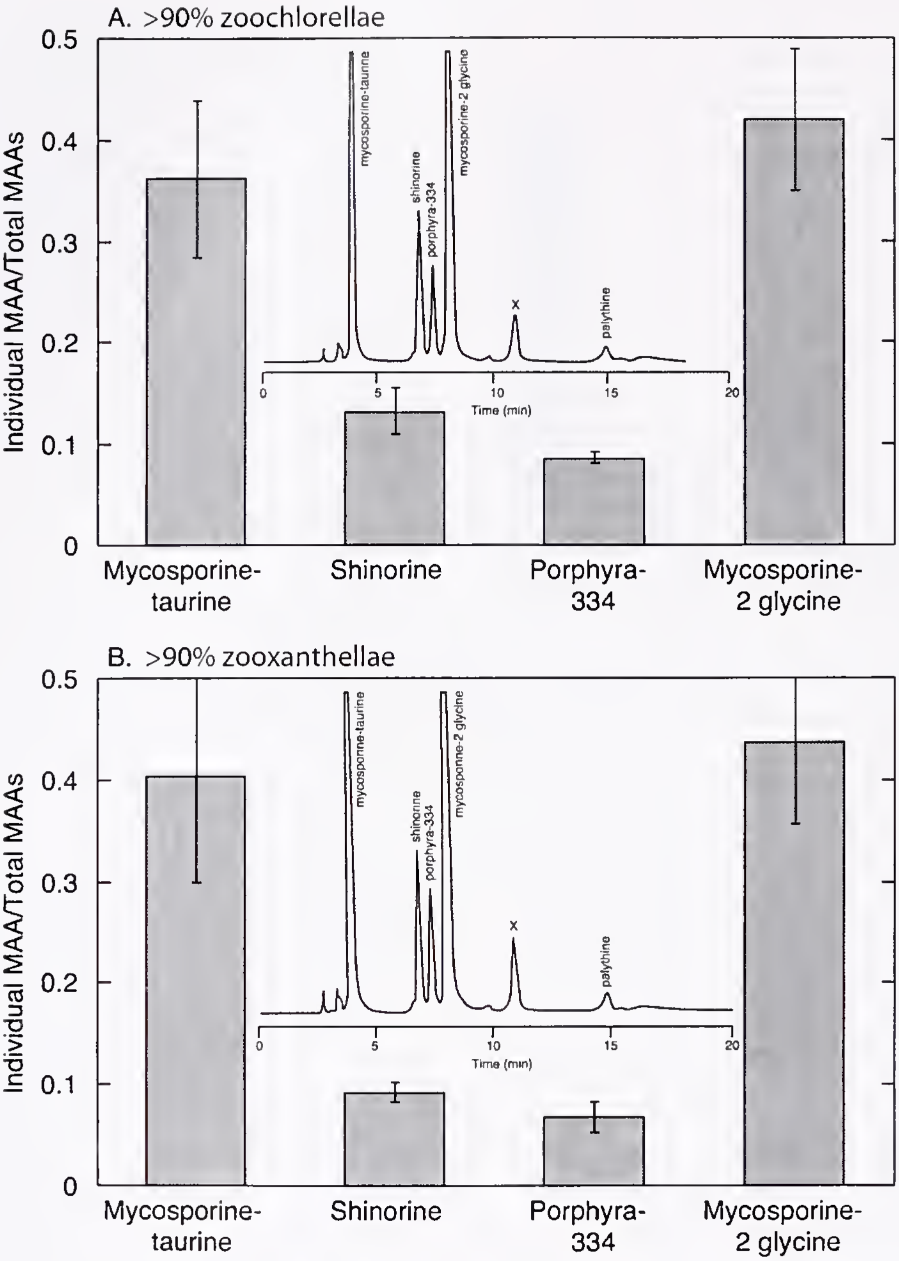

**Figure 3.** Proportions (molar fraction) of the major mycosporine-like amino acids (MAAs) in specimens of *Anthopleura elegantissima* collected at Fidalgo Island, Washington, in 1996. (A) Anemones in which the algal complement is >90% zoochlorellae. (B) Anemones in which the algal complement is >90% zooxanthellae. Only the proportion of shinorine differs significantly between predominantly zoochlorellate and predominantly zooxanthellate anemones ($t = 2.852$, $d.f. = 4$, $P = 0.046$). Vertical bars represent ± 1 standard deviation (SD), where $n = 3$ anemones in each group. Insets are HPLC chromatograms of the MAAs in a specimen that is 95% zoochlorellate (A) and in an entirely zooxanthellate individual (B); the peak indicated by an "X" is not an MAA.

concentration of MAAs [$t$ test, $P > 0.05$].) Student-Newmann-Keuls multiple comparison tests revealed the following relationships in the anemones from Santa Cruz. The asymbiotic species, *A. artemisia,* had the lowest absolute concentration of MAAs, overlapping with that in *A. sola,* which in turn overlapped with that in large specimens of *A. xanthogrammica.* The highest concentration occurred in *A. elegantissima* (whether zooxanthellate or aposymbiotic) and small specimens of *A. xanthogrammica.*

To facilitate interspecific comparisons, the molar propor-

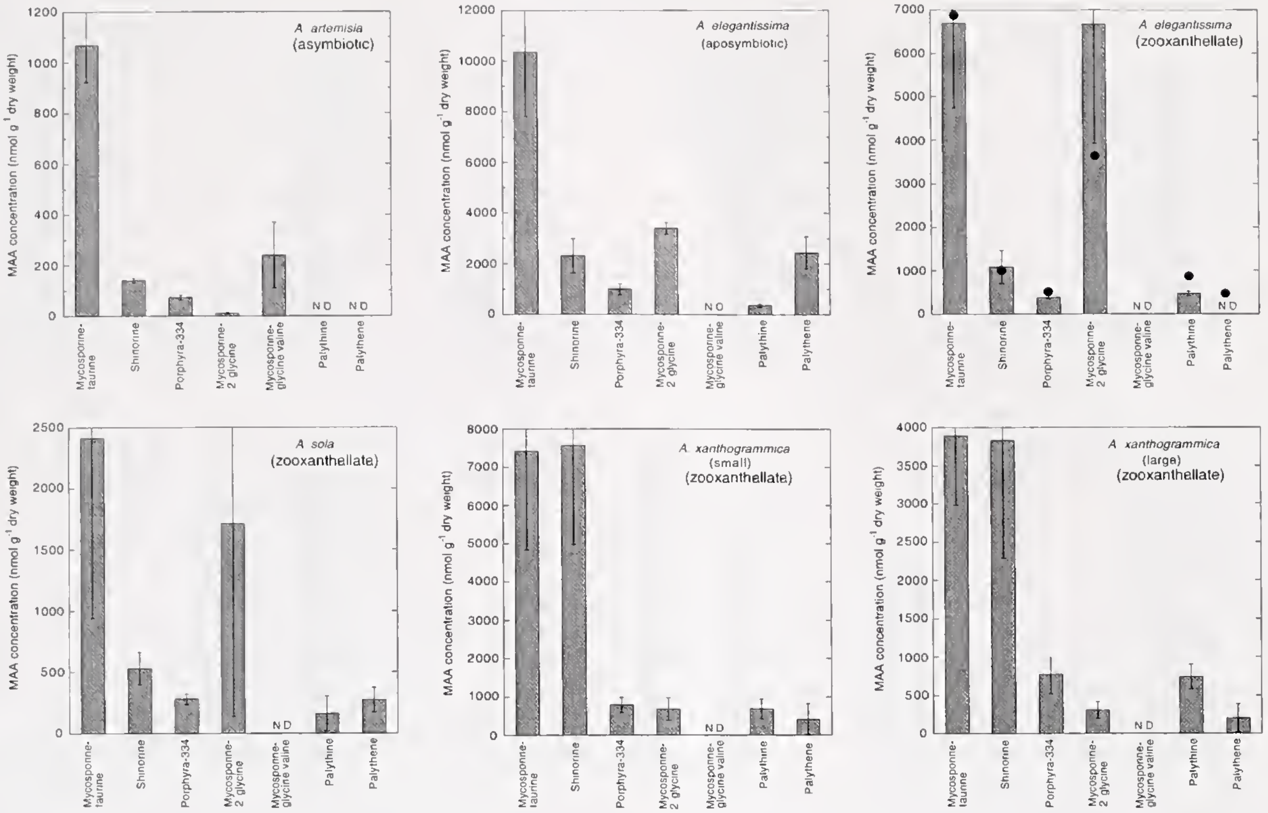

**Figure 4.** Concentrations of all quantifiable mycosporine-like amino acids (MAAs) in four species of *Anthopleura* collected in 1996 in Santa Cruz County, California, including aposymbiotic, laboratory-maintained specimens of *A. elegantissima*; $n = 3$ for each species or group. Solid points (●) represent MAA concentrations in a partially buried, bleached specimen of *A. elegantissima* collected from one of the same three clones from which the zooxanthellate specimens were taken. Vertical bars represent ± 1 standard deviation (SD).

tions of the four common MAAs in the Santa Cruz specimens are shown in Figure 6, where several patterns are evident. *A. elegantissima* presented the same relative distribution of MAAs as seen in the 1996 collection in Washington: approximately equal proportions of mycosporine-taurine and mycosporine-2 glycine, and intermediate proportions (≈0.05–0.15 molar fraction) of shinorine and porphyra-334. *A. xanthogrammica* was distinctly different, with mycosporine-taurine and shinorine each representing about 0.45 of the total MAAs. *A. artemisia* differed from both of the foregoing species in that mycosporine-taurine accounted for 0.8 of the total MAAs, and mycosporine-2 glycine was scarcely present. Aposymbiotic individuals of *A. elegantissima* showed an intermediate situation, having a proportion of mycosporine-2 glycine that was smaller than in zooxanthellate conspecifics but larger than in *A. artemisia* or *A. xanthogrammica*. *A. sola* evinced a proportion of mycosporine-2 glycine intermediate to that in *A. elegantissima* and the other species in the genus, amid much variation among individuals.

The phenogram (Fig. 7) based on the data in Figure 6 displays discrete clusters consistent with the foregoing qual-

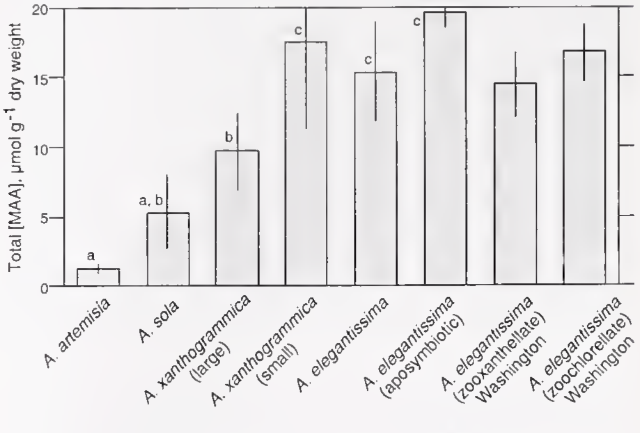

**Figure 5.** Total concentration of the four major mycosporine-like amino acids (MAAs) in *Anthopleura* spp. from Santa Cruz County, California, and in zoochlorellate and zooxanthellate specimens from Fidalgo Island, Washington; $n = 3$ for each group of California anemones, and $n = 5$ for both groups of Washington anemones (1996 data). Vertical bars represent ± 1 standard deviation (SD). Letters above each bar for the Santa Cruz anemones give the results of Student-Newmann-Keuls multiple comparison tests; groups having different letters differ significantly at $P = 0.05$. Washington anemones were not included in the ANOVA for the California populations of anemones, which were sympatric.

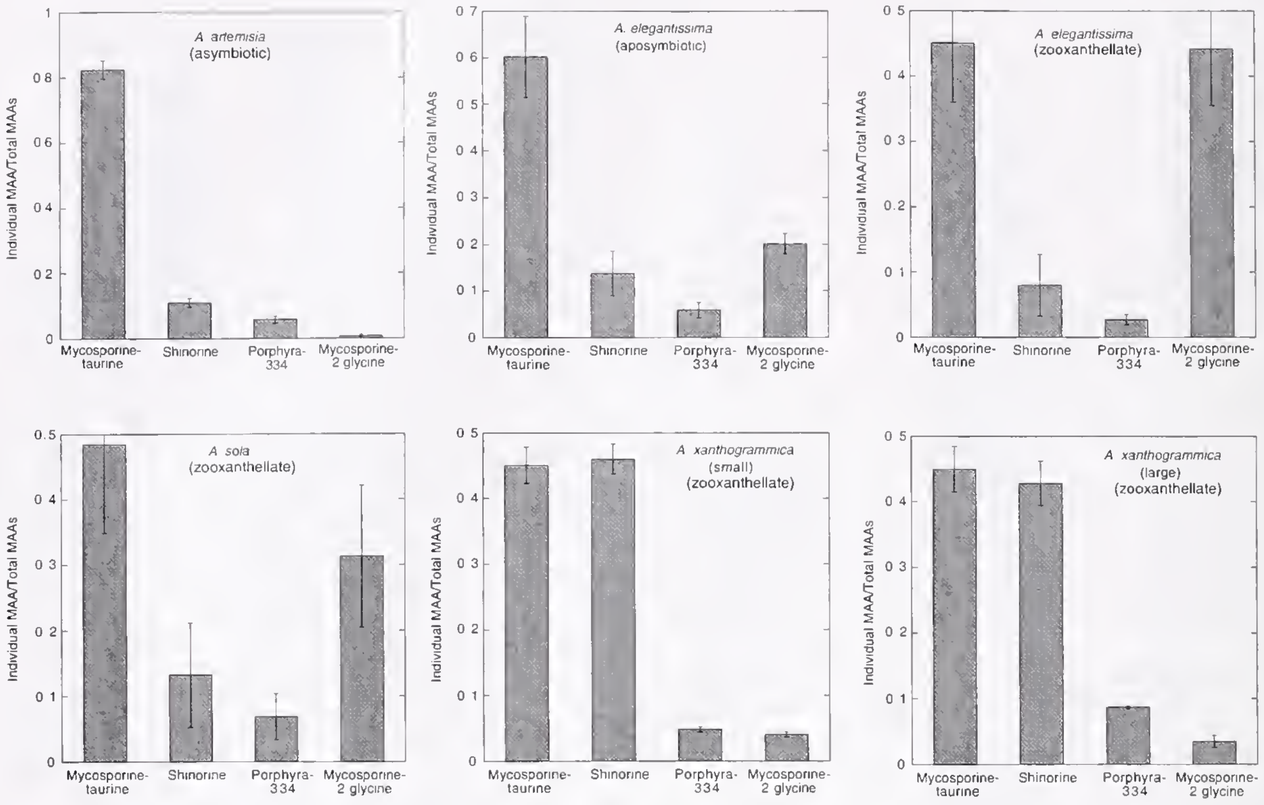

**Figure 6.** Proportional concentrations (molar fractions) of the four principal mycosporine-like amino acids (MAAs) common to all *Anthopleura* species from Santa Cruz County, California; $n = 3$ for each group. Vertical bars represent ± 1 standard deviation (SD). These data were used to construct the phenogram shown in Figure 7.

itative description. Specimens of both *A. artemisia* and *A. xanthogrammica* formed distinct clades. *A. sola* was not clearly separated from *A. elegantissima*. Aposymbiotic individuals of *A. elegantissima* presented a separate clade, and the occurrence of one specimen of *A. sola* in this clade was owing to its exceptionally low concentration of mycosporine-2 glycine (less than half the mean value for the group), yielding an MAA profile distinctly like that of aposymbiotic specimens of *A. elegantissima*. Large and small specimens of *A. xanthogrammica* were not separated by their molar fractions of MAAs used to construct the phenogram, but were separable by their absolute concentrations of MAAs (Figs. 4 and 5).

### *Feeding experiment*

Specimens of *A. elegantissima* readily ingested and retained the ocular lenses of *C. lumpus*. The fed anemones produced no visible fecal pellets or egesta, perhaps because the proteinaceous lenses (average $_{w}W = 23$ mg, which was ≈1% of the anemones' average fresh weight) were completely absorbed (a 1% ration of brine shrimps would be at least 90% absorbed: Zamer, 1986). These lenses contained principally palythene and usujirene, with a smaller amount of palythine and a trace of asterina-330 (not quantified). Unfed specimens of *A. elegantissima* from Bodega Bay contained the usual complement of MAAs seen in this species from the other locations, including palythine, and, exceptionally, usujirene, but no palythene. Clonemates of *A. elegantissima* given lumpfish lenses to eat did contain palythene 4 and 8 days after feeding (Fig. 8). Perhaps because of the relatively high endogenous concentrations of palythine in control anemones compared with the small amount available in a lens (Fig. 8A, B, top panel), the level of this MAA did not change significantly in fed anemones. The concentration of usujirene rose significantly by 4 days after feeding on a lens rich in this MAA, and declined to control levels by 8 days after a single meal of lumpfish lens. In those cases where ingesting a lumpfish lens led to a significant increase in the concentration of a particular MAA, the total change in that MAA was compared with the amount of that MAA available in the meal (Fig. 8B). For palythene, anemones eating a lens still contained 88% of this compound initially available in the lens (estimated from the MAA content of the second lens from the same fish) at 4 days, and 33% at 8 days after the meal. Perhaps because of the suboptimal chromatographic resolution of usujirene

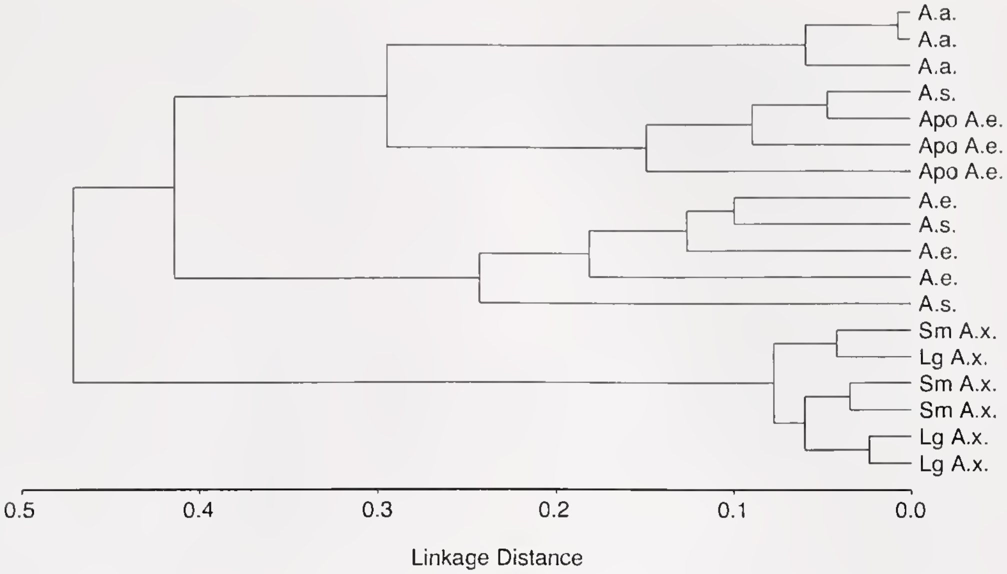

**Figure 7.** Similarity phenogram for three individual specimens of each *Anthopleura* species collected in Santa Cruz County, California, based on the proportional concentrations (molar fraction) of the four mycosporine-like amino acids (MAAs) shown in Figure 6. Similarity was determined by cluster analysis and is expressed as linked Euclidean distance. *A. a.* = *A. artemisia; A. e.* = *A. elegantissima;* Apo *A. e.* = aposymbiotic *A. elegantissima; A. s.* = *A. sola;* Lg *A. x.* = large *A. xanthogrammica;* Sm *A. x.* = small *A. xanthogrammica.*

in the anemone extracts, the significant elevation of this MAA at 4 days after feeding was apparently 20% greater than the amount available in the meal.

## Discussion

Our data show clearly, and for the first time, that the complement of MAAs in the four North American species of *Anthopleura* broadly reflects the taxonomic and phylogenetic differences among these species. This conclusion is supported by our other findings: that the profiles and concentrations of the major MAAs are independent of the presence or absence of algal endosymbionts, the taxon of the symbionts that are present, and of several environmental factors. Nevertheless, our evidence does suggest that *A. elegantissima* can accumulate MAAs from its food, which may explain the temporal and local variations seen in the MAA profile, and the occurrence of minor MAAs in some individuals. These findings and others (Shick and Dunlap, 2002) lead us, finally, to consider the possibility that MAAs are synthesized *de novo* by the sea anemones.

### *Phylogeny of* Anthopleura *spp. as deduced from their complements of MAAs*

In the phenogram (Fig. 7) based on the proportional complements of the four major MAAs in *Anthopleura* spp. from California, specimens of *A. artemisia* and *A. xanthogrammica* form distinct clades. However, unlike the phylogenetic tree of Geller and Walton (2001) based on mitochondrial DNA sequences, in which the three species having algal endosymbionts form an unresolved trichotomy, the MAA complements indicate that *A. elegantissima* and *A. sola* are more closely related to each other than either is to *A. xanthogrammica.*

*A. elegantissima* and *A. sola* are difficult to distinguish morphologically (Francis, 1979), and Smith and Potts (1987) were unable to distinguish them by allozymic analysis. The reproductive isolation of the two species was confirmed only by a more thorough genetic study using allozymes (McFadden *et al.*, 1997), and by the analysis of Geller and Walton (2001), which was able to separate them by fixed differences in base pairs. Our finding that *A. elegantissima* and *A. sola* cluster together, distinct from *A. xanthogrammica,* supports the view of Pearse and Francis (2000) that they are sibling species and the view of McFadden *et al.* (1997) that the speciation was probably relatively recent.

Although it is gratifying, the finding that MAAs may contribute to phylogenetic understanding renders problematic any interpretations of the environmental factors affecting the MAA composition in a species of *Anthopleura*—that is, discriminating between the expression of this character as enforced by natural selection or as an ancestral legacy (Mangum and Hochachka, 1998). Until the biochemical steps involved in synthesizing and modifying individual MAAs *in vivo* have been elucidated and the factors controlling their expression have been determined, the issue will not be resolved.

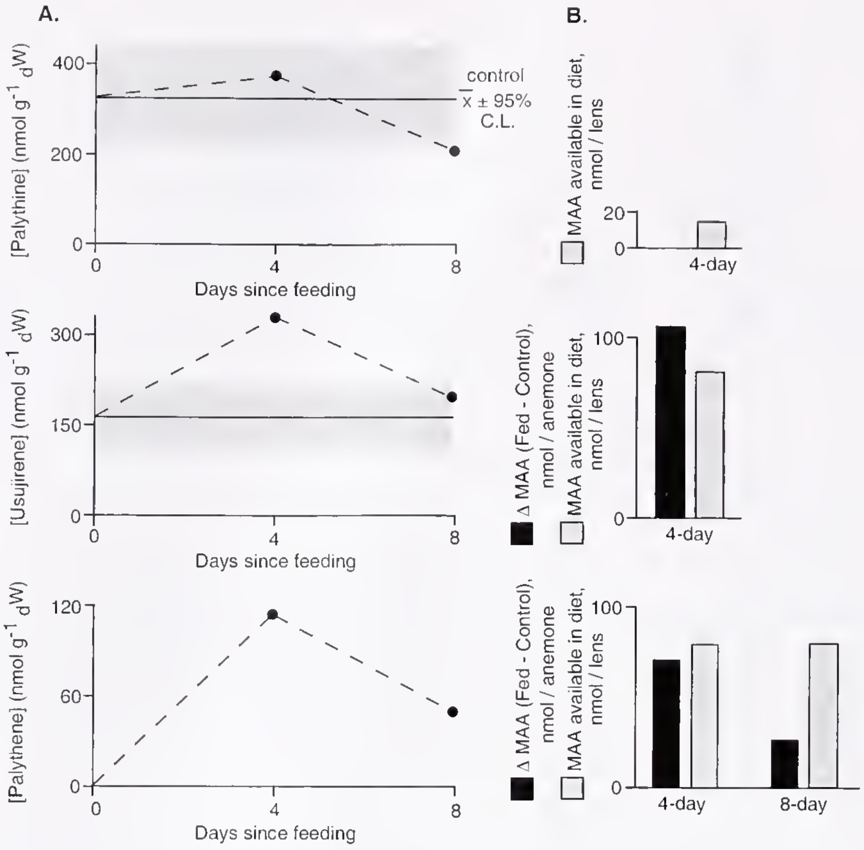

**Figure 8.** (A) Concentrations of the major mycosporine-like amino acids (MAAs) from the lenses of lumpfish (*Cyclopterus lumpus*) present in two specimens of *Anthopleura elegantissima* 4 and 8 days after ingesting a lens. Shaded area represents 95% confidence interval for pre-feeding concentrations of MAAs based on analyses of three unfed clonemates (controls) of the experimental anemones. Palythene was not present in the control anemones. (B) Where significant, the increase in total MAA content (ΔMAA, Fed minus Control) of an anemone eating a lens (solid bars) is compared with the amount of that MAA available in the contralateral lens (shaded bars) from the same fish.

### *Role of algal endosymbionts in determining the complements of MAAs in the anemones*

The foregoing says nothing of the possible role of the algal endosymbionts—another layer of genotypic complexity to be considered—although the adoption of symbiosis itself is a trait that has been important in the evolution of the genus (Geller and Walton, 2001). Our data for the Washington specimens of *A. elegantissima* that harbored exclusively zooxanthellae or zoochlorellae (the extremes of the continuum in Fig. 2B) clearly demonstrate that the identity of the alga does not qualitatively affect the MAAs that are present in the consortium. This in turn strongly suggests that, in these anemones, the algal endosymbionts are not the source of the MAAs in the consortium, although the algae might provide a necessary precursor (such as deoxygadusol: Shick and Dunlap, 2002). That the algae do not determine the MAA complement is also indicated by our finding that the same proportional MAA complement occurs in anemones harboring predominantly (>90%) one alga or the other (Fig. 3). It is conceivable that one type of alga produces MAAs and the other does not, so that the former, even if a minor proportion of the total algal complement, could produce the MAAs detected in the mixed symbiosis, but this would be inconsistent with our interpretation of the data for anemones harboring exclusively one alga or the other. Unfortunately, neither zoochlorellae nor *S. muscatinei* (the species of zooxanthella that occurs in Washington specimens of *A. elegantissima*: LaJeunesse and Trench, 2000) has been cultured successfully, so it is not known whether either can indeed produce MAAs. The placement of *S. muscatinei* in lineage B of the established phylotypes of *Symbiodinium* spp. (*e.g.*, Rowan, 1998; LaJeunesse, 2001) suggests that it does not produce MAAs, because none of the other species in this clade do (Banaszak *et al.*, 2000; LaJeunesse, 2001).

Because MAAs that have accumulated in animal tissues have a long residence time (Carroll and Shick, 1996; Adams and Shick, 1996, 2001; Newman *et al.*, 2000), it is also conceivable that the MAAs present in an anemone at a particular time are products not just of its population of symbionts at that time, but also of an earlier suite of symbionts. As has been shown in *A. elegantissima* (Saunders and Muller-Parker, 1997) and *A. xanthogrammica* (Bates, 2000), the symbiont population can change temporally, according to environmental factors. However, complete symbiont-switching has not been reported in *A. elegantissima*, and Weis and Levine (1996) found that naturally aposymbiotic specimens could not be experimentally infected with algae, and that anemones rendered aposymbiotic in the laboratory could be reinfected only with difficulty, and then only with the original algae. The most parsimonious explanation remains that zoochlorellae and *S. muscatinei* in Washington specimens of *A. elegantissima* are not the source of MAAs in those sea anemones.

In contrast to the foregoing conclusion, there are indications, at least in *A. elegantissima*, that the level of mycosporine-2 glycine in an anemone is associated with its density of zooxanthellae. Whereas the concentrations of MAAs did not differ among most Washington anemones having very different proportions of zoochlorellae and zooxanthellae, mycosporine-2 glycine was significantly elevated in individuals harboring *exclusively* zooxanthellae (Fig. 2B). Similarly, in the California anemones, aposymbiotic specimens of *A. elegantissima* had a lower proportion of mycosporine-2 glycine than zooxanthellate specimens (Fig. 6), which clearly separated the former from the latter, and, furthermore, placed the apozooxanthellate individuals nearer to the asymbiotic *A. artemisia* (Fig. 7), which scarcely contained any mycosporine-2 glycine. A lower level of mycosporine-2 glycine was also seen in a naturally bleached clonemate of one of the specimens of *A. elegantissima* from Santa Cruz (Fig. 4), as well as in naturally aposymbiotic individuals of *A. elegantissima* from Bodega Bay (Stochaj *et al.*, 1994) and Santa Barbara, California (Banaszak and Trench, 1995). The correspondence between the zooxanthellate condition and high levels of mycosporine-2 glycine was not absolute, however, because the levels of this MAA were relatively low in zooxanthellate specimens of *A. xanthogrammica*, and all specimens of all *Anthopleura* species contained some mycosporine-2 glycine (Fig. 2B and Fig. 4).

The situation is further complicated by the finding of Banaszak and Trench (1995) that *S. californium* isolated from *A. elegantissima* did not produce any MAAs in culture, nor indeed did these authors detect mycosporine-2 glycine in any species of zooxanthella cultured from diverse symbioses (Banaszak *et al.*, 2000). However, the mobile phase they used (25% aqueous, acidic methanol) would not have resolved mycosporine-2 glycine from porphyra-334, even if it were present (Stochaj *et al.*, 1994); and we (J. M. Shick and C. Ferrier-Pagès, unpubl. results) subsequently have found mycosporine-2 glycine in zooxanthellae cultured from the scleractinian coral *Galaxea fascicularis*.

The failure of *S. californium* to produce MAAs in culture is also strong evidence that zooxanthellae are not the source of the MAAs found in those symbiotic specimens of *A. elegantissima* from California that harbor this alga (Banaszak and Trench, 1995), nor perhaps in the sympatric *A. sola* and *A. xanthogrammica*, assuming that they also include *S. californium*. Because the anemones from Santa Cruz probably also harbor *S. muscatinei* (LaJeunesse and Trench, 2000), MAAs might originate with this species of zooxanthella; but as already mentioned, based on its phylotype it is doubtful that *S. muscatinei* can produce MAAs. Consider also that zooxanthellae cultured from a symbiosis may not reflect the entire complement of algal genotypes present *in hospite* (Santos *et al.*, 2001); thus, although *S. californium* in culture does not produce MAAs (Banaszak *et al.*, 2000), the host anemones might contain other phylotypes of *Symbiodinium* that do. Zooxanthellae might also provide an essential precursor, such as deoxygadusol, that the anemones use to synthesize MAAs (Shick and Dunlap, 2002).

Even if the endosymbiotic algae are not the source of the MAAs in *Anthopleura* species, might their presence stimulate the accumulation of MAAs (from whatever source) in the host anemone? Aposymbiotic and zooxanthellate anemones differ qualitatively in their expression of proteins (Weis and Levine, 1996; Stochaj and Grossman, 1997) induced by the algae, and the presence of zooxanthellae enhances the synthesis of carbonic anhydrase by the host in *A. elegantissima* (Weis and Reynolds, 1999). Might the presence of algal endosymbionts also affect the expression of host enzymes involved in the biosynthesis or modification of MAAs (especially mycosporine-2 glycine)? The specific enzymes involved in the metabolism of MAAs have not been identified to test this possibility.

### *Role of solar radiation in determining the concentrations of MAAs in* Anthopleura *spp.*

Are there environmental correlates that are consistent with a sunscreening role of the compounds? Again, the evidence is equivocal, which is not surprising in light of previous experiments showing that varying the exposure of the anemones to UVR did not affect the concentrations of MAAs in zooxanthellate or aposymbiotic individuals of *A. elegantissima* (Scelfo, 1988; Stochaj *et al.*, 1994; Banaszak and Trench, 1995). Nevertheless, concentrations of MAAs are lowest in *A. artemisia* (Fig. 4), which typically inhabits sheltered microhabitats, such as deep holes in rocks and rocks buried in sand, so that only its oral disc is visible (Hand, 1955; Pearse and Francis, 2000). Might constitutively low concentrations of MAAs reflect the restriction of this species to sheltered microhabitats? *A. sola* and large individuals of *A. xanthogrammica* exhibit the next-lowest concentrations of MAAs. These are low intertidal species that extend well into the subtidal or occur in tidepools and thus experience lower solar irradiances than does the characteristically intertidal *A. elegantissima*, which typically is exposed to direct sunlight during aerial exposure (Pearse, 1974; Shick and Dykens, 1984), and which has the highest concentrations of MAAs. Although low by comparison with the concentrations of MAAs in tropical corals ($\approx$150–1000 nmol MAA $mg^{-1}$ protein), those in *Anthopleura* species (Fig. 5: 10–20 $\mu$mol MAA $g^{-1}$ dry weight, equivalent to about 15–30 nmol MAA $mg^{-1}$ protein) are the same as in temperate red macroalgae ($\approx$10 $\mu$mol MAA $g^{-1}$ dry weight: Karsten *et al.*, 1998).

Several uncertainties temper this seemingly clear environmental correlation. Anemones from Fidalgo Island have concentrations of MAAs as high as those in specimens of *A. elegantissima* at Santa Cruz (Fig. 5). This is true even though the Fidalgo Island anemones live at a latitude 11° higher, and thus have lower daily and seasonal exposures to solar UVR (Madronich, 1993) than the Santa Cruz specimens (although the coastal fog in California in summer, and the early-morning timing of summer low tides, may diminish the dose of UVR there). Concentrations of MAAs in small specimens of *A. xanthogrammica* are just as high as those in *A. elegantissima;* however, small specimens of *A. xanthogrammica* settle in mussel beds, where ours were collected, and move to the low intertidal only as they grow in size. Thus, their relatively high levels of MAAs are not unexpected. We do not know whether concentrations in the former specimens changed while they were held in shallow outdoor aquaria for 3 months before analysis, although the aforementioned experiments with *A. elegantissima* suggest that they would not. Also, the concentration of MAAs in large specimens of *A. xanthogrammica* may be low compared with smaller specimens, because large individuals may have disproportionally greater amounts of extracellular mesoglea (Shick, 1991) relative to the mass of cells in which the MAAs are located, leading to a low mass-specific concentration of MAAs. The same may apply to large specimens of *A. sola*, as compared with small specimens of *A. elegantissima*. Finally, concentrations of MAAs in aposymbiotic individuals of *A. elegantissima* held in darkness in the laboratory for more than 1 year are just as high as or higher than in zooxanthellate specimens, as are those in a naturally bleached clonemate of the latter (Fig. 4; also see Stochaj *et al.*, 1994; and Banaszak and Trench, 1995). Thus, proximal environmental effects as determinants of MAA concentrations seem less important than these four species' evolutionary histories, including broad interspecific differences in habitat.

### *Other possible physiological functions of MAAs*

MAAs function as osmolytes in cyanobacteria (Oren, 1997; Portwich and Garcia-Pichel, 1999), but this role does not seem important in sea anemones, because in *A. elegantissima*, the concentration of MAAs is only 3% of that of free amino acids (FAAs), the principal organic intracellular osmotic effectors here (Shick, 1991; Shick and Dunlap, 2002).

Next, FAAs have been implicated as "host factors" that induce the release of photosynthate from the endosymbiotic algae (Gates *et al.*, 1995), and taurine in particular has been studied as such by Wang and Douglas (1997). Might mycosporine-taurine or other MAAs also have such a regulatory role in these symbioses, as proposed by Gates *et al.* (1995)? The concentrations of MAAs are lowest in the asymbiotic *A. artemisia* (Fig. 4 and Fig. 5) and are higher in the symbiotic species, and mycosporine-2 glycine varies with the proportion of zooxanthellae in *A. elegantissima* (Fig. 2B); these facts are consistent with a role of MAAs as a host factor. A high concentration of MAAs in aposymbiotic individuals of *A. elegantissima* does not necessarily argue against such a role because aposymbiosis is a secondary, environmentally imposed condition that would not *per se* affect the inherent capacity of the host to accumulate MAAs from exogenous sources. Nevertheless, it remains to be established whether mycosporine-taurine, mycosporine-2 glycine, or any other MAA at physiologically relevant concentrations effects the release of photosynthate by zooxanthellae or zoochlorellae.

Finally, because specimens of *A. elegantissima* harboring these different algae have identical complements of MAAs, these compounds are unlikely to account for the differential palatability of zoochlorellate and zooxanthellate specimens to a predatory fish (Augustine and Muller-Parker, 1998), and both types of anemones are readily eaten by a predatory nudibranch (Seavy and Muller-Parker, 2002). In short, a clear physiological (osmolyte or host factor) or defensive (sunscreening or feeding deterrent) role for MAAs that would explain their patterns of occurrence among species of *Anthopleura* remains to be elucidated.

### *The role of dietary MAAs*

Our experiments unequivocally show that *A. elegantissima* can absorb MAAs from its food and retain them for at least 8 days (Fig. 8). Not only does this result support a possible trophic origin of MAAs in sea anemones, but it also may explain local and temporal differences in the complement of minor and trace MAAs (*cf.* Stochaj *et al.*, 1994, and Banaszak and Trench, 1995), including the unusual and surprising occurrence of usujirene in specimens of *A. elegantissima* from Bodega Bay used in our feeding experiment. The possibility that unpredictable variations in diet can affect the complement of MAAs in a population must be borne in mind when interpreting qualitative field surveys of MAAs in diverse animal taxa, particularly if the data are intended to delineate broad phylogenetic patterns (Karentz, 2001). This seems particularly relevant in polyphagous opportunists such as sea anemones (Shick, 1991). Indeed, such stochastic variability in the minor MAAs (*e.g.*, we had never seen usujirene in diverse seasonal collections of *A. elegantissima* from Bodega Bay dating back to 1988) prompted us to use only the four MAAs that occur in all specimens of all species in constructing the phylogeny (although this obscured the qualitative differences between *A. artemisia* and the other three species: Fig. 4). Thus, like these compounds in cyanobacteria (Karsten and Garcia-Pichel, 1996), dinoflagellates (Carreto *et al.*, 2001), and cultured zooxanthellae (Banaszak *et al.*, 2000; LaJeunesse, 2001), the predominant MAAs in *Anthopleura* spp. do appear to be useful phylogenetic characters.

Determining the diet and ration in sea anemones is tedious work, but it has been done in *A. elegantissima* (Sebens, 1981; Zamer, 1986). To establish the relative importance of various food items in affecting the MAAs present in the anemones in nature would require long-term studies of the MAAs in their natural diet for comparison with their own time-averaged complement of MAAs. A single sample of the phytoplankton, zooplankton, and particulate detritus $>25$ $\mu$m diameter in the water column above the population of *A. elegantissima* at Bodega Bay (J.M. Shick, unpubl. data) revealed the presence of most major and minor MAAs found in the anemones (including usujirene). The exceptions were mycosporine-glycine:valine and mycosporine-taurine, the latter being the predominant MAA that apparently is unique to anemones in this genus. Thus, mycosporine-taurine may be produced by the anemones themselves, perhaps by modifying other MAAs, as seems to be the case for certain MAAs and their precursors in corals (Shick *et al.*, 1999), holothuroid echinoderms (Dunlap and Shick, 1998), fishes (Mason *et al.*, 1998), and red macroalgae (Franklin *et al.*, 1999).

As we have noted elsewhere (Stochaj *et al.*, 1994), taurine is by far the most concentrated component of the free amino acid pool in *Anthopleura* species. Although the biosynthetic origin of mycosporine-taurine remains enigmatic, it may result from the modification of a pre-existing (dietary) MAA or deoxygadusol by the substitution of taurine in the chromophore conjugation. Thus, the anemones may be exploiting the ready availability of this amino acid to synthesize mycosporine-taurine, which not only absorbs the shortest, most damaging UV wavelengths (309 nm) of any MAA, but which moreover is a moderate antioxidant (Shick *et al.*, 1996; Shick and Dunlap, 2002). This is an important consideration for a phototrophic symbiosis, in which the metazoan host experiences hyperoxia (Dykens and Shick, 1982), because this hyperoxia, together with exposure of the animal to solar UVR, leads to an enhanced flux of reactive oxygen species (Dykens *et al.*, 1992).

We deliberately collected the specimens from Santa Cruz in a habitat where all four species of *Anthopleura* are present in close proximity, to ensure that all of them potentially have access to the same prey. Although Sebens (1981) documented size-related differences between *A. elegantissima* and *A. xanthogrammica* in the prey that they capture, he also found considerable overlap between these species in their major food items. Therefore, if the MAA complements of these anemones are affected by their diets, their disparate MAA spectra are surprising, unless the heavier reliance of *A. xanthogrammica* on mussels (*Mytilus* spp.), which are rich in shinorine (Chioccara *et al.*, 1979, 1985; J. M. Shick, unpubl. data), enhances the concentration of this MAA in *A. xanthogrammica*.

*A. artemisia* consistently contained an MAA that we never saw in any of the other species—mycosporine-glycine:valine. This MAA is common in Antarctic phytoplankton and the krill that eat them (Karentz *et al.*, 1991; Dunlap *et al.*, 1995; Newman *et al.*, 2000); this substance has also been found in a red-tide dinoflagellate (Vernet and Whitehead, 1996) and in particulate organic matter (Whitehead and Vernet, 2000) in California coastal waters. Thus, mycosporine-glycine:valine probably is present in the plankton available to all of these *Anthopleura* species (although it was not in the assemblage of particulate material sampled at Bodega Bay), and its restriction to *A. artemisia* underscores the biochemical distinction of this species from its sympatric congeners. This finding of a unique MAA, together with the absence of palythine and palythene from this species alone of the four (Fig. 4), reinforces the phylogenetic conclusion of Geller and Walton (2001) that *A. artemisia* is not closely related to the other three species, but belongs to a western Pacific clade of the genus *Anthopleura*.

Diet does not explain the MAA complement in aposymbiotic specimens of *A. elegantissima* maintained in the laboratory. Stochaj *et al.* (1994) suggested a dietary source of MAAs in laboratory-maintained aposymbiotic specimens, but the UV-absorbing compounds in the squid fed to the anemones in that study subsequently proved not to be MAAs, and the MAA complement after month-long feeding on this diet was the same as in freshly collected specimens (J.M. Shick, unpubl. data). Aposymbiotic individuals maintained in the laboratory in Santa Cruz for more than 1 year and occasionally fed previously frozen adult brine shrimps (*Artemia* sp.) had the same MAA complement, although in different proportions, as zooxanthellate individuals fresh from the field (Fig. 6). Those brine shrimps were not analyzed for MAAs, but results for other samples of *Artemia* indicate that they probably contained principally shinorine, along with some asterina-330 and porphyra-334 (Grant *et al.*, 1985), and possibly mycosporine-2 glycine (J.M. Shick, unpubl. data); *Artemia* tissues also contain gadusols (Grant *et al.*, 1985), likely precursors of MAAs (Shick and Dunlap, 2002). The diet may provide the gadusols and certain MAAs that the sea anemones ultimately convert into the suites of MAAs that characterize the several species.

### De novo *biosynthesis of MAAs by cnidarians?*

As we have noted here and elsewhere (Shick and Dunlap, 2002), the same major MAAs occur in aposymbiotic and zooxanthellate individuals of *A. elegantissima*, and controlled diets fail to modify this pattern; moreover, zooxanthellae freshly isolated from *A. elegantissima* lack MAAs, and cultured *S. californium* apparently cannot synthesize MAAs (Banaszak and Trench, 1995). These considerations all suggest that the anemones themselves make these compounds. The tentative finding that scleractinian corals can synthesize aromatic amino acids (Fitzgerald and Szmant, 1997) may also point to the unexpected presence of the shikimic acid pathway in these metazoans. But like Fitzgerald and Szmant (1997), we might equivocate, suggesting that like aromatic amino acids, the MAAs originate in bacteria associated with the anemones, although only one marine bacterium has ever been reported to produce MAAs (Arai *et al.*, 1992). Alternatively, the algal endosymbionts and the food might be sources of deoxygadusol, which the animal host might use to produce MAAs. Testing these possibilities, and looking more rigorously in cnidarians for, especially, the early steps of the shikimic acid pathway (including the postulated branchpoint leading to MAAs *via* deoxygadusol), might clarify the otherwise unexplained presence of certain MAAs in these metazoans.

In summary, the complements of the MAAs in four species of *Anthopleura* seem more closely associated with their phylogenetic position than with other factors. Several lines of evidence indicate that the algal endosymbionts do not contribute the MAAs seen in the symbiotic anemones, although in *A. elegantissima* the level of mycosporine-2 glycine does seem to be affected by the predominance of zooxanthellae. The successful culturing of zoochlorellae and of *Symbiodinium muscatinei* would facilitate the analysis of their MAA complements and do much to resolve the uncertainty about their contributions to the suite of MAAs in the symbiosis. Identifying the enzymes involved in the biosynthesis of primary MAAs, and in the secondary structural modification of these, remains a major unresolved problem. Its solution would allow us to study the phylogenetic distribution of the enzymes in concert with the occurrence of particular MAAs, and would also permit us to study the factors that affect the expression and regulation of these enzymes.

## Acknowledgments

We thank Dr. Gisèle Muller-Parker for collecting the sea anemones in Washington, and Drs. James Clegg and Dennis Hedgecock for facilities and facilitation at the Bodega Marine Laboratory. We are grateful to Donald Mason, who first identified the MAAs present in lumpfish lenses, where the rare presence of usujirene suggested their use as a source of this dietary marker, and to Amy Carroll, who assisted in the laboratory. We appreciate Dr. Irv Kornfield's advice regarding the cluster analysis and his comments on the manuscript, and Francis Wihbey's assistance with producing the map. We thank the editors and two anonymous reviewers for their heroic efforts. This research was supported by U.S. National Science Foundation grant IBN-9316426 to J.M. Shick and W.C. Dunlap, and in part by a grant from the National Geographic Society to J.M. Shick.

## Literature Cited

**Adams, N. L., and J. M. Shick. 1996.** Mycosporine-like amino acids provide protection against ultraviolet radiation in eggs of the green sea urchin, *Strongylocentrotus droebachiensis. Photochem. Photobiol.* **64:** 149–158.

**Adams, N. L., and J. M. Shick. 2001.** Mycosporine-like amino acids prevent UVB-induced abnormalities during early development of the green sea urchin *Strongylocentrotus droebachiensis. Mar. Biol.* **138:** 267–280.

**Adams, N. L., J. M. Shick, and W. C. Dunlap. 2001.** Selective accumulation of mycosporine-like amino acids in ovaries of the green sea urchin, *Strongylocentrotus draebachiensis*, is not affected by ultraviolet radiation. *Mar. Biol.* **138:** 281–294.

**Arai, T., M. Nishijima, K. Adachi, and H. Sano. 1992.** Isolation and structure of a UV absorbing substance from the marine bacterium *Micrococcus* sp. AK-334. Pp. 88–94 in *MBI Report 1992*. Marine Biotechnology Institute, Tokyo.

**Augustine, L., and G. Muller-Parker. 1998.** Selective predation by the mosshead sculpin *Clinocottus globiceps* on the sea anemone *Anthopleura elegantissima* and its two algal symbionts. *Limnol. Oceanogr.* **43:** 711–715.

**Banaszak, A. T., and R. K. Trench. 1995.** Effects of ultraviolet (UV) radiation on marine microalgal-invertebrate symbioses. II. The synthesis of mycosporine-like amino acids in response to exposure to UV in *Anthopleura elegantissima* and *Cassiopeia xamachana. J. Exp. Mar. Biol. Ecol.* **194:** 233–250.

**Banaszak, A. T., T. C. LaJeunesse, and R. K. Trench. 2000.** The synthesis of mycosporine-like amino acids (MAAs) by cultured, symbiotic dinoflagellates. *J. Exp. Mar. Biol. Ecol.* **249:** 219–233.

**Bandaranayake, W. M. 1998.** Mycosporines: Are they nature's sunscreens? *Nat. Prod. Rep.* **15:** 159–172.

**Bates, A. 2000.** The intertidal distribution of two algal symbionts hosted by *Anthopleura xanthogrammica* (Brandt, 1835). *J. Exp. Mar. Biol. Ecol.* **249:** 249–262.

**Bentley, R. 1990.** The shikimate pathway—a metabolic tree with many branches. *Crit. Rev. Biochem. Mol. Biol.* **25:** 307–384.

**Carreto, J. I., M. O. Carignan, and N. G. Montoya. 2001.** Comparative studies on mycosporine-like amino acids, paralytic shellfish toxins and pigment profiles of the toxic dinoflagellates *Alexandrium tamarense, A. catenella* and *A. minutum. Mar. Ecol. Prog. Ser.* **223:** 49–60.

**Carroll, A. K., and J. M. Shick. 1996.** Dietary accumulation of mycosporine-like amino acids (MAAs) by the green sea urchin (*Strongylocentrotus droebachiensis*). *Mar. Biol.* **124:** 561–569.

**Chalker, B. E., W. C. Dunlap, A. T. Banaszak, and P. J. Moran. 1988.** UV-absorbing pigments in *Acanthaster planci:* photoadaptation during the life history of reef invertebrates. Page 15 in *Abstracts. Proceedings of the Sixth International Coral Reef Symposium.* J. H. Choat and O.

Bellwood, eds. Organizing Committee of the Sixth International Coral Reef Symposium, Townsville, Australia.

**Chioccara, F., G. Misuraca, E. Novellino, and G. Prota. 1979.** Occurrence of two new mycosporine-like aminoacids, mytilins A and B in the edible mussel, *Mytilus galloprovincialis*. *Tetrahedron Lett.* **34:** 3181–3182.

**Chioccara, F., G. Prota, and E. Novellino. 1985.** Occurrence and distribution of mycosporine-like amino acids in *Mytilus galloprovincialis* and related bivalv[e]s. *Gazz. Chim. Ital.* **115:** 643–647.

**Dunlap, W. C., and J. M. Shick. 1998.** Ultraviolet radiation-absorbing mycosporine-like amino acids in coral reef organisms: a biochemical and environmental perspective. *J. Phycol.* **34:** 418–430.

**Dunlap, W. C., D. M. Williams, B. E. Chalker, and A. T. Banaszak. 1989.** Biochemical photoadaptations in vision: UV-absorbing pigments in fish eye tissues. *Comp. Biochem. Physiol.* **93B:** 601–607.

**Dunlap, W. C., G. A. Rae, E. W. Helbling, V. E. Villafañe, and O. Holm-Hansen. 1995.** Ultraviolet absorbing compounds in natural assemblages of Antarctic phytoplankton. *Antarct. J. US* **30:** 323–325.

**Dykens, J. A., and J. M. Shick. 1982.** Oxygen production by endosymbiotic algae controls superoxide dismutase activity in their animal host. *Nature* **297:** 579–580.

**Dykens, J. A., J. M. Shick, C. Benoit, G. R. Buettner, and G. W. Winston. 1992.** Oxygen radical production in the sea anemone *Anthopleura elegantissima* and its endosymbiotic algae. *J. Exp. Biol.* **168:** 219–241.

**Favre-Bonvin, J., J. Bernillon, N. Salin, and N. Arpin. 1987.** Biosynthesis of mycosporines: mycosporine glutaminol in *Trichothecium roseum*. *Phytochemistry* **29:** 2509–2514.

**Fitzgerald, L. M., and A. M. Szmant. 1997.** Biosynthesis of "essential" amino acids by scleractinian corals. *Biochem. J.* **322:** 213–221.

**Francis, L. 1979.** Contrast between solitary and clonal lifestyles in the sea anemone *Anthopleura elegantissima*. *Am. Zool.* **19:** 669–681.

**Franklin, L. A., I. Yakoleva, U. Karsten, and K. Lüning. 1999.** Synthesis of mycosporine-like amino acids in *Chondrus crispus* (Florideophyceae) and the consequences for sensitivity to ultraviolet B radiation. *J. Phycol.* **35:** 682–693.

**Garcia-Pichel, F. 1994.** A model for internal self-shading in planktonic organisms and its implications for the usefulness of ultraviolet sunscreens. *Limnol. Oceanogr.* **39:** 1704–1717.

**Gates, R. D., O. Hoegh-Guldberg, M. J. McFall-Ngai, K. Y. Bil, and L. Muscatine. 1995.** Free amino acids exhibit anthozoan "host factor" activity: they induce the release of photosynthate from symbiotic dinoflagellates *in vitro*. *Proc. Natl. Acad. Sci. USA* **92:** 7430–7434.

**Geller, J. B., and E. D. Walton. 2001.** Breaking up and getting together: evolution of symbiosis and cloning by fission in sea anemones (genus *Anthopleura*). *Evolution* **55:** 1781–1794.

**Grant, P. T., C. Middleton, P. A. Plack, and R. H. Thomson. 1985.** The isolation of four aminocyclohexenimines (mycosporines) and a structurally related derivative of cyclohexane-1:3-dione (gadusol) from the brine shrimp, *Artemia*. *Comp. Biochem. Physiol.* **80B:** 755–759.

**Hand, C. 1955.** The sea anemones of central California. Part II. The endomyarian and mesomyarian anemones. *Wasmann J. Biol.* **13:** 37–99.

**Haslam, E. 1993.** *Shikimic Acid: Metabolism and Metabolites*. John Wiley, New York. 387 pp.

**Herrmann, K. M., and L. M. Weaver. 1999.** The shikimate pathway. *Annu. Rev. Plant Physiol.* **50:** 473–503.

**Karentz, D. 2001.** Chemical defenses of marine organisms against solar radiation exposure: UV-absorbing mycosporine-like amino acids and scytonemin. Pp. 481–520 in *Marine Chemical Ecology*, J. B. McClintock and B. J. Baker, eds. CRC Press, Boca Raton, FL.

**Karentz, D., F. S. McEuen, M. C. Land, and W. C. Dunlap. 1991.** Survey of mycosporine-like amino acid compounds in Antarctic marine organisms: potential protection from ultraviolet exposure. *Mar. Biol.* **129:** 157–166.

**Karsten, U., and F. Garcia-Pichel. 1996.** Carotenoids and mycosporine-like amino acid compounds in members of the genus *Microcoleus* (Cyanobacteria): a chemosystematic study. *System. Appl. Microbiol.* **19:** 285–294.

**Karsten, U., T. Sawall, D. Hanelt, K. Bischof, F. L. Figueroa, A. Flores-Moya, and C. Wiencke. 1998.** An inventory of UV-absorbing mycosporine-like amino acids in macroalgae from polar to warm-temperate regions. *Bot. Mar.* **41:** 443–453.

**Kishore, G. M., and D. M. Shah. 1988.** Amino acid biosynthesis inhibitors as herbicides. *Annu. Rev. Biochem.* **57:** 627–663.

**LaJeunesse, T. C. 2001.** Investigating the biodiversity, ecology, and phylogeny of endosymbiotic dinoflagellates in the genus *Symbiodinium* using the ITS region: in search of a "species" level marker. *J. Phycol.* **37:** 866–880.

**LaJeunesse, T. C., and R. K. Trench. 2000.** Biogeography of two species of *Symbiodinium* (Freudenthal) inhabiting the intertidal sea anemone *Anthopleura elegantissima* (Brandt). *Biol. Bull.* **199:** 126–134.

**Madronich, S. 1993.** The atmosphere and UV-B radiation at ground level. Pp. 1–39 in *Environmental UV Photobiology*, A. R. Young, ed. Plenum Press, New York.

**Mangum, C. P., and P. W. Hochachka. 1998.** New directions in comparative physiology and biochemistry: mechanisms, adaptations, and evolution. *Physiol. Zool.* **71:** 471–484.

**Mason, D. S., F. Schafer, J. M. Shick, and W. C. Dunlap. 1998.** Ultraviolet radiation-absorbing mycosporine-like amino acids (MAAs) are acquired from their diet by medaka fish (*Oryzias latipes*) but not by SKH-1 hairless mice. *Comp. Biochem. Physiol.* **120A:** 587–598.

**McFadden, C. S., R. K. Grosberg, B. B. Cameron, D. P. Karlton, and D. Secord. 1997.** Genetic relationships within and between clonal and solitary forms of the sea anemone *Anthopleura elegantissima* revisited: evidence for the existence of two species. *Mar. Biol.* **128:** 127–139.

**Muscatine, L. 1971.** Experiments on green algae coexistent with zooxanthellae in sea anemones. *Pacific Sci.* **25:** 13–21.

**Neale, P. J., A. T. Banaszak, and C. R. Jarriel. 1998.** Ultraviolet sunscreens in *Gymnodinium sanguineum* (Dinophyceae): mycosporine-like amino acids protect against inhibition of photosynthesis. *J. Phycol.* **34:** 928–938.

**Newman, S. J., W. C. Dunlap, S. Nicol, and D. Ritz. 2000.** Antarctic krill (*Euphausia superba*) acquire UV-absorbing mycosporine-like amino acids from dietary algae. *J. Exp. Mar. Biol. Ecol.* **255:** 93–110.

**O'Brien, T. L. 1980.** The symbiotic association between intracellular zoochlorellae (Chlorophyceae) and the coelenterate *Anthopleura xanthogrammica*. *J. Exp. Zool.* **211:** 343–355.

**O'Brien, T. L., and C. R. Wyttenbach. 1980.** Some effects of temperature on the symbiotic association between zoochlorellae (Chlorophyceae) and the sea anemone *Anthopleura xanthogrammica*. *Trans. Am. Microsc. Soc.* **99:** 221–225.

**Oren, A. 1997.** Mycosporine-like amino acids as osmotic solutes in a community of halophilic cyanobacteria. *Geomicrobiol. J.* **14:** 231–240.

**Pearse, V. B. 1974.** Modification of sea anemone behavior by symbiotic zooxanthellae: phototaxis. *Biol. Bull.* **147:** 630–640.

**Pearse, V. B., and L. Francis. 2000.** *Anthopleura sola*, a new species, solitary sibling species to the aggregating sea anemone, *A. elegantissima* (Cnidaria: Anthozoa: Actiniaria: Actiniidae). *Proc. Biol. Soc. Washington* **113:** 596–608.

**Portwich, A., and F. Garcia-Pichel. 1999.** Ultraviolet and osmotic stresses induce and regulate the synthesis of mycosporines in the cyanobacterium *Chlorogloeopsis* PCC 6912. *Arch. Microbiol.* **172:** 187–192.

**Rowan, R. 1998.** Diversity and ecology of zooxanthellae on coral reefs. *J. Phycol.* **34:** 407–417.

**Santos, S. R., D. J. Taylor, and M. A. Coffroth. 2001.** Genetic comparisons of freshly isolated *versus* cultured symbiotic dinoflagellates: implications for extrapolating to the intact symbiosis. *J. Phycol.* **37:** 900–912.

**Saunders, B. K., and G. Muller-Parker. 1997.** The effects of temperature and light on two algal populations in the temperate sea anemone *Anthopleura elegantissima* (Brandt, 1835). *J. Exp. Mar. Biol. Ecol.* **211:** 213–224.

**Scelfo, G. M. 1988.** Ultraviolet-B absorbing compounds in *Anthopleura elegantissima*. *Am. Zool.* **28:** 105A.

**Seavy, B. E., and G. Muller-Parker. 2002.** Chemosensory and feeding preferences of the nudibranch *Aeolidia papillosa* to the symbiotic sea anemone *Anthopleura elegantissima*. *Invertebr. Biol.* **121:** 115–125.

**Sebens, K. P. 1981.** The allometry of feeding, energetics, and body size in three sea anemone species. *Biol. Bull.* **161:** 152–171.

**Secord, D., and L. Augustine. 2000.** Biogeography and microhabitat variation in temperate algal-invertebrate symbioses: zooxanthellae and zoochlorellae in two Pacific intertidal sea anemones, *Anthopleura elegantissima* and *A. xanthogrammica*. *Invertebr. Biol.* **119:** 139–146.

**Sekikawa, I., C. Kubota, T. Hiraoki, and I. Tsujino. 1980.** Isolation and structure of a 357 nm UV-absorbing substance, usujirene, from the red alga *Palmaria palmata* (L) O. Kintzi. *Jpn. J. Phycol.* **34:** 185–188.

**Shick, J. M. 1991.** *A Functional Biology of Sea Anemones*. Chapman & Hall, London. 395 pp.

**Shick, J. M., and W. C. Dunlap. 2002.** Mycosporine-like amino acids and related gadusols: biosynthesis, accumulation, and UV-protective functions in aquatic organisms. *Annu. Rev. Physiol.* **64:** 223–262.

**Shick, J. M., and J. A. Dykens. 1984.** Photobiology of the symbiotic sea anemone, *Anthopleura elegantissima:* photosynthesis, respiration, and behavior under intertidal conditions. *Biol. Bull.* **166:** 608–619.

**Shick, J. M., W. C. Dunlap, and A. K. Carroll. 1996.** Mycosporine-like amino acids and small-molecule antioxidants in *Anthopleura* spp.: taxonomic and environmental patterns. *Am. Zool.* **36:** 72A

**Shick, J. M., S. Romaine-Lioud, C. Ferrier-Pagès, and J.-P. Gattuso. 1999.** Ultraviolet-B radiation stimulates shikimate pathway-dependent accumulation of mycosporine-like amino acids in the coral *Stylophora pistillata* despite decreases in its population of symbiotic dinoflagellates. *Limnol. Oceanogr.* **44:** 1667–1682.

**Smith, B. L., and D. C. Potts. 1987.** Clonal and solitary anemones (*Anthopleura*) of western North America: population genetics and systematics. *Mar. Biol.* **94:** 537–546.

**Sneath, P. H. A., and R. R. Sokal. 1973.** *Numerical Taxonomy*. W. H. Freeman, San Francisco. 573 pp.

**Stochaj, W. R., and A. R. Grossman. 1997.** Differences in the protein profiles of cultured and endosymbiotic *Symbiodinium* sp. (Pyrrophyta) from the anemone *Aiptasia pallida* (Anthozoa). *J. Phycol.* **33:** 44–53.

**Stochaj, W. R., W. C. Dunlap, and J. M. Shick. 1994.** Two new UV-absorbing mycosporine-like amino acids from the sea anemone *Anthopleura elegantissima* and the effects of zooxanthellae and spectral irradiance on chemical composition and content. *Mar. Biol.* **118:** 149–156.

**Verde, E. A., and L. R. McCloskey. 1996.** Photosynthesis and respiration of two species of algal symbionts in the anemone *Anthopleura elegantissima* (Brandt) (Cnidaria: Anthozoa). *J. Exp. Mar. Biol. Ecol.* **195:** 187–202.

**Vernet, M., and K. Whitehead. 1996.** Release of ultraviolet-absorbing compounds by the red-tide dinoflagellate *Lingulodinium polyedra*. *Mar. Biol.* **127:** 35–44.

**Wang, J.-T., and A. E. Douglas. 1997.** Nutrients, signals, and photosynthate release by symbiotic algae. The impact of taurine on the dinoflagellate alga *Symbiodinium* from the sea anemone *Aiptasia pulchella*. *Plant Physiol.* **114:** 631–636.

**Weis, V. M., and R. P. Levine. 1996.** Differential protein profiles reflect different lifestyles of symbiotic and aposymbiotic *Anthopleura elegantissima*, a sea anemone from temperate waters. *J. Exp. Biol.* **199:** 883–892.

**Weis, V. M., and W. S. Reynolds. 1999.** Carbonic anhydrase expression and synthesis in the sea anemone *Anthopleura elegantissima* are enhanced by the presence of dinoflagellate symbionts. *Physiol. Biochem. Zool.* **72:** 307–316.

**Whitehead, K., and M. Vernet. 2000.** Influence of mycosporine-like amino acids (MAAs) on UV absorption by particulate and dissolved organic matter in La Jolla Bay. *Limnol. Oceanogr.* **45:** 1788–1796.

**Zamer, W. E. 1986.** Physiological energetics of the intertidal sea anemone *Anthopleura elegantissima* I. Prey capture, absorption efficiency and growth. *Mar. Biol.* **92:** 299–314.

Reference: *Biol. Bull.* **203:** 331–337. (December 2002)

# Osmotic Induction of Stress-Responsive Gene Expression in the Lobster *Homarus americanus*

JEFFREY L. SPEES[1], SHARON A. CHANG, MARK J. SNYDER, AND ERNEST S. CHANG*

*Bodega Marine Laboratory, University of California, PO Box 247, Bodega Bay, California 94923*

**Abstract.** The American lobster, *Homarus americanus*, encounters osmotic stress throughout its life cycle. To understand the molecular basis of osmotic stress responses *in vivo*, we used homologous cDNA probes to characterize the mRNA patterns of lobster HSP70 (=70-kDa heat-shock protein), HSP90 (=90-kDa heat-shock protein), and polyubiquitin during hypo- and hyper-osmotic stress in abdominal muscle and hepatopancreas (a digestive tissue) at 30, 60, and 120 min of osmotic stress. Hypo- and hyper-osmotic stress significantly increased the levels of the mRNAs encoding HSP70 and HSP90 in abdominal muscle. Hyperosmotic stress increased HSP90 mRNA levels in hepatopancreas, but hypo-osmotic stress did not. Both abdominal muscle and hepatopancreas exhibited significant changes in polyubiquitin gene expression during osmotic stress. In abdominal muscle, polyubiquitin mRNA levels increased during both hypo- and hyper-osmotic stress. Hepatopancreas, however, showed a significant elevation in polyubiquitin mRNA only during hypo-osmotic stress.

## Introduction

The lobster life cycle includes several stages that experience osmotic stress. First, as pelagic larvae suspended at the surface of the water column, near-shore larval lobsters encounter hypo-osmotic stress during periods of rainfall (Ennis, 1995). As larvae (zoeal stages I-III), lobsters can tolerate reduced salinities. This tolerance, however, decreases as development proceeds to stages IV and V (Charmantier *et al.*, 1988). Following metamorphosis and settlement, intertidal juvenile lobsters can experience osmotic shifts due to springtime freshwater run-off, and these events can lead to mortality (reviewed in Charmantier *et al.*, 2001). Migrating seasonally into coves and estuaries to reproduce, adult lobsters may endure osmotic stress in brackish waters (Lawton and Lavalli, 1995). In contrast to pelagic larval life stages, juvenile and adult lobsters (primarily benthic organisms) are described as stenohaline and as poor osmoregulators (Dall, 1970), although they can survive in the laboratory at salinities as low as 8 ppt (McLeese, 1956) and may be exposed to salinities as low as 0 ppt during winter snow run-off (reviewed in Charmantier *et al.*, 2001).

Early studies of lobster environmental physiology were concerned with the determination of optimal and suboptimal conditions for maintaining lobsters in captivity. McLeese (1956) found that the survival of adult *Homarus americanus* was negatively impacted by various levels of hypo-osmotic stress. By acclimating lobsters over several reduced salinities, he determined that there were interactive effects of low salinity and temperature on survival (McLeese, 1956). Gonzalez and Bradley (1994) observed both up- and down-regulation in the synthesis of specific proteins in the copepod *Eurytemora affinis* in response to stress from low and high salinities.

To examine the osmotic stress response at the level of gene transcription, we used several homologous molecular probes now available for stress-responsive genes in *H. americanus* (Shean and Mykles, 1995; Chang *et al.*, 1999; Spees *et al.*, 2002). As indexes of lobster stress *in vivo*, we examined the levels of the mRNAs encoding the molecular chaperones HSP70 (= 70-kDa heat-shock protein) and HSP90 (=90-kDa heat-shock protein), and polyubiquitin. HSPs are well-characterized and pervasive "chaperones" of nascent peptides during protein synthesis; they also help to re-fold denatured proteins resulting from environmental

---

Received 5 February 2001; accepted 20 September 2002.

[1] Current address: Center for Gene Therapy, Tulane Health Sciences Center, New Orleans, LA 70112

* To whom correspondence should be addressed. E-mail: eschang@ucdavis.edu

*Abbreviations:* HSP, heat-shock protein; mos*M*, milliosmolar; SDS, sodium dodecyl sulfate; SSPE, sodium chloride, sodium phosphate, ethylenediaminetetraacetic acid.

perturbation of cells (reviewed in Morimoto *et al.*, 1990; Hartl, 1996; Nover and Scharf, 1997; Bukau and Horwich, 1998; Feder and Hofmann, 1999). HSP90 is one of the most abundant proteins in eukaryotic cells, accounting for as much as 1%–2% of total cytosolic protein even in the absence of stress (Welch and Feramisco, 1982; Parsell and Lindquist, 1993; Jakob and Buchner, 1994).

Although HSP70 appears to be a "chaperoning generalist" assisting in the folding and re-folding of most proteins, HSP90 chaperones specific targets, many of which require its presence for final maturation (Nathan *et al.*, 1997). Classical examples of HSP90 substrates include a variety of steroid hormone receptors, the aryl hydrocarbon receptor, kinases, the heat-shock transcription factor, and the tumor-suppressor protein p53 (Buchner, 1999). HSP90 plays dual roles in environmental stress responses (Buchner, 1999; Rutherford and Lindquist, 1999) and cellular signal transduction (Pratt, 1997, 1998). HSP90 is likely to regulate the crustacean ecdysteroid (steroid molting hormone) receptor as demonstrated in *Drosophila* (Arbeitman and Hogness, 2000). In the absence of environmental stress, lobster HSP90 mRNA may be induced by injections of ecdysteroid (20-hydroxyecdysone; Chang *et al.*, 1999) and increases significantly in claw muscle during premolt atrophy (an ecdysteroid-dependent process) (Spees *et al.*, unpubl.).

During cell stress, damaged proteins that cannot be salvaged by chaperones are no longer functional and are potentially cytotoxic (Feder, 1999). The process of destroying proteins and the recycling of useful peptides and amino acids occurs *via* the ubiquitin/proteasome pathway. Ubiquitin (a 76 amino acid peptide) is bound to targets through a multi-step enzyme cascade. The resulting pattern of moieties signals a degradation complex (26S proteasome) to remove targeted proteins or regulatory subunits from the cell (Varshavsky, 1997). To expedite the production of ubiquitin, eukaryotic genetic coding regions for multiple ubiquitin molecules are linked and transcribed as a single "polyubiquitin" transcript. The resulting polypeptide is post-translationally cleaved into functional ubiquitin units. Because its rapid and robust production is correlated with environmental stress, ubiquitin (ubiquitous in cells) was identified early as one of the first "stress proteins." In mussels (*Mytilus trossulus*), conjugation of ubiquitin has been used to quantify irreversible protein damage in nature (Hofmann and Somero, 1995). Polyubiquitin mRNA levels increase severalfold in both *Manduca sexta* (Myer and Schwartz, 1996) and *Drosophila* (Lee *et al.*, 1988) following thermal stress. Quantification of polyubiquitin mRNA has also been used to examine the degradation process during premolt claw atrophy in the land crab *Gecarcinus lateralis* (Shean and Mykles, 1995). Recently, increases in ubiquitin concentrations have been observed in grass shrimp following their exposure to heat shock, cadmium, and petroleum fuels (Downs *et al.*, 2001).

Osmotic conditions strongly affect the survival of *H. americanus* (McLeese, 1956). In response to acute osmotic stress, we hypothesized that stenohaline juvenile lobsters would upregulate mRNA levels of HSP70, HSP90, and polyubiquitin—stress-responsive genes often induced during protein synthesis or turnover.

## Materials and Methods

### *Animal care*

Lobsters were reared from larvae hatched in a flow-through aquaculture system at the Bodega Marine Laboratory, Bodega Bay, California. Detailed descriptions of our larval-rearing and aquaculture system are available elsewhere (Chang and Conklin, 1993; Conklin and Chang, 1993). Intermolt juvenile male lobsters were used for all experiments. Animals were molt-staged based upon microscopic examination of pleopod cuticular development (Aiken, 1973). Prior to the osmotic stress experiments, the salinity of the flow-through system was stable (32 ppt) for several weeks.

### *Osmotic stress*

Two-liter jars were fitted with air stones and filled with either 1.0 l of 100% seawater (controls; 32 ppt), 50% seawater (0.5 l seawater with 0.5 l distilled and 0.2 $\mu$m-filtered freshwater; 16 ppt), or 150% seawater (1.0 l total volume with 16 g additional dissolved sea salts; 48 ppt; Sigma). Salinity was determined with a refractometer. The jars were thermally equilibrated by partial submersion in the flow-through system at 15 °C, the rearing temperature of the juvenile lobsters. Lobsters ($n = 4$ for all treatments) were removed from their compartments and placed directly into the jars, where they remained for 30, 60, or 120 min. During these time points we have previously measured significantly elevated levels of HSP70 and HSP90 mRNAs in lobsters exposed to acute thermal stress (Spees *et al.*, 2002). Controls (100% seawater) were incubated for 30, 60, and 120 min in the same manner. Following all of the treatments (100% survival), animals were quickly removed from the jars and sacrificed. Samples of abdominal muscle and hepatopancreas (midgut gland) were dissected, frozen in liquid $N_2$, and stored at −70 °C.

We ran a parallel experiment to examine the effect of salinity on hemolymph osmolarity. Hemolymph (50 $\mu$l) was removed repeatedly from individual lobsters at 0, 30, 60, and 120 min of exposure to 50, 100, or 150% seawater ($n = 4$ for each time point), and osmolarity was measured with a vapor pressure osmometer (Wescor). The osmolarity of seawater from the flow-through system was 940 mos*M*. Student's *t* test was used to compare the hemolymph osmolarity of animals incubated in 100% seawater to that of animals incubated in 50% or 150% seawater.

*Northern analysis*

Total RNA was isolated from the abdominal muscle and hepatopancreas samples (RNAgents kit, Promega), quantified by absorbance at 260 nm with a spectrophotometer, and equally loaded (15 $\mu$g abdominal muscle total RNA; 25 $\mu$g hepatopancreas total RNA) onto denaturing (formaldehyde) 1% agarose gels. These gels were washed (15 min, diethylpyrocarbonate water); blotted overnight onto nylon membranes (Magnagraph, MSI), UV cross-linked; and prehybridized (2 h) in 5× SSPE buffer (0.75 $M$ NaCl, 50 m$M$ $NaH_2PO_4$, 5 m$M$ ethylenediaminetetraacetic acid, pH 7.4), 50% (w/v) formamide, 5× Denhardt's, 1% sodium dodecyl sulfate (SDS), and 100 $\mu$g/ml denatured sheared salmon sperm DNA at 42 °C. A partial lobster HSP90 clone (350 bp, cloning described in Chang *et al.*, 1999) was $^{32}$P-labeled (Prime-It RmT, Stratagene), added directly to the prehybridization solution, and allowed to hybridize overnight at 42 °C. Following hybridization, the blots were washed twice with 2× SSPE at room temperature and placed on film overnight at −70 °C.

Following exposure of the film, the blots were stripped with several washes of buffer (15 m$M$ NaCl, 1.5 m$M$ sodium citrate, pH 7, with 0.1% SDS at 65 °C) until background was minimal; they were then prehybridized, hybridized, and washed as above, except that a partial lobster polyubiquitin cDNA probe was added (690 bp fragment from *Acc* I digest of lobster polyubiquitin clone; described in Shean and Mykles, 1995). To check for equal loading of RNA, the blots were probed with a partial lobster actin cDNA (700 bp, Harrison and El Haj, 1994). Lastly, following similar washes and prehybridization, a partial lobster HSP70 cDNA probe was hybridized with the blots (500 bp, Spees *et al.*, 2002). Films were scanned on a high-resolution scanner, and densitometry was performed with NIH Image software. The signals from these northern blots were quantified, normalized against the actin signal to control for equal loading of RNA, and expressed as percent control mRNA level. All data were $\log_{10}$-transformed to normalize variance prior to statistical analysis. Student's $t$ test was used to identify differences between treatment and control mRNA levels. $P$ values ≤0.01 were considered significant for the mRNA experiments and ≤0.05 for the hemolymph osmolarity measurements.

## Results

*Hemolymph osmolarity during acute osmotic stress*

Hemolymph osmolarity differed significantly between control animals and those incubated in either hypo- or hyper-osmotic conditions at all time points examined after the start of the experiments (Fig. 1). As expected, the hemolymph osmolarity of animals incubated in 50% seawater decreased over time (30 min, $P < 0.001$; 60 min, $P = 0.029$; 120 min, $P < 0.001$; Fig. 1). In contrast, the hemolymph osmolarity of animals incubated in 150% seawater increased over time (30 min, $P = 0.002$; 60 min, $P < 0.001$; 120 min, $P < 0.001$; Fig. 1).

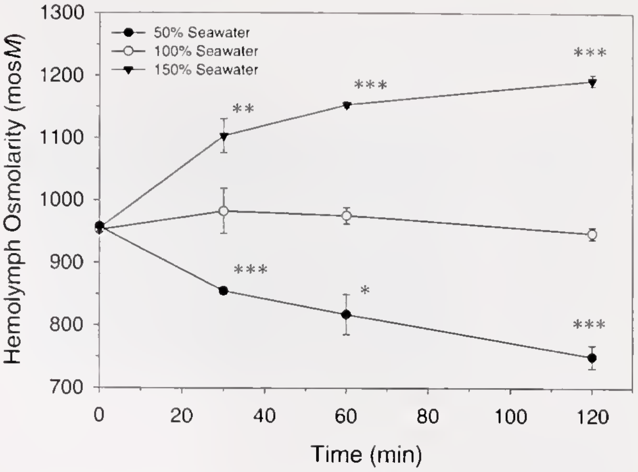

**Figure 1.** Hemolymph osmolarity (mos$M$) of individual lobsters repeatedly sampled at 0, 30, 60, and 120 min of exposure to control (100%), hypo-osmotic (50%), or hyper-osmotic (150%) seawater. For each time point, $n = 4$; error bars represent one standard deviation of the mean. Asterisks indicate significant difference between treatment and respective control at a given exposure time (*$P \leq 0.05$, **$P \leq 0.01$, ***$P \leq 0.001$).

*Gene expression in response to osmotic stress*

Representative northern blots from analysis of total RNA are shown for lobster abdominal muscle dissected from animals that received hypo- and hyper-osmotic stress for 30, 60, and 120 min (Fig. 2A-C). We had previously determined that transfer of lobsters from their rearing system into 2-l jars did not in itself alter HSP transcription levels (Spees *et al.*, 2002).

*HSP70 mRNA levels*

In abdominal muscle, HSP70 mRNA levels were significantly increased by both hypo- and hyper-osmotic stress (Fig. 3). HSP70 mRNA levels were significantly higher than control levels by 30 min of incubation in 50% seawater ($P = 0.002$) and continued to be elevated at 60 min of incubation ($P = 0.002$). Exposure to 150% seawater resulted in a significant elevation of abdominal muscle HSP70 mRNA levels over control levels at 60 min ($P = 0.004$). HSP70 mRNA levels returned to control levels in both salinity exposure groups by 120 min. HSP70 expression was not measured in hepatopancreas.

*HSP90 mRNA levels*

Both hypo- and hyper-osmotic stress significantly increased HSP90 mRNA levels in lobster abdominal muscle

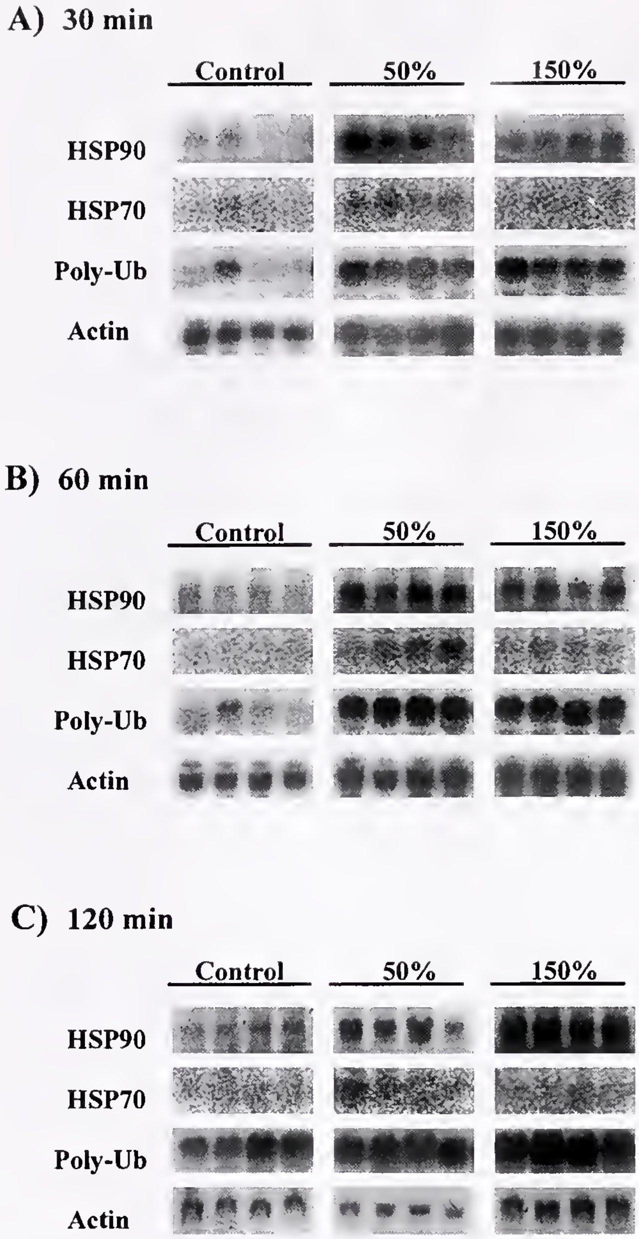

**Figure 2.** Northern analysis of total RNA showing HSP70, HSP90, and polyubiquitin gene expression in response to control (100% seawater), hypo-osmotic (50% seawater), or hyper-osmotic (150% seawater) stress in *Homarus americanus* abdominal muscle at (A) 30, (B) 60, and (C) 120 min of exposure. Northern blots were serially probed with $^{32}$P-labeled partial cDNAs for lobster HSP70, HSP90, polyubiquitin, and actin (indicator of equal loading). At each salinity and for each probe, RNA from a single lobster was run in each of the four lanes.

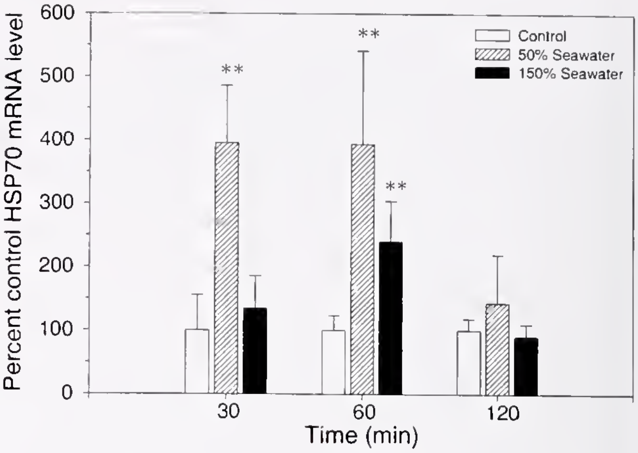

**Figure 3.** Quantitative analysis of lobster HSP70 gene expression in abdominal muscle during hypo- and hyper-osmotic stress (50% and 150% seawater) for 30, 60, and 120 min. Data are normalized against the actin signal (indicator of equal loading) and expressed as percent control (100% seawater) mRNA level. For all time points, $n = 4$; error bars represent one standard deviation of the mean. Significance between treatment and control HSP70 mRNA levels is indicated (**$P \leq 0.01$).

at all time points examined (Fig. 4). In 50% seawater, HSP90 mRNA levels were significantly greater than control levels by 30 min of exposure ($P < 0.001$). HSP90 mRNA levels also remained significantly elevated at the 60-min ($P < 0.001$) and 120-min ($P = 0.008$) time points of the hypo-osmotic treatment. In 150% seawater, abdominal muscle HSP90 mRNA levels were significantly increased over control levels by 30 min of exposure ($P = 0.001$) and remained elevated at the 60-min ($P = 0.009$) and 120-min ($P = 0.01$) time points.

Hepatopancreas responded differently to the hypo-osmotic treatment. In 50% seawater, HSP90 mRNA levels never rose significantly above control levels. Hepatopancreas HSP90 gene expression did, however, change in re-

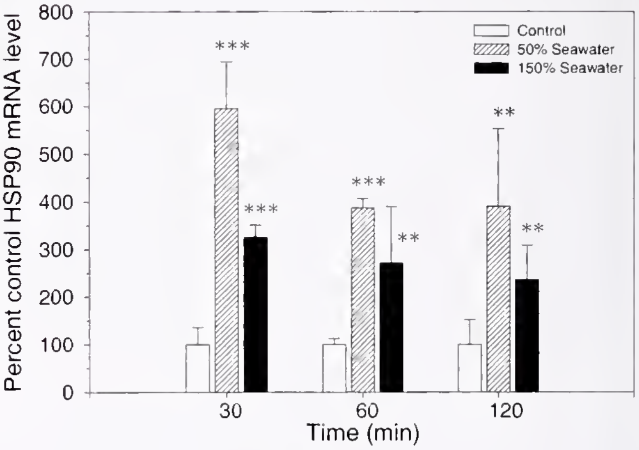

**Figure 4.** Quantitative analysis of lobster HSP90 gene expression during hypo- and hyper-osmotic stress (50% and 150% seawater) for 30, 60, and 120 min in abdominal muscle. Data are normalized against the actin signal (indicator of equal loading) and expressed as percent control (100% seawater) mRNA level. For all time points, $n = 4$; error bars represent one standard deviation of the mean. Significance between treatment and control HSP90 mRNA levels is indicated (**$P \leq 0.01$, ***$P \leq 0.001$).

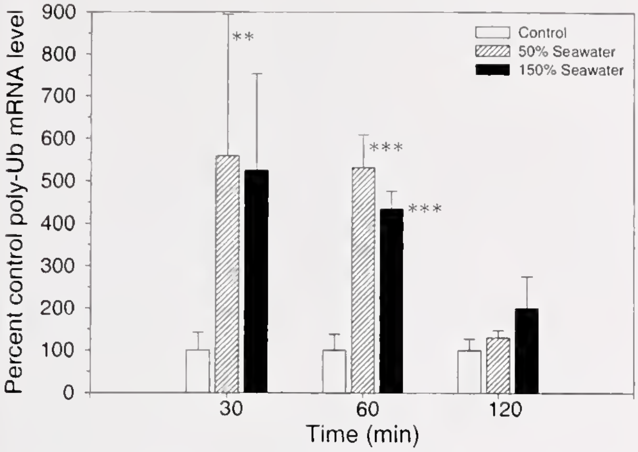

**Figure 5.** Quantitative analysis of lobster polyubiquitin gene expression during hypo- and hyper-osmotic stress (50% and 150% seawater) for 30, 60, and 120 min in abdominal muscle. Data are normalized against the actin signal (indicator of equal loading) and expressed as percent control (100% seawater) mRNA level. For all time points, $n = 4$; error bars represent one standard deviation of the mean. Significance between treatment and control HSP90 mRNA levels is indicated ($**P \leq 0.01$, $***P \leq 0.001$).

sponse to the hyper-osmotic treatment. In 150% seawater, HSP90 mRNA levels were significantly different than control levels at the 120-min time point ($P = 0.008$; mean ± standard deviation = 438% ± 205% of control values).

### *Polyubiquitin mRNA levels*

Hypo- and hyper-osmotic stress both significantly increased polyubiquitin mRNA levels in abdominal muscle (Fig. 5). Significant elevation over control levels was detectable by 30 min of exposure in 50% seawater ($P = 0.004$). Polyubiquitin mRNA levels were significantly elevated at 60 min of exposure to either salinity treatment (50% seawater, $P < 0.001$; 150% seawater, $P < 0.001$).

Significant elevation of hepatopancreas polyubiquitin mRNA was detected at 60 min of exposure to 50% seawater ($P = 0.007$; 227% ± 50.5% of control values). Hyper-osmotic stress did not lead to significant increases in hepatopancreas mRNA levels for any of the exposures we tested.

## Discussion

Our results demonstrate that, for *Homarus americanus*, (1) exposure to 50% or 150% seawater significantly alters hemolymph osmolarity, (2) hypo- and hyper-osmotic stress both can significantly elevate molecular chaperone gene expression, (3) osmotic effects on molecular chaperone mRNA levels may differ depending on duration of stress and tissue, and (4) polyubiquitin gene expression is also significantly increased by osmotic stress and similarly can differ on the basis of exposure duration and tissue.

### *Tissue-specific patterns of stress-responsive gene expression*

We observed tissue-specific patterns of lobster HSP90 expression following osmotic challenge. Whereas HSP90 expression was significantly increased in lobster abdominal muscle by hypo-osmotic treatments, expression in hepatopancreas was unaffected by any duration of hypo-osmotic stress that we tested. Both tissues, however, displayed significant elevations in HSP90 mRNA levels in response to hyper-osmotic stress. As the composite protein pools of abdominal muscle and hepatopancreas may differ considerably, variation in expression patterns may be due to differential stability of proteins arising from ionic or other solute interactions.

In lobster abdominal muscle and hepatopancreas, HSP70 and HSP90 mRNA levels are both raised by thermal stress (Chang *et al.*, 1999; Spees *et al.*, 2002) and by osmotic stress in this study (only HSP90 mRNA was examined in hepatopancreas). Abdominal muscle appears to be a more thermally stable tissue than hepatopancreas (*in vivo* expression of polyubiquitin does not occur in abdominal muscle from the same lobsters that do express it in the hepatopancreas during and after a 13 °C acute heat-shock; Spees *et al.*, 2002). In the present study, however, abdominal muscle did show an increase in expression of polyubiquitin during both hypo- and hyper-osmotic stress. In fact, it did so to a much greater extent than hepatopancreas, which did not show a significant increase in polyubiquitin mRNA levels in response to any duration of hyper-osmotic stress that we tested. Although less sensitive to thermal stress, abdominal muscle appears to be more sensitive than hepatopancreas to osmotic stress.

### *Does osmotic stress cause protein instability or denaturation* in vivo?

It is thought more likely that low availability of ions perturbs cells by affecting enzyme-ligand interactions rather than by altering enzyme conformations substantially (protein structure) (Somero and Yancey, 1997). The cations $Na^{+}$, $K^{+}$, $Mg^{+2}$, $Ca^{+2}$, and the anion $Cl^{-}$ are all present in seawater and are known to destabilize proteins at excessive concentrations (>1 *M*) (Somero and Yancey, 1997). *In vitro* results from 3T3 and SV-3T3 (rat) cells in culture show that the presence of the osmolyte betaine (*N*-trimethylglycine) reduces the production of HSP70 during hypertonic (500 mos*M*) incubation (Petronini *et al.*, 1993). Betaine also inhibits HSP70 protein induction in Madin-Darby canine kidney (MDCK) cells during thermal stress (Sheikh-Hamad *et al.*, 1994), suggesting that, as is commonly observed during thermal stress, some form of protein destabilization may occur during osmotic stress. Interestingly, the heat-shock transcription factor (HSF1) can be activated by either hyper- or hypo-osmotic stress in mammalian (HeLa) cells, but does not induce HSP70 mRNA, indicating that it may play a different role in regulating osmo-sensing pathways or osmotic stress proteins (Caruccio *et al.*, 1997).

Because the hypo- and hyper-osmotic conditions used in this study may not generate ionic conditions *in vivo* that have been observed to denature proteins *in vitro*, it is important to consider alternative hypotheses concerning osmotic stress and stress-responsive gene expression. In the rat kidney, both the mRNA and protein levels of HSP72 and HSP25/27 increase steeply along the corticopapillary axis in a pattern that matches tissue solute levels in the distal tubule. It is believed, however, that hypertonicity rather than hyperosmolarity *per se* is actually responsible for these patterns, because increased HSP synthesis correlates with the addition of relatively membrane-impermeable substances (NaCl) and not with the addition of membrane-permeable substances (urea). Thus, alterations in membrane fluidity or shrinking and swelling may influence HSP expression in some cellular systems without protein denaturation (reviewed in Beck *et al.*, 2000).

Increased molecular chaperone mRNA levels may be required in a particular tissue for signal transduction or osmolyte responses to intracellular ionic changes. Pan *et al.* (2000) found that, in salmon, hyper-osmotic stress could raise the levels of HSP90 mRNA in the branchial lamellae (both *in vitro* and *in vivo*), but not in the kidney. Because cortisol is believed to govern osmoregulatory capacity in salmon by influencing chloride cell differentiation and ATPase activity in the gill, and HSP90 is known to regulate glucocorticoid receptors, Pan *et al.* (2000) hypothesized that HSP90 might be playing a specific role in signal transduction during osmotic stress. In the lobster, there is evidence that molting hormone (ecdysteroid) titers can influence molecular chaperone gene expression (Chang *et al.*, 1999; Spees *et al.*, unpubl.).

The changes in lobster polyubiquitin gene expression we observed during osmotic stress indicate that protein turnover is occurring. Although the osmotic stress used in this study may not be excessive enough to denature proteins that have achieved their native state, it may have been enough to affect the folding of nascent proteins post-translation. As linear molecules arising from the ribosome, proteins may be more susceptible to ionic fluctuations. Improperly folded proteins in this case would be ubiquitinated and degraded by the 26S proteasome. Alternatively, the synthesis of proteins required for osmotic stress responses could account for the molecular chaperone gene expression we observed, while degradation (ubiquitination) of proteins that are unnecessary or detrimental during osmotic stress could account for increased polyubiquitin mRNA levels. Further study will be required to determine the effects on gene expression of osmotic stresses that are not as extreme as those that we used and that are more like the stresses encountered in nature. In addition, studies will be needed to elucidate the mechanisms responsible for our observations and the extent to which ionic fluctuations can alter protein stability *in vivo*.

## Acknowledgments

Special thanks are given to Prof. D. L. Mykles, Colorado State University, for supplying the polyubiquitin cDNA clone used in this study. We thank Prof. J. S. Clegg for helpful discussions and the reviewers for their useful comments. This research was funded in part by a grant from the National Sea Grant College System, National Oceanic and Atmospheric Administration, U.S. Department of Commerce, under grant number R/A-108, project number NA66RG0477, through the California Sea Grant College system, and in part by the California State Resources Agency (to M.J.S. and E.S.C.), project LR/LR-1 through the Connecticut Sea Grant College system (to E.S.C.), NSF grant 96-31128 (to M.J.S.), and Bodega Marine Laboratory student travel grants (to J.L.S.). The views expressed herein are those of the authors and do not necessarily reflect the views of NOAA or any of its sub-agencies. The U.S. Government is authorized to reproduce and distribute for governmental purposes. Contribution Number 2168, Bodega Marine Laboratory, University of California at Davis.

## Literature Cited

**Aiken, D. E. 1973.** Proecdysis, setal development, and molt prediction in the American lobster (*Homarus americanus*). *J. Fish. Res. Board Can.* **30:** 1337–1344.

**Arbeitman, M. N., and D. S. Hogness. 2000.** Molecular chaperones activate the *Drosophila* ecdysone receptor, an RXR heterodimer. *Cell* **101:** 67–77.

**Beck, F.-X., W. Neuhofer, and E. Müller. 2000.** Molecular chaperones in the kidney: distribution, putative roles, and regulation. *Am. J. Physiol. Renal Physiol.* **279:** F203–F215.

**Buchner, J. 1999.** HSP90 & Co.—a holding for folding. *Trends Biochem. Sci.* **24:** 136–141.

**Bukau, B., and A. L. Horwich. 1998.** The HSP70 and HSP60 chaperone machines. *Cell* **92:** 351–366.

**Caruccio, L., S. Bae, A. Y.-C. Liu, and K. Y. Chen. 1997.** The heat-shock transcription factor HSF1 is rapidly activated by either hyper- or hypo-osmotic stress in mammalian cells. *Biochem. J.* **327:** 341–347.

**Chang, E. S., and D. E. Conklin. 1993.** Larval culture of the American lobster (*Homarus americanus*). Pp. 489–495 in *CRC Handbook of Mariculture*, vol. 1, 2nd ed., J. P. McVey, ed. CRC Press, Boca Raton, FL.

**Chang, E. S., S. A. Chang, R. Keller, P. S. Reddy, M. J. Snyder, and J. L. Spees. 1999.** Quantification of stress in lobsters: crustacean hyperglycemic hormone, stress proteins, and gene expression. *Am. Zool.* **39:** 487–495.

**Charmantier, G., M. Charmantier-Daures, N. Bouaricha, P. Thuet, D. E. Aiken, and J. P. Trilles. 1988.** Ontogeny of osmoregulation and salinity tolerance in two decapod crustaceans: *Homarus americanus* and *Penaeus japonicus*. *Biol. Bull.* **175:** 102–110.

**Charmantier, G., C. Haond, J-H. Lignot, and M. Charmantier-Daures. 2001.** Ecophysiological adaptation to salinity throughout a lifecycle: a review in homarid lobsters. *J. Exp. Biol.* **204:** 967–977.

**Conklin, D. E., and E. S. Chang. 1993.** Culture of juvenile lobsters

(*Homarus americanus*). Pp. 497–510 in *CRC Handbook of Mariculture*, vol. 1, 2nd ed., J. P. McVey, ed. CRC Press, Boca Raton, FL.

**Dall, W. 1970.** Osmoregulation in the lobster *Homarus americanus*. *J. Fish Res. Board Can.* **27:** 1123–1130.

**Downs, C. A., J. E. Fauth, and C. M. Woodley. 2001.** Assessing the health of grass shrimp (*Palaeomonetes pugio*) exposed to natural and anthropogenic stressors: a molecular biomarker system. *Mar. Biotechnol.* **3:** 380–397.

**Ennis, G. P. 1995.** Larval and postlarval ecology. Pp. 23–46 in *Biology of the Lobster* Homarus americanus, J. R. Factor, ed. Academic Press, San Diego, CA.

**Feder, M. E. 1999.** Organismal, ecological, and evolutionary aspects of heat-shock proteins and the stress response: established conclusions and unresolved issues. *Am. Zool.* **39:** 857–864.

**Feder, M. E., and G. E. Hofmann. 1999.** Heat-shock proteins, molecular chaperones and the stress response: evolutionary and ecological physiology. *Annu. Rev. Physiol.* **61:** 243–282.

**Gonzalez, C. R. M., and B. P. Bradley. 1994.** Are there salinity stress proteins? *Mar. Environ. Res.* **39:** 205–208.

**Harrison, P., and A. J. El Haj. 1994.** Actin mRNA levels and myofibrillar growth in leg muscles of the European lobster (*Homarus gammarus*) in response to passive stretch. *Mol. Mar. Biol. Biotech.* **3:** 35–41.

**Hartl, F. U. 1996.** Molecular chaperones in protein folding. *Nature* **381:** 571–580.

**Hofmann, G. E., and G. N. Somero. 1995.** Evidence for protein damage at environmental temperatures: seasonal changes in levels of ubiquitin conjugates and hsp70 in the intertidal mussel *Mytilus trossulus*. *J. Exp. Biol.* **198:** 1509–1518.

**Jakob, U., and J. Buchner. 1994.** Assisting spontaneity: the role of hsp90 and small hsps as molecular chaperones. *Trends Biochem. Sci.* **19:** 205–211.

**Lawton, P., and K. Lavalli. 1995.** Postlarval, juvenile, adolescent, and adult ecology. Pp. 47–88 in *Biology of the Lobster* Homarus americanus, J. R. Factor, ed. Academic Press, San Diego, CA.

**Lee, H., J. A. Simon, and J. T. Lis. 1988.** Structure and expression of ubiquitin genes of *Drosophila melanogaster*. *Mol. Cell. Biol.* **8:** 4727–4735.

**McLeese, D. W. 1956.** Effects of temperature, salinity, and oxygen on the survival of the American lobster. *J. Fish Res. Board Can.* **13:** 247–272.

**Morimoto, R. I., A. Tissieres, and C. Georgopoulos. 1990.** *Stress Proteins in Biology and Medicine*. Cold Spring Harbor Laboratory Press, Cold Spring Harbor, NY.

**Myer, A., and L. M. Schwartz. 1996.** Allelic variation of the polyubiquitin gene in the tobacco hawkmoth, *Manduca sexta*, and its regulation by heat shock and programmed cell death. *Insect Biochem. Mol. Biol.* **26:** 1037–1046.

**Nathan, D. F., M. H. Vos, and S. Lindquist. 1997.** *In vivo* functions of the *Saccharomyces cerevisiae* Hsp90 chaperone. *Proc. Natl. Acad. Sci. USA* **94:** 12949–12956.

**Nover, L., and K.-D. Scharf. 1997.** Heat stress proteins and transcription factors. *Cell Mol. Life Sci.* **53:** 80–103.

**Pan, F., J. M. Zarate, G. C. Tremblay, and T. M. Bradley. 2000.** Cloning and characterization of salmon hsp90 cDNA: upregulation by thermal and hyperosmotic stress. *J. Exp. Zool.* **287:** 199–212.

**Parsell, D. A., and S. Lindquist. 1993.** The function of heat-shock proteins in stress tolerance: degradation and reactivation of damaged proteins. *Annu. Rev. Genet.* **27:** 437–496.

**Petronini, P. G., E. M. De Angelis, A. Borghetti, and K. P. Wheeler. 1993.** Effect of betaine on HSP70 expression and cell survival during adaptation to osmotic stress. *Biochem. J.* **293:** 553–558.

**Pratt, W. B. 1997.** The role of the hsp90-based chaperone system in signal transduction by nuclear receptors and receptors signaling *via* MAP kinase. *Annu. Rev. Pharmacol. Toxicol.* **37:** 297–326.

**Pratt, W. B. 1998.** The hsp90-based chaperone system: involvement in signal transduction from a variety of hormone and growth factor receptors. *Proc. Soc. Exp. Biol. Med.* **217:** 420–434.

**Rutherford, S. L., and S. Lindquist. 1999.** Hsp90 as a capacitor for morphological evolution. *Nature* **396:** 336–342.

**Shean, B. S., and D. L. Mykles. 1995.** Polyubiquitin in crustacean striated muscle: increased expression and conjugation during molt-induced claw muscle atrophy. *Biochim. Biophys. Acta* **126:** 312–322.

**Sheikh-Hamad, D., A. Garcia-Perez, J. D. Ferraris, E. M. Peters, and M. B. Burg. 1994.** Induction of gene expression by heat shock *versus* osmotic stress. *Am. J. Physiol.* **267:** F28–F34.

**Somero, G. N., and P. H. Yancey. 1997.** Osmolytes and cell-volume regulation: physiological and evolutionary principles. Pp. 441–484 in *Handbook of Physiology*, section 14, J. F. Hoffman and J. D. Jamieson, eds. Oxford University Press, New York.

**Spees, J. L., S. A. Chang, M. J. Snyder, and E. S. Chang. 2002.** Thermal acclimation and stress in the American lobster, *Homarus americanus*: equivalent temperature shifts elicit unique gene expression patterns for molecular chaperones and polyubiquitin. *Cell Stress Chaperones* **7:** 97–106.

**Varshavsky, A. 1997.** The ubiquitin system. *Trends Biochem. Sci.* **22:** 383–387.

**Welch, W. J., and J. R. Feramisco. 1982.** Purification of the major mammalian heat shock proteins. *J. Biol. Chem.* **257:** 14949–14959.

Reference: *Biol. Bull.* **203:** 338–346. (December 2002)

# Biochemical Differences Between Trail Mucus and Adhesive Mucus From Marsh Periwinkle Snails

ANDREW M. SMITH* AND MARTHA C. MORIN

*Department of Biology, Center for Natural Sciences, Ithaca College, Ithaca, New York 14850*

**Abstract.** The composition of the adhesive form of marsh periwinkle mucus was compared to the trail mucus used during locomotion. The trail mucus consists primarily of large, carbohydrate-rich molecules with some relatively small proteins. In contrast, the adhesive mucus has 2.7 times as much protein with no significant difference in carbohydrate concentration. The resulting gel has roughly equal amounts of protein and carbohydrate. This substantial increase in protein content is due to the additional presence of two proteins with molecular weights of 41 and 36 kD. These two proteins are absent from the trail mucus. Both proteins are glycosylated, have similar amino acid compositions, and have isoelectric points of 4.75. This change in composition corresponds to an order of magnitude increase in tenacity with little clear change in overall concentration. The difference between adhesive and non-adhesive mucus suggests that relatively small proteins are important for controlling the mechanics of periwinkle mucus.

## Introduction

It is generally believed that the fundamental structure of mucous gels consists of giant protein-polysaccharide complexes (Denny, 1983; Davies and Hawkins, 1998), and that mucous secretions can function as effective adhesives due to their viscoelasticity (Grenon and Walker, 1980, 1981). Recent research on limpets, however, has shown that mucus that is used for adhesion can differ substantially from other forms of mucus (Smith *et al.*, 1999). Thus, we investigated the adhesive mucus of the marsh periwinkle *Littorina irrorata*. This snail belongs to a different order of molluscs from limpets, yet it too uses mucus to create a powerful, temporary adhesion. Our goal was to identify specific biochemical characteristics that may be associated with adhesiveness in a mucous gel.

Marsh periwinkles use mucus to glue themselves down during periods of inactivity. During low tide, they forage along the substratum, using a typical, slimy mucous secretion to crawl upon. When the tide comes in, periwinkles migrate up cord grass stems and other marsh vegetation and secrete mucus to glue the lip of their shell to the plant stem. In this way, they can protect themselves from aquatic predators (Warren, 1985; Vaughn and Fisher, 1988). It is possible that the adhesiveness of the mucus results merely from it drying down to a hard film (Denny, 1984). Nevertheless, even when fully hydrated, the mucus used during adhesion creates strikingly stronger attachments than typical molluscan slime. Thus, like limpets (Smith, 1992), periwinkles alternate between active and glued states in a way that suggests a substantial change in the mechanics of their mucus.

There is currently no information on the biochemical structure of periwinkle mucus. As with most mucous secretions, it is probably a dilute gel containing more than 95% water. These gels are usually assumed to resemble mammalian mucus. The organic component of mammalian mucus consists primarily of megadalton-sized, carbohydrate-rich glycoproteins (Silberberg and Meyer, 1982; Allen *et al.*, 1984; Perez-Vilar and Hill, 1999). These fill a large volume and entangle to create a hydrogel. Limpet mucus is quite different, however; it consists of a similarly dilute gel made of much smaller proteins (20 to 220 kDa), only one of which has attached carbohydrate (Grenon and Walker, 1980; Smith *et al.*, 1999). To form a gel, the proteins in limpet mucus may link together through non-covalent bonds. Furthermore, the presence of a specific protein in limpet mucus is correlated with the change from a non-adhesive to an adhesive form (Smith *et al.*, 1999). Comparing periwinkle mucus to these other types of mucus may

Received 16 April 2002; accepted 4 September 2002.

* To whom correspondence should be addressed. E-mail: asmith@ithaca.edu

reveal structural features that are important for adhesion with a mucous-type secretion.

The primary goals of the present study were to determine the general structure of periwinkle mucus, and to see if there are specific features associated with the change to an adhesive mucus. To do this, the composition of adhesive mucus from the marsh periwinkle *Littorina irrorata* was compared to the composition of the normal mucus they use during locomotion, hereafter referred to as trail mucus. In addition, the tenacity of periwinkles using fully hydrated adhesive mucus was measured to confirm that there is a substantial functional change between the adhesive and trail mucus. Because of the unusual nature of these molluscan adhesive secretions, they could provide interesting insights into the structure and function of polymer gels and adhesives.

## Materials and Methods

### *Sample collection*

Samples were collected from roughly 200 individuals of the species *Littorina irrorata*. These animals were purchased from Gulf Specimen Marine Laboratories, Inc. (Panacea, Florida) in two separate shipments. They were maintained at 17 °C in a 29-gallon recirculating marine aquarium. The animals normally crawled above the waterline and glued the lip of their shell down at the top of the glass. The process of gluing took several minutes, and involved slowly swiping the entire sole of the foot across the uppermost edge of the shell as the foot retracted into the shell (Bingham, 1972). The resulting thin band of adhesive mucus formed a distinct bridge between the shell and the glass. When the animal was removed, it was easy to scrape this mucus from the glass or the lip of the shell. Trail mucus was collected from the same animals. For these samples, the animals were detached from the aquarium, soaked briefly in seawater, brushed with a paper towel to remove excess moisture, and placed on a glass plate. They were allowed to crawl over the plate for roughly 20 min. The resulting trails were clearly visible, and were scraped off with a clean razor blade. All samples of mucus were dehydrated for 30 min in a rotary Speed-Vac, without heat. Unless otherwise specified, each sample contained 2 to 5 mg dry weight, collected from roughly 20 animals. The snails survived well and continued to produce mucus for over 6 months, but the glue seemed weaker in the later months. Since this implied a possible decrease in quality of the mucus over time, all comparisons between the glue and the trail mucus were made between samples collected at the same time.

### *Protein and carbohydrate concentration*

The protein concentration of 10 dried samples each of adhesive mucus and trail mucus was measured with the bicinchoninic acid (BCA) assay (Pierce Chemical Co.). Several other assay methods were tested, including the Bradford assay (Bradford, 1976) and the ultraviolet absorbance (230 and 280 nm), but these suffered from unacceptable levels of interference from the buffers. In contrast, the BCA assay gave consistent results. Samples to be tested with the BCA assay were typically dissolved in 200–400 $\mu$l of 1% sodium dodecyl sulfate (SDS) per milligram of dried mucus. Assuming that half of each sample was dried salt (see results), this gave a mucus concentration of roughly 0.1% to 0.25%. To speed the solubilization, mucus samples were heated at least 10 min in a closed microcentrifuge tube at 80 °C, with occasional vortexing. Even under these conditions, the solution often gelled. In fact, the vortexing usually triggered gel formation. This tendency to gel complicated the assays. To avoid this, the solution was sonicated for less than a minute immediately before the assay. Calibration of the assay was performed with bovine serum albumen in the same buffer.

Several possible sources of error in the protein assay were examined. Though the mucus was mostly soluble in 1% SDS, the presence of a small amount of undissolved material meant that the assays underestimated the total protein. To account for this, the undissolved material from three glue samples and three trail mucus samples was collected by centrifugation. The supernatant was removed, and the pellet was dried in a rotary Speed-Vac. The resulting material was weighed and compared to the mass of the original sample. An additional source of error was that carbohydrates reacted in the BCA assay, slightly inflating the apparent protein concentration. To control for this, different carbohydrates were tested in the assay. Glucose, *N*-acetyl glucosamine, and glucuronic acid were tested separately and together. These carbohydrates gave 2% to 13% of the reaction that a comparable amount of protein gave. Glucuronic acid interfered more strongly than the other two carbohydrates, and the average interference with equal quantities of all three amounted to 8.5%.

The total carbohydrate concentrations of 12 dried samples of adhesive mucus and 9 dried samples of trail mucus were measured using the orcinol-sulfuric acid assay as described by Smith *et al.* (1999). Samples were either dissolved in 1% SDS and diluted to minimize interference, or dissolved directly in 0.1% SDS. Reducing agents were not used as they interfered with the assay. Samples were dissolved as described above. Before dilution, they were vortexed to suspend the remaining fine particles that did not fully dissolve. After addition of the orcinol-sulfuric acid reagent, all the suspended particles rapidly went into solution. Results from dissolution in 0.1% SDS and 1% SDS did not differ. The assay was calibrated with known amounts of glucose dissolved in the same buffer. Since commonly used colorimetric assays for carbohydrates vary in their sensitivity to different carbohydrates (Labare *et al.*, 1989), other standards were tested. These were glucuronic acid, *N*-acetylglucosamine, and potato starch.

### *Electrophoresis*

Samples were analyzed by SDS-polyacrylamide gel electrophoresis (SDS-PAGE). They were run on discontinuous gels, based on the method of Laemmli (1970) and the detailed protocols of Hames (1990). The gels were 10% acrylamide, and were 10 × 10 cm by 0.75 mm thick. They were stained with Coomassie blue R-250 and photographed with a Kodak EDAS-290 digital imaging system. The software allowed identification of protein bands and quantification of the relative intensity of staining of each band.

Several comparisons were performed. Samples of trail mucus were compared to samples of adhesive mucus ($n = 6$). In addition, samples dissolved in 2× SDS-PAGE sample buffer (0.125 *M* Tris-Cl, pH 6.8, 4% SDS, 10% 2-mercaptoethanol, 1.6 *M* urea) were compared to those dissolved in the same buffer without 2-mercaptoethanol ($n = 5$). Each sample contained mucus pooled from more than 10 snails. Samples were dissolved with heat and sonication as described above, and the same amount of sample was loaded into each lane. To control for possible damage to the samples from the dissolution conditions, some samples were dissolved at room temperature overnight in twice the volume of buffer without sonication or vortexing.

The presence of carbohydrates was determined by periodic acid Schiff (PAS) staining. After electrophoresis of trail mucus and adhesive mucus, the proteins were transferred to nitrocellulose using a semi-dry blotting system (Owl Scientific). Proteins were transferred in a Tris-borate buffer (22.5 m*M* Tris-borate, pH 8.3, 0.1 m*M* EDTA, 0.1% SDS and 25% methanol). Transfer conditions were 300 mA for 3 h. One lane of the transfer was stained with Coomassie blue G-250 (0.005% in 40% methanol), and destained with 40% methanol. The rest of the transfer was stained by PAS following the method of Strömqvist and Gruffman (1992). In addition, four gels were PAS stained directly without transfer, following the method of Zacharius *et al.* (1969). This procedure was performed to detect large carbohydrate-containing molecules in the stacking gel. These may go undetected when a blot is stained because they may not transfer well, and the stacking gel tends to stick to the membrane, interfering with the staining of the blot. The only changes to the published procedure were to double the duration of the incubations with periodic acid and with Schiff's reagent.

The extent of glycosylation was estimated using the method of Segrest and Jackson (1972). This involved running the sample on gels with different total acrylamide concentrations. In a low-percentage gel, proteins with more than 10% carbohydrate will run with a higher apparent molecular weight because the glycosylation inhibits SDS binding. At higher acrylamide concentrations, the effect of sieving determines the mobility more than the charge. Thus, the relative mobility of heavily glycosylated proteins will increase as the gel concentration increases, whereas there will be little effect on proteins with less than 10% carbohydrate. Samples were tested on 5%, 7.5%, 10%, and 15% gels.

### *Isoelectric focusing*

Isoelectric focusing was performed in vertical slab gels. Samples of mucus were dissolved in 50–100 μl of sample buffer (9 *M* urea, 2% CHAPS, and 5% 2-mercaptoethanol) per mg. They were heated at 80 °C in a closed microcentrifuge tube for at least 30 min, and sonicated for less than 1 min. The focusing gels contained the following components: 4.3% total acrylamide with an acrylamide to bisacrylamide ratio of 37.5:1, 9 *M* urea, 2% ampholytes (pH range 3–10), and 1% Triton X-100. The upper buffer chamber contained 20 m*M* NaOH, and the lower chamber contained 0.085% phosphoric acid. The gels were pre-run at 100 V for 15 min, 200 V for 15 min, then 300 V for 15 min. After the pre-run, the upper buffer was replaced with fresh buffer. The samples were run for 3 h at 300 V. One trial was run for 5 h, yielding the same results to within 0.05 pH units. After each run, a middle lane containing no sample was cut from the gel and sliced into 5-mm strips for determination of the pH gradient. Each of the 5-mm pieces was placed in 1 ml of 0.5% NaCl and left in a sealed test tube overnight with gentle agitation. The next day, the pH of the salt solution was measured with a digital pH meter. The remainder of the gel was stained using the Coomassie blue R-250/$CuSO_4$ method described by Righetti *et al.* (1990). This calibration procedure turned out to be more reliable than using standards, as many standards are not intended for use in gels with urea. The method gave pH as a nearly linear function of distance, with a precision of roughly 0.05 pH units.

### *Amino acid analysis*

Amino acid analysis was performed on the 41 and 36 kD proteins to determine whether or not they had specific features characteristic of mammalian mucin. The method described by Smith *et al.* (1999) was used. Briefly, this involved electrophoresis followed by a tank transfer in tris-borate to a PVDF membrane. Excised bands were hydrolyzed in 6 *M* HCl with 10% phenol and 10% trifluoroacetic acid under vacuum at 150 °C for 40 min. Amino acid compositions were determined on a Beckman System 6300 auto analyzer by the Laboratory for Macromolecular Structure at Purdue University.

### *Tenacity measurements*

The tenacity, defined as attachment force per unit area, of 12 marsh periwinkles was measured when they were using adhesive mucus that had not dried out. This was to confirm preliminary observations that adhesion involves a substantial difference in the functional properties of the mucus that is not related to the mucus drying. The snails were tested in an aquarium on glass and plastic surfaces. Preliminary observations showed no obvious difference in the tenacity on the two surfaces. The snails were detached primarily by shearing forces. No attempt was made to control for the direction of shear, though, and in some cases there was a significant normal component to the forces. This was because the snails tended to cluster under the lip of the aquarium and on the tubing and pumps, making it difficult to apply the force from a consistent direction. It was clear that detaching in some directions introduced substantial peeling forces, which would weaken the attachment. Nevertheless, the point of this experiment was merely to document a clear change in function from non-adhesive to adhesive rather than to get a precise measure of the tenacity.

Force was measured with a strain gauge force transducer similar to the one described by Smith (1991). The transducer was made of substantially thinner metal, to increase sensitivity, and a half-bridge circuit was used. The transducer was calibrated by hanging known weights from it. The response was linear, and the predictions of the calibration curve differed from the actual values by less than 2% in the range used in this study. Force was measured by connecting an elastic loop around the shell of the snail, connecting this to the transducer, and pulling so that the snails were detached primarily in shear.

The area of contact was estimated from two measurements: the area of shell that is glued down and the area of the mucous patch left on the surface after detachment. The lip of the shell is glued to the substratum only along one edge, resulting in a thin arc of adhesive mucus. The length of this arc was measured by laying a strip of paper marked with fine gradations along the edge of the shell and measuring that part of the lip that was glued down. The length was also estimated by using calipers to measure the mucous patch directly. The width of the mucous arc was estimated by measuring the thickness of the lip of the shell with calipers. The width of the mucous patch was also measured directly. Given the dimensions of the mucous patch and the fact that it is a dilute gel rather than a clearly defined solid, there was significant error in these measurements. For both methods, most of the error was in measuring the thickness, and based on the precision achievable with our measurements, the maximum error was roughly 30%. In some cases, the mucous patch was too distorted to measure. Therefore, since all the snails were the same size and the measurements of the area of adhesion were consistently the same given the limits of precision in the measurements, the same value was used in all the tenacity calculations (3.5 $mm^2$, based on 7-mm arc length, 0.5-mm width). Finally, as an additional check on the accuracy, the area was estimated from the mass of the collected mucus. The average mass of the samples was 1.8 mg ± a standard deviation (SD) of 1.0 mg. Assuming that mucus has the same density as water, a 1.8-mg patch of mucus 7 mm long by 0.5 mm wide would be approximately 0.5 mm tall. Visual inspection of the patches suggested that, indeed, the patch was about as tall as it was wide. Note that these estimates of area are likely to give a conservative estimate of tenacity because the mucus is stretched thinner between the shell and substratum during normal attachment.

After each tenacity measurement, the mucus was collected by scraping with a clean, dry razor blade and placed into a fresh microcentrifuge tube. The samples were immediately weighed on a digital balance to the nearest 0.1 mg. Then the amount of carbohydrate in each sample was determined using the orcinol-sulfuric acid assay. The total organic concentration was estimated assuming that the ratio of protein to carbohydrate was the same as measured in experiments described above.

For comparison, the shear tenacity of 23 active periwinkles was measured. This provided an estimate of the tenacity due to the trail mucus. Force was measured as described above. The area of the foot in contact with the substratum was calculated from the length and width of the foot as measured with calipers. The foot was assumed to have an elliptical outline. Note that this measurement will overestimate the tenacity due to the trail mucus alone, since a snail may use an active process such as suction to hold its foot down. In contrast, no such active process can augment the tenacity of a snail using adhesive mucus, since the foot is withdrawn into the shell. Furthermore, the band of adhesive mucus between the shell and substratum is often stretched in a way that weakens the adhesion, while the mucus under the foot of an active snail is in a thin layer, which would provide better adhesiveness. Thus, the difference between trail mucus and adhesive mucus is probably larger than estimated by these measurements.

## Results

### *Protein and carbohydrate concentration*

The compositions of the adhesive mucus and the trail mucus differed significantly even when both were fully dehydrated (Fig. 1). The primary difference was that the adhesive mucus had 2.7 times as much protein as the trail mucus (Student's $t$ test, $P < 0.001$). In contrast, the carbohydrate concentrations were not significantly different ($P = 0.15$). It is worth noting that the samples used in this comparison were from animals that had been in an aquarium for over 2 months. Several glue samples taken from recently collected animals had higher protein and carbohydrate concentrations. The same may have been true of the trail mucus, though this was not tested. The protein content of dried adhesive mucus from freshly collected animals was

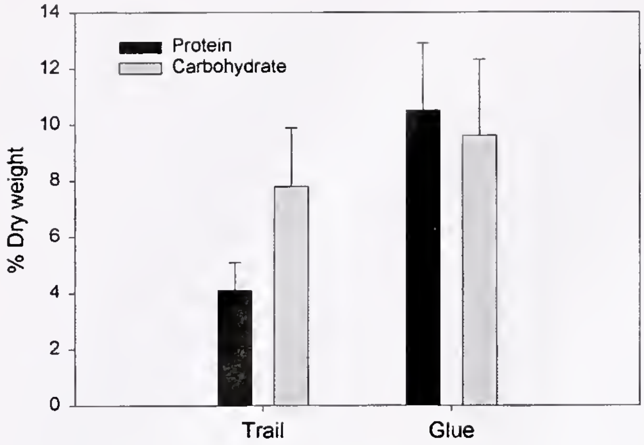

**Figure 1.** Comparison of the protein and carbohydrate content by dry weight of the two forms of periwinkle mucus. Six to ten pooled samples of each type were tested, with each pooled sample containing mucus from about 10 snails.

15.8% ± 2.5% (Mean ± SD, $n = 4$). The carbohydrate concentration was 17.1% ± 3.1% ($n = 5$).

The remainder of the dried sample was presumably inorganic material left over from evaporating seawater. Previous research on other marine mucous secretions found that roughly 50% of the dry weight was inorganic residue (Connor, 1986; Davies *et al.*, 1990). This figure can also be estimated from the percentage of inorganic salts in seawater (3.56%, Schmidt-Nielsen, 1990); for a typical marine mucus containing 96%–98% water, we would predict that inorganic material would make up 46%–64% of the dry weight.

The protein concentration is likely to be an underestimate. Since reducing agents could not be used in the protein assay, the solubilization was not total. The dried insoluble material amounted to 13% ± 7% of the total dry weight ($n = 6$), with similar results for trail mucus and glue. This undissolved material would not be detected by the assay. This error would only be partially offset by the slight increase in absorbance due to carbohydrate reacting with the assay. The interference from carbohydrates probably led to the protein values being as much as one percentage point above their actual value (*i.e.*, a calculated value of 11% may have actually been 10%, and 4% may have been 3%).

The value for carbohydrate content is also an underestimate. This is primarily due to differential sensitivity of the orcinol assay to different sugar derivatives. The calibration was based on glucose, so it should reflect the neutral sugars accurately. There were no significant differences between the assay's response to glucose and its response to glucuronic acid or starch (Student's $t$ test, $P = 0.49$ and 0.07 respectively). Thus, the assay should accurately account for uronic acid content, and it should not be significantly affected by degree of polymerization. The assay did not detect *N*-acetyl glucosamine though; 0–20 μg of this sugar produced absorbances that were within the normal variation of the blanks. Because amino sugars are common components of polysaccharides, and since many oligosaccharides are linked to proteins *via* amino sugars, they are likely to be present in mucus in significant quantities. In three studies of mucus-like gels from marine invertebrates, the quantity of amino sugars was equal to roughly half the neutral sugar (Grenon and Walker, 1980; Meikle *et al.*, 1988; Flammang *et al.*, 1998). Thus, the carbohydrate concentrations may be 50% greater than the values reported here. Finally, the presence of strong acid ensured that, unlike the protein assays, this assay did not have a problem with solubilization.

In the process of dissolving the samples it was noted that the adhesive mucus had different mechanical properties from the trail mucus. The most striking difference was that the trail mucus did not gel under the conditions used to dissolve samples for these assays. In contrast, the adhesive mucus formed gels ranging from viscous solutions to firm gels that did not flow when tipped upside down. At concentrations higher than 1 mg of dry material per 200 μl of buffer (*i.e.*, roughly 0.25% organic material), it was difficult to pipette. Furthermore, the dissolved mucus stuck to the pipet tip or any surface that it contacted, leaving fine, cobweb-like threads when the tip was pulled away.

### *Electrophoresis*

SDS-PAGE showed a clear difference between the protein compositions of adhesive mucus and trail mucus. The protein component of the adhesive mucus consisted almost entirely of a pair of proteins with molecular weights of 41 and 36 kD (Fig. 2). An analysis of digital images indicated that these proteins made up more than 95% of the total

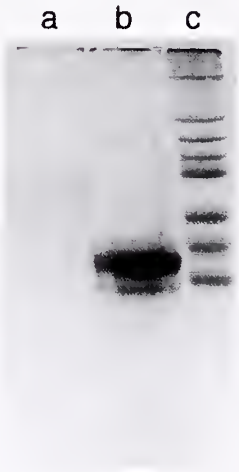

**Figure 2.** SDS-PAGE comparison of marsh periwinkle trail mucus (a) and adhesive mucus (b). Molecular weight markers are in lane c and have the following molecular weights: 205, 116, 97, 84, 66, 55, 45, and 36 kD. Both forms of mucus were fully dissolved by heating in the sample buffer.

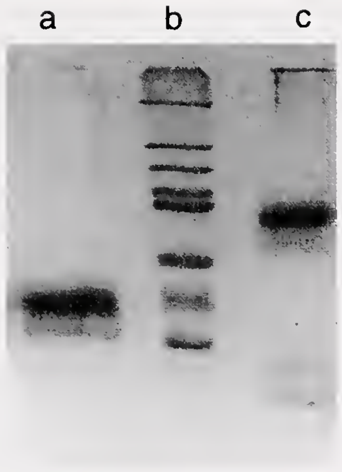

**Figure 3.** The effect of reducing agents on the proteins found in adhesive mucus. The sample in lane a was reduced prior to running on the gel, while the sample in lane c was not reduced. Molecular weight markers are in lane b and have the following weights: 205, 116, 97, 84, 66, 55, 45, and 36 kD.

protein in the adhesive, yet they were not present in the trail mucus. The proteins found in the trail mucus were different from those found in the adhesive mucus. The main proteins were 65, 63, and 59 kD (Fig. 2). Bands in this range occasionally showed up in the adhesive mucus, but only in relatively small amounts. In both forms of mucus, there was no material at the top of or within the stacking gel, and there were only a few faint bands near the top of the resolving gel. Finally, the overall difference in protein concentration that was detected by the BCA assay was also apparent in the stained gels.

Disulfide bonds affect the structure of the 41 and 36 kD proteins. When these bonds are not broken, the two primary bands show up at 64 and 59 kD (Fig. 3). Thus, disulfide bonds may change the protein structure or SDS binding to create a greater apparent molecular weight. Alternatively, the 41 and 36 kD proteins may be subunits of slightly larger proteins that are held together by disulfide bonds. The key finding, though, is that the proteins are not linked into giant complexes, unlike mammalian mucin. With disulfide bonds intact, there were faint bands at a lower molecular weight, but no significant bands above 64 kD in the resolving or stacking gel.

PAS staining showed that most of the carbohydrates in the mucus appear to be in the form of very large molecules (Fig. 4). There was distinct staining in the stacking gel or at the interface between the stacking and resolving gels. There was faint staining at the position of the 41 kD protein, but it was barely visible. Visual inspection of four stained gels showed no consistent difference between the amount of the large carbohydrates in the adhesive and trail mucus (Fig. 4). It is also possible that there were larger carbohydrate-containing molecules that could not even enter the gel. Finally, PAS staining of transfers showed that the 41 and 36 kD proteins and the trail mucus proteins were glycoproteins, but there was not enough carbohydrate to detect consistently with the in-gel staining.

When samples of adhesive mucus were run on gels with different acrylamide concentrations, there was no difference in the apparent molecular weight of the proteins. This is consistent with the previous results showing that the 41 and 36 kD proteins are not heavily glycosylated. On a 5% gel, all proteins less than 55 kD ran with the tracking dye. On 7.5%, 10%, and 15% gels, the proteins ran at 42.5, 43.5, and 41.5 and at 36, 35.5, and 36 respectively.

### *Isoelectric focusing and amino acid analysis*

All of the proteins in the mucus were acidic. The 41 and 36 kD proteins focused as a single band at a pI of 4.75. The proteins in trail mucus focused as two bands with pI values of 4.91 and 5.15. Because of the low concentrations, the similar molecular weights and isoelectric points, and the format of the gels, 2-dimensional electrophoresis was not performed. Thus, it is uncertain which of the proteins in trail mucus corresponded to which isoelectric points.

The amino acid compositions of the 41 and 36 kD proteins were similar to each other (Table 1). As calculated using the method of Marchalonis and Weltman (1971), the relatedness value between the proteins was 30; any value below 100 suggests relatedness. Proline, serine, and threonine make up 18% and 20% of the amino acids in these two proteins; in comparison, these typically constitute 40% of the amino acids in mammalian mucin (Allen *et al.*, 1984).

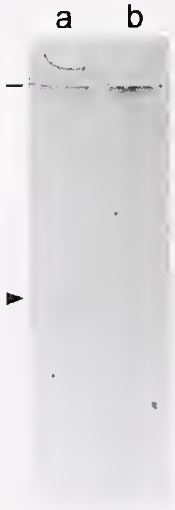

**Figure 4.** A PAS-stained polyacrylamide gel comparing the adhesive mucus (a) to the trail mucus (b). The arrowhead marks the expected location of the 41 kD protein, based on a lane stained with Coomassie blue. The horizontal line marks the boundary between the stacking and resolving gels.

**Table 1**

*Amino acid compositions of the proteins found in adhesive periwinkle mucus (values in residues per thousand)*

| Amino acid | 41-kD protein | 36-kD protein |
|---|---|---|
| ASX | 85 | 78 |
| GLX | 67 | 55 |
| SER | 51 | 56 |
| GLY | 72 | 42 |
| HIS | 24 | 12 |
| ARG | 63 | 59 |
| THR | 96 | 73 |
| ALA | 70 | 68 |
| PRO | 55 | 54 |
| TYR | 57 | 65 |
| VAL | 72 | 74 |
| MET | 29 | 42 |
| ILE | 49 | 64 |
| LEU | 70 | 88 |
| PHE | 61 | 77 |
| LYS | 80 | 91 |

### *Tenacity measurements*

The shear tenacity of marsh periwinkles using adhesive mucus was dramatically stronger than the shear tenacity of active periwinkles with trail mucus under their feet. This was true even though the adhesive mucus was fully hydrated. The average tenacity using adhesive mucus was 73 ± 43 kPa ($n = 12$). The highest tenacities were 130 to 140 kPa. These tended to occur when the detaching force applied little peeling component. The average carbohydrate concentration of the adhesive mucus that created these tenacities was only 1.0% ± 0.4% (w/w, $n = 11$). One of the samples was lost because it detached with the snail and ended up underwater. In contrast, the average shear tenacity of active periwinkles was 6.6 ± 3.1 kPa ($n = 23$). This is comparable to data reported for other periwinkle species by Davies and Case (1997).

## Discussion

The mucus used by marsh periwinkles for glue is distinctly different from the mucus used for locomotion. As is the case for limpets (Smith *et al.*, 1999), the key difference correlating with adhesion is the presence of one or two specific proteins. For marsh periwinkles, the change is much more striking than it is with limpets; the additional protein amounts to roughly half of the organic material in the mucus, while the trail mucus has relatively little protein. This correlation strongly suggests a role for these proteins in making the mucus adhesive.

In order to understand the function of these proteins, it is necessary to consider the biochemical structure of marsh snail mucus. Unlike limpet mucus, carbohydrates make up a substantial fraction of the material. The results from the assays on dried marsh periwinkle glue from recently collected animals were 16% protein and 17% carbohydrate. When the undissolved material in the protein assay, the error in the protein assay due to carbohydrates, and the undetected amino sugars are accounted for, it is likely that protein and carbohydrate each make up 20%–25% of the dried adhesive mucus, with the other 50%–60% being inorganic residue. The trail mucus has significantly less protein.

In both forms of mucus, most of the carbohydrates appear to be in the form of large polysaccharides. The carbohydrate assays and the PAS-stained gel showed no noticeable difference between the adhesive and trail mucus in the quantity of these carbohydrates. There was no protein staining associated with these carbohydrates, though the presence of a small amount of protein, as in proteoglycans, has not been ruled out. While it is possible that the carbohydrates at the top of the gel were actually smaller but had limited mobility because they were relatively neutral, this seems unlikely given what is known of gel structure and mucus biochemistry. Finally, only a relatively minor fraction of the carbohydrates are covalently linked to the smaller proteins seen in the adhesive mucus.

A reasonable model for the structure of trail mucus is a dilute, viscoelastic gel consisting primarily of giant carbohydrate-rich molecules. This is typical of most mucous secretions (Denny, 1983; Davies and Hawkins, 1998). The adhesive mucus appears to have a similar amount of giant carbohydrate-rich molecules, but in addition has substantial quantities of relatively small 41 and 36 kD proteins. This suggests that the 41 and 36 kD proteins cause the functional change, perhaps by changing the mechanics of the gel. For example, these proteins could cross-link with each other, with the carbohydrates, or both. Such cross-links would substantially affect the mechanics of the secretion (Denny, 1983). It is also possible that the large carbohydrates in the adhesive mucus have structural differences from those in the trail mucus, though this was not studied. For example, the uronic acid content or the degree of sulfation may differ. This leads to two primary hypotheses. First, the adhesive mucus may be a modified version of the trail mucus, with the 41 and 36 kD proteins added. Alternatively, the large carbohydrates in adhesive mucus may differ as well, which may contribute to adhesion. For example the carbohydrates may be a type that is more capable of interacting with each other or the 41 and 36 kD proteins. In either case, the striking change in protein content argues that these proteins play a key role. The relative importance of smaller, cross-linked proteins makes sense for an adhesive. It is desirable for many adhesives to be made of smaller polymers that can flow more readily to achieve intimate contact with a surface, then cross-link into a stiff network (Bikerman, 1958; Wake, 1982; Waite, 1983). The proteins found in the trail mucus may also play a role in the mechanics of that gel, though they are not present in a large quantity. The isoelectric point of these proteins falls in the range found for the 41 and 36 kD proteins and the proteins from limpet mucus (Smith *et al.*, 1999), suggesting that there may be some similarity among these proteins.

The change in the composition of mucus corresponds to a substantial functional change. The switch to the adhesive form of mucus increases the shear tenacity a full order of magnitude, from roughly 7 to 73 kPa. Furthermore, the difference is probably greater than these data indicate. The tenacity of snails using adhesive mucus is likely to be an underestimate, due to peeling and the conservative estimate of area that was used. It is likely that tenacities commonly exceed 100 kPa, as is seen with limpets (Smith, 1991, 1992). In contrast, the tenacity of active snails gives an overestimate of the adhesiveness of trail mucus, since much of the adhesive force at that time probably results from suction. This was the case for limpets (Smith, 1991, 1992).

This large increase in tenacity is achieved without concentrating the mucus appreciably. As measured by the orcinol assay, only 1% of the mass of the adhesive mucus was carbohydrate. Adding in carbohydrates that may have been undetected and protein, the total organic concentration of the adhesive mucus was roughly 2%–3% (w/w). This concentration is typical for normal mucous secretions. Thus, the adhesion is not due to changes in mucus concentration; it is more likely due to the differences in composition.

It should not be surprising that different forms of mucus have different compositions and different mechanical properties. There is wide variation in the gross composition of mucous secretions (Davies and Hawkins, 1998), and in their function (Denny, 1989). For example, some mucous secretions have roughly 10 times as much carbohydrate as protein, while in others the reverse is true (Meikle *et al.*, 1988; Davies and Hawkins, 1998; Smith *et al.*, 1999). The differences in function are similarly dramatic: some mucous secretions are designed for lubrication, whereas others are powerful adhesives. Furthermore, it is not unusual for a mollusc to have as many as 10 types of secretory cell on the epithelium of its foot (*e.g.*, Grenon and Walker, 1978). Given these facts, we have no reason to expect that all invertebrate mucous secretions will depend solely on the same type of giant glycoproteins.

There are probably a number of types of mucous gel. Meikle *et al.* (1988) found substantial differences between the mucus of six coral species. Some produce a carbohydrate-rich mucus consisting of megadalton-size glycoproteins with an amino acid composition dominated by serine and threonine, like mammalian mucin. Other corals produce a protein-rich mucus consisting of much smaller subunits (around 150 kD) whose amino acid composition has a high proportion of acidic amino acids. This resembles limpet mucus. Finally, some corals produce a mucus that appears to be dominated by large polysaccharides with very little protein. This may be similar to the mucus of the neogastropod *Nucella emarginata*, which contains 25% carbohydrate by dry weight and only 1% protein (Connor, 1986). The trail mucus produced by marsh periwinkles may also resemble this, whereas the adhesive mucus also contains smaller proteins that are superficially similar to those found in limpet mucus.

As Davies and Hawkins (1998) point out, relatively little is known about the structure of invertebrate mucous secretions. In particular, they note that almost no work has been done linking biochemical structure to function. Our research on marsh periwinkles provides a substantial step forward in this area. There appear to be different categories of mucus. Typical lubricating mucous gels whose mechanics depend solely on giant protein-polysaccharide complexes have been well studied. We have identified different molecules that may be used in situations where greater mechanical strength is needed. These relatively small, acidic proteins from limpet and periwinkle mucus are likely to have interesting structural and chemical properties.

## Acknowledgments

We thank S. Johnsen, W. M. Kier, and J. H. Waite for helpful comments. We also thank P. Cowley for assistance with the tenacity measurements. This work was supported in part by an Ithaca College Summer Grant for Faculty Research to AMS.

## Literature Cited

**Allen, A., D. A. Hutton, J. P. Pearson, and L. A. Sellers. 1984.** Mucus glycoprotein structure, gel formation and gastrointestinal mucus function. In *Mucus and Mucosa*, J. Nugent and M. O'Connor, eds. *Ciba Found. Symp.* **109:** 137–156.

**Bikerman, J. J. 1958.** The rheology of adhesion. Pp. 479–503 in *Rheology: Theory and Applications*, Vol. 3, F. R. Eirich, ed. Academic Press, New York.

**Bingham, F. O. 1972.** The mucus holdfast of *Littorina irrorata* and its relationship to relative humidity and salinity. *Veliger* **15:** 48–50.

**Bradford, M. M. 1976.** A rapid and sensitive method for the quantitation of microgram quantities of protein utilizing the principle of protein-dye binding. *Anal. Biochem.* **72:** 248–254.

**Connor, V. M. 1986.** The use of mucous trails by intertidal limpets to enhance food resources. *Biol. Bull.* **171:** 548–564.

**Davies, M. S., and C. M. Case. 1997.** Tenacity of attachment in two species of littorinid, *Littorina littorea* (L.) and *Littorina obtusata* (L.). *J. Molluscan Stud.* **63:** 235–244.

**Davies, M. S., and S. J. Hawkins. 1998.** Mucus from marine molluscs. *Adv. Mar. Biol.* **34:** 1–71.

**Davies, M. S., H. D. Jones, and S. J. Hawkins. 1990.** Seasonal variation in the composition of pedal mucus from *Patella vulgata* L. *J. Exp. Mar. Biol. Ecol.* **144:** 101–112.

**Denny, M. W. 1983.** Molecular biomechanics of molluscan mucous secretions. Pp. 431–465 in *The Mollusca*, Vol. 1, K. Wilbur, K. Simkiss, and P. W. Hochachka, eds. Academic Press, New York.

**Denny, M. W. 1984.** Mechanical properties of pedal mucus and their consequences for gastropod structure and performance. *Am. Zool.* **24:** 23–36.

**Denny, M. W. 1989.** Invertebrate mucous secretions: functional alternatives to vertebrate paradigms. In *Mucus and Related Topics*, E. Chantler and N. A. Ratcliffe, eds. *Symp. Soc. Exp. Biol.* **43:** 337–366.

**Flammang, P., A. Michel, A. V. Cauwenberge, H. Alexandre, and M. Jangoux. 1998.** A study of the temporary adhesion of the podia in the sea star *Asterias rubens* (Echinodermata, Asteroidea) through their footprints. *J. Exp. Biol.* **201:** 2383–2395.

**Grenon, J. F., and G. Walker. 1978.** The histology and histochemistry of the pedal glandular system of two limpets, *Patella vulgata* and *Acmaea tessulata* (Gastropoda: Prosobranchia). *J. Mar. Biol. Assoc. UK* **58:** 803–816.

**Grenon, J. F., and G. Walker. 1980.** Biomechanical and rheological properties of the pedal mucus of the limpet, *Patella vulgata* L. *Comp. Biochem. Physiol. B* **66:** 451–458.

**Grenon, J. F., and G. Walker. 1981.** The tenacity of the limpet, *Patella vulgata* L.: an experimental approach. *J. Exp. Mar. Biol. Ecol.* **54:** 277–308.

**Hames, B. D. 1990.** One dimensional polyacrylamide gel electrophoresis. Pp. 1–147 in *Gel Electrophoresis of Proteins: A Practical Approach*, B. D. Hames and D. Rickwood, eds. IRL Press, Oxford.

**Labare, M. P., K. Guthrie, and R. M. Weiner. 1989.** Polysaccharide exopolymer adhesives from periphytic marine bacteria. *J. Adhesion Sci. Technol.* **3:** 213–223.

**Laemmli, U. K. 1970.** Cleavage of structural proteins during the assembly of the head of bacteriophage T4. *Nature* **227:** 680–685.

**Marchalonis, J. J., and J. K. Weltman. 1971.** Relatedness among proteins: a new method of estimation and its application to immunoglobins. *Comp. Biochem. Physiol. B* **38:** 609–625.

**Meikle, P., G. N. Richards, and D. Yellowlees. 1988.** Structural investigations on the mucus from six species of coral. *Mar. Biol.* **99:** 187–193.

**Perez-Vilar, J., and R. L. Hill. 1999.** The structure and assembly of secreted mucins. *J. Biol. Chem.* **274:** 31751–31754.

**Righetti, P. G., E. Gianazza, C. Gelfi, and M. Chiari. 1990.** Isoelectric focusing. Pp. 149–216 in *Gel Electrophoresis of Proteins: A Practical Approach*, B. D. Hames and D. Rickwood, eds. IRL Press, Oxford.

**Schmidt-Nielsen, K. 1990.** *Animal Physiology: Adaptation and Environment*. Cambridge University Press, Cambridge. 607 pp.

**Segrest, J. P., and R. L. Jackson. 1972.** Molecular weight determination of glycoproteins by polyacrylamide gel electrophoresis in sodium dodecyl sulfate. Pp 54–63 in *Methods in Enzymology*, Vol 28B, V. Ginsburg, ed. Academic Press, New York.

**Silberberg, A., and F. A. Meyer. 1982.** Structure and function of mucus. In *Mucus in Health and Disease II*, E. N. Chantler, J. B. Elder, and M. Elstein, eds. *Adv. Exp. Med. Biol.* **144:** 53–74.

**Smith, A. M. 1991.** The role of suction in the adhesion of limpets. *J. Exp. Biol.* **161:** 151–169.

**Smith, A. M. 1992.** Alternation between attachment mechanisms by limpets in the field. *J. Exp. Mar. Biol. Ecol.* **160:** 205–220.

**Smith, A. M., T. J. Quick, and R. L. St. Peter. 1999.** Differences in the composition of adhesive and non-adhesive mucus from the limpet *Lottia limatula*. *Biol. Bull.* **196:** 34–44.

**Strömqvist, M., and H. Gruffman. 1992.** Periodic acid/Schiff staining of glycoproteins immobilized on a blotting matrix. *Biotechniques* **13:** 744–749.

**Vaughn, C. C., and F. M. Fisher. 1988.** Vertical migration as a refuge from predation in intertidal marsh snails: a field test. *J. Exp. Mar. Biol. Ecol.* **123:** 163–176.

**Waite, J. H. 1983.** Adhesion in byssally attached bivalves. *Biol. Rev. Camb. Philos. Soc.* **58:** 209–231.

**Wake, W. C. 1982.** *Adhesion and the Formulation of Adhesives*. Applied Science Publishers, London. 332 pp.

**Warren, J. H. 1985.** Climbing as an avoidance behaviour in the salt marsh periwinkle, *Littorina irrorata* (Say). *J. Exp. Mar. Biol. Ecol.* **89:** 11–28.

**Zacharius, R. M., T. E. Zell, J. H. Morrison, and J. J. Woodlock. 1969.** Glycoprotein staining following electrophoresis on acrylamide gels. *Anal. Biochem.* **30:** 148–152.

Reference: *Biol. Bull.* **203:** 347–357. (December 2002)

# Tests of Hypotheses on the Adaptive Value of an Extended Male Phase in the Hermaphroditic Shrimp *Lysmata wurdemanni* (Caridea: Hippolytidae)

RAYMOND T. BAUER

*Department of Biology, University of Louisiana at Lafayette, Lafayette, Louisiana 70504-2451*

**Abstract.** Hypotheses on delayed sex change in the protandric simultaneous hermaphrodite *Lysmata wurdemanni* were tested with observations from population samples, mating experiments, and experiments on sex change under optimal and suboptimal breeding conditions. Male-phase individuals (MPs) much larger than the minimum size of sex change were most frequent in a natural population from fall through early spring. The hypothesis was tested that some MPs delay sex change to the simultaneous hermaphrodite female-phase (FP) because MPs are more competitive in obtaining copulations with parturial FPs than are FPs mating as males (MFPs). In different experiments, parturial FPs were maintained with two potential male mating partners (large MP and MFP, small MP and MFP, large MP and small MP) through the parturial molt and spawning; activities were recorded with time-lapse video. MFPs gained the single copulation with the parturial FP as frequently as MPs, large or small, but large MPs copulated with more FPs than small MPs. The hypothesis of FP reversion to large MP was tested experimentally and rejected. Rate of change of MP to FP was much lower in large MPs maintained under suboptimal (fall/winter) than optimal (spring/summer) breeding conditions. The results presented here suggest that the occurrence of large MPs from the fall to early spring is better explained by abiotic proximate factors related to breeding than by socially mediated sex change in different demographic environments.

Received 16 April 2002; accepted 6 September 2002.

E-mail: rtbauer@louisiana.edu

*Abbreviations:* AG, androgenic gland; CL, carapace length; ESD, environmental sex determination; FP, female-phase individual (simultaneous hermaphrodite in *Lysmata wurdemanni*); MP, male-phase individual; MFP, a FP acting as a male mating partner; PFP, parturial FP; PSH, protandric simultaneous hermaphroditism; TR, transitional individual.

## Introduction

Many organisms, both plant and animal, partition reproductive output into male and female components. Such sex allocation may occur before fertilization or during embryonic development. In hymenopteran insects (ants, wasps, bees), haplodiploid sex determination allows females to produce male and female offspring in variable proportions (Wilson, 1976; Thornhill and Alcock, 1983). In turtles and some other reptiles such as alligators, sex determination is temperature dependent, so that females may control the sex ratio of offspring by the seasonal timing of egg laying or the location of nests (Bull, 1980; Ferguson and Joanen, 1982). Higher male fetal mortality may occur in mammalian females under stressful conditions, resulting in female-biased litters (Wilson, 1976; see also Charnov, 1982). In other organisms, sex allocation many occur after birth or hatching in the sexually mature organism. Simultaneous hermaphrodites may vary resources to male and female gamete production (Charnov, 1982). In sequential hermaphrodites, sexual function is partitioned ontogenetically because an individual first reproduces as one sex and then the other (sex changers; Ghiselin, 1969; Warner, 1975; Charnov, 1982; Policansky, 1982). Simultaneous and sequential hermaphroditism is found in many plant taxa, in most invertebrate groups (except insects), and in many fishes (Chan and Yeung, 1983; Ross, 1990). The direction of sex change (female to male; protogyny; male to female; protandry) is fairly well explained by the size-advantage model (Ghiselin, 1969), especially in fishes and crustaceans, two groups in which sequential hermaphroditism is relatively common (Warner, 1975). What is not often well explained, especially in decapod shrimps, is variation in the timing of sex change, *i.e.*, the amount of time spent as male and female.

Protandric hermaphroditism occurs in several genera and families of caridean shrimps (Bauer, 2000). In the simplest form of caridean protandry, all individuals develop first as males and then later change to breeding females. The sexual system may be more complex, with a mixture in the population of primary females, which develop only as females, and protandric individuals, as in *Pandalus jordani, P. borealis, P. eous, P. montagui,* and *P. danae* (Butler, 1980; Bergström, 2000). In other species, the population may consist of protandric individuals and primary males, individuals that never change to females, as in *Thor manningi* (Bauer, 1986) and *Athanas kominatoensis* (Nakashima, 1987).

Throughout the last century, *Lysmata seticaudata* was described as a completely protandric species (Spitschakoff, 1912; Dohrn, 1950; Charniaux-Cotton and Payen, 1985). Smaller individuals have external male characteristics, but the gonads are ovotestes with immature oocytes in the ovarian region. With increasing size, individuals lose external male characters and change to breeding females that incubate embryos. Unlike other protandric carideans, the female-phase individuals (FPs) retain the male ducts and testicular portion of the ovotestes, and sperm production continues (Berreur-Bonnenfant and Charniaux-Cotton, 1965; Charniaux-Cotton, 1975). The ability of *L. seticaudata* FPs to function as males was not addressed in these studies. However, FPs of *Lysmata wurdemanni* (Bauer and Holt, 1998) and *L. amboinensis* (Fiedler, 1998), with sexual changes during ontogeny similar to *L. seticaudata,* mate as males and fertilize other FPs, although they are unable to fertilize themselves. They are functional, outcrossing simultaneous hermaphrodites. Bauer (2000) termed this sexual system "protandric simultaneous hermaphroditism" (PSH), in which male-phase individuals (MPs) function only as males, but FPs are functional simultaneous hermaphrodites. Morphological and behavioral observations on these and other *Lysmata* spp. indicate that PSH is widespread in the genus (Bauer, 2000, 2001).

The size (age) of sex change in protandric species may be variable (Charnov *et al.,* 1978; Charnov, 1981; Charnov and Anderson, 1989; Bergström, 1997, 2000). The size of sex change may be a phenotypically flexible trait governed by the demographic environment in which an individual occurs (environmental sex determination, or ESD; Charnov *et al.,* 1978; Charnov, 1981; Charnov and Anderson, 1989). In *Pandalus* spp, for example, a male in a population with abundant females might gain more inseminations by delaying change to female because males can potentially inseminate several females during the breeding season. A *Pandalus* female, in contrast, produces only one brood per year. When females are not abundant in the population, a male might benefit by early change to female because insemination of a female's brood of eggs is assured. As a male, the individual would have to compete with numerous other males to inseminate one of the scarcer females. On the other hand, a male changing to female later in life would begin female production with larger broods, since female fecundity is correlated with size in carideans including *Pandalus* spp. (Bauer, 1991; Bergström, 2000). However, a later change to female might cause the loss of female breeding for an entire season, given only one brood per year, thus countering the fecundity advantage of late change to female. The relative proportions of males and females in the population, perceived by an individual through social interactions, would serve as the environmental factor stimulating or inhibiting male change to female.

However, the hypothesis of ESD in *Pandalus danae* was rejected by Marliave *et al.* (1993) after they conducted extensive experiments involving the rearing of a large number of young males in different demographic environments. They concluded that the sexual composition of the population has no effect on sex determination (change) in this protandric species. Other mating and rearing experiments led Marliave *et al.* (1993) to conclude that the timing of sex change was under genetic control. They proposed that any adaptive change in the proportions of sexual morphs would occur by between-generation selection on sexual genotypes rather than a within-generation, socially determined response as proposed by Charnov *et al.* (1978) and Charnov (1981). Bergström (1997), on the basis of results of a demographic analysis, concluded that the variable type and size of sex change in *Pandalus borealis* was best explained by frequency-dependent selection on genotypes for sex change at different ages (sizes). According to this hypothesis, different combinations of mortality, recruitment, and growth favor different sex-change genotypes. Conover and Munch (2002) showed experimentally in the fish *Menidia menidia* (Atherinidae) that size-dependent selection, like that acting on commercially fished populations, lowers the age of sexual maturity. Charnov *et al.* (1978) and Charnov (1981) reported a decrease in the size (age) of sex change in fished pandalids. This might result from size-related mortality (selection) (Conover and Munch, 2002) rather than from an adaptive response (decision) by individuals to demographic changes in the population. On the other hand, Zupo (2001) clearly showed that seasonal variations in diet of newly recruited shrimps determine whether or not sex change takes place in the protandric shrimp *Hippolyte inermis.*

In *Lysmata wurdemanni,* individuals from a natural population vary in size from 3–14 mm carapace length (CL) (Bauer and Holt, 1998; Bauer, 2002). Individuals enter the population as MPs and can change to FPs at a size as small as 6 mm CL; the majority change by 7.5 mm CL. However, there is frequently considerable overlap between MP and FP size-frequency distributions. Many MPs do not change sex until a much larger size, with some MPs becoming as large as the larger FPs (Bauer and Holt, 1998; Bauer, 2002). Some MPs might never change to FP, although all are morphologically capable of doing so (Bauer and Holt, 1998; Bauer, 2000; Lin and Zhang, 2001). Bauer and Holt (1998) and Bauer (2000, 2001) suggested that delayed change to the reproductively advantageous FP, a simultaneous hermaphrodite, might be selected for in certain demographic situations if large MPs were competitively superior to FPs (mating as males) and small MPs in inseminating FPs near spawning. Lin and Zhang (2001) reared MPs of *L. wurdemanni* singly and in groups of from 2 to 10 individuals, finding that change to FP increased with increasing MP group size. Replicate size was quite small in this experiment, varying from 2 to 9 replicates per treatment. The authors concluded that these results demonstrated social control of sex ratio. Furthermore, they proposed that persistence of MPs in some treatments suggested a mating advantage for large MPs in certain demographic situations.

Other explanations are possible for large MP size in *Lysmata wurdemanni*. Large MPs might be FPs that have reverted to the male phase. Bidirectional sex change is known in some animals, such as gobiid fishes (Munday, 2002) and polychaetes (Berglund, 1986). A secondary change back to male purportedly takes place in some females of the protandric alpheid *Athanas indicus* (Suzuki, 1970). In *L. wurdemanni*, abiotic factors related to female breeding might account for the seasonally related occurrence of large MPs. The largest MPs, including transitional MPs changing to FP, are found in winter and early spring (Bauer, 2002). Suboptimal conditions for breeding (lower water temperatures, short daylength) and presumably larval survival (planktonic food supply) occur during the late fall through early spring in this primarily tropical species studied near the northern edge of its range (Bauer and Holt, 1998; Bauer, 2002). Abiotic environmental conditions unfavorable for female breeding might cause a decrease in female hormone levels, resulting in a shift in female/male hormones in favor of the male system. Female-phase individuals, with both male and female reproductive systems, might molt back into a male phase, with male external sex characters. Alternatively, suboptimal breeding conditions might delay change to FP in MPs that reach the size of sex change during the fall, resulting in growth to the very large MPs observed by Bauer (2002) in the late winter and early spring.

The objective of this study was to examine components of hypotheses explaining the presence of large MPs in *Lysmata wurdemanni*. The male mating abilities of large MPs, small MPs, and FPs were compared to determine the possible male mating advantages of delayed sex change. The presence of large MPs might alternatively be explained by factors not related to the sexual composition of the population and socially determined sex change. The possible effects of seasonal abiotic factors unfavorable to female breeding resulting in either (a) reversion of FPs to large MPs or (b) delayed MP change to FPs were examined by maintaining (a) FPs and (b) MPs capable of sex change under suboptimal (nonbreeding season) and optimal (breeding season) conditions.

## Materials and Methods

Population samples and live specimens were collected from a population of *Lysmata wurdemanni* inhabiting the rock jetty at Mustang Island, Port Aransas, Texas (27° 50′ N, 97° 03′ W). Collection was during low tides at night (Bauer, 2002): when tides are lower than −0.5 ft mean sea level, the rock ledge and tidepool habitats of these shrimps are exposed, and the shrimps are active at night, moving out into pools and the perimeter of the jetty rocks where they can be taken with dipnets. Hand dipnets were used to take the shrimps from tidepools; long-handled dipnets were more effective in sweeping deep under rock ledges. All nets had a 1-mm mesh and were effective in collecting the smallest (= newly recruited) individuals of the population (Bauer, 2002). In any particular location, groups of individuals showed no apparent segregation by sexual morph or size, and the samples are assumed to represent a random sample of the population. Population samples were taken monthly from June 1999 through June 2000, and then bimonthly from August 2000 through June 2001 (Bauer, 2002). Shrimps collected in population samples were first preserved in 10% seawater formalin and later transferred to 70% ethanol for permanent storage. Live specimens for experiments were collected separately from population samples and transported in sealed collecting bags containing seawater oxygenated just before the 8–10-h trip from the collecting site to the home institution.

Sexual morphs were identified and classified as in Bauer and Holt (1998). Male-phase individuals (MPs) have cincinnuli (coupling hooks) on pleopod 1 endopods and appendices masculinae on pleopod 2 endopods. Transitionals (TRs) are MPs in which the ovarian portion of the ovotestes is filling with vitellogenic oocytes, which is easily observed through the carapace in living and preserved specimens. At the next molt, TRs change to FPs and spawn for the first time. Female-phase individuals (FPs) lack pleopod 1 cincinnuli and appendices masculinae. They are typical caridean females in external morphology, and they brood embryos. However, they can mate as males (simultaneous hermaphrodites) (Bauer and Holt, 1998). As in females of other carideans, FPs of *L. wurdemanni* near spawning (ovarian portion of gonad full of vitellogenic oocytes) become receptive to mating immediately after a prespawning (parturial) molt (Bauer and Holt, 1998; Bauer and Abdalla, 2001). As in other carideans, the male deposits an external spermatophore on the underside of the female, and there is no sperm storage (Bauer, 1976; Bauer and Holt, 1998). In this report, FPs very near or just completing the parturial molt are termed parturial FPs (PFPs).

Mating experiments tested the hypothesis of no difference in male mating ability among FPs (mating as males = MFPs), small MPs, and large MPs. In three experiments, competition for inseminating the PFP was between a large MP and a MFP, a small MP and a MFP, and a large MP and a small MP. Parturial FPs near the prespawning molt were identified by gonad condition (vitellogenic oocytes filling the cephalothoracic space behind the eyes and above the cardiac stomach) and developmental state of brooded embryos (near hatching, with large eyes and little or no yolk). MFPs carried embryos but, unlike PFPs, were not close to a parturial molt. Small and large MPs were defined as MPs $\leq$ 6.5 mm CL and $>$ 6.5 mm CL, respectively. The size of 6.5 mm CL was chosen to define "large" MP because MPs can change to FPs above this size (Bauer and Holt, 1998; Bauer, 2002).

In each replicate, a premolt PFP was placed with two potential mating partners. The median duration of replicates, from placement of individuals into the experimental chamber until spawning by the PFP, was 2 days (1–9 d, $n$ = 90). The MP or MFP that copulated with and inseminated the PFP was identified from time-lapse video recordings. Replicates in which the PFP copulated with more than one male mating partner (4 of 94 replicates) were not included in the data analyses. In all other replicates, there was only a single copulation, except for one replicate in which a MFP copulated twice with the PFP. Spawned PFPs were maintained alive for 5 days to determine if the attached brood of eggs had been fertilized and contained developing embryos (Bauer and Holt, 1998).

Replicates of mating experiments were conducted in aquaria partitioned into a space 20 cm wide × 25 cm long × 15 cm high to allow for sufficient magnification using the CCD surveillance video camera, which was equipped with an 8-mm lens sensitive to both low-intensity white and infrared light. Activities were recorded with a time-lapse video at a speed of 5 pictures per second (24-h recording mode). Fluorescent and infrared (880 nm) lamps provided day and night illumination, respectively. In replicates with a large and a small MP, individuals had to be marked to distinguish between them in videotapes, especially at night when most mating occurred. Small pieces of reflective tape were fixed with cyanoacrylate glue on the carapace of one MP and the posterior abdomen of the other, with position assigned at random. No marking was needed in replicates with a MP and a MFP because the latter could be identified by its brood of embryos. After hatching of embryos prior to the mating molt, the PFP was identified by the absence of embryos and the presence of vitellogenic ovotestes. Reflective tape, embryo broods, and vitellogenic gonads show clearly on videotapes recorded with infrared (nighttime) illumination. As in Bauer and Holt (1998), shrimps were maintained prior to and during experiments at water temperatures of 25–28 °C, salinities of 33–36 ppt, and a photoperiod of 14-h day: 10-h night. Shrimps were fed shrimp pellets daily.

The hypothesis that FPs may revert to large MPs was tested by an experiment in which FPs were maintained under favorable and less favorable breeding conditions for 9 weeks. In the "optimal" treatment (2 September through 2 November, 2000), 50 FPs with embryos were maintained in groups of 10 individuals occupying 38-l aquaria at a water temperature, controlled by aquarium heaters, of 26 °C and a photoperiod of 14-h light: 10-h dark. In the "suboptimal" treatment (22 September to 24 November, 2000), another 50 FPs with embryos were similarly maintained except without heaters so that water temperatures would be cooler than those in the optimal treatment. The ambient temperature of the aquatic laboratory during this period was 19 °C; the photoperiod was set at 10-h light: 14-h dark. Prior to the experiment, individuals used in both treatments were maintained at a salinity of 33–36 ppt and an optimal temperature (26 °C) and photoperiod (14-h light: 10-h dark). They were fed daily, and the aquarium water was partially changed weekly. To reduce cannibalism of newly molted shrimps, which was an observed source of mortality during this experiment, small concrete block shelters were placed in each aquarium for this thigmotactic species. Molts (exuviae) readily visible in the aquaria were removed and recorded daily. Absolute counts of molts were not feasible because (a) the shrimps may pick apart and eat some exuviae before they are observed, and (b) other exuviae are hidden by shelters and aquarium tubing and could not be observed without major disturbance of the aquarium environment. At the end of the experiment, all individuals were preserved and checked for sexual condition.

The hypothesis that sex change of large MPs to FPs is greater under optimal (spring/summer) than suboptimal (fall/winter) breeding conditions was tested with an experiment using a setup similar to that just described for the previous experiment. The MPs used in both treatments (all nontransitional) were maintained at optimal temperature and photoperiod prior to the beginning of the experiment. In the optimal treatment ($n$ = 46 MPs), water temperature was maintained with heaters at 26 °C, and photoperiod was 14-h light: 10-h dark. In the suboptimal treatment ($n$ = 45 MPs), cooler water temperatures were obtained by not using water heaters, with water temperature following the ambient air temperature of the laboratory, which was not under control of the investigator. The experiment was begun when a decrease in ambient laboratory temperature was predicted from outside weather conditions. Water temperature in the suboptimal treatment was 23 °C at the beginning of the experiment and decreased to 18–19 °C (weekly median temperature = 20 °C); photoperiod was 10-h light: 14-h dark. After 14 weeks (20 October 2001 to 23 January 2002), the laboratory air temperature and thus the water temperature of the suboptimal treatment began to rise. Heaters were then placed in aquaria of the suboptimal treatment to increase water temperature to that of the optimal treatment, and photoperiod was changed to 14-h light: 10-h dark, simulating a change from fall/winter to spring/summer conditions. The experiment then continued for another 8 weeks. The shrimps were maintained and checked for molts as in the previous experiment. Male-phase individuals that changed to FP (brood of embryos observed) were removed from the experiment and preserved. When only one MP remained in an aquarium, it was removed when it reached the late transitional stage (mature vitellogenic ovotestes), with the assumption that it would have transformed to FP at the next molt. This was done because it could not have produced a brood of embryos (visible evidence of sex change) upon molting to FP without a mating partner.

## Results

### *Occurrence of large MPs*

Large MPs, defined as MPs > 6.5 mm CL, composed 17.6% to 100% of the MP population (Fig. 1), with higher proportions of large MPs in the fall through early spring (Fig. 1). The proportions of large MPs ≥ 8.5 mm CL ("very large MPs") followed a similar pattern. Some (28.7%; $n$ = 150) of the very large MPs were transitionals that would change to the female phase at the next molt. The highest frequency of these very large transitionals occurred from mid-winter through late spring (Fig. 2).

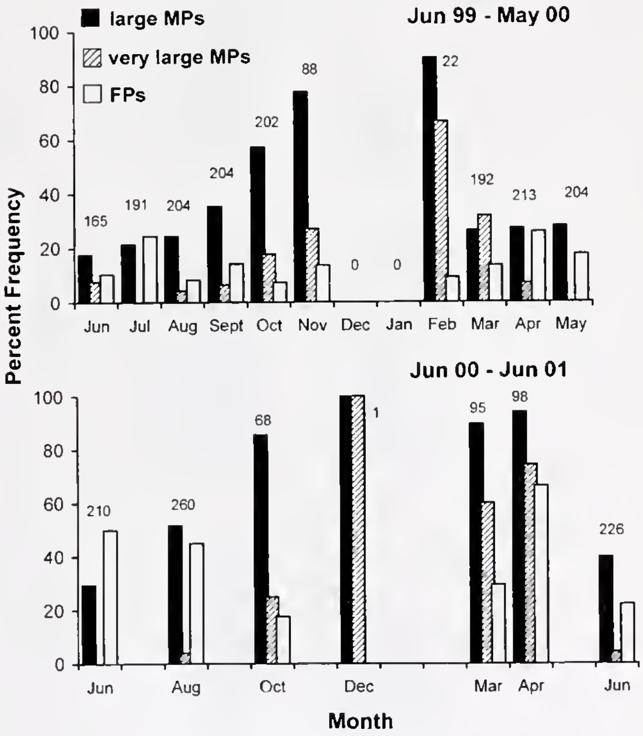

**Figure 1.** Temporal variation in percent frequency of large and very large male-phase (MP) individuals, and of female-phase (FP) individuals. Frequency (converted to percent) for large MPs = (# large MPs)/(# total MPs); very large MPs = (# very large MPs)/(# large MPs); FPs = (# FPs)/(total # individuals in population sample). Percent total MPs = 100 − % FPs. Months in which sampling occurred are listed on the abscissa. The number of individuals in population samples is given above the histogram bars for each month.

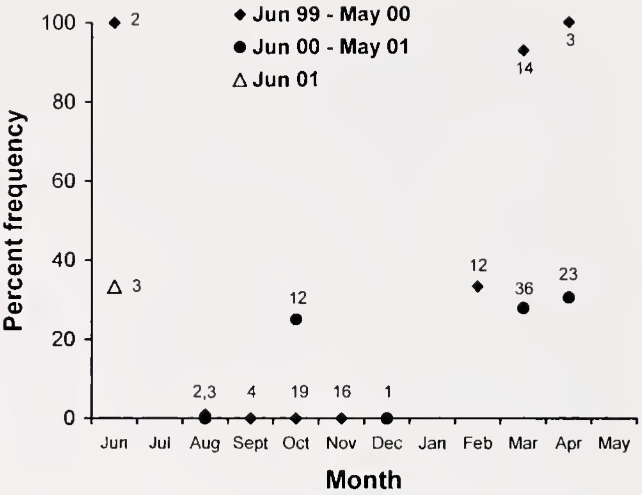

**Figure 2.** Temporal variation in percent frequency of very large MPs in the transitional stage (TR) to female-phase. The number with each data point is the sample size of large MPs on which frequencies were calculated.

### *Mating experiments*

Precopulatory and copulatory behaviors were qualitatively similar to those described in Bauer and Holt (1998), in which a single FP served as the male mating partner, except for the following observations. In this study, MPs and MFPs began to approach, follow, and remain near the PFP as the latter neared the parturial molt. These behaviors became obvious about 1 h before the PFP molt. In addition, another behavior was observed ("perching") in about 20% of the replicates, in which a MP or a MFP perched on the PFP from above and remained in that position as long as several seconds. Although individuals of *Lysmata wurdemanni* can be aggressive—for example, fighting over food particles using the third maxillipeds and anterior pereopods—no obvious aggressive behavior between the potential male mating partners over a parturial female was observed in the videotapes.

The hypothesis of no difference among sexual morphs in their ability to copulate with and inseminate parturial females (PFPs) was tested with mating experiments. In the experiment with large MPs and small MPs as potential male mating partners (Table 1), large MPs gained the single PFP copulation in more replicates than small FPs (Fig. 3A). The hypothesis of no difference from a 50:50 distribution of copulations between large MPs and small MPs was tested with chi-square and is rejected ($\chi^2_1$ = 6.53; $P$ = 0.01; $n$ =

**Table 1**

*Size data for potential male mating partners placed with newly molted parturial females in mating experiments*

| | Potential Male Mating Partners | | |
|---|---|---|---|
| Experiment | SMP | LMP | MFP |
| SMP *vs.* LMP | 5.4 (4.4, 6.4) | 7.4 (6.6, 9.4) | |
| LMP *vs.* MFP | | 7.7 (6.6, 9.7) | 8.2 (6.9, 10.0) |
| SMP *vs.* MFP | 5.6 (4.5, 6.5) | | 8.8 (7.2, 12.3) |

Size given is median carapace length (mm), with minimum and maximum values in parentheses ($n$ = 30 for all categories). LMP, large male-phase; MFP, non-parturial female-phase (simultaneous hermaphrodite); SMP, small male-phase.

30). In another experiment, large MPs and MFPs (Table 1) were equally successful in obtaining the PFP copulation (Fig. 3B) ($\chi^2_1 = 0$; $P = 1$; $n = 30$). In the 19 replicates in which the large MP was smaller than the MFP, the MP and MFP gained the PFP copulation equally ($n$ = 9, 10 respectively). Similarly, when the large MP was larger than the MFP ($n$ = 8 replicates), each gained the single PFP copulation in an equal number of replicates. In the small MP *vs.* MFP experiment (Table 1), MFPs obtained the PFP copulation in more replicates (Fig. 3C), but the difference is not statistically significant ($\chi^2_1 = 1.2$; $P = 0.27$; $n = 30$). The copulated PFP produced a fertile brood of embryos in 87 of the 90 replicates of the three experiments.

### *Correlations of large MP and FP relative abundance*

The effect of demographic influence (relative abundance of FPs) on the proportion of large MPs was investigated. From population samples, Spearman rank correlation coefficients ($r_s$) were calculated for possible correlations between % large MP and % FP, and % very large MP and % FP (Fig. 1). The null hypothesis of no correlation ($r_s = 0$) between % large MP and % FP and between very large MP and % FP was accepted ($r_s = 0.02$, $P \gg 0.20$ and $r_s = -0.32$, $P > 0.20$, respectively; $n$ = 17 months in both tests).

### *FP to MP sex change experiment*

This experiment tested the hypothesis that FPs may change back to large MPs. In the treatment with optimal breeding conditions, all surviving individuals (36 of 50) were FPs. Of these 36 FPs, 33 (91.6%) showed female reproductive activity, either incubating embryos (21) or, if without embryos, showing mature vitellogenic ovotestes (12), indicating spawning at their next molt. In the suboptimal treatment, the 39 survivors out of 50 were all FPs. Of these 39, 33 (84%) were reproductively active as females; 26 incubated embryos, and 7 without embryos had mature vitellogenic ovotestes. During the 9 weeks of the experiment, 93 exuviae were collected in the optimal treatment *vs.* 43 in the suboptimal treatment. The molting rate, adjusted for number of survivors per treatment, was 2.4 times greater in the optimal treatment.

### *Large MP to FP sex change experiment*

During first 14 weeks, 42 of 46 individuals in the optimal treatment changed to FP (including 2 solitary late-stage transitionals), 2 died, and 2 remained MP; in the suboptimal treatment only 23 of 45 changed (5 deaths). The rate of change was relatively constant in the optimal treatment compared to that of the suboptimal treatment (Fig. 4A), in which the rate of sex change slowed with decreasing ambient temperatures (Fig. 4C). Molting rates were always higher in the optimal treatment (Fig. 4B). The mean frequency of individuals molting per week was 31.2% in the optimal and 13.0% in the suboptimal treatment. Given that the period between molts may be estimated by the inverse of

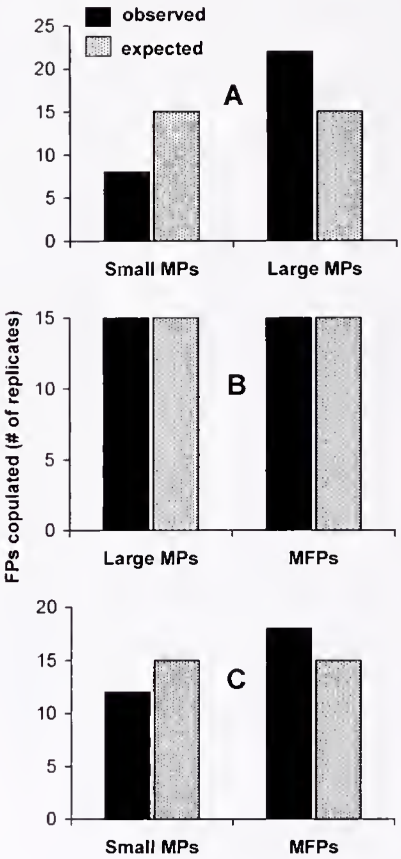

**Figure 3.** Comparative mating success of sexual morphs. The observed number of replicates (black fill) in which one or the other of two sexual morphs obtained the single copulation with the parturial female phase is figured and compared to the expected number (stippled fill) under the hypothesis of a 50:50 distribution. (A) small MP *vs.* large MP; (B) large MP *vs.* MFP; (C) small MP *vs.* MFP. $n$ = 30 replicates in each treatment.

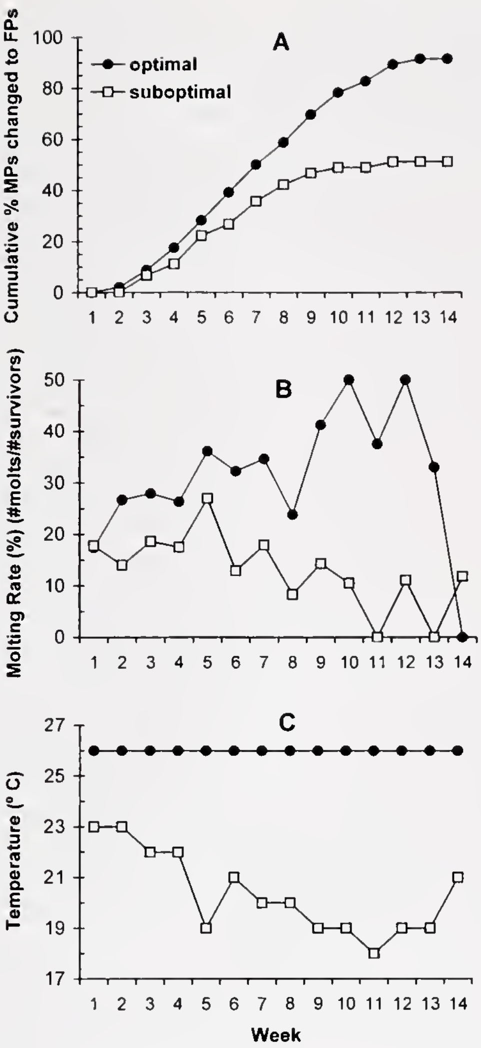

**Figure 4.** Change of large MPs to FPs under optimal and suboptimal conditions (treatments) during 14 weeks. (A) Cumulative percentage of large MPs changed to FP; (B) relative molting rates; (C) water temperatures.

the molting frequency, the average individual in the optimal treatment molted every 3.2 weeks *versus* every 7.7 weeks in the suboptimal treatment. Thus, during the first 14 weeks of the experiment, an average individual underwent at least 4 molts in the optimal and 1.8 molts in the suboptimal treatment.

After 14 weeks, only 2 MPs remained in the optimal treatment, but there were still 17 MPs in the suboptimal treatment. There had been no change to FP in the suboptimal treatment for 3 weeks (Figs. 4A, 5). At this time, the ambient laboratory temperature of the suboptimal treatment began to rise (Fig. 4C). To simulate a switch from suboptimal (fall/winter) to optimal (spring/summer) breeding conditions, the temperature and photoperiod of the suboptimal treatment was changed to equal that of the optimal. The experiment was followed for another 8 weeks. At the end of this time, the two MPs of the original optimal treatment had not changed sex (verified by examination of pleopods after preservation). In the suboptimal treatment, after 6 weeks without any sex change and 3 weeks after the switch to optimal conditions, MPs began to change and continued to do so until the experiment was terminated (Fig. 5). In the last 8 weeks, 10 of 17 had changed to FP, while 2 others were late-stage transitionals (close to FP change) when removed from the experiment. Three of the original MPs in the suboptimal experiment remained, including one mid-stage transitional. Two others died during the last 8 weeks of the experiment.

At the beginning of the experiment, the mean size of MPs in the suboptimal ($n = 45$) and optimal ($n = 46$) treatments was equal (7.5 mm CL; $t$ test, $P = 0.80$) (Fig. 6). The size of FPs (sex-changed individuals) was compared between the suboptimal (9.2 mm CL; $n = 33$) and optimal treatments (9.1 mm CL; $n = 40$) (Fig. 6), and the hypothesis of no difference is accepted ($t$ test, $P = 0.58$). The size of FPs from the suboptimal treatment that transformed in weeks 14–22 (mean = 9.4 mm CL, $n = 10$) was slightly larger than that of FPs from the optimal treatment (Fig. 6), but the means of these two groups are not significantly different ($t$ test, $P = 0.14$).

## Discussion

This study addressed components of different hypotheses about the timing and degree of sex change in *Lysmata wurdemanni* that might explain the presence of large MPs (male-phase individuals) in this species. *Lysmata* spp. have a unique protandric sexual system in which sex-changed "females" (FPs) retain the ability to mate as males—that is, are simultaneous hermaphrodites (Bauer, 2000). The size (age) of change from MP to FP might be socially determined, resulting in considerable variation in sex change in

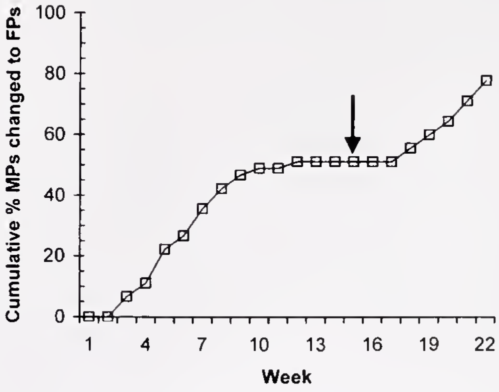

**Figure 5.** Change of large MPs to FPs in the suboptimal treatment during 22 weeks, first under suboptimal temperature and photoperiod for 14 weeks (as in Fig. 4A) and then after a change to optimal conditions (arrow) for the next 8 weeks.

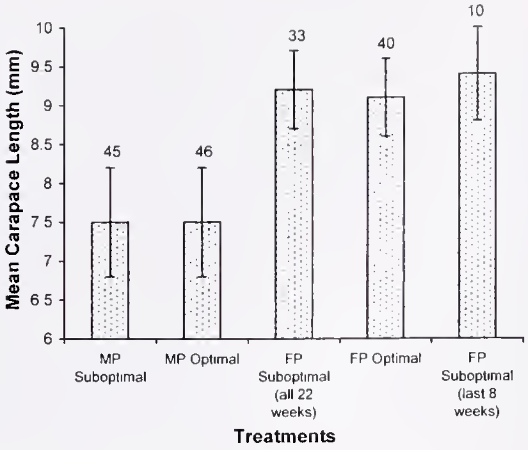

**Figure 6.** Sizes of MPs beginning experiment and of sex-changed individuals (FPs) in the large MP to FP sex change experiment. The number of individuals is given above each group. Error bars represent one standard deviation.

different demographic environments, as hypothesized for protandric pandalid shrimps (termed environmental sex determination, or ESD; Charnov *et al.*, 1978; Charnov, 1981; Charnov and Anderson, 1989). In ESD, the frequency of sexual morphs in the population (demographic environment), presumably perceived by contacts among individuals (socially mediated), influences the size and age at which males change to females. Delayed sex change might be advantageous to males in populations in which females are abundant. A sexually successful male might inseminate several females during the same period in which a female can produce only one brood of eggs, although those eggs are assured of fertilization by males.

However, "females" (FPs) of *L. wurdemanni* are simultaneous hermaphrodites that can mate as males (Bauer and Holt, 1998). The delayed sex change of MPs would only be adaptive, under an ESD hypothesis, if large MPs had a male mating advantage over the hermaphroditic FPs (Bauer and Holt, 1998; Bauer, 2000). In this study, I tested the relative male mating success of MPs and FPs by presenting a parturial FP simultaneously to a pair of potential male mating partners. Surprisingly, MFPs (FPs mating as males) were just as competitive as MPs, both large and small, in obtaining copulations from parturial FPs. Although these experiments demonstrated no male mating advantage of large MPs over FPs, large MPs were more successful than small MPs in obtaining the copulation of parturial FPs in a competitive situation. If FPs were not simultaneous hermaphrodites and thus could not mate as males, the superiority of large MPs over small MPs in inseminating parturial FPs would agree with an ESD explanation of delayed MP change to FP. However, there is no obvious benefit (selection pressure) favoring delayed change of a MP to a FP (a) whose male mating ability is equal to that of MPs, large and small, and (b) whose reproduction as a female is not only assured but, given spawning every 2 weeks, would be more productive if change to FP occurred as early in life as morphologically and physiologically possible. In a population with few FPs, large MPs would have the mating advantage over small MPs, but there would be few FPs to exercise that advantage with. In a population with abundant FPs, large MPs would have more parturial FPs to mate with, but also more FPs, mating as males, to compete with for the same parturial FPs. Not surprisingly, the percentage of large MPs in the population was not significantly correlated with either low or high percentage of FPs. These results are not concordant with a hypothesis of socially determined sex change in *L. wurdemanni*. However, only large-scale experiments in which sex change in different demographic environments is measured can give a definite answer about whether or not socially mediated ESD occurs in *L. wurdemanni* or other *Lysmata* spp. Based on such large-scale experiments and parentage studies, Marliave *et al.* (1993) rejected the hypothesis of socially determined sex change in the protandric hermaphroditic shrimp *Pandalus danae*.

The hypothesis that FPs may change back to MPs in *Lysmata* under certain conditions, accounting for large MPs, was suggested by the anecdotal observations of colleagues rearing *L. wurdemanni* and by work on *Athanas indicus* (Suzuki, 1970) in which reversion of protandric FPs to MP was reported. Control of sexual differentiation by the androgenic glands (AG), located on the distal vas deferens (ejaculatory duct), has been demonstrated in various malacostracan crustaceans (Charniaux-Cotton and Payen, 1985; Hasegawa *et al.*, 1993). Both males and females have primordia of the AG, but its development in genetic males causes growth of male external characters and testes. However, it is still not established that AG hormone is the only factor controlling sex differentiation in Crustacea (Sagi *et al.*, 1997). Study of AGs in caridean shrimps is limited. Disappearance of the AGs after change to the female phase was reported, on the basis of stereomicroscopical and histological observations, in *L. seticaudata* (Berreur-Bonnenfant and Charniaux-Cotton, 1965). In *L. amboinensis*, Fiedler (1998) reported an absence of AGs in FPs, but neither similar histological examination nor other observations on MP androgenic glands was given for comparison. However, as in *L. wurdemanni*, male ducts with sperm production are retained in FPs of both species. Fiedler (1998) showed that FPs of *L. amboinensis*, like those of *L. wurdemanni*, mate as males and inseminate prespawning FPs. A small number of *L. wurdemanni* FPs show external male characters (reduced appendices masculinae) (Bauer and Holt, 1998). Obviously, male function is maintained. Hormones maintaining male characters in FPs might still be produced by remnants of AGs retained from the MP stage but overlooked in histological studies. There must be a balance of male and female hormones in the FPs that allows simultaneous male and female function. Therefore, the possibility of change from FPs back to large MPs was tested in this study.

In the FP to MP sex change experiment, one group of FPs was maintained under optimal breeding conditions of high water temperature and long day length (Bauer and Holt, 1998; Lin and Zhang, 2001) approximating those found in late spring and summer at the collecting site (Bauer, 2002). Given the hypothesis of socially mediated ESD proposed for pandalid shrimps (Charnov, 1981), reversion to MP, if physiologically possible, might be expected in an all-FP group under optimal breeding conditions. However, mating experiments in this study showed no strong selective advantage for large MPs in a population with abundant FPs, and no reversion to the male phase was observed in the treatment with optimal breeding conditions.

The suboptimal treatment tested the possibility that FPs exposed to less favorable breeding conditions, such as lower water temperatures and short day length, might revert to large MPs. In many caridean species, females molt out of "breeding dress" (characters related to spawning and incubation) outside of the breeding season. In the simultaneous hermaphrodite FP of *L. wurdemanni*, it was hypothesized that suboptimal breeding conditions might tip the balance of male/female hormones away from the female phase back to the male phase. The FPs in this treatment were exposed to water temperatures and a photoperiod approximating late fall through early winter conditions in the natural habitat of the population sampled (Bauer, 2002). The less favorable breeding conditions of the suboptimal treatment are apparent from a comparison of the reproductive condition and molting rates between the suboptimal and optimal treatments. The percentage of FPs brooding embryos or preparing for spawning was only slightly higher in the optimal than in the suboptimal treatment. However, the molting rate of the optimal treatment, adjusted for number of FPs surviving, was more than twice that of the suboptimal treatment. In *L. wurdemanni* FPs, spawning occurs at every molt (Bauer and Holt, 1998), so that the higher molting of the optimal treatment indicates that more broods were produced. At the temperature and photoperiod of the optimal treatment, molting and spawning may occur every 10–14 days (Lin and Zhang, 2001; Bauer, pers. obs.). Using a figure of 12 days between spawning molts, a FP in the optimal treatment could have molted and spawned five times during the 9 weeks of the experiment. Molting in the suboptimal treatment was less than half of that in the optimal treatment, so that the number of FP molts in this treatment was about two, with a maximum of two spawns possible. Although breeding conditions were poorer in the suboptimal treatment, no reversion of FPs to MPs occurred. Given that change from MP to FP takes place within a single molt cycle, reversion of FPs back to a male phase could have taken place within a single molt cycle as well. In the suboptimal treatment, FPs passed through two molt cycles, sufficient opportunity for reversion to the male phase, which did not, however, occur.

The high relative abundance of large MPs from fall through early spring might be best explained by suppression of sex change to FPs because of suboptimal breeding conditions. In the fall, MPs that have grown to and beyond the minimum size of sex change may not transform as they enter a period of the year not favorable for embryo production and larval survival. The proximate factors that retard sex change may be seasonally related environmental conditions such as lower temperature or shorter day length. The change of large MPs to FPs was much higher in conditions simulating spring/summer than in those simulating fall/winter conditions. Nearly all large MPs changed to FPs in the optimal treatment during the first 14 weeks of observation. There was much less change to FP during the same time period (14 weeks) when MPs were maintained under suboptimal (fall/winter) conditions. Molting rates were lower, but MPs of sufficient size to change to FP require only one molt cycle to do so (Bauer and Holt, 1998). The average MP in this treatment molted twice during the first 14 weeks.

After 14 weeks, the conditions of the suboptimal treatment were changed to those of the optimal treatment to determine if the slower rate of sex change could be increased in the surviving MPs. After 3 weeks (6 weeks without any MP to FP change), MPs began again to change to FP, and a majority did change or were changing to FP by the end of the experiment. During the same period, neither of the two MPs remaining in the original optimal treatment changed. At the end of 22 weeks two MPs from the original suboptimal treatment had neither changed nor showed signs of change to FP in spite of a switch from suboptimal to optimal conditions during the last 8 weeks of observation. Lin and Zhang (2001) found that all MPs reared individually under optimal conditions became FPs; but when MPs were reared in groups of 10, as in this study, only 67% transformed to FP, much less than that observed in the present study. Lin and Zhang began with postlarvae (MPs), and the total period of observation was not specified. In the present study, the experiment began with MPs at or above the minimum size of change to FP. Although Lin and Zhang suggested that a rather high percentage of individuals never change sex (primary males), my results suggest that most, if not all, will change to FP sometime during their lifetime if they live out the maximum natural lifespan (about 1.5 years; A. W. Baldwin and R. T. Bauer, unpubl.). However, in both experimental groups in my study, a low percentage of individuals (4%) never changed under laboratory conditions.

The adaptive advantage of not changing to FP during the non-breeding season may be that reproductive effort will be wasted on embryo production during a period unfavorable to larvae. This energy might be channeled into maintenance and growth so that when spring arrives, the MP will change into a larger FP, with the benefit of a larger brood produced under conditions favorable to larval growth and survival. Brood size in *L. wurdemanni* is highly correlated with body size (Bauer, unpubl.), as in other carideans (Bauer, 1991). Suboptimal conditions did slow and then stop sex change in this study, explaining the presence of large and very large MPs during the fall through early spring in field samples. However, large MPs did not change to FP at a significantly larger size than large MPs reared under optimal (spring/summer) conditions.

In conclusion, mating experiments showed that FPs are competitive with MPs of any size in obtaining copulations with parturial FPs. There seems to be no mating advantage for an individual to remain a large MP, and under optimal breeding conditions, almost all change to FP. The proportion of large and very large MPs in the natural population studied is greatest from fall through early spring, and in the laboratory, change from MP to FP is slowed under the suboptimal breeding conditions of these seasons. Seasonal changes in abiotic proximate factors that regulate breeding, such as temperature and photoperiod, seem a more likely explanation for the occurrence of large MPs in *Lysmata wurdemanni* than does socially mediated ESD in different demographic situations. In *L. wurdemanni*, there may also be genetic variation in the size of sex change, although adaptive advantages to change at a larger size are not apparent from this and previous studies.

The proportion of FPs was often low in the *Lysmata wurdemanni* population sampled (Fig. 1). This is partly because all smaller (younger) individuals of this sex-changing species are male phase. In addition, as shown in this report and elsewhere (Bauer and Holt, 1998; Bauer, 2000), many large MPs capable of changing to FP do not do so for an extended period, so that the population often has a low proportion of FPs (Fig. 1). Therefore, the frequent occurrence of an extended male phase results in a lower number of FPs in the population (Fig. 1). This may affect the total output of larvae and subsequent recruitment potential of the population.

## Acknowledgments

This study was funded by the National Science Foundation (Biological Oceanography Program, grant OCE-99822466) and the Neptune Foundation. I thank student assistants Aaron Baldwin and Sara LaPorte for their careful work on the project. This is Contribution No. 91 of the Laboratory for Crustacean Research, University of Louisiana at Lafayette.

## Literature Cited

**Bauer, R. T. 1976.** Mating behaviour and spermatophore transfer in the shrimp *Heptacarpus pictus* (Stimpson) (Decapoda: Caridea: Hippolytidae). *J. Nat. Hist.* **10:** 415–440.

**Bauer, R. T. 1986.** Sex change and life history pattern in the shrimp *Thor manningi* (Decapoda: Caridea): a novel case of partial protandric hermaphroditism. *Biol. Bull.* **170:** 11–31.

**Bauer, R. T. 1991.** Analysis of embryo production in a caridean shrimp guild from a tropical seagrass meadow. Pp. 181–191 in *Crustacean Egg Production*, A. Wenner and A. Kuris, eds. A. A. Balkema, Rotterdam.

**Bauer, R. T. 2000.** Simultaneous hermaphroditism in caridean shrimps: a unique and puzzling sexual system in the Decapoda. *J. Crustac. Biol.* **20 (Special Number 2):** 116–128.

**Bauer, R. T. 2001.** Hermafroditismo en camarones: el sistema sexual y su relación con atributos socioecológicos. *Interciencia* **26:** 2–7.

**Bauer, R. T. 2002.** Reproductive ecology of a protandric simultaneous hermaphrodite, the shrimp *Lysmata wurdemanni* (Decapoda: Caridea: Hippolytidae). *J. Crustac. Biol.* **22:** 742–749.

**Bauer, R. T., and J. H. Abdalla. 2001.** Male mating tactics in the shrimp *Palaemonetes pugio* (Decapoda, Caridea): precopulatory mate guarding vs. pure searching. *Ethology* **107:** 185–200.

**Bauer, R. T., and G. J. Holt. 1998.** Simultaneous hermaphroditism in the marine shrimp *Lysmata wurdemanni* (Caridea: Hippolytidae): an undescribed sexual system in the decapod Crustacea. *Mar. Biol.* **132:** 223–235.

**Berglund, A. 1986.** Sex change by a polychaete: effects of social and reproductive costs. *Ecology* **67:** 837–845.

**Bergström, B. I. 1997.** Do protandric pandalid shrimp have environmental sex determination? *Mar. Biol.* **128:** 397–407.

**Bergström, B. I. 2000.** The biology of *Pandalus*. *Adv. Mar. Biol.* **38:** 1–245.

**Berreur-Bonnenfant, J., and H. Charniaux-Cotton. 1965.** Hermaphrodisme protérandrique et fonctionnemente de la zone germinative chez la crevette *Pandalus borealis* Kröyer. *Bull. Soc. Zool. Fr.* **90:** 240–259.

**Bull, J. J. 1980.** Sex determination in reptiles. *Q. Rev. Biol.* **55:** 3–21.

**Butler, T. H. 1980.** Shrimps of the Pacific coast of Canada. *Can. Bull. Fish. Aquat. Sci.* **202:** 1–280.

**Chan, S. T. H., and W. S. B. Yeung. 1983.** Sex control and sex reversal in fish under natural conditions. Pp. 171–221 in *Fish Physiology*, W. S. Hoar, D. J. Randall, and E. M. Donaldson, eds. Academic Press, New York.

**Charniaux-Cotton, H. 1975.** Hermaphroditism and gynandromorphism in malacostracan Crustacea. Pp. 91–105 in *Intersexuality in the Animal Kingdom*, R. Reinboth, ed. Springer Verlag, New York.

**Charniaux-Cotton, H., and G. Payen. 1985.** Sexual differentiation. Pp. 217–299 in *The Biology of Crustacea, Vol. 9, Integuments, Pigments, and Hormonal Processes*, D. E. Bliss and L. H. Mantel, eds. Academic Press, New York.

**Charnov, E. L. 1981.** Sex reversal in *Pandalus borealis*: effect of a fishery? *Mar. Biol. Lett.* **2:** 53–57.

**Charnov, E. L. 1982.** *The Theory of Sex Allocation.* Princeton University Press, Princeton, NJ. 355 pp.

**Charnov, E. L., and P. J. Anderson. 1989.** Sex change and population fluctuations in pandalid shrimp. *Am. Nat.* **134:** 824–827.

**Charnov, E. L., D. W. Gotshall, and J. G. Robinson. 1978.** Sex ratio: adaptive response to population fluctuations in pandalid shrimp. *Science* **200:** 204–206.

**Conover, O., and S. B. Munch. 2002.** Sustaining fisheries yields over evolutionary time scales. *Science* **297:** 94–96.

**Dohrn, P. F. R. 1950.** Studi sulla *Lysmata seticaudata* Risso (Hyppolytidae). I. Le condizioni normali della sessualita in natura. *Pubbl. Stn. Zool. Napoli* **22:** 257–272.

**Ferguson, M. W. J., and T. Joanen. 1982.** Temperature of egg incubation determines sex in *Alligator mississippiensis*. *Nature* **296:** 850–853.

**Fiedler, G. C. 1998.** Functional, simultaneous hermaphroditism in female-phase *Lysmata amboinensis* (Decapoda: Caridea: Hippolytidae). *Pac. Sci.* **52:** 161–169.

**Ghiselin, M. T. 1969.** The evolution of hermaphroditism among animals. *Q. Rev. Biol.* **44:** 189–208.

**Hasegawa, Y., E. Hirose, and Y. Katakura. 1993.** Hormonal control of sexual differentiation and reproduction in Crustacea. *Am. Zool.* **33:** 403–411.

**Lin, J., and D. Zhang. 2001.** Reproduction in a simultaneous hermaphroditic shrimp, *Lysmata wurdemanni*: any two will do? *Mar. Biol.* **139:** 919–922.

**Marliave, J. B., W. F. Gergits, and S. Aota. 1993.** $F_{10}$ pandalid shrimp: sex determination; DNA and dopamine as indicators of domestication; and outcrossing for wild pigment pattern. *Zoo Biol.* **12:** 435–451.

**Munday, P. L. 2002.** Bi-directional sex change: testing the growth-rate advantage model. *Behav. Ecol. Sociobiol.* **52:** 247–254.

**Nakashima, Y. 1987.** Reproductive strategies in a partially protandric shrimp, *Athanas kominatoensis* (Decapoda: Alpheidae): sex change as the best of a bad situation for subordinates. *J. Ethol.* **5:** 145–159.

**Policansky, D. 1982.** Sex change in plants and animals. *Annu. Rev. Ecol. Syst.* **13:** 471–495.

**Ross, R. M. 1990.** The evolution of sex-change mechanisms in fishes. *Environ. Biol. Fishes.* **29:** 81–93.

**Sagi, A., E. Snir, and I. Khalaila. 1997.** Sexual differentiation in decapod crustaceans: role of the androgenic gland. *Invertebr. Reprod. Dev.* **31:** 55–61.

**Spitschakoff, T. 1912.** *Lysmata seticaudata* Risso, als Beispiel eines echten Hermaphroditismus bei en Decapoden. *Z. Wiss. Zool.* **100:** 190–209.

**Suzuki, H. 1970.** Taxonomic review of four alpheid shrimps belonging to the genus *Athanas* with reference to their sexual phenomenona. *Sci. Rep. Yokohama Natl. Univ. Sect. II Biol. Geol. Sci.* **17:** 1–37.

**Thornhill, R., and J. Alcock. 1983.** *The Evolution of Insect Mating Systems.* Harvard University Press, Cambridge, MA. 547 pp.

**Warner, R. R. 1975.** The adaptive significance of sequential hermaphroditism in animals. *Am. Nat.* **109:** 61–82.

**Wilson, E. O. 1976.** *Sociobiology.* Harvard University Press, Cambridge, MA. 697 pp.

**Zupo, V. 2001.** Influence of diet on sex determination of *Hippolyte inermis* Leach (Decapoda: Natantia) in the field. *Hydrobiologia* **449:** 131–140.

# INDEX

A

Abundance, 263
Acetylcholine, 231
Acetylcholine mediates excitatory input to chromatophore motoneurons in the squid, *Loligo pealeii*, 231
Acid-base balance, 42
Actin filament, 206
Adams, C. E., see D. E. W. Arnolds, 188
Adhesion, 338
Air exposure, 42
Algal
  bloom, 244
  physiology, 1
Allen, Matt C., see Jeremy M. Testa, 255
Ammonium, 258
Amorphous calcium carbonate, 269
Amphipod, 248
Amplexus, 225
Anatomical correlates of venom production in *Conus californicus*, 27
Anderson, Don, see Jane La Du, 244
Anesthetic, 188
Anion channel, 194
Annual Report of the Marine Biological Laboratory, v. 203(1) R1
*Anomalocera ornata*, 307
*Anthopleura* spp., 315
Aplacophoran embryo, 87
Apoptosis, 70
Armstrong, Margaret T., see Peter B. Armstrong, 203
Armstrong, Peter B., Margaret T. Armstrong, R. L. Pardy, Alice Child, and Norman Wainwright, Immunohistochemical demonstration of a lipopolysaccharide in the cell wall of a eukaryote, the green alga *Chlorella*, 203
Arnolds, D. E. W., S. J. Zottoli, C. E. Adams, S. M. Dineen, S. Fevrier, Y. Guo, and A. J. Pascal, Physiological effects of tricaine on the supramedullary/dorsal neurons of the cunner, *Tautogolabrus adspersus*, 188
Arthropod relationships, 221
Atema, Jelle, see Sarah M. Rohrkasse, 235
Axon
  injury, 219
  perfused, 189
  repair, 219
  sealing, 219

B

Bacterioplankton, 251
Bacterioplankton community composition in flowing waters of the Ipswich River watershed, 251
Baker, Robert, see Werner Graf, 236
*Balanus*, 173
Barlow, R. B., see K. Smith, 222; C. Ridings, 224; Douglas Borst, 227
Barnacle, 173
Barnes, David K. A., Clade perseverance from Mesozoic to present: a multidisciplinary approach to interpretation of pattern and process, 161
Barron, Stacy, Carolyn Weber, Roxanne Marino, Eric Davidson, Gabrielle Tomasky, and Robert Howarth, Effects of varying salinity on phytoplankton growth in a low-salinity coastal pond under two nutrient conditions, 260
Barron, Stacy, see Carolyn F. Weber, 261
Bartman, Marc, see Robert B. Silver, 213
Bauer, Raymond T., Tests of hypotheses on the adaptive value of an extended male phase in the hermaphroditic shrimp *Lysmata wurdemanni* (Caridea: Hippolytidae), 347
Behavior, 112, 197, 224, 227, 232
  predatory, 241
  social, 240
Benthic community, 256
Bingham, Jon-Paul, see Jennifer Marshall, 27
Biochemical differences between trail mucus and adhesive mucus from marsh periwinkle snails, 338
Biochemistry, sea anemone, 315
Biomineralization, 269
Bittner, George D., see Christopher S. Eddleman, 219
Blade motion, 1
Blockade of an inward sodium current facilitates pharmacological study of hemi-gap-junctional currents in *Xenopus* oocytes, 192
Blood cell, 204
Bodznick, David, see John Montgomery, 238
Borley, Kimberly A., Herman T. Epstein, and Alan M. Kuzirian, Effects of a sensory block on calexcitin levels in the photoreceptors of *Hermissenda crassicornis*, 197
Borst, D., see C. Ridings, 224
Borst, Douglas, and Robert Barlow, Circadian rhythms in locomotor activity of juvenile horseshoe crabs, 227
Brackish water, 261
Braun, A., see K.-G. Lee, 204
Brown, Jeremiah R., Elizabeth M. Peacock-Villada, and George M. Langford, Globular tail fragment of myosin-V displaces vesicle-associated motor and blocks vesicle transport in squid nerve cell extracts, 210
Brumwell, Gordon B., and Vicki J. Martin, Immunocytochemically defined populations of neurons progressively increase in size through embryogenesis of *Hydra vulgaris*, 70
Buchsbaum, Robert, see John P. Ludlam, 250
Burnett, Louis, Nora Terwilliger, Amy Carroll, Darwin Jorgensen, and David Scholnick, Respiratory and acid-base physiology of the purple sea urchin, *Strongylocentrotus purpuratus*, during air exposure: presence and function of a facultative lung, 42
Bystrova, Olga A., see Marina G. Martynova, 104

C

$Ca^{2+}$ effects on myosin-II-mediated contraction of pseudo-contractile rings and transport of vesicles in extracts of clam oocytes, 206
*Calanopia americana*, 307
Calcium, 206, 213
  metabolism, 269
  storage, 269
Calcium-dependent phospholipase A2, 213
Calcium-independent phospholipase A2, 213
Calexcitin, 197
Canopy structure, 248
*Caranx latus*, 241
*Caranx latus* (Carangidae) chooses dock pilings to attack silverside schools: a tactic to interfere with stereotyped escape behavior of prey?, 241
Carbenoxolone, 192
Carbon, 228
Caridea, 347
Carmichael, Ruth H., see Dianne N. Suggs, 225; Emily F. Gaines, 228
Carroll, Amy, see Louis Burnett, 42

Carton, Guy, see John Montgomery, 238
Catalase, 212
Cell cycle, 58
Central pathways mediating oculomotor reflexes in an elasmobranch, *Scyliorhinus canicula*, 236
Central pattern generator, 152
*Centropages typicus*, 307
Cephalopod, 14, 231, 232
Cerebellar-like, 238
Cerebellum, 238
Cermak, Michael J., *Caranx latus* (Carangidae) chooses dock pilings to attack silverside schools: a tactic to interfere with stereotyped escape behavior of prey?, 241
Chaikhoutdinov, I., see K.-G. Lee, 204
Chang, Ernest S., see Jeffrey L. Spees, 331
Chang, Sharon A., see Jeffrey L. Spees, 331
Chaparro, R., J. L. Charpentier, and R. Collin, Embryonic velar structure and function of two sibling species of *Crepidula* with different modes of development, 80
Chappell, Richard L., see Stephen Redenti, 200
Charette, Matthew A., see Jeremy M. Testa, 255
Charpentier, J. L., see R. Chaparro, 80
Cheilostome, 161
Chemoreception, 235
Chiao, Chuan-Chin, see Melissa M. Grable, 232
Chikarmane, Hemant M., see Jennifer L. Hsieh, 266
Child, Alice, see Peter B. Armstrong, 203
*Chlorella*, 203
Chromatophore, 231
Circadian rhythms in locomotor activity of juvenile horseshoe crabs, 227
$Cl^-$ and glutamate$^-$ competition for a volume-regulated anion channel, 194
Clade, 161
Clade perseverance from Mesozoic to present: a multidisciplinary approach to interpretation of pattern and process, 161
Clam, 206, 208
Cleavage, spiral, 87
Cnidaria, 70
Cohen, Jonathan H., and Richard B. Forward, Jr., Spectral sensitivity of vertically migrating marine copepods, 307
Cohen, W., see K.-G. Lee, 204
Collin, R., see R. Chaparro, 80
Competition, 161, 173
  exploitation, 173
  interference, 173
Cone snail, 27
Conrad, M., see K.-G. Lee, 204
Contractile ring, 206, 208
Copepod, 307
Crab, estuarine, 289
Crawford, Karen, Culture method for *in vitro* fertilization to hatching of the squid, *Loligo pealeii*, 216
*Crepidula*
  *dilatata*, 80
  *fecunda*, 80
Crump, Byron C., see Uri Y. Levine, 251
Crustacean, 269
Culture, 216
Culture method for *in vitro* fertilization to hatching of the squid, *Loligo pealeii*, 216
Cuttlefish body patterns as a behavioral assay to determine polarization perception, 232
Cyanobacteria, 260
Cyclostome, 161
Cytoskeleton, 204

D

Davidson, Eric A., see Stacy Barron, 260; Carolyn F. Weber, 261
Deegan, Linda, see Sarah Twichell, 256
Delaney, Martha, Christopher Follet, Nick Ryan, Nick Hanney, Jenny Lusk-Yablick, and Gabriele Gerlach, Social interaction and distribution of female zebrafish *(Danio rerio)* in a large aquarium, 240
Delgado, Gabriel A., Robert A. Glazer, and Nicola J. Stewart, Predator-induced behavioral and morphological plasticity in the tropical marine gastropod *Strombus gigas*, 112
Denaturing gradient gel electrophoresis, 251
Denny, Mark, and Loretta Roberson, Blade motion and nutrient flux to the kelp, *Eisenia arborea*, 1
Denny, Mark W., Elizabeth K. Nelson, and Kristina S. Mead, Revised estimates of the effects of turbulence on fertilization in the purple sea urchin *Strongylocentrotus purpuratus*, 275
DeNobile, J., see K.-G. Lee, 204
DePina, Ana S., see Torsten Wöllert, 206, 208
Development
  molluscan, 278
  rate, 58
Development of the lateral eye of juvenile *Limulus*, 222
DGGE, 251
Diel vertical migration, 307
Diet, 228
Dineen, S. M., see D. E. W. Arnolds, 188
Dinoflagellate, 244
Dissolved iron cycling in the subterranean estuary of a coastal bay: Waquoit Bay, Massachusetts, 255
Dodge, F. A., see K. Smith, 222; C. Ridings, 224
Dorsal cell, 188
Dunlap, Walter C., see J. Malcolm Shick, 315
Dyhrman, Sonya, see Jane La Du, 244
Dysgerminoma, 265

E

Early neurogenesis in the horseshoe crab *Limulus polyphemus* and its implication for arthropod relationships, 221
Echinoderm, 42, 121
Eckelbarger, Kevin J., and Craig M. Young, Spermiogenesis and modified sperm morphology in the "seepworm" *Methanoaricia dendrobranchiata* (Polychaeta: Orbiniidae) from a methane seep environment in the Gulf of Mexico: implications for fertilization biology, 134
Eddleman, Christopher S., George D. Bittner, and Harvey M. Fishman, SEM comparison of severed ends of giant axons isolated from squid *(Loligo pealeii)* and crayfish *(Procambarus clarkii)*, 219
Edds-Walton, Peggy L., see Richard R. Fay, 195
Eelgrass habitat, 247
Effects of a sensory block on calexcitin levels in the photoreceptors of *Hermissenda crassicornis*, 197
Effects of haying on salt-marsh surface invertebrates, 250
Effects of individual size on pairing in horseshoe crabs, 225
Effects of varying salinity on phytoplankton growth in a low-salinity coastal pond under two nutrient conditions, 260
Egg
  capsule, 278
  envelope, 289
  laying, 289
  size, 58
*Eisenia arborea*, 1
Elasmobranch, 236
Embryo, 58, 70, 87, 278
  aplacophoran, 87
  attachment system, 289
  culture, 278
Embryogenesis and development of *Epimenia babai* (Mollusca Neomeniomorpha), 87
Embryonic velar structure and function of two sibling species of *Crepidula* with different modes of development, 80
Emersion, 42
Endotoxin, 203
Energy dissipation rate, 275
Enhancement, 200
Epidermal growth factor, 278
Epstein, Herman T., see Kimberly A. Borley, 197

Erdner, Deana, see Jane La Du, 244
ERG, 198, 200
Error-driven motor learning in fish, 238
Escape, 144
Escape jet, 14
Estuarine crab, 289
Estuarine–open-water comparison of fish community structure in eelgrass *(Zostera marina* L.) habitats of Cape Cod, 247
Ethyl-*m*-aminobenzoate, 188
Evolution, 58
  molluscan, 87
  sea anemone, 315
Evolution of fast development of planktonic embryos to early swimming, 58
Exploitation competition, 173
Extracts, 206, 208
Eye development, 222
Eyman, Maria, see Antonio Giuditta, 189

F

Facultative lung, 42
Farley, Gregory S., Helical nature of sperm swimming affects the fit of fertilization-kinetics models to empirical data, 51
Fay, Richard R., and Peggy L. Edds-Walton, Preliminary evidence for interpulse interval selectivity of cells in the torus semicircularis of the oyster toadfish *(Opsanus tau)*, 195
Fertilization, 51, 134, 275
  efficiency, 51
  kinetics, 51
  success, 275
Fevrier, S., see D. E. W. Arnolds, 188
Filter feeder, 173
Findley, Ann, see Earl Weidner, 212
Fish, 195, 238
Fish community structure, 247
Fishman, Harvey M., see Christopher S. Eddleman, 219
Fixed action pattern, 144
Flow, 1
Follet, Christopher, see Martha Delaney, 240
Food web, 228
Foraging, 248
Forward, Richard B., see Jonathan H. Cohen, 307
*Fundulus heteroclitus*, 248

G

Gaines, Emily F., Ruth H. Carmichael, Sara P. Grady, and Ivan Valiela, Stable isotopic evidence for changing nutritional sources of juvenile horseshoe crabs, 228
*Gammarus mucronatus*, 248
Gap junction, 192
Garber, Sarah S., and Mary M. Hoffman, $Cl^-$ and glutamate$^-$ competition for a volume-regulated anion channel, 194
Garritt, Robert, see Sarah Twichell, 256
Gastropod, 278
Gating currents, 190
Gene expression, 189
Gene expression in the squid giant axon: neurotransmitter modulation of RNA transfer from periaxonal glia to the axon, 189
General Scientific Meetings of the Marine Biological Laboratory, 185
  featured reports, 185
Geographic
  information system, 253
  variability, 161
Gerlach, Gabriele, see Martha Delaney, 240
Giblin, Anne, see Ketil Koop-Jakobsen, 258
Gilland, Edwin, see Werner Graf, 236
Gilles, Nicole L., see Melissa M. Grable, 232
Gilly, William F., see Jennifer Marshall, 27
GIS, 253
Giuditta, Antonio, Maria Eyman, and Barry B. Kaplan, Gene expression in the squid giant axon: neurotransmitter modulation of RNA transfer from periaxonal glia to the axon, 189
Glazer, Robert A., see Gabriel A. Delgado, 112
Glia, 189
Globular tail fragment of myosin-V displaces vesicle-associated motor and blocks vesicle transport in squid nerve cell extracts, 210
Goldberg, Jeffrey I., see Shihuan Kuang, 278
Gould, Robert M., see Nicholas Pahl, 217
Grable, Melissa M., Nadav Shashar, Nicole L. Gilles, Chuan-Chin Chiao, and Roger T. Hanlon, Cuttlefish body patterns as a behavioral assay to determine polarization perception, 232
Grady, Sara P., see Dianne N. Suggs, 225; Emily F. Gaines, 228
Graf, Werner, Edwin Gilland, Matt McFarlane, Laura Knott, and Robert Baker, Central pathways mediating oculomotor reflexes in an elasmobranch, *Scyliorhinus canicula*, 236
Groundwater, 255
Growth rate, 263
GTPase Rho is involved in myosin-II-mediated contraction of pseudocontractile rings and transport of vesicles in extracts of clam oocytes, 208
Guo, Y., see D. E. W. Arnolds, 188

H

Habitat structure, 241
Hammar, Katherine, see Gilad Twig, 198
Hanley, Janice, see Roxanna Smolowitz, 265
Hanlon, Roger T., see Melissa M. Grable, 232
Hanney, Nick, see Martha Delaney, 240
Haying, 250
Hearing, 195
Heat-shock protein, 331
Hecker, Arnaud, see Sefi Raz, 269
Helical nature of sperm swimming affects the fit of fertilization-kinetics models to empirical data, 51
Hemichannel, 192
Herbold, Craig W., see Jeremy M. Testa, 255
Hermaphroditism, 347
*Hermissenda*, 197
Histidine, 200
Hoffman, Mary M., see Sarah S. Garber, 194
Homsi, Sara, see Nicholas Pahl, 217
Horseshoe crab, see *Limulus*
Howarth, Robert, see Stacy Barron, 260; Carolyn F. Weber, 261
Hsieh, Jennifer L., Hemant M. Chikarmane, Roxanna Smolowitz, Kevin R. Uhlinger, W. Mebane, and Alan M. Kuzirian, Microbial analysis of ozone disinfection in a recirculating seawater system, 266
Huffaker, Diana, and R. Gil Pontius, Jr., Reconstruction of historical land cover in the Ipswich watershed, 253
Hughes, Jeffrey, see Kristin Hunter-Thomson, 247; Bradley S. Williams, 248
Hunter-Thomson, Kristin, see Bradley S. Williams, 248
Hunter-Thomson, Kristin, Jeffrey Hughes, and Bradley Williams, Estuarine–open-water comparison of fish community structure in eelgrass *(Zostera marina* L.) habitats of Cape Cod, 247
Hunting tactic, 241
Hydrostatic skeleton, 14

I

Immunocytochemically defined populations of neurons progressively increase in size through embryogenesis of *Hydra vulgaris*, 70
Immunocytochemistry, 197
Immunofluorescence, 204
Immunohistochemical demonstration of a lipopolysaccharide in the cell wall of a eukaryote, the green alga *Chlorella*, 203
Impulse, 14
Influence of epiphytic algal coverage on fish predation rates in simulated eelgrass habitats, 248
Injury-induced vesiculation, 219

Interference competition, 173
Intertidal sediments, 258
Intestine, 42
*In vitro* fertilization, 216
Ion
  permeation, 194
  strength, 194
Ipswich River watershed, 251; 253
Iron, 255

J

JD1, 70
Jorgensen, Darwin, see Louis Burnett, 42

K

Kaplan, Barry B., see Antonio Giuditta, 189
Kelley, Wayne P., see Jennifer Marshall, 27
Kelp, 1
Kier, William M., see Joseph T. Thompson, 14
Knott, Laura, see Werner Graf, 236
Koop-Jakobsen, Ketil, and Anne Giblin, Tidal flushing of ammonium from intertidal salt marsh sediments: the relative importance of adsorbed ammonium, 258
Kuang, Shihuan, Marette Regnier, and Jeffrey I. Goldberg, Long-term culture of decapsulated gastropod embryos: a transplantation study, 278
Kuzirian, Alan M., see Kimberly A. Borley, 197; Jennifer L. Hsieh, 266

L

*Labidocera aestiva*, 307
La Du, Jane, Deana Erdner, Sonya Dyhrman, and Don Anderson, Molecular approaches to understanding population dynamics of the toxic dinoflagellate *Alexandrium fundyense*, 244
LALF, 203
Land-use change, 253
Landowne, David, Perchlorate prevents sodium channel gating and sodium protects in the squid giant axon, 190
Langford, George M., see Torsten Wöllert, 206, 208; Jeremiah R. Brown, 210
Larva, 58, 87, 121
Laser ablation, 278
Lawrence, K.A., and W.H. Watson III, Swimming behavior of the nudibranch *Melibe leonina*, 144
Learning, 197, 238
Lee, K.-G., A. Braun, I. Chaikhoutdinov, J. DeNobile, M. Conrad, and W. Cohen, Rapid visualization of microtubules in blood cells and other cell types in marine model organisms, 204
Levine, Uri Y., and Byron C. Crump, Bacterioplankton community composition in flowing waters of the Ipswich River watershed, 251
Levy, Hanna, see Gilad Twig, 198
Life history classification, 247
Light, 307
Limit oscillator, 213
*Limulus*, 221, 222, 224, 225, 227, 228, 235
  anti-lipopolysaccharide factor (LALF), 203
  behavior, 224, 227
  ommatidia, 222
  vision, 222, 224, 227
Lipopolysaccharide, 203
Lobster, 331
Locomotion, 14, 227
Lohse, David P., Relative strengths of competition for space and food in a sessile filter feeder, 173
*Loligo*, 216
Long-term culture of decapsulated gastropod embryos: a transplantation study, 278
Low-salinity system, 260
Ludlam, John P., David H. Shull, and Robert Buchsbaum, Effects of haying on salt-marsh surface invertebrates, 250
Luquet, Gilles, see Sefi Raz, 269
Lusk-Yablick, Jenny, see Martha Delaney, 240
*Lysmata wurdemanni*, 347

M

MAAs, 315
Macroalgae, 1
Malchow, Robert Paul, see Gilad Twig, 198
Mantle, 14
Marginal band, 204
Marine Biological Laboratory
  Annual Report, v. 203(1) R1
  General Scientific Meetings, 185
Marine diversity, 161
Marino, Roxanne, see Stacy Barron, 260; Carolyn F. Weber, 261
Marshall, Jennifer, Wayne P. Kelley, Stanislav S. Rubakhin, Jon-Paul Bingham, Jonathan V. Sweedler, and William F. Gilly, Anatomical correlates of venom production in *Conus californicus*, 27
Martin, Vicki J., see Gordon B. Brumwell, 70
Martinetto, Paulina, see Melissa Millman, 263
Martynova, Marina G., and Olga A. Bystrova, Undifferentiated cells in the snail myocardium are capable of DNA synthesis and myodifferentiation, 104
Mass spectrometry, 27
Mate selection, 225
Mating, 347
McClintock, James B., see Minako Vickery, 121
McFarlane, Matt, see Werner Graf, 236
Mead, Kristina S., see Mark W. Denny, 275
Mebane, W., see Jennifer L. Hsieh, 266
*Melibe leonina*, 144, 152
Methane seep, 134
A metronome-like control of the calcium signal leading to nuclear envelope breakdown and mitosis in sand dollar *(Echinaracnius parma)* cells, 213
Microbial analysis of ozone disinfection in a recirculating seawater system, 266
Microbial sampling, 266
Microdomain, 213
Microtubule, 204
Midbrain, 195
Millman, Melissa, Mirta Teichberg, Paulina Martinetto, and Ivan Valiela, Response of shrimp populations to land-derived nitrogen in Waquoit Bay, Massachusetts, 263
Mitosis, 213
Mitotic apparatus, 213
Mittmann, Beate, Early neurogenesis in the horseshoe crab *Limulus polyphemus* and its implication for arthropod relationships, 221
Modeling, 253
Molecular approaches to understanding population dynamics of the toxic dinoflagellate *Alexandrium fundyense*, 244
Mollusc, 144, 152; 338
  development, 87, 278
  evolution, 87
Montgomery, John, Guy Carton, and David Bodznick, Error-driven motor learning in fish, 238
Morin, Martha A., see Andrew M. Smith, 338
Morphogenesis and organogenesis in the regenerating planktotrophic larvae of asteroids and echinoids, 121
Morphology, 112
Morrison, Hilary G., see Nicholas Pahl, 217
Motion and nutrient flux to the kelp, *Eisenia arborea*, 1
Motoneuron, 231
mRNAs located in *Squalus acanthias* (spiny dogfish) oligodendrocyte processes, 217
MS-222, 188
Mucus, 338
Muscle, 14

Mycosporine-like amino acid content in four species of sea anemones in the genus *Anthopleura* reflects phylogenetic but not environmental or symbiotic relationships, 315
Mycosporine-like amino acids (MAAs), 315
Myelination, 217
Myosin
  -II, 206, 208
  -V, 210

## N

Nelson, Elizabeth K., see Mark W. Denny, 275
Nerve cell extracts, 210
Nervous system development, 70
Neural correlates of swimming behavior in *Melibe leonina*, 152
Neurogenesis, 221
Neuron, supramedullary, 188
Neuropeptide expression, 70
Newcomb, James M., see Winsor H. Watson III, 152
Nitrogen, 228
  limitation, 261
A novel turtle retinal preparation for simultaneously measuring light-induced electrical activity and changes in metabolite levels, 198
Nudibranch, 144, 152
Nurse eggs, 80
Nutrient
  flux, 1
  limitation, 261
  loading, 256
Nutrient and freshwater inputs from sewage effluent discharge alter benthic algal and infaunal communities in a tidal salt marsh creek, 256
Nutrient limitation of phytoplankton growth in Vineyard Sound and Oyster Pond, Falmouth, Massachusetts, 261

## O

Oculomotor, 236
Okusu, Akiko, Embryogenesis and development of *Epimenia babai* (Mollusca Neomeniomorpha), 87
Oligodendrocyte, 217
Ommatidia, 222
Ontogeny, 14
Ontogeny of squid mantle function: changes in the mechanics of escape-jet locomotion in the oval squid, *Sepioteuthis lessoniana* Lesson, 1830, 14
Oocyte, 192, 206, 208
Open water, 247
Opposed band cilia, 80
*Orchestia*, 250
Osmoconformer, 42
Osmotic induction of stress-responsive gene expression in the lobster *Homarus americanus*, 331
Osphradium, 235
Ovigerous, 263
Oxygen, 198
Ozone disinfection, 266

## P

Pahl, Nicholas, Sara Homsi, Hilary G. Morrison, and Robert M. Gould, mRNAs located in *Squalus acanthias* (spiny dogfish) oligodendrocyte processes, 217
Pancreatic carcinoma, 265
Paralytic shellfish poisoning, 244
Pardy, R. L., see Peter B. Armstrong, 203
Pascal, A. J., see D. E. W. Arnolds, 188
Peacock-Villada, Elizabeth M., see Jeremiah R. Brown, 210
Pearse, John S., see J. Malcolm Shick, 315
Pearse, Vicki B., see J. Malcolm Shick, 315
Pelagic larval duration of the Caribbean wrasse, *Thalassoma bifasciatum*, 245
Perchlorate, 190
Perchlorate prevents sodium channel gating and sodium protects in the squid giant axon, 190
Perfused axon, 189
Perlman, Ido, see Gilad Twig, 198
Peroxisomal catalase in extrusion apparatus posterior vacuole of microsporidian spores, 212
pH, 198
Philibotte, Jason, Pelagic larval duration of the Caribbean wrasse, *Thalassoma bifasciatum*, 245
*Philoscia*, 250
Phosphate, 255
Physiological effects of tricaine on the supramedullary/dorsal neurons of the cunner, *Tautogolabrus adspersus*, 188
Phytoplankton, 260
Plankton, 58
Plum Island Sound, 250
Polychaete, 134
Polyubiquitin, 331
Pontius, R. Gil Jr., see Diana Huffaker, 253
Population dynamics, 244
Predator-induced behavioral and morphological plasticity in the tropical marine gastropod *Strombus gigas*, 112
Predatory behavior, 241
Preliminary evidence for interpulse interval selectivity of cells in the torus semicircularis of the oyster toadfish *(Opsanus tau)*, 195
Programmed cell death, 70
Protandry, 347

## Q

Qian, Haohua, see Harris Ripps, 192
Queen conch, 112
Quinine, 192

## R

Radula, 27
Rago, Adam, see Jeremy M. Testa, 255
Rapid visualization of microtubules in blood cells and other cell types in marine model organisms, 204
Raz, Sefi, Olivier Testeniere, Arnaud Hecker, Steve Weiner, and Gilles Luquet, Stable amorphous calcium carbonate is the main component of the calcium storage structures of the crustacean *Orchestia cavimana*, 269
Recirculating system, 266
Reconstruction of historical land cover in the Ipswich watershed, 253
Redenti, Stephen, and Richard L. Chappell, Zinc chelation enhances the zebrafish retinal ERG b-wave, 200
Redox, 255
Regeneration, 121
Regnier, Marette, see Shihuan Kuang, 278
Relative strengths of competition for space and food in a sessile filter feeder, 173
Respiration, 42
Respiratory and acid-base physiology of the purple sea urchin, *Strongylocentrotus purpuratus*, during air exposure: presence and function of a facultative lung, 42
Response of shrimp populations to land-derived nitrogen in Waquoit Bay, Massachusetts, 263
Retina, 198, 200
Retinoic acid, 192
Revised estimates of the effects of turbulence on fertilization in the purple sea urchin *Strongylocentrotus purpuratus*, 275
RFamide, 70
Rho GTPase, 208
Rhythm, 144
Richmond, Hazel, see Roxanna Smolowitz, 265
Ridings, C., see K. Smith, 222
Ridings, C., D. Borst, K. Smith, F. Dodge, and R. Barlow, Visual behavior of juvenile *Limulus* in their natural habitat and in captivity, 224

Ripps, Harris, Haohua Qian, and Jane Zakevicius, Blockade of an inward sodium current facilitates pharmacological study of hemi-gap-junctional currents in *Xenopus* oocytes, 192

RNA synthesis, 189

Roberson, Loretta, see Mark Denny, 1

Rohrkasse, Sarah M., and Jelle Atema, Tracking behavior of Busyconinae whelks, 235

Rubakhin, Stanislav S., see Jennifer Marshall, 27

Ryan, Nick, see Martha Delaney, 240

S

Saigusa, M., M. Terajima, and M. Yamamoto, Structure, formation, mechanical properties, and disposal of the embryo attachment system of an estuarine crab, *Sesarma haematocheir*, 289

Salinity, 260

Salt marsh, 250, 256, 258

Sand dollar, 213

Scholnick, David, see Louis Burnett, 42

Sea anemone
- biochemistry, 315
- evolution, 315
- symbiosis, 315

Sea star, 144

Sea urchin, 42, 275

SEM comparison of severed ends of giant axons isolated from squid *(Loligo pealeii)* and crayfish *(Procambarus clarkii)*, 219

Seminoma, 265

Sensory block, 197

Sensory-motor integration, 231

*Sepia*, 232

Severed axon structure, 219

Sewage input, 256

Sex
- change, 347
- determination, 347

Shark hindbrain, 236

Shashar, Nadav, see Melissa M. Grable, 232

Sheldon, Sallie, see Sarah Twichell, 256

Shick, J. Malcolm, Walter C. Dunlap, John S. Pearse, and Vicki B. Pearse, Mycosporine-like amino acid content in four species of sea anemones in the genus *Anthopleura* reflects phylogenetic but not environmental or symbiotic relationships, 315

Sholkovitz, Edward R., see Jeremy M. Testa, 255

Shrimp, 347

Shull, David H., see John P. Ludlam, 250

Silver, Robert B., and Marc Bartman, A metronome-like control of the calcium signal leading to nuclear envelope breakdown and mitosis in sand dollar *(Echinaracnius parma)* cells, 213

Silversides, 241

Siphon, 235

Smith, Andrew M., and Martha C. Morin, Biochemical differences between trail mucus and adhesive mucus from marsh periwinkle snails, 338

Smith, K., C. Ridings, F. A. Dodge, and R. B. Barlow, Development of the lateral eye of juvenile *Limulus*, 222

Smith, K., see C. Ridings, 224

Smith, Peter J. S., see Gilad Twig, 198

Smolowitz, Roxanna, see Jennifer L. Hsieh, 266

Smolowitz, Roxanna, Janice Hanley, and Hazel Richmond, A three-year retrospective study of abdominal tumors in zebrafish maintained in an aquatic laboratory animal facility, 265

Smotherman, Michael, Acetylcholine mediates excitatory input to chromatophore motoneurons in the squid, *Loligo pealeii*, 231

Snail myocardium, 104

Snyder, Mark J., see Jeffrey L. Spees, 331

Social interaction and distribution of female zebrafish *(Danio rerio)* in a large aquarium, 240

Sodium
- channel, 190
- current, 192

*Spartina*, 250

*Spraguea lophii*, 212

Spawning, 225

Spectral sensitivity, 307

Spectral sensitivity of vertically migrating marine copepods, 307

Spees, Jeffrey L., Sharon A. Chang, Mark J. Snyder, and Ernest S. Chang, Osmotic induction of stress-responsive gene expression in the lobster *Homarus americanus*, 331

Sperm
- -egg collision, 51
- development, 134
- swimming, 51

Spermiogenesis and modified sperm morphology in the "seepworm" *Methanoaricia dendrobranchiata* (Polychaeta: Orbiniidae) from a methane seep environment in the Gulf of Mexico: implications for fertilization biology, 134

Spiny dogfish, 217

Spiral cleavage, 87

Spore extrusion apparatus, 212

Squid, 189, 216
- giant axon, 190, 210

Stable amorphous calcium carbonate is the main component of the calcium storage structures of the crustacean *Orchestia cavimana*, 269

Stable isotopic evidence for changing nutritional sources of juvenile horseshoe crabs, 228

Staver, Jennifer M., and Richard R. Strathmann, Evolution of fast development of planktonic embryos to early swimming, 58

Stem cell, 104

Stewart, Nicola J., see Gabriel A. Delgado, 112

Stock enhancement, 112

Strathmann, Richard R., see Jennifer M. Staver, 58

Stress proteins, 331

*Strombus gigas*, 112

Structure, formation, mechanical properties, and disposal of the embryo attachment system of an estuarine crab, *Sesarma haematocheir*, 289

Subtractive hybridization, 217

Suggs, Dianne N., Ruth H. Carmichael, Sara P. Grady, and Ivan Valiela, Effects of individual size on pairing in horseshoe crabs, 225

Supramedullary neuron, 188

Sweedler, Jonathan V., see Jennifer Marshall, 27

Swim, 58

Swimming, 144, 152

Swimming behavior of the nudibranch *Melibe leonina*, 144

*Symbiodinium* spp., 315

Symbiosis, sea anemone, 315

T

Teichberg, Mirta, see Melissa Millman, 263

Temporal
- features, 195
- patterns, 195

Terajima, M., see M. Saigusa, 289

Terwilliger, Nora, see Louis Burnett, 42

Testa, Jeremy M., Matthew A. Charette, Edward R. Sholkovitz, Matt C. Allen, Adam Rago, and Craig W. Herbold, Dissolved iron cycling in the subterranean estuary of a coastal bay: Waquoit Bay, Massachusetts, 255

Testeniere, Olivier, see Sefi Raz, 269

Tests of hypotheses on the adaptive value of an extended male phase in the hermaphroditic shrimp *Lysmata wurdemanni* (Caridea: Hippolytidae), 347

*Thalassoma bifasciatum*, 245

Thompson, Joseph T., and William M. Kier, Ontogeny of squid mantle function: changes in the mechanics of escape-jet locomotion in the oval squid, *Sepioteuthis lessoniana* Lesson, 1830, 14

Thompson, Reid F., see Torsten Wöllert, 206, 208

Thompson, Stuart, see Winsor H. Watson III, 152

A three-year retrospective study of abdominal tumors in zebrafish maintained in an aquatic laboratory animal facility, 265

Tidal flushing, 258

Tidal flushing of ammonium from intertidal salt marsh sediments: the relative importance of adsorbed ammonium, 258
Tomasky, Gabrielle, see Stacy Barron, 260; Carolyn F. Weber, 261
Toxin, 27
Tracking behavior of Busyconinae whelks, 235
Transplantation, 278
Tricaine, 188
Tumor, 265
Turbulent mixing, 275
Twichell, Sarah, Sallie Sheldon, Linda Deegan, and Robert Garritt, Nutrient and freshwater inputs from sewage effluent discharge alter benthic algal and infaunal communities in a tidal salt marsh creek, 256
Twig, Gilad, Robert Paul Malchow, Katherine Hammar, Peter J. S. Smith, Hanna Levy, and Ido Perlman, A novel turtle retinal preparation for simultaneously measuring light-induced electrical activity and changes in metabolite levels, 198

U

Uhlinger, Kevin R., see Jennifer L. Hsieh, 266
Ultrastructure, 289
Undifferentiated cells in the snail myocardium are capable of DNA synthesis and myodifferentiation, 104
UV sunscreen, 315

V

Valiela, Ivan, see Dianne N. Suggs, 225; Emily F. Gaines, 228; Melissa Millman, 263
Velum, 80
Venom duct, 27
Vesicle transport, 206, 208, 210
Vesicular plug, 219
Vestibular, 236
Vickery, Michael C.L., see Minako Vickery, 121
Vickery, Minako, Michael C.L. Vickery, and James B. McClintock, Morphogenesis and organogenesis in the regenerating planktotrophic larvae of asteroids and echinoids, 121
Vision, 224, 227
Visual behavior of juvenile *Limulus* in their natural habitat and in captivity, 224
Visual perception, 232
Volume regulation, 194

W

Wainwright, Norman, see Peter B. Armstrong, 203
Watson, W. H. III, see K. A. Lawrence, 144
Watson, Winsor H. III, James M. Newcomb, and Stuart Thompson, Neural correlates of swimming behavior in *Melibe leonina*, 152
Weber, Carolyn, see Stacy Barron, 260
Weber, Carolyn F., Stacy Barron, Roxanne Marino, Robert W. Howarth, Gabrielle Tomasky, and Eric A. Davidson, Nutrient limitation of phytoplankton growth in Vineyard Sound and Oyster Pond, Falmouth, Massachusetts, 261
Weidner, Earl, and Ann Findley, Peroxisomal catalase in extrusion apparatus posterior vacuole of microsporidian spores, 212
Weiner, Steve, see Sefi Raz, 3381
Williams, Bradley, see Kristin Hunter-Thomson, 247
Williams, Bradley S., Jeffrey E. Hughes, and Kristin Hunter-Thomson, Influence of epiphytic algal coverage on fish predation rates in simulated eelgrass habitats, 248
Wöllert, Torsten, Ana S. DePina, Reid F. Thompson, and George M. Langford, $Ca^{2+}$ effects on myosin-II-mediated contraction of pseudo-contractile rings and transport of vesicles in extracts of clam oocytes, 206
Wöllert, Torsten, Ana S. DePina, Reid F. Thompson, and George M. Langford, GTPase Rho is involved in myosin-II-mediated contraction of pseudo-contractile rings and transport of vesicles in extracts of clam oocytes, 208

X

*Xenopus* oocyte, 192

Y

Yamamoto, M., see M. Saigusa, 289
Young, Craig M., see Kevin J. Eckelbarger, 134

Z

Zakevicius, Jane, see Harris Ripps, 192
Zebrafish, 200, 240, 265
  retina, 200
Zinc, 200
Zinc chelation enhances the zebrafish retinal ERG b-wave, 200
Zoochlorellae, 315
Zooxanthellae, 315
Zottoli, S. J., see D. E. W. Arnolds, 188

# THE BIOLOGICAL BULLETIN

## 2003 Subscription Rates
## Volumes 204-205

***Paid Subscriptions include both print and electronic subscriptions at:** www.biolbull.org

| | Institutional* | Individual* |
|---|---|---|
| **One year subscription (6 issues - 2 volumes)** | $280.00 | $105.00 |
| **Single volume (3 issues)** | $140.00 | $52.50 |
| **Single Issues** | $ 50.00 | $20.00 |

*Surface delivery included in above prices.
For prompt delivery, we encourage subscribers outside the U.S. to request airmail service.

**Airmail Delivery Charge**

| | |
|---|---|
| U.S. and Canada: | $ 25.00 |
| Mexico: | $ 60.00 |
| All other locations: | $100.00 |

**Orders Must Be Prepaid in U.S. Dollars, Check Payable to The Marine Biological Laboratory**

**About *The Biological Bulletin***
ISSN: 0006-3185
Frequency: Bimonthly
Number of issues per year: 6
Months of Publication: February, April, June, August, October, December
Subscriptions entered for calendar year
Volume indexes contained in June and December issues
Annual report of the Marine Biological Laboratory contained in August issue
Most back issues available
Claims handled upon receipt
No agency discounts
Internet:
www.biolbull.org

**Please address orders to:**
Wendy Child
Subscription Administrator
The Biological Bulletin
Marine Biological Laboratory
7 MBL Street
Woods Hole, MA 02543-1015 U.S.A.
Fax: 508-289-7922 Tel: 508-289-7402 Email: wchild@mbl.edu

Published by the Marine Biological Laboratory
Woods Hole, Massachusetts, 02543 U.S.A.

# THE BIOLOGICAL BULLETIN
# (www.biolbull.org)
# 2003 SUBSCRIPTION FORM
# (VOLUMES 204-205, 6 ISSUES)

**All subscriptions run on the calendar year; price includes both print and online journals.**

*(please print)*

NAME: ______________________________

INSTITUTION: ______________________________

ADDRESS: ______________________________

CITY: ______________ STATE: ______________

POSTAL CODE: ______________ COUNTRY: ______________

TELEPHONE: ______________ FAX: ______________

E-MAIL ADDRESS: ______________________________

☐ **Please send me a 2003 subscription to *The Biological Bulletin* at the rate indicated below:**

☐ Individual: $105.00 (6 ISSUES) ☐ Institutional: $280.00 (6 ISSUES)
☐ Individual: $ 52.50 (3 ISSUES) ☐ Institutional: $140.00 (3 ISSUES)
*Check one:* ☐ February, April, June or ☐ August, October, December

☐ **Please send me the following back issue(s):** ______________________________

☐ Individual: at $20.00 (PER ISSUE) ☐ Institutional: at $50.00 (PER ISSUE)

**Delivery Options**

_____ Surface Delivery (Surface delivery is included in the subscription price.)

_____ Air delivery (Please add the correct amount to your payment.)

☐ U.S. and Canada: $25.00 ☐ Mexico: $60.00 ☐ All other locations: $100.00

**Payment Options**

_____ Enclosed is my check or U.S. money order for $ ______ payable to The Marine Biological Laboratory

_____ Please send me an invoice. (Note: Payment must be received before subscription commences.)

_____ Please charge my ☐ VISA, ☐ MasterCard ☐ Discover Card $________

Account No.: ______________ Exp. Date: ______________

Signature: ______________ Date: ______________

5034 . 5

**Return this form with your check or credit card information to:**

Marine Biological Laboratory
Subscription Office ◆ The Biological Bulletin ◆ 7 MBL Street ◆ Woods Hole, MA 02543-1015

**Ludl Electronic Products Ltd.**

*Designers and manufacturers of precision microscope automation accessories for over 25 years*

Precision XY Stages

- Stepper or DC-servo motors
- Sizes from 3"x2" up to 10"x4"
- Flexible encoder options
- Precision ball-screws
- 0.05μm resolution
- Universal microscope mount

Microscope Automation

- Programmable filter wheels
- Focus/ Z-axis controls
- Lamp sockets and retrofits
- Lamp power supplies
- Custom designs

171 Brady Avenue • Hawthorne, NY 10532
(888) 769-6111 Tel. • (914) 769-4759 Fax
www.ludl.com • sales@ludl.com

---

**2003 SUMMER RESEARCH FELLOWSHIPS**

**FUNDING AVAILABLE FOR SUMMER RESEARCH AT THE MARINE BIOLOGICAL LABORATORY**

The Marine Biological Laboratory is pleased to announce the availability of funding for Summer Research Fellowships in 2003 for junior or senior investigators holding a Ph.D., M.D., or equivalent degree. These prestigious awards provide costs for research and housing, and also enable Fellows to benefit from the rich intellectual and interactive environment of the scientific community at the MBL.

Proposals for Fellowship support will be considered in, but are not limited to, the following fields of investigation:

**Cellular & Molecular Physiology**
**Neurobiology**
**Parasitology**
**Molecular Biology**
**Developmental Biology**
**Ecology**
**Microbiology**

Specific Fellowships in Cell & Developmental Biology are funded by the Laura and Arthur Colwin Fellowship Fund. Additional specific Fellowships also provide state-of-the-art microscopy support.

*Applications are encouraged from women and members of underrepresented minorities.*

ADDITIONAL INFORMATION IS AVAILABLE ON OUR WEB-SITE:

**http://www.mbl.edu/fellowships**

**APPLICATION DEADLINE FOR FELLOWSHIPS IS JANUARY 15, 2003**

Applications are reviewed by the MBL Fellowship Committee. Notification of decisions will be mailed by March 15.

FOR APPLICATION FORMS AND ADDITIONAL INFORMATION, PLEASE CONTACT:
Sandra Kaufmann
Fellowship Coordinator
508-289-7441: skaufman@mbl.edu

*The MBL is an EEO Affirmative Action Institution*

**Marine Biological Laboratory, 7 MBL Street, Woods Hole, Massachusetts 02543-1015**

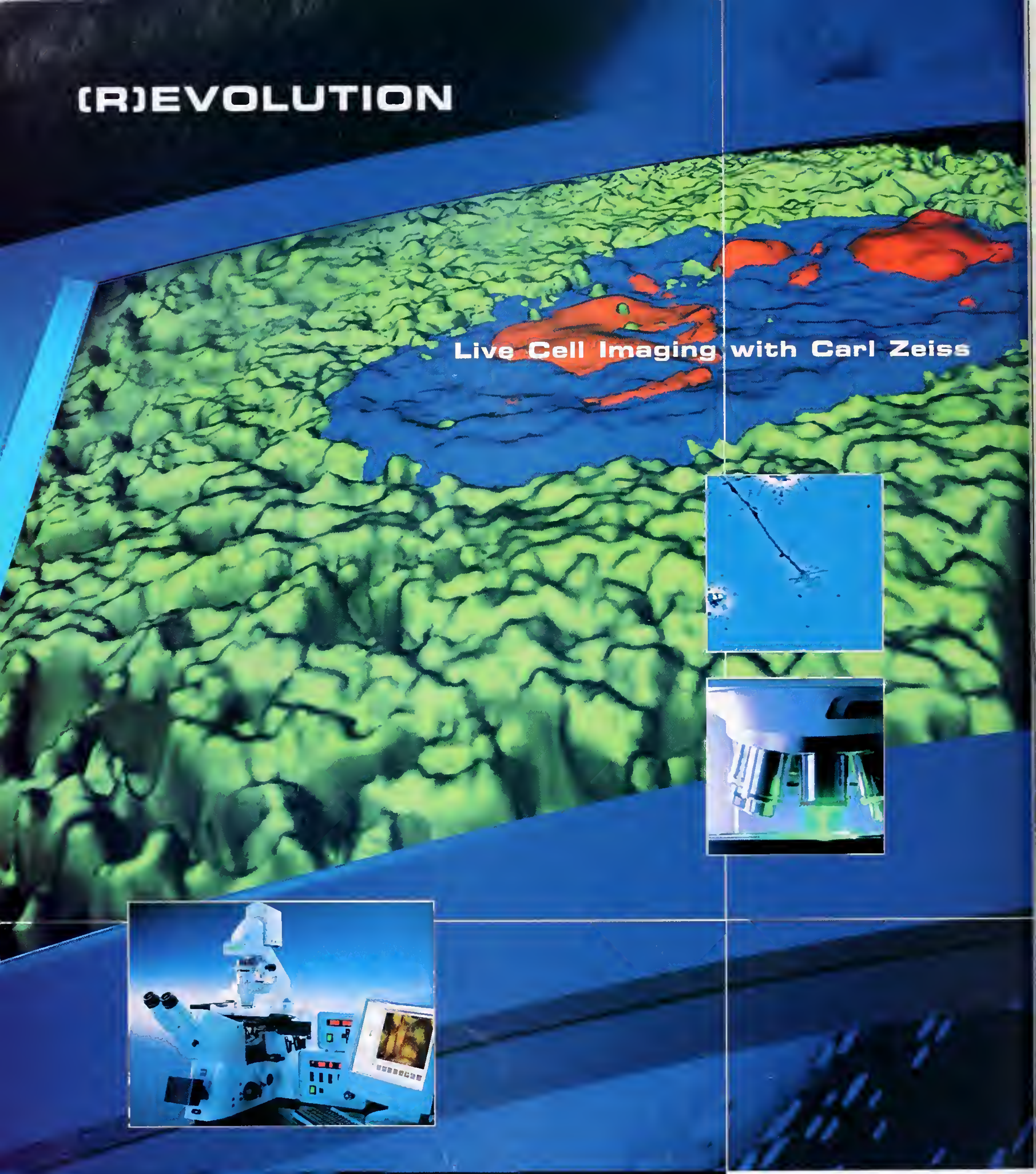

You need more than brilliant optics to uncover life's secrets. You need a revolutionary new system for live cell research: The Cell Observer™ from Carl Zeiss. This innovative system was developed specifically for the observation & digital documentation of living processes. It provides a powerful combination of perfectly matched high-performance components: microscopes, digital cameras, software & incubation peripherals. Carl Zeiss systems: so forward-thinking, we revolutionized the field.

For information about Zeiss products please call 800-233-2343 or visit us online: zeiss.com/micro.

Carl Zeiss MicroImaging, Inc. • Thornwood, NY 10594 • micro@zeiss.com

ZEISS

We make it visible.

MBL/WHOI LIBRARY
WH 1838 W